Advances in Experimental Medicine and Biology 1441

Silke Rickert-Sperling
Robert G. Kelly
Nikolaus Haas *Editors*

Congenital Heart Diseases: The Broken Heart

Clinical Features, Human Genetics and Molecular Pathways

Second Edition

Springer

Advances in Experimental Medicine and Biology

Volume 1441

Series Editors

Wim E. Crusio, Institut de Neurosciences Cognitives et Intégratives d'Aquitaine, CNRS and University of Bordeaux, Pessac Cedex, France

Haidong Dong, Departments of Urology and Immunology, Mayo Clinic, Rochester, MN, USA

Heinfried H. Radeke, Institute of Pharmacology and Toxicology, Clinic of the Goethe University Frankfurt Main, Frankfurt am Main, Hessen, Germany

Nima Rezaei, Research Center for Immunodeficiencies, Children's Medical Center, Tehran University of Medical Sciences, Tehran, Iran

Ortrud Steinlein, Institute of Human Genetics, LMU University Hospital, Munich, Germany

Junjie Xiao, Cardiac Regeneration and Ageing Lab, Institute of Cardiovascular Sciences, School of Life Science, Shanghai University, Shanghai, China

Advances in Experimental Medicine and Biology provides a platform for scientific contributions in the main disciplines of the biomedicine and the life sciences. This series publishes thematic volumes on contemporary research in the areas of microbiology, immunology, neurosciences, biochemistry, biomedical engineering, genetics, physiology, and cancer research. Covering emerging topics and techniques in basic and clinical science, it brings together clinicians and researchers from various fields.

Advances in Experimental Medicine and Biology has been publishing exceptional works in the field for over 40 years, and is indexed in SCOPUS, Medline (PubMed), EMBASE, BIOSIS, Reaxys, EMBiology, the Chemical Abstracts Service (CAS), and Pathway Studio.

2022 CiteScore: 6.2

Silke Rickert-Sperling • Robert G. Kelly • Nikolaus Haas
Editors

Congenital Heart Diseases: The Broken Heart

Clinical Features, Human Genetics and Molecular Pathways

Second Edition

Springer

Editors
Silke Rickert-Sperling
Cardiovascular Genetics
Charité - Universitätsmedizin Berlin
Berlin, Germany

Robert G. Kelly
Aix Marseille Université
Institut de Biologie du Dévelopment de Marseille
Marseille, France

Nikolaus Haas
LMU Ludwig Maximilian University,
Klinikum der Universität München
München, Bayern, Germany

ISSN 0065-2598 ISSN 2214-8019 (electronic)
Advances in Experimental Medicine and Biology
ISBN 978-3-031-44086-1 ISBN 978-3-031-44087-8 (eBook)
https://doi.org/10.1007/978-3-031-44087-8

© The Editor(s) (if applicable) and The Author(s), under exclusive license to Springer Nature Switzerland AG 2016, 2024
This work is subject to copyright. All rights are solely and exclusively licensed by the Publisher, whether the whole or part of the material is concerned, specifically the rights of translation, reprinting, reuse of illustrations, recitation, broadcasting, reproduction on microfilms or in any other physical way, and transmission or information storage and retrieval, electronic adaptation, computer software, or by similar or dissimilar methodology now known or hereafter developed.
The use of general descriptive names, registered names, trademarks, service marks, etc. in this publication does not imply, even in the absence of a specific statement, that such names are exempt from the relevant protective laws and regulations and therefore free for general use.
The publisher, the authors, and the editors are safe to assume that the advice and information in this book are believed to be true and accurate at the date of publication. Neither the publisher nor the authors or the editors give a warranty, expressed or implied, with respect to the material contained herein or for any errors or omissions that may have been made. The publisher remains neutral with regard to jurisdictional claims in published maps and institutional affiliations.

This Springer imprint is published by the registered company Springer Nature Switzerland AG
The registered company address is: Gewerbestrasse 11, 6330 Cham, Switzerland

If disposing of this product, please recycle the paper.

Foreword of the 1st Edition

As is indicated in its title, the book you are about to read is concerned with the congenitally malformed heart. Approximately eight neonates in every thousand born alive present with such a "broken heart". This number has changed little since Maude Abbott, when describing the first plate in her Atlas devoted to congenitally malformed hearts, commented that "An understanding of the elementary facts of human and comparative embryology is essential to an intelligent grasp of the ontogenetic problems of congenital cardiac disease". Paul Dudley White, when writing the foreword to her Atlas, commented that it had been left to Abbott to "make the subject one of such general and widespread interest that we no longer regard it with either disdain or awe as a mystery for the autopsy table alone to discover and to solve". It is perhaps surprising, therefore, to realise that it has taken nearly a century for us to achieve the necessary understanding of the "elementary facts" emphasised by Abbott. Indeed, it is not that long since, in company with my very good friend and collaborator Anton Becker, we suggested that interpretations based on embryology might prove to be a hindrance, rather than a help, in understanding the congenitally malformed heart. The contents of this book show how much has changed in the years that have passed since we made that comment, such that we now need to eat our words.

As is revealed by the multiple chapters of this book, the recent advances made in the fields of cardiac embryology and molecular genetics have been truly spectacular. It was these fields that were expertly summarised in the volumes edited by Rosenthal and Harvey. The details contained in the central part of this book, related to central molecular pathways, recapitulate and extend those reviews. Such extensive knowledge of the genetic and molecular background, however, is of limited value if these interpretations cannot properly be translated into the findings observed on a daily basis by those who diagnose and treat the individual cardiac lesions. The first part of this book, therefore, provides a necessarily brief overview of normal cardiac development, while the final chapters then incorporate the developmental and molecular findings into the clinical manifestations of the abnormal morphogenesis.

I know from my own experience how difficult it is to obtain such chapters from multiple authors, who nowadays are themselves under greater pressure to produce primarily in the peer-reviewed realm. The editors, therefore, are to be congratulated on assembling such a panoply of authoritative texts. As might be expected, not all of

the texts are of comparable length or content. The critical reader will note that several of the topics addressed remain contentious, and that opinions continue to vary between the chosen experts. This is no more than to be expected, since the topics remain very much moving targets. One hopes, therefore, that this is but the first edition of a work which itself, for the first time, seeks to provide in detail the scientific background to the specific lesions that continue to break the normal heart. As the pages of this book demonstrate, we still have much to do if we are fully to understand the mechanics of normal as opposed to abnormal cardiac development.

London, UK
August 2015

Robert H. Anderson

Foreword of the 2nd Edition

It has been now 8 years since the publication of the first edition of "The Broken Heart". In writing the foreword to the first edition, I cited the importance placed by Maude Abbott, certainly the first, if not the most influential, of dedicated pediatric cardiac morphologists, on an appreciation of normal cardiac development as the basis for understanding the anatomy of the congenitally malformed heart. It remains, of course, a firm grasp of the underlying anatomical substrate that underscores the correct diagnosis and treatment of the various phenotypes encountered when the heart is congenitally malformed. In continuing my foreword, I pointed to the time taken to achieve the necessary understanding of the elementary facts highlighted by Abbott. I then further emphasized how the contents of the first edition demonstrated the spectacular advances made in the fields of cardiac molecular genetics over the turn of the twenty-first century. Further improvements are now to be found in the revised chapters of this second edition.

In the first edition of the book, the important chapter on normal cardiac development had "necessarily been brief". It has been markedly expanded in the second edition. In this regard, I should acknowledge my bias, since I am one of the co-authors of this chapter. Its importance, nonetheless, lies in the fact that it is based on a detailed analysis of temporal development of the human heart during the embryonic period. It matches a companion study of the same material now published in "Communications in Biology", but accounts for the changes in systematic rather than longitudinal fashion. The two accounts are complementary. In my obviously biased opinions, I do believe that the chapter and its partner manuscript now provide all the material required to fulfill the expectations of Maude Abbott. Most importantly, it represents the necessary anatomical skeleton on which to assemble the extensive information provided in the central section of the book devoted to molecular and genetic advances. As the editors emphasize in their own preface, this central part has now also been expanded to include chapters on single-cell transcriptomics, stem cells, organoids, and cardiac metabolism. These initial parts of the book then set the scene for understanding the "meat" of the practice of pediatric cardiology, namely the clinical features, the underlying genetic alterations, the related animal models, and the molecular pathways of the different lesions that together make up congenital heart disease.

I have now been involved in the investigation of these various entities for more than half a century. It is encouraging to note that, slowly but surely, the controversies

that surrounded many of these lesions when I started in the field are being resolved. I commented on such controversies in my foreword to the first edition. I suggested that the topics remained as "moving targets". Readers of this second edition will discover that, in the period between the editions, the targets have become much easier to hit. This reflects the ability, developed over the past decade, for clinicians to provide three-dimensional illustrations of the underlying anatomy by means of virtual dissection, or creation of models, of datasets obtained during life. These advances also receive appropriate emphasis in this second edition. The appearance of this second edition itself points to the success of the first edition, which provided in detail the scientific background to the specific lesions that continue to break the normal heart. As the pages of the second edition demonstrate, we continue to increase our understanding of the mechanics of normal as opposed to abnormal cardiac development.

London, UK
July 2023

Robert H. Anderson

Preface

In the fifteenth century, Leonardo Da Vinci made the first drawing of partial anomalous pulmonary venous connection, and 300 years later, Karl von Rokitansky described ventricular septal defects. Since then, the understanding of congenital heart diseases (CHDs) has rapidly evolved, encompassing clinical recognition, therapeutic opportunities, and the exploration of their developmental and genetic origins.

The initial wave of progress focused on enhancing clinical diagnosis and therapy through anatomical, physiological, and surgical considerations. Consequently, the mortality rate for patients with CHD decreased to below 1 in 100,000 cases, giving rise to a new group of adult patients with corrected and palliated CHD.

The subsequent wave of progress shifted attention toward the developmental, genetic, and molecular aspects of CHDs. Valuable insights were gained by studying animal models alongside humans, leading to the discovery of numerous genes, signaling pathways, and other molecular and hemodynamic factors. The developmental perspective served as a crucial starting point for these investigations.

After decades of basic research primarily utilizing animal models, the focus has shifted toward the human phenotype. Technological advancements have overcome previous limitations, enabling the study of complex biological questions and systems. Additionally, there is a growing recognition that improving human health is a central aim of life science research. This book consolidates clinical, genetic, and molecular knowledge into a single volume, with a particular emphasis on the observed human phenotype during development and in the disease state. Its intended audience encompasses both basic scientists and physicians. Furthermore, it aims to contribute to the current third wave of progression, where the basic science of cardiovascular development is translated into clinical diagnosis and therapy of CHDs.

To achieve this goal, the book is structured into three main parts. The first part provides an introduction to the development of the heart and its vessels. The second part offers an overview of molecular pathways influencing the development of multiple cardiovascular structures. Lastly, the book adopts a textbook-like structure in the third part, focusing on different types of congenital heart diseases. Each chapter delves into their clinical features, underlying genetic alterations, related animal models, and pathways.

In this second edition, published eight years after the first edition, every chapter has been thoroughly updated to reflect the rapid pace of discovery and technological innovation in the field of CHD research. New chapters have been included, covering topics such as single-cell transcriptomics—a revolutionary approach that offers unprecedented insights into cellular heterogeneity and differentiation pathways. Stem cell and organoid approaches to study CHD are also discussed, as they accelerate mechanistic understanding and hold therapeutic potential. Additionally, cardiac metabolism has emerged as a highly dynamic driver of cardiac development and is explored in a dedicated chapter. Furthermore, the book presents the 3D-reconstruction of human heart development, showcasing both its beauty and complexity. Finally, the clinical chapters have been expanded significantly, incorporating additional pathological details and new illustrations. Each clinical chapter now features a section highlighting the diagnostic imaging approaches best suited for analyzing specific forms of CHD.

We extend our deepest gratitude to all the contributors to this volume, whose expertise and state-of-the-art accounts have enriched this book.

Berlin, Germany — Silke Rickert-Sperling
Marseille, France — Robert G. Kelly
Rochester, MN, USA — David J. Driscoll
Munich, Germany — Nikolaus Haas
April 2024

Contents

Part I Introduction

1 **Human Cardiac Development** 3
Jill P. J. M. Hikspoors, Nutmethee Kruepunga, Greet M. C. Mommen, S. Eleonore Köhler, Robert H. Anderson, and Wouter H. Lamers

2 **Human Genetics of Congenital Heart Defects** 57
Anna Wilsdon and Siobhan Loughna

3 **Cardiac Development and Animal Models of Congenital Heart Defects** 77
Robert G. Kelly

4 **Normal Cardiac Anatomy and Clinical Evaluation** 87
Nikolaus A. Haas, David J. Driscoll, and Silke Rickert-Sperling

Part II Development of the Heart and Its Vessels

5 **Cardiac Progenitor Cells of the First and Second Heart Fields** 103
Margaret Buckingham and Robert G. Kelly

6 **Neural Crest** 125
Bijoy D. Thattaliyath and Anthony B. Firulli

7 **Inflow Tract Development** 145
Andy Wessels

8 **Epicardium and Coronary Vessels** 155
Adrián Ruiz-Villalba, Juan Antonio Guadix, and José M. Pérez-Pomares

9 **Establishment of Cardiac Laterality** 167
George C. Gabriel, Yijen L. Wu, and Cecilia W. Lo

10 **Development of the Cardiac Conduction System** 185
Lieve E. van der Maarel and Vincent M. Christoffels

11 Hemodynamics During Development and Postnatal Life 201
Martina Gregorovicova, S. Samaneh Lashkarinia, Choon Hwai Yap, Viktor Tomek, and David Sedmera

12 Evolutionary Aspects of Chamber Formation and Septation 227
Bjarke Jensen and Antoon F. M. Moorman

13 Deciphering Congenital Heart Disease Using Human Induced Pluripotent Stem Cells 239
Hao Zhang and Joseph C. Wu

14 Cardiac Development at a Single-Cell Resolution 253
Nicholas Wei, Carissa Lee, Lauren Duan, Francisco X. Galdos, Tahmina Samad, Alireza Raissadati, William R. Goodyer, and Sean M. Wu

Part III Central Molecular and Cellular Pathways

15 Inter- and Intracellular Signaling Pathways 271
Gergana Dobreva and Joerg Heineke

16 Cardiac Transcription Factors and Regulatory Networks 295
Marcel Grunert, Cornelia Dorn, and Silke Rickert-Sperling

17 Posttranscriptional Regulation by Proteins and Noncoding RNAs 313
Amelia E. Aranega and Diego Franco

18 Epigenetics 341
Rajan Jain and Jonathan A. Epstein

19 Cardiac Metabolism 365
Silvia Martin-Puig and Ivan Menendez-Montes

20 Environmental Signals 397
George A. PorterJr

21 The Contractile Machines of the Heart 417
Ingo Morano

22 Technologies to Study Genetics and Molecular Pathways 435
Marcel Grunert, Cornelia Dorn, Ana Dopazo, Fátima Sánchez-Cabo, Jésus Vázquez, Silke Rickert-Sperling, and Enrique Lara-Pezzi

Part IV Atrial Septal Defect

23 Clinical Presentation and Therapy of Atrial Septal Defect 461
Nikolaus A. Haas, David J. Driscoll, and Silke Rickert-Sperling

24 Human Genetics of Atrial Septal Defect 467
Lars A. Larsen and Marc-Phillip Hitz

25 Molecular Pathways and Animal Models of Atrial Septal Defect 481
Rachel A. Magnan, Lillian Kang, Karl R. Degenhardt, Robert H. Anderson, and Patrick Y. Jay

Part V Ventricular Septal Defect

26 Clinical Presentation and Therapy of Ventricular Septal Defect 497
Nikolaus A. Haas, David J. Driscoll, and Silke Rickert-Sperling

27 Human Genetics of Ventricular Septal Defect 505
Andreas Perrot and Silke Rickert-Sperling

28 Ventricular Septal Defects: Molecular Pathways and Animal Models 535
Lucile Houyel

Part VI Atrioventricular Septal Defect

29 Clinical Presentation and Therapy of Atrioventricular Septal Defect 553
Nikolaus A. Haas, David J. Driscoll, and Silke Rickert-Sperling

30 Human Genetics of Atrioventricular Septal Defect 559
Cheryl L. Maslen

31 Molecular Pathways and Animal Models of Atrioventricular Septal Defect 573
Andy Wessels

Part VII Total Anomalous Pulmonary Venous Return

32 Clinical Presentation and Therapy of Total Anomalous Pulmonary Venous Return 587
Nikolaus A. Haas, David J. Driscoll, and Silke Rickert-Sperling

33 Total Anomalous Pulmonary Venous Connections, Human Genetics 593
R. E. Poelmann, M. R. M. Jongbloed, and M. C. DeRuiter

34 TAPVR: Molecular Pathways and Animal Models 599
Robert E. Poelmann, Monique R. M. Jongbloed, and Marco C. DeRuiter

Part VIII Tetralogy of Fallot and Double Outlet Right Ventricle

35 Clinical Presentation and Therapy of Tetralogy of Fallot and Double-Outlet Right Ventricle 617
Nikolaus A. Haas, David J. Driscoll, and Silke Rickert-Sperling

36 Human Genetics of Tetralogy of Fallot and Double-Outlet Right Ventricle 629
Cornelia Dorn, Andreas Perrot, Marcel Grunert, and Silke Rickert-Sperling

37 Molecular Pathways and Animal Models of Tetralogy of Fallot and Double Outlet Right Ventricle 645
Robert G. Kelly

Part IX d-Transposition of the Great Arteries

38 Clinical Presentation and Therapy of d-Transposition of the Great Arteries 663
Nikolaus A. Haas, David J. Driscoll, and Silke Rickert-Sperling

39 Human Genetics of d-Transposition of Great Arteries 671
Lucile Houyel

40 Molecular Pathways and Animal Models of d-Transposition of the Great Arteries 683
Eleanor Gill and Simon D. Bamforth

Part X Defects of Situs

41 Clinical Presentation and Therapy of Anomalies of the Situs 699
Nikolaus A. Haas, David J. Driscoll, and Silke Rickert-Sperling

42 Human Genetics of Defects of Situs 705
Andreas Perrot and Silke Rickert-Sperling

43 Molecular Pathways and Animal Models of Defects in Situs 719
George C. Gabriel and Cecilia W. Lo

Part XI Semilunar Valve and Aortic Arch Anomalies

44 Clinical Presentation and Therapy of Semilunar Valve and Aortic Arch Anomalies 741
Nikolaus A. Haas, David J. Driscoll, and Silke Rickert-Sperling

45 Human Genetics of Semilunar Valve and Aortic Arch Anomalies 761
Matina Prapa and Siew Yen Ho

46 Molecular Pathways and Animal Models of Semilunar Valve and Aortic Arch Anomalies 777
Eleanor Gill and Simon D. Bamforth

Part XII Coronary Artery Anomalies

47 Clinical Presentation and Therapy of Coronary Artery Anomalies 799
Nikolaus A. Haas, David J. Driscoll, and Silke Rickert-Sperling

48 The Genetics of Human Congenital Coronary Vascular Anomalies 811
Almudena Ortiz Garrido, Beatriz Picazo, Juan Antonio Guadix, Adrián Ruiz-Villalba, and José M. Pérez-Pomares

49 Congenital Coronary Blood Vessel Anomalies: Animal Models and the Integration of Developmental Mechanisms 817
Juan Antonio Guadix, Adrián Ruiz-Villalba, and José M. Pérez-Pomares

Part XIII Truncus Arteriosus

50 Clinical Presentation and Therapy of Truncus Arteriosus 835
Nikolaus A. Haas, David J. Driscoll, and Silke Rickert-Sperling

51 Human Genetics of Truncus Arteriosus 841
Hiroyuki Yamagishi

52 Molecular Pathways and Animal Models of Truncus Arteriosus 853
Eleanor Gill and Simon D. Bamforth

Part XIV Tricuspid Atresia and Univentricular Heart

53 Clinical Presentation and Therapy of Tricuspid Atresia and Univentricular Heart 869
Nikolaus A. Haas, David J. Driscoll, and Silke Rickert-Sperling

54 Human Genetics of Tricuspid Atresia and Univentricular Heart 875
Abdul-Karim Sleiman, Liane Sadder, and George Nemer

55 Molecular Pathways and Animal Models of Tricuspid Atresia and Univentricular Heart 885
Kamel Shibbani and George Nemer

Part XV Ebstein Anomaly

56 Clinical Presentation and Therapy of Ebstein Anomaly 903
Nikolaus A. Haas, David J. Driscoll, and Silke Rickert-Sperling

57 Human Genetics of Ebstein Anomaly 909
Farbod Sedaghat-Hamedani, Gregor U. Andelfinger, and Benjamin Meder

58 Molecular Pathways and Animal Models of Ebstein's Anomaly 915
Bjarke Jensen, Gregor U. Andelfinger, and Alex V. Postma

Part XVI Hypoplastic Left Heart Syndrome

59 Clinical Presentation and Therapy of Hypoplastic Left Heart Syndrome 931
Nikolaus A. Haas, David J. Driscoll, and Silke Rickert-Sperling

60 Human Genetics of Hypoplastic Left Heart Syndrome 937
Constanze Pfitzer, Katharina R. L. Schmitt, and Woodrow D. Benson

61 Molecular Pathways and Animal Models of Hypoplastic Left Heart Syndrome 947
Hisato Yagi, Xinxiu Xu, George C. Gabriel, and Cecilia Lo

Part XVII Cardiomyopathies

62 Clinical Presentation and Therapy of Cardiomyopathies 965
Nikolaus A. Haas, David J. Driscoll, and Silke Rickert-Sperling

63 Human Genetics of Cardiomyopathies 977
Arjan C. Houweling, Ronald H. Lekanne Deprez, and Arthur A. M. Wilde

64 Molecular Pathways and Animal Models of Cardiomyopathies . . . 991
Buyan-Ochir Orgil and Enkhsaikhan Purevjav

Part XVIII Arrhythmias

65 Clinical Presentation and Therapy of Arrhythmias 1023
Nikolaus A. Haas, David J. Driscoll, and Silke Rickert-Sperling

66 Human Genetics of Cardiac Arrhythmias 1033
Eric Schulze-Bahr and Sven Dittmann

67 Molecular Pathways and Animal Models of Arrhythmias 1057
Tyler L. Stevens, Sara Coles, Amy C. Sturm, Catherine A. Hoover, Maegen A. Borzok, Peter J. Mohler, and Mona El Refaey

Perspective 1091

Index 1095

Contributors

Gregor U. Andelfinger Cardiovascular Genetics, Department of Pediatrics, CHU Sainte Justine, Université de Montréal, Montréal, QC, Canada

Robert H. Anderson Institute of Genetic Medicine, Newcastle University, Newcastle upon Tyne, UK
Cardiovascular Research Center, Biosciences Institute, Newcastle University, Newcastle upon Tyne, UK

Amelia E. Aranega Cardiovascular Research Group, Department of Experimental Biology, University of Jaén, Jaén, Spain

Simon D. Bamforth Newcastle University Biosciences Institute, Newcastle upon Tyne, UK
Newcastle University, Newcastle upon Tyne, UK

Woodrow D. Benson Department of Pediatrics, Herma Heart Center, Children's Hospital of Wisconsin, Medical College of Wisconsin, Milwaukee, WI, USA

Maegen A. Borzok Department of Natural Sciences, Mansfield University of Pennsylvania, Mansfield, PA, USA

Margaret Buckingham Department of Developmental and Stem Cell Biology, CNRS UMR 3738, Institut Pasteur, Paris, France

Vincent M. Christoffels Department of Medical Biology, Amsterdam University Medical Center, University of Amsterdam, Amsterdam, The Netherlands

Sara Coles Division of Cardiology, Department of Medicine, Duke University Medical Center, Durham, NC, USA

Karl R. Degenhardt Division of Cardiology, Department of Pediatrics, Children's Hospital of Philadelphia, Perelman School of Medicine at the University of Pennsylvania, Philadelphia, PA, USA

Marco C. DeRuiter Department of Anatomy and Embryology, Leiden University Medical Center, Leiden, The Netherlands

Sven Dittmann Department of Cardiovascular Medicine, Institute for Genetics of Heart Diseases (IfGH), University Hospital Münster, Münster, Germany

Gergana Dobreva ECAS (European Center for Angioscience), Department of Cardiovascular Genomics and Epigenomics, Mannheim Faculty of Medicine, Heidelberg University, Mannheim, Germany
German Centre for Cardiovascular Research (DZHK) Partner Site, Heidelberg/ Mannheim, Germany

Ana Dopazo Genomics Unit, Centro Nacional de Investigaciones Cardiovasculares, Madrid, Spain

Cornelia Dorn Cardiovascular Genetics, Charité – Universitätsmedizin Berlin, Berlin, Germany

David J. Driscoll Division of Pediatric Cardiology, Department of Pediatrics, Mayo Clinic College of Medicine, Rochester, MN, USA

Lauren Duan Stanford University, Cardiovascular Institute, Stanford, CA, USA

Jonathan A. Epstein Departments of Medicine and Cell and Developmental Biology, Institute for Regenerative Medicine, Epigenetics Institute and the Cardiovascular Institute, Perelman School of Medicine at the University of Pennsylvania, Philadelphia, PA, USA

Anthony B. Firulli Herman B Wells Center for Pediatric Research, Department of Pediatrics, Indiana University School of Medicine, Indianapolis, IN, USA

Diego Franco Cardiovascular Research Group, Department of Experimental Biology, University of Jaén, Jaén, Spain

George C. Gabriel Department of Developmental Biology, University of Pittsburgh School of Medicine, Pittsburgh, PA, USA

Francisco X. Galdos Stanford University, Cardiovascular Institute, Stanford, CA, USA

Almudena Ortiz Garrido Hospital Materno Infantil-Hospital Carlos de Haya, Málaga, Spain

Eleanor Gill Newcastle University Biosciences Institute, Newcastle upon Tyne, UK
Newcastle University, Newcastle upon Tyne, UK

William R. Goodyer Department of Pediatrics, Stanford University, Stanford, CA, USA

Martina Gregorovicova Laboratory of Developmental Cardiology, Institute of Physiology, Czech Academy of Sciences, Prague, Czech Republic
Institute of Anatomy, First Faculty of Medicine, Charles University, Prague, Czech Republic

Marcel Grunert Cardiovascular Genetics, Charité – Universitätsmedizin Berlin, Berlin, Germany
DiNAQOR AG, Schlieren, Switzerland

Juan Antonio Guadix Department of Animal Biology, Faculty of Sciences, University of Málaga, Málaga, Spain
Andalusian Center for Nanomedicine and Biotechnology (BIONAND), Málaga, Spain
Instituto de Biomedicina de Málaga (IBIMA)-Hospital Carlos de Haya, Málaga, Spain

Nikolaus A. Haas Department of Pediatric Cardiology and Intensive Care, Ludwig Maximilians University, Munich, Germany

Joerg Heineke German Centre for Cardiovascular Research (DZHK) Partner Site, Heidelberg/Mannheim, Germany
ECAS (European Center for Angioscience), Department of Cardiovascular Physiology, Mannheim Faculty of Medicine, Heidelberg University, Mannheim, Germany

Jill P. J. M. Hikspoors Department of Anatomy & Embryology, Maastricht University, Maastricht, The Netherlands

Marc-Phillip Hitz Institute of Medical Genetics, University Medicine Oldenburg, Oldenburg, Germany
Department of Paediatric Cardiology, University Hospital Kiel, Kiel, Germany

Siew Yen Ho Cardiac Morphology, Royal Brompton & Harefield Hospitals, London, UK

Catherine A. Hoover Department of Natural Sciences, Mansfield University of Pennsylvania, Mansfield, PA, USA

Arjan C. Houweling Department of Clinical Genetics, Amsterdam University Medical Centers, University of Amsterdam, Amsterdam, The Netherlands

Lucile Houyel Pediatric and Congenital Cardiology Unit, Necker-Enfants Malades Hospital – M3C, University of Paris, Paris, France
Department of Congenital and Pediatric Cardiology, Necker-Enfants Malades Hospital–M3C, APHP, Paris, France
Université Paris Cité, Paris, France

Rajan Jain Departments of Medicine and Cell and Developmental Biology, Institute for Regenerative Medicine, Epigenetics Institute and the Cardiovascular Institute, Perelman School of Medicine at the University of Pennsylvania, Philadelphia, PA, USA

Patrick Y. Jay Alnylam Pharmaceuticals, Cambridge, MA, USA

Bjarke Jensen Department of Medical Biology, Amsterdam Cardiovascular Sciences, Amsterdam University Medical Centres, Amsterdam, The Netherlands

Monique R. M. Jongbloed Department of Cardiology, Leiden University Medical Center, Leiden, The Netherlands
Department of Anatomy and Embryology, Leiden University Medical Center, Leiden, The Netherlands

Lillian Kang Department of Surgery, Duke University, Durham, NC, USA

Robert G. Kelly Aix Marseille Université, Institut de Biologie du Dévelopment de Marseille, Marseille, France

S. Eleonore Köhler Department of Anatomy & Embryology, Maastricht University, Maastricht, The Netherlands

Nutmethee Kruepunga Department of Anatomy & Embryology, Maastricht University, Maastricht, The Netherlands
Department of Anatomy, Mahidol University, Bangkok, Thailand

Wouter H. Lamers Department of Anatomy & Embryology, Maastricht University, Maastricht, The Netherlands
Tytgat Institute for Liver and Intestinal Research, Academic Medical Center, Amsterdam, The Netherlands

Enrique Lara-Pezzi Myocardial Pathophysiology Area, Centro Nacional de Investigaciones Cardiovasculares, Madrid, Spain

Lars A. Larsen Department of Cellular and Molecular Medicine, University of Copenhagen, Copenhagen, Denmark

S. Samaneh Lashkarinia Department of Bioengineering, Imperial College, London, UK

Carissa Lee Stanford University, Cardiovascular Institute, Stanford, CA, USA

Ronald H. Lekanne Deprez Department of Clinical Genetics, Amsterdam University Medical Centers, University of Amsterdam, Amsterdam, The Netherlands

Cecilia W. Lo Department of Developmental Biology, University of Pittsburgh School of Medicine, Pittsburgh, PA, USA

Siobhan Loughna School of Life Sciences, University of Nottingham, Nottingham, UK

Lieve E. van der Maarel Department of Medical Biology, Amsterdam University Medical Center, University of Amsterdam, Amsterdam, The Netherlands

Rachel A. Magnan Department of Pediatrics, Goryeb Children's Hospital, Morristown, NJ, USA

Silvia Martin-Puig Department of Vascular Pathophysiology, National Center for Cardiovascular Research, CNIC, Madrid, Spain

Department of Metabolic, Immune and Cardiovascular Disease, Institute for Biomedical Research "Alberto Sols", National Spanish Research Council, CSIC, Madrid, Spain

Cheryl L. Maslen Knight Cardiovascular Institute, Oregon Health & Science University, Portland, OR, USA

Benjamin Meder Institute for Cardiomyopathies Heidelberg, Universitätsklinikum Heidelberg, Innere Medizin III - Kardiologie, Angiologie und Pneumologie, Heidelberg, Germany

Ivan Menendez-Montes Department of Internal Medicine, University of Texas Southwestern Medical Center, Dallas, TX, USA

Peter J. Mohler The Dorothy M. Davis Heart and Lung Research Institute, The Ohio State University Wexner Medical Center, Columbus, OH, USA
Department of Physiology and Cell Biology, The Ohio State University Wexner Medical Center, Columbus, OH, USA
Division of Cardiovascular Medicine, Department of Internal Medicine, The Ohio State University Wexner Medical Center, Columbus, OH, USA

Greet M. C. Mommen Department of Anatomy & Embryology, Maastricht University, Maastricht, The Netherlands

Antoon F. M. Moorman Department of Medical Biology, Amsterdam Cardiovascular Sciences, Amsterdam University Medical Centres, Amsterdam, The Netherlands

Ingo Morano Max-Delbrück Center for Molecular Medicine and University Medicine Charité Berlin, Berlin, Germany

George Nemer Faculty of Medicine, American University of Beirut, Beirut, Lebanon
College of Health and Life Sciences, Hamad bin Khalifa University, Doha, Qatar
Department of Biochemistry and Molecular Genetics, American University of Beirut, Beirut, Lebanon
Division of Genomics and Translational Biomedicine, Hamad Bin Khalifa University, Doha, Qatar

Buyan-Ochir Orgil Division of Cardiology, Department of Pediatrics, The Heart Institute, University of Tennessee Health Science Center, Memphis, TN, USA

José M. Pérez-Pomares Department of Animal Biology, Faculty of Sciences, University of Málaga, Málaga, Spain
Andalusian Center for Nanomedicine and Biotechnology (BIONAND), Málaga, Spain
Instituto de Biomedicina de Málaga (IBIMA)-Hospital Carlos de Haya, Málaga, Spain

Andreas Perrot Experimental and Clinical Research Center, a Cooperation Between the Max Delbrück Center for Molecular Medicine in the Helmholtz Association and Charité Universitätsmedizin Berlin, Berlin, Germany
Cardiovascular Genetics, Charité Universitätsmedizin Berlin, Berlin, Germany

Constanze Pfitzer Department of Congenital Heart Disease/Paediatric Cardiology, German Heart Center Berlin, Berlin, Germany

Beatriz Picazo Hospital Materno Infantil-Hospital Carlos de Haya, Málaga, Spain

Robert E. Poelmann Department of Integrative Zoology, Institute of Biology, University of Leiden, Leiden, The Netherlands

George A. Porter, Jr Departments of Pediatrics (Cardiology), Pharmacology and Physiology, and Medicine (Aab Cardiovascular Research Institute), University of Rochester Medical Center, Rochester, NY, USA

Alex V. Postma Department of Medical Biology, Amsterdam Cardiovascular Sciences, Amsterdam University Medical Centres, Amsterdam, The Netherlands
Department of Human Genetics, Amsterdam University Medical Centres, Amsterdam, The Netherlands

Matina Prapa Department of Clinical Genetics, St George's University Hospitals NHS Foundation Trust, London, UK

Enkhsaikhan Purevjav Division of Cardiology, Department of Pediatrics, The Heart Institute, University of Tennessee Health Science Center, Memphis, TN, USA

Alireza Raissadati Stanford University, Cardiovascular Institute, Stanford, CA, USA

Mona El Refaey The Dorothy M. Davis Heart and Lung Research Institute, The Ohio State University Wexner Medical Center, Columbus, OH, USA
Division of Cardiac Surgery, Department of Surgery, The Ohio State University Wexner Medical Center, Columbus, OH, USA

Silke Rickert-Sperling Cardiovascular Genetics, Charité – Universitätsmedizin Berlin, Berlin, Germany

Adrián Ruiz-Villalba Department of Animal Biology, Faculty of Sciences, University of Málaga, Málaga, Spain
Andalusian Center for Nanomedicine and Biotechnology (BIONAND), Málaga, Spain
Instituto de Biomedicina de Málaga (IBIMA)-Hospital Carlos de Haya, Málaga, Spain

Liane Sadder Faculty of Medicine, American University of Beirut, Beirut, Lebanon

Tahmina Samad Stanford University, Cardiovascular Institute, Stanford, CA, USA

Fátima Sánchez-Cabo Bioinformatics Unit, Centro Nacional de Investigaciones Cardiovasculares, Madrid, Spain

Katharina R. L. Schmitt Department of Congenital Heart Disease/Paediatric Cardiology, German Heart Center Berlin, Berlin, Germany

Erik Schulze-Bahr Department of Cardiovascular Medicine, Institute for Genetics of Heart Diseases (IfGH), University Hospital Münster, Münster, Germany

Farbod Sedaghat-Hamedani Institute for Cardiomyopathies Heidelberg (ICH), University Hospital Heidelberg, Heidelberg, Germany

David Sedmera Laboratory of Developmental Cardiology, Institute of Physiology, Czech Academy of Sciences, Prague, Czech Republic
Institute of Anatomy, First Faculty of Medicine, Charles University, Prague, Czech Republic

Kamel Shibbani Division of Cardiology, Department of Pediatrics, University of Iowa Hospitals and Clinics, Iowa City, IA, USA

Abdul-Karim Sleiman Faculty of Medicine, American University of Beirut, Beirut, Lebanon

Tyler L. Stevens The Dorothy M. Davis Heart and Lung Research Institute, The Ohio State University Wexner Medical Center, Columbus, OH, USA
Department of Physiology and Cell Biology, The Ohio State University Wexner Medical Center, Columbus, OH, USA

Amy C. Sturm Genomic Medicine Institute, Geisinger, Danville, PA, USA

Bijoy D. Thattaliyath Department of Pediatrics, Stead Family Children's Hospital, University of Iowa, Iowa, IA, USA

Viktor Tomek Pediatric Cardiology, Motol University Hospital, Prague, Czech Republic

Jésus Vázquez Proteomics Unit, Centro Nacional de Investigaciones Cardiovasculares, Madrid, Spain

Nicholas Wei Stanford University, Cardiovascular Institute, Stanford, CA, USA

Andy Wessels Department of Regenerative Medicine and Cell Biology, Medical University of South Carolina, Charleston, SC, USA

Arthur A. M. Wilde Department of Clinical and Experimental Cardiology, Academic Medical Center, Amsterdam, The Netherlands

Anna Wilsdon School of Life Sciences, University of Nottingham, Nottingham, UK
Clinical Geneticist at Nottingham Clinical Genetics Department, Nottingham University Hospitals, City Hospital, Nottingham, UK

Joseph C. Wu Stanford Cardiovascular Institute, Stanford, CA, USA
Division of Cardiovascular Medicine, Department of Medicine, Stanford, CA, USA
Department of Radiology, Stanford University School of Medicine, Stanford, CA, USA

Sean M. Wu Stanford University, Cardiovascular Institute, Stanford, CA, USA

Yijen L. Wu Department of Developmental Biology, University of Pittsburgh School of Medicine, Pittsburgh, PA, USA

Xinxiu Xu Department of Developmental Biology, University of Pittsburgh School of Medicine, Pittsburgh, PA, USA

Hisato Yagi Department of Developmental Biology, University of Pittsburgh School of Medicine, Pittsburgh, PA, USA

Hiroyuki Yamagishi Division of Pediatric Cardiology, Department of Pediatrics, Keio University School of Medicine, Tokyo, Japan

Choon Hwai Yap Department of Bioengineering, Imperial College, London, UK

Hao Zhang Stanford Cardiovascular Institute, Stanford, CA, USA

List of Abbreviations

22q11DS	22q11.2 deletion syndrome
A	Atrium
AAA	Aortic arch anomalies
ACTC1	Cardiac alpha-actin
ACVR	Activin A receptor
AD	Arterial duct
ADAM19	ADAM metallopeptidase domain 19
ADAR	Adenosine deaminase that acts on RNA
ADP	Adenosine diphosphate
AGS	Alagille syndrome
AICD	Automatic internal cardiac defibrillator
ALCAPA	Anomalous origin of the left coronary artery from the pulmonary artery
AKT	V-akt murine thymoma viral oncogene homolog
AngII	Angiotensin II
ANP	Atrial natriuretic peptide
ANK2	Ankyrin B
ANKRD1/CARP	Ankyrin repeat domain 1, cardiac muscle
Ao	Aorta
AP	Action potential
ARVC	Arrhythmogenic right ventricular cardiomyopathy
ASD	Atrial septal defect
ATFB	Atrial fibrillation
ATP	Adenosine triphosphate
AV	Atrioventricular
AVB	Atrioventricular bundle
AVC	Atrioventricular canal
AVN	Atrioventricular node
AVSD	Atrioventricular septal defect
BA	Bulbus arteriosus
BAF	Brg1-associated factor
BAV	Bicuspid aortic valve
BBS	Bardet-Biedl syndrome

BDM	2,3-butanedione monoxime
BET	Bromodomain and extra terminal
BMP	Bone morphogenetic protein
BNP	Brain natriuretic peptide
bpm	Beat per minutes
BRAF	v-Raf murine sarcoma viral oncogene homolog B
BRG1	SWI/SNF-related, matrix-associated, actin-dependent regulator of chromatin, subfamily a, member 4 (also known as brahma-related gene 1)
BRGDA	Brugada syndrome
BWIS	Baltimore Washington Infant Study
CAA	Coronary artery anomalies
CACN	Calcium channel, voltage-dependent, L type
CAD	Coronary atherosclerotic disease
CaMK	Calmodulin-dependent kinase
cAMP	Cyclic adenosine monophosphate
CALM	Calmodulin
CASQ	Calsequestrin
CAT	Common arterial trunk
CAVV	Common atrioventricular valve
CBP	CREB-binding protein
CC	Cardiac crescent
CCDC	Coiled-coil domain containing
CCS	Cardiac conduction system
CCV	Common cardiac vein
CCVA	Congenital coronary vascular anomalies
CF	Cephalic folds
CFC1	Cripto, FRL-1, Cryptic family 1 (CRYPTIC)
CFD	Computational fluid dynamics
CGH	Comparative genomic hybridization
CHARGE	*C*oloboma of the eye, *H*eart defects, *A*tresia of the nasal choanae, *R*etarded growth and/or development, *G*enital and/or urinal abnormalities, and *E*ar anomalies
CHD	Congenital heart disease/defect
CHD7	Chromodomain helicase DNA-binding protein 7
CHF	Congestive heart failure
ChIP	Chromatin immunoprecipitation
CITED2	Cbp/P300-interacting transactivator, with Glu/Asp-rich carboxy-terminal domain 2
CNCCs	Cardiac neural crest cells
CNV	Copy number variation
CoA	Celiac artery
CoA	Coarctation of the aorta
CPVT	Catecholaminergic polymorphic ventricular tachycardia
CRE	Cre recombinase

CRELD1	Cysteine-rich protein with EGF-like domains 1
CRISPR	Clustered regularly interspaced short palindromic repeats
CTD	Conotruncal defects
CTGF	Connective tissue growth factor
CTVM	Canine tricuspid valve malformation
CX	Connexin
DA	Dorsal artery
DCM	Dilated cardiomyopathy
DGC	Dystrophin-glycoprotein complex
DMP	Dorsal mesenchymal protrusion
DNA	Deoxyribonucleic acid
DNAH	Dynein, axonemal, heavy chain
DNMT	DNA methyltransferases
DORV	Double outlet right ventricle
dpf	Days post fertilization
DPF3	D4 Zinc and double PHD fingers family 3 (also known as Baf45c)
DSC2	Desmocollin 2
DSG2	Desmoglein 2
DSP	Desmoplakin
Dvl2	Disheveled segment polarity protein 2
E	Embryonic day
ECs	Endocardial cushions
ECG	Electrocardiogram
ECM	Extracellular matrix
EGFR	Epidermal growth factor receptor
ELC	Essential myosin light chain
ELN	Elastin
EMT	Epithelial-to-mesenchymal transition
ENU	N-ethyl-N-nitrosourea
EPDC	Epicardially derived cells
EPO	Erythropoietin
ErbB	Erythroblastic leukemia viral oncogene homolog
ERK	Extracellular signal-regulated kinase
ERS	Early repolarization syndrome
ESC	Embryonic stem cells
ET1	Endothelin 1
EVC	Ellis-van-Creveld
FA	Folic acid
FACS	Fluorescence-activated cell sorting
FDA	Food and Drug Administration
FGF	Fibroblast growth factor
FGFR	Fibroblast growth factor receptor
FHF	First heart field
FHL1	Four and a half LIM domains protein 1

FISH	Fluorescence in situ hybridization
FOX	Forkhead box
FOG2	Friend of GATA 2
GATA	GATA binding protein
GATA4	GATA-binding protein 4
GBX	Gastrulation brain homeobox
GDF1	Growth differentiation factor
GFP	Green fluorescent protein
GJA5	Gap junction protein, alpha 5, 40 kDa (connexin 40)
GPCR	G-protein coupled receptors
GRP	Gastrocoel roof plate
GWAS	Genome-wide association study
H3K4me3	Trimethylation of histone H3 at lysine 4
H3K4me2	Dimethylation of histone H3 at lysine 4
H3K4me1	Monomethylation of histone H3 at lysine 4
H3K24ac	Acetylation of histone H3 at lysine 24
H3K27ac	Acetylation of histone H3 at lysine 27
H3K27me3	Trimethylation of histone H3 at lysine 27
HAND	Heart and neural crest derivatives expressed
HAT	Histone acetyltransferase
HDAC	Histone deacetylase
HCM	Hypertrophic cardiomyopathy
HCN4	Hyperpolarization activated cyclic nucleotide-gated potassium channel 4
HE	Hematoxylin and eosin
HES1	Hes family BHLH transcription factor 1
HEY	Hes-related family bHLH transcription factor with YRPW motif
HH	Hamburger—Hamilton stage
HIF	Hypoxia-inducible factor
HLHS	Hypoplastic left heart syndrome
HOX	Homeobox genes
hpf	Hours post fertilization
HT	Heart tube
HV	Hepatic vein
IAA	Interrupted aortic arch
IC	Inner curvature
IGF1	Insulin-like growth factor 1
INO80	Inositol requiring 80
IP3	Inositol-1,4,5-triphosphate
IPCCC	International Pediatric and Congenital Cardiac Code
iPSCs	Induced pluripotent stem cells
IRX	Iroquois homeobox
ISL1	ISL LIM homeobox 1 (Islet 1)
IUGR	Intrauterine growth restrictions
IVC	Inferior caval vein

IVF	Idiopathic ventricular fibrillation
IVS	Interventricular septum
JAG1	Jagged 1
JNK	c-Jun N-terminal kinase
JUP	Junctional plakoglobin
KLF	Krüppel-like factor
KLF2	Krüppel-like factor 2
KCNE	Potassium channel, voltage-gated subfamily E regulatory beta subunit
KCNJ	Potassium channel, inwardly rectifying subfamily J
KCNQ	Potassium channel, voltage-gated KQT-like subfamily Q
LA	Left atrium
LAL	Left atrial ligation
LAo	Left aortic arch
LBB	Left bundle branch
LCC	Left common carotid
LEFTY	Left-right determination factor
LEOPARD	*L*entigenes, *E*CG conduction abnormalities, *O*cular hypertelorism, *P*ulmonic stenosis, *A*bnormal genitalia, *R*etardation of growth and sensorineural *D*eafness
LIF	Leukemia inhibitory factor
LMNA	Lamin A/C
lncRNA	Long non-coding RNA
LPA	Left pulmonary artery
LPM	Lateral plate mesoderm
LLPM	Left lateral plate mesoderm
LPu	Left pulmonary artery
LQTS	Long QT syndrome
L-R	Left-to-right shunt
LRO	Left-right organizer
LSA	Left subclavian artery
LTCC	L-type calcium channel
LV	Left ventricle
LVNC	Left ventricular noncompaction
MAPCA	Major aortopulmonary collateral arteries
MBD	Methyl-CpG binding domain-based
MDM2	Murine double minute 2
MED13L	Mediator complex subunit 13-like
MEF2C	Myocyte enhancer factor 2C
MEK2	kinase 2
MERS	Middle east respiratory syndrome
MESP1	Mesoderm posterior 1 homolog
MHC	Myosin heavy chain
MI	Myocardial infarction
MMP	Matrix metalloproteinases

MLC	Myosin light chain
MLL2	Mixed-lineage leukemia protein 2
miRNA	MicroRNA
MOs	Morpholino oligonucleotides
MPES	Mid-pharyngeal endothelial strand
MRI	Magnetic resonance imaging
mRNA	Messenger RNA
MS	Mass spectrometry
MSX	Msh homeobox
MuRF	Muscle RING finger protein
MyoD	Myogenic differentiation factor
MYBPC3	Cardiac myosin-binding protein C
MYH6	Cardiac alpha-myosin heavy chain
MYH7	Cardiac beta-myosin heavy chain
NADPH	Nicotinamide adenine dinucleotide phosphate
NCC	Neural crest cells
NCCM	Noncompaction cardiomyopathy
NCX	Sodium/Calcium exchanger
ncRNA	Non-coding RNA
NDD	Neurodevelopmental delay
NF1	Neurofibromatosis type 1
NFAT	Nuclear factor of activated T-cells
NGS	Next-generation sequencing
NKA	Sodium/Potassium ATPase
NKX2-5	NK2 homeobox 5
NKX2-6	NK2 homeobox 6
NMD	Nonsense mediated decay
NMR	Nuclear magnetic resonance spectroscopy
NODAL	Nodal growth differentiation factor
NOS3	Nitric oxide synthase 3
NPC	Nuclear pore complexes
NPHP	Nephronophthisis
NPPA	Natriuretic peptide A
NRG1	Neuregulin 1
NR2F2	Nuclear receptor subfamily2/group F
NSAID	Nonsteroidal anti-inflammatory drugs
NS-CHD	Non-syndromic congenital heart disease/defect
NVP	Nodal vesicular parcels
OCT	Optical coherence tomography
OFT	Outflow tract
OPT	Optical projection tomography
OR	Odds ratio
OSI	Oscillatory shear index
OSS	Oscillatory shear stress
OR	Odds ratios

p300	E1A binding protein p300
PA	Pulmonary artery
PA	Pulmonary atresia
PAAs	Pharyngeal arch arteries
PACHD	Pancreatic agenesis and congenital heart defects
PAPVC	Partial anomalous pulmonary venous connections
PAX3	Paired box 3
PCD	Primary ciliary dyskinesia
PCG-1α	Peroxisome proliferator-activated receptor-gamma coactivator-1α
PCP	Planar cell polarity
PCR	Polymerase chain reaction
PDA	Patent ductus arteriosus
PDA	Persistent ductus arteriosus
PDGF	Platelet-derived growth factor
PDK1	Phosphoinositide-dependent kinase1
PECAM1	Platelet endothelial cell adhesion molecule 1
PFO	Patent foramen ovale
PFOS	Perfluorooctane sulfonate
PGD	Preimplantation genetic diagnosis
PI3K	Phosphoinositide 3-kinase
PITX2	Paired-like homeodomain 2
PKA	Protein kinase A
PKC	Protein kinase C
PKD2	Polycystic kidney disease 2 (polycystin 2)
PKP2	Plakophilin 2
PLN	Phospholamban
PLXN	Plexin
$PM_{2.5}$	Particulate matter < 2.5 microns
PM_{10}	Particulate matter < 10 microns
PRDM16	PR domain containing 16
PRLL	Pregnancy and Lactation Labeling (Drugs) Final Rule
PPS	Peripheral pulmonic stenosis
PS	Pulmonary stenosis
PSS	Pulsatile shear stress
PTA	Persistent truncus arteriosus
PTPN11	Protein tyrosine phosphatase, non-receptor type 11
PTC	Premature termination codon
PVCS	Peripheral ventricular conduction system
PVs	Pulmonary veins
QT	QT interval (electrocardiogram)
RA	Right atrium
RA	Retinoic acid
RAA	Right aortic arch
RAAS	Renin-angiotensin-aldosterone system

RAo	Right aortic arch
Ras/MAPK	Rat sarcoma viral oncogene homolog/mitogen-activated protein kinase
RBB	Right bundle branch
RBPs	RNA-binding proteins
RCC	Right common carotid
RCM	Restrictive cardiomyopathy
RLC	Regulatory myosin light chain
RNA	ribonucleic acid
RNAi	RNA interference
RNP	Ribonucleoprotein
ROS	Reactive oxygen species
RPA	Right pulmonary artery
RPu	Right pulmonary artery
R-L	Right-to-left shunt
RSA	Right subclavian artery
rRNA	Ribosomal RNA
RR	Relative risk
RV	Right ventricle
RVOTO	Right ventricular outflow tract obstruction
RYR	Ryanodine receptor
S-CHD	Syndromic congenital heart disease/defect
S1	First heart sound
S2	Second heart sound
S3	Third heart sound
SAN	Sinoatrial node
SARS	Severe acute respiratory syndrome
SARSr-CoV-2	Severe acute respiratory syndrome–related coronavirus 2
SCN	Sodium channel, voltage gated
SCN5A	Sodium channel voltage-gated type V alpha subunit
SCN10A	Sodium channel voltage-gated type X alpha subunit
SDF1	Stromal cell-derived factor 1
SENP	SUMO/sentrin-specific proteases
SEMA3C	Semaphorin 3C
SERCA	Sarcoplasmic/endoplasmic reticulum calcium ATPase
SHF	Second heart field
SHH	Sonic hedgehog
SHOX2	Short stature homeobox 2
SNPs	Single nucleotide polymorphisms
snRNA	Small nuclear RNA
snoRNA	Small nucleolar RNA
SPIM	Selective plane illumination microscopy
SQTS	Short QT syndrome
SMAD4	SMAD family member 4
SMC	Smooth muscle cells

SRF	Serum response factor
SSRI	Selective serotonin reuptake inhibitor
STAT3	Signal transducer and activator of transcription 3
SUMO	Small ubiquitin-like modifier
SV	Sinus venosus
SVC	Superior vena cava
SVAS	Supravalvar aortic stenosis
SWI/SNF	Switching defective/sucrose nonfermenting complex
TA	Truncus arteriosus
TAC	Transverse aortic constriction
TALEN	Transcription activator-like effector nucleases
TAPVR	Total anomalous pulmonary venous return
TBX	T-box
TEMED	Tetramethylethylenediamine
TF	Transcription factor
Tg	Transgenic
TGA	Transposition of the great arteries
TGFβ	Transforming growth factor-β
TMEM43	Transmembrane protein 43
Tn	Troponin
TNFα	Tumor necrosis factor alpha
TOF	Tetralogy of Fallot
tRNA	Transfer RNA
TTN	Titin
UPS	Ubiquitin proteasome system
UTRs	Untranslated regions
V	Ventricle
VACTERL	*V*ertebral defects, *A*nal atresia, *C*ardiovascular anomalies, *T*racheo-*E*sophageal fistula, *R*adial and renal anomalies, and *L*imb defects
VANGL2	VANGL planar cell polarity protein 2
VCFS	Velocardiofacial syndrome
VEGF	Vascular endothelial growth factor
VP	Venous pole
VS	Ventricular septum
VSD	Ventricular septal defect
VSMC	Vascular smooth muscle cells
VT	Ventricular tachycardia
VUS	Variants of unknown significance
WBS	Williams-Beuren syndrome
WES	Whole exome sequencing
WGS	Whole genome sequencing
WPW	Wolff-Parkinson-White syndrome
Wnt	Wingless and Int-1
WNT	Wingless-type MMTV integration site family

WSS	Wall shear stress
WT	Wild type
XB	Cross-bridges
Y2H	Yeast-two-hybrid
ZIC	Zic family member
ZFN	Zinc finger nucleases
ZFPM2	Zinc finger protein, FOG family member 2

Part I

Introduction

Human Cardiac Development

1

Jill P. J. M. Hikspoors, Nutmethee Kruepunga, Greet M. C. Mommen, S. Eleonore Köhler, Robert H. Anderson, and Wouter H. Lamers

Abstract

Many aspects of heart development are topographically complex and require three-dimensional (3D) reconstruction to understand the pertinent morphology. We have recently completed a comprehensive primer of human cardiac development that is based on firsthand segmentation of structures of interest in histological sections. We visualized the hearts of 12 human embryos between their first appearance at 3.5 weeks and the end of the embryonic period at 8 weeks. The models were presented as calibrated, interactive, 3D portable document format (PDF) files. We used them to describe the appearance and the subsequent remodeling of around 70 different structures incrementally for each of the reconstructed stages. In this chapter, we begin our account by describing the formation of the single heart tube, which occurs at the end of the fourth week subsequent to conception. We describe its looping in the fifth week, the formation of the cardiac compartments in the sixth week, and, finally, the septation of these compartments into the physically separated left- and right-sided circulations in

J. P. J. M. Hikspoors (✉) · G. M. C. Mommen · S. E. Köhler
Department of Anatomy & Embryology, Maastricht University, Maastricht, The Netherlands
e-mail: jill.hikspoors@maastrichtuniversity.nl

N. Kruepunga
Department of Anatomy & Embryology, Maastricht University, Maastricht, The Netherlands

Present address: Department of Anatomy, Mahidol University, Bangkok, Thailand

R. H. Anderson
Institute of Genetic Medicine, Newcastle University, Newcastle upon Tyne, UK

W. H. Lamers
Department of Anatomy & Embryology, Maastricht University, Maastricht, The Netherlands

Tytgat Institute for Liver and Intestinal Research, Academic Medical Center, Amsterdam, The Netherlands

© The Author(s), under exclusive license to Springer Nature Switzerland AG 2024

S. Rickert-Sperling et al. (eds.), *Congenital Heart Diseases: The Broken Heart*,
Advances in Experimental Medicine and Biology 1441,
https://doi.org/10.1007/978-3-031-44087-8_1

the seventh and eighth weeks. The phases are successive, albeit partially overlapping. Thus, the basic cardiac layout is established between 26 and 32 days after fertilization and is described as Carnegie stages (CSs) 9 through 14, with development in the outlet component trailing that in the inlet parts. Septation at the venous pole is completed at CS17, equivalent to almost 6 weeks of development. During Carnegie stages 17 and 18, in the seventh week, the outflow tract and arterial pole undergo major remodeling, including incorporation of the proximal portion of the outflow tract into the ventricles and transfer of the spiraling course of the subaortic and subpulmonary channels to the intrapericardial arterial trunks. Remodeling of the interventricular foramen, with its eventual closure, is complete at CS20, which occurs at the end of the seventh week. We provide quantitative correlations between the age of human and mouse embryos as well as the Carnegie stages of development. We have also set our descriptions in the context of variations in the timing of developmental features.

Keywords

Growth · Staging · Cardiac loop · Cardiac compartment · Embryonic ventricle · Cardiac septation · Developmental timing

1.1 Introduction

1.1.1 Sharing of Digitized Collections Allows for Higher-Quality Data

Progress in understanding the development of the amniotic heart can be mostly made by perusing studies of avian embryos, notably those of chicken and quail, but also increasingly by studies of mammalian embryos, in particular mice. Our knowledge of the developing human heart, to date, has largely relied on extrapolation of the findings in experimental and descriptive studies of mammalian and avian embryonic hearts and on histological sections of human embryos. Usually, such sections are stained with classical dyes. High-quality histological sections are necessary, therefore, to identify and follow critical structures at the developmental stage. Because sectioning disrupts the spatial aspects of a structure, and because histological techniques introduce artifacts that differ from section to section, we estimate that at most one-quarter of the specimens in most collections of human embryos are of sufficiently high histological quality to permit reconstruction of the third dimension and allow comparisons to be made between individual specimens of the same or different developmental stages. The initiative of Dr. Mark Hill, from the University of New South Wales in Australia, to create a facility to digitize sections of a high-quality series of human embryos from a number of established collections [1] is to be lauded because it makes more high-quality specimens accessible for study. The Virtual Human Embryo project was initiated by Dr. Ray Gasser [2] but is more generally known as the Digitally Reproduced Embryonic Morphology (DREM)

project. The DREM database is based on the Carnegie collection and contains one embryo for each Carnegie stage (CS). Our own database of digitized sections is based on the historical collections of the Departments of Anatomy in Leiden, Amsterdam, and Nijmegen and now contains 32 complete embryos and early fetuses between 4.5 and 15 weeks of development. We benefitted from Mark Hill's initiative and were able to study the entire digitized Blechschmidt collection housed in Göttingen [3], which contains 27 high-quality embryos. Having several specimens with a closely spaced developmental age available for study is an absolute necessity for accurate descriptions.

1.1.2 Sources of Additional Information

In addition to serial sections of high histological quality, access to immunologically stained sections is invaluable. Once one has seen the histological features of a structure highlighted, it becomes much easier to define distinctive histological features, which can also be recognized in series stained with standard techniques. We had access to the immunostained series of human embryonic hearts collected by Wessels and Viragh [4–6], Sizarov [7–11], and Ya [9]. Unfortunately, the immunological protocol introduces many histological artifacts, which make this staining method less suitable for reconstructions.

1.1.3 A Combination of Text and Three-Dimensional (3D) Images Is Necessary for Effective Communication

Since nomenclature in the developing heart is notoriously variable, a combination of text and illustrations is necessary to provide an understandable account. Reconstruction of the third dimension is, therefore, a key step to enable meaningful discussions about developmental features and processes. It is a truism that a picture is worth a 1000 words. Reconstruction methods were developed soon after the study of microscopic sections became more widely used. Born's *Die Plattenmodellirmethode* is now almost 150 years old and remains the basis of reconstruction techniques, but the labor intensity of methods based on his technique has long been a limiting factor. This issue was largely resolved with the advent of computer-aided reconstruction methods, which reduced the production time of reconstructions by almost 10-fold. A recent example of large-scale production of reconstructions has been the digital atlas of human development produced by the Amsterdam group [12], which contains 14 specimens. This atlas does not, however, address the development of the heart in any detail.

1.1.4 This Study

To our knowledge, no primer of heart development based on firsthand segmentation of structures of interest in histological sections is available. Therefore, we visualized cardiac development in 12 reconstructions of human embryos between 3.5 and 8 weeks of development. This correlates with the 9th through the 23rd Carnegie stages [13]. We used the DREM database of human embryos as templates for segmentation and reconstruction because the embryos that constitute this database are part of the Carnegie collection. They were staged a long time ago by experienced embryologists who did not have heart development in mind when assigning a stage to an embryo. Because we were not involved in the staging, we were able to assign critical events in heart development to specific Carnegie stages of human embryonic development. After reconstructing the hearts with the widely used Amira software, we processed the models with the Cinema 4D remodeling software to remove noise from imperfect matching or segmentation between consecutive paraffin sections. A total of 75 structures were reconstructed (Table 2 in reference [13]. Of these, 10 serve as reference structures for axial orientation and establishment of segmental levels, such as somites or spinal ganglia, the central nervous system, the gut, and so on, whereas the remainder are cardiovascular structures. The 3D reconstructions used in reference [13] are presented as freely accessible, fully interactive, 3D portable document format (PDF) files, which can be inspected on any computer with a PDF reader installed. The reconstructed models can be translated, rotated, and magnified. Each of the structures in a particular reconstruction is present as a clickable item in the so-called "model tree." It can be used as a search and identification tool. Structures can be visualized in a semitransparent mode so as to better appreciate topography. Throughout the series, each structure retains the same color code while a scale cube permits an estimation of its size.

In an earlier study [13], we described the developmental appearance, and the subsequent remodeling, of all structures incrementally per developmental stage, using sequential segmental analysis [14] as our template. In this communication, we will take a different approach. We begin by accounting for the formation of the single heart tube, which occurs at the end of the fourth week subsequent to fertilization. We then describe its looping in the fifth week, the formation of the cardiac compartments in the sixth week, and, finally, the septation of these compartments into the physically separated left- and right-sided circulations during the seventh and eighth weeks. The phases are sequential, albeit partially overlapping. We have used the criteria of O'Rahilly, as modified in 2010, to relate the Carnegie stage of development to age in terms of days subsequent to fertilization [15]. The description of developmental processes in human embryos is, wherever possible, underscored with experimental data from other mammals, in particular mice, and, if such data were not available, then with data from chicks. Comparison of human and mouse developmental stages (Fig. 1.1) was based on the conversion of Theiler's stages into horizons, the precursor of Carnegie stages [16]. As is shown in Fig. 1.1, these relations are remarkably linear, with approximately two Carnegie stages per mouse day and two human days per Carnegie stage over the period studied. A single mouse

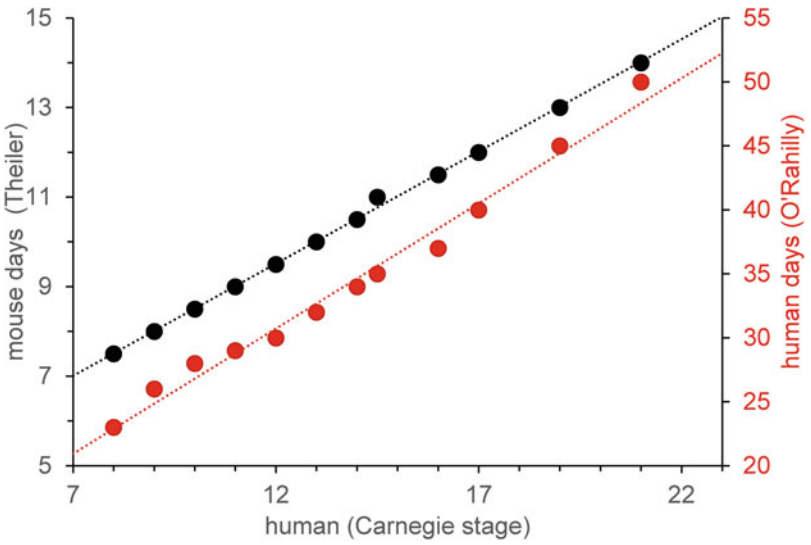

Fig. 1.1 Relationship between developmental stages and age in men and mice. Carnegie stages are shown on the *X*-axis and the corresponding mouse and human ages postfertilization are on the left and right *Y*-axes, respectively. One Carnegie stage lasts 0.5 mouse ($Y = 0.50X$) and ~2 human embryonic days ($Y = 1.96X$) in the age period studied. Sources for the regression analysis were references [15, 16]

day, therefore, is comparable to four human days [13]. The pictorial evidence for the text can be inspected in the interactive 3D PDF files (Supplemental Figs. 1–12 of Hikspoors et al. [13]). We encourage our readers to simultaneously read the text and inspect the corresponding interactive PDFs. This is because the rotational options of the files, producing relatively "live" images, allow a much better understanding of the complex local topography than do "still" images and text.

1.2 Formation of the Single Heart Tube (CS9–CS10)

1.2.1 Formation of Bilateral Heart Anlagen

At Carnegie stage 8, equivalent to ~23 days of development, the embryo is a dorsally convex disc that is sandwiched between the yolk sac ventrally and the amniotic sac dorsally. At this stage, the onset of gastrulation, a highly conserved process in vertebrates [17], establishes the body plan. Among the structures defined in the early phase of gastrulation are the bilateral heart fields, which are also known as the cardiogenic plates. These fields form craniolaterally in the mesoderm [18]. They give rise to the precursors of most of the cardiac structures, albeit not all are determined at once. The initial expression of the transcription factor Mesp1 marks the most primitive cardiac progenitors [19, 20]. At the transition from stage 8 to

Table 1.1 The early heart grows by the serial addition of cells from the caudal and cranial second heart field. The first structure to develop is the embryonic left ventricle, followed by the common atrium and embryonic right ventricle, and, finally, the myocardial outflow tract and the venous sinus. The non-myocardial arterial component of the heart forms last. See text for details. LV, left ventricle; OFT, outflow tract; RV, right ventricle

Structure	Tissue	Appearance
Not part of the heart	Non-myocardial	CS15
Distal OFT	Non-myocardial	CS15
Middle OFT	Myocardial	CS12
Proximal OFT	Myocardial	CS11
Embryonic RV	Myocardial	CS10
Embryonic LV	Myocardial	CS9
R and L atriums	Myocardial	CS10–11
Venous sinus	Myocardial	CS12

9, the newly formed Mesp1-positive cells produce the so-called first heart field, or lineage, which is characterized by the expression of the transcription factor Tbx5 [21, 22] and the ion channel Hcn4 [23, 24]. This field gives rise to cells of the embryonic left ventricle, three-quarters of those in the atrioventricular canal, half of those in the atriums, and a still smaller part of the right ventricle. Toward the end of stage 9, the Mesp1-positive cells produce the second heart field, which is characterized by the expression of the transcription factor *Isl1* [25]. This second field gives rise to virtually all cardiomyocytes of the outflow tract, the majority of cardiomyocytes in the right ventricle, half of the cardiomyocytes in the atriums, and one-quarter of the atrioventricular canal [19, 26]. The systemic venous sinus is the last part to be determined. It does not express the early cardiogenic transcription factor Nkx2–5 but does express Tbx18 [27–29]. The timing and sequence of development of the respective cardiac components is shown in Table 1.1.

1.2.2 Appearance of the Vascular Network and Myocyte Contractility

The heart, foregut, brain, and the first four somites all make their morphological appearance almost simultaneously at the 9th stage, equivalent to ~26 days of development [30–33]. At this initial stage, the most prominent components are the horseshoe-shaped pericardial cavity with its cardiogenic visceral wall, the cardiac jelly, and the endothelial precursors at the cranial margin of the embryo [30]. Cardiomyocyte contractility develops in the lateral regions of the cardiac crescents of mouse embryos as soon as sarcomeric assembly and Ca^{2+} transients can be demonstrated [34–36]. It is at this stage that the vascular precursors acquire a lumen [37]. Features are established with the appearance of the first somites [35], whereas contractions become visible when three somites have formed [38]. During the formation of the next three somites, networks of small endothelial vessels appear

around the developing foregut, at the boundary between the endoderm and yolk sac and around the allantois in the connecting stalk [30, 37, 39]. Other reconstructions [9, 12] of embryos at this stage all show that the heart region initially consists of two networks of narrow vascular channels. They course ventrolateral to the early foregut, extending from the cranial intestinal portal caudally, through the relatively wide arteries forming cranially in the first pharyngeal arch arteries, and terminating cranially in the dorsal aortas. The channels are covered by partially merged, longitudinal bulges of cardiac jelly, themselves covered by the visceral layer of the pericardial cavity. The extent of the jelly, produced by the endoderm and the myocardium-forming visceral pericardial wall [40], reflects the location of the boundaries of the differentiating left ventricular myocardium.

1.2.3 The Single Cardiac Tube

Transformation to a heart with only a single endothelial channel between the still-bilateral venous and arterial vessels occurs during the formation of the fourth through eighth somites. This is the tenth Carnegie stage and equates to ~28 days of development (Figure 1.2e–g). By this time, the vascular webs at the venous and arterial poles have consolidated, giving the lumen of the heart an hourglass configuration. At this stage, it is possible to distinguish the embryonic left ventricle, which arises from the first heart field. It is flanked by inflow and outflow tracts that have predominantly arisen from the caudal venous and cranial arterial parts of the second heart field, respectively. On the venous side, the umbilical vein occupies the junction of the embryonic disk and the amnion, whereas the vitelline plexus develops on the yolk sac. At the level of the fourth somite, at the future junction of the head and neck, these venous channels merge to form bilateral hepatocardiac channels [41]. These, in turn, connect to the inflow tract. The two arms of the inflow tract then merge at the midline of the caudal junction between the first and second heart fields [42], which will eventually become the atrioventricular canal. The developing myocardial wall surrounds the tube as a dorsally open cloak. The area lacking myocardium is the dorsal mesocardium. This connects the heart with the pharyngeal mesenchyme between the pericardial reflections. At the level of the narrow part of the hourglass-shaped endocardial lumen, the dorsal mesocardium disappears, producing the transverse pericardial sinus. This site marks the transition from the descending to the ascending limb of the cardiac loop and also the embryonic left ventricle derived from the first heart field and the outflow tract formed from the cranial second heart field [43]. The cranial boundary of the cardiac jelly coincides with the transition from the arterial pole of the heart into the arteries of the first pharyngeal arch.

1.2.4 The Pericardial Cavity and the Transverse Septum

The transverse septum, which will become the diaphragm, extends forward when first seen as a shelf of thick mesoderm between the pericardial cavity and the

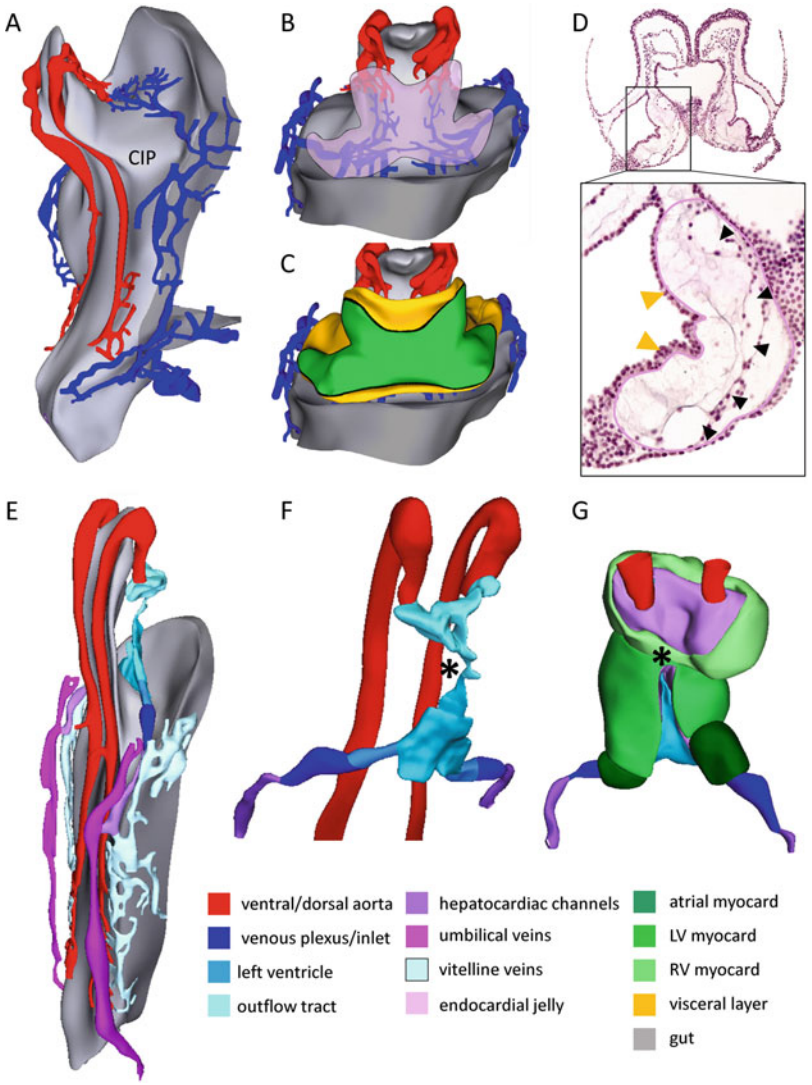

Fig. 1.2 Formation of the single heart tube. (a, e) Right dorsal, (b, c) cranial, (f) ventral, and (g) dorsal views of CS9 (a–d) and CS10 (e and f) human embryos. The heart forms during CS9 in front of the cranial intestinal pore (CIP; panels a–d) from separate left and right cardiovascular plexuses (a and b) that are covered by endocardial jelly (b (transparent pink)). It should be noted that the venous and arterial vessels are relatively wide compared to the endocardial tubes. The primary myocardium differentiates into a dumbbell-shaped visceral layer of the pericardial cavity that covers the endocardial jelly (green area in panel c). Panel d shows the cardiogenic area near the cranial intestinal portal with the black arrowheads pointing to small vessels and the orange arrowhead to the differentiating primary myocardium. At CS10, the hepatocardiac channels that drain blood from the umbilical and vitelline veins into the bilateral inflow tract become identifiable. Furthermore, the dorsal mesocardium ruptures between the descending and ascending portions of the developing heart loop to form the transverse pericardial sinus (*)

endoderm that will form the caudal foregut (Fig. 1.3). Both the developing inflow tract and left ventricle rest on the transverse septum. Due to the rapid growth of dorsal structures between CS9 and CS14, such as the nervous system and the foregut, the transverse septum gradually achieves a more caudal position in the embryo. As a result of this effective descent, the plane through the transverse septum relative to that of the body axis gradually changes from frontal at CS9 to transverse at CS13. Its caudal boundary descends from being cranial to somite 1 at CS9 to somite 8 at CS13. Between CS11 and CS13, the liver and transverse septum expand very rapidly in the lateral and dorsal directions, with hepatoblasts populating the septum [41]. Lateral expansion of the liver primordium results in engulfment of the vitelline veins. Dorsal expansion means that the common cardinal veins change from having a near-transverse orientation at CS12, when they are first seen, to becoming near to frontal at CS13 (Fig. 1.4). The umbilical veins are engulfed by the liver primordium during early CS14, whereas the venous return of the liver is restricted to the right-sided hepatocardiac channel during the late stage 14 [41].

1.3 Looping of the Heart (CS10–CS12)

1.3.1 Asymmetry of the Loop

The formation of a heart tube with its single lumen and the appearance of the transverse pericardial sinus coincide with the loss of bilateral symmetry in the developing heart. By stage 10, the embryonic left ventricle tilts slightly leftward and the arterial pole slightly rightward (Fig. 1.5) [44]. By stage 11, corresponding to ~29 days of development, the cells of the second heart field separate to become the inflow and outflow tracts [45]. By this stage, the cranial parts of the inflow tract are covered by cardiac jelly, whereas the atrioventricular junction has become a relatively narrow left-sided true canal. These changes presage the development of the right and left atrial chambers from the caudal second heart field [45, 46], with their cardiomyocytes differing in both lineage [29] and gene expression [47, 48] from those derived from the first heart field.

1.3.2 Elongation of the Loop

During stage 11, there is ventral and tangential expansion of the cardiac tube at around 45° relative to the sagittal plane between the left-sided atrioventricular junction and the right-sided arterial pole. This is known as cardiac looping. The changes reflect a higher rate of proliferation and myocardial differentiation of the epithelial layer of the second heart field in the dorsal mesocardium [49], along with subsequent second heart field-derived cell addition at the venous and arterial poles of the heart [9, 50–53]. The resulting asymmetry reflects the higher rate of proliferation [53, 54], and possibly hypertrophy [55], of cardiomyocytes in the right caudal second heart field. It is the breakdown of the dorsal mesocardium and the subsequent

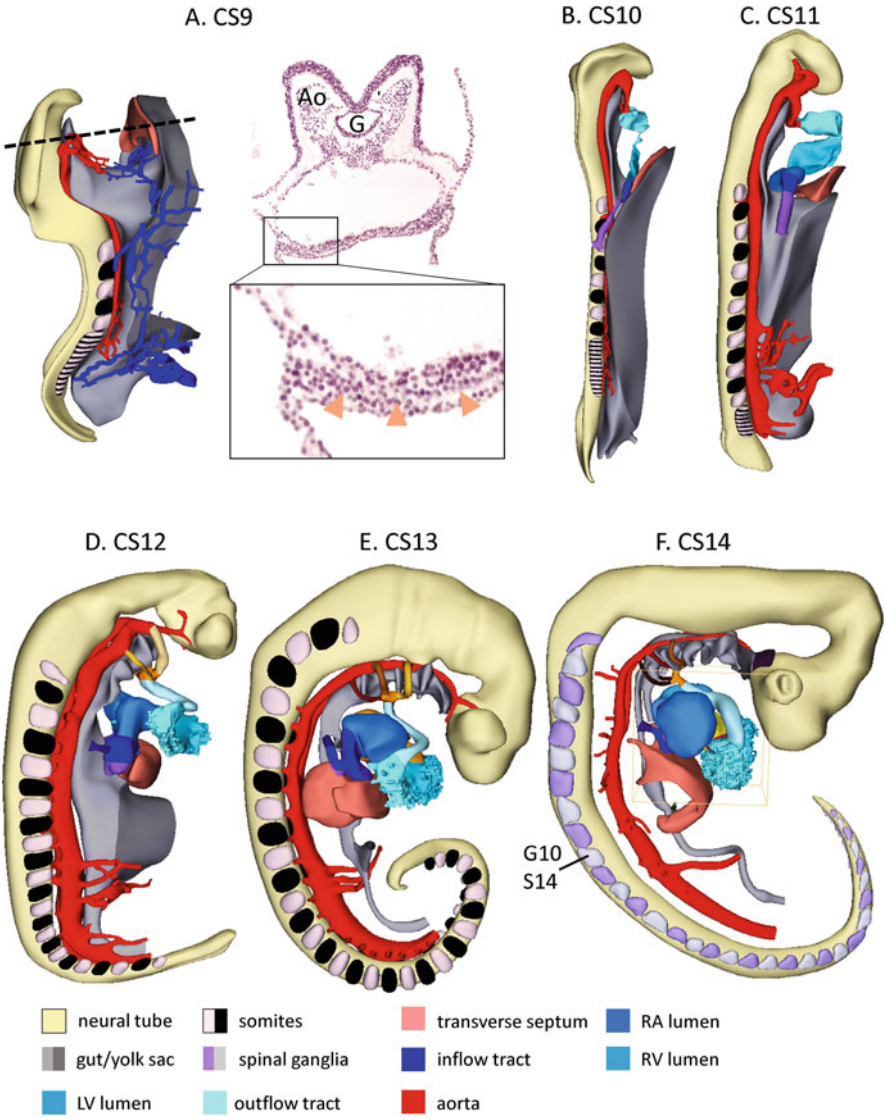

Fig. 1.3 Position of the heart relative to the body axis. (a–f) Right-sided views of CS9–14 human embryos with the cardiac lumen exposed. The dotted line in panel (a) shows a histological section of the transverse septum (arrowheads) between the pericardial cavity (upper space) and the yolk sac (lower space). The growth in the dorsal part of the embryo exceeds that around the umbilical cord, which results in a dorsally convex bending of the head and tail regions. Consequently, the heart appears to descend by three somite lengths per stage, but it should be noted that the caudal end of the pharynx retains its topographic relation with both the cranial somite and the arterial pole of the heart. In contrast, the venous pole of the heart, which is associated with the transverse septum, descends relative to the somites, concomitantly with the lengthening of the caudal foregut. It should be noted that the most cranial somites are no longer identifiable at CS14 and are replaced by spinal ganglia as topographic reference. Since the first four somites do not produce ganglia, ganglion 10 (G10) corresponds with somite 14 (S14). Ao, aorta; G, gut

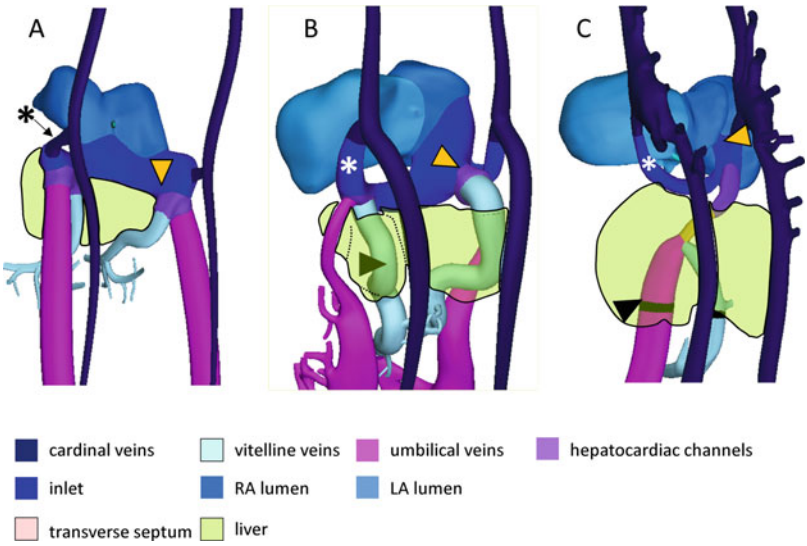

Fig. 1.4 From a bilateral to a right-sided venous inflow tract. (a–c) Dorsal views of the cardiac lumen of CS12–14 human embryos. Due to almost exclusive dorsal growth, the common cardinal veins (asterisks) change from transverse structures at CS12 to near-frontal structures at CS13. The expanding liver engulfs the vitelline veins at CS13 (panel b, black arrowhead) followed by the umbilical veins at CS14 (panel c, black arrowhead). Meanwhile, symmetry is lost as only the right-sided hepatocardiac channel persists and drains into the now right-sided inflow tract (panels a–c, white arrowhead)

looping of the heart tube that permits the separation of the second heart field into its caudal and cranial portions [45]. The conversion and reorientation of the cells of the second heart field into the elongating inflow and outflow tracts is mediated by the planar cell polarity pathway [49, 56, 57] (see Sect. 1.5.4.9 Formation of the Non-Myocardial Intercalated Ridges (or Tongues) and Swellings). The descending and ascending parts of the heart loop meet at the midline, ventral to the transverse pericardial sinus, whereas the position of the venous and arterial connections of the heart is retained through their connections to the dorsal mesocardium and, hence, their anchorage to the pharyngeal mesenchyme [53].

1.3.3 Chirality of the Heart Loop

By Carnegie stage 12, at ~30 days of development, the primordium of the developing right ventricle can be recognized as ballooning from the ascending, or outlet, part of the ventricular loop. This part further extends in a rightward and dorsal direction to form the new apex of the loop (Fig. 1.5). The left side of the caudal second heart field, as marked by Pitx2 [46, 58, 59], and the spiraling of the ridges, or cushions, in the outflow tract [60–62], reveal the helical bending of the loop, which is clockwise

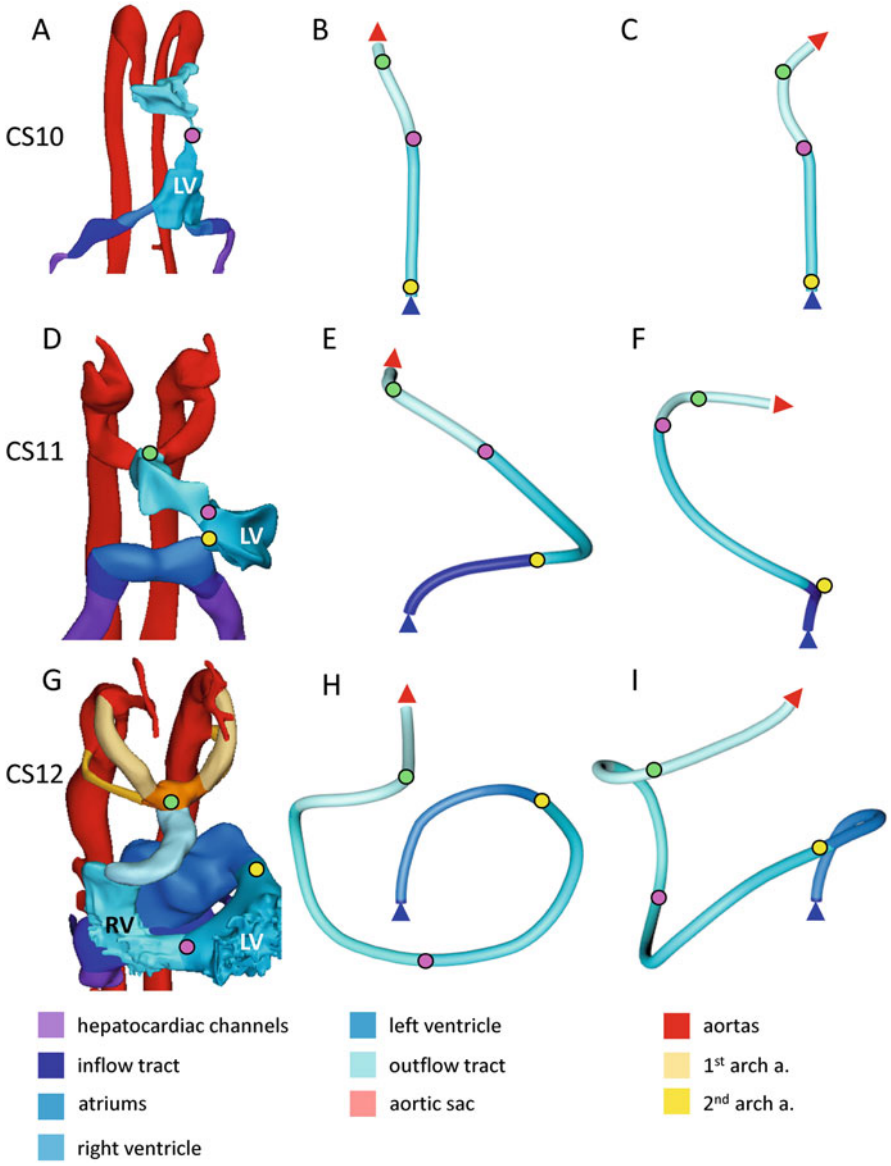

Fig. 1.5 The phases of cardiac looping. (a, d, g) Right ventral, (b, e, h) ventral, and (c, f, i) left-sided views. Wire loops through the axis of the endocardial heart tube show that cardiac looping starts at CS10, when the transition from the embryonic left ventricle to the outflow tract shifts slightly to the left (panel b, pink dot). The ventrally expanding cardiac loop (panel c) shifts the descending limb containing the embryonic left ventricle to the left (panel e, region between the pink and yellow dots). It should be noted that the inflow tract (below the yellow dot) and the distal OFT (above the green dot) remain at the midline (panels b, e, h). At CS12, the embryonic right ventricle becomes identifiable as a further loop with a perpendicular orientation relative to the cranial and caudal parts of the loop (cf. panels f and i, line between the pink and green dots)

when followed downstream [63]. The helical course is probably the product of a rightward displacement of the elongating heart tube due to a slight rotation of the arterial pole [53, 64]. The extent of bending may further explain the appearance of the so-called "bayonet" [65] or "dog-leg" bend [66] between the proximal, or "conal," and distal or "truncal" portions of the developing outflow tract [67] (Fig. 1.5). The bend is associated with valveless pumping in these early hearts [68]. The entire outflow tract, at this early stage, is myocardial to the margins of the pericardial cavity. With subsequent addition of the distal non-myocardial part at stage 15, reflecting ongoing growth from the second heart field, the outflow tract can be described as having both proximal and middle myocardial parts and a non-myocardial distal part (Table 1.1; see Sect. 1.5.4.4 The Growth Pattern of the Early Outflow Tract).

1.4 Formation of the Cardiac Compartments (CS11–CS14)

1.4.1 Cardiac Compartments Originate by "Ballooning" of the Heart Tube

As emphasized above, it is the greater rate of proliferation of the cardiomyocytes in the outer compared to the inner curvature of the heart tube that underscores looping. Continued, but now localized, increases in myocyte proliferation in the outer curvature then induce the formation of the so-called "chamber" components of the ventricles and atriums [9, 51, 52, 69, 70]. This so-called "ballooning" mainly increases the relative size of the trabecular components of the ventricles and the pectinated atrial appendages (Fig. 1.6 [69, 71–73]). Ballooning is first seen in the right atrium and left ventricle of CS11 embryos. The developing right and left atriums differentiate as separate compartments in the inflow tract. They are initially of similar size. The developing left ventricle, in contrast, remains larger and is further differentiated than its right ventricular counterpart up to stage 16 (Fig. 1.7; see next section). The inner curvature of the heart loop hardly grows [51, 74, 75]. It does not participate in the ballooning and formation of trabeculations, and, so, the boundaries of the respective "chamber" compartments can only be distinguished along the outer curvature.

1.4.2 Formation of Ventricular Trabeculations

Trabeculation in the left ventricle passes through the phases of endocardial sprouting into the cardiac jelly, "touchdown" of these sprouts on the outer layer of the myocardial wall, radial extension of the trabeculations, and eventual termination of trabecular growth [76]. Sprouting starts in the left ventricle at stage 11 (Fig. 1.6i). These sprouts increase in number, pass through holes that develop in the inner layer of the bilayered myocardium, and achieve touchdown with the outer myocardial layer at stage 12. The endocardial sprouts then spread between the myocardial

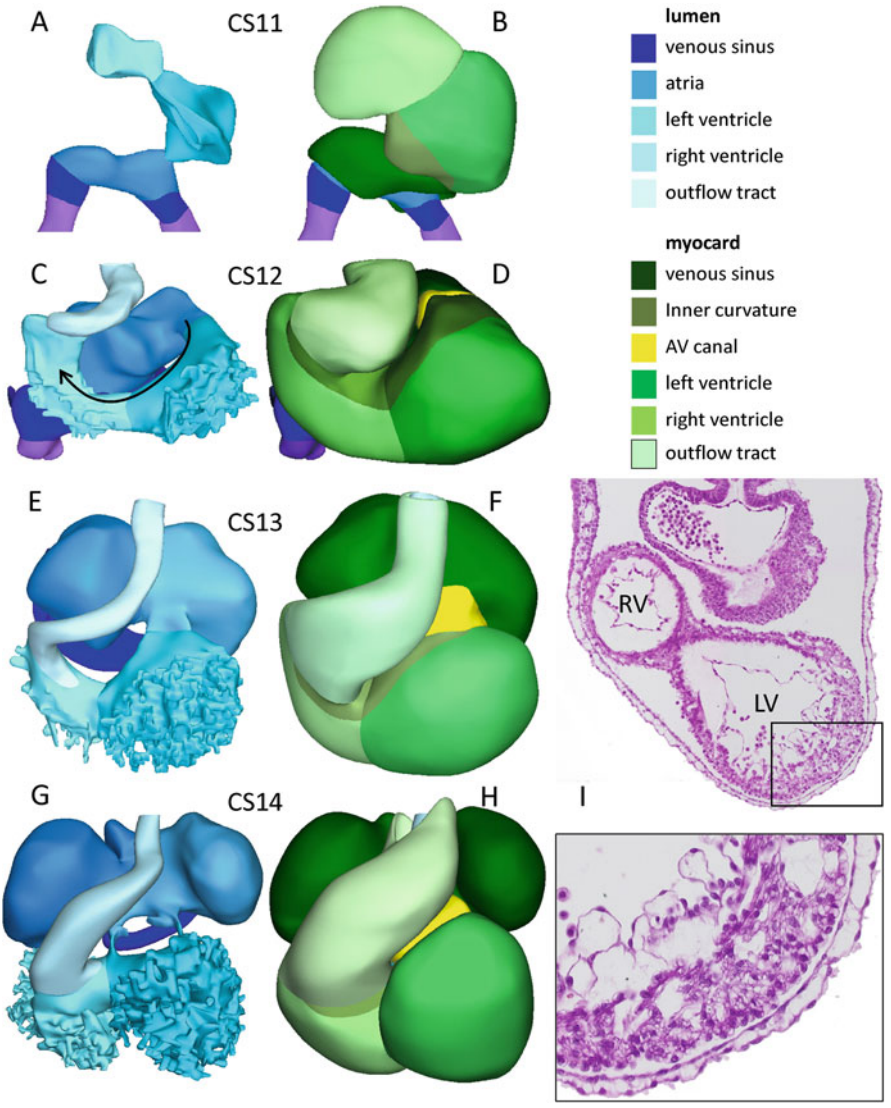

Fig. 1.6 Formation of cardiac compartments. (a–h) Ventral views. The blue gradient in panels (a, c, e, g) shows the lumen of the developing cardiac compartments and panels (b, d, f, h) the corresponding myocardial layer. Ballooning of the outer curvature occurs between CS12 and CS14, resulting in four compartments (panels e–h). The darker-shaded myocardium along the inner curvature (black arrow in panel c) does not balloon but temporarily retains its primary myocardial properties. Panel i shows the later onset of trabecularization in the right than in the left ventricle and a detail of the morphology of the left ventricular trabeculae (for details, see main text) at CS12. RV, right ventricle; LV, left ventricle

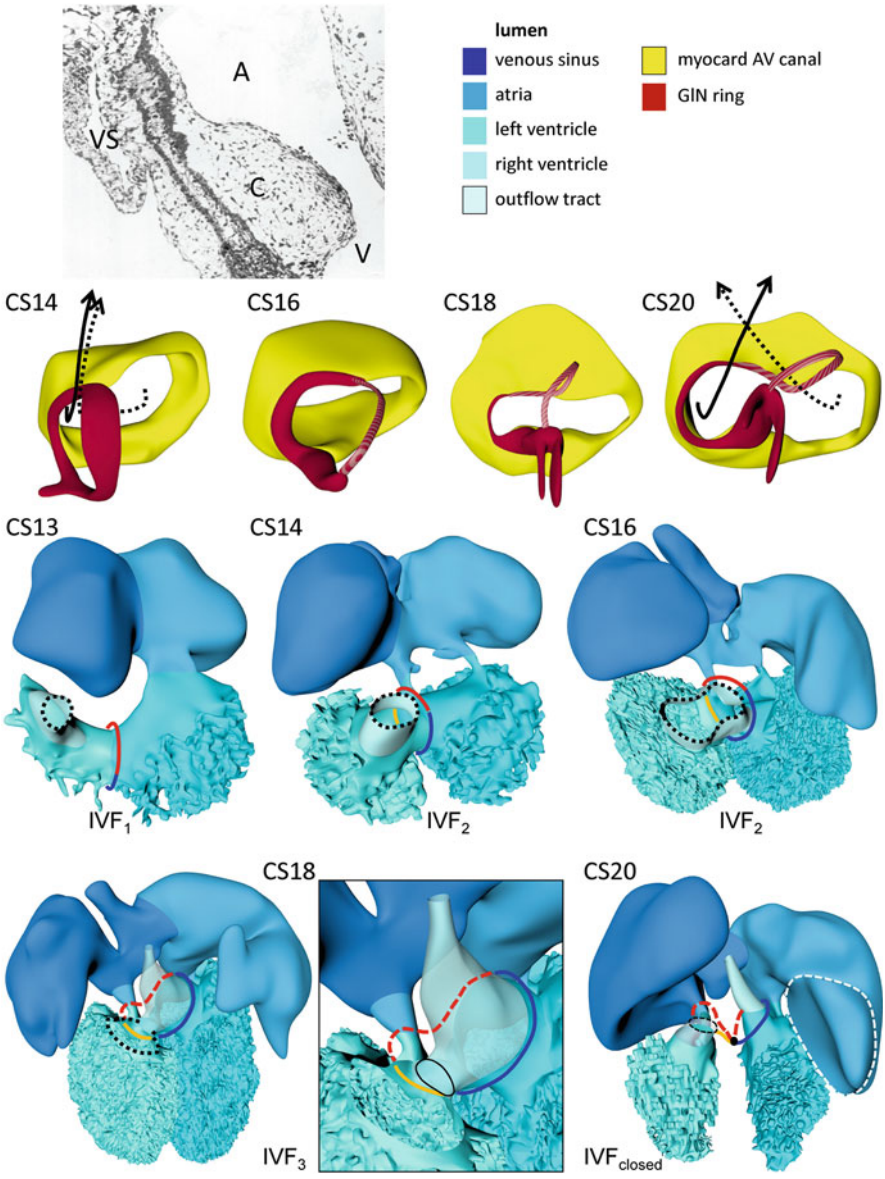

Fig. 1.7 Development of the conduction system and the interventricular foramen. The upper left panel shows the typical double-layered architecture of the primary myocardium (courtesy Dr. Szabolcs Viragh; abbreviations: VS, venous sinus; A, atrium; V, ventricle; C, atrioventricular cushion; for details, see text). Selective staining of the ventricular conduction system shows that it develops from an interventricular ring that becomes visible at CS14. The subsequent changes in the shape of the ring reveal that rightward extension of the atrioventricular canal and leftward and dorsal extension of the ventriculo-arterial junction (CS16 and CS18 configurations shown) align the right atrium with the right ventricle and the left ventricle with the subaortic channel of the outflow tract. This configuration allows completion of septation at CS20 (the curved black arrows indicate

layers, by stage 13, after ~32 days, forming radial columns, or bubbles, covered apically by the extracellular matrix and endocardium. Further radial spread occurs during stage 14, representing almost 5 weeks of development, with resolution of the bubbles by stage 15, equivalent to ~36 days of development. Trabeculation requires *Nrg1*-mediated myocardial synthesis of the extracellular matrix and, subsequently, *Notch1*-mediated degradation of the extracellular matrix [76]. Trabecular development in the developing right ventricle is delayed by approximately two Carnegie stages relative to that in the left ventricle. Mature ventricular trabeculations have a complex 3D structure with fractal properties [72]. Their relatively well-developed myofibers [77], and gap-junctional contacts [78, 79], enhance contraction and conduction in the embryonic heart [80, 81]. Due to the outward, ballooning growth of the ventricles, the trabeculations do not disrupt the contour of the original primary endocardial tube in the ventricles until they stop forming at stage 16. At this stage, representing ~38 days subsequent to fertilization, multiplication of cardiomyocytes at the epicardial side of the ventricular walls begins to exceed that in the trabecular layer. This presages the formation of the compact myocardium [71]. There is no evidence to suggest that the compact layer forms by coalescence of the trabecular meshwork. Instead, the compaction layer itself increases in thickness [82]. The left ventricular apex becomes identifiable at stage 17, approximately 40 days after conception.

1.4.3 Development of the Pectinate Muscles of the Atriums

The expansion of the cavity of the initial atrial component of the heart tube in the dorsal direction, and also in the cranial and ventral directions, produces an atrial appendage located on each side of the outflow tract (Fig. 1.6). This expansion can be first seen at stage 14 but becomes more pronounced by stage 16, with the appendages accounting for the major component of the atrial volumes at stage 20. Pectinate muscles can be recognized in the right appendage by stage 16, and in the left appendage by stage 19, equivalent to almost 7 weeks of development. The pectinate muscles remain initially shallow but become a well-developed plexus by stage 22. Their formation differs from that of the ventricular trabeculations, since they form in the areas of the atrial component of the initial heart tube, which is devoid of cardiac jelly.

Fig. 1.7 (continued) blood flow in the CS14 and CS20 models). The upper row shows the transformation of the interventricular ring into the ventricular cardiac conduction system. The portion of the interventricular ring that loses expression of specific markers in mammals is hatched. In the middle and lower rows, the fate of the interventricular foramen (IVF) as deduced from the changes in the shape of the ring is shown. Red identifies the retro-aortic portion, blue the ventral portion, and yellow the caudal portion. The interrupted parts indicate the invisible portions or the ring. The interrupted black lines represent the plane of OFT removal, and the interrupted white line indicates removal of the left atrial auricle to visualize the left ventricle

1.4.4 Formation of the Muscular Ventricular Septum

The ballooning of apical trabecular components at the outer curvature of the ventricular loop [69, 83] induces the formation of the muscular ventricular septum between them. This septum grows along its apicobasal axis [84]. Subsequent to the appearance of the septum, the primary interventricular foramen can be recognized between the inner curvature and the tip of the newly formed septum. The septum makes symmetrical right- and left-sided contributions until proliferation of the compact components of the ventricular walls sets in at stage 16, equivalent to 38 days of development. Thereafter, the contribution of cardiomyocytes from the left ventricle exceeds that of the right ventricle, in particular in its caudal portion [84].

1.4.5 Formation of the Definitive Left and Right Ventricles

Tracing studies have shown that the trabeculated component of the left ventricle extends upstream by recruitment of cells from the atrioventricular canal in both birds and mammals [85–87]. Tracing studies in birds also indicate that the right ventricular trabeculations extend downstream at the expense of the proximal outflow tract [88, 89]. The arterial valves eventually form from the endocardial ridges in the middle part of the outflow tract (see Sect. 1.5.4.8 Septation of the Middle Outflow Tract [90–92]). Subsequent to this process, the proximal part of the outflow tract gets incorporated into the definitive ventricles as the smooth-walled infundibular portion of the right ventricle and the short aortic vestibule of the left ventricle. These data show that the boundaries of the eventual ventricular mass, extending between the atrioventricular and ventriculo-arterial junctions, do not co-localize with the boundaries of the "embryonic" ventricles, which are determined by the complementary distributions of ventricular trabeculations and endocardial cushions or ridges. Throughout these changes, furthermore, the inner curvature of the ventricular loop retains a smooth myocardial phenotype with the functional properties of the primary myocardium [69]. It cannot, for this reason, precisely be assigned to a compartment. Thus, while the first heart field forms the entirety of the "embryonic" left ventricle, its contribution to the "definitive" left ventricle is restricted to the left side of the muscular septum and the apex subsequent to the incorporation of Tbx2- and Tbx3-positive cardiomyocytes from the initial atrioventricular canal [86, 87]. In both ventricles, the papillary muscles begin to form in the eighth week by consolidation of aggregating trabeculations, with coalescence starting at the level of the developing valvar leaflets and extending outward in the direction of the compact ventricular walls. At CS20, the left ventricle develops an apex.

1.4.6 The Conduction System

All components of the cardiac conduction system, except the peripheral ramifications of the ventricular pathways, derive from *Tbx3*-positive, poorly differentiated cardiomyocytes that border or separate the newly formed atrial or ventricular compartments of the primary heart tube [9, 87]. A *Tbx3*-positive myocardium is found on the wall of the atrioventricular canal, and on the common floor of the left and right atriums up to the pulmonary vein, up to and including the sinoatrial junction [9, 93]. Morphologically, the distribution of a Tbx3-positive primary myocardium corresponds with a typically bilayered myocardium, with a mesh of thin myocardial strands in between as found in the atrioventricular canal and on the atrial floor (Fig. 1.7). Tbx3 represses differentiation, but, until stage 16, a substantial fraction of Tbx2- and Tbx3-positive cardiomyocytes escapes from this repression and differentiates into a normal Gja5 (Cx40)-positive working myocardium.

1.4.6.1 The Sinus Node

The sinus node becomes an identifiable entity during stage 13, appearing as the slightly thickened wall of the right common cardinal vein (Fig. 1.8). Any development along the left common cardinal vein is repressed by Pitx2 [47]. The node extends cranially from the entrance of the common cardinal vein into the pericardial cavity and caudally toward the junction of the systemic venous sinus and the inferior caval vein, with the tail extending along the right venous valve [47, 94]. The working myocardium in this region will become the terminal crest. The node does not change its position during embryonic development, but its relative size and thickness decline.

1.4.6.2 The Atrioventricular Node

The embryonic atrioventricular canal is characterized not only by the presence of atrioventricular cushions but also by slow conduction of the atrial depolarizing impulse. The transition of atrial cardiomyocytes into those of the Tbx2- and Tbx3-positive atrioventricular canal [8, 93, 95] is gradual. It is characterized by a progressively lower expression of channels associated with rapid depolarization and conduction, with this producing the working myocardium, which expresses the Scn5a or Nav1.5 genes and the Gja1 or Cx43 connexins. The persisting primary myocardium, in contrast, shows a higher expression of genes associated with automaticity and slow conduction, namely, Hcn4 and Tbx3. This arrangement accounts for the bilateral inferior extensions of the atrioventricular node [96]. The compact node itself derives in its entirety from the Tbx3-positive atrioventricular canal musculature [97], without contributions from the myocardium of the coronary sinus [98], although its connections with the atrial septum are derived from the myocardialized vestibular spine and mesenchymal cap [97]. The definitive electrical insulation of atriums and ventricles is established by an interruption of the myocardial continuity between the atrioventricular canal and the ventricles, followed by the fusion of the epicardial connective tissue in the atrioventricular grooves with that of the

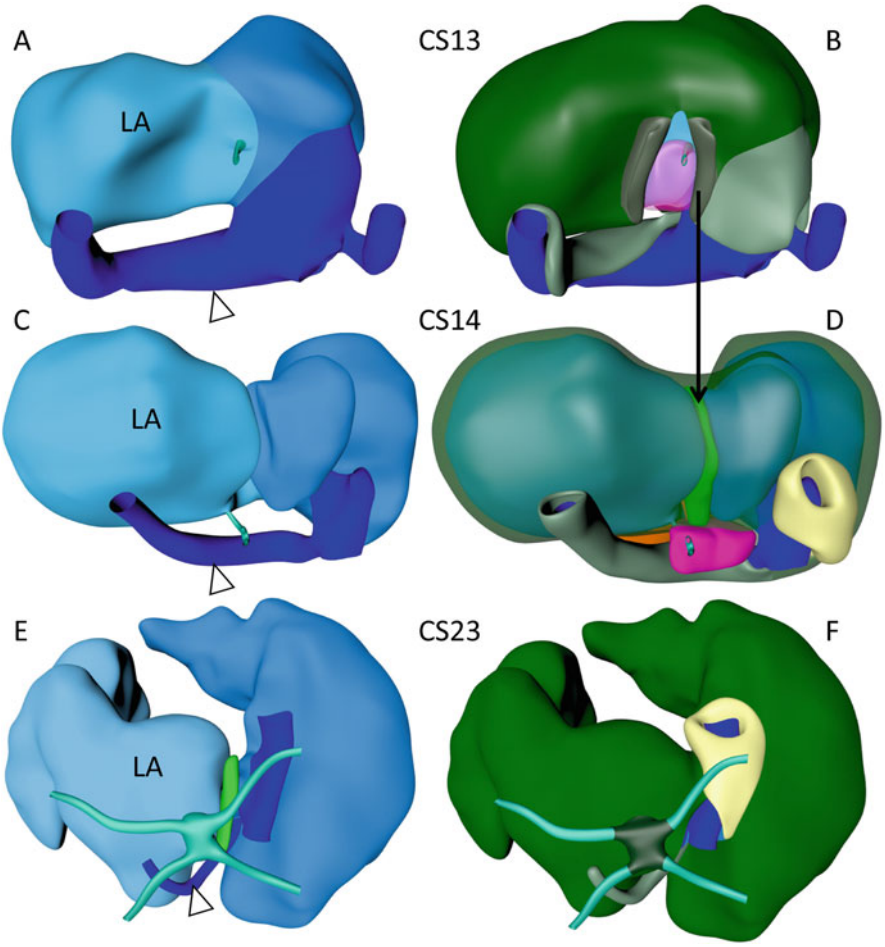

Fig. 1.8 Development and position of the pulmonary veins. (a–f) Dorsal views. Panels (a, c, and e) show the lumen of both atriums and venous sinus, whereas panels (b, d, and f) show the surrounding myocardium in green. The dorsal mesenchymal protrusion (pink) carries the pulmonary vein and is flanked by mesenchymal ridges (gray). The right ridge is continuous with the primary interatrial septum (panels b and d, black arrow) and commits the pulmonary vein to the left side. Up to CS23, the four pulmonary veins first drain into a common proximal portion before emptying into the left atrium (LA). It should be noted that this proximal portion is surrounded by the myocardium (panel e; dark green). The panels also show the development of the sinoatrial node and its tail (light yellow) along the right common cardinal vein. The declining diameter of the left common cardinal vein (coronary sinus) between CS13 and CS23 (arrowheads) should also be noted

atrioventricular endocardial cushions [99, 100]. This process starts at stage 18 in the right atrioventricular junction and is largely completed at stage 23, with the only persisting myocardial connection remaining at the site of the so-called penetrating bundle of His.

1.4.6.3 The Ventricular Conduction System

The transition of the compact atrioventricular node into the atrioventricular bundle is characterized by the expression of the genes associated with rapid conduction, namely, *Scn5a* and *Gja5* or Cx40 [97]. The position of the atrioventricular bundle and bundle branches can be visualized in human embryos with antibodies, variously known as GlN, HNK1, or LEU7, which all recognize a terminal 3-sulfated glucuronic acid epitope on macromolecules. At stage 14, the antibodies stain a ring of cardiomyocytes that encircles the primary interventricular foramen (Fig. 1.7 [6]). The myocardium of this interventricular ring has an extremely dense appearance, permitting its recognition in routine histological sections from stage 14 onward [8, 99]. In the lesser curvature, the GlN-positive ring is located at the right half of the atrioventricular canal. Parts of this ring subsequently differentiate to become the fast ventricular conduction system. Subsequent to the beginning of transfer of the aortic root to the left ventricle, at stage 15 in mammals, the ventral part of the initial ring no longer stains with the GlN antibody and loses its characteristic histological structure. It persists in birds [101, 102]. In a minority of cases, nonetheless, the ring may extend as a "dead-end tract" on the crest of the muscular ventricular septum beyond the origin of the right and left bundle branches [103]. As we will describe, the site of the components of the initial GlN-positive myocardial ring provides an excellent marker with which to follow ventricular septation ([104]; see Sect. 1.5.5 The Final Step in Septation).

1.4.7 Appearance of the Coronary Vessels

1.4.7.1 The Proepicardial Organ

The proepicardial organ plays a key role in the development of the coronary vessels. This temporary bilateral villous structure is found during stages 11 and 12 on the pericardial surface of the transverse septum, near the inflow tract (Fig. 1.9). Its cells proliferate to form vesicles, which spread across the surface of the heart to form the epicardium [105–107]. The spread is first seen in the adjacent atrioventricular grooves during stage 13, extending into the interventricular grooves during stage 14, and then expanding over the entire heart surface during stages 15 and 16 [108, 109]. Remaining thickest in the atrioventricular and interventricular grooves, the epicardial layer, derived from the proepicardial organ, induces the development of the coronary vessels, their vascular smooth muscle cells, and cardiac fibroblasts [110].

1.4.7.2 Formation of the Coronary Arteries

By the end of stage 16, an initially blind vascular network develops in the subepicardial space surrounding the aorta, whereas endothelial outgrowths protrude from the aortic base just distal to the border of the myocardial middle part of the outflow tract [111, 112]. The subepicardial network forms clusters of endothelial cells near the coronary arterial sprouts during stages 17 and 18 [112]. The remaining coronary aortic sprouts co-localize with the myocardial tongues at the distal outflow

tract (see Sect. 1.4.7.2 Formation of the Coronary Arteries). At CS18, the left coronary artery stem connects with the ventricular plexus, whereas the right coronary artery does so at CS19 (Fig. 1.9; [113–115]). The left coronary orifice, therefore, forms ~2 days earlier than does the right orifice. The main trunks of the coronary arteries are formed within the relatively thick epicardial areas in the atrioventricular and interventricular grooves, with the left anterior descending artery becoming evident during stages 20 and 21 [115]. This timeline shows that the coronary arteries appear after completion of epicardial development [108], septation at the arterial orifice level [114], and the onset of proliferation of the compact layers of the ventricular walls [115–119]. The coronary arterial endothelium largely derives from the Apln-expressing endothelium of the venous sinus [111, 120], with a contribution of the ventricular endocardium [121]. Scx-/Sema3D-expressing proepicardial cells form the endothelium of the coronary arteriovenous connections [122, 123].

1.4.7.3 Development of the Coronary Arterial Walls

Once the epicardium is enveloped by the myocardium, a subset of epicardially derived cells undergoes a process of epithelial-to-mesenchymal transition, migrating

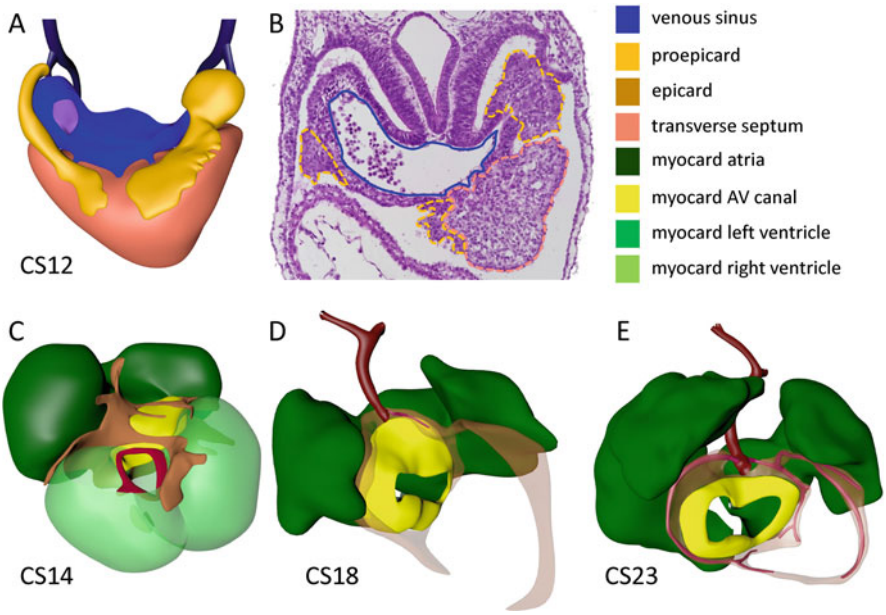

Fig. 1.9 Development of the coronary arteries. (a) Top and (c–e) right ventral views. The bilateral pro-epicardium is located on the pericardial wall of the transverse septum (panels a and b) and covers the venous sinus. The epicardium is first visible along the atrioventricular and interventricular grooves at CS14 (panel c). It will cover the entire heart surface, but only the thick parts are shown in panels d and e. The developing coronary arteries follow the course of this thick epicardium

into the subepicardial space [124, 125] to give rise to coronary pericytes or smooth muscle cells [126, 127]. The newly formed main stems of the coronary arteries are covered by only a single layer of vascular smooth muscle cells. Further recruitment and assembly of vascular smooth muscle cells occurs first at the orifices of the arterial stems and progresses distally. The orifices, when initially formed, arise from the tubular aorta. It is only with ongoing formation of the valvar sinuses of the aortic root that the orifices get incorporated proximal to the sinotubular junction. At stage 19, furthermore, vascular smooth muscle cells have yet to be recruited to clothe the branches of the main coronary arteries. The process is similar in mice [105, 128, 129].

1.4.7.4 Formation of the Cardiac Veins

Little is known about the development of the cardiac veins, which drain to the coronary sinus, except that the middle cardiac vein is reported to be identifiable as a bud of the left sinus horn at stage 16 [113, 118].

1.5 Septation of the Heart (CS14–CS20)

1.5.1 The Phylotypic Stage and the Onset of Septation

The body plan is laid down during gastrulation in the so-called phylotypic stage of embryos. At this stage, the morphological features and profiles of gene expression are most similar among vertebrate embryos [17]. This lack of diversity may reflect strong constraints on gene regulation and interactions during this process. In mammalian embryos, the end of the phylotypic stage is represented by Carnegie stage 13. By this stage, it is possible to recognize the beginning of formation of the so-called segments, which balloon from the outer curvature of the helically twisted myocardial tube. As we will describe in our next section, the molding of the endocardial jelly within the tube, from the outset, allows for two parallel bloodstreams. Structural separation of these bloodstreams and the development of one-way valves, however, only occur during the septation phase of development. Septation proceeds centripetally from the venous and arterial poles toward the interventricular foramen. It primarily occurs by the remodeling of those parts of the primary myocardium that have not yet differentiated and which are concentrated in the inner curvature of the heart [130].

1.5.2 Structural Changes in the Preseptational Heart

Separate left and right bloodstreams can be observed in the outflow tract soon after the appearance of the right ventricle at stage 12 [131, 132]. In the hearts of mice [133] and chicken [131, 132, 134, 135] prior to septation, the blood flow is laminar and mixing is limited. During the stage of formation of the ventricular trabeculations in humans [71, 136], mice [72, 136], and chicken [137]), the conduction velocity

increases. At the same time, ventricular activation changes from a base-to-apex to an apex-to-base sequence [138–140]. In addition, cardiac pumping switches from a suction, or impedance, to a pulsatile piston mechanism [141]. As a result, cardiac output increases [142], with the appearance of vortical streaming patterns [143] and mixing of bloodstreams. This is especially true downstream of the relatively narrow and still slowly contracting atrioventricular canal and distal outflow tract [132, 135]. The relationship between cardiac load and contraction pattern appears to be causal [144]. It is, therefore, probably not coincidental that the increasing functional effectivity of human [145] and chick hearts [146, 147] is temporally associated with septation, although many of the details on how rheology regulates cardiac morphogenesis remain to be clarified.

1.5.3 Septation of the Venous Pole

1.5.3.1 Septation of the Veins

The systemic veins enter the right atrium via the systemic venous sinus, with the pulmonary veins entering the left atrium through the remnant of the dorsal mesocardium. The floor of the initial atrial part of the primary tube has a characteristic bilayered appearance of its myocardium, with the cardiomyocytes themselves expressing Tbx3 [93, 98]. This part of the wall is initially a caudal extension of the atrioventricular canal. By stages 10 and 11, however, the left and right parts of the developing atrial component are already mostly separate structures with respect to their lineage and gene expression profile. The myocardium surrounding the entrance of the pulmonary vein derives, like the atrial myocardium, from a Nkx2–5-positive, Tbx18-negative lineage. The myocardium of the systemic venous sinus, in contrast, derives from a lineage negative for Nkx2–5 but positive for Tbx18 [27–29, 47]. Ang-1/Tie1 signaling is involved in the development of the right-sided components [148], whereas Pitx2 is expressed in the left-sided venous structures [58, 149]. The systemic venous sinus itself, by stage 12, becomes asymmetric, with a smaller left-sided and a larger right-sided component. Its entrance is restricted to the right atrium during stage 13 (Figs. 1.4 and 1.8). The junction between the sinus and the developing right atrium becomes slit-shaped and, by stage 14, is guarded by left and right venous valves. This configuration subsequently increases in size, but its shape remains largely conserved between 5 and 7 weeks of development. The primordium of the pulmonary vein is first seen at stage 12 as a wedge of mesenchyme between the legs of the inflow tract at the level of the caudal dorsal mesocardium [150, 151]. As the strand canalizes, its entrance into the developing left atrium is flanked by mesenchymal ridges (Fig. 1.8). It is growth of the right-sided ridge, which becomes the vestibular spine, or dorsal mesenchymal protrusion, and its fusion to the primary atrial septum (see next paragraph) that commits the orifice of the pulmonary vein to the left atrium [151–153]. The myocardium then surrounds the stem of the vein at stage 17. Thereafter, the myocardial stem expands radially, suggesting an increase in blood flow. By stage 20, the first bifurcation of the pulmonary vein has also acquired a myocardial wall, whereas the myocardium

surrounds the pulmonary veins up to their second division at stage 23. The diameter of the stem of the pulmonary veins continues to increase, which presages the incorporation of the pulmonary veins as two separate tributaries into the roof of the left atrium in the 9th week of development and as four tributaries in the 14th week [151]. The incorporation of the veins into the roof of the left atrium then underscores the formation of the superior interatrial fold, often incorrectly identified as the second atrial septum. It is the fold, nonetheless, against which the primary atrial septum abuts to close the oval foramen.

The Fate of the Left Cranial Cardinal Vein

Between stages 14 and 23, the diameter of the left half of the systemic venous sinus, also known as the left sinus horn, does not change (Fig. 1.8). This implies that it receives an increasingly smaller percentage of the systemic venous blood. Accordingly, the left cranial cardinal vein starts to attenuate between the junction of the left subclavian and jugular veins cranially and its passage in the left atrial ridge between the left inferior pulmonary vein and the left atrial appendage caudally [154]. Meanwhile, the brachiocephalic vein forms from merging the venous spaces that arise between both jugular veins just cranial to the aortic arch. Remodeling occurs during stages 20 and 21, with only a small left common cardinal vein present at stage 22, the lumen of which has disappeared by stage 23. The distal obliterated part of the left sinus horn remains as the ligament of Marshall [155]. The remaining proximal part becomes the coronary sinus.

1.5.3.2 The Atrial Septum

The atrial extensions of the cranial and caudal atrioventricular endocardial cushions begin to demarcate the interatrial foramen between the developing right and left sides of the atrial component of the primary heart tube at stage 12. By stage 14, the myocardial primary atrial septum can be recognized as a midline bud on the atrial roof, growing toward the atrioventricular canal. Its leading edge is covered by an extension of the cranial atrioventricular endocardial cushion, known as the mesenchymal cap [156]. At the dorsal side of the primary atrial septum, where the atrial extensions of the atrioventricular cushions approach each other, the atrial lumen is directly bordered by a cranial extension of the dorsal mesocardium. With continuing caudal expansion of the atrium, by stage 16, the cranial end of the dorsal mesocardium becomes spine-shaped. The spine protrudes on the atrial floor, extending toward the atrioventricular canal between the atrial extensions of the atrioventricular endocardial cushions. On the basis of its shape and position, the structure is known as the vestibular spine [157] or the dorsal mesenchymal protrusion [153, 158, 159]. Caudal to the opening of the pulmonary vein, the spine, or protrusion, is continuous with the dorsal mesocardium surrounding the sinus horns and, more caudally, with the ventral mesentery of the foregut. By stage 18, cardiomyocytes begin to populate both the spine and the mesenchymal cap, thus forming the well-developed ventrocaudal muscular rim, or buttress, of the interatrial septum [157]. It is this process that produces the true second atrial septum. The primary atrial septum then persists as the floor of the oval fossa. It is the superior

infolding produced by incorporation of the pulmonary veins to the roof of the left atrium that then provides the fold against which the primary septum will eventually abut to close the oval foramen in postnatal life. The myocardialization of the mesenchymal protrusion proceeds concurrently with that in the ridges of the proximal outflow tract, even though both sites are physically separated.

1.5.3.3 Atrioventricular Septation

Reflecting atrial growth, the myocardial atrioventricular canal changes from tubular to funnel-shaped in appearance between stages 16 and 18, becoming the vestibules of the atrioventricular valves. The superior and inferior atrioventricular endocardial cushions fuse during the same period to septate the atrioventricular canal [60, 160]. The atrial extensions of the cushions, which surround the primary interatrial foramen, also fuse and close this foramen. Coincident with the closure of the primary foramen, the muscular primary atrial septum undergoes extensive dorsal fenestration to provide the secondary interatrial foramen. Only later, in the eighth and tenth weeks of development, does a secondary atrial pseudoseptum develop gradually as a muscular fold in the cranial wall of the right atrium between the right pulmonary vein and the left venous valve [151, 157]. This fold forms the cranial rim of the secondary interatrial foramen, thus completing the formation of the oval fossa. It is the muscularized spine and mesenchymal cap that form the true second septum, serving to bind the primary septum to the newly separated atrioventricular junctions. Opposite the contact zone of the superior and inferior atrioventricular cushions, two smaller lateral endocardial cushions become identifiable during stage 18. By stage 20, the superior and inferior atrioventricular cushions are no longer separately distinguishable [161]. The leaflets and papillary muscles of the atrioventricular valves can then be recognized while tendinous cords begin to develop at stage 23 [162].

1.5.3.4 Growth of the Ventricles and Formation of the Muscular Ventricular Septum

The ventricular septum becomes a morphological entity at stage 12, when the right ventricle forms by ballooning from the outlet part of the ventricular loop [163]. During the looping phase, the heart tube elongates along its longitudinal, veno-arterial axis, but, during the ballooning phase, its growth along its radial axis becomes more important [52, 70]. The initially tiny right ventricle expands faster than the larger left ventricle, but it is not until stage 16, at around 49 days, that the ventricular cavities acquire a similar size (Figs. 1.6 and 1.7). Accordingly, ventricular growth is regulated independently, both qualitatively via expression of the transcription factor Hand2 or Hand1 [164] and quantitatively by the level of expression of the transcription factor Tbx5 [21]. Tbx5 is a marker of the first heart field. If deficient, it causes left ventricular hypoplasia, but, if highly expressed, it suppresses right ventricular growth [22, 165]. Separate left and right bloodstreams appear in the outflow tract soon after the appearance of the right ventricle at stage 12 [131, 132], but whether an increase in blood flow contributes to the selective growth of the right ventricle is not known.

1.5.4 Septation of the Arterial Pole

Septation of the arterial pole proceeds centripetally from the aortic sac toward the interventricular foramen.

1.5.4.1 Development of the Temporary Arteries of the Cranial Pharyngeal Arches

Between stages 9 and 11, representing 26 through 29 days of development, and before any segmentation of the pharynx is visible, there is already formation of a relatively large first pair of pharyngeal arch arteries. The ventral aortas feeding this first pair of arch arteries originate in the arterial pole of the heart. In both birds [166] and mammals [167], they run ventral to the pharynx in the cranial direction, continuing dorsolaterally to form the dorsal aortas (Fig. 1.10). The dorsal aortas, in turn, course caudally round the dorsolateral wall of the pharynx to form a plexus where somites are in the process of forming. With ongoing development, pharyngeal pouches form caudal to the corresponding pharyngeal arch. By stage 12, equivalent to day 30, and concomitant with the appearance of the second pharyngeal pouch, a second pair of arch arteries is formed. Meanwhile, an endothelial-lined space, the aortic sac, connects the lumen of the outflow tract with the lumens of the arteries now running through the pharyngeal arches, thus replacing the ventral aortas. The endothelial lining of the first two pharyngeal arches shares its lineage with that of the dorsal and ventral aortas but differs from that of the three caudal arch arteries [168]. The common mesodermal origin of the muscles of the heart with those of the two cranial pharyngeal arches may underlie this finding. Thus, the second heart field first gives rise to mesodermal cells that produce both the embryonic right ventricle and the muscles of the first pharyngeal arch. Then, slightly later, it produces mesodermal cells that give rise to the myocardium of the outflow tract and the muscles of the second pharyngeal arch [169, 170]. Because of the dual fate of their constituting cells, the cardiogenic fields are now often referred to as the cardiopharyngeal field [171]. The specification of the neural crest of the first two pharyngeal arches also differs from that of the more caudal pharyngeal arches [172].

1.5.4.2 Development of the Permanent Caudal Arch Arteries

By stage 13, after ~32 days of development, the first pair of arch arteries disappears, whereas the arteries coursing through the third and fourth arches can now be recognized (Fig. 1.10). After 34 days, by stage 14, the second pair of arch arteries also gets interrupted, whereas the ultimate pair is formed. This final pair of arteries is traditionally known as the arteries of the sixth arch. At no stage of development, however, is there any formation of a fifth pharyngeal pouch. Only four discrete arches are seen with the ultimate pair of arteries percolating through the mesenchyme caudal to the fourth pouch. These ultimate arch arteries will give rise, at stage 15, or ~36 days of development, to the right and left pulmonary arteries. We will refer to the final pair of arch arteries, therefore, as occupying the pulmonary arches. The caudal three pairs of arch arteries are modified in the developing embryo but persist into adult life. Their endothelium derives from the Tbx1-positive caudal

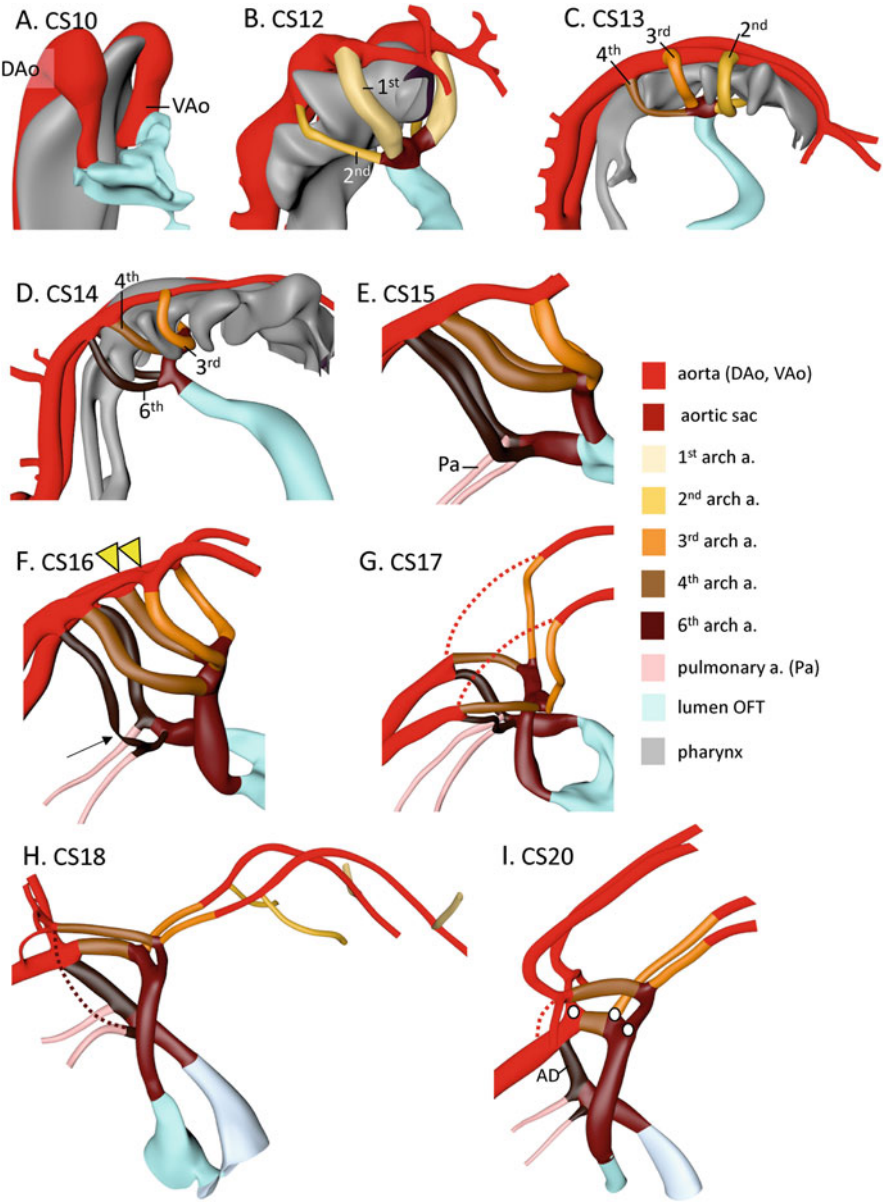

Fig. 1.10 Aortic arch development. Panels a and b are seen from cranial and right, and the remaining panels from the right. Arch artery 1 (AA-1) is present ab initio (a), AA-2 appears at CS12 (b), AAs-3 and AA-4 appear, and AA-1 disappears at CS13 (c), whereas the terminal arch artery ("sixth") appears and AA-2 disappears at CS14 (d). Up to CS11, the ventral aortas are interposed between the arterial pole and the first 2 AAs. The pulmonary arteries appear at CS15 (panel e). AAs develop concomitantly with the corresponding pharyngeal pouches (b–d). Arterial symmetry disappears during and after CS16, when the right terminal AA just distal to the branching of the pulmonary artery (arrow; panel f) and the dorsal aortae between the third and fourth AAs ("carotid ducts") become markedly thinner (yellow arrowhead). The carotid ducts disappear at

second heart field [168, 173], with their smooth muscle coats derived from the cardiac neural crest [174, 175]. Neither in birds nor mammals is there any formation of a fifth arch [176].

1.5.4.3 The Fate of the Dorsal Aortas

By stage 12, the dorsal aortas begin to merge in the caudal direction from the level of somites 8 through 10, corresponding to the fourth and sixth cervical segments. By stage 13, this fusion rapidly reaches the level of the umbilical arteries, at the 4th lumbar segment and the 32nd somite. Intersegmental arteries are now recognizable, branching away from both the dorsal aortas and between adjacent somites. By stage 14, the seventh cervical segmental arteries, which are also known as the sixth cervical intersegmental arteries [177], become larger than the adjacent intersegmental vessels and can be used as a segmental landmark. Both dorsal aortas also develop cranial extensions, which will become the internal carotid arteries and which temporarily terminate as a bifurcation on both sides of the optic stalk. Stage 15 is the most advanced stage in which the arteries within the pharyngeal arches retain their symmetry. Between stages 15 and 16, the portions of both dorsal aortas between the entrances of the third and fourth pair of pharyngeal arch arteries, known as the "carotid duct" [178], attenuate. This component disappears by stage 17 (Fig. 1.10). The symmetry, while obvious until stage 16, is rapidly lost during the sixth and seventh weeks, over stages 17 through 20, due to the retarded development of the arteries on the right side. The distal part of the right pulmonary arch artery between the right pulmonary artery and the dorsal aorta attenuates during stage 17. It disappears at stage 18 so that the right pulmonary artery arises directly from the pulmonary trunk. The right dorsal aorta tapers off distal to the seventh segmental artery and disappears at stage 20, equivalent to 49 days of development. The left-sided dorsal aorta remains intact, although its axial length between the entrance of the fourth arch artery and the root of the seventh segmental artery does not increase subsequent to stage 13 [11]. During these stages, nonetheless, the origin of the left seventh segmental artery, which becomes the subclavian artery, crosses the union with the left pulmonary arch artery, which persists until postnatal life as the arterial duct. At 7 weeks of development, therefore, the major arterial vessels adopt their definitive configuration.

Fig. 1.10 (continued) CS17 (panel g: interrupted line) and the right terminal AA distal to the pulmonary artery at CS18 (panel h: interrupted lines). At CS18, the right dorsal aorta distal to the seventh segmental artery also becomes thinner and disappears at CS20 (panel i: stippled line). CS20 represents the adult configuration, with the brachiocephalic, left carotid arteries, and left subclavian arteries as direct aortic branches (panel i: white dots). The left terminal AA (AD, arterial duct) disappears after birth

1.5.4.4 The Growth Pattern of the Early Outflow Tract

Coinciding with the appearance of the first pharyngeal pouch at stage 11, the second heart field starts to contribute cells to the arterial pole of the heart [26, 45]. This addition of cells to the early outflow tract increases its length around fourfold over the period of 8 days between stages 12 and 16. This transforms it into a long and slender tubular midline structure extending perpendicular to the pharynx. At stage 12, with two arches and pouches formed, the appearance of endocardial sprouting into the cardiac jelly marks the ballooning of the developing apical part of the right ventricle from the outlet part of the initial ventricular loop. Meanwhile, the remaining downstream part of the outflow tract acquires a pronounced bend, known as the "bayonet" [65] or "dog-leg" bend [66]. This bend is possibly a critical structural element for efficient valveless pumping [68]. By stage 13, the developing right ventricle can be delineated by its external contour and the distribution of its apical trabeculations. We use the downstream boundary of the trabeculations, and the upstream boundary of the outflow tract ridges or cushions, as a marker for the junction of the right ventricle and the definitive outflow tract. Our reconstructions show that, due to continued axial growth of the outflow tract, the initially obvious dog-leg bend disappears, with the outflow tract straightening between stages 12 and 15.

1.5.4.5 The Remarkable Subsequent Change in the Shape of the Late Outflow Tract

Between stages 15 and 20, there is minimal growth of the myocardium of the outflow tract in either rodent [51, 74] or human embryos [13, 73]. In the overall architecture, nonetheless, it undergoes an impressive change in appearance. Within 2 days, between stages 16 and 17, its length declines to around two-fifths of its maximum [13, 179] due to its transformation from a fairly narrow tube to a wide entity with a figure-of-eight configuration when seen on the short axis. The waist in the figure-of-eight then represents the developing separation between the subpulmonary and subaortic channels (Fig. 1.11). At the same time, the outflow tract becomes progressively wedge-shaped, with its greatest length along the subpulmonary channel and its shortest length along the subaortic channel. The decrease in length occurs mostly in the proximal portion of the heart, also known as the conal part [179]. The change in length and shape cannot be ascribed to apoptosis. Cell death in mouse embryos is 10-fold more intense in the fusing endocardial cushions than in the myocardium and peaks between embryonic days 12.5 and 13.5, equivalent to Carnegie stages 17 through 19 [180, 181]. Furthermore, starting at stage 12, the boundary between the right ventricle and the proximal outflow tract shifts distally as the outflow myocardium is incorporated into the right ventricle [88, 89]. The change in the size and shape of the developing right ventricle by inclusion of the outflow tract myocardium can be compared to the recruitment by the developing left ventricle of cardiomyocytes initially belonging to the atrioventricular canal. There is a difference, nonetheless, in timeline. It continues on the right side for around 3½ weeks, whereas recruitment on the left side is completed in half a week [87]. The inclusion

of the myocardium into the embryonic ventricles changes the compartmental boundaries and explains why we distinguish embryonic from definitive ventricles.

1.5.4.6 Invasion of Neural Crest Cells and Establishment of Spiraling Ridges

The septation of the junction of the outflow tract and the aortic sac is complex. Up to, and including, stage 13, the distal myocardial boundary reaches the pericardial reflection. At this stage, the lumen of the outflow tract is approximately circular, surrounded by homogeneously thick endocardial jelly sparsely populated by cells. Until stage 13, the wall of the aortic sac, like that of the dorsal aortas, is composed only of the endothelium and the supporting homogeneous pharyngeal mesenchyme. Between stages 13 and 14, corresponding to 32–34 days of development, the appearance of the cardiac neural crest, and the formation of the intercalated non-myocardial ridges or tongues, changes the architecture of the aortic sac and the myocardial portion of the outflow tract. In this regard, the non-myocardial intercalated ridges should not be confused with the mesenchymal ridges, which spiral through the myocardial outflow tract. In mouse embryos, the cardiac neural crest originates almost exclusively at the level of the first and second somites and migrates from there through the caudal three pharyngeal arches to reach the arterial pole of the heart [175]. At the arterial pole, the neural crest cells embrace the aortic sac, invading the endocardial jelly from distal to proximal as left- and right-sided columns [182, 183]. Endocardial cells that undergo epithelial-to-mesenchymal transformation also populate the endocardial jelly, in particular those that will eventually form the leaflets of the arterial valves [184, 185]. The ridges produced by the neural crest cells in the endocardial jelly are more distinct [61]. It is the presence of neural crest cells that distinguishes the endocardial ridges in the outflow tract from the endocardial cushions in the atrioventricular canal. When traced proximally, these entities are attached to the myocardium of the outflow tract parietally and septally. They follow a clockwise spiraling course through ~180° when traced from the base of the outflow tract toward the aortic sac (Fig. 1.12 [60, 61]).

1.5.4.7 Formation of the Aortopulmonary Septum in the Distal Outflow Tract

Neural crest cells that aggregate around the endothelially lined aortic sac indent its dorsal wall to form the so-called aortopulmonary septum as a protrusion between the openings of the fourth and the ultimate pair of pharyngeal arch arteries. When first observed, at stage 14, the protrusion has a transverse orientation. As it grows ventrally through the aortic sac during stage 15, its orientation gradually changes in the anticlockwise direction when seen from the ventral aspect, thus following the bloodstream. In consequence, the aortic and pulmonary components of the aortic sac, respectively, acquire dextrocranial and sinistrocaudal positions at stage 16 and become right- and left-sided at stage 17 (Fig. 1.12). Concurrently, the aortic and pulmonary components of the aortic sac elongate and transform into the ascending aorta and pulmonary trunk, respectively (see Sect. 1.5.4.10 Appearance of the

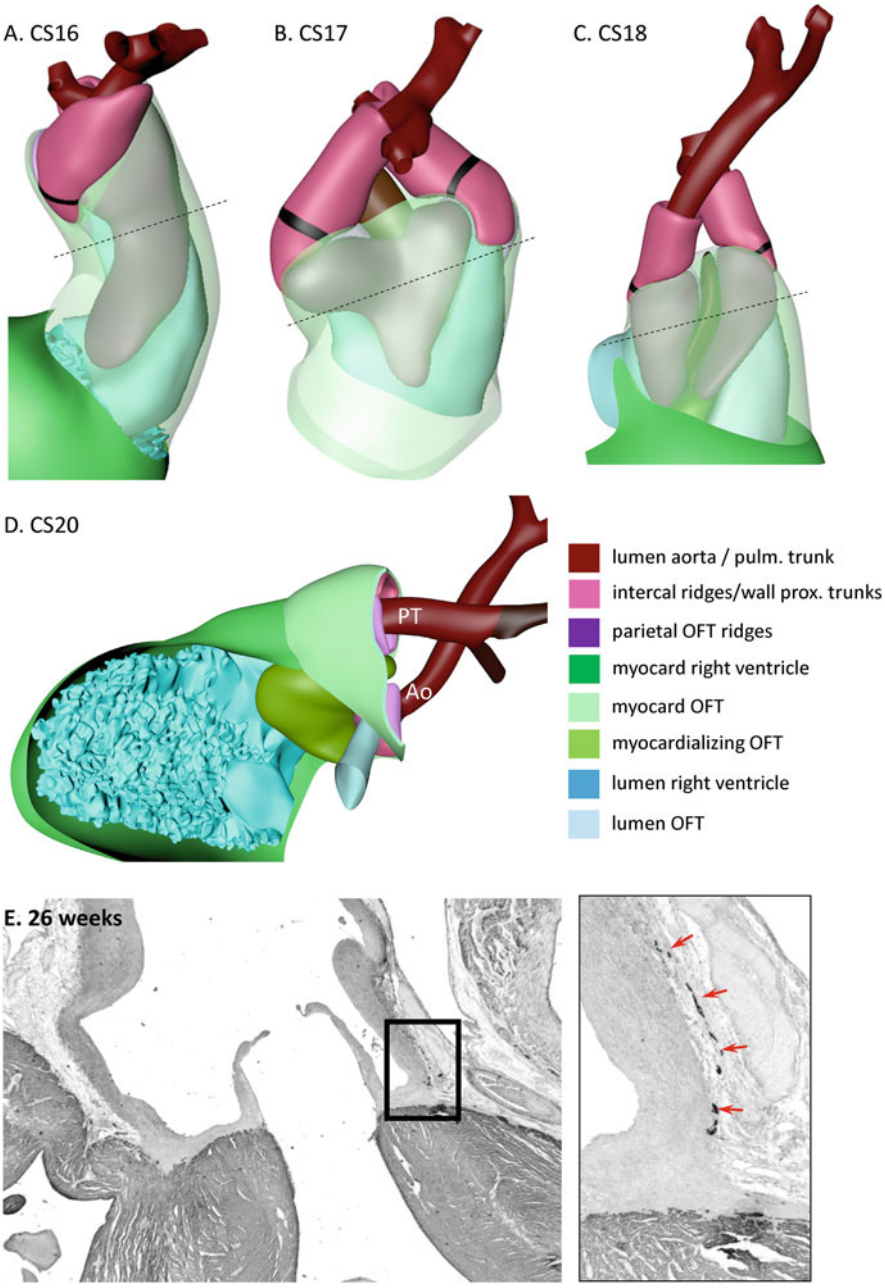

Fig. 1.11 Remodeling of the outflow tract. (a–d) Right-sided views of the heart with the myocardial OFT rendered translucent (CS16–18) or after removal of the free wall of the right ventricle (CS20). The changes in the shape of the parietal outflow tract ridge also reflect the change in the shape of the myocardial OFT. The black bands indicate the boundary between the wall of the

Arterial Trunks). The change in position of the future pulmonary trunk is sometimes interpreted as a rotation in the distal outflow tract [62]. Since a rotation in the distal outflow tract would require a compensatory counterrotation upstream, we interpret the change as a consequence of the asymmetric growth of the aortopulmonary septum (Fig. 1.12). In agreement, the change in position accompanies the increasing arterial asymmetry due to the right-sided regression of the dorsal aorta and pulmonary arch artery after stage 15.

1.5.4.8 Septation of the Middle Outflow Tract

The reorientation of the aortopulmonary septum between stages 15 and 17 provides access to the systemic arteries, on the one hand, and the pulmonary arch arteries, on the other, in line with the forming aortic and pulmonary channels [182, 186]. This remodeling, therefore, is a precondition for the fusion of the aortopulmonary septum with the adjacent distal ends of the outflow tract ridges of cushions and the subsequent septation from distal to proximal in the outflow tract [10, 11]. Septation reaches the valvar area in CS15 embryos while fusion of the aortopulmonary septum with the endocardial ridges is about to occur just distal to the developing valves in CS16 embryos. Fusion in the middle part of the outflow tract, which at this stage has retained its myocardial wall, occurs during stage 17. Fusion in the proximal myocardial outflow tract takes place during stage 18. The distal-to-proximal fusion of the endocardial ridges appears to occur exclusively in the endothelium overlying the "prongs" of neural crest cells. Subsequently, both prongs also fuse to become an extremely dense, central "whorl" in the outflow tract. In support of this notion, it is well-established that ablation of the contribution made by the neural crest to the outflow tract interferes with its septation [187].

1.5.4.9 Formation of the Non-Myocardial Intercalated Ridges (or Tongues) and Swellings

The cranial second heart field produces two waves of progenitor cells that contribute to the outflow tract. The first wave arises at stage 10. It contributes to the cranial wall of the muscular outflow tract until stage 14 and to the intrapericardial component of the ascending aorta thereafter. The second wave evolves slightly later, and more gradually, between stages 11 and 15. This wave contributes to the caudal wall of the muscular outflow tract and, after stage 14, to the pulmonary trunk [57, 188]. The cranial, or aortic, column is short when traced into the pharyngeal floor. The caudal, or pulmonary, column is continuous dorsally with, and probably originates from, a

Fig. 1.11 (continued) arterial trunks and the intercalated non-myocardial ridges. The interrupted lines show the approximate boundary between the proximal and middle myocardial outflow tracts. With the extension of the myocardialized septum of the proximal outflow tract to the valve region (Fig. 1.10) and the regression of the myocardium surrounding the valves (panel e), the distal myocardial rim of the subpulmonary outflow tract transforms into the freestanding infundibulum of the right ventricle

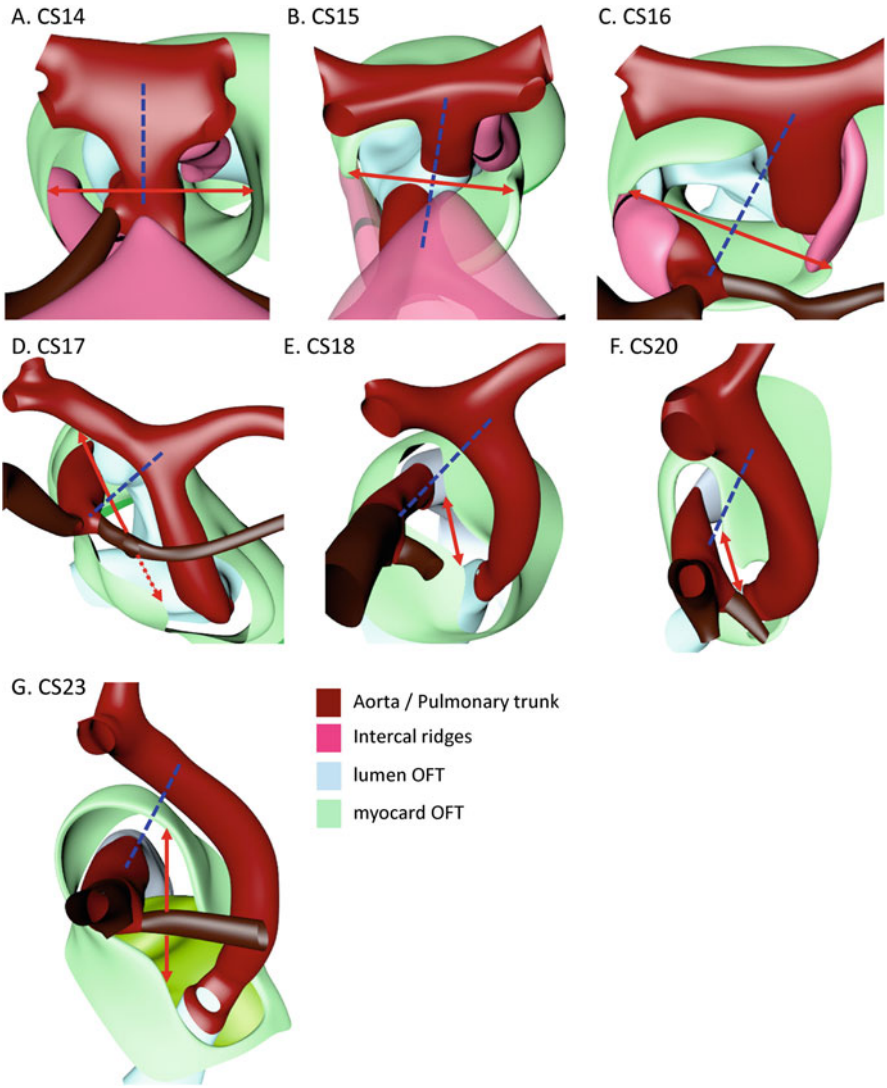

Fig. 1.12 Spiraling of the arterial channels distal to the arterial valves. Dorsal views of arterial trunks in CS14–23 embryos. The blue line connects the center of the distal ends of the ascending aorta and pulmonary trunk, whereas the red line connects both (developing) arterial valves. Both sets of lines rotate clockwise across ~90° between CS14 and CS18, which reflects the formation and realignment of the aortopulmonary septum in this period (see main text for details). Between CS18 and CS23, there is no further rotation

phenotypically similar mass of pharyngeal mesenchyme, which surrounds the trachea [183, 189–191]. This mesenchymal club forms during stage 13, remains identifiable during stages 14 and 15, but disappears at stage 16. With ongoing

development, the groups of progenitor cells converge. They can be traced as columns of cells that move toward, and then into, the relatively narrow outflow tract before differentiating locally [49, 56, 57]. Their convergent extension is mediated by the planar cell polarity pathway.

When new cardiomyocytes cease to enter the outflow tract at stage 14, non-myocardial cells start to contribute to the distal portion of the outflow tract. It is these cells that insert themselves cranially and caudally as columns, or tongues, between the remaining myocardial walls [10, 60, 192]. Hence, they are also known as intercalated ridges (Fig. 1.11). Histologically, the cranial non-myocardial intercalated ridge or tongue is continuous with the mesenchyme of the third and fourth pharyngeal arches, whereas the caudal intercalated ridge or tongue is continuous with the mesenchymal club that surrounds the trachea and foregut [13, 191]. Since the intercalated ridges are non-myocardial, but the myocardium remains present over the endocardial ridges, the distal myocardial border can be likened to a fishmouth. The non-myocardial intercalated ridges abut, but do not penetrate, the small endocardial swellings between the septal and parietal ridges. These entities are known as intercalated swellings [67, 193]. Cranial, or aortic, swelling differs from caudal, or pulmonary, swelling, in that it is slightly bigger and is invaded by some neural crest cells [186]. The intercalated swellings remain relatively small during stages 14 and 15 but increase in size from stage 16 onward as they begin their transformation into the nonadjacent leaflets of the arterial roots at stage 18. Taken together, and viewed on the short axis, the columns produced by the endocardial ridges and the swellings create the primordia for the formation of the arterial roots in the middle outflow tract. Unlike the endocardial ridges, the intercalated swellings do not extend into the proximal outflow tract.

1.5.4.10 Appearance of the Arterial Trunks

The fishmouth distal border of the myocardial walls of the outflow can still be seen at stage 17, equivalent to 40 days of development, but, by this stage, the endocardial ridges, along with their myocardial coverings, no longer reach the pericardial reflection due to addition of further non-myocardial tissues from the pharyngeal floor to the developing arterial trunks. The intrapericardial part of the systemic component can be labeled with Mef2c-Cre [194], a marker of the cranial second heart field. This will become the intrapericardial component of the ascending aorta. The lateral horns of the aortic sac remain unlabeled and become the extrapericardial part of the ascending aorta, the brachiocephalic trunk, and the initial part of the transverse aortic arch. The pulmonary component becomes the pulmonary trunk, an entirely intrapericardial vessel. It is the ventral extension of the aortopulmonary septum, therefore, which initiates the anatomical separation of the arterial pole of the heart [10, 11]. As we have already explained, by stage 16, the connections of the subaortic and subpulmonary channels within the middle part of the outflow tract and the ascending aorta and pulmonary trunk occupy the left and right positions, respectively (Fig. 1.12 [62, 178, 195]). Axial growth of the pulmonary trunk ceases after stage 16, coincidently with the depletion of the peritracheal mesenchymal club. Whether or not this striking correlation is causal needs further investigation. The

ascending aorta, in contrast, continues to increase in length well beyond stage 23. The increasingly spiraling course of the intrapericardial arterial trunks corresponds in time with the unwinding of the spiraling course of the muscular outflow tract and its endocardial ridges [196]. The inner layer of the smooth muscular wall of both arterial trunks derives from the neural crest and the outer layer from the second heart field. The wall of the ascending aorta, however, mainly derives from the neural crest [188, 194, 197], whereas the wall of the pulmonary trunk predominantly originates from the second heart field [57, 188, 190].

1.5.4.11 The "Arterial" Epicardium

The epicardium that covers the intrapericardial arterial trunks resembles the pericardium but differs from that which covers the myocardial walls of the outflow tract. The difference, in chicken and mice, is both morphological, in terms of densely packed cuboidal as opposed to squamous cells, and molecular according to the expression of WT1 [198–200]. The cells that form the non-myocardial intercalated ridges, in contrast, express Isl1 [183, 189]. The epicardium that envelops the arterial trunks, furthermore, forms independently of the pro-epicardial body [201].

1.5.4.12 The Arterial Valves

The appearance at stage 15, corresponding to ~36 days of development, of two increasingly narrow parts in the endothelial channels of the distal outflow tract identifies the site of formation of the arterial roots. These passages are histologically recognizable by their intensely staining, cobble stone-shaped endocardial lining. Both channels are found within the middle, myocardial portion of the outflow tract. The narrowing results from the local apposition of the endocardial ridges and the intercalated swellings. Although septation has not yet extended into the valvar complex, and both channels remain in continuity at the midline at stage 15, the topography reveals that excavation of the distal margins of the septal and parietal ridges will form the right and left leaflets of the arterial valves, respectively. The cranial intercalated swelling will form the nonadjacent leaflet of the pulmonary arterial valve, whereas the caudal swelling will produce the nonadjacent leaflet of the aortic valve [67]. Septation passes through the valvar area during stage 16 and is complete in the middle part of the outflow tract by stage 17. The distal parts of the septal and parietal ridges now assume a heart-shaped configuration with wide downstream "ears" separated by a median furrow that presages its separation and allocation to the left and right leaflets of the aortic and pulmonary roots, respectively (Fig. 1.11). Between stages 17 and 23, the valvar leaflets become more slender. The arterial valves were previously positioned at the dog-leg bend [67, 91, 92]. This bend, however, is recognizable only until stage 16. Thereafter, the transition of the myocardium of the middle into the proximal portion becomes marked by the transition of the thin layer of the myocardium that surrounds the middle outflow tract into the much thicker myocardium of the proximal outflow tract that surrounds the now myocardializing outflow tract ridges. The difference in appearance and the progressively shorter length of the myocardium of the middle compared to the proximal portion of the outflow tract reflect the slow proliferation of the middle

portion [50, 51]. The increasingly prominent sinuses develop within the middle outflow tract. The sinotubular junction is eventually located at the distal end of the endocardial cushions [202]. Concurrent with formation of the valvar leaflets, growth of the myocardial middle outflow tract slows down [74]. The initially still plumb leaflets, however, remain surrounded by the dense and regressing myocardium of the middle outflow tract, perhaps to support closure. As development progresses, however, the myocardial valvar cuff regresses (Fig. 1.11).

1.5.4.13 Septation of the Proximal Outflow Tract

Septation of the proximal, or conal, part of the outflow tract begins during stage 16. It is at this stage that the overall outflow tract undergoes its profound change in shape, assuming a wedge-shaped, figure-of-eight-like configuration. Its base is then along the outer curvature, and its apex lies in the lesser curvature of the heart. At stage 17, only a small myocardial contribution is left between the inner curvature and the most proximal edge of the aortic intercalated swelling. By then, the septal and parietal endocardial ridges have fused, except near the interventricular foramen. The site of fusion of the ridges is marked by the location of the central whorl of neural crest cells, which forms after fusion of the prongs of neural crest cells (see Sect. 1.5.4.8 Septation of Middle Outflow Tract). The whorl is relatively large as long as the outflow tract ridges fuse but disappears by apoptosis when myocardialization reaches the subvalvar part of the ridges during stages 21 and 22 [181, 182, 203]. Some neural crest cells, nonetheless, persist in the leaflets of the arterial valves [186], with other remnants sometimes persisting as the so-called conus tendon [204, 205]. Proximally, cardiomyocytes originating in the adjacent ventricular walls invade the remaining mesenchymal shell of the fused ridges. In this way, they form a dumbbell-shaped muscular wall between the subaortic and subpulmonary channels (Fig. 1.13 [203]). The myocardializing area is continuous on its medial side with the crest of the muscular ventricular septum and on its lateral side with the parietal wall of the myocardial outflow tract. This myocardialization occurs in both mammals [90, 206] and birds [207].

1.5.4.14 Formation of the Supraventricular Crest and Free-Standing Infundibulum

Until the completion of septation, the fused outflow tract ridges, or cushions, provide a myocardial outlet septum. Extension of the myocardialization toward the developing arterial roots changes the shape of this temporary septum. If development proceeds normally, then the septum transforms into the supraventricular crest and the free-standing muscular infundibulum, which supports the leaflets of the pulmonary valve [179, 204, 208]. Concurrently, the smooth-walled proximal outflow tract is incorporated into the right ventricle as its infundibulum and into the left ventricle as its aortic vestibule [89, 179, 207]. At this stage, the outlet septum can no longer be considered a septum between the subpulmonary and subaortic outlets but instead is largely incorporated into the right ventricular infundibulum. The incorporation of the

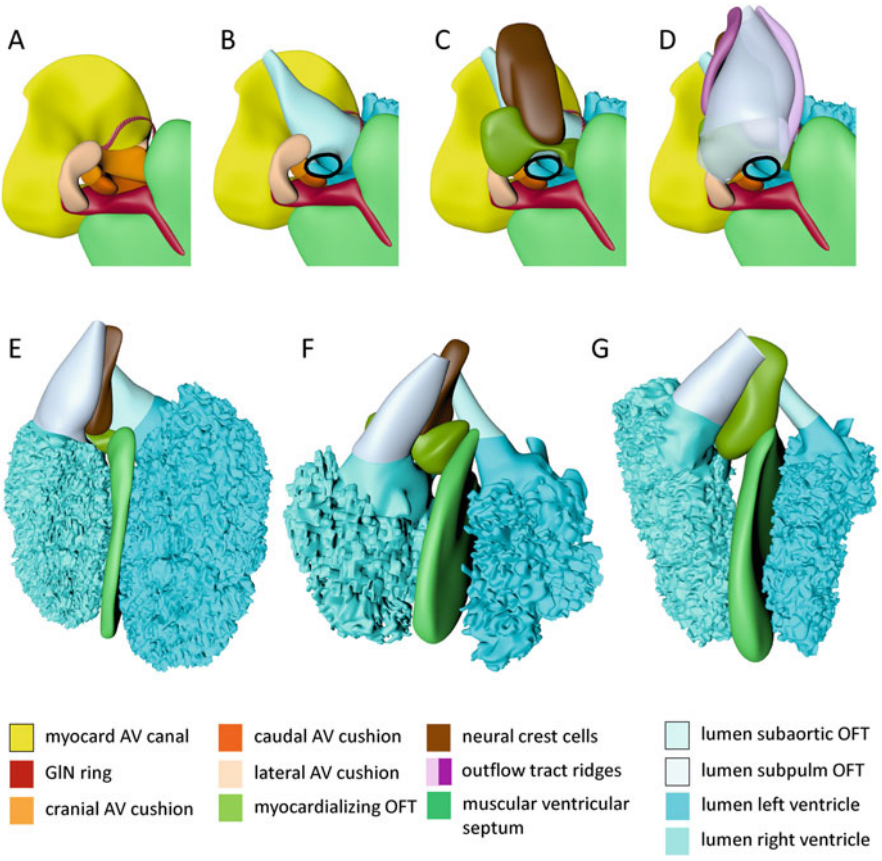

Fig. 1.13 Ventricular septation. (a–d) Dextro-ventral and (e–g) ventral views. Top row: CS18. Panels b–d are identical to panel a but with the addition of the subaortic outflow tract (b), the muscular outlet septum and whorl of the neural crest (c), and the subpulmonary outflow tract (d). The black line represents the remaining intermediate part of the interventricular foramen. The septal structures of the ventricles and the outflow tract of CS18, CS20, and CS23 hearts are shown in panels e–g. The muscular ventricular septum does not change much, but the muscular outflow tract septum (olive green) expands toward the arterial pole at the expense of the neural crest cells (brown). It should be noted that the outlet septum becomes a largely right ventricular structure that separates only the distal ends of the subaortic and subpulmonary channels

embryonic muscular septum of the outflow tract as a subsequent right ventricular structure [209] can be appreciated if the ventricular cavities, the free-standing infundibulum, and the subaortic and subpulmonary channels are observed from the ventral aspect (Figure 1.13e–g). The developmental events underlying this transformation remain poorly understood.

1.5.5 The Final Step in Septation

Septation at the venous and arterial poles simultaneously moves toward the initial interventricular foramen between the developing left and right ventricles, where the systemic and pulmonary circulations eventually become definitively separated. As stated earlier, the atrioventricular endocardial cushions have already functionally separated the bloodstream through the atrioventricular canal into left and right flow channels at stage 14. At that time, the interventricular foramen is a single, round connection between the crest of the muscular ventricular septum and the inner curvature (Figs. 1.6 and 1.7). Blood from the right atrium passes through the foramen to reach the right ventricle, whereas blood from the left ventricle passes through the same foramen to reach the subaortic outflow tract. During septation, both bloodstreams become physically separated. The obvious, and indeed the actual, evolution of events is the breaking up of the interventricular foramen into peri-tricuspid and peri-aortic portions. The junction between these parts is eventually closed by the membranous septum as a newly formed tissue bridge.

1.5.5.1 The Changing Shape of the Interventricular Foramen

The myocardium surrounding the interventricular foramen is the first component of the second heart field that differentiates at the boundary with the developing left ventricle [87]. As we have already described, the fate of the surrounding of this primary interventricular foramen can be traced by following the location of the GlN monoclonal antibody (see Sect. 1.4.6 The Conduction System) [6, 104]. Up to, and including, stage 15, the GlN-positive ring occupies a sagittal plane. At stage 16, when fusion of the atrioventricular endocardial cushions leads to physical separation of the right- and left-sided bloodstreams in the atrioventricular canal, the common part of the atrioventricular canal and the interventricular foramen begins to expand locally to the right to form a direct connection between the right atrium and right ventricle [206]. This is the so-called tricuspid gully. Subsequent to this expansion, it is in the remaining part of the interventricular foramen that the peri-subaortic outlet for the left ventricle forms. It is mainly guarded by the superior endocardial cushion. The junction between the newly formed right ventricular inlet, now represented by the gully, and the outlet is formed by the fusing superior and right-lateral endocardial cushions. At this stage, the middle part of the tripartite interventricular foramen is bordered by the crest of the muscular ventricular septum, the rightward margins of the atrioventricular cushions, and the myocardializing ventricular ends of the fused outflow ridges. This channel, which is between the cavity of the right ventricle and the developing aortic root, begins to narrow and eventually closes during stage 20 [209] (Fig. 1.7). Due to the leftward and dorsal expansion of the subaortic outlet portion of the interventricular foramen between CS15 and CS23 [209], the peri-aortic portion of the interventricular ring acquires a more or less perpendicular plane relative to the peri-tricuspid portion of the ring.

1.5.5.2 Formation of the Membranous Septum

The middle portion of the interventricular foramen between the subaortic outlet and the tricuspid inlet is positioned on the right ventricular side of the crest of the muscular ventricular septum [209]. The junctional portion decreases in diameter after stage 16 by progressive fusion of the septal and parietal ridges in the proximal outflow tract. Closure of the interventricular foramen itself is mediated by fusion of the local atrioventricular endocardial cushions [67, 210]. The septal outflow tract ridge expands cranially over the right side of the crest of the interventricular septum, whereas the parietal outflow tract ridge fuses with the superior atrioventricular cushion. Fusion and, hence, septation is complete at stage 20 (Fig. 1.5). The newly formed septum does not myocardialize. It is known as the membranous ventricular septum [67, 211–213]. While the foramen closes, fragmentation of the myocardial floor of the gully gives atrial blood full access to the right ventricular cavity via conduits that pass by the septomarginal trabeculation through a preexisting cranial channel and a newly formed caudal channel on the disrupted floor of the tricuspid gully [206]. The net result is that the left ventricular blood flow enters the caudal subaortic part of the outflow tract, whereas the right ventricular blood flows through the cranial part. In other words, the streams spiral clockwise through 90°. The membranous septum closes the initial space between the two parts.

1.6 Coda

1.6.1 Accuracy of the Assignments of Stages to Successive Phases of Heart Development

We have described the morphological development of the human heart from its first appearance at Carnegie stage 9 up to stage 23, when all structures of the definitive heart have formed. Heart development is often separated, as in our account, into a phase of formation of the single, straight heart tube, which represents stages 9 and 10. This is followed by looping, at stages 11 and 12, the formation of the cardiac chambers during stages 12 through 14, and subsequent septation extending to stage 20. Parenthetically, we have denoted the stages during which conformational changes that characterize the four phases are most pronounced. If we include asymmetric growth, which is a requirement for successful septation, then this process has already started at stage 11. This example shows that assignment of stages to a developmental feature is inevitably subjective and prone to be biased. Cardiac development, therefore, involves a series of more or less successive projects of renovation. Our decision to describe phases in heart development originates, therefore, mostly from our wish to keep the description comprehensible.

1.6.2 Carnegie Stages 1–18 Obey Different Criteria than do Stages 19–23

We have not provided reconstructions of Carnegie stages 19, 21, and 22 [13]. We did not do so because Streeter changed his staging system from one based on qualitative, morphological criteria, extending to stage 18, to one from then to stage 23 based on a more quantitative assessment of organ development [214]. With fewer features changed qualitatively, we have reconstructed only stages 20 and 23. Stage 20 is reached when around 7 weeks have passed since fertilization [15].

1.6.3 Accuracy of the Assignments of Stages to Developmental Events

We have followed the developmental changes in the heart as we observed them in our series of 12 reconstructions [13]. Questions can justifiably be posed regarding the strictness of the timeline of these developmental events. As far as we are aware, only Hutchins and colleagues have surveyed the entire Carnegie collection, which contains several hundreds of embryos, and assigned a Carnegie stage to developmental features, with a focus on the heart [160–162, 215] and the digestive tract. This survey, summarized in Table 1.2, shows that two Carnegie stages, encompassing around 4 days, are usually necessary to complete any developmental process in the majority of embryos. An example is the first appearance of the pulmonary arteries. We have assigned this event to stage 15, whereas we observed these arteries at stage 14 in an earlier study [7]. Our assignment of features, therefore, can vary by one Carnegie stage. This variation usually affects just a single event, with other features being in line with the assigned stage. We have not included a "confidence interval" in our text. Hutchins and colleagues studied fewer events and sometimes offered a different aspect of an event.

Acknowledgments We thank John Cork (New Orleans, LA) for making extra sections of embryos included in the DREM collection available. Special thanks goes to Els Terwindt (MU) for technical assistance. Furthermore, we also thank our bachelor students, who worked on heart development as part of their academic internship. The financial support from "Stichting Rijp" is gratefully acknowledged.

Table 1.2 Carnegie stage of appearance of 27 morphological features and 6 histological qualifications in human embryos. It should be noted that the developmental events take ~2 Carnegie stages or ~4 days to take place. The data were modified from references [160–162, 215]. Initially, 602 "good quality" embryos between CS9 and CS23 were analyzed [160], but fewer embryos, sometimes from a different source, were included in the later studies (e.g., 329 embryos in references [161, 162]). The numbers used to prepare this table are medians. We have retained the terminology of Hutchins *cs*, with AV, IVS, OFT, and LSCV referring to atrioventricular, interventricular septum, outflow tract, and left superior caval vein, respectively

Carnegie stage	9	10	11	12	13	14	15	16	17	18	19	20	21	22	23
Myocardium fuses	67	100													
Ruptured dorsal mesocardium		33	95	100											
Heart tube asymmetry			92	100											
Trabeculated LV			63	100											
Trabeculated RV			47	100											
IVS present			18	92	100										
Septum primum				28	100										
Ostium primum present				28	100	100	100	87	20	0					
Pulmonary capillaries					84	100									
Pulmonary vein (1)					68	100									
His bundle identified					14	93	88	100							
Pulmonary arteries						78	100								
OFT cushions						51	97	95	100						
Coronary capillaries						11	77	100							
Ostium secundum							57	81	97						
Aortic sac disappears							30	92	100						
Semilunar valves							10	86	100						
Coronary veins							3	32	93						
Ostium primum disappears								87	20	0					
OFT cushions join								71	97	100					
AV cushions join								50	84	100					
Parietal pericardium								3	69	97	100				

(continued)

Table 1.2 (continued)

Carnegie stage	9	10	11	12	13	14	15	16	17	18	19	20	21	22	23
Coronary arteries										50	100				
Memb IVS “closes”										24	60	88	100		
Pulmonary veins (≥2)										16	74	100			
Oblit LSCV													12	56	86
Chordae tendineae formed														13	50
AV cushions															
Cushion_jelly					100	90	44	0							
Cushion_cellular						20	56	100	97	84	53	0			
Cushion_fibrocellular									3	16	47	100			
OFT cushions															
OFT septum_cellular								72	96	18	0				
OFT septum_cells & myocytes										70	60	6	0		
OFT septum_myocytes										12	40	94	100		

References

1. Hill MA. Two web resources linking major human embryology collections worldwide. Cells Tissue Organs. 2018;205:293–302.
2. Gasser RF, Cork RJ, Stillwell BJ, McWilliams DT. Rebirth of human embryology. Dev Dyn. 2014;243:621–8. https://doi.org/10.1002/dvdy.24110.
3. Markert M. Ethical aspects of human embryo collections: a historically grounded approach to the blechschmidt collection at the University of Gottingen. Cells Tissues Organs. 2020;209:189–99. https://doi.org/10.1159/000513176.
4. Wessels A, et al. Spatial distribution of "tissue-specific" antigens in the developing human heart and skeletal muscle. I. An immunohistochemical analysis of creatine kinase isoenzyme expression patterns. Anat Rec. 1990;228:163–76. https://doi.org/10.1002/ar.1092280208.
5. Wessels A, et al. Spatial distribution of "tissue-specific" antigens in the developing human heart and skeletal muscle. II. An immunohistochemical analysis of myosin heavy chain isoform expression patterns in the embryonic heart. Anat Rec. 1991;229:355–68. https://doi.org/10.1002/ar.1092290309.
6. Wessels A, et al. Spatial distribution of "tissue-specific" antigens in the developing human heart and skeletal muscle. III. An immunohistochemical analysis of the distribution of the neural tissue antigen GlN2 in the embryonic heart; implications for the development of the atrioventricular conduction system. Anat Rec. 1992;232:97–111. https://doi.org/10.1002/ar.1092320111.
7. Sizarov A, Anderson RH, Christoffels VM, Moorman AF. Three-dimensional and molecular analysis of the venous pole of the developing human heart. Circulation. 2010;122:798–807. https://doi.org/10.1161/CIRCULATIONAHA.110.953844.
8. Sizarov A, et al. Molecular analysis of patterning of conduction tissues in the developing human heart. Circ Arrhythm Electrophysiol. 2011;4:532–42. https://doi.org/10.1161/CIRCEP.111.963421.
9. Sizarov A, et al. Formation of the building plan of the human heart: morphogenesis, growth, and differentiation. Circulation. 2011;123:1125–35. https://doi.org/10.1161/CIRCULATIONAHA.110.980607.
10. Sizarov A, et al. Three-dimensional and molecular analysis of the arterial pole of the developing human heart. J Anat. 2012;220:336–49. https://doi.org/10.1111/j.1469-7580.2012.01474.x.
11. Rana MS, Sizarov A, Christoffels VM, Moorman AF. Development of the human aortic arch system captured in an interactive three-dimensional reference model. Am J Med Genet A. 2014;164A:1372–83. https://doi.org/10.1002/ajmg.a.35881.
12. de Bakker BS, et al. An interactive three-dimensional digital atlas and quantitative database of human development. Science. 2016;354:aag0053. https://doi.org/10.1126/science.aag0053.
13. Hikspoors JPJM, et al. A pictorial account of heart development: spatial and temporal aspects of the human embryonic heart between 3.5 and 8 weeks of development. Commun Biol. 2021;5:226.
14. Anderson RH, et al. Sequential segmental analysis of congenital heart disease. Pediatr Cardiol. 1984;5:281–7. https://doi.org/10.1007/BF02424973.
15. O'Rahilly R, Muller F. Developmental stages in human embryos: revised and new measurements. Cells Tissues Organs. 2010;192:73–84. https://doi.org/10.1159/000289817.
16. Theiler K. The house mouse. Development and normal stages from fertilization to 4 weeks of age. Springer-Verlag; 1972.
17. Irie N, Kuratani S. Comparative transcriptome analysis reveals vertebrate phylotypic period during organogenesis. Nat Commun. 2011;2:248. https://doi.org/10.1038/ncomms1248.
18. Tam PP, Parameswaran M, Kinder SJ, Weinberger RP. The allocation of epiblast cells to the embryonic heart and other mesodermal lineages: the role of ingression and tissue movement during gastrulation. Development. 1997;124:1631–42.

19. Lescroart F, et al. Early lineage restriction in temporally distinct populations of Mesp1 progenitors during mammalian heart development. Nat Cell Biol. 2014;16:829–40. https://doi.org/10.1038/ncb3024.
20. Devine WP, Wythe JD, George M, Koshiba-Takeuchi K, Bruneau BG. Early patterning and specification of cardiac progenitors in gastrulating mesoderm. Elife. 2014;3:e03848. https://doi.org/10.7554/eLife.03848.
21. Bruneau BG, et al. Chamber-specific cardiac expression of Tbx5 and heart defects in Holt-Oram syndrome. Dev Biol. 1999;211:100–8. https://doi.org/10.1006/dbio.1999.9298.
22. Takeuchi JK, et al. Tbx5 specifies the left/right ventricles and ventricular septum position during cardiogenesis. Development. 2003;130:5953–64. https://doi.org/10.1242/dev.00797.
23. Liang X, et al. HCN4 dynamically marks the first heart field and conduction system precursors. Circ Res. 2013;113:399–407. https://doi.org/10.1161/CIRCRESAHA.113.301588.
24. Spater D, et al. A HCN4+ cardiomyogenic progenitor derived from the first heart field and human pluripotent stem cells. Nat Cell Biol. 2013;15:1098–106. https://doi.org/10.1038/ncb2824.
25. Cai CL, et al. Isl1 identifies a cardiac progenitor population that proliferates prior to differentiation and contributes a majority of cells to the heart. Dev Cell. 2003;5:877–89.
26. Meilhac SM, Esner M, Kelly RG, Nicolas JF, Buckingham ME. The clonal origin of myocardial cells in different regions of the embryonic mouse heart. Dev Cell. 2004;6:685–98. https://doi.org/10.1016/s1534-5807(04)00133-9.
27. Christoffels VM, et al. Formation of the venous pole of the heart from an Nkx2-5-negative precursor population requires Tbx18. Circ Res. 2006;98:1555–63. https://doi.org/10.1161/01.RES.0000227571.84189.65.
28. Mommersteeg MT, et al. The sinus venosus progenitors separate and diversify from the first and second heart fields early in development. Cardiovasc Res. 2010;87:92–101. https://doi.org/10.1093/cvr/cvq033.
29. Lescroart F, Mohun T, Meilhac SM, Bennett M, Buckingham M. Lineage tree for the venous pole of the heart: clonal analysis clarifies controversial genealogy based on genetic tracing. Circ Res. 2012;111:1313–22. https://doi.org/10.1161/CIRCRESAHA.112.271064.
30. Davis CL. Development of the human heart from its first appearance to the stage found in embryos of twenty paired somites. Contrib Embryol Carnegie Inst. 1927;107:247–84.
31. O'Rahilly R. The timing and sequence of events in the development of the human digestive system and associated structures during the embryonic period proper. Anat Embryol. 1978;153:123–36. https://doi.org/10.1007/BF00343369.
32. Muller F, O'Rahilly R. The first appearance of the major divisions of the human brain at stage 9. Anat Embryol. 1983;168:419–32. https://doi.org/10.1007/BF00304278.
33. O'Rahilly R, Muller F. Somites, spinal ganglia, and centra. Enumeration and interrelationships in staged human embryos, and implications for neural tube defects. Cells Tissues Organs. 2003;173:75–92. https://doi.org/10.1159/000068948.
34. Kobayashi T, et al. The beginning of the calcium transient in rat embryonic heart. J Physiol Sci. 2011;61:141–9. https://doi.org/10.1007/s12576-010-0131-x.
35. Tyser RC, et al. Calcium handling precedes cardiac differentiation to initiate the first heartbeat. Elife. 2016;5:e17113. https://doi.org/10.7554/eLife.17113.
36. Ivanovitch K, Temino S, Torres M. Live imaging of heart tube development in mouse reveals alternating phases of cardiac differentiation and morphogenesis. Elife. 2017;6:e30668. https://doi.org/10.7554/eLife.30668.
37. Kaufman MH, Navaratnam V. Early differentiation of the heart in mouse embryos. J Anat. 1981;133:235–46.
38. Nishii K, Shibata Y. Mode and determination of the initial contraction stage in the mouse embryo heart. Anat Embryol. 2006;211:95–100. https://doi.org/10.1007/s00429-005-0065-x.
39. O'Rahilly R. The timing and sequence of events in human cardiogenesis. Acta Anat. 1971;79:70–5.

40. Manasek FJ. Macromolecules of the extracellular compartment of embryonic and mature hearts. Circ Res. 1976;38:331–7.
41. Hikspoors JPJM, et al. The fate of the vitelline and umbilical veins during the development of the human liver. J Anat. 2017;231:718–35. https://doi.org/10.1111/joa.12671.
42. Buckingham M, Meilhac S, Zaffran S. Building the mammalian heart from two sources of myocardial cells. Nat Rev Genet. 2005;6:826–35. https://doi.org/10.1038/nrg1710.
43. Miquerol L, Kelly RG. Organogenesis of the vertebrate heart. Wiley Interdiscip Rev Dev Biol. 2013;2:17–29. https://doi.org/10.1002/wdev.68.
44. Biben C, Harvey RP. Homeodomain factor Nkx2-5 controls left/right asymmetric expression of bHLH gene eHand during murine heart development. Genes Dev. 1997;11:1357–69.
45. De Bono C, et al. T-box genes and retinoic acid signaling regulate the segregation of arterial and venous pole progenitor cells in the murine second heart field. Hum Mol Genet. 2018;27:3747–60. https://doi.org/10.1093/hmg/ddy266.
46. Dominguez JN, Meilhac SM, Bland YS, Buckingham ME, Brown NA. Asymmetric fate of the posterior part of the second heart field results in unexpected left/right contributions to both poles of the heart. Circ Res. 2012;111:1323–35. https://doi.org/10.1161/CIRCRESAHA.112.271247.
47. Mommersteeg MT, et al. Pitx2c and Nkx2-5 are required for the formation and identity of the pulmonary myocardium. Circ Res. 2007;101:902–9. https://doi.org/10.1161/CIRCRESAHA.107.161182.
48. Galli D, et al. Atrial myocardium derives from the posterior region of the second heart field, which acquires left-right identity as Pitx2c is expressed. Development. 2008;135:1157–67. https://doi.org/10.1242/dev.014563.
49. Francou A, De Bono C, Kelly RG. Epithelial tension in the second heart field promotes mouse heart tube elongation. Nat Commun. 2017;8:14770. https://doi.org/10.1038/ncomms14770.
50. van den Berg G, et al. A caudal proliferating growth center contributes to both poles of the forming heart tube. Circ Res. 2009;104:179–88. https://doi.org/10.1161/CIRCRESAHA.108.185843.
51. de Boer BA, van den Berg G, de Boer PA, Moorman AF, Ruijter JM. Growth of the developing mouse heart: an interactive qualitative and quantitative 3D atlas. Dev Biol. 2012;368:203–13. https://doi.org/10.1016/j.ydbio.2012.05.001.
52. Meilhac SM, Esner M, Kerszberg M, Moss JE, Buckingham ME. Oriented clonal cell growth in the developing mouse myocardium underlies cardiac morphogenesis. J Cell Biol. 2004;164:97–109. https://doi.org/10.1083/jcb.200309160.
53. Le Garrec JF, et al. A predictive model of asymmetric morphogenesis from 3D reconstructions of mouse heart looping dynamics. Elife. 2017;6:e28951. https://doi.org/10.7554/eLife.28951.
54. Bayraktar M, Manner J. Cardiac looping may be driven by compressive loads resulting from unequal growth of the heart and pericardial cavity. Observations on a physical simulation model. Front Physiol. 2014;5:112. https://doi.org/10.3389/fphys.2014.00112.
55. Shi Y, et al. Bending and twisting the embryonic heart: a computational model for c-looping based on realistic geometry. Front Physiol. 2014;5:297. https://doi.org/10.3389/fphys.2014.00297.
56. Ramsbottom SA, et al. Vangl2-regulated polarisation of second heart field-derived cells is required for outflow tract lengthening during cardiac development. PLoS Genet. 2014;10:e1004871. https://doi.org/10.1371/journal.pgen.1004871.
57. Li D, Angermeier A, Wang J. Planar cell polarity signaling regulates polarized second heart field morphogenesis to promote both arterial and venous pole septation. Development. 2019;146:dev181719. https://doi.org/10.1242/dev.181719.
58. Campione M, et al. Pitx2 expression defines a left cardiac lineage of cells: evidence for atrial and ventricular molecular isomerism in the iv/iv mice. Dev Biol. 2001;231:252–64. https://doi.org/10.1006/dbio.2000.0133.

59. Furtado MB, Biben C, Shiratori H, Hamada H, Harvey RP. Characterization of Pitx2c expression in the mouse heart using a reporter transgene. Dev Dyn. 2011;240:195–203. https://doi.org/10.1002/dvdy.22492.
60. de Vries PA, de Cusance Morant Saunders JB. Development of the ventricles and spiral outflow tract in the human heart : a contribution to the development of the human heart from age group IX to age group XV. Contrib Embryol. 1962;37:87–114.
61. Webb S, Qayyum SR, Anderson RH, Lamers WH, Richardson MK. Septation and separation within the outflow tract of the developing heart. J Anat. 2003;202:327–42.
62. Bajolle F, et al. Rotation of the myocardial wall of the outflow tract is implicated in the normal positioning of the great arteries. Circ Res. 2006;98:421–8. https://doi.org/10.1161/01.RES.0000202800.85341.6e.
63. Manner J. On the form problem of embryonic heart loops, its geometrical solutions, and a new biophysical concept of cardiac looping. Ann Anat. 2013;195:312–23. https://doi.org/10.1016/j.aanat.2013.02.008.
64. Honda H, Abe T, Fujimori T. The chiral looping of the embryonic heart is formed by the combination of three axial asymmetries. Biophys J. 2020;118:742–52. https://doi.org/10.1016/j.bpj.2019.11.3397.
65. Orts-Llorca F, Puerta Fonolla J, Sobrado J. The formation, septation and fate of the truncus arteriosus in man. J Anat. 1982;134:41–56.
66. Anderson RH, Webb S, Brown NA, Lamers W, Moorman A. Development of the heart: (3) formation of the ventricular outflow tracts, arterial valves, and intrapericardial arterial trunks. Heart. 2003;89:1110–8.
67. Kramer TC. The partitioning of the truncus and conus and the formation of the membranous portion of the interventricular septum in the human heart. Am J Anat. 1942;71:343–70.
68. Hiermeier F, Manner J. Kinking and torsion can significantly improve the efficiency of valveless pumping in periodically compressed tubular conduits. Implications for understanding of the form-function relationship of embryonic heart tubes. J Cardiovasc Dev Dis. 2017;4:19. https://doi.org/10.3390/jcdd4040019.
69. Christoffels VM, et al. Chamber formation and morphogenesis in the developing mammalian heart. Dev Biol. 2000;223:266–78. https://doi.org/10.1006/dbio.2000.9753.
70. Meilhac SM, et al. A retrospective clonal analysis of the myocardium reveals two phases of clonal growth in the developing mouse heart. Development. 2003;130:3877–89.
71. Van Mierop LH, Alley RD, Kausel HW, Stranahan A. Pathogenesis of transposition complexes. I. Embryology of the ventricles and great arteries. Am J Cardiol. 1963;12:216–25.
72. Captur G, et al. Morphogenesis of myocardial trabeculae in the mouse embryo. J Anat. 2016;229:314–25. https://doi.org/10.1111/joa.12465.
73. Faber JW, Hagoort J, Moorman AFM, Christoffels VM, Jensen B. Quantified growth of the human embryonic heart. Biol Open. 2021;10:bio057059. https://doi.org/10.1242/bio.057059.
74. Knaapen MW, Vrolijk BC, Wenink AC. Growth of the myocardial volumes of the individual cardiac segments in the rat embryo. Anat Rec. 1995;243:93–100. https://doi.org/10.1002/ar.1092430111.
75. de Boer BA, et al. Measurement and 3D-visualization of cell-cycle length using double labelling with two thymidine analogues applied in early heart development. PLoS One. 2012;7:e47719. https://doi.org/10.1371/journal.pone.0047719.
76. Del Monte-Nieto G, et al. Control of cardiac jelly dynamics by NOTCH1 and NRG1 defines the building plan for trabeculation. Nature. 2018;557:439–45. https://doi.org/10.1038/s41586-018-0110-6.
77. Wenink AC, Knaapen MW, Vrolijk BC, VanGroningen JP. Development of myocardial fiber organization in the rat heart. Anat Embryol. 1996;193:559–67.
78. Van Kempen MJ, et al. Developmental changes of connexin40 and connexin43 mRNA distribution patterns in the rat heart. Cardiovasc Res. 1996;32:886–900.
79. Kaba RA, et al. Comparison of connexin 43, 40 and 45 expression patterns in the developing human and mouse hearts. Cell Commun Adhes. 2001;8:339–43.

80. Sedmera D, McQuinn T. Embryogenesis of the heart muscle. Heart Fail Clin. 2008;4:235–45. https://doi.org/10.1016/j.hfc.2008.02.007.
81. Samsa LA, Yang B, Liu J. Embryonic cardiac chamber maturation: trabeculation, conduction, and cardiomyocyte proliferation. Am J Med Genet C Semin Med Genet. 2013;163C:157–68. https://doi.org/10.1002/ajmg.c.31366.
82. Chin TK, Perloff JK, Williams RG, Jue K, Mohrmann R. Isolated noncompaction of left ventricular myocardium. A study of eight cases. Circulation. 1990;82:507–13. https://doi.org/10.1161/01.cir.82.2.507.
83. Van Mierop LH, Kutsche LM. Development of the ventricular septum of the heart. Heart Vessel. 1985;1:114–9.
84. Franco D, et al. Left and right ventricular contributions to the formation of the interventricular septum in the mouse heart. Dev Biol. 2006;294:366–75. https://doi.org/10.1016/j.ydbio.2006.02.045.
85. De La Cruz MV, Sanchez-Gomez C, Palomino MA. The primitive cardiac regions in the straight tube heart (stage 9) and their anatomical expression in the mature heart: an experimental study in the chick embryo. J Anat. 1989;165:121–31.
86. Aanhaanen WT, et al. The Tbx2+ primary myocardium of the atrioventricular canal forms the atrioventricular node and the base of the left ventricle. Circ Res. 2009;104:1267–74. https://doi.org/10.1161/CIRCRESAHA.108.192450.
87. Mohan RA, et al. Embryonic Tbx3(+) cardiomyocytes form the mature cardiac conduction system by progressive fate restriction. Development. 2018;145:dev167361. https://doi.org/10.1242/dev.167361.
88. Rana MS, et al. Trabeculated right ventricular free wall in the chicken heart forms by ventricularization of the myocardium initially forming the outflow tract. Circ Res. 2007;100:1000–7. https://doi.org/10.1161/01.RES.0000262688.14288.b8.
89. Lazzarini R, et al. The proximal segment of the embryonic outflow (conus) does not participate in aortic vestibule development. PLoS One. 2018;13:e0209930. https://doi.org/10.1371/journal.pone.0209930.
90. Ya J, et al. Normal development of the outflow tract in the rat. Circ Res. 1998;82:464–72.
91. Oostra RJ, Steding G, Lamers WH, Moorman AFM. Steding's and Virágh's scanning electron microscopy atlas of the developing human heart. Springer; 2007.
92. Steding G. The anatomy of the human embryo; a scanning electron-microscopic atlas, Ch. 3.1. Karger; 2009. p. 204–53.
93. Hoogaars WM, et al. The transcriptional repressor Tbx3 delineates the developing central conduction system of the heart. Cardiovasc Res. 2004;62:489–99. https://doi.org/10.1016/j.cardiores.2004.01.030.
94. Wiese C, et al. Formation of the sinus node head and differentiation of sinus node myocardium are independently regulated by Tbx18 and Tbx3. Circ Res. 2009;104:388–97. https://doi.org/10.1161/CIRCRESAHA.108.187062.
95. Aanhaanen WT, et al. Defective Tbx2-dependent patterning of the atrioventricular canal myocardium causes accessory pathway formation in mice. J Clin Invest. 2011;121:534–44. https://doi.org/10.1172/JCI44350.
96. Anderson RH, et al. The inferior extensions of the atrioventricular node. Arrhythmia Electrophysiol Rev. 2021;10(4):262.
97. Aanhaanen WT, et al. Developmental origin, growth, and three-dimensional architecture of the atrioventricular conduction axis of the mouse heart. Circ Res. 2010;107:728–36. https://doi.org/10.1161/CIRCRESAHA.110.222992.
98. Bakker ML, et al. Transcription factor Tbx3 is required for the specification of the atrioventricular conduction system. Circ Res. 2008;102:1340–9. https://doi.org/10.1161/CIRCRESAHA.107.169565.
99. Wessels A, et al. The development of the atrioventricular junction in the human heart. Circ Res. 1996;78:110–7. https://doi.org/10.1161/01.res.78.1.110.

100. Wessels A, et al. Epicardially derived fibroblasts preferentially contribute to the parietal leaflets of the atrioventricular valves in the murine heart. Dev Biol. 2012;366:111–24. https://doi.org/10.1016/j.ydbio.2012.04.020.
101. Vassall-Adams PR. The development of the atrioventricular bundle and its branches in the avian heart. J Anat. 1982;134:169–83.
102. Lamers WH, De Jong F, De Groot IJ, Moorman AF. The development of the avian conduction system, a review. Eur J Morphol. 1991;29:233–53.
103. Kurosawa H, Becker AE. Dead-end tract of the conduction axis. Int J Cardiol. 1985;7:13–20. https://doi.org/10.1016/0167-5273(85)90166-4.
104. Lamers WH, et al. New findings concerning ventricular septation in the human heart. Implications for maldevelopment. Circulation. 1992;86:1194–205. https://doi.org/10.1161/01.cir.86.4.1194.
105. Viragh S, Challice CE. The origin of the epicardium and the embryonic myocardial circulation in the mouse. Anat Rec. 1981;201:157–68. https://doi.org/10.1002/ar.1092010117.
106. Rodgers LS, Lalani S, Runyan RB, Camenisch TD. Differential growth and multicellular villi direct proepicardial translocation to the developing mouse heart. Dev Dyn. 2008;237:145–52. https://doi.org/10.1002/dvdy.21378.
107. Simoes FC, Riley PR. The ontogeny, activation and function of the epicardium during heart development and regeneration. Development. 2018;145:dev155994. https://doi.org/10.1242/dev.155994.
108. Hirakow R. Epicardial formation in staged human embryos. Kaibogaku Zasshi. 1992;67:616–22.
109. Risebro CA, Vieira JM, Klotz L, Riley PR. Characterisation of the human embryonic and foetal epicardium during heart development. Development. 2015;142:3630–6. https://doi.org/10.1242/dev.127621.
110. Nakajima Y, Imanaka-Yoshida K. New insights into the developmental mechanisms of coronary vessels and epicardium. Int Rev Cell Mol Biol. 2013;303:263–317. https://doi.org/10.1016/B978-0-12-407697-6.00007-6.
111. Chen HI, et al. VEGF-C and aortic cardiomyocytes guide coronary artery stem development. J Clin Invest. 2014;124:4899–914. https://doi.org/10.1172/JCI77483.
112. Theveniau-Ruissy M, et al. Coronary stem development in wild-type and Tbx1 null mouse hearts. Dev Dyn. 2016;245:445–59. https://doi.org/10.1002/dvdy.24380.
113. Hirakow R. Development of the cardiac blood vessels in staged human embryos. Acta Anat. 1983;115:220–30. https://doi.org/10.1159/000145693.
114. Bogers AJ, Gittenberger-de Groot AC, Dubbeldam JA, Huysmans HA. The inadequacy of existing theories on development of the proximal coronary arteries and their connexions with the arterial trunks. Int J Cardiol. 1988;20:117–23. https://doi.org/10.1016/0167-5273(88)90321-x.
115. Tomanek RJ. Developmental progression of the coronary vasculature in human embryos and fetuses. Anat Rec. 2016;299:25–41. https://doi.org/10.1002/ar.23283.
116. Conte G, Pellegrini A. On the development of the coronary arteries in human embryos, stages 14-19. Anat Embryol. 1984;169:209–18. https://doi.org/10.1007/bf00303151.
117. Hutchins GM, Kessler-Hanna A, Moore GW. Development of the coronary arteries in the embryonic human heart. Circulation. 1988;77:1250–7. https://doi.org/10.1161/01.cir.77.6.1250.
118. Red-Horse K, Ueno H, Weissman IL, Krasnow MA. Coronary arteries form by developmental reprogramming of venous cells. Nature. 2010;464:549–53. https://doi.org/10.1038/nature08873.
119. Wu B, et al. Endocardial cells form the coronary arteries by angiogenesis through myocardial-endocardial VEGF signaling. Cell. 2012;151:1083–96. https://doi.org/10.1016/j.cell.2012.10.023.
120. Su T, et al. Single-cell analysis of early progenitor cells that build coronary arteries. Nature. 2018;559:356–62. https://doi.org/10.1038/s41586-018-0288-7.

121. Zhang H, et al. Endocardium minimally contributes to coronary endothelium in the embryonic ventricular free walls. Circ Res. 2016;118:1880–93. https://doi.org/10.1161/CIRCRESAHA.116.308749.
122. Katz TC, et al. Distinct compartments of the proepicardial organ give rise to coronary vascular endothelial cells. Dev Cell. 2012;22:639–50. https://doi.org/10.1016/j.devcel.2012.01.012.
123. Cano E, et al. Extracardiac septum transversum/proepicardial endothelial cells pattern embryonic coronary arterio-venous connections. Proc Natl Acad Sci U S A. 2016;113:656–61. https://doi.org/10.1073/pnas.1509834113.
124. Acharya A, et al. The bHLH transcription factor Tcf21 is required for lineage-specific EMT of cardiac fibroblast progenitors. Development. 2012;139:2139–49. https://doi.org/10.1242/dev.079970.
125. Sharma B, Chang A, Red-Horse K. Coronary artery development: progenitor cells and differentiation pathways. Annu Rev Physiol. 2017;79:1–19. https://doi.org/10.1146/annurev-physiol-022516-033953.
126. Cai CL, et al. A myocardial lineage derives from Tbx18 epicardial cells. Nature. 2008;454:104–8. https://doi.org/10.1038/nature06969.
127. Volz KS, et al. Pericytes are progenitors for coronary artery smooth muscle. Elife. 2015;4:e10036. https://doi.org/10.7554/eLife.10036.
128. Tian X, et al. Subepicardial endothelial cells invade the embryonic ventricle wall to form coronary arteries. Cell Res. 2013;23:1075–90. https://doi.org/10.1038/cr.2013.83.
129. Tian X, Pu WT, Zhou B. Cellular origin and developmental program of coronary angiogenesis. Circ Res. 2015;116:515–30. https://doi.org/10.1161/CIRCRESAHA.116.305097.
130. Lamers WH, Moorman AF. Cardiac septation: a late contribution of the embryonic primary myocardium to heart morphogenesis. Circ Res. 2002;91:93–103.
131. Yoshida H, Manasek F, Arcilla RA. Intracardiac flow patterns in early embryonic life. A reexamination. Circ Res. 1983;53:363–71.
132. Bharadwaj KN, Spitz C, Shekhar A, Yalcin HC, Butcher JT. Computational fluid dynamics of developing avian outflow tract heart valves. Ann Biomed Eng. 2012;40:2212–27. https://doi.org/10.1007/s10439-012-0574-8.
133. Phoon CK, Aristizabal O, Turnbull DH. Spatial velocity profile in mouse embryonic aorta and doppler-derived volumetric flow: a preliminary model. Am J Physiol Heart Circ Physiol. 2002;283:H908–16. https://doi.org/10.1152/ajpheart.00869.2001.
134. Al-Roubaie S, Jahnsen ED, Mohammed M, Henderson-Toth C, Jones EA. Rheology of embryonic avian blood. Am J Physiol Heart Circ Physiol. 2011;301:H2473–81. https://doi.org/10.1152/ajpheart.00475.2011.
135. Yalcin HC, Shekhar A, McQuinn TC, Butcher JT. Hemodynamic patterning of the avian atrioventricular valve. Dev Dyn. 2011;240:23–35. https://doi.org/10.1002/dvdy.22512.
136. Jensen B, et al. The hypertrabeculated (noncompacted) left ventricle is different from the ventricle of embryos and ectothermic vertebrates. Biochim Biophys Acta. 1863;1696-1706:2016. https://doi.org/10.1016/j.bbamcr.2015.10.018.
137. Sedmera D, Pexieder T, Vuillemin M, Thompson RP, Anderson RH. Developmental patterning of the myocardium. Anat Rec. 2000;258:319–37.
138. Rentschler S, et al. Visualization and functional characterization of the developing murine cardiac conduction system. Development. 2001;128:1785–92.
139. Valderrabano M, et al. Atrioventricular ring reentry in embryonic mouse hearts. Circulation. 2006;114:543–9. https://doi.org/10.1161/CIRCULATIONAHA.106.633727.
140. Chen F, et al. Atrioventricular conduction and arrhythmias at the initiation of beating in embryonic mouse hearts. Dev Dyn. 2010;239:1941–9. https://doi.org/10.1002/dvdy.22319.
141. Manner J, Wessel A, Yelbuz TM. How does the tubular embryonic heart work? Looking for the physical mechanism generating unidirectional blood flow in the valveless embryonic heart tube. Dev Dyn. 2010;239:1035–46. https://doi.org/10.1002/dvdy.22265.
142. Makikallio K, Jouppila P, Rasanen J. Human fetal cardiac function during the first trimester of pregnancy. Heart. 2005;91:334–8. https://doi.org/10.1136/hrt.2003.029736.

143. Santhanakrishnan A, Nguyen N, Cox JG, Miller LA. Flow within models of the vertebrate embryonic heart. J Theor Biol. 2009;259:449–61. https://doi.org/10.1016/j.jtbi.2009.04.020.
144. Reckova M, et al. Hemodynamics is a key epigenetic factor in development of the cardiac conduction system. Circ Res. 2003;93:77–85. https://doi.org/10.1161/01.RES.0000079488.91342.B7.
145. Wloch A, et al. Doppler study of the embryonic heart in normal pregnant women. J Matern Fetal Neonatal Med. 2007;20:533–9. https://doi.org/10.1080/14767050701434747.
146. Hu N, Clark EB. Hemodynamics of the stage 12 to stage 29 chick embryo. Circ Res. 1989;65:1665–70.
147. Midgett M, Chivukula VK, Dorn C, Wallace S, Rugonyi S. Blood flow through the embryonic heart outflow tract during cardiac looping in HH13-HH18 chicken embryos. J R Soc Interface. 2015;12:20150652. https://doi.org/10.1098/rsif.2015.0652.
148. Loughna S, Sato TN. A combinatorial role of angiopoietin-1 and orphan receptor TIE1 pathways in establishing vascular polarity during angiogenesis. Mol Cell. 2001;7:233–9. https://doi.org/10.1016/s1097-2765(01)00171-x.
149. Ai D, et al. Pitx2 regulates cardiac left-right asymmetry by patterning second cardiac lineage-derived myocardium. Dev Biol. 2006;296:437–49. https://doi.org/10.1016/j.ydbio.2006.06.009.
150. Neill CA. Development of the pulmonary veins; with reference to the embryology of anomalies of pulmonary venous return. Pediatrics. 1956;18:880–7.
151. Webb S, Kanani M, Anderson RH, Richardson MK, Brown NA. Development of the human pulmonary vein and its incorporation in the morphologically left atrium. Cardiol Young. 2001;11:632–42.
152. Auer J. The development of the human pulmonary vein and its major variations. Anat Rec. 1948;101:581–94.
153. Wessels A, et al. Atrial development in the human heart: an immunohistochemical study with emphasis on the role of mesenchymal tissues. Anat Rec. 2000;259:288–300.
154. Cabrera JA, Ho SY, Climent V, Sanchez-Quintana D. The architecture of the left lateral atrial wall: a particular anatomic region with implications for ablation of atrial fibrillation. Eur Heart J. 2008;29:356–62. https://doi.org/10.1093/eurheartj/ehm606.
155. Kim DT, et al. The ligament of Marshall: a structural analysis in human hearts with implications for atrial arrhythmias. J Am Coll Cardiol. 2000;36:1324–7. https://doi.org/10.1016/s0735-1097(00)00819-6.
156. Mommersteeg MT, et al. Two distinct pools of mesenchyme contribute to the development of the atrial septum. Circ Res. 2006;99:351–3. https://doi.org/10.1161/01.RES.0000238360.33284.a0.
157. Anderson RH, Brown NA, Webb S. Development and structure of the atrial septum. Heart. 2002;88:104–10.
158. Snarr BS, et al. Isl1 expression at the venous pole identifies a novel role for the second heart field in cardiac development. Circ Res. 2007;101:971–4. https://doi.org/10.1161/CIRCRESAHA.107.162206.
159. Snarr BS, Wirrig EE, Phelps AL, Trusk TC, Wessels A. A spatiotemporal evaluation of the contribution of the dorsal mesenchymal protrusion to cardiac development. Dev Dyn. 2007;236:1287–94. https://doi.org/10.1002/dvdy.21074.
160. McBride RE, Moore GW, Hutchins GM. Development of the outflow tract and closure of the interventricular septum in the normal human heart. Am J Anat. 1981;160:309–31. https://doi.org/10.1002/aja.1001600308.
161. Teal SI, Moore GW, Hutchins GM. Development of aortic and mitral valve continuity in the human embryonic heart. Am J Anat. 1986;176:447–60. https://doi.org/10.1002/aja.1001760407.
162. Magovern JH, Moore GW, Hutchins GM. Development of the atrioventricular valve region in the human embryo. Anat Rec. 1986;215:167–81. https://doi.org/10.1002/ar.1092150210.

163. Kelly RG, Brown NA, Buckingham ME. The arterial pole of the mouse heart forms from Fgf10-expressing cells in pharyngeal mesoderm. Dev Cell. 2001;1:435–40.
164. McFadden DG, et al. The Hand1 and Hand2 transcription factors regulate expansion of the embryonic cardiac ventricles in a gene dosage-dependent manner. Development. 2005;132:189–201. https://doi.org/10.1242/dev.01562.
165. Bruneau BG, et al. A murine model of Holt-Oram syndrome defines roles of the T-box transcription factor Tbx5 in cardiogenesis and disease. Cell. 2001;106:709–21. https://doi.org/10.1016/s0092-8674(01)00493-7.
166. Hiruma T, Hirakow R. Formation of the pharyngeal arch arteries in the chick embryo. Observations of corrosion casts by scanning electron microscopy. Anat Embryol. 1995;191:415–23. https://doi.org/10.1007/bf00304427.
167. Hiruma T, Nakajima Y, Nakamura H. Development of pharyngeal arch arteries in early mouse embryo. J Anat. 2002;201:15–29. https://doi.org/10.1046/j.1469-7580.2002.00071.x.
168. Wang X, et al. Endothelium in the pharyngeal arches 3, 4 and 6 is derived from the second heart field. Dev Biol. 2017;421:108–17. https://doi.org/10.1016/j.ydbio.2016.12.010.
169. Tzahor E, Evans SM. Pharyngeal mesoderm development during embryogenesis: implications for both heart and head myogenesis. Cardiovasc Res. 2011;91:196–202. https://doi.org/10.1093/cvr/cvr116.
170. Lescroart F, et al. Clonal analysis reveals a common origin between nonsomite-derived neck muscles and heart myocardium. Proc Natl Acad Sci U S A. 2015;112:1446–51. https://doi.org/10.1073/pnas.1424538112.
171. Diogo R, et al. A new heart for a new head in vertebrate cardiopharyngeal evolution. Nature. 2015;520:466–73. https://doi.org/10.1038/nature14435.
172. Depew MJ, Simpson CA, Morasso M, Rubenstein JL. Reassessing the dlx code: the genetic regulation of branchial arch skeletal pattern and development. J Anat. 2005;207:501–61. https://doi.org/10.1111/j.1469-7580.2005.00487.x.
173. Li P, Pashmforoush M, Sucov HM. Mesodermal retinoic acid signaling regulates endothelial cell coalescence in caudal pharyngeal arch artery vasculogenesis. Dev Biol. 2012;361:116–24. https://doi.org/10.1016/j.ydbio.2011.10.018.
174. Fukiishi Y, Morriss-Kay GM. Migration of cranial neural crest cells to the pharyngeal arches and heart in rat embryos. Cell Tissue Res. 1992;268:1–8. https://doi.org/10.1007/BF00338048.
175. Chan WY, Cheung CS, Yung KM, Copp AJ. Cardiac neural crest of the mouse embryo: axial level of origin, migratory pathway and cell autonomy of the splotch (Sp2H) mutant effect. Development. 2004;131:3367–79. https://doi.org/10.1242/dev.01197.
176. Graham A, Poopalasundaram S, Shone V, Kiecker C. A reappraisal and revision of the numbering of the pharyngeal arches. J Anat. 2019;235:1019–23. https://doi.org/10.1111/joa.13067.
177. Padget DH. Designation of the embryonic intersegmental arteries in reference to the vertebral artery and subclavian stem. Anat Rec. 1954;119:349–56. https://doi.org/10.1002/ar.1091190306.
178. Congdon ED. Transformation of the aortic-arch system during the development of the human embryo. Contrib Embryol Carnegie Inst Wash. 1922;14:47–110.
179. Goor DA, Dische R, Lillehei CW. The conotruncus. I. Its normal inversion and conus absorption. Circulation. 1972;46:375–84. https://doi.org/10.1161/01.cir.46.2.375.
180. Zhao Z, Rivkees SA. Programmed cell death in the developing heart: regulation by BMP4 and FGF2. Dev Dyn. 2000;217:388–400. https://doi.org/10.1002/(SICI)1097-0177(200004)217:4<388::AID-DVDY6>3.0.CO;2-N.
181. Sharma PR, Anderson RH, Copp AJ, Henderson DJ. Spatiotemporal analysis of programmed cell death during mouse cardiac septation. Anat Rec A Discov Mol Cell Evol Biol. 2004;277:355–69. https://doi.org/10.1002/ar.a.20006.
182. Jiang X, Rowitch DH, Soriano P, McMahon AP, Sucov HM. Fate of the mammalian cardiac neural crest. Development. 2000;127:1607–16.

183. Yang YP, et al. Second heart field and the development of the outflow tract in human embryonic heart. Develop Growth Differ. 2013;55:359–67. https://doi.org/10.1111/dgd.12050.
184. de Lange FJ, et al. Lineage and morphogenetic analysis of the cardiac valves. Circ Res. 2004;95:645–54. https://doi.org/10.1161/01.RES.0000141429.13560.cb.
185. Lincoln J, Alfieri CM, Yutzey KE. Development of heart valve leaflets and supporting apparatus in chicken and mouse embryos. Dev Dyn. 2004;230:239–50. https://doi.org/10.1002/dvdy.20051.
186. Phillips HM, et al. Neural crest cells are required for correct positioning of the developing outflow cushions and pattern the arterial valve leaflets. Cardiovasc Res. 2013;99:452–60. https://doi.org/10.1093/cvr/cvt132.
187. Kirby ML, Waldo KL. Role of neural crest in congenital heart disease. Circulation. 1990;82:332–40. https://doi.org/10.1161/01.cir.82.2.332.
188. Jin H, et al. Differential contribution of the two waves of cardiac progenitors and their derivatives to aorta and pulmonary artery. Dev Biol. 2019;450:82–9. https://doi.org/10.1016/j.ydbio.2019.03.019.
189. Liang S, et al. Pulmonary endoderm, second heart field and the morphogenesis of distal outflow tract in mouse embryonic heart. Develop Growth Differ. 2014;56:276–92. https://doi.org/10.1111/dgd.12129.
190. Zhou Z, et al. Temporally distinct Six2-positive second heart field progenitors regulate mammalian heart development and disease. Cell Rep. 2017;18:1019–32. https://doi.org/10.1016/j.celrep.2017.01.002.
191. Wang JJ, et al. Isl-1 positive pharyngeal mesenchyme subpopulation and its role in the separation and remodeling of the aortic sac in embryonic mouse heart. Dev Dyn. 2019;248:771–83. https://doi.org/10.1002/dvdy.68.
192. Eley L, et al. A novel source of arterial valve cells linked to bicuspid aortic valve without raphe in mice. Elife. 2018;7:e34110. https://doi.org/10.7554/eLife.34110.
193. Tandler J. In: Keibel F, Mall FP, editors. Manual of human embryology, vol. II, Ch. XVIII. J. B. Lippincott Co; 1912. p. 534–70.
194. Sawada H, Rateri DL, Moorleghen JJ, Majesky MW, Daugherty A. Smooth muscle cells derived from second heart field and cardiac neural crest reside in spatially distinct domains in the media of the ascending aorta-brief report. Arterioscler Thromb Vasc Biol. 2017;37:1722–6. https://doi.org/10.1161/ATVBAHA.117.309599.
195. Bajolle F, et al. Myocardium at the base of the aorta and pulmonary trunk is prefigured in the outflow tract of the heart and in subdomains of the second heart field. Dev Biol. 2008;313:25–34. https://doi.org/10.1016/j.ydbio.2007.09.023.
196. Yashiro K, Shiratori H, Hamada H. Haemodynamics determined by a genetic programme govern asymmetric development of the aortic arch. Nature. 2007;450:285–8. https://doi.org/10.1038/nature06254.
197. Harmon AW, Nakano A. Nkx2-5 lineage tracing visualizes the distribution of second heart field-derived aortic smooth muscle. Genesis. 2013;51:862–9. https://doi.org/10.1002/dvg.22721.
198. Manner J. Does the subepicardial mesenchyme contribute myocardioblasts to the myocardium of the chick embryo heart? A quail-chick chimera study tracing the fate of the epicardial primordium. Anat Rec. 1999;255:212–26. https://doi.org/10.1002/(sici)1097-0185(19990601)255:2<212::aid-ar11>3.3.co;2-o.
199. Perez-Pomares JM, Phelps A, Sedmerova M, Wessels A. Epicardial-like cells on the distal arterial end of the cardiac outflow tract do not derive from the proepicardium but are derivatives of the cephalic pericardium. Dev Dyn. 2003;227:56–68. https://doi.org/10.1002/dvdy.10284.
200. Gittenberger-de Groot AC, et al. The arterial and cardiac epicardium in development, disease and repair. Differentiation. 2012;84:41–53. https://doi.org/10.1016/j.diff.2012.05.002.

201. Gittenberger-de Groot AC, Vrancken Peeters MP, Bergwerff M, Mentink MM, Poelmann RE. Epicardial outgrowth inhibition leads to compensatory mesothelial outflow tract collar and abnormal cardiac septation and coronary formation. Circ Res. 2000;87:969–71. https://doi.org/10.1161/01.res.87.11.969.
202. Spicer DE, Bridgeman JM, Brown NA, Mohun TJ, Anderson RH. The anatomy and development of the cardiac valves. Cardiol Young. 2014;24:1008–22. https://doi.org/10.1017/S1047951114001942.
203. Okamoto N, Akimoto N, Satow Y, Hidaka N, Miyabara S. Role of cell death on conal ridges of developing human heart, vol. 5. Raven Press; 1981. p. 127–37.
204. Merrick AF, Yacoub MH, Ho SY, Anderson RH. Anatomy of the muscular subpulmonary infundibulum with regard to the Ross procedure. Ann Thorac Surg. 2000;69:556–61. https://doi.org/10.1016/s0003-4975(99)01300-4.
205. Anderson RH, et al. Myths and realities relating to development of the arterial valves. J Cardiovasc Dev Dis. 2014;1:177–200.
206. Lamers WH, Viragh S, Wessels A, Moorman AF, Anderson RH. Formation of the tricuspid valve in the human heart. Circulation. 1995;91:111–21.
207. van den Hoff MJ, et al. Myocardialization of the cardiac outflow tract. Dev Biol. 1999;212:477–90. https://doi.org/10.1006/dbio.1999.9366.
208. de la Cruz MV, Sanchez Gomez C, Arteaga MM, Arguello C. Experimental study of the development of the truncus and the conus in the chick embryo. J Anat. 1977;123:661–86.
209. Anderson RH, Spicer DE, Mohun TJ, Hikspoors J, Lamers WH. Remodeling of the embryonic interventricular communication in regard to the description and classification of ventricular septal defects. Anat Rec. 2019;302:19–31. https://doi.org/10.1002/ar.24020.
210. Anderson RH, Spicer DE, Brown NA, Mohun TJ. The development of septation in the four-chambered heart. Anat Rec. 2014;297:1414–29. https://doi.org/10.1002/ar.22949.
211. Odgers PN. The development of the pars membranacea septi in the human heart. J Anat. 1938;72:247–59.
212. Goor DA, Edwards JE, Lillehei CW. The development of the interventricular septum of the human heart; correlative morphogenetic study. Chest. 1970;58:453–67. https://doi.org/10.1378/chest.58.5.453.
213. Allwork SP, Anderson RH. Developmental anatomy of the membranous part of the ventricular septum in the human heart. Br Heart J. 1979;41:275–80. https://doi.org/10.1136/hrt.41.3.275.
214. Streeter GL. In: Heuser CH, Corner GW, editors. Ch. 165 Contrib Embryol, vol. 34. Carnegie Inst Wash; 1951. p. 165–96.
215. Lomonico MP, Moore GW, Hutchins GM. Rotation of the junction of the outflow tract and great arteries in the embryonic human heart. Anat Rec. 1986;216:544–9. https://doi.org/10.1002/ar.1092160412.

Human Genetics of Congenital Heart Defects

2

Anna Wilsdon and Siobhan Loughna

Abstract

Congenital heart diseases (or congenital heart defects/disorders; CHDs) are structural abnormalities of the heart and/or great vessels that are present at birth. CHDs include an extensive range of defects that may be minor and require no intervention or may be life-limiting and require complex surgery shortly after birth. This chapter reviews the current knowledge on the genetic causes of CHD.

Keywords

Congenital heart disease · Congenital heart defects · Exome sequencing · Genetics · Genome sequencing · Inherited · Life span · Pediatric cardiology · Reduced penetrance · Screening

2.1 Introduction

Congenital heart disease (CHD) is the most common congenital abnormality, with a high mortality in those with the most severe defects. It affects 9.4 in every 1000 live births [1]; though if lesions such as a bicuspid aortic valve (BAV) are included, then the incidence rises to 2–3% [2]. Almost 58% of individuals with CHD have an atrial

A. Wilsdon (✉)
School of Life Sciences, University of Nottingham, Nottingham, UK

Clinical Geneticist at Nottingham Clinical Genetics Department, Nottingham University Hospitals, City Hospital, Nottingham, UK
e-mail: anna.wilsdon1@nhs.net

S. Loughna
School of Life Sciences, University of Nottingham, Nottingham, UK
e-mail: siobhan.loughna@nottingham.ac.uk

© The Author(s), under exclusive license to Springer Nature Switzerland AG 2024

S. Rickert-Sperling et al. (eds.), *Congenital Heart Diseases: The Broken Heart*,
Advances in Experimental Medicine and Biology 1441,
https://doi.org/10.1007/978-3-031-44087-8_2

septal defect (ASD), a ventricular septal defect (VSD), or patent ductus arteriosus (PDA) [1].

The prevalence of both milder and more complex lesions rose by around 10% between 2010 and 2017, predominantly due to improved detection and diagnosis [1]. Individuals with CHD are living longer due to better medical and surgical care, with more than 90% of them reaching adulthood [3]. Given that CHD is a common congenital abnormality with many individuals requiring lifelong specialist medical care, it is an important issue for those providing healthcare. Their needs range from complex and multiple surgeries to lifelong surveillance to monitor for late complications, as some types of CHDs are associated with high levels of morbidity and mortality during adulthood [4]. Given that there is a significant genetic component to CHD, and individuals are now more likely to survive to reproductive age, they may ask about the risks of their children also being affected by CHD. Genetic testing and counseling should be made available and be factored into health-care provision [5].

2.2 Patterns of Inheritance and the Etiology of CHD

A genetic cause can be identified in approximately 40% of people with CHD [6]; these can be a single gene de novo and inherited variants, chromosomal aneuploidies, or copy number variants. However, a genetic association is more likely to be found in those who have CHD in combination with extra-cardiac defects, including neurodevelopmental disability (NDD) [7–9]. CHD in combination with NDD or other congenital abnormalities is often referred to as syndromic CHD (S-CHD). This is in contrast to non-syndromic CHD (NS-CHD), where CHD is seen in isolation; it accounts for a much larger proportion of individuals with CHD.

CHD is usually only seen in a single individual within a family; however, there is an increased risk of first-degree family members also being affected. The overall sibling recurrence risk is 4.1–4.4%, with certain types of more severe CHD defects having higher rates of recurrence [10, 11]. In addition, twins have a higher risk of CHD compared to singletons. The risk is highest in monochorionic twins with twin–twin transfusion syndrome (TTTS) [4, 12, 13]. However, monozygotic twins without TTTS also have an increased risk of CHD. In addition, dizygotic twins also have a higher incidence of CHD than do singletons, suggesting that additional factors within the maternal environment influence cardiac development [14].

2.3 Single-Gene Variants and CHD

A number of CHD genes have been identified by the analysis of families with a Mendelian pattern of CHD. Two of the first genes to be associated with CHD were transcription factors: *TBX5* in S-CHD and *NKX2.5* in NS-CHD. Pathogenic variants in *TBX5* were associated with limb defects and a number of heart defects such as ASDs in Holt–Oram syndrome [15], whereas *NKX2.5* was associated with a range of

cardiac anomalies, including ASD and atrioventricular conduction block [16]. Another well-described example of S-CHD is Noonan syndrome, one of the RASopathies that results from pathogenic variants in the Ras/mitogen-associated protein kinase (Ras/MAPK) pathway. Noonan syndrome is most commonly caused by heterozygous gain-of-function mutations in *PTPN11*; the phenotype is variable, though characteristically wide-set eyes, ptosis, short stature, and pulmonary stenosis are described [17, 18]. However, this classical pedigree displaying Mendelian inheritance is uncommon; the majority of individuals with CHD display a complex pattern of inheritance. The mechanisms underlying CHD are complicated, with the correct expression of a range of genes necessary for normal heart development.

Traditionally, studies have relied on linkage or sequencing of specific candidate genes, often followed by further targeted sequencing of those genes in additional cohorts of individuals with the same type of CHD or syndromic phenotype. This approach has allowed the definition of strong genotype–phenotype associations and the identification of many genes that cause CHDs; however, this method leads to ascertainment bias. Non-targeted testing using whole exome sequencing (WES) or whole genome sequencing (WGS) to detect single nucleotide variants and indels can prove useful in identifying novel genes and help elucidate the full phenotypic spectrum of a gene. Sequencing in a cohort of individuals with a single CHD or multiple types of CHDs is now at the forefront of research to discover novel CHD genes [9, 19–25]. Genome-wide association studies may also help identify new candidate genes [26]. This approach requires a close collaboration between clinicians and research groups, in order to assemble large enough cohorts that are necessary to fully understand the genetic basis of this complex group of disorders.

Currently, examples of single-gene causes of CHD include transcription factors, protein kinases (such as *CDK13*) [19], genes encoding structural proteins (e.g., *MYH6* and *TPM1*) [27, 28], chromatin modifiers (*CHD4*, for example) [19], cilia-related genes [29], and genes in a variety of signaling pathways (such as Notch) [30–32]. For review articles describing many of the single-gene causes, see [22, 33, 34]. Many of these genes are necessary for normal cardiogenesis. Most of the identified genetic causes result in S-CHD.

2.4 Structural Variants as a Cause of CHD

CHD can also result from structural variation, in the form of chromosomal or copy number aberrations. The exact proportion of CHD occurring as a result of chromosomal abnormalities varies depending on the CHD population assessed. In a large study of 4430 live-born and fetal deaths with CHD, 12.3% had a causative chromosomal abnormality [35], whereas up to 23% of severe CHD in 919 fetuses and live-born infants were due to aneuploidy [36]. Some of the typical cardiac defects associated with these and other genetic conditions are included in Table 2.1. Given the large number of developmentally important genes affected by these chromosomal abnormalities, it is not unexpected that these diagnoses are often associated with multiple noncardiac congenital abnormalities and NDD.

Table 2.1 Common CHD defects and examples of genetic etiologies

Ventricular septal defect (VSD)	This is the most common type of CHD (1.5–53.2 per 1000 live births) [123]. A VSD represents communication between the two ventricles. Classification is complex but can be broadly divided into those affecting the muscular and membranous septum [124] VSDs are commonly seen in trisomies 13, 18, and 21 [125, 126], 22q11.2 deletions [127], fetal alcohol syndrome (FAS) [128], and maternal diabetes mellitus [129]. Non-syndromic VSDs may be associated with mutations in genes such as *GATA4* [130, 131] and *NKX2.5* [132]	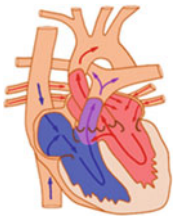
Atrial septal defect (ASD)	The atrial septum is formed from the superior and inferior atrioventricular cushions, the primary atrial septum, the mesenchymal cap, and the dorsal mesenchymal protrusion [133]. ASDs occur at different locations in the septum and are likely to have different mechanisms leading to their formation. Defects include patent foramen ovale, ostium primum, ostium secundum, sinus venosus, coronary sinus defects, and the common atrium [134] ASDs are seen as part of trisomy 13 [126], trisomy 21 [125], and FAS [128]. It is also a feature of syndromes such as Holt–Oram syndrome (HOS) [15]. ASD is also seen in isolation as a result of mutations in, for example, *GATA4, NKX2.5* [135], *GATA6* [136], and *ACTC1* [137]	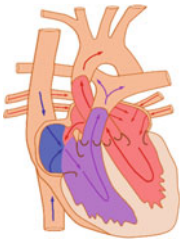
Atrioventricular septal defect (AVSD)	AVSDs constitute a variable spectrum of defects involving the atrial and ventricular septa and the mitral and tricuspid valves, resulting in either a common atrioventricular orifice or one that is partially separated [138]. It includes ostium primum defects. AVSDs result from defective formation of the endocardial cushions The risk of AVSDs is high in trisomy 21, where 20–45% are affected by this defect [139–141], compared with around 1 in 10,000 without chromosomal abnormalities [142]. AVSDs are also seen in a number of ciliopathy syndromes [143]. Mutations in *GATA4* are also linked to AVSDs [131, 144]	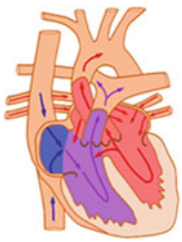
Tetralogy of Fallot (TOF)	CHD is comprised of cyanotic and non-cyanotic lesions. Cyanotic lesions allow mixing of oxygen-rich and oxygen-poor blood, resulting in lower oxygen levels and cyanosis. TOF is the most common cyanotic form of CHD, with a prevalence of 0.356 per 1000 live births [1]. TOF is a combination of VSD, anterocephalad deviation of the outflow septum, which results in an overriding aorta, and variable obstruction of the outflow tract	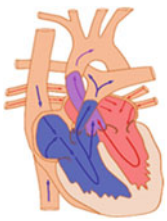

(continued)

Table 2.1 (continued)

	(pulmonary stenosis). This obstruction results in hypertrophy of the right ventricle TOF is a feature of a number of syndromes, including 22q11 deletion syndrome, where 17–22% have this defect [145–147], and 2–2.6% of individuals with trisomy 21 [125, 148]. Other associated genes include *NOTCH1*, *FLT4* [21], *NKX2.5* [149], and *ZFPM2* (*FOG2*) [150]	
Coarctation of the aorta (CoA)	CoA is a narrowing of the aorta, most commonly distal to the left subclavian artery. It results in upper limb hypertension and radiofemoral delay (the femoral pulse is felt later than the radial pulse) CoA occurs in around 7–18% of individuals with Turner syndrome (45X) [47, 151]. To date, only a few genes, such as *TBL1Y* [152], *JAG1* [153], and *MYH6* [154], have been associated with CoA	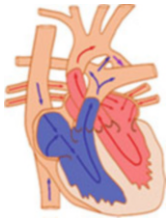

Trisomy 13 (Patau syndrome), 18 (Edwards syndrome), and 21 (Down syndrome) and monosomy X (Turner syndrome) are common chromosomal causes of antenatally detected CHD [37]. The majority of affected fetuses will miscarry during pregnancy. A proportion of fetuses with trisomy 13 and trisomy 18 do survive to term, but have a poor prognosis, and the vast majority do not survive the neonatal period. Up to 87% will have CHD [38–42] in combination with multiple extracardiac abnormalities. Trisomy 21 is the most common live-born trisomy, with an immediately recognizable facial gestalt and 40–50% of individuals having CHD [43, 44]. It is a far more variable condition than is trisomy 13 or 18, and prognosis is dependent on the presence and type of CHD, and other congenital abnormalities [45]. Another well-recognized aneuploidy associated with CHD is Turner syndrome (45X and mosaic variants). Up to 50% of individuals have a structural heart defect, most commonly BAV and coarctation of the aorta [46, 47]. Aortic dilatation and dissection can occur, and cardiovascular abnormalities are one of the most common causes of early mortality in this condition [46, 48].

Copy number variations (CNVs) are structural deletions and duplications that vary in size and which affect in the region of 12% of the genome [49, 50]. Like chromosomal defects, the reported contribution of CNVs to the pathogenesis of CHD is variable, due to the different CHD populations studied, the size of the CNVs considered, and the difficulty in determining pathogenicity due to reduced penetrance. It is apparent, however, that there is an increased burden of rare CNVs in individuals with CHD (around 10%), compared to controls [20, 51, 52]. CNVs are detected more commonly in syndromic than in non-syndromic CHDs [53].

Some CNVs, such as the 22q11.2 deletion syndrome (also known as velocardiofacial syndrome or DiGeorge syndrome), are a well-established cause of CHD and can be detected using fluorescence in situ hybridization (FISH) or microarray. Clinical features result from a large deletion of 1.5–3 Mb, of the long arm of chromosome 22 [54]. Haploinsufficiency of *Tbx1* contained within this

deletion results in abnormal third and fourth pharyngeal arch development because of abnormal neural crest migration [55–58]. The resulting features include conotruncal CHD, specifically type B-interrupted aortic arch [55, 59, 60].

Another well-described cause of syndromic CHD is Williams syndrome, which is caused by a deletion of about 23 protein-coding genes on the long arm of chromosome 7 (7q11.23) [61, 62]. Deletion of the elastin (*ELN*) gene in these individuals results in a phenotype of supravalvular aortic stenosis [63]. Subsequently, single nucleotide variants in *ELN* were found to cause non-syndromic supravalvular aortic stenosis [64].

With more widespread use of microarray technology, an increasing number of microdeletion and microduplication syndromes have now been described in association with CHD [51, 65–68]. Some of these CNVs cause haploinsufficiency of known cardiac transcription factors (such as *GATA4* in individuals with 8p23.1 deletions) [69].

2.5 Reduced Penetrance and Other Mechanisms

CHD, like many genetic conditions, shows variable expressivity and reduced penetrance. In studies of families with CHD, non-penetrance is evident in obligate carriers [70], and, when recurrences do occur, family members are more likely to show discordant than concordant phenotypes [71]. Variable expression is demonstrated in even the most well-established CHD syndromes resulting from copy number variations [72] and single-gene mutations [73]. There is also mounting evidence of reduced penetrance with seemingly deleterious mutations in established CHD-causing genes [19, 21, 74, 75].

This raises the possibility that additional genetic and nongenetic factors may be involved and contribute to the development of CHD. Proposed mechanisms to explain this variability include oligogenic (a few genes contribute to the CHD phenotype) or polygenic inheritance (many low-penetrance genes contribute to the phenotype) [6, 76]. The presence of multiple variants in CHD genes may result in a more severe phenotype [77].

We are also increasingly aware of the contribution of epigenetic factors to CHD, and non-coding de novo variants may play a significant role in the occurrence of CHD [25, 78]. Epigenetic factors may explain some of the phenotypic variability in 22q11.2 deletion syndrome, where haploinsufficiency of the known developmentally important coding genes alone cannot explain the phenotypic variability [79]. Abnormal methylation of *NKX2–5* and *HAND1* in individuals with sporadic tetralogy of Fallot (TOF) [80] and significant differences in promotor methylation have been identified in CHD candidate genes in individuals with TOF [81]. It is not clear, however, whether this altered methylation is associated with, or contributes to, the development of TOF. Methylation patterns of genes involved in cardiogenesis change throughout development, suggesting roles of methylation in the control of transcription [82]. Importantly, there is an emerging role of genes involved in chromatin modification [9, 19, 23] in addition to already established CHD genes

such as *CHD7* (CHD7 Disorder, CHARGE Syndrome (coloboma, heart defects, atresia of the choanae, retarded growth and/or development, genital anomalies, and ear abnormalities and hearing loss) syndrome) and *KMT2D* and *KDM6A* (Kabuki syndrome). Currently, somatic variants are considered to play only a small role in the pathogenesis of CHD, although there is limited literature investigating this.

Additional maternal and environmental factors are likely to be involved in the variable degrees of penetrance and expressivity in CHD [83–85]. Such factors are important to understand, as they are potentially modifiable. A statement from the American Heart Association council summarized the literature on potential fetal exposures, which could alter the risk of CHD [86]. Heart formation predominantly occurs between 2 and 7 weeks of gestation, so maternal factors during this period and the 3 months leading up to conception (the periconceptional period) were considered. Maternal factors, which clearly and consistently showed an increased risk of CHD, include exposure to certain medications (such as anticonvulsants, sulfasalazine, thalidomide, and vitamin A/retinoids), influenza, rubella, and exposure to certain organic solvents (see Jenkins et al. [86] and the references therein). There is also a possible protective effect caused by multivitamin intake with folic acid in the periconceptional period [86]. Consistent with this, the beginning of fortification of food with folic acid was associated with a trend toward a lower incidence of CHD [87, 88]. The exact mechanism by which folic acid could influence cardiogenesis is unclear, but it may play a role in the migration of cardiac neural crest cells [89, 90].

Furthermore, when the mother has a pathogenic variant in the phenylalanine hydroxylase gene, which causes phenylketonuria (PKU), or she has pregestational diabetes, there is an increased risk of CHD [86]. However, the risk in babies whose mothers have either of these conditions can be reduced if carefully managed periconceptionally and during pregnancy. Interestingly, the risk of CHD in a diabetic mother's offspring is not significantly different between those with type 1 or type 2 diabetes [83], but the type of CHD does differ. Atrioventricular septal defects and conotruncal lesions are more commonly associated with type 1 diabetes and heterotaxy and left ventricular outflow tract obstruction with type 2 [91]. Other factors such as moderate consumption of caffeine or alcohol were either not found to have an association or there was a paucity of data to determine the risk [86]. In addition, in contrast to the study by Jenkins et al., recent studies have found a risk with cigarette smoking [92], obesity, and gestational diabetes [93]. Maternal age was also not considered to have enough data to consider it a risk factor [86]. Interestingly, mouse studies have suggested that a predisposition to developing CHD is greater when combined with increased maternal age [94].

2.6 Techniques and Benefits of Genetic Testing

In the majority of individuals, CHD occurs in isolation (NS-CHD), but it is important to look for other features that might suggest a syndromic diagnosis. Even in well-defined genetic conditions such as Noonan syndrome, the features can be subtle and

it is likely that milder phenotypes have been underdiagnosed historically. Examination by a clinical geneticist can be helpful if a syndromic diagnosis is suspected. It is also important to inquire about a family history and consider possible teratogens and infections in pregnancy [95]. Management should ideally involve a multidisciplinary team, which includes a geneticist (to evaluate for a syndromic diagnosis and facilitate testing) and a cardiologist (to ensure that the heart defect is characterized as accurately as possible to determine the recurrence risk [95]).

Genetic testing may be appropriate in some cases (NHS England » National Genomic Test Directory) [96]. Generally, it is restricted to those with S-CHD, a family history of CHD, or specific types of CHDs such as conotruncal defects, due to low yield in simplex (an isolated case within a family) NS-CHD [95]. FISH has been widely used for detection of specific deletions such as 22q11 deletion syndrome, by looking for loss-of-probe hybridization. Nowadays, microarray may be used (https://www.england.nhs.uk/publication/national-genomic-test-directories/). A microarray is often used as a first line test for congenital abnormalities [97] and will detect chromosomal aneuploidies as well as smaller microdeletions and duplications. If a specific syndromic diagnosis is suspected, then a gene panel test may be appropriate [5]. This uses either WES or WGS, followed by targeted analysis of the relevant genes with related phenotypes. In some cases, analysis may be based on a non-targeted approach. Careful variant annotation and classification, and correlation with clinical findings, are essential to ensure that a correct genetic diagnosis is made. Moving forward, genetic testing in CHD may become more commonplace once more robust recommendations are put in place, but this must be aligned with careful phenotyping and genetic counseling [5, 98].

Identifying a genetic diagnosis and providing genetic counseling have important benefits for the family and individual [99, 100]. It enables the clinician to provide more specific advice on prognosis [101], including neurodevelopmental outcomes [9], and may guide additional investigations [102]. It also opens up options for testing in other family members. This can be especially helpful in instances where CHD is not the only phenotype. For example, pathogenic variants in *ACTC1* can cause CHD in one individual and a later-onset arrhythmia or hypertrophic cardiomyopathy in another [103].

Genetic counseling is important for individuals with CHD when planning a family, and a proportion may alter their decision on whether or not to have a family after counseling [100]. Making a diagnosis in the antenatal period is especially challenging due to the difficulty in characterizing the heart lesion and detecting other abnormalities on scans. It is difficult to predict neurodevelopmental outcomes, even if structural malformations of the brain are present. This diagnostic uncertainty is especially difficult when you consider the significance of decisions being made about a pregnancy at this point.

Antenatal genetic testing can be carried out by taking a sample of the placenta (chorionic villus sampling) or fluid from around the fetus (amniocentesis) under ultrasound guidance [104]. This is possible because the placental cells and amniocytes derive from the same cell population as the fetus. However, both chorionic villus sampling and amniocentesis are associated with a small risk of

inducing preterm labor or miscarriage due to their invasive nature. This risk needs to be balanced against the benefit of making a diagnosis and the subsequent clinical actions.

Quantitative fluorescent polymerase chain reaction (PCR) can be used to perform a rapid check for trisomies. Prenatal microarray tests are used in the main, but single, gene, and gene panel tests, untargeted WES or WGS, and targeted testing for a known familial pathogenic variant may all be possible depending on the clinical situation [105, 106]. An in vitro fertilization (IVF)-based technology called preimplantation genetic diagnosis (PGD) is now also available; it allows implantation of unaffected embryos when a couple is at risk of having a child with a known genetic diagnosis [107]. A newer technology is noninvasive prenatal diagnosis or testing, which analyzes free fetal DNA that circulates in the maternal bloodstream [108, 109]. This is performed on a blood sample taken only from the mother, and, therefore, there is no associated risk of preterm labor. Its use in clinical situations is currently limited to specific conditions and circumstances due to the challenges filtering out the fetal from the maternal variants but is likely to expand in the future [109, 110].

2.7 Limitations of Genetic Testing

There are a number of possible outcomes from a genetic test. The first is that a pathogenic variant that causes a recognizable phenotype is identified, which would explain the individual's phenotype. The second possibility is that a causative variant is not identified. This does not exclude a genetic diagnosis, as variant detection is dependent on filtering pipelines and some variants are more difficult to detect than are others [111]. The third possibility is that a variant of uncertain significance is found. Whilst a formalized process is available to aid variant classification [112], it is important to discuss this possibility with individuals undergoing genetic testing and be aware that the classification of a variant may change over time.

Individuals may be concerned about how the results of their genetic test may influence their ability to access insurance. A number of policies and moratoriums to prevent discrimination based on genetic test results are in place, but these vary around the world depending on the type of insurance being offered [113, 114] (https://assets.publishing.service.gov.uk/government/uploads/system/uploads/attachment_data/file/751230/code-on-genetic-testing-and-insurance.pdf). It is also important to discuss secondary or incidental findings. These are pathogenic variants in other clinically significant genes, unrelated to the initial indication for testing (e.g., in a tumor suppressor gene, carrier status) [115–117].

2.8 Future Challenges

Despite being the most common congenital abnormality, CHD can be one of the most difficult lesions to provide genetic counseling for, due to its complex inheritance and potentially multifactorial etiology. With increasing availability of untargeted genetic testing, the ability to discover new genetic causes of CHD and expand the phenotypic spectrum of even well-described conditions will continue to increase. To maximize discoveries and improve clinical care, it is important that researchers and clinicians work together. An ongoing concern is that most research involves individuals of European descent; this results in a lack of understanding of the genetic causes and difficulty in interpreting variants in other populations [118, 119].

The potential for precision medicine in CHD is emerging. Whilst genetic-based treatments for CHD may be some way off, rapid genetic diagnosis can still guide treatment options and provide valuable information for families now. The presence of a damaging de novo variant can impact surgical outcomes and survival, through and independently of additional extra-cardiac abnormalities [120]. Increasing our understanding of the genetic mechanisms underlying CHD may help in the development of tailored therapies in the future [121, 122].

2.9 Summary

The genetic etiology of CHD is complex and does not follow a Mendelian pattern in most. Understanding the genetic etiology of CHD can help provide information about the prognosis and allow clinicians to provide appropriate genetic counseling and advice about the recurrence risk. In the future, genetic information may be used to support precision medicine in those with both syndromic and non-syndromic CHD.

Acknowledgments We thank Professor David Brook for the insight, guidance, and collegiality that he has shown us over the many years we have worked with him. In addition, we express our gratitude to all of those who have worked in the labs of S.L. and Professor Brook. Many thanks to Aseel Abbad for editorial assistance. We also express our appreciation to The British Heart Foundation, who has funded our research.

References

1. Liu Y, Chen S, Zühlke L, Black GC, Choy MK, Li N, et al. Global birth prevalence of congenital heart defects 1970-2017: updated systematic review and meta-analysis of 260 studies. Int J Epidemiol. 2019;48(2):455–63. https://doi.org/10.1093/ije/dyz009.
2. Gelb BD. Genetic discovery for congenital heart defects. In: Nakanishi T, Markwald RR, Baldwin HS, Keller BB, Srivastava D, Yamagishi H, editors. Etiology and morphogenesis of congenital heart disease: from gene function and cellular interaction to morphology. Tokyo: Springer; 2016. p. 355–60.

3. Diller GP, Arvanitaki A, Opotowsky AR, Jenkins K, Moons P, Kempny A, et al. Lifespan perspective on congenital heart disease research: JACC state-of-the-art review. J Am Coll Cardiol. 2021;77(17):2219–35. https://doi.org/10.1016/j.jacc.2021.03.012.
4. Best KE, Rankin J. Long-term survival of individuals born with congenital heart disease: a systematic review and meta-analysis. J Am Heart Assoc. 2016;5(6):e002846. https://doi.org/10.1161/JAHA.115.002846.
5. De Backer J, Bondue A, Budts W, Evangelista A, Gallego P, Jondeau G, et al. Genetic counselling and testing in adults with congenital heart disease: a consensus document of the ESC Working Group of Grown-Up Congenital Heart Disease, the ESC Working Group on Aorta and Peripheral Vascular Disease and the European Society of Human Genetics. Eur J Prev Cardiol. 2020;27(13):1423–35. https://doi.org/10.1177/2047487319854552.
6. Akhirome E, Walton NA, Nogee JM, Jay PY. The complex genetic basis of congenital heart defects. Circ J. 2017;81(5):629–34. https://doi.org/10.1253/circj.CJ-16-1343.
7. Cowan JR, Tariq M, Shaw C, Rao M, Belmont JW, Lalani SR, et al. Copy number variation as a genetic basis for heterotaxy and heterotaxy-spectrum congenital heart defects. Philos Trans R Soc Lond Ser B Biol Sci. 2016;371(1710):20150406. https://doi.org/10.1098/rstb.2015.0406.
8. Patel A, Costello JM, Backer CL, Pasquali SK, Hill KD, Wallace AS, et al. Prevalence of noncardiac and genetic abnormalities in neonates undergoing cardiac operations: analysis of the Society of Thoracic Surgeons Congenital Heart Surgery Database. Ann Thorac Surg. 2016;102(5):1607–14. https://doi.org/10.1016/j.athoracsur.2016.04.008.
9. Homsy J, Zaidi S, Shen Y, Ware JS, Samocha KE, Karczewski KJ, et al. De novo mutations in congenital heart disease with neurodevelopmental and other congenital anomalies. Science. 2015;350(6265):1262–6. https://doi.org/10.1126/science.aac9396.
10. Peyvandi S, Ingall E, Woyciechowski S, Garbarini J, Mitchell LE, Goldmuntz E. Risk of congenital heart disease in relatives of probands with conotruncal cardiac defects: an evaluation of 1,620 families. Am J Med Genet A. 2014;164a(6):1490-5:1490. https://doi.org/10.1002/ajmg.a.36500.
11. Brodwall K, Greve G, Leirgul E, Tell GS, Vollset SE, Øyen N. Recurrence of congenital heart defects among siblings-a nationwide study. Am J Med Genet A. 2017;173(6):1575–85. https://doi.org/10.1002/ajmg.a.38237.
12. Manning N, Archer N. A study to determine the incidence of structural congenital heart disease in monochorionic twins. Prenat Diagn. 2006;26(11):1062–4. https://doi.org/10.1002/pd.1556.
13. Gijtenbeek M, Shirzada MR, Ten Harkel ADJ, Oepkes D, M CH. Congenital heart defects in monochorionic twins: a systematic review and meta-analysis. J Clin Med. 2019;8(6):902. https://doi.org/10.3390/jcm8060902.
14. Caputo S, Russo MG, Capozzi G, Morelli C, Argiento P, Di Salvo G, et al. Congenital heart disease in a population of dizygotic twins: an echocardiographic study. Int J Cardiol. 2005;102(2):293–6. https://doi.org/10.1016/j.ijcard.2004.05.018.
15. Li QY, Newbury-Ecob RA, Terrett JA, Wilson DI, Curtis AR, Yi CH, et al. Holt-Oram syndrome is caused by mutations in TBX5, a member of the Brachyury (T) gene family. Nat Genet. 1997;15(1):21–9.
16. Schott JJ, Benson DW, Basson CT, Pease W, Silberbach GM, Moak JP, et al. Congenital heart disease caused by mutations in the transcription factor NKX2-5. Science. 1998;281(5373):108–11.
17. Tartaglia M, Kalidas K, Shaw A, Song X, Musat DL, van der Burgt I, et al. PTPN11 mutations in Noonan syndrome: molecular spectrum, genotype-phenotype correlation, and phenotypic heterogeneity. Am J Hum Genet. 2002;70(6):1555–63. https://doi.org/10.1086/340847.
18. Allen MJ, Sharma S. Noonan syndrome. Treasure Island; 2021.
19. Sifrim A, Hitz MP, Wilsdon A, Breckpot J, Turki SH, Thienpont B, et al. Distinct genetic architectures for syndromic and nonsyndromic congenital heart defects identified by exome sequencing. Nat Genet. 2016;48(9):1060–5. https://doi.org/10.1038/ng.3627.

20. Audain E, Wilsdon A, Breckpot J, Izarzugaza JMG, Fitzgerald TW, Kahlert AK, et al. Integrative analysis of genomic variants reveals new associations of candidate haploinsufficient genes with congenital heart disease. PLoS Genet. 2021;17(7):e1009679. https://doi.org/10.1371/journal.pgen.1009679.
21. Page DJ, Miossec MJ, Williams SG, Monaghan RM, Fotiou E, Cordell HJ, et al. Whole exome sequencing reveals the major genetic contributors to nonsyndromic tetralogy of Fallot. Circ Res. 2019;124(4):553–63. https://doi.org/10.1161/circresaha.118.313250.
22. Zaidi S, Brueckner M. Genetics and genomics of congenital heart disease. Circ Res. 2017;120 (6):923–40. https://doi.org/10.1161/circresaha.116.309140.
23. Zaidi S, Choi M, Wakimoto H, Ma L, Jiang J, Overton JD, et al. De novo mutations in histone-modifying genes in congenital heart disease. Nature. 2013;498(7453):220–3. https://doi.org/10.1038/nature12141.
24. Jin SC, Homsy J, Zaidi S, Lu Q, Morton S, DePalma SR, et al. Contribution of rare inherited and de novo variants in 2,871 congenital heart disease probands. Nat Genet. 2017;49(11): 1593–601. https://doi.org/10.1038/ng.3970.
25. Richter F, Morton SU, Kim SW, Kitaygorodsky A, Wasson LK, Chen KM, et al. Genomic analyses implicate noncoding de novo variants in congenital heart disease. Nat Genet. 2020;52 (8):769–77. https://doi.org/10.1038/s41588-020-0652-z.
26. Lahm H, Jia M, Dreßen M, Wirth F, Puluca N, Gilsbach R, et al. Congenital heart disease risk loci identified by genome-wide association study in European patients. J Clin Invest. 2021;131 (2):e141837. https://doi.org/10.1172/jci141837.
27. Ching YH, Ghosh TK, Cross SJ, Packham EA, Honeyman L, Loughna S, et al. Mutation in myosin heavy chain 6 causes atrial septal defect. Nat Genet. 2005;37(4):423–8.
28. England J, Granados-Riveron J, Polo-Parada L, Kuriakose D, Moore C, Brook JD, et al. Tropomyosin 1: multiple roles in the developing heart and in the formation of congenital heart defects. J Mol Cell Cardiol. 2017;106:1–13. https://doi.org/10.1016/j.yjmcc.2017.03.006.
29. Watkins WS, Hernandez EJ, Wesolowski S, Bisgrove BW, Sunderland RT, Lin E, et al. De novo and recessive forms of congenital heart disease have distinct genetic and phenotypic landscapes. Nat Commun. 2019;10(1):4722. https://doi.org/10.1038/s41467-019-12582-y.
30. Garg V, Muth AN, Ransom JF, Schluterman MK, Barnes R, King IN, et al. Mutations in NOTCH1 cause aortic valve disease. Nature. 2005;437(7056):270–4. https://doi.org/10.1038/nature03940.
31. Li L, Krantz ID, Deng Y, Genin A, Banta AB, Collins CC, et al. Alagille syndrome is caused by mutations in human Jagged1, which encodes a ligand for Notch1. Nat Genet. 1997;16(3): 243–51. https://doi.org/10.1038/ng0797-243.
32. Oda T, Elkahloun AG, Pike BL, Okajima K, Krantz ID, Genin A, et al. Mutations in the human Jagged1 gene are responsible for Alagille syndrome. Nat Genet. 1997;16(3):235–42.
33. Williams K, Carson J, Lo C. Genetics of congenital heart disease. Biomolecules. 2019;9:12. https://doi.org/10.3390/biom9120879.
34. Morton SU, Quiat D, Seidman JG, Seidman CE. Genomic frontiers in congenital heart disease. Nat Rev Cardiol. 2022;19(1):26–42. https://doi.org/10.1038/s41569-021-00587-4.
35. Hartman RJ, Rasmussen SA, Botto LD, Riehle-Colarusso T, Martin CL, Cragan JD, et al. The contribution of chromosomal abnormalities to congenital heart defects: a population-based study. Pediatr Cardiol. 2011;32(8):1147–57. https://doi.org/10.1007/s00246-011-0034-5.
36. van Nisselrooij AEL, Lugthart MA, Clur SA, Linskens IH, Pajkrt E, Rammeloo LA, et al. The prevalence of genetic diagnoses in fetuses with severe congenital heart defects. Genet Med. 2020;22(7):1206–14. https://doi.org/10.1038/s41436-020-0791-8.
37. Wimalasundera RC, Gardiner HM. Congenital heart disease and aneuploidy. Prenat Diagn. 2004;24(13):1116–22. https://doi.org/10.1002/pd.1068.
38. Lin HY, Lin SP, Chen YJ, Hsu CH, Kao HA, Chen MR, et al. Clinical characteristics and survival of trisomy 13 in a medical center in Taiwan, 1985-2004. Pediatr Int. 2007;49(3): 380–6. https://doi.org/10.1111/j.1442-200X.2007.02377.x.

39. Musewe NN, Alexander DJ, Teshima I, Smallhorn JF, Freedom RM. Echocardiographic evaluation of the spectrum of cardiac anomalies associated with trisomy 13 and trisomy 18. J Am Coll Cardiol. 1990;15(3):673–7. https://doi.org/10.1016/0735-1097(90)90644-5.
40. Wyllie JP, Wright MJ, Burn J, Hunter S. Natural history of trisomy 13. Arch Dis Child. 1994;71(4):343–5. https://doi.org/10.1136/adc.71.4.343.
41. Embleton ND, Wyllie JP, Wright MJ, Burn J, Hunter S. Natural history of trisomy 18. Arch Dis Child Fetal Neonatal Ed. 1996;75(1):F38–41. https://doi.org/10.1136/fn.75.1.f38.
42. Springett A, Wellesley D, Greenlees R, Loane M, Addor MC, Arriola L, et al. Congenital anomalies associated with trisomy 18 or trisomy 13: a registry-based study in 16 European countries, 2000-2011. Am J Med Genet A. 2015;167a(12):3062–9. https://doi.org/10.1002/ajmg.a.37355.
43. Bull MJ. Health supervision for children with down syndrome. Pediatrics. 2011;128(2):393–406. https://doi.org/10.1542/peds.2011-1605.
44. Pierpont ME, Brueckner M, Chung WK, Garg V, Lacro RV, McGuire AL, et al. Genetic basis for congenital heart disease: revisited: a scientific statement from the American Heart Association. Circulation. 2018;138(21):e653–711. https://doi.org/10.1161/cir.0000000000000606.
45. Bell R, Rankin J, Donaldson LJ. Down's syndrome: occurrence and outcome in the north of England, 1985-99. Paediatr Perinat Epidemiol. 2003;17(1):33–9. https://doi.org/10.1046/j.1365-3016.2003.00463.x.
46. Gravholt CH, Andersen NH, Conway GS, Dekkers OM, Geffner ME, Klein KO, et al. Clinical practice guidelines for the care of girls and women with Turner syndrome: proceedings from the 2016 Cincinnati International Turner Syndrome Meeting. Eur J Endocrinol. 2017;177(3):G1–g70. https://doi.org/10.1530/eje-17-0430.
47. Silberbach M, Roos-Hesselink JW, Andersen NH, Braverman AC, Brown N, Collins RT, et al. Cardiovascular health in Turner syndrome: a scientific statement from the American Heart Association. Circ Genom Prec Med. 2018;11(10):e000048. https://doi.org/10.1161/hcg.0000000000000048.
48. Fuchs MM, Attenhofer Jost C, Babovic-Vuksanovic D, Connolly HM, Egbe A. Long-term outcomes in patients with turner syndrome: a 68-year follow-up. J Am Heart Assoc. 2019;8(11):e011501. https://doi.org/10.1161/jaha.118.011501.
49. Redon R, Ishikawa S, Fitch KR, Feuk L, Perry GH, Andrews TD, et al. Global variation in copy number in the human genome. Nature. 2006;444(7118):444–54. https://doi.org/10.1038/nature05329.
50. Gibbs RA, Belmont JW, Hardenbol P, Willis TD, Yu F, Yang H, et al. The international HapMap project. Nature. 2003;426(6968):789–96. https://doi.org/10.1038/nature02168.
51. Glessner JT, Bick AG, Ito K, Homsy J, Rodriguez-Murillo L, Fromer M, et al. Increased frequency of de novo copy number variants in congenital heart disease by integrative analysis of single nucleotide polymorphism array and exome sequence data. Circ Res. 2014;115(10):884–96. https://doi.org/10.1161/circresaha.115.304458.
52. Soemedi R, Wilson IJ, Bentham J, Darlay R, Töpf A, Zelenika D, et al. Contribution of global rare copy-number variants to the risk of sporadic congenital heart disease. Am J Hum Genet. 2012;91(3):489–501. https://doi.org/10.1016/j.ajhg.2012.08.003.
53. Breckpot J, Thienpont B, Arens Y, Tranchevent LC, Vermeesch JR, Moreau Y, et al. Challenges of interpreting copy number variation in syndromic and non-syndromic congenital heart defects. Cytogenet Genome Res. 2011;135(3–4):251–9. https://doi.org/10.1159/000331272.
54. Morrow BE, McDonald-McGinn DM, Emanuel BS, Vermeesch JR, Scambler PJ. Molecular genetics of 22q11.2 deletion syndrome. Am J Med Genet A. 2018;176(10):2070–81. https://doi.org/10.1002/ajmg.a.40504.
55. Jerome LA, Papaioannou VE. DiGeorge syndrome phenotype in mice mutant for the T-box gene, Tbx1. Nat Genet. 2001;27(3):286–91. https://doi.org/10.1038/85845.

56. Merscher S, Funke B, Epstein JA, Heyer J, Puech A, Lu MM, et al. TBX1 is responsible for cardiovascular defects in velo-cardio-facial/DiGeorge syndrome. Cell. 2001;104(4):619–29. https://doi.org/10.1016/s0092-8674(01)00247-1.
57. Calmont A, Ivins S, Van Bueren KL, Papangeli I, Kyriakopoulou V, Andrews WD, et al. Tbx1 controls cardiac neural crest cell migration during arch artery development by regulating Gbx2 expression in the pharyngeal ectoderm. Development. 2009;136(18):3173–83. https://doi.org/10.1242/dev.028902.
58. Lindsay EA, Vitelli F, Su H, Morishima M, Huynh T, Pramparo T, et al. Tbx1 haploinsufficieny in the DiGeorge syndrome region causes aortic arch defects in mice. Nature. 2001;410(6824):97–101. https://doi.org/10.1038/35065105.
59. Lewin MB, Lindsay EA, Jurecic V, Goytia V, Towbin JA, Baldini A. A genetic etiology for interruption of the aortic arch type B. Am J Cardiol. 1997;80(4):493–7. https://doi.org/10.1016/s0002-9149(97)00401-3.
60. Arnold JS, Werling U, Braunstein EM, Liao J, Nowotschin S, Edelmann W, et al. Inactivation of Tbx1 in the pharyngeal endoderm results in 22q11DS malformations. Development. 2006;133(5):977–87. https://doi.org/10.1242/dev.02264.
61. Kozel BA, Barak B, Kim CA, Mervis CB, Osborne LR, Porter M, et al. Williams syndrome. Nat Rev Dis Primers. 2021;7(1):42. https://doi.org/10.1038/s41572-021-00276-z.
62. Firth HV, Richards SM, Bevan AP, Clayton S, Corpas M, Rajan D, et al. DECIPHER: database of chromosomal imbalance and phenotype in humans using ensembl resources. Am J Hum Genet. 2009;84(4):524–33. https://doi.org/10.1016/j.ajhg.2009.03.010.
63. Nickerson E, Greenberg F, Keating MT, McCaskill C, Shaffer LG. Deletions of the elastin gene at 7q11.23 occur in approximately 90% of patients with Williams syndrome. Am J Hum Genet. 1995;56(5):1156–61.
64. Li DY, Toland AE, Boak BB, Atkinson DL, Ensing GJ, Morris CA, et al. Elastin point mutations cause an obstructive vascular disease, supravalvular aortic stenosis. Hum Mol Genet. 1997;6(7):1021–8. https://doi.org/10.1093/hmg/6.7.1021.
65. Greenway SC, Pereira AC, Lin JC, DePalma SR, Israel SJ, Mesquita SM, et al. De novo copy number variants identify new genes and loci in isolated sporadic tetralogy of Fallot. Nat Genet. 2009;41(8):931–5. https://doi.org/10.1038/ng.415.
66. Wat MJ, Shchelochkov OA, Holder AM, Breman AM, Dagli A, Bacino C, et al. Chromosome 8p23.1 deletions as a cause of complex congenital heart defects and diaphragmatic hernia. Am J Med Genet A. 2009;149a(8):1661–77. https://doi.org/10.1002/ajmg.a.32896.
67. Bernier R, Steinman KJ, Reilly B, Wallace AS, Sherr EH, Pojman N, et al. Clinical phenotype of the recurrent 1q21.1 copy-number variant. Genet Med. 2016;18(4):341–9. https://doi.org/10.1038/gim.2015.78.
68. Rosenfeld JA, Lacassie Y, El-Khechen D, Escobar LF, Reggin J, Heuer C, et al. New cases and refinement of the critical region in the 1q41q42 microdeletion syndrome. Eur J Med Genet. 2011;54(1):42–9. https://doi.org/10.1016/j.ejmg.2010.10.002.
69. Pehlivan T, Pober BR, Brueckner M, Garrett S, Slaugh R, Van Rheeden R, et al. GATA4 haploinsufficiency in patients with interstitial deletion of chromosome region 8p23.1 and congenital heart disease. Am J Med Genet. 1999;83(3):201–6.
70. Ellesøe SG, Workman CT, Bouvagnet P, Loffredo CA, McBride KL, Hinton RB, et al. Familial co-occurrence of congenital heart defects follows distinct patterns. Eur Heart J. 2018;39(12):1015–22. https://doi.org/10.1093/eurheartj/ehx314.
71. Øyen N, Poulsen G, Boyd HA, Wohlfahrt J, Jensen PK, Melbye M. Recurrence of congenital heart defects in families. Circulation. 2009;120(4):295–301. https://doi.org/10.1161/circulationaha.109.857987.
72. Michaelovsky E, Frisch A, Carmel M, Patya M, Zarchi O, Green T, et al. Genotype-phenotype correlation in 22q11.2 deletion syndrome. BMC Med Genet. 2012;13:122. https://doi.org/10.1186/1471-2350-13-122.

73. Zenker M, Buheitel G, Rauch R, Koenig R, Bosse K, Kress W, et al. Genotype-phenotype correlations in Noonan syndrome. J Pediatr. 2004;144(3):368–74. https://doi.org/10.1016/j.jpeds.2003.11.032.
74. Li AH, Hanchard NA, Furthner D, Fernbach S, Azamian M, Nicosia A, et al. Whole exome sequencing in 342 congenital cardiac left sided lesion cases reveals extensive genetic heterogeneity and complex inheritance patterns. Genome Med. 2017;9(1):95. https://doi.org/10.1186/s13073-017-0482-5.
75. Blue GM, Kirk EP, Giannoulatou E, Sholler GF, Dunwoodie SL, Harvey RP, et al. Advances in the genetics of congenital heart disease: a Clinician's guide. J Am Coll Cardiol. 2017;69(7):859–70. https://doi.org/10.1016/j.jacc.2016.11.060.
76. Edwards JJ, Gelb BD. Genetics of congenital heart disease. Curr Opin Cardiol. 2016;31(3):235–41. https://doi.org/10.1097/hco.0000000000000274.
77. Liu X, Yagi H, Saeed S, Bais AS, Gabriel GC, Chen Z, et al. The complex genetics of hypoplastic left heart syndrome. Nat Genet. 2017;49(7):1152–9. https://doi.org/10.1038/ng.3870.
78. Wu Y, Jin X, Zhang Y, Zheng J, Yang R. Genetic and epigenetic mechanisms in the development of congenital heart diseases. World J Pediatr Surg. 2021;4(2):e000196. https://doi.org/10.1136/wjps-2020-000196.
79. Du Q, de la Morena MT, van Oers NSC. The genetics and epigenetics of 22q11.2 deletion syndrome. Front Genet. 2019;10:1365. https://doi.org/10.3389/fgene.2019.01365.
80. Sheng W, Qian Y, Wang H, Ma X, Zhang P, Diao L, et al. DNA methylation status of NKX2-5, GATA4 and HAND1 in patients with tetralogy of Fallot. BMC Med Genet. 2013;6:46. https://doi.org/10.1186/1755-8794-6-46.
81. Sheng W, Qian Y, Zhang P, Wu Y, Wang H, Ma X, et al. Association of promoter methylation statuses of congenital heart defect candidate genes with Tetralogy of Fallot. J Transl Med. 2014;12:31. https://doi.org/10.1186/1479-5876-12-31.
82. Chamberlain AA, Lin M, Lister RL, Maslov AA, Wang Y, Suzuki M, et al. DNA methylation is developmentally regulated for genes essential for cardiogenesis. J Am Heart Assoc. 2014;3(3):e000976. https://doi.org/10.1161/jaha.114.000976.
83. Øyen N, Diaz LJ, Leirgul E, Boyd HA, Priest J, Mathiesen ER, et al. Prepregnancy diabetes and offspring risk of congenital heart disease: a nationwide cohort study. Circulation. 2016;133(23):2243–53. https://doi.org/10.1161/circulationaha.115.017465.
84. Liu S, Liu J, Tang J, Ji J, Chen J, Liu C. Environmental risk factors for congenital heart disease in the Shandong Peninsula, China: a hospital-based case-control study. J Epidemiol. 2009;19(3):122–30. https://doi.org/10.2188/jea.je20080039.
85. Kalisch-Smith JI, Ved N, Sparrow DB. Environmental risk factors for congenital heart disease. Cold Spring Harb Perspect Biol. 2020;12(3):a037234. https://doi.org/10.1101/cshperspect.a037234.
86. Jenkins KJ, Correa A, Feinstein JA, Botto L, Britt AE, Daniels SR, et al. Noninherited risk factors and congenital cardiovascular defects: current knowledge: a scientific statement from the American Heart Association Council on Cardiovascular Disease in the Young: endorsed by the American Academy of Pediatrics. Circulation. 2007;115(23):2995–3014. https://doi.org/10.1161/circulationaha.106.183216.
87. Ionescu-Ittu R, Marelli AJ, Mackie AS, Pilote L. Prevalence of severe congenital heart disease after folic acid fortification of grain products: time trend analysis in Quebec, Canada. BMJ. 2009;338:b1673. https://doi.org/10.1136/bmj.b1673.
88. Liu S, Joseph KS, Luo W, León JA, Lisonkova S, Van den Hof M, et al. Effect of folic acid food fortification in Canada on congenital heart disease subtypes. Circulation. 2016;134(9):647–55. https://doi.org/10.1161/circulationaha.116.022126.
89. van Beynum IM, Kapusta L, den Heijer M, Vermeulen SH, Kouwenberg M, Daniëls O, et al. Maternal MTHFR 677C>T is a risk factor for congenital heart defects: effect modification by periconceptional folate supplementation. Eur Heart J. 2006;27(8):981–7. https://doi.org/10.1093/eurheartj/ehi815.

90. Tang LS, Wlodarczyk BJ, Santillano DR, Miranda RC, Finnell RH. Developmental consequences of abnormal folate transport during murine heart morphogenesis. Birth Defects Res A Clin Mol Teratol. 2004;70(7):449–58. https://doi.org/10.1002/bdra.20043.
91. Liu S, Joseph KS, Lisonkova S, Rouleau J, Van den Hof M, Sauve R, et al. Association between maternal chronic conditions and congenital heart defects: a population-based cohort study. Circulation. 2013;128(6):583–9. https://doi.org/10.1161/circulationaha.112.001054.
92. Zhao L, Chen L, Yang T, Wang L, Wang T, Zhang S, et al. Parental smoking and the risk of congenital heart defects in offspring: an updated meta-analysis of observational studies. Eur J Prev Cardiol. 2020;27(12):1284–93. https://doi.org/10.1177/2047487319831367.
93. Helle E, Priest JR. Maternal obesity and diabetes mellitus as risk factors for congenital heart disease in the offspring. J Am Heart Assoc. 2020;9(8):e011541. https://doi.org/10.1161/jaha.119.011541.
94. Winston JB, Schulkey CE, Chen IB, Regmi SD, Efimova M, Erlich JM, et al. Complex trait analysis of ventricular septal defects caused by Nkx2-5 mutation. Circ Cardiovasc Genet. 2012;5(3):293–300. https://doi.org/10.1161/circgenetics.111.961136.
95. Ison HE, Griffin EL, Parrott A, Shikany AR, Meyers L, Thomas MJ, et al. Genetic counseling for congenital heart disease - practice resource of the national society of genetic counselors. J Genet Couns. 2021;31:9–33. https://doi.org/10.1002/jgc4.1498.
96. Griffin EL, Nees SN, Morton SU, Wynn J, Patel N, Jobanputra V, et al. Evidence-based assessment of congenital heart disease genes to enable returning results in a genomic study. Circ Genom Prec Med. 2023;16(2):e003791. https://doi.org/10.1161/circgen.122.003791.
97. Miller DT, Adam MP, Aradhya S, Biesecker LG, Brothman AR, Carter NP, et al. Consensus statement: chromosomal microarray is a first-tier clinical diagnostic test for individuals with developmental disabilities or congenital anomalies. Am J Hum Genet. 2010;86(5):749–64. https://doi.org/10.1016/j.ajhg.2010.04.006.
98. De Backer J, Muiño ML. Genetic testing in patients with congenital heart disease: you do no harm when using the right tools! Circ Genom Prec Med. 2023;16(2):e004104. https://doi.org/10.1161/circgen.123.004104.
99. Blue GM, Kasparian NA, Sholler GF, Kirk EP, Winlaw DS. Genetic counselling in parents of children with congenital heart disease significantly improves knowledge about causation and enhances psychosocial functioning. Int J Cardiol. 2015;178:124–30. https://doi.org/10.1016/j.ijcard.2014.10.119.
100. van Engelen K, Baars MJ, Felix JP, Postma AV, Mulder BJ, Smets EM. The value of the clinical geneticist caring for adults with congenital heart disease: diagnostic yield and patients' perspective. Am J Med Genet A. 2013;161a(7):1628-37:1628. https://doi.org/10.1002/ajmg.a.35973.
101. Mercer-Rosa L, Pinto N, Yang W, Tanel R, Goldmuntz E. 22q11.2 Deletion syndrome is associated with perioperative outcome in tetralogy of Fallot. J Thorac Cardiovasc Surg. 2013;146(4):868–73. https://doi.org/10.1016/j.jtcvs.2012.12.028.
102. Simmons MA, Brueckner M. The genetics of congenital heart disease. . . understanding and improving long-term outcomes in congenital heart disease: a review for the general cardiologist and primary care physician. Curr Opin Pediatr. 2017;29(5):520–8. https://doi.org/10.1097/mop.0000000000000538.
103. Frank D, Yusuf Rangrez A, Friedrich C, Dittmann S, Stallmeyer B, Yadav P, et al. Cardiac α-actin (ACTC1) gene mutation causes atrial-septal defects associated with late-onset dilated cardiomyopathy. Circ Genom Prec Med. 2019;12(8):e002491. https://doi.org/10.1161/circgen.119.002491.
104. Van den Veyver IB. Recent advances in prenatal genetic screening and testing. F1000Research. 2016;5:2591. https://doi.org/10.12688/f1000research.9215.1.
105. Chong HP, Hamilton S, Mone F, Cheung KW, Togneri FS, Morris RK, et al. Prenatal chromosomal microarray testing of fetuses with ultrasound structural anomalies: a prospective cohort study of over 1000 consecutive cases. Prenat Diagn. 2019;39(12):1064–9. https://doi.org/10.1002/pd.5545.

106. Mone F, Stott BK, Hamilton S, Seale AN, Quinlan-Jones E, Allen S, et al. The diagnostic yield of prenatal genetic technologies in congenital heart disease: a prospective cohort study. Fetal Diagn Ther. 2021;48:1–8. https://doi.org/10.1159/000512488.
107. Vermeesch JR, Voet T, Devriendt K. Prenatal and pre-implantation genetic diagnosis. Nat Rev Genet. 2016;17(10):643–56. https://doi.org/10.1038/nrg.2016.97.
108. Skrzypek H, Hui L. Noninvasive prenatal testing for fetal aneuploidy and single gene disorders. Best Pract Res Clin Obstet Gynaecol. 2017;42:26–38. https://doi.org/10.1016/j.bpobgyn.2017.02.007.
109. Scotchman E, Chandler NJ, Mellis R, Chitty LS. Noninvasive prenatal diagnosis of single-gene diseases: the next frontier. Clin Chem. 2020;66(1):53–60. https://doi.org/10.1373/clinchem.2019.304238.
110. Gregg AR, Skotko BG, Benkendorf JL, Monaghan KG, Bajaj K, Best RG, et al. Noninvasive prenatal screening for fetal aneuploidy, 2016 update: a position statement of the American College of Medical Genetics and Genomics. Genet Med. 2016;18(10):1056–65. https://doi.org/10.1038/gim.2016.97.
111. Lincoln SE, Hambuch T, Zook JM, Bristow SL, Hatchell K, Truty R, et al. One in seven pathogenic variants can be challenging to detect by NGS: an analysis of 450,000 patients with implications for clinical sensitivity and genetic test implementation. Genet Med. 2021;23:1673. https://doi.org/10.1038/s41436-021-01187-w.
112. Richards S, Aziz N, Bale S, Bick D, Das S, Gastier-Foster J, et al. Standards and guidelines for the interpretation of sequence variants: a joint consensus recommendation of the American College of Medical Genetics and Genomics and the Association for Molecular Pathology. Genet Med. 2015;17(5):405–24. https://doi.org/10.1038/gim.2015.30.
113. Godard B, Raeburn S, Pembrey M, Bobrow M, Farndon P, Aymé S. Genetic information and testing in insurance and employment: technical, social and ethical issues. Eur J Hum Genet. 2003;11(Suppl 2):S123–42. https://doi.org/10.1038/sj.ejhg.5201117.
114. Clifton JM, VanBeuge SS, Mladenka C, Wosnik KK. The genetic information nondiscrimination act 2008: what clinicians should understand. J Am Acad Nurse Pract. 2010;22(5):246–9. https://doi.org/10.1111/j.1745-7599.2010.00504.x.
115. van El CG, Cornel MC, Borry P, Hastings RJ, Fellmann F, Hodgson SV, et al. Whole-genome sequencing in health care: recommendations of the European Society of Human Genetics. Eur J Hum Genet. 2013;21(6):580–4. https://doi.org/10.1038/ejhg.2013.46.
116. ACMG Board of Directors. ACMG policy statement: updated recommendations regarding analysis and reporting of secondary findings in clinical genome-scale sequencing. Genet Med. 2015;17(1):68–9. https://doi.org/10.1038/gim.2014.151.
117. Green RC, Berg JS, Grody WW, Kalia SS, Korf BR, Martin CL, et al. ACMG recommendations for reporting of incidental findings in clinical exome and genome sequencing. Genet Med. 2013;15(7):565–74. https://doi.org/10.1038/gim.2013.73.
118. Mullen M, Zhang A, Lui GK, Romfh AW, Rhee JW, Wu JC. Race and genetics in congenital heart disease: application of iPSCs, omics, and machine learning technologies. Front Cardiovas Med. 2021;8:635280. https://doi.org/10.3389/fcvm.2021.635280.
119. Mudd-Martin G, Cirino AL, Barcelona V, Fox K, Hudson M, Sun YV, et al. Considerations for cardiovascular genetic and genomic research with marginalized racial and ethnic groups and indigenous peoples: a scientific statement from the American Heart Association. Circ Genom Prec Med. 2021;14(4):e000084. https://doi.org/10.1161/hcg.0000000000000084.
120. Boskovski MT, Homsy J, Nathan M, Sleeper LA, Morton S, Manheimer KB, et al. De novo damaging variants, clinical phenotypes, and post-operative outcomes in congenital heart disease. Circ Genom Prec Med. 2020;13(4):e002836. https://doi.org/10.1161/circgen.119.002836.
121. Krane M, Dreßen M, Santamaria G, My I, Schneider CM, Dorn T, et al. Sequential defects in cardiac lineage commitment and maturation cause hypoplastic left heart syndrome. Circulation. 2021;144(17):1409–28. https://doi.org/10.1161/circulationaha.121.056198.

122. Gelb BD. Prospects for precision genetic medicine in congenital heart disease. Curr Opin Genet Dev. 2022;77:101983. https://doi.org/10.1016/j.gde.2022.101983.
123. Minette MS, Sahn DJ. Ventricular septal defects. Circulation. 2006;114(20):2190–7. https://doi.org/10.1161/circulationaha.106.618124.
124. Lopez L, Houyel L, Colan SD, Anderson RH, Béland MJ, Aiello VD, et al. Classification of ventricular septal defects for the eleventh iteration of the international classification of diseases-striving for consensus: a report from the International Society for Nomenclature of Paediatric and Congenital Heart Disease. Ann Thorac Surg. 2018;106(5):1578–89. https://doi.org/10.1016/j.athoracsur.2018.06.020.
125. Bergström S, Carr H, Petersson G, Stephansson O, Bonamy AK, Dahlström A, et al. Trends in congenital heart defects in infants with down syndrome. Pediatrics. 2016;138(1):e20160123. https://doi.org/10.1542/peds.2016-0123.
126. Diaz D, Benjamin RH, Navarro Sanchez ML, Mitchell LE, Langlois PH, Canfield MA, et al. Patterns of congenital anomalies among individuals with trisomy 13 in Texas. Am J Med Genet A. 2021;185(6):1787–93. https://doi.org/10.1002/ajmg.a.62175.
127. Toscano A, Anaclerio S, Digilio MC, Giannotti A, Fariello G, Dallapiccola B, et al. Ventricular septal defect and deletion of chromosome 22q11: anatomical types and aortic arch anomalies. Eur J Pediatr. 2002;161(2):116–7. https://doi.org/10.1007/s00431-001-0877-5.
128. Burd L, Deal E, Rios R, Adickes E, Wynne J, Klug MG. Congenital heart defects and fetal alcohol spectrum disorders. Congenit Heart Dis. 2007;2(4):250–5. https://doi.org/10.1111/j.1747-0803.2007.00105.x.
129. Correa A, Gilboa SM, Besser LM, Botto LD, Moore CA, Hobbs CA, et al. Diabetes mellitus and birth defects. Am J Obstet Gynecol. 2008;199(3):237.e1–9. https://doi.org/10.1016/j.ajog.2008.06.028.
130. Yang YQ, Wang J, Liu XY, Chen XZ, Zhang W, Wang XZ, et al. Novel GATA4 mutations in patients with congenital ventricular septal defects. Med Sci Monit. 2012;18(6):Cr344–50. https://doi.org/10.12659/msm.882877.
131. Zhang W, Li X, Shen A, Jiao W, Guan X, Li Z. GATA4 mutations in 486 Chinese patients with congenital heart disease. Eur J Med Genet. 2008;51(6):527–35. https://doi.org/10.1016/j.ejmg.2008.06.005.
132. Peng T, Wang L, Zhou SF, Li X. Mutations of the GATA4 and NKX2.5 genes in Chinese pediatric patients with non-familial congenital heart disease. Genetica. 2010;138(11–12):1231–40. https://doi.org/10.1007/s10709-010-9522-4.
133. Briggs LE, Kakarla J, Wessels A. The pathogenesis of atrial and atrioventricular septal defects with special emphasis on the role of the dorsal mesenchymal protrusion. Differentiation. 2012;84(1):117–30. https://doi.org/10.1016/j.diff.2012.05.006.
134. Celermajer DS. Atrial septal defects: even simple congenital heart diseases can be complicated. Eur Heart J. 2018;39(12):999–1001. https://doi.org/10.1093/eurheartj/ehx633.
135. Hirayama-Yamada K, Kamisago M, Akimoto K, Aotsuka H, Nakamura Y, Tomita H, et al. Phenotypes with GATA4 or NKX2.5 mutations in familial atrial septal defect. Am J Med Genet A. 2005;135(1):47–52. https://doi.org/10.1002/ajmg.a.30684.
136. Lin X, Huo Z, Liu X, Zhang Y, Li L, Zhao H, et al. A novel GATA6 mutation in patients with tetralogy of Fallot or atrial septal defect. J Hum Genet. 2010;55(10):662–7. https://doi.org/10.1038/jhg.2010.84.
137. Matsson H, Eason J, Bookwalter CS, Klar J, Gustavsson P, Sunnegardh J, et al. Alpha-cardiac actin mutations produce atrial septal defects. Hum Mol Genet. 2008;17(2):256–65.
138. Rastelli G, Kirklin JW, Titus JL. Anatomic observations on complete form of persistent common atrioventricular canal with special reference to atrioventricular valves. Mayo Clin Proc. 1966;41(5):296–308.
139. Tubman TR, Shields MD, Craig BG, Mulholland HC, Nevin NC. Congenital heart disease in Down's syndrome: two year prospective early screening study. BMJ. 1991;302(6790):1425–7. https://doi.org/10.1136/bmj.302.6790.1425.

140. Benhaourech S, Drighil A, Hammiri AE. Congenital heart disease and Down syndrome: various aspects of a confirmed association. Cardiovasc J Afr. 2016;27(5):287–90. https://doi.org/10.5830/cvja-2016-019.
141. Freeman SB, Taft LF, Dooley KJ, Allran K, Sherman SL, Hassold TJ, et al. Population-based study of congenital heart defects in Down syndrome. Am J Med Genet. 1998;80(3):213–7.
142. Hartman RJ, Riehle-Colarusso T, Lin A, Frías JL, Patel SS, Duwe K, et al. Descriptive study of nonsyndromic atrioventricular septal defects in the National Birth Defects Prevention Study, 1997-2005. Am J Med Genet A. 2011;155a(3):555–64. https://doi.org/10.1002/ajmg.a.33874.
143. Digilio MC, Pugnaloni F, De Luca A, Calcagni G, Baban A, Dentici ML, et al. Atrioventricular canal defect and genetic syndromes: the unifying role of sonic hedgehog. Clin Genet. 2019;95(2):268–76. https://doi.org/10.1111/cge.13375.
144. Rajagopal SK, Ma Q, Obler D, Shen J, Manichaikul A, Tomita-Mitchell A, et al. Spectrum of heart disease associated with murine and human GATA4 mutation. J Mol Cell Cardiol. 2007;43(6):677–85. https://doi.org/10.1016/j.yjmcc.2007.06.004.
145. Campbell IM, Sheppard SE, Crowley TB, McGinn DE, Bailey A, McGinn MJ, et al. What is new with 22q? An update from the 22q and You Center at the Children's Hospital of Philadelphia. Am J Med Genet A. 2018;176(10):2058–69. https://doi.org/10.1002/ajmg.a.40637.
146. Cancrini C, Puliafito P, Digilio MC, Soresina A, Martino S, Rondelli R, et al. Clinical features and follow-up in patients with 22q11.2 deletion syndrome. J Pediatr. 2014;164(6):1475–80.e2. https://doi.org/10.1016/j.jpeds.2014.01.056.
147. Poirsier C, Besseau-Ayasse J, Schluth-Bolard C, Toutain J, Missirian C, Le Caignec C, et al. A French multicenter study of over 700 patients with 22q11 deletions diagnosed using FISH or aCGH. Eur J Hum Genet. 2016;24(6):844–51. https://doi.org/10.1038/ejhg.2015.219.
148. Bermudez BE, Medeiros SL, Bermudez MB, Novadzki IM, Magdalena NI. Down syndrome: prevalence and distribution of congenital heart disease in Brazil. Sao Paulo Med J. 2015;133(6):521–4. https://doi.org/10.1590/1516-3180.2015.00710108.
149. Goldmuntz E, Geiger E, Benson DW. NKX2.5 mutations in patients with tetralogy of Fallot. Circulation. 2001;104(21):2565–8.
150. De Luca A, Sarkozy A, Ferese R, Consoli F, Lepri F, Dentici ML, et al. New mutations in ZFPM2/FOG2 gene in tetralogy of Fallot and double outlet right ventricle. Clin Genet. 2011;80(2):184–90. https://doi.org/10.1111/j.1399-0004.2010.01523.x.
151. Donadille B, Rousseau A, Zenaty D, Cabrol S, Courtillot C, Samara-Boustani D, et al. Cardiovascular findings and management in Turner syndrome: insights from a French cohort. Eur J Endocrinol. 2012;167(4):517–22. https://doi.org/10.1530/eje-12-0434.
152. Tagariello A, Breuer C, Birkner Y, Schmidt S, Koch AM, Cesnjevar R, et al. Functional null mutations in the gonosomal homologue gene TBL1Y are associated with non-syndromic coarctation of the aorta. Curr Mol Med. 2012;12(2):199–205. https://doi.org/10.2174/156652412798889027.
153. McElhinney DB, Krantz ID, Bason L, Piccoli DA, Emerick KM, Spinner NB, et al. Analysis of cardiovascular phenotype and genotype-phenotype correlation in individuals with a JAG1 mutation and/or Alagille syndrome. Circulation. 2002;106(20):2567–74. https://doi.org/10.1161/01.cir.0000037221.45902.69.
154. Bjornsson T, Thorolfsdottir RB, Sveinbjornsson G, Sulem P, Norddahl GL, Helgadottir A, et al. A rare missense mutation in MYH6 associates with non-syndromic coarctation of the aorta. Eur Heart J. 2018;39(34):3243–9. https://doi.org/10.1093/eurheartj/ehy142.

Cardiac Development and Animal Models of Congenital Heart Defects

3

Robert G. Kelly

Abstract

The major events of cardiac development, including early heart formation, chamber morphogenesis and septation, and conduction system and coronary artery development, are briefly reviewed together with a short introduction to the animal species commonly used to study heart development and model congenital heart defects (CHDs).

Keywords

Cardiac crescent · Heart tube · Venous pole · Arterial pole · Cardiac progenitor cells · Pharyngeal mesoderm · Second heart field · Outflow tract · Pharyngeal arch arteries · T-box 1 · Left–right axis · Tetralogy of Fallot · Double outlet right ventricle · Atrioventricular septal defect · Looping · Endocardial cushions · Atrioventricular canal · Atrioventricular cushions · Cardiac neural crest cells · Septation · Cardiac conduction system · Purkinje fibers · Trabeculae · Endocardium · Epicardium · Mouse · Chick · Xenopus · *N*-ethyl-*N*-nitrosourea · Zebrafish · *Ciona intestinalis* · *Drosophila melanogaster* · NKX2–5 · Common arterial trunk

R. G. Kelly (✉)
Aix Marseille Université, Institut de Biologie du Dévelopment de Marseille, Marseille, France
e-mail: Robert.Kelly@univ-amu.fr

© The Author(s), under exclusive license to Springer Nature Switzerland AG 2024

S. Rickert-Sperling et al. (eds.), *Congenital Heart Diseases: The Broken Heart*,
Advances in Experimental Medicine and Biology 1441,
https://doi.org/10.1007/978-3-031-44087-8_3

3.1 Introduction

This chapter provides a brief overview of the major events of cardiac development and the animal models used to study the developing heart. We will focus on the sequence of events that occur during mouse heart development and the principal animal model used for genetic studies of heart development. Mouse heart development and the structure of the definitive mouse heart are highly conserved with humans, with evident differences in scale, both temporal and spatial [1]. The advantages of using mouse models are discussed in the animal models section below, and these have led to the generation of numerous mouse congenital heart defect (CHD) models [2, 3]. The goal here is to provide a brief introduction to the chapters in Part I as well as to the pathways and models sections; the majority of the references in this introductory chapter are reviews, to which the reader seeking further information is directed. For a detailed description of human heart development, the reader is referred to the chapter by Lamers and colleagues as well as to embryology textbooks such as Larsen's *Human Embryology* or Langman's *Medical Embryology* [4, 5].

3.2 From the Cardiac Crescent to the Embryonic Heart Tube

The middle week of mouse gestation, corresponding approximately to weeks 2–5 of human embryonic development, spans the onset of cardiac differentiation through to the completion of cardiac septation (Fig. 3.1). Cardiomyocytes first differentiate in the most anterior lateral region of the splanchnic mesoderm underlying the neural folds [6]. Bilateral cardiac progenitor populations converge at the ventral midline to generate the cardiac crescent by embryonic day (E) 7.5 (Figure 3.1a). These myocardial cells are specified by a combination of positive intercellular signals from surrounding embryonic tissues, including foregut endoderm and surface ectoderm, and negative signals from midline structures. These inputs result in the precise activation of cardiac transcription factors that combinatorially drive the cardiomyogenic program in the cardiac crescent [7].

The cardiac crescent gives rise to a transiently linear heart tube, with a posterior venous pole and an anterior arterial pole, surrounding an endocardial tube; these early differentiating cardiomyocytes contribute to the apex of the left ventricle in the definitive heart (Figure 3.1b). Cardiac progenitor cells in the pharyngeal mesoderm adjacent to the early heart tube subsequently add to the growing cardiac poles, giving rise to right ventricular and outflow tract myocardium at the arterial pole and atrial myocardium at the venous pole [8]. These progenitor cells, known as the second heart field (Chap. 5) and discovered in 2001, thus form the major part of the heart, including the entire outflow tract or conotruncal region, connected to the pharyngeal arch arteries. Progressive addition of second heart field cells is regulated by diverse signals from pharyngeal epithelia and neural crest-derived mesenchyme, which are, in turn, integrated by transcription factors such as that encoded by the 22q11.2

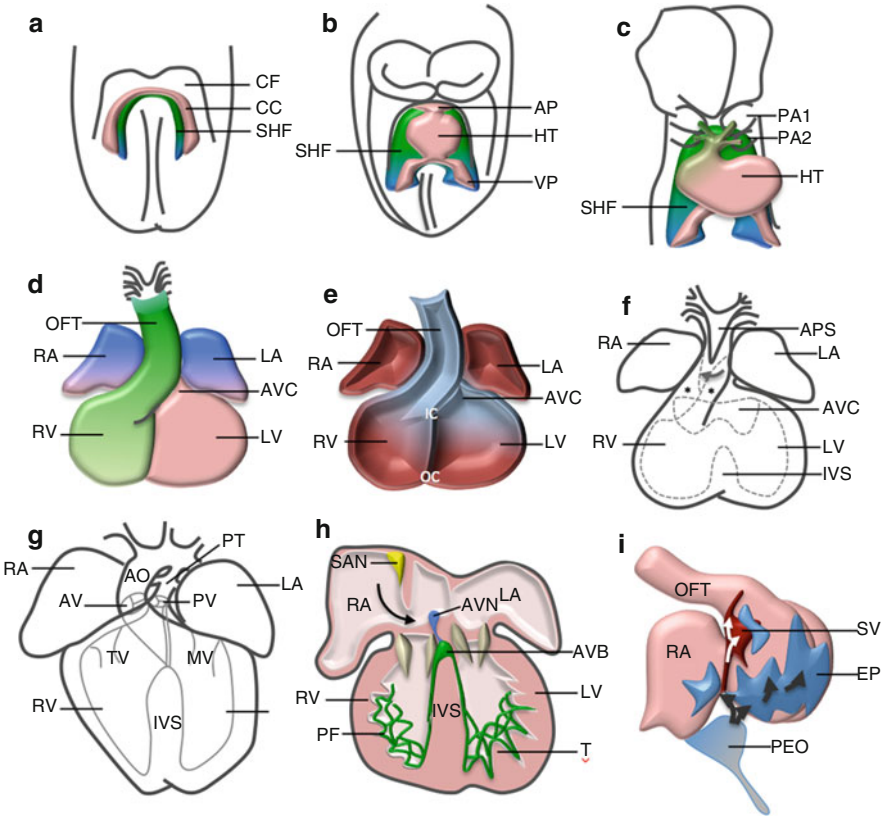

Fig. 3.1 Mouse heart development. Cartoon showing the major events in mouse heart development. (a–d) From the cardiac crescent (E7.5, A), through linear (E8, b) and looping (E8.5, c) stages to the mid-gestation embryonic heart tube (E10.5, d). The cardiac crescent and its linear heart tube and left ventricular derivatives are pink, and the second heart field and derivatives are green (arterial pole) and blue (venous pole). At mid-gestation, the atrial and ventricular chamber myocardium (red) expands by proliferation at the outer curvature of the heart tube (e). Cardiac septation is underway at E11.5 (f); the interventricular and aorticopulmonary septa and outflow tract cushions (asterisks) are evident, and the outflow tract rotates in a counterclockwise direction (arrow). Cardiac septation is complete by E14.5 (g), including division of the outflow tract into the ascending aorta and pulmonary trunk. Cardiac cushions have remodeled to form atrioventricular (tricuspid and mitral) and outlet valves (aortic and pulmonary). At this stage, differentiation of the cardiac conduction system is underway (h); the arrow shows the direction of propagation of the electrical signal in atrial myocardium. The epicardium spreads over the ventricular surface from the proepicardial organ from E10.5 (i, right lateral view), and sinus venosus-derived cells contribute to coronary vascular endothelium. Cartoons (a–i) adapted from [1]. Key: CF cephalic fold, AO aorta, AP arterial pole, APS aorticopulmonary septum, AV aortic valve, AVB atrioventricular bundle, AVC atrioventricular canal, AVN atrioventricular node, CC cardiac crescent, EP epicardium, IC inner curvature, IVS interventricular septum, LA left atrium, LV left ventricle, MV mitral valve, NT heart tube, OC outer curvature, OFT outflow tract, PA1 first pharyngeal arch, PA2 second pharyngeal arch, PEO proepicardial organ, PF Purkinje fiber network, PT pulmonary trunk, PV pulmonary valve, RA right atrium, RV right ventricle, SAN sinoatrial node, SHF second heart field, SV sinus venosus-derived endothelial cells, T trabeculae, TV tricuspid valve, VP venous pole

deletion (or DiGeorge) syndrome gene *TBX1* [9–12]. Defective addition of second heart field cells results in a spectrum of common congenital heart defects, ranging from conotruncal anomalies such as tetralogy of Fallot and double outlet right ventricle to venous poles defects, including atrial and atrioventricular septal defects. Rightward looping of the elongating heart tube is the first morphological manifestation of the embryonic left–right axis (Figure 3.1c). The left–right axis (Chap. 9) is established in the node during gastrulation and results in the activation of lateralized signaling information that is transmitted to asymmetrically developing organs such as the heart [13]. Dissection of the regulation of second heart field deployment and the establishment and transmission of laterality information are considered to be key steps in understanding the mechanisms underlying common forms of CHDs [14]. Indeed, the second heart field has recently been identified as a driving force that provides directionality to the heart loop [15].

3.3 Ballooning Morphogenesis and Cardiac Septation

By mid-gestation (E10.5), looping and heart tube extension are complete (Figure 3.1d). Subsequent growth of the heart occurs by proliferation of atrial and ventricular cardiomyocytes in the outer curvature of the heart tube, a process known as the ballooning model of chamber morphogenesis (Figure 3.1e). Patterned proliferation in the embryonic heart is regulated by transcription factors, in particular members of the T-box family, which are expressed in overlapping patterns in the early heart and define the atrioventricular canal and outflow tract as regions of low proliferation where endocardial cushions develop [16]. Cushions contain mesenchymal cells that are derived from the endocardium by a process of epithelial-to-mesenchymal transformation in response to overlying myocardial signals. The atrioventricular canal and outflow tract regulate directional blood flow through the early heart by valve-like cushion function and reduced myocardial electrical coupling. At this stage, cardiac septation initiates, dividing the heart into separate left and right chambers. The primary atrial septum converges with the developing endocardial cushions in the atrioventricular region. Addition of second heart field progenitor cells at the venous pole (Chap. 7) of the heart is essential for formation of a structure termed the dorsal mesenchymal protrusion that forms the muscular base of the primary atrial septum and plays a critical role in atrioventricular septation [17]. Atrioventricular cushions also connect with the interventricular septum, developing at the interface between the linear heart tube and second heart field-derived myocardium, i.e., future left (systemic) and right (pulmonary) ventricles. At the arterial pole, the influx of cardiac neural crest cells (Chap. 6) is essential for division of the outflow tract into the ascending aorta and pulmonary trunk (outlets of the left and right ventricles, respectively) through formation of the aorticopulmonary septum and outflow tract cushion fusion (Figure 3.1f). Neural crest cells also play a critical role in regulating progenitor cell deployment during heart tube elongation. Defects in neural crest cell development result in a spectrum of conotruncal defects, including common arterial trunk [18].

The endocardial cushions are remodeled during septation to form the definitive tricuspid, mitral, aortic, and pulmonary valves that regulate blood to and from the ventricular chambers (Figure 3.1g). The conotruncal region rotates in a counter-clockwise direction under influence of the embryonic laterality cascade and the aorta aligns with the left ventricle through a process termed wedging. Perturbation of cardiac septation results in failure to make the exclusive connection between the ascending aorta and left ventricle, which is essential for separating the systemic and pulmonary circulatory systems at birth. Defects in either heart tube elongation, which generates the template for septation, or in the septation process itself, thus result in a range of CHDs. Systemic and pulmonary circulatory systems are fully isolated at birth by the closure of the oval foramen and ductus arteriosus.

3.4 Development of the Conduction System and Coronary Circulation

Chamber development is accompanied by establishment of the definitive cardiac conduction system (Chap. 10) that regulates cardiac rhythm (Figure 3.1h). Electrical activity is triggered by the pacemaker, or sinoatrial node, in the sinus venous region. Conduction between the atria and ventricles is delayed by the atrioventricular node, ensuring sequential atrial and ventricular contraction. The electrical signal initiates apical ventricular contraction through the atrioventricular bundle, bundle branches, and the Purkinje fiber network. Conductive cells are specialized myocytes and share common progenitor cells with nonconducting myocytes [19]. Defects in the establishment of the electrical wiring of the heart result in arrhythmias and conduction blocks. The Purkinje fiber system develops adjacent to the ventricular lumen in trabecular myocytes, transient projections of the myocardium that form by signal exchange between the myocardial wall and endocardium. Trabeculae are present in the mouse heart from mid-gestation to fetal stages when a process of compaction generates the definitive ventricular wall. Failure of this step results in non-compaction cardiomyopathy.

From E10.5, a third cell layer, the epicardium (Chap. 8), covers the external surface of the heart (Figure 3.1i). The epicardium originates from the proepicardial organ and forms an epithelium from which cells undergo a mesenchymal transition and invade the myocardium, giving rise to smooth muscle cells associated with coronary arteries and cardiac fibroblasts. Signal exchange between the epicardium, epicardially derived fibroblasts, and myocardium plays an important role in regulating myocardial proliferation and differentiation. Coronary vasculature, essential for the delivery of oxygen and nutrients to the myocardium, develops during fetal stages [20]. The origin of coronary endothelial cells is controversial; however, the sinus venosus endothelium and endocardial trapping during compaction are believed to be the two major sources. Coronary smooth muscle cells originate from the epicardium and neural crest-derived cells. Coronary arteries connect with the base of the ascending aorta to form right and left coronary ostia. Abnormal proximal

coronary artery patterning, often associated with conotruncal CHD, is a cause of sudden cardiac death [21].

3.5 Animal Models of Heart Development

The above summary of heart development focuses on the mouse, where cardiogenesis is highly conserved with the human embryo. The mouse provides the advantages of a highly tractable organism for genetic studies [22–24]. Gene targeting, either using homologous recombination in embryonic stem cells or the more recent transcription activator-like effector nuclease (TALEN) or clustered regularly interspaced short palindromic repeat (CRISPR)/CRISPR-associated protein 9 (Cas9) strategies, allows detailed investigation of loss-of-function or potential disease-causing alleles [25, 26]. Conditional and inducible gene inactivation using, for example, Cre recombinase, permits precise temporal and spatial evaluation of gene function. In addition to these reverse genetic approaches, forward genetic screens following mutagenesis with, for example, *N*-ethyl-*N*-nitrosourea (ENU), allow the identification of novel developmental regulators. Powerful state-of-the-art genotyping and phenotyping technologies for characterizing mouse mutants with congenital heart defects are detailed in Chap. 16. In addition, transgenic mice can be used to study the function of gene regulatory sequences, modify gene dosage, or trace genetic lineages to distinct cardiac structures [27]. Organoid models of cardiovascular development using mouse and human cells provide highly tractable in vitro systems for high-throughput screens and disease modeling and can be generated using patient-derived pluripotent stem cells. Recent examples of such approaches include gastruloid and cardioid models that have recapitulate steps of heart development through self-organized or directed differentiation [28, 29]. Mouse embryos can be cultured ex vivo for short periods of time, and the development of microscopic techniques for live imaging of cultured mouse embryos has begun to provide unprecedented resolution of cell dynamics during early heart development [30, 31]. However, despite recent technological advances allowing embryo culture through to fetal stages [32], in utero embryonic development has made the mouse a poor model for experimental embryology. In contrast, the avian system is the model of choice for manipulation of the developing embryo, such as ablation studies, electroporation, or chick-to-quail transplantation experiments [33]. The avian heart is also four-chambered, although great artery development diverges from the mammalian configuration. Although transgenic chick lines are now available and gene and regulatory sequence function can be evaluated by electroporation, the chick is currently not a good model for genetic studies.

Other vertebrate models that will be referred to in the following chapters include the frog and fish [34]. Xenopus has a three-chambered heart, with ventricular septation being incomplete; it is, however, like the chick, a good model for experimental embryology. The zebrafish has two muscular cardiac chambers and is a highly tractable model for questions concerning formation and looping of the heart tube, atrial and ventricular patterning or myocardial differentiation, but not for

studies of cardiac septation, defects of which account for the majority of common human CHDs [35]. The zebrafish is also an extremely powerful system for forward genetic screens and has become the model of choice for the study of cardiac regeneration, which can occur in adult zebrafish, yet is restricted to the days after birth in mammals [36–38]. Finally, two invertebrate models have provided extremely important insights into the genetic regulation of heart development. The protochordate *Ciona intestinalis* has recently been shown to have two cardiac precursor cell populations, similar to the mammalian heart, regulated by conserved transcription factors and signaling pathways, and, evolutionarily more distant, dissection of cardiac development in the fruit fly *Drosophila melanogaster* has revealed that fly and mammalian heart development are regulated by a set of homologous genes [39, 40]. Furthermore, the convergence of cardiac progenitor cells at the dorsal midline of the *Drosophila* embryo is similar to that of cardiac progenitor cells during formation of the vertebrate linear heart tube. Discovery of the fly *Nkx2–5* homologue *Tinman*, a gene essential for formation of the fly heart, was a founding event in the molecular study of heart development [41–43]. Subsequent analysis of *NKX2–5* led to the first mutations identified in human CHD patients, and NKX2–5 remains the most commonly mutated gene in patients with a diverse spectrum of heart defects, thus illustrating the importance of animal models of heart development for the study of CHD [44, 45].

References

1. Miquerol L, Kelly RG. Organogenesis of the vertebrate heart. Wiley Interdiscip Rev Dev Biol. 2013;2:17–29.
2. Moon A. Mouse models of congenital cardiovascular disease. Curr Top Dev Biol. 2008;84:171–248.
3. Houyel L, Meilhac SM. Heart development and congenital structural heart defects. Annu Rev Genomics Hum Genet. 2021;22:257–84.
4. Schoenwolf GC, Bleyl SB, Brauer PR, Francis-West PH. Larsen's Human Embryology. 6th ed. Philadelphia: Elsevier; 2021.
5. Sadler TW. Langman's medical embryology. 12th ed. Philadeplhia: Wolters Kluwer; 2015.
6. Harvey RP. Patterning the vertebrate heart. Nat Rev Genet. 2002;3:544–56.
7. Srivastava D. Making or breaking the heart: from lineage determination to morphogenesis. Cell. 2006;126:1037–48.
8. Kelly RG. The second heart field. Curr Top Dev Biol. 2012;100:33–65.
9. Rochais F, Mesbah K, Kelly RG. Signaling pathways controlling second heart field development. Circ Res. 2009;104:933–42.
10. Dyer LA, Kirby ML. Sonic hedgehog maintains proliferation in secondary heart field progenitors and is required for normal arterial pole formation. Dev Biol. 2009;330:305–17.
11. Vincent SD, Buckingham ME. How to make a heart: the origin and regulation of cardiac progenitor cells. Curr Top Dev Biol. 2010;90:1–41.
12. Baldini A, Fulcoli FG, Illingworth E. Tbx1: transcriptional and developmental functions. Curr Top Dev Biol. 2017;122:223–43.
13. Hamada H. Molecular and cellular basis of left-right asymmetry in vertebrates. Proc Jpn Acad Ser B Phys Biol Sci. 2020;96:273–96.
14. Epstein JA, Franklin H, Lecture E. Cardiac development and implications for heart disease. N Engl J Med. 2010;363:1638–47.

15. Desgrange A, Le Garrec JF, Bernheim S, Bonnelykke TH, Meilhac SM. Transient nodal signaling in left precursors coordinates opposed asymmetries shaping the heart loop. Dev Cell. 2020;55:413–31 e6.
16. Greulich F, Rudat C, Kispert A. Mechanisms of T-box gene function in the developing heart. Cardiovasc Res. 2011;91:212–22.
17. Briggs LE, Kakarla J, Wessels A. The pathogenesis of atrial and atrioventricular septal defects with special emphasis on the role of the dorsal mesenchymal protrusion. Differentiation. 2012;84:117–30.
18. Hutson MR, Kirby ML. Neural crest and cardiovascular development: a 20-year perspective. Birth Defects Res C Embryo Today. 2003;69:2–13.
19. Miquerol L, Moreno-Rascon N, Beyer S, Dupays L, Meilhac SM, Buckingham ME, et al. Biphasic development of the mammalian ventricular conduction system. Circ Res. 2010;107: 153–61.
20. Tian X, Zhou B. Coronary vessel formation in development and regeneration: origins and mechanisms. J Mol Cell Cardiol. 2022;167:67–82.
21. Perez-Pomares JM, de la Pompa JL, Franco D, Henderson D, Ho SY, Houyel L, et al. Congenital coronary artery anomalies: a bridge from embryology to anatomy and pathophysiology--a position statement of the development, anatomy, and pathology ESC Working Group. Cardiovasc Res. 2016;109:204–16.
22. Hogan B, Costantini F, Lacy E. Manipulating the mouse embryo: a laboratory manual. Cold Spring Harbor: Cold Spring Harbor Laboratory Press; 1986.
23. Papaioannou VE, Behringer R. Mouse phneotypes: a handbook of mutation analysis. Cold Spring Harbor: Cold Spring Harbor Laboratory Press; 2005.
24. Gridley T, Murray SA. Mouse mutagenesis and phenotyping to generate models of development and disease. Curr Top Dev Biol. 2022;148:1–12.
25. Sommer D, Peters AE, Baumgart AK, Beyer M. TALEN-mediated genome engineering to generate targeted mice. Chromosom Res. 2015;23:43–55.
26. Yang H, Wang H, Jaenisch R. Generating genetically modified mice using CRISPR/Cas-mediated genome engineering. Nat Protoc. 2014;9:1956–68.
27. Buckingham ME, Meilhac SM. Tracing cells for tracking cell lineage and clonal behavior. Dev Cell. 2011;21:394–409.
28. Rossi G, Broguiere N, Miyamoto M, Boni A, Guiet R, Girgin M, et al. Capturing Cardiogenesis in Gastruloids. Cell Stem Cell. 2021;28:230–40 e6.
29. Hofbauer P, Jahnel SM, Papai N, Giesshammer M, Deyett A, Schmidt C, et al. Cardioids reveal self-organizing principles of human cardiogenesis. Cell. 2021;184:3299–317 e22.
30. Ivanovitch K, Temino S, Torres M. Live imaging of heart tube development in mouse reveals alternating phases of cardiac differentiation and morphogenesis. eLife. 2017;6:e30668.
31. McDole K, Guignard L, Amat F, Berger A, Malandain G, Royer LA, et al. In Toto imaging and reconstruction of post-implantation mouse development at the single-cell level. Cell. 2018;175: 859–76 e33.
32. Aguilera-Castrejon A, Oldak B, Shani T, Ghanem N, Itzkovich C, Slomovich S, et al. Ex utero mouse embryogenesis from pre-gastrulation to late organogenesis. Nature. 2021;593:119–24.
33. Serralbo O, Picard CA, Marcelle C. Long-term, inducible gene loss-of-function in the chicken embryo. Genesis. 2013;51:372–80.
34. Evans SM, Yelon D, Conlon FL, Kirby ML. Myocardial lineage development. Circ Res. 2010;107:1428–44.
35. Bakkers J. Zebrafish as a model to study cardiac development and human cardiac disease. Cardiovasc Res. 2011;91:279–88.
36. Poss KD, Wilson LG, Keating MT. Heart regeneration in zebrafish. Science. 2002;298:2188–90.
37. Porrello ER, Mahmoud AI, Simpson E, Hill JA, Richardson JA, Olson EN, et al. Transient regenerative potential of the neonatal mouse heart. Science. 2011;331:1078–80.

38. Tzahor E, Poss KD. Cardiac regeneration strategies: staying young at heart. Science. 2017;356:1035–9.
39. Stolfi A, Gainous TB, Young JJ, Mori A, Levine M, Christiaen L. Early chordate origins of the vertebrate second heart field. Science. 2010;329:565–8.
40. Medioni C, Senatore S, Salmand PA, Lalevee N, Perrin L, Semeriva M. The fabulous destiny of the Drosophila heart. Curr Opin Genet Dev. 2009;19:518–25.
41. Bodmer R. The gene tinman is required for specification of the heart and visceral muscles in Drosophila. Development. 1993;118:719–29.
42. Azpiazu N, Frasch M. Tinman and bagpipe: two homeo box genes that determine cell fates in the dorsal mesoderm of Drosophila. Genes Dev. 1993;7:1325–40.
43. Bruneau BG. The developing heart: from the wizard of Oz to congenital heart disease. Development. 2020;147(21):dev194233.
44. Schott JJ, Benson DW, Basson CT, Pease W, Silberbach GM, Moak JP, et al. Congenital heart disease caused by mutations in the transcription factor NKX2-5. Science. 1998;281:108–11.
45. McCulley DJ, Black BL. Transcription factor pathways and congenital heart disease. Curr Top Dev Biol. 2012;100:253–77.

Normal Cardiac Anatomy and Clinical Evaluation

4

Nikolaus A. Haas, David J. Driscoll, and Silke Rickert-Sperling

4.1 Introduction to Normal Heart Anatomy

The heart is positioned in the middle, superior, and posterior regions of the mediastinum. Although it is a midline structure, the apex of the heart is typically situated to the left of the midline (Fig. 4.1).

4.1.1 Venous Return to the Heart

The heart receives venous return from multiple sources: the body, lungs, and from its own muscle tissue. Systemic venous return from the body occurs through the right atrium via the superior vena cava (SVC) and inferior vena cava. Typically, both the superior and inferior vena cava are right-sided structures. Venous return from the lungs enters the left atrium through the pulmonary veins. Normally, there are four pulmonary veins, two from each side, although variations with three or five pulmonary veins can also occur. Venous return from the heart muscle itself is facilitated by

N. A. Haas (✉)
Department of Pediatric Cardiology and Intensive Care, Ludwig Maximilians University, Munich, Germany
e-mail: Nikolaus.haas@med.uni-muenchen.de

D. J. Driscoll
Division of Pediatric Cardiology, Department of Pediatrics, Mayo Clinic College of Medicine, Rochester, MN, USA
e-mail: driscoll.david@mayo.edu

S. Rickert-Sperling
Cardiovascular Genetics, Charité – Universitätsmedizin Berlin, Berlin, Germany
e-mail: silke.sperling@charite.de

© The Author(s), under exclusive license to Springer Nature Switzerland AG 2024

S. Rickert-Sperling et al. (eds.), *Congenital Heart Diseases: The Broken Heart*,
Advances in Experimental Medicine and Biology 1441,
https://doi.org/10.1007/978-3-031-44087-8_4

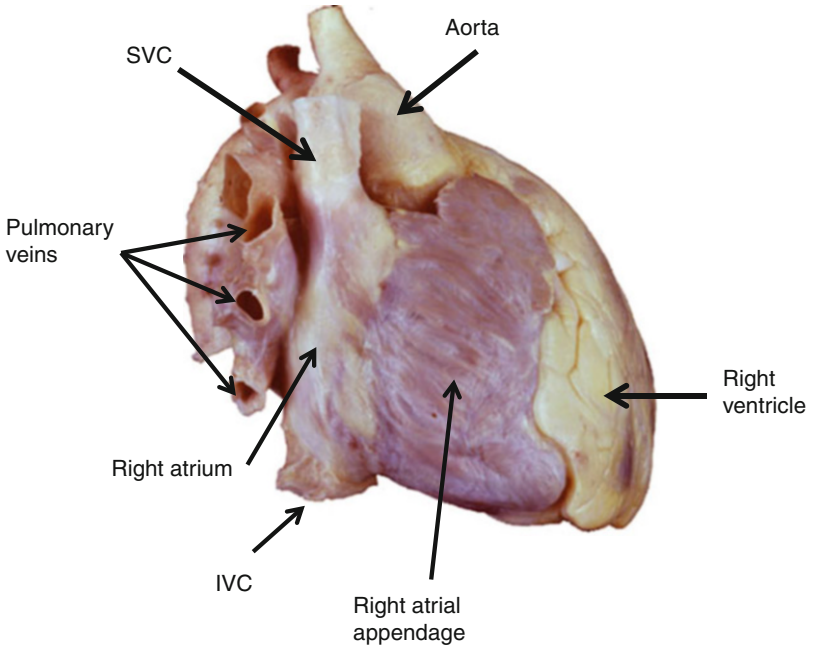

Fig. 4.1 A right anterior oblique external view of the human heart (photograph courtesy of Dr. William Edwards)

the coronary sinus, which drains into the right atrium. Additionally, sinusoidal veins directly within the right ventricle are involved in this venous return.

4.1.2 The Atria

The atria of the heart, namely, the right atrium and left atrium, are not named solely based on their position within the chest but rather on their morphological features. Typically, a morphological right atrium is located on the right side of the body, whereas a morphological left atrium is on the left side. However, certain cardiac anomalies can result in the morphological right atrium being situated on the left side and the morphological left atrium on the right side.

A right atrium is characterized by specific features, including the presence of the limbus of the fossa ovalis, a large pyramidal-shaped atrial appendage with a broad base connected to the right atrium, and that of the crista terminalis and pectinate muscles as well as the ability to receive blood from the superior vena cava and coronary sinus. Typically, there is only one superior vena cava on the right side (RSVC), but, in a small percentage of individuals, a left-sided vena cava (LSCV) may be present, connecting to the coronary sinus.

On the other hand, a left atrium is distinguished by a small atrial appendage, the absence of a crista terminalis, and the lack of pectinate muscles. The morphology of

the left atrial appendage may vary and is not always finger-like. It is now classified based on its shape as the windsock, cactus, cauliflower, or chicken-wing variant.

4.1.3 The Atrioventricular (AV) Valves

In the heart, there are two atrioventricular valves responsible for regulating blood flow. In a normal heart, the tricuspid valve allows blood to pass from the right atrium to the right ventricle, whereas the mitral valve permits blood movement from the left atrium to the left ventricle. However, in congenital heart classification, the AV valves are associated with their respective ventricles rather than the atria. This means that a mitral valve is linked to the left ventricle and that a tricuspid valve is connected to the right ventricle. Both valves can be connected to either a right or left atrium.

The tricuspid valve, as its name suggests, consists of three leaflets, whereas the mitral valve, also known as the bicuspid valve, consists of two leaflets. The annuli of both valves attach to the ventricular septum, with the mitral valve attaching in a more superior position compared to the tricuspid valve. This positioning creates a septum that separates the left ventricle and the right atrium, known as the "atrioventricular septum." One distinctive feature of the tricuspid valve is the presence of a papillary muscle attached to the ventricular septum, whereas the mitral valve lacks such attachments.

In summary, the tricuspid valve has three leaflets and a papillary muscle connected to the ventricular septum, whereas the mitral valve has two leaflets and does not have papillary muscles on the ventricular septum (Fig. 4.2).

4.1.4 The Ventricles

The heart consists of an anatomical right ventricle and an anatomical left ventricle. Their names are not simply based on their relative positions (right and left) but rather on their distinct morphological and functional characteristics. The right ventricle is located anteriorly and to the right of the left ventricle.

Morphologically, the right ventricle differs from the left ventricle. It has thinner walls and a triangular shape with distinct components: an inflow portion, a body, and an outflow portion. The distribution of muscle in the right ventricle allows for greater compliance, making it a more adaptable chamber that can accommodate changes in volume. On the other hand, the left ventricle has a more rounded or ellipsoid form, thicker walls, and is less compliant compared to the right ventricle. Its muscle fibers are oriented in a way that enables it to pump blood at higher pressures.

Furthermore, the right ventricle exhibits a more prominent trabecular pattern, resulting in a more textured appearance, whereas the left ventricle has a smoother surface.

In summary, the right ventricle and left ventricle are anatomically and functionally distinct. The right ventricle is thinner-walled, triangular, and compliant and is

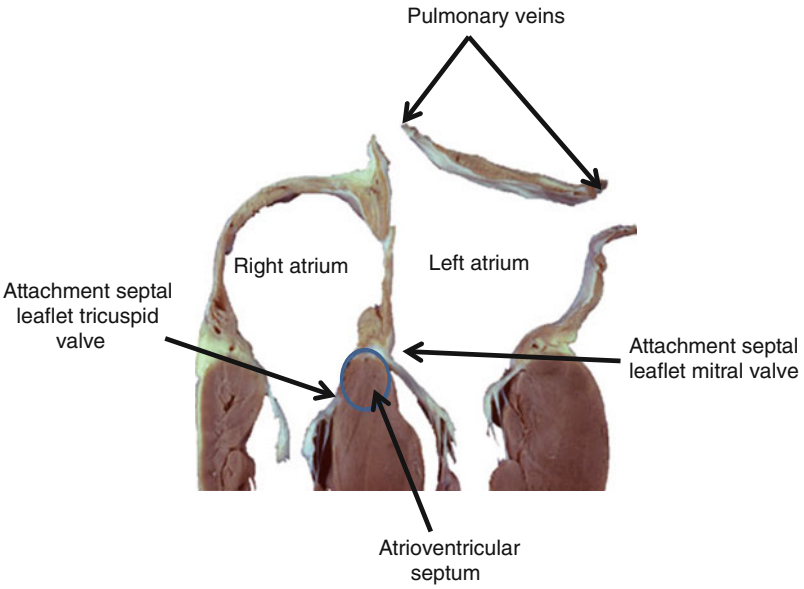

Fig. 4.2 A four-chamber view of a human heart. It should be noted that the septal leaflet of the mitral valve attaches more cephalad than the septal leaflet of the tricuspid valve (photographs courtesy of Dr. William Edwards)

designed to accommodate changes in volume. In contrast, the left ventricle is thicker-walled, more rounded, and less compliant and is specialized in pumping blood at higher pressures. Additionally, the right ventricle displays more prominent trabecularization compared to the left ventricle.

4.1.5 The Semilunar Valves

There are two semilunar valves in the heart: the pulmonary valve and the aortic valve. Typically, both valves have three cusps, although variations with two or four cusps can exist. The pulmonary valve is positioned above a muscular structure called the "conus," which creates a separation between the annulus of the pulmonary valve and the annulus of the tricuspid valve. On the other hand, the annulus of the aortic valve is continuous with the annulus of the mitral valve. This distinction is significant when dealing with various congenital heart anomalies.

In terms of orientation, the aortic valve is positioned to the right and posterior to the pulmonary valve. The coronary arteries originate from the aorta in the vicinity of the cusps of the aortic valve. The cusps of both the aortic valve and the pulmonary valve are associated with dilations known as the sinuses. Specifically, the dilated regions near the cusps of the aortic valve are referred to as the sinuses of Valsalva. Similarly, there are dilations adjacent to the cusps of the pulmonary valve known as

the sinuses of the pulmonary valve. It is important to note that these sinuses of the pulmonary valve should not be confused with the sinuses of Valsalva.

4.1.6 The Great Arteries

The cardiovascular system includes two major arteries: the pulmonary artery and the aorta. The pulmonary artery originates from the right ventricle and divides into the right and left pulmonary arteries. On the other hand, the aorta arises from the left ventricle. The initial branches of the aorta are the right and left coronary arteries. Moving forward, the innominate artery branches off from the aortic arch, giving rise to the right carotid artery and the right subclavian artery. Following this, the left carotid artery and the left subclavian artery emerge as the subsequent branches of the aortic arch.

In the fetal stage, there exists a connection between the aorta and the pulmonary artery called the ductus arteriosus. Normally, this structure should close within a few days after birth. However, in approximately 1 out of 2500–5000 live births, the ductus arteriosus remains patent (known as patent ductus arteriosus (PDA)). Among premature infants, the incidence is higher at 8 out of 1000 live births. PDA accounts for about 9–12% of all congenital heart defects.

When the ductus arteriosus remains open, it results in an abnormal blood flow between the systemic and pulmonary circulation, leading to an excess volume of blood passing through the pulmonary circulation, the left atrium, and the left ventricle. This can manifest as signs and symptoms of congestive heart failure. If the PDA is large and not treated promptly, then it can cause long-term complications such as pulmonary hypertension, which is characterized by increased pressure and resistance in the pulmonary vasculature.

Therefore, it is essential to close a clinically significant patent ductus arteriosus. Currently, the preferred method for closure is through the use of a transvenous device, and surgical intervention is rarely necessary. This approach ensures that the excessive pressure and volume load on the pulmonary vasculature are relieved, preventing the development of secondary pulmonary vascular obstructive disease.

4.1.7 The Coronary Arteries

The coronary artery system consists of two main arteries: the right coronary artery (RCA) and the left coronary artery (LCA) (Fig. 4.3; see also Chap. 43). The LCA originates from the left sinus of Valsalva, positioned posteriorly and to the left, whereas the RCA arises from the right sinus of Valsalva, situated anteriorly and to the right. The LCA branches into two major vessels, namely, the circumflex coronary artery and the left anterior descending coronary artery. Additionally, the LCA gives rise to numerous other branches. In about 80% of cases, the RCA gives off the posterior descending coronary artery. Furthermore, the RCA features a conal branch as well as arteries that supply the sinus node and AV node. It is important to note that

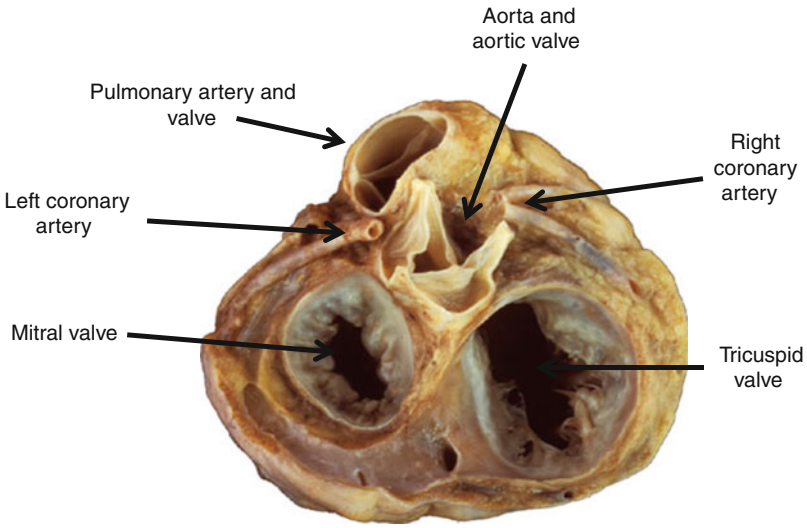

Fig. 4.3 A pathological specimen demonstrating the relationships of the four valves of the heart with each other and the location of the proximal coronary arteries (photographs courtesy of Dr. William Edwards)

in congenital heart defects, there can be significant variation in the anatomy of the coronary arteries, which may have implications for surgical or interventional procedures.

4.1.8 The Electrical System

The heart's electrical system comprises the sinus node, atrioventricular (AV) node, and the His–Purkinje system. Initiation of electrical activity occurs in the sinus node (Fig. 4.4), which is situated at the junction of the superior vena cava (SVC) and the right atrium. From there, the electrical impulses propagate through both the atria. Under normal circumstances, the sole route for electrical conduction from the atria to the ventricles is through the AV node and the bundle of His. The AV node serves as a collection point for electrical activity from both sides of the atria, resulting in a relatively slower conduction. This delay is responsible for the PR segment seen on an electrocardiogram (ECG). The AV node is located within the triangle of Koch, bordered by the tricuspid valve annulus, the tendon of Todaro, and the coronary sinus.

Following the AV node and His bundle, the electrical activity spreads across the ventricles through the right and left bundle branches as well as the Purkinje system. It is worth noting that certain congenital heart diseases may present with variations in the sinus node, including a second node or the absence of one. Additionally, the anatomical location of the AV node can differ depending on the specific congenital heart defect.

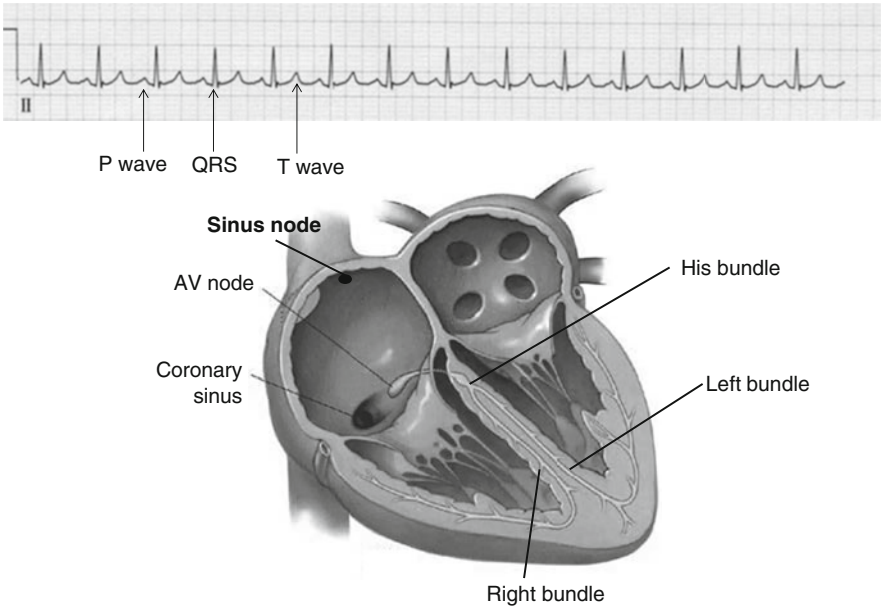

Fig. 4.4 A diagram of the cardiac conduction system. Reproduced from Mayo Clinic, 2009

4.2 Techniques, History, and Physical Examination

4.2.1 History

The historical points of interest vary depending on the patient's age and presenting signs, symptoms, and complaints. When evaluating cardiovascular problems, certain aspects are relevant to consider. In the prenatal history, factors like the method of conception (spontaneous or assisted reproduction), prenatal ultrasound scans, exposure to infections or potential teratogenic toxins, and genetic testing may be significant. For infants, it is important to inquire about any family history of congenital heart disease or premature death. Clinically, the focus is on assessing feeding patterns, signs of heart failure (excessive sweating, rapid breathing or shortness of breath, poor weight gain, cyanosis detected through pulse oximetry screening), or a history of acute life-threatening events (ALTEs).

In the case of older patients, the presence of age-related cardiac symptoms is crucial. These may include dyspnea, reduced exercise capacity, palpitations, syncope, chest pain, and other relevant symptoms.

4.2.2 Physical Examination

During a physical examination, four components are involved: inspection, palpation, auscultation, and percussion.

Inspection allows for the assessment of various factors such as the patient's general condition, respiratory rate, presence of chest retractions, pallor, clubbing, cyanosis, sweating, quality of fat stores, presence of dysmorphic features (e.g., syndromes like trisomy 21), presence of edema, and abnormal superficial vascular patterns.

Palpation involves evaluating pulse volume, comparing pulses between the arms and legs, detecting precordial impulses, assessing for thrills, evaluating temperature, assessing liver and spleen size, checking for peripheral edema, and detecting the presence of ascites.

Percussion is a useful technique to determine the presence of pleural effusion and ascites and assess the size and position of the liver and spleen.

Cardiac auscultation involves more than identifying the presence of murmurs. It includes describing heart sounds, clicks, and rubs in addition to murmurs. The intensity (loudness) of the first (S1) and second (S2) heart sounds is noted, to assess whether they are normal, reduced, or increased. The intensity of S2 may be increased in conditions such as a thin chest wall, pulmonary hypertension, or when the aorta is relatively anterior (e.g., transposition of the great arteries, tetralogy of Fallot, pulmonary atresia). Normally, S2 splits with inspiration and becomes single or nearly single with expiration. A widely split and never-single S2 may indicate the presence of an atrial septal defect (ASD) or right bundle branch block.

The presence of a third heart sound (S3) is normal in children but must be distinguished from abnormal sounds like a mitral murmur or tricuspid diastolic flow murmur.

Heart murmurs result from turbulent blood flow within the heart. They are described by intensity (loudness), frequency or pitch, timing within the cardiac cycle, location on the chest wall, and effects of the patient's position on the murmur quality. Systolic murmurs are graded from 1 to 6/6 based on intensity, with higher grades indicating increasing loudness. Diastolic murmurs are graded from 1 to 4/4. The change in intensity throughout the duration of the murmur is also important, such as a crescendo–decrescendo systolic murmur typical of aortic or pulmonary stenosis.

The frequency or pitch describes the quality of the sound, classified as low, mid, or high. For example, a larger ventricular septal defect (VSD) may produce a low-frequency murmur, whereas a small muscular VSD may be high-pitched. The quality of murmurs can change during the course of a disease, indicating hemodynamic changes.

4.2.3 The Electrocardiogram

An electrocardiogram (ECG) is a diagnostic tool used to measure the electrical activity of the heart, allowing for the evaluation of the heart's rhythm. Additionally, the voltage of the electrical signals provides information about the thickness of the heart muscle, enabling the detection of hypertrophy. During an ECG, leads are placed on all four extremities and six leads are positioned on the chest (Fig. 4.5). Each lead represents different regions of the heart, enabling the identification of atrial or ventricular abnormalities (such as ectopic beats) as well as left- or right-sided issues (such as hypertrophy) or lesions (such as ischemia). The ECG serves as a valuable tool for assessing the electrical and structural aspects of the heart.

4.2.4 Chest X-Rays

A chest X-ray is a valuable diagnostic tool for evaluating cardiac conditions. It helps determine the presence of cardiac enlargement and provides information about pulmonary blood flow. Additionally, certain characteristic appearances of the cardiac silhouette can indicate specific heart defects (e.g., tetralogy of Fallot) or cardiovascular abnormalities (e.g., coarctation of the aorta). By analyzing the chest X-ray, health-care professionals can gain insights into the structural aspects of the heart and identify potential cardiac or vascular abnormalities.

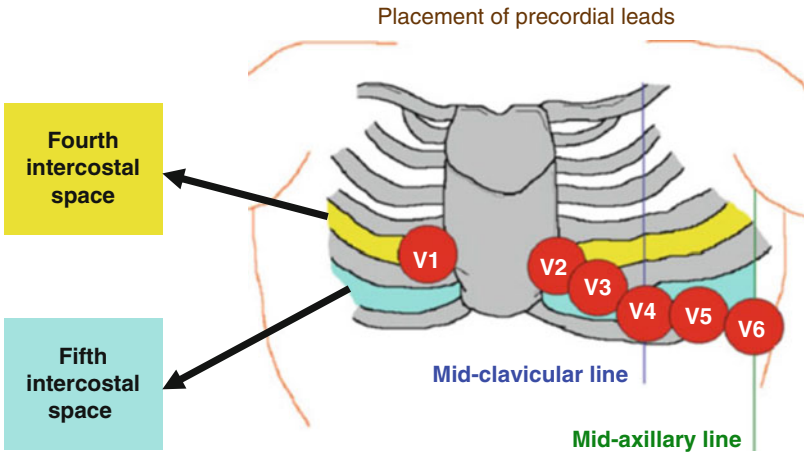

Fig. 4.5 A diagram of the placement of the precordial chest leads for recording an electrocardiogram

4.2.5 Echocardiography

Echocardiography is now the preferred imaging modality for primary screening of children of all ages due to its exceptional accuracy. This noninvasive technique, also known as cardiac ultrasound, enables visualization of the heart and provides detailed information about its anatomy, including the identification of congenital cardiac anomalies (Figs. 4.6 and 4.7). Moreover, with the aid of M-mode and Doppler technology, echocardiography allows for the assessment and measurement of cardiac function, determination of cardiac output and shunts, mapping of blood flow through the heart, and calculation of pressure gradients within the heart and/or vessels. This comprehensive evaluation of the heart's structure and function makes echocardiography an invaluable tool for diagnosing and monitoring cardiovascular conditions.

4.2.6 Cardiac Catheterization

Prior to the introduction of echocardiography, diagnostic cardiac catheterization was the primary method used to assess the presence, severity, and extent of cardiac defects. This invasive procedure involved the insertion of a catheter through the femoral vein, which was then advanced into the various chambers of the heart. By measuring blood oxygen saturations and pressures in different parts of the heart and blood vessels (Figs. 4.8 and 4.9), valuable diagnostic information could be obtained.

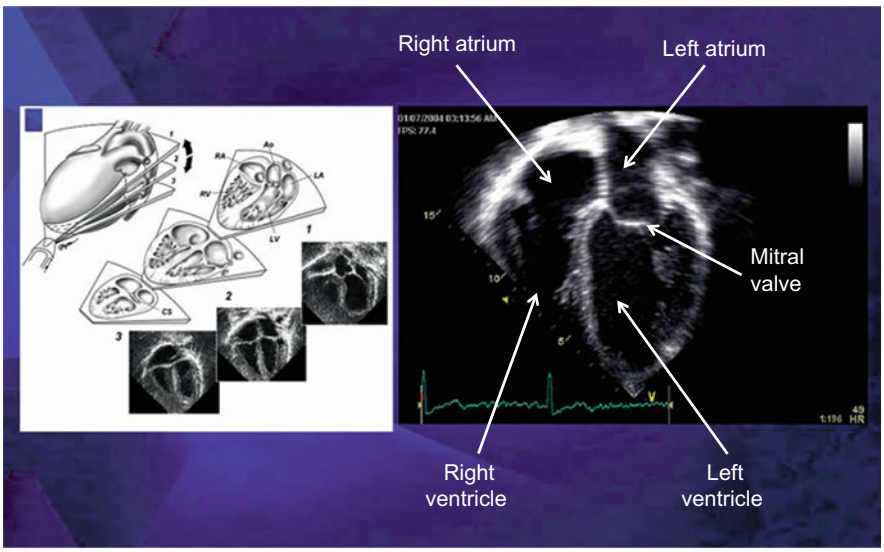

Fig. 4.6 A four-chamber echocardiographic view of the normal heart. Reproduced from Mayo Clinic, 2009

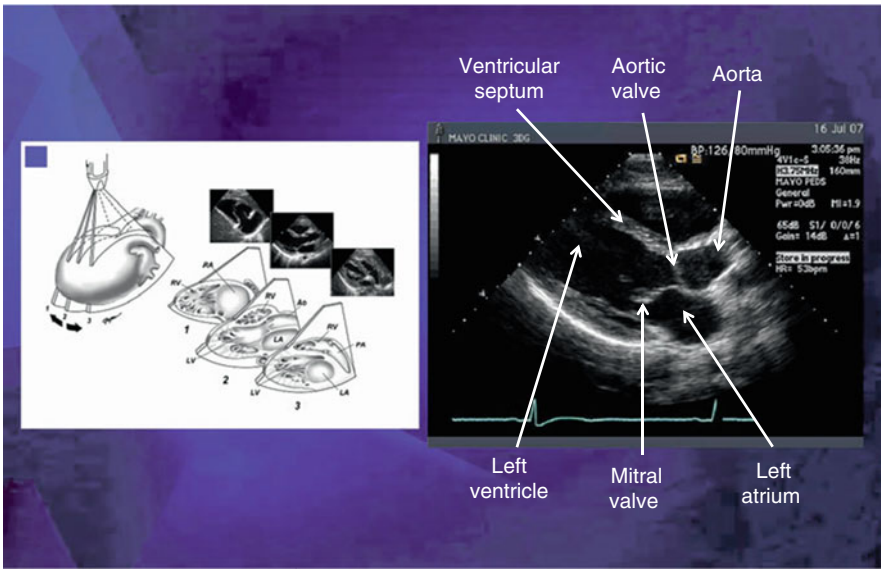

Fig. 4.7 A long-axis echocardiographic view of the normal heart. Reproduced from Mayo Clinic, 2009

Additionally, contrast dye could be injected to produce angiographic images of the heart and blood vessels.

However, with the advancements in echocardiography, the need for diagnostic cardiac catheterization has significantly reduced in determining the extent of cardiac anomalies. Echocardiography provides detailed visualization of the heart's structure and function, allowing for noninvasive assessment. Cardiac catheterization is now reserved for cases where specific information on blood flow, pressures, and resistances is required for further management of the patient.

In the last 25 years, interventional cardiac catheterization has significantly evolved, offering nonsurgical treatment options for various congenital heart defects. This has reduced the need for open-chest surgeries in many cases. Currently, approximately 70–75% of pediatric cardiac catheterizations involve interventional procedures, whereas only 22–30% are performed solely for diagnostic purposes.

Interventional cardiac catheterization provides a wide range of treatment options. Stenotic valves can be dilated, and balloon valvuloplasty has become the primary treatment for pulmonic or aortic stenosis. Catheter-based techniques, such as percutaneous pulmonary valve implantation (PPVI), are now used to replace pulmonic valves in children, adolescents, and adults. Aortic valve replacement (transcatheter aortic valve implantation, TAVI) has become routine in many adult cardiac centers. Vascular narrowing, such as peripheral pulmonary stenosis or coarctation of the aorta, can be treated by balloon dilation or stent insertion to maintain vessel patency.

Specific defects, such as atrial septal defects (ASDs) and ventricular septal defects (VSDs), can be closed using dedicated devices implanted through catheter

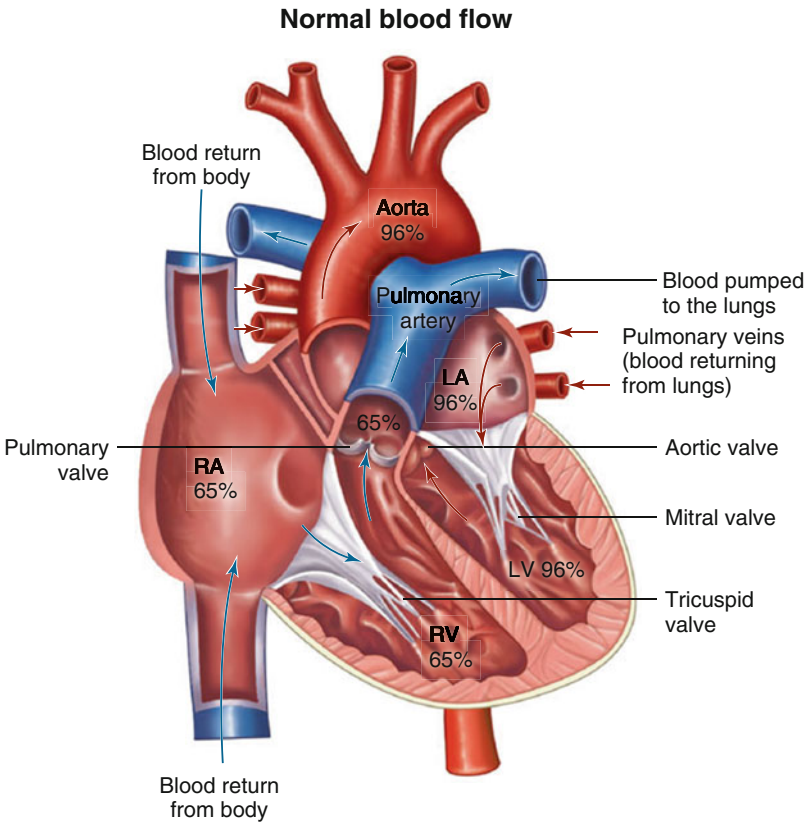

Fig. 4.8 Normal blood saturations in the human heart. A heart diagram demonstrating blood oxygen saturations in a normal heart. It should be noted that the blood oxygen saturation is 65% as it returns to the heart and remains at that level until it returns to the heart from the lungs. Since it becomes oxygenated in the lungs, the blood returning to the left atrium from the lungs is 96% and remains at that level as it passes through the left ventricle and is pumped into the aorta and subsequently delivered to the body

techniques. Fistulas can be closed, and closed structures can be opened as necessary (e.g., Rashkind atrial balloon septostomy). These interventional techniques are now not only used as standalone alternatives to surgery but can also complement surgical procedures by preparing the surgical field, thereby reducing surgical and bypass times. Furthermore, they can improve surgical follow-up by facilitating procedures such as dilation of surgical scars.

Overall, interventional cardiac catheterization has revolutionized the management of congenital heart defects, offering minimally invasive treatment options that have significantly impacted patient care and outcomes.

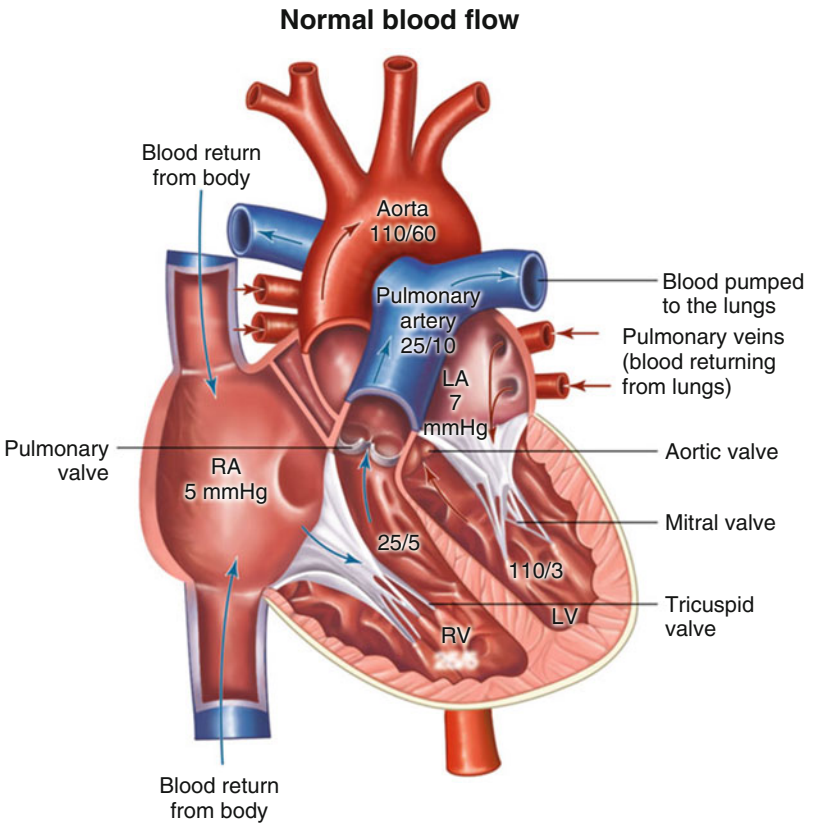

Fig. 4.9 Normal blood pressures in the human heart. A heart diagram with intracardiac pressures in a normal heart

4.2.7 Magnetic Resonance Imaging (MRI) and Computed Tomography (CT) Imaging

Over the past 20 years, cardiac MRI has emerged as the method of choice when echocardiography may not provide accurate results. It offers excellent imaging quality, particularly in adult patients, and allows for two-dimensional pictures, three-dimensional (3D) reconstruction, and even four-dimensional (4D) flow visualization of blood flow across cardiovascular structures. Cardiac MRI enables precise measurement of blood flow, making it the gold standard for assessing cardiac function. Contrast MRI techniques, utilizing gadolinium enhancement, are employed for tissue assessment and differentiation of vital myocardium, myocarditis, scars, and edema.

Cardiac CT (computed tomography) offers the advantage of reduced acquisition times, enabling imaging without the need for general anesthesia in children. However, it utilizes ionizing radiation, although the doses used today are significantly

smaller compared to those used 20 years ago. Cardiac CT provides excellent spatial resolution and striking 3D reconstruction quality. It is commonly used for surgical planning, particularly in complex cases, and has replaced invasive diagnostic catheter investigations.

These advanced imaging modalities, namely, cardiac MRI and cardiac CT, have revolutionized the field of cardiovascular imaging. They offer invaluable insights into cardiac structure and function, aiding in precise diagnosis, treatment planning, and follow-up care. Although each modality has its specific advantages and considerations, their utilization has significantly improved the accuracy and noninvasive assessment of cardiac conditions.

4.2.8 Electrophysiology

With the advancements in modern catheter equipment, interventional therapy for electrical abnormalities, such as arrhythmias, has become a routine procedure today. Diagnostic catheters utilize mapping techniques combined with computer-aided 3D reconstruction to visualize the electrical currents across cardiac structures. Subsequently, specific ablation catheters are guided to the targeted area of interest, allowing for the precise elimination or destruction of vulnerable regions using various methods.

One approach is electroablation, in which electrical heat is applied to the tissue to eliminate the problematic areas. Another technique is cryoablation, where the tissue is cooled to −80° to achieve the same goal. These ablation techniques have shown high success rates in treating various forms of supraventricular and ventricular arrhythmias.

By precisely identifying and eliminating the source of abnormal electrical activity within the heart, these interventional procedures have revolutionized the treatment of arrhythmias. They offer a minimally invasive alternative to traditional open-heart surgeries and have significantly improved patient outcomes.

Part II

Development of the Heart and Its Vessels

Cardiac Progenitor Cells of the First and Second Heart Fields

5

Margaret Buckingham and Robert G. Kelly

Abstract

The heart forms from the first and second heart fields, which contribute to distinct regions of the myocardium. This is supported by clonal analyses, which identify corresponding first and second cardiac cell lineages in the heart. Progenitor cells of the second heart field and its sub-domains are controlled by a gene regulatory network and signaling pathways, which determine their behavior. Multipotent cells in this field can also contribute cardiac endothelial and smooth muscle cells. Furthermore, the skeletal muscles of the head and neck are clonally related to myocardial cells that form the arterial and venous poles of the heart. These lineage relationships, together with the genes that regulate the heart fields, have major implications for congenital heart disease.

5.1 Introduction and Historical Perspective

The heart is the first organ to form and plays a vital role in pumping nutrients and removing waste as soon as the embryo reaches a size where passive diffusion is no longer sufficient to ensure cell survival. Early heart defects are a frequent source of mortality, estimated to account for as many as 30% of embryos/fetuses lost before birth in humans [1]. As many as 0.8% of newborn children in developed countries

M. Buckingham (✉)
Department of Developmental and Stem Cell Biology, CNRS UMR 3738, Institut Pasteur, Paris, France
e-mail: margaret.buckingham@pasteur.fr

R. G. Kelly (✉)
Aix Marseille Université, Institut de Biologie du Dévelopment de Marseille, Marseille, France
e-mail: Robert.Kelly@univ-amu.fr

© The Author(s), under exclusive license to Springer Nature Switzerland AG 2024

S. Rickert-Sperling et al. (eds.), *Congenital Heart Diseases: The Broken Heart*,
Advances in Experimental Medicine and Biology 1441,
https://doi.org/10.1007/978-3-031-44087-8_5

have some form of congenital heart malformation. These figures reflect the complex process of cardiogenesis, which involves the integration of different cell populations with precise spatial and temporal control as the heart undergoes morphogenesis [2] (Fig. 5.1). In the mouse embryo, which provides a mammalian model suitable for genetic manipulation, the early heart tube forms and begins beating at about embryonic day (E) 8, which is equivalent to 3 weeks of human gestation. At this stage, the tube is linear, with an anterior outflow tract (OFT) and a posterior inflow region, connecting to the circulatory system. As it grows, the cardiac tube rapidly loops to the right so that the mature outflow and inflow tracts, the arterial and venous poles, respectively, are aligned anteriorly. The cardiac chambers grow out from the looped tube in a process described as ballooning [3], with formation of septa and valves to control blood flow within the heart. By this stage, the neural crest cells of neuroectodermal origin migrate into the cardiac tube, which is composed of a myocardium surrounded by an inner layer of endocardium and an outer epicardium, all of mesodermal origin.

Cardiomyocytes proliferate within the heart tube, and it was previously believed that this accounted for heart growth, with different regions of the early tube prefiguring the future atria and ventricles, in a segmental model of cardiogenesis [4]. However, classic experiments in the chick embryo had already pointed to the addition of cells to the growing heart tube [5]. Investigators subsequently showed that cells are added to the outflow region of the avian heart from adjacent mesoderm [6, 7]. At the same time, in 2001, addition of cells from the pharyngeal mesoderm, marked by expression of a transgene integrated upstream of the *Fibroblast growth*

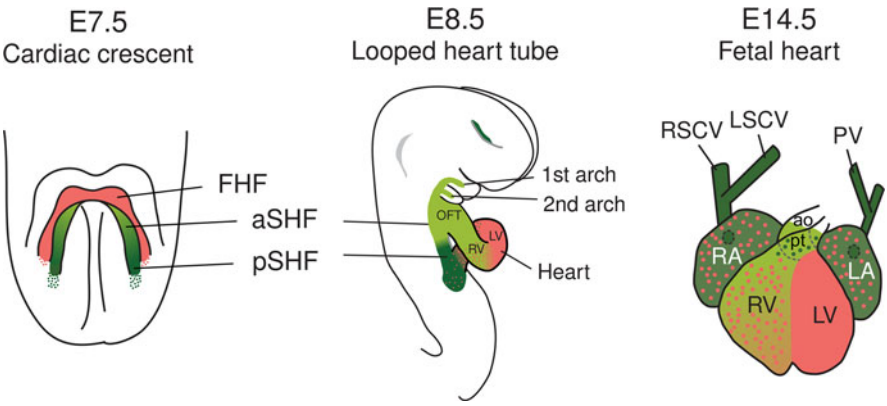

Fig. 5.1 Formation of the heart from the first and second heart fields. Schematic representation of cardiogenesis showing the contribution of the first heart field (FHF—red), located in the cardiac crescent, to the myocardium of the left ventricle and other parts of the heart and the anterior second heart field (aSHF—light green) and posterior second heart field (pSHF—dark green) to the myocardium of the arterial and venous poles of the heart as well as the right ventricle and atria. LA, left atrium; RA, right atrium; LV, left ventricle; RV, right ventricle; OFT, outflow tract; ao, aorta; pt, pulmonary trunk; PV, pulmonary vein; RSV, right superior caval vein; LSV, left superior caval vein; E, embryonic day of mouse development

factor (Fgf) 10 locus, was demonstrated to contribute to the outflow tract and right ventricular myocardium in the mouse embryo [8]. The transcription factor Islet1 also marks these cells and its expression pattern, together with the *Islet1* mutant phenotype, indicated a contribution to both the venous and arterial poles of the heart [9]. This was later confirmed by explant experiments and tracking of cells labeled by dye injection in cultured embryos [10], which also showed that the early heart tube mainly has a left ventricular identity [11]. These findings regarding cardiac progenitor cells that form the developing heart tube were complemented by a different experimental approach examining myocardial cell lineages in the mouse embryo. Retrospective clonal analysis demonstrated that the myocardium derives from two cell lineages. The first lineage is the source of the left ventricular myocardium, whereas the second lineage is the source of the myocardium of the outflow tract and most of the right ventricle (RV) and also contributes to the atria, which are derived from both lineages [12]. Thus, cardiac progenitor cells of the first heart field (FHF) form the early cardiac tube, whereas cells of the second heart field (SHF) subsequently enter the developing tube and constitute the second lineage contribution to the heart [2] (Fig. 5.2).

The distinction between these two cell populations is underlined by the early segregation of the first and second lineages, previously estimated to take place at the onset of gastrulation or earlier [12]. This conclusion was drawn from a genetic approach to clonal analysis that depends on a random recombination event in a progenitor cell that converts an inactive *laacZ* reporter to an active *lacZ* sequence. In this case, the reporter was targeted to an allele of the *cardiac actin* gene, resulting in β-galactosidase expression in clonally related daughter cells in the myocardium. The size of the clone provides an estimation of the time of recombination. However, this is only approximative. Other genetic approaches to clonal analysis have made it possible to more precisely estimate the timing of clonal segregation and also to follow all mesodermal cell types in the heart. One such approach was based on a conditional *confetti* multicolor reporter and brief induction of a Cre recombinase that activates a single-colored reporter in a progenitor cell and its descendants [13]. In this case, *Cre* is controlled by the *Mesoderm posterior 1 homolog* (*Mesp1)* gene, which is expressed in the primitive streak in gastrulating mesodermal cells that will contribute to all compartments of the heart [14]. These experiments confirmed that two myocardial cell lineages form the heart, as previously described, and demonstrated that the first lineage can be distinguished by E6.25–E6.75, at the onset of gastrulation, whereas the second lineage that gives rise to SHF derivatives is marked when Cre is induced at E6.75–E7.25. A similar genetic approach based on a mosaic analysis with double markers (MADMs) also showed distinct segregation of the two lineages [15]. The common progenitor that gives rise to the two lineages is therefore present prior to activation of *Mesp1* early in gastrulation, before day 12 of human embryonic development. Left and right ventricular cardiomyocytes, derived from the FHF and SHF, respectively, originate from *Foxa2*-expressing progenitor cells [16]. However, recent genetic tracing experiments using inducible Cre recombinase have shown that *Foxa2* is activated independently in left and right ventricular progenitor cells at the time of gastrulation [17].

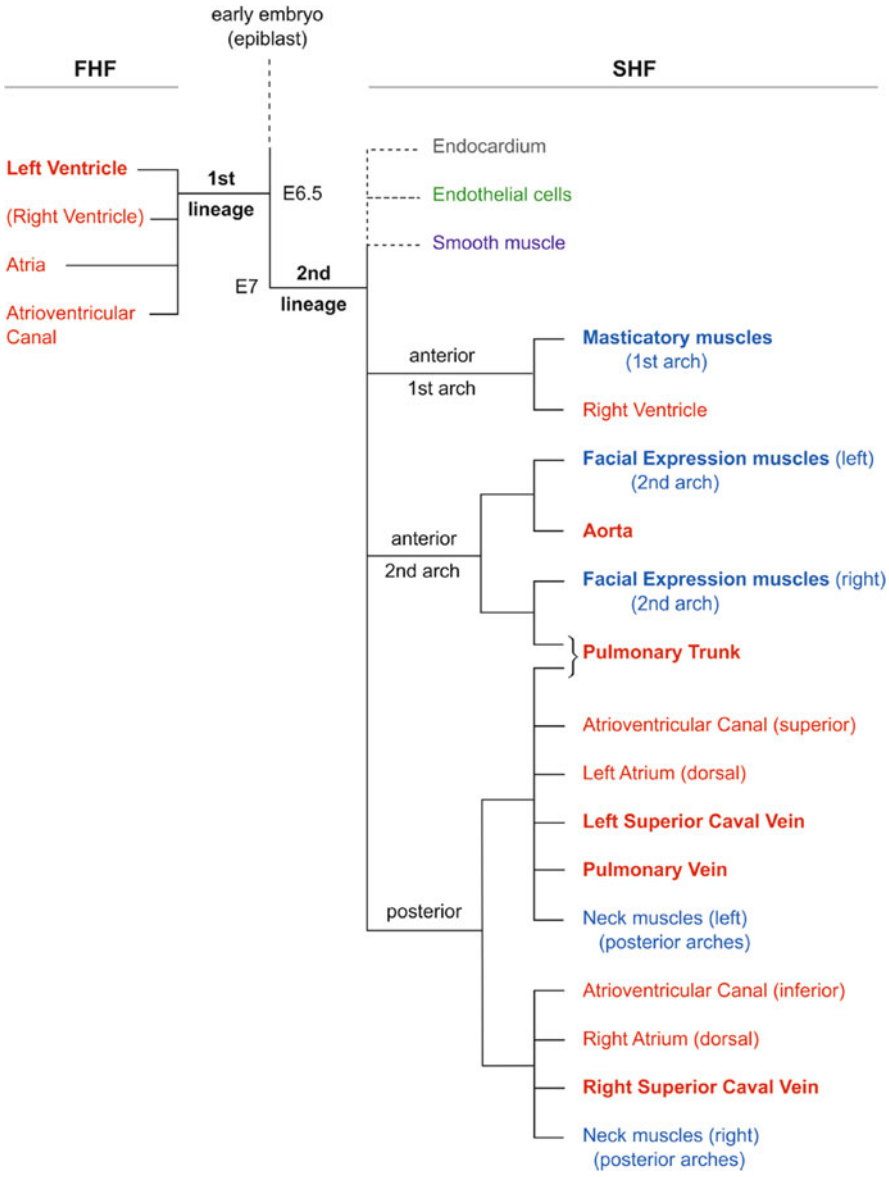

Fig. 5.2 A lineage tree for the heart. Schematic representation of the contribution of first and second cell lineages to the mouse heart. FHF, first heart field; SHF, second heart field. Myocardial derivatives are in red and skeletal muscle in blue, with bold type indicating that this is the major source, for example, the first lineage/FHF for the left ventricle or the second lineage/SHF for head muscles, whereas not all neck muscles derive from this source. Other second lineage (SHF) derivatives are indicted with dotted lines since their precise relation to each other or to the tree for myocardium and skeletal muscle is not yet clearly defined: endocardium, endothelial cells, and smooth muscle. The approximate timing of lineage segregation from a common progenitor, present in the epiblast is indicated—E, embryonic day of mouse development

5.2 The First Heart Field

The first differentiated cells expressing cardiac muscle markers are detected prior to formation of the heart tube, in a region under the head folds that spans the midline of the embryo, known as the cardiac crescent. The early heart tube forms as a result of fusion of the crescent at the midline. This process not only reflects the morphogenetic movements of the underlying endoderm as the embryo develops but also depends on genes expressed in the cardiac mesoderm, which control cell migration and fusion of the crescent. Not much is known about the underlying cell biology in mammals; however, a number of mutations that perturb the process have been identified. Failure to migrate leads to cardiac bifida where two hearts begin to develop on either side of the embryo. Mutation of the gene encoding the transcription factor GATA-binding protein 4 (Gata4) provides a classic example of this phenotype [2]. The early heart tube expresses transgenic markers for the left ventricular myocardium, and dye labeling of these cells followed by embryo culture showed that they will mainly contribute to the left ventricle [11]. Markers of cells in the crescent that distinguish the first from the second heart field have been elusive. For example, the transcription factor T-box (Tbx) 5, implicated in Holt–Oram syndrome [18] is not only present in FHF cells but also marks the posterior subdomain of the SHF [19] and is dynamically expressed in the forming heart tube before showing left ventricular localization. The *hyperpolarization activated cyclic nucleotide-gated potassium channel 4* (*Hcn4)* gene, which is later expressed in the conduction system, is transitorily activated specifically in the cardiac crescent and thus provides an interesting early marker [20]. However, it is probably expressed in myocardial cells at this stage rather than in the FHF progenitors. Induction of a *Mesp1-green fluorescent protein* (*GFP)* transgene at the early (E6.5) and later (E.7.5) time points, when progenitors for the first and then the second heart fields can be distinguished [13], makes it possible to separate these cell populations by flow cytometry and to perform transcriptome analysis. This approach has already identified a number of differentially expressed genes and should lead to novel markers. Such experiments also open the way to functional analysis, not only for FHF cells present in the crescent but also at earlier stages as they progress through the primitive streak, exit it, and then migrate anteriorly to take up their position under the head folds.

5.3 The Second Heart Field

The cardiac progenitor cells of the SHF (Fig. 5.1) are located medially to the cardiac crescent, extending posteriorly. As the crescent fuses to form the early heart tube, these cells come to lie behind the tube and also anteriorly, adjacent to the outflow tract, and posteriorly, adjacent to the sinus venosus and venous pole as it develops. Initially, the tube is not completely closed and there is continuity with the underlying dorsal mesocardium, which is attached to the pericardial wall, with some differentiating cells entering the heart dorsally from the SHF [12]. Subsequently,

the dorsal mesocardium breaks down as the tube closes. The cardiac tube is suspended in the pericardial cavity, with cells of the SHF continuing to feed from the dorsal pericardial wall into the poles of the heart to form the myocardium. Recent dynamic imaging of heart tube formation in mouse embryo culture has identified a pause in heart tube growth that precedes the onset of SHF cell addition to the heart tube [21]. This delay may be necessary to accommodate the morphogenetic transition linked to dorsal mesocardial breakdown.

SHF deployment continues over several days in the mouse embryo, with the myocardium at the base of the pulmonary and caval veins still being formed as late as E12.5 (40 days of human development). The SHF provides a pool of cardiac progenitor cells, which are maintained as a proliferating, non-differentiated population. The transcription factors and signaling pathways that mark these cells play a critical role in regulating this behavior [22]. Temporally regulated genetic labeling, using inducible Cre recombinase expressed in progenitor cells, or differentiated myocardium, illustrates the progressive addition of SHF cells to the RV and OFT as well as to the venous pole [23, 24]. Mutations in the regulators of SHF development lead to major arterial pole defects and also to venous pole defects, which may be more subtle, thus reflecting the fact that the outflow tract is exclusively derived from the second myocardial cell lineage and is thus entirely dependent on the SHF contribution. In newborn children with a congenital heart defect, 30% have a malformation of the arterial pole of the heart. Fortunately, this can be usually corrected surgically and the child survives. However, a small proportion of babies die after surgery, and reexamination of the records indicates that in a number of cases there was also a venous pole defect that had not been detected [25]. It is therefore important to check for subtle venous pole defects, which can be repaired at the same time as surgery is performed to correct a defect at the arterial pole.

5.3.1 Regulation of Proliferation and Differentiation

Cells in the SHF are highly proliferative so that the pool of cardiac progenitor cells is maintained as the heart grows. Fibroblast growth factor (FGF), canonical Wnt (wingless-related integration site), Notch, and Hedgehog signaling all promote proliferation [22, 26]. Differentiation of SHF cells is triggered as they enter the poles of the heart. Bone morphogenetic protein (BMP) signaling plays an important role in this process, antagonizing FGF signaling [27, 28] and promoting the deployment and differentiation of cells that will contribute to the arterial pole. Notch and non-canonical Wnt signaling are also implicated in cardiac differentiation [22, 26]. At the venous pole of the heart, canonical Wnt, Hedgehog, and BMP signaling all orchestrate the critical balance between proliferation and differentiation, where Hedgehog signaling promotes the migration of cells to the heart tube and also their proliferation [29, 30]. These pathways are activated by signals from the surrounding tissues and by cell autonomous signaling within the SHF [31]. Thus, the midline structures (the neural tube and notochord) are sources of canonical Wnt and Hedgehog signaling, promoting SHF proliferation. Hedgehog signaling also comes

from the endoderm, whereas FGF signals come from the surrounding endoderm and ectoderm as well as from the SHF itself. Neural crest cells, which migrate through the SHF into the arterial pole, mediate BMP inhibition of FGF signaling, such that in the absence of neural crest cells, excessive SHF cell proliferation results in reduced cardiomyocyte differentiation and defective growth of the heart. BMP signals are also produced by cells in the SHF, promoting neural crest survival, and by cardiomyocytes, promoting recruitment to the poles of the heart.

An extensive gene regulatory network operates in the SHF to control cardiac progenitor cell behavior [22]. Key transcription factors modulate signaling pathways, illustrated by Tbx1 interference with the BMP signaling cascade to delay differentiation [31, 32] or Tbx1 activation of enhancers that control *Fgf8* and *Fgf10* expression in the SHF [31–33]. Islet1 also activates the *Fgf10* enhancer [33] and has an SHF enhancer, which is itself controlled by forkhead box (Fox) c2 [22]. In addition, Hopx, encoding a homeodomain-only transcription factor, has been shown to play a role in balancing pro-proliferative Wnt and pro-differentiation BMP signaling as progenitor cells enter the elongating OFT [34].

Some genes expressed in the SHF are specific to the progenitor cell population in this cardiac context. Foxc2, for example, marks SHF progenitors and Islet1 has long been considered to be a key marker of this field. However, more sensitive reporters now indicate that *Islet1* is also expressed at a low level in FHF progenitors, although the *Islet1* mutant phenotype suggests that it is mainly functional in the SHF [22].

Genes that are involved in myocardial differentiation are also expressed in the SHF. These include genes coding for the transcription factors, NK2 homeobox 5 (Nkx2–5), Gata4, Mef2c, serum response factor (SRF), Tbx5, and the chromatin remodeling protein SWI/SNF-related, matrix-associated, actin-dependent regulator of chromatin, subfamily D, member 3 (Smarcd3; also called 60-kDa BRG-1/Brm-associated factor subunit C1; Baf60c), which marks a subset of early Mesp1-positive cardiac progenitors [22]. These genes are expressed in the differentiating cells of the cardiac crescent and in regions of the heart, where combinations of them activate sarcomeric genes. The ectopic expression of Gata4, Tbx5, and Smarcd3 in non-cardiogenic regions of the mouse embryo has been shown to activate cardiac muscle formation [35], indicating the role of these factors in cardiac progenitor cell determination and in cardiac differentiation. Their targets in the SHF are not well-understood, although transcriptome analysis of *Nkx2–5*-expressing cells provides some insights [36, 37]. Notably, Nkx2–5 functions in a negative feedback loop with BMP2/Smad1 signaling that controls cardiac progenitor cell behavior, which is probably of importance in the etiology of Nkx2–5-related human congenital heart defects [36]. Different combinations of factors are one reason why targets may differ between cardiac progenitors and the myocardium. Another consideration is the level of expression, which may affect function. The potential importance of modulating the level of these factors is indicated by Tbx1 downregulation of SRF and Tbx5 in the SHF [19, 32]. In the *Tbx1* mutant, abnormal cardiac differentiation of SHF progenitors in the dorsal pericardial wall probably reflects this effect and deregulation of the balance between BMP and FGF signaling [31]. The SHF enhancer of the *Fgf10* gene provides an example of how levels and combinations of transcription

factors can be functionally important [33]. In this enhancer, both Islet1 and Nkx2–5 bind to the same sites. In the SHF, Islet1 levels are high and successfully compete for binding, leading to activation of *Fgf10*, which also depends on Tbx1. Islet1 has been shown to interact with Smarcd3 and acts as a pioneering factor driving lineage commitment [38]. In the heart, on the other hand, Nkx2–5 levels are extremely high and displace Islet1 [33]. This leads to downregulation of *Fgf10* in keeping with the repressive function of Nkx2–5 observed for SHF genes, including *Islet1*, in the heart [36]. Since Nkx2–5 also functions as a transcriptional activator in the myocardium, this dual role again depends on the combinatorial effects of other factors.

Most transcription factors and components of signaling pathways that play a role in cardiogenesis are not cardiac-specific. This is in contrast to the skeletal muscle where the myogenic regulatory factors of the myogenic differentiation (MyoD) family are only expressed during myogenesis [39]. Analysis of mutant phenotypes is informative for the heart only when the gene does not play a vital role during early embryogenesis. Islet1 or Mesp1, for example, are mainly important for formation of the heart in the early stages of development, whereas Fgf8 is required for gastrulation and conditional mutation of *Fgf8* directed toward cardiac progenitors is essential for understanding its role in the SHF. Mesp1–Cre lines [14] have proved to be extremely valuable for targeting all cardiac progenitors, whereas an enhancer of the *Mef2c* gene targets cells in the SHF [40]. It follows that in the human population, many mutations in cardiac regulatory genes may be early embryonic lethal or may result in multiple effects as seen in a number of syndromes where the heart is affected. This is the case, for example, of mutations in *TBX1*, which give rise to 22q11.2 deletion (or DiGeorge) syndrome [41]. This includes major defects at the arterial pole of the heart, such as the common arterial trunk or persistent truncus arteriosus as well as craniofacial abnormalities, due to the function of Tbx1 in the SHF as well as in the endoderm and ectoderm in the pharyngeal region, which is important for cardiac and cranial neural crest development. Unless there is some cardiac-specific aspect of function, mutations in the enhancers that direct gene transcription toward the cardiac progenitors of the first or second heart field are the best candidates for defects that are restricted to the formation of the heart. Many such enhancers, which specifically direct transcription in the SHF, have now been identified for genes such as *Fgf8*, *Fgf10*, *Islet1*, *Nkx2–5*, or *Mef2c* [22]. They are regulated by combinations of SHF transcription factors, as for *Fgf10* [33].

5.3.2 Patterning the SHF

The SHF is patterned on the anterior/posterior axis where regional heterogeneity is apparent. The anterior part of the SHF is marked by genes that are not expressed throughout the field [22]. This is the case for *Fgf8* or *Fgf10* and also for the SHF *Mef2c* enhancer, which is not active in the posterior SHF. This anterior/posterior distinction correlates with the contribution of cells expressing these genes to the arterial or venous pole, respectively. This is also illustrated in the anterior SHF, where *Tbx1* is mainly expressed in cells that will contribute to the myocardium at the

base of the pulmonary trunk [31], in contrast to *Fgf8/10* or the *Mef2c* enhancer, which marks progenitors of the right ventricle and the outflow tract myocardium, including the pulmonary trunk and the aorta. Differences in the origin of the myocardium at the base of these arteries are reflected by differential gene expression [19]. The pulmonary trunk myocardium, for example, is marked by *Semaphorin 3c (Sema3c)* gene expression. In *Tbx1* mutants, the pulmonary trunk myocardium is reduced [31], which is probably the early abnormality that underlies the development of tetralogy of Fallot and other cardiac defects in 22q11.2 deletion (DiGeorge) syndrome patients. Use of an inducible *Mef2c* enhancer-driven *Cre* has shown that these different regions of the OFT arise from temporally distinct progenitor populations [42]. Future myocardium at the base of the aorta arises early, at E7.5, whereas future pulmonary trunk myocardium is progressively added to the arterial pole from E8.5. Continued addition of sub-pulmonary myocardium from the SHF up to E12.5 has been proposed to drive arterial pole rotation, essential for correct alignment of the ventricular outlets, through a pulmonary-push mechanism [43].

The posterior SHF is also marked by distinct gene expression profiles. Homeobox (*Hox)* genes, differentially expressed along the axis of the embryo, are classically involved in anterior/posterior patterning. Anterior members of the *Hox* gene clusters such as *Hoxb1* are expressed in the posterior SHF, under the control of retinoic acid signaling. When this signaling pathway is perturbed, *Hox* gene expression is affected and the posterior boundary of the SHF is modified [44]. *Tbx5* is expressed in cardiac progenitor cells in the posterior SHF. In addition to atrial myocardium, the dorsal mesenchymal protrusion also derives from the posterior SHF, from cells expressing *Tbx5* and *Islet1*, and its development depends on Hedgehog and BMP signaling [29, 30]. This structure is important in the context of congenital heart malformations since it provides the muscular base of the atrial septum and anomalies in its formation from the posterior SHF leads to atrial and atrioventricular septal defects. *Tbx18* is expressed in a particular lateral domain of the posterior SHF, which is also distinguished by the lack of *Nkx2–5* and *Islet1* expression [45]. This domain, which has been proposed to constitute a third heart field, contributes the caval vein myocardium, which is marked by continuing *Tbx18* expression. Retrospective clonal analysis distinguishes sub-lineages of the second myocardial cell lineage (equated with the SHF), which contribute to the myocardium at the arterial or venous poles of the heart. However, this clonal analysis does not distinguish a particular sub-lineage contributing to only the caval vein myocardium, as might be expected if this arises from a third heart field [46].

The distinction between the anterior and posterior domains of the SHF is made on the basis of gene expression; however, cells may move between these domains during SHF deployment. This was first indicated by genetic tracing of cells that had expressed *Hoxb1* in the posterior SHF [44], leading to labeling of myocardial derivatives at the venous pole. Unexpectedly, the Tbx1-dependent myocardium at the base of the pulmonary trunk was also labeled [19]. In keeping with this result, dye labeling of small groups of cells in the posterior domain of the SHF showed, after embryo culture, that some labeled cells were located in the outflow tract and had therefore moved anteriorly, expressing markers of the anterior SHF, as indicated

by *Fgf10* reporter gene expression [47]. Most cells do not appear to move extensively within the SHF, and clonal analysis suggests coherent, rather than dispersed, cell growth as the heart forms [2]. However, lineage studies for the venous pole of the heart showed unexpected clonality between the myocardium at the left side of the venous pole (the pulmonary vein, left caval vein, and left atrium) and the pulmonary trunk myocardium at the arterial pole [46]. This is consistent with the anterior movement of a subset of progenitor cells located on the left side of the posterior SHF from which the left venous pole myocardium derives. Cre genetic tracing experiments show that the classic anterior SHF markers, *Tbx1* [48] and the *Mef2c* SHF enhancer [49], are transiently expressed in progenitor cells giving rise to the atrial septum and dorsal mesenchymal protrusion. Indeed, loss of function of *Tbx1* impacts not only the anterior SHF but also the posterior SHF, resulting in venous and arterial pole defects [19]. The development of the dorsal mesenchymal protrusion is affected, leading to ostium primum atrial septal defects, a class of atrioventricular septal defects. In addition to its roles in promoting proliferation and limiting differentiation in the SHF, *Tbx1* is required for the segregation of cells to the arterial and venous poles of the heart from a common early progenitor population expressing *Tbx1*, the *Mef2c*-enhancer transgene, and *Hoxb1* [19]. From E8–8.5, *Tbx5*, a regulator of FHF and venous pole progenitor cells, is activated in a subpopulation of *Tbx1*-expressing cells in the dorsal pericardial wall that will contribute to atrial septal structures [50]. Transient co-expression of *Tbx1* and *Tbx5* is followed by downregulation of the anterior SHF program (Fig. 5.3). Distinct *Tbx1*-expressing arterial pole and *Tbx5*-expressing venous pole progenitor populations thus emerge in the dorsal pericardial wall. Retinoic acid is required to activate *Tbx5* in *Tbx1*-expressing cells, and blocking this signaling pathway during the E8–8.5 developmental window also leads to ostium primum atrial septal defects [50]. Tbx5 in the posterior SHF is critically required to drive the expression of canonical Wnt ligands, Wnt2 and Wnt2b, in venous pole progenitor cells [51]. In addition, *Hoxb1*, a direct target of retinoic acid signaling, has been shown to negatively regulate differentiation in the posterior SHF during heart tube elongation and is required, together with its paralogue Hoxa1, for development of the dorsal mesenchymal protrusion and atrial septation [52].

In addition to patterning on the anterior/posterior axis, the SHF also shows left/right patterning. This is driven by the Nodal signaling pathway, which leads to expression of the transcription factor paired-like homeodomain 2 (Pitx2) in cells on the left side of the SHF. Pitx2 is highly expressed in the posterior SHF where it promotes a left myocardial cell fate by repressing the acquisition of the right atrial identity [10]. It also tends to repress proliferation so that the left SHF and sinus venosus are less proliferative than the right. At later stages, Pitx2 is implicated, in conjunction with Nkx2–5, in initiating the formation of pulmonary vein myocardium at the left venous pole [53]. Pitx2 in the left anterior SHF also plays a role in the formation of the arterial pole of the heart [54, 55]. The rotation of the outflow tract, which is essential for the correct juxtaposition of the pulmonary trunk and aorta, depends on *Pitx2*, and, prior to this, genetic interactions with *Tbx1* have been demonstrated in the SHF [56]. Foxh1 is another transcription factor that plays a

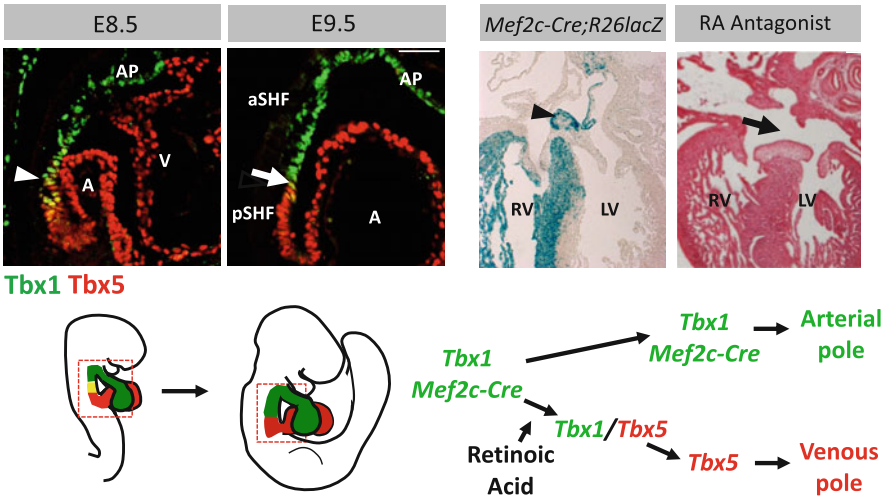

Fig. 5.3 Patterning the second heart field. Left: Immunofluorescence showing Tbx1 (green) and Tbx5 (red) expression in the anterior (aSHF) and posterior (pSHF) SHF in sections corresponding to the boxed regions in the schema below. Note the overlap present at E8.5 (arrowhead) and formation of a sharp boundary by E9.5 (arrow). Right, top: Expression of a conditional *lacZ* reporter gene at E14.5 showing *Mef2c–AHF–Cre* lineage contributions to atrial septal structures, including the dorsal mesenchymal protrusion (arrowhead) and the right ventricle. Blocking retinoic acid signaling during the time window of Tbx5 activation results in loss of the dorsal mesenchymal protrusion and a primum-type atrial septal defect (arrow). Right, bottom: A diagram illustrating SHF cell segregation to the alternate poles of the heart tube. Adapted from De Bono et al. [50]. A, atrium; AP, arterial pole; V, ventricle; RV, right ventricle; LV, left ventricle; RA, retinoic acid

role in the development of the anterior SHF [57], and mutations in *FOXH1* have been linked to arterial pole defects in humans [58]. This reflects a modification of left/right signaling since Foxh1 functions in the Nodal pathway. Upstream of Nodal, Hedgehog signaling is important for the establishment of left/right asymmetry in the embryo and *Shh* mutants have arterial pole defects, resembling tetralogy of Fallot [59]. These mutants have bilateral expression of Pitx2 and left atrial isomerism [60]. Nodal-expressing progenitor cells in the left SHF have been shown to direct cardiac looping to the right by coordinating asymmetry at the cardiac poles, acting upstream of the proliferative and differentiation pathways [61].

Recent studies have investigated the cell biology and biomechanics of SHF cardiac progenitor cells in the dorsal pericardial wall. SHF cells constitute an atypical epithelium with apical junctions and mesenchymal-like basolateral cell domains characterized by dynamic filopodia (Fig. 5.4) [62]. N-cadherin-mediated epithelial adhesion in the SHF is required to prevent premature progenitor cell differentiation [63]. In the absence of Tbx1, SHF cells are more rounded and have elevated apical markers and reduced filopodial structures [62]. Consistent with these observations, Tbx1 has been shown to promote focal adhesion and regulate expression of the focal adhesion protein Paxillin [64]. Tbx1 also regulates expression of the

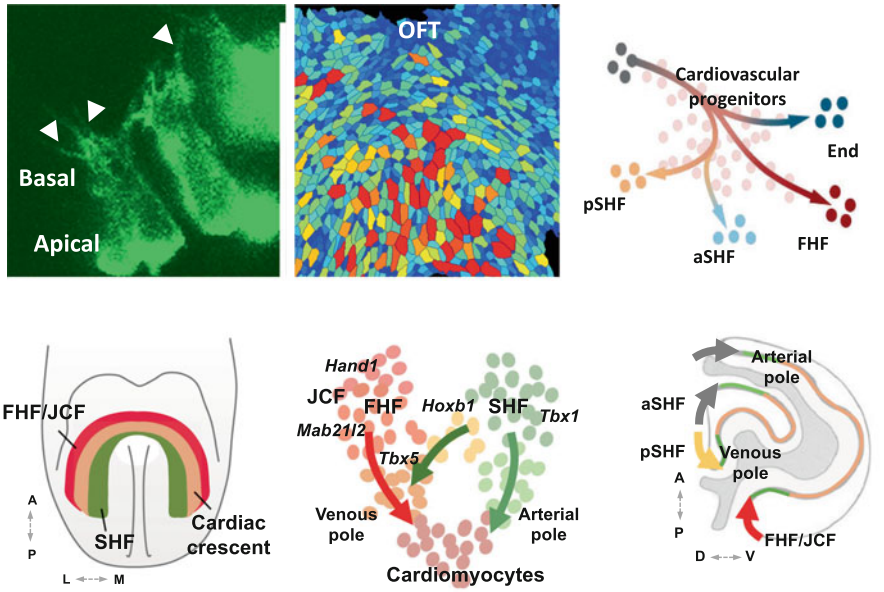

Fig. 5.4 Morphology and single-cell transcriptomic analysis of cardiac progenitor cells. Top, left: SHF cells, here expressing a Utrophin GFP fusion protein at E9.5, constitute an atypical epithelium with dynamic basal filopodia (arrowheads). Adapted from Francou et al. [62]. Top, middle: A segmented ventral view of the dorsal pericardial wall showing that cells, color-coded for surface area, are elongated in the posterior SHF and oriented toward the outflow tract (OFT). Adapted from Francou et al. [70]. Top right: A scheme showing two-dimensional representation of single-cell transcriptomes at E6.5; the emergence of distinct cardiac progenitor cells, including anterior (aSHF) and posterior (pSHF) SHF populations, from a multilineage-primed progenitor pool should be noted. Adapted from Lescroart et al. [80]. FHF, first heart field; End, endocardium. Bottom, left: A cartoon showing the lateral and medial locations of the FHF/juxtacardiac (JCF) and SHF progenitor populations adjacent to the cardiac crescent at E7.5. Bottom, middle: Trajectories from the FHF and SHF to the myocardium based on the single-cell transcriptomic analyses of Tyser et al. and Zhang et al. [83, 84]. Bottom, right: A cartoon showing the deployment of cells to the elongating heart tube. Bottom panels adapted from Kelly [85]

gene encoding the non-canonical Wnt ligand Wnt5a in the SHF [65]. Like Tbx1, Wnt5a is required for bidirectional SHF cell addition to the cardiac poles and has been proposed to promote progenitor cell intercalation in the dorsal pericardial wall, contributing, potentially together with elevated proliferation, to a pushing force that may drive SHF deployment [66–68]. Increased adhesion in the anterior SHF close to the arterial pole has been proposed to create an additional pulling force [69]. Indeed, patterned epithelial tension has been documented across the dorsal pericardial wall during SHF deployment, with elevated tension in *Tbx1*-expressing cells in the lateral posterior region of the dorsal pericardial wall where cells are oriented toward the elongating outflow tract (Fig. 5.4) [70]. Increased tension is associated with nuclear YAP/TAZ (yes-associated protein/PDZ-binding motif) localization that may in turn promote proliferation in a biomechanical regulatory loop, thus driving rapid heart

tube elongation. In addition, planar cell polarity pathway genes have been shown to regulate the epithelial status of SHF cells as they differentiate in a transition zone at the cardiac poles and are required for maximal heart tube elongation [71].

5.4 Non-Myocardial Derivatives of the First and Second Lineages: Endocardium, Epicardium, and Vascular Endothelial and Smooth Muscle Cells

As the heart tube forms, other cell types of mesodermal origin, in addition to myocardial cells, participate in its development. The endocardium, marked by *Nfatc1* expression, constitutes the inner layer of the cardiac tube and chambers as they develop [22]. Endocardium provides an important source of signals that promote ventricular trabeculation and is also important for valve formation, initiated by delamination of endocardial cells from the cardiac cushions. The source of the endocardium has been controversial. It derives from cells that express *Islet1* and *Nkx2–5*, suggesting a SHF origin.

The epicardium forms the outer layer of the cardiac tube [22]. Epicardial cells delaminate and enter the underlying myocardium where they form the smooth muscle of the coronary blood vessels as well as interstitial fibroblasts of the heart. The epicardium derives from the proepicardial organ, a transitory mesenchymal structure located near the venous pole of the heart. When cultured, epicardial cells can form the myocardium; however, whether this is the case in vivo is controversial. Cells in the proepicardial organ express *Islet1* and *Nkx2–5*, and the latter is required for its formation. However, the relation between the SHF and the epicardium remains unclear.

At the arterial pole of the heart, the arterial tree derives from the pharyngeal arch arteries. Pharyngeal arches 1 to 6 are transitory structures of the pharyngeal region that bulge out as pouches on either side of the embryo from E9. Their mesodermal core can be regarded as an extension of the SHF where cells express anterior SHF genes [22]. Dye labeling of cells in arch 2, in cultured mouse embryos, has shown that they contribute to the outflow tract myocardium. The posterior arches give rise to endothelial cells of the arch arteries, and, as expected for SHF derivatives, targeted mutations in genes like *Fgf8/10* [72] or *positive regulatory domain I-binding factor 1* (*Prdm1)* [73] lead to malformations of the arterial tree as well as affecting aorta and pulmonary trunk development. Clonal analysis and genetic tracing have shown that SHF endothelial fates include coronary lymphatic endothelial cells that differentiate within a vasculogenic niche at the base of the pulmonary trunk [74]. These cells contribute in particular to lymphatic endothelial cells on the ventral side of the heart, the development of which is *Tbx1*-dependent [75].

Isolation of cells, marked by *Islet1* expression, for example, from the embryo shows that they give rise to myocardial, smooth muscle, and endothelial derivatives and this has also been reported at the single-cell level [31, 76]. Embryonic stem (ES) cell lines, when directed toward a cardiac fate, give rise to progenitors expressing *Islet1* and *Nkx2–5* [76]. When cloned, these cells prove to be multipotent

by again forming vascular and myocardial derivatives. However, this does not establish that cardiac progenitors in vivo give rise to more than one cell type. Clonal analysis, using an inducible *Mesp1–Cre* and the conditional multicolor *confetti* reporter [13], has clarified this issue during cardiogenesis. Cells of the first myocardial cell lineage, which constitute the first heart field, were found to give rise only to myocardial cells. In contrast, cells of the second lineage that populate the second heart field were found to be multipotent, with clones contributing to the endocardium and to endothelial or smooth muscle of blood vessels as well as to the myocardium. Most clones in the epicardium did not show labeling with the myocardium, pointing to the existence of a unipotent population of epicardial progenitors.

Refinement of pluripotent stem cell approaches has enabled the differentiation of FHF and SHF lineages to be followed outside the embryo, providing an in vitro system to explore interactions during cardiogenesis. For example, the independent emergence of complementary FHF and SHF progenitor populations was followed using fluorescent reporter genes under the control of *Tbx1* and *Hcn4* regulatory elements in a precardiac organoid model, identifying *Cxcr4* as a marker of SHF cells [77]. Subsequent genetic studies in mice have confirmed the importance of Cxcr4 and Cxcr2 chemotactic signaling in SHF deployment [78]. Early steps in cardiogenesis have been recapitulated under conditions of structured organoid differentiation to mimic gastrulation and cardiac induction, including formation of a crescent-like structure expressing FHF markers and an adjacent SHF cell population [79]. Comparison of the transcriptome of single cells isolated from these gastruloids with the situation in the embryo suggests that such pluripotent stem cell-derived cardiac models will provide tractable systems to study the emergence of cardiac progenitor cells for high-throughput analyses.

5.5 Insights into Heart Fields from Single-Cell Transcriptomics

Single-cell RNA sequencing (scRNA-seq) provides a high-resolution view of cell heterogeneity and transcriptome-based lineage diversification of particular importance in dissecting developmental processes. Over the past 5 years, the power of this technology has been brought to bear on the emergence of cardiac progenitor cells in the early embryo. In a study of *Mesp1*-expressing progenitor cells emerging from gastrulation, the divergence of molecularly distinct SHF cells and early differentiating FHF cells could be inferred within a multilineage-primed progenitor population (Fig. 5.4) [80]. Early divergence of cells with characteristics of anterior and posterior SHF subpopulations was also observed in this study.

Subsequent scRNA-seq studies have confirmed and extended prior understanding of the two lineage model of heart morphogenesis. These studies have contributed to defining progenitor cell-state transitions during cardiogenesis [81] and have highlighted the importance of regional regulators of fate acquisition, identifying a role of *Hand2*, for example, in the right ventricular lineage, where it mediates retinoic acid antagonism in anterior progenitor cells [82]. In addition, *Hand1*-expressing progenitor cells, originating at the embryonic–extraembryonic boundary,

have been shown to contribute to the FHF and give rise to part of the left ventricle [83]. In this study, distinct trajectories to a left ventricular fate were inferred, with a second contribution from a predicted lineage related to SHF cells [83]. This is consistent with prior evidence based on genetic tracing for *Mef2c–Cre* lineage contributions to the left side of the interventricular septum [15, 49]. In another study, a *Mab21l2*-expressing progenitor cell population has been defined that contributes to the left ventricle and may correspond to late-differentiating FHF progenitor cells from the *Hand1* lineage that contribute to the growing heart tube across the lateral borders of the cardiac crescent, as opposed to the medial contribution of SHF cells (Fig. 5.4) [84]. *Mab21l2*-expressing progenitor cells have been termed the "juxtacardiac field" and also contribute to the epicardium. Trajectory analysis based on these datasets reveals FHF and SHF contributions to the arterial and venous poles of the developing heart, with the FHF contributing to the ventral venous pole and the SHF to the arterial and dorsal venous poles (Fig. 5.4) [83–85]. Recent scRNA-seq analysis of gastrulating embryos, coupled with high-resolution immunofluorescence and live imaging, has shown that FHF and SHF lineages emerge from spatially and molecularly distinct pools of cells as the mesoderm forms in the primitive streak at gastrulation [17]. An ongoing challenge concerns relating transcriptionally defined trajectories from such studies to our understanding of clonal and genetic lineages during cardiac morphogenesis. An additional challenge is to precisely map the embryonic location of different subpopulations of cells defined by single-cell sequencing. The development of high-resolution spatial transcriptomics approaches will contribute to resolving this latter point.

5.6 Cardiopharyngeal Mesoderm

Skeletal muscles of the trunk and limbs derive from somites, segments of the paraxial mesoderm located on either side of the neural tube along the anterior/posterior axis of the embryo. Their formation depends on a gene regulatory network in which the transcription factor paired box 3 (Pax3) acts upstream of the myogenic regulatory factors of the MyoD family that are required for cell entry into the skeletal muscle program [39]. Head muscles have a non-somitic origin, and, although the myogenic regulatory factors also control myogenic determination and differentiation, Pax3 is not implicated in the upstream gene regulatory network [39]. Extraocular muscles form from the anterior pre-chordal mesoderm, but most head muscles derive from the mesoderm of the first two pharyngeal (also referred to as branchial) arches, such that masticatory or facial expression muscles derive from the first or second arches, respectively. The progenitors of these muscles have expressed genes, such as *Islet1*, which characterize the anterior SHF. Mutation of *Tbx1*, for example, leads to abnormalities in the jaw muscles and to malformation of the arterial pole of the heart [86]. Within the mesodermal core of the arches, cells that have activated myogenic regulatory factors are located in the more distal region compared to cardiac progenitors, which continue to express SHF markers in the

proximal pharyngeal mesoderm [87]. These observations point to the cardiopharyngeal mesoderm as a source of cardiac and skeletal muscles, with overlapping expression of SHF genes in the progenitor cells that give rise to the heart and head muscles [88]. Retrospective clonal analysis shows that both types of muscles derive from a common progenitor. The *cardiac actin* gene, which was used to drive transcription of the *lacZ* reporter, is expressed in the developing skeletal muscles and throughout the myocardium. First arch-derived head muscles are clonally related to the right ventricular myocardium, whereas second arch-derived head muscles share a common clonal origin with the arterial pole of the heart, masticatory muscles on the left side of the head with the myocardium at the base of the pulmonary trunk, and those on the right side with the myocardium at the base of the aorta [89]. The clonal relationship between head muscles and the heart was also borne out by the observation of co-labeling of cells in the *Mesp1–Cre/confetti* system for genetically tracking clones [13]. The results of a clonal analysis of the myocardium at the venous pole of the heart indicated unexpected clonality between the components of the left venous pole and the pulmonary trunk myocardium. This sub-lineage does not include the head muscles, leading to the conclusion that two progenitor cell populations contribute to myocardium at the base of the pulmonary trunk. Since defects in the formation of the pulmonary trunk are frequent in congenital heart disease, this dual origin is important for diagnosis and prognosis.

The neck constitutes a transition zone where some muscles are somite-derived and others, like the trapezius, sternocleidomastoid, or laryngeal muscles, are marked by genetic tracing with regulatory elements of genes also expressed in the SHF [90]. Clonal analysis of these muscles shows that they share common progenitors with venous pole myocardium derived from the SHF [91]. Again, there is right/left lineage segregation such that the muscles on the right side of the neck are clonally related to the myocardium at the right venous pole and the left neck muscles to the left venous pole. This sub-lineage includes pulmonary trunk myocardium at the arterial pole of the heart. SHF-derived neck muscles show no clonal relationship with head muscles. These lineage relationships further underline the dual origin of the pulmonary trunk myocardium (Fig. 5.2). Esophageal skeletal muscle has also been shown to have a cardiopharyngeal genetic origin [92], although the lineage relationship with the heart and other craniofacial muscles remains to be determined. Extending the known derivatives of cells expressing SHF regulators, recent genetic lineage studies using the *Mef2–Cre*-enhancer transgene and *Tbx1–Cre* have shown that the connective tissue of the somite-derived neck muscles is in part derived from cardiopharyngeal mesoderm [93]. This finding highlights the integration of the head and trunk developmental programs in the neck region. Moreover, defective attachment of somite-derived neck muscles is observed in *Tbx1*-haploinsufficient mice, suggesting a role of cardiopharyngeal mesoderm in muscle patterning.

A discussion of the evolution of the heart and heart fields is outside the scope of this chapter. However, it is notable that other vertebrates have a second heart field. In birds and fish, this is an important source of cells for the arterial pole of the heart [31]. A basic gene regulatory network, with similarities to that in the mammalian SHF, which involves genes including *Tbx1*, functions in cardiopharyngeal

mesoderm in the invertebrate chordate *Ciona*, the sea squirt [94]. Progenitor cells in this mesoderm also give rise to muscle and heart-like structures, pointing to the ancient origins of the relationship between cranial muscles and the myocardium [88].

5.7 Conclusions

The clonal relationships between progenitor cells that form the heart are important for understanding the potential links between different cardiac malformations. This is illustrated by the SHF contribution to both the arterial and the venous poles of the heart [25]. In the context of the SHF, perturbation of the two different sub-lineages that contribute to pulmonary trunk myocardium, one that also gives rise to the head muscles and the other to the venous pole of the heart and neck muscles, will have different clinical manifestations. Effects on the myocardium derived from the second (SHF), as compared to the first (FHF) lineage, may also be associated with endocardial or cardiovascular defects. These considerations are important for diagnosis and prognosis. Defects that reflect cell lineage relationships also relate to gene expression. *Tbx1* mutations, for example, impact pulmonary trunk myocardium and also affect head muscles. Genes that regulate the posterior SHF and affect the venous pole may also affect the formation of pulmonary trunk myocardium and, in this case, be associated with neck muscle defects, processes also perturbed in *Tbx1* mutant embryos. Perturbation of mesodermal FGF signaling [72] provides an example of how interference with cells of the anterior SHF, where this signaling pathway plays a key role in proliferation, affects both the myocardium at the base of the great vessels and the formation of the arterial tree by affecting endothelial cells derived from the posterior arches.

Congenital heart defects due to mutations in genes coding for regulatory factors or signaling pathways that control cardiogenesis are likely to reflect perturbations in the later SHF contribution to the poles of the heart, since earlier effects are more likely to result in embryonic lethality. However, perturbations in the FHF contribution to the atria or the right ventricle, for example, may be compensated by the SHF-derived myocardium, thus leading to less drastic malformations. Furthermore, depending on the mutation and on the genetic compensatory mechanisms, the cellular source, whether FHF or SHF, may be only partially compromised. Continuing work on the mouse genetic model, as well as on organisms as apparently far removed as *Ciona* [95], should continue to provide insights into the origins of congenital heart defects, their diagnosis, and their prognosis, with the possibility of correction by post- or prenatal surgery and in the future by gene or cell therapy, perhaps even in utero.

Acknowledgments M.B. acknowledges support from the Pasteur Institute and the CNRS (UMR 3738). Research in R.K.'s lab is supported by the Agence National pour la Recherche (Heartbox, Heartbound and PP-heart projects), AFM-Telethon, and Fondation Leducq (Transatlantic Network of Excellence 15CVD01).

References

1. Bruneau BG. The developmental genetics of congenital heart disease. Nature. 2008;451(7181):943–8.
2. Buckingham M, Meilhac S, Zaffran S. Building the mammalian heart from two sources of myocardial cells. Nat Rev Genet. 2005;6(11):826–35.
3. Christoffels VM, et al. Chamber formation and morphogenesis in the developing mammalian heart. Dev Biol. 2000;223(2):266–78.
4. Brand T. Heart development: molecular insights into cardiac specification and early morphogenesis. Dev Biol. 2003;258(1):1–19.
5. de la Cruz MV, Sanchez Gomez C, Arteaga MM, Arguello C. Experimental study of the development of the truncus and the conus in the chick embryo. J Anat. 1977;123(Pt 3):661–86.
6. Mjaatvedt CH, Nakaoka T, Moreno-Rodriguez R, Norris RA, Kern MJ, Eisenberg CA, Turner D, Markwald RR. The outflow tract of the heart is recruited from a novel heart-forming field. Dev Biol. 2001;238(1):97–109.
7. Waldo KL, Kumiski DH, Wallis KT, Stadt HA, Hutson MR, Platt DH, Kirby ML. Conotruncal myocardium arises from a secondary heart field. Development. 2001;128(16):3179–88.
8. Kelly RG, Brown NA, Buckingham ME. The arterial pole of the mouse heart forms from Fgf10-expressing cells in pharyngeal mesoderm. Dev Cell. 2001;1(3):435–40.
9. Cai CL, Liang X, Shi Y, Chu PH, Pfaff SL, Chen J, Evans S. Isl1 identifies a cardiac progenitor population that proliferates prior to differentiation and contributes a majority of cells to the heart. Dev Cell. 2003;5(6):877–89.
10. Galli D, Dominguez JN, Zaffran S, Munk A, Brown NA, Buckingham ME. Atrial myocardium derives from the posterior region of the second heart field, which acquires left-right identity as Pitx2c is expressed. Development. 2008;135(6):1157–67.
11. Zaffran S, Kelly RG, Meilhac SM, Buckingham ME, Brown NA. Right ventricular myocardium derives from the anterior heart field. Circ Res. 2004;95(3):261–8.
12. Meilhac SM, Esner M, Kelly RG, Nicolas JF, Buckingham ME. The clonal origin of myocardial cells in different regions of the embryonic mouse heart. Dev Cell. 2004;6(5):685–98.
13. Lescroart F, et al. Early lineage restriction in temporally distinct populations of Mesp1 progenitors during mammalian heart development. Nat Cell Biol. 2014;16(9):829–40.
14. Saga Y, Miyagawa-Tomita S, Takagi A, Kitajima S, Miyazaki J, Inoue T. MesP1 is expressed in the heart precursor cells and required for the formation of a single heart tube. Development. 1999;126(15):3437–47.
15. Devine WP, Wythe JD, George M, Koshiba-Takeuchi K, Bruneau BG. Early patterning and specification of cardiac progenitors in gastrulating mesoderm. Elife. 2014;3:e03848. https://doi.org/10.7554/eLife.03848.
16. Bardot E, et al. Foxa2 identifies a cardiac progenitor population with ventricular differentiation potential. Nat Commun. 2017;8:14428.
17. Ivanovitch K, et al. Ventricular, atrial, and outflow tract heart progenitors arise from spatially and molecularly distinct regions of the primitive streak. PLoS Biol. 2021;19(5):e3001200.1.
18. Bruneau BG, et al. A murine model of Holt-Oram syndrome defines roles of the T-box transcription factor Tbx5 in cardiogenesis and disease. Cell. 2001;106(6):709–21.
19. Rana MS, et al. Tbx1 coordinates addition of posterior second heart field progenitor cells to the arterial and venous poles of the heart. Circ Res. 2014;115(9):790–9.
20. Liang X, et al. HCN4 dynamically marks the first heart field and conduction system precursors. Circ Res. 2013;113(4):399–407.
21. Ivanovitch K, Temino S, Torres M. Live imaging of heart tube development in mouse reveals alternating phases of cardiac differentiation and morphogenesis. Elife. 2017;6:6. https://doi.org/10.7554/eLife.30668.
22. Vincent SD, Buckingham ME. How to make a heart: the origin and regulation of cardiac progenitor cells. Curr Top Dev Biol. 2010;90:1–41.

23. Zhou Z, Wang J, Guo C, Chang W, Zhuang J, Zhu P, Li X. Temporally distinct Six2-positive second heart field progenitors regulate mammalian heart development and disease. Cell Rep. 2017;18(4):1019–32.
24. Choquet C, Marcadet L, Beyer S, Kelly RG, Miquerol L. Segregation of central ventricular conduction system lineages in early SMA+ cardiomyocytes occurs prior to heart tube formation. J Cardiovasc Dev Dis. 2016;3(1):1.
25. Bajolle F, Zaffran S, Losay J, Ou P, Buckingham M, Bonnet D. Conotruncal defects associated with anomalous pulmonary venous connections. Arch Cardiovasc Dis. 2009;102(2):105–10.
26. Rochais F, Mesbah K, Kelly RG. Signaling pathways controlling second heart field development. Circ Res. 2009;104(8):933–42.
27. Hutson MR, Zeng XL, Kim AJ, Antoon E, Harward S, Kirby ML. Arterial pole progenitors interpret opposing FGF/BMP signals to proliferate or differentiate. Development. 2010;137(18):3001–11.
28. Tirosh-Finkel L, Zeisel A, Brodt-Ivenshitz M, Shamai A, Yao Z, Seger R, Domany E, Tzahor E. BMP-mediated inhibition of FGF signaling promotes cardiomyocyte differentiation of anterior heart field progenitors. Development. 2010;137(18):2989–3000.
29. Xie L, Hoffmann AD, Burnicka-Turek O, Friedland-Little JM, Zhang K, Moskowitz IP. Tbx5-hedgehog molecular networks are essential in the second heart field for atrial septation. Dev Cell. 2012;23(2):280–91.
30. Briggs LE, Phelps AL, Brown E, Kakarla J, Anderson RH, van den Hoff MJ, Wessels A. Expression of the BMP receptor Alk3 in the second heart field is essential for development of the dorsal mesenchymal protrusion and atrioventricular septation. Circ Res. 2013;112(11):1420–32.
31. Kelly RG. The second heart field. Curr Top Dev Biol. 2012;100:33–65.
32. Chen L, Fulcoli FG, Tang S, Baldini A. Tbx1 regulates proliferation and differentiation of multipotent heart progenitors. Circ Res. 2009;105(9):842–51.
33. Watanabe Y, Zaffran S, Kuroiwa A, Higuchi H, Ogura T, Harvey RP, Kelly RG, Buckingham M. Fibroblast growth factor 10 gene regulation in the second heart field by Tbx1, Nkx2-5, and Islet1 reveals a genetic switch for down-regulation in the myocardium. Proc Natl Acad Sci U S A. 2012;109(45):18273–80.
34. Jain R, et al. Integration of Bmp and Wnt signaling by Hopx specifies commitment of cardiomyoblasts. Science. 2015;348(6242):aaa6071.
35. Takeuchi JK, Bruneau BG. Directed transdifferentiation of mouse mesoderm to heart tissue by defined factors. Nature. 2009;459(7247):708–11.
36. Prall OW, et al. An Nkx2-5/Bmp2/Smad1 negative feedback loop controls heart progenitor specification and proliferation. Cell. 2007;128(5):947–59.
37. Bouveret R, et al. NKX2-5 mutations causative for congenital heart disease retain functionality and are directed to hundreds of targets. Elife. 2015;4:4. https://doi.org/10.7554/eLife.06942.
38. Gao R, et al. Pioneering function of Isl1 in the epigenetic control of cardiomyocyte cell fate. Cell Res. 2019;29(6):486–501.
39. Buckingham M, Rigby PW. Gene regulatory networks and transcriptional mechanisms that control myogenesis. Dev Cell. 2014;28(3):225–38.
40. Dodou E, Verzi MP, Anderson JP, Xu SM, Black BL. Mef2c is a direct transcriptional target of ISL1 and GATA factors in the anterior heart field during mouse embryonic development. Development. 2004;131(16):3931–42.
41. Papangeli I, Scambler P. The 22q11 deletion: DiGeorge and velocardiofacial syndromes and the role of TBX1. Wiley Interdiscip Rev Dev Biol. 2013;2(3):393–403.
42. Jin H, et al. Differential contribution of the two waves of cardiac progenitors and their derivatives to aorta and pulmonary artery. Dev Biol. 2019;450(2):82–9.
43. Scherptong RW, Jongbloed MR, Wisse LJ, Vicente-Steijn R, Bartelings MM, Poelmann RE, Schalij MJ, Gittenberger-De Groot AC. Morphogenesis of outflow tract rotation during cardiac development: the pulmonary push concept. Dev Dyn. 2012;241(9):1413–22.

44. Bertrand N, Roux M, Ryckebusch L, Niederreither K, Dolle P, Moon A, Capecchi M, Zaffran S. Hox genes define distinct progenitor sub-domains within the second heart field. Dev Biol. 2011;353(2):266–74.
45. Christoffels VM, et al. Formation of the venous pole of the heart from an Nkx2-5-negative precursor population requires Tbx18. Circ Res. 2006;98(12):1555–63.
46. Lescroart F, Mohun T, Meilhac SM, Bennett M, Buckingham M. Lineage tree for the venous pole of the heart: clonal analysis clarifies controversial genealogy based on genetic tracing. Circ Res. 2012;111(10):1313–22.
47. Dominguez JN, Meilhac SM, Bland YS, Buckingham ME, Brown NA. Asymmetric fate of the posterior part of the second heart field results in unexpected left/right contributions to both poles of the heart. Circ Res. 2012;111(10):1323–35.
48. Huynh T, Chen L, Terrell P, Baldini A. A fate map of Tbx1 expressing cells reveals heterogeneity in the second cardiac field. Genesis. 2007;45(7):470–5.
49. Verzi MP, McCulley DJ, De Val S, Dodou E, Black BL. The right ventricle, outflow tract, and ventricular septum comprise a restricted expression domain within the secondary/anterior heart field. Dev Biol. 2005;287(1):134–45.
50. De Bono C, et al. T-box genes and retinoic acid signaling regulate the segregation of arterial and venous pole progenitor cells in the murine second heart field. Hum Mol Genet. 2018;27(21):3747–60.
51. Steimle JD, et al. Evolutionarily conserved Tbx5-Wnt2/2b pathway orchestrates cardiopulmonary development. Proc Natl Acad Sci U S A. 2018;115(45):E10615–24.
52. Stefanovic S, et al. Hox-dependent coordination of mouse cardiac progenitor cell patterning and differentiation. Elife. 2020;9:e55124. https://doi.org/10.7554/eLife.55124.
53. Mommersteeg MT, Brown NA, Prall OW, de Gier-de Vries C, Harvey RP, Moorman AF, Christoffels VM. Pitx2c and Nkx2-5 are required for the formation and identity of the pulmonary myocardium. Circ Res. 2007;101(9):902–9.
54. Liu C, Liu W, Palie J, Lu MF, Brown NA, Martin JF. Pitx2c patterns anterior myocardium and aortic arch vessels and is required for local cell movement into atrioventricular cushions. Development. 2002;129(21):5081–91.
55. Bajolle F, Zaffran S, Kelly RG, Hadchouel J, Bonnet D, Brown NA, Buckingham ME. Rotation of the myocardial wall of the outflow tract is implicated in the normal positioning of the great arteries. Circ Res. 2006;98(3):421–8.
56. Nowotschin S, Liao J, Gage PJ, Epstein JA, Campione M, Morrow BE. Tbx1 affects asymmetric cardiac morphogenesis by regulating Pitx2 in the secondary heart field. Development. 2006;133(8):1565–73.
57. von Both I, et al. Foxh1 is essential for development of the anterior heart field. Dev Cell. 2004;7(3):331–45.
58. Roessler E, et al. Reduced NODAL signaling strength via mutation of several pathway members including FOXH1 is linked to human heart defects and holoprosencephaly. Am J Hum Genet. 2008;83(1):18–29.
59. Washington Smoak I, Byrd NA, Abu-Issa R, Goddeeris MM, Anderson R, Morris J, Yamamura K, Klingensmith J, Meyers EN. Sonic hedgehog is required for cardiac outflow tract and neural crest cell development. Dev Biol. 2005;283(2):357–72.
60. Hildreth V, Webb S, Chaudhry B, Peat JD, Phillips HM, Brown N, Anderson RH, Henderson DJ. Left cardiac isomerism in the Sonic hedgehog null mouse. J Anat. 2009;214(6):894–904.
61. Desgrange A, Le Garrec JF, Bernheim S, Bonnelykke TH, Meilhac SM. Transient Nodal signaling in left precursors coordinates opposed asymmetries shaping the heart loop. Dev Cell. 2020;55(4):413–431 e6.
62. Francou A, Saint-Michel E, Mesbah K, Kelly RG. TBX1 regulates epithelial polarity and dynamic basal filopodia in the second heart field. Development. 2014;141(22):4320–31.
63. Soh BS, et al. N-cadherin prevents the premature differentiation of anterior heart field progenitors in the pharyngeal mesodermal microenvironment. Cell Res. 2014;24(12):1420–32.

64. Alfano D, Altomonte A, Cortes C, Bilio M, Kelly RG, Baldini A. Tbx1 regulates extracellular matrix-cell interactions in the second heart field. Hum Mol Genet. 2019;28(14):2295–308.
65. Chen L, Fulcoli FG, Ferrentino R, Martucciello S, Illingworth EA, Baldini A. Transcriptional control in cardiac progenitors: Tbx1 interacts with the BAF chromatin remodeling complex and regulates Wnt5a. PLoS Genet. 2012;8(3):e1002571.
66. Sinha T, Li D, Theveniau-Ruissy M, Hutson MR, Kelly RG, Wang J. Loss of Wnt5a disrupts second heart field cell deployment and may contribute to OFT malformations in DiGeorge syndrome. Hum Mol Genet. 2015;24(6):1704–16.
67. Sinha T, Wang B, Evans S, Wynshaw-Boris A, Wang J. Disheveled mediated planar cell polarity signaling is required in the second heart field lineage for outflow tract morphogenesis. Dev Biol. 2012;370(1):135–44.
68. Li D, Angermeier A, Wang J. Planar cell polarity signaling regulates polarized second heart field morphogenesis to promote both arterial and venous pole septation. Development. 2019;146(20):dev181719.
69. Li D, Sinha T, Ajima R, Seo HS, Yamaguchi TP, Wang J. Spatial regulation of cell cohesion by Wnt5a during second heart field progenitor deployment. Dev Biol. 2016;412(1):18–31.
70. Francou A, De Bono C, Kelly RG. Epithelial tension in the second heart field promotes mouse heart tube elongation. Nat Commun. 2017;8:14770.
71. Ramsbottom SA, Sharma V, Rhee HJ, Eley L, Phillips HM, Rigby HF, Dean C, Chaudhry B, Henderson DJ. Vangl2-regulated polarisation of second heart field-derived cells is required for outflow tract lengthening during cardiac development. PLoS Genet. 2014;10(12):e1004871.
72. Watanabe Y, Miyagawa-Tomita S, Vincent SD, Kelly RG, Moon AM, Buckingham ME. Role of mesodermal FGF8 and FGF10 overlaps in the development of the arterial pole of the heart and pharyngeal arch arteries. Circ Res. 2010;106(3):495–503.
73. Vincent SD, Mayeuf-Louchart A, Watanabe Y, Brzezinski JAT, Miyagawa-Tomita S, Kelly RG, Buckingham M. Prdm1 functions in the mesoderm of the second heart field, where it interacts genetically with Tbx1, during outflow tract morphogenesis in the mouse embryo. Hum Mol Genet. 2014;23(19):5087–101.
74. Lioux G, Liu X, Temino S, Oxendine M, Ayala E, Ortega S, Kelly RG, Oliver G, Torres M. A second heart field-derived vasculogenic niche contributes to cardiac lymphatics. Dev Cell. 2020;52(3):350–363 e6.
75. Martucciello S, Turturo MG, Bilio M, Cioffi S, Chen L, Baldini A, Illingworth E. A dual role for Tbx1 in cardiac lymphangiogenesis through genetic interaction with Vegfr3. FASEB J. 2020;34 (11):15062–79.
76. Moretti A, et al. Multipotent embryonic isl1+ progenitor cells lead to cardiac, smooth muscle, and endothelial cell diversification. Cell. 2006;127(6):1151–65.
77. Andersen P, et al. Precardiac organoids form two heart fields via Bmp/Wnt signaling. Nat Commun. 2018;9(1):3140.
78. Xiong H, et al. Single-cell transcriptomics reveals chemotaxis-mediated Intraorgan crosstalk during Cardiogenesis. Circ Res. 2019;125(4):398–410.
79. Rossi G, Broguiere N, Miyamoto M, Boni A, Guiet R, Girgin M, Kelly RG, Kwon C, Lutolf MP. Capturing Cardiogenesis in Gastruloids. Cell Stem Cell. 2021;28(2):230–40.
80. Lescroart F, et al. Defining the earliest step of cardiovascular lineage segregation by single-cell RNA-seq. Science. 2018;359(6380):1177–81.
81. Jia G, et al. Single cell RNA-seq and ATAC-seq analysis of cardiac progenitor cell transition states and lineage settlement. Nat Commun. 2018;9(1):4877.
82. de Soysa TY, et al. Single-cell analysis of cardiogenesis reveals basis for organ-level developmental defects. Nature. 2019;572(7767):120–4.
83. Zhang Q, Carlin D, Zhu F, Cattaneo P, Ideker T, Evans SM, Bloomekatz J, Chi NC. Unveiling complexity and multipotentiality of early heart fields. Circ Res. 2021;129:474–87.
84. Tyser RCV, et al. Characterization of a common progenitor pool of the epicardium and myocardium. Science. 2021;371(6533):10.1126.

85. Kelly RG. The heart field transcriptional landscape at single-cell resolution. Dev Cell. 2023;58 (4):257–66.
86. Kelly RG, Jerome-Majewska LA, Papaioannou VE. The del22q11.2 candidate gene Tbx1 regulates branchiomeric myogenesis. Hum Mol Genet. 2004;13(22):2829–40.
87. Nathan E, Monovich A, Tirosh-Finkel L, Harrelson Z, Rousso T, Rinon A, Harel I, Evans SM, Tzahor E. The contribution of Islet1-expressing splanchnic mesoderm cells to distinct branchiomeric muscles reveals significant heterogeneity in head muscle development. Development. 2008;135(4):647–57.
88. Diogo R, Kelly RG, Christiaen L, Levine M, Ziermann JM, Molnar JL, Noden DM, Tzahor E. A new heart for a new head in vertebrate cardiopharyngeal evolution. Nature. 2015;520 (7548):466–73.
89. Lescroart F, Kelly RG, Le Garrec JF, Nicolas JF, Meilhac SM, Buckingham M. Clonal analysis reveals common lineage relationships between head muscles and second heart field derivatives in the mouse embryo. Development. 2010;137(19):3269–79.
90. Theis S, et al. The occipital lateral plate mesoderm is a novel source for vertebrate neck musculature. Development. 2010;137(17):2961–71.
91. Lescroart F, Hamou W, Francou A, Theveniau-Ruissy M, Kelly RG, Buckingham M. Clonal analysis reveals a common origin between nonsomite-derived neck muscles and heart myocardium. Proc Natl Acad Sci U S A. 2015;112(5):1446–51.
92. Gopalakrishnan S, Comai G, Sambasivan R, Francou A, Kelly RG, Tajbakhsh S. A cranial mesoderm origin for esophagus striated muscles. Dev Cell. 2015;34(6):694–704.
93. Adachi N, Bilio M, Baldini A, Kelly RG. Cardiopharyngeal mesoderm origins of musculoskeletal and connective tissues in the mammalian pharynx. Development. 2020;147(3):10.1242.
94. Wang W, Razy-Krajka F, Siu E, Ketcham A, Christiaen L. NK4 antagonizes Tbx1/10 to promote cardiac versus pharyngeal muscle fate in the ascidian second heart field. PLoS Biol. 2013;11(12):e1001725.
95. Wang W, Niu X, Stuart T, Jullian E, Mauck WM 3rd, Kelly RG, Satija R, Christiaen L. A single-cell transcriptional roadmap for cardiopharyngeal fate diversification. Nat Cell Biol. 2019;21(6):674–86.

Neural Crest

6

Bijoy D. Thattaliyath and Anthony B. Firulli

Abstract

This chapter discusses the role of cardiac neural crest cells in the formation of the septum that divides the cardiac arterial pole into separate systemic and pulmonary arteries. Further, cardiac neural crest cells directly support the normal development and patterning of derivatives of the caudal pharyngeal arches, including the great arteries, thymus, thyroid, and parathyroids. Recently, cardiac neural crest cells have also been shown to indirectly influence the development of the secondary heart field, another derivative of the caudal pharynx, by modulating signaling in the pharynx. The contribution and function of the cardiac neural crest cells has been learned in avian models; most of the genes associated with cardiac neural crest function have been identified using mouse models. Together these studies show that the neural crest cells may not only critical for normal cardiovascular development but also may be involved secondarily because they represent a major component in the complex tissue interactions in the caudal pharynx and outflow tract. Cardiac neural crest cells span from the caudal pharynx into the outflow tract, and therefore may be susceptible to any perturbation in or by other cells in these regions. Thus, understanding congenital cardiac outflow malformations in human sequences of malformations resulting from genetic and/or environmental insults necessarily requires better understanding the role of cardiac neural crest cells in cardiac development.

B. D. Thattaliyath
Department of Pediatrics, Stead Family Children's Hospital, University of Iowa, Iowa, IA, USA
e-mail: bijoy-thattaliyath@uiowa.edu

A. B. Firulli (✉)
Herman B Wells Center for Pediatric Research, Department of Pediatrics, Indiana University School of Medicine, Indianapolis, IN, USA
e-mail: tfirulli@iu.edu

© The Author(s), under exclusive license to Springer Nature Switzerland AG 2024

S. Rickert-Sperling et al. (eds.), *Congenital Heart Diseases: The Broken Heart*,
Advances in Experimental Medicine and Biology 1441,
https://doi.org/10.1007/978-3-031-44087-8_6

Keywords

Cardiac neural crest cells · CNCCs · Neural tube · Nervous system · Ectomesenchymal cells · Thymus · Thyroid gland · Parathyroid gland · Pharyngeal arch arteries · Outflow tract · Aorta · Pulmonary trunk · Pax3 · ZIC1 · Snail · AP-2 · SRY · Epithelial-to-mesenchymal transition · EMT · E-cadherin · Semaphorin · Connexin 43 · Ectoderm · Endoderm · Patent ductus arteriosus · Endothelin-1 · Heart looping · Conduction system · 22q11.2 deletion syndrome · DiGeorge syndrome · Velocardiofacial syndrome · CHARGE syndrome · LEOPARD syndrome · Noonan syndrome · Treacher Collins syndrome · Jacobsen syndrome · SOX10 · TWIST1 · Cardiac regeneration

6.1 Introduction

Cardiac neural crest cells (CNCCs) were first defined by Kirby et al. in 1983 [1]. The "cardiac" region of neural crest cells (NCCs), extending from the axial level of the mid-otic placode to the third somite, was extensively documented using quail chick chimeras and ablation studies. This region was defined as the "cardiac neural crest" [2] because the cells were found to be critical for several aspects of normal cardiovascular development. Significantly, ablation of this region resulted in persistent truncus arteriosus (failure of outflow tract (OFT) septation), mispatterning of the great vessels, and hypoplasia or aplasia of the pharyngeal glands. This constellation of defects is observed in patients with congenital heart defects often associated with microdeletions of chromosome 22q11.2 (DiGeorge syndrome (DGS) or velocardiofacial syndrome (VCFS)) as well as CHARGE (coloboma, heart disease, atresia of the choanae, retarded growth and mental development, genital anomalies, and ear malformations and hearing loss), Noonan, and LEOPARD syndromes. These initial observations were followed by multiple studies in the mouse using transgenic methods that allowed the neural crest cells to be marked genetically by neural crest-specific promoters driving *lacZ* or *GFP* expression as well as by Cre recombinase (Cre-lox) technology to lineage trace neural crest cells in mouse embryos. These genetic tools also allowed for tissue-specific ablation of many genes within the neural crest cell lineage to address the functional importance of various transcription factors and signaling pathways that impact neural crest and cardiovascular development.

We begin with a description of CNCCs in normal development, including their function in remodeling the pharyngeal arch arteries, outflow tract septation, valvulogenesis, development of the cardiac conduction system, and the interaction of CNCCs with the second heart field (SHF), which is important for normal outflow tract alignment and septation. We also discuss more recent data revealing the potential roles of CNCCs in the formation of cardiomyocytes and cardiac regeneration. Finally, we discuss many of the human syndromes associated with aberrant CNCC development.

6.2 An Overview of CNCC Derivatives

NCCs are a population of multipotent cells that originate and delaminate from the dorsal neural tube. Once free of the neural tube, they emigrate to numerous locations throughout the developing embryo, where they ultimately differentiate into diverse cells types, including melanocytes, cartilage, bone, connective tissue, smooth muscle, and neurons. NCCs are divided rostrally to caudally into two large axial populations: the cranial and trunk NCCs. CNCCs are a caudal subpopulation of the cranial NCCs and represent a transitional region between the cranial and trunk NCC populations. While both the cranial and trunk NCCs give rise to melanocytes and the peripheral nervous system, only cranial NCCs give rise to ectomesenchymal cells. These ectomesenchymal cells contribute to the development of a wide variety of structures within the head, neck, and heart. The pre-otic cranial NCCs contribute significantly to development of the skeletal structures of the face. The ectomesenchyme derived from the post-otic or CNCC region migrates into the caudal pharyngeal arches 3, 4, and 6 and contribute to cardiovascular development and the formation of the thymus, thyroid, and parathyroid glands (Fig. 6.1) [3]. Some of these CNCCs will condense to form the sheath of smooth muscle (or tunica media) around the pharyngeal arch arteries. Importantly, CNCCs are also critical for the repatterning of the bilaterally symmetrical pharyngeal arch arteries to form the asymmetric great arteries of the head and neck (Fig. 6.1) [4]. An additional subpopulation of CNCCs in the caudal pharyngeal arches will further migrate into the developing cardiac outflow tract where they differentiate into a condensed mesenchyme at the junction of the presumptive aortic and pulmonary myocardium of the outflow tract (Fig. 6.2) [5, 6]. This condensed mesenchyme, termed the "aorticopulmonary septation complex," will divide the most distal outflow into the base of the aorta and pulmonary trunk and the middle outflow into the aortic and pulmonary semilunar valve regions. CNCCs also further migrate into the most proximal outflow tract where they may be involved in closure of the membranous ventricular outflow septum. Another population of pre-otic NCCs that migrate through the anterior pharyngeal arches has been observed to contribute to the smooth muscle of the coronary arteries in mouse and chick [7] and are, therefore, arguably also CNCCs. Finally, some of the CNCCs destined for the outflow tract contribute to the cardiac ganglia as well as the surrounding and insulating the bundle of His, which transmits conduction signals to the cardiac ventricles [8, 9].

6.3 Signaling Pathways Regulating Early CNCC Migration

CNCCs require a wide variety of environmental signals to orchestrate their specification, migration, proliferation, and, when at their final destination, differentiation. The complex molecular cascades required to establish the migratory and multipotent nature of NCCs are not fully understood. NCCs specify at the border of the non-neural ectoderm and the neural plate. Secreted extracellular signaling molecules that include *Wnts*, bone morphogenetic proteins (*Bmps*), and fibroblast growth

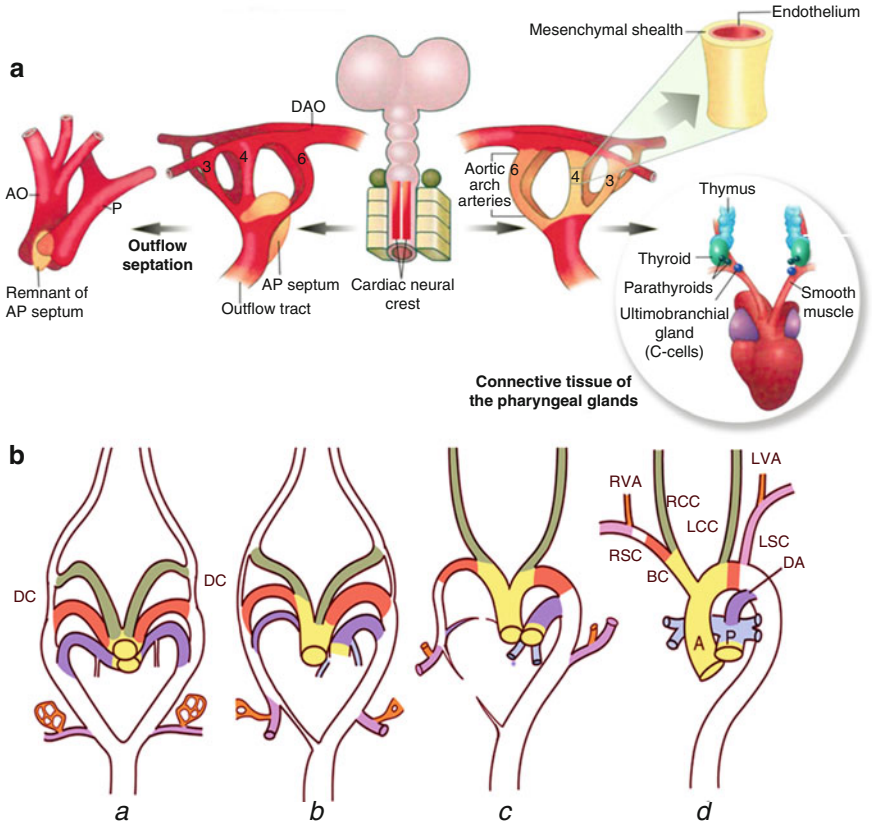

Fig. 6.1 (a) Derivatives of cardiac neural crest cells (CNCCs). CNCCs originate in the dorsal neural tube and migrate to pharyngeal arches 3, 4, and 6 and into the outflow tract to form the aorticopulmonary septum (*AP*). The AP septum divides the single outflow tract into the aorta (*AO*) and pulmonary trunk (*P*). CNCCs form a mesenchymal sheath around the aortic arch arteries and the connective tissue of the pharyngeal glands. (b) Schematic of the development of the paired aortic arch arteries and the subsequent remodeling to form the mature pattern of the great vessels (a–d). (*a* and *b*) Diagram of the bilaterally symmetrical aortic arch arteries that carry the early cardiac output to the dorsal aorta, which then distributes blood to the mouse or human embryo. (c and d) The early symmetry is lost when these vessels are remodeled to be the adult great arteries of the thorax. The third aortic arch arteries (green) form the right and left common carotid arteries (*RCC* and *LCC*, respectively). The left fourth aortic arch artery (*red*) forms part of the transverse arch of the aorta. The right fourth forms the base of the right subclavian artery (*RSC*). The left sixth aortic arch artery (*purple*) forms the ductus arteriosus (*DA*). The seventh dorsal intersegmental arteries (*pink*) form most of the RSC and left subclavian (*LSC*) arteries. Abbreviations: BC brachiocephalic artery, LVA and RVA left and right vertebral arteries, respectively; A aorta, P pulmonary trunk, DOA dorsal aorta, DC ductus caroticus (adapted from [62, 63])

factors (*Fgfs*) separate the non-neural ectoderm from the neural plate during neural induction [10]. For example, downregulation of *Bmp* signaling within the neural plate accompanied by an increase in *Bmp* signaling in the surface ectoderm results in

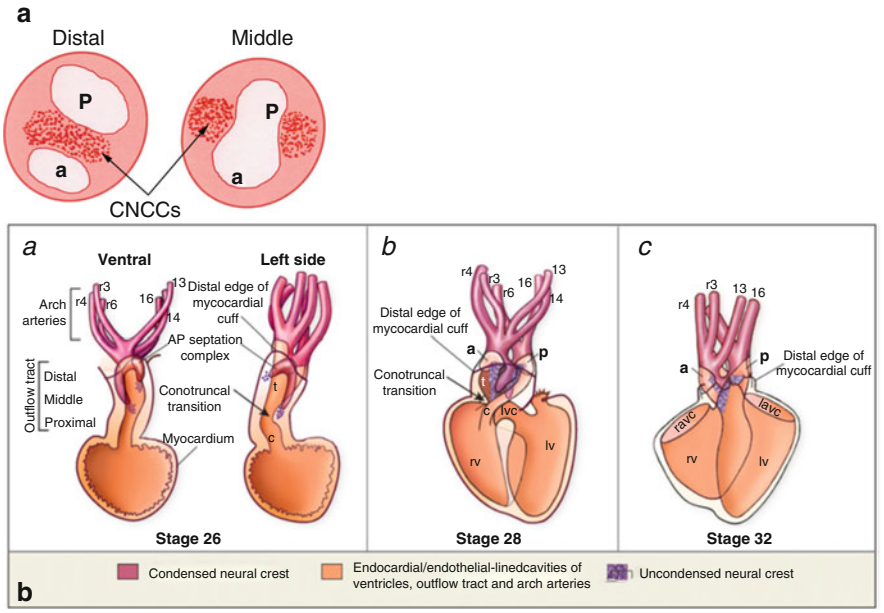

Fig. 6.2 (a) Cardiac neural crest cells (*CNCCs*) in the outflow cushions. Cross section through the distal and middle outflow tract shows the position of the condensed CNCC-derived mesenchyme within the cushions to form the future aorta (*a*) and pulmonary trunk (*p*). (b) Stages of outflow septation in the chick. (*a*) An U-shaped septation complex straddles the aortic sac between the fourth and sixth aortic arch arteries. (*b*) The septation complex grows at the expense of the prongs. (*c*) Septation of the conus (adapted from Hutson and Kirby[62])

the transcriptional activation of the gene encoding the snail family zinc finger transcription factor *Slug* in cells at the border between the two tissues. These cells subsequently become specified as NCCs. Induction is heralded by the expression of *Pax3* and Zic family member 1 (*Zic1*) transcription factor genes expressed within the dorsal neural tube, followed by activation of established NCC specification genes that encode transcription factors: *Snail*, *Slug*, AP-2 (*AP-2*), SRY (sex-determining region Y)-box 9 (*Sox9*) and *Sox10* [11], and forkhead box (*Fox*) D within the newly specified NCCs [10].

Once induced, the NCCs require another set of overlapping signaling pathways to disassociate and emigrate from the dorsal neural tube. This process is called epithelial-to-mesenchymal transition (EMT). SOX9 activates *Snai2* expression that facilitates NCC EMT [12]. During EMT, specified NCCs lose their cell–cell contacts with the cells of the neural tube, reorganize their cytoskeleton, and acquire filipodia that allow them to migrate through the developing embryo. One of the downstream effectors of BMP signaling is Smad-interacting protein 1 (*Sip1*). SIP1, an E-box-binding zinc finger transcriptional repressor expressed by pre-migratory and migrating cranial NCCs, is known to directly repress the cell adhesion protein E-cadherin within epithelial cells and thus represses cell–cell adhesion [13]. Downregulation of

E-cadherin is necessary for NCC EMT and subsequent migration from the neural tube. Thus, one of the major roles of BMP signaling in the CNCCs is to activate *Sip1*, which suppresses expression of *E-cadherin*, allowing the cells to detach from their neighbors.

Release from cell–cell contacts with adjacent cells allows the CNCCs to interact in three dimensions with extracellular matrix components. Migratory NCCs are now "mesenchymal" in phenotype, they express the intermediate filament protein vimentin, and are flattened cells with both visible filopodia and lamellipodia that facilitate cell movement. CNCCs also express a complex collection of integrins, which are cell surface receptors that mediate attachments between other cells and the extracellular matrix. Integrins are important for conveying cell signaling and also influence cell shape and mobility in addition to regulation of the cell cycle [14]. In addition to a role in induction, *Wnt* signaling also plays a role in CNCC migration. *Wnt1* is expressed within early migrating NCCs and is rapidly downregulated as the NCCs leave the neural tube. Mutations in the mouse *Dishevelled2* gene, a downstream component of *Wnt* signaling, results in cardiac defects similar to those observed after cardiac NCC (cNCC) ablation and include persistent truncus arteriosus, an extreme defect of the outflow tract where the pulmonary artery and dorsal aorta fail to separate their circulations [15].

Once NCCs migrate away from the neural tube, they travel along distinct migratory pathways to specific tissue destinations. In conjunction with *FGF* signaling, members of the *ephrin* family of ligands and receptors, semaphorins, and gap junction protein connexin 43, define these specific CNCC migration pathways. Ephrin signaling appears more important for directing migration of CNCCs into the pharyngeal arches rather than guiding away from the neural tube where semaphorins have an important role. Semaphorins are a family of secreted ligands, and their receptors (plexins and neuropilins) are also important players in the targeted migration of the CNCCs to the outflow tract of the heart. The semaphorin receptors plexin-A2, plexin-D1, and neuropilin-1 (*Nrp1*) are expressed in CNCCs. SEMA6A and SEMA6B ligands have been shown to repel NCCs, whereas SEMA3C attracts NCCs. *Sema3C* is expressed in the outflow tract, whereas *Sema6A* and *Sema6B* are expressed in the dorsal neural tube and lateral aspects of the pharyngeal mesenchyme [16]. These observations suggests that CNCCs migrate from the neural tube through a combination of SEMA6A and 6B repulsion, and SEMA3C attractions to their target, the outflow tract. Studies that show downregulation of each semaphorin receptor in NCCs by RNA interference (RNAi) knockdown reveal a failure of the NCCs to normally migrate into the cardiac outflow tract [16].

An interesting study by Vincentz et al. suggests a role of the basic helix–loop–helix (bHLH) transcription factor TWIST1 in determining cell lineage commitment to either the ectoderm or mesoderm after CNCCs have migrated into the OFT [17]. NCCs migrate in the developing embryo and commit to CNCCs that migrate to the developing mesoderm and contribute to septation of the OFT [1, 18]. NCCs also migrate into the ectoderm and contribute to the formation of the autonomic nervous system [19]. Bone morphogenetic proteins (BMPs), as previously

described, which are present in the milieu of this differentiation, upregulate the bHLH transcription factors *Twist1*, *Hand1*, and *Hand2*. These factors may play a role in pre-migratory differentiation [20]. In NCC-conditional *Twist1* knockout (CKO) mice, using both *Wnt1-Cre* (pre-migration) and $Hand1^{Cre}$ (post-migration) alleles leads to the ectopic neural tissue resembling sympathetic ganglia. On further dissection of the TWIST1 pathway, it was found to directly repress the homeobox transcription factor PHOX2B and its upstream regulator SOX10. Disruption of TWIST1 function leads to the upregulation of *Phox2b* and, consequently, the formation of ectopic neurons [17]. These data suggest that CNCCs are not solely specified at their origin on the neural tube and that transcription factors such as TWIST1 actively guide CNCC fate determination and downstream differentiation to the mesodermal versus ectodermal tissue.

In a later study, the roles of the related HAND1 and HAND2 transcription factors were interrogated within both CNCCs and SHF during mouse OFT development [21]. *Hand1* NCC-conditional deletion mice are viable [22] but exhibit low penetrance OFT phenotypes, including aberrant origin of the right subclavian artery, as well as atrial (ASD) and ventricular septal (VSD) defects [21]. *Hand2* NCC-conditional deletion mice exhibit misalignment of the aortic arch arteries and present with a double outlet right ventricle (DORV) and an accompanying VSD [23]. Heterozygous null *Hand1* or *Hand2* mice are phenotypically normal. However, compound $Hand1^{fx/-}$;$Hand2^{fx/-}$ all present with a DORV, thus showing that cumulative *Hand* gene dosage is also essential for maintaining normal CNCC differentiation and OFT morphogenesis. This is patently evident in double NCC knockout (*Wnt1-Cre;* $Hand1^{fx/-}$;$Hand2^{fx/-}$) mice in which there is a 100% penetrance of persistent truncus arteriosus (PTA) and impaired cardiac function, resulting in a dilatated/hypertrophic left ventricle [21]. Mechanistically, HAND factors appear to regulate CNCC localization within the forming OFT where NCC lineage analysis and expression of *Sema3C* show that the CNCCs are present but move to inappropriate locations [21]. Together, these data show that Twist-family bHLH factors modulate both CNCC fate and morphological positioning within the forming OFT contributing to cardiac phenotypes when misregulated.

6.4 CNCCs and Pharyngeal Arch Artery Remodeling

CNCCs migrate and populate pharyngeal arches 3, 4, and 6 and participate in the development of the pharyngeal arch arteries. Specifically, the CNCCs migrate between the pharyngeal ectoderm and endoderm, proliferate, and envelope the endothelial vessels of the nascent aortic arch arteries. The pharyngeal arch arteries initially form as a bilaterally symmetrical series of arteries that connect the aortic sac to the paired dorsal aortas (Fig. 6.1). Remodeling of the pharyngeal arteries requires programmed asymmetrical expansion, regression, persistence, and change of the relative position of the different vascular segments (Fig. 6.1). Pharyngeal arch arteries 3–6 are remodeled into the asymmetric great arteries, including the common carotid, definitive aortic arch, and the ductus arteriosus. The right and left common

carotid arteries are derived from the right and left third arch artery, respectively. The arch of the aorta is derived from the left fourth arch artery. The left sixth arch artery gives rise to the ductus arteriosus [24]. CNCCs form the smooth muscle tunica media of these arteries [25]. Interestingly, CNCC ablation studies show that CNCCs are not required for aortic arch artery formation but are required for their repatterning [4]. Defects in fourth arch artery remodeling include the interrupted aortic arch (IAA), double aortic arch, and aberrant (retroesophageal) subclavian artery. Patent ductus arteriosus and proximal pulmonary artery hypoplasia arise from defects in the sixth arch artery.

Several signaling pathways have been implicated in aortic arch artery patterning. Mutations in the Endothelin 1 (*ET1*) pathway in mouse models result in patterning defects of the great arteries and outflow despite normal migration of the neural crest cells [26–30]. Haploinsufficiency for the transcriptional regulator T-box (*Tbx*) 1, by contrast, affects the initial growth and patterning of the arch arteries, the fourth arch artery in particular. Vessel growth failure, poor smooth muscle differentiation, and abnormal CNCC migration have all been implicated in contributing to the observed defects [31]. Interestingly, *Tbx1* is not expressed within the CNCCs but in the pharyngeal endoderm, ectoderm, and mesoderm (second heart field; see below). Loss of *Tbx1* indirectly affects the CNCCs by impacting tissue-specific gene expression and altering the CNCC migration environment [29, 32, 33]. This in turn impacts signaling between the NCCs and surrounding tissues, ultimately leading to abnormal pharyngeal arch patterning.

6.5 CNCCs and Septation of the Cardiac Outflow Tract and Valvulogenesis

After CNCCs migrate into the caudal pharynx, a subpopulation of these cells continues to further migrate into the cardiac outflow cushions (Fig. 6.2). The cushions are cardiac jelly (extracellular matrix)-filled ridges that spiral within the outflow tract. The outflow cushions are largely populated by two distinct groups of mesenchymal cells, depending on the proximal-distal location within the outflow tract. In the proximal or conal outflow tract, the cushions are populated by endocardial cells that undergo an EMT induced by the conal myocardium. These mesenchymal cells will form the bulk of the semilunar valve leaflets. CNCCs move into the distal or truncal cushions and form two condensed columns of cells that are joined by a shelf of condensed CNCCs at the aortic sac (Figs. 6.1 and 6.2). The horseshoe-shaped aorticopulmonary septation complex is positioned between the origins of the fourth and sixth pairs of the arch arteries where it will divide the pulmonary and systemic circulation [34]. Septation proceeds as the aorticopulmonary septation complex elongates into the distal outflow tract at the expense of the prongs [5, 35]. This splits the common arterial trunk into the aorta and pulmonary trunk (Fig. 6.2). Once the aortic sac and truncal portion of the outflow is divided, the proximal outflow septum in the conus closes in a zipper-like process from distal to proximal, toward the ventricles. This is accomplished by the invasion of myocardial

cells into the cushions in a process called myocardialization [36]. After division of the outflow tract, the cushion mesenchyme is remodeled to form the aortic and pulmonary semilunar valves. Each valve has three cusps or leaflets. The valve leaflets receive a major contribution from the endocardial-derived mesenchymal cells. CNCCs are observed at the tip of the semilunar valve leaflets and have been shown play a role in valve remodeling and maturation [37–39]. However, it is unclear to what extent CNCCs play a role in initial valve formation, though apoptosis and alterations in the extracellular matrix have been described in the process of semilunar valvulogenesis in mouse models [40–42].

6.6 The Role of Interaction Between CNCCs and the Secondary Heart Field

An unexpected finding from chick CNCC ablation experiments is that CNCCs are required not only for outflow septation but also for normal heart looping. Abnormal looping is one of the earliest defects observed after cardiac neural crest ablation and can be observed days before the CNCCs actually reach the outflow tract. The defective cardiac looping is caused by the failure of addition of a new outflow myocardium to the growing heart tube. The source of these new cardiomyocytes is a domain termed the "secondary heart field," which is a subpopulation of the second heart field. During cardiac looping, the secondary heart field is located in the ventral caudal pharynx, directly dorsal of the outflow attachment to the pharynx. Secondary heart field-derived cells add to the outflow and lengthen the growing heart tube to ultimately contribute to both the myocardium and smooth muscle at the level of the semilunar valves (Fig. 6.2). Lengthening of the outflow tract allows for the proper alignment of the aorta and pulmonary trunk with the left and right ventricles. An abnormally shortened heart loop results in arterial pole malalignment defects, such as a double outlet right ventricle (DORV) and an overriding aorta [43]. Thus, the looping defects observed after CNCC ablation suggest that CNCCs [44] are required for normal deployment of the second heart field.

As discussed above, outflow alignment and outflow septation involve distinct cell populations, the second heart field derivatives, and CNCCs. The ablation studies suggest that both these cell populations must act together to form the normal divided outflow tract. Indeed, after CNCC ablation, proliferation within the secondary heart field cells is increased due to elevated levels of FGF8, indicating that the CNCCs influence FGF signaling within the pharynx [45, 46]. Conversely, inhibition of NOTCH signaling within the second heart field results in abnormal migration of CNCCs into the outflow tract, suggesting that a NOTCH-dependent signal originating from the SHF can modulate CNCC behavior [47]. Thus, coordinated morphogenesis of these two cell populations is essential to form both the myocardium and the septation complex that divides the outflow tract.

6.7 CNCCs in Cardiac Innervation and Conduction

CNCCs form the entire parasympathetic innervation of the heart [1]. While the components of the cardiac conduction system are largely innervated by neural crest-derived cardiac ganglia, the essential components of the cardiac conduction system are specialized cardiomyocytes [48, 49]. Lineage analysis showed that some cells of His–Purkinje fibers lack mesoderm posterior 1 homolog (*Mesp-1*), implying that some of these conduction cells may be of CNCC in origin; however, variation in Cre expression cannot be ruled out as an explanation of these findings [50]. Retroviral lineage studies in chick and Cre lineage analysis in mouse show a contribution of CNCCs to the inflow region proximal to the cardiac conduction system [51, 52], but CNCC contribution to the inflow has not been demonstrated using quail chick chimeras [5]. Another lineage analysis using the established NCC-specific *Wnt1-Cre* mouse suggested that the CNCCs contribute to the central conduction system [53].

Irrespective of whether CNCCs contribute directly to the His–Purkinje conduction system, they are required for the normal development and maturation of the cardiac conduction system. A large number of fibroblasts derived from the epicardium, endocardium, and NCCs, reside within the mature conduction system and function to insulate the ventricular pathways. Following ablation of CNCCs in chick embryos, there is an observed delay in the maturation of conduction system function stemming from a failure of the conduction bundles to condense [9]. This finding is supported by mouse studies in which deletion of the transcription factor Sp4 (*Sp4/Hf1b*) specifically within NCCs results in atrial and atrioventricular conduction dysfunction resulting from deficiencies in the neurotrophin tyrosine kinase receptor 3 (*Ntrk3/trkC*) [54].

6.8 The Potential Role of CNCCs in Cardiac Regeneration

CNCCs have been proposed to play a significant role in adult cardiomyocyte regeneration in experimentally injured zebrafish hearts [55–57]. Similarly, lineage-tracing studies have suggested the contribution of CNCCs to the formation of cardiomyocytes in chick embryo hearts; however, data are contradictory.

CNCCs are multipotent in nature and arise from the neural tube and migrate ventrally and differentiate and commit to form a wide variety of tissues and organs during early embryonic development [58]. Recent exciting yet somewhat controversial studies have shown the capability of CNCCs to differentiate into cardiomyocytes [59]. Studies involving resection of the ventricular apex showed impressive and complete repair and regeneration of the zebrafish ventricle [57]. Subsequent studies demonstrated that these regenerative cardiomyocytes were derived from preexisting mature cardiomyocytes [60]. A number of studies have now shown the role of Sox10 in zebrafish cardiac regeneration [59, 61] (Fig. 6.3) via the activation of the embryonic cardiomyocyte gene regulatory network [59]. To further delineate the contribution of embryonically derived *sox10*+ lineage versus adult *sox10*-expressing

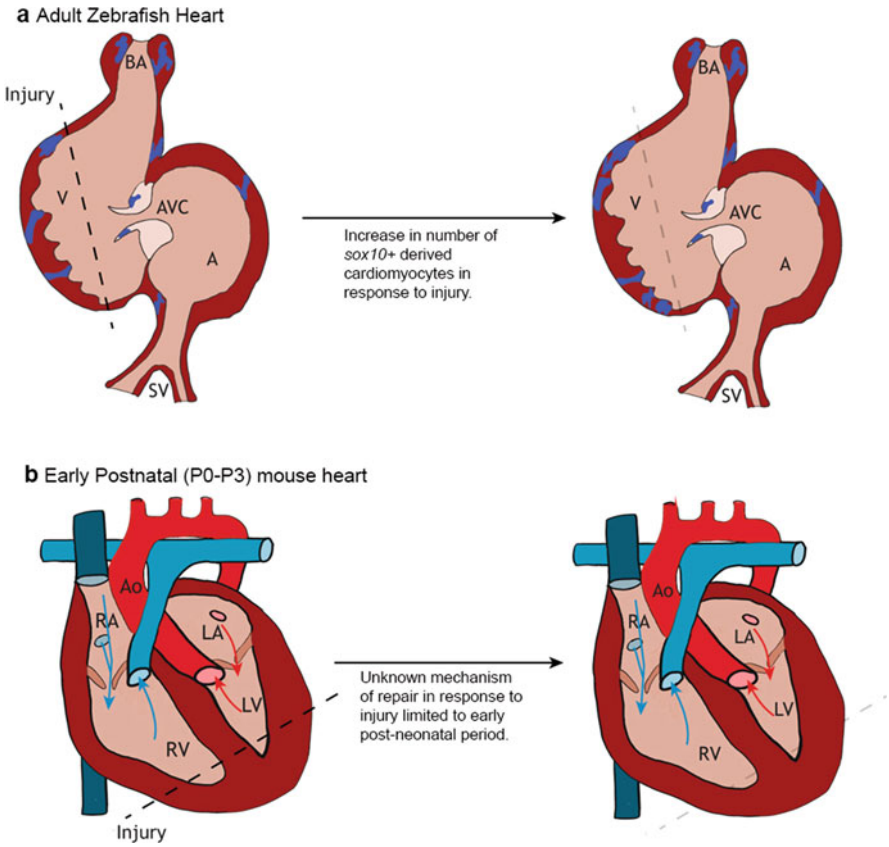

Fig. 6.3 Cardiac neural crest cells (CNCCs) in heart regeneration. (a) Injury to the ventricle (dashed line) in an adult zebrafish heart leads to an increase in the number of *sox10*+ lineage-derived cardiomyocytes (blue). Alternatively, activated SOX10 expression within neighboring cardiomyocytes could account for the effect. Specifically, these cardiomyocytes are seen close to the site of injury. The myocardium and lumen are in red and light red, respectively. (b) Injury to the ventricle in the postnatal mouse heart from P0 to P3 results in successful repair. The contribution of cNCCs or *Sox10*+ cells to cardiac repair in the mouse heart is still controversial. A atrium, Ao aorta, AVC atrioventricular junction, BA bulbus arteriosus, LA left atrium, LV left ventricle, RA right atrium, RV right ventricle, SV sinus venosus, V ventricle (adapted from George et al. [82] with permission)

cardiomyocytes in cardiomyocyte regeneration post-injury, Mercader and colleagues used *sox10*-driven tamoxifen-inducible Cre [62, 63] and noted an increase of 0.7% cells expressing *sox10* to 5% of cells expressing *sox10*, 14 days post-injury with an increase in cell proliferation and motility. Ablation of *sox10*+ cardiomyocytes prior to cardiac injury resulted in lower numbers of replacement of cardiomyocytes accompanied by larger fibrotic scars [62]. These findings suggest the significant contribution of *sox10*+ CNCC-derived cardiomyocytes in zebrafish cardiac regeneration. While these studies are highly encouraging, this mechanism is

currently not observed in mammals and it does not account for the possibility that renewing fish cardiomyocytes outside the CNCC lineage can upregulate SOX10, thus confounding the data interpretation.

Studies in the amphibian *Xenopus laevis* have shown that they possess a three-chambered heart and a common outflow trunk. Reporter Red Fluorescent Protein (RFP) co-labeled with a cardiomyocyte-specific marker MF20 failed to show any cNCC contribution to outflow tract septation [64]. Hence, *Xenopus* lacks septation of the OFT and has a common truncus with no anatomical separation of oxygenated and non-oxygenated blood.

Data demonstrating cardiomyocyte regeneration in the mouse model are limited. Partial surgical resection of mouse heart apex regenerates in 1-day old mice, and the regenerative potential diminishes by P2 and P3 and is completely lost by the first week of life [65]. A recent study has found that transcription factor *Isl*+ expressing CNCCs, though highly proliferative and active in the IFT (inflow tract) during mammalian cardiac morphogenesis, loses its clonal amplification properties in the postnatal period [66]. It will be especially interesting to see whether further analysis shows that this observation holds true.

6.9 Cardiac and Extracardiac Congenital Defects Due to Defective CNCC Development

6.9.1 Failure of Outflow Septation: Persistent Truncus Arteriosus

Persistent truncus arteriosus (PTA) is found in 2–4% of congenital heart disease patients [67]. It results from a failure of outflow septation stemming from a failure of the CNCCs in the formation/function of the aorticopulmonary septation complex. This defect is characterized by a single large vessel and a common valve (the truncal valve) that originates from the base of the heart supplying the systemic, coronary, and pulmonary circulation. A large ventricular septal defect (VSD) due to malalignment of the OFT usually accompanies PTA. Furthermore, a substantial proportion of patients with PTA have associated IAA, which almost always occurs between the left common carotid and the left subclavian arteries.

6.9.2 DiGeorge Syndrome (22q11.2 Deletion Syndrome)

DiGeorge syndrome (DGS) is caused by hemizygous deletions of chromosome 22q11.2 [68]. The cardiovascular defects in this syndrome include the IAA (interrupted aortic arch), PTA, tetralogy of Fallot, or DORV, implicating defective neural crest development. DGS is also often associated with a hypoplastic thymus and varying levels of immunodeficiency. In this syndrome, varying degrees of craniofacial defects, VSD, aberrant origin of the right subclavian artery, hypothyroidism, psychosis, cleft lip, and cleft palate are usually seen. Besides deletions of 22q11.2, this syndrome can also be caused by other deletions or translocations

involving chromosome 22q11 [69]. Occasionally, no deletions are found. Gene penetrance is variable, and phenotypic expression of the same deletion may have a variable clinical picture. Interestingly, *TBX1* is one of the genes included in the deleted region. *Tbx1* deficiency in mouse models recapitulates the cardiovascular phenotypes of DGS. As mentioned above, while *Tbx1* is not expressed within CNCCs, it is expressed in the pharyngeal epithelia and the second heart field and impacts tissue-specific gene expression, thus altering the environment through which the CNCCs migrate and differentiate. Tbx1 deletion alters the downstream expression of *Gbx2*. This results in the defective migration of CNCCs and abnormal pharyngeal arch development [70], leading to an interrupted aortic arch. There is also defective development of the second heart field, causing a hypoplastic or misaligned OFT [71, 72].

6.9.3 CHARGE Syndrome

CHARGE syndrome is characterized by the following defects: coloboma of the eye, heart defects, atresia of the nasal choanae, retarded growth and/or development, genital abnormalities, and ear anomalies. The collective anomalies associated with CHARGE syndrome overlap with DGS-associated defects. The thyroid and parathyroid glands are often absent and accompany aortic arch artery and outflow defects, suggesting that NCC development is affected in this syndrome. More than 90% of individuals affected by CHARGE syndrome have heterozygous mutations in *CHD7*, a member of the chromodomain helicase DNA-binding gene family [73]. Animal studies show that *CHD7* is required for activation of critical NCC genes, including *Sox9*, *Slug*, and *Twist* family bHLH transcription factor (*Twist1*), and genetically interacts with Tbx1 [74, 75].

6.9.4 LEOPARD and Noonan Syndromes

Noonan and LEOPARD syndromes have considerable phenotypic similarities. Noonan syndrome manifests as growth retardation, facial dysmorphism, skeletal abnormalities, hypertrophic cardiomyopathy, and congenital heart defects, including pulmonary stenosis, ventricular septal defect, and aortic coarctation. LEOPARD syndrome is characterized by lentigenes, electrocardiogram (ECG) conduction abnormalities, ocular hypertelorism, pulmonic stenosis, abnormal genitalia, retardation of growth, and sensorineural deafness. Both of these syndromes are caused by mutations within the *PTPN11* gene that encodes for the protein tyrosine phosphatase, non-receptor type 11 (SHP2 phosphatase). Approximately half of Noonan syndrome patients present with an activating mutation in *PTPN11* that results in increased SHP2 phosphatase activity, thus altering signaling through the Ras/mitogen-activated protein kinase (Ras/MAPK) pathway. Conversely, the vast majority of individuals with LEOPARD syndrome carry *PTPN11* mutations [76, 77] that produce catalytically inactive SHP2 that exhibit dominant-negative effects. In animal

models, abnormal SHP2 activity results in defectives in both NCC migration and differentiation.

6.9.5 Treacher Collins Syndrome (TCS)

Treacher Collins syndrome (TCS) is rare congenital disorder with severe craniofacial defects. Clinical features of TCS are due to the abnormal development of the first and second pharyngeal arches [78]. *TCOF1* gene mutation results in abnormal messenger RNA (mRNA) expression in NCCs. Cardiac defects include septal defects (ventricular and atrial) and patent ductus arteriosus (PDA) [79]. Using small interfering RNA (siRNA) in human-induced pluripotent stem cells, Serrano et al. were able to disrupt *TCOF1* expression, resulting in aberrant migration of NCCs and a TCS-like phenotype [80].

6.9.6 Jacobsen Syndrome

Jacobsen syndrome is a rare chromosomal disorder characterized by deletion of genes on the q arm of chromosome 11, resulting in a phenotype with congenital heart defects, dysmorphic features, developmental delay, and bleeding disorders. Cardiac defects include large membranous ventricular septal defects and hypoplastic left ventricle. Ye and colleagues demonstrated that gene-targeted disruption of the *ETS-1* gene in E10.5 mouse embryos resulted in defective migration of CNCCs and a large ventricular septal defect similar to a DORV phenotype [81].

6.10 Conclusions

Over the last four decades, since the discovery of CNCCs, we have come to better understand their role in cardiovascular development. Like any other organ system or pathway, the functions of neural crest cells cannot be completely understood in isolation—rather the role of CNCCs in the heart reflects dynamic interactions with other cells and tissues. The varying severity of cardiac defects with single-gene mutations or identical chromosomal microdeletions reflects the importance of other factors that form the pharyngeal microenvironment with the neural crest cells. The future directions of this field will include deciphering the cross talk between CNCCs and other cells in the pharyngeal region and heart, deciphering the role of CNCCs in mammalian cardiomyocyte regeneration if any, and determining the gene regulatory networks involved.

References

1. Kirby ML, Gale TF, Stewart DE. Neural crest cells contribute to normal aorticopulmonary septation. Science. 1983;220(4601):1059–61. https://doi.org/10.1126/science.6844926.

2. Kirby ML, Turnage KL 3rd, Hays BM. Characterization of conotruncal malformations following ablation of "cardiac" neural crest. Anat Rec. 1985;213(1):87–93. https://doi.org/10.1002/ar.1092130112.
3. Bockman DE, Kirby ML. Dependence of thymus development on derivatives of the neural crest. Science. 1984;223(4635):498–500. https://doi.org/10.1126/science.6606851.
4. Bockman DE, Redmond ME, Waldo K, Davis H, Kirby ML. Effect of neural crest ablation on development of the heart and arch arteries in the chick. Am J Anat. 1987;180(4):332–41. https://doi.org/10.1002/aja.1001800403.
5. Waldo K, Miyagawa-Tomita S, Kumiski D, Kirby ML. Cardiac neural crest cells provide new insight into septation of the cardiac outflow tract: aortic sac to ventricular septal closure. Dev Biol. 1998;196(2):129–44. https://doi.org/10.1006/dbio.1998.8860.
6. Bajolle F, Zaffran S, Meilhac SM, Dandonneau M, Chang T, Kelly RG, et al. Myocardium at the base of the aorta and pulmonary trunk is prefigured in the outflow tract of the heart and in subdomains of the second heart field. Dev Biol. 2008;313(1):25–34. https://doi.org/10.1016/j.ydbio.2007.09.0236.
7. Arima Y, Miyagawa-Tomita S, Maeda K, Asai R, Seya D, Minoux M, et al. Preotic neural crest cells contribute to coronary artery smooth muscle involving endothelin signalling. Nat Commun. 2012;3:1267. https://doi.org/10.1038/ncomms22587.
8. Miyagawa-Tomita S, Waldo K, Tomita H, Kirby ML. Temporospatial study of the migration and distribution of cardiac neural crest in quail-chick chimeras. Am J Anat. 1991;192(1):79–88. https://doi.org/10.1002/aja.1001920109.
9. Gurjarpadhye A, Hewett KW, Justus C, Wen X, Stadt H, Kirby ML, et al. Cardiac neural crest ablation inhibits compaction and electrical function of conduction system bundles. Am J Physiol Heart Circ Physiol. 2007;292(3):H1291–300. https://doi.org/10.1152/ajpheart.01017.20063.
10. Sauka-Spengler T, Bronner-Fraser M. A gene regulatory network orchestrates neural crest formation. Nat Rev Mol Cell Biol. 2008;9(7):557–68. https://doi.org/10.1038/nrm24285.
11. Aoki Y, Saint-Germain N, Gyda M, Magner-Fink E, Lee YH, Credidio C, et al. Sox10 regulates the development of neural crest-derived melanocytes in Xenopus. Dev Biol. 2003;259(1):19–33. https://doi.org/10.1016/s0012-1606(03)00161-15.
12. Sakai D, Suzuki T, Osumi N, Wakamatsu Y. Cooperative action of Sox9, Snail2 and PKA signaling in early neural crest development. Development. 2006;133(7):1323–33. https://doi.org/10.1242/dev.022975.
13. Van de Putte T, Maruhashi M, Francis A, Nelles L, Kondoh H, Huylebroeck D, et al. Mice lacking ZFHX1B, the gene that codes for Smad-interacting protein-1, reveal a role for multiple neural crest cell defects in the etiology of Hirschsprung disease-mental retardation syndrome. Am J Hum Genet. 2003;72(2):465–70. https://doi.org/10.1086/3460927.
14. Jones JL, Walker RA. Integrins: a role as cell signalling molecules. Mol Pathol. 1999;52(4):208–13. https://doi.org/10.1136/mp.52.4.2081.
15. Hamblet NS, Lijam N, Ruiz-Lozano P, Wang J, Yang Y, Luo Z, et al. Dishevelled 2 is essential for cardiac outflow tract development, somite segmentation and neural tube closure. Development. 2002;129(24):5827–38. https://doi.org/10.1242/dev.001640.
16. Toyofuku T, Yoshida J, Sugimoto T, Yamamoto M, Makino N, Takamatsu H, et al. Repulsive and attractive semaphorins cooperate to direct the navigation of cardiac neural crest cells. Dev Biol. 2008;321(1):251–62. https://doi.org/10.1016/j.ydbio.2008.06.0284.
17. Vincentz JW, Firulli BA, Lin A, Spicer DB, Howard MJ, Firulli AB. Twist1 controls a cell-specification switch governing cell fate decisions within the cardiac neural crest. PLoS Genet. 2013;9(3):e1003405. https://doi.org/10.1371/journal.pgen.10034059.
18. Brown CB, Baldwin HS. Neural crest contribution to the cardiovascular system. Adv Exp Med Biol. 2006;589:134–54. https://doi.org/10.1007/978-0-387-46954-6_89.
19. Howard MJ. Mechanisms and perspectives on differentiation of autonomic neurons. Dev Biol. 2005;277(2):271–86. https://doi.org/10.1016/j.ydbio.2004.09.0344.

20. Nelms BL, Labosky PA. Transcriptional control of neural crest development. San Rafael: Developmental Biology; 2010.
21. Vincentz JW, Firulli BA, Toolan KP, Osterwalder M, Pennacchio LA, Firulli AB. HAND transcription factors cooperatively specify the aorta and pulmonary trunk. Dev Biol. 2021;476:1–10. https://doi.org/10.1016/j.ydbio.2021.03.0111.
22. Barbosa AC, Funato N, Chapman S, McKee MD, Richardson JA, Olson EN, et al. Hand transcription factors cooperatively regulate development of the distal midline mesenchyme. Dev Biol. 2007;310(1):154–68. https://doi.org/10.1016/j.ydbio.2007.07.0360.
23. Holler KL, Hendershot TJ, Troy SE, Vincentz JW, Firulli AB, Howard MJ. Targeted deletion of Hand2 in cardiac neural crest-derived cells influences cardiac gene expression and outflow tract development. Dev Biol. 2010;341(1):291–304. https://doi.org/10.1016/j.ydbio.2010.02.0018.
24. Frisdal A, Trainor PA. Development and evolution of the pharyngeal apparatus. Wiley Interdiscip Rev Dev Biol. 2014;3(6):403–18. https://doi.org/10.1002/wdev.1470.
25. Bergwerff M, Verberne ME, DeRuiter MC, Poelmann RE, Gittenberger-de Groot AC. Neural crest cell contribution to the developing circulatory system: implications for vascular morphology? Circ Res. 1998;82(2):221–31. https://doi.org/10.1161/01.res.82.2.221.
26. Clouthier DE, Williams SC, Hammer RE, Richardson JA, Yanagisawa M. Cell-autonomous and nonautonomous actions of endothelin-A receptor signaling in craniofacial and cardiovascular development. Dev Biol. 2003;261(2):506–19. https://doi.org/10.1016/s0012-1606(03)00128-36.
27. Clouthier DE, Williams SC, Yanagisawa H, Wieduwilt M, Richardson JA, Yanagisawa M. Signaling pathways crucial for craniofacial development revealed by endothelin-A receptor-deficient mice. Dev Biol. 2000;217(1):10–24. https://doi.org/10.1006/dbio.1999.95272.
28. Clouthier DE, Hosoda K, Richardson JA, Williams SC, Yanagisawa H, Kuwaki T, et al. Cranial and cardiac neural crest defects in endothelin-A receptor-deficient mice. Development. 1998;125(5):813–24.
29. Morishima M, Yanagisawa H, Yanagisawa M, Baldini A. Ece1 and Tbx1 define distinct pathways to aortic arch morphogenesis. Dev Dyn. 2003;228(1):95–104. https://doi.org/10.1002/dvdy.103583.
30. Yanagisawa T, Urade M, Yamamoto Y, Furuyama J. Increased expression of human DNA repair genes, XRCC1, XRCC3 and RAD51, in radioresistant human KB carcinoma cell line N10. Oral Oncol. 1998;34(6):524–8. https://doi.org/10.1016/s1368-8375(98)00045-1.
31. Papangeli I, Scambler PJ. Tbx1 genetically interacts with the transforming growth factor-beta/bone morphogenetic protein inhibitor Smad7 during great vessel remodeling. Circ Res. 2013;112(1):90–102. https://doi.org/10.1161/CIRCRESAHA.112.2702233.
32. Kochilas L, Merscher-Gomez S, Lu MM, Potluri V, Liao J, Kucherlapati R, et al. The role of neural crest during cardiac development in a mouse model of DiGeorge syndrome. Dev Biol. 2002;251(1):157–66. https://doi.org/10.1006/dbio.2002.08195.
33. Lindsay EA, Vitelli F, Su H, Morishima M, Huynh T, Pramparo T, et al. Tbx1 haploinsufficieny in the DiGeorge syndrome region causes aortic arch defects in mice. Nature. 2001;410(6824):97–101. https://doi.org/10.1038/350651059.
34. Keyte A, Hutson MR. The neural crest in cardiac congenital anomalies. Differentiation. 2012;84(1):25–40. https://doi.org/10.1016/j.diff.2012.04.0056.
35. Waldo KL, Lo CW, Kirby ML. Connexin 43 expression reflects neural crest patterns during cardiovascular development. Dev Biol. 1999;208(2):307–23. https://doi.org/10.1006/dbio.1999.92197.
36. van den Hoff MJ, Moorman AF, Ruijter JM, Lamers WH, Bennington RW, Markwald RR, et al. Myocardialization of the cardiac outflow tract. Dev Biol. 1999;212(2):477–90. https://doi.org/10.1006/dbio.1999.93666.
37. Jiang X, Rowitch DH, Soriano P, McMahon AP, Sucov HM. Fate of the mammalian cardiac neural crest. Development. 2000;127(8):1607–167.

38. Jain R, Engleka KA, Rentschler SL, Manderfield LJ, Li L, Yuan L, et al. Cardiac neural crest orchestrates remodeling and functional maturation of mouse semilunar valves. J Clin Invest. 2011;121(1):422–30. https://doi.org/10.1172/JCI442440.
39. Phillips HM, Mahendran P, Singh E, Anderson RH, Chaudhry B, Henderson DJ. Neural crest cells are required for correct positioning of the developing outflow cushions and pattern the arterial valve leaflets. Cardiovasc Res. 2013;99(3):452–60. https://doi.org/10.1093/cvr/cvt1324.
40. Nakajima Y, Yamagishi T, Hokari S, Nakamura H. Mechanisms involved in valvuloseptal endocardial cushion formation in early cardiogenesis: roles of transforming growth factor (TGF)-beta and bone morphogenetic protein (BMP). Anat Rec. 2000;258(2):119–27. https://doi.org/10.1002/(SICI)1097-0185(20000201)258:2<119::AID-AR1>3.0.CO;2-U9.
41. Butcher JT, Markwald RR. Valvulogenesis: the moving target. Philos Trans R Soc Lond Ser B Biol Sci. 2007;362(1484):1489–503. https://doi.org/10.1098/rstb.2007.21300.
42. Combs MD, Yutzey KE. Heart valve development: regulatory networks in development and disease. Circ Res. 2009;105(5):408–21. https://doi.org/10.1161/CIRCRESAHA.109.2015666.
43. Yelbuz TM, Waldo KL, Kumiski DH, Stadt HA, Wolfe RR, Leatherbury L, et al. Shortened outflow tract leads to altered cardiac looping after neural crest ablation. Circulation. 2002;106(4):504–10. https://doi.org/10.1161/01.cir.0000023044.44974.8a3.
44. Ward C, Stadt H, Hutson M, Kirby ML. Ablation of the secondary heart field leads to tetralogy of Fallot and pulmonary atresia. Dev Biol. 2005;284(1):72–83. https://doi.org/10.1016/j.ydbio.2005.05.0033.
45. Waldo KL, Hutson MR, Stadt HA, Zdanowicz M, Zdanowicz J, Kirby ML. Cardiac neural crest is necessary for normal addition of the myocardium to the arterial pole from the secondary heart field. Dev Biol. 2005;281(1):66–77. https://doi.org/10.1016/j.ydbio.2005.02.0119.
46. Hutson MR, Zhang P, Stadt HA, Sato AK, Li YX, Burch J, et al. Cardiac arterial pole alignment is sensitive to FGF8 signaling in the pharynx. Dev Biol. 2006;295(2):486–97. https://doi.org/10.1016/j.ydbio.2006.02.0526.
47. High FA, Jain R, Stoller JZ, Antonucci NB, Lu MM, Loomes KM, et al. Murine Jagged1/Notch signaling in the second heart field orchestrates Fgf8 expression and tissue-tissue interactions during outflow tract development. J Clin Invest. 2009;119(7):1986–96. https://doi.org/10.1172/JCI389226.
48. Miquerol L, Beyer S, Kelly RG. Establishment of the mouse ventricular conduction system. Cardiovasc Res. 2011;91(2):232–42. https://doi.org/10.1093/cvr/cvr0697.
49. Kirby ML, Stewart DE. Neural crest origin of cardiac ganglion cells in the chick embryo: identification and extirpation. Dev Biol. 1983;97(2):433–43. https://doi.org/10.1016/0012-1606(83)90100-8.
50. Kitajima S, Miyagawa-Tomita S, Inoue T, Kanno J, Saga Y. Mesp1-nonexpressing cells contribute to the ventricular cardiac conduction system. Dev Dyn. 2006;235(2):395–402. https://doi.org/10.1002/dvdy.206403.
51. Poelmann RE, Gittenberger-de Groot AC. A subpopulation of apoptosis-prone cardiac neural crest cells targets to the venous pole: multiple functions in heart development? Dev Biol. 1999;207(2):271–86. https://doi.org/10.1006/dbio.1998.91663.
52. Poelmann RE, Jongbloed MR, Molin DG, Fekkes ML, Wang Z, Fishman GI, et al. The neural crest is contiguous with the cardiac conduction system in the mouse embryo: a role in induction? Anat Embryol. 2004;208(5):389–93. https://doi.org/10.1007/s00429-004-0401-63.
53. Nakamura T, Colbert MC, Robbins J. Neural crest cells retain multipotential characteristics in the developing valves and label the cardiac conduction system. Circ Res. 2006;98(12):1547–54. https://doi.org/10.1161/01.RES.0000227505.19472.692.
54. St Amand TR, Lu JT, Zamora M, Gu Y, Stricker J, Hoshijima M, et al. Distinct roles of HF-1b/Sp4 in ventricular and neural crest cells lineages affect cardiac conduction system development. Dev Biol. 2006;291(2):208–17. https://doi.org/10.1016/j.ydbio.2005.10.0181.
55. Poss KD. Getting to the heart of regeneration in zebrafish. Semin Cell Dev Biol. 2007;18(1):36–45. https://doi.org/10.1016/j.semcdb.2006.11.0099.

56. Major RJ, Poss KD. Zebrafish heart regeneration as a model for cardiac tissue repair. Drug Discov Today Dis Models. 2007;4(4):219–25. https://doi.org/10.1016/j.ddmod.2007.09.0027.
57. Poss KD, Wilson LG, Keating MT. Heart regeneration in zebrafish. Science. 2002;298(5601): 2188–90. https://doi.org/10.1126/science.10778576.
58. Dupin E, Calloni GW, Coelho-Aguiar JM, Le Douarin NM. The issue of the multipotency of the neural crest cells. Dev Biol. 2018;444(Suppl 1):S47–59. https://doi.org/10.1016/j.ydbio.2018.03.0241.
59. Tang W, Martik ML, Li Y, Bronner ME. Cardiac neural crest contributes to cardiomyocytes in amniotes and heart regeneration in zebrafish. Elife. 2019;8:e47929. https://doi.org/10.7554/eLife.479294.
60. Jopling C, Sleep E, Raya M, Marti M, Raya A, Izpisua Belmonte JC. Zebrafish heart regeneration occurs by cardiomyocyte dedifferentiation and proliferation. Nature. 2010;464(7288): 606–9. https://doi.org/10.1038/nature088995.
61. Cavanaugh AM, Huang J, Chen JN. Two developmentally distinct populations of neural crest cells contribute to the zebrafish heart. Dev Biol. 2015;404(2):103–12. https://doi.org/10.1016/j.ydbio.2015.06.0021.
62. Hutson M, Kirby M. Role of cardiac neural crest in the development of the caudal pharyngeal arches, the cardiac outflow and disease. In: Rosenthal N, Harvey RP, editors. Heart development and regeneration. Amsterdam: Academic Press; 2010. p. 441–46.
63. Kirby M. Cardiac development. Oxford, UK; 2007. p. 1–273.
64. Lee YH, Saint-Jeannet JP. Cardiac neural crest is dispensable for outflow tract septation in Xenopus. Development. 2011;138(10):2025–34. https://doi.org/10.1242/dev.0616148.
65. Porrello ER, Mahmoud AI, Simpson E, Hill JA, Richardson JA, Olson EN, et al. Transient regenerative potential of the neonatal mouse heart. Science. 2011;331(6020):1078–80. https://doi.org/10.1126/science.12007089.
66. Hatzistergos KE, Durante MA, Valasaki K, Wanschel A, Harbour JW, Hare JM. A novel cardiomyogenic role for Isl1(+) neural crest cells in the inflow tract. Sci Adv. 2020;6(49): eaba9950. https://doi.org/10.1126/sciadv.aba99504.
67. Calder L, Van Praagh R, Van Praagh S, Sears WP, Corwin R, Levy A, et al. Truncus arteriosus communis. Clinical, angiocardiographic, and pathologic findings in 100 patients. Am Heart J. 1976;92(1):23–38. https://doi.org/10.1016/s0002-8703(76)80400-0.
68. Shprintzen RJ. Velo-cardio-facial syndrome: 30 years of study. Dev Disabil Res Rev. 2008;14 (1):3–10. https://doi.org/10.1002/ddrr.21.
69. Scambler PJ. 22q11 deletion syndrome: a role for TBX1 in pharyngeal and cardiovascular development. Pediatr Cardiol. 2010;31(3):378–90. https://doi.org/10.1007/s00246-009-9613-01.
70. Calmont A, Ivins S, Van Bueren KL, Papangeli I, Kyriakopoulou V, Andrews WD, et al. Tbx1 controls cardiac neural crest cell migration during arch artery development by regulating Gbx2 expression in the pharyngeal ectoderm. Development. 2009;136(18):3173–83. https://doi.org/10.1242/dev.0289021.
71. Theveniau-Ruissy M, Dandonneau M, Mesbah K, Ghez O, Mattei MG, Miquerol L, et al. The del22q11.2 candidate gene Tbx1 controls regional outflow tract identity and coronary artery patterning. Circ Res. 2008;103(2):142–8. https://doi.org/10.1161/CIRCRESAHA.108.1721894.
72. Kelly RG, Papaioannou VE. Visualization of outflow tract development in the absence of Tbx1 using an FgF10 enhancer trap transgene. Dev Dyn. 2007;236(3):821–8. https://doi.org/10.1002/dvdy.210635.
73. Bergman JE, Janssen N, Hoefsloot LH, Jongmans MC, Hofstra RM, van Ravenswaaij-Arts CM. CHD7 mutations and CHARGE syndrome: the clinical implications of an expanding phenotype. J Med Genet. 2011;48(5):334–42. https://doi.org/10.1136/jmg.2010.0871069.
74. Bajpai R, Chen DA, Rada-Iglesias A, Zhang J, Xiong Y, Helms J, et al. CHD7 cooperates with PBAF to control multipotent neural crest formation. Nature. 2010;463(7283):958–62. https://doi.org/10.1038/nature087337.

75. Randall V, McCue K, Roberts C, Kyriakopoulou V, Beddow S, Barrett AN, et al. Great vessel development requires biallelic expression of Chd7 and Tbx1 in pharyngeal ectoderm in mice. J Clin Invest. 2009;119(11):3301–10. https://doi.org/10.1172/JCI375614.
76. Diman NY, Remacle S, Bertrand N, Picard JJ, Zaffran S, Rezsohazy R. A retinoic acid responsive Hoxa3 transgene expressed in embryonic pharyngeal endoderm, cardiac neural crest and a subdomain of the second heart field. PLoS One. 2011;6(11):e27624. https://doi.org/10.1371/journal.pone.00276247.
77. Lepore AC, Neuhuber B, Connors TM, Han SS, Liu Y, Daniels MP, et al. Long-term fate of neural precursor cells following transplantation into developing and adult CNS. Neuroscience. 2006;142(1):287–304. https://doi.org/10.1016/j.neuroscience.2005.12.0678.
78. Dixon J, Jones NC, Sandell LL, Jayasinghe SM, Crane J, Rey JP, et al. Tcof1/Treacle is required for neural crest cell formation and proliferation deficiencies that cause craniofacial abnormalities. Proc Natl Acad Sci U S A. 2006;103(36):13403–8. https://doi.org/10.1073/pnas.06037301038.
79. Dobrilovic N, Fernandez AB, Lin A, Singh AK. Treacher Collins syndrome: sinus of Valsalva aneurysm. Circulation. 2013;128(2):e12–3. https://doi.org/10.1161/CIRCULATIONAHA.113.0015883.
80. Serrano F, Bernard WG, Granata A, Iyer D, Steventon B, Kim M, et al. A novel human pluripotent stem cell-derived neural crest model of Treacher Collins syndrome shows defects in cell death and migration. Stem Cells Dev. 2019;28(2):81–100. https://doi.org/10.1089/scd.2017.02344.
81. Ye M, Coldren C, Liang X, Mattina T, Goldmuntz E, Benson DW, et al. Deletion of ETS-1, a gene in the Jacobsen syndrome critical region, causes ventricular septal defects and abnormal ventricular morphology in mice. Hum Mol Genet. 2010;19(4):648–56. https://doi.org/10.1093/hmg/ddp5320.
82. George RM, Maldonado-Velez G, Firulli AB. The heart of the neural crest: cardiac neural crest cells in development and regeneration. Development. 2020;147(20):dev188706. https://doi.org/10.1242/dev.1887066.

Inflow Tract Development

7

Andy Wessels

Abstract

The development of the inflow tract is undoubtedly one of the most complex remodeling events in the formation of the four-chambered heart. It involves the creation of two separate atrial chambers, the formation of an atrial/atrioventricular (AV) septal complex, the incorporation of the caval veins and coronary sinus into the right atrium, and the remodeling events that result in pulmonary venous return draining into the left atrium. In these processes, the atrioventricular mesenchymal complex, consisting of the major atrioventricular (AV) cushions, the mesenchymal cap on the primary atrial septum (pAS), and the dorsal mesenchymal protrusion (DMP), plays a crucial role.

Keywords

Venous pole · Pulmonary venous return · Left atrium · Coronary sinus · Dorsal mesenchymal protrusion · Outflow tract · OFT · Dorsal mesocardium · Mesenchymal cap · Atrioventricular cushion · AV cushion · Bone morphogenetic protein 2 · BMP2 · Transforming growth factor-β 2 · TGFb2 · Pulmonary vein · Sinus venosus · Islet1 · Nkx2-5 · AVSD · Septum primum · Septum secundum · Ostium primum · Patent foramen ovale · PFO · First heart field · FHF · Second heart field · SHF

A. Wessels (✉)
Department of Regenerative Medicine and Cell Biology, Medical University of South Carolina, Charleston, SC, USA
e-mail: wesselsa@musc.edu

© The Author(s), under exclusive license to Springer Nature Switzerland AG 2024

S. Rickert-Sperling et al. (eds.), *Congenital Heart Diseases: The Broken Heart*,
Advances in Experimental Medicine and Biology 1441,
https://doi.org/10.1007/978-3-031-44087-8_7

7.1 Introduction

During the initial phase of heart development, the first heart field (FHF) generates the cell populations that form the primary heart tube. After its formation, this tubular heart consists of an outer myocardial wall and an inner lining of endocardial cells. These two cell layers are separated by an acellular space filled with extracellular matrix (ECM) components, generally referred to as the cardiac jelly. In the earliest stages of heart development, the primary heart tube hangs suspended over its entire length from the rest of the embryo by the dorsal mesocardium. As the heart expands, it starts to loop. During this process, the dorsal mesocardium disintegrates in the anterior and midsection of the tube. When this process is completed, the only remaining part of the dorsal mesocardium is found at the junction of the sinus venosus and atria. Here, it becomes a key anatomical structure playing a central role in several events that determine the final architecture of the inflow tract.

7.2 The Venous Pole

The growth of the early embryonic heart is, for a large part, the result of addition of cells from the second heart field (SHF), which is especially prominent at the arterial pole of the heart (see Chap. 3). The use of mouse models that allow the tracing of SHF-derived cells has demonstrated that the entire outflow tract (OFT), the right ventricle, and a significant part of the interventricular septum (IVS) are derivatives of the SHF [16]. At the inflow tract (or the venous pole), the SHF contributes to parts of the atria, to the primary atrial septum (pAS), and to the formation of the dorsal mesenchymal protrusion (DMP). The cardiac venous pole is the region of the heart that receives the blood returning from the rest of the body. This includes the left atrium, where the oxygenated blood from the lungs is transported through the pulmonary veins, and the right atrium, where the deoxygenated blood returning from the rest of the body via the caval veins and the coronary sinus is collected. In a properly formed four-chambered heart, oxygenated and deoxygenated blood are at the atrial level kept physically separated by the atrial septal complex.

7.3 Development of the Venous Pole

The development of the venous pole involves a series of interrelated remodeling events. We will only review a few of the major steps, primarily as they relate to atrial/atrioventricular (AV) septation. It is important to note that there is no universal agreement among cardiovascular developmental biologists regarding the details of the respective mechanisms involved in atrial development (or even the nomenclature of individual structures). The statements provided in this chapter reflect our own insights into this topic based on what has been published in the literature and our own research on this topic.

7.3.1 The Sinus Venosus

As described in the Introduction section, after the initial formation of the tubular heart, tissues are subsequently added at the arterial and venous poles during looping. During this process, the sinus venosus is formed. Once formed, the sinus venosus consists of a left and right sinus horn and can be seen as a prominent structure in the developing human heart [21]. It receives the venous return from the left and right anterior and posterior cardinal veins. In the human embryo, the connections of the left-sided cardinal vein and other left-sided venous structures associated with the left sinus horn normally regress. This process is responsible for the formation of the coronary sinus. Failure of the left sinus horn to regress leads to a condition known as persistent left superior vena cava. It is noteworthy that this regression of the left sinus horn does not occur in the mouse and that a left superior caval vein is part of the normal murine cardiovascular anatomy. As development progresses, the sinus venosus becomes largely incorporated into the posterior wall of the right atrium, resulting in the formation of the sinus venarum and the incorporation of the orifices of the superior and inferior caval veins, derivatives of the right-sided cardinal veins as well as the orifice of the coronary sinus.

7.3.2 The Pulmonary Vein

After formation of the looped heart, a strand of endothelial cells can be found within the persisting dorsal mesocardium. This midline structure, which is contiguous with the endocardial lining of the heart, is known as the mid-pharyngeal strand [6]. The invagination of the endocardium/endothelium into the dorsal mesocardium creates an indentation, known as the "pulmonary pit" that is easily recognized in histological specimens (Fig. 7.1a,b) and by scanning electron microscopy [17, 18]. The mid-pharyngeal strand will eventually become the primitive (or common) pulmonary vein. During this process, the primitive pulmonary vein coalesces with the endothelial network in the developing lung, which results in the formation of the network of pulmonary veins that return oxygenated blood from the lung to the heart [2]. Whereas the primitive pulmonary vein is initially located at the midline of the venous pole [18], the development of the DMP (see below) to the right of the pulmonary vein [3] in concert with a series of subsequent remodeling events eventually translocate the orifice of the pulmonary vein into the posteroinferior wall of the left atrium [21] (Fig. 7.1c,d).

7.3.3 The Atrioventricular Cushions

The atrial and ventricular chambers of the early embryonic heart expand during the looping phase as the result of a process sometimes referred to as "ballooning" [1]. During this process, the chambers gradually lose most of the cardiac jelly initially found between the myocardium and endocardium in earlier stages.

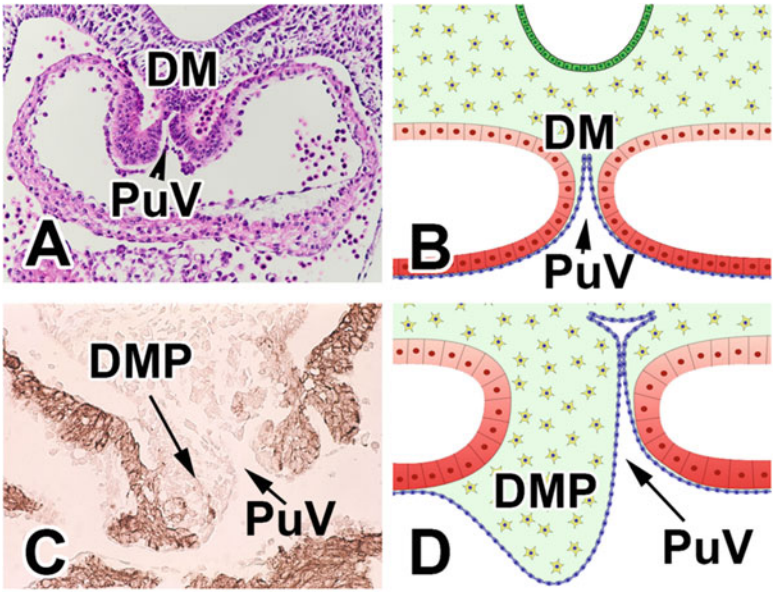

Fig. 7.1 The dorsal mesenchymal protrusion and the development of the primitive pulmonary vein. Panel (**a**) shows an hematoxylin/eosin-stained histological section of the venous pole of an E9.5 mouse heart, demonstrating the central location of the primitive pulmonary vein located within the dorsal mesocardium. The cartoon in panel (**b**) is a schematic representation of this situation. Panel (**c**) shows the same area in a section of an E10.5 mouse heart, which is immunohistochemically stained for a myocardial marker. The dorsal mesenchymal protrusion starts to develop between the right mesocardial reflection and the pulmonary vein, resulting in a leftward shift of the pulmonary vein away from the midline toward the future left atrium. This situation is schematically depicted in panel (**d**). Abbreviations: DM, dorsal mesocardium; DMP, dorsal mesenchymal protrusion; PuV, pulmonary vein (adapted from Blom et al. [6])

However, at the AV junction and in the outflow tract (OFT), the cardiac jelly accumulates in the subendocardial spaces, resulting in the formation of prominent swellings, generally referred to as "endocardial cushions." While the extracellular matrix-rich cushions in the early stage of their development do not contain cells, an endocardial-to-mesenchymal transformation/transition (endMT) of the endocardial lining of the cushions results in the generation of mesenchymal cells that gradually migrate into the cushions. The process of endMT has been well-studied, and a variety of molecular mechanisms have been identified in its regulation. This includes signaling by bone morphogenetic protein 2 (BMP2) and transforming growth factor-β 2 (TGFb2) [8, 9, 14].

In this chapter, we will concentrate on the development of the cushions at the AV junction. The two major AV cushions are the first to form. The inferior AV cushion develops adjacent to the dorsal AV myocardium, whereas the superior AV cushion is attached to the ventral AV myocardium. As the major AV cushions grow in size and eventually fuse, they divide the common AV canal into a left and right AV orifice. As this process is taking place, two smaller AV cushions start to develop at the

lateral walls of the AV canal. These AV cushions are known as the lateral AV cushions [19, 20]. Each of the four AV cushions plays a specific and important role in valvuloseptal development and has a specific fate. While the fate of the lateral AV cushions seems mainly confined to the formation of AV valve leaflets on the parietal walls of the AV junction, the major AV cushions also play, in addition to their role in the formation of leaflets associated with the AV septum, a crucial role in atrial and atrioventricular septation as they, together with the DMP and the mesenchymal cap on the pAS, eventually form the AV mesenchymal complex [11].

7.3.4 The Dorsal Mesenchymal Protrusion

The atrial septal complex functionally separates the left atrium from the right atrium. In recent years, it has become increasingly clear that atrial septation is intrinsically associated with the development of the tissues at the AV junction [11, 13]. Incomplete formation of elements of the AV mesenchymal complex results in atrial and atrioventricular septal defects [4, 7, 12, 15]. The DMP, also known as the vestibular spine, plays a critical role in atrial and atrioventricular septation. The mesenchymal structure, now known as the DMP, was first described in studies of the developing human heart [21] where it was reported that the mesenchyme of the DMP was immunohistochemically distinct from the endocardially derived mesenchyme of the AV cushions. This observation suggests that the cells that form the DMP are of a different origin than those of the AV cushions. The development of Cre-recombinase transgenic mouse technology has enabled developmental biologists to perform cell fate studies. Using Cre mouse models that allowed the tracing of cells derived from the endocardium and cells derived from the SHF, it was determined that the mesenchyme of the DMP was not, as suggested by its immunohistochemical characteristics, endocardially derived [10, 11] but instead a derivative of the SHF [4, 7, 12]. During its development, the DMP extends ventrally into the common atrium using the dorsal mesocardium as its portal of entry (Fig. 7.1c,d). Whereas the DMP initially develops as a mesenchymal tissue, after completion of atrial septation, the SHF-derived mesenchyme of the DMP eventually undergoes a mesenchymal-to-myocardial differentiation, characterized by a decrease in the expression of islet 1 (Isl1) and an increase in NKX2.5 in DMP-derived cells. This myocardialized DMP becomes the muscular inferior rim at the base of the atrial septum [12].

7.3.5 The Mesenchymal Cap of the Primary Atrial Septum

The mesenchymal cap of the developing primary atrial septum is a critical component of the AV mesenchymal complex. It forms a mesenchymal arch that connects the inferior AV cushion and DMP in the posteroinferior aspect of the common atrium to the superior AV cushion in the anterosuperior part of the common chamber. While a lot of research has been conducted on the AV cushions and DMP, very little work has been carried out on the development of the mesenchymal

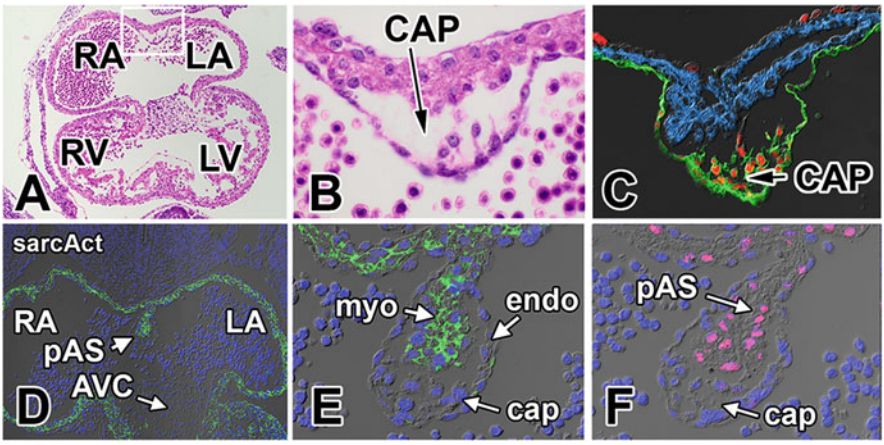

Fig. 7.2 The mesenchymal cap. Panel (**a**) shows a transverse section of an E9.5 embryonic day. The boxed area is enlarged in panel (**b**), showing the cap as a small cushion with invading mesenchymal cells. Panel (**c**) shows a section of a heart at the same age in which endocardial and endocardially derived cells are depicted in green (cell fate tracing with an endocardial-specific Tie2-Cre mouse). The endocardially derived cell within the cap express the transcription factor Sox9. The images in panels (**d–f**) are all from heart at E11.5 and are immunofluorescently stained for either sarcomeric actin (green in panels **d** and **e**) or the transcription factor Nkx2.5 to demonstrate the myocardial character of the core of the primary atrial septum. Abbreviations: AVC, atrioventricular cushion; cap, mesenchymal cap; endo, endocardium; LA, left atrium; LV, left ventricle; myo, myocardium; pAS, primary atrial septum; RA, right atrium; RV, right ventricle

cap. The cap initially develops as a small cushion on the roof of the common atrium at the site where the primary atrial septum will develop (Fig. 7.2a,b). Cell fate-tracing studies have shown that the mesenchyme within the developing cap is primarily endocardially derived and expresses genes that are also typically seen in the endocardially derived mesenchyme of the AV cushions (Fig. 7.2c). A few SHF-derived cells are found in the cap as well, which is not surprising as from the earliest stages at which it can be recognized, the DMP is in mesenchymal continuity with the cap [5]. As the primary atrial septum develops, the cap is found on its leading edge (Fig. 7.2d–h). Eventually, as the primary septum descends, the cap will fuse with the AV cushions.

7.4 The Role of the AV Mesenchymal Complex in the Formation of the Atrial Septum and the Pathogenesis of Atrial Septal Defects

After the embryonic heart has completed looping, the atrial and ventricular components are still unseptated. A more detailed description of how septation of the cardiac chambers takes place can be found elsewhere in this volume. Here, we provide a synopsis of atrial septation and the involvement of the structures described

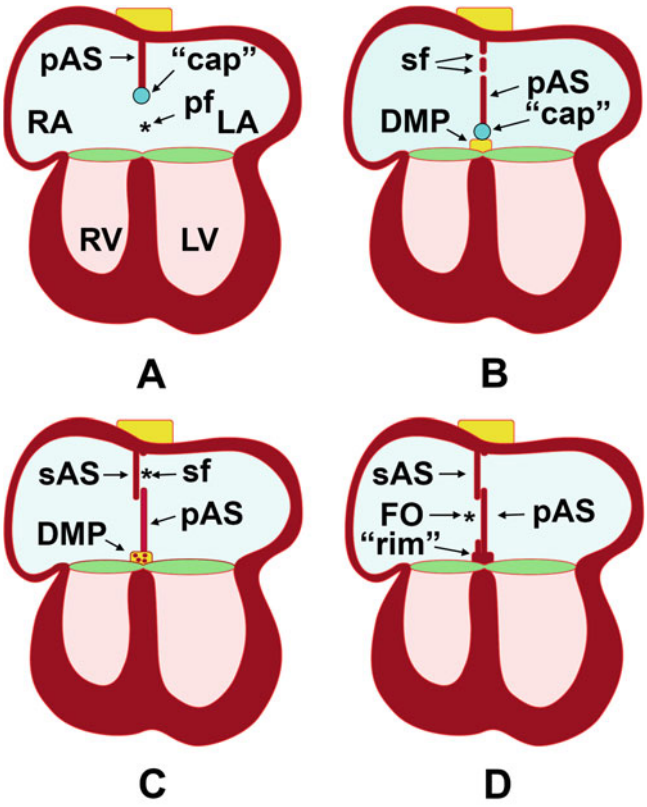

Fig. 7.3 Atrial septation. In this cartoon, the series of events that lead to the formation of the atrial septal complex are presented in simplified diagrams. A more detailed explanation of the individual steps is provided in the text of this chapter. It is important to note that atrial septation is a complex three-dimensional event and that the panels in this figure do not truly do justice to this event (additional information can be found in the study by Snarr et al. [11]). The asterisk in panel **a** marks the primary foramen (the ostium primum). Abbreviations: DMP, dorsal mesenchymal protrusion; FO, foramen ovale; LA, left atrium; LV, left ventricle; pAS, primary atrial septum; RA, right atrium; RV, right ventricle; rim, muscular rim at the base of the atrial septum; sAS, secondary atrial septum, sf, secondary foramen

above. In the first step, the primary atrial septum ("septum primum") develops as a thin myocardial curtain that gradually grows down from the left myocardial "reflection" of the dorsal mesocardium into the, yet undivided, common atrium toward the AV junction (Fig. 7.3a). At this early stage, in the atrial septation process, the left and right atria are still in communication with each other through the opening, the primary interatrial foramen ("ostium primum"), which is still present between the primary atrial septum and the major AV cushions. The primary foramen eventually closes when the cushions, the cap, and the DMP completely fuse [11] (Fig. 7.3b). During this process, a second interatrial communication forms in the upper part of the primary atrial septum. This secondary interatrial foramen ("ostium secundum"),

allows continuous shunting of blood from the right to left atrium, critical for the embryonic circulation. Around the same time, a secondary atrial septum ("septum secundum") starts to develop (Fig. 7.3c). As this septum descends into the atrial cavity, it starts to cover the secondary foramen. As a result, the primary atrial septum basically becomes a one-way valve, temporarily allowing shunting from right to left during fetal development but limiting/preventing left-to-right shunting (Fig. 7.3d). It is interesting to note that the mechanism by which the secondary septum develops appears to be different between humans and mice. In humans, the secondary septum primarily develops by the infolding of the atrial roof, whereas in mice, the secondary septum appears to form as a result of active myocardial growth.

Perturbation of the respective processes involved in atrial septation, as briefly described above, can lead to a number of atrial septal defects. The mildest of defects is a condition known as patent foramen ovale (PFO). In the majority of the human population, the secondary and the primary septum eventually fuse, preventing right–left or left–right shunting of blood at the atrial level after birth. However, in a significant percentage (25%) of human individuals, the two septa will not fuse, allowing for a right–left shunt after birth. Although a PFO is not considered a serious congenital heart defect, it is being associated with a number of conditions, most notably cryptogenic stroke (i.e., a stroke of unknown cause), as an estimated 50% of individuals with a cryptogenic stroke have a PFO. PFOs are considered a subclass of "ostium secundum defects" (or secondary atrial septal defects, sASDs). In more serious forms of sASDs, one can find large defects in the upper part of the atrial septal complex allowing shunting between the two atria. These defects can, for instance, result from failure of the secondary atrial septum to form correctly or as a result of disturbances in the formation of the secondary interatrial foramen. In a primary atrial septal defect (pASD), or "ostium primum defect," the primary atrial septum has not developed properly and has failed to fuse with the major AV cushions.

References

1. Anderson RH, Brown NA, Moorman AF. Development and structures of the venous pole of the heart. Dev Dyn. 2006;235:2–9.
2. Blom NA, Gittenberger-de Groot AC, Jongeneel TH, et al. Normal development of the pulmonary veins in human embryos and formulation of a morphogenetic concept for sinus venosus defects. Am J Cardiol. 2001;87:305–9.
3. Briggs LE, Kakarla J, Wessels A. The pathogenesis of atrial and atrioventricular septal defects with special emphasis on the role of the dorsal mesenchymal protrusion. Differentiation. 2012;84:117–30.
4. Briggs LE, Phelps AL, Brown E, et al. Expression of the BMP receptor Alk3 in the second heart field is essential for development of the dorsal mesenchymal protrusion and atrioventricular septation. Circ Res. 2013;112:1420–32.
5. Deepe R, Fitzgerald F, Wolters R, et al. The mesenchymal cap of the atrial septum and atrial and atrioventricular septation. J Cardiovasc Dev Dis. 2000;7(50):1–21.
6. DeRuiter MC, Poelmann RE, Mentink MM, et al. Early formation of the vascular system in quail embryos. Anat Rec. 1993;235:261–74.

7. Goddeeris MM, Rho S, Petiet A, et al. Intracardiac septation requires hedgehog-dependent cellular contributions from outside the heart. Development. 2008;135:1887–95.
8. Kruithof BP, Duim SN, Moerkamp AT, et al. TGFbeta and BMP signaling in cardiac cushion formation: lessons from mice and chicken. Differentiation. 2012;84:89–102.
9. Ma L, Lu MF, Schwartz RJ, et al. Bmp2 is essential for cardiac cushion epithelial-mesenchymal transition and myocardial patterning. Development. 2005;132:5601–11.
10. Mommersteeg MT, Soufan AT, de Lange FJ, et al. Two distinct pools of mesenchyme contribute to the development of the atrial septum. Circ Res. 2006;99:351–3.
11. Snarr BS, Wirrig EE, Phelps AL, et al. A spatiotemporal evaluation of the contribution of the dorsal mesenchymal protrusion to cardiac development. Dev Dyn. 2007;236:1287–94.
12. Snarr BS, O'Neal JL, Chintalapudi MR, et al. Isl1 expression at the venous pole identifies a novel role for the second heart field in cardiac development. Circ Res. 2007;101:971–4.
13. Snarr BS, Kern CB, Wessels A. Origin and fate of cardiac mesenchyme. Dev Dyn. 2008;237:2804–19.
14. Sugi Y, Yamamura H, Okagawa H, et al. Bone morphogenetic protein-2 can mediate myocardial regulation of atrioventricular cushion mesenchymal cell formation in mice. Dev Biol. 2004;269:505–18.
15. Tian Y, Yuan L, Goss AM, et al. Characterization and in vivo pharmacological rescue of a Wnt2-Gata6 pathway required for cardiac inflow tract development. Dev Cell. 2010;18:275–87.
16. Verzi MP, McCulley DJ, De Val S, et al. The right ventricle, outflow tract, and ventricular septum comprise a restricted expression domain within the secondary/anterior heart field. Dev Biol. 2005;287:134–45.
17. Webb S, Brown NA, Wessels A, et al. Development of the murine pulmonary vein and its relationship to the embryonic venous sinus. Anat Rec. 1998;250(3):325–34.
18. Wessels A, Markwald R. Cardiac morphogenesis and dysmorphogenesis. I. Normal development. Methods Mol Biol. 2000;136:239–59.
19. Wessels A, Sedmera D. Developmental anatomy of the heart: a tale of mice and man. Physiol Genomics. 2003;15:165–76.
20. Wessels A, Markman MW, Vermeulen JL, et al. The development of the atrioventricular junction in the human heart. Circ Res. 1996;78:110–7.
21. Wessels A, Anderson RH, Markwald RR, et al. Atrial development in the human heart: an immunohistochemical study with emphasis on the role of mesenchymal tissues. Anat Rec. 2000;259:288–300.

Epicardium and Coronary Vessels

8

Adrián Ruiz-Villalba, Juan Antonio Guadix, and José M. Pérez-Pomares

Abstract

Congenital anomalies and acquired diseases of the coronary blood vessels are of great clinical relevance. The early diagnosis of these conditions remains, however, challenging. In order to improve our knowledge of these ailments, progress has to be achieved in the research of the molecular and cellular mechanisms that control development of the coronary vascular bed. The aim of this chapter is to provide a succint account of the key elements of coronary blood vessel development, especially in the context of the role played by the epicardium and epicardial cellular derivatives. We will discuss the importance of the epicardium in coronary blood vessel morphogenesis, from the contribution of the epicardially derived mesenchyme to these blood vessels to its role as an instructive signaling center, attempting to relate these concepts to the origin of coronary disease.

Keywords

Epicardium · Embryo · Coronary arteries · Coronary veins

A. Ruiz-Villalba · J. A. Guadix · J. M. Pérez-Pomares (✉)
Department of Animal Biology, Faculty of Sciences, University of Málaga, Málaga, Spain

Instituto de Biomedicina de Málaga (IBIMA)—Plataforma BIONAND, Campanillas (Málaga), Spain
e-mail: jmperezp@uma.es

© The Author(s), under exclusive license to Springer Nature Switzerland AG 2024

S. Rickert-Sperling et al. (eds.), *Congenital Heart Diseases: The Broken Heart*,
Advances in Experimental Medicine and Biology 1441,
https://doi.org/10.1007/978-3-031-44087-8_8

8.1 Introduction

Coronary artery disease (CAD), also known as coronary atherosclerosis, is the leading cause of death worldwide, sparing no nation, ethnicity, or economic stratum [1]. Globally, CAD affects 126 million individuals (1655 per 100,000), with its prevalence in Europe being even higher (3547 per 100,000) [2]. Chronic conditions such as CAD significantly contribute to the estimated expense of 192,000 million €/year invested by the European Union to treat cardiovascular diseases.

Together with adult coronary artery disease, widely regarded as an "acquired" ailment, congenital anomalies of the coronary blood vessels (arteries and veins) have a significant incidence in newborns, with a prevalence ranging between 0.21 and 5.79%, depending upon the definition of the anomaly and the diagnostic criteria [3]. Coronary anomalies strongly correlate with adult sudden death [4]. However, despite the enormous clinical relevance of coronary blood vessel disease, not much is known about the embryonic developmental mechanisms that control the formation of coronary arteries and veins. Moreover, the genetic networks and molecular signals involved in normal coronary blood vessel morphogenesis and coronary disease pathophysiology are poorly understood. The main aim of this chapter is to provide a comprehensive account of the information on these topics available in the literature.

8.2 The Embryonic Epicardium and Forming Coronary Vessels Constitute a Developmental Unit

8.2.1 Tissue Interaction During Embryonic Development

The epicardium is a monolayered epithelium covering the heart surface. For different reasons, the embryonic formation of the coronary vascular system is inextricably related to epicardial development [5–8]. First, the epicardium provides the milieu in which the first coronary vascular structures form [9, 10]. This environment is known as the subepicardium and is an extracellular matrix-rich space that forms between the outer myocardium and the epicardium. Second, as soon as the epicardium forms, it becomes the source of new mesenchymal cells, many of which will get incorporated into the nascent coronary vessels. Third, epicardial cells and epicardially derived cells (EPDCs) are known to behave as a signaling center that coordinate coronary morphogenesis and other key developmental phenomena like the growth of the compact ventricular myocardium. This latter aspect is quite relevant, since molecular interactions between different tissues are instrumental to understanding embryonic development, organ homeostasis, and, in consequence, the origin of disease. This should not be forgotten when attempting to study the pathophysiology of a disease, most especially a congenital anomaly, since the tissues carrying the genetic alterations that cause the defect and the tissues displaying the morphological and/or physiological anomalies are not the same. In summary, our knowledge of normal embryonic development is essential to guide us toward the causes of

postnatal and adult cardiovascular disease [11, 12]. Thus, understanding coronary blood vessel development will prove critical to improve our diagnostic and clinical approaches to coronary diseases.

In order to complete these fundamental participations in coronary development, two essential cellular processes need to be accomplished: (1) formation of the epicardium from its extracardiac progenitors and (2) epicardial epithelial-to-mesenchymal transition (EMT). The next two sections of this chapter will focus on these events.

8.2.2 Formation of the Epicardial Epithelium from Proepicardial Progenitor Cells

The origin of the epicardium remained a mystery for decades. We now know that the epicardial epithelium forms from the proepicardium, a proliferative mass of mesodermal cells protruding from the coelomic epithelium that covers the septum transversum area, i.e., the planar sheet of the splanchnic mesoderm that separates the thoracic and abdominal cavities. In order to form the primitive monolayered epicardium, constituting squamous epithelial cells, proepicardial cells, located caudally to the early heart, are transferred to the myocardial surface. Transference, adhesion, and spreading of proepicardial cells over cardiomyocytes are governed by poorly known mechanisms that differ between the animal models considered, ranging from the release of free-floating clusters of proepicardial cells to the pericardial cavity to the persistent bridging and attachment of the proepicardium to the myocardial surface [13, 14]. In the case of mammals, integrins, especially α4β1 integrin, have been suggested to be critical to proepicardial cell attachment to the outer cardiomyocytes [15–17]. Moreover, several lines of evidence suggest that the migration of primitive epicardial cells over the myocardium is highly patterned, but little information has been reported on this fascinating process [14, 18–20]. Furthermore, systematic studies are required to improve our current knowledge of these critical steps in coronary development.

8.2.3 Epicardial EMT

Once the epicardium forms over the myocardium, it undergoes a process of epithelial-to-mesenchymal transition that transforms subsets of epicardial epithelial cells into a heterogeneous population of mesenchymal cells referred to as epicardially derived cells (EPDCs). Although for the sake of simplicity it is stated that the EMT is initiated after epicardium formation, multiple lines of evidence suggest that events required for EMT to occur (such as loss of cell–cell adhesion and disruption of apicobasal polarity) can already be identified in the epithelial component of pro-pericardial cells [21, 22]. It is not the aim of this chapter to define the starting point of EMT in the epicardial cell lineage, but it seems important to consider that some of the molecular mechanisms governing epicardial EMT might

have been activated before epicardial cells make contact with the heart muscle. Such mechanisms include the controversial involvement of the cadherin repressor Snail in the loss of cell junctions [23, 24], the activation of extracellular matrix degradation necessary to enable mesenchymal cell migration [25, 26], or even complex transcriptional changes following β-catenin translocation to the cellular nucleus [27]. As soon as proepicardial cells contact and spread over the myocardium to form the primitive epicardium, they undergo EMT. This highly regulated process involves the full phenotypical conversion of epicardial cells into mesenchymal ones. Interestingly enough, not all epicardial epithelial cells seem to be competent to transform into mesenchymal cells.

How is epicardial EMT regulated? The causes of the differential competence of epicardial cells to transform into the mesenchyme are unknown. Furthermore, the nature of the signals that trigger epicardial EMT continues to be a matter of debate. Two decades ago, some studies tested in vitro the impact of some growth factors in the activation of epicardial EMT (please refer to the next section for additional information on this point) [28]. Recently, a proteomic analysis of the in vitro EPDC secretome has revealed the transforming growth factor-β2 (TGFβ2)- and Platelet Derived Growth Factor-B PDGFBB-mediated roles of nuclear factor kappa b (NF-Kb) in the activation of EMT and the inhibitor of several relevant epicardial genes, including the Wilms tumor suppressor gene (*Wt1*) [29]. However, it remains unclear whether these signals can activate EMT in vivo, and lines of evidence point to the joint activation of epicardial EMT by more than one molecule [30].

The study of the molecular effectors of epicardial EMT also deserves attention. Different transcription factors such as Wt1, a well-known classic (pro)epicardial marker, has been reported to be involved in the epicardial EMT process. Of them, Wt1 seems to be directly involved in the development of the epicardium and the coronary plexus through the direct regulation of different molecular pathways, including Wnt canonical/β-catenin signaling [31, 32] or myocardin-related transcription factors (MRTFs) [10, 33]. Recently, the use of high-throughput technologies such as spatial transcriptomics and single-cell RNA sequencing has been crucial to identify new molecules involved in epicardial EMT. For example, the epicardial deletion of the WD Repeat Containing Planar Cell Polarity Effector (*Wdpcp*), a gene involved in ciliogenesis, has been shown to enhance the chemotactic response to Shh, reducing EMT and EPDC migration and thus altering subepicardial coronary plexus formation [34]. A recent study has also shown that the downregulation of protein arginine methyltransferase 1 (PRMT1) leads to the accumulation of nuclear p53, which inhibits the degradation of Slug/Snail and blocks the EMT [35]. Additionally, the inhibition of the axis PRMT1/p53 also modifies the transcriptomic profile and EPDC formation, resulting in anomalous development of the coronary vessels. Similarly, the absence of agrin, a component of the ECM, induces the downregulation of Wt1 and, consequently, both the epicardial EMT and the formation of the coronary plexus [17].

8.2.4 Epicardium–Myocardium Molecular Cross Talk

Epicardial–myocardial juxtacrine/paracrine interactions are crucial to the development of the two tissues and have a clear impact on coronary vascular morphogenesis. First, the epicardium is known to produce a largely uncharacterized retinoic acid- and erythropoietin-dependent secretome, which is necessary for the compact ventricular myocardium to grow and for proper coronary vessel maturation [36–39]. Different epicardially secreted growth factors like some fibroblast growth factors (FGF9, FGF16, and FGF20) or insulin-like growth factor 2 (IGF2) have been reported to form part of this secretome [40, 41]. The myocardium also secretes provascular vascular endothelial growth factor (VEGF) under the control of Hedgehog [42], directly modulating coronary vascular development and patterning by defining a transmural growth factor gradient [43, 44]. The complexity of the molecular networks that control epicardial–myocardial interaction is emphasized by the severe epicardial and coronary defects found in mice mutants for the myocardially (but not epicardially) expressed the gene Friend of Gata 2 (Fog2) and VANGL planar cell polarity protein 2 (Vangl2) [45, 46], encoding a co-factor for Gata transcription factors and a transduction element of non-canonical Planar Cell Polarity (PCP) Wnt signaling, respectively.

In addition to the molecules that initiate epicardial EMT, different molecules are important for the spatiotemporal patterning of EPDC migration and contribution to cardiac tissues. In this regard, $CXCR4^+$ endothelial cells (ECs) are responsive to CXCL12 secreted by the epicardium and EPDCs, promoting the spatial distribution of the coronary plexus [47, 48]. In addition, Jagged1+ endothelial cells recruit Notch3+ epicardium-derived pericytes that participate in the maturation of the coronary vessels [49].

8.3 Diversity of Coronary Cell Lineages

8.3.1 The Developmental Potential of Epicardial Cells

Most of the recent epicardial/coronary research has focused on the developmental differentiation potential of epicardial cells or, more precisely, on cells in the epicardial lineage, from proepicardial progenitors to EPDCs. Controversies remain as to whether or not the proepicardium/epicardium contains a multipotent progenitor population that is able to differentiate into multiple cell types or, on the contrary, cell fate commitment precedes the proepicardial stage. Relevant to this discussion, a recent study has described a pool of $Mab21l2^+$ progenitor cells, named the juxtacardiac field (JCF), as a common precursor of the epicardium and the myocardium [50]. Some of these JCF cells persist in the proepicardium, suggesting a possible molecular preconditioning for cell fate determination of, at least, a subpopulation of proepicardial cells. This point is of especial interest if we take into account the current efforts to identify reliable sources of cardiovascular cells that can be used to repair or regenerate the injured heart and blood vessels.

The proepicardium has been shown to display quite different abilities in vivo and in vitro. Whereas mouse-cultured proepicardial cells robustly differentiate into smooth muscle cells and fibroblasts [51–53], in vivo genetic tracing of (pro)-epicardial cells in mouse embryos indicates that the contribution of this cell lineage to these cell types is quite different. Endothelial contribution of epicardial cells to the coronary endothelium (CoE) seems to be limited, although relevant for proper coronary formation [8]. In accordance with these findings, Paik et al. carried out a single-cell RNA sequencing (RNA-Seq) analysis that revealed Wt1 as the top gene defining the transcriptomic signature of murine cardiac endothelial cells as compared with the transcriptional signatures of endothelial cells isolated from other 11 organs. Notably, these results were confirmed for human fetal endothelial cells [54]. The same study also reveals that cardiac ECs are characterized by the enrichment in the genes annotated to the axon guidance pathways, a finding that has been recently associated with a potential role of specific EPDCs in the patterning of the coronary vasculature during the development [10, 54]. Relevant to this discussion, a recent work by Tang et al. has indicated that 61% of all cardiac endothelial cells derive from Sca1+ cardiac progenitors, thus pointing to the impact of embryonic cell progenitors in adult cardiac homeostasis and responses to pathological stimuli [55].

On a final note, some of the studies discussed above rely on the use of genetic cell-tracing technologies, especially the de Cre/LoxP one. This is a powerful tool that should nonetheless be used carefully, as the efficiency in the recombination of the transgenes can be quite variable depending on the Cre driver used so that there is an intrinsic variation in the number of cells tagged in every specific case [56].

8.3.2 Hierarchical Differentiation of Coronary Blood Vessel Cell Progenitors

An intense debate about the arteriovenous patterning of the coronary vascular system remains open. Coronary arteries and coronary veins are morphologically different and join the systemic circulation at opposed anatomical positions, since the coronary veins drain to the coronary sinus, derived from the posterior (venous) pole of the embryonic heart, and coronary arteries are connected to the aortic root, derived from the anterior (arterial) pole of the developing heart. Not only are coronary arteries and veins anatomically distinct entities, but anomalies in these two vessel types are linked to different cardiac conditions, arteries to sudden death [57], and veins to arrhythmias [58].

A possible strategy to understand the mechanics of coronary artery versus vein development is to dissect the diversity of cell lineages contributing to coronary blood vessel morphogenesis. Recent data have suggested that the coronary endothelium (CoE) develops from multiple embryonic cell sources, including different endocardial subpopulations (sinus venosus and ventricular endocardium), (pro)epicardial cells outflow tract-derived cells, and erythro-myeloid progenitors (EMPs) coming from the yolk sac [59–64]. However, contributions from other sources to the CoE should not be ruled out because vascular progenitors are known to be extremely

plastic in the modulation of their phenotype. In this regard, it has been recently demonstrated that the GATA4^{+} hematopoietic progenitor cells contribute to adult mouse endothelium in both early embryonic and postnatal stages [65].

All these data, taken together, strongly suggest that building the complex arteriovenous coronary vascular tree, which develops independently from the aortic root, i.e., the point of eventual connection of the coronary circulation to the systemic one, requires a large variety of endothelial cell progenitors. This is in accordance with the differentiation mechanics of the coronary arterial primary vascular plexus, which forms in isolation from the coronary venosus component. Furthermore, a molecular mechanism for the pre-arterial specification of sinus venosus endocardial cells based on the inhibition of the venous gene *Coup-tf2* and the activation of *Dach1* has been recently reported [63, 66]. Unfortunately, the lack of specific Cre lines for genetic tracing of defined cardiac chamber-specific endocardial populations prevents us from making definitive conclusions on this point.

Additional controversy exists on the cellular origin of the new blood vessels that appear during the latter phase of trabecular compaction in newborn hearts. Using Nfatc1-Cre^{ERT};Rosa26^{RFP} mice, Tian et al. described a significant contribution of neonatal endocardial cells to this coronary vascular subset, which is located on the inner myocardial wall [67]. In contrast, results from a different study using a natriuretic peptide receptor 3 (Npr3)-CreER line indicates that these specific intramural coronary vessels are formed from the angiogenesis of the preexisting embryonic coronary plexus via DLL4–NOTCH1 signaling and do not derive from the neonatal endocardium [68]. In any case, the contribution of the embryonic coronary plexus is essential for the development and maturation of the coronary circulatory system.

Definitive pattering of the coronary blood vessels requires the stable formation of the blood vessel medial wall. Coronary smooth muscle cells (CoSMCs) are, for the major part, epicardial derivatives, although other alternative sources (e.g., the neural crest) have been suggested [69]. In this line, Volz et al. suggested that CoSMCs differentiate from epicardium-derived pericytes in response to Notch signaling at arterial remodeling zones [49]. CoSMC follow CoE differentiation, being the maturation of the vessel smooth muscle wall a late event that is triggered by the initiation of effective coronary circulation. This physiological delay in the differentiation of CoSMCs is regulated by epicardial retinoids, working synergistically with VEGF to promote early vascular morphogenesis at the expense of blood vessel muscularization [70]. It has been interpreted that late formation of the vascular wall permits CoE remodeling and proper patterning from an intricate, immature capillary network, to give rise to the characteristic "inverted crown"-shaped adult coronary vascular system. In this regard, anomalous muscularization of CoE during embryonic development could explain part of the known coronary congenital malformation phenotypes, especially those involving anomalous coronary artery course and termination [3].

A much neglected coronary cell type is that of coronary fibroblasts. Differentiation of coronary adventitial fibroblasts (CoFs) takes place once CoSMCs have initiated their maturation to form the fibrous adventitia layer that appears in the

coronary arteries of large caliber. This adventitial layer includes a high number of epicardium-derived fibroblasts, a cell type characterized by the early expression of the transcription factor Tcf21 [71], although it cannot be ruled out that heart fibroblasts of a non-epicardial origin, such as the endocardium, neural crest, or bone marrow (see Zeisberg and Kalluri [72]), can also locally contribute to the formation of the coronary adventitia.

Epicardium-derived CoFs are ontogenetically related to ventricular interstitial fibroblasts [51], but their distinct location and different responses to cardiovascular diseases such as perivascular fibrosis followed by intermuscular interstitial fibrosis in pressure-overload models versus the massive, acute inflammation-induced fibrosis of the ischemic heart [73, 74] suggest that these two cardiac fibroblast (CF) populations have diverged during their differentiation and maturation from common progenitors. Deciphering the signals that elicit specific fibrotic responses from different cardiac fibroblast populations is an important future challenge in the cardiovascular field, and some recent reports have undertaken the important task of identifying the origin of distinct populations of CFs as related to specific cardiac disease [53, 64, 75, 76]. A summary of the developmental origins and the cellular and molecular events that control coronary morphogenesis is provided in (Fig. 8.1).

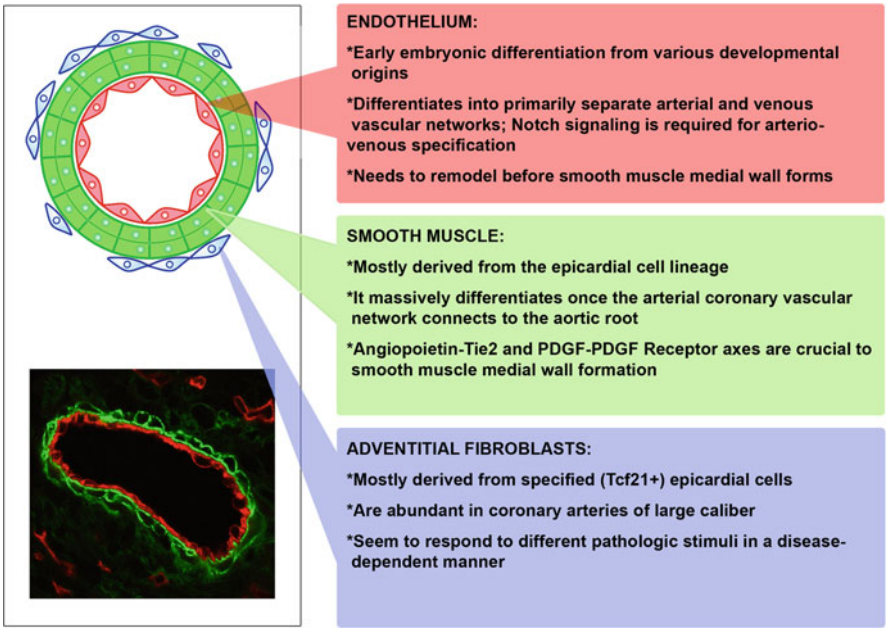
ENDOTHELIUM:
*Early embryonic differentiation from various developmental origins
*Differentiates into primarily separate arterial and venous vascular networks; Notch signaling is required for arterio-venous specification
*Needs to remodel before smooth muscle medial wall forms
SMOOTH MUSCLE:
*Mostly derived from the epicardial cell lineage
*It massively differentiates once the arterial coronary vascular network connects to the aortic root
*Angiopoietin-Tie2 and PDGF-PDGF Receptor axes are crucial to smooth muscle medial wall formation
ADVENTITIAL FIBROBLASTS:
*Mostly derived from specified (Tcf21+) epicardial cells
*Are abundant in coronary arteries of large caliber
*Seem to respond to different pathologic stimuli in a disease-dependent manner

Fig. 8.1 A graphic summary of the basic developmental aspects of coronary blood vessel development in relation to epicardial development. The upper left cartoon reproduces the characteristic concentric arrangement of embryonic coronary blood vessels (lower left panel)

8.4 Conclusions

We have shown that multi-lineage contribution to coronary blood vessel development during the normal patterning of the embryonic and prenatal coronary blood vessel system may be a substrate for the initiation of adverse responses to pathological stimuli. Furthermore, we have highlighted the importance of cell and tissue interactions during coronary blood vessel formation and have identified the characteristic transcriptional and signaling networks whose disruption could drive diverse forms of coronary disease, to finally conclude that extensive research in the field is required to increase our knowledge of coronary blood vessel disease.

References

1. Musunuru K, Kathiresan S. Genetics of common, complex coronary artery disease. Cell. 2019;177(1):132–45.
2. Khan MA, Hashim MJ, Mustafa H, et al. Global epidemiology of ischemic heart disease: results from the global burden of disease study. Cureus. 2020;12(7):e9349.
3. Angelini P. Coronary artery anomalies: an entity in search of an identity. Circulation. 2007;115:1296–305.
4. Hill S, Sheppard M. Non-atherosclerotic coronary artery disease associated with sudden cardiac death. Heart. 2010;96:1119–25.
5. Pérez-Pomares JM, de la Pompa JL. Signaling during epicardium and coronary vessel development. Circ Res. 2011;109:1429–42.
6. Lavine KJ, Ornitz DM. Fibroblast growth factors and hedgehogs: at the heart of the epicardial signaling center. Trends Genet. 2008;24:33–40.
7. Von Gise A, Pu WT. Endocardial and epicardial epithelial to mesenchymal transitions in heart development and disease. Circ Res. 2012;110:1628–45.
8. Cano E, Carmona R, Ruiz-Villalba A, et al. Extracardiac septum transversum/proepicardial endothelial cells pattern embryonic coronary arterio-venous connections. Proc Natl Acad Sci U S A. 2016;113(3):656–61.
9. Wessels A, Pérez-Pomares JM. The epicardium and epicardially derived cells (EPDCs) as cardiac stem cells. Anat Rec A Discov Mol Cell Evol Biol. 2004;276(1):43–57.
10. Quijada P, Trembley MA, Misra A, et al. Coordination of endothelial cell positioning and fate specification by the epicardium. Nat Commun. 6. 2021;12(1):4155.
11. Luxán G, Casanova JC, Martínez-Poveda B, et al. Mutations in the NOTCH pathway regulator MIB1 cause left ventricular noncompaction cardiomyopathy. Nat Med. 2013;19:193–201.
12. Rentschler S, Yen AH, Lu J, et al. Myocardial Notch signaling reprograms cardiomyocytes to a conduction-like phenotype. Circulation. 2012;126:1058–66.
13. Männer J, Pérez-Pomares JM, Macías D, Muñoz-Chápuli R. The origin, formation and developmental significance of the epicardium: a review. Cells Tissues Organs. 2001;169:89–103.
14. Peralta M, Steed E, Harlepp S, et al. Heartbeat-driven pericardiac fluid forces contribute to epicardium morphogenesis. Curr Biol. 2013;23:1726–35.
15. Yang JT, Rayburn H, Hynes RO. Cell adhesion events mediated by alpha 4 integrins are essential in placental and cardiac development. Development. 1995;121:549–60.
16. Pae SH, Dokic D, Dettman RW. Communication between integrin receptors facilitates epicardial cell adhesion and matrix organization. Dev Dyn. 2008;237:962–78.
17. Sun X, Malandraki-Miller S, Kennedy T, et al. The extracellular matrix protein agrin is essential for epicardial epithelial-to-mesenchymal transition during heart development. Development. 2021;148(9):dev197525.

18. Vrancken Peeters MP, Mentink MM, Poelmann RE, Gittenberger-de Groot AC. Cytokeratins as a marker for epicardial formation in the quail embryo. Anat Embryol (Berl). 1995;191(6): 503–8.
19. Yue MS, Plavicki JS, Li XY, et al. A co-culture assay of embryonic zebrafish hearts to assess migration of epicardial cells in vitro. BMC Dev Biol. 2015;29(15):50.
20. Tran JR, Zheng X, Zheng Y. Lamin-B1 contributes to the proper timing of epicardial cell migration and function during embryonic heart development. Mol Biol Cell. 15. 2016;27(25): 3956–63.
21. Dettman RW, Denetclaw W, Ordahl CP, Bristow J. Common epicardial origin of coronary vascular smooth muscle, perivascular fibroblasts, and intermyocardial fibroblasts in the avian heart. Dev Biol. 1998;193:169–81.
22. Pérez-Pomares JM, Macías D, García-Garrido L, Muñoz-Chápuli R. The origin of the subepicardial mesenchyme in the avian embryo: an immunohistochemical and quail-chick chimera study. Dev Biol. 1998;200:57–68.
23. Martínez-Estrada OM, Lettice L, Essafi A, et al. Wt1 is required for cardiovascular progenitor cell formation through transcriptional control of Snail and E-cadherin. Nat Genet. 2010;42:89–93.
24. Casanova JC, Travisano S, de la Pompa JL. Epithelial-to-mesenchymal transition in epicardium is independent of Snail1. Genesis. 2013;51:32–40.
25. Guadix JA, Carmona R, Muñoz-Chápuli R, Pérez-Pomares JM. In vivo and in vitro analysis of the vasculogenic potential of avian proepicardial and epicardial cells. Dev Dyn. 2006;235: 1014–26.
26. Ruiz-Villalba A, Ziogas A, Ehrbar M, Pérez-Pomares JM. Characterization of Epicardial-derived cardiac interstitial cells: differentiation and mobilization of heart fibroblast progenitors. PLoS One. 2013;8:e53694.
27. Von Gise A, Zhou B, Honor LB, et al. WT1 regulates epicardial epithelial to mesenchymal transition through β-catenin and retinoic acid signaling pathways. Dev Biol. 2011;356:421–31.
28. Morabito CJ, Dettman RW, Kattan J, et al. Positive and negative regulation of epicardial-mesenchymal transformation during avian heart development. Dev Biol. 2001;234(1):204–15.
29. Li Y, Urban A, Midura D, et al. Proteomic characterization of epicardial-myocardial signaling reveals novel regulatory networks including a role for NF-κB in epicardial EMT. PLoS One. 2017;12(3):e0174563. 29. Red-Horse K, Ueno H, Weissman IL, Krasnow M (2010) Coronary arteries form by developmental reprogramming of venous cells. Nature 464:549–53.
30. Krainock M, Toubat O, Danopoulos S, et al. Epicardial epithelial-to-mesenchymal transition in heart development and disease. J Clin Med. 2016;5(2):27.
31. Zamora M, Männer J, Ruiz-Lozano P. Epicardium-derived progenitor cells require beta-catenin for coronary artery formation. Proc Natl Acad Sci U S A. 2007;104(46):18109–14.
32. Wu M, Smith CL, Hall JA, et al. Epicardial spindle orientation controls cell entry into the myocardium. Dev Cell. 2010;19(1):114–25.
33. Trembley MA, Velasquez LS, de Mesy Bentley KL, Small EM. Myocardin-related transcription factors control the motility of epicardium-derived cells and the maturation of coronary vessels. Development. 2015;142(1):21–30.
34. Liu X, Wang Y, Liu F, et al. Wdpcp promotes epicardial EMT and epicardium-derived cell migration to facilitate coronary artery remodeling. Sci Signal. 2018;11(519):eaah5770.
35. Jackson-Weaver O, Ungvijanpunya N, Yuan Y, et al. PRMT1-p53 pathway controls Epicardial EMT and invasion. Cell Rep. 2020;31(10):107739.
36. Chen T, Chang TC, Kang JO, et al. Epicardial induction of fetal cardiomyocyte proliferation via a retinoic acid-inducible trophic factor. Dev Biol. 2002;250(1):198–207.
37. Stuckmann I, Evans S, Lassar AB. Erythropoietin and retinoic acid, secreted from the epicardium, are required for cardiac myocyte proliferation. Dev Biol. 2003;255(2):334–49.
38. Guadix JA, Ruiz-Villalba A, Lettice L, et al. Wt1 controls retinoic acid signalling in embryonic epicardium through transcriptional activation of Raldh2. Development. 2011;138(6):1093–7.

39. Quijada P, Trembley MA, Small EM. The role of the epicardium during heart development and repair. Circ Res. 2020;126(3):377–94.
40. Lavine KJ, White AC, Park C, et al. Fibroblast growth factor signals regulate a wave of hedgehog activation that is essential for coronary vascular development. Genes Dev. 2006;20:1651–66.
41. Brade T, Kumar S, Cunningham TJ, et al. Retinoic acid stimulates myocardial expansion by induction of hepatic erythropoietin which activates epicardial Igf2. Development. 2011;148: 139–48.
42. White AC, Lavine KJ, Ornitz DM. FGF9 and SHH regulate mesenchymal Vegfa expression and development of the pulmonary capillary network. Development. 2007;134:3743–52.
43. Pennisi DJ, Mikawa T. Normal patterning of the coronary capillary plexus is dependent on the correct transmural gradient of FGF expression in the myocardium. Dev Biol. 2005;279:378–90.
44. Wu B, Zhang Z, Lui W, et al. Endocardial cells form the coronary arteries by angiogenesis through myocardial-endocardial VEGF signaling. Cell. 2012;151:1083–96.
45. Tevosian SG, Deconinck AE, Tanaka M, et al. FOG-2, a cofactor for GATA transcription factors, is essential for heart morphogenesis and development of coronary vessels from epicardium. Cell. 2000;101:729–39.
46. Phillips HM, Rhee HJ, Murdoch JN, et al. Disruption of planar cell polarity signaling results in congenital heart defects and cardiomyopathy attributable to early cardiomyocyte disorganization. Circ Res. 2007;101:137–45.
47. Harrison MR, Bussmann J, Huang Y, et al. Chemokine-guided angiogenesis directs coronary vasculature formation in zebrafish. Dev Cell. 2015;33(4):442–54.
48. Cavallero S, Shen H, Yi C, et al. CXCL12 signaling is essential for maturation of the ventricular coronary endothelial plexus and establishment of functional coronary circulation. Dev Cell. 2015;33(4):469–77.
49. Volz KS, Jacobs AH, Chen HI, et al. Pericytes are progenitors for coronary artery smooth muscle. elife. 2015;4:e10036.
50. Tyser RCV, Ibarra-Soria X, McDole K, et al. Characterization of a common progenitor pool of the epicardium and myocardium. Science. 2021;371(6533):eabb2986.
51. Wessels A, van den Hoff MJB, Adamo RF, et al. Epicardially derived fibroblasts preferentially contribute to the parietal leaflets of the atrioventricular valves in the murine heart. Dev Biol. 2012;366:111–24.
52. Kanisicak O, Khalil H, Ivey MJ, et al. Genetic lineage tracing defines myofibroblast origin and function in the injured heart. Nat Commun. 2016;7:12260.
53. Ruiz-Villalba A, Simón AM, Pogontke C, et al. Interacting resident epicardium-derived fibroblasts and recruited bone marrow cells form myocardial infarction scar. J Am Coll Cardiol. 2015;65(19):2057–66.
54. Paik DT, Tian L, Williams IM, et al. Single-cell RNA sequencing unveils unique transcriptomic signatures of organ-specific endothelial cells. Circulation. 2020;142(19):1848–62.
55. Tang J, Li Y, Huang X, et al. Fate mapping of Sca1+ cardiac progenitor cells in the adult mouse heart. Circulation. 2018;138(25):2967–9.
56. Niderla-BieliŃska J, Jankowska-Steifer E, Flaht-Zabost A, et al. Proepicardium: current understanding of its structure, induction, and fate. Anat Rec (Hoboken). 2019;302(6):893–903.
57. Basso C, Maron BJ, Corrado D, Thiene G. Clinical profile of congenital coronary artery anomalies with origin from the wrong aortic sinus leading to sudden death in young competitive athletes. J Am Coll Cardiol. 2000;35:1493–501.
58. Sun Y. Coronary sinus-ventricular accessory connections producing Posteroseptal and left posterior accessory pathways: incidence and electrophysiological identification. Circulation. 2002;106:1362–7.
59. Palmquist-Gomes P, Guadix JA, Pérez-Pomares JM. Avian embryonic coronary arterio-venous patterning involves the contribution of different endothelial and endocardial cell populations. Dev Dyn. 2018;247(5):686–98.

60. Palmquist-Gomes P, Pérez-Pomares JM, Guadix JA. Proepicardial origin of developing coronary vessels. Rev Esp Cardiol (Engl Ed). 2019;72(2):163.
61. Stone OA, Zhou B, Red-Horse K, Stainier DYR. Endothelial ontogeny and the establishment of vascular heterogeneity. BioEssays. 2021;43(7):e2100036.
62. Plein A, Fantin A, Denti L, et al. Erythro-myeloid progenitors contribute endothelial cells to blood vessels. Nature. 2018;562(7726):223–8.
63. Su T, Stanley G, Sinha R, et al. Single-cell analysis of early progenitor cells that build coronary arteries. Nature. 2018;559:356–62.
64. Forte E, Skelly DA, Chen M, et al. Dynamic interstitial cell response during myocardial infarction predicts resilience to rupture in genetically diverse mice. Cell Rep. 2020;30(9): 3149–3163.e6.
65. Carmona R, Moral SDD, Barrena S, Muñoz-Chápuli R. Contribution of a GATA4-expressing hematopoietic progenitor lineage to the adult mouse endothelium. Cell. 2020;9(5):1257.
66. Raftrey B, Williams I, Rios Coronado PE, a. Dach1 extends artery networks and protects against cardiac injury. Circ Res. 2021;129(7):702–16.
67. Tian X, Hu T, Zhang H, et al. Vessel formation. De novo formation of a distinct coronary vascular population in neonatal heart. Science. 2014;345(6192):90–4.
68. Lu P, Wang Y, Liu Y, et al. Perinatal angiogenesis from pre-existing coronary vessels via DLL4-NOTCH1 signalling. Nat Cell Biol. 2021;23(9):967–77.
69. Arima Y, Miyagawa-Tomita S, Maeda K, et al. Preotic neural crest cells contribute to coronary artery smooth muscle involving endothelin signalling. Nat Commun. 2012;3:1267.
70. Azambuja AP, Portillo-Sánchez V, Rodrigues M, et al. Retinoic acid and VEGF delay smooth muscle relative to endothelial differentiation to coordinate inner and outer coronary vessel wall morphogenesis. Circ Res. 2010;107:204–16.
71. Acharya A, Baek ST, Huang G, et al. The bHLH transcription factor Tcf21 is required for lineage-specific EMT of cardiac fibroblast progenitors. Development. 2012;139:2139–49.
72. Zeisberg E, Kalluri R. Origins of cardiac fibroblasts. Circ Res. 2011;107:1304–12.
73. Creemers EE, Pinto YM. Molecular mechanisms that control interstitial fibrosis in the pressure-overloaded heart. Cardiovasc Res. 2011;89:265–72.
74. Kai H, Kuwahara F, Tokuda K, Imaizumi T. Diastolic dysfunction in hypertensive hearts: roles of perivascular inflammation and reactive myocardial fibrosis. Hypertens Res. 2005;28:483–90.
75. Moore-Morris T, Guimarães-Camboa N, Banerjee I, et al. Resident fibroblast lineages mediate pressure overload – induced cardiac fibrosis. J Clin Investig. 2014;124:2921–34.
76. Marín-Sedeño E, de Morentin XM, Pérez-Pomares JM, et al. Understanding the adult mammalian heart at single-cell RNA-Seq resolution. Front Cell Dev Biol. 2021;12(9):645276.

Establishment of Cardiac Laterality

9

George C. Gabriel, Yijen L. Wu, and Cecilia W. Lo

Abstract

Formation of the vertebrate heart with its complex arterial and venous connections is critically dependent on patterning of the left–right axis during early embryonic development. Abnormalities in left–right patterning can lead to a variety of complex life-threatening congenital heart defects. A highly conserved pathway responsible for left–right axis specification has been uncovered. This pathway involves initial asymmetric activation of a nodal signaling cascade at the embryonic node, followed by its propagation to the left lateral plate mesoderm and activation of left-sided expression of the Pitx2 transcription factor specifying visceral organ asymmetry. Intriguingly, recent work suggests that cardiac laterality is encoded by intrinsic cell and tissue chirality independent of Nodal signaling. Thus, Nodal signaling may be superimposed on this intrinsic chirality, providing additional instructive cues to pattern cardiac situs. The impact of intrinsic chirality and the perturbation of left–right patterning on myofiber organization and cardiac function warrants further investigation. We summarize recent insights gained from studies in animal models and also some human clinical studies in a brief overview of the complex processes regulating cardiac asymmetry and their impact on cardiac function and the pathogenesis of congenital heart defects.

Keywords

Left–right patterning · Cardiac asymmetry · Situs solitus · Situs inversus · Heterotaxy · Dextrocardia · Atrial situs · Heart looping · Great arteries · Atrial

G. C. Gabriel · Y. L. Wu · C. W. Lo (✉)
Department of Developmental Biology, University of Pittsburgh School of Medicine, Pittsburgh, PA, USA
e-mail: cel36@pitt.edu

© The Author(s), under exclusive license to Springer Nature Switzerland AG 2024

S. Rickert-Sperling et al. (eds.), *Congenital Heart Diseases: The Broken Heart*,
Advances in Experimental Medicine and Biology 1441,
https://doi.org/10.1007/978-3-031-44087-8_9

isomerism · Primary cilia · Mesocardia · Zebrafish · Bone morphogenetic protein · Left lateral plate mesoderm · Pitx2 · Zic family members · Primary ciliary dyskinesia · Laterality defects · Joubert syndrome · Kartagener syndrome · Motile cilia

9.1 Introduction

Studies using animal models have rapidly advanced our knowledge of the mechanisms driving cardiac morphogenesis, a process in which a left–right asymmetric, four-chambered heart is formed from an initially symmetric heart tube. It is now recognized that the developmental specification of cardiac asymmetry is a complex and dynamic process that begins very early in development with breaking of symmetry at the embryonic node. This comprises an organizing center that induces asymmetric gene expression that is propagated to the surrounding tissue to define distinct asymmetric patterning of visceral organ situs. Normal development results in visceral organ situs referred to as situs solitus where the heart, stomach, and spleen are on the left, with three lung lobes on the right and two on the left, and a stereotypical pattern of liver lobation and gut rotation. With defects in left–right patterning, the left–right body axis can become mirror symmetric, referred to as situs inversus totalis, or situs can be affected differently across multiple organs in the thoracic and abdominal cavities, causing heterotaxy.

Heterotaxy patients are known to suffer high morbidity and mortality. This is often due to the co-occurrence of congenital heart defects. In fact, a recent epidemiological study found that of 517 cases of laterality defects, 82.2% had some form of congenital heart disease [1]. More specifically, of the heterotaxy patients examined, 96.6% presented with congenital heart disease [1]. These findings highlight the importance of left–right patterning in cardiac morphogenesis. In addition to congenital heart disease, heterotaxy patients may also suffer other visceral organ defects such as gut malrotation, biliary atresia (the bile duct is considered to be a right-sided structure), or asplenia/polysplenia (the spleen is a left-sided structure) [2]. High morbidity and mortality can also be seen with gut malrotation and biliary atresia, with biliary atresia often requiring liver transplant as the only effective palliation.

9.2 Cardiac Asymmetry and Oxygenation of Blood

The heart is the most left–right asymmetric organ in the human body, sitting in the left side of the chest cavity and with the apex pointing to the left, i.e. levocardia (Figs. 9.1 and 9.2). The pattern of blood flow through the four-chamber heart highlights the striking anatomical and functional asymmetries that have evolved to separate the systemic and pulmonary circulation. Thus, deoxygenated blood flows from the body to the right side of the heart, and then on to the lung, and oxygenated blood flows from the lung back to the left side of the heart and systemically back to

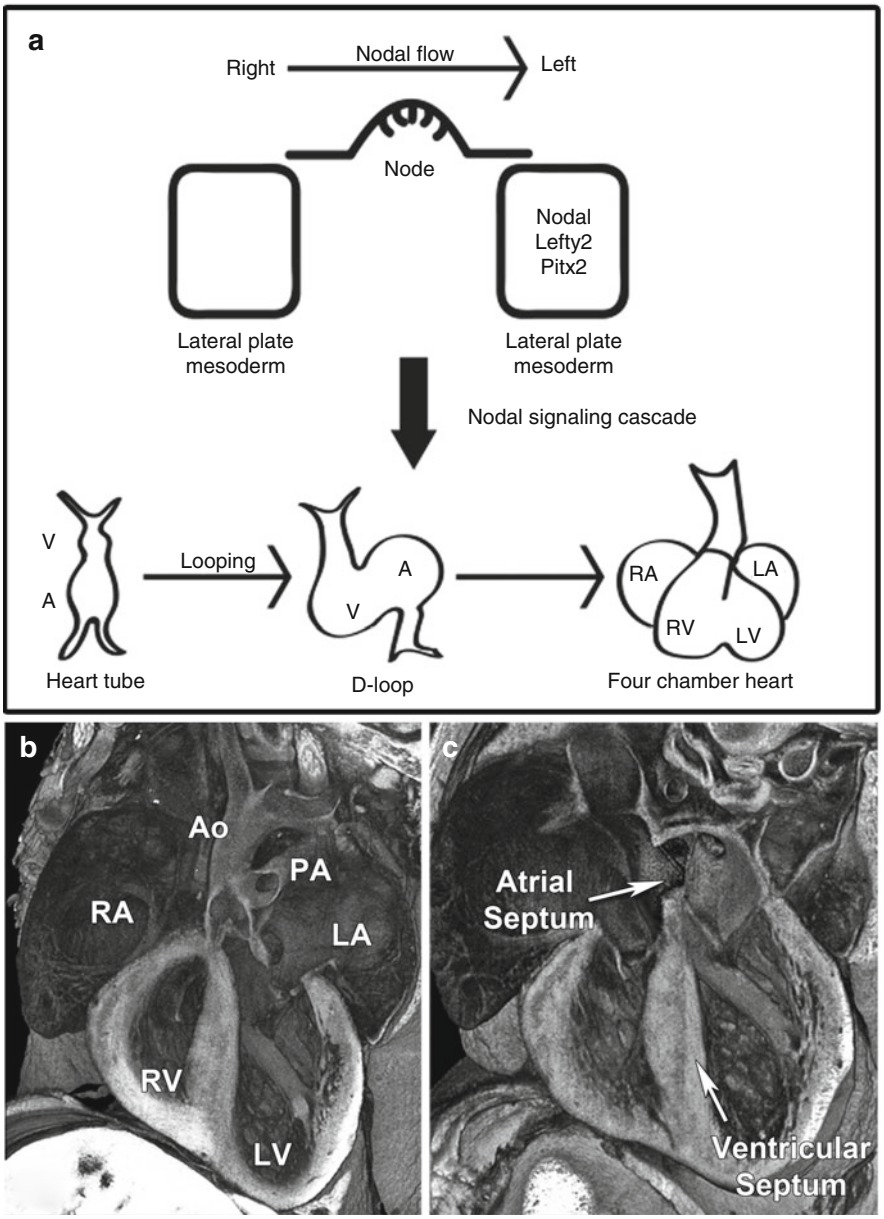

Fig. 9.1 Specification of cardiac asymmetry
(a) Cilia generated leftward flow at the embryonic node initiates an asymmetric signaling cascade in which nodal, lefty2, and pitx2 are expressed exclusively in the left lateral plate mesoderm. This left-sided expression has important consequences for heart looping; a process in which the symmetric heart tube undergoes dextral looping to form the four-chambered heart
(b) A representative image of normal intracardiac anatomy obtained by histopathology reveals the four chambers and two great arteries of the mouse heart
(c) A representative image of normal intracardiac anatomy obtained by histopathology

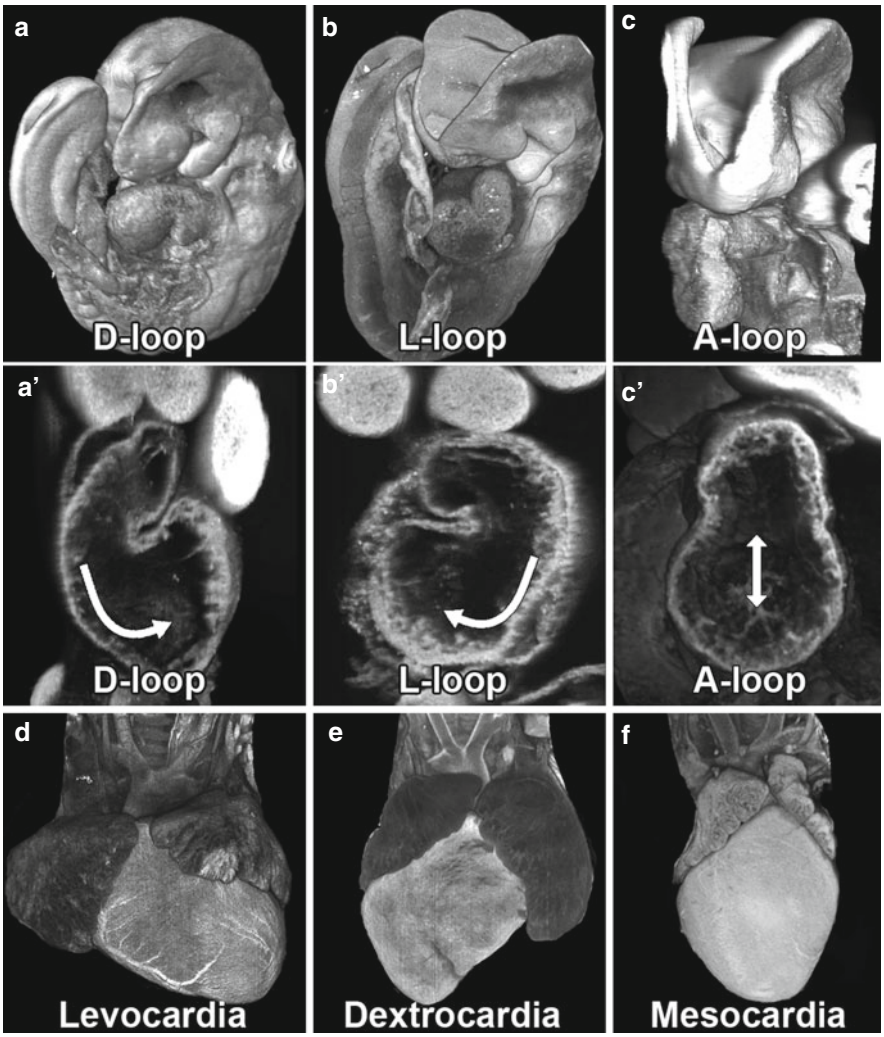

Fig. 9.2 Heart looping and heart situs
Normally, the linear heart tube undergoes dextral heart looping (**a**, **a**'). Defects in left–right axis specification can perturb heart looping resulting in abnormities such as reversed heart looping (L-loop; **b**, **b**′) or no looping (A-loop, **c**, **c**′). Ultimately, the normal heart will exhibit levocardia with the apex pointing leftward (**d**). Problems in heart looping can result in dextrocardia, in which the heart apex points toward the right (**e**) or mesocardia, in which the heart apex is midline (**f**)

Fig. 9.1 (continued) reveals the interatrial and interventricular septums
V, ventricle; A, atria; RA, right atria; LA, left atria; RV, right ventricle; LV, left ventricle; Ao, aorta; PA, pulmonary artery

the rest of the body. This pattern of systemic and pulmonary blood flow connected as a circuit in series allows efficient oxygenation of blood from the lung. A disruption of this pattern of segregated blood flow from the right vs. left side of the heart can cause high morbidity and mortality. This can arise from failure in partitioning of the atrial and/or ventricular chambers, outflow tract malalignment, septation defects, or defects in cardiac valve development required for unidirectional blood flow. Interestingly, the asymmetric looping of the heart tube that initiates the patterning of left–right asymmetry in the heart can be observed not only in airbreathing land mammals but this is also observed in fish, suggesting that looping of the heart tube might have other adaptive functions.

9.3 Complex Congenital Heart Disease and Heterotaxy

The finding of complex congenital heart disease in patients or mice with heterotaxy is well described. Mice are ideally suited for modeling human congenital heart disease; as being air-breathing animals, they have an identical four-chamber cardiac anatomy to humans [3]. Some examples of congenital heart defects found in mutant mouse models with heterotaxy are shown in Fig. 9.3. Compared to normal levocardia (Fig. 9.3a), mice with laterality defects can exhibit mirror image dextrocardia, which is the complete reversal of a normal heart structure (Fig. 9.3b). Aberrant left–right patterning can also lead to more complex phenotypes, such as ventricular dextroversion in which the heart exhibits dextrocardia, but ventricular chamber placement and outflow tract alignment are not altered (Fig. 9.3c). Other examples of phenotypes associated with abnormal left–right patterning include transposition of the great arteries (TGA), a condition in which the connections between the ventricles and the outflow tracts are reversed (Fig. 9.3d), double outlet right ventricle (DORV) in which both outflow tracts originate from the right ventricle (Fig. 9.3e), and atrioventricular septal defect (AVSD) with complete failure of the atrioventricular septum to form, resulting in a hole that allows communication between all four cardiac chambers.

9.4 Modular Assembly of Cardiac Asymmetry

While surgical palliation now allows many congenital heart disease patients to survive their initial acute cardiovascular deficits, even those with complex structural heart defects, there remains high morbidity and mortality in this patient population. To track and study the emergence of cardiac asymmetry and its disturbance, Van Praagh developed the “segmental” approach for the classification of cardiac asymmetry [4]. This approach utilizes a three-part lettering system to describe: (1) the atrial situs, (2) the direction of heart looping, and (3) the relationship of the great arteries [5]. In this manner, atrioventricular and inflow/outflow tract identities can be summarized and tabulated across a patient cohort. Thus, normal cardiac situs would be described as (S,D,S)—solitus (S) or normal atria situs, normal dextral (D) looping

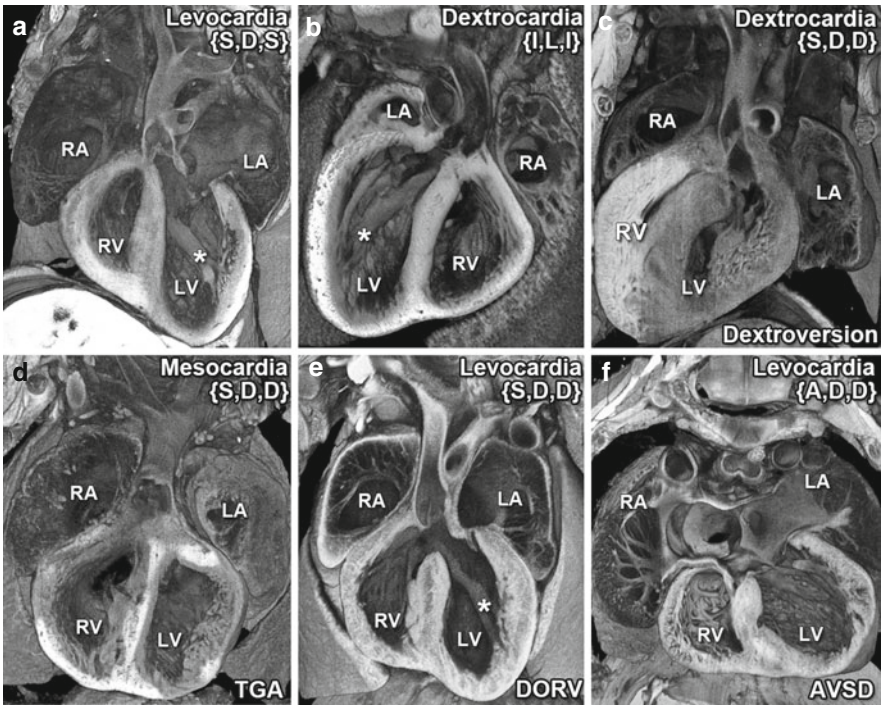

Fig. 9.3 Congenital heart defects associated with abnormal left–right patterning Compared to normal levocardia (**a**), mice with laterality defects can exhibit congenital heart diseases such as mirror image dextrocardia, or the complete reversal of normal heart structure (**b**), dextroversion, a special case of dextrocardia in which the ventricular and outflow positions are not altered (**c**), transposition of the great arteries (TGA), in which the connections between the ventricles and the outflow tracts are reversed (**d**), double outlet right ventricle (DORV), in which both outflow tracts originate from the RV (e), or atrialventricular septal defect (AVSD), in which the atrial septum fails to form (**f**). Van Praagh segmentation for each heart is given in brackets. * denotes the free wall papillary muscle, which is defining for the left ventricle. RA, right atria; LA, left atria; RV, right ventricle; LV, left ventricle; Ao, aorta; PA, pulmonary artery

of the heart, and solitus (S) or normal arrangement of the great arteries. What is striking with regard to patterning of cardiac asymmetry captured by the Van Praagh classification scheme is that left–right patterning of the different segments of the heart, i.e., the atria, ventricle, and outflow tract, can be specified in a modular fashion independent of each other. Thus, it is possible to have a heart with two left or two right atria (referred to as left or right atrial isomerism) or a left atrium connected to a right ventricle, but on the body's right or left side. It is also possible to have the pulmonary trunk connected to the left ventricle and the aorta to the right ventricle, i.e., transposition of the great arteries, and this can occur with the ventricles positioned in their normal left–right position (D-TGA) or in an inverted orientation (L-TGA). Such complex shuffling of cardiac situs can cause not only mixing of oxygenated with deoxygenated blood, but in some instances, blood flow is also

routed in two parallel circuits such that the systemic blood flow bypasses the lung altogether. These findings suggest that understanding how left–right asymmetry is established during cardiac morphogenesis is of great importance for elucidating the etiology of congenital heart disease.

9.5 Left–Right Patterning

Patterning of left–right asymmetry is a developmental process highly conserved in evolution. In the vertebrate embryo, the initial break in symmetry occurs via signaling mediated by a transient, ciliated organ, known as the embryonic node in mouse embryos. At the embryonic node, monociliated pit cells have rotating motile cilia and are surrounded by perinodal crown cells harboring nonmotile primary cilia [6, 7]. Motile cilia of the pit cells rotate clockwise, generating a leftward flow, resulting in propagation of a signal that establishes the left–right axis through asymmetric expression of nodal, a Tgfβ ligand, on the left side, and its inhibitor Dand5 on the right side of the embryonic node [8]. Further studies investigating how the leftward nodal flow is perceived and propagated has led to three distinct models: an accumulation of morphogens on the left side of the embryo, an asymmetric distribution of node vesicular parcels containing hedgehog proteins and retinoic acid, or detection of fluid flow by the nonmotile cilia of the crown cells leading to asymmetric calcium signaling via Pkd2 and Pkd111 [9–13, 43]. Most intriguing is recent evidence from our laboratory resulting from analysis of a novel *Dnah5* mutant, indicating that nodal flow may be necessary but not sufficient for establishing the left–right axis (Unpublished results).

9.6 Heart Looping and Development of Cardiac Asymmetry

Cardiac morphogenesis begins with migration of cells comprising the primary heart field in the cardiac crescent to the axial midline, forming a hollow linear heart tube. This is followed by a distinct rightward or dextral (D) looping of the heart tube, the first evidence of cardiac asymmetry. Defects in the specification of left–right patterning can perturb heart looping, causing reversed looping (L-loop) or no looping (A-loop) which can result in dextrocardia (L-loop) or mesocardia (A-loop), respectively (Fig. 9.2) [14]. The process of heart looping also serves to initiate cardiac chamber formation such that the initially posteriorly positioned atrial segment is brought to a cranial position relative to the primitive ventricles, establishing the anterior or superior positioning of the atrial segment of the heart tube relative to the ventricle as seen in the mature heart (Fig. 9.1) [14]. While the primitive heart tube is formed by cells from the primary heart field, these cells will only give rise to future left ventricle, while most of the remainder of the heart, the right ventricle, outflow tract, and atria are derived from another cardiac progenitor cell population, the second heart field [15, 16]. These cells migrate into the looped heart tube via the dorsal pericardial wall and are added at the arterial and venous pole of the heart over

a period of several days during embryogenesis [17]. These second heart field cells play an important role in elaboration of the four-chamber heart and contribute cells that form the atrial septum [18].

Studies carried out in zebrafish, a model organism which breaks symmetry via a ciliated organ functionally homologous to the mouse embryonic node, the Kupffer's Vesicle (KV), have helped to elucidate the connection between early asymmetries in gene expression and heart looping [19]. While the zebrafish has only a two-chamber heart, it still undergoes cardiac looping and exhibits cardiac and visceral organ asymmetry. The transparency of the zebrafish embryo and its development externally has made it possible to study cardiac looping at the single cell level. Such studies have indicated that activation of nodal signaling in the left LPM may direct heart looping by modulating directional migration of cardiac progenitor cells [20]. This is mediated through left-sided inhibition of BMP signaling by a nodal regulated extra cellular matrix protein Has-2. As a result, a left–right difference in cell motility emerges in the zebrafish embryo, with the left side of the embryo exhibiting increased cell motility driving asymmetric looping of the heart tube [21]. Whether this same mechanism is conserved in the regulation of heart looping in the mouse embryo remains to be determined.

9.7 Developmental Signaling in the Specification of Cardiac Asymmetry

The specification of cardiac asymmetry occurs during early embryogenesis, mediated by the same developmental processes that specify the entire left–right body axis. While the initial breaking of symmetry occurs at the embryonic node, signaling initiated at the node must be propagated to the left lateral plate mesoderm (LPM), resulting in left-sided LPM expression of Nodal, followed by left-sided expression of Lefty1/Lefty2 (nodal inhibitors), and then left-sided expression of Pitx2, a paired-like homeodomain transcription factor [7]. This asymmetric gene expression cascade is essential for left–right organization of the entire embryo, with left-sided Pitx2 expression persisting in all of the visceral organ primordia throughout development. This is thought to regulate a gene expression program specifying left-sided differentiation (Fig. 9.1) [7, 22]. Since cells of the first and second heart field are found in both the left and right lateral plate mesoderm, it is likely that the early LPM asymmetric gene expression pattern may drive cardiac asymmetry and the coding of left–right patterning in the first and second heart field [23]. Consistent with this, Pitx2 expression persists exclusively on the left side of the developing heart, impacting patterning of the second heart field [24]. Expression of Pitx2 is also required in the pharyngeal arch mesenchyme later in development for the formation of the aorta and pulmonary artery [25]. In addition, Pitx2 has been shown to regulate cell proliferation and cell migration, which may also impact heart looping and contribute to specification of cardiac left–right asymmetries (Fig. 9.1) [26].

9.8 Intrinsic Chirality and the Regulation of Heart Looping

Studies using zebrafish and chick embryos have provided evidence of heart looping encoded by intrinsic chirality independent of the nodal signaling cascade driving visceral organ patterning. Thus, a zebrafish mutant carrying a mutation in the nodal-related gene *southpaw* showed retention of normal dextral heart looping even as gut and brain asymmetry were randomized [27]. Furthermore, dextral heart looping in both the zebrafish and chick embryos was maintained in heart tubes explanted and cultured in vitro. This intrinsic chirality requires nonmuscle myosin II and actin and is independent of cardiac contractility [27]. These findings demonstrate that heart looping is hardwired and is likely regulated by a tissue intrinsic mechanism driven by actomyosin [27].

Studies in chicken embryos further showed that this chirality is specified at the cellular level. Thus, cardiomyocytes explanted from the chick heart tube before and during heart looping showed rightward rotation [28]. Furthermore, a rightward bias in cell alignment and Golgi orientation were observed together with asymmetric distribution of *N*-cadherin and nonmuscle myosin II in cardiomyocytes within the chick heart prior to looping of the heart tube [29, 30]. Together these observations suggest that intrinsic chirality in cardiomyocytes may drive heart looping. This is corroborated by the finding that reversal of this intrinsic chirality is associated with reversal of heart looping direction [29]. The further finding in the mouse heart of regional polarization of cells would suggest that this mechanism has broader relevance for heart looping in mammals [29].

As primitive chordates such as Ascidians exhibit asymmetric Nodal expression that is associated with brain and gut asymmetry, but no asymmetry is observed in the heart, this suggests that cardiac asymmetry may have emerged in evolution independently of Nodal signaling [30]. Instead, a mechanism involving the specification of intrinsic cell chirality may have emerged to establish cardiac laterality. Nevertheless, as Nodal signaling does contribute to patterning of cardiac asymmetry in higher vertebrates, it provides instructive signals superimposed on the intrinsic chirality of cardiomyocytes to pattern left–right asymmetry in the cardiovascular system of higher organisms.

9.9 Impact of Cardiac Mechanics

Defects in left–right patterning have been shown to be associated with abnormal organization of muscle bundles in the heart, suggesting possible disturbance on cardiac mechanics. This was first reported by the pioneering pediatric cardiologist Dr. Helen Taussig with direct visualization of two human heart specimens with situs inversus totalis (SIT) [31]. She reported that the deep muscle bundles of these hearts were arranged differently from that of the normal heart. In the normal situs solitus (SS) heart, a helical arrangement of the myocardial fibers arranged in opposing direction are observed at the outer/epicardial vs. inner/endocardial layers of the ventricle. As the left ventricle (LV) contracts with a twisting motion in systole,

potential energy is stored for driving ventricular ejection, while the untwisting (recoil) in diastole releases energy to promote relaxation and ventricular filling. This provides a wringing motion that allows for effective emptying of the heart and its subsequent unwinding allows efficient filling of the heart.

Quantification of the angles of systolic twist and diastolic untwist with echocardiography showed in the wildtype mouse heart, coherent systolic twist (positive radial displacement representing counterclockwise rotation) and diastolic untwist (negative radial displacement representing clockwise rotation) throughout different short-axis planes [32–38]. Thus, coherent systolic twist is associated with positive radial displacement reflecting the counterclockwise rotation of the myocardial fibers, while diastolic untwisting causes negative radial displacement with clockwise rotation (Fig. 9.4a). In comparison, in *Pkd1L1*$^{m/m}$ mutant mice, which display situs inversus totalis (SIT) (Fig. 9.4b), rotation of the heart is incoherent in all short-axis planes. Furthermore, quantification of the angular displacement of cardiac rotation showed additional twists deviating from normal rotation in the SIT heart (Fig. 9.4).

These ultrasound findings were corroborated with diffusion MRI for tracking directional water diffusion to map local fiber orientations and the myofiber architecture of the heart [39–42, 44]. In WT hearts, fiber tractography showed that each myofiber bundle has coherent helical organization with specific angular organization (Fig. 9.5). In contrast, the heart of a *Pkd1L1*$^{m/m}$ mutant with SIT showed dispersed and incoherent myofiber bundle formation deviating from the normal helical arrangements (Fig. 9.5). This is associated with incoherent rotation in the short-axis plane. Some short-axis planes also displayed additional twists deviating from normal rotation. The clinical relevance of these findings was demonstrated in a study of eight patients with situ inversus totalis (SIT) by Delhaas and associates. They showed that rotation of the heart in human subjects with SIT vs. normal hearts is

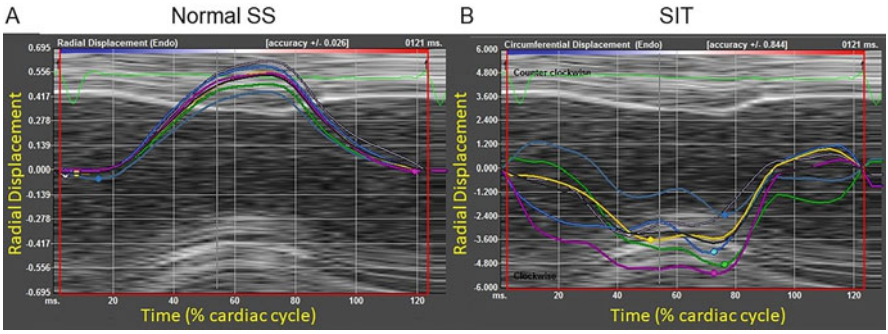

Fig. 9.4 Echocardiography shows abnormal rotation of *Pdk1l1*$^{m/m}$ mutant mouse heart
Echocardiography was conducted to examine cardiac rotation in a wildtype mouse with normal situs solitus (SS) heart (**a**) and *Pkd1l1*$^{m/m}$ mutant mouse with situs inversus totalis (SIT) heart (**b**). Each colored line represents a short-axis plane showing radial displacement through the cardiac cycle, with negative displacement representing clockwise rotation and positive displacement, counterclockwise rotation. Note the very abnormal rotation of the SIT heart as compared to the wildtype SS heart. X-axis: time in a cardiac cycle. Y-axis: radial displacement

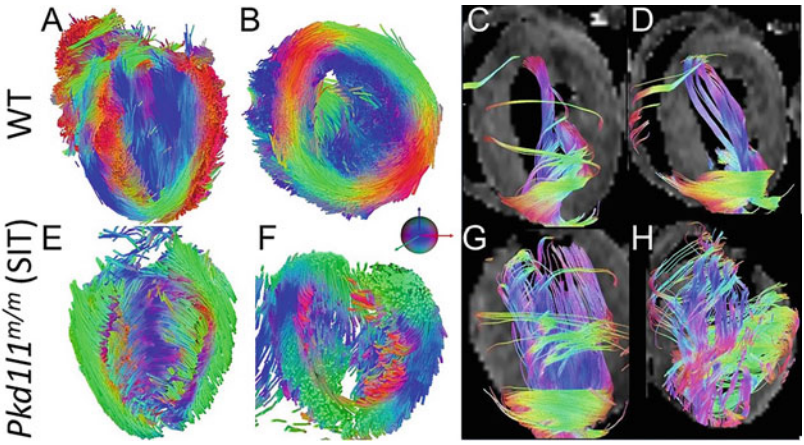

Fig. 9.5 *Pkd1l1*$^{m/m}$ mutant hearts with situs inversus totalis displayed aberrant myofiber organization
Myofiber tractography of adult heart using ex vivo MRI in a WT (**a**–**d**) and ***Pkd1l1***$^{m/m}$ mutant (**e**–**h**) with situs inversus totalis. The fiber tracts obtained are shown in long-axis (**a**,**e**) or short-axis (**b**,**f**) views, or with partial visualization of the fibers (**c**, **d**, **g**, **h**). Color-coding tensor vectors indicate myofiber orientation: red: X, green: Y, blue: Z. The diffusion images were acquired on a Bruker BioSpec GmbH 7-Tesla scanner with 35 mm quadrature coil

considerably different [38, 45–48]. Together these findings suggest that left–right patterning plays an important role in patterning of myofiber organization in the heart, and its disturbance can result in altered cardiac mechanics. The possible role of intrinsic chirality on myofiber architecture has not been investigated. Additional studies are also needed to investigate the impact of left–right patterning defects on cardiac mechanics and its potential physiological impact, such as in exercise tolerance.

9.10 Cilia, Left–Right Patterning, and Congenital Heart Defects

The important role of cilia in left–right patterning and in establishing cardiac asymmetry has implicated disruption of cilia as a potential key contributor to congenital heart disease. Mutations in Zic2 and Zic3, transcription factors known to regulate cilia formation in the embryonic node, can cause cardiac situs anomalies and congenital heart defects in conjunction with heterotaxy [49, 50]. Consistent with the important role of the cilium in cardiac morphogenesis and the establishment of cardiac asymmetry, we recovered many ciliome genes from a large-scale mouse mutagenesis screen for mutations causing congenital heart disease [51]. This included both genes required for motile and primary cilia function. Some examples include *Mks1, Cep290, Dnah5, Dnai1, Dnah11, Drc1, Dyx1c1, Ccdc151,* and *Armc4* [52–58]. Many of these genes are known to cause primary ciliary dyskinesia (PCD), a sinopulmonary disease arising from mucociliary clearance defects due to

defects in motile cilia in the airway. This reflects the shared requirement for motile cilia in airway clearance and left–right patterning. Hence, some PCD patients can exhibit situs inversus totalis (Kartagener's syndrome) or heterotaxy, with the heterotaxy/PCD patients usually also exhibiting congenital heart defects [59]. As expected, congenital heart defects are often observed in conjunction with heterotaxy. However, we also recovered many mutations affecting ciliogenesis or cilia formation that caused isolated congenital heart disease without laterality defects, such as *Wdpcp* and *Jbts17* [60, 61]. These mutations are primarily associated with phenotypes that suggest the disturbance of primary cilia transduced cell signaling, such as in Tgfβ, Wnt, or Shh signaling, all pathways known to play important roles in cardiovascular development [62]. Disruption of these cell signaling pathways has been shown to cause congenital heart defects in mutant mouse models [63–65]. Thus, cilia play a fundamental role in cardiac morphogenesis beyond a role in patterning cardiac asymmetry, and this can involve both motile and primary cilia.

9.11 Complex Genetic Architecture of Human Laterality Defects

While many studies have highlighted the role of cilia and cilia transduced signaling in laterality defects and congenital heart defects, in patients presenting with laterality phenotypes, a genetic cause is often not identified. Recent work has shown that variants contributing to laterality defects can only account for approximately 20% of cases [66]. In patients, congenital heart disease associated with heterotaxy is hereditary and recessive transmission of disease has been demonstrated. Damaging recessive variants in cilia-related genes are enriched in CHD patients, and this can be observed with or without accompanying laterality defects [67, 68]. Additionally, recent work has demonstrated that both laterality disorders and congenital heart disease phenotypes can have a complex multigenic etiology, complicating efforts to elucidate the genetic causes of congenital heart disease associated with heterotaxy [66, 69, 70].

9.12 Summary

Patterning left–right asymmetries of the heart is a complex and dynamic process dependent on early embryonic events that break symmetry and establish the left–right body axis. Disruption of this process can result in congenital heart disease composed of a wide spectrum of defects involving atrial, ventricular, or outflow tract anomalies. Defects in left–right asymmetry in the heart have been observed to present in a modular fashion, such that each segment of the heart (atrium, ventricle, and outflow tract) can be structurally either left- or right-sided. Given this modular construction, complex congenital heart disease associated with heterotaxy can be composed of many different right- and/or left-sided atria/ventricle/outflow combinations. Thus, it is perhaps not surprising that structural heart defects associated with heterotaxy are associated with high morbidity and mortality. While

further work is needed to elucidate how the earliest events in left–right axis specification are transmitted to the cardiac precursor cells, and how the different segments of the heart are patterned, studies in animal models have shown that cilia, both motile and nonmotile, play a critical role in these processes. More recent work has further shown the involvement of intrinsic chirality at the cellular and tissue level in the patterning of cardiac laterality. The impact of left–right patterning and intrinsic chirality on myofiber architecture and cardiac mechanics warrant further investigations. A better understanding of the mechanisms underlying the specification of cardiac asymmetry will help elucidate not only the developmental etiology of complex congenital heart disease but also aid in its diagnosis and clinical management.

References

1. Lin AE, Krikov S, Riehle-Colarusso T, Frias JL, Belmont J, Anderka M, et al. Laterality defects in the national birth defects prevention study (1998-2007): birth prevalence and descriptive epidemiology. Am J Med Genet A. 2014;164A(10):2581–91. https://doi.org/10.1002/ajmg.a.36695.
2. Pepes S, Zidere V, Allan LD. Prenatal diagnosis of left atrial isomerism. Heart. 2009;95(24):1974–7. https://doi.org/10.1136/hrt.2009.165514.
3. Krishnan A, Samtani R, Dhanantwari P, Lee E, Yamada S, Shiota K, et al. A detailed comparison of mouse and human cardiac development. Pediatr Res. 2014;76(6):500–7. https://doi.org/10.1038/pr.2014.128.
4. Praagh RV. Diagnosis of complex congenital heart disease: Morphologic-anatomic method and terminology. Cardiovascular and Interventional Radiology. 1984;7(3–4):115–20.
5. Erica K, Schallert GHD, Kardon R, Young DA. Describing congenital heart disease by using three-part segmental notation. Radiographics. 2013;33(2):E33–46. https://doi.org/10.1148/rg.332125086.
6. Nonaka S, Tanaka Y, Okada Y, Takeda S, Harada A, Kanai Y, et al. Randomization of left–right asymmetry due to loss of nodal cilia generating leftward flow of extraembryonic fluid in mice lacking KIF3B motor protein. Cell. 1998;95(6):829–37. https://doi.org/10.1016/s0092-8674(00)81705-5.
7. Hamada H, Meno C, Watanabe D, Saijoh Y. Establishment of vertebrate left-right asymmetry. Nat Rev Genet. 2002;3(2):103–13. https://doi.org/10.1038/nrg732.
8. Oki S, Kitajima K, Marques S, Belo JA, Yokoyama T, Hamada H, et al. Reversal of left-right asymmetry induced by aberrant nodal signaling in the node of mouse embryos. Development. 2009;136(23):3917–25. https://doi.org/10.1242/dev.039305.
9. Tanaka Y, Okada Y, Hirokawa N. FGF-induced vesicular release of sonic hedgehog and retinoic acid in leftward nodal flow is critical for left-right determination. Nature. 2005;435(7039):172–7. https://doi.org/10.1038/nature03494.
10. McGrath J, Somlo S, Makova S, Tian X, Brueckner M. Two populations of node Monocilia initiate left-right asymmetry in the mouse. Cell. 2003;114(1):61–73. https://doi.org/10.1016/s0092-8674(03)00511-7.
11. McGrath J. Cilia are at the heart of vertebrate left–right asymmetry. Curr Opin Genet Dev. 2003;13(4):385–92. https://doi.org/10.1016/s0959-437x(03)00091-1.
12. Field S, Riley KL, Grimes DT, Hilton H, Simon M, Powles-Glover N, et al. Pkd1l1 establishes left-right asymmetry and physically interacts with Pkd2. Development. 2011;138(6):1131–42. https://doi.org/10.1242/dev.058149.

13. Kamura K, Kobayashi D, Uehara Y, Koshida S, Iijima N, Kudo A, et al. Pkd1l1 complexes with Pkd2 on motile cilia and functions to establish the left-right axis. Development. 2011;138(6):1121–9. https://doi.org/10.1242/dev.058271.
14. Srivastava D, Olson EN. A genetic blueprint for cardiac development. Nature. 2000;407(6801):221–6. https://doi.org/10.1038/35025190.
15. Kathiriya IS, Srivastava D. Left-right asymmetry and cardiac looping: implications for cardiac development and congenital heart disease. Am J Med Genet. 2000;97(4):271–9. https://doi.org/10.1002/1096-8628(200024)97:4<271::Aid-Ajmg1277>3.0.Co;2-O.
16. Brand T. Heart development: molecular insights into cardiac specification and early morphogenesis. Dev Biol. 2003;258(1):1–19. https://doi.org/10.1016/s0012-1606(03)00112-x.
17. Buckingham M, Meilhac S, Zaffran S. Building the mammalian heart from two sources of myocardial cells. Nat Rev Genet. 2005;6(11):826–35. https://doi.org/10.1038/nrg1710.
18. Francou A, Saint-Michel E, Mesbah K, Theveniau-Ruissy M, Rana MS, Christoffels VM, et al. Second heart field cardiac progenitor cells in the early mouse embryo. Biochim Biophys Acta. 2013;1833(4):795–8. https://doi.org/10.1016/j.bbamcr.2012.10.003.
19. Xie L, Hoffmann AD, Burnicka-Turek O, Friedland-Little JM, Zhang K, Moskowitz IP. Tbx5-hedgehog molecular networks are essential in the second heart field for atrial septation. Dev Cell. 2012;23(2):280–91. https://doi.org/10.1016/j.devcel.2012.06.006.
20. Bakkers J, Verhoeven MC, Abdelilah-Seyfried S. Shaping the zebrafish heart: from left-right axis specification to epithelial tissue morphogenesis. Dev Biol. 2009;330(2):213–20. https://doi.org/10.1016/j.ydbio.2009.04.011.
21. Smith KA, Chocron S, von der Hardt S, de Pater E, Soufan A, Bussmann J, et al. Rotation and asymmetric development of the zebrafish heart requires directed migration of cardiac progenitor cells. Dev Cell. 2008;14(2):287–97. https://doi.org/10.1016/j.devcel.2007.11.015.
22. Veerkamp J, Rudolph F, Cseresnyes Z, Priller F, Otten C, Renz M, et al. Unilateral dampening of Bmp activity by nodal generates cardiac left-right asymmetry. Dev Cell. 2013;24(6):660–7. https://doi.org/10.1016/j.devcel.2013.01.026.
23. Jeffrey J, Essner WWB, Zhang J, Yost HJ. Mesendoderm and left-right brain, heart and gut development are differentially regulated by pitx2 isoforms. Development. 2000;127(5):1081–93.
24. Ramsdell AF. Left-right asymmetry and congenital cardiac defects: getting to the heart of the matter in vertebrate left-right axis determination. Dev Biol. 2005;288(1):1–20. https://doi.org/10.1016/j.ydbio.2005.07.038.
25. Vincent SD, Buckingham ME. How to make a heart: the origin and regulation of cardiac progenitor cells. Curr Top Dev Biol. 2010;90:1–41. https://doi.org/10.1016/s0070-2153(10)90001-x.
26. Yashiro K, Shiratori H, Hamada H. Haemodynamics determined by a genetic programme govern asymmetric development of the aortic arch. Nature. 2007;450(7167):285–8. https://doi.org/10.1038/nature06254.
27. Kioussi C, Briata P, Baek SH, Rose DW, Hamblet NS, Herman T, et al. Identification of a Wnt/Dvl/β-catenin → Pitx2 pathway mediating cell-type-specific proliferation during development. Cell. 2002;111(5):673–85. https://doi.org/10.1016/s0092-8674(02)01084-x.
28. Noël ES, Verhoeven M, Lagendijk AK, Tessadori F, Smith K, Choorapoikayil S, et al. A nodal-independent and tissue-intrinsic mechanism controls heart-looping chirality. Nat Commun. 2013;4(1):2754. https://doi.org/10.1038/ncomms3754.
29. Ray P, Chin AS, Worley KE, Fan J, Kaur G, Wu M, et al. Intrinsic cellular chirality regulates left–right symmetry breaking during cardiac looping. Proc Natl Acad Sci. 2018;115(50):E11568–E77. https://doi.org/10.1073/pnas.1808052115.
30. de Boer BA, van den Berg G, de Boer PA, Moorman AF, Ruijter JM. Growth of the developing mouse heart: an interactive qualitative and quantitative 3D atlas. Dev Biol. 2012;368(2):203–13. https://doi.org/10.1016/j.ydbio.2012.05.001.

31. Signore IA, Palma K, Concha ML. Nodal signalling and asymmetry of the nervous system. Philos Trans R Soc Lond Ser B Biol Sci. 2016;371(1710):20150401. https://doi.org/10.1098/rstb.2015.0401.
32. Taussig HB. The anatomy of the heart in two cases of situs transversus. Johns Hopkins Med J. 1977;140(4):143–5.
33. Jeung MY, Germain P, Croisille P, El ghannudi S, Roy C, Gangi A. Myocardial tagging with MR imaging: overview of normal and pathologic findings. Radiographics: a review publication of the Radiological Society of North America, Inc. 2012;32(5):1381–98. https://doi.org/10.1148/rg.325115098.
34. Grotenhuis HB, Nyns ECA, Kantor PF, Dipchand AI, Greenway SC, Yoo SJ, et al. Abnormal myocardial contractility after pediatric heart transplantation by cardiac MRI. Pediatr Cardiol. 2017;38(6):1198–205. https://doi.org/10.1007/s00246-017-1642-5.
35. Musa TA, Uddin A, Swoboda PP, Fairbairn TA, Dobson LE, Singh A, et al. Cardiovascular magnetic resonance evaluation of symptomatic severe aortic stenosis: association of circumferential myocardial strain and mortality. J Cardiovasc Magn Reson. 2017;19(1):13. https://doi.org/10.1186/s12968-017-0329-7.
36. Schneeweis C, Lapinskas T, Schnackenburg B, Berger A, Hucko T, Kelle S, et al. Comparison of myocardial tagging and feature tracking in patients with severe aortic stenosis. J Heart Valve Dis. 2014;23(4):432–40.
37. Ahmed MI, Desai RV, Gaddam KK, Venkatesh BA, Agarwal S, Inusah S, et al. Relation of torsion and myocardial strains to LV ejection fraction in hypertension. J Am Coll Cardiol Img. 2012;5(3):273–81. https://doi.org/10.1016/j.jcmg.2011.11.013.
38. Fuchs E, Muller MF, Oswald H, Thony H, Mohacsi P, Hess OM. Cardiac rotation and relaxation in patients with chronic heart failure. Eur J Heart Fail. 2004;6(6):715–22. https://doi.org/10.1016/j.ejheart.2003.12.018.
39. Delhaas T, Kroon W, Decaluwe W, Rubbens M, Bovendeerd P, Arts T. Structure and torsion of the normal and situs inversus totalis cardiac left ventricle. I. Experimental data in humans. Am J Physiol Heart Circ Physiol. 2008;295(1):H197–201. https://doi.org/10.1152/ajpheart.00876.2007.
40. Wu YL, Yu C, Liu X, Yeh F, Hitchens T, Gabriel GC, et al. Diffusion-tensor imaging study of myocardial architecture of Situs Inversus and Situs Solitus mutant mouse hearts. 23rd International Soceity of Magnetic Resonance in Medicine Annual Meeting; 2015; Toronto, Ontario, Canada.
41. Wu YL, Yeh F, Tadros S, Lo C. How Can Situs Inversus Totalis Hearts Work: From Genes, Myocardial Micro-architecture, to Cardiac Function. Soceity of Cardiovascular Magnetic Resonance SCMR Annual Meeting; 2017; Washington, D. C.
42. Behrens TE, Woolrich MW, Jenkinson M, Johansen-Berg H, Nunes RG, Clare S, et al. Characterization and propagation of uncertainty in diffusion-weighted MR imaging. Magn Reson Med. 2003;50(5):1077–88. https://doi.org/10.1002/mrm.10609.
43. Wedeen VJ, Rosene DL, Wang R, Dai G, Mortazavi F, Hagmann P, et al. The geometric structure of the brain fiber pathways. Science. 2012;335(6076):1628–34. 335/6076/1628 [pii]. https://doi.org/10.1126/science.1215280.
44. Behrens TEJ, Berg HJ, Jbabdi S, Rushworth MFS, Woolrich MW. Probabilistic diffusion tractography with multiple fibre orientations: what can we gain? NeuroImage. 2007;34(1):144–55.
45. Delhaas T, Kroon W, Bovendeerd P, Arts T. Left ventricular apical torsion and architecture are not inverted in situs inversus totalis. Prog Biophys Mol Biol. 2008;97(2–3):513–9. https://doi.org/10.1016/j.pbiomolbio.2008.02.004.
46. Kroon W, Delhaas T, Bovendeerd P, Arts T. Structure and torsion in the normal and situs inversus totalis cardiac left ventricle. II. Modeling cardiac adaptation to mechanical load. Am J Physiol Heart Circ Physiol. 2008;295(1):H202–10. https://doi.org/10.1152/ajpheart.00877.2007.

47. Pluijmert M, Kroon W, Rossi AC, Bovendeerd PH, Delhaas T. Why SIT works: normal function despite typical myofiber pattern in situs Inversus Totalis (SIT) hearts derived by shear-induced myofiber reorientation. PLoS Comput Biol. 2012;8(7):e1002611. https://doi.org/10.1371/journal.pcbi.1002611.
48. Rossi AC, Pluijmert M, Bovendeerd PH, Kroon W, Arts T, Delhaas T. Assessment and comparison of left ventricular shear in normal and situs inversus totalis hearts by means of magnetic resonance tagging. Am J Physiol Heart Circ Physiol. 2015;308(5):H416–23. https://doi.org/10.1152/ajpheart.00502.2014.
49. Barratt KS, Glanville-Jones HC, Arkell RM. The Zic2 gene directs the formation and function of node cilia to control cardiac situs. Genesis. 2014;52(6):626–35. https://doi.org/10.1002/dvg.22767.
50. Sutherland MJ, Wang S, Quinn ME, Haaning A, Ware SM. Zic3 is required in the migrating primitive streak for node morphogenesis and left-right patterning. Hum Mol Genet. 2013;22(10):1913–23. https://doi.org/10.1093/hmg/ddt001.
51. Liu X, Francis R, Kim AJ, Ramirez R, Chen G, Subramanian R, et al. Interrogating congenital heart defects with noninvasive fetal echocardiography in a mouse forward genetic screen. Circ Cardiovasc Imaging. 2014;7(1):31–42. https://doi.org/10.1161/CIRCIMAGING.113.000451.
52. Cui C, Chatterjee B, Francis D, Yu Q, SanAgustin JT, Francis R, et al. Disruption of Mks1 localization to the mother centriole causes cilia defects and developmental malformations in Meckel-Gruber syndrome. Dis Model Mech. 2011;4(1):43–56. https://doi.org/10.1242/dmm.006262.
53. Kennedy MP, Omran H, Leigh MW, Dell S, Morgan L, Molina PL, et al. Congenital heart disease and other heterotaxic defects in a large cohort of patients with primary ciliary dyskinesia. Circulation. 2007;115(22):2814–21. https://doi.org/10.1161/CIRCULATIONAHA.106.649038.
54. Tan SY, Rosenthal J, Zhao XQ, Francis RJ, Chatterjee B, Sabol SL, et al. Heterotaxy and complex structural heart defects in a mutant mouse model of primary ciliary dyskinesia. J Clin Invest. 2007;117(12):3742–52. https://doi.org/10.1172/JCI33284.
55. Tarkar A, Loges NT, Slagle CE, Francis R, Dougherty GW, Tamayo JV, et al. DYX1C1 is required for axonemal dynein assembly and ciliary motility. Nat Genet. 2013;45(9):995–1003. https://doi.org/10.1038/ng.2707.
56. Hjeij R, Lindstrand A, Francis R, Zariwala MA, Liu X, Li Y, et al. ARMC4 mutations cause primary ciliary dyskinesia with randomization of left/right body asymmetry. Am J Hum Genet. 2013;93(2):357–67. https://doi.org/10.1016/j.ajhg.2013.06.009.
57. Francis RJ, Christopher A, Devine WA, Ostrowski L, Lo C. Congenital heart disease and the specification of left-right asymmetry. Am J Physiol Heart Circ Physiol. 2012;302(10):H2102–11. https://doi.org/10.1152/ajpheart.01118.2011.
58. Rim Hjeij AO, Watson CM, Slagle CE, Klena NT, Dougherty GW, Kurkowiak M, Loges NT, Diggle CP, Morante NFC, Gabriel GC, Lemke KL, Li Y, Pennekamp P, Menchen T, Konert F, Martin JK, Mans DA, Letteboer SJF, Werner C, Burgoyne T, Westermann C, Rutman A, Carr IM, O'Callaghan C, Moya E, Chung EMK, UK10K, Sheridan E, Nielsen KG, Roepman R, Bartscherer K, Burdine RD, Lo CW, Omran H, Mitchison HM. CCDC151 mutations cause primary ciliary dyskinesia by disruption of the outer dynein arm docking complex formation. Am J Hum Genet. 2014;95(3):257–74. https://doi.org/10.1016/j.ajhg.2014.08.005.
59. Nakhleh N, Francis R, Giese RA, Tian X, Li Y, Zariwala MA, et al. High prevalence of respiratory ciliary dysfunction in congenital heart disease patients with heterotaxy. Circulation. 2012;125(18):2232–42. https://doi.org/10.1161/CIRCULATIONAHA.111.079780.
60. Cui C, Chatterjee B, Lozito TP, Zhang Z, Francis RJ, Yagi H, et al. Wdpcp, a PCP protein required for ciliogenesis, regulates directional cell migration and cell polarity by direct modulation of the actin cytoskeleton. PLoS Biol. 2013;11(11):e1001720. https://doi.org/10.1371/journal.pbio.1001720.
61. Damerla CC R, Gabriel G, Liu X, Gibbs B, Francis R, Li Y, Chatterjee B, Srour M, Michaud JL, Pazour GJ, Lo CW. Mutation in the mouse homolog of C5ORF42 disrupts ciliogenesis and

causes cerebellar defects and other Joubert Syndrome phenotypes associated with the disruption of SHH signaling (3162W). Presented at the Joubert Syndrome Biennial Conference 2013; 2013.
62. Rochais F, Mesbah K, Kelly RG. Signaling pathways controlling second heart field development. Circ Res. 2009;104(8):933–42. https://doi.org/10.1161/CIRCRESAHA.109.194464.
63. Arthur HM, Bamforth SD. TGFbeta signaling and congenital heart disease: insights from mouse studies. Birth Defects Res A Clin Mol Teratol. 2011;91(6):423–34. https://doi.org/10.1002/bdra.20794.
64. Cohen ED, Tian Y, Morrisey EE. Wnt signaling: an essential regulator of cardiovascular differentiation, morphogenesis and progenitor self-renewal. Development. 2008;135(5):789–98. https://doi.org/10.1242/dev.016865.
65. Hildreth V, Webb S, Chaudhry B, Peat JD, Phillips HM, Brown N, et al. Left cardiac isomerism in the sonic hedgehog null mouse. J Anat. 2009;214(6):894–904. https://doi.org/10.1111/j.1469-7580.2009.01087.x.
66. Li AH, Hanchard NA, Azamian M, D'Alessandro LCA, Coban-Akdemir Z, Lopez KN, et al. Genetic architecture of laterality defects revealed by whole exome sequencing. Eur J Hum Genet. 2019;27(4):563–73. https://doi.org/10.1038/s41431-018-0307-z.
67. Jin SC, Homsy J, Zaidi S, Lu Q, Morton S, DePalma SR, et al. Contribution of rare inherited and de novo variants in 2,871 congenital heart disease probands. Nat Genet. 2017;49(11):1593–601. https://doi.org/10.1038/ng.3970.
68. Watkins WS, Hernandez EJ, Wesolowski S, Bisgrove BW, Sunderland RT, Lin E, et al. De novo and recessive forms of congenital heart disease have distinct genetic and phenotypic landscapes. Nat Commun. 2019;10(1):4722. https://doi.org/10.1038/s41467-019-12582-y.
69. Liu X, Yagi H, Saeed S, Bais AS, Gabriel GC, Chen Z, et al. The complex genetics of hypoplastic left heart syndrome. Nat Genet. 2017;49(7):1152–9. https://doi.org/10.1038/ng.3870.
70. Li Y, Yagi H, Onuoha EO, Damerla RR, Francis R, Furutani Y, et al. DNAH6 and its interactions with PCD genes in Heterotaxy and primary ciliary dyskinesia. PLoS Genet. 2016;12(2):e1005821. https://doi.org/10.1371/journal.pgen.1005821.

Development of the Cardiac Conduction System

10

Lieve E. van der Maarel and Vincent M. Christoffels

Abstract

The electrical impulses that coordinate the sequential, rhythmic contractions of the atria and ventricles are initiated and tightly regulated by the specialized tissues of the cardiac conduction system. In the mature heart, these impulses are generated by the pacemaker cardiomyocytes of the sinoatrial node, propagated through the atria to the atrioventricular node where they are delayed and then rapidly propagated to the atrioventricular bundle, right and left bundle branches, and finally, the peripheral ventricular conduction system. Each of these specialized components arise by complex patterning events during embryonic development. This chapter addresses the origins and transcriptional networks and signaling pathways that drive the development and maintain the function of the cardiac conduction system.

Keywords

Conduction system · Cardiac conduction system · Sinoatrial node · Atrioventricular node · Atrioventricular bundle · Bundle branches · Ventricular conduction system · Atrioventricular junction · Bundle of His · Purkinje Fiber · Pacemaker · Atrioventricular canal · peripheral ventricular conduction system · Sinus venosus

L. E. van der Maarel · V. M. Christoffels (✉)
Department of Medical Biology, Amsterdam University Medical Center, University of Amsterdam, Amsterdam, The Netherlands
e-mail: v.m.christoffels@amsterdamumc.nl

© The Author(s), under exclusive license to Springer Nature Switzerland AG 2024

S. Rickert-Sperling et al. (eds.), *Congenital Heart Diseases: The Broken Heart*,
Advances in Experimental Medicine and Biology 1441,
https://doi.org/10.1007/978-3-031-44087-8_10

10.1 Introduction

During the early stages of embryonic development, the heart begins to generate and propagate electrical impulses, coordinating the rhythmic contractions that distribute essential nutrients and oxygen throughout the body. These rhythmic contractions arise from the coordinated depolarization of electrically coupled atrial and ventricular cardiomyocytes. The activating electrical impulse is initiated and distributed through the heart by the specialized tissues of the cardiac conduction system (CCS) (Fig. 10.1). These specialized tissues can be further categorized into pacemaker-like components that generate and delay the impulse and components that rapidly propagate and distribute the impulse throughout the heart [1].

The sinoatrial node (SAN) is the primary pacemaker of the heart, situated in vertebrates at the junction of the systemic venous return and the right atrium. Here, the electrical impulse that initiates contraction is generated by specialized pacemaker cardiomyocytes. This impulse is rapidly spread across the atrial myocardium toward the atrioventricular (AV) node, where the impulse slows down, allowing for the contraction of the atria and filling of the ventricles. The impulse then enters the ventricular conduction system (VCS) via the AV bundle (bundle of His), the only electrical passage between the atria and ventricles. The impulse is dispersed deep into the ventricles, rapidly spreading across the ventricular septum via the left and right bundle branches (BBs), and through the Purkinje fiber network (PFN), resulting in synchronized ventricular working myocardial excitation–contraction and the expulsion of blood into the aorta and pulmonary artery.

Severe arrhythmias can arise from impaired CCS development or function, necessitating (invasive) surgical or therapeutic interventions. Currently, the only long-term intervention for the management of cardiac function in patients with bradycardia resulting from SAN dysfunction or AV block is the implantation of an electronic pacemaker. Electronic pacemakers are life-saving devices, but may malfunction, are insensitive to autonomic modulation, and are associated with inflammation and infection risks [2]. Biological pacemakers are a less invasive and promising alternative that may overcome these limitations. While great strides

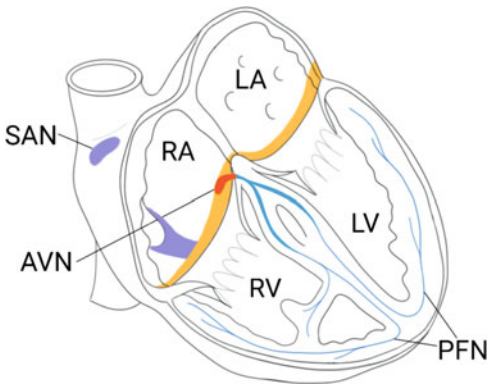

Fig. 10.1 The adult cardiac conduction system: the impulse is initiated in the sinoatrial node (SAN) and is propagated through the atria to the atrioventricular node (AVN), atrioventricular bundle, right and left bundle branches, and the Purkinje fiber network (PFN) that forms the peripheral ventricular conduction system. Adapted from [1]

have been made in our understanding of CCS composition and function, further interrogation of the molecular mechanisms governing CCS development and maintenance is essential for the realization of such therapeutic interventions [1].

10.2 CCS Development

The development of the CCS has been reviewed extensively [1, 3, 4]. Early in development, fusion of two bilateral regions in the cardiogenic mesoderm at the craniolateral side of the forming embryo leads to the formation of the cardiac crescent. Spontaneous, asynchronous calcium oscillations can already be observed at this stage, which are soon followed by the first contractions of the differentiating cardiomyocytes [5]. Subsequent fusion of the crescent at the midline, embryonic folding, and foregut elongation together guide the formation the primary heart tube.

The cardiomyocytes of the inflow tract (IFT) region of the primary heart tube spontaneously depolarize at the highest rate, forming a pacemaking center generating electrical impulses that are slowly conducted toward the outflow tract (OFT), giving rise to slow, peristaltic contractions (Fig. 10.2). The primary heart tube grows by addition of progenitor cells originating from the second heart field (SHF) at both poles [6, 7]. The cells of the first heart field contribute to the definitive left ventricle (LV) and atrioventricular canal (AVC), while SHF-derived cells added to the venous pole will form the sinus venosus (SV), and those added to the arterial pole will form the right ventricle (RV) and outflow tract (OFT) [8–10]. The definitive SAN will form within the SV myocardium, while the definitive AVN, AV rings, and part of the LV develop from embryonic AVC myocardium. Cells at the arterial pole of the early heart tube will form the interventricular ring, which includes the interventricular septum with the AVB at its crest and the proximal BBs [11, 12]. PFN progenitors are located in the ventricular trabecular myocardium [13] (Fig. 10.2).

While the elongating heart tube initially does not proliferate, specific regions initiate rapid proliferation during looping morphogenesis and activate the chamber myocardial gene program associated with rapid conduction and high contractility. Key markers of the chamber myocardium include gap junction subunits CX40 and CX43 (encoded by *Gja5* and *Gja1*), natriuretic peptide A (*Nppa*), SERCA2A (*Atp2a2*), and the sodium channel Nav1.5 (*Scn5a*) [1, 14]. The rapid expansion of these myocardial regions forms the working myocardial atria and ventricles. Conversely, the working myocardial gene program is repressed in adjacent areas, including the developing SV, the AVC, and the inner curvature of the heart. These "nodal" regions will retain their low proliferation rates as well as their automaticity and slow conduction properties.

The dominant pacemaker activity at the inflow tract (IFT) (or SV once it has been formed) together with the fast-conducting atria and ventricles separated by a slow-conducting AVC ensures a unidirectional activation pattern (SV, atria, AVC, ventricle, and OFT) with an AV delay. This basic activation pattern, established by approximately embryonic day (E) 9.5 in mouse and Hamburger Hamilton

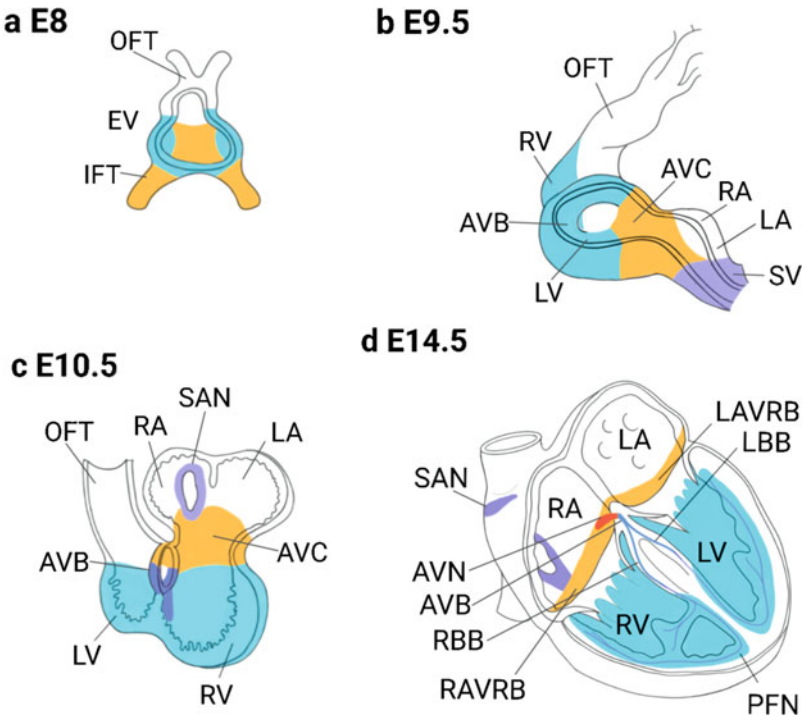

Fig. 10.2 Cardiac conduction system development in endothermic vertebrates. (**a**) Nascent contractions begin around embryonic day (E) 8 in the murine primary heart tube. OFT, outflow tract; EV, embryonic ventricle; IFT, inflow tract. (**b**) By E9.5, the working myocardium undergoes rapid expansion, forming the atria and ventricles (blue) and the primary heart tube elongates by the addition of second heart field progenitors. (**c**) At E10.5, the sinoatrial node (SAN) forms in the sinus venosus (SV, purple) and the outer curvatures of the working myocardium continue to expand, giving rise to the left atrium (LA), right atrium (RA), left ventricle (LV), and the right ventricle (RV). The atrioventricular bundle (AVB) forms at the crest of the interventricular septum. (**d**) At E14.5, the Purkinje fiber network (PFN) arises from the ventricular trabecular myocardium. At this stage, the right bundle branch (RBB) and left bundle branch (LBB) (blue) arise from septal trabeculae. Adapted from [1]

(HH) stage 13 in the chick, closely resembles that of the mature heart long before the definitive components of the CCS are morphologically distinguishable [14, 15].

10.3 Development of the Sinus Venosus and Sinoatrial Node

The adult mammalian heart contains approximately 10 billion cells, of which <10,000 are cardiac pacemaker cells that reside in the SAN and autonomously generate the impulse [16]. Macroscopically, in developing mammals, the SAN has an elongated structure consisting of two domains: the "head," wrapped around the superior caval vein and the "tail," extending into the atrium along the venous valve

[17]. At the cellular level, the SAN has a highly complex and heterogeneous structure consisting of different subsets of pacemaker cells, fibroblasts, endothelial cells, and connective tissue and is extensively innervated by autonomic nerves. Transcriptome analyses of the developing and adult SAN illustrate this heterogeneity, revealing distinct clusters of SAN cells alongside a core pacemaker gene program [18–22].

In mice, the first spontaneous calcium oscillations are seen in the cardiac crescent by E7.75, initiating the first contractions by E8 [5]. However, these early centers of automaticity do not represent the progenitors of the SAN. Instead, as the primary heart tube elongates by the addition of SHF-derived cells, the dominant pacemaker activity will shift into these newly added cells at the caudal pole [23, 24] coinciding with a caudal shift in *Hcn4* expression [25–27]. The actual SAN progenitors are present in the HH8 chicken lateral plate mesoderm caudal of the region that has initiated the cardiogenic program at this stage (cardiac crescent) [28], indicating that they will differentiate and be recruited to the heart tube at a later developmental stage. Once formed, the *Hcn4*$^{+}$ horns of the SV will become the main functional pacemaking centers. Developing within the SV, the SAN will become the dominant functional pacemaking center of the >HH28 chicken heart and the E12.5 mouse heart [18, 29, 30], while the SV acquires an atrial gene program [31].

In the mouse, the SV and SAN progenitors can be recognized as a *Tbx18*$^{+}$, *Isl1*$^{+}$, and *Nkx2-5*$^{-}$ SHF population caudal of the forming heart tube [32]. These progenitors form the SV, including the SAN anlage, at E9-E9.5 of mouse development [17, 31]. Once *Tbx3* expression has been initiated, the SAN progenitors (*Tbx3*$^{+}$) can be distinguished within the SV [11, 31]. Indeed, genetic lineage analyses have revealed that distinct gene expression boundaries divide the SAN and the bordering atrial domain from the onset of SAN development (Fig. 10.2, Fig. 10.3).

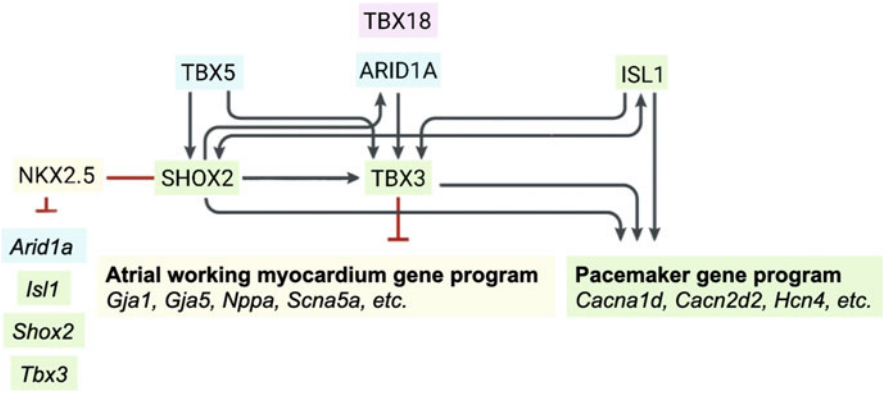

Fig. 10.3 Pacemaker gene program vs. atrial working myocardium gene program. Distinct gene expression boundaries define the sinoatrial node and the adjacent atrial working myocardium. Transcription factors SHOX2, TBX3, and ISL1 drive the pacemaker gene program in the TBX18-dependent sinus venosus myocardium, while NKX2-5 drives the atrial working myocardium gene program. Adapted from [1]

Atrial *Nppa*$^{+}$ descendants do not enter the SAN domain [33], while SAN *Shox2*$^{+}$, *Tbx3*$^{+}$, and *Tbx18*$^{+}$ descendants do not enter the atrial domain [11, 17, 34]. However, during late embryonic development and early fetal development, a subpopulation of transitional pacemaker cells surrounding the core SAN domain and bordering the atrial myocardium (including the tail domain that descends along the venous valve) will initiate *Nkx2-5* expression. These cells are a phenotypic intermediate between atrial and SAN cardiomyocytes and are essential for SAN function [22, 35]. *Nkx2-5* depletion in the developing heart extends the SV/SAN gene program into the atrial domain [31], while ectopic *Nkx2-5* expression in the SAN domain results in atrialization of the SAN domain [36].

10.4 Transcriptional Regulatory Network of the Sinoatrial Node

Both murine and human SAN regions are enriched for transcription factors SHOX2, ISL1, TBX3, TBX18, HOXA family members, and for BMP and Notch effectors as well as for calcium-binding proteins (SMOC2, VSNL1), genes associated with neuronal development, and ECM organization [18, 19, 21, 22]. The transcription factors SHOX2, ISL1, and TBX3 are key drivers of the pacemaker gene program. SV-restricted SHOX2 expression regulates the pacemaker gene program via the activation of *Isl1* and repression of *Nkx2-5*, maintaining SAN fate and preventing the atrialization of the SAN [36–39]. Initially expressed by all cardiac progenitors until their cardiac differentiation, ISLl1 expression becomes restricted to the SAN where it is maintained into adulthood [40]. In the SAN, ISL1 directly regulates genes required for normal SAN development and function, including *Hcn4*, *Shox2*, and *Tbx3* [41]. TBX3, too, is expressed in the developing and adult SAN where it maintains the pacemaker gene program and represses that of the working myocardium [33, 42]. Ectopic atrial TBX3 expression imposes the pacemaker program on atrial myocytes, inducing the formation of ectopic functional pacemakers [33, 43]. GATA6 has been recently identified as a key regulator of SAN development, promoting pacemaker identity by activating *Tbx3*, *Tbx5,* and *Tbx18* expression in the developing SAN, with its loss resulting in SAN hypoplasia and upregulation of atrial working myocardial genes like *Nkx2-5* and *Nppa* [44]. The transcription factor PITX2, expressed in the left side of asymmetric organs such as the heart, imposes left-specific organogenesis. *Pitx2c*-deficient mouse embryos develop right-sided isomerism of the atria and SV, with SANs forming in the right and left atria [31]. Mechanistically, PITX2c suppresses *Shox2* and *Tbx3* expression, restricting the SAN anlage to the right SV [45, 46].

The cis-regulatory architecture of the SAN has only recently begun to be revealed. Van Eif et al. and Galang et al. have identified and functionally validated the role of several pacemaker cell-specific regulatory elements of the *Shox2*, *Isl1*, and *Tbx3* loci in transgenic mice and zebrafish [47, 48].

Cell signaling pathways further coordinate the gene regulatory changes that drive SAN development. Pacemaker cell progenitors in the cardiac mesoderm respond to Wnt5b, inducing the pacemaker phenotype by activating *Isl1* and *Tbx18*, and repressing *Nkx2-5* [49]. Conversely, perturbation of Wnt/β-catenin signaling in

these progenitors changes their fate to that of the NKX2-5^{+} atrial cardiomyocyte lineage. Endocardial Notch1 signaling has been found to regulate SAN development via myocardial Wnt and Nrg1 signaling, with loss of NOTCH1 resulting in a marked reduction in *Hcn4* expression, indicating underdevelopment of the SAN, alongside reduced *Tbx3* and *Tbx5* expression [50]. Furthermore, ISL1-regulated spatially restricted Wnt/β-catenin signaling activity controls heart rate by regulating pacemaker cell response to parasympathetic stimuli in zebrafish [51]. RHOA-Rock signaling has been implicated in the restriction of the pacemaker gene program in the SV to the right [30]. Hedgehog (Hh) signaling controls pacemaker progenitor cell commitment, regulating the expression of *Isl1*, *Shox2*, *Tbx3*, *Hcn4*, but not *Tbx18* in the developing heart, with loss of smoothened impairing the differentiation potential of the SHF due to the downregulation of *Tbx5* [52].

10.5 Development of the Atrioventricular Canal

The AVC, taking shape at the center of the developing heart as the ventricular and atrial chambers begin to expand, is highly conserved across vertebrate species from fish to mammals [53]. Its formation involves localized repression of the chamber myocardial gene program. The AVC is the first CCS precursor component to develop and, in mammals and birds, will give rise to the base of the LV and the AV junction, including the AV ring bundles (AVRBs) and the AV node [9, 54, 55]. The AVC is the principal slow-conducting electrical connection between the atria and ventricles, ensuring delayed propagation of the impulse to the ventricles. In mammals and birds, the annulus fibrosus forms during fetal development and electrically separates the atria and ventricles. Dorsally, at the level of the AV node in the AVC, this separation does not occur, maintaining the only electrical connection between the atria and ventricles.

In the adult heart, the AV node confers a critical conduction delay that not only mediates the sequential contraction of the atria and ventricles but also prevents the transmission of atrial tachyarrhythmias through to the VCS [56]. Unlike the atrial and ventricular working myocardium that initiates expression of *Gja5* (CX40), *Gja1* (CX43), *Scna5a* (Nav1.5), and *Nppa* (ANF), cells of the AVJ myocardium retain their primitive slow conducting phenotype [57], expressing slow conductance gap junctions CX45 and CX30.2 [58, 59]. As the AV node shares pacemaker properties with the SAN, it can act as a secondary pacemaker, activating the ventricles upon SAN failure.

10.6 Gene Regulatory Mechanisms for AVC Development and Function

AVC development is orchestrated by a network of core cardiac transcription factors, including NKX2-5, TBX5, GATA4, and GATA6, and localized transcription factors including TBX2 and TBX3. In the AVC, bone morphogenetic proteins (BMP2 in

mammals and birds) activate *Tbx3* and its functional homolog and paralog, *Tbx2*. Together, these transcription factors suppress the working myocardial gene program and activate the nodal gene program in a dose-dependent manner [42, 43, 60–65]. Loss of expression of *Tbx2* from the myocardium causes failure to maintain the slow conducting property of the AVC, resulting in ventricular pre-excitation [66]. BMP2, TBX2, and TBX3 also induce AV cushion formation, contributing to the development of the valves and AV insulation [62, 63]. A recent genome-wide search for TBX3-dependent AV regulatory DNA elements emphasizes the significance of TBX3-dependent regulatory networks in the AV conduction system and indicates how these networks contribute to healthy heart electrophysiology [65].

The core cardiac transcription factor network drives the development and homeostasis of the AV conduction system. *Tbx5* haplo insufficient mice present with a fetal-like AVC [67]. This may indicate that a disturbance of the balance between the chamber myocardial gene activating factor TBX5 and nodal gene activator TBX3 disrupts AVC homeostasis. Furthermore, heterozygous loss of NKX2-5 causes AV block in mouse and human [68, 69], while the heterozygous loss of *Gata4* accelerates atrioventricular conduction by diminishing CX30.2 expression [70] and *Gata6*$^{-/-}$ mice feature slower atrioventricular conduction [71]. Furthermore, GATA4 and GATA6 can bind AVC-specific enhancers and, in combination with nuclear SMADs downstream of BMP signaling, recruit histone acetyltransferases, activating the AVC gene program. In the working myocardium of the chambers, however, GATA4 and GATA6, in combination with HEY1 or HEY2, recruit histone deacetylases, thus suppressing AVC-specific genes in chamber myocardium [72].

Notch and Wnt/β-catenin signaling, together, control the structural and electrical properties of the AVJ myocardium upstream of *Tbx2* and *Tbx3*. The demarcation of the boundary between AVC chamber myocardium and atrial/ventricular myocardium is, at least in part, governed by TBX20 and Notch signaling. TBX20 confines TBX2 expression to the AVC by interfering with Bmp/Smad signaling in the chambers [73]. In chamber myocardium, Notch signaling activates HEY1 and HEY2, inhibiting *Bmp2* and *Tbx2* expression, while, in the AVC, TBX2 represses *Hey1* and *Hey2*, further delimiting the AVC [74–76]. During later stages of AVC maturation, the absence of Notch signaling impedes AVN development, characterized by a selective loss of slow-conducting CX30.2^{+} cells, and causes a loss of the AV conduction delay [77]. Wnt/β-catenin signaling within the AVJ also regulates the maturation of the AVC and maintains the AVC myocardial phenotype [78]. Ectopic Wnt/β-catenin signaling in the ventricular myocardium imposes an AVJ-like phenotype alongside elevated *Tbx3* expression, while *Bmp2* and *Tbx2* expression are unaffected. Ectopic Notch activation in the AVJ reprograms the AVJ myocardium toward chamber-like myocardium and downregulates Wnt/β-catenin signaling in the AVJ [78]. Within the AVJ, Wnt/β-catenin signaling regulates AVC maturation, driving AV cushion formation, proper patterning of the developing myocardium, and the establishment of AV electrophysiological properties [78–80].

10.7 Development of the Ventricular Conduction System

The VCS, including CCS components distal to the AVN (AVB, left and right BBS, and the PFN), only represents ~1–2% of the total ventricular mass [13]. Yet, its fast and near-simultaneous depolarization, mediated by sodium channels (Nav1.5) and fast-conducting gap junctions composed of subunits CX40 and CX43, orchestrates the coordinated contraction of the ventricles.

At approximately E10.5 of mouse development, epicardial breakthrough of the impulse is seen at the apex [81], consistent with the notion that the impulse is propagated by the relatively fast-conducting $CX40^+$ and $Nav1.5^+$ trabecular myocardium [53]. While the definitive AVN arises from the $Tbx2^+$ AVC, the AVB and the BB arise from $Mef2c\text{-}enhancer\text{-}Cre^+$ progenitors, suggesting that VCS precursors segregate early in development [9]. The interventricular ring that includes the future AVB and proximal BB derives from $Tbx3^+$ cells at the arterial pole of the E8 heart tube. This population moves into the heart, while the right ventricle and definitive OFT are recruited from the SHF at the arterial pole [11]. The crest of the ventricular septal segment of the $G1N2^+/TBX3^+$ primary interventricular ring gives rise to the AVB, while $G1N2^+Tbx3^+$ subendocardial trabeculae that develop in the ventricular septum give rise to the BBs [82, 83]. By E12.5, two distinct ventricular activation patterns appear in mice, indicating the development of discrete left and right BBs [81]. The trabecular myocardium serves as the fast-conducting network in the vertebrate embryonic ventricles, harboring the precursors of the PFN that forms in mammals and birds (ectothermic vertebrates maintain trabecular ventricles) [53]. The precursors of the PFN are also committed to the PFN fate as early as the onset of heart tube formation (E7.5 in mice) [84]. The VCS will further continue its functional maturation postnatally [85, 86].

10.8 Transcriptional Regulatory Network of the Ventricular Conduction System

The development of the VCS is driven by the expression of cardiac transcription factors including *Nkx2-5*, *Tbx2*, *Tbx3*, *Tbx5*, *Id2*, *Etv1*, and *Irx3*. Together, these drive the fast-conduction gene program of the VCS [87–91]. The severe VCS dysfunction caused by loss of *Tbx5* expression in the mature murine VCS is characterized by a loss of fast conduction and arrhythmias, culminating in sudden death [92]. The expression of key mediators of the fast conduction gene program of the VCS including *Scn5a* and *Gja5* is dependent on TBX5 [92]. TBX5 and NKX2-5, together with ID2, form an important transcriptional network that drives the differentiation of ventricular cardiomyocytes into specialized VCS cells [87]. Maximal NKX2-5 expression is essential during the late fetal stages of PFN development when newly committed PF cells are rapidly added to the early scaffold via a non-cell autonomous mechanism [84]. The balance between *Tbx5* and *Tbx3* expression drives the regional specialization of the developing VCS. TBX3 is an early marker of the AVB and BB, preventing the differentiation of AVB and BB precursors into

working ventricular myocardium [88]. TBX3 represses the fast conduction gene program of the working myocardium and competes with TBX5 to interact with NKX2-5 and the regulatory elements of shared target genes [65, 93]. Indeed, while the AVB features a high TBX5:TBX3 expression ratio, the AVN possesses a low TBX5:TBX3 expression ratio. Changing the relative expression of these transcription factors in favor of TBX3 activates the nodal gene program and transforms the AVB into a slow, nodal-like conduction network [64]. IRX3 induces the fast conduction gene program, possibly through interaction with TBX5 and NKX2-5, to regulate the expression of VCS-enriched genes including *Gja5* [86, 90]. The spatiotemporal regulation of gene regulatory networks in the developing VCS gives rise to the morphological asymmetry of the mature VCS [94]. bHLH transcription factor HAND1 expression is restricted to the LV where it suppresses the differentiation of progenitors towards the conduction lineage and may regulate the electrical continuity and intrinsic electrophysiological properties of conduction cells [95]. Interestingly, a genetic variant in the *Hand1* locus associated with VCS function in humans colocalizes with a GATA-dependent LV-specific *Hand1* enhancer, and the deletion of the orthologue of this enhancer in the mouse genome results in a RBB block-like phenotype [96].

Notch activation in the ventricles transforms chamber cardiac progenitors into specialized, Purkinje-like conduction cells with increased *Tbx5*, *Nkx2-5*, and *Scn5a* expression [97]. Indeed, juxtacrine signaling between cardiac fibroblasts and ventricular cardiomyocytes, triggered by Notch signaling, activates the fast conduction gene program, transforming ventricular cardiomyocytes into VCS-like cells [98]. Notch signaling also influences ventricular trabecular development by modulating downstream regulators like BMP10 and Neuregulin 1 (NRG1). Endocardial Notch signaling modulates proliferation in the trabecular myocardium via BMP10 activation [99]. Abrogation of BMP10 expression by E9.5 also rapidly reduces *Nkx2-5* and *Mef2c* expression in the ventricles resulting in severely impaired cardiac function [100]. The *Nrg1-ErbB1/4-Erk1/2* signaling axis maintains the gene regulatory network of ventricular myocardium, and variable *Nrg1* expression levels are thought to account for the graded differentiation across the ventricular wall [101]. NRG1 signaling, activated by Notch signaling, induces and activates the fast conduction gene program by upregulating *Nkx2-5*, *Gja5*, *Scn5a*, and *Irx3* expression [89]. The NRG1-responsive transcription factor Etv1highly expressed in the atrial myocardium and VCS cardiomyocytes regulates the fast conduction gene program (*Nkx2-5*, *Gja5,* and *Scn5a*) [89].

10.9 Conclusion

Recent developments in our understanding of key transcriptional networks, the origin, and the composition of the CCS are currently laying the groundwork for a better understanding of the molecular mechanisms that govern CCS development and function. It is clear that functionally robust gene regulatory networks ensure that a relatively small population of cells can faithfully initiate and coordinate the

heartbeat throughout life. Common genetic variants associated with conduction velocity or arrhythmia are found in non-coding genomic regions close to genes important for CCS development and function, such as *TBX3, TBX5*, *HAND1, NKX2-5, SCN5A,* and *SCN10A* [102–105]. These variants likely influence the activity of regulatory elements controlling the expression of these genes, thus influencing the gene regulatory network and potentially contributing to disease susceptibility. Indeed, functional links have been found between variants located up to one million base pairs away from *TBX3*, *TBX3* expression and CCS function, illustrating yet another layer of complexity [46, 106]. Together, our growing understanding of CCS development is paving the way to new therapeutic interventions, CCS disease models, and drug testing.

References

1. van Eif VWW, Devalla HD, Boink GJJ, Christoffels VM. Transcriptional regulation of the cardiac conduction system. Nat Rev Cardiol. 2018;15(7):1–14.
2. Cingolani E, Goldhaber JI, Marban E. Next-generation pacemakers: from small devices to biological pacemakers. Nat Rev Cardiol. 2018;15(3):139–50.
3. Park DS, Fishman GI. Development and Function of the Cardiac Conduction System in Health and Disease. J Cardiovasc Dev Dis. 2017;4(2).
4. Bhattacharyya S, Munshi NV. Development of the Cardiac Conduction System. Cold Spring Harbor perspectives in biology. 2020.
5. Tyser RC, Miranda AM, Chen CM, Davidson SM, Srinivas S, Riley PR. Calcium handling precedes cardiac differentiation to initiate the first heartbeat. elife. 2016;5:e17113.
6. van den Berg G, Abu-Issa R, de Boer BA, Hutson MR, de Boer PA, Soufan AT, et al. A caudal proliferating growth center contributes to both poles of the forming heart tube. CircRes. 2009;104(2):179–88.
7. Meilhac SM, Buckingham ME. The deployment of cell lineages that form the mammalian heart. Nat Rev Cardiol. 2018;15(11):705–24.
8. Miquerol L, Bellon A, Moreno N, Beyer S, Meilhac SM, Buckingham M, et al. Resolving cell lineage contributions to the ventricular conduction system with a Cx40-GFP allele: a dual contribution of the first and second heart fields. Dev Dyn. 2013;242(6):665–77.
9. Aanhaanen WT, Brons JF, Dominguez JN, Rana MS, Norden J, Airik R, et al. The Tbx2+ primary myocardium of the atrioventricular canal forms the atrioventricular node and the base of the left ventricle. CircRes. 2009;104(11):1267.
10. Kelly RG, Buckingham ME, Moorman AF. Heart fields and cardiac morphogenesis. Cold Spring Harb Perspect Med. 2014;4(10):1–11.
11. Mohan RA, Mommersteeg MTM, Dominguez JN, Choquet C, Wakker V, de Gier-de Vries C, et al. Embryonic Tbx3+ cardiomyocytes form the mature cardiac conduction system by progressive fate restriction. Development. 2018;145:1–12.
12. Moorman AF, Christoffels VM. Development of the cardiac conduction system: a matter of chamber development. NovartisFoundSymp. 2003;250:25–34.
13. Miquerol L, Moreno-Rascon N, Beyer S, Dupays L, Meilhac SM, Buckingham ME, et al. Biphasic development of the mammalian ventricular conduction system. Circ Res. 2010;107 (1):153–61.
14. Moorman AFM, Christoffels VM. Cardiac chamber formation: development, genes and evolution. PhysiolRev. 2003;83(4):1223–67.
15. Van Mierop LH, Bertuch CJ Jr. Development of arterial blood pressure in the chick embryo. Am J Phys. 1967;212(1):43–8.

16. Bleeker WK, Mackaay AJC, Masson-Pevet M, Bouman LN, Becker AE. Functional and morphological organization of the rabbit sinus node. CircRes. 1980;46(1):11–22.
17. Wiese C, Grieskamp T, Airik R, Mommersteeg MT, Gardiwal A, de Gier-de VC, et al. Formation of the sinus node head and differentiation of sinus node myocardium are independently regulated by tbx18 and tbx3. CircRes. 2009;104(3):388–97.
18. van Eif VWW, Stefanovic S, van Duijvenboden K, Bakker M, Wakker V, de Gier-de VC, et al. Transcriptome analysis of mouse and human sinoatrial node cells reveals a conserved genetic program. Development. 2019;146(8):1–15.
19. Liang D, Xue J, Geng L, Zhou L, Lv B, Zeng Q, et al. Cellular and molecular landscape of mammalian sinoatrial node revealed by single-cell RNA sequencing. Nat Commun. 2021;12 (1):287.
20. Linscheid N, Logantha S, Poulsen PC, Zhang S, Schrolkamp M, Egerod KL, et al. Quantitative proteomics and single-nucleus transcriptomics of the sinus node elucidates the foundation of cardiac pacemaking. Nat Commun. 2019;10(1):2889.
21. Vedantham V, Galang G, Evangelista M, Deo RC, Srivastava D. RNA sequencing of mouse sinoatrial node reveals an upstream regulatory role for Islet-1 in cardiac pacemaker cells. Circ Res. 2015;116(5):797–803.
22. Goodyer WR, Beyersdorf BM, Paik DT, Tian L, Li G, Buikema JW, et al. Transcriptomic profiling of the developing cardiac conduction system at single-cell resolution. Circ Res. 2019;125(4):379–97.
23. van Mierop LHS. Localization of pacemaker in chick embryo heart at the time of initiation of heartbeat. Am J Physiol. 1967;212:407–15.
24. Christoffels VM, Smits GJ, Kispert A, Moorman AF. Development of the pacemaker tissues of the heart. Circ Res. 2010;106(2):240–54.
25. Stieber J, Herrmann S, Feil S, Loster J, Feil R, Biel M, et al. The hyperpolarization-activated channel HCN4 is required for the generation of pacemaker action potentials in the embryonic heart. Proc Natl Acad Sci USA. 2003;100(25):15235–40.
26. Garcia-Frigola C, Shi Y, Evans SM. Expression of the hyperpolarization-activated cyclic nucleotide-gated cation channel HCN4 during mouse heart development. Gene Expr Patterns. 2003;3(6):777–83.
27. Liang X, Wang G, Lin L, Lowe J, Zhang Q, Bu L, et al. HCN4 dynamically marks the first heart field and conduction system precursors. Circ Res. 2013;113(4):399–407.
28. Bressan M, Liu G, Mikawa T. Early mesodermal cues assign avian cardiac pacemaker fate potential in a tertiary heart field. Science. 2013;340(6133):744–8.
29. Yi T, Wong J, Feller E, Sink S, Taghli-Lamallem O, Wen J, et al. Electrophysiological mapping of embryonic mouse hearts: mechanisms for developmental pacemaker switch and internodal conduction pathway. J Cardiovasc Electrophysiol. 2012;23(3):309–18.
30. Vicente-Steijn R, Kelder TP, Tertoolen LG, Wisse LJ, Pijnappels DA, Poelmann RE, et al. RHOA-ROCK signalling is necessary for lateralization and differentiation of the developing sinoatrial node. Cardiovasc Res. 2017;113(10):1186–97.
31. Mommersteeg MT, Hoogaars WM, Prall OW, de Gier-de VC, Wiese C, Clout DE, et al. Molecular pathway for the localized formation of the sinoatrial node. Circ Res. 2007;100(3): 354–62.
32. Mommersteeg MT, Dominguez JN, Wiese C, Norden J, de Gier-de VC, Burch JB, et al. The sinus venosus progenitors separate and diversify from the first and second heart fields early in development. Cardiovasc Res. 2010;87(1):92–101.
33. Hoogaars WM, Engel A, Brons JF, Verkerk AO, de Lange FJ, Wong LY, et al. Tbx3 controls the sinoatrial node gene program and imposes pacemaker function on the atria. Genes Dev. 2007;21(9):1098–112.
34. Sun C, Zhang T, Liu C, Gu S, Chen Y. Generation of Shox2-Cre allele for tissue specific manipulation of genes in the developing heart, palate, and limb. Genesis. 2013;51(7):515–22.

35. Li H, Li D, Wang Y, Huang Z, Xu J, Yang T, et al. Nkx2-5 defines a subpopulation of pacemaker cells and is essential for the physiological function of the sinoatrial node in mice. Development. 2019;146(14):dev178145.
36. Espinoza-Lewis RA, Liu H, Sun C, Chen C, Jiao K, Chen Y. Ectopic expression of Nkx2.5 suppresses the formation of the sinoatrial node in mice. Dev Biol. 2011;356(2):359–69.
37. Hoffmann S, Berger IM, Glaser A, Bacon C, Li L, Gretz N, et al. Islet1 is a direct transcriptional target of the homeodomain transcription factor Shox2 and rescues the Shox2-mediated bradycardia. Basic Res Cardiol. 2013;108(2):339.
38. Espinoza-Lewis RA, Yu L, He F, Liu H, Tang R, Shi J, et al. Shox2 is essential for the differentiation of cardiac pacemaker cells by repressing Nkx2-5. Dev Biol. 2009;327(2):378–85.
39. Ye W, Wang J, Song Y, Yu D, Sun C, Liu C, et al. A common Shox2-Nkx2-5 antagonistic mechanism primes the pacemaker cell fate in the pulmonary vein myocardium and sinoatrial node. Development. 2015;142(14):2521–32.
40. Sun Y, Liang X, Najafi N, Cass M, Lin L, Cai CL, et al. Islet 1 is expressed in distinct cardiovascular lineages, including pacemaker and coronary vascular cells. Dev Biol. 2007;304(1):286–96.
41. Liang X, Zhang Q, Cattaneo P, Zhuang S, Gong X, Spann NJ, et al. Transcription factor ISL1 is essential for pacemaker development and function. J Clin Investig. 2015;125(8):3256–68.
42. Frank DU, Carter KL, Thomas KR, Burr RM, Bakker ML, Coetzee WA, et al. Lethal arrhythmias in Tbx3-deficient mice reveal extreme dosage sensitivity of cardiac conduction system function and homeostasis. Proc Natl Acad Sci U S A. 2011;109(3):E154–E63.
43. Bakker ML, Boink GJ, Boukens BJ, Verkerk AO, van den Boogaard M, den Haan AD, et al. T-box transcription factor TBX3 reprograms mature cardiac myocytes into pacemaker-like cells. Cardiovasc Res. 2012;94(13):439–49.
44. Gharibeh L, Yamak A, Whitcomb J, Lu AZ, Joyal M, Komati H, et al. GATA6 is a regulator of sinus node development and heart rhythm. Proc Natl Acad Sci U S A. 2021;118(1):e2007322118.
45. Wang J, Klysik E, Sood S, Johnson RL, Wehrens XH, Martin JF. Pitx2 prevents susceptibility to atrial arrhythmias by inhibiting left-sided pacemaker specification. Proc Natl Acad Sci U S A. 2010;107(21):9753–8.
46. Wang J, Bai Y, Li N, Ye W, Zhang M, Greene SB, et al. Pitx2-microRNA pathway that delimits sinoatrial node development and inhibits predisposition to atrial fibrillation. Proc Natl Acad Sci U S A. 2014;111(25):9181–6.
47. van Eif VWW, Protze SI, Bosada FM, Yuan XF, Sinha T, van Duijvenboden K, et al. Genome-wide analysis identifies an essential human TBX3 pacemaker enhancer. Circ Res. 2020;127(12):1522–35.
48. Galang G, Mandla R, Ruan HM, Jung C, Sinha T, Stone NR, et al. ATAC-Seq reveals an Isl1 enhancer that regulates sinoatrial node development and function. Circ Res. 2020;127(12):1502–18.
49. Ren J, Han P, Ma X, Farah EN, Bloomekatz J, Zeng XI, et al. Canonical Wnt5b signaling directs outlying Nkx2.5+ mesoderm into pacemaker Cardiomyocytes. Dev Cell. 2019;50(6):729–43 e5.
50. Wang YD, Lu PF, Jiang LP, Wu BR, Zhou B. Control of sinus venous valve and sinoatrial node development by endocardial NOTCH1. Cardiovasc Res. 2020;116(8):1473–86.
51. Burkhard SB, Bakkers J. Spatially resolved RNA-sequencing of the embryonic heart identifies a role for Wnt/beta-catenin signaling in autonomic control of heart rate. elife. 2018;7:e31515.
52. Zhang C, Li Y, Cao J, Yu B, Zhang K, Li K, et al. Hedgehog signalling controls sinoatrial node development and atrioventricular cushion formation. Open Biol. 2021;11(6):210020.
53. Jensen B, Boukens BJ, Postma AV, Gunst QD, van den Hoff MJ, Moorman AF, et al. Identifying the evolutionary building blocks of the cardiac conduction system. PLoS One. 2012;7(9):e44231.

54. Mohan RA, Boukens BJ, Christoffels VM. Developmental origin of the cardiac conduction system: insight from lineage tracing. Pediatr Cardiol. 2018;39(6):1107–14.
55. De la Cruz MV, Markwald RR. In: Markwald RR, editor. Living morphogenesis of the heart, vol. 1. Basel: Birkhäuser; 1998 1998.
56. Dobrzynski H, Nikolski VP, Sambelashvili AT, Greener ID, Yamamoto M, Boyett MR, et al. Site of origin and molecular substrate of atrioventricular junctional rhythm in the rabbit heart. Circ Res. 2003;93(11):1102–10.
57. de Jong F, Opthof T, Wilde AA, Janse MJ, Charles R, Lamers WH, et al. Persisting zones of slow impulse conduction in developing chicken hearts. Circ Res. 1992;71(2):240–50.
58. Coppen SR, Gourdie RG, Severs NJ. Connexin45 is the first connexin to be expressed in the central conduction system of the mouse heart. Exp Clin Cardiol. 2001;6:17–23.
59. Kreuzberg MM, Willecke K, Bukauskas FF. Connexin-mediated cardiac impulse propagation: connexin 30.2 slows atrioventricular conduction in mouse heart. Trends Cardiovasc Med. 2006;16(8):266–72.
60. Habets PEMH, Moorman AFM, Clout DEW, van Roon MA, Lingbeek M, Lohuizen M, et al. Cooperative action of Tbx2 and Nkx2.5 inhibits ANF expression in the atrioventricular canal: implications for cardiac chamber formation. Genes Dev. 2002;16(10):1234–46.
61. Harrelson Z, Kelly RG, Goldin SN, Gibson-Brown JJ, Bollag RJ, Silver LM, et al. Tbx2 is essential for patterning the atrioventricular canal and for morphogenesis of the outflow tract during heart development. Development. 2004;131(20):5041–52.
62. Ma L, Lu MF, Schwartz RJ, Martin JF. Bmp2 is essential for cardiac cushion epithelial-mesenchymal transition and myocardial patterning. Development. 2005;132(24):5601–11.
63. Singh R, Hoogaars WM, Barnett P, Grieskamp T, Rana MS, Buermans H, et al. Tbx2 and Tbx3 induce atrioventricular myocardial development and endocardial cushion formation. Cell Mol Life Sci. 2012;69(8):1377–89.
64. Burnicka-Turek O, Broman MT, Steimle JD, Boukens BJ, Petrenko NB, Ikegami K, et al. Transcriptional patterning of the ventricular cardiac conduction system. Circ Res. 2020;127 (3):E94–E106.
65. Mohan RA, Bosada FM, van Weerd JH, van Duijvenboden K, Wang J, Mommersteeg MTM, et al. T-box transcription factor 3 governs a transcriptional program for the function of the mouse atrioventricular conduction system. Proc Natl Acad Sci U S A. 2020;117(31): 18617–26.
66. Aanhaanen WT, Boukens BJ, Sizarov A, Wakker V, de Gier-de VC, van Ginneken AC, et al. Defective Tbx2-dependent patterning of the atrioventricular canal myocardium causes accessory pathway formation in mice. J Clin Invest. 2011;121(2):534–44.
67. Moskowitz IPG, Pizard A, Patel VV, Bruneau BG, Kim JB, Kupershmidt S, et al. The T-box transcription factor Tbx5 is required for the patterning and maturation of the murine cardiac conduction system. Development. 2004;131(16):4107–16.
68. Schott J-J, Benson DW, Basson CT, Pease W, Silberbach GM, Moak JP, et al. Congenital heart disease caused by mutations in the transcription factor NKX2-5. Science. 1998;281 (5373):108–11.
69. Jay PY, Harris BS, Maguire CT, Buerger A, Wakimoto H, Tanaka M, et al. Nkx2-5 mutation causes anatomic hypoplasia of the cardiac conduction system. J Clin Invest. 2004;113(8): 1130–7.
70. Munshi NV, McAnally J, Bezprozvannaya S, Berry JM, Richardson JA, Hill JA, et al. Cx30.2 enhancer analysis identifies Gata4 as a novel regulator of atrioventricular delay. Development. 2009;136(15):2665–74.
71. Liu F, Lu MM, Patel NN, Schillinger KJ, Wang T, Patel VV. GATA-binding factor 6 contributes to atrioventricular node development and function. Circ Cardiovasc Genet. 2015;8(2):284–93.
72. Stefanovic S, Barnett P, van Duijvenboden K, Weber D, Gessler M, Christoffels VM. GATA-dependent regulatory switches establish atrioventricular canal specificity during heart development. Nat Commun. 2014;5:3680.

73. Singh R, Horsthuis T, Farin HF, Grieskamp T, Norden J, Petry M, et al. Tbx20 interacts with smads to confine tbx2 expression to the atrioventricular canal. Circ Res. 2009;105(5):442–52.
74. Rutenberg JB, Fischer A, Jia H, Gessler M, Zhong TP, Mercola M. Developmental patterning of the cardiac atrioventricular canal by notch and hairy-related transcription factors. Development. 2006;133(21):4381–90.
75. Kokubo H, Tomita-Miyagawa S, Hamada Y, Saga Y. Hesr1 and Hesr2 regulate atrioventricular boundary formation in the developing heart through the repression of Tbx2. Development. 2007;134(4):747–55.
76. Miao L, Li J, Li J, Tian X, Lu Y, Hu S, et al. Notch signaling regulates Hey2 expression in a spatiotemporal dependent manner during cardiac morphogenesis and trabecular specification. Sci Rep. 2018;8(1):2678.
77. Rentschler S, Harris BS, Kuznekoff L, Jain R, Manderfield L, Lu MM, et al. Notch signaling regulates murine atrioventricular conduction and the formation of accessory pathways. J Clin Investig. 2011;121(2):525–33.
78. Gillers BS, Chiplunkar A, Aly H, Valenta T, Basler K, Christoffels VM, et al. Canonical wnt signaling regulates atrioventricular junction programming and electrophysiological properties. Circ Res. 2015;116(3):398–406.
79. Hurlstone AFL, Haramis APG, Wieholds E, Begthel H, Korving J, van Eeden F, et al. The Wnt/B -catenin pathway regulates cardiac valve formation. Nature. 2003;425:633–7.
80. Verhoeven MC, Haase C, Christoffels VM, Weidinger G, Bakkers J. Wnt signaling regulates atrioventricular canal formation upstream of BMP and Tbx2. Birth Defects Res A Clin Mol Teratol. 2011;91(6):435–40.
81. Rentschler S, Vaidya DM, Tamaddon H, Degenhardt K, Sassoon D, Morley GE, et al. Visualization and functional characterization of the developing murine cardiac conduction system. Development. 2001;128(10):1785–92.
82. Wessels A, Vermeulen JLM, Verbeek FJ, Virágh S, Kálmán F, Lamers WH, et al. Spatial distribution of "tissue-specific" antigens in the developing human heart and skeletal muscle: III. An immunohistochemical analysis of the distribution of the neural tissue antigen G1N2 in the embryonic heart; implications for the development of the atrioventricular conduction system. Anat Rec. 1992;232(1):97–111.
83. Hoogaars WMH, Tessari A, Moorman AFM, de Boer PAJ, Hagoort J, Soufan AT, et al. The transcriptional repressor Tbx3 delineates the developing central conduction system of the heart. Cardiovasc Res. 2004;62(3):489–99.
84. Choquet C, Kelly RG, Miquerol L. Nkx2-5 defines distinct scaffold and recruitment phases during formation of the murine cardiac Purkinje fiber network. Nat Commun. 2020;11(1):5300.
85. Meysen S, Marger L, Hewett KW, Jarry-Guichard T, Agarkova I, Chauvin JP, et al. Nkx2.5 cell-autonomous gene function is required for the postnatal formation of the peripheral ventricular conduction system. Dev Biol. 2007;303(2):740–53.
86. Kim KH, Rosen A, Hussein SM, Puviindran V, Korogyi AS, Chiarello C, et al. Irx3 is required for postnatal maturation of the mouse ventricular conduction system. Sci Rep. 2016;6:19197.
87. Moskowitz IP, Kim JB, Moore ML, Wolf CM, Peterson MA, Shendure J, et al. A molecular pathway including id2, tbx5, and nkx2-5 required for cardiac conduction system development. Cell. 2007;129(7):1365–76.
88. Bakker ML, Boukens BJ, Mommersteeg MTM, Brons JF, Wakker V, Moorman AFM, et al. Transcription factor Tbx3 is required for the specification of the atrioventricular conduction system. Circ Res. 2008;102(11):1340–9.
89. Shekhar A, Lin X, Liu FY, Zhang J, Mo H, Bastarache L, et al. Transcription factor ETV1 is essential for rapid conduction in the heart. J Clin Investig. 2016;126(12):4444–59.
90. Zhang SS, Kim KH, Rosen A, Smyth JW, Sakuma R, Delgado-Olguin P, et al. Iroquois homeobox gene 3 establishes fast conduction in the cardiac his-Purkinje network. Proc Natl Acad Sci U S A. 2011;108(33):13576–81.

91. Koizumi A, Sasano T, Kimura W, Miyamoto Y, Aiba T, Ishikawa T, et al. Genetic defects in a His-Purkinje system transcription factor, IRX3, cause lethal cardiac arrhythmias. Eur Heart J. 2016;37(18):1469–75.
92. Arnolds DE, Liu F, Fahrenbach JP, Kim GH, Schillinger KJ, Smemo S, et al. TBX5 drives Scn5a expression to regulate cardiac conduction system function. J Clin Investig. 2012;122(7): 2509–18.
93. van den Boogaard M, Wong LY, Tessadori F, Bakker ML, Dreizehnter LK, Wakker V, et al. Genetic variation in T-box binding element functionally affects SCN5A/SCN10A enhancer. J Clin Investig. 2012;122(7):2519–30.
94. Miquerol L, Beyer S, Kelly RG. Establishment of the mouse ventricular conduction system. Cardiovasc Res. 2011;91(2):232–42.
95. Firulli BA, George RM, Harkin J, Toolan KP, Gao HY, Liu YL, et al. HAND1 loss-of-function within the embryonic myocardium reveals survivable congenital cardiac defects and adult heart failure. Cardiovasc Res. 2020;116(3):605–18.
96. Vincentz JW, Firulli BA, Toolan KP, Arking DE, Sotoodehnia N, Wan J, et al. Variation in a left ventricle-specific Hand1 enhancer impairs GATA transcription factor binding and disrupts conduction system development and function. Circ Res. 2019;125(6):575–89.
97. Rentschler S, Yen AH, Lu J, Petrenko NB, Lu MM, Manderfield LJ, et al. Myocardial notch signaling reprograms cardiomyocytes to a conduction-like phenotype. Circulation. 2012;126 (9):1058–66.
98. da Silva AR, Neri EA, Turaca LT, Dariolli R, Fonseca-Alaniz MH, Santos-Miranda A, et al. NOTCH1 is critical for fibroblast-mediated induction of cardiomyocyte specialization into ventricular conduction system-like cells in vitro. Sci Rep. 2020;10(1):16163.
99. D'Amato G, Luxan G, de la Pompa JL. Notch signalling in ventricular chamber development and cardiomyopathy. FEBS J. 2016;283(23):4223–37.
100. Chen H, Shi S, Acosta L, Li W, Lu J, Bao S, et al. BMP10 is essential for maintaining cardiac growth during murine cardiogenesis. Development. 2004;131(9):2219–31.
101. Lai D, Liu X, Forrai A, Wolstein O, Michalicek J, Ahmed I, et al. Neuregulin 1 sustains the gene regulatory network in both trabecular and nontrabecular myocardium. Circ Res. 2010;107(6):715–27.
102. Pfeufer A, van Noord C, Marciante KD, Arking DE, Larson MG, Smith AV, et al. Genome-wide association study of PR interval. Nat Genet. 2010;42(2):153–9.
103. Sotoodehnia N, Isaacs A, de Bakker PI, Dorr M, Newton-Cheh C, Nolte IM, et al. Common variants in 22 loci are associated with QRS duration and cardiac ventricular conduction. Nat Genet. 2010;42(12):1068–76.
104. van Setten J, Brody JA, Jamshidi Y, Swenson BR, Butler AM, Campbell H, et al. PR interval genome-wide association meta-analysis identifies 50 loci associated with atrial and atrioventricular electrical activity. Nat Commun. 2018;9(1):2904.
105. Verweij N, Leach IM, van den Boogaard M, van Veldhuisen DJ, Christoffels VM, Hillege HL, et al. Genetic determinants of P wave duration and PR segment. Circ Cardiovasc Genet. 2014;7(4):475–81.

Hemodynamics During Development and Postnatal Life

11

Martina Gregorovicova, S. Samaneh Lashkarinia, Choon Hwai Yap, Viktor Tomek, and David Sedmera

Abstract

A well-developed heart is essential for embryonic survival. There are constant interactions between cardiac tissue motion and blood flow, which determine the heart shape itself. Hemodynamic forces are a powerful stimulus for cardiac growth and differentiation. Therefore, it is particularly interesting to investigate how the blood flows through the heart and how hemodynamics is linked to a particular species and its development, including human. The appropriate patterns and magnitude of hemodynamic stresses are necessary for the proper formation of cardiac structures, and hemodynamic perturbations have been found to cause malformations via identifiable mechanobiological molecular pathways. There are significant differences in cardiac hemodynamics among vertebrate species, which go hand in hand with the presence of specific anatomical structures. However, strong similarities during development suggest a common pattern for cardiac hemodynamics in human adults. In the human fetal heart, hemodynamic abnormalities during gestation are known to progress to congenital heart malformations by birth. In this chapter, we discuss the current state of the knowledge of the prenatal cardiac hemodynamics, as discovered through small and large animal models, as well as from clinical investigations, with parallels

M. Gregorovicova · D. Sedmera (✉)
Laboratory of Developmental Cardiology, Institute of Physiology, Czech Academy of Sciences, Prague, Czech Republic

Institute of Anatomy, First Faculty of Medicine, Charles University, Prague, Czech Republic
e-mail: David.Sedmera@lf1.cuni.cz

S. S. Lashkarinia · C. H. Yap
Department of Bioengineering, Imperial College, London, UK

V. Tomek
Pediatric Cardiology, Motol University Hospital, Prague, Czech Republic

© The Author(s), under exclusive license to Springer Nature Switzerland AG 2024

S. Rickert-Sperling et al. (eds.), *Congenital Heart Diseases: The Broken Heart*,
Advances in Experimental Medicine and Biology 1441,
https://doi.org/10.1007/978-3-031-44087-8_11

gathered from the poikilotherm vertebrates that emulate some hemodynamically significant human congenital heart diseases.

Keywords

Chick embryo · Fetal heart · Hyperplasia · Hypertrophy · Pressure overload · Volume overload · Developing myocardium · Zebrafish · Axolotl · Reptile · Hemodynamics · Embryogenesis · Endothelin 1 · ET1 · Nitric oxide synthase 3 · NOS3 · Krüppel-like factor 2 · KLF2 · VSD · DORV · HLHS · Hypoplastic left heart syndrome · Lamb · Guinea pig · Mouse · Rat

11.1 Introduction

Cardiogenesis is a highly dynamic process consisting of the migration and induction of precursor cells into a linear heart tube [1]. During development, the heart tube is bent and partitioned to become a multichambered and unidirectional myogenic pump [2]. Many structural and functional heart features are similar in all vertebrates [3], especially during early development [4]. However, there is a big variance in functional diversity connected with behavior and environment [5].

A properly developed heart is crucial for embryo survival. Constant interactions between cardiac tissue motion and blood flow dynamics shape the heart [6]. Blood flow within the heart forms two types of forces: shear stress, which is a force tangential to the vessel wall, and pressure, which creates a circumferential stretch perpendicular to the vessel wall [7]. If there is an absence of blood flow, the heart does not develop properly [8]. Such deviations from normal hemodynamic conditions can lead to grave cardiac malformations [9, 10] but are also observed in ectothermic vertebrates [11, 12]. We will organize this chapter according to models used to perform hemodynamics studies, briefly summarizing their advantages and limitations, then follow with clinical observations and phylogenetic parallels (more of which are discussed in the following chapter).

11.2 Studies in Developing Zebrafish

The zebrafish embryo is a useful model for cardiac hemodynamics studies because tissue translucency provides good optical access for imaging and investigation. The ease of genetic manipulation in the species further conferred advantages for mechanobiological studies of cardiac development.

The zebrafish embryonic heart tube starts exhibiting clear beating by 22 h post fertilization (hpf), and circulation starts at 24 hpf [12]. Studies of the 26 hpf heart tube in the zebrafish embryo led to an intriguing but controversial proposal by Forouhar et al. that the early heart tube functions as an impedance pump rather than a peristaltic pump [2]. An impedance pump relies on impedance mismatch at the inlet and outlet and wave reflections at these boundaries to produce net

directional flow and typically has strong nonlinear responses at resonance pumping frequencies. To substantiate the proposal, Forouhar et al. cited observations that bidirectional rather than unidirectional waves traversed the endocardial layer, that blood flow velocities exceeded those expected for peristaltic pump, and that nonlinear peaks in flow responses occurred at resonance frequencies. However, opponents to the proposal [13] cited examples of gastric peristaltic pumps being able to generate flow velocities exceeding those of peristaltic waves, and that simulation results showed that a presumed peristaltic heart tube could still generate pulsatile waveforms not expected of a strictly peristaltic pump due to the presence of endocardial cushions [14].

The general hemodynamic characteristics of the zebrafish embryo has been well-investigated. The heart rate of the zebrafish embryonic heart was reported to increase in a roughly linear manner from 54 ± 2 bpm at 30 hpf to 149 ± 20 bpm at 120 hpf [15]. Gierten et al. developed a high throughput method for measuring heart rates of zebrafish embryos via bright-field microscopy and image processing [16], which could track heart rate over long incubation periods, and they recorded dips in heart rate at night with the circadian rhythm, as well as increasing heart rate with temperature. 3D microscopy measurements of cardiac and vascular sizes and function were performed by Bagatto and Burggren [17], who found that dorsal aortic flow velocities increased from 291 ± 35 to 766 ± 55 μm/s from 2 to 6 days post fertilization (dpf) in a power law trend (increasing rate of change with increasing age), but ventricular volumes increased roughly linearly from approximately ~0.4 ± 0.02 to ~0.75 ± 0.025 nl over the same period. Stroke volume was found to increase from 0.146 ± 0.016 to 0.297 ± 0.040 nl over the same period, in a roughly linear manner. The authors also reported that 3D cardiac output measurements were different from a 2D approach, pointing out the inadequacy of 2D approaches, which are frequently used in the literature. Intraventricular pressure in the embryo was measured via a glass micropipette connected to the servo null pressure system (designed to measure small pressure fluctuations by setting the zero to a fluid pool near the site of measurements), and the peak systolic ventricular pressure was found to increase from 7.52 ± 0.77 mmHg at 72 hpf to 11.26 ± 1.31 mmHg at 120 hpf, while end diastolic ventricular pressure remained roughly constant at 1.28–1.36 mmHg [18].

There is a substantial interest in using the zebrafish embryonic model to study heart valve development, and several studies provided evidence that normal heart valve development requires the appropriate biomechanical stimuli from blood flow. For example, Bartman et al. examined the silent heart mutant embryo, which lacked a heartbeat due to cardiac troponin T mutations, and found that endocardial cushions, the precursors to heart valves, failed to form [19]. Vermot et al. proposed that both the forward and retrograde flow naturally observed at the atrioventricular junction at 48 hpf are necessary for proper valve formation and reported that in *gata* morpholino embryos, where the characteristics of the retrograde flow were altered, abnormal valve leaflets were more frequently observed concurrently with altered *klf2* expression [20]. Banjo et al. demonstrated that miR-21 was rapidly switched on and off by blood flow in their experiments where they modulated flow stimuli using troponin T

morpholino, the silent heart mutant, and 2,3-butanedione monoxime (BDM, a myosin inhibitor preventing contraction) drug treatment [21]. They also demonstrated that flow-dependent expression of miR-21 governed valvulogenesis by regulating proliferation. Steed et al. demonstrated that blood flow and flow-dependent klf2a expression controlled a coordinated set of tissue movements and fibronectin1b expression, which were necessary for valve leaflet morphogenesis [22].

For this reason, there is substantial interest in characterizing the fluid dynamics and stresses at the endocardial cushions and atrioventricular junctions. Microparticle image velocimetry measurements by Hove et al. reported that the wall shear stresses at the atrioventricular canal ranged from 2.5 dyn/cm^2 at the 37 hpf to 76 dyn/cm^2 at the 108 hpf [8]. A 2D microscopy-based computational fluid dynamics (CFD) study reported that Reynolds number at the atrioventricular canal increased linearly from 0.07–0.23 to 30–120 hpf, while the Womersley number remained at around 0.14 over the same period, and that peak wall shear stresses increased approximately from ~3 ± 1 to ~82 ± 15 dyn/cm^2 in a steep linear manner from 20–30 hpf to 110–120 hpf. The authors noted that cardiac looping at 40–50 hpf was associated with a nearly threefold increase in wall shear stress magnitude from conditions at 20–30 hpf [15]. The Reynolds number describes how much momentum is present in the flow compared to the damping effects of viscosity, while the Womersley number describes how much periodic pulsatile flow inertia is present compared to the effects of viscosity. Here, both measures are very small in the embryonic heart, indicating a very stable and orderly flow environment that is dominated by viscosity.

Hsu et al. performed moving-wall CFD based on 4D light-sheet imaging to determine effects contractility changes on ventriculobulbar valve development [23]. Results showed that the augmentation of myocardial contractility with isoproterenol increased wall shear stresses from approximately ~20 ± 7 to ~45 ± 10 dyn/cm^2, which was associated with increased Notch1b activity in the developing outflow tract and resulted in ventriculobulbar valve hyperplasia. Increasing blood viscosity through EPO mRNA injection increased wall shear stress to ~32 ± 4 dyn/cm^2 in the outflow tract and resulted again in valve hyperplasia. Conversely, BDM reduction of contractility and wall shear stress was associated with reduced Notch1b activity and an absence of ventriculobulbar valve leaflet formation (Fig. 11.1).

Motivated by the limitations of 2D approaches, dynamic 3D whole ventricular simulations were conducted by some investigators to further characterize the zebrafish embryonic heart fluid dynamics. Foo et al. conducted 4D microscopy-based CFD simulations of the zebrafish embryonic ventricle at 120 hpf [24] and demonstrated a bimodal wall shear stress versus time waveform over the cardiac cycle corresponding to inflow and outflow and high spatial variation of wall shear stresses, which peaked at 48–130 dyn/cm^2 at the inflow and outflow regions but were in the range of 4–11 dyn/cm^2 in the mid-ventricular region. They also demonstrated the wave-like contractile motion of the heart that produced energy savings. Lee et al. conducted dynamic mesh CFD studies in both wildtype and mutant zebrafish embryos with defects of trabecular formation (*gata1a*, *wea,* and *erbB2* mutants) [25]. They reported that wild-type ventricles experienced higher wall shear stresses

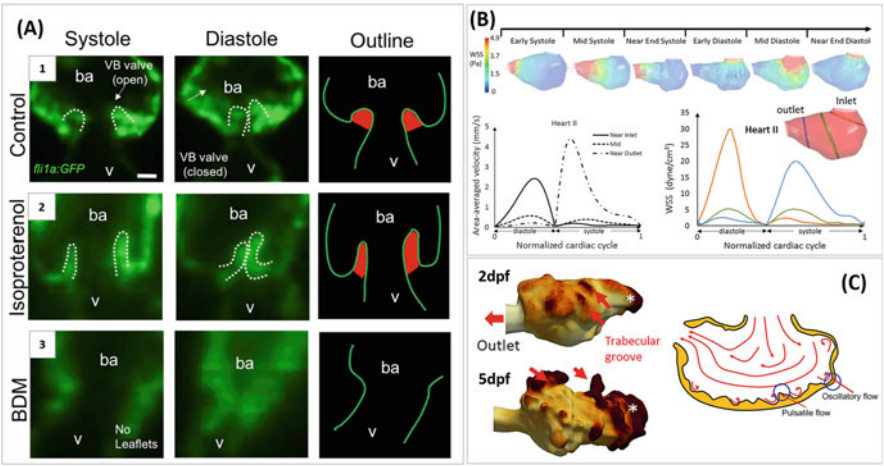

Fig. 11.1 Hemodynamic studies in larval zebrafish. (**a**) Effects of changes in hemodynamic shear force on ventriculobulbar valve leaflet formation. SPIM images of ventriculobulbar valves during ventricular systole and diastole at 120 hpf, with corresponding outline of the endocardium/endothelium (with valve leaflets highlighted in red), are shown [23]. (**b**) Contour maps of wall shear stress and velocity vectors along the longitudinal cross section in three normal ventricles over the cardiac cycle [24]. Plots of flow velocity averaged over cross-sectional area versus time were demonstrated for three cross sections. Wall sheer stress (WSS) averaged across the cross section plotted over the course of the cardiac cycle [23]. (**c**) Elevated oscillatory shear index (OSI) values developed in trabecular ridges and are dependent on ventricular surface roughness at 2 dpf; elevated OSI values were interspersed between trabecular ridges and grooves in the WT embryos. At 5 dpf, high OSI values are associated with the formation of the trabecular network. Trabecular ridges were exposed to pulsatile shear stress (PSS), while trabecular grooves were exposed to oscillatory shear stress (OSS). An elevated OSI developed as a result of flow trapped between the two trabecular ridges [25]

compared to the mutant embryos and noted that these corresponded to the non-trabeculation phenotypes in the mutants. They further reported that wall shear stresses were higher on the ridges of the trabeculations than in the grooves, while oscillatory indices were much higher in the grooves compared to the ridges and proposed the idea that the trabeculation has the function of acting as cushions to dissipate inflow kinetic energy. In interpreting results of CFD simulations in the zebrafish embryonic model, however, it should be noted that there is a lack of information on embryonic blood viscosity and studies have used estimates based on hematocrit measurements or adult fish values [24] and should be interpreted with care.

It is further known that flow stimuli are necessary for the formation of trabeculations, and specific mechanobiological pathways have been demonstrated. Peshkovsky et al. demonstrated that in the *wea* mutant where atrial contractions are inhibited, ventricular flow is weakened and this inhibited trabeculation formation [26]. They further demonstrated that the nrg/ErbB signaling was necessary for trabecular development. Rasouli et al. extended this study by demonstrating that

blood flow and contractility were necessary for *nrg2a* expression and that the noncontractile heart failed to form trabeculae [27]. These observations motivated studies into the fluid dynamics of the trabeculations, such as by Lee et al., as explained above [25], and by Battista et al., who reported that the trabeculation height had an impact on intratrabecular vorticity dynamics [28].

11.3 Avian Embryonic Heart Hemodynamics

The avian embryo is frequently used for cardiac hemodynamic studies, as both visualization of the beating heart by video microscopy and more sophisticated functional evaluation (pressure monitoring, high-frequency ultrasound and Doppler, optical coherence tomography) are relatively straightforward. Unlike the zebrafish embryonic heart, it forms ultimately four-chamber morphology and is thus more similar to the human embryonic heart. This allows models of septation defect or with side-specific lesions, such as left or right ventricular hypoplasia. The avian embryo is larger than the zebrafish embryo, and surgical manipulations to the heart are more easily accomplished. It is also easily accessible by opening the eggshell or by incubating the embryo in an ex ovo environment [29] and in this regard is more advantageous compared to rodents.

Early stages of development of the avian heart tube can be imaged with high spatial resolution with the OCT, achieving 3D scans of 10–15 μm resolution [30], and with a highspeed version, 10 volumes per heartbeat [31]. Peterson et al. computed wall shear stresses on the HH13 quail embryonic heart tube, using a validated technique involving 4D Doppler OCT images and assumptions on blood viscosity and flow directions, and found that wall shear stresses could be as high as 7.7 Pa, where the inner curvature region experiences much higher shear stresses than the outer curvature region [32].

Hu et al. performed morphological and flow measurements on the chick embryonic heart from stages 12–29, corresponding to 2–6 days of gestation [33]. The increase with age of the weight of the ventricle and whole embryo could best be modeled as a power law model, but the ratio of ventricle to embryo weight decreased from ~0.045 ± 0.007 at stage 12 to ~0.012 ± 0.002 at stage 21, where it remained until stage 29. Heart rate was found to increase from 103 ± 2 to 208 ± 5 bpm from Hamburger–Hamilton (HH) stage 12–21 in a roughly linear manner, while stroke volume increased from 0.01 ± 0.003 mm [3] to 0.69 ± 0.03 mm^3 over the same period, also in a roughly linear manner. The increase in arterial pressure over the stages was found to be roughly linearly, from 0.28 ± 0.01 mmHg to 1.51 ± 0.04 mmHg from HH stages 12 to 29. From these measurements, they estimated that the vascular resistance to decrease via an inverse power law from 24.71 to 0.63 mmHg/mm [3], while cardiac work done increased in a positive power law from 0.04 ± 0.02 to 13.89 ± 0.69 dyn.mm, over the same stages. Midgett et al. performed Doppler measurements at the outflow tract and found that peak velocities increased from ~30 ± 1 to ~40 ± 3 mm/s from HH stage 13 to 18 [34]. Oosterbaan et al. performed similar measurements at HH stages 18, 21, and 23, and reported

inflow tract velocities increased from 59 ± 17 to 89 ± 20 mm/s from stages 18 to 23, and significant reversed flow velocities at the atrioventricular junction at end diastole just before the closure of the endocardial cushions [35].

4D high-frequency ultrasound imaging of the HH25 chick embryonic heart was conducted by Ho et al. [36, 37], who subsequently used the images for 4D dynamic-mesh CFD flow simulations to understand the hemodynamics. They found that the embryonic atrial appendages were among the most contractile regions of the heart and speculated that it serves the function of enhancing atrial pumping. Highly laminar flow was observed, but with high spatial and temporal variations of wall shear stresses, with the spatial average peaking at 0.2–0.5 Pa. The atrioventricular junction and outflow tract experienced the highest shear stresses which averaged at around 1 Pa. Oscillatory indices were in the range of 0.13–0.27 but can be as high as 0.44 in the atrial appendages.

Flow simulations were also conducted in the outflow tract (OFT) by various investigators. Liu et al. performed 4D OCT imaging of the HH18 chick embryonic outflow tract [38] and quantified strains of up to 50% at the endocardial layer, wall stresses of up to 400–600 Pa. They then performed 4D simulations of the OFT flow for 50% of the cardiac cycle and reported wall shear stresses in the range of 1–11 Pa at various locations of the OFT during peak flow phase. Bharadwaj et al. performed micro-CT imaging of corrosion casted mounds of the blood spaces within the OFT of embryos between HH stages of 16–30, as well as Doppler measurements of flow velocities, and performed transient flow CFD simulations on nondynamic geometries [39]. They reported peak wall shear stresses that increased exponentially from 18.16 ± 3.18 to 671.24 ± 211.46 dyn/cm [2] from HH16 to HH30. Ho et al. performed 4D high-frequency ultrasound imaging of the OFT of the HH25 embryo to support 4D dynamic mesh flow simulations [40]. They reported that peak wall shear stress of 0.7 to 6.3 Pa but reported that because of the periodic collapse of the OFT at two locations, substantial oscillatory flow and wall stresses were observed and oscillatory indices were especially high near the cushion locations. Due to the curvature of the OFT centerline, a dual counter-rotating helical flow pattern was observed, where the dividing axis of the two helical flow structures coincided with the eventual septation orientation, suggesting a relationship between flow patterns and development.

There has further been a substantial interest in understanding the role of hemodynamics on the development of the pharyngeal aortic arches. Kowalski et al. performed 3D pulsatile flow simulations on the aortic arches between stages HH18 and HH24 [41] and found quantitative correlation between hemodynamic wall shear stresses and the aortic arch diameters and proposed that such flow stresses guide vascular growth, in a homeostatic manner where growth attempts to restore a normative wall shear stress environment. Lindsey et al. used guided femtosecond laser to occlude specific aortic arches to investigate if the subsequent vascular remodeling would be guided by flow stresses predicted by CFD [42]. However, while predictions were qualitatively accurate, they were not as accurate quantitatively, suggesting that more complex factors could be involved in addition to flow stresses.

Several models of congenital malformations and cardiac dysfunction have been developed in the chick embryo model and have led to improved understanding of the effects of hemodynamics disturbances on cardiac development. Hogers et al. introduced a venous clip model that mimics placental infarction and observed the resulting changes in intracardiac blood flow patterns [43], where a unilateral ligation of the right vitelline vein frequently led to abnormal morphogenesis translating in incomplete ventricular septation (VSD), valve abnormalities and pharyngeal arch artery malformations. After the ligation, venous Indian ink allowed observations of intracardiac flow patterns, which were observed to be altered and were postulated to be the cause of the malformations.

A second model is the constriction of the outflow tract (conotruncal banding), which was used as a model of increased pressure load of the embryonic ventricle [44]. The banding resulted in high lethality and defects in survivors. These included VSD, with either double outlet right ventricle or persistent truncus arteriosus [44, 45], which could be due to the mechanical effects of the suture and to the hypoplasia of the conotruncal ridges due to altered intracardiac flow patterns [9]. The ventricle also showed dilation and spiraling of trabeculae in the left ventricle, which could reflect adaptations to increased functional demands [46]. There was also increased compact myocardium thickness within 48 h [9], corroborating with literature that increased pressure loading at this stage is a powerful stimulus for active myocardial growth based on cell proliferation [44, 47, 48]. There were also anomalies in coronary arteries, but interestingly, the growth of capillaries matched that of the myocytes, so the ratio was kept constant [49]. Flow simulations and OCT imaging in this model have also been conducted to quantify elevations of flow wall shear stresses on banding [50], and banding was also found to disrupt the normal peristaltic motion of the OFT.

Another popular model with a long history is the left atrial clipping or ligation (LAL) [9, 51], which is a model of restricted inflow into the left ventricle and shunting of blood into the right side of the heart. A main feature of this model is the underdevelopment of the LV and the overdevelopment of the RV, bearing similarities to the clinical hypoplastic left heart syndrome (HLHS) [52] (Fig. 11.2). The ventricle also experiences changes to myofiber angle distribution, ventricular wall stiffness, myocardium thickness, and ventricular dimensions [9, 46, 48, 52, 53]. Interestingly, the LAL left ventricle was also found to have a significant thickening of subendocardial fibrous tissues [54], similar to clinical observations of endocardial fibroelastosis in fetal aortic stenosis and evolving HLHS [55]. Further, surgical clipping of the right atrial appendage following LAL has been found to normalize the hemodynamics and rapidly resulted in increased myocyte proliferation in the LV, thus normalizing and rescuing the small LV volume caused by the LAL [56] (Fig. 11.2). This observation reinforces the notion that hemodynamics affects development and demonstrates the feasibility of fetal intervention aimed at mitigating human fetal cardiac malformations [57, 58].

The fluid dynamics of the LAL model has been investigated in detail by Ho et al., who performed 4D dynamic mesh CFD simulations based on 4D high-frequency ultrasound imaging at HH25 [59] (Fig. 11.2c, d). They found that the ligation

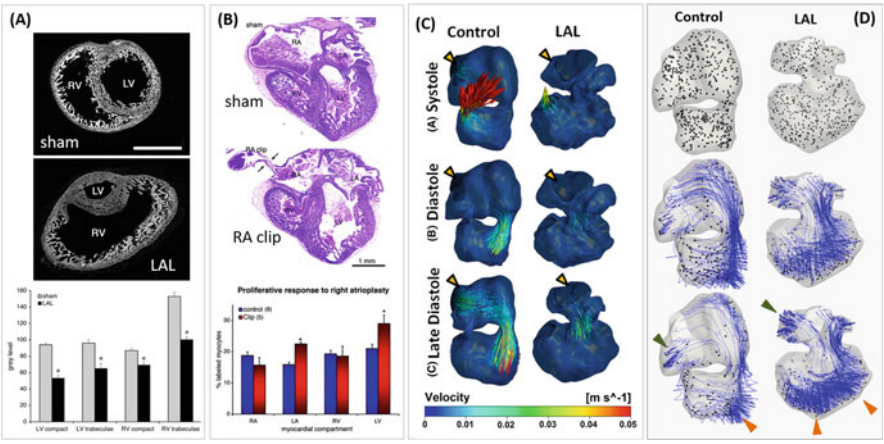

Fig. 11.2 Hemodynamic studies in the chick embryonic model of HLHS. (**a**) Left atrial ligation (LAL) at the presentation stage produces a hypoplastic LV and hyperplastic RV, from [48]. (**b**) Heart morphology in normal HH35 embryos 24 h after placement of the right atrial clip. The clip was removed before processing, and its position on the right atrium is indicated by the arrows. Note the enlargement of the left ventricular cavity. Bar chart shows a significant increase in percentage of labeled myocytes in the left heart structures, from [56]. (**c**–**d**) Fluid dynamics simulations shortly after LAL revealed weak and oscillatory flow patterns near the LV free wall, which may play a role in this outcome [59]

compromised the atrial function and led to weaker velocities in the ventricle. Concurrently, anatomical changes after the ligation, including a medial shift of the atrioventricular junction and a sharper primitive ventricle apex, led to a sluggish flow at the LV free wall that generated weak and oscillatory wall shear stresses, and subsequently, the LV was observed to become hypoplastic despite septation not being complete. These findings suggested that the altered flow stresses on the LV to play a role in LV the hypoplasia.

11.4 Studies in Rodent Embryos

Rodent embryos are widely used in research, due to their similarity to human embryos, an excellent range of mutants that are available to model diseases, and comprehensive biological assays applicable to the species and genomic annotations. Early work in assessing mouse hemodynamics was performed by Keller and associates, who imaged embryonic hearts from E10.5 to E14.5 with light microscopy after externalization and surgical exposure, and performed doppler measurements of flow velocities via pulsed Doppler velocimetry [60]. Later, with the advent of high-frequency ultrasound, hemodynamics in the mouse embryo has become well-characterized. Yu et al. performed measurements of 2D anatomic sizes, heart rate, flow velocities in the heart, and durations of cardiac cycle phases and assessed

systolic function of the mouse embryonic hearts from E12.5 to E19.5, using large sample sizes [61]. 2D quantification of the heart area found it to be roughly proportional to the fetus area measured from the sagittal plane. Heart rate was observed to increase gradually from 190 ± 12 to 245 ± 20 bpm from E12.5 to E19.5. Throughout the late gestational of the mouse, A-wave (active filling phase due to atrial contraction, or "kick") mitral inflow velocity was stronger than E-wave (passive filling due to ventricular suction in early diastole) velocity, which is consistent with the trends in human fetuses. E-wave velocity was observed to increase gradually with gestational age (0.06 ± 0.02 to 0.15 ± 0.03 m/s from E12.5 to E19.5), but A-wave velocity decreased slowly (0.37 ± 0.06 to 0.34 ± 0.05 m/s over the same period), leading to E/A ratio that increases from 0.19 ± 0.05 to 0.44 ± 0.06 from E12.5 to E19.5. Peak aortic velocity increases from 0.29 ± 0.102 to 0.38 ± 0.08 m/s over the same gestational period, which is very similar to peak pulmonary velocity. With the increasing heart rate, ejection duration, isovolumic contraction and relaxation durations, and diastolic durations all decreased with age. Ejection time stayed constant at roughly 41% of the cardiac cycle duration across all ages, while the other durations in terms of percentage of the cardiac cycle all decreased with age. LV pressures have been measured invasively with glass micropipettes attached to servo-null pressure transducers by Le et al. [71] and was found to be 10 ± 2 mmHg at E18, but increased gradually to 58 ± 6 mmHg at P14. During the same period, heart rate was observed to increase quickly to roughly 470 ± 30 bpm.

In the early-stage mouse embryo, 4D imaging has been performed by Wang et al., who performed OCT anatomic and Doppler imaging of the dissected E9.0 embryo and yolk sac in culture media [62]. Velocity waveforms were obtained in the primitive atrium, the primitive ventricle, and bulbus cordis, and both strong forward flow velocities as well as substantial retrograde flow velocities were observed, likely due to the immaturity of valve and cushions to control flow directions. However, this suggested that strong wall shear stresses can be induced by flows in both directions, and given that retrograde flow was found to be important for valve development in the zebrafish embryonic heart [20], it is likely that retrograde flow here is important for development as well. Hoog et al. performed optical projection tomography (OPT) and histology on E8.5 mouse embryonic hearts after dissection [63]. They developed a technique for reducing hematocrit in the embryo and thereby reducing hemodynamics forces on the cardiovascular system, though the injection of acrylamide and TEMED into the yolk save blood island vessels. They found that reduced hemodynamic loading led to reduced heart volume, myocardial thickness, trabeculation, and cardiac looping thus demonstrating the importance of hemodynamics loading on the proper early cardiac development in the mouse model. An elegant surgical study was performed in fetal guinea pigs [64]. The fetuses in the third trimester were accessed by hysterotomy, and their ascending aorta was constricted to 50% of its original diameter. The heart to body weight ratio and left ventricular wall thickness increased significantly in the constricted group. There was also a significant increase in proliferating cells (Ki-67-positive) in both ventricles

with no changes in apoptosis, suggesting the existence of an adaptation mechanism similar to that observed in the chick model [48, 65].

Recently, a mouse model of hypoplastic left heart syndrome was induced by microsurgery in the mouse fetuses at ED14.5 (post-septation) [66]. Hemodynamic perturbation caused by micro-embolization of the left atrium under ultrasound guidance created a phenocopy of the chick presentation model of HLHS [56], so hopefully will allow testing feasibility of prenatal therapeutic intervention also in a mammalian model. Hemodynamics and its role in changing gene expression resulting in asymmetric remodeling of aortic arches were also studied in the mouse [67]. The authors examined the link between laterality determination (dependent upon *Pitx2* expression) and asymmetric regression of the sixth branchial arch arteries. They proposed a model, in which the asymmetric *Pitx2* expression leads to spiraling of the developing outflow tract, resulting in asymmetric distribution of the blood flow into the sixth aortic arches, resulting (via asymmetric PDFG and VEGFR2 expression) into regression of the right sixth arch artery and persistence of the left one. This theory was supported by experimental manipulations using mechanical insults (selective ligations) and chemical inhibitors (of growth factor signaling or decreasing the heart rate and contractility via propranolol) and helps to explain frequent occurrence of aortic arch defects in mutants with laterality problems.

11.5 Large Animal Models

Compared to small animal fetal and embryonic studies, the large animal fetal models provide a system that is closer to human fetuses in terms of size, anatomy, and physiology, which was the motivation for such investigations. Studies of fetal hearts in large animal models were mostly performed on the lamb and have focused on investigating intrauterine development of the cardiopulmonary system, modeling congenital heart malformations and fetal heart dysfunctions, and testing the effects of various prenatal interventions.

Early surgical studies were conducted by putting the lamb fetus on extracorporeal cardiac bypass, with the goal of eventually enabling surgical corrections of fetal hearts with congenital malformations. Initial attempts encountered placenta dysfunction, but improvements to the fetal extracorporeal circuitry and technique resolved this [68], with the promising outcome of 8 out of 9 fetal lambs surviving to birth. The feasibility of fetal cardiac bypass was later confirmed in the goat model [69]. More recently, rather than an open-heart surgery, catheter-based fetal heart intervention was clinically attempted and was found promising in preventing mid-gestational cardiac abnormalities from progressing to malformations at birth [70]. The lamb fetal model was used to test improved interventional approaches [71] and to train interventionalists [72]. New devices were also tested for fetal heart intervention in the fetal lamb model, including atrial septal stents [73] and tissue-engineered transcatheter pulmonary valve [74].

Large animal fetal experiments have also successfully developed models of congenital heart malformations and demonstrated that altered fetal hemodynamics could adversely impact cardiac growth and development. Fishman et al. experimented with both LV inflow and outflow obstruction in the lamb fetuses between 90 and 100 days of gestation. Inflow obstruction was achieved by inflating a permanent balloon in the left atrium, while outflow obstruction was achieved via aortic banding and found that both approaches resulted in hypoplastic LV [75]. Inflow obstruction decreased LV output to 30% of the control values and caused a LV/RV weight ratio to decrease by 30%. Outflow obstruction initially caused a large LV mass increase, but over the longer term, drastically decreased the LV/RV weight ratio. The inflow obstruction model was later corroborated by Wong et al., who performed foramen ovale occlusion in the lamb model at 104–117 days of gestation and evaluated outcomes 3–5 weeks later [76]. They found that the occlusion, which decreased LV strain function, caused a significantly smaller LV size at the experimental endpoint, having a decrease in various LV anatomical dimensions. Together with clinical association of restrictive foramen ovale to HLHS malformations [77], and with observations that critical fetal aortic stenosis will mostly progress to HLHS by birth [78], these works suggest that abnormal LV hemodynamics can lead to abnormal LV growth and to HLHS births. However, it is noteworthy that a more recent effort at investigating the effects of aortic outflow obstruction at an earlier time point (mean of 53 days of gestation) found no growth retardation or abnormal fibrosis of the LV, suggesting that responses at different gestational ages can vary [79].

The sheep fetal model has also been used to study the effects of intrauterine growth restrictions (IUGRs) on cardiac function and development. Techniques to induce IUGR include maternal hyperthermia, placenta embolization or caruncles (parts of ungulate placenta) removal, and uterine artery ligation [80]. Generally, these studies found that cardiomyocyte growth and maturation are impaired, where the fetal heart weighs less, has myocytes that are smaller and less active in cell cycle, and has a higher proportion of mononuclear myocytes [81, 82]. These changes are likely consequent to altered cardiac hemodynamics and cardiac dysfunction consequent to elevated placenta circulation resistance, based on clinical studies of IUGR fetal hearts [83], but the direct investigation of the cardiac hemodynamics characteristics of IUGR fetal lambs is lacking in the literature. A notable study conducted by Lawrence et al. performed ex utero incubation of fetal lambs via a novel fetal circulatory support system [84] and found that hypoxia leads to reduced cardiac output of both ventricles and that cardiac output has a negative correlation with oxygen delivery. Reduced myocyte size and increased myocardial capillary density were also observed in the hypoxic fetal group.

11.6 Human Fetal Hemodynamics

The fetal circulation differs fundamentally from that of a newborn. Fetoplacental circulation is characterized by: (1) low systemic vascular resistance provided by the low resistance placenta containing 40% of fetal blood, (2) high pulmonary vascular resistance due to fluid-filled lungs with a hypoxic environment, (3) preferential supply of the most saturated blood from the umbilical vein to the left side of the heart via the foramen ovale and thereby the brain and heart, and (4) preferential supply of the most unsaturated blood from the body via the RV and the arterial duct to the placenta (Fig. 11.3). Due to physiological shunts, the fetal circulation occurs in a parallel arrangement rather than in series (as postnatally). Cardiac output in the fetus reflects an increasing dominant contribution of the right ventricle during gestation.

However, the regulation of the fetal circulation is complex and not fully understood. Limited knowledge about fetal hemodynamics comes from experimental studies of fetal animal models with simulated alterations to the circulation and from recent Doppler-derived ultrasound or MRI measurements of hemodynamic in human fetuses. Both demonstrated how congenital heart defects may affect the fetal

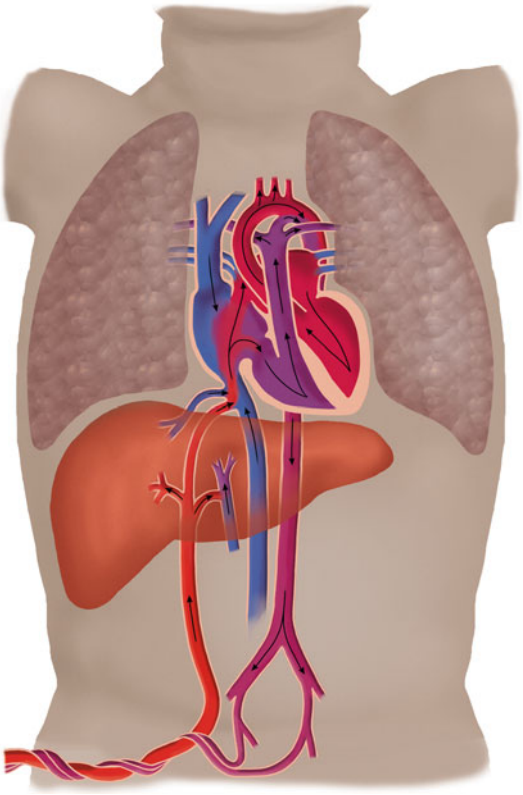

Fig. 11.3 Diagram of fetal circulation in human. Arrows indicate the direction of blood flow, color relative to blood saturation by oxygen. Original drawing by Ivan Helekal, based on various sources

circulation and influence development of the fetal heart. Data on placental–fetal interactions, placental metabolism and placental transfer function, and capacity were translated from animal models (most commonly the sheep) to human fetuses. Not all information can be simply translated, and some critical approach is required. For example: the brain in human is larger than that in lamb resulting in higher output of the left ventricle (40–45% versus 33% of combined cardiac output), and the estimated combined cardiac output of the human fetus (550 ml/kg/min) is higher than that of sheep (450 ml/kg/min) [85].

Fetal physiological shunts are essential for normal circulation, and their prenatal restriction or closure in structurally normal hearts is associated with serious consequences. Closure of the foramen ovale in early or midgestation leads to reduced left ventricular preload and prevents further development of the left heart resulting in HLHS or fetal death [76, 77]. Premature closure in the third trimester has been associated with right ventricle dilation (increased preload), heart failure, and intrauterine demise. Although it may not lead to decompensation of fetal circulation, distribution of more oxygenated blood through the right ventricle and ductus arteriosus decreases the materno-fetal oxygen gradient and reduces the fetal extraction of oxygen from the placenta [86]. Prenatal closure of the ductus arteriosus increases pulmonary artery blood flow with remodeling of pulmonary artery wall, right ventricular dysfunction (increased afterload), and pulmonary artery hypertension at birth carrying significant morbidity and mortality [87].

Fetal hemodynamics is basically dependent upon normal heart rate as the fetal myocardium is less compliant, operating near the upper end of the Frank–Starling curve with less response to preload changes. Fetal heart rates exceeding the range between 50 and 200 bpm cannot be compensated by stroke volume changes to maintain an adequate cardiac output and sufficient tissue perfusion [88]. Thus, long lasting supraventricular or rare ventricular tachyarrhythmias as well as complete atrioventricular block with a ventricular rate below 50 bpm often result in fetal heart failure, hydrops, and demise. In tachyarrhythmias, the heart failure is induced by inadequate filling time and impaired myocardial perfusion. Low ventricular rate in complete atrioventricular block limits the cardiac output due to fetal inability to substantially increase stroke volume. In addition to importance of heart rate and preload, cardiac output is dependent on afterload as well. The fetal heart appears to be highly sensitive to changes in afterload, represented by arterial pressure. Studies on fetal lambs indicated a fetal increase in afterload decrease stroke volume [89]. With increasing atrial pressure, the cardiac output plateaus at a much lower pressure in the fetus than postnatally. Decreased cardiac output with inversely increased placental resistance typically occurs in fetuses with growth restriction due to placental dysfunction [90]. Generally reduced ability of the fetal myocardium to contract and generate force contributes to a decreased cardiac reserve in response to stress and easily leads to fetal heart failure.

Various congenital heart lesions influence fetal circulation by altering patterns and volumes of flow through cardiac chambers and great vessels. They often lead to different distribution of blood flow and altered levels of blood saturation delivered to various organs. Those changes likely affect fetal development, growth, and postnatal

outcome. Heart anomalies, especially those with valvular regurgitation (typically in tricuspid insufficiency), or conditions compromising fetal circulation (twin to twin transfusion syndrome, atrioventricular fistula, anemia, etc.) may result in heart failure and fetal demise [91]. The final result of altered pathways is the elevation of end-diastolic ventricular pressure, atrial, and central venous pressure. In the fetus, even a small increase in filling pressure alters fetal organ function and may induce fetal hydrops.

In case of ventricular hypoplasia, cardiac output is maintained only by the one developed ventricle preserving the blood flow to all organs. However, fetal compensatory mechanisms in univentricular circulation are not complete. MRI studies demonstrated that the combined cardiac output in fetuses with HLHS was decreased by 20% compared with controls [92]. Similarly decreased combined cardiac output was detected in other groups of fetuses with various forms of univentricular heart. A different distribution of fetal blood flow in left-sided obstructed heart lesions (HLHS, severe aortic stenosis) resulted in increased placental vascular resistance and decreased cerebral resistance improving cerebral oxygen delivery sought to be protective for neurodevelopment [93]. On the contrary, current studies in fetuses with d-transposition of great arteries (TGA) demonstrated higher combined cardiac output. Left ventricular blood with higher oxygen level in those fetuses flows to the pulmonary artery lowering pulmonary vascular resistance [94]. Increased pulmonary flow results in increased combined cardiac output and in elevated left atrial pressure which may lead to restriction at the level of the atrial communication, as often seen in newborns with TGA.

Even heart lesions causing minor alterations to the fetal circulation may result in complex changes limiting long-term postnatal outcome. Coarctation of the aorta seems to be a local narrowing to the aortic isthmus but leads to high afterload of left ventricle and compensatory increased right ventricular output. It seems to be responsible for an observed thickening of pulmonary arterial muscle wall related to frequent pulmonary arterial hypertension [95].

Congenital heart diseases (Fig. 11.4), regardless of the type of anomaly, are often associated with a relatively high prevalence of abnormal brain development, reduced cranial size, and increased brain perfusion with reduction in brain oxygenated blood supply [96]. Changes in plasma concentration of angiogenic factors in various heart lesions imply a higher risk of impaired placental angiogenesis with subsequent low birth weights [97].

11.7 Postnatal Hemodynamics

Abrupt changes in circulation occurring after birth have been the subject of numerous studies, and there is a considerable variation among species in, e.g., mechanisms of closure of the foramen ovale (cell proliferation closing multiple foramina in birds or flap-like valve sealing the double septum in mammals [98]). In the adult body, the following remnants of prenatal shunts (Fig. 11.3) can be found. The arterial duct (ductus arteriosus), connecting the pulmonary artery with the aortic arch, obliterates

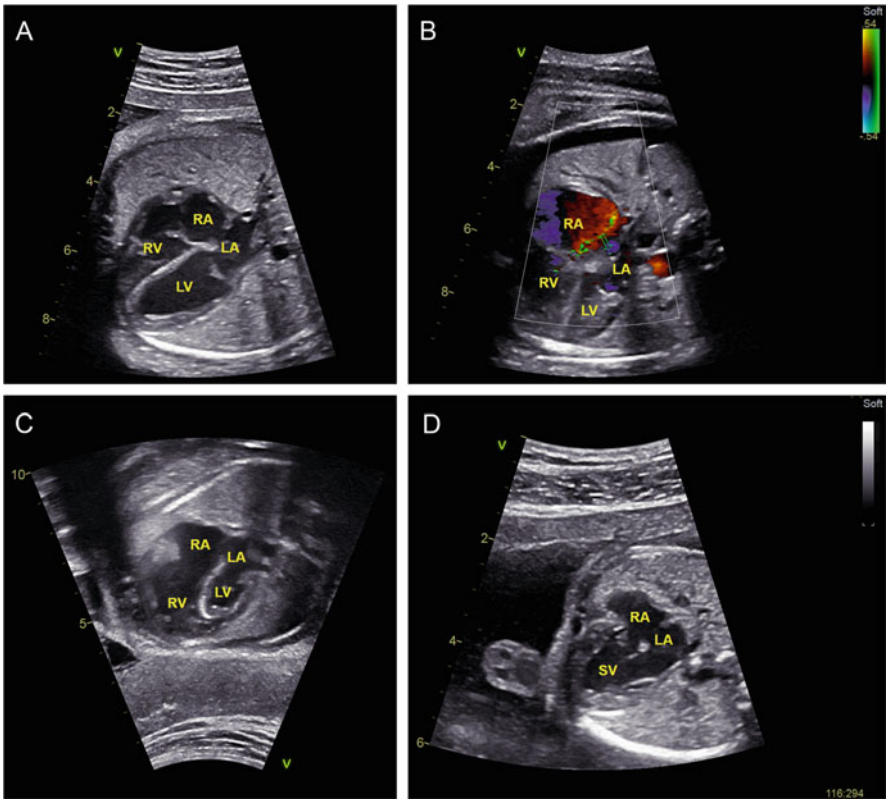

Fig. 11.4 Examples of hemodynamically significant human fetal heart anomalies discovered during fetal ultrasonographic evaluation. (**a**) Normal heart morphology, physiological fetal circulation. Symmetry of left (LA) and right atrium (RA), left (LV) and right ventricle (RV). (**b**) Premature closure of foramen ovale (arrow) resulting to dilation of right ventricle (RV), right atrium (RA), severe tricuspid regurgitation, and pleural effusions. Left atrium (LA) and left ventricle (LV) with reduced volume. (**c**) HLHS with small fibroelastic left ventricle (LV) and left atrium (LA). Compensatory enlargement of right ventricle (RV) and right atrium (RA). Compare with Fig. 11.2. (**d**). Single ventricle (SV)—double inlet left, left atrium (LA), right atrium (RA)

and becomes the arterial ligament (ligamentum arteriosum); persistence of this communication (PDA, persistent ductus arteriosus) is by some regarded as the most common (extracardiac) congenital heart disease, fortunately easily correctable nowadays either pharmacologically or via transcathetral approach [99]. The umbilical artery obliterates as well and becomes the round ligament of the liver (the segment between the umbilicus and entrance to the liver) and ligamentum venosum (between the porta hepatis and inferior caval vein), respectively. The obliterated umbilical arteries create peritoneal folds on the anterior abdominal wall called the medial umbilical ligaments. In the interatrial septum, the oval foramen leaves a depression called the oval fossa. Persistence or inadequate anatomical closure of this structure is called a patent foramen ovale (PFO) and may be found in up to 20% of the general population.

Interesting parallels can be gathered by comparing some forms of congenital heart disease with situation found in the poikilotherm vertebrates (Fig. 11.5).

In the fish (see Fig. 11.5**a**), the circulatory system with a single ventricle pumps blood to the gills, where it becomes oxygenated and is distributed to the rest of the body, could be compared to Fontan circulation. The fundamental difference is that in this palliation, it is the low-pressure pulmonary circulation that is perfused without the direct pumping force. The main anatomical difference between a typical adult fish and amphibian heart lies in the presence of the two atria instead of one, with a conus arteriosus, which partially divides the outflow tract [100, 101]. This conus arteriosus delivers equal pressures to the parallel pulmocutaneous and systemic vascular circuits [102, 103]. When we compare ectothermic vertebrates with endotherms, the amphibian hemodynamical pattern is similar to that of the chick embryo [33] except for the heart rate, which has a decreasing tendency in amphibians [104, 105]. However, amphibian cardiac hemodynamics and morphology is also connected with metamorphosis and the transition from aquatic lifestyle as well as with changes linked to breathing by lungs/skin [106, 107]. This should be taken into consideration as well.

Reptiles played an essential role in the evolution of mammals and birds [108, 109]. The reptilian heart takes specific position among the vertebrate cardiovascular systems by possession of different ventricular septation levels (Fig. 11.5b) from nonseptated (e.g. leopard geckos) [110], almost septated (pythons and monitor lizards) [111], to fully septated ventricle (crocodylians) [112, 113]. A fundamental feature of all reptilian circulatory systems lies in the ability to regulate the distribution of cardiac output between systemic and pulmonary circuits via the cardiac shunts [114]. In addition, reptiles have complete right and left aortic arches, unique among Amniota [115, 116]. Thanks to this specific reptilian heart morphology, the mixing of oxygenated and deoxygenated blood results in the hemodynamical specific blood flows—the cardiac shunts. The cardiac shunts can be described as Left–Right (L-R) and Right–Left (R-L) shunts, which are determined by the direction of blood flow [114, 117]. A R-L shunt represents recirculation of systemic deoxygenated blood back into the systemic arterial circulation by bypassing the lungs. In contrast, a L-R shunt represents the recirculation of pulmonary oxygenated blood to the pulmonary circulation [118].

Incomplete septation in the reptilian ventricle mimics ventricular septum defects in mammals (Fig. 11.5**c**). Since the crocodylians have full ventricular septation, the L-R shunt is not possible [119, 120]. Moreover, except the R-L cardiac shunt, there is also possibility of mixing the oxygenated and deoxygenated blood via the foramen of Panizza, which is extracardiac between the right and left aortic arches in crocodylians [121]. However, surgical closure of this shunt [117] did not in any measurable way impede growth and survival of young alligators. This arrangement is reminiscent of aortic-pulmonary window, and the double aortic arch is also sometimes encountered in humans, where it can cause breathing and swallowing difficulties by constricting the aorta and esophagus, respectively (Fig. 11.5**c**). In endotherms (birds and mammals), cardiac shunts are detrimental, but in reptiles this condition is often considered as a derived trait, which, however, could arise from

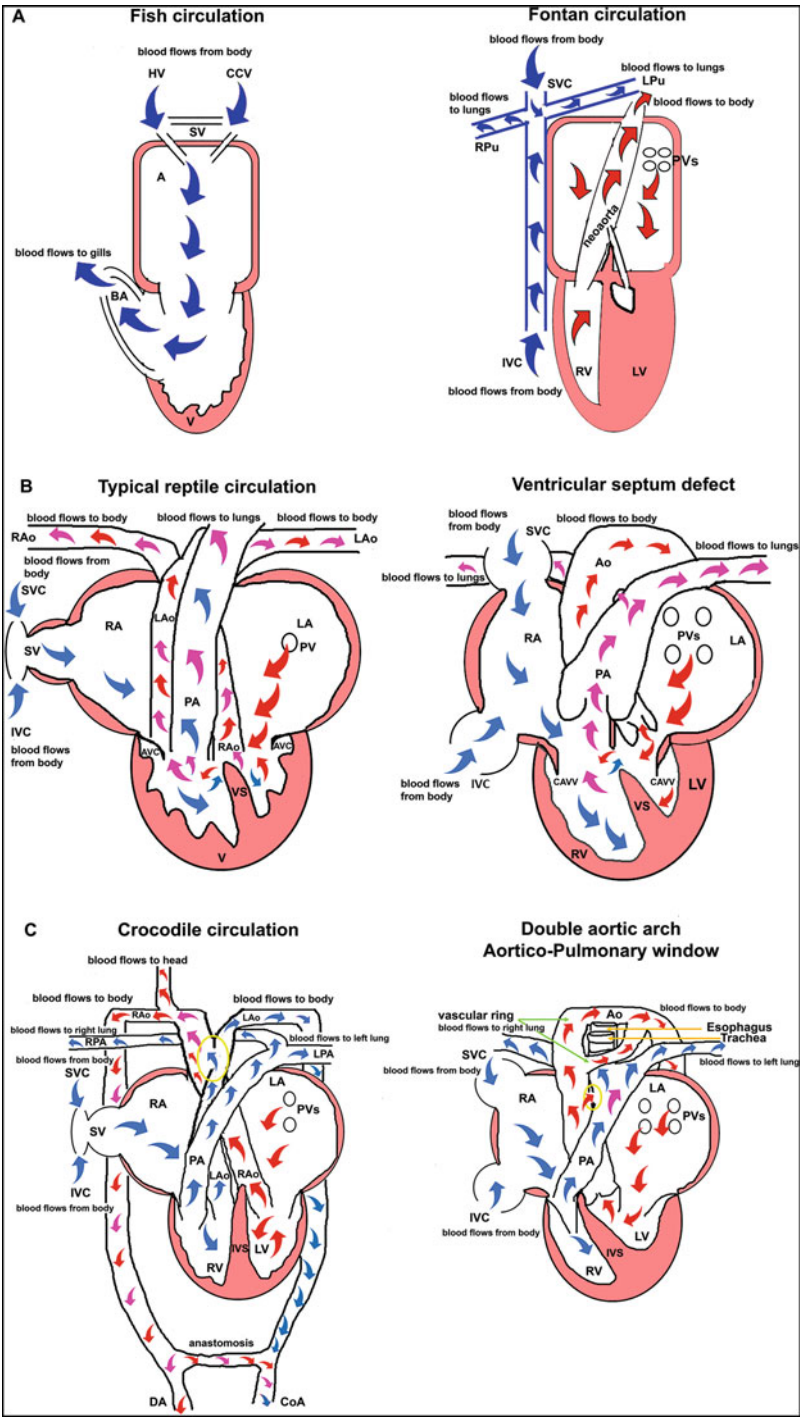

Fig. 11.5 Comparison of poikilotherm hearts with some examples of human congenital heart disease. (**a**) Fontan circulation is similar to the arrangement known in fish, except that the fish heart

embryonic development [111, 114]. Regardless of species, mechanisms for regulating intracardiac shunting involve changes in the balance between peripheral resistance of the pulmonary and systemic circulations and adjustments in cardiac performance [122]. The presence of two aortae also does not cause them any problems, as they never join into a single dorsal aorta (Fig. 11.5c). Thus, the arrangement of the heart of the poikilotherms is optimized for their lifestyle but is not suitable for active homeotherms with two differentially pressurized circuits. This restricts the range of conditions compatible with survival in congenitally malformed hearts.

11.8 Conclusions

Hemodynamic studies can help us to understand the etiology of cardiac birth defects in humans because they also imply that fluctuations in blood flow in utero could have significant consequences for cardiac morphogenesis [123]. This might be a promising avenue for searching novel pathways in cardiac regeneration, especially when coupled with the phylogenetic approach. There are strong similarities in hemodynamics in different vertebrate species during development, despite considerable differences among adults. Modeling fluid dynamics could help us to make quantitative predictions prior to actual surgical procedures altering blood flow patterns.

Acknowledgments This study was supported by the Next Generation EU EXCELES, ID: LX22NPO5104, Ministry of Education PROGRES-Q38/LF1/5, Cooperation 207029 Cardiovascular Science, and institutional funding from the Academy of Sciences of the Czech Republic RVO: 67985823. Further support comes from the Grant Agency of the Czech Republic 18-03461S and 22-05271S, and the Czech Health Research Council NU21-02-00402. Royal Society Newton International Fellowship funded under the Newton Fund: NIF\R1\202197.

Fig. 11.5 (continued) is venous, while the Fontan heart pumps the oxygenated blood. (**b**) Comparison of a typical reptilian heart with a ventricular septum defect (VSD). The reason while the later causes symptoms is different regulation of vascular tone and larger difference in systemic and pulmonary resistance in homeotherms. (**c**). Crocodylian heart, while fully septated, presents a secondary possibility of blood shunting, potentially advantageous in diving; similar situation in humans results in unfavorable left-to-right shunting. The diagram also shows how keeping both fourth aortic arches in reptiles does not interfere with the respiration or swallowing due to their different anatomical arrangement

A, atrium; Ao, aorta; AVC, atrioventricular canal; BA, bulbus arteriosus; CAVV, common atrioventricular valve; CCV, common cardiac vein; CoA, coeliac artery; DA, dorsal artery; HV, hepatic vein; IVC, inferior caval vein; IVS, interventricular septum; LA, left atrium; LAo, left aortic arch; LPA, left pulmonary artery; LPu, left pulmonary artery; LV, left ventricle; PA, pulmonary artery; PVs, pulmonary veins; RA, right atrium; RAo, right aortic arch; RPA, right pulmonary artery; RPu, right pulmonary artery; RV, right ventricle; SV, sinus venosus; SVC, superior caval vein; V, ventricle; VS, ventricular septum; red arrows, oxygenated blood; blue arrows, deoxygenated blood; magenta arrows, mixed blood

References

1. van den Hoff MJ, Kruithof BP, Moorman AF, Markwald RR, Wessels A. Formation of myocardium after the initial development of the linear heart tube. Dev Biol. 2001;240:61–76.
2. Forouhar AS, Liebling M, Hickerson A, Nasiraei-Moghaddam A, Tsai HJ, Hove JR, Fraser SE, Dickinson ME, Gharib M. The embryonic vertebrate heart tube is a dynamic suction pump. Science. 2006;312:751–3.
3. Harvey RP. Patterning the vertebrate heart. Nat Rev Genet. 2002;3:544–56.
4. Jensen B, Christoffels VM. Reptiles as a model system to study heart development, vol. 12. Cold Spring Harb Perspect Biol; 2020. p. a037226.
5. Lillywhite HB, Zippel KC, Farrell AP. Resting and maximal heart rates in ectothermic vertebrates. Comp Biochem Physiol A Mol Integr Physiol. 1999;124:369–82.
6. Goenezen S, Rennie MY, Rugonyi S. Biomechanics of early cardiac development. Biomech Model Mechanobiol. 2012;11:1187–204.
7. Jones EA, le Noble F, Eichmann A. What determines blood vessel structure? Genetic prespecification vs. hemodynamics. Physiology (Bethesda). 2006;21:388–95.
8. Hove JR, Koster RW, Forouhar AS, Acevedo-Bolton G, Fraser SE, Gharib M. Intracardiac fluid forces are an essential epigenetic factor for embryonic cardiogenesis. Nature. 2003;421:172–7.
9. Sedmera D, Pexieder T, Rychterova V, Hu N, Clark EB. Remodeling of chick embryonic ventricular myoarchitecture under experimentally changed loading conditions. Anat Rec. 1999;254:238–52.
10. Midgett M, Rugonyi S. Congenital heart malformations induced by hemodynamic altering surgical interventions. Front Physiol. 2014;5:287.
11. Jensen B, Wang T. Hemodynamic consequences of cardiac malformations in two juvenile ball pythons (Python regius). J Zoo Wildl Med. 2009;40:752–6.
12. Stainier DY, Fouquet B, Chen JN, Warren KS, Weinstein BM, Meiler SE, Mohideen MA, Neuhauss SC, Solnica-Krezel L, Schier AF, Zwartkruis F, Stemple DL, Malicki J, Driever W, Fishman MC. Mutations affecting the formation and function of the cardiovascular system in the zebrafish embryo. Development. 1996;123:285–92.
13. Manner J, Wessel A, Yelbuz TM. How does the tubular embryonic heart work? Looking for the physical mechanism generating unidirectional blood flow in the valveless embryonic heart tube. Dev Dyn. 2010;239:1035–46.
14. Taber LA, Zhang J, Perucchio R. Computational model for the transition from peristaltic to pulsatile flow in the embryonic heart tube. J Biomech Eng. 2007;129:441–9.
15. Lee J, Moghadam ME, Kung E, Cao H, Beebe T, Miller Y, Roman BL, Lien CL, Chi NC, Marsden AL, Hsiai TK. Moving domain computational fluid dynamics to interface with an embryonic model of cardiac morphogenesis. PLoS One. 2013;8:e72924.
16. Gierten J, Pylatiuk C, Hammouda OT, Schock C, Stegmaier J, Wittbrodt J, Gehrig J, Loosli F. Automated high-throughput heartbeat quantification in medaka and zebrafish embryos under physiological conditions. Sci Rep. 2020;10:2046.
17. Bagatto B, Burggren W. A three-dimensional functional assessment of heart and vessel development in the larva of the zebrafish (Danio rerio). Physiol Biochem Zool. 2006;79:194–201.
18. Salehin N, Villarreal C, Teranikar T, Dubansky B, Lee J, Chuong CJ. Assessing pressure-volume relationship in developing heart of zebrafish in-vivo. Ann Biomed Eng. 2021;49:2080–93.
19. Bartman T, Walsh EC, Wen KK, McKane M, Ren J, Alexander J, Rubenstein PA, Stainier DY. Early myocardial function affects endocardial cushion development in zebrafish. PLoS Biol. 2004;2:E129.
20. Vermot J, Forouhar AS, Liebling M, Wu D, Plummer D, Gharib M, Fraser SE. Reversing blood flows act through klf2a to ensure normal valvulogenesis in the developing heart. PLoS Biol. 2009;7:e1000246.

21. Banjo T, Grajcarek J, Yoshino D, Osada H, Miyasaka KY, Kida YS, Ueki Y, Nagayama K, Kawakami K, Matsumoto T, Sato M, Ogura T. Haemodynamically dependent valvulogenesis of zebrafish heart is mediated by flow-dependent expression of miR-21. Nat Commun. 2013;4:1978.
22. Steed E, Faggianelli N, Roth S, Ramspacher C, Concordet JP, Vermot J. klf2a couples mechanotransduction and zebrafish valve morphogenesis through fibronectin synthesis. Nat Commun. 2016;7:11646.
23. Hsu JJ, Vedula V, Baek KI, Chen C, Chen J, Chou MI, Lam J, Subhedar S, Wang J, Ding Y, Chang CC, Lee J, Demer LL, Tintut Y, Marsden AL, Hsiai TK. Contractile and hemodynamic forces coordinate Notch1b-mediated outflow tract valve formation. JCI Insight. 2019;5:e124460.
24. Foo YY, Pant S, Tay HS, Imangali N, Chen N, Winkler C, Yap CH. 4D modelling of fluid mechanics in the zebrafish embryonic heart. Biomech Model Mechanobiol. 2020;19:221–32.
25. Lee J, Vedula V, Baek KI, Chen J, Hsu JJ, Ding Y, Chang CC, Kang H, Small A, Fei P, Chuong CM, Li R, Demer L, Packard RRS, Marsden AL, Hsiai TK. Spatial and temporal variations in hemodynamic forces initiate cardiac trabeculation. JCI Insight. 2018;3:e96672.
26. Peshkovsky C, Totong R, Yelon D. Dependence of cardiac trabeculation on neuregulin signaling and blood flow in zebrafish. Dev Dyn. 2011;240:446–56.
27. Rasouli SJ, Stainier DYR. Regulation of cardiomyocyte behavior in zebrafish trabeculation by Neuregulin 2a signaling. Nat Commun. 2017;8:15281.
28. Battista NA, Lane AN, Liu J, Miller LA. Fluid dynamics in heart development: effects of hematocrit and trabeculation. Math Med Biol. 2018;35:493–516.
29. Ribatti D. The chick embryo chorioallantoic membrane (CAM). A multifaceted experimental model. Mech Dev. 2016;141:70–7.
30. Jenkins MW, Rothenberg F, Roy D, Nikolski VP, Hu Z, Watanabe M, Wilson DL, Efimov IR, Rollins AM. 4D embryonic cardiography using gated optical coherence tomography. Opt Express. 2006;14:736–48.
31. Jenkins MW, Adler DC, Gargesha M, Huber R, Rothenberg F, Belding J, Watanabe M, Wilson DL, Fujimoto JG, Rollins AM. Ultrahigh-speed optical coherence tomography imaging and visualization of the embryonic avian heart using a buffered Fourier domain mode locked laser. Opt Express. 2007;15:6251–67.
32. Peterson LM, Jenkins MW, Gu S, Barwick L, Watanabe M, Rollins AM. 4D shear stress maps of the developing heart using Doppler optical coherence tomography. Biomed Opt Express. 2012;3:3022–32.
33. Hu N, Clark EB. Hemodynamics of the stage 12 to stage 29 chick embryo. Circ Res. 1989;65:1665–70.
34. Midgett M, Chivukula VK, Dorn C, Wallace S, Rugonyi S. Blood flow through the embryonic heart outflow tract during cardiac looping in HH13-HH18 chicken embryos. J R Soc Interface. 2015;12:20150652.
35. Oosterbaan AM, Ursem NT, Struijk PC, Bosch JG, van der Steen AF, Steegers EA. Doppler flow velocity waveforms in the embryonic chicken heart at developmental stages corresponding to 5-8 weeks of human gestation. Ultrasound Obstet Gynecol. 2009;33:638–44.
36. Ho S, Chan WX, Phan-Thien N, Yap CH. Organ dynamics and hemodynamic of the whole HH25 avian embryonic heart, revealed by ultrasound biomicroscopy, boundary tracking, and flow simulations. Sci Rep. 2019;9:18072.
37. Ho S, Tan GXY, Foo TJ, Phan-Thien N, Yap CH. Organ dynamics and fluid dynamics of the HH25 Chick embryonic cardiac ventricle as revealed by a novel 4D high-frequency ultrasound imaging technique and computational flow simulations. Ann Biomed Eng. 2017;45:2309–23.
38. Liu A, Yin X, Shi L, Li P, Thornburg KL, Wang R, Rugonyi S. Biomechanics of the chick embryonic heart outflow tract at HH18 using 4D optical coherence tomography imaging and computational modeling. PLoS One. 2012;7:e40869.
39. Bharadwaj KN, Spitz C, Shekhar A, Yalcin HC, Butcher JT. Computational fluid dynamics of developing avian outflow tract heart valves. Ann Biomed Eng. 2012;40:2212–27.

40. Ho S, Chan WX, Rajesh S, Phan-Thien N, Yap CH. Fluid dynamics and forces in the HH25 avian embryonic outflow tract. Biomech Model Mechanobiol. 2019;18:1123–37.
41. Kowalski WJ, Dur O, Wang Y, Patrick MJ, Tinney JP, Keller BB, Pekkan K. Critical transitions in early embryonic aortic arch patterning and hemodynamics. PLoS One. 2013;8: e60271.
42. Lindsey SE, Menon PG, Kowalski WJ, Shekhar A, Yalcin HC, Nishimura N, Schaffer CB, Butcher JT, Pekkan K. Growth and hemodynamics after early embryonic aortic arch occlusion. Biomech Model Mechanobiol. 2015;14(4):735–51.
43. Hogers B, DeRuiter MC, Gittenberger-de Groot AC, Poelmann RE. Unilateral vitelline vein ligation alters intracardiac blood flow patterns and morphogenesis in the chick embryo. Circ Res. 1997;80:473–81.
44. Clark EB, Hu N, Frommelt P, Vandekieft GK, Dummett JL, Tomanek RJ. Effect of increased pressure on ventricular growth in stage 21 chick embryos. Am J Phys. 1989;257:H55–61.
45. Clark EB, Hu N, Rosenquist GC. Effect of conotruncal constriction on aortic-mitral valve continuity in the stage 18, 21 and 24 chick embryo. Am J Cardiol. 1984;53:324–7.
46. Tobita K, Garrison JB, Li JJ, Tinney JP, Keller BB. Three-dimensional myofiber architecture of the embryonic left ventricle during normal development and altered mechanical loads. Anat Rec A Discov Mol Cell Evol Biol. 2005;283:193–201.
47. Taber LA, Chabert S. Theoretical and experimental study of growth and remodeling in the developing heart. Biomechan Model Mechanobiol. 2002;1:29–43.
48. Sedmera D, Hu N, Weiss KM, Keller BB, Denslow S, Thompson RP. Cellular changes in experimental left heart hypoplasia. Anat Rec. 2002;267:137–45.
49. Tomanek RJ, Hu N, Phan B, Clark EB. Rate of coronary vascularization during embryonic chicken development is influenced by the rate of myocardial growth. Cardiovasc Res. 1999;41:663–71.
50. Chivukula VK, Goenezen S, Liu A, Rugonyi S. Effect of outflow tract banding on embryonic cardiac hemodynamics. J Cardiovasc Dev Dis. 2016;3:1.
51. Rychter Z, Rychterova V, Lemez L. Formation of the heart loop and proliferation structure of its wall as a base for ventricular septation. Herz. 1979;4:86–90.
52. Tobita K, Keller BB. Right and left ventricular wall deformation patterns in normal and left heart hypoplasia chick embryos. Am J Physiol Heart Circ Physiol. 2000;279:H959–69.
53. Tobita K, Schroder EA, Tinney JP, Garrison JB, Keller BB. Regional passive ventricular stress-strain relations during development of altered loads in chick embryo. Am J Physiol Heart Circ Physiol. 2002;282:H2386–96.
54. Pesevski Z, Kvasilova A, Stopkova T, Nanka O, Drobna Krejci E, Buffinton C, Kockova R, Eckhardt A, Sedmera D. Endocardial Fibroelastosis is secondary to hemodynamic alterations in the Chick embryonic model of Hypoplastic left heart syndrome. Dev Dyn. 2018;247:509–20.
55. McElhinney DB, Vogel M, Benson CB, Marshall AC, Wilkins-Haug LE, Silva V, Tworetzky W. Assessment of left ventricular endocardial fibroelastosis in fetuses with aortic stenosis and evolving hypoplastic left heart syndrome. Am J Cardiol. 2010;106:1792–7.
56. deAlmeida A, McQuinn T, Sedmera D. Increased ventricular preload is compensated by myocyte proliferation in normal and hypoplastic fetal chick left ventricle. Circ Res. 2007;100:1363–70.
57. Friedman KG, Sleeper LA, Freud LR, Marshall AC, Godfrey ME, Drogosz M, Lafranchi T, Benson CB, Wilkins-Haug LE, Tworetzky W. Improved technical success, postnatal outcome and refined predictors of outcome for fetal aortic valvuloplasty. Ultrasound Obstet Gynecol. 2018;52:212–20.
58. Tworetzky W, McElhinney DB, Marx GR, Benson CB, Brusseau R, Morash D, Wilkins-Haug LE, Lock JE, Marshall AC. In utero Valvuloplasty for pulmonary atresia with Hypoplastic right ventricle: techniques and outcomes. Pediatrics. 2009;124:e510–8.
59. Ho S, Chan WX, Yap CH. Fluid mechanics of the left atrial ligation chick embryonic model of hypoplastic left heart syndrome. Biomech Model Mechanobiol. 2021;20:1337–51.

60. Keller BB, MacLennan MJ, Tinney JP, Yoshigi M. In vivo assessment of embryonic cardiovascular dimensions and function in day-10.5 to −14.5 mouse embryos. Circ Res. 1996;79:247–55.
61. Yu Q, Leatherbury L, Tian X, Lo CW. Cardiovascular assessment of fetal mice by in utero echocardiography. Ultrasound Med Biol. 2008;34:741–52.
62. Wang S, Lakomy DS, Garcia MD, Lopez AL 3rd, Larin KV, Larina IV. Four-dimensional live imaging of hemodynamics in mammalian embryonic heart with Doppler optical coherence tomography. J Biophotonics. 2016;9:837–47.
63. Hoog TG, Fredrickson SJ, Hsu CW, Senger SM, Dickinson ME, Udan RS. The effects of reduced hemodynamic loading on morphogenesis of the mouse embryonic heart. Dev Biol. 2018;442:127–37.
64. Saiki Y, Konig A, Waddell J, Rebeyka IM. Hemodynamic alteration by fetal surgery accelerates myocyte proliferation in fetal Guinea pig hearts. Surgery. 1997;122:412–9.
65. Sedmera D, Kucera P, Kolar F, Thompson RP. Proliferative responses to myocardial remodeling in the developing heart. In: Artman M, Benson DW, Srivastava D, Nakazawa M, editors. Cardiovascular development and congenital malformations: molecular and genetic mechanisms. Malden: Blackwell Publishing; 2005. p. 47–51.
66. Rahman A, DeYoung T, Cahill LS, Yee Y, Debebe SK, Botelho O, Seed M, Chaturvedi RR, Sled JG. A mouse model of hypoplastic left heart syndrome demonstrating left heart hypoplasia and retrograde aortic arch flow. Dis Model Mech. 2021;14:dmm049077.
67. Yashiro K, Shiratori H, Hamada H. Haemodynamics determined by a genetic programme govern asymmetric development of the aortic arch. Nature. 2007;450:285–8.
68. Reddy VM, Liddicoat JR, Klein JR, Wampler RK, Hanley FL. Long-term outcome after fetal cardiac bypass: fetal survival to full term and organ abnormalities. J Thorac Cardiovasc Surg. 1996;111:536–44.
69. Liu XB, Zhou CB, Chen JM, Cen JZ, Xu G, Zhuang J. A fetal goat model of cardiopulmonary bypass with cardioplegic arrest and hemodynamic assessment. J Thorac Cardiovasc Surg. 2011;142:1562–6.
70. Strainic J. Fetal cardiac intervention for right sided heart disease: pulmonary atresia with intact ventricular septum. Birth Defects Res. 2019;111:395–9.
71. Edwards A, Menahem S, Veldman A, Schranz D, Chan Y, Nitsos I, Wong F. Fetal cardiac catheterization using a percutaneous transhepatic access technique: preliminary experience in a lamb model. Ultrasound Obstet Gynecol. 2013;42:58–63.
72. Emery SP, Kreutzer J, McCaffrey FM, Sherman FS, Simhan HN, Keller BB. The learning curve for a fetal cardiac intervention team. Minim Invasive Surg. 2010;2010:674185.
73. Edwards A, Veldman A, Nitsos I, Chan Y, Brew N, Teoh M, Menahem S, Schranz D, Wong FY. Percutaneous fetal cardiac catheterization technique for stenting the foramen ovale in a midgestation lamb model. Circ Cardiovasc Interv. 2015;8:e001967.
74. Zakko J, Blum KM, Drews JD, Wu YL, Hatoum H, Russell M, Gooden S, Heitkemper M, Conroy O, Kelly J, Carey S, Sacks M, Texter K, Ragsdale E, Strainic J, Bocks M, Wang Y, Dasi LP, Armstrong AK, Breuer C. Development of tissue engineered heart valves for percutaneous Transcatheter delivery in a fetal ovine model. JACC Basic Transl Sci. 2020;5:815–28.
75. Fishman NH, Hof RB, Rudolph AM, Heymann MA. Models of congenital heart disease in fetal lambs. Circulation. 1978;58:354–64.
76. Wong FY, Veldman A, Sasi A, Teoh M, Edwards A, Chan Y, Graupner O, Enzensberger C, Axt-Fliedner R, Black MJ, Schranz D. Induction of left ventricular hypoplasia by occluding the foramen ovale in the fetal lamb. Sci Rep. 2020;10:880.
77. Donofrio MT, Bremer YA, Moskowitz WB. Diagnosis and management of restricted or closed foramen ovale in fetuses with congenital heart disease. Am J Cardiol. 2004;94:1348–51.
78. Makikallio K, McElhinney DB, Levine JC, Marx GR, Colan SD, Marshall AC, Lock JE, Marcus EN, Tworetzky W. Fetal aortic valve stenosis and the evolution of hypoplastic left heart syndrome: patient selection for fetal intervention. Circulation. 2006;113:1401–5.

79. Eghtesady P, Michelfelder E, Altaye M, Ballard E, Hirsh R, Beekman RH 3rd. Revisiting animal models of aortic stenosis in the early gestation fetus. Ann Thorac Surg. 2007;83:631–9.
80. Morrison JL. Sheep models of intrauterine growth restriction: fetal adaptations and consequences. Clin Exp Pharmacol Physiol. 2008;35:730–43.
81. Jonker SS, Kamna D, LoTurco D, Kailey J, Brown LD. IUGR impairs cardiomyocyte growth and maturation in fetal sheep. J Endocrinol. 2018;239:253–65.
82. Morrison JL, Botting KJ, Dyer JL, Williams SJ, Thornburg KL, McMillen IC. Restriction of placental function alters heart development in the sheep fetus. Am J Physiol Regul Integr Comp Physiol. 2007;293:R306–13.
83. Niewiadomska-Jarosik K, Zamojska J, Zamecznik A, Wosiak A, Jarosik P, Stanczyk J. Myocardial dysfunction in children with intrauterine growth restriction: an echocardiographic study. Cardiovasc J Afr. 2017;28:36–9.
84. Lawrence KM, Hennessy-Strahs S, McGovern PE, Mejaddam AY, Rossidis AC, Baumgarten HD, Bansal E, Villeda M, Han J, Gou Z, Zhao S, Rychik J, Peranteau WH, Davey MG, Flake AW, Gaynor JW, Bartoli CR. Fetal hypoxemia causes abnormal myocardial development in a preterm ex utero fetal ovine model. JCI Insight. 2018;3:e124338.
85. De Smedt MC, Visser GH, Meijboom EJ. Fetal cardiac output estimated by Doppler echocardiography during mid- and late gestation. Am J Cardiol. 1987;60:338–42.
86. Sharland GK, Chita SK, Fagg NL, Anderson RH, Tynan M, Cook AC, Allan LD. Left ventricular dysfunction in the fetus: relation to aortic valve anomalies and endocardial fibroelastosis. Br Heart J. 1991;66:419–24.
87. Levin DL, Mills LJ, Weinberg AG. Hemodynamic, pulmonary vascular, and myocardial abnormalities secondary to pharmacologic constriction of the fetal ductus arteriosus. A possible mechanism for persistent pulmonary hypertension and transient tricuspid insufficiency in the newborn infant. Circulation. 1979;60:360–4.
88. Rudolph AM, Heymann MA. Cardiac output in the fetal lamb: the effects of spontaneous and induced changes of heart rate on right and left ventricular output. Am J Obstet Gynecol. 1976;124:183–92.
89. Hawkins J, Van Hare GF, Schmidt KG, Rudolph AM. Effects of increasing afterload on left ventricular output in fetal lambs. Circ Res. 1989;65:127–34.
90. Hecher K, Snijders R, Campbell S, Nicolaides K. Fetal venous, intracardiac, and arterial blood flow measurements in intrauterine growth retardation: relationship with fetal blood gases. Am J Obstet Gynecol. 1995;173:10–5.
91. Oberhoffer R, Cook AC, Lang D, Sharland G, Allan LD, Fagg NL, Anderson RH. Correlation between echocardiographic and morphological investigations of lesions of the tricuspid valve diagnosed during fetal life. Br Heart J. 1992;68:580–5.
92. Al Nafisi B, van Amerom JF, Forsey J, Jaeggi E, Grosse-Wortmann L, Yoo SJ, Macgowan CK, Seed M. Fetal circulation in left-sided congenital heart disease measured by cardiovascular magnetic resonance: a case-control study. J Cardiovasc Magn Reson. 2013;15:65.
93. Williams IA, Fifer C, Jaeggi E, Levine JC, Michelfelder EC, Szwast AL. The association of fetal cerebrovascular resistance with early neurodevelopment in single ventricle congenital heart disease. Am Heart J. 2013;165:544–550 e1.
94. Rudolph AM. Aortopulmonary transposition in the fetus: speculation on pathophysiology and therapy. Pediatr Res. 2007;61:375–80.
95. Levin DL, Mills LJ, Parkey M. Morphologic development of the pulmonary vascular bed in experimental coarctation of the aorta. Circulation. 1979;60:349–54.
96. Ruiz A, Cruz-Lemini M, Masoller N, Sanz-Cortes M, Ferrer Q, Ribera I, Martinez JM, Crispi F, Arevalo S, Gomez O, Perez-Hoyos S, Carreras E, Gratacos E, Llurba E. Longitudinal changes in fetal biometry and cerebroplacental hemodynamics in fetuses with congenital heart disease. Ultrasound Obstet Gynecol. 2017;49:379–86.
97. Llurba E, Sanchez O, Ferrer Q, Nicolaides KH, Ruiz A, Dominguez C, Sanchez-de-Toledo J, Garcia-Garcia B, Soro G, Arevalo S, Goya M, Suy A, Perez-Hoyos S, Alijotas-Reig J,

Carreras E, Cabero L. Maternal and foetal angiogenic imbalance in congenital heart defects. Eur Heart J. 2014;35:701–7.
98. Jensen B, Joyce W, Gregorovicova M, Sedmera D, Wang T, Christoffels VM. Low incidence of atrial septal defects in nonmammalian vertebrates. Evol Dev. 2019;22:e12322.
99. Zaidi M, Sorathia N, Abbasi H, Khashkhusha A, Harky A. Interventions on patent ductus arteriosus and its impact on congenital heart disease. Cardiol Young. 2020;30:1566–71.
100. Putnam JJC. *Anatomy of the heart of the Amphibia. I. Siren Lacertina.*; 1977.
101. Sedmera D, Reckova M, DeAlmeida A, Sedmerova M, Biermann M, Volejnik J, Sarre A, Raddatz E, McCarthy RA, Gourdie RG, Thompson RP. Functional and morphological evidence for a ventricular conduction system in the zebrafish and Xenopus heart. Am J Physiol Heart Circ Physiol. 2003;284:H1152–60.
102. Hillman SS, Hedrick MS, Kohl ZF. Net cardiac shunts in anuran amphibians: physiology or physics? J Exp Biol. 2014;217:2844–7.
103. Wang T, Hedrick MS, Ihmied YM, Taylor EW. Control and interaction of the cardiovascular and respiratory systems in anuran amphibians. Comp Biochem Physiol A Mol Integr Physiol. 1999;124:393–406.
104. Hou PC, Burggren WW. Cardiac output and peripheral resistance during larval development in the anuran amphibian Xenopus laevis. Am J Phys. 1995;269:R1126–32.
105. Shelton G, Jones DR. A comparative study of central blood pressures in five amphibians. J Exp Biol. 1968;49:631–43.
106. Burggren WW, Pinder AW. Ontogeny of cardiovascular and respiratory physiology in lower vertebrates. Annu Rev Physiol. 1991;53:107–35.
107. Olejnickova V, Kolesova H, Bartos M, Sedmera D, Gregorovicova M. The tale-tell heart: evolutionary tetrapod shift from aquatic to terrestrial life-style reflected in heart changes in axolotl (Ambystoma mexicanum). Dev Dyn. 2021;251(6):1004–14.
108. Laurin M, Reisz RR. A reevaluation of early Amniote phylogeny. Zool J Linn Soc-Lond. 1995;113:165–223.
109. Modesto SP, Anderson JS. The phylogenetic definition of reptilia. Syst Biol. 2004;53:815–21.
110. Gregorovicova M, Sedmera D, Jensen B. Relative position of the atrioventricular canal determines the electrical activation of developing reptile ventricles. J Exp Biol. 2018;221 (Pt 11):jeb178400.
111. Hanemaaijer J, Gregorovicova M, Nielsen JM, Moorman AFM, Wang T, Planken RN, Christoffels VM, Sedmera D, Jensen B. Identification of the building blocks of ventricular septation in monitor lizards (Varanidae). Development. 2019;146:dev177121.
112. Kvasilova A, Olejnickova V, Jensen B, Christoffels VM, Kolesova H, Sedmera D, Gregorovicova M. The formation of the atrioventricular conduction axis is linked in development to ventricular septation. J Exp Biol. 2020;223:jeb229278.
113. Jensen B, Boukens BJ, Crossley DA 2nd, Conner J, Mohan RA, van Duijvenboden K, Postma AV, Gloschat CR, Elsey RM, Sedmera D, Efimov IR, Christoffels VM. Specialized impulse conduction pathway in the alligator heart. elife. 2018;7:e32120.
114. Hicks JW. The physiological and evolutionary significance of cardiovascular shunting patterns in reptiles. News Physiol Sci. 2002;17:241–5.
115. Poelmann RE, Gittenberger-de Groot AC, Biermans MWM, Dolfing AI, Jagessar A, van Hattum S, Hoogenboom A, Wisse LJ, Vicente-Steijn R, de Bakker MAG, Vonk FJ, Hirasawa T, Kuratani S, Richardson MK. Outflow tract septation and the aortic arch system in reptiles: lessons for understanding the mammalian heart. EvoDevo. 2017;8:9.
116. White FN. Functional anatomy of the heart of reptiles. Am Zool. 1968;8:211–9.
117. Eme J, Gwalthney J, Blank JM, Owerkowicz T, Barron G, Hicks JW. Surgical removal of right-to-left cardiac shunt in the American alligator (Alligator mississippiensis) causes ventricular enlargement but does not alter apnoea or metabolism during diving. J Exp Biol. 2009;212:3553–63.
118. Stephenson A, Adams JW, Vaccarezza M. The vertebrate heart: an evolutionary perspective. J Anat. 2017;231:787–97.

119. Axelsson M, Franklin C, Ouml FC, Nilsson S, Grigg G. Dynamic anatomical study of cardiac shunting in crocodiles using high-resolution angioscopy. J Exp Biol. 1996;199:359–65.
120. Eme J, Gwalthney J, Owerkowicz T, Blank JM, Hicks JW. Turning crocodilian hearts into bird hearts: growth rates are similar for alligators with and without right-to-left cardiac shunt. J Exp Biol. 2010;213:2673–80.
121. Axelsson M, Franklin CE. The calibre of the foramen of Panizza in Crocodylus porosus is variable and under adrenergic control. J Comp Physiol B. 2001;171:341–6.
122. Burggren W. Form and function in reptilian ciruclations. Am Zool. 1987;27:5–19.
123. Sidhwani P, Yelon D. Fluid forces shape the embryonic heart: insights from zebrafish. Curr Top Dev Biol. 2019;132:395–416.

Evolutionary Aspects of Chamber Formation and Septation

12

Bjarke Jensen and Antoon F. M. Moorman

Abstract

The formed hearts of vertebrates are widely different in anatomy and performance, yet their embryonic hearts are surprisingly similar. Developmental and molecular biology are making great advances in reconciling these differences by revealing an evolutionarily conserved building plan to the vertebrate heart. This suggests that perspectives from evolution may improve our understanding of the formation of the human heart. Here, we exemplify this approach by discussing atrial and ventricular septation and the associated processes of remodeling of the atrioventricular junction and formation of the atrioventricular insulating plane.

Keywords

Heart development · Evolution · Reptiles

12.1 Introduction

With an output of 5 L per minute at rest and a systolic blood pressure of 120 mmHg, the formed human left ventricle clearly outperforms the slow beating and low-pressure ventricles of ectothermic or cold-blooded vertebrates [1]. Architecturally, the human heart is different from the heart of a shark, where pulmonary circulation is absent and four chambers are aligned in series from the sinus venosus, atrium, and ventricle to the myocardial outflow tract. Yet, the embryos of all vertebrates form an early heart with a single atrium and a single trabeculated

B. Jensen (✉) · A. F. M. Moorman
Department of Medical Biology, Amsterdam Cardiovascular Sciences, Amsterdam University Medical Centres, Amsterdam, The Netherlands
e-mail: b.jensen@amsterdamumc.nl

© The Author(s), under exclusive license to Springer Nature Switzerland AG 2024

S. Rickert-Sperling et al. (eds.), *Congenital Heart Diseases: The Broken Heart*,
Advances in Experimental Medicine and Biology 1441,
https://doi.org/10.1007/978-3-031-44087-8_12

ventricle. Further, the electrocardiograms of embryonic and adult vertebrate hearts are strikingly similar, all with distinct P, QRS, and T waves [2, 3]. The question then arises whether the vast differences in cardiac performance and structure across adult vertebrates are simply variations of an evolutionarily conserved design? We will argue that this is the case and we will exemplify how an evolutionary perspective is informative for our understanding of congenital malformations of the human heart with regard to the late embryonic events of ventricular septation, remodeling of the atrioventricular junction, and formation of the insulating atrioventricular plane. Our understanding of the evolution of the early embryonic event of forming the heart tube from distinct populations of mesoderm, the so-called heart fields, has recently been greatly advanced and for this discussion we refer to Chap. 2.

12.2 An Evolutionarily Conserved Building Plan of the Developing Heart

During development, all vertebrates form a heart tube with no anatomically distinct pacemaker. Instead, a gradient of automaticity is present from the intake to the outflow so that the heartbeat initiates at the venous pole [4]. Soon thereafter, the heart tube loops and acquires an atrium and a ventricle by ballooning at the outer curvatures (Fig. 12.1**a**–**b**). The flanking regions remain tube-like; these are the sinu-atrial border, the floor of the atrium, the atrioventricular canal, the inner curvature of the ventricle, and the myocardial outflow tract (Fig. 12.1**b**). The ballooning atrium and ventricle consist of "working myocardium" and have faster electrical propagation and contraction than the remaining heart tube myocardium. There are no valves, but only cushions in the embryonic heart. Therefore, the slow and sustained contractions of the heart tube myocardium of the atrioventricular canal and the myocardial outflow tract are important to maintain unidirectional flow [5]. This "electrophysiological patterning" of the heart is known to reflect in the working myocardium the rich expression of genes involved in the propagation of the depolarizing impulse (calcium and sodium channels with voltage sensitivity), conduction (gap junction proteins), and excitation–contraction coupling (sarcomeric and calcium handling proteins) (Fig. 12.1**b**) [6, 7].

The division of the embryonic heart into fast and slow propagating chambers and junctions can give rise to an almost adult-like ECG with distinct P, QRS, and T waves [8]. Similar regions are present in the adult hearts of fishes and amphibians, except in the oldest lineages of extant vertebrates (hagfishes) where a myocardial outflow tract is absent. Also, in most teleost bony fishes, e.g., the zebrafish, the myocardial outflow tract is feebly developed and the cardiac inflow is almost devoid of myocardium [9, 10].

Differentiation of the working myocardium relies on broadly expressed transcription factors like GATA binding protein 4 (*Gata4*), NK2 homeobox 5 transcription factor (*Nkx2-5*), and T-box transcription factors *Tbx5* and *Tbx20* that are expressed in gradients from inflow-to-outflow and outflow-to-inflow, respectively [11]. The remaining heart tube myocardium escapes differentiation into working myocardium

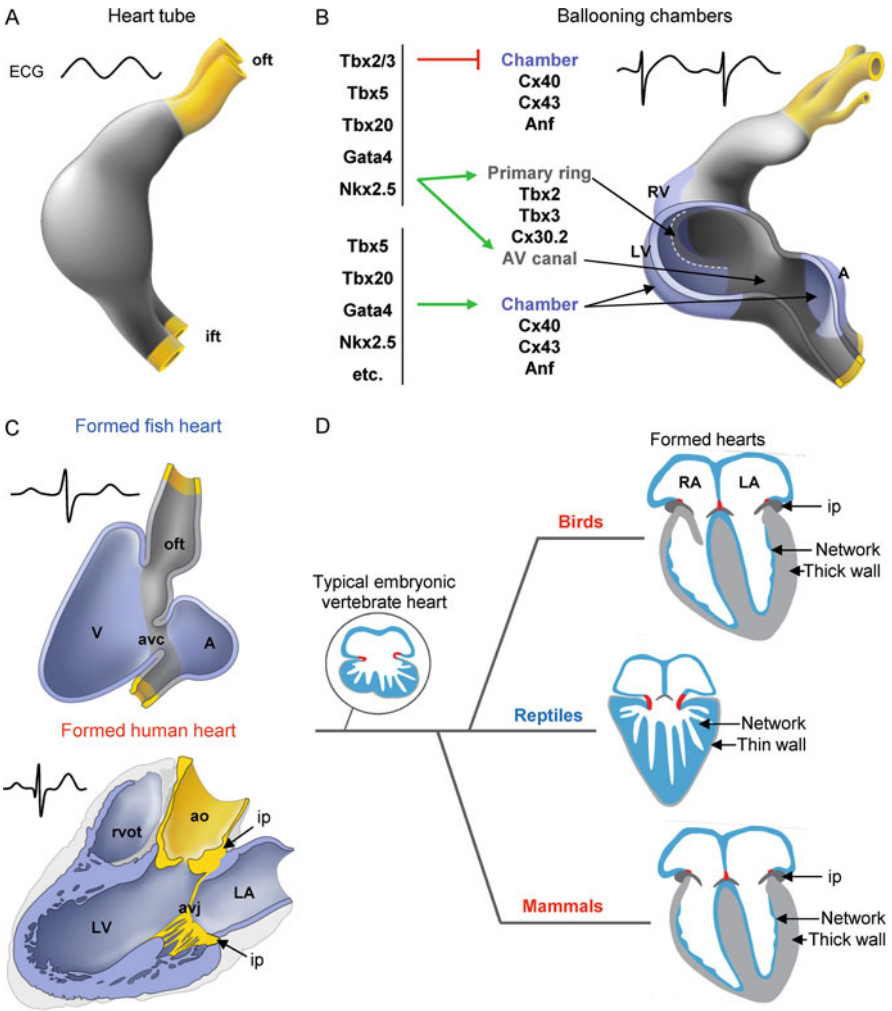

Fig. 12.1 The evolutionarily conserved building plan of the heart. (**a**) All vertebrate embryos form a heart tube with slow propagating peristaltic contractions reflected in a sinusoid ECG. (**b**) Atrial and ventricular compartments with a distinct molecular phenotype balloon out (blue) and due to faster propagation, there the electrocardiogram (ECG) acquires an adult-like profile. Full ventricular septation in mammals and birds coincides with a primary ring that expresses the Bmp2/Tbx3 pathway. (**c**) The configuration of (**b**) is essentially the scaffold of the adult fish heart, except that there is no primary ring, and it even resembles the systemic side of the formed human heart. (**d**) The atrioventricular conduction axis is established in the embryo with a slow propagating atrioventricular canal (red) and a fast propagating trabeculated ventricle (blue) with a thin compact wall (light grey). This design is maintained in ectothermic vertebrates and modified in birds and mammals by the presence of the ventricular septum, thickened ventricular walls, and an insulating plane (ip). Modified from [50]

due to transcriptional repression. The repressive action of the pathway of bone morphogenetic protein 2/4 (*Bmp2/4*)-*Tbx2/3* appears very important [12] and is regulated upstream by the signaling pathways of Notch [13], Wnt/β-catenin [14], and activated by colocalization with *Gata4* [15] (Fig. 12.1**b**). This model of transcriptional regulation of chamber formation largely has been unraveled in mechanistic studies in mice, but we and others have shown a similar pattern of expression of transcription factors in all vertebrate classes investigated, ranging from lampreys, bony fishes, amphibians, reptiles, birds to mammals [16, 17]. During further development of mammals and birds, the non-chamber regions may acquire the phenotypes of the cardiac conduction system and *Tbx3* is expressed in the sinus node, the atrioventricular node, the His bundle, and its bundle branches [18] and functions in a very dosage-sensitive manner [19]. The Purkinje fibers, the terminal branches of the ventricular conduction system, share the molecular phenotype of the trabeculations of the embryonic ventricle and the fully formed ventricle of the ectotherms (Fig. 12.1**d**) [17]. The cardiac conduction system, thus, is built on the old scaffold of the vertebrate heart, and this may explain the great similarity in the ECGs from very different vertebrates and developmental stages (see also Chap. 7).

12.3 Origins of Chamber Septation

In mammals and birds, the early atrial and ventricular septa have a mesenchymal cap that expresses the *Bmp2/Tbx3* pathway [18, 20]. This mesenchyme is continuous with the mesenchymal cushions of the atrioventricular canal and the so-called dorsal mesenchymal protrusion (or spina vestibuli of His the elder) that harbors the orifice of the pulmonary vein and contributes to the completion of atrial septation (Fig. 12.2**a**) [21, 22] (see also Part V). It is remarkable that a very similar mesenchymal configuration can be found in the heart of lungfishes (Fig. 12.2b–d). A prominent ventricular septum of trabeculated myocardium develops in the lungfishes of Africa and South America (Fig. 12.2d), but not in the heart of the Australian lungfish, which nonetheless has a pronounced mesenchymal guide in development (Fig. 12.2b–c). Benninghoff called this mesenchyme a "Leitbahn," or guide, for septation [23]. Lungfishes are the extant vertebrates that likely resemble the tetrapod ancestors the most, and they are the only fish where the heart displays partial septation of the atrium, ventricle, and outflow. Lungfish cardiogenesis, however, has only been studied morphologically [24–26], and whether the heart is in fact patterned by the *Bmp2/Tbx3* pathway, for example, is not known. Although zebrafish have a quite distant relation to tetrapods, their heart has a molecular sidedness that resembles that of mammals [27], as revealed by the expression of genes such as *meis2b* and *pitx2c* in the left side of the atrium [28] and contributions of both the first and second heart field to the ventricle [29]. This could indicate the presence of a genetic blueprint that can be co-opted for dividing the cardiac chambers and which is much older than the lungfish lineage (Dipnoi).

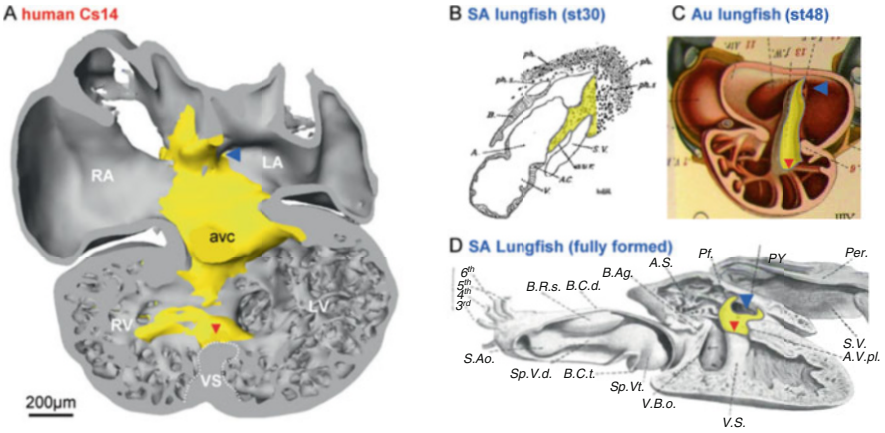

Fig. 12.2 Mesenchyme reflects the embryonic cardiac building plan. (**a**) Dorsal half of the embryonic human heart with mesenchyme (yellow) associated with the orifice of the pulmonary vein (blue arrowhead), atrial septum, cushions of the atrioventricular canal (avc), and the crest of the ventricular septum (red arrowhead). (**b**) In the embryonic South American lungfish, a dorsal mesenchymal protrusion harboring the pulmonary vein precursors enters the atrium. (**c**) The cardiac mesenchyme in the embryo of the Australian lungfish associates with the orifice of the pulmonary vein, atrial septum, cushion of the atrioventricular canal, and ventricular trabeculations (red arrowhead). (**d**) Right half of the fully formed heart of the South American lungfish showing the guiding mesenchyme associated with the orifice of the pulmonary vein, the perforated atrial septum (A.S.), and the crest of the ventricular septum (V.S.). (**b**, **d**) are modified from [26], (**c**) is modified from [24]

12.4 Atrial Septation

Human and other placental mammals, or Eutherians, are the only tetrapods to form the atrial septum from the merger of the primary and secondary atrial septum (Fig. 12.3a) (see Part III for an in-depth description of atrial septation in mouse and human). The primary atrial septum is the only atrial septum in all other tetrapods, that is, amphibians, reptiles, birds, and monotreme and marsupial mammals [30, 31] (Fig. 12.3b–c). Interestingly, these animals have a lower incidence of interatrial shunts than the incidence of persistent foramen ovale which occurs in approximately one-quarter of most placental mammals [32]. Paradoxically, it appears that placental mammals have evolved a less efficient formation of the atrial septum.

The first stages of atrial septation are the same in tetrapods, and they occur together with the first appearance of the atriums (Fig. 12.3d, schemes a-c). The secondary atrial septum of placental mammals, in contrast, develops prenatally in mouse and in the second trimester in human and thus much later. Nonetheless, it appears that all components of the primary and secondary atrial septums can be found in reptiles (Fig. 12.3d, schemes b and c'), including myocardialization of mesenchyme [32]. Only these components may be less developed. The most

important role of the secondary septum is after birth, when it is needed to close the foramen ovale (Fig. 12.3d, schemes e–f). In fact, it is the foramen ovale that appears unique to placental mammals [31]. The foramen ovale develops from the miniscule secondary perforations to primary atrial septum (Fig. 12.3d, schemes c-d). Similar secondary perforations develop in other terapods, and they are closed after birth, or hatching, by growth of the surrounding tissues (Fig. 12.3e). In ungulates, which are placental mammals, the foramen ovale appears as a vast expansion of the primary septum, whereas the foramen ovale as a single orifice occurs in rodents and human (Fig. 12.3f–h). A large foramen ovale, or foramens, is likely a low-resistance conduit for nutrient and oxygen-rich blood to reach the cardiac left side. Indeed, neonates of placental mammals can be larger than neonates of any other vertebrate group [31]. This may be the advantage that offsets the disadvantage of a less efficient formation of the atrial septum.

12.5 Evolution of Ventricular Septation and Atrioventricular Remodeling

A complete ventricular septum, including a membranous septum, is found only in mammals, crocodylians, and birds [8]. In hearts of other tetrapods, for example of the skink shown in Fig. 12.3c in which the label "ven" is positioned in lumen between ventricular muscle and the atrioventricular valve, there is no full ventricular septum. Full ventricular septum formation relies on firstly ballooning and, at least in the reptiles and birds, coalescence or compaction of trabeculations (see also Part IV) [33, 34]. Tbx5 associates with septal defects, and it is expressed in a left-right gradient over the ventricular septum of mammals, chicken, and crocodylians [35, 36], but the evolutionary precursors of the full ventricular septum are mostly identified on morphology [27, 37]. When ventricular septum formation commences in mammals and birds, the atrioventricular canal is positioned on the left of the body midline as in reptiles (Fig. 12.4a–b). Soon after, the atrioventricular canal expands and shifts rightward so that the right atrium remains in communication with the right ventricle (Fig. 12.4c). This process does not occur in ectothermic vertebrates (crocodylians excluded) [24] (Fig. 12.4d). In monitor lizards, ventricular septation is not full but it is nonetheless so developed that there is a separation of the left and right side of the ventricle in systole allowing for mammal-like blood pressures to develop [38]. Proportionally, however, the atrioventricular canal is the same as in other reptiles, suggesting that only full ventricular septation necessitates atrioventricular remodeling (Fig. 12.4d). Thus, the width of the atrioventricular canal almost doubles in mammals and birds, but not in the incompletely septated reptile hearts (Fig. 12.4d). The remodeling not only maintains the communication of the right atrium to the right ventricle in the face of full septation but it also widens the atrioventricular junction which may then better accommodate the several fold increase in cardiac output that characterizes endotherms [39].

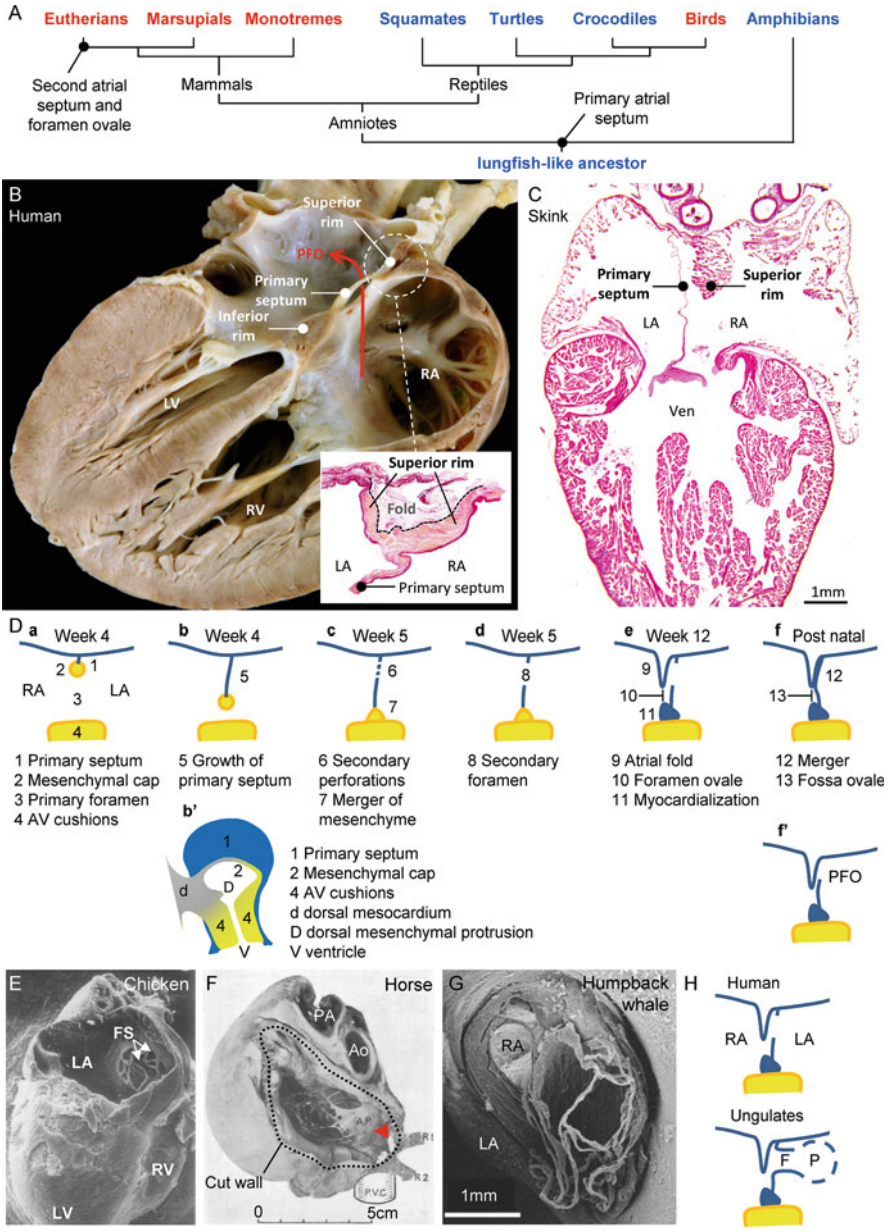

Fig. 12.3 Atrial septation. (**a**) Phylogeny of tetrapods with ectotherms in blue, endotherms in red, indicating the second atrial septum and foramen ovale evolved in placental mammals (Eutherians) only. (**b**) Anterior half of a human heart, showing PFO (patent foramen ovale), bounded by the inferior and superior rim of the second septum. Note that the histology of the insert shows that the superior rim comprises both relatively thick muscle and a fold, or the Waterston groove [51, 52], of the atrial wall. Adapted from [53], insert is adapted from [54]. (**c**) In reptiles (here a skink), the

12.6 Congenital Malformations to the Atrioventricular Junction That Resemble Embryonic and Evolutionary Primitive States

Congenital malformations of the human heart such as double inlet left ventricle and tricuspid dysplasia and atresia may be considered as an incomplete rightward shift and expansion of the atrioventricular canal [57] (see also Part XII). Indeed, tricuspid atresia is not confined to man and has been reported in multiple mammalian species [40]. It is therefore crucial to know the mechanisms and forces that underlie the rightward shift and expansion of the atrioventricular canal in animals with complete ventricular septation. In formed crocodiles and birds, the mural leaflet of the right atrioventricular junction is largely myocardial and in mammals it is only late in gestation that the mural leaflet loses its myocardium and is exclusively composed of connective tissue. In Ebstein's anomaly, which has also been reported for multiple mammalian species [40], the mural leaflet has persisting myocardium [41] (see also Part XIII).

12.7 Evolutionary Perspectives on the Atrioventricular Insulating Plane

After the onset of ventricular septation, an insulating plane of fibro-fatty tissue will form in between the atria and ventricles. Only mammals, crocodilians and birds develop an insulating plane [36, 42, 43] and only they have a complete ventricular septum and an expanded atrioventricular junction with large mural leaflets (Fig. 12.1c–d). Formation of the mural leaflets of the atrioventricular junction includes a large contribution of migrating cells derived from the atrioventricular sulcus [44]. It is then possible to view the insulating plane of fibro-fatty tissue as a settling of the migrating cells of the atrioventricular sulcus. In evolution, there may

Fig. 12.3 (continued) primary atrial septum is the only atrial septum, even if a superior rim-like large aggregate of trabecular muscle is present. Notice that the label "ven" (ventricle) is positioned between the atrioventricular valve and ventricular muscle, thus indicating that there is no full ventricular septum in this heart. Adapted from [32]. (**d**) Development of the atrial septum (time in weeks refer to human gestation). Schemes a-c occur in mammals, birds, and reptiles, whereas schemes d-f characterizes placental mammals, even if in reptiles a superior rim-like structure can form (scheme e, structure 9) and mesenchyme can myocardialize (scheme e, structure 11). (**e**) Secondary perforations (FS) in the primary atrial septum of chicken after 6 days of incubation. Adapted with permission from [55]. (**f**) Primary atrial septum (red arrowhead) of a recently born fowl, showing multiple large foramens. Adapted from [56]. (**g**) Primary atrial septum of a fetal whale, seen from the left atrial cavity, showing multiple large foramens. Adapted with permission from [57]. (**h**) While human (and rodents) have a large foramen ovale, the foramen ovale (F) of ungulates is typically a deep invagination of the primary atrial septum (P) that has multiple large foramens. Ao, aorta; LA, left atrium; LV, left ventricle; PA, pulmonary artery; RA, right atrium; RV, right ventricle

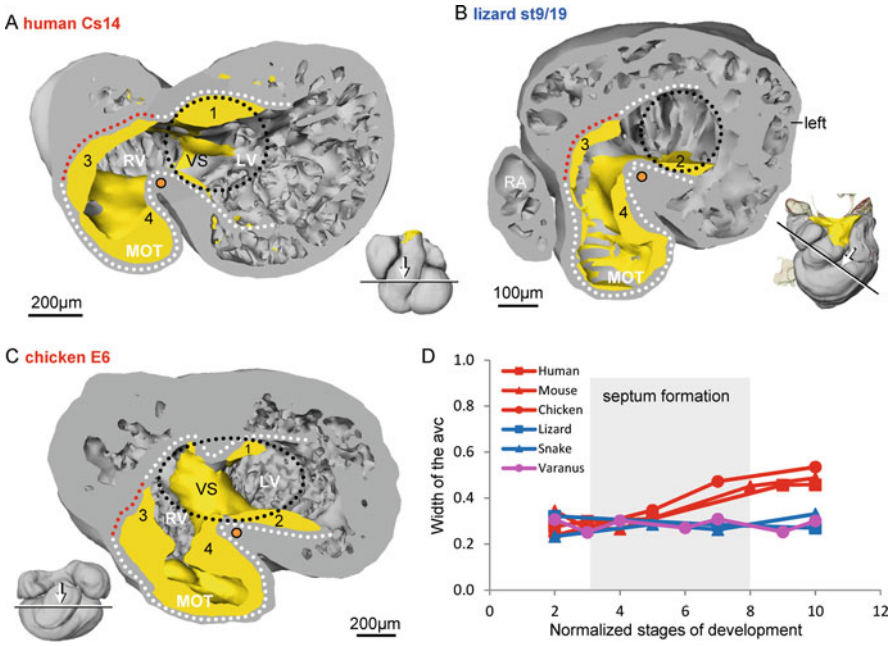

Fig. 12.4 Ventricular septation and atrioventricular remodeling. (**a**–**b**) In early embryos of all amniote vertebrates, the atrioventricular canal (outlined by black dots) is to the left of the bulboventricular fold (orange dot) as exemplified by human (**a**) and lizard (**b**). (**c**) In later embryonic stages of species with complete ventricular septation, exemplified by the chicken, the atrioventricular canal will expand to the right of the bulboventricular fold. (**d**) Quantification of the width of the atrioventricular canal. Each point is one measurement from a "four-chamber" section of the maximal width (diameter) of the atrioventricular canal and ventricle. Stage 2 is at the onset of ventricular trabeculation, stages 3–8 encompass initiation and completion of ventricular septation in the endotherms. Notice that the atrioventricular canal in monitor lizards (Varanus, in magenta) is proportionally the same as in the other reptiles, despite monitors have a functional separation of the ventricular left and right side

have been a causal chain from septum formation, to formation of large mural leaflets, and then formation of the insulating plane. In this view, the insulating plane may be of little significance for electrical insulation. The conjecture is supported by many observations that show ectothermic vertebrates have no insulating plane, while their ECGs have the same deflections as the human ECG, including a several hundred millisecond delay between atrial and ventricular activation [2, 45]. In fact, the mammal atrioventricular delay is four-fold shorter than that of reptiles and there is then a correlation between the formation of an insulating plane and shortening of the atrioventricular delay [46]. Further, studies in mice strongly suggest that the key to proper atrioventricular insulation, rather than an insulating plane, is the evolutionarily conserved molecular patterning of the atrioventricular myocardium by *Tbx2* to repress the formation of working myocardium [11, 13, 29, 47]. The insulating plane may therefore not be necessary for insulation, albeit it may provide another layer of

safety. Alternatively, it may be important to anchor the atrioventricular valves in the presence of large pressure gradients. The high-pressure ventricle of tuna fish (ca. 100 mmHg) seemingly negates this alternative because there is no insulating plane and the atrioventricular valves are imbedded in the atrioventricular myocardium [48, 49]. It is not clear whether the cells of the atrioventricular valves of ectothermic vertebrates are coupled to cardiomyocytes or are supported by the interstitial fibroblasts between the cardiomyocytes of the atrioventricular canal.

12.8 Conclusion

There are vast differences in the performance and anatomy of the hearts of endothermic and ectothermic vertebrates. Conversely, there are striking similarities between electrocardiograms and cardiac embryology of all vertebrates. Recent molecular studies are harmonizing these discrepancies by revealing an evolutionarily conserved building plan to the heart. Such advances challenge common notions and may enable us to better answer not only how, but why, the human heart acquired the particular features that are necessary for a healthy life and are prone to diseases.

Acknowledgments This space is intentionally left blank.

References

1. Burggren W, Farrell A, Lillywhite H. Vertebrate cardiovascular systems. In: Comprehensive physiology. New York: John Wiley & Sons, Inc; 2010. p. 215–308.
2. Jensen B, et al. Evolution of the sinus venosus from fish to human. J Cardiovasc Dev Dis. 2014;1:14–28.
3. Moorman AF, Christoffels VM. Cardiac chamber formation: development, genes, and evolution. Physiol Rev. 2003;83(4):1223–67.
4. Arrenberg AB, et al. Optogenetic control of cardiac function. Science. 2010;330(6006):971–4.
5. Burggren WW, et al. Comparative cardiovascular physiology: future trends, opportunities and challenges. Acta Physiol. 2014;210(2):257–76.
6. Boukens BJ, Christoffels VM. Electrophysiological patterning of the heart. Pediatr Cardiol. 2012;33(6):900–6.
7. Dobrzynski H, et al. Structure, function and clinical relevance of the cardiac conduction system, including the atrioventricular ring and outflow tract tissues. Pharmacol Ther. 2013;139(2): 260–88.
8. Poelmann RE, Gittenberger-de Groot AC. Development and evolution of the metazoan heart. Dev Dyn. 2019;248(8):634–56.
9. Icardo JM. Heart morphology and anatomy. Fish Physiol. 2017;36:1–54.
10. Satchell GH. Physiology and form of fish circulation. Cambridge: Cambridge University Press; 1991.
11. Olson EN. Gene regulatory networks in the evolution and development of the heart. Science. 2006;313(5795):1922–7.
12. Singh R, et al. Tbx2 and Tbx3 induce atrioventricular myocardial development and endocardial cushion formation. Cell Mol Life Sci. 2011;69(8):1377–89.
13. Rentschler S, et al. Notch signaling regulates murine atrioventricular conduction and the formation of accessory pathways. J Clin Invest. 2011;121(2):525–33.

14. Verhoeven MC, et al. Wnt signaling regulates atrioventricular canal formation upstream of BMP and Tbx2. Birth Defects Res A Clin Mol Teratol. 2011;91(6):435–40.
15. Stefanovic S, et al. GATA-dependent regulatory switches establish atrioventricular canal specificity during heart development. Nat Commun. 2014;5:3680.
16. Kokubo N, et al. Mechanisms of heart development in the Japanese lamprey, Lethenteron japonicum. Evol Dev. 2010;12(1):34–44.
17. Jensen B, et al. Identifying the evolutionary building blocks of the cardiac conduction system. PLoS One. 2012;7(9):e44231.
18. Hoogaars WMH, et al. The transcriptional repressor Tbx3 delineates the developing central conduction system of the heart. Cardiovasc Res. 2004;62(3):489–99.
19. Frank DU, et al. Lethal arrhythmias in Tbx3-deficient mice reveal extreme dosage sensitivity of cardiac conduction system function and homeostasis. Proc Natl Acad Sci U S A. 2012;109(3): E154–63.
20. Yamada M, et al. Expression of chick Tbx-2, Tbx-3, and Tbx-5 genes during early heart development: evidence for BMP2 induction of Tbx2. Dev Biol. 2000;228(1):95–105.
21. Mommersteeg MT, et al. The sinus venosus progenitors separate and diversify from the first and second heart fields early in development. Cardiovasc Res. 2010;87(1):92–101.
22. Briggs LE, Kakarla J, Wessels A. The pathogenesis of atrial and atrioventricular septal defects with special emphasis on the role of the dorsal mesenchymal protrusion. Differentiation. 2012;84(1):117–30.
23. Benninghoff A. Das Herz. In: Bolk L, et al., editors. Handbuch der vergleichende Anatomie der Wirbeltiere. Berlin: Urban & Schwarzenberg; 1933. p. 467–555.
24. Greil A. Entwickelungsgeschichte des Kopfes und des Blutgefässsystemes von Ceratodus forsteri. II. Die epigenetischen Erwerbungen während der Stadien 39–48, vol. 9. Denkschriften der Medizinisch-Naturwissenschaftlichen Gesellschaft zu Jena; 1913. p. 935–1492.
25. Greil A. Entwickelungsgeschichte des Kopfes und des Blutgefässsystemes von Ceratodus forsteri. I. Gesammtenentwickelung bis zum Beginn der Blutzirkulation. Denkschriften der Medizinisch-Naturwissenschaftlichen Gesellschaft zu Jena. 1908;4:661–934.
26. Robertson JI. The development of the heart and vascular system of Lepidosiren paradoxa. Quart J Micr Sci. 1913:53–132.
27. Katano W, et al. Cardiac septation in heart development and evolution. Develop Growth Differ. 2019;61(1):114–23.
28. Guerra A, et al. Distinct myocardial lineages break atrial symmetry during cardiogenesis in zebrafish. elife. 2018;7:e32833.
29. De Pater E, et al. Distinct phases of cardiomyocyte differentiation regulate growth of the zebrafish heart. Development. 2009;136(10):1633–41.
30. Röse C. Beitrage zur vergleichenden Anatomie des Herzens der Wirbelthiere. Morphol Jahrb. 1890;16:27–96.
31. Jensen B, Wang T, Moorman AFM. Evolution and development of the atrial septum. Anat Rec. 2019;302(1):32–48.
32. Jensen B, et al. Low incidence of atrial septal defects in nonmammalian vertebrates. Evol Dev. 2019;22:e12322.
33. Wessels A, Sedmera D. Developmental anatomy of the heart: a tale of mice and man. Physiol Genomics. 2003;15(3):165–76.
34. Hanemaaijer J, et al. Identification of the building blocks of ventricular septation in monitor lizards (Varanidae). Development. 2019;146:dev.177121.
35. Koshiba-Takeuchi K, et al. Reptilian heart development and the molecular basis of cardiac chamber evolution. Nature. 2009;461(7260):95–8.
36. Jensen B, et al. Specialized impulse conduction pathway in the alligator heart. elife. 2018;7: e32120.
37. Jensen B. Commemoration of comparative cardiac anatomy of the Reptilia I-IV. J Morphol. 2019;280(4):623–6.

38. Burggren WW, Johansen K. Ventricular hemodynamics in the monitor lizard Varanus exanthematicus: pulmonary and systemic pressure separation. J Exp Biol. 1982;96:343–54.
39. Jensen B. *The atrioventricular valve in the animal kingdom.* In: Wells FCA, Anderson RH, editors. *Mitral valve disease. Basic sciences and current approaches to management*. Basel: Springer Nature; 2021. p. 63–79.
40. Michaëlsson M, Ho SY. Congenital heart malformations in mammals. Singapore: World Scientific Publishing Company; 2000.
41. Sylva M, van den Hoff MJ, Moorman AF. Development of the human heart. Am J Med Genet A. 2014;164A(6):1347–71.
42. Davies F, Francis ET, King TS. The conducting (connecting) system of the crocodilian heart. J Anat. 1952;86(2):152–61.
43. Jensen B, et al. Development of the hearts of lizards and snakes and perspectives to cardiac evolution. PLoS One. 2013;8(6):e63651.
44. Wessels A, et al. Epicardially derived fibroblasts preferentially contribute to the parietal leaflets of the atrioventricular valves in the murine heart. Dev Biol. 2012;366(2):111–24.
45. Abramochkin DV, Matchkov V, Wang T. A characterization of the electrophysiological properties of the cardiomyocytes from ventricle, atrium and sinus venosus of the snake heart. J Comp Physiol B. 2020;190(1):63–73.
46. Boukens BJ, Kristensen DL, Filogonio R, Carreira LBT, Sartori MR, Abe AS, Currie S, Joyce W, Conner J, Opthof T, Crossley DA II, Wang T, Jensen B. The electrocardiogram of vertebrates: evolutionary changes from ectothermy to endothermy. Prog Biophys Mol Biol. 2019;144:16–29.
47. Aanhaanen WT, et al. Defective Tbx2-dependent patterning of the atrioventricular canal myocardium causes accessory pathway formation in mice. J Clin Invest. 2011;121(2):534–44.
48. Brill RW, Bushnell PG. In: Stevens E, editor. *The cardiovascular system of tunas*, in *fish physiology. Tuna: physiology, ecology, and evolution*, B.B.A. Cambridge: Academic Press; 2001. p. 79–120.
49. Icardo JM, Colvee E. The atrioventricular region of the teleost heart. A distinct heart segment. Anat Rec (Hoboken). 2011;294(2):236–42.
50. Jensen B, et al. Evolution and development of the building plan of the vertebrate heart. Biochim Biophys Acta. 2013;1833(4):783–94.
51. Naqvi N, McCarthy KP, Ho SY. Anatomy of the atrial septum and interatrial communications. J Thorac Dis. 2018;10(Suppl 24):S2837–47.
52. Cabrera JA, Sanchez-Quintana D. Cardiac anatomy: what the electrophysiologist needs to know. Heart. 2013;99(6):417–31.
53. Cook AC, et al. Sequential segmental analysis of the crocodilian heart. J Anat. 2017;231 (4):484–99.
54. Jensen B, Christoffels VM, Moorman AFM. An appreciation of anatomy in the molecular world. J Cardiovasc Dev Dis. 2020;7(4):44.
55. Hendrix MJ, Morse DE, Atrial septation. I. Scanning electron microscopy in the chick. Dev Biol. 1977;57(2):345–63.
56. Franklin KJ, et al. The valve of the foramen Ovale its relation to pulmonary vein entries. Veterinary J (1900). 1942;98(2):29–41.
57. Faber JW, Buijtendijk MF, Klarenberg H, Vink AS, Coolen BF, Moorman AF, Christoffels VM, Clur SA, Jensen B. Fetal tricuspid valve agenesis/atresia: testing predictions of the embryonic etiology. Pediatric Cardiology. 2022:1–11.

Deciphering Congenital Heart Disease Using Human Induced Pluripotent Stem Cells

13

Hao Zhang and Joseph C. Wu

Abstract

Congenital heart disease (CHD) is a leading cause of birth defect-related death. Despite significant advances, the mechanisms underlying the development of CHD are complex and remain elusive due to a lack of efficient, reproducible, and translational model systems. Investigations relied on animal models have inherent limitations due to interspecies differences. Human induced pluripotent stem cells (iPSCs) have emerged as an effective platform for disease modeling. iPSCs allow for the production of a limitless supply of patient-specific somatic cells that enable advancement in cardiovascular precision medicine. Over the past decade, researchers have developed protocols to differentiate iPSCs to multiple cardiovascular lineages, as well as to enhance the maturity and functionality of these cells. With the development of physiologic three-dimensional cardiac organoids, iPSCs represent a powerful platform to mechanistically dissect CHD and serve as a foundation for future translational research.

Keywords

Congenital heart disease (CHD) · Heart development · Induced pluripotent stem cells (iPSCs) · Cardiac organoid · Disease modeling · Differentiation

H. Zhang
Stanford Cardiovascular Institute, Stanford, CA, USA

J. C. Wu (✉)
Stanford Cardiovascular Institute, Stanford, CA, USA

Department of Medicine, Division of Cardiovascular Medicine, Stanford, CA, USA

Department of Radiology, Stanford University School of Medicine, Stanford, CA, USA
e-mail: joewu@stanford.edu

© The Author(s), under exclusive license to Springer Nature Switzerland AG 2024

S. Rickert-Sperling et al. (eds.), *Congenital Heart Diseases: The Broken Heart*,
Advances in Experimental Medicine and Biology 1441,
https://doi.org/10.1007/978-3-031-44087-8_13

13.1 Introduction

Congenital heart disease (CHD) is a leading cause of birth defect-related death that affects 1% of live births in the United States [1]. CHD is characterized by morphological abnormalities in the cardiac chambers, septum, valves, and great vessels arising from the heart. Congenital malformations of all aspects of the heart have been described, and the most common types of CHD can be classified into the following categories: (1) hypoplasia, (2) septal defects, (3) aortic arch artery anomalies, (4) valve defects, and (5) syndromic CHD with other congenital anomalies and/or neurodevelopmental defects [2].

Various risk factors contribute to CHD, including genetic/familial and nongenetic/environmental elements. With the advances in massively parallel sequencing, the genetics of CHD has been aggressively explored in the past decade. A recent genome-wide association study (GWAS) identified several genetic risk factors, including Macrod2, Gosr2, Wnt3, and Msx1, which were associated with CHD from 4034 patients and 8486 healthy controls [3]. Although normal embryonic heart development is a carefully choreographed and robust process, it is nonetheless vulnerable to perturbation by extrinsic factors, including toxic substances, drugs, or the lack of essential nutrients [4].

The mechanisms underlying the development of CHD are complex and remain elusive. There are limited animal models to study the developmental genetics of CHD, and transgenic mice carrying human variants do not always recapitulate the clinical phenotypes of CHD [5]. The human induced pluripotent stem cell (iPSC) technology has allowed us to efficiently produce human cells with specific patient and disease characteristics, enabling advancement in precision medicine [6]. Genome editing using clustered regularly interspaced short palindromic repeats (CRISPR) can precisely regulate gene expression in iPSC derivatives, facilitating our understanding of the genotype–phenotype correlation [7, 8].

In this review, we will first describe the stepwise differentiation protocol of iPSC-derived cardiovascular cell types, which can be used for recapitulating heart development. We will then discuss the current progress in using iPSCs to decipher molecular mechanisms of various types of CHD. We will also explore the application of cardiac organoids incorporating multiple cell types and organized structures in modeling complex CHD (Fig. 13.1).

13.2 Recapitulation of Heart Development by Stepwise Differentiation of iPSCs

The methods of differentiating iPSCs to various cardiovascular cell types have been established by mimicking their development program (Fig. 13.2). As CHD results from disruption of normal heart development by intrinsic or extrinsic factors, the iPSC differentiation process can be leveraged to delineate the role of pathogenic factors during in vivo cardiac development in an in vitro setting.

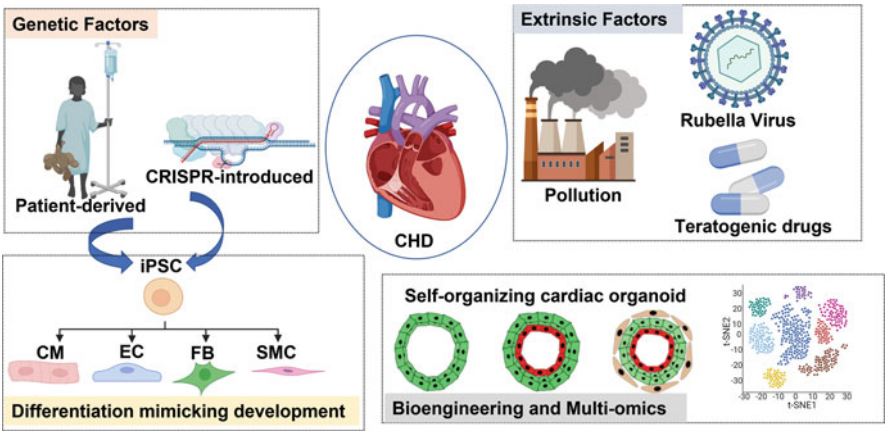

Fig. 13.1 Application of induced pluripotent stem cells in CHD research
Human iPSCs provide an effective platform for deciphering the mechanisms of congenital heart diseases (CHDs). First, heart development can be recapitulated by stepwise differentiation of iPSCs to cardiac cells, including cardiomyocytes (CMs), endocardial/endothelial cells (ECs), cardiac fibroblasts (FBs), and smooth muscle cells (SMCs). The developmental origin is a major determinant for regional propensity and different types of CHD. Second, iPSCs can recapitulate patient-specific clinical phenotype in vitro, resulting in accurate genotype-to-phenotype correlation. In addition, CRISPR-Cas9 genome editing offers a valuable tool to study rare genetic diseases by introducing designated mutations into iPSCs. Third, the pathogenic role of extrinsic factors of CHD, such as pollution, virus, and teratogenic drugs, can be determined by exposing these factors to iPSC cardiac differentiation process. Last, iPSC-derived cardiovascular cells can be engineered into three-dimensional organoids to mimic morphological complexity of the developing human fetal heart and dissect the mechanisms with single-cell multi-omics technology

The iPSC-derived cardiomyocyte (iPSC-CM) differentiation is induced by the manipulation of several signaling pathways essential for cardiac development, recapitulating embryonic cardiac differentiation process: from pluripotent stage (OCT4, SOX2), to mesodermal lineage (KDR, MESP1), to cardiac progenitor lineage (ISL1, MESP1), and finally to relatively immature beating CMs (TNNT2, ACTN2) [9]. As CHD affects distinct chambers of the heart, it is necessary to develop methods to generate chamber-specific iPSC-CM cellular subtypes. Recent studies have described how to modulate retinoic acid signaling during CM differentiation to derive atrial- and ventricular-like CMs [10]. Generation of a double-reporter iPSC line of $TBX5^{Clover2}$ and $NKX2–5^{RFP}$ enables isolation of cells from first and second heart fields, distinguishing atrial and ventricular iPSC-CMs, epicardial cells, and endothelial cells (ECs) [11, 12].

The developmental origin of smooth muscle cells (SMCs) is a major determinant for regional propensity and different types of congenital vascular diseases, such as bicuspid aortic valve, Marfan, and Loeys–Dietz syndrome [13, 14]. One of the first induction protocols to systemically derive lineage-specific iPSC-SMC subtypes was developed by the Sinha group, which generated origin-specific SMCs from iPSCs through three intermediate lineages—neuroectoderm, lateral plate mesoderm, and paraxial mesoderm [15].

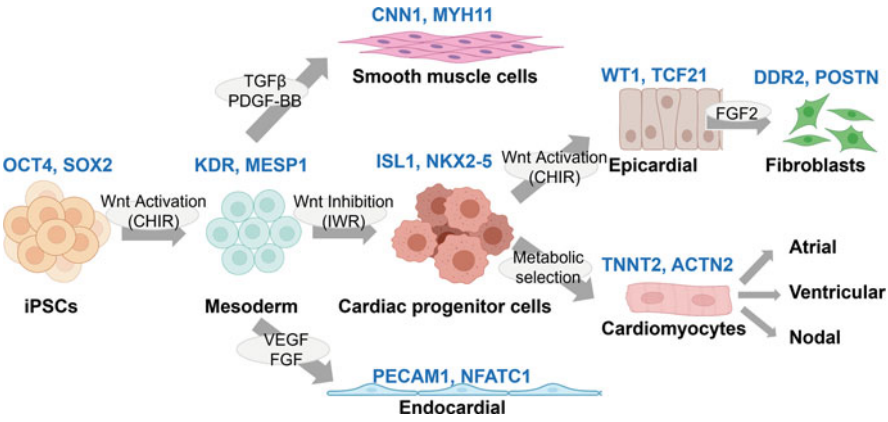

Fig. 13.2 Generation of cardiovascular cells from human induced pluripotent stem cells
Human iPSCs are pushed to mesodermal lineage (KDR1, MESP1) via Wnt activation (e.g., CHIR99021). Smooth muscle cells (CNN1, MYH11) and endocardial cells (PECAM1, NFATC1) are generated from mesoderm by treatment with unique sets of growth factors and small molecules such as TGFβ/PDGF-BB and VEGF/FGF, respectively. Following mesoderm differentiation, cardiac progenitor cells (ISL1, NKX2-5) are derived via canonical Wnt signaling inhibition (e.g., IWR1). Functional cardiomyocytes (TNNT2, ACTN2) are generated and purified with metabolic selection. Recently, methods to generate atrial, ventricular, and nodal cardiomyocytes have been described. Epicardial cells (WT1, TCF21) can also be generated from cardiac progenitor cells following Wnt activation (e.g., IWR1), which can then be differentiated to cardiac fibroblasts (DDR2, POSTN) with FGF2

The majority of cardiac fibroblasts derives from epicardial, defined by the expression of the marker genes Tcf21 [16]. As such, human iPSC-derived cardiac fibroblasts (iPSC-CFs) were successfully generated after intermediate cell types of cardiac progenitor cells and epicardial cells had been sequentially differentiated (Fig. 13.2) [17]. A second, minor developmental source of fibroblasts from the second heart field progenitors (SHFPs) constitutes ~10% of the tissue-resident fibroblasts, in particular regions such as ventricular septum and right ventricle. Following this pathway, a protocol was generated to drive iPSC-CFs via SHFPs using sequential inhibition of GSK3βμto activate canonical Wnt signaling followed by stimulation with FGF2 [18]. The formation of valves during embryogenesis originates from endocardial cells lining the myocardium [19]. Recently, a protocol to differentiate iPSC-derived endocardial cells was developed and demonstrated to be a representative model to study human valvulogenesis [19].

13.3 Patient-Specific iPSCs for Modeling Genetic of CHD

Patient-derived iPSCs carrying genetic variants enable researchers to study the disease mechanisms in a Petri dish (Table 13.1) [44–46]. By analyzing genome-wide transcriptomic profiles of iPSC-CMs, two studies identified distinctive

Table 13.1 Current iPSC models for studying disease mechanisms of genetic CHD

CHD	Variants	Cell types	Disease phenotypes	Corrections	Reference
HLHS	Unknown	CMs	Lower cardiomyogenic differentiation	Co-transfection of NKX2-5, HAND1, and NOTCH1	Kobayashi et al. [20]
	Unknown	CMs	Lower cardiomyogenic differentiation, Myofibrillar disorganization, persistence of a fetal gene expression pattern	/	Jiang et al. [21]
	NOTCH1	CMs	Lower cardiomyogenic differentiation, myofibrillar disorganization	/	Theis et al. [22]
	NOTCH	CMs	Lower cardiomyogenic differentiation, myofibrillar disorganization, blunted response to isoprenaline	Addition of jagged peptide ligand	Yang et al. [23]
	NOTCH1	CMs	Lower cardiomyogenic differentiation	Potentiation of NO signaling with small molecules	Hrstka et al. [24]
	MYH6	CMs	Lower cardiomyogenic differentiation, increased expression of MYH7	/	Tomita et al. [25]
	MYH6	CMs	Lower cardiomyogenic differentiation, myofibrillar disorganization, impaired contractility	CRISPR/Cas9 gene correction	Kim et al. [26]
	LRP2	CMs, drosophila, and zebrafish	Reduced CMs proliferation	/	Theis et al. [27]
	Unknown	Endocardium	Abnormal endothelial-to-mesenchymal transition, disrupting fibronectin–integrin signaling	FN1 supplementation or ETS1 overexpression	Miao et al. [28]
LVNC	TBX20	CMs	Decreased CMs proliferative capacity	Inhibition of TGF-βμsignaling and genome correction of the TBX20 mutation	Kodo et al. [29]
	MKL2, MYH7, and NKX2-5	CMs, mice	Increased CMs aggregate size	/	Gifford et al. [30]
ASD	GATA4	CMs	Defect in CMs proliferation	Gene correction, overexpression of FGF16	Ye et al. [31]
Septal defects	GATA4	CMs	Impaired contractility, calcium handling, and metabolic activity	/	Ang et al. [32]

(continued)

Table 13.1 (continued)

CHD	Variants	Cell types	Disease phenotypes	Corrections	Reference
VSD	TBX5	CMs	Lower cardiomyogenic differentiation, myofibrillar disorganization	/	Kathiriya et al. [33]
BAV	GATA4	ECs	Impaired the transition from endothelial cells into mesenchymal cells	/	Yang et al. [34]
	Unknown	SMCs	Impaired contraction	Inhibition of mTOR pathway using rapamycin	Jiao et al. [35]
	NOTCH1	SMCs, ECs	Immature morphology with smaller size of SMCs, defective differentiation of ECs	/	Jiao et al. [36]
Marfan	FBN1	SMCs	Defects in fibrillin-1 accumulation, extracellular matrix degradation, transforming growth factor-βμ signaling, contraction, and apoptosis	Gene correction	Granata et al. [37]
	FBN1	CMs	Stiffer of CMs, impaired contraction	Gene correction	Aalders et al. [38]
Noonan	SOS1	CMs	Myofibrillar disorganization, impaired contraction	/	Gurusamy et al. [39]
	LZTR1	CMs	Cellular hypertrophy	Intronic CRISPR repair	Hanses et al. [40]
	RAF1	CMs	Myofibrillar disorganization, cellular hypertrophy	Gene correction	Jaffré et al. [41]
	Unknown	CMs	Cellular hypertrophy, higher diastolic intracellular calcium concentration	Pyr3, a transient receptor potential channel 3 channel inhibitor	Sakai et al. [42]
	Introduced R276W mutation	CMs	Reduced viability	/	Ward et al. [43]

iPSC, human induced pluripotent stem cell; *CHD*, congenital heart disease; *HLHS,* hypoplastic left heart syndrome; *LVNC,* left ventricular noncompaction cardiomyopathy; *ASD,* atrial septal defect; *VSD,* ventricular septal defect; *BAV,* bicuspid aortic valve; *CMs,* iPSC-derived cardiomyocytes; *ECs,* iPSC-derived endothelial cells; *SMCs,* iPSC-derived smooth muscle cells

transcriptomes in single ventricle diseases and tetralogy of Fallot, uncovering the complex molecular mechanisms in patients with CHD [5, 47]. In combination with human iPSCs and animal models, an integrated high-throughput phenotypical platform was developed to test large numbers of CHD candidates in human iPSC-CMs and drosophila [48].

13.4 Hypoplasia

Hypoplastic left heart syndrome (HLHS) is a rare disease in which the left side of the heart is severely underdeveloped, and it was the first CHD being investigated on the iPSC platform back in 2014 [20, 21]. Early studies found a number of cardiac marker expression and functional differences between HLHS iPSC-CMs and control iPSC-CMs, providing evidence that cardiac-specific genes might influence the risk of HLHS [20, 21]. NOTCH1 was the first variation being investigated. Patient-specific iPSC-CMs exhibited diminished transcript levels of NOTCH1 signaling pathway components, along with impaired myocardiogenesis and myofilament disorganization [22, 49]. Activation of NOTCH signaling via the addition of Jagged peptide ligand or potentiation of NO signaling restored cardiogenesis in vitro, providing potential therapeutic targets for HLHS [23, 24]. Another rare variant in the α-myosin heavy chain (MYH6) gene in HLHS was also investigated using iPSC-CMs, which displayed a dysmorphic sarcomere structure and increased compensatory MYH7 expression [25, 26]. A multi-species high-throughput platform was recently established to rapidly evaluate candidate genes and their interactions in HLHS by leveraging human iPSCs and model organisms, such as drosophila and zebrafish [27]. In addition, Miao et al. highlighted the contribution of endocardial defects to the pathogenesis of HLHS using patient iPSCs and single-cell RNA sequencing of human fetuses with underdeveloped left ventricles. This study suggested that endocardial defects lead to abnormal endothelial-to-mesenchymal transition and reduced cardiomyocyte proliferation and maturation by disrupting fibronectin–integrin signaling [28].

Left ventricular noncompaction cardiomyopathy (LVNC) is a rare congenital disease of heart muscle that affects both children and adults. It results from abnormal prenatal development of heart muscle [29]. iPSC-CMs generated from LVNC patients carrying a mutation in the cardiac transcription factor TBX20 have decreased proliferative capacity and are associated with perturbed transforming growth factor-beta (TGF-β) signaling. Inhibition of TGF-βμsignaling and genome correction of the TBX20 mutation were sufficient to reverse the disease phenotype [29]. Human iPSC-CMs and mice models revealed that endocardial angiocrines regulated cardiomyocyte development and maturation and induce features of ventricular non-compaction [50]. Besides single variant, cardiac anomalies can be caused by a combination of rare, inherited mutations. For example, offspring with childhood-onset LVNC from a family were found to have three missense single-nucleotide variants in the MKL2, MYH7, and NKX2-5 genes [30]. Analysis of murine hearts and iPSC-CMs provided histologic and molecular evidence that

MKL2 and NKX2-5 contributed as genetic modifiers of the phenotype in the presence of the MYH7 variant [30].

13.5 Septal Defects

Genetic mutations of developmentally regulated cardiac transcription factors have long been implicated in cardiac septal defects. iPSC-CMs derived from a familial atrial septal defect (ASD) carrying a hereditary mutation in GATA4 gene (T280M) exhibited an obvious defect in cell proliferation [31]. The T280M mutation obstructed GATA4 occupancy at the FGF16 promoter region, leading to impaired activation of FGF16 transcription, and overexpression of FGF16 in GATA4-mutant cardiomyocytes rescued the cell proliferation defect [31]. In another study, iPSC-CMs from subjects with GATA4-G296S missense mutation showed impaired contractility, calcium handling, and metabolic activity [32]. The GATA4-G296S mutation disrupted TBX5 recruitment, leading to dysregulation of genes related to cardiac septation [32]. Kathiriya et al. further demonstrated the exquisite and diverse sensitivity to TBX5 dosage in heterogeneous subsets of iPSC-CMs, with implications for quantitative transcriptional regulation in the gene regulatory network of CHD [33].

13.6 Valve Defects

Bicuspid aortic valve (BAV) and mitral valve prolapse (MVP) are the most common types of congenital valve malformation [51, 52]. A GWAS scan of 466 BAV cases and 4660 age-, sex-, and ethnicity-matched controls identified the association with a noncoding variant 151 kb from GATA4 [34]. The molecular mechanism was then delineated by disruption of GATA4 by CRISPR-Cas9 in iPSC-ECs, revealing impairment of the transition from endothelial cells into mesenchymal cells, a critical step in the heart valve development [34]. On the other hand, iPSC-SMCs from BAV patients showed immature morphology with smaller size and decreased expression of contractile proteins, which accounts for the aortopathy associated with BAV [35, 36]. As valve developed from endocardial, iPSC-derived endocardial cells represented a faithful model of human valvulogenesis and recapitulated key features of MVP, suggesting dysregulated sonic hedgehog pathway as a putative therapeutic target [19].

13.7 Large Vessel Defects

Marfan syndrome (MFS) is a genetic disorder that affects the connective tissue, leading to aortic dilation and aneurysm [37]. The MFS iPSC-SMCs recapitulated the pathology seen in Marfan aorta and identified novel targets for treatment, such as p38 and KLF4 [37]. Myocardial dysfunction has been reported in MFS patients, but

little is known about the intrinsic effect on the CMs [53]. Aalders et al. reported that MFS iPSC-CMs are stiffer compared to corrected CMs, revealing that abnormalities in the behavior of MFS CMs were related to matrix defects [38]. More common vessel defects, such as coarctation of the aorta, transposition of great arteries, and pulmonary artery atresia, will be expected to be recapitulated with the advancement of engineered blood vessels from iPSCs in the future.

13.8 CHD in Systemic Syndrome

Syndromic CHD is defined as heart defects accompanied by other congenital anomalies, neurodevelopmental defects, and/or dysmorphic features [2]. Syndromic CHD may be caused by aneuploidy, copy number variants, or single gene defects. Noonan syndrome (NS) is a genetic disorder presenting unusual facial features, short height, bleeding problems, skeletal malformations, and CHD, classified into five types based on different gene mutations [54]. Type 3, 4, and 5 NS, associated with LZTR1, SOS1, and RAF1 mutation, respectively, have been recapitulated using the iPSC platform, exhibiting structurally and functionally compromised in iPSC-CMs [39–41]. Phenotypic screening revealed that Pyr3, a transient receptor potential channel 3 inhibitor, decreased cell size and diastolic intracellular calcium concentration in iPSC-CMs, suggesting a novel treatment for NS patients [42].

CRISPR-Cas9 genome editing offers us a valuable tool to study rare genetic diseases by introducing designated mutations into iPSCs [6]. For example, truncating variants in N-alpha-acetylation (NAA15) is a rare syndrome associated with intellectual disability, autism spectrum disorder, and congenital anomalies [43]. However, the modulated proteins responsible for NAA15-haploinsufficiency-mediated CHD have not been determined. Using CRISPR-Cas9, genetically engineered iPSCs with introduced NAA15 mutation provided a platform to evaluate the consequences of variants of unknown significance on NAA15 function [43]. In the future, we expect that studies in complex CHD, such as Down syndrome, will require a 3-dimensional (3D) organoid model consisting of multiple cell types, which allows for elucidation of cell interaction and more comprehensive pathogenetic mechanisms.

13.9 iPSCs for Modeling Extrinsic Factors for CHD

Although solid evidence for environmental causes of CHD has been available for almost 80 years, the underlying molecular mechanisms have not been elucidated [55]. Several studies have attempted to solve this issue by exposing extrinsic factors during the iPSC cardiac differentiation process. Rubella virus (RV) infection commonly leads to defects in ear, heart, and eye development. In the presence of RV, profound alterations of the epigenetic landscape were found during endodermal differentiation of RV-infected iPSCs [56]. Ribavirin has been proven to be an antiviral treatment with risks of congenital malformation. Exposure to ribavirin

significantly inhibited the proliferation and differentiation of iPSCs from mesoderm to cardiac progenitor cells, and from cardiac progenitor cells to cardiomyocytes, providing evidence of its cardiac developmental toxicity [57]. In the future, we expect that iPSCs can be used as a drug testing platform to evaluate the potential teratogenic effect.

13.10 Cardiac Organoid for Modeling CHD

CHD modeling faces challenges in recapitulating cellular complexity and animal-to-human translation due to the limitations of conventional 2D cell culture and inter-species differences. The development of human cardiac organoid technologies has helped resolve these challenges by mimicking in vivo organ functions and incorporating multiple cell types in the organized 3D structure [58, 59]. By constructing human cardiac organoids from iPSCs derived from patients with specific known genotypes and phenotypes, more complex and robust in vitro tools have recently become available for disease modeling [60–63].

Most recently, Yonatan et al. have generated cardiac organoids through a three-step Wnt signaling modulation strategy using chemical inhibitors and growth factors [64]. Heart organoids developed sophisticated internal chambers with well-organized multi-lineage cardiac cell types, mimicked heart field formation, developed a complex vasculature, and exhibited robust functional activity. This organoid platform recreated complex metabolic disorders such as pregestational diabetes-induced CHD [64]. Pablo et al. established a similar cardiac organoid model that intrinsically patterns into chamber-like structures, incorporating separated layers of CMs, ECs, and epicardial cells from iPSCs [65]. The cavity morphogenesis is governed by a mesodermal Wnt-BMP signaling axis and requires its target HAND1, a transcription factor linked to developmental heart chamber defects [65]. Taken together, cardiac organoid models effectively recapitulate morphological and functional complexity of the developing human fetal heart, including chamber formation, atrioventricular specification, electrophysiological activity, and vascularization.

13.11 Conclusion

In summary, by utilizing advances in CRISPR genome editing, 3D tissue engineering, and single-cell RNA sequencing technologies on human iPSCs, an innovative platform was developed to address the molecular mechanisms of CHD. One of the major limitations of iPSCs is the immaturity of the cells. iPSC-CMs do not have mature structures of myofibrils and T-tubule, and they are misaligned compared to rod-shaped adult cardiomyocytes. To date, researchers have attempted to use hormone/steroid, culture substrate, genetic, 3D tissue engineering, mechanical-, and electrical-based methods to generate mature iPSC-CMs [66]. Integrative of single-cell analysis and iPSC model identified developmental trajectories and non-coding

mutations in congenital heart disease [67]. Successful efforts on these fronts will enable us to mechanistically dissect more complex CHD and serve as a foundation for future translational research.

References

1. Lopez KN, Morris SA, Sexson Tejtel SK, Espaillat A, Salemi JL. US mortality attributable to congenital heart disease across the lifespan from 1999 through 2017 exposes persistent racial/ethnic disparities. Circulation. 2020;142(12):1132–47.
2. Lin H, McBride KL, Garg V, Zhao MT. Decoding genetics of congenital heart disease using patient-derived induced pluripotent stem cells (iPSCs). Front Cell Dev Biol. 2021;9:630069.
3. Lahm H, Jia M, Dreßen M, Wirth F, Puluca N, Gilsbach R, et al. Congenital heart disease risk loci identified by genome-wide association study in European patients. J Clin Invest. 2021;131(2):e141837.
4. Kalisch-Smith JI, Ved N, Sparrow DB. Environmental risk factors for congenital heart disease. Cold Spring Harb Perspect Biol. 2020;12(3)a037234.
5. Kitani T, Tian L, Zhang T, Itzhaki I, Zhang JZ, Ma N, et al. RNA sequencing analysis of induced pluripotent stem cell-derived Cardiomyocytes from congenital heart disease patients. Circ Res. 2020;126(7):923–5.
6. Paik DT, Chandy M, Wu JC. Patient and disease-specific induced pluripotent stem cells for discovery of personalized cardiovascular drugs and therapeutics. Pharmacol Rev. 2020;72(1):320–42.
7. Nishiga M, Liu C, Qi LS, Wu JC. The use of new CRISPR tools in cardiovascular research and medicine. Nat Rev Cardiol. 2022;19(8):505–21.
8. Guo H, Liu L, Nishiga M, Cong L, Wu JC. Deciphering pathogenicity of variants of uncertain significance with CRISPR-edited iPSCs. Trends Genet. 2021;37(12):1109–23.
9. Burridge PW, Matsa E, Shukla P, Lin ZC, Churko JM, Ebert AD, et al. Chemically defined generation of human cardiomyocytes. Nat Methods. 2014;11(8):855–60.
10. Lee JH, Protze SI, Laksman Z, Backx PH, Keller GM. Human pluripotent stem cell-derived atrial and ventricular cardiomyocytes develop from distinct mesoderm populations. Cell Stem Cell. 2017;21(2):179–94.e4.
11. Pezhouman A, Engel JL, Nguyen NB, Skelton RJP, Gilmore WB, Qiao R, et al. Isolation and characterization of hESC-derived heart field-specific cardiomyocytes unravels new insights into their transcriptional and electrophysiological profiles. Cardiovasc Res. 2021;118(3):828–43.
12. Zhang JZ, Termglinchan V, Shao NY, Itzhaki I, Liu C, Ma N, et al. A human iPSC double-reporter system enables purification of cardiac lineage subpopulations with distinct function and drug response profiles. Cell Stem Cell. 2019;24(5):802–11.e5.
13. Dobnikar L, Taylor AL, Chappell J, Oldach P, Harman JL, Oerton E, et al. Disease-relevant transcriptional signatures identified in individual smooth muscle cells from healthy mouse vessels. Nat Commun. 2018;9(1):4567.
14. Shen M, Quertermous T, Fischbein MP, Wu JC. Generation of vascular smooth muscle cells from induced pluripotent stem cells: methods, applications, and considerations. Circ Res. 2021;128(5):670–86.
15. Cheung C, Bernardo AS, Trotter MW, Pedersen RA, Sinha S. Generation of human vascular smooth muscle subtypes provides insight into embryological origin-dependent disease susceptibility. Nat Biotechnol. 2012;30(2):165–73.
16. Tallquist MD, Molkentin JD. Redefining the identity of cardiac fibroblasts. Nat Rev Cardiol. 2017;14(8):484–91.
17. Zhang H, Tian L, Shen M, Tu C, Wu H, Gu M, et al. Generation of quiescent cardiac fibroblasts from human induced pluripotent stem cells for in vitro modeling of cardiac fibrosis. Circ Res. 2019;125(5):552–66.

18. Zhang J, Tao R, Campbell KF, Carvalho JL, Ruiz EC, Kim GC, et al. Functional cardiac fibroblasts derived from human pluripotent stem cells via second heart field progenitors. Nat Commun. 2019;10(1):2238.
19. Neri T, Hiriart E, van Vliet PP, Faure E, Norris RA, Farhat B, et al. Human pre-valvular endocardial cells derived from pluripotent stem cells recapitulate cardiac pathophysiological valvulogenesis. Nat Commun. 2019;10(1):1929.
20. Kobayashi J, Yoshida M, Tarui S, Hirata M, Nagai Y, Kasahara S, et al. Directed differentiation of patient-specific induced pluripotent stem cells identifies the transcriptional repression and epigenetic modification of NKX2-5, HAND1, and NOTCH1 in hypoplastic left heart syndrome. PLoS One. 2014;9(7):e102796.
21. Jiang Y, Habibollah S, Tilgner K, Collin J, Barta T, Al-Aama JY, et al. An induced pluripotent stem cell model of hypoplastic left heart syndrome (HLHS) reveals multiple expression and functional differences in HLHS-derived cardiac myocytes. Stem Cells Transl Med. 2014;3(4):416–23.
22. Theis JL, Hrstka SC, Evans JM, O'Byrne MM, de Andrade M, O'Leary PW, et al. Compound heterozygous NOTCH1 mutations underlie impaired cardiogenesis in a patient with hypoplastic left heart syndrome. Hum Genet. 2015;134(9):1003–11.
23. Yang C, Xu Y, Yu M, Lee D, Alharti S, Hellen N, et al. Induced pluripotent stem cell modelling of HLHS underlines the contribution of dysfunctional NOTCH signalling to impaired cardiogenesis. Hum Mol Genet. 2017;26(16):3031–45.
24. Hrstka SC, Li X, Nelson TJ. NOTCH1-dependent nitric oxide signaling deficiency in Hypoplastic left heart syndrome revealed through patient-specific phenotypes detected in bioengineered cardiogenesis. Stem Cells. 2017;35(4):1106–19.
25. Tomita-Mitchell A, Stamm KD, Mahnke DK, Kim MS, Hidestrand PM, Liang HL, et al. Impact of MYH6 variants in hypoplastic left heart syndrome. Physiol Genomics. 2016;48(12):912–21.
26. Kim MS, Fleres B, Lovett J, Anfinson M, Samudrala SSK, Kelly LJ, et al. Contractility of induced pluripotent stem cell-cardiomyocytes with an MYH6 head domain variant associated with hypoplastic left heart syndrome. Front Cell Dev Biol. 2020;8:440.
27. Theis JL, Vogler G, Missinato MA, Li X, Nielsen T, Zeng XI, et al. Patient-specific genomics and cross-species functional analysis implicate LRP2 in hypoplastic left heart syndrome. elife. 2020;9:e59554.
28. Miao Y, Tian L, Martin M, Paige SL, Galdos FX, Li J, et al. Intrinsic endocardial defects contribute to Hypoplastic left heart syndrome. Cell Stem Cell. 2020;27(4):574–89.e8.
29. Kodo K, Ong SG, Jahanbani F, Termglinchan V, Hirono K, InanlooRahatloo K, et al. iPSC-derived cardiomyocytes reveal abnormal TGF-β signalling in left ventricular non-compaction cardiomyopathy. Nat Cell Biol. 2016;18(10):1031–42.
30. Gifford CA, Ranade SS, Samarakoon R, Salunga HT, de Soysa TY, Huang Y, et al. Oligogenic inheritance of a human heart disease involving a genetic modifier. Science. 2019;364(6443):865–70.
31. Ye L, Yu Y, Zhao ZA, Zhao D, Ni X, Wang Y, et al. Patient-specific iPSC-derived cardiomyocytes reveal abnormal regulation of FGF16 in a familial atrial septal defect. Cardiovasc Res. 2021;118(3):859–71.
32. Ang YS, Rivas RN, Ribeiro AJS, Srivas R, Rivera J, Stone NR, et al. Disease model of GATA4 mutation reveals transcription factor cooperativity in human cardiogenesis. Cell. 2016;167(7):1734–49.e22.
33. Kathiriya IS, Rao KS, Iacono G, Devine WP, Blair AP, Hota SK, et al. Modeling human TBX5 haploinsufficiency predicts regulatory networks for congenital heart disease. Dev Cell. 2021;56(3):292–309.e9.
34. Yang B, Zhou W, Jiao J, Nielsen JB, Mathis MR, Heydarpour M, et al. Protein-altering and regulatory genetic variants near GATA4 implicated in bicuspid aortic valve. Nat Commun. 2017;8:15481.

35. Jiao J, Xiong W, Wang L, Yang J, Qiu P, Hirai H, et al. Differentiation defect in neural crest-derived smooth muscle cells in patients with aortopathy associated with bicuspid aortic valves. EBioMedicine. 2016;10:282–90.
36. Jiao J, Tian W, Qiu P, Norton EL, Wang MM, Chen YE, et al. Induced pluripotent stem cells with NOTCH1 gene mutation show impaired differentiation into smooth muscle and endothelial cells: implications for bicuspid aortic valve-related aortopathy. J Thorac Cardiovasc Surg. 2018;156(2):515–22.e1.
37. Granata A, Serrano F, Bernard WG, McNamara M, Low L, Sastry P, et al. An iPSC-derived vascular model of Marfan syndrome identifies key mediators of smooth muscle cell death. Nat Genet. 2017;49(1):97–109.
38. Aalders J, Léger L, Van der Meeren L, Van den Vreken N, Skirtach AG, Sinha S, et al. Effects of fibrillin mutations on the behavior of heart muscle cells in Marfan syndrome. Sci Rep. 2020;10(1):16756.
39. Gurusamy N, Rajasingh S, Sigamani V, Rajasingh R, Isai DG, Czirok A, et al. Noonan syndrome patient-specific induced cardiomyocyte model carrying SOS1 gene variant c.1654A>G. Exp Cell Res. 2021;400(1):112508.
40. Hanses U, Kleinsorge M, Roos L, Yigit G, Li Y, Barbarics B, et al. Intronic CRISPR repair in a preclinical model of Noonan syndrome-associated cardiomyopathy. Circulation. 2020;142(11):1059–76.
41. Jaffré F, Miller CL, Schänzer A, Evans T, Roberts AE, Hahn A, et al. Inducible pluripotent stem cell-derived cardiomyocytes reveal aberrant extracellular regulated kinase 5 and mitogen-activated protein kinase kinase 1/2 signaling concomitantly promote hypertrophic cardiomyopathy in RAF1-associated Noonan syndrome. Circulation. 2019;140(3):207–24.
42. Sakai T, Naito AT, Kuramoto Y, Ito M, Okada K, Higo T, et al. Phenotypic screening using patient-derived induced pluripotent stem cells identified Pyr3 as a candidate compound for the treatment of infantile hypertrophic cardiomyopathy. Int Heart J. 2018;59(5):1096–105.
43. Ward T, Tai W, Morton S, Impens F, Van Damme P, Van Haver D, et al. Mechanisms of congenital heart disease caused by NAA15 haploinsufficiency. Circ Res. 2021;128(8):1156–69.
44. Mullen M, Zhang A, Lui GK, Romfh AW, Rhee JW, Wu JC. Race and genetics in congenital heart disease: application of iPSCs, omics, and machine learning technologies. Front Cardiovasc Med. 2021;8:635280.
45. Lee J, Termglinchan V, Diecke S, Itzhaki I, Lam CK, Garg P, Lau E, Greenhaw M, Seeger T, Wu H, Zhang JZ. Activation of PDGF pathway links LMNA mutation to dilated cardiomyopathy. Nature. 2019;572(7769):335–40.
46. Zhang H, Ren L, Wu JC. New insights into the therapy for Lamin-associated dilated cardiomyopathy. Basic Transl Sci. 2022;7(12):1246–8.
47. Grunert M, Appelt S, Schönhals S, Mika K, Cui H, Cooper A, et al. Induced pluripotent stem cells of patients with tetralogy of Fallot reveal transcriptional alterations in cardiomyocyte differentiation. Sci Rep. 2020;10(1):10921.
48. Schroeder AM, Allahyari M, Vogler G, Missinato MA, Nielsen T, Yu MS, et al. Model system identification of novel congenital heart disease gene candidates: focus on RPL13. Hum Mol Genet. 2019;28(23):3954–69.
49. Ye S, Wang C, Xu Z, Lin H, Wan X, Yu Y, Adhicary S, Zhang JZ, Zhou Y, Liu C, Alonzo M. Impaired human cardiac cell development due to NOTCH1 deficiency. Circ Res. 2023;132(2):187–204.
50. Rhee S, Paik DT, Yang JY, Nagelberg D, Williams I, Tian L, Roth R, Chandy M, Ban J, Belbachir N, Kim S. Endocardial/endothelial angiocrines regulate cardiomyocyte development and maturation and induce features of ventricular non-compaction. Eur Heart J. 2021;42(41):4264–76.
51. Michelena HI, Della Corte A, Evangelista A, Maleszewski JJ, Edwards WD, Roman MJ, et al. Summary: international consensus statement on nomenclature and classification of the congenital bicuspid aortic valve and its aortopathy, for clinical, surgical, interventional, and research purposes. J Thorac Cardiovasc Surg. 2021;162(3):781–97.

52. Pavon AG, Monney P, Schwitter J. Mitral valve prolapse, arrhythmias, and sudden cardiac death: the role of multimodality imaging to detect high-risk features. Diagnostics (Basel). 2021;11(4):683.
53. Muiño-Mosquera L, De Backer J. Cardiomyopathy in genetic aortic diseases. Front Pediatr. 2021;9:682390.
54. Rodríguez F, Gaete X, Cassorla F. Etiology and treatment of growth delay in Noonan syndrome. Front Endocrinol (Lausanne). 2021;12:691240.
55. Darbar D. Unraveling the genomic basis of congenital heart disease. J Clin Invest. 2021;131(2): e145377.
56. Bilz NC, Willscher E, Binder H, Böhnke J, Stanifer ML, Hübner D, et al. Teratogenic rubella virus alters the endodermal differentiation capacity of human induced pluripotent stem cells. Cell. 2019;8(8):870.
57. Ye D, Bao Z, Yu Y, Han Z, Yu Y, Xu Z, et al. Inhibition of cardiomyocyte differentiation of human induced pluripotent stem cells by ribavirin: implication for its cardiac developmental toxicity. Toxicology. 2020;435:152422.
58. Liu C, Oikonomopoulos A, Sayed N, Wu JC. Modeling human diseases with induced pluripotent stem cells: from 2D to 3D and beyond. Development. 2018;145(5):dev156166.
59. Zushin PJ, Mukherjee S, Wu JC. FDA modernization Act 2.0: transitioning beyond animal models with human cells, organoids, and AI/ML-based approaches. J Clin Invest. 2023;133(21)
60. Nugraha B, Buono MF, von Boehmer L, Hoerstrup SP, Emmert MY. Human cardiac organoids for disease modeling. Clin Pharmacol Ther. 2019;105(1):79–85.
61. Cho S, Discher DE, Leong KW, Vunjak-Novakovic G, Wu JC. Challenges and opportunities for the next generation of cardiovascular tissue engineering. Nat Methods. 2022;19(9):1064–71.
62. Kim H, Kamm RD, Vunjak-Novakovic G, Wu JC. Progress in multicellular human cardiac organoids for clinical applications. Cell Stem Cell. 2022;29(4):503–14.
63. Thomas D, Choi S, Alamana C, Parker KK, Wu JC. Cellular and engineered organoids for cardiovascular models. Circ Res. 2022;130(12):1780–802.
64. Lewis-Israeli YR, Wasserman AH, Gabalski MA, Volmert BD, Ming Y, Ball KA, et al. Self-assembling human heart organoids for the modeling of cardiac development and congenital heart disease. Nat Commun. 2021;12(1):5142.
65. Hofbauer P, Jahnel SM, Papai N, Giesshammer M, Deyett A, Schmidt C, et al. Cardioids reveal self-organizing principles of human cardiogenesis. Cell. 2021;184(12):3299–317.e22.
66. Feyen DAM, McKeithan WL, Bruyneel AAN, Spiering S, Hörmann L, Ulmer B, et al. Metabolic maturation media improve physiological function of human iPSC-derived cardiomyocytes. Cell Rep. 2020;32(3):107925.
67. Ameen M, Sundaram L, Shen M, Banerjee A, Kundu S, Nair S, Shcherbina A, Gu M, Wilson KD, Varadarajan A, Vadgama N. Integrative single-cell analysis of cardiogenesis identifies developmental trajectories and non-coding mutations in congenital heart disease. Cell. 2022;185(26):4937–53.

Cardiac Development at a Single-Cell Resolution

14

Nicholas Wei, Carissa Lee, Lauren Duan, Francisco X. Galdos, Tahmina Samad, Alireza Raissadati, William R. Goodyer, and Sean M. Wu

Abstract

Mammalian cardiac development is a complex, multistage process. Though traditional lineage tracing studies have characterized the broad trajectories of cardiac progenitors, the advent and rapid optimization of single-cell RNA sequencing methods have yielded an ever-expanding toolkit for characterizing heterogeneous cell populations in the developing heart. Importantly, they have allowed for a robust profiling of the spatiotemporal transcriptomic landscape of the human and mouse heart, revealing the diversity of cardiac cells—myocyte and non-myocyte—over the course of development. These studies have yielded insights into novel cardiac progenitor populations, chamber-specific developmental signatures, the gene regulatory networks governing cardiac development, and, thus, the etiologies of congenital heart diseases. Furthermore, single-cell RNA sequencing has allowed for the exquisite characterization of distinct cardiac populations such as the hard-to-capture cardiac conduction system and the intracardiac immune population. Therefore, single-cell profiling has also resulted in new insights into the regulation of cardiac regeneration and injury repair. Single-cell multiomics approaches combining transcriptomics, genomics, and epigenomics may uncover an even more comprehensive atlas of human cardiac biology. Single-cell analyses of the developing and adult mammalian heart offer

N. Wei · C. Lee · L. Duan · F. X. Galdos · T. Samad · A. Raissadati · S. M. Wu (✉)
Stanford University, Cardiovascular Institute, Stanford, CA, USA
e-mail: carislee@stanford.edu; laurduan@stanford.edu; fxgaldos@stanford.edu; fyrdowse@stanford.edu; ali.raissadati@stanford.edu; smwu@stanford.edu

W. R. Goodyer
Stanford University, Department of Pediatrics, Stanford, CA, USA
e-mail: wgoodyer@stanford.edu

© The Author(s), under exclusive license to Springer Nature Switzerland AG 2024

S. Rickert-Sperling et al. (eds.), *Congenital Heart Diseases: The Broken Heart*,
Advances in Experimental Medicine and Biology 1441,
https://doi.org/10.1007/978-3-031-44087-8_14

an unprecedented look into the fundamental mechanisms of cardiac development and the complex diseases that may arise from it.

Keywords

Heart development · Single-cell RNA sequencing · Chamber morphogenesis · Myocardial trabeculation · Bioinformatics

14.1 Introduction

In mammals, the heart is the first organ of the body to develop and cardiogenesis is a complex, multistage process that begins during embryonic gastrulation. While much has been studied in the mechanism of heart development in model organisms such as flies, chicks, and mice, human heart development has been more difficult to investigate. Available data support the formation of the three embryonic germ layers—endoderm, mesoderm, and ectoderm—at approximately 3 weeks of human gestation. The pluripotent epiblast cells that collectively give rise to the body undergo gastrulation at this time as they migrate and ingress through the groove of the primitive streak to form the mesoderm [1]. The heart itself develops from two distinct, mesoderm-derived groups of progenitor cells called the first (FHF) and second heart fields (SHF) [2]. FHF progenitors contribute significantly to the left ventricle (LV) and rapidly migrate anterolaterally to become the cardiac crescent, which fuses at the midline to become the primitive linear heart tube (HT) [3]. SHF progenitors, which ultimately give rise to cells in the right ventricle (RV) and outflow tract (OFT), differentiate later than FHF progenitors to aid in dorsal closure of the HT [4]. Subsequent elongation and rightward looping of HT establish the structural foundation for the four chambers of the heart: right atrium (RA), right ventricle (RV), left atrium (LA), and left ventricle (LV). Cardiac trabeculation also begins after looping, forming specialized projections of cardiomyocytes (CMs) and endocardial cells—collectively called trabeculae—responsible for the majority of pumping action in the early fetal heart [5].

Cardiac septation, occurring between weeks 4 and 7 in human development, closes primitive connections between the RA and LA and between ventricles and subarterial channels and creates new junctions in preparation for neonatal circulation [6]. OFT septation, initiated by migration of cardiac neural crest cells through the aortic arches, results in separation of the aorta and pulmonary trunk. These septation processes have recently been shown to give rise to transcriptionally distinct, chamber-specific CM and nonmyocyte populations [7].

Later stages of cardiac development are characterized by immense growth and increasing diversity of cardiac cell types. CMs that make up the sinoatrial and atrioventricular nodes of the cardiac conduction system, for example, display unique transcriptional profiles [8]. Formation of epicardium, cardiac valves, and coronary vasculature is characterized by dynamic processes such as epithelial-to-mesenchymal (EMT) and endothelial-to-mesenchymal (EndMT) transitions, which further

contribute to nonmyocyte diversity as migrating cells differentiate into new subpopulations [9]. The final process of trabecular compaction results in the compaction of the outer ventricular myocardium, increasing the ratio of compact CMs to their transcriptionally distinct trabecular counterparts and enabling greater contractile strength in anticipation for neonatal circulation [10].

While vertebrate cardiac morphogenesis has been well-studied since the 1920s, technological limitations have hindered high-resolution studies of developmental cell types until recent years [11]. Thus, the transcriptional heterogeneity of early developmental cardiac cell populations has generated interest in the use of emerging single-cell tools, including high-throughput transcriptomic and epigenomic sequencing techniques, to profile these cell types and better characterize their effects on disease phenotypes.

14.2 Single-Cell Tools and Approaches

The development of the single-cell RNA sequencing (scRNA-seq) technology in recent years has provided significant insights into the key regulatory processes of early cardiogenesis and the pathophysiological mechanisms involved in heart disease. The first step in performing a high-quality scRNA-seq experiment is to ensure the highest quality and integrity of the mRNA transcripts in each single cell. Different sources of tissues require different concentrations and duration of exposure to proteolytic enzymes (i.e., a proteinases and collagenases) for single-cell isolation. Cell count of isolated viable cells should be more than sufficient for the technology employed. In comparison to the murine heart, the human heart is more fibrous which makes it more challenging to isolate CMs [12]. Furthermore, postnatal CMs beyond the neonatal window are too rigid and ensconced within the extracellular matrix and non-myocytes to be digested successfully for scRNA-seq. Thus, most single-cell cardiac studies involving postnatal CMs employ single nucleus RNA sequencing (snRNA-seq). While the total cell/nuclear count is often higher in snRNA-seq, the number of unique mRNA per cell/nucleus is generally lower compared to scRNA-seq [13].

From a technical point-of-view, single-cell capture can be performed utilizing various methods (Fig. 14.1, **step 3**). Fluorescence-activated cell sorting (FACS) utilizes scatter and fluorescence signals to sort cells into 96- or 384-well plates. The use of fluorescence signals enables selection of cells of interest and filtering of dead cells [14]. Because of the size of the nozzle, cells less than 50 μm in diameter can be sorted with minimal damage; thus, a robust number of viable fetal CMs and other smaller cells such as endothelial cells (ECs) and fibroblasts (Fbs) can be sorted [15]. Adult CMs would be damaged in the process due to their large size (>100 μm in diameter along the major axis). However, Gladka et al. have recently successfully used a larger nozzle size (130 μm) with a large particle sorter in order to obtain RNA sequencing data from single CMs from adult murine tissue [16].

Another method for single-cell capture employs an integrated microfluidic circuit (e.g., Fluidigm C1), which isolates single cells into individual reaction chambers in

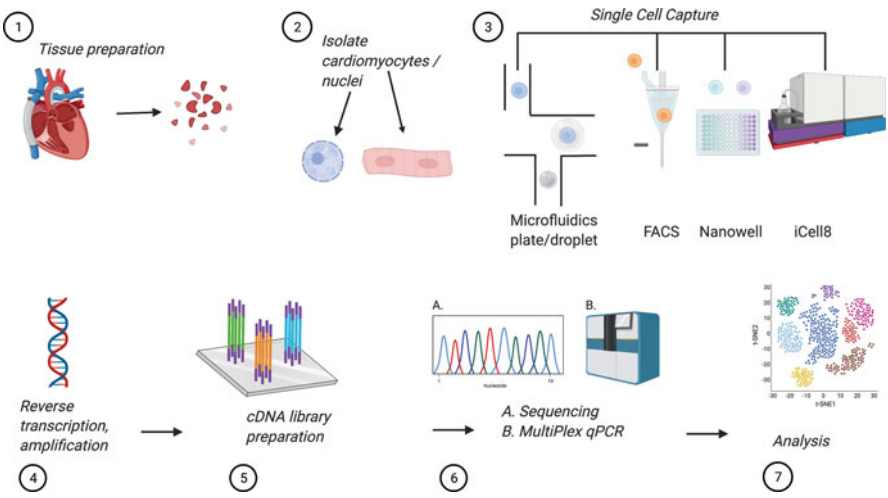

Fig. 14.1 Steps to single-cell RNA sequencing. (1) Dissociation of the cardiac tissue using optimal digestion protocol. (2) Isolate whole cell cardiomyocyte or nuclei. (3) Single-cell capture via various methods of single-cell capture. (4) Reverse transcription of sc-RNA and PCR amplification. (5) cDNA library preparation. (6) (A) Next-generation sequencing or (B) Multiplex qPCR generates readout. (7) Alignment, quality control and analysis.Adapted from Seminars in Cell & Developmental Biology, Vol. 118, T. Samad & S.M. Wu, "Single cell RNA sequencing approaches to cardiac development and congenital heart disease", pp. 129–135, Copyright Elsevier (2021), with permission from Elsevier

an automated fashion. This approach can simultaneously isolate hundreds of single cells within a defined range of cell size and shape [17]. Following cell capture, the microfluidic platform automatically lyses the cell within each micro-chamber and the cDNA pools are processed immediately for subsequent library generation and high-throughput sequencing. Since the cell lysis, reverse transcription, mRNA fragmentation, and cell barcoding steps all occur within the micro-chamber, the technique has the advantage of being able to capture full-length mRNA in each cell.

When compared to the microfluid plate system, the microfluid droplet method (i.e.,10x Genomics) is less time-consuming and more cost-effective on a per cell basis [18]. Cells of various sizes can be captured using this system, and greater than 20,000 cells can often be processed with each run (though cells must be smaller than ~50 μm in diameter) [19–21]. In this system, each cell is captured in a droplet, typically within an oil emulsion that also contains the necessary reagents for cell barcoding and reverse transcription into first strand cDNA. These reagents may be incorporated in the form of a thermosensitive gel bead. This system enables 3′-end or 5′-end sequencing of single cells with increased scale and throughput [20]. The disadvantage of the droplet-based system includes a lower overall unique transcript recovery rate when compared to other methods: ~500 to 2500 genes detected per cell versus 1000–4000 genes per cell when utilizing the microfluid plate-based platform [18, 22]. Additional limitations include droplet fragility, risk of leakage, poor cell capturing efficiency due to initial low cell density, or clogging the system due to high

initial cell concentration resulting in increased doublets in each droplet. These technical issues can usually be addressed by using the Nanowell (i.e. iCell8) or Microwell-seq approaches [23].

The iCell8 system consists of a 5184-nanowell-containing microchip to capture and process 1300–1800 single cells each run [24, 25]. Each nanowell contains preprinted oligonucleotides encoding poly-d(T), a unique well barcode, and a unique molecular identifier. The iCell8 system uses imaging software to identify nanowells containing viable single cells, and only wells with single cells are processed into sequencing libraries. The advantages of this system include the ability to process small number of cells for applications in rare cell capture and ability to distinguish between mono- and multinucleate CMs by microscopic imaging of each cell for pre-cell identification before lysis and reverse transcription [17].

The Microwell-seq system utilizes agarose-constructed Nanowells to profile 100–10,000 cells in each run and provides a comprehensive transcriptome consisting of full-length cDNA coverage. Each magnetic bead is loaded into a well and retrieved by a magnet after capturing single-cell mRNAs. The amplification method consists of template switching-based PCR where reverse transcription, amplification, and library preparation can be performed following the Smart-seq 2 protocol [19]. This technology is also able to identify and disqualify doublet cells based on imaging prior to sample lysis for scRNA-seq, which provides an extra layer of reassurance. Disadvantages of this system include the non-fully automated processing and lower throughput than the droplet-based system.

Following the single-cell capture, reverse transcription, amplification, and cDNA libraries generation steps, the DNA library undergoes high-throughput next-generation sequencing to generate readouts that are then aligned to a reference genome. After alignment, quality control of the data ensures that readouts consist of highly abundant (generally $>80\%$) non-mitochondrial genes in each single viable cell. Each cell cluster is then assigned a cell type identity based on cell markers, mitochondrial gene percentage, and total gene count [20, 21]. The data generated are then visualized and analyzed using software for scRNA-seq data processing (i.e., Seurat version 4.0, an R package; Monocle; Scanpy; Scater; and SINCERA) via a nonlinear reduction algorithm such as t-distributed stochastic neighboring embedding (t-SNE) or uniform manifold approximation and projection (UMAP).

In summary, when designing experiments for single-cell or single-nucleus sequencing, many options are available and customization to optimize quality of data is key. Greater incorporation of this technology in the future will bring us one step closer to attaining the ultimate goal of precision and personalized medicine.

14.3 Trajectory of Cardiac Development from scRNA-Seq Studies

Over the past decade, advances in scRNA-seq technologies have unlocked the ability for investigators to profile thousands of cells across multiple time points during embryonic development. Traditionally, developmental biologists have relied on

complex genetic lineage tracing and labeling experiments to study cellular differentiation in vivo [26]. As the scale of scRNA-seq experiments increases, however, investigators are now able to reconstruct the complex differentiation trajectories that arise during organogenesis using in silico lineage trajectory analysis tools [27–31]. These novel informatic tools are enabling the study of the transcriptional events that occur during organogenesis and are advancing our understanding of the complex gene regulatory networks that may be implicated in developmental defects.

As noted earlier, the heart is a multichambered organ that is derived from two progenitor pools, the FHF and SHF [32–35], the outflow tract, and the atria [2, 36]. Due to these distinct embryologic origins, a significant interest has risen to understand the unique transcriptional networks that regulate the development of these progenitor populations into distinct cardiac chambers. In 2016, Li et al. [37] and DeLaughter et al. [38] published the first comprehensive scRNA-seq datasets profiling cells from distinct cardiac chambers and time points during cardiac development [37, 38]. These studies demonstrated the unique gene expression profiles exhibited by distinct CM subpopulations among each chamber while also revealing the heterogeneity of cell types present in the developing mouse heart across multiple time points of development. These studies also revealed the unique expression profiles present across cardiac chambers derived from the cardiac progenitor populations. For example, at E10.5, the LV and RV could be distinguished transcriptomically demonstrating the early and unique differences between structures derived from distinct progenitor subtypes [37, 38].

With advances in scRNA-seq, multiple groups have sought to better understand the transcriptional events governing the earliest stages of cardiac differentiation including the origins of the cardiac progenitors themselves. In 2018, Lescroart et al. demonstrated the scRNA-seq of Mesp1^{+} mesodermal progenitors where FHF and SHF arise from two temporally separated waves of early mesodermal progenitors [32, 39]. More recently, multiple groups have profiled developing mouse hearts by scRNA-seq to extensively characterize early cardiac progenitors [40–42], cardiac chambers [8, 40, 43], and the cardiac conduction system [8, 44]. Importantly, gene knockout studies have been conducted in mouse embryos and profiled by scRNA-seq to demonstrate the disruption of cell identities during development [32, 37, 40, 43, 45, 46]. Nkx2.5 gene knockout studies have shown an atrialization of ventricular CMs by scRNA-seq [37], while Hand2 knockout mice show disruption of anterior and posterior patterning [40]. These profiling studies have been further extended to unraveling the origins of additional structures of the heart such as the coronary arteries, where scRNA-seq has uncovered the transcriptional mechanisms by which vein cells give rise to coronary arteries [47].

scRNA-seq studies continue to reveal a diversity of cell types during cardiac development including cell types present in fetal and adult human hearts as well as adult murine hearts [48–52]. Recent studies have not only confirmed the identity of known progenitor populations but have also revealed a diversity of mesenchymal cell types as well as distinct origins of valvular cells during development [43, 53]. Interestingly, one study suggested the presence of a common cardiac progenitor giving rise to both epicardial and myocardial cells, which illustrates the

potential for scRNA-seq tools to uncover novel cell types during cardiac development [54]. Overall, the ability to understand the transcriptional and cellular changes occurring during cardiac development at the single-cell level is providing unprecedented insight into the gene regulatory networks that drive the differentiation of distinct cardiac cell types. By uncovering novel cell types, a more accurate delineation of the gene regulatory network that governs cardiac development can be created that provides newer insights into the etiology of congenital and adult heart diseases.

14.4 Single-Cell Profiling of the Cardiac Conduction System

The cardiac conduction system (CCS) is made up of specialized CMs that allow for the rhythmic beating of the heart [55]. This intricate system is composed of distinct components, each with their own electrophysiologic properties, including the sinoatrial node (SAN), atrioventricular node (AVN), His bundle (His), bundle branches (BBs), and Purkinje fibers (PFs) [56]. The CCS is essential for both the formation and normal function of the heart, and importantly, disturbance to any part of the CCS can result in decreased cardiac output and life-threatening arrhythmias [55]. Despite the importance of the CCS, progress in our understanding of its intricate cellular and molecular landscape has, until recently with the advent of single-cell techniques, remained limited for several reasons, including: (1) low conduction cell numbers within the heart; (2) intra- and intercomponent cell type heterogeneity; (3) challenges in conduction cell isolation; and (4) complexity of the three-dimensional anatomy of the CCS [57].

Early studies into CCS transcriptional regulation involved painstaking evaluation of heart tissue sections using immunofluorescence and resulted in the discovery of a handful of markers [58, 59]. More recently, alternative approaches including transgenic murine reporter lines coupled with FACS [60] or laser capture [55, 61] have been employed to perform bulk RNA sequencing analyses. Despite these important early studies into the molecular regulators of CCS development and function, a reliance on bulk tissue analysis continued to prevent further resolution due to contamination by non-CCS cells as well as a plateau in our ability to isolate and distinguish between rare conduction cell types.

Recent efforts using scRNA-seq, however, have circumvented the aforementioned technical hurdles and advanced our ability to characterize the vast cell type heterogeneity within the CCS. In 2019, Goodyer et al. used a combined approach involving microdissection and scRNA-seq to generate the first comprehensive transcriptome analysis of the entire CCS at single-cell resolution [8]. In this study, unsupervised weighted co-expression gene network analyses were used to: (1) confirm successful isolation of all major CCS components using previously reported markers; (2) identify and validate a host of novel genes not previously associated with the CCS; and (3) begin to characterize the transcriptional profile and anatomical architecture of subdomains within each CCS component [8]. For instance, evaluation of the SAN cluster of cells revealed two distinct subpopulations consisting of *compact* and *transitional* SAN cells. The *transitional* cell population, consistent

with its hypothesized role as a cellular bridge to the surrounding working myocardium, demonstrated a hybrid phenotype by expressing hallmark SAN markers at similar (e.g., *Shox2* and *Gjc1*) or lower (e.g., *Hcn4, Tbx3,* and *Isl1*) levels while also showing enrichment for certain atrial CM markers (e.g., *Scn5a* and *Cx40*). While no one marker was specific to the SAN transitional cells, their identity can now be confirmed by a combination of established ($Hcn4^{low}$, $Isl1^{low/neg}$, $Shox2^{+}$, and $Tbx3^{low}$) and novel ($Igfbp5^{+}$, $Cpne5^{+}$, $Smoc2^{+}$, and $Rgs6^{+}$) markers. Subcluster analyses of the *compact* SAN cells revealed two distinct clusters consistent with the Head ($Hcn4^{+}$, $Shox2^{+}$, $Tbx18^{+}$, *and* $Nkx2\text{-}5^{neg}$) and Tail ($Hcn4^{+}$, $Shox2^{+}$, $Tbx18^{neg}$, *and* $Nkx2\text{-}5^{+}$) cells [62]. These two functional SAN subdomains have long been recognized, with the Head representing the leading pacemaker region that can shift to the Tail in response to various stimuli, both physiologic and extrinsic [63, 64], thereby providing a "fail-safe" to prevent rhythm failure [65]. For the first time, the single-cell approach enabled an in-depth analysis of the transcriptional variation between these rare and distinct cell types.

Efforts to deconstruct the AVN/His and Purkinje fiber (PF) regions have similarly revealed significant inter- and intra-component cell type heterogeneity. For instance, the AVN/His region could be broken down into six transcriptionally distinct and clinically relevant subpopulations of cells including the compact AVN, nodal extensions, transitional cells, His bundle, and AVN ring [8]. Consistently, Bhattacharyya et al. [66] also identified similar AV nodal cell clusters from single cells isolated from AVN tissue of a *Cx30.2*-tdTomato mouse reporter line. Finally, scRNA-seq of the PF region revealed two distinct cell populations including standard and transitional PF cells, the latter consistent with cells with a hybrid-like phenotype [8]. Further validation of these and other markers in vivo will advance our basic understanding of the ventricular conduction system and may allow for a greater appreciation of the mechanisms that drive clinical arrhythmias such as AVN, heart block, and PF-derived ventricular arrhythmias. For a broader overview of the transcriptional regulation of the CCS, we recommend additional recent reviews [67, 68].

Despite the progress made in elucidating the molecular landscape of the CCS, much work remains to be done both in the validation of uncovered genes and demonstration of their functional relevance in vivo. Cross-referencing existing datasets between species, in particular human, and various developmental time points can help to narrow down the list of evolutionarily conserved genes necessary in the development and/or maturation of the CCS.

14.5 Single-Cell Profiling of Immune Cells in the Heart

In contrast to the adult heart, the neonatal myocardium has robust regeneration capabilities orchestrated by multiple native cardiac cells and infiltrating cell populations. A droplet-based scRNA-seq technology is a powerful way to characterize different types of cells present during cardiac regeneration as it allows for the

dissection of the complex cellular heterogeneity and dynamic intercellular genetic landscape involved in this process.

scRNA-seq of injured neonatal mouse cardiac tissue has identified at least 13 types of cardiac cells based on their defined gene expression signatures, each with their respective subpopulations. These include CMs, ECs, Fbs, epicardial cells, smooth muscle cells (SMCs), pericytes, macrophages, monocytes, dendritic cells, granulocytes, T cells, and glial cells. Intracardiac immune cell populations are characterized by S100 calcium binding protein A9 expression along with concomitant expression of adhesion G protein-coupled receptor E1 for macrophages, monocytes, and dendritic cells. In addition, CD3g and membrane spanning 4-domains A1 (MS4A1) gene expression are used to further define T and B cells, respectively [69].

In a mouse myocardial ischemic injury model, there is a rapid and robust increase in the intracardiac numbers of immune cell populations, including macrophages, monocytes, lymphocytes, and granulocytes, signifying swift local expansion and cardiac infiltration of circulating immune cells [69]. In fact, there is an abundance of immune cells in the homeostatic heart, spanning the full repertoire of the major leukocyte classes, including mononuclear phagocytes, neutrophils, B-cells, and T-cells [70]. Resident macrophages have experienced a growing recognition regarding both their homeostatic and pathophysiologic cardiac functions [71–73]. Four subclasses of intracardiac macrophages have been identified through detailed cell surface marker profiling. All subsets express $CD45^{+}F4/80^{+}CD11b^{+}CD64^{+}MERTK^{+}$ but differ in their expression of MHC-II molecules, CCR2, and Ly6C [74–77]. Fate mapping studies have demonstrated that $CCR2^{-}$ and $Ly6C^{+}$ cardiac macrophages populate the cardiac tissue during embryogenesis before the start of hematopoiesis and self-renew locally without input from circulating cells. Intramyocardial $CCR2^{+}$ populations, on the other hand, are established through circulating precursors [78–80]. In general, however, most human and mouse cardiac macrophages are derived locally and not from circulating progenitors [71].

Unsurprisingly, the intracardiac macrophage population sees the highest increase in their numbers following myocardial injury, with high-resolution single-cell clustering separating the macrophage population into M1 and M2 subsets. The M1 subset is characterized by a proinflammatory phenotype and defined by high expression of CD86 [69, 81–84]. These cells participate in the initial inflammatory phase of cardiac regeneration, digesting, and removing necrotic debris through the release of proinflammatory cytokines, proteolytic enzymes, and reactive oxygen species. M2 macrophages, on the other hand, possess an anti-inflammatory and wound-healing phenotype and are characterized by Arg1 gene expression, witnessing a sharp increase in their numbers early following myocardial injury and contributing to tissue healing and revascularization through the expression of chemokines and growth factors such as TGFβ and PDGF-B. Monocytes, however, express low levels of macrophage maturation marker ADGRE1 but are highly enriched in PLAC8 and ITGAL and function to replenish particularly the proinflammatory $MHC\text{-}II^{high}CCR2^{+}$ intracardiac macrophage population, the depletion of which preserved myocardial function after injury [69, 81, 85]. Current evidence pinpoints

these immune cells as the most prominent source of myocardial injury-enriched genes, highlighting their importance in the neonatal cardiac regeneration process. Specifically, macrophage and monocyte clusters express Areg, CCL24, and CLCF1—all regulators of cardiomyocyte proliferation, the depletion of which blocks neonatal heart regeneration [81, 86, 87]. Similarly, regulatory $CD4^+FOXP3^+$ T cells have been identified as important mediators of cardiac regeneration in the neonatal mouse heart, mitigating the profibrotic functions of M2 macrophages and instead promoting cardiomyocyte proliferation. Inflammatory $CD4^+FOXP3^-$ T cells, on the other hand, drive a profibrotic response, which is mitigated after their ablation [87, 88].

14.6 Future Directions in Single-Cell Multiomic Studies

Since their emergence in the mid-2000s, large-scale genome-wide association studies (GWASs) have been an instrumental tool for understanding population genetics and biology of disease [89]. However, it has since become apparent that GWAS and high-throughput genotyping cannot fully explain causes of disease for several reasons. The discovery of polygenic inheritance patterns, epigenetic regulation from noncoding regions of the genome, pleiotropy, and the influence of environmental factors all represent challenges to inferring causality of genetic variants from genomics data alone [90]. Capitalizing on advancements in high-throughput technologies to provide a molecular basis for gene causality, recent studies have adopted a "multiomics" approach in examining gene-trait associations. Multiomics analysis refers to the simultaneous integration of data from multiple omics technologies, including but not limited to genomics, transcriptomics, epigenomics, proteomics, metabolomics, and microbiomics [91].

Current multiomics strategies are highly diverse in application and frequently applied in the context of human disease. With regard to the heart, multiomics approaches have integrated genomic data from existing GWAS and expression quantitative trait locus (eQTL) studies with transcriptomic mRNA sequencing data or epigenomic assay for transpose-accessible chromatin sequencing (ATAC-seq) data to identify biomarkers for coronary artery disease and cardiac hypertrophy [91–93]. Studies combining transcriptomic data and liquid chromatography with tandem mass spectrometry (LC-MS) data examined the effects of cardiac hypertrophy on proteome dynamics as well as the metabolomic landscape of heart regeneration in mice [94, 95]. Advancements in single-cell technologies have also generated novel multiomics pipelines for simultaneous data collection across multiple modalities, including joint scRNA-seq and single-cell ATAC-seq as well as multimodal cellular indexing of transcriptomes and epitopes by sequencing (CITE-seq) [96, 97].

Single-cell applications have received considerable attention as higher resolution data enable identification of heterogeneity within cell types and quantification of tissue-level changes due to changes in cell type composition over time [90]. This potential for pseudotime analysis has popularized the use of these approaches to generate spatiotemporal maps of cellular heterogeneity [98, 99]. Perhaps the largest-

scale example to date, the Human Cell Atlas is an international collaborative effort inspired by The Human Genome Project that aims to construct multimodal profiles for all cell types in healthy human tissue across various physiological states [100].

In summary, by providing more precise methods for identification of causal genes, emerging multiomics techniques represent a potential solution to the critical gaps left by GWAS. While existing studies have predominantly focused on the integration of genomics, transcriptomics, and epigenomics, future studies utilizing meta-transcriptomics and metagenomics are highly likely given the rapid growth of the field. Finally, the advent of single-cell multiomics analysis posits the creation of large-scale, comprehensive atlases of whole organs or organ systems, which, in addition to contributing highly nuanced reference datasets for the scientific community, may have important clinical implications for illuminating chains of causality from genetic variation to manifestation of disease.

References

1. Brade T, Pane LS, Moretti A, Chien KR, Laugwitz K-L. Embryonic heart progenitors and cardiogenesis. Cold Spring Harb Perspect Med. 2013;3(10):a013847. https://doi.org/10.1101/cshperspect.a013847.
2. Meilhac SM, Buckingham ME. The deployment of cell lineages that form the mammalian heart. Nat Rev Cardiol. 2018;15(11):705–24. https://doi.org/10.1038/s41569-018-0086-9.
3. Ivanovitch K, Temiño S, Torres M. Live imaging of heart tube development in mouse eveals alternating phases of cardiac differentiation and morphogenesis. elife. 2017;6:e30668. https://doi.org/10.7554/elife.30668.
4. Lin C-J, Lin C-Y, Chen C-H, Zhou B, Chang C-P. Partitioning the heart: mechanisms of cardiac septation and valve development. Development. 2012;139(18):3277–99. https://doi.org/10.1242/dev.063495.
5. Wu M. Mechanisms of trabecular formation and specification during Cardiogenesis. Pediatr Cardiol. 2018;39(6):1082–9. https://doi.org/10.1007/s00246-018-1868-x.
6. Lamers WH, Moorman AFM. Cardiac Septation: a late contribution of the embryonic primary myocardium to heart morphogenesis. Circ Res. 2002;91(2):93–103. https://doi.org/10.1161/01.RES.0000027135.63141.89.
7. Tucker NR, Chaffin M, Fleming SJ, Hall AW, Parsons VA, Bedi KC, et al. Transcriptional and cellular diversity of the human heart. Circulation. 2020;142(5):466–82. https://doi.org/10.1161/CIRCULATIONAHA.119.045401.
8. Goodyer W, Beyersdorf B, Paik D, Tian L, Li G, Buikema J, et al. Transcriptomic profiling of the developing cardiac conduction system at single-cell resolution. Circ Res. 2019;125(4):379–97. https://doi.org/10.1161/CIRCRESAHA.118.314578.
9. Zhou B, Pu WT. More than a cover: epicardium as a novel source of cardiac progenitor cells. Regen Med. 2008;3(5):633–5. https://doi.org/10.2217/17460751.3.5.633.
10. Samsa LA, Yang B, Liu J. Embryonic cardiac chamber maturation: Trabeculation, conduction, and cardiomyocyte proliferation. Am J Med Genet C Semin Med Genet. 2013;163C(3):157–68. https://doi.org/10.1002/ajmg.c.31366.
11. Van Vliet P, Wu SM, Zaffran S, Puceat M. Early cardiac development: a view from stem cells to embryos. Editor's choice. 2012;96(3):352–62. https://doi.org/10.1093/cvr/cvs270.
12. Pimpalwar N, Czuba T, Smith ML, Nilsson J, Gidlöf O, Smith JG. Methods for isolation and transcriptional profiling of individual cells from the human heart. Heliyon. 2020;6(12):e05810-e. https://doi.org/10.1016/j.heliyon.2020.e05810.

13. Cao J, O'Day DR, Pliner HA, Kingsley PD, Deng M, Daza RM, et al. A human cell atlas of fetal gene expression. Science. 2020;370(6518):eaba7721. https://doi.org/10.1126/science.aba7721.
14. Liao X, Makris M, Luo XM. Fluorescence-activated cell sorting for purification of Plasmacytoid dendritic cells from the mouse bone marrow. J Vis Exp. 2016;117:54641. https://doi.org/10.3791/54641.
15. Samad T, Wu SM. Single cell RNA sequencing approaches to cardiac development and congenital heart disease. Semin Cell Dev Biol. 2021;118:129–35. https://doi.org/10.1016/j.semcdb.2021.04.023.
16. Gladka MM, Molenaar B, Ruiter H, Svd E, Tsui H, Versteeg D, et al. Single-cell sequencing of the healthy and diseased heart reveals cytoskeleton-associated protein 4 as a new modulator of fibroblasts activation. Circulation. 2018;138(2):166–80. https://doi.org/10.1161/CIRCULATIONAHA.117.030742.
17. DeLaughter DM. The use of the Fluidigm C1 for RNA expression analyses of single cells. Curr Protoc Mol Biol. 2018;122(1):e55. https://doi.org/10.1002/cpmb.55.
18. Papalexi E, Satija R. Single-cell RNA sequencing to explore immune cell heterogeneity. Nat Rev Immunol. 2018;18(1):35–45. https://doi.org/10.1038/nri.2017.76.
19. Bakken TE, Hodge RD, Miller JA, Yao Z, Nguyen TN, Aevermann B, et al. Single-nucleus and single-cell transcriptomes compared in matched cortical cell types. PLoS One. 2018;13(12):e0209648. https://doi.org/10.1371/journal.pone.0209648.
20. Paik DT, Cho S, Tian L, Chang HY, Wu JC. Single-cell RNA sequencing in cardiovascular development, disease and medicine. Nat Rev Cardiol. 2020;17(8):457–73. https://doi.org/10.1038/s41569-020-0359-y.
21. Kashima Y, Sakamoto Y, Kaneko K, Seki M, Suzuki Y, Suzuki A. Single-cell sequencing techniques from individual to multiomics analyses. Exp Mol Med. 2020;52(9):1419–27. https://doi.org/10.1038/s12276-020-00499-2.
22. Yamada S, Nomura S. Review of single-cell RNA sequencing in the heart. Int J Mol Sci. 2020;21(21):8345. https://doi.org/10.3390/ijms21218345.
23. Choi JR, Yong KW, Choi JY, Cowie AC. Single-cell RNA sequencing and its combination with protein and DNA analyses. Cell. 2020;9(5):1130. https://doi.org/10.3390/cells9051130.
24. Goldstein LD, Chen Y-JJ, Dunne J, Mir A, Hubschle H, Guillory J, et al. Massively parallel nanowell-based single-cell gene expression profiling. BMC Genomics. 2017;18(1):519. https://doi.org/10.1186/s12864-017-3893-1.
25. Yekelchyk M, Guenther S, Preussner J, Braun T. Mono- and multi-nucleated ventricular cardiomyocytes constitute a transcriptionally homogenous cell population. Basic Res Cardiol. 2019;114(5):36. https://doi.org/10.1007/s00395-019-0744-z.
26. Kretzschmar K, Watt FM. Lineage tracing. Cell. 2012;148(1):33–45. https://doi.org/10.1016/j.cell.2012.01.002.
27. Cao J, Spielmann M, Qiu X, Huang X, Ibrahim DM, Hill AJ, et al. The single-cell transcriptional landscape of mammalian organogenesis. Nature. 2019;566(7745):496–502. https://doi.org/10.1038/s41586-019-0969-x.
28. Farrell JA, Wang Y, Riesenfeld SJ, Shekhar K, Regev A, Schier AF. Single-cell reconstruction of developmental trajectories during zebrafish embryogenesis. Science. 2018;360(6392):eaar3131. https://doi.org/10.1126/science.aar3131.
29. Haghverdi L, Buettner F, Theis FJ. Diffusion maps for high-dimensional single-cell analysis of differentiation data. Bioinformatics. 2015;31(18):2989–98. https://doi.org/10.1093/bioinformatics/btv325.
30. Street K, Risso D, Fletcher RB, Das D, Ngai J, Yosef N, et al. Slingshot: cell lineage and pseudotime inference for single-cell transcriptomics. BMC Genomics. 2018;19(1):477. https://doi.org/10.1186/s12864-018-4772-0.
31. Wolf FA, Hamey FK, Plass M, Solana J, Dahlin JS, Göttgens B, et al. PAGA: graph abstraction reconciles clustering with trajectory inference through a topology preserving map of single cells. Genome Biol. 2019;20(1):59. https://doi.org/10.1186/s13059-019-1663-x.

32. Lescroart F, Chabab S, Lin X, Rulands S, Paulissen C, Rodolosse A, et al. Early lineage restriction in temporally distinct populations of Mesp1 progenitors during mammalian heart development. Nat Cell Biol. 2014;16(9):829–40.
33. Meilhac SM, Esner M, Kelly RG, Nicolas J-F, Buckingham ME. The clonal origin of myocardial cells in different regions of the embryonic mouse heart. Dev Cell. 2004;6(5):685–98.
34. Zaffran S, Kelly RG, Meilhac SM, Buckingham ME, Brown NA. Right ventricular myocardium derives from the anterior heart field. Circ Res. 2004;95(3):261–8.
35. Zhou L, Liu J, Olson P, Zhang K, Wynne J, Xie L. Tbx5 and Osr1 interact to regulate posterior second heart field cell cycle progression for cardiac septation. J Mol Cell Cardiol. 2015;85:1–12.
36. Cai C-L, Liang X, Shi Y, Chu P-H, Pfaff SL, Chen J, et al. Isl1 identifies a cardiac progenitor population that proliferates prior to differentiation and contributes a majority of cells to the heart. Dev Cell. 2003;5(6):877–89.
37. Li G, Xu A, Sim S, Priest JR, Tian X, Khan T, et al. Transcriptomic profiling maps anatomically patterned subpopulations among single embryonic cardiac cells. Dev Cell. 2016;39(4):491–507.
38. DeLaughter DM, Bick AG, Wakimoto H, McKean D, Gorham JM, Kathiriya IS, et al. Single-cell resolution of temporal gene expression during heart development. Dev Cell. 2016;39(4):480–90.
39. Scialdone A, Tanaka Y, Jawaid W, Moignard V, Wilson NK, Macaulay IC, et al. Resolving early mesoderm diversification through single-cell expression profiling. Nature. 2016;535(7611):289–93.
40. de Soysa TY, Ranade SS, Okawa S, Ravichandran S, Huang Y, Salunga HT, et al. Single-cell analysis of cardiogenesis reveals basis for organ-level developmental defects. Nature. 2019;572(7767):120–4.
41. Jia G, Preussner J, Chen X, Guenther S, Yuan X, Yekelchyk M, et al. Single cell RNA-seq and ATAC-seq analysis of cardiac progenitor cell transition states and lineage settlement. Nat Commun. 2018;9(1):4877. https://doi.org/10.1038/s41467-018-07307-6.
42. Xiong H, Luo Y, Yue Y, Zhang J, Ai S, Li X, et al. Single-cell transcriptomics reveals chemotaxis-mediated intraorgan crosstalk during cardiogenesis. Circ Res. 2019;125(4):398–410.
43. Hill MC, Kadow ZA, Li L, Tran TT, Wythe JD, Martin JF. A cellular atlas of Pitx2-dependent cardiac development. Development. 2019;146(12):dev180398. https://doi.org/10.1242/dev.180398.
44. Liang D, Xue J, Geng L, Zhou L, Lv B, Zeng Q, et al. Cellular and molecular landscape of mammalian sinoatrial node revealed by single-cell RNA sequencing. Nat Commun. 2021;12(1):1–15.
45. Hofbauer P, Jahnel SM, Papai N, Giesshammer M, Deyett A, Schmidt C, et al. Cardioids reveal self-organizing principles of human cardiogenesis. Cell. 2021;184(12):3299–3317.e22.
46. Rhee S, Paik DT, Yang JY, Nagelberg D, Williams I, Tian L, et al. Endocardial/endothelial angiocrines regulate cardiomyocyte development and maturation and induce features of ventricular non-compaction. bioRxiv. 2020;42(41):4264–76.
47. Su T, Stanley G, Sinha R, D'Amato G, Das S, Rhee S, et al. Single-cell analysis of early progenitor cells that build coronary arteries. Nature. 2018;559(7714):356–62.
48. Asp M, Giacomello S, Larsson L, Wu C, Fürth D, Qian X, et al. A spatiotemporal organ-wide gene expression and cell atlas of the developing human heart. Cell. 2019;179(7):1647–60. e19
49. Cui Y, Zheng Y, Liu X, Yan L, Fan X, Yong J, et al. Single-cell transcriptome analysis maps the developmental track of the human heart. Cell Rep. 2019;26(7):1934–50. e5
50. Litviňuková M, Talavera-López C, Maatz H, Reichart D, Worth CL, Lindberg EL, et al. Cells of the adult human heart. Nature. 2020;588(7838):466–72.

51. Marín-Sedeño E, de Morentin XM, Pérez-Pomares JM, Gómez-Cabrero D, Ruiz-Villalba A. Understanding the adult mammalian heart at single-cell RNA-Seq resolution. Front Cell Dev Biol. 2021;9:645276.
52. Schaum N, Karkanias J, Neff NF, May AP, Quake SR, Wyss-Coray T, et al. Single-cell transcriptomics of 20 mouse organs creates a tabula Muris. Nature. 2018;562(7727):367–72. https://doi.org/10.1038/s41586-018-0590-4.
53. Wang L, Yu P, Zhou B, Song J, Li Z, Zhang M, et al. Single-cell reconstruction of the adult human heart during heart failure and recovery reveals the cellular landscape underlying cardiac function. Nat Cell Biol. 2020;22(1):108–19.
54. Tyser RC, Ibarra-Soria X, McDole K, Jayaram SA, Godwin J, van den Brand TA, et al. Characterization of a common progenitor pool of the epicardium and myocardium. Science. 2021;371(6533):eabb2986.
55. Vedantham V. New approaches to biological pacemakers: links to sinoatrial node development. Trends Mol Med. 2015;21(12):749–61.
56. Christoffels VM, Smits GJ, Kispert A, Moorman AF. Development of the pacemaker tissues of the heart. Circ Res. 2010;106(2):240–54.
57. Liang X, Evans SM, Sun Y. Development of the cardiac pacemaker. Cell Mol Life Sci. 2017;74(7):1247–59.
58. Liang X, Wang G, Lin L, Lowe J, Zhang Q, Bu L, et al. HCN4 dynamically marks the first heart field and conduction system precursors. Circ Res. 2013;113(4):399–407.
59. Pallante BA, Giovannone S, Fang-Yu L, Zhang J, Liu N, Kang G, et al. Contactin-2 expression in the cardiac Purkinje fiber network. Circ Arrhythm Electrophysiol. 2010;3(2):186–94.
60. Liang X, Zhang Q, Cattaneo P, Zhuang S, Gong X, Spann NJ, et al. Transcription factor ISL1 is essential for pacemaker development and function. J Clin Invest. 2015;125(8):3256–68.
61. Vedantham V, Galang G, Evangelista M, Deo RC, Srivastava D. RNA sequencing of mouse sinoatrial node reveals an upstream regulatory role for Islet-1 in cardiac pacemaker cells. Circ Res. 2015;116(5):797–803.
62. Wiese C, Grieskamp T, Airik R, Mommersteeg MT, Gardiwal A, de Gier-de Vries C, et al. Formation of the sinus node head and differentiation of sinus node myocardium are independently regulated by Tbx18 and Tbx3. Circ Res. 2009;104(3):388–97.
63. Monfredi O, Dobrzynski H, Mondal T, Boyett MR, Morris GM. The anatomy and physiology of the sinoatrial node—a contemporary review. Pacing Clin Electrophysiol. 2010;33(11):1392–406.
64. Verheijck EE, van Kempen MJ, Veereschild M, Lurvink J, Jongsma HJ, Bouman LN. Electrophysiological features of the mouse sinoatrial node in relation to connexin distribution. Cardiovasc Res. 2001;52(1):40–50.
65. Li N, Hansen BJ, Csepe TA, Zhao J, Ignozzi AJ, Sul LV, et al. Redundant and diverse intranodal pacemakers and conduction pathways protect the human sinoatrial node from failure. Sci Transl Med. 2017;9(400):eaam5607.
66. Bhattacharyya S, Duan J, Wang L, Li B, Bhakta M, Fernandez-Perez A, et al. Using Gjd3-CreEGFP mice to examine atrioventricular node morphology and composition. Sci Rep. 2019;9(1):1–15.
67. Mantri S, Wu SM, Goodyer WR. Molecular profiling of the cardiac conduction system: the Dawn of a new era. Curr Cardiol Rep. 2021;23(8):1–11.
68. van Eif VW, Devalla HD, Boink GJ, Christoffels VM. Transcriptional regulation of the cardiac conduction system. Nat Rev Cardiol. 2018;15(10):617–30.
69. Wang Z, Cui M, Shah AM, Tan W, Liu N, Bassel-Duby R, et al. Cell-type-specific gene regulatory networks underlying murine neonatal heart regeneration at single-cell resolution. Cell Rep. 2020;33(10):108472.
70. Ramos GC, van den Berg A, Nunes-Silva V, Weirather J, Peters L, Burkard M, et al. Myocardial aging as a T-cell–mediated phenomenon. Proc Natl Acad Sci. 2017;114(12):E2420–E9.

71. Bajpai G, Schneider C, Wong N, Bredemeyer A, Hulsmans M, Nahrendorf M, et al. The human heart contains distinct macrophage subsets with divergent origins and functions. Nat Med. 2018;24(8):1234–45.
72. Honold L, Nahrendorf M. Resident and monocyte-derived macrophages in cardiovascular disease. Circ Res. 2018;122(1):113–27.
73. Hulsmans M, Clauss S, Xiao L, Aguirre AD, King KR, Hanley A, et al. Macrophages facilitate electrical conduction in the heart. Cell. 2017;169(3):510–22.e20.
74. Pinto AR, Paolicelli R, Salimova E, Gospocic J, Slonimsky E, Bilbao-Cortes D, et al. An abundant tissue macrophage population in the adult murine heart with a distinct alternatively-activated macrophage profile. PLoS One. 2012;7(5):e36814.
75. Epelman S, Lavine KJ, Beaudin AE, Sojka DK, Carrero JA, Calderon B, et al. Embryonic and adult-derived resident cardiac macrophages are maintained through distinct mechanisms at steady state and during inflammation. Immunity. 2014;40(1):91–104.
76. Epelman S, Lavine KJ, Randolph GJ. Origin and functions of tissue macrophages. Immunity. 2014;41(1):21–35.
77. Epelman S, Liu PP, Mann DL. Role of innate and adaptive immune mechanisms in cardiac injury and repair. Nat Rev Immunol. 2015;15(2):117–29.
78. Heidt T, Courties G, Dutta P, Sager HB, Sebas M, Iwamoto Y, et al. Differential contribution of monocytes to heart macrophages in steady-state and after myocardial infarction. Circ Res. 2014;115(2):284–95.
79. Molawi K, Wolf Y, Kandalla PK, Favret J, Hagemeyer N, Frenzel K, et al. Progressive replacement of embryo-derived cardiac macrophages with age. J Exp Med. 2014;211(11):2151–8.
80. Ensan S, Li A, Besla R, Degousee N, Cosme J, Roufaiel M, et al. Self-renewing resident arterial macrophages arise from embryonic CX3CR1+ precursors and circulating monocytes immediately after birth. Nat Immunol. 2016;17(2):159–68.
81. Aurora AB, Porrello ER, Tan W, Mahmoud AI, Hill JA, Bassel-Duby R, et al. Macrophages are required for neonatal heart regeneration. J Clin Invest. 2014;124(3):1382–92.
82. Biswas SK, Gangi L, Paul S, Schioppa T, Saccani A, Sironi M, et al. A distinct and unique transcriptional program expressed by tumor-associated macrophages (defective NF-κB and enhanced IRF-3/STAT1 activation). Blood. 2006;107(5):2112–22.
83. Martinez FO, Gordon S. The M1 and M2 paradigm of macrophage activation: time for reassessment. F1000 Prime Rep. 2014;6:13.
84. Murray PJ, Allen JE, Biswas SK, Fisher EA, Gilroy DW, Goerdt S, et al. Macrophage activation and polarization: nomenclature and experimental guidelines. Immunity. 2014;41(1):14–20.
85. Lavine KJ, Epelman S, Uchida K, Weber KJ, Nichols CG, Schilling JD, et al. Distinct macrophage lineages contribute to disparate patterns of cardiac recovery and remodeling in the neonatal and adult heart. Proc Natl Acad Sci. 2014;111(45):16029–34.
86. Wang Z, Cui M, Shah AM, Ye W, Tan W, Min Y-L, et al. Mechanistic basis of neonatal heart regeneration revealed by transcriptome and histone modification profiling. Proc Natl Acad Sci. 2019;116(37):18455–65.
87. Li J, Yang KY, Tam RCY, Chan VW, Lan HY, Hori S, et al. Regulatory T-cells regulate neonatal heart regeneration by potentiating cardiomyocyte proliferation in a paracrine manner. Theranostics. 2019;9(15):4324.
88. Li J, Liang C, Yang KY, Huang X, Han MY, Li X, et al. Specific ablation of CD4+ T-cells promotes heart regeneration in juvenile mice. Theranostics. 2020;10(18):8018.
89. Visscher PM, Wray NR, Zhang Q, Sklar P, McCarthy MI, Brown MA, et al. 10 years of GWAS discovery: biology, function, and translation. Am J Hum Genet. 2017;101(1):5–22. https://doi.org/10.1016/j.ajhg.2017.06.005.
90. Hasin Y, Seldin M, Lusis A. Multi-omics approaches to disease. Genome Biol. 2017;18(1):83. https://doi.org/10.1186/s13059-017-1215-1.

91. Leon-Mimila P, Wang J, Huertas-Vazquez A. Relevance of multi-omics studies in cardiovascular diseases. Front Cardiovasc Med. 2019;6:91. https://doi.org/10.3389/fcvm.2019.00091.
92. Liu B, Pjanic M, Wang T, Nguyen T, Gloudemans M, Rao A, et al. Genetic regulatory mechanisms of smooth muscle cells map to coronary artery disease risk loci. Am J Hum Genet. 2018;103(3):377–88. https://doi.org/10.1016/j.ajhg.2018.08.001.
93. Santolini M, Romay MC, Yukhtman CL, Rau CD, Ren S, Saucerman JJ, et al. A personalized, multiomics approach identifies genes involved in cardiac hypertrophy and heart failure. NPJ Sys Biol App. 2018;4(1):12–3. https://doi.org/10.1038/s41540-018-0046-3.
94. Lalowski MM, Björk S, Finckenberg P, Soliymani R, Tarkia M, Calza G, et al. Characterizing the key metabolic pathways of the neonatal mouse heart using a quantitative combinatorial omics approach. Front Physiol. 2018;9:365. https://doi.org/10.3389/fphys.2018.00365.
95. Lau E, Cao Q, Lam MPY, Wang J, Ng DCM, Bleakley BJ, et al. Integrated omics dissection of proteome dynamics during cardiac remodeling. Nat Commun. 2018;9(1):120. https://doi.org/10.1038/s41467-017-02467-3.
96. Gayoso A, Steier Z, Lopez R, Regier J, Nazor KL, Streets A, et al. Joint probabilistic modeling of single-cell multi-omic data with totalVI. Nat Methods. 2021;18(3):272–82. https://doi.org/10.1038/s41592-020-01050-x.
97. Stoeckius M, Hafemeister C, Stephenson W, Houck-Loomis B, Chattopadhyay PK, Swerdlow H, et al. Simultaneous epitope and transcriptome measurement in single cells. Nat Methods. 2017;14(9):865–8. https://doi.org/10.1038/nmeth.4380.
98. Schlotter F, Halu A, Goto S, Blaser M, Body S, Lee L, et al. Spatiotemporal multi-omics mapping generates a molecular atlas of the aortic valve and reveals networks driving disease. Circulation. 2018;138(4):377–93. https://doi.org/10.1161/CIRCULATIONAHA.117.032291.
99. Zhu C, Zhang Y, Li YE, Lucero J, Behrens MM, Ren B. Joint profiling of histone modifications and transcriptome in single cells from mouse brain. Nat Methods. 2021;18(3):283–92. https://doi.org/10.1038/s41592-021-01060-3.
100. Regev A, Teichmann SA, Lander ES, Amit I, Benoist C, Birney E, et al. Science forum : the human cell atlas. elife. 2017;6:e27041.

Part III

Central Molecular and Cellular Pathways

Inter- and Intracellular Signaling Pathways 15

Gergana Dobreva and Joerg Heineke

Abstract

Cardiovascular diseases, both congenital and acquired, are the leading cause of death worldwide, associated with significant health consequences and economic burden. Due to major advances in surgical procedures, most patients with congenital heart disease (CHD) survive into adulthood but suffer from previously unrecognized long-term consequences, such as early-onset heart failure. Therefore, understanding the molecular mechanisms resulting in heart defects and the lifelong complications due to hemodynamic overload are of utmost importance. Congenital heart disease arises in the first trimester of pregnancy, due to defects in the complex morphogenetic patterning of the heart. This process is coordinated through a complicated web of intercellular communication between the epicardium, the endocardium, and the myocardium. In the postnatal heart, similar crosstalk between cardiomyocytes, endothelial cells, and fibroblasts exists during pathological hemodynamic overload that emerges as a consequence of a congenital heart defect. Ultimately, communication between cells triggers the activation

G. Dobreva (✉)
ECAS (European Center for Angioscience), Department of Cardiovascular Genomics and Epigenomics, Mannheim Faculty of Medicine, Heidelberg University, Mannheim, Germany

German Centre for Cardiovascular Research (DZHK) Partner Site, Heidelberg/Mannheim, Germany
e-mail: gergana.dobreva@medma.uni-heidelberg.de

J. Heineke (✉)
German Centre for Cardiovascular Research (DZHK) Partner Site, Heidelberg/Mannheim, Germany

ECAS (European Center for Angioscience), Department of Cardiovascular Physiology, Mannheim Faculty of Medicine, Heidelberg University, Mannheim, Germany
e-mail: Joerg.Heineke@medma.uni-heidelberg.de

© The Author(s), under exclusive license to Springer Nature Switzerland AG 2024

S. Rickert-Sperling et al. (eds.), *Congenital Heart Diseases: The Broken Heart*,
Advances in Experimental Medicine and Biology 1441,
https://doi.org/10.1007/978-3-031-44087-8_15

of intracellular signaling circuits, which allow fine coordination of cardiac development and function. Here, we review the inter- and intracellular signaling mechanisms in the heart as they were discovered mainly in genetically modified mice.

15.1 Introduction

Cardiac development is a tightly coordinated morphogenetic process that requires precise specification, expansion, migration, and differentiation of cardiovascular progenitor cells into the various cardiac cell types [1, 2]. These distinct cardiac cell types are in a constant crosstalk, which enables them to coordinate their activity that is essential for cardiac morphogenesis, postnatal cardiac growth, contractile performance, and rhythmicity [3]. Specific growth factors are released from a particular cell type in a precise spatiotemporal manner during development to direct and control the differentiation, proliferation, or migration of one or multiple neighboring cell types. In this way, endocardial cells release, for example, Neuregulin1 to induce trabeculation and proliferation of the adjacent myocardium. Similar signaling circuits originate from cardiomyocytes to impact endocardial cells and also exist between epicardial cells and the myocardium. Defects in these events (e.g., as a consequence of an inherited gene mutation) are a common reason for congenital heart disease. On the other hand, the existence of congenital heart disease puts an extra burden (i.e., pressure or volume-overload) on the right or left ventricle (depending on the type of defect), which—in order to reduce wall stress—mounts a pathological hypertrophic response of the myocardium. Pathological hypertrophy, although compensatory in the short term, constitutes a common and important risk factor for the development of chronic heart failure. Heart failure is a serious condition, in which the heart, due to decreased pump function, is unable to pump enough blood into the circulation to meet systemic demands and is associated with high morbidity and mortality. The severity and clinical implications of hypertrophy or heart failure depend, to a large degree, on the type and severity of the underlying cardiac defect. Pathological myocardial growth is associated with activation and proliferation of fibroblasts, which secrete extracellular matrix. Similarly, endothelial cells initially proliferate, and angiogenesis is increased to deliver sufficient oxygen and nutrients to the growing cardiac myocytes, although in end-stage heart failure capillary rarefaction exists. Recently, it has emerged that fibroblasts as well as endothelial cells serve an important regulatory role in the myocardium during chronic stress exposure in the adult through secretion of growth factors and extracellular matrix proteins—similar to their role in heart development. These growth factors and extracellular matrix components act on cardiac myocytes and trigger intracellular signaling during intrauterine or postnatal physiological growth as well as under conditions of pathological hypertrophy and heart failure. Although signaling circuits are inherently complex and abundant, this chapter will highlight the central inter- and intracellular pathways and effectors that mediate cardiac development and the growth response in cardiomyocytes.

15.2 Intercellular Signaling in Cardiac Development and Physiological Growth

15.2.1 Endocardial–Myocardial Signaling

During embryogenesis, endocardial endothelial cell (EC) and myocardial precursors arise bilaterally within the mesoderm and through migration and overall embryo folding coalesce at the ventral midline to form a primitive heart tube consisting of an inner endocardial layer and an outer myocardial layer. The two layers are separated by a dense extracellular matrix, termed cardiac jelly, but continue to communicate through paracrine signals. Soon afterward, second heart field (SHF) progenitor cells are added to the arterial and venous poles of the heart tube allowing its continuous growth and complex morphogenetic patterning [4]. Perturbation of SHF development and deployment results in a spectrum of congenital heart defects, including conotruncal and atrial septal defects [2, 5, 6]. These SHF precursors are multipotent and give rise to the distinct lineages in the heart, including the myocardium and the endocardium [4, 7–9]. The endocardium has recently gained attention due to its remarkable cellular plasticity and important contribution to the distinct heart cell types as well as signaling function during heart development, disease, and regeneration [10]. On one hand, it forms a vascular endothelial layer contiguous with the rest of the vasculature, which provides nutrients and oxygen to the heart. On the other hand, it receives and secretes signals that instruct heart morphogenesis and function, e.g., trabeculation, cardiac valve, septum formation, and myocardial compaction [3, 11, 12]. Lack of the endocardium results in failed myocardial maturation, with reduced cardiomyocyte proliferation and lack of myocardial trabeculation that together leads to embryonic heart failure and death. Trabeculae are folds of the myocardium that help to direct blood flow in the ventricular chambers and increase contractility. The trabeculae later contribute to the formation of papillary muscle, interventricular septum, and the cardiac conduction system. Increased or persistent trabeculation (hypertrabeculation) is associated with left ventricular non-compaction, a class of inherited cardiomyopathy [13]. The key importance of endocardial cells for heart development has been demonstrated by endothelial-specific gene inactivation of different components of the Notch, vascular endothelial growth factor (VEGF), fibroblast growth factor (FGF), Neuregulin-1 (Nrg1)/ErbB2/B4, and angiopoietin-1 signaling pathways, among others. Many of these pathways are tightly interconnected and can induce distinct temporal and spatial outcomes in the developing heart.

Neuregulin1 (NRG1) belongs to the epidermal growth factor family and is secreted specifically by endocardial cells during midgestation (Fig. 15.1). The tyrosine kinase receptors v-erb-b2 avian erythroblastic leukemia viral oncogene homolog (ErbB)2 and ErbB4 on cardiomyocytes act as Neuregulin1 receptors, (hetero-)dimerize upon ligand binding, and induce ERK1/2 MAP Kinase or protein kinase B/Akt-dependent signaling in these cells (see below) [14]. NRG1-knock-out mice die in the middle of embryogenesis (E10.5) due to lack of normal trabeculation

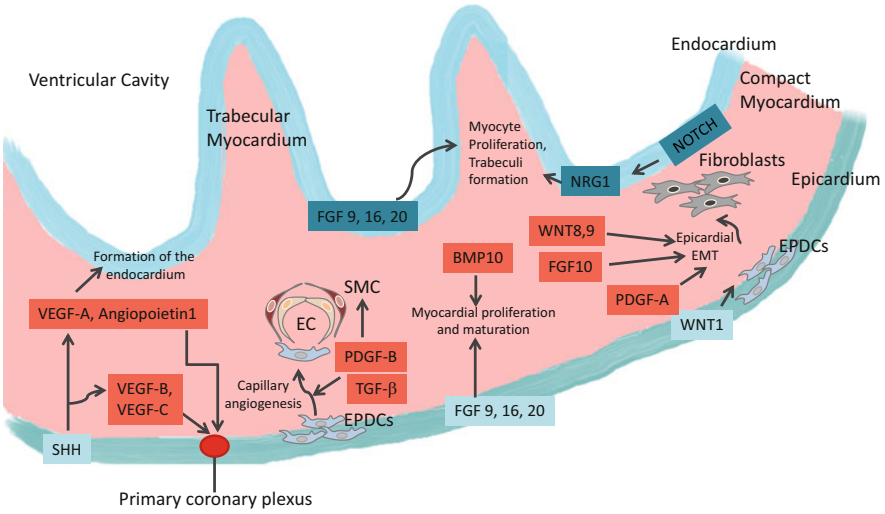

Fig. 15.1 Growth factor signaling between epicardium, endocardium, and myocardium during midgestation. Sonic hedgehog (SHH) is released from the epicardium and triggers the production of angiogenic cytokines (like VEGF-A, Angiopoietin1, VEGF-B, and VEGF-C) in the myocardium, which in turn promote coronary vessel development. FGF9, 16, and 20 are secreted from the endocardial cells and induce myocyte proliferation and formation of the trabeculi, a process that is also supported by Notch/Neuregulin-1 (NRG1) signaling. Similarly, FGF9, 16, and 20 are released from the epicardium and together with BMP10 drive myocardial maturation and proliferation in the compact layer. Myocardial fibroblasts and vascular smooth muscle cells are generated from epicardial cells by epithelial to mesenchymal transition (EMT). This process is activated by WNT8/9, FGF10, PDGF-A, WNT1 for myocardial fibroblasts, and PDGF-B, TGF-β for vascular smooth muscle cells

of the ventricles and ErbB2 and ErbB4 null mice also lack ventricular trabeculation [3, 14]. Conversely, NRG1 injection into the developing heart leads to hypertrabeculation of the ventricles [15]. Thus, endocardial-derived NRG1 induces trabeculation of the myocardium. In addition, it is important for the maintenance of myocardial-specific gene expression in both the trabecular and non-trabecular myocardium. Studies in isolated cardiomyocytes further revealed that Neuregulin1 directly induces cell survival, hypertrophy, and proliferation. Insulin-like growth factor 1 (IGF1) is also secreted by the endocardium and acts together with NRG1. In addition, endocardial NRG1 promotes the development of the cardiac conduction system (CCS) in a tight spatiotemporal manner [16]. Together with NRG1, endothelin-1 (ET-1), also produced by the endothelial cells, is instrumental for the development of the CCS by inducing cardiomyocyte conversion into impulse-conducting Purkinje fibers [17]. Neuregulin1 expression is regulated at least in part by endocardial Notch signaling [18]: Notch is an evolutionary conserved transmembrane receptor family (Notch1-4). Upon ligand binding, the intracellular domain of the Notch receptor (NICD) translocates to the nucleus to act as a cofactor

of the transcription factor recombination signal binding protein for immunoglobulin kappa J region (RBPJK). The membrane-bound proteins of the Delta or Jagged family are ligands of Notch. The expression of Delta4, Notch1, and Notch4 has been detected in the endocardium. Ablation of Notch signaling in the endocardium leads to hypotrabeculation as a result of reduced ephrinB2 expression (direct target of Notch), which in turn leads to reduced NRG1 expression. Endocardial Notch activation triggers the expression of BMP10 in the myocardium, which induces proliferation of cardiomyocytes within the trabeculae. In accordance with these data, over-activation of endocardial Notch leads to myocardial hypertrabeculation [19]. In addition, endocardial Notch1 signaling triggers endothelial-to-mesenchymal transition (EndoMT), which is essential for proper endocardial cushion and valve formation. Mechanistically, N1ICD (Notch1 intracellular domain) activation induces the expression of Snail1 and Snail2, known to inhibit VE-cadherin (Cdh5) levels, thereby resulting in loss of endocardial cell–cell junctions and acquisition of a motile, mesenchymal phenotype [20]. Consistent with the important function of Notch1 signaling in endocardial cushion and valve formation, mutations in NOTCH1 result in a variety of aortic valve anomalies as well as severe valve calcification [21]. Fibroblast growth factor (FGF) 9, 16, and 20 is also expressed in the endocardium (and in the epicardium, see below), but not in the myocardium during midgestation. They act on the myocardial FGF receptors FGFR1 and FGFR2c, to induce cardiomyocyte proliferation and differentiation [22].

15.2.2 Myocardial–Endocardial Signaling

The myocardium plays an important paracrine and autocrine role on the endocardium as well as on endothelial cells during cardiogenesis. It was demonstrated, for example, that cardiomyocytes are the main source of Vascular Endothelial Growth Factor A (VEGF-A), which is one of the most potent angiogenesis inducing factors [23]. Cardiomyocyte-specific VEGF-A knock-out reduces the level of VEGF-A mRNA to $<15\%$ of the wild-type level and leads to significant embryonic mortality and hypovascular, thin-walled hearts [23]. VEGF-A mainly binds and activates the receptor tyrosine kinase VEGF receptor2 (VEGFR2, also called Flk1), which is the major mediator of VEGF-A-dependent mitogenic, angiogenic, and permeability enhancing effects. VEGFR2 is expressed in endothelial cells including the endocardium. VEGFR2 knock-out mice die at embryonic day E8.5–E9.5 and completely lack the endocardium, blood vessels, and cardiac trabeculation [24]. Thus, myocardial-derived VEGF-A is functionally important for the formation of the endocardium, which in turn provides crucial signals for myocardial development (Fig. 15.1). In a similar manner, cardiomyocyte-derived angiopoietin-1 binds to its receptor Tie2 (expressed on endothelial and endocardial cells) to induce the formation of the endocardium [3]. Consistent with this, ablation of Tie2 specifically in the endocardium leads to decreased endocardial cell proliferation and decreased endocardial sprouting. On the other hand, it results in enhanced myocardial proliferation and hyperplastic trabeculae due to the upregulation of Bmp10 and increased retinoic

acid signaling in the trabecular myocardium [25]. Thus, Tie2 signaling is required in an autocrine manner to support endocardial growth and in paracrine manner to inhibit trabecular cardiomyocyte proliferation. Moreover, cardiomyocyte-derived angiopoietin-1 activation of endocardial Tie2 is important for cardiac jelly degradation and chamber expansion [26].

An important anatomical signaling hub between the endocardium and myocardium is found in the development of endocardial cushions in the outflow tract (OFT) and the atrioventricular canal (AVC) that later form the cardiac valves [27]. The endocardial cushions are expansions of the cardiac jelly and become visible at embryonic day E9 of mouse development. Endocardial cells lining these cushions become mesenchymal cells and move into the cushions to form the future valve interstitial cells. This process is called endothelial to mesenchymal transition (EndMT) and is triggered by myocardial signals, for example, by bone morphogenic protein (BMP)2, which is expressed first in the myocardium surrounding the AVC [27]. Its importance for EndMT is shown in cardiomyocyte-specific BMP2 deleted mice, which exerts disturbed AV cushion formation [28]. BMPs bind to type I (in the myocardium ALK2/3) and type II receptors (in the myocardium encoded by *Bmpr2*) at the surface of its target cell and trigger SMAD1/5/8-dependent signaling. Endocardial-specific ablation of *Alk2*, *Alk3,* or *Bmp2r* results in strongly impaired EndMT [27]. Mechanistically, myocardial BMP2 through Alk3 in the endocardium augments the expression of factors triggering EndoMT, such as Twist1, Msx1, and Msx2. BMP4 is also required for proper valve development by regulating atrioventricular (AV) septation after cushions have been formed and conditional ablation of Bmp4 in cardiomyocytes results in AV septum and valve defects [29]. Cardiomyocyte-derived transforming growth factor (TGF) β2 and VEGF-A are similarly involved in the regulation of EndMT, whereby it has been suggested that precise levels of VEGF-A are essential for this process, since both overexpression and inhibition of VEGF-A lead to impaired EndMT [27]. In this regard, deregulated myocardial VEGF-A levels were proposed to account for endocardial cushion defects due to environmental stresses or Down syndrome.

Some cardiomyocyte-derived growth factors also act in an autocrine fashion to regulate formation of the ventricular myocardium. Cardiomyocyte-derived BMP10, for instance, induces cardiomyocyte proliferation and maintains a normal expression level of key cardiogenic factors like NK2 homeobox 5 (NKX2-5) and myocyte enhancer factor 2c (MEF2c); lack of BMP10 in mice results in embryonic mortality between E9.5 and E10.5 with a hypoplastic myocardium [30].

15.2.3 Epicardial–Myocardial Signaling

During midgestation, around E10.5, the epicardium is beginning to form as the outmost epithelial layer that ensheathes the heart [27]. Before that time point, the linear and looping heart tube consists only of two layers, the outer myocardium and an inner layer of endothelial cells (endocardium). The developing epicardium promotes cardiomyocyte proliferation and thereby the proper development of the

myocardial compact layer, which is extremely thin after experimental removal of the epicardium in chick embryos. This regulatory role is mainly mediated by the release of paracrine factors: FGF 9, FGF16, and FGF20 are produced in the epicardium and act on FGFR1/FGFR2 on cardiomyocytes in the adjacent compact layer to induce cellular proliferation and modulate differentiation (Fig. 15.1) [3]. FGF effects in the myocardium also trigger activation of hedgehog (HH) signaling [31]; this circuit is composed of three ligands: sonic (S)HH, indian (I)HH, and desert D(HH), which are all expressed in the embryonic and adult heart, SHH being the most abundant. At midgestation, SHH is expressed in the epicardium, but not in the myocardium. HH ligands bind to the cell surface receptor patched (PTC). In the absence of ligand, PTC inhibits the activation of the multi-transmembrane protein Smoothened (Smo). Upon HH ligand binding, Smo triggers downstream signaling that culminates in activation of GLI transcription factors. Epicardial-derived SHH binds to PTC, which is expressed on cardiomyoblasts and perivascular mesenchymal cells in the myocardium and induces the expression and release of multiple proangiogenic molecules, especially VEGF-A, VEGF-B, VEGF-C, and Angiopoietin2 from its target cells. These factors, in turn, promote coronary vascular development, which starts in the subepicardial space with the formation of the primary vascular plexus (between E11.5 and E13.5) that is later remodeled and expands into the myocardium to form the mature coronary tree. Inhibition of HH signaling in whole heart cultures with the specific inhibitor cyclopamine completely blunts coronary plexus formation, while transgenic overexpression of the HH transcription factor GLI2 in the myocardium at E13.5 increased the vessel density in the subepicardium [32]. Interestingly, HH signaling is still important for maintenance of the coronary vasculature in adult mice, as induced genetic deletion of PTC in cardiomyocytes leads to diminution of cardiac capillarization, aggravation of cardiac hypoxia, cardiomyocyte cell death, subsequent heart failure, and death. Inhibition of HH signaling after myocardial infarction (MI) triggers increased scarring, heart failure, and lethality. Of note, the ligand SHH is expressed in perivascular and interstitial fibroblasts in the myocardium of adult mice, which are cells that are originally mainly derived from the epicardium. In addition, the epicardium itself becomes reactivated and expands after MI and starts to release paracrine factors like WNT1, VEGF-A, FGF, TGFβ2, stromal cell-derived factor 1 (SDF-1), and monocyte chemoattractant protein 1 (MCP-1) [33, 34]. These factors play a protective role when administered to the myocardium after MI [34].

15.2.4 Myocardial–Epicardial Signaling

During embryonic development, the epicardium does not only play a prominent regulatory role via the release of paracrine factors, but also contributes to different cell types (mainly fibroblasts and vascular smooth muscle cells) in the heart through epithelial to mesenchymal transition (EMT). Epicardial cells start to undergo EMT (starting at around E11.5 in mice) to form mesenchymal cells known as epicardium-derived cells (EPDCs, Fig. 15.1) [27, 31]. EPDCs reside in the subepicardial space

and also migrate into the myocardium to form a subset of cardiac fibroblasts and vascular smooth muscle cells. Although it was thought previously that all capillary endothelial cells also arise from EPDCs, recent data revealed that only a small fraction of these cells originate from the epicardium [31]. The majority of vascular endothelial cells are derived from the endocardium and the sinus venosus. Epicardial EMT is mainly triggered by myocardial-derived growth factors. In this regard, not only Wnt ligands (WNTs) from the myocardium (e.g., WNT8a or WNT9) but also autocrine epicardial WNT1 act on the epicardium [3]. In their canonical signaling mode, WNTs bind to a co-receptor complex consisting of frizzled (Fzd) family seven-pass transmembrane proteins and the lipoprotein receptor-related 5/6 (LRP5/6), which ultimately leads to stabilization and nuclear translocation of β-catenin. β-Catenin forms a complex with LEF/TCF family DNA binding proteins to activate the transcription of WNT target genes. Elimination of β-catenin from the epicardium with a Gata5-Cre leads to embryonic mortality in mice between embryonic day 15 and birth, whereby the mutant mice display a defective coronary artery development, but normal veins and microvasculature. This phenotype is the consequence of failed expansion of the subepicardial space and impaired differentiation of epicardium-derived coronary smooth muscle cells, indicating a defective EMT in response to ablation of WNT signaling. In a similar manner, FGF10 from the myocardium might act on FGF receptors-1/2 on epicardial cells. Elimination of this signaling axis leads to myocardial hypoplasia and a defect in cardiac fibroblast formation, although this was disputed in one study [35, 36]. In a third important pathway, platelet-derived growth factor (PDGF) signaling from the myocardium regulates epicardial EMT. When both epicardial PDGF receptors α and β are eliminated from epicardial cells, the process of EMT is blocked with a complete lack of EPDCs. However, as revealed by a selective knock-out of the α- and β- form of the receptor in the epicardium, both receptors also have independent functions: the PDGF receptor α promotes the development of myocardial fibroblasts, while the PDGF receptor β promotes the formation of coronary vascular smooth muscle cells. TGF-β ligands also promote epicardial EMT, stimulate hyaluronic acid production, which is required for epicardial migration, and promote smooth muscle cell differentiation [37]. Epicardial cell proliferation and activation as well as EMT also occur during myocardial injury such as MI also in adult mice. This leads to a thickened epicardial layer on the cardiac surface, but in contrast to embryonic development, not to an invasion of the subjacent myocardium.

15.3 Intercellular Signaling During Pathological Cardiac Growth

While intercellular coordination during the embryonic phase, when the developing heart is still small, depends mainly on signals from the epicardium and endocardium, in the adult heart—due to larger distances—interspersed cells such as fibroblasts and capillary endothelial cells become a more important source of regulatory growth factors that affect cardiac myocytes. In general, intercellular interactions are strong

early in disease (for example, 1 week after the induction of pressure overload) but reduce in the chronic phase [38].

15.3.1 Communication Between Cardiomyocytes

Although in terms of cell number, cardiomyocytes represent only 30–45% (depending on species) of all heart cells because of their size they contribute to more than 90% of the heart's volume. Rich communication takes place among cardiomyocytes. Importantly, cardiac myocytes are directly coupled via gap junction at the intercalated disk (Fig. 15.2) [39]. Mainly ions (Ca^{++}) and small solutes pass through gap junction to promote impulse conduction in the cardiac conduction system and the working myocardium. The gap junctions in adult mice are constituted by connexin40 in myocytes of the conduction system, but by connexin43 in the working myocardium. Besides impulse conduction, the connexins are important for cardiac morphogenesis, since heterozygous and homozygous deletion of connexin40 leads to developmental abnormalities of the heart, including double-outlet right

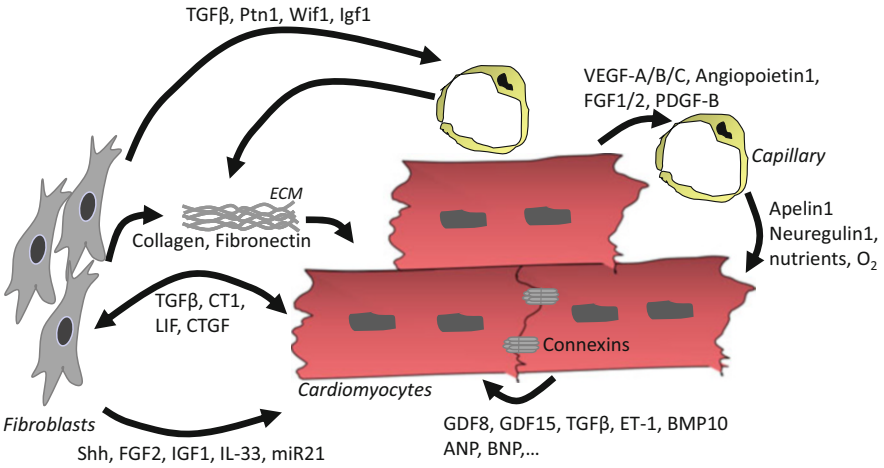

Fig. 15.2 Intercellular communication in the adult myocardium as it occurs during hemodynamic overload. Cardiomyocytes are directly coupled by gap junctions that are constituted by connexins and allow passage of calcium ions for electrical coupling between myocytes. In addition, secreted proteins like GDF8, GDF15 and ANP influence neighboring myocytes. Cardiomyocytes also release angiogenic cytokines (e.g. VEGF-A/B/C, FGF1/2) that promote capillary angiogenesis. In turn, capillaries produce proteins like Apelin1 and Neuregulin1 and thereby influence cardiac growth and cardiac function. Capillary endothelial cells also receive signals from a subset of fibroblasts to regulate angiogenesis and to trigger mesenchymal activation, during which endothelial cells contribute to fibrosis. In addition, a direct communication exists between cardiac fibroblasts and myocytes. While the profibrotic cytokines TGF-β and CTGF can be released from both cell types, Shh and IGF-1, for example, are produced mainly in fibroblasts and were shown to influence myocyte survival and hypertrophy. Extracellular matrix (ECM) affects cardiomyocytes by interfering with myocyte coupling and oxygen diffusion from capillaries

ventricle, tetralogy of Fallot and endocardial cushion defects [40]. Cardiomyocyte-specific deletion of connexin43 results in outflow tract abnormalities and cardiac hypertrophy after birth.

Cardiomyocytes secrete various growth factors, which either act in an autocrine fashion on the secreting cell, thus neighboring cardiomyocytes or on non-cardiomyocytes. Among the myocyte-derived factors with functional autocrine effects are for example endothelin-1, ANP, and BNP as well as multiple TGFβ family members, including TGFβ1 and 2, BMP10, growth differentiation factor (GDF) 15, and myostatin (GDF8). Ablation of the TGFβ receptor (R)2 specifically in cardiac myocytes strongly reduced cardiac hypertrophy, fibrosis, and improved cardiac function during experimental pressure overload in mice by transverse aortic constriction (TAC). In this procedure, which is often used as a model of human disease in mice, a ligature is placed between the left common carotid artery and the right innominate artery around the ascending aortic arch. This leads to a robust mechanical pressure overloading of the left ventricle with cardiac hypertrophy (+30–60% in heart weight) within two weeks and reduced cardiac function within 4–8 weeks after surgery. The data from cardiomyocyte-specific Tgfβr2 knock-out mice indicate that intrinsic cardiomyocyte TGFβ signaling is a strong promoter of pathological hypertrophy and dysfunction under these circumstances. In contrast, cardiomyocyte GDF15 acts to inhibit hypertrophy and death in these cells. Myocardial Myostatin is crucial for the maintenance of cardiac homeostasis, as its selective-induced genetic ablation under baseline conditions resulted in hypertrophy, heart failure, and death associated with metabolic imbalance and over-activation of the AMP-activated kinase (AMPK) [41]. In response to stress, cardiomyocytes also upregulate the expression of collagens (i.e., Col1a1 and Col3a1) and cell adhesion genes (like Thbs1/4 and Fn1), which could act on other cardiomyocytes [38].

During hypertrophic heart disease in humans, cardiomyocyte appears to receive less signals not only from other cell types (e.g., endothelial cells and fibroblasts), but also from other cardiomyocytes, while enhancing outgoing signals to endothelial cells and fibroblasts.

15.3.2 Endothelial-Cardiomyocyte Crosstalk

As an organ highly dependent on oxidative energy production, the capillary density in the heart is high and each cardiomyocyte is supplied roughly by one capillary [42]. Capillary endothelial cells are closely associated with cardiomyocytes in an ideal diffusion range not only for capillary-derived nutrients and oxygen but also for reciprocal paracrine signals between these cells. It has been demonstrated that cardiomyocytes regulate the formation and adaptation of the myocardial capillary network and that angiogenesis (i.e., the formation of capillaries from pre-existing endothelial cells) is enhanced during increased hemodynamic load and cardiac hypertrophy in multiple different species (mice, sheep, and humans). In fact, this increase in myocardial capillaries (by about 30–50%) is important for the preservation of cardiac function during hypertrophy. How is myocardial angiogenesis

regulated, especially during pathological overload? As stated above, around 85% of the VEGF-A within the heart is produced by cardiac myocytes [23]. Similarly, expression of pro-angiogenic growth factors like VEGF-B, VEGF-C, Angiopoietin1, FGF1, FGF2, EGF, matrix metallo-proteinase (MMP) 9 as well as PDGF-B has been reported in cardiac myocytes (Fig. 15.2). Expression of these molecules is triggered in cardiomyocytes by signaling molecules, transcription factors, and transcriptional coregulators. In this regard, the transcription factor GATA4, which is activated by mechanical overload in cardiomyocytes, directly binds and activates the *Vegfa* promoter [43]. Consequently, cardiomyocyte-specific GATA4 overexpression induces VEGF-A and capillary angiogenesis in the myocardium of mice, while in turn, genetic deletion of GATA4 in cardiac myocytes reduces myocardial angiogenesis and also leads to heart failure. In parallel, the hypoxia sensitive transcription factor HIF1-α, which is a known direct regulator of VEGF-A and other angiogenic growth factors, becomes activated early in the course of cardiac pressure-overload, when cardiomyocyte growth exceeds the ability of the existing capillary network to deliver enough oxygen for the muscle cells and hypoxia emerges [44]. Other cardiomyocyte-based regulators with positive effects on myocardial capillary growth include the transcriptional coregulator peroxisome proliferator-activated receptor gamma, coactivator 1 alpha (PGC1α), the transcription factor signal transducer and activator of transcription 3 (STAT3), and protein kinase B/Akt. Although capillary growth in the heart is enhanced during the initial compensatory phase of cardiac overload, capillary density decreases with disease progression and capillary rarefaction is ultimately present in terminal heart failure. This might, at least in part, be due to the fact that cardiomyocyte GATA4 activation decreases and Hif1-α becomes inhibited by p53 in persisting pressure overload. Increasing capillary density under these conditions, for example, by the delivery of angiogenic growth factors like a combination of VEGFA and angiopoietin-1 or VEGF-B alone, improves cardiac function, indicating that sufficient angiogenesis is crucial for the maintenance of heart function under pathological stress [43–45].

How do endothelial cells influence cardiomyocytes to maintain their function? First and foremost, they deliver oxygen and nutrients (i.e., amino acids, glucose, and fatty acids) to enable the production of ATP by myocytes. In fact, cardiomyocytes rely on fatty acid transporter expression (e.g., CD36 and Fabp4) by endothelial cells for the uptake of fatty acids from the circulation, otherwise heart failure develops [46]. Second, paracrine factors released by the endothelial cells play an important role for cardiac homeostasis and survival. In a co-culture system of cardiomyocytes and endothelial cells, in which oxygen and nutrient delivery by capillaries naturally does not play a role, endothelial cells are essential for the survival of myocytes and also trigger their spatial organization and rhythmic contraction. As endothelial-derived paracrine factors, Neuregulin1, which acts on ErbB2 and ErbB4 receptors on cardiomyocytes and which promotes myocyte survival and hypertrophy, as well as Apelin1, which induces a strong positive inotropic response via its G-protein coupled receptor APJ on cardiomyocytes, has been identified [14, 39]. Interestingly, both Neuregulin1 and Apelin1 are being evaluated as therapy in patients with heart failure.

On the other hand, endothelial cells might also contribute to the progression of heart failure during pathological circumstances. It is currently emerging mainly from single cell sequencing studies in mouse models that a subset of cardiac endothelial cells transiently proliferate and upregulate extracellular matrix as well as proinflammatory genes between 3 and 14 days after myocardial infarction or pressure overload [38, 47]. Despite attaining transient mesenchymal characteristics, cardiac endothelial cells appear not to fully transdifferentiate into fibroblasts. Although it is assumed that this transient endothelial-mesenchymal activation process (as it is called) promotes myocardial fibrosis and/or cardiac dysfunction, whether and to which extent this holds true, remains unknown.

15.3.3 Fibroblast-Derived Crosstalk

Cardiac fibroblasts are spindle-shaped cells that specifically express the PDGF receptor α, Tcf21 as well as vimentin [48]. They arise through EMT from the epicardium, from the neural crest as well as the endocardium during embryonic development [49]. They constitute around 10% of all cardiac cells under homeostatic conditions. The primary function of cardiac fibroblasts is to synthesize (and degrade) extracellular matrix, which forms a three-dimensional structural network that supports cohesion of myocardial cells, cardiac shape, and function. Extracellular matrix (ECM) in the heart consists mainly of collagen I and III, fibronectin, proteoglycans, and glycoproteins [50]. In addition, fibroblasts express and secrete many protein ligands and thereby entertain a rich network of intercellular communication by interacting with receptors expressed on neighboring cells, such as other fibroblasts, cardiomyocytes, endothelial cells, and immune cells. Intercellular communication occurs via the release of specific growth factors, through extracellular matrix proteins, extracellular vesicles (EVs) and even more directly by forming connexin containing gap junction between these two different cell types.

In the embryonic heart, release of fibronectin, EGF-like growth factor, and collagen by fibroblasts promotes cardiac myocyte proliferation, by stimulating β1-integrin-dependent signaling in these cells [51]. In the healthy adult heart, fibroblasts are mainly quiescent but become activated in response to mechanical overload, ischemic injury, and profibrotic molecules like TGF-β, Periostin, and connective tissue growth factor (CTGF), which are expressed in fibroblasts as well as cardiomyocytes (Fig. 15.2). Activation leads to a dramatic increase in fibroblast proliferation, secretion of extracellular matrix proteins, and growth factors. In addition, a fraction of fibroblasts (around 15% in murine pressure overload, but close to 90% after myocardial infarction) become myofibroblasts, which is a contractile cell type, characterized by the expression of α-smooth-muscle actin. Myofibroblasts can be found in the infarct scar mainly in the first week after myocardial infarction; α-smooth-muscle actin expression seizes thereafter and the cells turn into a more quiescent, new molecular and stable differentiated state, termed the matrifibrocyte that persists in the infarct scar for a long term [52]. Coculture with adult heart fibroblasts leads to hypertrophy in cardiomyocytes

[51]. One of the growth factor responsible for this effect could be TGFβ1, which is released abundantly from myocytes as well as fibroblasts and which induces hypertrophy and dysfunction in cardiomyocytes and extracellular matrix production in fibroblasts. Interestingly, the endogenous prohypertrophic agonist Angiotensin II primarily acts on the Angiotensin type 1 receptor on cardiac fibroblasts and triggers cardiomyocyte growth indirectly through the induction of TGFβ1 and FGF2. FGF2 is mainly produced in myocardial fibroblasts and induces hypertrophy of adjacent cardiomyocytes. In support of this, FGF2 knock-out mice showed reduced hypertrophy during pressure overload. Cardiac IGF1 is predominantly derived from fibroblasts, where its expression is induced by the transcription factor Krüppel-like factor 5 (KLF5) [53]. Fibroblast IGF1 promotes cardiomyocyte hypertrophy and myocardial fibrosis but is also essential for preventing heart failure and mortality during pressure overload in mice. Members of the IL-6 family like cardiotrophin-1 and leukemia inhibitory factor (LIF) are synthesized by cardiac fibroblasts and myocytes and signal through the transmembrane gp130 receptor to induce cardiomyocyte hypertrophy. In addition, CT-1 also promotes fibroblast migration, while LIF inhibits myofibroblast transition and collagen synthesis. Fibroblasts do not only release factors that induce growth in cardiac myocytes. Interleukin-33 (IL-33), which is expressed by cardiac fibroblast in response to mechanical load, inhibits cardiomyocyte hypertrophy in a paracrine and dose-dependent manner by binding to its receptor STL2. Similarly, cardiac fibroblasts release metallothioneins to protect the myocardium from increased loading, for example, during exercise. Metallothioneins are taken up by cardiomyocytes where they reduce oxidative damage-induced cell death [54]. Fibroblast are the most ligand providing cell type to endothelial cells. For instance, single cell expression profiling uncovered a distinct type of activated fibroblasts that expressed paracrine factors (like Wif1, Timp3, Ptn, Mdk, Apoe, Igf1 etc.) binding to receptors on endothelial cells to regulate angiogenesis. In addition, myofibroblasts release GM-CSF upon cardiac injury instructing resident macrophages to recruit other inflammatory cells and trigger myocardial inflammation.

Therefore, fibroblast regulate different adaptive as well as maladaptive features in the myocardium after injury or overload. Research is ongoing to uncover fibroblast inherent master regulators of these different effects. While for example the transcription factors SOX9, YAP/TAZ, or MEOX1 promote fibrogenic and proinflammatory responses, NRF2 or GATA4 and GATA6 promote adaptive features like antioxidative gene expression and angiogenesis, respectively [55–58].

The cardiomyocyte–fibroblast crosstalk is not only regulated by proteins but also by noncoding RNA molecules such as micro-RNAs (miRs) [59]. MiRs are short (17–25 nucleotides) noncoding RNAs that function mainly to inhibit gene expression of specific mRNAs. They are processed from 60–70 nucleotides pre-miRs, which are exported to the cytosol where they are cleaved by the enzyme Dicer to produce the mature duplex miR, consisting of a guide strand and a passenger strand. Mainly the guide strand targets cellular mRNA for silencing. miR133a is predominantly expressed in cardiomyocytes, where it blocks the expression of the profibrotic factor CTGF. As a result, miR133 knock-out mice develop heart failure with

massive myocardial fibrosis, while cardiomyocyte-specific overexpression protected the mice from cardiac fibrosis after pressure-overload. miR21, in contrast, was found to be specifically upregulated in fibroblasts of failing hearts, where it targets intracellular signaling and the paracrine influence on cardiomyocytes. Inhibition of miR21 by an antagomiR (small, chemically modified RNA) reduces cardiac fibrosis and hypertrophy after pressure overload. Fibroblasts also release the passenger strand of miR21 in exosomes (small vesicles), which are taken up by cardiomyocytes, and thereby induce hypertrophy in these cells.

15.4 Cardiomyocyte Intracellular Signaling During Pathological and Physiological Heart Growth

Cardiomyocytes have a very low ability to divide after birth, and myocardial growth then occurs through enlargement (i.e., hypertrophy) of these cells [60]. Indeed, physiological hypertrophy drives the normal growth of the heart from birth to early adulthood and during professional exercise and pregnancy. Physiological hypertrophy is characterized by a balanced growth of chambers and ventricular walls and is not associated with dysfunction or fibrosis. In contrast, pathological hypertrophy occurs in response to disease associated stimuli like pressure or volume overload, characteristic for patients with congenital heart disease. During pressure overload, cardiomyocytes become mainly thicker and concentric hypertrophy (thick ventricular walls and small chambers) develops. Eccentric hypertrophy (with dilated chambers and thin walls) is the consequence of volume overload and cardiomyocyte elongation. All forms of pathological hypertrophy are only partially reversible, associated with ventricular dysfunction, exert interstitial and perivascular fibrosis, and often lead to heart failure.

15.4.1 Signaling Cascades in Physiological Heart Growth

Insulin, growth hormone and IGF1 are prominent inducers of physiological cardiac growth (Fig. 15.3) [61, 62]. Insulin binds and activates the tyrosine kinase insulin receptor, which leads to the recruitment and phosphorylation of the adaptor proteins insulin receptor substrate 1 (IRS1) and IRS2 that in turn activate phosphoinositide 3-kinase (PI3K)α/AKT signaling (see below) at the plasma membrane. IGF1 binds to the insulin receptor and the IGF1 receptor, which also leads to the activation of PI3Kα. PI3K converts the plasma-membrane lipid phosphatidylinositol-4,5-bisphosphate to phosphatidylinositol-3,4,5-trisphosphate. PI3Kα is a heterodimer that consists of a p85 regulatory subunit and a p110α subunit. It is functionally important, as cardiomyocyte-specific over-expression of a dominant negative form of p110α inhibited physiological cardiac hypertrophy during postnatal growth and during swimming exercise, while over-expression of a constitutive active p110α produced physiological cardiac hypertrophy. PI3K activation results in the sarcolemmal recruitment of the kinases AKT/PKB and phosphoinositide-dependent

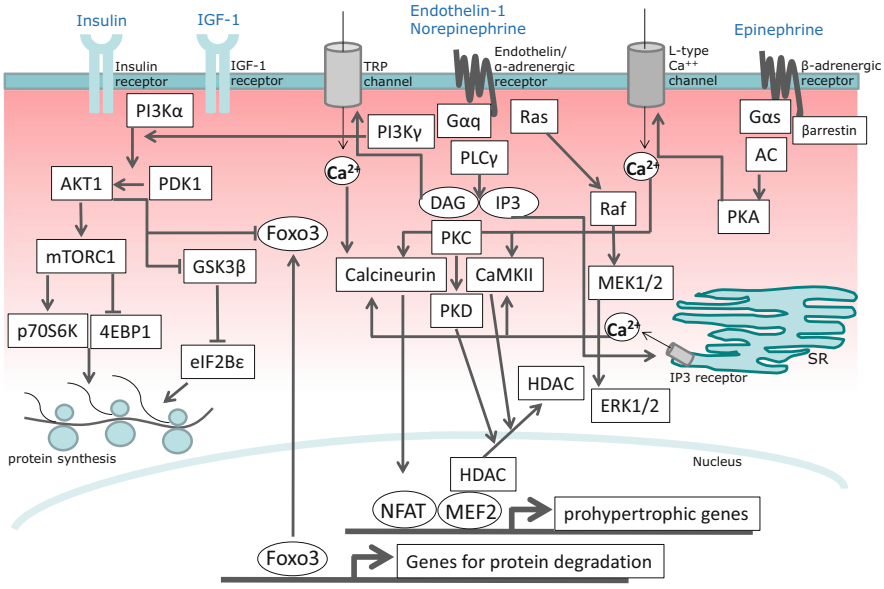

Fig. 15.3 Prohypertrophic intracellular signal transduction in cardiac myocytes. Growth factors like Insulin, IGF-1, or epinephrine act on receptors on the cardiomyocyte surface. A complicated web of intracellular signal transduction molecules becomes activated that leads to activation of prohypertrophic transcription factors like NFAT or MEF2 or the inhibition of anti-hypertrophic transcription factors like FOXO3. Calcium is released from the sarcoplasmatic reticulum or enters the cells through TRP or L-type channels and triggers activation of calcium-dependent signaling molecules like the phosphatase calcineurin or the calmodulin-dependent kinase (CamKII). Abbreviations not mentioned in the text: AC, adenylat cyclase; p70S6K, p70 S6 kinase

kinase1 (PDK1) through their pleckstrin-homology domains. When PDK1 and AKT are brought into close proximity, PDK1 phosphorylates and activates AKT. AKT1 and AKT2 are expressed in the heart. AKT1 is necessary for the induction of physiological hypertrophy, as *Akt1* knock-out mice were defective in exercise-induced hypertrophy. In response to pathological pressure overload, AKT1 KO mice displayed cardiac dilation and dysfunction, indicating that AKT1 promotes cardiac compensation in this setting. Short-term (two weeks) transgenic overexpression of AKT in the heart leads to physiological cardiac hypertrophy, while this hypertrophy acquires pathological features when it persists for six weeks, indicating that AKT in principal can induce pathological as well as physiological hypertrophy depending on the duration of the stimulus. Mechanistically, AKT1 directly promotes protein translation, in part by inhibiting constitutive GSK3β activity, which negatively regulates eukaryotic translation initiation factor 2Bε (eIF2Bε), as well as by indirectly activating the protein kinase mechanistic target of rapamycin (mTOR). In addition, AKT inactivates the transcription factors Forkhead box protein O3 (FOXO3) and thereby decreases the expression of

ubiquitin ligases like Atrogin-1. This reduces the rate of cellular protein degradation and therefore favors the net protein accumulation needed for hypertrophy.

mTOR as part of the so-called mTOR complex 1 (mTORC1, together with the proteins RAPTOR and Lst8) can be activated by AKT as well as for example by amino acids. Lack of cellular energy during fasting or starvation leads to activation of the AMP-dependent protein kinase, which inhibits mTORC1. mTORC1 promotes ribosomal protein production through activation of S6 kinases and by inhibiting the eIF4E-binding protein1 (4EBP1). Pharmacological inhibition of mTOR by rapamycin reverses not only cardiac hypertrophy induced by AKT overexpression but also pathological hypertrophy in response to pressure overload. Genetic deletion of *Mtor* in cardiomyocytes results in heart failure without an initial phase of hypertrophy.

The cardiac myocyte expression of CITED4 (CBP/p300-interacting transactivators with E/D-rich carboxyterminal domain) is increased not only during swimming exercise but also after TAC. CITED4 is sufficient to induce physiological heart hypertrophy with preserved ventricular function and is on the other hand necessary for cardiac compensation not only during strenuous exercise but also during pressure overload. CITED4 acts by regulating transcription through interaction with DNA-binding factors (as it lacks an own DNA-binding domain). It appears to promote mTOR signaling, but the exact molecular mechanisms remain unknown [63].

15.4.2 Signaling in Pathological Heart Growth

During pathological overload of the heart, Angiotensin II, Endothelin-1, and α-adrenergic catecholamines bind to seven-transmembrane-spanning receptors that are coupled to heterotrimeric G proteins of the Gαq/α11 subclass and activate phospholipase Cβ (PLCβ, Fig. 15.3) [62]. This induces the generation of diacylglycerol (DAG), which functions as an intracellular ligand for protein kinase C (PKC), leading to PKC activation and induction of inositol-1,4,5-triphosphate (IP3). IP3 leads to the mobilization of internal calcium by direct binding to the IP3 receptor at the sarcoplasmatic reticulum or the nuclear envelope. DAG and IP3 also trigger opening of transient receptor potential (TRPC) channels, which leads to influx of sodium and mainly calcium into cardiac myocytes. Increase in this signaling-associated calcium occurs in cellular microdomains associated with specialized lipid rafts (termed caveolae) or in proximity to plasma membrane invaginations, called T-tubules [64]. Signaling-associated calcium is shielded from the highly abundant and mainly sarcoplasmatic reticulum-based calcium that activates cardiomyocyte contraction by binding to contractile filaments ("contractile calcium"). Signaling calcium binds to calmodulin and subsequently activates prohypertrophic downstream signaling by the calmodulin-dependent kinase (CaMK) II and the phosphatase calcineurin. Gαq triggered signaling also leads to the activation of MAPK (exact mechanisms not known) and AKT through the PI3Kγ. The β-adrenergic receptor initiates prohypertrophic signaling as well: it is

associated with Gαs dependent activation of the adenylate cyclase and subsequent activation of protein kinase A (PKA). PKA induces calcium influx from the extracellular space through the L-type calcium channel, thereby also contributing to signaling calcium to activate CaMKII and calcineurin. In addition, the scaffold protein β-arrestin associates with the intracellular portion of the β-receptor to activate CaMKII and MAP kinase signaling.

CaMKII is induced in expression and becomes activated in response to pressure overload in the myocardium [65]. Among its different isoforms, CaMKIIδ is the most abundant in the heart, although CaMKIIγ is also expressed there. CaMKII is a serine/threonine kinase that is directly activated by calcium/calmodulin binding and by reactive oxygen species. The splice variant CaMKIIδB is localized to the nucleus, while CaMKIIδC is found in the cytosol. Genetic ablation of CaMKIIδ reduced cardiac hypertrophy, fibrosis, and dysfunction in mice. Cardiomyocyte-specific overexpression of CaMKII, in turn, leads to cardiac hypertrophy (in the case of CaMKIIδB) or dilated cardiomyopathy (CaMKIIδC). CaMKII directly phosphorylates the histone deacetylase (HDAC) 4 and thereby promotes binding of the chaperone 14-3-3 to cause export of HDAC4 from the nucleus. Reduction of nuclear HDAC4 leads to enhanced activation of the prohypertrophic transcription factor MEF2, which usually is directly repressed by class II HDACs. It was recently demonstrated that HDAC4 (and especially an N-terminal HDAC4 fragment that can be released from the molecule) protects for example from diabetic cardiomyopathy and exercise-induced cardiac strain [66, 67]. Class IIa HDACs (HDACS 4, 5, 7, 9) are known to inhibit cardiac hypertrophy, and mice lacking HDAC5 or HDAC9 exert myocardial hypertrophy with aging or exaggerated hypertrophy in response to pressure overload. Nuclear export of class IIa HDACs can also be induced through phosphorylation by protein kinase D. In contrast, class I HDACs like HDAC 1, 2 and 3, which are constitutively present in the nucleus, are not regulated by kinases, and promote cardiac hypertrophy and failure, as demonstrated with specific pharmacological inhibitors like apicidin that improve adverse remodeling in mice.

The calcium-dependent serine/threonine protein-phosphatase calcineurin consists of a catalytic subunit (CnA) and a 19-kDa regulatory subunit (CnB) [62, 64]. The dimeric protein becomes activated in response to increased calcium concentrations through direct binding of calcium-bound calmodulin. Activated calcineurin dephosphorylates the transcription factor nuclear factor of activated T-cells (NFAT) in proximity to the cardiomyocyte plasma membrane, where calcineurin is anchored by the small adaptor protein CIB1. Upon dephosphorylation, NFAT translocates into the nucleus to induce the expression of hypertrophy inducing genes. Myocardial calcineurin/NFAT signaling appears to be selectively activated in pathological hypertrophy and heart failure, but not under conditions of physiological hypertrophy. Genetic ablation of the CnAβ isoform in mice, which is upregulated in the heart during pressure overload, blunts pathological hypertrophy, similar to genetic elimination of NFATc3 and NFATc2 [68–70].

Among the MAP kinases, mainly the activation of ERK1/2 contributes to the development of cardiac hypertrophy. Activation of ERK kinases occurs downstream of G-protein coupled receptors, receptor tyrosine kinases (e.g., IGF1 and FGF

receptors), receptor serine/threonine kinases (TGFβ receptors), gp130 receptors as well as integrins in response to mechanical stretch [23]. Downstream of these receptors, the small G protein Ras is activated, which then recruits the MAP kinase (MAP3K) Raf-1 to the plasma membrane. Raf-1 then activates the dual-specificity kinases MEK1 and MEK2 (MAP2K) that finally phosphorylate and activate ERK1/2. Constitutive expression of an activated MEK1 mutant in cardiomyocytes results in a concentric from of hypertrophy with increased myocyte width, but lack of cardiac fibrosis or dysfunction. Genetic elimination of cardiomyocyte ERK1 and ERK2, in turn, leads to spontaneous eccentric cardiac hypertrophy (i.e., cardiac dilation with cardiomyocyte elongation at the microscopic level) and ventricular dysfunction [71]. Thus, ERK1/2 promotes a compensated form of concentric cardiac hypertrophy. The other MAP kinases p38 and JNK, which are also activated in response to pathological stress, appear to inhibit cardiomyocyte hypertrophy by rephosphorylating NFAT and thereby promoting its export from the nucleus. Casein kinase 2α, in contrast, is a kinase that promotes cardiac hypertrophy through phosphorylation of the tumor suppressor protein p27, which is degraded in response, as well as through the activation of HDAC2 [72, 73].

Beside NFAT and MEF2, other transcription factors with prohypertrophic effects in cardiomyocyte include GATA4, GATA6, serum response factor (SRF), and nuclear factor (NF)-κB. Single cardiomyocyte sequencing at multiple time points during persisting overload revealed a bifurcation into adaptive and failing cardiomyocytes, whereby p53 signaling drives mitochondrial inhibition, cellular elongation, and expression of a heart failure gene program [74].

Noncoding RNAs, mainly miRs and long-noncoding RNAs (lncRNAs) are currently emerging as regulators of cardiac hypertrophy and failure. Because miRs often inhibit multiple mRNAs related to the same pathway, they can be very potent regulators of cardiomyocyte hypertrophy. Prohypertrophic miRNAs are for example miR-195 and miR-208, while miR-133 counteracts hypertrophy. Because miRNAs can effectively be targeted by specific antagonists, for example, antagomiRs upon their systemic administration are considered as promising therapeutic targets. lncRNAs are longer than 200 bp and interact with RNA or DNA (in a sequence-specific manner) and also specifically bind proteins. With that molecular properties, they act on cellular gene expression, for example, by directing or diverting transcription factors or epigenetic regulators to/from specific sites of the genome, by scaffolding miRNAs or also by bringing promoter and enhancer regions together and thereby enhancing gene expression.

For example, the muscle-enriched lncRNA H19 suppresses cardiac hypertrophy by interacting with the polycomb repressive complex 2 to suppress H3K27 trimethylation of the anti-hypertrophic Tescalcin locus that in turn leads to reduced NFAT expression and activity. As another example, a cluster of lncRNAs described in antisense direction from the Myh7 locus (encoding for the β-myosin heavy chain gene), called Myheart (Mhrt), inhibit cardiac hypertrophy by binding and diverting the chromatin remodeling factor Brg1 from recognizing its genomic DNA targets and thereby preventing prohypertrophic gene expression [75].

Another level of complexity is added in terms of prohypertrophic signaling mechanisms when considering that regulation of gene expression occurs only in part at the level of transcription, but as well at the post-transcriptional level. In fact, profiling of mRNAs that are bound to the ribosome (and therefore are currently actively translated) versus RNA sequencing from hearts after TAC showed that a subset of mRNAs (related to protein quality control, metabolism, and translation) are predominantly regulated at the translational level [76]. Importantly, extensive translational regulation was also detected in human hearts by ribosome profiling, which also revealed microprotein production from characterized lncRNAs [77]. The microproteins can be implicated in mitochondrial and other cellular processes. Gene-therapeutic overexpression of the tumor suppressor gene TIP30 in mice counteracts cardiac hypertrophy and failure in multiple mouse disease models by interfering with translational elongation and cardiomyocyte protein synthesis [78]. This, post-transcriptional regulation might also entail novel therapeutic approaches.

15.5 Conclusions

Complex signaling circuits between and within cells coordinate not only cardiac development and growth but also the adaptation in response to disease causing stimuli. Perturbation of these pathways, for example, as a consequence of inherited gene mutations or environmental stimuli triggers and perpetuates heart failure. Understanding how intercellular and intracellular signaling determines cardiac cell identity and plasticity that is critical for proper cardiac morphogenesis and tissue healing following environmental stress will likely constitute a major area for future research. Integration of multiomics technologies (epigenomic, metabolomic, transcriptomic, and proteomic) in spatial and single-cell resolution will be instrumental in clarifying the signals and downstream molecular networks instructing proper heart morphogenesis and postnatal heart growth, and how these pathways go awry in congenital heart disease. The hope exists that specific targeting of signaling molecules or circuits for instance by small molecules or gene therapy will one day improves the outcome of individuals with congenital heart defects.

References

1. Meilhac SM, Buckingham ME. The deployment of cell lineages that form the mammalian heart. Nat Rev Cardiol. 2018;15:705–24.
2. Vincent SD, Buckingham ME. How to make a heart: the origin and regulation of cardiac progenitor cells. Curr Top Dev Biol. 2010;90:1–41.
3. Tian Y, Morrisey EE. Importance of myocyte-nonmyocyte interactions in cardiac development and disease. Circ Res. 2012;110:1023–34.
4. Cai CL, Liang X, Shi Y, Chu PH, Pfaff SL, Chen J, Evans S. Isl1 identifies a cardiac progenitor population that proliferates prior to differentiation and contributes a majority of cells to the heart. Dev Cell. 2003;5:877–89.

5. Caputo L, Witzel HR, Kolovos P, Cheedipudi S, Looso M, Mylona A, van IJcken WF, Laugwitz KL, Evans SM, Braun T, Soler E, Grosveld F, Dobreva G. The Isl1/Ldb1 complex orchestrates genome-wide chromatin organization to instruct differentiation of multipotent cardiac progenitors. Cell Stem Cell. 2015;17:287–99.
6. Gao R, Liang X, Cheedipudi S, Cordero J, Jiang X, Zhang Q, Caputo L, Gunther S, Kuenne C, Ren Y, Bhattacharya S, Yuan X, Barreto G, Chen Y, Braun T, Evans SM, Sun Y, Dobreva G. Pioneering function of Isl1 in the epigenetic control of cardiomyocyte cell fate. Cell Res. 2019;29:486–501.
7. He Z, Grunewald M, Dor Y, Keshet E. VEGF regulates relative allocation of Isl1(+) cardiac progenitors to myocardial and endocardial lineages. Mech Dev. 2016;142:40–9.
8. Milgrom-Hoffman M, Harrelson Z, Ferrara N, Zelzer E, Evans SM, Tzahor E. The heart endocardium is derived from vascular endothelial progenitors. Development. 2011;138:4777–87.
9. Moretti A, Caron L, Nakano A, Lam JT, Bernshausen A, Chen Y, Qyang Y, Bu L, Sasaki M, Martin-Puig S, Sun Y, Evans SM, Laugwitz KL, Chien KR. Multipotent embryonic isl1+ progenitor cells lead to cardiac, smooth muscle, and endothelial cell diversification. Cell. 2006;127:1151–65.
10. Zhang H, Lui KO, Zhou B. Endocardial cell plasticity in cardiac development, diseases and regeneration. Circ Res. 2018;122:774–89.
11. Kim H, Wang M, Paik DT. Endothelial-myocardial Angiocrine signaling in heart development. Front Cell Dev Biol. 2021;9:697130.
12. Qu X, Harmelink C, Baldwin HS. Endocardial-myocardial interactions during early cardiac differentiation and trabeculation. Front Cardiovasc Med. 2022;9:857581.
13. Towbin JA. Left ventricular noncompaction: a new form of heart failure. Heart Fail Clin. 2010;6:453–69. viii
14. Lemmens K, Doggen K, De Keulenaer GW. Role of neuregulin-1/ErbB signaling in cardiovascular physiology and disease: implications for therapy of heart failure. Circulation. 2007;116:954–60.
15. Hertig CM, Kubalak SW, Wang Y, Chien KR. Synergistic roles of neuregulin-1 and insulin-like growth factor-I in activation of the phosphatidylinositol 3-kinase pathway and cardiac chamber morphogenesis. J Biol Chem. 1999;274:37362–9.
16. Rentschler S, Zander J, Meyers K, France D, Levine R, Porter G, Rivkees SA, Morley GE, Fishman GI. Neuregulin-1 promotes formation of the murine cardiac conduction system. Proc Natl Acad Sci U S A. 2002;99:10464–9.
17. Gourdie RG, Wei Y, Kim D, Klatt SC, Mikawa T. Endothelin-induced conversion of embryonic heart muscle cells into impulse-conducting Purkinje fibers. Proc Natl Acad Sci U S A. 1998;95:6815–8.
18. Niessen K, Karsan A. Notch signaling in cardiac development. Circ Res. 2008;102:1169–81.
19. Chen H, Zhang W, Sun X, Yoshimoto M, Chen Z, Zhu W, Liu J, Shen Y, Yong W, Li D, Zhang J, Lin Y, Li B, VanDusen NJ, Snider P, Schwartz RJ, Conway SJ, Field LJ, Yoder MC, Firulli AB, Carlesso N, Towbin JA, Shou W. Fkbp1a controls ventricular myocardium trabeculation and compaction by regulating endocardial Notch1 activity. Development. 2013;140:1946–57.
20. MacGrogan D, D'Amato G, Travisano S, Martinez-Poveda B, Luxan G, Del Monte-Nieto G, Papoutsi T, Sbroggio M, Bou V, Gomez-Del Arco P, Gomez MJ, Zhou B, Redondo JM, Jimenez-Borreguero LJ, de la Pompa JL. Sequential ligand-dependent notch signaling activation regulates valve primordium formation and morphogenesis. Circ Res. 2016;118:1480–97.
21. Garg V, Muth AN, Ransom JF, Schluterman MK, Barnes R, King IN, Grossfeld PD, Srivastava D. Mutations in NOTCH1 cause aortic valve disease. Nature. 2005;437:270–4.
22. Lavine KJ, Yu K, White AC, Zhang X, Smith C, Partanen J, Ornitz DM. Endocardial and epicardial derived FGF signals regulate myocardial proliferation and differentiation in vivo. Dev Cell. 2005;8:85–95.

23. Giordano FJ, Gerber HP, Williams SP, VanBruggen N, Bunting S, Ruiz-Lozano P, Gu Y, Nath AK, Huang Y, Hickey R, Dalton N, Peterson KL, Ross J Jr, Chien KR, Ferrara N. A cardiac myocyte vascular endothelial growth factor paracrine pathway is required to maintain cardiac function. Proc Natl Acad Sci U S A. 2001;98:5780–5.
24. Shalaby F, Rossant J, Yamaguchi TP, Gertsenstein M, Wu XF, Breitman ML, Schuh AC. Failure of blood-island formation and vasculogenesis in Flk-1-deficient mice. Nature. 1995;376:62–6.
25. Qu X, Harmelink C, Baldwin HS. Tie2 regulates endocardial sprouting and myocardial trabeculation. JCI Insight. 2019;4:5.
26. Kim KH, Nakaoka Y, Augustin HG, Koh GY. Myocardial Angiopoietin-1 controls atrial chamber morphogenesis by spatiotemporal degradation of cardiac jelly. Cell Rep. 2018;23: 2455–66.
27. von Gise A, Pu WT. Endocardial and epicardial epithelial to mesenchymal transitions in heart development and disease. Circ Res. 2012;110:1628–45.
28. Ma L, Lu MF, Schwartz RJ, Martin JF. Bmp2 is essential for cardiac cushion epithelial-mesenchymal transition and myocardial patterning. Development. 2005;132:5601–11.
29. Jiao K, Kulessa H, Tompkins K, Zhou Y, Batts L, Baldwin HS, Hogan BL. An essential role of Bmp4 in the atrioventricular septation of the mouse heart. Genes Dev. 2003;17:2362–7.
30. Chen H, Shi S, Acosta L, Li W, Lu J, Bao S, Chen Z, Yang Z, Schneider MD, Chien KR, Conway SJ, Yoder MC, Haneline LS, Franco D, Shou W. BMP10 is essential for maintaining cardiac growth during murine cardiogenesis. Development. 2004;131:2219–31.
31. Lavine KJ, Ornitz DM. Shared circuitry: developmental signaling cascades regulate both embryonic and adult coronary vasculature. Circ Res. 2009;104:159–69.
32. Lavine KJ, White AC, Park C, Smith CS, Choi K, Long F, Hui CC, Ornitz DM. Fibroblast growth factor signals regulate a wave of Hedgehog activation that is essential for coronary vascular development. Genes Dev. 2006;20:1651–66.
33. Duan J, Gherghe C, Liu D, Hamlett E, Srikantha L, Rodgers L, Regan JN, Rojas M, Willis M, Leask A, Majesky M, Deb A. Wnt1/βcatenin injury response activates the epicardium and cardiac fibroblasts to promote cardiac repair. EMBO J. 2011;31:429–42.
34. Zhou B, Honor LB, He H, Ma Q, Oh JH, Butterfield C, Lin RZ, Melero-Martin JM, Dolmatova E, Duffy HS, Gise A, Zhou P, Hu YW, Wang G, Zhang B, Wang L, Hall JL, Moses MA, McGowan FX, Pu WT. Adult mouse epicardium modulates myocardial injury by secreting paracrine factors. J Clin Invest. 2011;121:1894–904.
35. Rudat C, Norden J, Taketo MM, Kispert A. Epicardial function of canonical Wnt-, Hedgehog-, Fgfr1/2-, and Pdgfra-signalling. Cardiovasc Res. 2013;100:411–21.
36. Vega-Hernandez M, Kovacs A, De Langhe S, Ornitz DM. FGF10/FGFR2b signaling is essential for cardiac fibroblast development and growth of the myocardium. Development. 2011;138:3331–40.
37. Cao Y, Duca S, Cao J. Epicardium in heart development, vol. 12. Cold Spring Harb Perspect Biol; 2020. p. 12.
38. Froese N, Cordero J, Abouissa A, Trogisch FA, Grein S, Szaroszyk M, Wang Y, Gigina A, Korf-Klingebiel M, Bosnjak B, Davenport CF, Wiehlmann L, Geffers R, Riechert E, Jurgensen L, Boileau E, Lin Y, Dieterich C, Forster R, Bauersachs J, Ola R, Dobreva G, Volkers M, Heineke J. Analysis of myocardial cellular gene expression during pressure overload reveals matrix based functional intercellular communication. iScience. 2022;25: 103965.
39. Tirziu D, Giordano FJ, Simons M. Cell communications in the heart. Circulation. 2010;122: 928–37.
40. Gu H, Smith FC, Taffet SM, Delmar M. High incidence of cardiac malformations in connexin40-deficient mice. Circ Res. 2003;93:201–6.
41. Biesemann N, Mendler L, Wietelmann A, Hermann S, Schafers M, Kruger M, Boettger T, Borchardt T, Braun T. Myostatin regulates energy homeostasis in the heart and prevents heart failure. Circ Res. 2014;115:296–310.

42. Heineke J. Wag the dog: how endothelial cells regulate cardiomyocyte growth. Arterioscler Thromb Vasc Biol. 2012;32:545–7.
43. Heineke J, Auger-Messier M, Xu J, Oka T, Sargent MA, York A, Klevitsky R, Vaikunth S, Duncan SA, Aronow BJ, Robbins J, Crombleholme TM, Molkentin JD. Cardiomyocyte GATA4 functions as a stress-responsive regulator of angiogenesis in the murine heart. J Clin Invest. 2007;117:3198–210.
44. Sano M, Minamino T, Toko H, Miyauchi H, Orimo M, Qin Y, Akazawa H, Tateno K, Kayama Y, Harada M, Shimizu I, Asahara T, Hamada H, Tomita S, Molkentin JD, Zou Y, Komuro I. p53-induced inhibition of Hif-1 causes cardiac dysfunction during pressure overload. Nature. 2007;446:444–8.
45. Kivela R, Hemanthakumar KA, Vaparanta K, Robciuc M, Izumiya Y, Kidoya H, Takakura N, Peng X, Sawyer DB, Elenius K, Walsh K, Alitalo K. Endothelial cells regulate physiological cardiomyocyte growth via VEGFR2-mediated paracrine signaling. Circulation. 2019;139:2570–84.
46. Jabs M, Rose AJ, Lehmann LH, Taylor J, Moll I, Sijmonsma TP, Herberich SE, Sauer SW, Poschet G, Federico G, Mogler C, Weis EM, Augustin HG, Yan M, Gretz N, Schmid RM, Adams RH, Grone HJ, Hell R, Okun JG, Backs J, Nawroth PP, Herzig S, Fischer A. Inhibition of endothelial notch signaling impairs fatty acid transport and leads to metabolic and vascular remodeling of the adult heart. Circulation. 2018;137:2592–608.
47. Tombor LS, John D, Glaser SF, Luxan G, Forte E, Furtado M, Rosenthal N, Baumgarten N, Schulz MH, Wittig J, Rogg EM, Manavski Y, Fischer A, Muhly-Reinholz M, Klee K, Looso M, Selignow C, Acker T, Bibli SI, Fleming I, Patrick R, Harvey RP, Abplanalp WT, Dimmeler S. Single cell sequencing reveals endothelial plasticity with transient mesenchymal activation after myocardial infarction. Nat Commun. 2021;12:681.
48. Nicin L, Wagner JUG, Luxan G, Dimmeler S. Fibroblast-mediated intercellular crosstalk in the healthy and diseased heart. FEBS Lett. 2022;596:638–54.
49. Moore-Morris T, Guimaraes-Camboa N, Banerjee I, Zambon AC, Kisseleva T, Velayoudon A, Stallcup WB, Gu Y, Dalton ND, Cedenilla M, Gomez-Amaro R, Zhou B, Brenner DA, Peterson KL, Chen J, Evans SM. Resident fibroblast lineages mediate pressure overload-induced cardiac fibrosis. J Clin Invest. 2014;124:2921–34.
50. Kakkar R, Lee RT. Intramyocardial fibroblast myocyte communication. Circ Res. 2010;106:47–57.
51. Ieda M, Tsuchihashi T, Ivey KN, Ross RS, Hong TT, Shaw RM, Srivastava D. Cardiac fibroblasts regulate myocardial proliferation through beta1 integrin signaling. Dev Cell. 2009;16:233–44.
52. Fu X, Khalil H, Kanisicak O, Boyer JG, Vagnozzi RJ, Maliken BD, Sargent MA, Prasad V, Valiente-Alandi I, Blaxall BC, Molkentin JD. Specialized fibroblast differentiated states underlie scar formation in the infarcted mouse heart. J Clin Invest. 2018;128:2127–43.
53. Takeda N, Manabe I, Uchino Y, Eguchi K, Matsumoto S, Nishimura S, Shindo T, Sano M, Otsu K, Snider P, Conway SJ, Nagai R. Cardiac fibroblasts are essential for the adaptive response of the murine heart to pressure overload. J Clin Invest. 2010;120:254–65.
54. Lighthouse JK, Burke RM, Velasquez LS, Dirkx RA Jr, Aiezza A 2nd, Moravec CS, Alexis JD, Rosenberg A, Small EM. Exercise promotes a cardioprotective gene program in resident cardiac fibroblasts. JCI Insight. 2019;4:4.
55. Xiao Y, Hill MC, Li L, Deshmukh V, Martin TJ, Wang J, Martin JF. Hippo pathway deletion in adult resting cardiac fibroblasts initiates a cell state transition with spontaneous and self-sustaining fibrosis. Genes Dev. 2019;33:1491–505.
56. Alexanian M, Przytycki PF, Micheletti R, Padmanabhan A, Ye L, Travers JG, Gonzalez-Teran B, Silva AC, Duan Q, Ranade SS, Felix F, Linares-Saldana R, Li L, Lee CY, Sadagopan N, Pelonero A, Huang Y, Andreoletti G, Jain R, McKinsey TA, Rosenfeld MG, Gifford CA, Pollard KS, Haldar SM, Srivastava D. A transcriptional switch governs fibroblast activation in heart disease. Nature. 2021;595:438–43.

57. Scharf GM, Kilian K, Cordero J, Wang Y, Grund A, Hofmann M, Froese N, Wang X, Kispert A, Kist R, Conway SJ, Geffers R, Wollert KC, Dobreva G, Bauersachs J, Heineke J. Inactivation of Sox9 in fibroblasts reduces cardiac fibrosis and inflammation. JCI Insight. 2019;4:5.
58. Dittrich GM, Froese N, Wang X, Kroeger H, Wang H, Szaroszyk M, Malek-Mohammadi M, Cordero J, Keles M, Korf-Klingebiel M, Wollert KC, Geffers R, Mayr M, Conway SJ, Dobreva G, Bauersachs J, Heineke J. Fibroblast GATA-4 and GATA-6 promote myocardial adaptation to pressure overload by enhancing cardiac angiogenesis. Basic Res Cardiol. 2021;116:26.
59. Viereck J, Bang C, Foinquinos A, Thum T. Regulatory RNAs and paracrine networks in the heart. Cardiovasc Res. 2014;102:290–301.
60. Bergmann O, Bhardwaj RD, Bernard S, Zdunek S, Barnabe-Heider F, Walsh S, Zupicich J, Alkass K, Buchholz BA, Druid H, Jovinge S, Frisen J. Evidence for cardiomyocyte renewal in humans. Science. 2009;324:98–102.
61. Maillet M, van Berlo JH, Molkentin JD. Molecular basis of physiological heart growth: fundamental concepts and new players. Nat Rev Mol Cell Biol. 2013;14:38–48.
62. Heineke J, Molkentin JD. Regulation of cardiac hypertrophy by intracellular signalling pathways. Nat Rev Mol Cell Biol. 2006;7:589–600.
63. Lerchenmuller C, Rabolli CP, Yeri A, Kitchen R, Salvador AM, Liu LX, Ziegler O, Danielson K, Platt C, Shah R, Damilano F, Kundu P, Riechert E, Katus HA, Saffitz JE, Keshishian H, Carr SA, Bezzerides VJ, Das S, Rosenzweig A. CITED4 protects against adverse remodeling in response to physiological and pathological stress. Circ Res. 2020;127:631–46.
64. Heineke J, Ritter O. Cardiomyocyte calcineurin signaling in subcellular domains: from the sarcolemma to the nucleus and beyond. J Mol Cell Cardiol. 2012;52:62–73.
65. Kreusser MM, Backs J. Integrated mechanisms of CaMKII-dependent ventricular remodeling. Front Pharmacol. 2014;5:36.
66. Kronlage M, Dewenter M, Grosso J, Fleming T, Oehl U, Lehmann LH, Falcao-Pires I, Leite-Moreira AF, Volk N, Grone HJ, Muller OJ, Sickmann A, Katus HA, Backs J. O-GlcNAcylation of histone deacetylase 4 protects the diabetic heart from failure. Circulation. 2019;140:580–94.
67. Lehmann LH, Jebessa ZH, Kreusser MM, Horsch A, He T, Kronlage M, Dewenter M, Sramek V, Oehl U, Krebs-Haupenthal J, von der Lieth AH, Schmidt A, Sun Q, Ritterhoff J, Finke D, Volkers M, Jungmann A, Sauer SW, Thiel C, Nickel A, Kohlhaas M, Schafer M, Sticht C, Maack C, Gretz N, Wagner M, El-Armouche A, Maier LS, Londono JEC, Meder B, Freichel M, Grone HJ, Most P, Muller OJ, Herzig S, Furlong EEM, Katus HA, Backs J. A proteolytic fragment of histone deacetylase 4 protects the heart from failure by regulating the hexosamine biosynthetic pathway. Nat Med. 2018;24:62–72.
68. Bourajjaj M, Armand AS, da Costa Martins PA, Weijts B, van der Nagel R, Heeneman S, Wehrens XH, De Windt LJ. NFATc2 is a necessary mediator of calcineurin-dependent cardiac hypertrophy and heart failure. J Biol Chem. 2008;283:22295–303.
69. Wilkins BJ, De Windt LJ, Bueno OF, Braz JC, Glascock BJ, Kimball TF, Molkentin JD. Targeted disruption of NFATc3, but not NFATc4, reveals an intrinsic defect in calcineurin-mediated cardiac hypertrophic growth. Mol Cell Biol. 2002;22:7603–13.
70. Bueno OF, Lips DJ, Kaiser RA, Wilkins BJ, Dai YS, Glascock BJ, Klevitsky R, Hewett TE, Kimball TR, Aronow BJ, Doevendans PA, Molkentin JD. Calcineurin Abeta gene targeting predisposes the myocardium to acute ischemia-induced apoptosis and dysfunction. Circ Res. 2004;94:91–9.
71. Kehat I, Davis J, Tiburcy M, Accornero F, Saba-El-Leil MK, Maillet M, York AJ, Lorenz JN, Zimmermann WH, Meloche S, Molkentin JD. Extracellular signal-regulated kinases 1 and 2 regulate the balance between eccentric and concentric cardiac growth. Circ Res. 2011;108:176–83.
72. Hauck L, Harms C, An J, Rohne J, Gertz K, Dietz R, Endres M, von Harsdorf R. Protein kinase CK2 links extracellular growth factor signaling with the control of p27(Kip1) stability in the heart. Nat Med. 2008;14:315–24.

73. Eom GH, Cho YK, Ko JH, Shin S, Choe N, Kim Y, Joung H, Kim HS, Nam KI, Kee HJ, Kook H. Casein kinase-2α1 induces hypertrophic response by phosphorylation of histone deacetylase 2 S394 and its activation in the heart. Circulation. 2011;123:2392–403.
74. Nomura S, Satoh M, Fujita T, Higo T, Sumida T, Ko T, Yamaguchi T, Tobita T, Naito AT, Ito M, Fujita K, Harada M, Toko H, Kobayashi Y, Ito K, Takimoto E, Akazawa H, Morita H, Aburatani H, Komuro I. Cardiomyocyte gene programs encoding morphological and functional signatures in cardiac hypertrophy and failure. Nat Commun. 2018;9:4435.
75. Lozano-Vidal N, Bink DI, Boon RA. Long noncoding RNA in cardiac aging and disease. J Mol Cell Biol. 2019;11:860–7.
76. Doroudgar S, Hofmann C, Boileau E, Malone B, Riechert E, Gorska AA, Jakobi T, Sandmann C, Jurgensen L, Kmietczyk V, Malovrh E, Burghaus J, Rettel M, Stein F, Younesi F, Friedrich UA, Mauz V, Backs J, Kramer G, Katus HA, Dieterich C, Volkers M. Monitoring cell-type-specific gene expression using ribosome profiling in vivo during cardiac hemodynamic stress. Circ Res. 2019;125:431–48.
77. van Heesch S, Witte F, Schneider-Lunitz V, Schulz JF, Adami E, Faber AB, Kirchner M, Maatz H, Blachut S, Sandmann CL, Kanda M, Worth CL, Schafer S, Calviello L, Merriott R, Patone G, Hummel O, Wyler E, Obermayer B, Mucke MB, Lindberg EL, Trnka F, Memczak S, Schilling M, Felkin LE, Barton PJR, Quaife NM, Vanezis K, Diecke S, Mukai M, Mah N, Oh SJ, Kurtz A, Schramm C, Schwinge D, Sebode M, Harakalova M, Asselbergs FW, Vink A, de Weger RA, Viswanathan S, Widjaja AA, Gartner-Rommel A, Milting H, Dos Remedios C, Knosalla C, Mertins P, Landthaler M, Vingron M, Linke WA, Seidman JG, Seidman CE, Rajewsky N, Ohler U, Cook SA, Hubner N. The translational landscape of the human heart. Cell. 2019;178:242–260.e29.
78. Grund A, Szaroszyk M, Korf-Klingebiel M, Malek Mohammadi M, Trogisch FA, Schrameck U, Gigina A, Tiedje C, Gaestel M, Kraft T, Hegermann J, Batkai S, Thum T, Perrot A, Remedios CD, Riechert E, Volkers M, Doroudgar S, Jungmann A, Bauer R, Yin X, Mayr M, Wollert KC, Pich A, Xiao H, Katus HA, Bauersachs J, Muller OJ, Heineke J. TIP30 counteracts cardiac hypertrophy and failure by inhibiting translational elongation. EMBO Mol Med. 2019;11:e10018.

Cardiac Transcription Factors and Regulatory Networks

16

Marcel Grunert, Cornelia Dorn, and Silke Rickert-Sperling

Abstract

Cardiac development is a fine-tuned process governed by complex transcriptional networks, in which transcription factors (TFs) interact with other regulatory layers. In this chapter, we introduce the core cardiac TFs including Gata, Hand, Nkx2, Mef2, Srf, and Tbx. These factors regulate each other's expression and can also act in a combinatorial manner on their downstream targets. Their disruption leads to various cardiac phenotypes in mice, and mutations in humans have been associated with congenital heart defects. In the second part of the chapter, we discuss different levels of regulation including *cis*-regulatory elements, chromatin structure, and microRNAs, which can interact with transcription factors, modulate their function, or are downstream targets. Finally, examples of disturbances of the cardiac regulatory network leading to congenital heart diseases in human are provided.

Keywords

Transcription factors · Gata4 · Hand1 · Hand2 · Nkx2-5 · Mef2 · Tbx1 · Tbx2 · Tbx3 · Tbx5 · Tbx18 · Tbx20 · Tead1 · Srf · *cis*-regulatory elements · Chromatin structure · MicroRNAs · Transcriptional network · *Drosophila* · Isl1 · Tetralogy of Fallot · TOF · Left ventricular noncompaction · Double outlet right ventricle · DORV · Ebstein's anomaly · MyoD · HDAC · HAT · Knockout mice · Atrioventricular septal defects · AVSD · Truncus arteriosus · Common atrioventricular canal · First heart field · Second heart field · FHF · SHF ·

M. Grunert
Cardiovascular Genetics, Charité – Universitätsmedizin Berlin, Berlin, Germany

C. Dorn · S. Rickert-Sperling (✉)
Cardiovascular Genetics, Charité – Universitätsmedizin Berlin, Berlin, Germany
e-mail: silke.sperling@charite.de

© The Author(s), under exclusive license to Springer Nature Switzerland AG 2024

S. Rickert-Sperling et al. (eds.), *Congenital Heart Diseases: The Broken Heart*,
Advances in Experimental Medicine and Biology 1441,
https://doi.org/10.1007/978-3-031-44087-8_16

Embryonic stem cells · Myocardin · ENCODE · Regulatory elements · Enhancers · Silencers · Histone · DNA methylation · miR-133 · miR-143 · miR-145 · Notch1 · Genome-wide association studies · GWAS · SCN10A · SCN5A

16.1 Transcription Factor Networks Driving Heart Development

A multitude of studies has revealed a set of myogenic transcription factors (TFs) that is at the core of an evolutionary conserved regulatory network defining cardiac cell fate, myogenic differentiation, and cardiac morphogenesis. These transcription factors are functionally highly interconnected with each other and operate in concert with upstream signaling pathways and downstream target genes. The transcriptional network involved in heart development is highly conserved across vast phylogenetic distances, and the first heart-like organ is believed to have appeared over 500 million years ago in an ancestral bilaterian. So, the emergence of hearts with increasing complexity occurred through modification and expansion of an ancestral network of transcription factors and their *cis*-regulatory elements. During evolution, the heart evolved from a single-layered tube with peristaltic contractility to a powerful multichambered pump. *Drosophila* has provided a model to delineating the architecture of the cardiac regulatory network, due to the lack of functional redundancies in the network. Mutations of cardiac transcription factors in *Drosophila* often result in dramatic phenotypes, whereas mutations of individual paralogs of these genes in mammals affect specific substructures of the heart that do not exist in insects. The core cardiac transcription factor network in *Drosophila* consists of NK-2 (tinman), MEF2, TBX (mid-H15), GATA (Pannier), and HAND and corresponds to the vertebrate paralogs Nkx2-5 (NK2 homeobox 5), Mef2 (myocyte enhancer factor 2), Tbx (T-box) 1/2/3/5/18/20, Gata-4 (GATA binding protein 4), and Hand1/2 (heart and neural crest derivatives expressed 1 and 2) as core factors of the mammalian heart. In an evolutionary context, the linear heart tube gives rise to the left ventricle of the heart, which is the ancestral chordate cardiac component, whereas the right ventricular chamber and outflow tract are later evolutionary additions formed from an adjacent population of progenitor cells, referred to as the second heart field [1]. Along with the addition of the second heart field, a further transcription factor named Isl1 joined this core transcription network; however, Isl1 is not cardiac specific and functionally requires combinatorial mechanisms with other factors [2, 3].

Core cardiac transcription factors cross-regulate and autoregulate their expression. Thus, activation of one or a few factors within the network may ultimately activate them all, as well as common sets of downstream targets [4]. One of the first large-scale studies on cardiac transcription networks used an integrative approach to predict regulatory subnetworks in patients with diverse cardiac malformations. In applying linear models, specific disease-associated transcription profiles were identified in cardiac biopsies. Moreover, the combination with predicted transcription factor binding sites leads to the identification of regulatory subnetworks, which

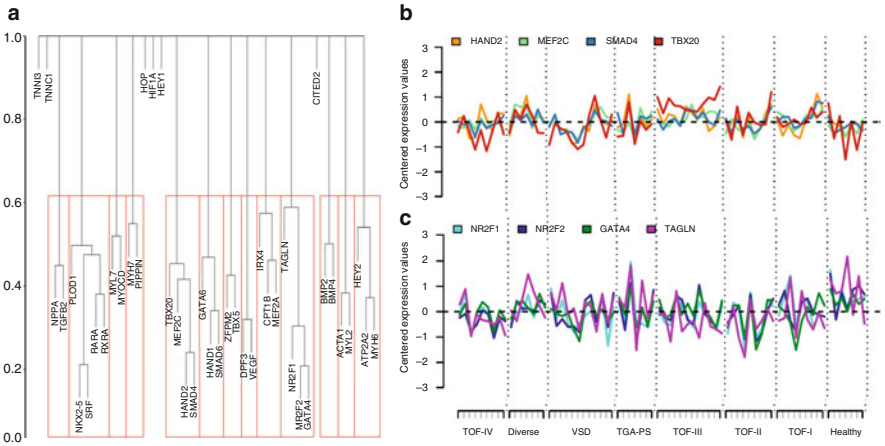

Fig. 16.1 Correlated gene groups. (**a**) Cluster dendrogram showing 13 correlated gene groups. Clustering was derived by cutting the cluster tree at the 0.001 quantile of a random distribution. The cluster distances are indicated on the y-axis. (**b**, **c**) Example of two correlated gene groups showing highly correlated patterns of expression in samples of patients and healthy individuals. Centered expression vectors were sorted by defined meta-phenotypes (Figure adapted from Toenjes et al. [5])

were further validated by chromatin immunoprecipitation followed by microarray analysis (ChIP-chip) and literature mining. For example, two correlated gene groups comprising HAND2, MEF2C, SMAD4 (SMAD family member 4), and TBX20 as well as GATA4, NR2F1/2 (nuclear receptor subfamily 2, group F, member 1 and 2) and TAGLN (transgelin) were shown to extensively regulate each other's expression and function, showing the complex molecular architecture underlying heart development (Fig. 16.1) [5].

In a further study by Schlesinger et al., the global transcription network driven by Gata4, Mef2a, Nkx2-5, and Srf (serum response factor) was investigated in the mouse cardiomyocyte cell line HL-1. ChIP-chip data demonstrated that the combinatorial regulation by these TFs and RNAi knockdown experiments showed that they partially compensate each other's function. In detail, genes bound by multiple TFs in their promoter and/or enhancer region are less likely differentially expressed in the knockdown of one respective factor, demonstrating the buffering capacity of the network [6]. Finally, the genome-wide combinatorial binding of Gata4, Nkx2-5, Tbx5, Srf, Mef2a, as well as the histone acetyltransferase p300 determined by ChIP followed by next-generation sequencing (ChIP-seq) in HL-1 cells has also been used to identify cardiac enhancer regions. Interestingly, the majority of loci bound by multiple cardiac TFs did not overlap with loci bound by p300 [7], a transcriptional coactivator commonly used to identify cardiac enhancers [8].

To dissect the spatiotemporal protein networks driving human heart development, another study constructed functional clusters from over 250 cardiac development genes based on morphological subgroups corresponding to the specific phenotype associated with their mutation [9]. In general, increased complexity of the heart

during development is accompanied by a higher complexity at the molecular level. This is reflected by a higher number of functional modules in networks associated with "late phenotypes" compared to "early phenotypes." The TFs GATA4, TBX5, and NKX2-5 were found to be involved in the majority of networks in almost all stages of cardiogenesis, demonstrating their central role in the cardiac transcription network. Interestingly, the respective modules show a high degree of variation in their complexity and protein composition, leading to a flexible and combinatorial regulation by the core cardiac transcription factors. Moreover, integrating transcriptomic, DNA-occupancy, and epigenomic datasets during cardiac reprogramming revealed context-specific roles for Gata4, Mef2c, and Tbx5, which includes the ability of Mef2c and Tbx5 to independently promote chromatin remodeling at previously inaccessible sites. In addition, there is supporting evidence for cooperative facilitation and refinement of the individual TF binding in a combinatorial manner [10]. Taken together, these results underline the dynamics of cardiac transcription networks and are consistent with the striking phenotypic variability that can result from alterations of a single factor [11, 12].

Another key regulator of cardiac expression is TEAD1, formerly known as TEF-1, which is generally not included among the core cardiac TFs [13]. However, in addition to its role in multiple cell types of Hippo/Yap signaling [14], TEAD1 is required for heart development and is even associated with it as one of the first TFs [15]. Moreover, its motif is located at muscle gene promoters, and it was recently shown that TEAD1 collaborate with other cardiac TFs, especially NKX2-5, to regulate cardiac gene expression and core cardiomyocyte-specific functions such as contraction and metabolism [13]. It shows that TEAD1 is an essential element of the cardiac transcriptional network.

16.2 Core Myogenic Transcription Factors

16.2.1 Nkx2-5

The transcription factor Nkx2-5 (NK2 homeobox 5) is essential for multiple aspects of heart development [16]. It is expressed in early heart progenitor cells, and expression remains high in adult hearts [17]. NOTCH1 knockout in human iPSC-derived cardiovascular progenitor cells showed a reduced expression of NKX2-5, ISL1, and MYOD, which suggests an impaired cardiac lineage differentiation [18]. Nkx2-5 physically interacts with other core cardiac TFs in a combinatorial manner. For example, Gata4, Tbx5, and Nkx2-5 synergistically activate the *ANF* promoter [19]. Moreover, Nkx2-5 interacts with Hand2 and Mef2c to determine ventricular identity [20, 21]. In combination with Srf and Gata4, it further activates the expression of sarcomeric genes [22]. Mice lacking *Nkx2-5* show abnormal morphogenesis of the heart tube as well as failure of left ventricular development and die early during embryonic development (lethality at E9.5) [23]. In addition, Nkx2-5 functions in the development and maintenance of the conduction system, demonstrated by progressive atrioventricular (AV) block observed in *Nkx2-5*

heterozygous mice [24]. NKX2-5 is one of the most commonly mutated genes in CHD including AV block, septal defects, TOF, left ventricular noncompaction, double outlet right ventricle (DORV), AS, and Ebstein's anomaly [25, 26].

16.2.2 Mef2

Myocyte enhancer factor 2 (Mef2) proteins are a family of TFs that play a central role in cellular differentiation. They contain both a highly conserved MADS box and an immediately adjacent motif, the MEF2 domain, which together mediate dimerization, DNA binding, and cofactor interactions [27]. The *MEF2* genes *MEF2A*, *MEF2B*, *MEF2C*, and *MEF2D* are all expressed in every stage of the developing human heart [28] and are crucial for the expression of muscle-specific genes [29]. They interact with other key cardiac TFs, particularly to regulate the expression of contractile proteins via interacting with members of the MyoD (myogenic differentiation) family, which play a key role in regulating muscle differentiation. For example, Mef2c regulates the expression of Dpf3 (D4, zinc and double PHD fingers, family 3, also known as BAF45c) [30], a heart- and muscle-specific subunit of the BAF chromatin remodeling complex, and moreover interacts with Tbx5 to activate the expression of the *Myh6* (cardiac alpha-myosin heavy chain 6) gene [31]. Within cardiac muscle lineages, the expression of Mef2 itself is in turn regulated by NK2 proteins [32]. Moreover, the different Mef2 proteins can partly compensate each other's functions [33]. In addition to other TFs, Mef2 proteins can also interact with HATs (histone acetyltransferase, e.g., p300) and HDACs (histone deacetylase, e.g., HDAC4) to activate or repress the transcription of downstream targets [34]. HDAC4 expression is further repressed by the myogenic microRNA miR-1, which leads to an activation of Mef2 that together with MyoD initiates miR-1 expression in a feedback loop [35].

Mef2a is predominantly expressed in postnatal cardiac muscle cells, and mice lacking *Mef2a* die within the first week after birth due to myofibrillar fragmentation, mitochondrial disorganization, and impaired myocyte differentiation [36]. Mutations in Mef2a identified in patients implicate its signaling pathway in the pathogenesis of coronary artery disease and myocardial infarction [37]. In *Mef2c* null mice, failure to undergo cardiac looping and formation of the right ventricle have been reported [38] and a Mef2c enhancer has been defined that drives gene expression in the second heart field and has been widely used for conditional gene inactivation [39].

16.2.3 Tbx

Tbx proteins are characterized by a conserved 180 amino acid long region termed the T-box [40]. Members of this family including Tbx1, Tbx2, Tbx3, Tbx5, Tbx18, and Tbx20 are involved in early cardiac lineage determination, chamber specification, and the development of the conduction system [41]. Tbx2 and Tbx3 act redundantly during outflow tract (OFT) development and repress Tbx1 expression in ventral

pharyngeal endoderm, while their own spatial expression is regulated by a feedback loop by Tbx1. Thus, the three factors form a crucial regulatory network for pharyngeal and OFT development, which is demonstrated by severe cardiac defects caused by knockout of *Tbx1* and either *Tbx2* or *Tbx3* [42]. Alterations in TBX3 showed a reduced transcriptional activation of the MEF2C promoter resulting in conotruncal heart malformation [43]. Tbx5 is involved in multiple pathways and combinatorial interactions with other TFs [44]. For example, it physically interacts with Nkx2-5 to control gene expression in cells of the cardiac conduction system [45] or forms a transcriptional complex with Mef2c required for early heart development [31]. Finally, Tbx20 interacts with Gata4 to activate both *Mef2c* and *Nkx2-5* enhancers [46].

Heterozygous *Tbx5* knockout mice suffer from septation defects and AV block, similar to heterozygous *Nkx2-5* knockout mice [45]. Similar to the human *GATA4* mutant phenotype, double heterozygous *Tbx5* and *Gata4* knockout mice show atrioventricular septal defects (AVSDs) and myocardial thinning. In humans, *TBX5* missense mutations cause Holt–Oram [47] syndrome [48], which is characterized by heart and limb malformations. Moreover, a homozygous variation in the *TBX5* enhancer abrogating the cardiac expression of the gene was observed in a patient with isolated VSD [49]. Hemizygosity of *TBX1* is the major cause for the CHD phenotype in 22q11.2 deletion syndrome patients, which is characterized by conotruncal defects like TOF, DORV, and truncus arteriosus (TA) [50]. Mutations in *TBX3* [51] and *TBX20* [52] as well as in the *TBX18* promoter region [53] have also been identified in different CHD types. Moreover, TBX20 mutations can result in disturbances of cardiac electrical/conductance systems by affected downstream gene expression alterations of KCNH2 channel [54].

16.2.4 Gata4

The zinc finger transcription factor Gata4 (GATA binding protein 4) is essential for cardiac development and plays a critical role for embryo survival [55, 56]. The Gata family of zinc finger TFs consists of six members, which all bind the DNA sequence "A/G GATA A/T." Gata4, Gata5, and Gata6 are expressed in the developing heart, and Gata4 and Gata6 remain expressed in adult cardiac myocytes. Both Gata4 and Gata6 regulate the expression of several cardiac-specific genes, and Gata4 is crucial for cardiac morphogenesis during mouse embryonic development [56]. Gata4 can physically interact with other cardiac TFs like Hand2 [57], Nkx2-5 [58], Mef2 [59], Srf [60], and Tbx5 [61]. In combination with Isl1 and Tbx20, Gata4 actives Mef2c and Nkx2-5 expression in the second heart field (SHF) [46]. Furthermore, Gata4 is known to regulate the transcription of several muscle-specific genes encoding contractile elements like the α- and β-myosin heavy chain (α- and β-MHC) proteins and α-actin as well as signaling molecules like atrial natriuretic factor (ANF) and brain natriuretic peptide (BNP) [62]. Gata4 DNA-binding affinity is enhanced by the HAT p300 [63], while it is negatively regulated by HDAC4, a transcriptional repressor of muscle gene expression [64]. In addition, Gata4 binds and participates

in establishing active chromatin regions by stimulating histone 3 lysine 24 acetylation (H3K24ac) deposition [65].

Homozygous *Gata4* null mice die between embryonic day E7.0 and E9.5 because of severe morphogenic defects in heart tube formation [66]. Cardiogenesis is sensitive to Gata4 dosage, and graded reduction of the TF results in DORV, common atrioventricular canal (CAVC), and hypoplastic ventricular myocardium [67]. In human, *GATA4* mutations cause CHD including septal defects, tetralogy of Fallot (TOF), and pulmonary stenosis (PS) [16]. One *GATA4* mutation described in a family with septation defects specifically disrupted the interaction with TBX5, while the binding to NKX2-5 remained unaffected, suggesting a concerted role for GATA4 and TBX5 in cardiac septation [61].

16.2.5 Hand

Hand1 and Hand2 (heart and neural crest derivatives expressed 1 and 2) are basic helix-loop-helix transcription factors, which are expressed early in derivatives of the first and second heart field (FHF and SHF), respectively [1]. They are asymmetrically expressed in the developing ventricular chambers and play an important role in cardiac morphogenesis. *Hand2* knockout mice show abnormalities in the formation of the right ventricle, most probably due to the loss of the SHF [68, 69]. Embryonic stem cells (ESCs) lacking *Hand1* are unable to contribute to the outer curvature of the heart that gives rise to the left ventricle [70]. In developing mouse hearts, the deletion of *Hand1* has been associated with CHD including ventricular septal defect (VSD), atrioventricular valve malformation, hypoplastic ventricles, and outflow tract abnormalities 1 [71]. Nkx2-5 regulates the expression of Hand1 in the FHF, and double knockout of *Nkx2-5* and *Hand2* ablates both ventricular chambers, leaving only an atrial remnant [1]. In human, mutations in *HAND1* cause septation defects, while *HAND2* mutations have been identified in patients with TOF, DORV, and PS [16]. Furthermore, it has been shown that HAND2 in combination with GATA2, MEF2c, and TBX5 can enhance direct reprogramming of human cardiomyocytes from fibroblast with better quality of cardiomyocytes at faster differentiation rate [72].

16.2.6 Isl1 and Srf

The LIM homeodomain transcription factor Isl1 (Isl LIM homeobox 1) is a well-described cardiomyocyte progenitor marker with temporal expression [73–75] and is required for the contribution of the SHF progenitor cells to cardiogenesis [2]. Isl1 represents a key factor of the transcriptional network regulating SHF development. The central role of Isl1 for cardiac development is demonstrated by knockout mice, which completely lack the derivatives of the SHF, namely the outflow tract, right ventricle, and much of the atria [2]. Isl1 directly activates the expression of Mef2c [76, 77] or together with TBX20 [46]. Several *ISL1* single nucleotide

polymorphisms (SNPs) have been associated with CHD in a large patient cohort [78]; however, their functional impact awaits further exploration.

The widely expressed serum response factor (Srf) is like Mef2, a MADS-box TF important for heart and muscle development. Srf is well-known to bind to a specific DNA motif, the CArG box, with the consensus sequence "$CC(A/T)_6GG$" in promoters of its target genes [79]. Several studies demonstrated the crucial role of Srf for heart and muscle development. For example, cardiac-specific deletion of *Srf* in mice results in embryonically lethal cardiac defects including abnormally thin myocardium, dilated cardiac chambers, poor trabeculation, and a disorganized interventricular septum [80]. Srf autoregulates its own expression [81] and is suggested to be a master regulator of the actin cytoskeleton and contractile apparatus [79]. Since Srf is ubiquitously expressed and has relatively low intrinsic transcriptional activity, its ability to regulate cardiac transcription is highly dependent on its interaction with both positive and negative coregulators. For example, the combinatorial expression of Gata4, Nkx2-5, and Srf directs early cardiac gene activity [22]. Moreover, Srf enhances muscle gene expression in association with myocardin (Myocd), a smooth and cardiac muscle-specific transcriptional coactivator [82]. The Srf/Myocd complex recruits p300 to Srf-binding sites, which induces histone 3 acetylation (H3ac) and actives gene expression [83]. Furthermore, a strong correlation was found between the presence of H3ac, histone 2 lysine 4 dimethylation (H3K4me2), and Srf and p300 *in vivo* [84]. In addition, the homeodomain protein Hopx, which does not directly bind DNA, can inhibit SRF-dependent transcription by recruiting HDAC2 to Srf target genes, thereby modulating growth and proliferation of cardiomyocytes [85]. Similar to Mef2, Srf acts in feedback loop with miR-133 to modulate muscle proliferation and differentiation [35]. Furthermore, Srf regulates the transcription of other microRNAs like the smooth muscle-relevant miR-143 and miR-145, which in turn cooperatively targeted a network of transcription factors including Myocd to promote differentiation and repress proliferation of smooth muscle cells [86]. In addition, Tbx1 promotes posttranscriptional regulation of Srf levels by proteasome-mediated degradation [87].

16.3 *Cis*-Regulatory Elements and Chromatin Structures

In humans, the number of protein-coding genes is only about 20,500 based on the Ensembl human gene catalog (Dec 2021), whereas the human body consists of about 10^{14} cells and approximately 200 different cell types, which originated from one pluripotent cell via numerous intermediate cellular stages. Thus, it seems reasonable that a large fraction of the sequence space is occupied by regulatory sequence elements defining spatiotemporal gene expression and protein functionality by "coding" for *cis*-regulatory elements and short and long non-coding RNAs modulating transcription, translation, and posttranslational modification. In fact, ~99% of the human genome does not code for proteins (known as the genome's "dark matter") and has been investigated by major international efforts led by the ENCODE consortium [88, 89]. Thus, a vertebrate gene is typically associated with a

proximal promoter and multiple transcriptional regulatory elements (enhancers and silencers or even insulators). These *cis*-regulatory elements are often distant from the promoter and sometimes act across intermediate genes. Moreover, regulatory sequences can affect their target genes without regard to orientation and often over long distances in cis or in trans. Forty thousand human heart enhancers have been postulated [90], which are potential targets for DNA-binding transcription factors and consist of short sequence motifs recognized by them. Moreover, transcriptional enhancers are often marked by H3K27ac and P300 occupancy [8, 91], and an integrative analysis of over 35 genome-wide H3K27ac or P300 profiles from mouse or human heart samples revealed more than 80,000 cardiac enhancers [92]. The specific sequence of a motif and interacting proteins, RNA cofactors, local physical properties of the DNA fiber, and surrounding chromatin determine the binding affinity of TFs and thereby modulate TF function. The chromatin structure is modulated, for example, by posttranslational modifications and variants of histones, presence of DNA methylation or chromatin-related proteins, and RNAs. Thus, a complex molecular network of *cis*- and *trans-acting* elements directs spatiotemporal gene expression.

16.4 MicroRNAs as Downstream Targets

Downstream targets mediate a considerable multiplication effect of transcription factor function. Only a small proportion of differentially expressed genes in loss-of-function experiments are direct targets of the respective transcription factors [6]. The transcription factor Srf represents a well-studied example for regulating muscle-specific microRNAs like the cardiac-specific miR-1 and miR-133 as well as miR-143 and miR-145 [35]. RNAi-mediated knockdown of Srf supported the role of Srf as a microRNA activator such that the majority of the differentially expressed microRNAs were found to be downregulated. The differential expression of these microRNAs explained more than two-third of the differentially expressed downstream target genes in Srf knockdown [6]. Figure 16.2 shows the Srf-based transcription network integrating Srf-binding events, H3ac, microRNAs, and differential expression in Srf knockdown. A further and more global study investigated the relationship between tissue-specific microRNAs and TFs across multiple tissues, including the heart and skeletal muscle. Using ChIP-seq data for transcription factor binding sites (TFBS) from the ENCODE project, 2,347 interactions between TFs and tissue-specific microRNAs were identified, with the majority of the microRNAs being regulated by non-tissue-specific TFs. Moreover, TF-microRNA regulatory networks integrating verified or predicted interactions and expression data were constructed for each tissue. In the heart, the network comprises 33 TFs and 10 tissue-specific microRNAs, while in skeletal muscle, 9 microRNAs are regulated by 52 TFs [93].

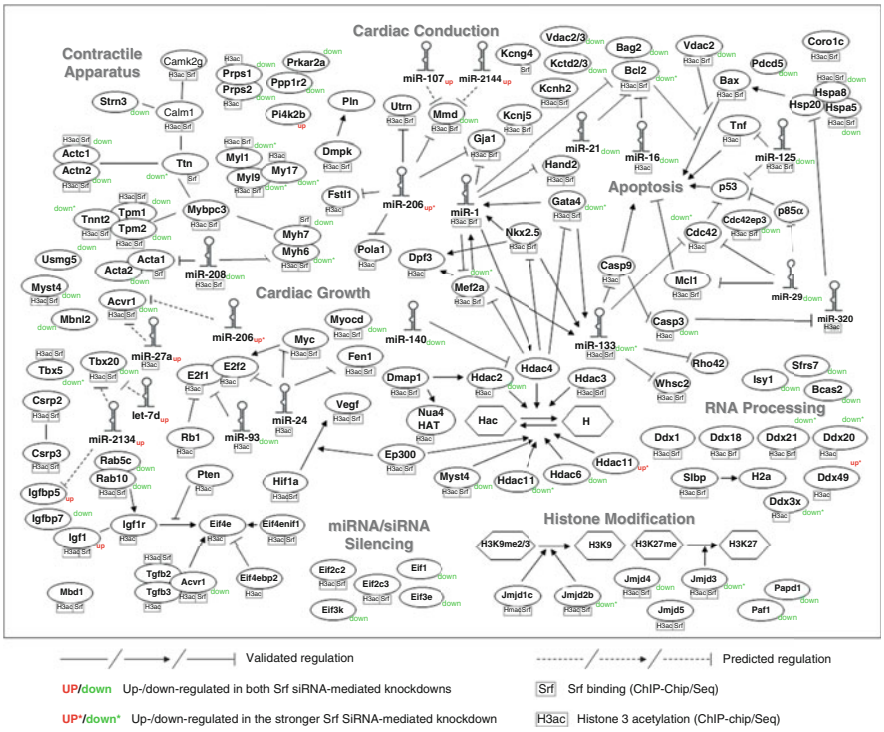

Fig. 16.2 Srf-based transcription network integrating Srf-binding events, histone 3 acetylation, microRNAs, and differential expression in Srf knockdown. The network is based on a literature search and findings from the Srf and histone 3 acetylation (*H3ac*), chromatin immunoprecipitation (*ChIP*), and Srf siRNA-mediated knockdown experiments in mouse cardiomyocytes. Srf binding and H3ac occurrence are depicted in small boxes, and up- (*red*) or downregulation (*green*) in Srf knockdown is further indicated (Figure adapted from Schlesinger et al. [6])

16.5 Disturbance of the Regulatory Network Underlying Congenital Heart Disease

Almost two decades ago, Kaynak et al. provided the first evidence that distinct types of congenital heart diseases are characterized by distinct gene expression profiles at a global scale [94]. With the development of the next-generation sequencing technology, it became feasible to study the entire exome and genome in patients. It is now apparent that the majority of CHDs, which are sporadic and nonsyndromic, are based on multiple genomic alterations, which in concert alter the molecular network [95, 96]. These are not limited to cardiac-specific factors nor to the coding part of the genome. It is highly likely that network alterations driven by alterations in non-coding sequences will emerge and have a significant impact in driving the disease state. In general, human diseases including CHDs are often caused by

heterozygous genetic variants that quantitatively affect dosage of the functional encoded gene product, as it is the case for copy number variations or haploinsufficiency [97, 98]. An example is Notch1 haploinsufficiency causing bicuspid aortic valve and severe aortic calcifications in related adults. Heterozygous nonsense mutations in Notch1 cause disruption of the epigenetic architecture, which results in derepression of latent pro-osteogenic and pro-inflammatory gene networks and triggers aortic valve calcification depending on the hemodynamic shear stress [98].

Insights of the impact of non-coding variations have, for example, been gained by genome-wide association studies (GWASs) assessing the association between genetic variants and a phenotypic trait of interest in many individuals. The TBX3-TBX5 locus and the NKX2-5 locus are frequently implicated regions in GWAS analysis of conduction anomalies. A meta-analysis of 14 GWAS on QRS duration in individuals of European descent implicated an intronic region of the *SCN10A* (sodium channel, voltage gated, type X, alpha subunit) gene as a major risk region for prolonged QRS duration [99]. Intriguingly, SCN10A is located next to SCN5A, which encodes the alpha subunit of the cardiac voltage-gated sodium channel and is known to cause several types of heritable arrhythmogenic disorders. In a close examination of this risk region in SCN10A-containing rs6801957, the sentinel SNP frequently found in ECG GWAS reveals that it is occupied by TBX3, TBX5, NKX2-5, and several enhancer-associated coactivators, such as p300 and PolII, in the adult mouse heart. Analysis of the risk allele showed that the SNP alters the sequence of the *cis*-regulatory motif for TBX3/TBX5, which inhibits the response of the enhancer to these factors and decreases the activity of the enhancer in zebrafish *in vivo*, thus potentially reducing the expression level and dosage of SCN5A [100].

16.6 Conclusion

Cardiac development is tightly controlled by transcription factors that lead to correct temporal and spatial gene expression. The core cardiac transcription factors regulate each other's expression and can act in a combinatorial manner, resulting in a buffering capacity of the network. Moreover, co-regulators, epigenetic marks, and posttranscriptional regulators like microRNAs control their expression and functional activity. While transcription factors are clearly a main driving force for gene regulation, a number of studies now show the importance of multiple regulatory levels with a high degree of interdependency leading to a fine-tuned balance of gene expression. Disruption of cardiac transcription networks can lead to dramatic consequences for cardiogenesis and results in congenital heart disease. However, the realization of the complexity of the network and most importantly its buffering capacity at different levels provide hope that we might be able to find ways to modulate it to arrive at a more favorable state without the need for genetic corrections. One focus could be the role of targetable epigenetic mechanisms driven by genetic alterations or environmental factors to reduce the burden of CHDs and most importantly improve the long-term outcome.

References

1. Buckingham M, Meilhac S, Zaffran S. Building the mammalian heart from two sources of myocardial cells. Nat Rev Genet. 2005;6(11):826–35.
2. Cai CL, Liang X, Shi Y, Chu PH, Pfaff SL, Chen J, et al. Isl1 identifies a cardiac progenitor population that proliferates prior to differentiation and contributes a majority of cells to the heart. Dev Cell. 2003;5(6):877–89.
3. Engleka KA, Manderfield LJ, Brust RD, Li L, Cohen A, Dymecki SM, et al. Islet1 derivatives in the heart are of both neural crest and second heart field origin. Circ Res. 2012;110(7):922–6.
4. Kathiriya IS, Nora EP, Bruneau BG. Investigating the transcriptional control of cardiovascular development. Circ Res. 2015;116(4):700–14.
5. Toenjes M, Schueler M, Hammer S, Pape UJ, Fischer JJ, Berger F, et al. Prediction of cardiac transcription networks based on molecular data and complex clinical phenotypes. Mol BioSyst. 2008;4(6):589–98.
6. Schlesinger J, Schueler M, Grunert M, Fischer JJ, Zhang Q, Krueger T, et al. The cardiac transcription network modulated by Gata4, Mef2a, Nkx2.5, Srf, histone modifications, and microRNAs. PLoS Genet. 2011;7(2):e1001313.
7. He A, Kong SW, Ma Q, Pu WT. Co-occupancy by multiple cardiac transcription factors identifies transcriptional enhancers active in heart. Proc Natl Acad Sci U S A. 2011;108(14):5632–7.
8. Visel A, Blow MJ, Li Z, Zhang T, Akiyama JA, Holt A, et al. ChIP-seq accurately predicts tissue-specific activity of enhancers. Nature. 2009;457(7231):854–8.
9. Lage K, Mollgard K, Greenway S, Wakimoto H, Gorham JM, Workman CT, et al. Dissecting spatio-temporal protein networks driving human heart development and related disorders. Mol Syst Biol. 2010;6:381.
10. Stone NR, Gifford CA, Thomas R, Pratt KJB, Samse-Knapp K, Mohamed TMA, et al. Context-specific transcription factor functions regulate epigenomic and transcriptional dynamics during cardiac reprogramming. Cell Stem Cell. 2019;25(1):87–102.e9.
11. Takeuchi JK, Bruneau BG. Directed transdifferentiation of mouse mesoderm to heart tissue by defined factors. Nature. 2009;459(7247):708–11.
12. Ieda M, Fu JD, Delgado-Olguin P, Vedantham V, Hayashi Y, Bruneau BG, et al. Direct reprogramming of fibroblasts into functional cardiomyocytes by defined factors. Cell. 2010;142(3):375–86.
13. Akerberg BN, Gu F, VanDusen NJ, Zhang X, Dong R, Li K, et al. A reference map of murine cardiac transcription factor chromatin occupancy identifies dynamic and conserved enhancers. Nat Commun. 2019;10(1):4907.
14. Zhao B, Ye X, Yu J, Li L, Li W, Li S, et al. TEAD mediates YAP-dependent gene induction and growth control. Genes Dev. 2008;22(14):1962–71.
15. Chen Z, Friedrich GA, Soriano P. Transcriptional enhancer factor 1 disruption by a retroviral gene trap leads to heart defects and embryonic lethality in mice. Genes Dev. 1994;8(19):2293–301.
16. McCulley DJ, Black BL. Transcription factor pathways and congenital heart disease. Curr Top Dev Biol. 2012;100:253–77.
17. Kamohara H, Sakamoto K, Ishiko T, Mita S, Masuda Y, Abe T, et al. Human carcinoma cell lines produce biologically active leukemia inhibitory factor (LIF). Res Commun Mol Pathol Pharmacol. 1994;85(2):131–40.
18. Jiao J, Tian W, Qiu P, Norton EL, Wang MM, Chen YE, et al. Induced pluripotent stem cells with NOTCH1 gene mutation show impaired differentiation into smooth muscle and endothelial cells: implications for bicuspid aortic valve-related aortopathy. J Thorac Cardiovasc Surg. 2018;156(2):515–22 e1.
19. Takeuchi JK, Ohgi M, Koshiba-Takeuchi K, Shiratori H, Sakaki I, Ogura K, et al. Tbx5 specifies the left/right ventricles and ventricular septum position during cardiogenesis. Development. 2003;130(24):5953–64.

20. Yamagishi H, Yamagishi C, Nakagawa O, Harvey RP, Olson EN, Srivastava D. The combinatorial activities of Nkx2.5 and dHAND are essential for cardiac ventricle formation. Dev Biol. 2001;239(2):190–203.
21. Vincentz JW, Barnes RM, Firulli BA, Conway SJ, Firulli AB. Cooperative interaction of Nkx2.5 and Mef2c transcription factors during heart development. Dev Dyn. 2008;237(12): 3809–19.
22. Sepulveda JL, Vlahopoulos S, Iyer D, Belaguli N, Schwartz RJ. Combinatorial expression of GATA4, Nkx2-5, and serum response factor directs early cardiac gene activity. J Biol Chem. 2002;277(28):25775–82.
23. Lyons I, Parsons LM, Hartley L, Li R, Andrews JE, Robb L, et al. Myogenic and morphogenetic defects in the heart tubes of murine embryos lacking the homeo box gene Nkx2-5. Genes Dev. 1995;9(13):1654–66.
24. Jay PY, Harris BS, Maguire CT, Buerger A, Wakimoto H, Tanaka M, et al. Nkx2-5 mutation causes anatomic hypoplasia of the cardiac conduction system. J Clin Invest. 2004;113(8): 1130–7.
25. Clark KL, Yutzey KE, Benson DW. Transcription factors and congenital heart defects. Annu Rev Physiol. 2006;68:97–121.
26. Benson DW. Genetic origins of pediatric heart disease. Pediatr Cardiol. 2010;31(3):422–9.
27. Potthoff MJ, Olson EN. MEF2: a central regulator of diverse developmental programs. Development. 2007;134(23):4131–40.
28. Iida K, Hidaka K, Takeuchi M, Nakayama M, Yutani C, Mukai T, et al. Expression of MEF2 genes during human cardiac development. Tohoku J Exp Med. 1999;187(1):15–23.
29. Amacher SL, Buskin JN, Hauschka SD. Multiple regulatory elements contribute differentially to muscle creatine kinase enhancer activity in skeletal and cardiac muscle. Mol Cell Biol. 1993;13(5):2753–64.
30. Lange M, Kaynak B, Forster UB, Tonjes M, Fischer JJ, Grimm C, et al. Regulation of muscle development by DPF3, a novel histone acetylation and methylation reader of the BAF chromatin remodeling complex. Genes Dev. 2008;22(17):2370–84.
31. Ghosh TK, Song FF, Packham EA, Buxton S, Robinson TE, Ronksley J, et al. Physical interaction between TBX5 and MEF2C is required for early heart development. Mol Cell Biol. 2009;29(8):2205–18.
32. Olson EN. Gene regulatory networks in the evolution and development of the heart. Science. 2006;313(5795):1922–7.
33. Karamboulas C, Dakubo GD, Liu J, De Repentigny Y, Yutzey K, Wallace VA, et al. Disruption of MEF2 activity in cardiomyoblasts inhibits cardiomyogenesis. J Cell Sci. 2006;119(Pt 20):4315–21.
34. Lu J, McKinsey TA, Zhang CL, Olson EN. Regulation of skeletal myogenesis by association of the MEF2 transcription factor with class II histone deacetylases. Mol Cell. 2000;6(2): 233–44.
35. Chen JF, Mandel EM, Thomson JM, Wu Q, Callis TE, Hammond SM, et al. The role of microRNA-1 and microRNA-133 in skeletal muscle proliferation and differentiation. Nat Genet. 2006;38(2):228–33.
36. Naya FJ, Black BL, Wu H, Bassel-Duby R, Richardson JA, Hill JA, et al. Mitochondrial deficiency and cardiac sudden death in mice lacking the MEF2A transcription factor. Nat Med. 2002;8(11):1303–9.
37. Wang L, Fan C, Topol SE, Topol EJ, Wang Q. Mutation of MEF2A in an inherited disorder with features of coronary artery disease. Science. 2003;302(5650):1578–81.
38. Lin Q, Schwarz J, Bucana C, Olson EN. Control of mouse cardiac morphogenesis and myogenesis by transcription factor MEF2C. Science. 1997;276(5317):1404–7.
39. Verzi MP, McCulley DJ, De Val S, Dodou E, Black BL. The right ventricle, outflow tract, and ventricular septum comprise a restricted expression domain within the secondary/anterior heart field. Dev Biol. 2005;287(1):134–45.

40. Nemer M. Genetic insights into normal and abnormal heart development. Cardiovasc Pathol. 2008;17(1):48–54.
41. Plageman TF Jr, Yutzey KE. T-box genes and heart development: putting the "T" in heart. Dev Dyn. 2005;232(1):11–20.
42. Mesbah K, Rana MS, Francou A, van Duijvenboden K, Papaioannou VE, Moorman AF, et al. Identification of a Tbx1/Tbx2/Tbx3 genetic pathway governing pharyngeal and arterial pole morphogenesis. Hum Mol Genet. 2012;21(6):1217–29.
43. Xie H, Zhang E, Hong N, Fu Q, Li F, Chen S, et al. Identification of TBX2 and TBX3 variants in patients with conotruncal heart defects by target sequencing. Hum Genomics. 2018;12(1): 44.
44. Hatcher CJ, Basson CT. Specification of the cardiac conduction system by transcription factors. Circ Res. 2009;105(7):620–30.
45. Bruneau BG, Nemer G, Schmitt JP, Charron F, Robitaille L, Caron S, et al. A murine model of Holt-Oram syndrome defines roles of the T-box transcription factor Tbx5 in cardiogenesis and disease. Cell. 2001;106(6):709–21.
46. Takeuchi JK, Mileikovskaia M, Koshiba-Takeuchi K, Heidt AB, Mori AD, Arruda EP, et al. Tbx20 dose-dependently regulates transcription factor networks required for mouse heart and motoneuron development. Development. 2005;132(10):2463–74.
47. Maitra M, Schluterman MK, Nichols HA, Richardson JA, Lo CW, Srivastava D, et al. Interaction of Gata4 and Gata6 with Tbx5 is critical for normal cardiac development. Dev Biol. 2009;326(2):368–77.
48. Basson CT, Bachinsky DR, Lin RC, Levi T, Elkins JA, Soults J, et al. Mutations in human TBX5 [corrected] cause limb and cardiac malformation in Holt-Oram syndrome. Nat Genet. 1997;15(1):30–5.
49. Smemo S, Campos LC, Moskowitz IP, Krieger JE, Pereira AC, Nobrega MA. Regulatory variation in a TBX5 enhancer leads to isolated congenital heart disease. Hum Mol Genet. 2012;21(14):3255–63.
50. Merscher S, Funke B, Epstein JA, Heyer J, Puech A, Lu MM, et al. TBX1 is responsible for cardiovascular defects in velo-cardio-facial/DiGeorge syndrome. Cell. 2001;104(4):619–29.
51. Meneghini V, Odent S, Platonova N, Egeo A, Merlo GR. Novel TBX3 mutation data in families with ulnar-mammary syndrome indicate a genotype-phenotype relationship: mutations that do not disrupt the T-domain are associated with less severe limb defects. Eur J Med Genet. 2006;49(2):151–8.
52. Kirk EP, Sunde M, Costa MW, Rankin SA, Wolstein O, Castro ML, et al. Mutations in cardiac T-box factor gene TBX20 are associated with diverse cardiac pathologies, including defects of septation and valvulogenesis and cardiomyopathy. Am J Hum Genet. 2007;81(2):280–91.
53. Ma L, Li J, Liu Y, Pang S, Huang W, Yan B. Novel and functional variants within the TBX18 gene promoter in ventricular septal defects. Mol Cell Biochem. 2013;382(1–2):121–6.
54. Caballero R, Utrilla RG, Amoros I, Matamoros M, Perez-Hernandez M, Tinaquero D, et al. Tbx20 controls the expression of the KCNH2 gene and of hERG channels. Proc Natl Acad Sci U S A. 2017;114(3):E416–E25.
55. Peterkin T, Gibson A, Loose M, Patient R. The roles of GATA-4, -5 and -6 in vertebrate heart development. Semin Cell Dev Biol. 2005;16(1):83–94.
56. Pikkarainen S, Tokola H, Kerkela R, Ruskoaho H. GATA transcription factors in the developing and adult heart. Cardiovasc Res. 2004;63(2):196–207.
57. Dai YS, Cserjesi P, Markham BE, Molkentin JD. The transcription factors GATA4 and dHAND physically interact to synergistically activate cardiac gene expression through a p300-dependent mechanism. J Biol Chem. 2002;277(27):24390–8.
58. Lee Y, Shioi T, Kasahara H, Jobe SM, Wiese RJ, Markham BE, et al. The cardiac tissue-restricted homeobox protein Csx/Nkx2.5 physically associates with the zinc finger protein GATA4 and cooperatively activates atrial natriuretic factor gene expression. Mol Cell Biol. 1998;18(6):3120–9.

59. Morin S, Charron F, Robitaille L, Nemer M. GATA-dependent recruitment of MEF2 proteins to target promoters. EMBO J. 2000;19(9):2046–55.
60. Belaguli NS, Sepulveda JL, Nigam V, Charron F, Nemer M, Schwartz RJ. Cardiac tissue enriched factors serum response factor and GATA-4 are mutual coregulators. Mol Cell Biol. 2000;20(20):7550–8.
61. Garg V, Kathiriya IS, Barnes R, Schluterman MK, King IN, Butler CA, et al. GATA4 mutations cause human congenital heart defects and reveal an interaction with TBX5. Nature. 2003;424(6947):443–7.
62. Moorman AF, Christoffels VM. Cardiac chamber formation: development, genes, and evolution. Physiol Rev. 2003;83(4):1223–67.
63. Kouzarides T. Chromatin modifications and their function. Cell. 2007;128(4):693–705.
64. Davis FJ, Gupta M, Camoretti-Mercado B, Schwartz RJ, Gupta MP. Calcium/calmodulin-dependent protein kinase activates serum response factor transcription activity by its dissociation from histone deacetylase, HDAC4. Implications in cardiac muscle gene regulation during hypertrophy. J Biol Chem. 2003;278(22):20047–58.
65. He A, Gu F, Hu Y, Ma Q, Ye LY, Akiyama JA, et al. Dynamic GATA4 enhancers shape the chromatin landscape central to heart development and disease. Nat Commun. 2014;5:4907.
66. Molkentin JD, Lin Q, Duncan SA, Olson EN. Requirement of the transcription factor GATA4 for heart tube formation and ventral morphogenesis. Genes Dev. 1997;11(8):1061–72.
67. Pu WT, Ishiwata T, Juraszek AL, Ma Q, Izumo S. GATA4 is a dosage-sensitive regulator of cardiac morphogenesis. Dev Biol. 2004;275(1):235–44.
68. Srivastava D, Thomas T, Lin Q, Kirby ML, Brown D, Olson EN. Regulation of cardiac mesodermal and neural crest development by the bHLH transcription factor, dHAND. Nat Genet. 1997;16(2):154–60.
69. Tsuchihashi T, Maeda J, Shin CH, Ivey KN, Black BL, Olson EN, et al. Hand2 function in second heart field progenitors is essential for cardiogenesis. Dev Biol. 2011;351(1):62–9.
70. Riley PR, Gertsenstein M, Dawson K, Cross JC. Early exclusion of hand1-deficient cells from distinct regions of the left ventricular myocardium in chimeric mouse embryos. Dev Biol. 2000;227(1):156–68.
71. McFadden DG, Barbosa AC, Richardson JA, Schneider MD, Srivastava D, Olson EN. The Hand1 and Hand2 transcription factors regulate expansion of the embryonic cardiac ventricles in a gene dosage-dependent manner. Development. 2005;132(1):189–201.
72. Muraoka N, Nara K, Tamura F, Kojima H, Yamakawa H, Sadahiro T, et al. Role of cyclooxygenase-2-mediated prostaglandin E2-prostaglandin E receptor 4 signaling in cardiac reprogramming. Nat Commun. 2019;10(1):674.
73. Bu L, Jiang X, Martin-Puig S, Caron L, Zhu S, Shao Y, et al. Human ISL1 heart progenitors generate diverse multipotent cardiovascular cell lineages. Nature. 2009;460(7251):113–7.
74. Pandur P, Sirbu IO, Kuhl SJ, Philipp M, Kuhl M. Islet1-expressing cardiac progenitor cells: a comparison across species. Dev Genes Evol. 2013;223(1–2):117–29.
75. Churko JM, Garg P, Treutlein B, Venkatasubramanian M, Wu H, Lee J, et al. Defining human cardiac transcription factor hierarchies using integrated single-cell heterogeneity analysis. Nat Commun. 2018;9(1):4906.
76. Dodou E, Verzi MP, Anderson JP, Xu SM, Black BL. Mef2c is a direct transcriptional target of ISL1 and GATA factors in the anterior heart field during mouse embryonic development. Development. 2004;131(16):3931–42.
77. Laugwitz KL, Moretti A, Caron L, Nakano A, Chien KR. Islet1 cardiovascular progenitors: a single source for heart lineages? Development. 2008;135(2):193–205.
78. Stevens KN, Hakonarson H, Kim CE, Doevendans PA, Koeleman BP, Mital S, et al. Common variation in ISL1 confers genetic susceptibility for human congenital heart disease. PLoS One. 2010;5(5):e10855.
79. Miano JM, Long X, Fujiwara K. Serum response factor: master regulator of the actin cytoskeleton and contractile apparatus. Am J Physiol Cell Physiol. 2007;292(1):C70–81.

80. Parlakian A, Tuil D, Hamard G, Tavernier G, Hentzen D, Concordet JP, et al. Targeted inactivation of serum response factor in the developing heart results in myocardial defects and embryonic lethality. Mol Cell Biol. 2004;24(12):5281–9.
81. Belaguli NS, Schildmeyer LA, Schwartz RJ. Organization and myogenic restricted expression of the murine serum response factor gene. A role for autoregulation. J Biol Chem. 1997;272 (29):18222–31.
82. Wang D, Chang PS, Wang Z, Sutherland L, Richardson JA, Small E, et al. Activation of cardiac gene expression by myocardin, a transcriptional cofactor for serum response factor. Cell. 2001;105(7):851–62.
83. Cao D, Wang Z, Zhang CL, Oh J, Xing W, Li S, et al. Modulation of smooth muscle gene expression by association of histone acetyltransferases and deacetylases with myocardin. Mol Cell Biol. 2005;25(1):364–76.
84. Schueler M, Zhang Q, Schlesinger J, Tonjes M, Sperling SR. Dynamics of Srf, p300 and histone modifications during cardiac maturation in mouse. Mol BioSyst. 2012;8(2):495–503.
85. Kook H, Lepore JJ, Gitler AD, Lu MM, Wing-Man Yung W, Mackay J, et al. Cardiac hypertrophy and histone deacetylase-dependent transcriptional repression mediated by the atypical homeodomain protein Hop. J Clin Invest. 2003;112(6):863–71.
86. Cordes KR, Sheehy NT, White MP, Berry EC, Morton SU, Muth AN, et al. miR-145 and miR-143 regulate smooth muscle cell fate and plasticity. Nature. 2009;460(7256):705–10.
87. Chen L, Fulcoli FG, Tang S, Baldini A. Tbx1 regulates proliferation and differentiation of multipotent heart progenitors. Circ Res. 2009;105(9):842–51.
88. Consortium EP, Birney E, Stamatoyannopoulos JA, Dutta A, Guigo R, Gingeras TR, et al. Identification and analysis of functional elements in 1% of the human genome by the ENCODE pilot project. Nature. 2007;447(7146):799–816.
89. Ernst J, Kellis M. Interplay between chromatin state, regulator binding, and regulatory motifs in six human cell types. Genome Res. 2013;23(7):1142–54.
90. Narlikar L, Sakabe NJ, Blanski AA, Arimura FE, Westlund JM, Nobrega MA, et al. Genome-wide discovery of human heart enhancers. Genome Res. 2010;20(3):381–92.
91. Nord AS, Blow MJ, Attanasio C, Akiyama JA, Holt A, Hosseini R, et al. Rapid and pervasive changes in genome-wide enhancer usage during mammalian development. Cell. 2013;155(7): 1521–31.
92. Dickel DE, Ypsilanti AR, Pla R, Zhu Y, Barozzi I, Mannion BJ, et al. Ultraconserved enhancers are required for Normal development. Cell. 2018;172(3):491–9 e15.
93. Guo Z, Maki M, Ding R, Yang Y, Zhang B, Xiong L. Genome-wide survey of tissue-specific microRNA and transcription factor regulatory networks in 12 tissues. Sci Rep. 2014;4:5150.
94. Kaynak B, von Heydebreck A, Mebus S, Seelow D, Hennig S, Vogel J, et al. Genome-wide array analysis of normal and malformed human hearts. Circulation. 2003;107(19):2467–74.
95. Zaidi S, Choi M, Wakimoto H, Ma L, Jiang J, Overton JD, et al. De novo mutations in histone-modifying genes in congenital heart disease. Nature. 2013;498(7453):220–3.
96. Grunert M, Dorn C, Schueler M, Dunkel I, Schlesinger J, Mebus S, et al. Rare and private variations in neural crest, apoptosis and sarcomere genes define the polygenic background of isolated tetralogy of Fallot. Hum Mol Genet. 2014;23(12):3115–28.
97. Greenway SC, Pereira AC, Lin JC, DePalma SR, Israel SJ, Mesquita SM, et al. De novo copy number variants identify new genes and loci in isolated sporadic tetralogy of Fallot. Nat Genet. 2009;41(8):931–5.
98. Theodoris CV, Li M, White MP, Liu L, He D, Pollard KS, et al. Human disease modeling reveals integrated transcriptional and epigenetic mechanisms of NOTCH1 haploinsufficiency. Cell. 2015;160(6):1072–86.

99. Sotoodehnia N, Isaacs A, de Bakker PI, Dorr M, Newton-Cheh C, Nolte IM, et al. Common variants in 22 loci are associated with QRS duration and cardiac ventricular conduction. Nat Genet. 2010;42(12):1068–76.
100. van den Boogaard M, Wong LY, Tessadori F, Bakker ML, Dreizehnter LK, Wakker V, et al. Genetic variation in T-box binding element functionally affects SCN5A/SCN10A enhancer. J Clin Invest. 2012;122(7):2519–30.

Posttranscriptional Regulation by Proteins and Noncoding RNAs

17

Amelia E. Aranega and Diego Franco

Abstract

Posttranscriptional regulation comprises those mechanisms occurring after the initial copy of the DNA sequence is transcribed into an intermediate RNA molecule (i.e., messenger RNA) until such a molecule is used as a template to generate a protein. A subset of these posttranscriptional regulatory mechanisms essentially are destined to process the immature mRNA toward its mature form, conferring the adequate mRNA stability, providing the means for pertinent introns excision, and controlling mRNA turnover rate and quality control check. An additional layer of complexity is added in certain cases, since discrete nucleotide modifications in the mature RNA molecule are added by RNA editing, a process that provides large mature mRNA diversity. Moreover, a number of posttranscriptional regulatory mechanisms occur in a cell- and tissue-specific manner, such as alternative splicing and noncoding RNA-mediated regulation. In this chapter, we will briefly summarize current state-of-the-art knowledge of general posttranscriptional mechanisms, while major emphases will be devoted to those tissue-specific posttranscriptional modifications that impact on cardiac development and congenital heart disease.

Keywords

Messenger RNA · mRNA · Posttranscriptional regulation · Mature RNA · Immature mRNA · RNA editing · RNA-binding proteins · Ribonucleoprotein · Pre-mRNA splicing · Translation · RNA maturation · Nonsense-mediated decay · NMD · RNA guanylyltransferase and 5′ triphosphatase · RNA methyltransferase ·

A. E. Aranega · D. Franco (✉)
Cardiovascular Research Group, Department of Experimental Biology, University of Jaén, Jaén, Spain
e-mail: dfranco@ujaen.es

© The Author(s), under exclusive license to Springer Nature Switzerland AG 2024

S. Rickert-Sperling et al. (eds.), *Congenital Heart Diseases: The Broken Heart*,
Advances in Experimental Medicine and Biology 1441,
https://doi.org/10.1007/978-3-031-44087-8_17

mRNA capping · Cap-binding protein · *S. cerevisiae* · *S. pombe* · 5′end capping · Splicing · Polyadenylation · Poly-A site · Premature translation termination codons · ADAR · Alternative splicing · Spliceosome · PITX2 · GATA4 · ZIC3 · SCN5A · Noncoding RNA · Ribosomal RNAs · rRNAs · Transfer RNAs · tRNAs · Small nuclear RNAs · snRNAs · Small nucleolar RNAs · snoRNAs · microRNA · miRNA

17.1 Introduction

Posttranscriptional regulation comprises those mechanisms occurring after the initial copy of the DNA sequence is transcribed into an intermediate RNA molecule (i.e., messenger RNA) until such a molecule is used as a template to generate a protein. Posttranscriptional regulation is mainly mediated by distinct RNA-binding proteins (RBPs). RBPs are key components in RNA metabolism, regulating the temporal, spatial, and functional dynamics of RNAs. RBPs form dynamic interactions with coding, untranslated, and non-protein-coding RNAs in functional units called ribonucleoprotein (RNP) complexes [1, 2]. This enables the RBPs within RNP complexes to remain stably bound to the RNA throughout its journey from synthesis to degradation or to associate with the RNAs in a temporally and spatially specific manner. RNA molecules are constantly accompanied by RBPs, which are intimately involved in every step of RNA biology, including transcription, editing, splicing, transport and localization, stability, and translation. Altering the expression of RBPs has profound implications for cellular physiology, affecting RNA processes from pre-mRNA splicing to protein translation [1, 3]. RBPs therefore have opportunities to shape gene expression at multiple levels. This capacity is particularly important during development, when dynamic chemical and physical changes give rise to complex organs and tissues [2].

Modification of the nascent mRNA is a general mechanism that occurs in all cells within an organism. A subset of these posttranscriptional regulatory mechanisms is essentially destined to process the immature mRNA toward its mature form, conferring the adequate mRNA stability including modifications at the 5′ and 3′ ends (5′ capping and 3′ polyadenylation) as well as excision of pertinent introns by pre-mRNA splicing. mRNA turnover rate and quality control checking are performed by the nonsense-mediated decay (NMD) surveillance pathway. An additional layer of complexity is added in certain cases, since discrete nucleotide modifications in the mature RNA molecule are added by RNA editing, a process that provides large mature mRNA diversity. Given the fact that these posttranscriptional modifications would affect all RNA molecules, there are a very limited number of cases in which a discrete tissue layer or an organ, such as the heart, is affected since impairment impacts at the level of the organism. On the other hand, a number of posttranscriptional regulatory mechanisms occur in a cell- and tissue-specific manner, such as alternative splicing and noncoding RNA-mediated regulation. Alternative splicing is a major driver of mRNA diversity and consequently protein diversity, affecting

almost all genes within an organism. The use of alternative promoters or the generation of alternative mRNA species from a single gene locus has been reported widely in almost every biological context, providing extensive mRNA, and thus protein, diversity. In recent years, a novel layer of regulation has been identified mediated by noncoding RNAs. Currently, short and long noncoding RNAs have been implicated modulating RNA expression at distinct biological levels, acting both as cis- and trans-acting factors. Importantly, tissue-specific expression of these short and long noncoding RNAs has been widely reported. In this chapter, we will briefly summarize current state-of-the-art knowledge of general posttranscriptional mechanisms, while major emphases will be devoted to those tissue-specific post-transcriptional modifications that impact on cardiac development and congenital heart disease. While these processes are presented in the following subheadings as discrete events, it is important to highlight the intricate interrelationship between different posttranscriptional regulatory mechanisms.

17.2 mRNA Maturation: Generating Stability and Quality Control

The maturation of mRNA transcripts, from the time they are transcribed in the nucleus until they are exported into the cytoplasm, is accompanied by a series of general structural modifications (Fig. 17.1). A large number of RNA-binding proteins interact with the nascent transcript leading to the addition of modifications at the 5′ and 3′ ends as well along the coding sequence to basically stabilize the transcript and promote splicing whenever required [1, 2]. If impaired processing occurs, the NMD surveillance system is rapidly activated. In particular cases, editing of the nascent RNA transcript also occurs. Over the last years, we have gained much knowledge about the basic regulatory mechanisms orchestrating these events in eukaryotic cells, particularly in *Saccharomyces cerevisiae* and *Saccharomyces pombe*, while our understanding in metazoan cells has lagged behind.

17.2.1 5′ End Capping

Eukaryotic mRNAs are modified by the addition of a 7-methylguanosine “cap” to the first transcribed nucleotide in the nucleus (Fig. 17.1). This modification is necessary for efficient gene expression and cell viability from yeast to humans. The 7-methylguanosine cap is required for transcription elongation, splicing, translation, and general mRNA stability. On the other hand, the 5′ cap seems to be required for polyadenylation and nuclear export of mRNA in *S. cerevisiae* [4], but not in metazoan cells [5, 6]. Several factors have been reported to regulate mRNA cap methylation in yeast [7]. Triphosphatases such as Cet1p and Pct1 direct the hydrolyzation of RNA 5′ triphosphate to a diphosphate-RNA. Guanylyltransferases, such as Ceg1p and Pch1, catalyze the addition of CMP to the diphosphate-RNA to produce the guanosine cap [8], while the methylation of the guanosine cap is

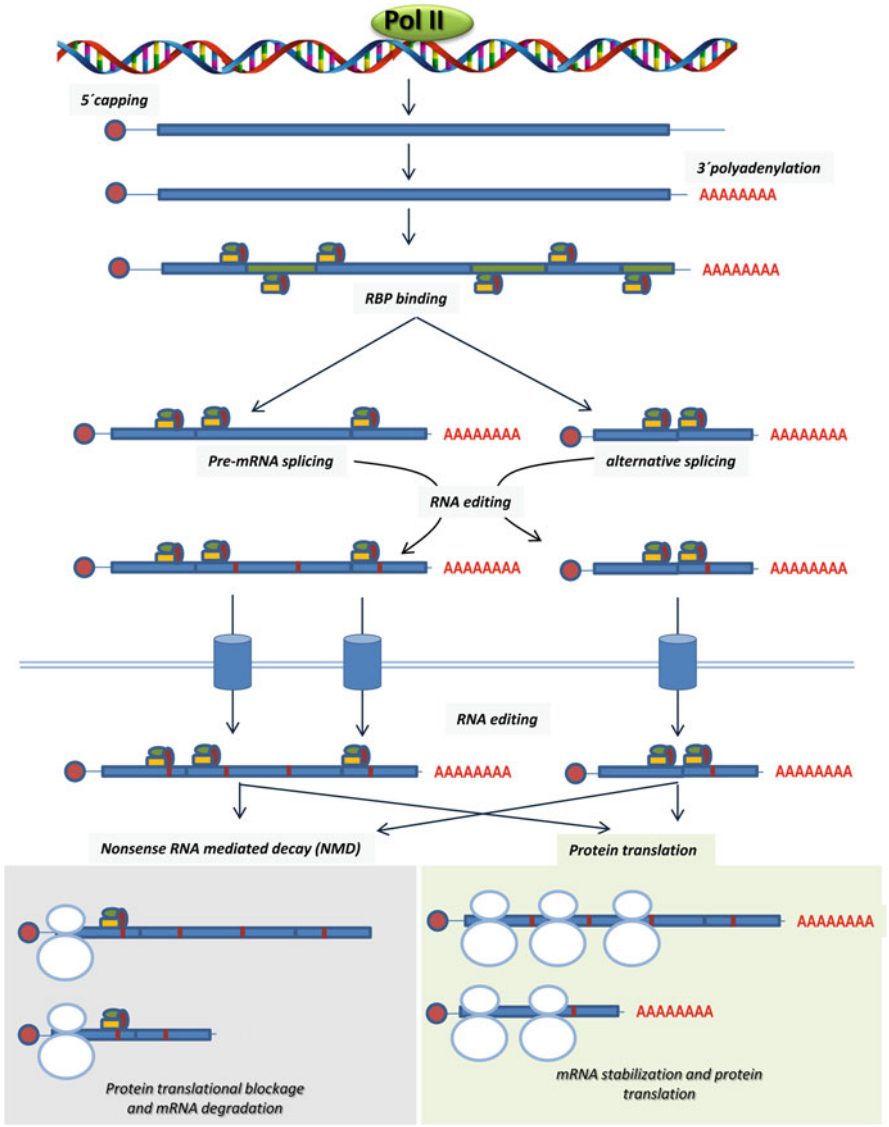

Fig. 17.1 Graphical representation of the distinct posttranscriptional regulatory mechanisms operating during the transcription, splicing, editing, quality control checking, and maturation of mRNA transcripts

mediated by Abd1 and Pcm1. In mammals, the triphosphate and guanylyltransferase activities are found within the same peptide [9, 10], the capping enzyme of RNA guanylyltransferase and 5′ triphosphatase (RNGTT), while the RNA methyltransferase (RNMT) is encoded by a distinct protein [9–13]. Interestingly,

guanylyltransferase and methyltransferase are highly conserved in structure and function from yeast to humans, yet triphosphatases are widely divergent.

mRNA capping and cap methylation occur "co-transcriptionally," that is, the cap methyltransferase is recruited to RNA polymerase II as the RNA is being transcribed, thus providing the means to promote transcription elongation [7]. Pre-RNA splicing is dependent on the 5′ cap since the splicing reaction has been demonstrated to be inhibited by the presence of free 7-methylguanosine [14]. The dependency of splicing on the 5′ cap is mediated by the cap-binding complex, which is a heteromeric complex formed by cap-binding protein (CBP) 80 and CBP20. From yeast to humans, the 5′ cap is necessary for the translation of almost all mRNAs, with the exception of mRNAs translated by an internal ribosome entry site [15]. The presence of a 5′ cap can also protect mRNA from degradation in *X. laevis* [16–18], while in *S. cerevisiae,* inhibition of guanosine capping *in vivo* provoked rapid degradation in some but not all mRNAs, demonstrating the necessity for a guanosine cap to stabilize at a least a subset of mRNAs [4, 7, 19, 20]. Similarly, mRNA polyadenylation and nuclear export appear to be largely independent of the 5′ capping in *S. cerevisiae* [3] but dependent in other species such as *X. laevis* and humans [6, 21]. Thus, while the influence of 5′ capping is pivotal for subsequent mRNA biogenic steps such as transcriptional elongation, pre-mRNA splicing, and translation, species-specific differences seem to occur for degradation protection and mRNA polyadenylation. Given the essential role of 5′ capping in basal mRNA biogenesis, to date no specific defects affecting heart morphogenesis and/or muscle development have been reported.

17.2.2 3′ End Polyadenylation

Polyadenylation is a two-step nuclear process that involves an endonucleolytic cleavage of the pre-mRNA at the 3′-end and the polymerization of a poly-adenosine (polyA) tail (Fig. 17.1), which is fundamental for mRNA stability, nuclear export, and efficient translation during development [22]. The core molecular machinery responsible for the definition of a poly-A site includes several recognition, cleavage, and polyadenylation factors that identify and act on a given poly-A signal present in a pre-mRNA, usually an AAUAAA hexamer [22]. This mechanism is tightly regulated by both cis- and trans-acting factors, and its impairment can cause inefficient gene expression and thus disease. Previous studies have indicated that more than half of the human genes possess multiple polyadenylation sites [23], dubbed APA, which may produce mRNA isoforms with different protein-coding regions or 3′ UTRs of variable length. Interestingly, such a property is also documented in yeast [24]. The differential recognition of polyadenylation signals leads to long or short 3′ UTR of the transcripts. Usage of alternative poly(A) sites influences the fate of mRNAs by altering the availability of RNA-binding protein sites and miRNA binding sites. Abnormalities in the 3′-end processing mechanisms thus represent a common feature among many oncological, immunological, neurological, and hematological disorders [23, 25, 26], and the usage of APA and alterations in

polyadenylation are beginning to be discovered and studied in human diseases [27, 28], including cardiovascular diseases [29].

17.2.3 Nonsense-Mediated Decay

Nonsense-mediated decay (NMD) is an evolutionary conserved surveillance pathway present in all eukaryotes studied to date. NMD plays an important role in the posttranscriptional control of gene expression. Approximately one-third of human genes generate pre-mRNAs that undergo alternative splicing, and similarly one-third of alternatively spliced transcripts are targeted for elimination by the NMD pathway [30]. Most alternatively spliced NMD targets appear to be generated in error [31], yet NMD also downregulates the level of other apparently normal transcripts [32–34]. NMD targets premature translation termination codons (PTC)-containing transcripts for rapid degradation (Fig. 17.1), thus protecting the organism from deleterious gain- or loss-of-function (dominant-negative effects) effects of the resulting truncated proteins [35–37]. As a rule, NMD degrades newly synthesized mRNAs during a pioneer round of translation [38–41] and occurs when a PTC is located more than 50–55 nucleotides upstream of the last exon–exon junction within the mRNA, and at least one intron and components of translation are present [42]. Importantly, there is a growing body of evidence supporting that mRNA decay in eukaryotes requires an exit from translation so that the mRNA is accessible to degradative activities [43–46].

The role of NMD in genetic diseases is emerging progressively. A pivotal role for NMD in cystic fibrosis as well as in Duchenne muscular dystrophy (DMD) has been documented (see for a review [47]) yet has only begun to be recognized in cardiac genetic diseases. Geiger et al. [48] recently reported that insufficient clearance of lamin A/C truncated mutations by NMD underlies the development of dilated cardiomyopathy in a human kindred. Similar findings have also been reported for nonsense mutations in hERG in the context of human long QT syndrome [49–51]. Importantly, an intricate relationship between NMD and the ubiquitin–proteasome system as well as its contribution to mediate myosin binding protein C3 (MYBPC3) premature termination codon mutations [52] has been recently demonstrated in the context of hypertrophic cardiomyopathy [50], opening new ways to understand the complex RNA–protein interphase. In the context of congenital heart diseases, involvement of NMD has been proven for GATA binding protein 6 (*GATA6*) regulation in the setting of ventricular septal defect, patent ductus arteriosus, and congenital diaphragmatic hernia [53] and suspected in a kindred of syndromic patent ductus arteriosus as consequence the generation of aberrant transcription factor AP-2 beta (*TFAP2B*) splice variants [54].

17.3 mRNA Maturation: Generating Diversity (RNA Editing and Pre-mRNA Splicing)

17.3.1 RNA Editing

RNA editing relates to those molecular processes by which the RNA nucleotide sequence is conspicuously modified (Fig. 17.1). To date, such changes have been observed in tRNA, rRNA, and mRNA molecules of eukaryotes, but not prokaryotes. RNA editing can modify an A-to-I (inosine) by the action of adenosine deaminase that acts on RNA (ADAR), and similarly a C-to-U modification can be elicited by a protein complex composed by APOBEC-1 (apolipoprotein B mRNA editing enzyme, catalytic polypeptide 1), an RNA cytidine deaminase, and APOBEC-1 complementation factor (ACF). This C-to-U editing holoenzyme (APOBEC-1/ACF) is also in part regulated by CELF2 [55, 56].

Inosine is an essential modification introduced by specialized enzymes in a highly regulated manner generating thereafter transcriptome diversity. Adenosine to inosine (A-to-I) modification by the ADAR (i.e., ADAR1 and ADAR2) enzymes performs the most common type of RNA editing in metazoans [57], while C-to-U modifications seem to be confined to more discrete transcripts [55, 58–61]. A-to-I RNA editing most frequently targets repetitive RNA sequences located within introns and 5′ and 3′ untranslated regions (UTRs). ADARs use double-stranded RNA as substrates but allow structure interruptions such as bulges and loops. It is well known that these enzymes can use messenger RNA as targets for A-to-I editing and thereby recode the transcript. Both ADAR1 and ADAR2 have been proven to be able to also target short double-stranded RNA molecules, i.e., microRNAs and their precursors. Since the editing activity is found both in the nucleus and the cytoplasm, there are several steps during the microRNA maturation pathway that can be targeted for modification [62]. Although the biological significance of noncoding RNA editing remains largely unknown, several possibilities have been proposed, including its role in the control of endogenous short interfering RNAs [63].

RNA editing involving C-to-U modifications has been reported extensively to play a pivotal role in virus-associated human diseases, including human T lymphotropic virus (HTLV), hepatitis C virus (HCV), hepatitis B virus (HBV), and Epstein–Barr virus (EBV), among others [64, 65]. Furthermore, more recently, a possible role in cancer development has also been proposed [65]. However, to date, no abnormalities in C-to-U RNA editing have been reported in cardiovascular diseases.

A-to-I RNA defective editing has been reported in various human diseases including viral infection susceptibility, cancer, and neurological and psychiatric disorders [66–71]. Involvement of defective RNA editing is recently emerging also in cardiovascular development [72–74]. Moore et al. [73] recently demonstrated that cardiomyocyte-specific deletion of Adar1 in mice resulted in embryonic lethality, due to impaired cardiomyocyte survival and proliferation. Furthermore, the importance of A-to-I RNA editing is also emerging in human embryogenesis, yet only a limited number of events have been thoroughly tested [74]. A-to-I RNA

editing is also relevant in cardiovascular diseases, particularly atherosclerosis [75], blood pressure control [76], and arrhythmogenic right ventricular displasia [77], and emerging evidences are becoming available in congenital heart diseases [78].

17.3.2 Pre-mRNA Splicing and Alternative Splicing

RNA splicing is the molecular process by which introns are deleted from nascent immature mRNA providing the means to successfully link exons back together and thus form a single mature mRNA molecule. RNA splicing is carried out by the assembly of over a hundred core proteins and five small nuclear RNAs into large ribonucleoprotein complexes, named spliceosomes [79]. Regulation of splicing is a complex process [80–82], and alterations of splicing potential have major consequences in distinct human diseases [83].

Alternative splicing is a major driver of protein diversity and allows for the generation of distinct proteins from a single gene. It is estimated that almost 85% of genes within the human genome undergo alternative splicing. Distinct mechanisms such as exon exclusion, intron retention, and the usage of alternative splice sites contribute to modify protein structure, localization, regulation, and function [84, 85]. Interestingly, genetic mutations in distinct spliceosome components have been reported in human families with distinct cardiac diseases such as myocardial infarction [86, 87] and dilated cardiomyopathy [88, 89], suggesting a functional link. Importantly, alternative splicing also plays a pivotal role during embryonic development. Differential expression of distinct spliceosome components has been reported during heart development [90]. Postnatal excitation–contraction coupling impairment has been reported in genetically engineered mice lacking ASF/SF2 spliceosome component [91], and mutant mice for SRp38, a spliceosome regulator, display early embryonic cardiac resulting in impaired calcium handling [92].

On the other hand, alternatively spliced variants have been documented widely in cardiovascular diseases such as cardiomyopathies, arrhythmias, and vascular defects leading to differential expression of sarcomeric proteins, ion channels, and cell signaling proteins [84, 85, 93–99]. An example of the impact of alternative splicing in adult heart physiology is illustrated by the diversity and functional consequences of alternative spliced variants of the troponin–tropomyosin complex (see for a review [100]) and titin [101–104]. Multiple alternatively spliced variants are formed from each of the troponin isoforms as well as from titin, and deregulation of spliced variant expression is linked to dilated cardiomyopathy in different species [101–107]. Similarly, impaired ion channel splice variants also contribute to cardiac arrhythmogenesis, as reported for distinct components of the calcium handling [94, 96, 108, 109] and plasma membrane cardiac pumps [96, 110, 111].

Multiple transcription factors, with critical roles in cardiac development, are alternatively spliced, such as T-box genes [112–114], myocardin [115], myocyte enhancer factor (Mef)-2 [116, 117], pituitary homeobox (Pitx)-2 [118–120], and GATA binding protein 4 (Gata4) [121]. In this context, Yehya et al. [122] identified

an intronic retention variant of the *NFATC1* (nuclear factor of activated T cells, cytoplasmic, calcineurin-dependent 1) gene in patients with ventricular septal defects, suggesting that such a spliced variant might be a VSD-susceptibility gene. More recently, Fardoun et al. [123] described a novel somatic variant of HEY2 that leads to a novel alternative spliced variant linked to ventricular septal defects. Bedard et al. [124] reported spliced variants of *ZIC3* (Zic family member 3) linked to patients with heterotaxy and congenital heart diseases. McCright et al. [125] reported that aberrant Notch2 alternative spliced variants lead to myocardial hypoplasia as well as eye and kidney defects. More recently, Ricci et al. [126] demonstrate that multiple genes were differentially spliced in hypoplastic left heart syndrome, suggesting a deregulation of cell metabolism and cytoskeleton and cell adherence. Interestingly, impaired alternative splicing in other genes also results in cardiac alterations. Impaired fibronectin splicing is associated with thoracic aortic aneurysm in patients with bicuspid aortic valve [127], while abnormal *SCN5A* (sodium channel, voltage gated, type V, alpha subunit) alternative spliced variants lead to fetal arrhythmias [128]. Furthermore, impaired expression of alternatively spliced *NXT2* (nuclear transport factor 2-like export factor 2) variants, a protein involved in nuclear RNA export, has also been proven to affect cardiac development, particularly valve formation [129]. Ver Heyen et al. [130] reported that genetic engineered disruption of *SERCA2a/2b* (sarcoplasmic/endoplasmic reticulum calcium ATPase 2a/b) alternative splicing leads to 20% increase in embryonic and neonatal mortality, as consequence of severe cardiac malformations. Buyon et al. [131] describes a spliced variant of congenital heart block-associated 52 kb autoantigen which is maximal at the time of fetal heart block, suggesting a putative role in its pathophysiology. These reports exemplify the potential causative role of impaired alternative spliced variants as key regulatory modulators of cardiac development. Increasing evidence of this is expected in the coming years as deep-sequencing technologies depict the magnitude of the alternative spliced transcriptome in congenital heart diseases.

17.4 Noncoding RNA-Mediated Posttranscriptional Control

Noncoding RNAs (ncRNAs) constitute a highly diverse group of RNA molecules in structure and function (see for a recent review [132]). Currently, ncRNAs are broadly classified according to their size. Small ncRNAs are generally defined as those that are <200 nucleotides, whereas long noncoding RNAs (lncRNAs) can extend to tens or even hundreds of thousands of nucleotides in length. Small ncRNAs display a rather homogeneous structure, whereas lcnRNAs have more complex secondary structures. ncRNAs, such as ribosomal RNAs (rRNAs) and transfer RNAs (tRNAs), have been extensively studied given their prominent roles as components of the translational machinery. A similar situation occurs with small nuclear RNAs (snRNAs) and small nucleolar RNAs (snoRNAs) given their essential role in splicing. (Fig 17.2) Over the last decade, great interest has arisen in a class of small regulatory ncRNAs that directly affect the expression and/or function of

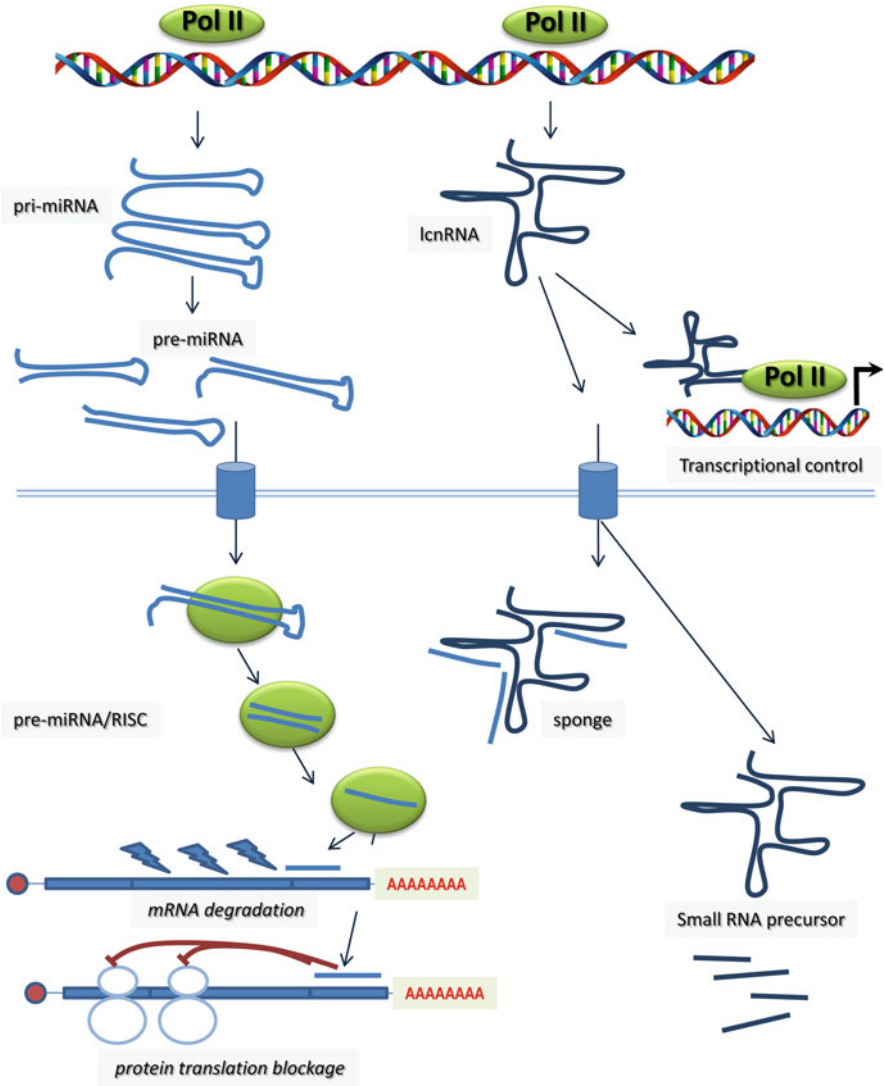

Fig. 17.2 Graphical representation of the microRNAs and long noncoding RNAs (lcnRNA) biosynthetic pathway and their functional roles during transcriptional and posttranscriptional regulation. microRNAs can elicit mRNA degradation and/or protein translation blockage. lncRNAs have been reported to actively contribute to transcriptional regulation and serve as sequestering small RNA system (sponge) or as a template to generate smaller RNA molecules with, to date, poorly characterized functions

protein-coding genes, i.e., microRNAs (miRNAs). miRNAs were discovered in the early 1990s and since then represent the most extensively studied class of ncRNA. microRNAs display an average length of 22–24 nucleotides and are capable of

interacting with the 3′ untranslated region of coding RNAs (mRNAs) eliciting blockage of protein translation and/or mRNA degradation [133]. Understanding of microRNA biogenesis has moved rapidly [134], whereas insights into the functional role of microRNAs are progressively emerging at a slower pace. Nonetheless, the functional relevance of distinct microRNAs in multiple aspects of cardiac development and diseases is now widely documented (see for recent reviews [135–137]).

Differential expression of microRNAs has been documented widely during embryonic [138–141], postnatal [142–144], and the aging heart [145–147] suggesting a pivotal role for microRNAs during different stages of heart development. Similarly, investigators have reported impaired microRNA expression in a large variety of cardiovascular physiopathological conditions, such as hypertrophic and/or dilated cardiomyopathy [148–159], heart failure [155, 160–166], atrial fibrillation [167–174], and aortic aneurism [175–182]. The importance of microRNAs in congenital heart diseases is manifested by the embryonic defects observed in genetically engineered mice. Conditional deletion of Dicer, an endonuclease required for the microRNA processing, with distinct Cre drivers, demonstrated the critical role of microRNA biogenesis in distinct temporal and tissue-specific contexts during cardiovascular development. Conditional ablation using an early cardiogenic deletor mouse strain (*Nkx2-5-Cre* mice) led to embryonic lethality due to cardiac hypoplasia [183], whereas ablation with myocardial-specific Cre driver line *(αMHC-Cre*) resulted in outflow tract defects and impaired chamber formation [184]. More recently, Singh et al. [185] demonstrated that Dicer deletion in pro-epicardial cells compromised cardiac vascular development. In addition, germline deletion of discrete microRNAs such as miR-1-2 resulted in ventricular septal defects and early embryonic lethality [183], whereas miR-126 deletion leads to embryonic lethality due to vascular leakage [186]. These studies highlight the importance of microRNA biology for congenital heart diseases. In this context, an increasing number of studies are providing the impaired microRNA signature of distinct congenital heart diseases [187–194], such as ventricular septal defects [195], tetralogy of Fallot [196–199], corrected transposition of great arteries [200], univentricular left hearts [201], bicuspid aortic valves [202, 203], and DiGeorge syndrome [204]. These studies provide novel insights for the prospective use of microRNA signature as biomarkers of prenatal diagnosis [205–208]. While, in most cases, the impaired regulatory networks modulated by these microRNAs remain to be fully elucidated, there is increasing evidence of the particular role of distinct microRNAs in these settings. Pang et al. [209] reported that miR-592 modulates Notch signaling by upregulating Kctd10 protecting therein from developing hypoplastic heart and thus congenital heart disease in mice, while miR-182 alleviates the development of cyanotic congenital heart by decreasing Hes1 expression [210]. Notch signaling is also modulated by miR-34a, yet their consequences on congenital heart disease remains to be established [211]. In the coming years, we shall see an explosion on the understanding and functional consequences of microRNA regulation, with great hopes as to their therapeutic potential, including pediatric cardiology [159, 207, 208, 212].

In addition to microRNAs, lncRNAs and circular RNAs are also emerging as posttranscriptional modulators. lcnRNAs might undergo alternative splicing and in some cases, but not in others, can be polyadenylated. lncRNAs can not only be located within the nucleus but also can be found within the cytoplasm thus potentially exerting a large number of biological functions. lncRNAs have been reported in a wide range of functions beyond posttranscriptional regulation such as cell cycle progression, differentiation, apoptosis, structural, or cellular trafficking, as well as serving as precursors for smaller RNAs (see for a recent review [132, 213–218]). Differential expression of lncRNAs has been reported in the developing [219–221], adult [222, 223], and aging [224, 225] heart as well as in ventricular cardiac hypertrophy [226, 227], heart failure [228, 229], myocardial infarction [230–234], and cardiac ischemia [231, 235–237]. Interestingly, a pivotal role for distinct lncRNAs has been reported in recent years in the context of cardiac hypertrophy, including Myheart [238–240], Tug1 [241–243], H19 [244–246], Miat [247, 248] among others [249–261] (for a recent review, see [262–264]). Furthermore, their molecular mechanisms are also emerging, such as in the case of Myheart that modulates the miR-145/Klf4/myocardin axis [240] or Tug1 that regulates miR-24/Dkk1/Wnt-beta-catenin [241], miR-29b [242], and miR-497/Mef2c [244] regulating cardiac hypertrophy. Importantly, differentially expression of lcnRNAs has also been reported in hearts with congenital heart defects [265–267], such as ventricular septal defect [268, 269] and tetralogy of Fallot [270–272]. Overall, these data suggest a plausible role for lncRNAs in congenital heart diseases, and the first evidences for this have recently been reported. Seminal works demonstrated that genetic deletion of *Fendrr*, *Braveheart,* and *Upperhand* three cardiac-enriched lncRNAs, respectively, leads to impaired cardiogenesis [273–276]. In recent years, an explosion of studies has focused on dissecting the differential expression profiles of circRNAs in cardiac pathology, such as hypertrophic and dilated cardiomyopathy [277, 278] and heart failure [279], revealing some recent insights on the functional role of circular RNAs, e.g., acting as microRNA sponges [279–287]. However, scarce information is yet available for circRNAs in the context of cardiac development and congenital heart diseases [288, 289]. In the coming years, it is expected that unraveling the functional roles of lcnRNAs and circular RNAs will guide toward the understanding of the etiology of distinct cardiovascular diseases, including that in congenital heart diseases.

17.5 Conclusion

Posttranscriptional regulation is a complex process. This chapter has highlighted distinct processes that sequentially modify the nascent mRNA molecule into a mature form with, in many cases, multiple distinct variants. It is important to emphasize that complex regulatory networks between these processes are well documented such as for the multiple roles of 5′ capping and 3′ polyadenylation in mRNA stabilization, elongation, and translation among others, but importantly emerging evidence demonstrates that microRNAs, lncRNAs, and/or circRNAs

also participate in these intricately interlinked regulatory mechanisms [290], i.e., modulating alternative splicing [291]. Thus, we could foresee that in coming years, impaired posttranscriptional regulatory networks would be linked to distinct congenital heart diseases, as recently reported [292–295] and their molecular mechanisms unraveled.

References

1. Lukong KE, Chang KW, Khandjian EW, et al. RNA-binding proteins in human genetic disease. Trends Genet. 2008;24:416–25.
2. Blech-Hermoni Y, Ladd AN. RNA binding proteins in the regulation of heart development. Int J Biochem Cell Biol. 2013;45:2467–78.
3. Forget A, Chartrand P. Cotranscriptional assembly of mRNP complexes that determine the cytoplasmic fate of mRNA. Transcription. 2011;2:86–90.
4. Fresco LD, Buratowski S. Conditional mutants of the yeast mRNA capping enzyme show that the cap enhances, but is not required for, mRNA splicing. RNA. 1996;2:584–96.
5. Shatkin AJ, Manley JL. The ends of the affair: capping and polyadenylation. Nat Struct Biol. 2000;7:838–42.
6. Glover-Cutter K, Kim S, Espinosa J, et al. RNA polymerase II pauses and associates with pre-mRNA processing factors at both ends of genes. Nat Struct Mol Biol. 2008;15:71–8.
7. Cowling VH. Regulation of mRNA cap methylation. Biochem J. 2009;425:295–302.
8. Suh MH, Meyer PA, Gu M, et al. A dual interface determines the recognition of RNA polymerase II by RNA capping enzyme. J Biol Chem. 2010;285:34027–38.
9. Yue Z, Maldonado E, Pillutla R, et al. Mammalian capping enzyme complements mutant Saccharomyces cerevisiae lacking mRNA guanylyltransferase and selectively binds the elongating form of RNA polymerase II. Proc Natl Acad Sci U S A. 1997;94:12898–903.
10. Tsukamoto T, Shibagaki Y, Niikura Y, et al. Cloning and characterization of three human cDNAs encoding mRNA (guanine-7-)-methyltransferase, an mRNA cap methylase. Biochem Biophys Res Commun. 1998;251:27–34.
11. Yamada-Okabe T, Doi R, Shimmi O, et al. Isolation and characterization of a human cDNA for mRNA 5′-capping enzyme. Nucleic Acids Res. 1998;26:1700–6.
12. Pillutla RC, Shimamoto A, Furuichi Y, et al. Human mRNA capping enzyme (RNGTT) and cap methyltransferase (RNMT) map to 6q16 and 18p11.22-p11.23, respectively. Genomics. 1998;1998(54):351–3.
13. Ishikawa K, Nagase T, Nakajima D, et al. Prediction of the coding sequences of unidentified human genes. VIII. 78 new cDNA clones from brain which code for large proteins in vitro. DNA Res. 1997;4:307–13.
14. Konarska MM, Padgett RA, Sharp PA. Recognition of cap structure in splicing in vitro of mRNA precursors. Cell. 1984;38:731–6.
15. Spriggs KA, Stoneley M, Bushell M, et al. Re-programming of translation following cell stress allows IRES-mediated translation to predominate. Biol Cell. 2008;100:27–38.
16. Furuichi Y, LaFiandra A, Shatkin AJ. 5′-Terminal structure and mRNA stability. Nature. 1977;266:235–9.
17. Shimotohno K, Kodama Y, Hashimoto J, et al. Importance of 5′-terminal blocking structure to stabilize mRNA in eukaryotic protein synthesis. Proc Natl Acad Sci U S A. 1977;74:2734–8.
18. Murthy KG, Park P, Manley JL. A nuclear micrococcal-sensitive, ATP-dependent exoribonuclease degrades uncapped but not capped RNA substrates. Nucleic Acids Res. 1991;19:2685–92.
19. Schwer B, Shuman S. Conditional inactivation of mRNA capping enzyme affects yeast pre-mRNA splicing in vivo. RNA. 1996;2:574–83.

20. Schwer B, Mao X, Shuman S. Accelerated mRNA decay in conditional mutants of yeast mRNA capping enzyme. Nucleic Acids Res. 1998;26:2050–7.
21. Flaherty SM, Fortes P, Izaurralde E, et al. Participation of the nuclear cap binding complex in pre-mRNA 3′ processing. Proc Natl Acad Sci U S A. 1997;94:11893–8.
22. Curinha A, Braz SO, Pereira-Castro I, et al. Implications of polyadenylation in health and disease. Nucleus. 2014;5:508–19.
23. Tian B, Hu J, Zhang H, Lutz CS. A large-scale analysis of mRNA polyadenylation of human and mouse genes. Nucleic Acids Res. 2005;33:201–12.
24. Pelechano V, Wei W, Steinmetz LM. Extensive transcriptional heterogeneity revealed by isoform profiling. Nature. 2013;497:127–31.
25. Carpenter S, Ricci EP, Mercier BC, et al. Post-transcriptional regulation of gene expression in innate immunity. Nat Rev Immunol. 2014;14:361–76.
26. Griseri P, Pagès G. Regulation of the mRNA half-life in breast cancer. World J Clin Oncol. 2014;5:323–34.
27. Chatterjee S, Pal JK. Role of 5′- and 3′-untranslated regions of mRNAs in human diseases. Biol Cell. 2009;101:251–62.
28. Rehfeld A, Plass M, Krogh A, et al. Alterations in polyadenylation and its implications for endocrine disease. Front Endocrinol. 2013;4:53.
29. Zhang Q, He X, Yao S, Lin T, Zhang L, Chen D, Chen C, Yang Q, Li F, Zhu YM, Guan MX. Ablation of Mto1 in zebrafish exhibited hypertrophic cardiomyopathy manifested by mitochondrion RNA maturation deficiency. Nucleic Acids Res. 2021 May 7;49(8):4689–704.
30. Lewis BP, Green RE, Brenner SE. Evidence for the widespread coupling of alternative splicing and nonsense-mediated mRNA decay in humans. Proc Natl Acad Sci U S A. 2003;100:189–92.
31. Pan Q, Saltzman AL, Kim YK, et al. Quantitative microarray profiling provides evidence against widespread coupling of alternative splicing with nonsense-mediated mRNA decay to control gene expression. Genes Dev. 2006;20:153–8.
32. Mendell JT, Sharifi NA, Meyers JL, et al. Nonsense surveillance regulates expression of diverse classes of mammalian transcripts and mutes genomic noise. Nat Genet. 2004;36:1073–8.
33. Wittmann J, Hol EM, Jäck HM. hUPF2 silencing identifies physiologic substrates of mammalian nonsense-mediated mRNA decay. Mol Cell Biol. 2006;26:1272–87.
34. Ni JZ, Grate L, Donohue JP, et al. Ultraconserved elements are associated with homeostatic control of splicing regulators by alternative splicing and nonsense-mediated decay. Genes Dev. 2007;21:708–18.
35. Chang YF, Imam JS, Wilkinson MF. The nonsense-mediated decay RNA surveillance pathway. Annu Rev Biochem. 2007;76:51–74.
36. Maquat LE. Nonsense-mediated mRNA decay in mammals. J Cell Sci. 2005;118:1773–6.
37. Garneau NL, Wilusz J, Wilusz CJ. The highways and byways of mRNA decay. Nat Rev Mol Cell Biol. 2007;8:113–26.
38. Ishigaki Y, Li X, Serin G, Maquat LE. Evidence for a pioneer round of mRNA translation: mRNAs subject to nonsense-mediated decay in mammalian cells are bound by CBP80 and CBP20. Cell. 2001;106:607–17.
39. Lejeune F, Ishigaki Y, Li X, Maquat LE. The exon junction complex is detected on CBP80-bound but not eIF4E-bound mRNA in mammalian cells: dynamics of mRNP remodeling. EMBO J. 2002;21:3536–45.
40. Lejeune F, Ranganathan AC, Maquat LE. eIF4G is required for the pioneer round of translation in mammalian cells. Nat Struct Mol Biol. 2004;11:992–1000.
41. Chiu SY, Lejeune F, Ranganathan AC, et al. The pioneer translation initiation complex is functionally distinct from but structurally overlaps with the steady-state translation initiation complex. Genes Dev. 2004;18:745–54.

42. Zhang J, Sun X, Qian Y, et al. At least one intron is required for the nonsense-mediated decay of triosephosphate isomerase mRNA: a possible link between nuclear splicing and cytoplasmic translation. Mol Cell Biol. 1998;18:5272–83.
43. Coller J, Parker R. Eukaryotic mRNA decapping. Annu Rev Biochem. 2004;73:861–90.
44. Coller J, Parker R. General translational repression by activators of mRNA decapping. Cell. 2005;122:875–86.
45. Ferraiuolo MA, Basak S, Dostie J, et al. A role for the eIF4E-binding protein 4E-T in P-body formation and mRNA decay. Cell Biol. 2005;170:913–24.
46. Braun KA, Young ET. Coupling mRNA synthesis and decay. Mol Cell Biol. 2014;34:4078–87.
47. Linde L, Kerem B. Introducing sense into nonsense in treatments of human genetic diseases. Trends Genet. 2008;24:552–63.
48. Geiger SK, Bar H, Ehlermann P, et al. Incomplete nonsense-mediated decay of mutant lamin A/C mRNA provokes dilated cardiomyopathy and ventricular tachycardia. J Mol Med. 2008;86:281–9.
49. Gong Q, Zhang L, Vincent GM, et al. Nonsense mutations in hERG cause a decrease in mutant mRNA transcripts by nonsense-mediated mRNA decay in human long-QT syndrome. Circulation. 2007;116:17–24.
50. Zarraga IG, Zhang L, Stump MR, et al. Nonsense-mediated mRNA decay caused by a frameshift mutation in a large kindred of type 2 long QT syndrome. Heart Rhythm. 2011;8:1200–6.
51. Gong Q, Zhou Z. Nonsense-Mediated mRNA Decay of hERG Mutations in Long QT Syndrome. Methods Mol Biol. 2018;1684:37–49.
52. Seeger T, Shrestha R, Lam CK, Chen C, McKeithan WL, Lau E, Wnorowski A, McMullen G, Greenhaw M, Lee J, Oikonomopoulos A, Lee S, Yang H, Mercola M, Wheeler M, Ashley EA, Yang F, Karakikes I, Wu JC. A premature termination codon mutation in MYBPC3 causes hypertrophic cardiomyopathy via chronic activation of nonsense-mediated decay. Circulation. 2019 Feb 5;139(6):799–811.
53. Suzuki S, Nakao A, Sarhat AR, et al. A case of pancreatic agenesis and congenital heart defects with a novel GATA6 nonsense mutation: evidence of haploinsufficiency due to nonsense-mediated mRNA decay. Am J Med Genet A. 2014;164A(2):476–9.
54. Mani A, Radhakrishnan J, Farhi A, et al. Syndromic patent ductus arteriosus: evidence for haploinsufficient TFAP2B mutations and identification of a linked sleep disorder. Proc Natl Acad Sci U S A. 2005;102:2975–9.
55. Chen Z, Eggerman TL, Patterson AP. ApoB mRNA editing is mediated by a coordinated modulation of multiple apoB mRNA editing enzyme components. Am J Physiol Gastrointest Liver Physiol. 2007;292:G53–65.
56. Wedekind JE, Dance GS, Sowden MP, et al. Messenger RNA editing in mammals: new members of the APOBEC family seeking roles in the family business. Trends Genet. 2003;19:207–16.
57. Galeano F, Tomaselli S, Locatelli F, et al. A-to-I RNA editing: the "ADAR" side of human cancer. Semin Cell Dev Biol. 2012;23:244–50.
58. Anant S, Henderson J, Mukhopadhyay D, et al. Novel role for RNA-binding protein CUGBP2 in mammalian RNA editing. J Biol Chem. 2001;276:47338–51.
59. Blanc V, Davidson NO. C-to-U RNA editing: mechanisms leading to genetic diversity. J Biol Chem. 2003;278:1395–8.
60. Zhang H. The inhibitory effect of apolipoprotein B mRNA-editing enzyme catalytic polypeptide-like 3G (APOBEC3G) and its family members on the activity of cellular microRNAs. Prog Mol Subcell Biol. 2010;50:71–83.
61. Dasgupta T, Ladd AN. The importance of CELF control: molecular and biological roles of the CUG-BP, Elav-like family of RNA-binding proteins. Wiley Interdiscip Rev RNA. 2012;3:104–21.

62. Ohman M. A-to-I editing challenger or ally to the microRNA process. Biochimie. 2007;89: 1171–6.
63. Nishikura K. Functions and regulation of RNA editing by ADAR deaminases. Annu Rev Biochem. 2010;79:321–49.
64. Franca R, Spadari S, Maga G. APOBEC deaminases as cellular antiviral factors: a novel natural host defense mechanism. Med Sci Monit. 2006;12:RA92–8.
65. Vieira VC, Soares MA. The role of cytidine deaminases on innate immune responses against human viral infections. Biomed Res Int. 2013;2013:683095.
66. van den Hoogen BG, van Boheemen S, de Rijck J, et al. Excessive production and extreme editing of human metapneumovirus defective interfering RNA is associated with type I IFN induction. J Gen Virol. 2014;95:1625–33.
67. Sarvestani ST, Tate MD, Moffat JM, et al. Inosine-mediated modulation of RNA sensing by Toll-like receptor 7 (TLR7) and TLR8. J Virol. 2014;88:799–810.
68. Clerzius G, Shaw E, Daher A, et al. The PKR activator, PACT, becomes a PKR inhibitor during HIV-1 replication. Retrovirology. 2013;10:96.
69. Avesson L, Barry G. The emerging role of RNA and DNA editing in cancer. Biochim Biophys Acta. 2014;1845:308–16.
70. Dominissini D, Moshitch-Moshkovitz S, Amariglio N, et al. Adenosine-to-inosine RNA editing meets cancer. Carcinogenesis. 2011;2011(32):1569–77.
71. Picardi E, Manzari C, Mastropasqua F, Aiello I, D'Erchia AM, Pesole G. Profiling RNA editing in human tissues: towards the inosinome Atlas. Sci Rep. 2015 Oct 9;5:14941.
72. Lichtner P, Attié-Bitach T, Schuffenhauer S, et al. Expression and mutation analysis of *Brunol3*, a candidate gene for heart and thymus developmental defects associated with partial monosomy 10p. J Mol Med. 2002;80:431–42.
73. Moore JB 4th, Sadri G, Fischer AG, Weirick T, Militello G, Wysoczynski M, Gumpert AM, Braun T, Uchida S. The A-to-I RNA editing enzyme *Adar1* is essential for normal embryonic cardiac growth and development. Circ Res. 2020 Jul 31;127(4):550–2.
74. Shtrichman R, Germanguz I, Mandel R, Ziskind A, Nahor I, Safran M, Osenberg S, Sherf O, Rechavi G, Itskovitz-Eldor J. Altered A-to-I RNA editing in human embryogenesis. PLoS One. 2012;7(7):e41576.
75. Uchida S, Jones SP. RNA editing: unexplored opportunities in the cardiovascular system. Circ Res. 2018 Feb 2;122(3):399–401.
76. Jain M, Mann TD, Stulić M, Rao SP, Kirsch A, Pullirsch D, Strobl X, Rath C, Reissig L, Moreth K, Klein-Rodewald T, Bekeredjian R, Gailus-Durner V, Fuchs H, Hrabě de Angelis M, Pablik E, Cimatti L, Martin D, Zinnanti J, Graier WF, Sibilia M, Frank S, Levanon EY, Jantsch MF. RNA editing of Filamin A pre-mRNA regulates vascular contraction and diastolic blood pressure. EMBO J. 2018 Oct 1;37(19):e94813.
77. Li D, Bachinski L, Roberts R. Genomic organization and isoform-specific tissue expression of human NAPOR (CUGBP2) as a candidate gene for familial arrhythmogenic right ventricular dysplasia. Genomics. 2001;74:396–401.
78. Borik S, Simon AJ, Nevo-Caspi Y, Mishali D, Amariglio N, Rechavi G, Paret G. Increased RNA editing in children with cyanotic congenital heart disease. Intensive Care Med. 2011 Oct;37(10):1664–71.
79. Wang Z, Burge CB. Splicing regulation: from a parts list of regulatory elements to an integrated splicing code. RNA. 2008;14:802–13.
80. Burge CB, Tuschl T, Sharp PA. Splicing of precursors to mRNAs by the spliceosomes. In: Gesteland RF, et al., editors. The RNA world. Cold Spring Harbor: Cold Spring Harbor Press; 1999. p. 525–60.
81. Hastings ML, Krainer AR. Pre-mRNA splicing in the new millennium. Curr Opin Cell Biol. 2001;13:302–9.
82. Black DL. Mechanisms of alternative pre-messenger RNA splicing. Annu Rev Biochem. 2003;72:291–336.

83. Nissim-Rafinia M, Kerem B. Splicing regulation as a potential genetic modifier. Trends Genet. 2002;18:123–7.
84. Han J, Xiong J, Wang D, et al. Pre-mRNA splicing: where and when in the nucleus. Trends Cell Biol. 2011;21:336–43.
85. Lara-Pezzi E, Gómez-Salinero J, Gatto A, García-Pavía P. The alternative heart: impact of alternative splicing in heart disease. J Cardiovasc Transl Res. 2013;6:945–55.
86. Ria M, Eriksson P, Boquist S, et al. Human genetic evidence that OX40 is implicated in myocardial infarction. Biochem Biophys Res Commun. 2006;339:1001–6.
87. Maatz H, Jens M, Liss M, et al. RNA-binding protein RBM20 represses splicing to orchestrate cardiac pre-mRNA processing. J Clin Invest. 2014;124:3419–30.
88. Brauch KM, Karst ML, Herron KJ, et al. Mutations in ribonucleic acid binding protein gene cause familial dilated cardiomyopathy. J Am Coll Cardiol. 2009;54:930–41.
89. Rimessi P, Fabris M, Bovolenta M, et al. Antisense modulation of both exonic and intronic splicing motifs induces skipping of a DMD pseudo-exon responsible for x-linked dilated cardiomyopathy. Hum Gene Ther. 2010;21:1137–46.
90. Ruiz-Lozano P, Doevendans P, Brown A, et al. Developmental expression of the murine spliceosome-associated protein mSAP49. Dev Dyn. 1997;208:482–90.
91. Xu X, Yang D, Ding JH, et al. ASF/SF2-regulated CaMKIIdelta alternative splicing temporally reprograms excitation-contraction coupling in cardiac muscle. Cell. 2005;120:59–72.
92. Feng Y, Valley MT, Lazar J, et al. SRp38 regulates alternative splicing and is required for Ca (2+) handling in the embryonic heart. Dev Cell. 2009;16:528–38.
93. Dally S, Corvazier E, Bredoux R, et al. Multiple and diverse coexpression, location, and regulation of additional SERCA2 and SERCA3 isoforms in nonfailing and failing human heart. J Mol Cell Cardiol. 2010;48:633–44.
94. Schroeter A, Walzik S, Blechschmidt S, et al. Structure and function of splice variants of the cardiac voltage-gated sodium channel Na(v)1.5. J Mol Cell Cardiol. 2010;49:16–24.
95. Valadkhan S, Jaladat Y. The spliceosomal proteome: at the heart of the largest cellular ribonucleoprotein machine. Proteomics. 2010;10:4128–41.
96. Zhang SS, Shaw RM. Multilayered regulation of cardiac ion channels. Biochim Biophys Acta. 2013;1833:876–85.
97. Kjellqvist S, Maleki S, Olsson T, et al. A combined proteomic and transcriptomic approach shows diverging molecular mechanisms in thoracic aortic aneurysm development in patients with tricuspid- and bicuspid aortic valve. Mol Cell Proteomics. 2013;12:407–25.
98. Murata K, Lu W, Hashimoto M, Ono N, Muratani M, Nishikata K, Kim JD, Ebihara S, Ishida J, Fukamizu A. PRMT1 deficiency in mouse juvenile heart induces dilated cardiomyopathy and reveals cryptic alternative splicing products. iScience. 2018 Oct 26;8:200–13.
99. Zahr HC, Jaalouk DE. Exploring the crosstalk between *LMNA* and splicing machinery gene mutations in dilated cardiomyopathy. Front Genet. 2018 Jul 9;9:231.
100. Sheng JJ, Jin JP. Gene regulation, alternative splicing, and posttranslational modification of troponin subunits in cardiac development and adaptation: a focused review. Front Physiol. 2014;5:165.
101. Gi WT, Haas J, Sedaghat-Hamedani F, Kayvanpour E, Tappu R, Shirvani LDH, Samani O, Wisdom M, Keller A, Katus HA, Meder B. Epigenetic regulatio of alternative mRNA splicing in dilated cardiomyopathy. J Clin Med. 2020 Mar 16;9(5):1499.
102. Liu J, Kong X, Zhang M, Yang X, Xu X. RNA binding protein 24 deletion disrupts global alternative splicing and causes dilated cardiomyopathy. Protein Cell. 2019 Jun;10(6):405–16.
103. Watanabe T, Kimura A, Kuroyanagi H. Alternative Splicing Regulator RBM20 and Cardiomyopathy. Front Mol Biosci. 2018 Nov 28;5:105.
104. Boeckel JN, Möbius-Winkler M, Müller M, Rebs S, Eger N, Schoppe L, Tappu R, Kokot KE, Kneuer JM, Gaul S, Bordalo DM, Lai A, Haas J, Ghanbari M, Drewe-Boss P, Liss M, Katus HA, Ohler U, Gotthardt M, Laufs U, Streckfuss-Bömeke K, Meder B. SLM2 is a novel cardiac splicing factor involved in heart failure due to dilated cardiomyopathy. Genomics Proteomics Bioinformatics. 2021 Jul 14;20(1):129–46.

105. Biesiadecki BJ, Elder BD, Yu ZB, Jin JP. Cardiac troponin T variants produced by aberrant splicing of multiple exons in animals with high instances of dilated cardiomyopathy. J Biol Chem. 2002;277:50275–85.
106. Biesiadecki BJ, Jin JP. Exon skipping in cardiac troponin T of turkeys with inherited dilated cardiomyopathy. J Biol Chem. 2002;277:18459–68.
107. Wei B, Gao J, Huang XP, Jin JP. Mutual rescues between two dominant negative mutations in cardiac troponin I and cardiac troponin T. J Biol Chem. 2010;285:27806–16.
108. Duran J, Nickel L, Estrada M, Backs J, van den Hoogenhof MMG. CaMKIIδ splice variants in the healthy and diseased heart. Front Cell Dev Biol. 2021 Mar 11;9:644630.
109. van den Hoogenhof MMG, Beqqali A, Amin AS, van der Made I, Aufiero S, Khan MAF, Schumacher CA, Jansweijer JA, van Spaendonck-Zwarts KY, Remme CA, Backs J, Verkerk AO, Baartscheer A, Pinto YM, Creemers EE. RBM20 mutations induce an arrhythmogenic dilated cardiomyopathy related to disturbed calcium handling. Circulation. 2018 Sep 25;138 (13):1330–42.
110. Pang PD, Alsina KM, Cao S, Koushik AB, Wehrens XHT, Cooper TA. CRISPR-mediated expression of the fetal Scn5a isoform in adult mice causes conduction defects and arrhythmias. J Am Heart Assoc. 2018 Oct 2;7(19):e010393.
111. Freyermuth F, Rau F, Kokunai Y, Linke T, Sellier C, Nakamori M, Kino Y, Arandel L, Jollet A, Thibault C, Philipps M, Vicaire S, Jost B, Udd B, Day JW, Duboc D, Wahbi K, Matsumura T, Fujimura H, Mochizuki H, Deryckere F, Kimura T, Nukina N, Ishiura S, Lacroix V, Campan-Fournier A, Navratil V, Chautard E, Auboeuf D, Horie M, Imoto K, Lee KY, Swanson MS, de Munain AL, Inada S, Itoh H, Nakazawa K, Ashihara T, Wang E, Zimmer T, Furling D, Takahashi MP, Charlet-Berguerand N. Splicing misregulation of SCN5A contributes to cardiac-conduction delay and heart arrhythmia in myotonic dystrophy. Nat Commun. 2016 Apr 11;7:11067.
112. Hoogaars WM, Barnett P, Rodriguez M, et al. TBX3 and its splice variant TBX3 + exon 2a are functionally similar. Pigment Cell Melanoma Res. 2008;21:379–87.
113. Georges R, Nemer G, Morin M, et al. Distinct expression and function of alternatively spliced Tbx5 isoforms in cell growth and differentiation. Mol Cell Biol. 2008;28:4052–67.
114. DeBenedittis P, Jiao K. Alternative splicing of T-box transcription factor genes. Biochem Biophys Res Commun. 2011;412:513–7.
115. Ueyama T, Kasahara H, Ishiwata T, et al. Myocardin expression is regulated by Nkx2.5, and its function is required for cardiomyogenesis. Mol Cell Biol. 2003;23:9222–32.
116. Iida K, Hidaka K, Takeuchi M, et al. Expression of MEF2 genes during human cardiac development. Tohoku J Exp Med. 1999;187:15–23.
117. Zhu B, Gulick T. Phosphorylation and alternative pre-mRNA splicing converge to regulate myocyte enhancer factor 2C activity. Mol Cell Biol. 2004;24:8264–75.
118. Schweickert A, Campione M, Steinbeisser H, et al. Pitx2 isoforms: involvement of Pitx2c but not Pitx2a or Pitx2b in vertebrate left-right asymmetry. Mech Dev. 2000;90:41–51.
119. Yu X, St Amand TR, Wang S, et al. Differential expression and functional analysis of Pitx2 isoforms in regulation of heart looping in the chick. Development. 2001;128:1005–13.
120. Lamba P, Hjalt TA, Bernard DJ. Novel forms of Paired-like homeodomain transcription factor 2 (PITX2): generation by alternative translation initiation and mRNA splicing. BMC Mol Biol. 2008;9:31.
121. Mazaud Guittot S, Bouchard MF, Robert-Grenon JP, et al. Conserved usage of alternative 5′ untranslated exons of the GATA4 gene. PLoS One. 2009;4(12):e8454.
122. Yehya A, Souki R, Bitar F, et al. Differential duplication of an intronic region in the NFATC1 gene in patients with congenital heart disease. Genome. 2006;49:1092–8.
123. Fardoun M, Dehaini H, Kamar A, Bitar F, Majdalani M, El-Rassi I, Nemer G, Arabi M. A novel somatic variant in HEY2 unveils an alternative splicing isoform linked to ventricular septal defect. Pediatr Cardiol. 2019 Jun;40(5):1084–91.

124. Bedard JE, Haaning AM, Ware SM. Identification of a novel ZIC3 isoform and mutation screening in patients with heterotaxy and congenital heart disease. PLoS One. 2011;6(8): e23755.
125. McCright B, Gao X, Shen L, et al. Defects in development of the kidney, heart and eye vasculature in mice homozygous for a hypomorphic Notch2 mutation. Development. 2001;128:491–502.
126. Ricci M, Xu Y, Hammond HL, et al. Myocardial alternative RNA splicing and gene expression profiling in early stage hypoplastic left heart syndrome. PLoS One. 2012;7(1):e29784.
127. Paloschi V, Kurtovic S, Folkersen L, et al. Impaired splicing of fibronectin is associated with thoracic aortic aneurysm formation in patients with bicuspid aortic valve. Arterioscler Thromb Vasc Biol. 2011;31:691–7.
128. Murphy LL, Moon-Grady AJ, Cuneo BF, et al. Developmentally regulated SCN5A splice variant potentiates dysfunction of a novel mutation associated with severe fetal arrhythmia. Heart Rhythm. 2012;9:590–7.
129. Ver Heyen M, Heymans S, Antoons G, et al. Replacement of the muscle-specific sarcoplasmic reticulum Ca(2+)-ATPase isoform SERCA2a by the nonmuscle SERCA2b homologue causes mild concentric hypertrophy and impairs contraction-relaxation of the heart. Circ Res. 2001;89:838–46.
130. Huang H, Zhang B, Hartenstein PA, et al. NXT2 is required for embryonic heart development in zebrafish. BMC Dev Biol. 2005;5:7.
131. Buyon JP, Tseng CE, Di Donato F, et al. Cardiac expression of 52beta, an alternative transcript of the congenital heart block-associated 52-kd SS-A/Ro autoantigen, is maximal during fetal development. Arthritis Rheum. 1997;40:655–60.
132. Schonrock N, Harvey RP, Mattick JS. Long noncoding RNAs in cardiac development and pathophysiology. Circ Res. 2012;111:1349–62.
133. Bartel DP. MicroRNAs: genomics, biogenesis, mechanism, and function. Cell. 2004;116:281–97.
134. Bauersachs J, Thum T. Biogenesis and regulation of cardiovascular microRNAs. Circ Res. 2011;109(3):334–47.
135. Espinoza-Lewis RA, Wang DZ. MicroRNAs in heart development. Curr Top Dev Biol. 2012;100:279–317.
136. Chen J, Wang DZ. microRNAs in cardiovascular development. J Mol Cell Cardiol. 2012;52: 949–57.
137. Bonet F, Hernandez-Torres F, Franco D. Towards the therapeutic usage of microRNAs in cardiac disease and regeneration. Exp Clin Cardiol. 2014;20:720–56.
138. Chinchilla A, Lozano E, Daimi H, et al. MicroRNA profiling during mouse ventricular maturation: a role for miR-27 modulating Mef2c expression. Cardiovasc Res. 2011;89:98–108.
139. Vacchi-Suzzi C, Hahne F, Scheubel P, et al. Heart structure-specific transcriptomic atlas reveals conserved microRNA-mRNA interactions. PLoS One. 2013;8:e52442.
140. Saxena S, Mathur P, Shukla V, Rani V. Differential expression of novel MicroRNAs from developing fetal heart of Gallus gallus domesticus implies a role in cardiac development. Mol Cell Biochem. 2019 Dec;462(1–2):157–65.
141. Poon EN, Hao B, Guan D, Jun Li M, Lu J, Yang Y, Wu B, Wu SC, Webb SE, Liang Y, Miller AL, Yao X, Wang J, Yan B, Boheler KR. Integrated transcriptomic and regulatory network analyses identify microRNA-200c as a novel repressor of human pluripotent stem cell-derived cardiomyocyte differentiation and maturation. Cardiovasc Res. 2018 May 1;114(6):894–906.
142. Porrello ER, Mahmoud AI, Simpson E, et al. Regulation of neonatal and adult mammalian heart regeneration by the miR-15 family. Proc Natl Acad Sci U S A. 2013;110:187–92.
143. Hsu J, Hanna P, Van Wagoner DR, et al. Whole genome expression differences in human left and right atria ascertained by RNA sequencing. Circ Cardiovasc Genet. 2012;5:327–35.
144. Raso A, Dirkx E, Sampaio-Pinto V, El Azzouzi H, Cubero RJ, Sorensen DW, Ottaviani L, Olieslagers S, Huibers MM, de Weger R, Siddiqi S, Moimas S, Torrini C, Zentillin L, Braga L,

Nascimento DS, da Costa Martins PA, van Berlo JH, Zacchigna S, Giacca M, De Windt LJ. A microRNA program regulates the balance between cardiomyocyte hyperplasia and hypertrophy and stimulates cardiac regeneration. Nat Commun. 2021 Aug 10;12(1):4808.
145. Boon RA, Iekushi K, Lechner S, et al. MicroRNA-34a regulates cardiac ageing and function. Nature. 2013;495:107–10.
146. Dimmeler S, Nicotera P. MicroRNAs in age-related diseases. EMBO Mol Med. 2013;5(2): 180–90.
147. Wang J, Zhang J, Ding X, Wang Y, Li Z, Zhao W, Jia J, Zhou J, Ge J. Differential microRNA expression profiles and bioinformatics analysis between young and aging spontaneously hypertensive rats. Int J Mol Med. 2018 Mar;41(3):1584–94.
148. van Rooij E, Sutherland LB, Liu N, et al. A signature pattern of stress-responsive microRNAs that can evoke cardiac hypertrophy and heart failure. Proc Natl Acad Sci U S A. 2006;103: 18255–60.
149. Care A, Catalucci D, Felicetti F, et al. MicroRNA-133 controls cardiac hypertrophy. Nat Med. 2007;13:613–8.
150. Sayed D, Hong C, Chen IY, et al. MicroRNAs play an essential role in the development of cardiac hypertrophy. Circ Res. 2007;100:416–24.
151. Fernandes T, Hashimoto NY, Magalhães FC, et al. Aerobic exercise training-induced left ventricular hypertrophy involves regulatory microRNAs, decreased angiotensin-converting enzyme-angiotensin ii, and synergistic regulation of angiotensin-converting enzyme 2-angiotensin. Hypertension. 2011;58:182–9.
152. Yang KC, Ku YC, Lovett M, Nerbonne JM. Combined deep microRNA and mRNA sequencing identifies protective transcriptomal signature of enhanced PI3Kα signaling in cardiac hypertrophy. J Mol Cell Cardiol. 2012;53:101–12.
153. Reddy S, Zhao M, Hu DQ, et al. Dynamic microRNA expression during the transition from right ventricular hypertrophy to failure. Physiol Genomics. 2012;44:562–75.
154. Shi H, Li J, Song Q, Cheng L, Sun H, Fan W, Li J, Wang Z, Zhang G. Systematic identification and analysis of dysregulated miRNA and transcription factor feed-forward loops in hypertrophic cardiomyopathy. J Cell Mol Med. 2019 Jan;23(1):306–16.
155. Shao X, Zhang X, Yang L, Zhang R, Zhu R, Feng R. Integrated analysis of mRNA and microRNA expression profiles reveals differential transcriptome signature in ischaemic and dilated cardiomyopathy induced heart failure. Epigenetics. 2021 Aug;16(8):917–32.
156. Zaragoza C, Saura M, Hernández I, Ramirez-Carracedo R, García-García F, Zamorano JL, Mangas A, Toro R. Differential expression of circulating miRNAs as a novel tool to assess BAG3-associated familial dilated cardiomyopathy. Biosci Rep. 2019 Mar 15;39(3): BSR20180934.
157. Calderon-Dominguez M, Belmonte T, Quezada-Feijoo M, Ramos M, Calderon-Dominguez J, Campuzano O, Mangas A, Toro R. Plasma microrna expression profile for reduced ejection fraction in dilated cardiomyopathy. Sci Rep. 2021 Apr 6;11(1):7517.
158. Huang K, Wen S, Huang J, Wang F, Pang L, Wang Y, Sun X. Integrated analysis of hub genes and miRNAs in dilated cardiomyopathy. Biomed Res Int. 2020 Sep 15;2020:8925420.
159. Hailu FT, Karimpour-Fard A, Toni LS, Bristow MR, Miyamoto SD, Stauffer BL, Sucharov CC. Integrated analysis of miRNA-mRNA interaction in pediatric dilated cardiomyopathy. Pediatr Res. 2022 Jul;92(1):98–108.
160. van Rooij E, Sutherland LB, Thatcher JE, et al. Dysregulation of microRNAs after myocardial infarction reveals a role of miR-29 in cardiac fibrosis. Proc Natl Acad Sci U S A. 2008;105: 13027–32.
161. Drake JI, Bogaard HJ, Mizuno S, et al. Molecular signature of a right heart failure program in chronic severe pulmonary hypertension. Am J Respir Cell Mol Biol. 2011;45(6):1239–47.
162. Yang KC, Yamada KA, Patel AY, et al. Deep RNA sequencing reveals dynamic regulation of myocardial noncoding RNAs in failing human heart and remodeling with mechanical circulatory support. Circulation. 2014;129:1009–21.

163. Meiri E, Volinsky N, Dromi N, Kredo-Russo S, Benjamin H, Tabak S, Marmor H, Motin M, Lebanony D, Lithwick-Yanai G, Kadosh E, Kreader C, Grosman-Rimon L, Amir O. Differential expression of microRNA in serum fractions and association of Argonaute 1 microRNAs with heart failure. J Cell Mol Med. 2020 Jun;24(12):6586–95.
164. D'Alessandra Y, Chiesa M, Carena MC, Beltrami AP, Rizzo P, Buzzetti M, Ricci V, Ferrari R, Fucili A, Livi U, Aleksova A, Pompilio G, Colombo GI. Differential role of circulating microRNAs to track progression and pre-symptomatic stage of chronic heart failure: a pilot study. Biomedicines. 2020 Dec 11;8(12):597.
165. Chen F, Yang J, Li Y, Wang H. Circulating microRNAs as novel biomarkers for heart failure. Hellenic J Cardiol. 2018 Jul–Aug;59(4):209–14.
166. Witvrouwen I, Gevaert AB, Possemiers N, Beckers PJ, Vorlat A, Heidbuchel H, Van Laere SJ, Van Craenenbroeck AH, Van Craenenbroeck EM. Circulating microRNA as predictors for exercise response in heart failure with reduced ejection fraction. Eur J Prev Cardiol. 2021 Dec 29;28(15):1673–81.
167. Lu Y, Zhang Y, Wang N, et al. MicroRNA-328 contributes to adverse electrical remodeling in atrial fibrillation. Circulation. 2010;122:2378–87.
168. Xiao J, Liang D, Zhang Y, et al. MicroRNA expression signature in atrial fibrillation with mitral stenosis. Physiol Genomics. 2011;43:655–64.
169. Cooley N, Cowley MJ, Lin RC, et al. Influence of atrial fibrillation on microRNA expression profiles in left and right atria from patients with valvular heart disease. Physiol Genomics. 2012;44:211–9.
170. Liu Z, Zhou C, Liu Y, et al. The expression levels of plasma microRNAs in atrial fibrillation patients. PLoS One. 2012;7(9):e44906.
171. Nishi H, Sakaguchi T, Miyagawa S, et al. Impact of microRNA expression in human atrial tissue in patients with atrial fibrillation undergoing cardiac surgery. PLoS One. 2013;8: e73397.
172. Wei Z, Bing Z, Shaohuan Q, Yanran W, Shuo S, Bi T, Feiyu Z, Heng Z, Qin G, Pinfang K. Expression of miRNAs in plasma exosomes derived from patients with atrial fibrillation. Clin Cardiol. 2020 Dec;43(12):1450–9.
173. Yan Y, Shi R, Yu X, Sun C, Zang W, Tian H. Identification of atrial fibrillation-associated microRNAs in left and right atria of rheumatic mitral valve disease patients. Genes Genet Syst. 2019 Apr 9;94(1):23–34.
174. Zhu P, Li H, Zhang A, Li Z, Zhang Y, Ren M, Zhang Y, Hou Y. MicroRNAs sequencing of plasma exosomes derived from patients with atrial fibrillation: miR-124-3p promotes cardiac fibroblast activation and proliferation by regulating AXIN1. J Physiol Biochem. 2022 Feb;78 (1):85–98.
175. Liu G, Huang Y, Lu X, et al. Identification and characteristics of microRNAs with altered expression patterns in a rat model of abdominal aortic aneurysms. Tohoku J Exp Med. 2010;222:187–93.
176. Lareyre F, Clément M, Moratal C, Loyer X, Jean-Baptiste E, Hassen-Khodja R, Chinetti G, Mallat Z, Raffort J. Differential micro-RNA expression in diabetic patients with abdominal aortic aneurysm. Biochimie. 2019 Jul;162:1–7.
177. Zalewski DP, Ruszel KP, Stępniewski A, Gałkowski D, Bogucki J, Komsta Ł, Kołodziej P, Chmiel P, Zubilewicz T, Feldo M, Kocki J, Bogucka-Kocka A. Dysregulation of microRNA modulatory network in abdominal aortic aneurysm. J Clin Med. 2020 Jun 24;9(6):1974.
178. Yang P, Cai Z, Wu K, Hu Y, Liu L, Liao M. Identification of key microRNAs and genes associated with abdominal aortic aneurysm based on the gene expression profile. Exp Physiol. 2020 Jan;105(1):160–73.
179. Ji J, Xu Q, He X, Chen XL, Yang J. MicroRNA microarray analysis to detect biomarkers of aortic dissection from paraffin-embedded tissue samples. Interact Cardiovasc Thorac Surg. 2020 Aug 1;31(2):239–47.
180. Torres-Do Rego A, Barrientos M, Ortega-Hernández A, Modrego J, Gómez-Gordo R, Álvarez-Sala LA, Cachofeiro V, Gómez-Garre D. Identification of a plasma microRNA

signature as biomarker of subaneurysmal aortic dilation in patients with high cardiovascular risk. J Clin Med. 2020 Aug 28;9(9):2783.
181. Su Y, Li Q, Zheng Z, Wei X, Hou P. Integrative bioinformatics analysis of miRNA and mRNA expression profiles and identification of associated miRNA-mRNA network in aortic dissection. Medicine (Baltimore). 2019 Jun;98(24):e16013.
182. Tian L, Hu X, He Y, Wu Z, Li D, Zhang H. Construction of lncRNA-miRNA-mRNA networks reveals functional lncRNAs in abdominal aortic aneurysm. Exp Ther Med. 2018 Nov;16(5):3978–86.
183. Zhao Y, Ransom JF, Li A, et al. Dysregulation of cardiogenesis, cardiac conduction, and cell cycle in mice lacking miRNA-1-2. Cell. 2007;129:303–17.
184. Saxena A, Tabin CJ. miRNA-processing enzyme Dicer is necessary for cardiac outflow tract alignment and chamber septation. Proc Natl Acad Sci U S A. 2010;107:87–91.
185. Singh MK, Lu MM, Massera D, et al. MicroRNA-processing enzyme Dicer is required in epicardium for coronary vasculature development. J Biol Chem. 2011;286:41036–45.
186. Fish JE, Santoro MM, Morton SU, et al. miR-126 regulates angiogenic signaling and vascular integrity. Dev Cell. 2008;15:272–84.
187. Xing HJ, Li YJ, Ma QM, et al. Identification of microRNAs present in congenital heart disease associated copy number variants. Eur Rev Med Pharmacol Sci. 2013;17(15):2114–20.
188. Nagy O, Baráth S, Ujfalusi A. The role of microRNAs in congenital heart disease. EJIFCC. 2019 Jun 24;30(2):165–78.
189. Dueñas A, Expósito A, Aranega A, Franco D. The role of non-coding RNA in congenital heart diseases. J Cardiovasc Dev Dis. 2019 Apr 1;6(2):15.
190. Pulignani S, Andreassi MG. MicroRNAs and Congenital Heart Disease: Where Are We Now? Rev Esp Cardiol (Engl Ed). 2019 Jan;72(1):7–9.
191. Zloto K, Tirosh-Wagner T, Bolkier Y, Bar-Yosef O, Vardi A, Mishali D, Paret G, Nevo-Caspi Y. Preoperative miRNA-208a as a predictor of postoperative complications in children with congenital heart disease undergoing heart surgery. J Cardiovasc Transl Res. 2020 Apr;13(2):245–52.
192. Zhang YZ, Li G, Yan DL, Liu YL. MicroRNA-98 can serve as a diagnostic marker for congenital heart disease-associated pulmonary artery hypertension. Chin Med J (Engl). 2020 Nov 5;133(24):3007–9.
193. Song Y, Higgins H, Guo J, Harrison K, Schultz EN, Hales BJ, Moses EK, Goldblatt J, Pachter N, Zhang G. Clinical significance of circulating microRNAs as markers in detecting and predicting congenital heart defects in children. J Transl Med. 2018 Feb 27;16(1):42.
194. Gu H, Chen L, Xue J, Huang T, Wei X, Liu D, Ma W, Cao S, Yuan Z. Expression profile of maternal circulating microRNAs as non-invasive biomarkers for prenatal diagnosis of congenital heart defects. Biomed Pharmacother. 2019 Jan;109:823–30.
195. Li D, Ji L, Liu L, et al. Characterization of circulating microRNA expression in patients with a ventricular septal defect. PLoS One. 2014;9:e106318.
196. Zhang J, Chang JJ, Xu F, et al. MicroRNA deregulation in right ventricular outflow tract myocardium in nonsyndromic tetralogy of fallot. Can J Cardiol. 2013;29:1695–703.
197. You G, Zu B, Wang B, Fu Q, Li F. Identification of miRNA-mRNA-TFs Regulatory Network and Crucial Pathways Involved in Tetralogy of Fallot. Front Genet. 2020 Jun;12(11):552.
198. Abu-Halima M, Meese E, Keller A, Abdul-Khaliq H, Rädle-Hurst T. Analysis of circulating microRNAs in patients with repaired Tetralogy of Fallot with and without heart failure. J Transl Med. 2017 Jul 10;15(1):156.
199. Zhang J, Chang JJ, Xu F, Ma XJ, Wu Y, Li WC, Wang HJ, Huang GY, Ma D. MicroRNA deregulation in right ventricular outflow tract myocardium in nonsyndromic tetralogy of fallot. Can J Cardiol. 2013 Dec;29(12):1695–703.
200. Lai CT, Ng EK, Chow PC, et al. Circulating microRNA expression profile and systemic right ventricular function in adults after atrial switch operation for complete transposition of the great arteries. BMC Cardiovasc Disord. 2013;13:73.

201. Yu ZB, Han SP, Bai YF, et al. microRNA expression profiling in fetal single ventricle malformation identified by deep sequencing. Int J Mol Med. 2012;29:53–60.
202. Nigam V, Sievers HH, Jensen BC, et al. Altered microRNAs in bicuspid aortic valve: a comparison between stenotic and insufficient valves. J Heart Valve Dis. 2010;19:459–65.
203. Sabatino J, Wicik Z, De Rosa S, Eyileten C, Jakubik D, Spaccarotella C, Mongiardo A, Postula M, Indolfi C. MicroRNAs fingerprint of bicuspid aortic valve. J Mol Cell Cardiol. 2019 Sep;134:98–106.
204. de la Morena MT, Eitson JL, Dozmorov IM, et al. Signature MicroRNA expression patterns identified in humans with 22q11.2 deletion/DiGeorge syndrome. Clin Immunol. 2013;147:11–22.
205. Zhu S, Cao L, Zhu J, et al. Identification of maternal serum microRNAs as novel non-invasive biomarkers for prenatal detection of fetal congenital heart defects. Clin Chim Acta. 2013;424:66–72.
206. Yu Z, Han S, Hu P, et al. Potential role of maternal serum microRNAs as a biomarker for fetal congenital heart defects. Med Hypotheses. 2011;76:424–6.
207. Paul S, Ruiz-Manriquez LM, Ledesma-Pacheco SJ, Benavides-Aguilar JA, Torres-Copado A, Morales-Rodríguez JI, De Donato M, Srivastava A. Roles of microRNAs in chronic pediatric diseases and their use as potential biomarkers: a review. Arch Biochem Biophys. 2021 Mar 15;699:108763.
208. Toni LS, Hailu F, Sucharov CC. Dysregulated micro-RNAs and long noncoding RNAs in cardiac development and pediatric heart failure. Am J Physiol Heart Circ Physiol. 2020 May 1;318(5):H1308–15.
209. Pang XF, Lin X, Du JJ, Zeng DY. Downregulation of microRNA-592 protects mice from hypoplastic heart and congenital heart disease by inhibition of the Notch signaling pathway through upregulating KCTD10. J Cell Physiol. 2019 May;234(5):6033–41.
210. Zhang Y, Peng B, Han Y. MiR-182 alleviates the development of cyanotic congenital heart disease by suppressing HES1. Eur J Pharmacol. 2018 Oct 5;836:18–24.
211. Wu KH, Xiao QR, Yang Y, Xu JL, Zhang F, Liu CM, Zhang ZM, Lu YQ, Huang NP. MicroRNA-34a modulates the Notch signaling pathway in mice with congenital heart disease and its role in heart development. J Mol Cell Cardiol. 2018 Jan;114:300–8.
212. Omran A, Elimam D, Webster KA, et al. MicroRNAs: a new piece in the paediatric cardiovascular disease puzzle. Cardiol Young. 2013;23:642–55.
213. Ounzain S, Pezzuto I, Micheletti R, et al. Functional importance of cardiac enhancer-associated noncoding RNAs in heart development and disease. J Mol Cell Cardiol. 2014;76:55–70.
214. Scheuermann JC, Boyer LA. Getting to the heart of the matter: long non-coding RNAs in cardiac development and disease. EMBO J. 2013;32:1805–16.
215. Caley DP, Pink RC, Trujillano D, et al. Long noncoding RNAs, chromatin, and development. Sci World J. 2010;10:90–102.
216. Quinn JJ, Chang HY. Unique features of long non-coding RNA biogenesis and function. Nat Rev Genet. 2016 Jan;17(1):47–62.
217. Ransohoff JD, Wei Y, Khavari PA. The functions and unique features of long intergenic non-coding RNA. Nat Rev Mol Cell Biol. 2018 Mar;19(3):143–57.
218. Dykes IM, Emanueli C. Transcriptional and post-transcriptional gene regulation by long non-coding RNA. Genomics Proteomics Bioinformatics. 2017 Jun;15(3):177–86.
219. Zhu S, Hu X, Han S, et al. Differential expression profile of long non-coding RNAs during differentiation of cardiomyocytes. Int J Med Sci. 2014;11:500–7.
220. Zhu JG, Shen YH, Liu HL, et al. Long noncoding RNAs expression profile of the developing mouse heart. J Cell Biochem. 2014;115:910–8.
221. García-Padilla C, Domínguez JN, Aránega AE, Franco D. Differential chamber-specific expression and regulation of long non-coding RNAs during cardiac development. Biochim Biophys Acta Gene Regul Mech. 2019 Oct;1862(10):194435.

222. Kaushik K, Leonard VE, Kv S, et al. Dynamic expression of long non-coding RNAs (lncRNAs) in adult zebrafish. PLoS One. 2013;8:e83616.
223. Touma M, Kang X, Zhao Y, Cass AA, Gao F, Biniwale R, Coppola G, Xiao X, Reemtsen B, Wang Y. Decoding the long noncoding RNA during cardiac maturation: roadmap for functional discovery. Circ Cardiovasc Genet. 2016 Oct;9(5):395–407.
224. Shen S, Jiang H, Bei Y, Xiao J, Li X. Long non-coding RNAs in cardiac remodeling. Cell Physiol Biochem. 2017;41(5):1830–7.
225. Devaux Y, Zangrando J, Schroen B, Creemers EE, Pedrazzini T, Chang CP, Dor GW 2nd, Thum T, Heymans S, Cardiolinc Network. Long noncoding RNAs in cardiac development and ageing. Nat Rev Cardiol. 2015 Jul;12(7):415–25.
226. Zhang L, Hamad EA, Vausort M, et al. Identification of candidate long noncoding RNAs associated with left ventricular hypertrophy. Clin Transl Sci. 2015;8:100–6.
227. Pant T, Dhanasekaran A, Bai X, Zhao M, Thorp EB, Forbess JM, Bosnjak ZJ, Ge ZD. Genome-wide differential expression profiling of lncRNAs and mRNAs associated with early diabetic cardiomyopathy. Sci Rep. 2019 Oct 25;9(1):15345.
228. Ounzain S, Micheletti R, Beckmann T, et al. Genome-wide profiling of the cardiac transcriptome after myocardial infarction identifies novel heart-specific long non-coding RNAs. Eur Heart J. 2015;36:353–68.
229. Omura J, Habbout K, Shimauchi T, Wu WH, Breuils-Bonnet S, Tremblay E, Martineau S, Nadeau V, Gagnon K, Mazoyer F, Perron J, Potus F, Lin JH, Zafar H, Kiely DG, Lawrie A, Archer SL, Paulin R, Provencher S, Boucherat O, Bonnet S. Identification of Long Noncoding RNA H19 as a New Biomarker and Therapeutic Target in Right Ventricular Failure in Pulmonary Arterial Hypertension. Circulation. 2020 Oct 13;142(15):1464–84.
230. Di Salvo TG, Guo Y, Su YR, Clark T, Brittain E, Absi T, Maltais S, Hemnes A. Right ventricular long noncoding RNA expression in human heart failure. Pulm Circ. 2015 Mar;5(1):135–61.
231. Zhong Z, Hou J, Zhang Q, Li B, Li C, Liu Z, Yang M, Zhong W, Zhao P. Differential expression of circulating long non-coding RNAs in patients with acute myocardial infarction. Medicine (Baltimore). 2018 Dec;97(51):e13066.
232. Zhao P, Wu H, Zhong Z, Zhang Q, Zhong W, Li B, Li C, Liu Z, Yang M. Expression profiles of long noncoding RNAs and mRNAs in peripheral blood mononuclear cells of patients with acute myocardial infarction. Medicine (Baltimore). 2018 Oct;97(41):e12604.
233. Sheng X, Fan T, Jin X. Identification of key genes involved in acute myocardial infarction by comparative transcriptome analysis. Biomed Res Int. 2020 Oct 6;2020:1470867.
234. Li H, Cheng Z, Tang Y, Feng M, Yin A, Zhang H, Xu J, Zhang Q, Zhang J, Qian L. Expression profile of long non-coding RNAs in cardiomyocytes exposed to acut ischemic hypoxia. Mol Med Rep. 2019 Jan;19(1):302–8.
235. Li H, Cheng Z, Tang Y, Feng M, Yin A, Zhang H, Xu J, Zhang Q, Zhang J, Qian L. Expression profile of long non-coding RNAs in cardiomyocytes exposed to acute ischemic hypoxia. Mol Med Rep. 2019 Jan;19(1):302–8.
236. Liu Y, Li G, Lu H, et al. Expression profiling and ontology analysis of long noncoding RNAs in post-ischemic heart and their implied roles in ischemia/reperfusion injury. Gene. 2014;543:15–21.
237. Zhang R, Wang J, Liu B, Wang W, Fan X, Zheng B, Yuan Q, Xue M, Xu F, Guo P, Chen Y. Differentially expressed lncRNAs, miRNAs and mRNAs with associated ceRNA networks in a mouse model of myocardial ischemia/reperfusion injury. Mol Med Rep. 2020 Sep;22(3):2487–95.
238. Liu J, Wang DZ. An epigenetic "LINK(RNA)" to pathological cardiac hypertrophy. Cell Metab. 2014;20:555–7.
239. Han P, Li W, Lin CH, et al. A long noncoding RNA protects the heart from pathological hypertrophy. Nature. 2014;514:102–6.
240. Xu Y, Luo Y, Liang C, Zhang T. LncRNA-Mhrt regulates cardiac hypertrophy by modulating the miR-145a-5p/KLF4/myocardin axis. J Mol Cell Cardiol. 2020 Feb;139:47–61.

241. Fang Q, Liu T, Yu C, Yang X, Shao Y, Shi J, Ye X, Zheng X, Yan J, Xu D, Zou X. LncRNA TUG1 alleviates cardiac hypertrophy by targeting miR-34a/DKK1/Wnt-β-catenin signalling. J Cell Mol Med. 2020 Mar;24(6):3678–91.
242. Zou X, Wang J, Tang L, Wen Q. LncRNA TUG1 contributes to cardiac hypertrophy via regulating miR-29b-3p. In Vitro Cell Dev Biol Anim. 2019 Aug;55(7):482–90.
243. Zhang G, Ni X. Knockdown of TUG1 rescues cardiomyocyte hypertrophy through targeting the miR-497/MEF2C axis. Open Life Sci. 2021 Mar 16;16(1):242–51.
244. Su W, Huo Q, Wu H, Wang L, Ding X, Liang L, Zhou L, Zhao Y, Dan J, Zhang H. The function of LncRNA-H19 in cardiac hypertrophy. Cell Biosci. 2021 Aug 3;11(1):153.
245. Viereck J, Bührke A, Foinquinos A, Chatterjee S, Kleeberger JA, Xiao K, Janssen-Peters H, Batkai S, Ramanujam D, Kraft T, Cebotari S, Gueler F, Beyer AM, Schmitz J, Bräsen JH, Schmitto JD, Gyöngyösi M, Löser A, Hirt MN, Eschenhagen T, Engelhardt S, Bär C, Thum T. Targeting muscle-enriched long non- coding RNA H19 reverses pathological cardiac hypertrophy. Eur Heart J. 2020 Sep 21;41(36):3462–74.
246. Hobuß L, Foinquinos A, Jung M, Kenneweg F, Xiao K, Wang Y, Zimmer K, Remke J, Just A, Nowak J, Schmidt A, Pich A, Mazlan S, Reamon-Buettner SM, Ramos GC, Frantz S, Viereck J, Loyer X, Boulanger C, Wollert KC, Fiedler J, Thum T. Pleiotropic cardiac functions controlled by ischemia-induced lncRNA H19. J Mol Cell Cardiol. 2020 Sep;146:43–59.
247. Yang L, Deng J, Ma W, Qiao A, Xu S, Yu Y, Boriboun C, Kang X, Han D, Ernst P, Zhou L, Shi J, Zhang E, Li TS, Qiu H, Nakagawa S, Blackshaw S, Zhang J, Qin G. Ablation of lncRNA *Miat* attenuates pathological hypertrophy and heart failure. Theranostics. 2021 Jul 6;11(16): 7995–8007.
248. Li Z, Liu Y, Guo X, Sun G, Ma Q, Dai Y, Zhu G, Sun Y. Long noncoding RNA myocardial infarction-associated transcript is associated with the microRNA-150-5p/P300 pathway in cardiac hypertrophy. Int J Mol Med. 2018 Sep;42(3):1265–72.
249. Sun XL, Lv JL, Dou L, Chen D, Zhu YC, Hu X. LncRNA NEAT1 promotes cardiac hypertrophy through microRNA-19a-3p/SMYD2 axis. Eur Rev Med Pharmacol Sci. 2020 Feb;24(3):1367–77.
250. Wen ZQ, Li SH, Shui X, Tang LL, Zheng JR, Chen L. LncRNA PEG10 aggravates cardiac hypertrophy through regulating HOXA9. Eur Rev Med Pharmacol Sci. 2019 Aug;23 (3 Suppl):281–6.
251. Cheng Z, Liu L, Li Q. lncRNA ZEB2-AS1 stimulates cardiac hypertrophy by downregulating PTEN. Exp Ther Med. 2020 Nov;20(5):92.
252. Yu J, Yang Y, Xu Z, Lan C, Chen C, Li C, Chen Z, Yu C, Xia X, Liao Q, Jose PA, Zeng C, Wu G. Long noncoding RNA *Ahit* protects against cardiac hypertrophy through SUZ12 (suppressor of Zeste 12 protein homolog)-mediated downregulation of MEF2A (myocyte enhancer factor 2A). Circ Heart Fail. 2020 Jan;13(1):e006525.
253. Lv L, Li T, Li X, Xu C, Liu Q, Jiang H, Li Y, Liu Y, Yan H, Huang Q, Zhou Y, Zhang M, Shan H, Liang H. The lncRNA Plscr4 controls cardiac hypertrophy by regulating miR-214. Mol Ther Nucleic Acids. 2018 Mar 2;10:387–97.
254. Chen ZQ, Chen F, Li L. LncRNA GAS5 aggravates pathological cardiac hypertrophy by targeting miR-135b to mediate apoptosis. Int J Cardiol. 2019 Nov 1;294:56.
255. Zhang J, Liang Y, Huang X, Guo X, Liu Y, Zhong J, Yuan J. STAT3-induced upregulation of lncRNA MEG3 regulates the growth of cardiac hypertrophy through miR-361-5p/HDAC9 axis. Sci Rep. 2019 Jan 24;9(1):460.
256. Li C, Zhou G, Feng J, Zhang J, Hou L, Cheng Z. Upregulation of lncRNA VDR/CASC15 induced by facilitates cardiac hypertrophy through modulating miR-432-5p/TLR4 axis. Biochem Biophys Res Commun. 2018 Sep 18;503(4):2407–14.
257. Li Y, Wang J, Sun L, Zhu S. LncRNA myocardial infarction-associated transcript (MIAT) contributed to cardiac hypertrophy by regulating TLR4 via miR-93. Eur J Pharmacol. 2018 Jan 5;818:508–17.

258. Yan SM, Li H, Shu Q, Wu WJ, Luo XM, Lu L. LncRNA SNHG1 exerts a protective role in cardiomyocytes hypertrophy via targeting miR-15a-5p/HMGA1 axis. Cell Biol Int. 2020 Apr;44(4):1009–19.
259. Xiao L, Gu Y, Sun Y, Chen J, Wang X, Zhang Y, Gao L, Li L. The long noncoding RNA XIST regulates cardiac hypertrophy by targeting miR-101. J Cell Physiol. 2019 Aug;234(8): 13680–92.
260. Chen Y, Zhang Z, Zhu D, Zhao W, Li F. Knockdown of KCNQ1OT1 attenuates cardiac hypertrophy through modulation of the miR-2054/AKT3 axis. J Thorac Dis. 2020 Sep;12(9): 4771–80.
261. Zhang Q, Wang F, Wang F, Wu N. Long noncoding RNA MAGI1-IT1 regulates cardiac hypertrophy by modulating miR-302e/DKK1/Wnt/beta-catenin signaling pathway. J Cell Physiol. 2020 Jan;235(1):245–53.
262. Liu L, Zhang D, Li Y. LncRNAs in cardiac hypertrophy: from basic science to clinical application. J Cell Mol Med. 2020 Oct;24(20):11638–45.
263. Li Y, Liang Y, Zhu Y, Zhang Y, Bei Y. Noncoding RNAs in cardiac hypertrophy. J Cardiovasc Transl Res. 2018 Dec;11(6):439–49.
264. Sun J, Wang C. Long non-coding RNAs in cardiac hypertrophy. Heart Fail Rev. 2020 Nov;25 (6):1037–45.
265. Jiang Y, Mo H, Luo J, Zhao S, Liang S, Zhang M, Yuan J. HOTAIR is a potential novel biomarker in patients with congenital heart diseases. Biomed Res Int. 2018 Mar 7;2018: 2850657.
266. Ma J, Chen S, Hao L, Sheng W, Chen W, Ma X, Zhang B, Ma D, Huang G. Long non-coding RNA SAP30-2:1 is downregulated in congenital heart disease and regulates cell proliferation by targeting HAND2. Front Med. 2021 Feb;15(1):91–100.
267. Song G, Shen Y, Zhu J, et al. Integrated analysis of dysregulated lncRNA expression in fetal cardiac tissues with ventricular septal defect. PLoS One. 2013;8:e77492.
268. Jiang Y, Zhuang J, Lin Y, Wang X, Chen J, Han F. Long noncoding RNA SNHG6 contributes to ventricular septal defect formation via negative regulation of miR-101 and activation of Wnt/β-catenin pathway. Pharmazie. 2019 Jan 1;74(1):23–8.
269. O'Brien JE Jr, Kibiryeva N, Zhou XG, et al. Noncoding RNA expression in myocardium from infants with tetralogy of Fallot. Circ Cardiovasc Genet. 2012;5:279–86.
270. Ma J, Chen S, Hao L, Sheng W, Chen W, Ma X, Zhang B, Ma D, Huang G. Hypermethylation-mediated down-regulation of lncRNA TBX5-AS1:2 in Tetralogy of Fallot inhibits cell proliferation by reducing TBX5 expression. J Cell Mol Med. 2020 Jun;24 (11):6472–84.
271. Wang Q, Wang Z, Wu C, Pan Z, Xiang L, Liu H, Jin X, Tong K, Fan S, Jin X. Potential association of long noncoding RNA HA117 with tetralogy of Fallot Genes Dis. 2018 Mar 10;5 (2):185–90.
272. Zhang X, Gao Y, Zhang X, Zhang X, Xiang Y, Fu Q, Wang B, Xu Z. FGD5-AS1 is a hub lncRNA ceRNA in hearts with tetralogy of fallot which regulates congenital heart disease genes transcriptionally and epigenetically. Front Cell Dev Biol. 2021 May 11;9:630634.
273. Grote P, Wittler L, Hendrix D, et al. The tissue-specific lncRNA Fendrr is an essential regulator of heart and body wall development in the mouse. Dev Cell. 2013;24:206–14.
274. Klattenhoff CA, Scheuermann JC, Surface LE, et al. Braveheart, a long noncoding RNA required for cardiovascular lineage commitment. Cell. 2013;152:570–83.
275. Anderson KM, Anderson DM, McAnally JR, Shelton JM, Bassel-Duby R, Olson EN. Transcription of the non-coding RNA upperhand controls Hand2 expression and heart development. Nature. 2016 Nov 17;539(7629):433–6.
276. Han X, Zhang J, Liu Y, Fan X, Ai S, Luo Y, Li X, Jin H, Luo S, Zheng H, Yue Y, Chang Z, Yang Z, Tang F, He A, Shen X. The lncRNA *Hand2os1/Uph* locus orchestrates heart development through regulation of precise expression of *Hand2*. Development. 2019 Jul 4;146(13):dev176198.

277. Chouvarine P, Photiadis J, Cesnjevar R, Scheewe J, Bauer UMM, Pickardt T, Kramer HH, Dittrich S, Berger F, Hansmann G. RNA expression profiles and regulatory networks in human right ventricular hypertrophy due to high pressure load. iScience. 2021 Feb 27;24(3):102232.
278. Lin Z, Zhao Y, Dai F, Su E, Li F, Yan Y. Analysis of changes in circular RNA expression and construction of ceRNA networks in human dilated cardiomyopathy. J Cell Mol Med. 2021 Mar;25(5):2572–83.
279. Sun Y, Jiang X, Lv Y, Liang X, Zhao B, Bian W, Zhang D, Jiang J, Zhang C. Circular RNA expression profiles in plasma from patients with heart failure related to platelet activity. Biomolecules. 2020 Jan 25;10(2):187.
280. Li H, Xu JD, Fang XH, Zhu JN, Yang J, Pan R, Yuan SJ, Zeng N, Yang ZZ, Yang H, Wang XP, Duan JZ, Wang S, Luo JF, Wu SL, Shan ZX. Circular RNA circRNA_000203 aggravates cardiac hypertrophy via suppressing miR-26b-5p and miR-140-3p binding to Gata4. Cardiovasc Res. 2020 Jun 1;116(7):1323–34.
281. Wang K, Long B, Liu F, Wang JX, Liu CY, Zhao B, Zhou LY, Sun T, Wang M, Yu T, Gong Y, Liu J, Dong YH, Li N, Li PF. A circular RNA protects the heart from pathological hypertrophy and heart failure by targeting miR-223. Eur Heart J. 2016 Sep 1;37(33):2602–11.
282. Yang MH, Wang H, Han SN, Jia X, Zhang S, Dai FF, Zhou MJ, Yin Z, Wang TQ, Zang MX, Xue LX. Circular RNA expression in isoproterenol hydrochloride-induced cardiac hypertrophy. Aging (Albany NY). 2020 Feb 5;12(3):2530–44.
283. Xu X, Wang J, Wang X. Silencing of circHIPK3 Inhibits Pressure Overload-Induced Cardiac Hypertrophy and Dysfunction by Sponging miR-185-3p. Drug Des Devel Ther. 2020 Dec 29;14:5699–710.
284. Lim TB, Aliwarga E, Luu TDA, Li YP, Ng SL, Annadoray L, Sian S, Ackers- Johnson MA, Foo RS. Targeting the highly abundant circular RNA circSlc8a1 in cardiomyocytes attenuates pressure overload induced hypertrophy. Cardiovasc Res. 2019 Dec 1;115(14):1998–2007.
285. Schulte C, Barwari T, Joshi A, Theofilatos K, Zampetaki A, Barallobre- Barreiro J, Singh B, Sörensen NA, Neumann JT, Zeller T, Westermann D, Blankenberg S, Marber M, Liebetrau C, Mayr M. Comparative analysis of circulating noncoding RNAs versus protein biomarkers in the detection of myocardial injury. Circ Res. 2019 Jul 19;125(3):328–40.
286. Pan J, Xu Z, Guo G, Xu C, Song Z, Li K, Zhong K, Wang D. Circ_nuclear factor I X (circNfix) attenuates pressure overload-induced cardiac hypertrophy via regulating miR-145-5p/ATF3 axis. Bioengineered. 2021 Dec;12(1):5373–85.
287. Guo HM, Liu ZP. Up-regulation of circRNA_0068481 promotes right ventricular hypertrophy in PAH patients via regulating miR-646/miR-570/miR-885. J Cell Mol Med. 2021 Apr;25(8):3735–43.
288. Wu J, Li J, Liu H, Yin J, Zhang M, Yu Z, Miao H. Circulating plasma circular RNAs as novel diagnostic biomarkers for congenital heart disease in children. J Clin Lab Anal. 2019 Nov;33(9):e22998.
289. Liu H, Hu Y, Zhuang B, Yin J, Chen XH, Wang J, Li MM, Xu J, Wang XY, Yu ZB, Han SP. Differential expression of CircRNAs in embryonic heart tissue associated with ventricular septal defect. Int J Med Sci. 2018 May 14;15(7):703–12.
290. Matkovich SJ, Edwards JR, Grossenheider TC, et al. Epigenetic coordination of embryonic heart transcription by dynamically regulated long noncoding RNAs. Proc Natl Acad Sci U S A. 2014;111(33):12264–9.
291. Kalsotra A, Wang K, Li PF, et al. MicroRNAs coordinate an alternative splicing network during mouse postnatal heart development. Genes Dev. 2010;24:653–8.
292. Xu J, Hu Z, Xu Z, et al. Functional variant in microRNA-196a2 contributes to the susceptibility of congenital heart disease in a Chinese population. Hum Mutat. 2009;30:1231–6.
293. Vignier N, Schlossarek S, Fraysse B, et al. Nonsense-mediated mRNA decay and ubiquitin-proteasome system regulate cMyBP-C mutant levels in cardiomyopathic mice. Circ Res. 2009;105:239–48.
294. Kalsotra A, Wang K, Li PF et al (2010) MicroRNAs coordinate an alternative splicing network during mouse postnatal heart development. Genes Dev 24:653–658
295. Xu J, Hu Z, Xu Z et al (2009) Functional variant in microRNA-196a2 contributes to the susceptibility of congenital heart disease in a Chinese population. Hum Mutat 30:1231–1236

Epigenetics

18

Rajan Jain and Jonathan A. Epstein

Abstract

Epigenetics is the study of heritable changes to the genome and gene expression patterns that are not caused by direct changes to the DNA sequence. Examples of these changes include posttranslational modifications to DNA-bound histone proteins, DNA methylation, and remodeling of nuclear architecture. Collectively, epigenetic changes provide a layer of regulation that affects transcriptional activity of genes while leaving DNA sequences unaltered. Sequence variants or mutations affecting enzymes responsible for modifying or sensing epigenetic marks have been identified in patients with congenital heart disease (CHD), and small-molecule inhibitors of epigenetic complexes have shown promise as therapies for adult heart diseases. Additionally, transgenic mice harboring mutations or deletions of genes encoding epigenetic enzymes recapitulate aspects of human cardiac disease. Taken together, these findings suggest that the evolving field of epigenetics will inform our understanding of congenital and adult cardiac disease and offer new therapeutic opportunities.

Keywords

Epigenetics · Epigenetic marks · Chromatin · Nucleosome · Euchromatic · Methylation · DNA methylation · MECP2 · Histone · Acetylation · Histone methyltransferase · Histone deacetylase · CHD7 · Embryonic stem cell · Histone modification · Jumonji · Histone acetyltransferase · HAT · Smyd · MLL2 · Kabuki syndrome · HDAC · HDAC1 · HDAC2 · HDAC3 · HDAC5 · HDAC9 · HDAC7 ·

R. Jain (✉) · J. A. Epstein (✉)
Departments of Medicine and Cell and Developmental Biology, Institute for Regenerative Medicine, Epigenetics Institute and the Cardiovascular Institute, Perelman School of Medicine at the University of Pennsylvania, Philadelphia, PA, USA
e-mail: jainr@pennmedicine.upenn.edu; epsteinj@upenn.edu

© The Author(s), under exclusive license to Springer Nature Switzerland AG 2024

S. Rickert-Sperling et al. (eds.), *Congenital Heart Diseases: The Broken Heart*,
Advances in Experimental Medicine and Biology 1441,
https://doi.org/10.1007/978-3-031-44087-8_18

Sirtuins · Histone methylation · Wolf–Hirschhorn syndrome · Brg1-associated factor · BAF · Chromatin remodeler complex · SWI/SNF complex · Brg1 · Baf45c · Chromatin organization · Lamins · Nuclear lamina · Nucleoporin · BET · Ino80 · Cohesin

18.1 Introduction

Coordinated expression of genes coded by the DNA sequence of the genome requires precise temporal and spatial interactions between protein factors in the nucleus and DNA. Studies over the last half century have revealed that these interactions are highly influenced by the manner in which DNA is packaged and organized as chromatin. The basic unit of chromatin is the nucleosome, a complex of 147 bases of DNA wound around an octameric core of histone proteins. The spacing and number of nucleosomes determine chromatin density, with the DNA within highly dense heterochromatin being less accessible to nuclear factors than sequences within relaxed, less dense euchromatin. As a result, genes within heterochromatic regions tend to be silenced, while euchromatic loci are typically active. Clusters of nucleosomes are further condensed so that the genome can be packaged efficiently into the nucleus.

The first epigenetic modification to be identified was methylation of DNA itself. Methylation of cytosine residues is typically associated with transcriptional silencing, and a number of enzymes are responsible for adding and removing these methyl groups. Another type of epigenetic modification involves posttranslational modifications of histone proteins, including methylation and acetylation of lysine residues. These modifications modulate the recruitment of additional protein complexes that regulate chromatin density and conformation. A host of "writer" and "eraser" enzymes exists to add and remove specific modifications from histone tails, and the description of these growing families of enzymes is evolving rapidly (Fig. 18.1). Histone methyltransferases and deacetylases are among the most studied of these "writer" and "eraser" enzymes, respectively, in the context of cardiac development and disease. Covalent modifications of histone proteins are recognized by "reader" proteins that affect downstream changes in chromatin in response to changes in epigenetic marks (Fig. 18.1). Included in this class of proteins are chromodomain-containing proteins such as CHD7, a member of a larger family of ATP-dependent chromatin-remodeling complexes. Mutations in the gene-encoding CHD7 have been recently identified in patients with congenital heart disease [1]. This chapter will provide an overview of epigenetic changes during cardiovascular development and highlight the various families of epigenetic proteins and their roles in congenital heart disease. Additionally, we will highlight how changes in nuclear architecture may influence cardiac development.

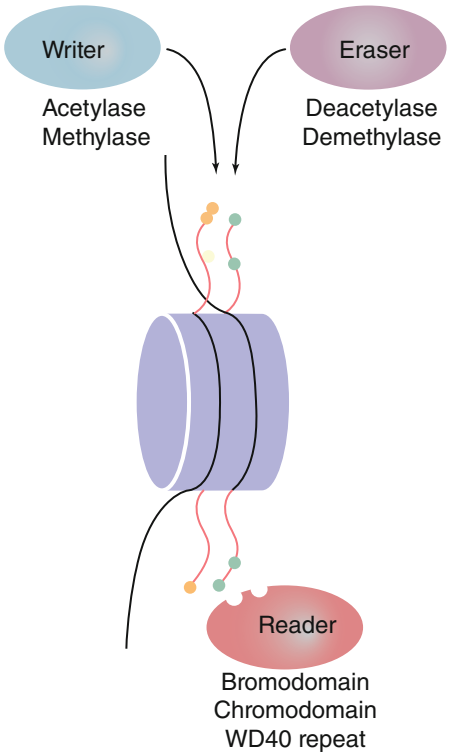

Fig. 18.1 Epigenetic regulators modify histone tails of a nucleosome. Epigenetic factors can be categorized into "writers," "erasers," and "readers." Writers add specific modifications to the histone tails of a nucleosome, while erasers remove these modifications. Readers function to recognize epigenetic modifications and can recruit other regulatory factors. Examples of each class of epigenetic regulator are provided

18.2 Epigenetic Changes During Cardiac Development

The explosion of next-generation sequencing technologies coupled with the improved efficiency of directed differentiation of embryonic stem cells into cardiac lineages has enabled mapping of the landscape of histone modifications over the course of cardiac differentiation. Most prominently, studies by Paige et al. and Wamstad et al. have shed significant light on the dynamics of gene activation and repression during cardiac specification [2, 3]. By taking snapshots at a series of well-defined time points in mouse and human ESC differentiation, these groups defined the presence of various histone modifications across the genome during cardiogenesis using chromatin immunoprecipitation coupled with massively paralleled sequencing (ChIP-Seq). Specifically, they observed unique histone modifications marking transcription start sites (trimethylation of histone H3 at lysine 4; H3K4me3), enhancers (monomethylation of histone H3 at lysine 4; H3K4me1, and acetylation of histone H3 at lysine 27; H3K27ac), and inactive chromatin (trimethylation of histone H3 at lysine 27; H3K27me3), thus providing an initial "map" of the dynamic epigenetic landscape during cardiac development. A theme that emerges from these surveys is that genes specific to noncardiac lineages such as

endoderm and ectoderm derivatives are rapidly marked by repressive histone modifications, resulting in the repression of these lineages. These findings support the hypothesis that cell differentiation requires active silencing of alternative lineages. More recent studies, discussed below, have extended this to human iPSC-differentiation into cardiac cell types as well as from human myocardial specimens in various pathologic conditions.

18.3 Histone Modifications

Epigenetic studies have focused on understanding how histone proteins undergo posttranslational modifications, in which amino acid residues are subject to these modifications, and how various combinations of modifications affect gene expression. Methylation and acetylation are two of the most common and well-studied histone modifications. Histones can be methylated on a variety of residues, and Jumonji domain-containing proteins act as demethylases. Histone acetyltransferases (HATs) acetylate lysine residues primarily on histone tails and histone deacetylase enzymes (Hdacs) reverse this process. Additional forms of histone modification have been described and continue to be discovered, though application to cardiac development and disease awaits further study [4].

18.3.1 Histone Deacetylase Enzymes

Histone deacetylases (Hdacs) remove acetyl groups from lysine residues, typically resulting in compaction of chromatin and repression of gene expression. Histones represent only one type of the many possible substrates for Hdacs, which can also remove acetyl groups from lysine residues of many other proteins, including tumor protein 53 (p53) and GATA binding protein 4 (Gata4) [5, 6]. Hence, these enzymes are more accurately known as lysine deacetylases (Ldacs) and nonhistone targets likely account for many important developmental functions that remain to be fully elucidated. There are five classes of Hdac proteins: I, IIa, IIb, III, and IV. Class I includes Hdacs 1, 2, 3, and 8, and these enzymes are expressed in most tissues [7–9]. Hdacs 1 and 2 are members of several repressive complexes including the Sin3 deacetylase, repressor element-1 silencing transcription factor corepressor 1/deacetylase (CoREST), nucleosome-remodeling deacetylase (NuRD), and polycomb-repressive complex 2 (PRC2) complexes [10]. Hdacs 4, 5, 7, and 9 comprise the class IIa subfamily of Hdacs. Class IIa Hdacs exhibit minimal deacetylase activity in vivo and in vitro due to evolutionary divergence of a critical tyrosine residue within the catalytic pocket. These Hdacs are characterized by a highly conserved myocyte enhancer factor 2-binding domain (Mef2). In addition, class IIa Hdacs act as signal integrators through interactions with 14-3-3 chaperone proteins to facilitate shuttling in and out of the nucleus [9]. Class III sirtuins require NAD^+ for deacetylation activity and have been studied in the context of cardiac

hypertrophy [11, 12]. Hdac11 is the sole member of class IV and is expressed in the heart; however, its function remains poorly described [13].

18.3.1.1 Hdac1 and Hdac2

Hdac1 and Hdac2 share a large degree of amino acid homology, are thought to have mostly redundant functions, and are both expressed in the myocardium [14, 15]. Global *Hdac1*-null mice die in utero at approximately E10.5, but myocardial specific deletion of *Hdac1* does not result in gross cardiac abnormality [14]. Global *Hdac2* deletion by a gene trap allele results in partial lethality, but surviving mutants exhibit only slightly thickened myocardial walls under homeostatic conditions [15]. However, these mutant mice are resistant to the cardiac hypertrophy that results from β-adrenergic stimulation or transaortic constriction. Montgomery et al. generated a floxed allele of Hdac2, and global deletion of *Hdac2* (by crossing the floxed allele to a cytomegalovirus-Cre recombinase mouse) results in lethality of all mice within 24 h of birth [14]. The differences between the phenotypes of the gene trap and floxed alleles are likely due to differences in genetic background and/or efficiencies of *Hdac2* inactivation. Combined deletion of *Hdac1* and *Hdac2* in cardiomyocytes results in death within 2 weeks of birth due to cardiac arrhythmias and cardiomyopathy, along with ectopic expression of fetal ion channels and contractile proteins [14]. It should be noted that compound deletion of *Hdac1* and *Hdac2* just a few days earlier in cardiac development leads to intrauterine demise, highlighting the changing role of Hdacs during cardiac development, especially during critical times of progenitor cell commitment, proliferation, and differentiation.

18.3.1.2 Hdac3

Like other class I Hdacs, Hdac3 is expressed in the myocardium throughout development and into adulthood. Germline deletion leads to lethality during gastrulation, before the heart is formed, and any cardiac phenotype can be appreciated [16]. Specifically, genetic deletion of *Hdac3* in early cardiac progenitors results in embryonic lethality late in gestation and ventricular hypoplasia [17]. Hdac3 acts as a repressor of T-box transcription factor 5 (Tbx5), a known driver of cardiogenesis, which also plays critical roles in the development of the cardiac conduction system and atrial septation [5, 18, 19], though it is unclear if deacetylation of Tbx5 protein by Hdac3 is required for cardiogenesis. Myocyte-specific deletion of *Hdac3* during mid-late gestation with alpha–myosin heavy chain-Cre recombinase (αMHC-Cre) permits survival until 3–4 months of age when mice succumb to severe cardiac hypertrophy and fibrosis [20]. Interestingly, deleting *Hdac3* in postnatal myocardium and skeletal muscle with myosin creatine kinase-Cre (MCK-Cre) results in a very mild phenotype and no lethality unless the mice are stressed by a high-fat diet [21]. Switching the mice from normal chow to a high-fat diet results in severe hypertrophic cardiomyopathy and fibrosis followed by death of all animals within several weeks. Myocyte-specific deletion of *Hdac3* is also characterized by extensive metabolic dysregulation of both lipid and glucose processing. Consistent with these findings, Hdac3 is unique among Hdacs for its interaction with the nuclear receptor

corepressor-silencing mediator for retinoid and thyroid receptor (NCoR/SMRT) complex that has been previously implicated in metabolic regulation [22–24].

Hdac3 is also a potent regulator of cell proliferation and directly regulates p21 [25, 26]. Previous work in transformed cells and hematopoiesis implicated Hdac3 in regulating cell cycle progression and DNA replication [26, 27]. Transgenic overexpression of *Hdac3* in cardiomyocytes causes increased proliferation and ventricular hyperplasia [25]. Expression analysis indicated that Hdac3 represses several cyclin-dependent kinase inhibitors, reducing levels of these cell cycle checkpoints, and promoting rapid proliferation of cardiomyocytes.

18.3.1.3 Hdac5 and Hdac9

These two class II Hdacs are expressed in the myocardium and skeletal muscle, and individual genetic loss yields viable adult mice without an overt cardiac phenotype under homeostatic conditions [28, 29]. However, combined deletion of *Hdac5* and *Hdac9* results in sensitivity to hypertrophic signals, phenotypically opposite to that of *Hdac2*-null animals. Loss of *Hdac5/9* leads to overactive Mef2 signaling in response to calcineurin-dependent signaling, which normally leads to export of class IIa Hdacs from the nucleus and inhibition of Mef2 activity. The absence of *Hdac5/9* leaves Mef2 within the nucleus where it can activate hypertrophic gene programs [29]. Class IIa Hdacs also modulate other transcription factor complexes, including serum response factor (SRF), myocardin, and calmodulin-binding transcription activator 2 [30], and it is likely that deletion of both *Hdac5* and *Hdac9* has effects on these regulators and Mef2 throughout development.

18.3.1.4 Hdac7

Global deletion of *Hdac7* leads to midgestation death at E11.5 due to vascular defects [31]. Mutant mice have vascular leak and lack smooth muscle cells around the dorsal aorta. Hdac7 complexes with Mef2 to repress matrix metalloproteinase 10 (Mmp10) in endothelium, which has been shown to influence the integrity of surrounding smooth muscle [31]. Consistent with a primary role of Hdac7 in endothelial cells, knockdown studies of *Hdac7* in endothelial cell cultures result in abnormal cellular morphology and tube formation [32].

18.3.1.5 Sirtuins

Sirtuins are class III Hdacs and require nicotinamide adenine dinucleotide (NAD) for their catalytic activity. There are seven sirtuins in mammals with various expression patterns, cellular localizations, and functions [11, 12]. Sirt1 is the best-studied sirtuin and is located in the nucleus and cytoplasm [33, 34], while Sirt2 is restricted to the cytoplasm [35]. Sirt3, Sirt4, and Sirt5 are localized to the mitochondria primarily [36]. Sirt6 and Sirt7 are localized to the nucleus [37, 38]. Sirt6 is involved in deacetylation of H3K9 and H3K56 [38], while Sirt7 modulates gene transcription dependent on RNA polymerase-I [37]. Multiple sirtuin proteins have been implicated in the pathogenesis of cardiac hypertrophy, but to our knowledge, there is no clear role for sirtuins in the most common forms of congenital heart disease.

18.3.2 HAT Proteins: Histone Acetyltransferases

Histone acetyltransferase enzymes catalyze the addition of acetyl groups to lysine residues of histone tails. This results in relaxation of chromatin, greater accessibility of the transcriptional machinery to DNA, and an increase in gene expression.

The most well-studied HAT is p300, with genetic deletion resulting in a generalized lack of cell proliferation, myocardial thinning, and death between E9.5 and E11.5 [39]. A single amino acid mutation abrogating the acetyltransferase activity results in myocardial thinning as well, but these mutants live to E12.5–E15.5 [40]. p300 also acetylates nonhistone proteins, including Gata4, which plays multiple roles in cardiac myocyte specification, differentiation, and proliferation [5, 41]. Acetylation of Gata4 enhances its transcriptional activity [42]. Interestingly, Hdac2, functioning with the atypical homeodomain protein, Hopx, can deacetylate Gata4 and represses its transcriptional activity [5]. This pathway is important in cell cycle exit and reducing the proliferative capacity of myocytes in late gestation. More recent studies have shown that Hopx marks a subset of cardiac progenitors committed to the cardiac myocyte lineage during cardiac development and promotes cardiac differentiation by physically interacting with an activated SMAD complex to repress WNT signaling [43]. These are examples of traditional "epigenetic" factors acting on nonhistone proteins to indirectly affect cardiac gene expression.

18.4 Histone Methylation

Multiple arginine and lysine residues on histone proteins are methylated. Gene activation or gene repression is dependent on which residue of the histone tail is methylated. Gene activation is associated with methylation at lysine (K) 4, K36, and K79 of histone H3, while gene repression is associated with methylation of K9 and K27 [4]. To date, histone methyltransferases and demethylases have not been studied as comprehensively in the context of cardiac development as Hdac and HAT proteins.

18.4.1 Jumonji Proteins

Methyl groups are removed from histone tails by a family of proteins containing Jumonji C domains. Two members of this family, jumonji AT-rich interactive domain 2 (Jarid2) and jumonji domain-containing 6 (Jmjd6), have important roles in cardiac outflow tract septation. Jarid2 is expressed in the developing myocardium of mice, as early as E8.0. The developing outflow tract, ventricular septum, and ventricular walls express relatively high levels of Jarid2 as compared to the atria. Jarid2 remains expressed in the myocardium in the adult mouse but at lower levels than during development. Global deletion of *Jarid2* results in hypertrabeculation of myocardium and outflow tract defects, including double outlet right ventricle (DORV) [44, 45]. Jarid2 controls expression of Notch1, and its downstream target,

Neureglin1, both implicated in the control of trabecular growth [45]. Similarly, *Jmjd6* knockout mice demonstrate DORV [46]. The nature of the defects suggests that these proteins affect neural crest function, though conditional deletion in the neural crest will be necessary to establish the tissue-specific roles of these proteins.

18.4.2 *WHSCI1* and Wolf–Hirschhorn Syndrome

Wolf–Hirschhorn syndrome is characterized by mental retardation, epilepsy, craniofacial abnormalities, and myocardial septal defects. Genetically, this syndrome is correlated with mutations and/or translocations of *WHSC1* (Wolf–Hirschhorn syndrome candidate 1), which encodes a histone methyltransferase that specifically methylates H3K36 and H4K20 [47]. Knockout *Whsc1* mice are characterized by myocardial septal defects, bone defects, and growth delay. However, haploinsufficiency of *Whsc1* in murine models does not result in the overt features associated with the clinical syndrome [48]. Whsc1 is known to associate with NK2 homeobox 5 (Nkx2–5), and compound haploinsufficiency of *Whsc1* and *Nkx2–5* in murine models recapitulates the atrial and ventricular septal defects associated with the clinical syndrome [48]. Some human mutations involve deletions of large pieces of chromosome 4, including the nearby Msh Homeobox 1 (*MSX1*) gene, which is highly expressed in the mesenchyme that contributes to craniofacial structures including teeth. Some of the typical craniofacial features of Wolf–Hirschhorn syndrome, such as dental abnormalities and cleft lip and/or palate, are more prominent in patients when *MSX1* is lost as well [49].

18.4.3 Smyd Proteins

The SET and MYND (Smyd) proteins are a family of five proteins characterized by a SET domain, which catalyzes methyltransferase activity, and a protein–protein interaction MYND domain [50]. The MYND domain allows Smyd proteins to interact with Hdacs, and Smyd1 represses gene transcription in an Hdac-dependent manner [51]. Interestingly, multiple Smyd family members have been detected in the cytoplasm and can be shuttled into the nucleus. This suggests that Smyd proteins likely have nonnuclear functions such as methylation of nonhistone proteins [50]. Smyd1 is the founding member of this family of proteins, and knockout studies in mice demonstrate a critical role in cardiac myocyte maturation and morphogenesis of the right ventricle [51]. This defect may be due to, at least in part, Smyd1 regulation of *Heart and Neural Crest Derivatives Expressed 2* (*Hand2*) and *Iroquois Homeobox 4* (*Irx4*) expression [51]. Zebrafish studies confirm a critical role for *smyd1b*, one of the two zebrafish orthologues; knockdown of *smyd1b* results in mispatterning of myofibers and lack of myocardial contraction [52, 53]. Smyd2, known to associate with the Sin3 complex [54], is strongly expressed in the embryonic myocardium and highly related to Smyd1 [55]. *Smyd2* knockdown in zebrafish results in cardiac dysfunction and myocyte disorganization [56]. However,

knockout studies in mice demonstrate that Smyd2 is dispensable for normal cardiogenesis [55]. *Smyd3* knockdown in zebrafish results in abnormal cardiac looping and defective expression of essential myocyte genes [57].

18.4.4 MLL2 and Kabuki Syndrome

Kabuki syndrome is an autosomal dominant syndrome characterized by mental retardation, distinctive craniofacial abnormalities, skeletal anomalies, and short stature [58]. The incidence of congenital heart disease in patients with Kabuki syndrome is 30–55%. There is a wide spectrum of reported defects including aortic coarctation, septal defects (atrial and ventricular), and hypoplastic left ventricle [59, 60]. Type I Kabuki syndrome is associated with mutations in the mixed-lineage leukemia protein 2 (*MLL2*), a histone methyltransferase belonging to the Trithorax family of proteins [61]. MLL2 is required for methylation of H3K4 [62, 63]. Mutations in *MLL2* have been detected in 48–75% of Kabuki patients, and nonsense or frameshift mutations are the most common types of mutations detected. Type II Kabuki syndrome, a more rare form of the disorder, is associated with mutations in *KDM6A*, a histone demethylase that specifically acts on H3K27 [64].

18.5 Epigenetic Gene Variants and Sporadic Congenital Heart Disease

The study by Zaidi et al., as part of the Pediatric Cardiac Genomics Consortium, provided a fundamental advance in our understanding of epigenetics and congenital heart disease by sequencing the exomes of 362 trios (affected patients and their parents) with a variety of congenital heart disorders, along with a cohort of 264 unaffected trios [1]. Interestingly, there was an overrepresentation of mutations or variants in genes encoding epigenetic enzymes in affected patients when compared to unaffected controls. Cohorts were largely composed of patients of European ancestry. Probands were affected by a variety of forms of congenital heart disease, but mostly composed of conotruncal defects ($n = 153$ patients, transposition of the great arteries, DORV, TOF, partial truncus arteriosus, and aortic arch abnormalities), LV obstructive lesions ($n = 132$, hypoplastic left heart syndrome, aortic coarctation, and bicuspid aortic valve), and heterotaxy ($n = 70$). Extracardiac abnormalities including craniofacial defects were present in 22% of probands. The authors identified mutations predicted to be pathologic in 28 genes. These predictions depended on whether the mutations resulted in premature termination, splicing variants, and/or frameshift of the coding sequence. The analyses also demonstrated that these mutated genes were among the highest expressed genes in the developing heart (25% percentile or higher). Mutations in five genes were specifically associated with histone methylation of H3K4: *MLL2*, *WDR5*, *CHD7*, *KDM5A*, and *KDM5B*. H3K4me is known to mark active promoters and genes "poised" to be expressed.

MLL2, as previously discussed, deposits the methylation of H3K4 [63]. The gene products of KDM5A and KDM5B, JARID1A and JARID1B, are responsible for removing methyl groups on H3K4, and CHD7 recognizes this histone modification [65]. Additionally, WD repeat domain 5 (WDR5) has been identified as part of the MLL complex [66]. Interestingly, the proband identified with a *CHD7* mutation did not manifest typical features of the CHARGE syndrome, though a patient with *MLL2* mutation did display characteristic craniofacial abnormalities typical of Kabuki syndrome. The group also identified mutations in *ring finger protein 20* (*RNF20*) and *ubiquitin-conjugating enzyme E2B* (*UBE2B*), factors involved in the ubiquitination of H2BK120, which is required for H3K4 methylation. Interestingly, a follow-up study by the Pediatric Cardiac Genomics Consortium revealed an enrichment of de novo pathogenic variants in genes involved in transcription and chromatin biology in children with congenital heart disease and neurodevelopmental disabilities [67]. Genes implicated included *CHD7, KMT2D,* and *RBFOX2*. These data raise the intriguing possibility of a common epigenetic underpinning to some forms of congenital heart disease and neurodevelopmental disorders.

18.6 DNA Methylation

In addition to histone proteins, the C5 position of cytosine nucleotides can be directly methylated (5-mC). The DNMT family of proteins (DNA methyltransferases) is composed of three proteins that catalyze transfer of methyl groups onto DNA in CpG islands. DNMT1 recognizes previously methylated DNA to reinforce existing patterns after DNA replication. DNMT3a and DNMT3b are de novo DNMTs and catalyze methylation of previously unmethylated cytosines [68]. More recently, it was discovered that the methylcytosine dioxygenase (TET) family of proteins catalyzes DNA demethylation through the conversion of 5-mC to 5-hmC as well as 5-formylcytosine (5fC) and 5-carboxylcytosine (5caC) [68]. Methyl-CpG-binding domain proteins, including MeCP2, recognize methylated DNA and recruit histone-modifying complexes. Mutations in *MECP2* have been implicated in the pathogenesis of Rett syndrome, a condition characterized by regression of skills, significant neurological difficulties, and stereotypical movements [69]. However, it was recently determined that approximately 20% of patients with Rett syndrome have a prolonged QT interval on their electrocardiogram, which can lead to sudden cardiac death in some patients [70]. Further work is needed to determine if mutations in TET proteins or DNMTs in humans are associated with congenital heart disease.

18.7 Nuclear Architecture

The organization and three-dimensional structure of chromatin have emerged as an important regulator of gene transcription. Dense, heterochromatic regions are associated with repressed gene activity, and euchromatic regions with a more open

conformation permit increased access by transcription factors to the DNA and are associated with increased gene transcription. Regulating higher order chromatin structure in this way allows for simultaneous control of large genomic regions and coordination of gene expression—a requirement for large-scale processes such as cell differentiation and stress response. For example, epigenetic mapping has demonstrated that as cells exit pluripotency during development and become more lineage restricted, levels of heterochromatin increase and the genome becomes more compact, while cell fates stabilize [71, 72]. Chromatin-remodeling complexes such as Brg1-associated factor (BAF), CHD, and inositol requiring 80 (INO80) contain ATPase domains that catalyze nucleosome restructuring–detaching histone proteins from the DNA helix and reassembly of the complex elsewhere. In addition, these complexes may contain domains for sensing histone modifications or other epigenetic marks and reorganize the chromatin accordingly. Finally, emerging evidence has also identified three-dimensional positioning of chromatin within the nucleus as an additional layer of regulation of chromatin structure and gene expression.

18.7.1 ATP-Dependent Chromatin Remodelers

Chromatin remodeling complexes are a class of "writers" that are characterized by SWI-like ATP-dependent catalytic activity. There are several classes of chromatin remodeling complexes including the switching defective/sucrose nonfermenting (SWI/SNF), chromodomain, helicase, DNA binding (CHD), and INO80 complexes. These complexes all contain a core ATPase domain that serves to disassemble the DNA-histone contacts to restructure and reposition nucleosomes. The complexes also serve as bridges to other regulatory factors and readers of histone modifications, making them important regulators of chromatin architecture and organization.

18.7.2 SWI/SNF Complex

The SWI/SNF complex was identified and purified in yeast with a vertebrate homolog BAF composed of 12 subunits. The core ATPase subunit is encoded by one of two highly homologous genes, SWI/SNF-related, matrix-associated, actin-dependent regulator of chromatin, subfamily a, member 4 (also known as brahma-related gene 1; *Brg1*) and SWI/SNF-related, matrix-associated, actin-dependent regulator of chromatin, subfamily a, member 2 (*Brm*); however, most studies suggest that Brg1 is the dominant ATPase in cardiovascular development [73].

Brg1 is expressed from the onset of embryogenesis, and *Brg1*-null embryos do not advance past implantation [74]. Endothelial-specific deletion of *Brg1* results in embryonic lethality at E10.5 and deficient yolk sac vasculogenesis [75]. Loss of *Brg1* in the endocardium results in hypertrabeculation. Further analysis revealed that Brg1 acts to repress a metalloproteinase, *Adamts1*, responsible for breakdown of the cardiac jelly present in the early embryonic heart. Loss of *Brg1* allows premature expression of Adamts1, early degradation of the cardiac jelly, and lack of normal

trabeculation. Deletion of *Brg1* in cardiac myocytes results in reduced cell proliferation and thin compact myocardium, ventricular septal defects, and lethality at E11.5 [73]. In developing cardiomyocytes, Brg1 complexes with Hdacs and poly (ADP-ribose) polymerases (PARP) to repress the adult isoform of myosin heavy chain and activate the fetal form, permitting normal embryogenesis. Loss of *Brg1* induces premature expression of the adult myosin isoform and leads myocytes to exit the fetal state too rapidly. Conditional deletion of *Brg1* results in hypoplastic right ventricle, shortened outflow tract, and embryonic lethality at E11.5 [73]. Smooth muscle depletion of *Brg1* leads to reduction of contractile proteins and dilated cardiomyopathy secondary to patent ductus arteriosus [76–79]. Taken together, these tissue-specific deletions suggest that Brg1 is an essential regulator of cardiac development as a core ATPase of the BAF complex, and its abrogation can lead to a variety of congenital heart defects in animal models.

Polybromo 1 (Baf180) is another subunit of the BAF complex critical for normal cardiac development. Baf180 contains six bromodomains and serves as a "reader" of acetylated histone tails. Global deletion of *Baf180* is embryonic lethal by E15.5 with ventricular hypoplasia and ventricular septal defects [80]. Epicardium-specific deletion disrupts normal vasculogenesis, resulting in coronary artery abnormalities [81]. Further analysis reveals that Baf180 is required for normal expression of elements of the retinoic acid pathway, a core regulatory mechanism of myocardial patterning. D4, zinc and double PHD fingers, family 3 (Baf45c or Dpf3) is a BAF subunit that also serves as a "reader," in this case of histone tails modified by the addition of acetyl and methyl groups. Knockdown in zebrafish results in abnormal cardiac looping and poor cardiac function [82]. Notably, human patients with tetralogy of Fallot (TOF) exhibit increased expression of Baf45c in the right ventricle [83]. Cui et al. showed that Baf45c is also upregulated in the hypertrophied left ventricle of patients with aortic stenosis and hypertrophic cardiomyopathy [84]. Mechanistically, phosphorylation of Baf45c (Dpf3a) by casein kinase 2 induces hypertrophy by releasing HEY repressors from chromatin [84].

SWI/SNF-related, matrix-associated, actin-dependent regulator of chromatin, subfamily d, member 3 (Baf60c) has been shown to interact with Nkx2-5, Tbx5, and Gata4 to activate multiple genes critical for cardiogenesis [85]. Loss-of-function studies in mice and zebrafish have confirmed that Baf60c regulates multiple steps of cardiogenesis including cardiac looping and morphogenesis [86–88]. Recent lineage tracing studies suggest that Baf60c-expressing cells give rise to the majority of the heart, in addition to extracardiac structures [89].

Williams syndrome is an autosomal dominant disorder notable for growth deficiency, dysmorphic facies, and cardiovascular abnormalities including pulmonary artery stenosis, supravalvular aortic stenosis, bicuspid aortic valve, aortic coarctation, and ASD [90]. Williams syndrome is marked by loss of 7q11.23 encompassing 23 genes including Williams syndrome transcription factor (*WSTF*), which is recruited into the BAF complex [91].

18.7.3 CHD Chromodomain Proteins

The CHD chromatin remodelers are complexes made up of at least a chromodomain, helicase, and DNA-binding domain. *CHD7* has been implicated in human disease as its haploinsufficiency results in CHARGE syndrome [65]. The syndrome features several cardiac defects including septal defects, endocardial cushion abnormalities, and conotruncal malformations. Furthermore, the aforementioned study by Zaidi et al. implicated *CHD7* as a genetic cause of congenital heart disease. Studies in mice reveal that loss of one copy of *Chd7* results in congenital heart disease including truncus arteriosus and interrupted aortic arch [92]. Recent studies suggest that this phenotype is mediated by a genetic interaction with Tbx1.

18.7.4 INO80 Complexes

Inositol requiring 80 (INO80) complexes contain DNA helicases to unwind double-stranded DNA. In vertebrates, pontin and reptin are two closely related helicases that commonly complex with one another and have been extensively studied in zebrafish. Disruption of either of these enzymes disrupts INO80 chromatin-remodeling activity and affects cardiac morphogenesis in fish [93]. Pontin represses cardiomyocyte proliferation, and Reptin plays an opposite role to promote proliferation through counteracting effects on the β-catenin pathway. Currently, little is known of their functions in mammalian heart development and disease.

18.7.5 BET Proteins: Chromatin "Readers"

The bromodomain and extra terminal (BET) family of proteins consist of three ubiquitously expressed members (Brd2-4) and a testis-specific isoform, BrdT. BET proteins are characterized by tandem bromodomains that allow for recognition of acetylated lysine residues on histone tails and other nuclear proteins. The "reader" activity of BET proteins allows them to recruit the basal transcriptional machinery, thereby promoting gene expression. The carboxy-terminus of BRD4 also interacts with pTEF-B, and thus BRD4 has been shown to mediate pause-release [94]. Recent data reveals a role for BRD4 in maintaining higher-order chromatin structure [95]. Pharmacologic inhibition of BET family members with the small molecule inhibitor JQ1 is sufficient to inhibit development of pathologic cardiac hypertrophy [96, 97]. JQ1 can competitively bind the bromodomains of BET family proteins, thereby inhibiting the "reader" ability [98]. Inhibition of cardiac hypertrophy was postulated to be secondary to inhibition of transcription at cohorts of genes relevant to a pro-hypertrophic phenotype. However, this phenotype may not be mediated by BRD4 in cardiac myocytes. Recent studies show that deletion of BRD4 in cardiac myocytes results in lethality and loss of mitochrondrial homeostasis [99, 100]. Interestingly, BET inhibition in fibroblasts ameliorates pathogenic cardiac fibrosis, suggesting a critical role for BET proteins in fibroblasts in cardiac pathobiology

[101]. Undoubtedly, modulating and/or repurposing the immune system may be an attractive way to control cardiac fibrosis [102, 103]. *Brd2* deficiency in mice leads to defective neural tube closure and death at approximately E13.5 [104, 105], while global *Brd4* deficiency in mice leads to death shortly after implantation [106].

18.8 Spatial Positioning of the Genome in the Nucleus

An emerging concept within the field of chromatin organization is that the localization of genes within the nucleus can affect gene expression. Several recent studies have revealed, for example, that the conformation of chromatin at the nuclear periphery versus in the nucleoplasm is very different [107]. More specifically, peripheral chromatin bound at the nuclear pore complex tends to be more transcriptionally active than chromatin at the nuclear membrane between the pores, where gene expression is repressed [108–110]. The inner surface of the nuclear membrane is coated by a thin layer of intermediate filament proteins called lamins. Chromatin found at the nuclear lamina has been termed lamina-associated domains (LADs) and tends to be transcriptionally silent, and forced tethering of reporter genes to the nuclear periphery can result in repression [111, 112]. Genome-wide mapping studies have revealed that the organization of chromatin at the nuclear lamina versus the interior of the nucleus/nucleoplasm is dynamic and varies over the course of cell differentiation [113, 114]. Our groups recently demonstrated that cardiogenesis is associated with a repositioning of the genome, and cardiac genes reposition from the nuclear lamina to the nuclear interior during cardiogenesis [115]. This is, in part, mediated by an interaction between Hdac3 and Lap2β, a protein restricted to the nuclear membrane. A specific DNA sequence has not been found to be sufficient nor necessary to position chromatin to the nuclear lamina. However, our group and others have shown that a specific histone post-translational modification is enriched on chromatin positioned at the nuclear lamina, dimethylation of Lysine 9 on Histone 3, H3K9me2 [116–120]. Thus, this raises the intriguing possibility that a histone post-translational modification may underlie aspects of positioning of chromatin to the periphery, which has been supported by studies utilizing non-traditional cells [119]. In addition, multiple studies have revealed different types of chromatin based on gene content and histone post-translational modifications, including that positioned at the nuclear lamina [121, 122]. Specifically, chromatin enriched for H3K9me2 but relatively depleted for LaminB1 occupancy is enriched for enhancers as opposed to other regulatory elements [123], and future studies will delineate if this constitutes an especially dynamic subset of peripheral chromatin during lineage restriction.

The significance of these changes to cardiac disease is still a matter of intense study; however, it is clear that several diseases with cardiac manifestations, including cardiomyopathy and arrhythmogenesis, are caused by mutations in nuclear lamina-associated proteins. These laminopathies include Hutchinson–Gilford progeria syndrome and Emery–Dreifuss muscular dystrophy and are due to mutations in genes encoding lamin A and its interacting protein emerin, respectively

[124, 125]. Multiple recent studies have demonstrated that pathogenic *LMNA* variants associated cardiomyopathy result in a loss of genome organization and LAD maintenance at the nuclear periphery in iPSC-derived cardiomyocytes [126, 127]. In addition, our study demonstrated that changes in genome organization at the nuclear periphery induced by missense mutants are cell type-specific. Specifically, *LMNA* variants resulted in a loss of lamina occupancy and expression of non-myocyte genes [127], in accord with a different study utilizing a haploinsufficient model of laminopathy [128]. New synthetic biology approaches will be key to restore nuclear architecture to define the consequence of disorganized genome organization in cardiac laminopathies on calcium flux and contraction.

In addition to lamina filaments, the nuclear membrane is also decorated with thousands of nuclear pore complexes (NPCs). These large protein complexes of at least 30 different nucleoporin proteins are typically thought of as regulators of selective transport in and out of the nucleus [129]. In addition to this transport role, nuclear pore proteins interact with chromatin, and genome-wide surveys have demonstrated that nuclear pore complexes tend to associate with transcriptionally active chromatin [110, 130, 131]. Much work remains to clarify the role of the nuclear pore complex in development and transcriptional regulation, although interesting connections have begun to emerge. For example, screens have identified several chromatin-remodeling complexes including chromatin structure remodeling (RSC) as interacting partners with the NPC [132]. Mutations in *nucleoporin 155 kDa* (*Nup155*) in mice results in atrial arrhythmias [133]. Hdac4 can physically interact with Nup155, and this interaction is necessary for Hdac4-mediated gene regulation at least in some settings [134].

18.9 Higher-Order Genome Structure

Genome compaction and organization are highly regulated processes, and causative links between high-order chromatin structure and function are being established. Chromosomes occupy specific locations within the nucleus and fold into defined territories. Territories are broadly divided into two classes: the A compartment, frequently euchromatic [135], and the B compartment, usually late replicating, heterochromatic, and transcriptionally silent [136]. Recent data using chromosome conformation capture techniques have shown that a subset of the genome switches compartments during cardiac lineage restriction [128, 137, 138]. Compartmentalization often correlates with histone post-translational modifications associated with euchromatin or heterochromatin [139], and it is possible that multiple types of compartments exist similar to the various chromatin states [139, 140].

An additional layer of chromatin organization involves domains which are enriched for self-interaction, termed Topological Associated Domains (TADs) [141, 142]. TADs are relatively insulated from each other, and a subset is cell type-specific and is disrupted in several diseases [143]. Chromatin looping, for example between enhancers and promoters, has been shown to be largely constrained within individual TADs [140, 143]. Manipulation of TAD boundaries

via induction of aberrant epigenetic modifications and/or genetic deletion (whether induced or naturally occurring) results in abnormal TAD formation and/or gene expression [144–146]. Consistently, emerging studies suggest changes in chromatin interactions in the pathogenesis of congestive heart failure and other cardiac pathologies [147–150]. The decreasing cost of sequencing will provide opportunities for more deeply sequenced datasets which will undoubtedly provide greater resolution into cell type-specific differences among TADs. Moreover, super-resolution imaging has revealed incredible heterogeneity amongst TADs at the single cell level [151–153].

CTCF (CCCTC-binding factor) is a zinc-finger nucleic acid binding protein whose binding is enriched at TAD boundaries. The orientation of CTCF binding sites is critical to forming TADs, and incorrect orientation of CTCF binding results in abnormal TAD formation and gene expression [135, 146, 154]. Degradation of CTCF protein in murine ESCs resulted in a loss of insulation between neighboring TADs [155]. In addition, the cohesin complex, a ring complex of proteins, has been found to be critical in loop formation and TAD stability in interphase cells [139, 156–159]. This effect on higher-order structure is likely mediated through the ability of cohesin to ensnare a piece of DNA and extrude the genome through it allowing for chromatin contacts to be dynamically established (often referred to as the loop extrusion hypothesis) [160, 161]. Related to cardiac development, several syndromes with etiologies in mutations in cohesin, including Cornelia de Lange Syndrome, are associated with congenital heart defects [162–164]. These syndromes are collectively referred to as cohesinopathies and frequently involve neurodevelopmental delay and stereotypical craniofacial abnormalities. *NIPBL* is most frequently mutated in Cornelia de Lange Syndrome, and NIPBL has been shown to facilitate the loading of cohesin onto chromatin as well as regulate its loop extrusion activity [165–168]. Our recent studies show that BRD4 regulates association of NIPBL with chromatin. Loss of BRD4 decreases chromatin-bound NIPBL and is accompanied by compromised maintenance of loops, TADs, and loop extrusion. This role for BRD4 in genome folding is critical for differentiation of neural crest progenitor cells into smooth muscle [95]. Thus, there is a nascent but rapidly growing appreciation of the regulation of chromatin topology that is likely to impact gene expression, lineage stability, cellular competence, and cellular identity. Future studies will undoubtedly leverage recent advances in super-resolution imaging to understanding how nuclear architecture influences cardiac development in vivo.

18.10 Conclusion

The rapidly growing appreciation of the complex array of enzymes and associated proteins that mediate epigenetic regulation of gene expression has transformed our understanding of the etiology of congenital heart disease. The specific functions of various subclasses of epigenetic modifiers during heart development remain poorly elucidated, and the range of interacting proteins, RNA molecules, and other moieties have not been fully defined. Nevertheless, gain and loss of function studies in animal

models, and human genetic studies strongly suggest that the developing cardiovascular system is acutely sensitive to epigenetic perturbations, and it seems likely that these sensitivities are further modulated by environmental exposures. Epigenetic regulation of cardiovascular development is a rapidly evolving field that will gain increasing relevance for the understanding and treatment of cardiac disorders in the future.

References

1. Zaidi S, Choi M, Wakimoto H, et al. De novo mutations in histone-modifying genes in congenital heart disease. Nature. 2013;498:220–3.
2. Paige SL, Thomas S, Stoick-Cooper CL, et al. A temporal chromatin signature in human embryonic stem cells identifies regulators of cardiac development. Cell. 2012;151:221–32.
3. Wamstad JA, Alexander JM, Truty RM, et al. Dynamic and coordinated epigenetic regulation of developmental transitions in the cardiac lineage. Cell. 2012;151:206–20.
4. Huang H, Sabari BR, Garcia BA, et al. SnapShot: histone modifications. Cell. 2014;159:458–458.e451.
5. Trivedi CM, Zhu W, Wang Q, et al. Hopx and Hdac2 interact to modulate Gata4 acetylation and embryonic cardiac myocyte proliferation. Dev Cell. 2010;19:450–9.
6. Zhao Y, Lu S, Wu L, et al. Acetylation of p53 at lysine 373/382 by the histone deacetylase inhibitor depsipeptide induces expression of p21(Waf1/Cip1). Mol Cell Biol. 2006;26:2782–90.
7. Taunton J, Hassig CA, Schreiber SL. A mammalian histone deacetylase related to the yeast transcriptional regulator Rpd3p. Science. 1996;272:408–11.
8. Yang XJ, Seto E. The Rpd3/Hda1 family of lysine deacetylases: from bacteria and yeast to mice and men. Nat Rev Mol Cell Biol. 2008;9:206–18.
9. Haberland M, Montgomery RL, Olson EN. The many roles of histone deacetylases in development and physiology: implications for disease and therapy. Nat Rev Genet. 2009;10:32–42.
10. Yang XJ, Seto E. Collaborative spirit of histone deacetylases in regulating chromatin structure and gene expression. Curr Opin Genet Dev. 2003;13:143–53.
11. Guarente L. Sirtuins as potential targets for metabolic syndrome. Nature. 2006;444:868–74.
12. Schwer B, Verdin E. Conserved metabolic regulatory functions of sirtuins. Cell Metab. 2008;7:104–12.
13. Gao L, Cueto MA, Asselbergs F, et al. Cloning and functional characterization of HDAC11, a novel member of the human histone deacetylase family. J Biol Chem. 2002;277:25748–55.
14. Montgomery RL, Davis CA, Potthoff MJ, et al. Histone deacetylases 1 and 2 redundantly regulate cardiac morphogenesis, growth, and contractility. Genes Dev. 2007;21:1790–802.
15. Trivedi CM, Luo Y, Yin Z, et al. Hdac2 regulates the cardiac hypertrophic response by modulating Gsk3 beta activity. Nat Med. 2007;13:324–31.
16. Bhaskara S, Chyla BJ, Amann JM, et al. Deletion of histone deacetylase 3 reveals critical roles in S phase progression and DNA damage control. Mol Cell. 2008;30:61–72.
17. Lewandowski SL, Janardhan HP, Smee KM, et al. Histone deacetylase 3 modulates Tbx5 activity to regulate early cardiogenesis. Hum Mol Genet. 2014;23:3801–9.
18. Bruneau BG, Nemer G, Schmitt JP, et al. A murine model of Holt-Oram syndrome defines roles of the T-box transcription factor Tbx5 in cardiogenesis and disease. Cell. 2001;106:709–21.
19. Li QY, Newbury-Ecob RA, Terrett JA, et al. Holt-Oram syndrome is caused by mutations in TBX5, a member of the Brachyury (T) gene family. Nat Genet. 1997;15:21–9.
20. Montgomery RL, Potthoff MJ, Haberland M, et al. Maintenance of cardiac energy metabolism by histone deacetylase 3 in mice. J Clin Invest. 2008;118:3588–97.

21. Sun Z, Singh N, Mullican SE, et al. Diet-induced lethality due to deletion of the Hdac3 gene in heart and skeletal muscle. J Biol Chem. 2011;286:33301–9.
22. Codina A, Love JD, Li Y, et al. Structural insights into the interaction and activation of histone deacetylase 3 by nuclear receptor corepressors. Proc Natl Acad Sci U S A. 2005;102:6009–14.
23. Guenther MG, Barak O, Lazar MA. The SMRT and N-CoR corepressors are activating cofactors for histone deacetylase 3. Mol Cell Biol. 2001;21:6091–101.
24. Sun Z, Miller RA, Patel RT, et al. Hepatic Hdac3 promotes gluconeogenesis by repressing lipid synthesis and sequestration. Nat Med. 2012;18:934–42.
25. Trivedi CM, Lu MM, Wang Q, et al. Transgenic overexpression of Hdac3 in the heart produces increased postnatal cardiac myocyte proliferation but does not induce hypertrophy. J Biol Chem. 2008;283:26484–9.
26. Wilson AJ, Byun DS, Popova N, et al. Histone deacetylase 3 (HDAC3) and other class I HDACs regulate colon cell maturation and p21 expression and are deregulated in human colon cancer. J Biol Chem. 2006;281:13548–58.
27. Summers AR, Fischer MA, Stengel KR, et al. HDAC3 is essential for DNA replication in hematopoietic progenitor cells. J Clin Invest. 2013;123:3112–23.
28. Zhang CL, McKinsey TA, Chang S, et al. Class II histone deacetylases act as signal-responsive repressors of cardiac hypertrophy. Cell. 2002;110:479–88.
29. Chang S, McKinsey TA, Zhang CL, et al. Histone deacetylases 5 and 9 govern responsiveness of the heart to a subset of stress signals and play redundant roles in heart development. Mol Cell Biol. 2004;24:8467–76.
30. Song K, Backs J, McAnally J, et al. The transcriptional coactivator CAMTA2 stimulates cardiac growth by opposing class II histone deacetylases. Cell. 2006;125:453–66.
31. Chang S, Young BD, Li S, et al. Histone deacetylase 7 maintains vascular integrity by repressing matrix metalloproteinase 10. Cell. 2006;126:321–34.
32. Mottet D, Bellahcene A, Pirotte S, et al. Histone deacetylase 7 silencing alters endothelial cell migration, a key step in angiogenesis. Circ Res. 2007;101:1237–46.
33. Michishita E, Park JY, Burneskis JM, et al. Evolutionarily conserved and nonconserved cellular localizations and functions of human SIRT proteins. Mol Biol Cell. 2005;16:4623–35.
34. Tanno M, Sakamoto J, Miura T, et al. Nucleocytoplasmic shuttling of the NAD + -dependent histone deacetylase SIRT1. J Biol Chem. 2007;282:6823–32.
35. Inoue T, Hiratsuka M, Osaki M, et al. SIRT2, a tubulin deacetylase, acts to block the entry to chromosome condensation in response to mitotic stress. Oncogene. 2007;26:945–57.
36. He W, Newman JC, Wang MZ, et al. Mitochondrial sirtuins: regulators of protein acylation and metabolism. Trends Endocrinol Metab. 2012;23:467–76.
37. Ford E, Voit R, Liszt G, et al. Mammalian Sir2 homolog SIRT7 is an activator of RNA polymerase I transcription. Genes Dev. 2006;20:1075–80.
38. Schwer B, Schumacher B, Lombard DB, et al. Neural sirtuin 6 (Sirt6) ablation attenuates somatic growth and causes obesity. Proc Natl Acad Sci U S A. 2010;107:21790–4.
39. Yao TP, Oh SP, Fuchs M, et al. Gene dosage-dependent embryonic development and proliferation defects in mice lacking the transcriptional integrator p300. Cell. 1998;93:361–72.
40. Shikama N, Lutz W, Kretzschmar R, et al. Essential function of p300 acetyltransferase activity in heart, lung and small intestine formation. EMBO J. 2003;22:5175–85.
41. Rojas A, Kong SW, Agarwal P, et al. GATA4 is a direct transcriptional activator of cyclin D2 and Cdk4 and is required for cardiomyocyte proliferation in anterior heart field-derived myocardium. Mol Cell Biol. 2008;28:5420–31.
42. Takaya T, Kawamura T, Morimoto T, et al. Identification of p300-targeted acetylated residues in GATA4 during hypertrophic responses in cardiac myocytes. J Biol Chem. 2008;283:9828–35.
43. Jain R, et al. HEART DEVELOPMENT. Integration of Bmp and Wnt signaling by Hopx specifies commitment of cardiomyoblasts. Science. 2015;348:aaa6071. https://doi.org/10.1126/science.aaa6071.

44. Lee Y, Song AJ, Baker R, et al. Jumonji, a nuclear protein that is necessary for normal heart development. Circ Res. 2000;86:932–8.
45. Mysliwiec MR, Bresnick EH, Lee Y. Endothelial Jarid2/Jumonji is required for normal cardiac development and proper Notch1 expression. J Biol Chem. 2011;286:17193–204.
46. Schneider JE, Bose J, Bamforth SD, et al. Identification of cardiac malformations in mice lacking Ptdsr using a novel high-throughput magnetic resonance imaging technique. BMC Dev Biol. 2004;4:16.
47. Marango J, Shimoyama M, Nishio H, et al. The MMSET protein is a histone methyltransferase with characteristics of a transcriptional corepressor. Blood. 2008;111:3145–54.
48. Nimura K, Ura K, Shiratori H, et al. A histone H3 lysine 36 trimethyltransferase links Nkx2-5 to Wolf-Hirschhorn syndrome. Nature. 2009;460:287–91.
49. Paradowska-Stolarz AM. Wolf-Hirschhorn syndrome (WHS) – literature review on the features of the syndrome. Adv Clin Exp Med. 2014;23:485–9.
50. Du SJ, Tan X, Zhang J. SMYD proteins: key regulators in skeletal and cardiac muscle development and function. Anat Rec. 2014;297:1650–62.
51. Gottlieb PD, Pierce SA, Sims RJ, et al. Bop encodes a muscle-restricted protein containing MYND and SET domains and is essential for cardiac differentiation and morphogenesis. Nat Genet. 2002;31:25–32.
52. Li H, Zhong Y, Wang Z, et al. Smyd1b is required for skeletal and cardiac muscle function in zebrafish. Mol Biol Cell. 2013;24:3511–21.
53. Tan X, Rotllant J, Li H, et al. SmyD1, a histone methyltransferase, is required for myofibril organization and muscle contraction in zebrafish embryos. Proc Natl Acad Sci U S A. 2006;103:2713–8.
54. Brown MA, Sims RJ 3rd, Gottlieb PD, et al. Identification and characterization of Smyd2: a split SET/MYND domain-containing histone H3 lysine 36-specific methyltransferase that interacts with the Sin3 histone deacetylase complex. Mol Cancer. 2006;5:26.
55. Diehl F, Brown MA, van Amerongen MJ, et al. Cardiac deletion of Smyd2 is dispensable for mouse heart development. PLoS One. 2010;5:e9748.
56. Voelkel T, Andresen C, Unger A, et al. Lysine methyltransferase Smyd2 regulates Hsp90-mediated protection of the sarcomeric titin springs and cardiac function. Biochim Biophys Acta. 2013;1833:812–22.
57. Fujii T, Tsunesumi S, Yamaguchi K, et al. Smyd3 is required for the development of cardiac and skeletal muscle in zebrafish. PLoS One. 2011;6:e23491.
58. Bogershausen N, Wollnik B. Unmasking Kabuki syndrome. Clin Genet. 2013;83:201–11.
59. Yuan SM. Congenital heart defects in Kabuki syndrome. Cardiol J. 2013;20:121–4.
60. Digilio MC, Marino B, Toscano A, et al. Congenital heart defects in Kabuki syndrome. Am J Med Genet. 2001;100:269–74.
61. Ng SB, Bigham AW, Buckingham KJ, et al. Exome sequencing identifies MLL2 mutations as a cause of Kabuki syndrome. Nat Genet. 2010;42:790–3.
62. Wan X, Liu L, Ding X, et al. Mll2 controls cardiac lineage differentiation of mouse embryonic stem cells by promoting H3K4me3 deposition at cardiac-specific genes. Stem Cell Rev. 2014;10:643–52.
63. Schuettengruber B, Chourrout D, Vervoort M, et al. Genome regulation by polycomb and trithorax proteins. Cell. 2007;128:735–45.
64. Lederer D, Grisart B, Digilio MC, et al. Deletion of KDM6A, a histone demethylase interacting with MLL2, in three patients with kabuki syndrome. Am J Hum Genet. 2012;90:119–24.
65. Vissers LE, van Ravenswaaij CM, Admiraal R, et al. Mutations in a new member of the chromodomain gene family cause CHARGE syndrome. Nat Genet. 2004;36:955–7.
66. Song JJ, Kingston RE. WDR5 interacts with mixed lineage leukemia (MLL) protein via the histone H3-binding pocket. J Biol Chem. 2008;283:35258–64.

67. Homsy J, et al. De novo mutations in congenital heart disease with neurodevelopmental and other congenital anomalies. Science. 2015;350:1262–6. https://doi.org/10.1126/science.aac9396.
68. Smith ZD, Meissner A. DNA methylation: roles in mammalian development. Nat Rev Genet. 2013;14:204–20.
69. Amir RE, Van den Veyver IB, Wan M, et al. Rett syndrome is caused by mutations in X-linked MECP2, encoding methyl-CpG-binding protein 2. Nat Genet. 1999;23:185–8.
70. McCauley MD, Wang T, Mike E, et al. Pathogenesis of lethal cardiac arrhythmias in Mecp2 mutant mice: implication for therapy in Rett syndrome. Sci Transl Med. 2011;3:113ra125.
71. Li G, Reinberg D. Chromatin higher-order structures and gene regulation. Curr Opin Genet Dev. 2011;21:175–86.
72. Meister P, Mango SE, Gasser SM. Locking the genome: nuclear organization and cell fate. Curr Opin Genet Dev. 2011;21:167–74.
73. Hang CT, Yang J, Han P, et al. Chromatin regulation by Brg1 underlies heart muscle development and disease. Nature. 2010;466:62–7.
74. Bultman S, Gebuhr T, Yee D, et al. A Brg1 null mutation in the mouse reveals functional differences among mammalian SWI/SNF complexes. Mol Cell. 2000;6:1287–95.
75. Stankunas K, Hang CT, Tsun ZY, et al. Endocardial Brg1 represses ADAMTS1 to maintain the microenvironment for myocardial morphogenesis. Dev Cell. 2008;14:298–311.
76. Zhou J, Zhang M, Fang H, et al. The SWI/SNF chromatin remodeling complex regulates myocardin-induced smooth muscle-specific gene expression. Arterioscler Thromb Vasc Biol. 2009;29:921–8.
77. Zhang M, Fang H, Zhou J, et al. A novel role of Brg1 in the regulation of SRF/MRTFA-dependent smooth muscle-specific gene expression. J Biol Chem. 2007;282:25708–16.
78. Zhang M, Chen M, Kim JR, et al. SWI/SNF complexes containing Brahma or Brahma-related gene 1 play distinct roles in smooth muscle development. Mol Cell Biol. 2011;31:2618–31.
79. Huang J, Cheng L, Li J, et al. Myocardin regulates expression of contractile genes in smooth muscle cells and is required for closure of the ductus arteriosus in mice. J Clin Invest. 2008;118:515–25.
80. Wang Z, Zhai W, Richardson JA, et al. Polybromo protein BAF180 functions in mammalian cardiac chamber maturation. Genes Dev. 2004;18:3106–16.
81. Huang X, Gao X, Diaz-Trelles R, et al. Coronary development is regulated by ATP-dependent SWI/SNF chromatin remodeling component BAF180. Dev Biol. 2008;319:258–66.
82. Lange M, Kaynak B, Forster UB, et al. Regulation of muscle development by DPF3, a novel histone acetylation and methylation reader of the BAF chromatin remodeling complex. Genes Dev. 2008;22:2370–84.
83. Kaynak B, von Heydebreck A, Mebus S, et al. Genome-wide array analysis of normal and malformed human hearts. Circulation. 2003;107:2467–74.
84. Cui H, Schlesinger J, Schoenhals S, et al. Phosphorylation of the chromatin remodeling factor DPF3a induces cardiac hypertrophy through releasing HEY repressors from DNA. Nucleic Acids Res. 2015;44:2538. https://doi.org/10.1093/nar/gkv1244.
85. Takeuchi JK, Bruneau BG. Directed transdifferentiation of mouse mesoderm to heart tissue by defined factors. Nature. 2009;459:708–11.
86. Lickert H, Takeuchi JK, Von Both I, et al. Baf60c is essential for function of BAF chromatin remodelling complexes in heart development. Nature. 2004;432:107–12.
87. Lou X, Deshwar AR, Crump JG, et al. Smarcd3b and Gata5 promote a cardiac progenitor fate in the zebrafish embryo. Development. 2011;138:3113–23.
88. Takeuchi JK, Lickert H, Bisgrove BW, et al. Baf60c is a nuclear Notch signaling component required for the establishment of left-right asymmetry. Proc Natl Acad Sci U S A. 2007;104:846–51.
89. Devine WP, Wythe JD, George M, et al. Early patterning and specification of cardiac progenitors in gastrulating mesoderm. Elife. 2014;3:e03848. https://doi.org/10.7554/eLife.03848.

90. Lu X, Meng X, Morris CA, et al. A novel human gene, WSTF, is deleted in Williams syndrome. Genomics. 1998;54:241–9.
91. Oya H, Yokoyama A, Yamaoka I, et al. Phosphorylation of Williams syndrome transcription factor by MAPK induces a switching between two distinct chromatin remodeling complexes. J Biol Chem. 2009;284:32472–82.
92. Randall V, McCue K, Roberts C, et al. Great vessel development requires biallelic expression of Chd7 and Tbx1 in pharyngeal ectoderm in mice. J Clin Invest. 2009;119:3301–10.
93. Rottbauer W, Saurin AJ, Lickert H, et al. Reptin and pontin antagonistically regulate heart growth in zebrafish embryos. Cell. 2002;111:661–72.
94. Filippakopoulos P, Knapp S. Targeting bromodomains: epigenetic readers of lysine acetylation. Nat Rev Drug Discov. 2014;13:337–56. https://doi.org/10.1038/nrd4286.
95. Linares-Saldana R, et al. BRD4 orchestrates genome folding to promote neural crest differentiation. Nat Genet. 2021;53:1480–92. https://doi.org/10.1038/s41588-021-00934-8.
96. Spiltoir JI, Stratton MS, Cavasin MA, et al. BET acetyl-lysine binding proteins control pathological cardiac hypertrophy. J Mol Cell Cardiol. 2013;63:175–9.
97. Anand P, Brown JD, Lin CY, et al. BET bromodomains mediate transcriptional pause release in heart failure. Cell. 2013;154:569–82.
98. Filippakopoulos P, Qi J, Picaud S, et al. Selective inhibition of BET bromodomains. Nature. 2010;468:1067–73.
99. Kim SY, et al. Epigenetic reader BRD4 (Bromodomain-containing protein 4) governs nucleus-encoded mitochondrial transcriptome to regulate cardiac function. Circulation. 2020;142:2356–70. https://doi.org/10.1161/CIRCULATIONAHA.120.047239.
100. Padmanabhan A, et al. BRD4 (Bromodomain-containing protein 4) interacts with GATA4 (GATA binding protein 4) to govern mitochondrial homeostasis in adult cardiomyocytes. Circulation. 2020;142:2338–55. https://doi.org/10.1161/CIRCULATIONAHA.120.047753.
101. Alexanian M, et al. A transcriptional switch governs fibroblast activation in heart disease. Nature. 2021;595:438–43. https://doi.org/10.1038/s41586-021-03674-1.
102. Aghajanian H, et al. Targeting cardiac fibrosis with engineered T cells. Nature. 2019;573:430–3. https://doi.org/10.1038/s41586-019-1546-z.
103. Vagnozzi RJ, et al. An acute immune response underlies the benefit of cardiac stem cell therapy. Nature. 2020;577:405–9. https://doi.org/10.1038/s41586-019-1802-2.
104. Gyuris A, Donovan DJ, Seymour KA, et al. The chromatin-targeting protein Brd2 is required for neural tube closure and embryogenesis. Biochim Biophys Acta. 2009;1789:413–21.
105. Shang E, Wang X, Wen D, et al. Double bromodomain-containing gene Brd2 is essential for embryonic development in mouse. Dev Dyn. 2009;238:908–17.
106. Houzelstein D, Bullock SL, Lynch DE, et al. Growth and early postimplantation defects in mice deficient for the bromodomain-containing protein Brd4. Mol Cell Biol. 2002;22:3794–802.
107. Schermelleh L, Carlton PM, Haase S, et al. Subdiffraction multicolor imaging of the nuclear periphery with 3D structured illumination microscopy. Science. 2008;320:1332–6.
108. Guelen L, Pagie L, Brasset E, et al. Domain organization of human chromosomes revealed by mapping of nuclear lamina interactions. Nature. 2008;453:948–51.
109. Akhtar A, Gasser SM. The nuclear envelope and transcriptional control. Nat Rev Genet. 2007;8:507–17.
110. Capelson M, Liang Y, Schulte R, et al. Chromatin-bound nuclear pore components regulate gene expression in higher eukaryotes. Cell. 2010;140:372–83.
111. Reddy KL, Zullo JM, Bertolino E, et al. Transcriptional repression mediated by repositioning of genes to the nuclear lamina. Nature. 2008;452:243–7.
112. Andrulis ED, Neiman AM, Zappulla DC, et al. Perinuclear localization of chromatin facilitates transcriptional silencing. Nature. 1998;394:592–5.
113. Peric-Hupkes D, Meuleman W, Pagie L, et al. Molecular maps of the reorganization of genome-nuclear lamina interactions during differentiation. Mol Cell. 2010;38:603–13.

114. Meister P, Towbin BD, Pike BL, Ponti A, Gasser SM. The spatial dynamics of tissue-specific promoters during C. elegans development. Genes Dev. 2010;24:766–82. https://doi.org/10.1101/gad.559610.
115. Poleshko A, et al. Genome-nuclear lamina interactions regulate cardiac stem cell lineage restriction. Cell. 2017;171:573–587.e514. https://doi.org/10.1016/j.cell.2017.09.018.
116. Kind J, et al. Single-cell dynamics of genome-nuclear lamina interactions. Cell. 2013;153:178–92. https://doi.org/10.1016/j.cell.2013.02.028.
117. See K, et al. Lineage-specific reorganization of nuclear peripheral heterochromatin and H3K9me2 domains. Development. 2019;146(3):dev174078. https://doi.org/10.1242/dev.174078.
118. Poleshko A, et al. H3K9me2 orchestrates inheritance of spatial positioning of peripheral heterochromatin through mitosis. Elife. 2019;8:e49278. https://doi.org/10.7554/eLife.49278.
119. Smith CL, Lan Y, Jain R, Epstein JA, Poleshko A. Global chromatin relabeling accompanies spatial inversion of chromatin in rod photoreceptors. Sci Adv. 2021;7:eabj3035. https://doi.org/10.1126/sciadv.abj3035.
120. Shah PP, Keough KC, Gjoni K, et al. An atlas of lamina-associated chromatin across twelve human cell types reveals an intermediate chromatin subtype. Genome Biol. 2023;24(1):16. https://doi.org/10.1186/s13059-023-02849-5
121. Filion GJ, et al. Systematic protein location mapping reveals five principal chromatin types in Drosophila cells. Cell. 2010;143:212–24. https://doi.org/10.1016/j.cell.2010.09.009.
122. Ernst J, Kellis M. ChromHMM: automating chromatin-state discovery and characterization. Nat Methods. 2012;9:215–6. https://doi.org/10.1038/nmeth.1906.
123. Smith CL, Poleshko A, Epstein JA. The nuclear periphery is a scaffold for tissue-specific enhancers. Nucleic Acids Res. 2021;49:6181–95. https://doi.org/10.1093/nar/gkab392.
124. Ho CY, Jaalouk DE, Vartiainen MK, et al. Lamin A/C and emerin regulate MKL1-SRF activity by modulating actin dynamics. Nature. 2013;497:507–11.
125. Gruenbaum Y, Margalit A, Goldman RD, et al. The nuclear lamina comes of age. Nat Rev Mol Cell Biol. 2005;6:21–31.
126. Lee J, et al. Activation of PDGF pathway links LMNA mutation to dilated cardiomyopathy. Nature. 2019;572:335–40. https://doi.org/10.1038/s41586-019-1406-x.
127. Shah PP, et al. Pathogenic LMNA variants disrupt cardiac lamina-chromatin interactions and de-repress alternative fate genes. Cell Stem Cell. 2021;28:938–954.e939. https://doi.org/10.1016/j.stem.2020.12.016.
128. Bertero A, et al. Chromatin compartment dynamics in a haploinsufficient model of cardiac laminopathy. J Cell Biol. 2019;218:2919–44. https://doi.org/10.1083/jcb.201902117.
129. Alber F, Dokudovskaya S, Veenhoff LM, et al. The molecular architecture of the nuclear pore complex. Nature. 2007;450:695–701.
130. Vaquerizas JM, Suyama R, Kind J, et al. Nuclear pore proteins nup153 and megator define transcriptionally active regions in the Drosophila genome. PLoS Genet. 2010;6:e1000846.
131. Kalverda B, Pickersgill H, Shloma VV, et al. Nucleoporins directly stimulate expression of developmental and cell-cycle genes inside the nucleoplasm. Cell. 2010;140:360–71.
132. Titus LC, Dawson TR, Rexer DJ, et al. Members of the RSC chromatin-remodeling complex are required for maintaining proper nuclear envelope structure and pore complex localization. Mol Biol Cell. 2010;21:1072–87.
133. Zhang X, Chen S, Yoo S, et al. Mutation in nuclear pore component NUP155 leads to atrial fibrillation and early sudden cardiac death. Cell. 2008;135:1017–27.
134. Kehat I, Accornero F, Aronow BJ, et al. Modulation of chromatin position and gene expression by HDAC4 interaction with nucleoporins. J Cell Biol. 2011;193:21–9.
135. Lieberman-Aiden E, et al. Comprehensive mapping of long-range interactions reveals folding principles of the human genome. Science. 2009;326:289–93. https://doi.org/10.1126/science.1181369.

136. Ryba T, et al. Evolutionarily conserved replication timing profiles predict long-range chromatin interactions and distinguish closely related cell types. Genome Res. 2010;20:761–70. https://doi.org/10.1101/gr.099655.109.
137. Zhang Y, et al. Transcriptionally active HERV-H retrotransposons demarcate topologically associating domains in human pluripotent stem cells. Nat Genet. 2019;51:1380–8. https://doi.org/10.1038/s41588-019-0479-7.
138. Bertero A, et al. Dynamics of genome reorganization during human cardiogenesis reveal an RBM20-dependent splicing factory. Nat Commun. 2019;10:1538. https://doi.org/10.1038/s41467-019-09483-5.
139. Rao SSP, et al. Cohesin loss eliminates all loop domains. Cell. 2017;171:305–320.e324. https://doi.org/10.1016/j.cell.2017.09.026.
140. Yu M, Ren B. The three-dimensional organization of mammalian genomes. Annu Rev Cell Dev Biol. 2017;33:265–89. https://doi.org/10.1146/annurev-cellbio-100616-060531.
141. Dixon JR, et al. Topological domains in mammalian genomes identified by analysis of chromatin interactions. Nature. 2012;485:376–80. https://doi.org/10.1038/nature11082.
142. Nora EP, et al. Spatial partitioning of the regulatory landscape of the X-inactivation Centre. Nature. 2012;485:381–5. https://doi.org/10.1038/nature11049.
143. Beagan JA, Phillips-Cremins JE. On the existence and functionality of topologically associating domains. Nat Genet. 2020;52:8–16. https://doi.org/10.1038/s41588-019-0561-1.
144. Flavahan WA, et al. Insulator dysfunction and oncogene activation in IDH mutant gliomas. Nature. 2016;529:110–4. https://doi.org/10.1038/nature16490.
145. Hnisz D, et al. Activation of proto-oncogenes by disruption of chromosome neighborhoods. Science. 2016;351:1454–8. https://doi.org/10.1126/science.aad9024.
146. Narendra V, et al. CTCF establishes discrete functional chromatin domains at the Hox clusters during differentiation. Science. 2015;347:1017–21. https://doi.org/10.1126/science.1262088.
147. Rosa-Garrido M, et al. High-resolution mapping of chromatin conformation in cardiac myocytes reveals structural remodeling of the epigenome in heart failure. Circulation. 2017;136:1613–25. https://doi.org/10.1161/CIRCULATIONAHA.117.029430.
148. Hocker JD, et al. Cardiac cell type-specific gene regulatory programs and disease risk association. Sci Adv. 2021;7 https://doi.org/10.1126/sciadv.abf1444.
149. Lee DP, et al. Robust CTCF-based chromatin architecture underpins epigenetic changes in the heart failure stress-gene response. Circulation. 2019;139:1937–56. https://doi.org/10.1161/CIRCULATIONAHA.118.036726.
150. Tan WLW, et al. Epigenomes of human hearts reveal new genetic variants relevant for cardiac disease and phenotype. Circ Res. 2020;127:761–77. https://doi.org/10.1161/CIRCRESAHA.120.317254.
151. Su JH, Zheng P, Kinrot SS, Bintu B, Zhuang X. Genome-scale imaging of the 3D organization and transcriptional activity of chromatin. Cell. 2020;182:1641–1659.e1626. https://doi.org/10.1016/j.cell.2020.07.032.
152. Bintu B, et al. Super-resolution chromatin tracing reveals domains and cooperative interactions in single cells. Science. 2018; 362. https://doi.org/10.1126/science.aau1783
153. Mateo LJ, et al. Visualizing DNA folding and RNA in embryos at single-cell resolution. Nature. 2019;568:49–54. https://doi.org/10.1038/s41586-019-1035-4.
154. Rao SS, et al. A 3D map of the human genome at kilobase resolution reveals principles of chromatin looping. Cell. 2014;159:1665–80. https://doi.org/10.1016/j.cell.2014.11.021.
155. Nora EP, et al. Targeted degradation of CTCF decouples local insulation of chromosome domains from genomic compartmentalization. Cell. 2017;169:930–944.e922. https://doi.org/10.1016/j.cell.2017.05.004.
156. Haarhuis JHI, et al. The Cohesin release factor WAPL restricts chromatin loop extension. Cell. 2017;169:693–707.e614. https://doi.org/10.1016/j.cell.2017.04.013.
157. Hansen AS, Pustova I, Cattoglio C, Tjian R, Darzacq X. CTCF and cohesin regulate chromatin loop stability with distinct dynamics. Elife. 2017;6 https://doi.org/10.7554/eLife.25776.

158. Schwarzer W, et al. Two independent modes of chromatin organization revealed by cohesin removal. Nature. 2017;551:51–6. https://doi.org/10.1038/nature24281.
159. Wutz G, et al. Topologically associating domains and chromatin loops depend on cohesin and are regulated by CTCF, WAPL, and PDS5 proteins. EMBO J. 2017;36:3573–99. https://doi.org/10.15252/embj.201798004.
160. Vian L, et al. The energetics and physiological impact of Cohesin extrusion. Cell. 2018;173:1165–1178.e1120. https://doi.org/10.1016/j.cell.2018.03.072.
161. Fudenberg G, et al. Formation of chromosomal domains by loop extrusion. Cell Rep. 2016;15:2038–49. https://doi.org/10.1016/j.celrep.2016.04.085.
162. Chatfield KC, et al. Congenital heart disease in Cornelia de Lange syndrome: phenotype and genotype analysis. Am J Med Genet A. 2012;158A:2499–505. https://doi.org/10.1002/ajmg.a.35582.
163. Piche J, Van Vliet PP, Puceat M, Andelfinger G. The expanding phenotypes of cohesinopathies: one ring to rule them all! Cell Cycle. 2019;18:2828–48. https://doi.org/10.1080/15384101.2019.1658476.
164. Kline AD, et al. Diagnosis and management of Cornelia de Lange syndrome: first international consensus statement. Nat Rev Genet. 2018;19:649–66. https://doi.org/10.1038/s41576-018-0031-0.
165. Ciosk R, et al. Cohesin's binding to chromosomes depends on a separate complex consisting of Scc2 and Scc4 proteins. Mol Cell. 2000;5:243–54. https://doi.org/10.1016/s1097-2765(00)80420-7.
166. Tonkin ET, Wang TJ, Lisgo S, Bamshad MJ, Strachan T. NIPBL, encoding a homolog of fungal Scc2-type sister chromatid cohesion proteins and fly Nipped-B, is mutated in Cornelia de Lange syndrome. Nat Genet. 2004;36:636–41. https://doi.org/10.1038/ng1363.
167. Kim Y, Shi Z, Zhang H, Finkelstein IJ, Yu H. Human cohesin compacts DNA by loop extrusion. Science. 2019;366:1345–9. https://doi.org/10.1126/science.aaz4475.
168. Davidson IF, et al. DNA loop extrusion by human cohesin. Science. 2019;366:1338–45. https://doi.org/10.1126/science.aaz3418.

Cardiac Metabolism

19

Silvia Martin-Puig and Ivan Menendez-Montes

Abstract

The heart is composed of a heterogeneous mixture of cellular components perfectly intermingled and able to integrate common environmental signals to ensure proper cardiac function and performance. Metabolism defines a cell context-dependent signature that plays a critical role in survival, proliferation, or differentiation, being a recognized master piece of organ biology, modulating homeostasis, disease progression, and adaptation to tissue damage. The heart is a highly demanding organ, and adult cardiomyocytes require large amount of energy to fulfill adequate contractility. However, functioning under oxidative mitochondrial metabolism is accompanied with a concomitant elevation of harmful reactive oxygen species that indeed contributes to the progression of several cardiovascular pathologies and hampers the regenerative capacity of the mammalian heart. Cardiac metabolism is dynamic along embryonic development and substantially changes as cardiomyocytes mature and differentiate within the first days after birth. During early stages of cardiogenesis, anaerobic glycolysis is the main energetic program, while a progressive switch toward oxidative phosphorylation is a hallmark of myocardium differentiation. In response to cardiac injury, different signaling pathways participate in a metabolic rewiring to reactivate embryonic bioenergetic programs or the utilization of alternative substrates,

S. Martin-Puig (✉)
Department of Metabolic and Immune Diseases, Institute for Biomedical Research "Sols-Morreale", National Spanish Research Council, CSIC, Madrid, Spain

Cardiac Regeneration Program, National Center for Cardiovascular Research, CNIC, Madrid, Spain
e-mail: smartinp@cnic.es; smpuig@iib.uam.es

I. Menendez-Montes
Department of Internal Medicine, University of Texas Southwestern Medical Center, Dallas, TX, USA

© The Author(s), under exclusive license to Springer Nature Switzerland AG 2024

S. Rickert-Sperling et al. (eds.), *Congenital Heart Diseases: The Broken Heart*,
Advances in Experimental Medicine and Biology 1441,
https://doi.org/10.1007/978-3-031-44087-8_19

reflecting the flexibility of heart metabolism and its central role in organ adaptation to external factors. Despite the well-established metabolic pattern of fetal, neonatal, and adult cardiomyocytes, our knowledge about the bioenergetics of other cardiac populations like endothelial cells, cardiac fibroblasts, or immune cells is limited. Considering the close intercellular communication and the influence of nonautonomous cues during heart development and after cardiac damage, it will be fundamental to better understand the metabolic programs in different cardiac cells in order to develop novel interventional opportunities based on metabolic rewiring to prevent heart failure and improve the limited regenerative capacity of the mammalian heart.

Keywords

Cardiac metabolism · Glycolysis · Fatty acid oxidation · Pentose phosphate pathway · Hypoxia · Oxidative stress · Cardiac development · Cardiac regeneration

19.1 Introduction

When mentioning metabolism, one usually thinks of hundreds of bioenergetic intermediates, enzymes, and a complex map of cycles, fluxes, etc., remembering the old times of biochemistry lessons at university. However, nowadays, metabolism is considered a keystone in biological processes, from immune regulation to organ development and regeneration or disorders, opening attractive opportunities for therapeutic intervention in many diseases such as cancer. In the setting of the cardiovascular system, research on cardiac metabolism opened a new field to better understand the physiology of the heart in homeostasis and during pathological conditions.

Most of the studies performed on cardiac metabolism so far have focused on cardiomyocytes; while understanding the metabolic programs governing other cardiac populations, like endothelial cells or cardiac fibroblasts, both, in resting conditions and upon an insult, will bring fundamental information for an integrative view of cardiovascular pathophysiology. Moreover, the increasing knowledge on how the metabolic status influences the differentiation and functional capabilities of different inflammatory cell types opens the question of whether certain developmental or pathological conditions might be associated with a specific bioenergetic signature in a subset of immune cells.

Here, we will review our current knowledge on cardiac metabolism, including the metabolic signature during embryonic stages and the changes required for cardiac differentiation and myocardial growth until adult maturation. Moreover, we will review the most recent discoveries connecting bioenergetics and cardiovascular regeneration and comment on the perspectives toward therapeutic applications for heart repair based on the metabolic modulation.

19.2 Cardiac Metabolism During Heart Development

Immature cardiomyocytes mainly rely on anaerobic use of glucose as a metabolic substrate in contrast to the use of glucose oxidation and fatty acid oxidation (FAO) in the mitochondria as the principal energy source in the adult heart [1]. This is essentially due to the combination of three main factors. First, the fact is that cardiogenesis occurs under low oxygen conditions, especially during its early stages [2]. Second, the low availability of free FA in the fetal blood [3], together with the immaturity of FAO enzymatic machinery in the embryonic heart [4]. Finally, glycolysis being not just a metabolic fuel but also a source of building blocks to support biosynthetic processes and cell growth during fast organ development [5]. In addition to substrate availability, there are specific regulations of glycolytic components that direct adenosine triphosphate (ATP) production, such as differential association of hexokinase isoforms with mitochondria between the fetal and adult stages [6].

The fact is that the embryonic myocardium largely relies on the anaerobic utilization of glucose and lactate, while the adult heart mostly functions under oxidative mitochondrial metabolism, implying the existence of a metabolic switch in between those stages. Interestingly, this bioenergetic reprogramming also occurs during in vitro differentiation of stem cells into cardiomyocytes, where the metabolic switch from glycolysis to mitochondrial oxidation of substrates is an essential step of cardiac differentiation [7].

As mentioned above, hypoxia and thus oxygen levels represent important aspects of the embryonic cardiac microenvironment governing cardiac metabolism. Initially, the embryonic heart was described globally as a hypoxic structure [2]. However, more recent studies demonstrated that Hypoxia Inducible Factor (HIF) signaling, the main cellular pathway mediating the transcriptional response to hypoxia, is not uniformly activated in all cardiac cell types and in contrast shows a well-defined spatiotemporal expression pattern during heart development [8, 9]. Thus, in early stages, around E9.0, when the heart is mainly formed by few layers of cardiomyocytes, HIF1α is expressed along the whole myocardium, correlating with a highly active glycolytic signature. However, as development progresses, the ventricular myocardium starts to differentiate into two distinct subpopulations: the *compact myocardium* that retains high expression of HIF1α and glycolytic enzymes and the *trabecular myocardium*, where HIF1 signaling and glycolytic signature are downregulated, in parallel with the enhanced mitochondrial activity in cardiomyocytes of this embryonic heart layer [9, 10]. Interestingly, this spatial regulation of HIF1 signaling and the metabolic compartmentalization of the embryonic myocardium also exhibit a temporal control through which HIF1α protein levels on the compact myocardium progressively diminish from E9.5 to E14.5, when it is barely detected. The influence of HIF1 signaling over embryonic cardiac metabolism occurs directly through HIF1-mediated gene expression of glycolytic enzymes [8–10] and also indirectly through the regulation of metabolic master regulatory pathways, such as PGC1a, Mxi1, or Hand1 [9, 11].

This embryonic metabolic shift is accompanied by a maturation of cardiac mitochondria. It has been described that mitochondria increases in number and

complexity as the embryonic heart develops. Between E9.5 and E13.5, at early stages, mitochondria show immature cristae and expanded matrix, while later on mitochondria develop more organized cristae and a compacted matrix, reflecting the increased reliance on mitochondrial oxidative metabolism for energy production. In addition, the intracellular distribution of the mitochondria also changes, from a perinuclear pattern by E9.5 to a more established network aligned with the sarcomeric apparatus by E13.5 [12]. This mitochondrial maturation has direct implications in myocyte maturation, raising the connection between metabolism and cardiac differentiation. The closure of the mitochondrial permeability transition pore (mPTP) that happens from E9.5 to E11.5-13.5 reduces the amount of reactive oxygen species (ROS) released by the mitochondria, directly enhancing myocyte differentiation [12]. Respiratory complexes start to assemble in the cardiac mitochondria around E11.5-E12.5, with compact mitochondrial matrices and increased number of respirasomes in the cristae [13–15]. This progressive maturation of the mitochondrial network in the embryonic heart ensures the presence of the adequate bioenergetic machinery to allow the initiation of FAO and aerobic glycolysis by midgestation (around E14.5). Mitochondria maturation is also regulated in a spatial manner, with trabecular cardiomyocytes displaying increased mitochondrial content and activity relative to the compact myocardium, holding reduced mitochondrial number with more immature features [9]. This embryonic metabolic switch, and drop in HIF1α levels in the compact myocardium, is essential for proper cardiac development. Indeed, sustained HIF1 signaling by elimination of hypoxia main negative regulator, Von Hippel Lindau (VHL), causes growth arrest, thinning of the myocardial wall, chamber dilation, and immature conduction system, ultimately leading to embryonic lethality, which is rescued by double deletion of VHL and HIF1α [9]. These results clearly show that a progressive decrease in ventricular HIF1 signaling, in parallel with the onset of FAO and mitochondrial oxidative phosphorylation, is required for proper cardiac development and ventricular chamber formation (Fig. 19.1).

Despite its crucial role in establishing metabolic boundaries in the developing myocardium as highlighted by the findings on the hypoxia gain of function model mentioned above, blunting glycolysis upon elimination of *Hif1a* in cardiovascular progenitors showed that in mice, activation of the glycolytic program is dispensable for proper cardiac development and function [10]. Indeed, *Hif1a* loss results in a metabolic rewiring consisting in increased mitochondrial content and enhanced use of amino acids as anaplerotic source of energy and building blocks by E12.5. Interestingly, this adaptation is transient and does not preclude the establishment of embryonic FAO by E14.5 [10]. Overall, these results demonstrate that while sustained glycolysis is detrimental for heart development, premature loss of glucose utilization ability is not critical for proper cardiogenesis in mammals. In contrast, glycolytic requirements seem to be different in the zebrafish, where embryonic cardiac trabeculation requires an active glycolytic metabolic program, mainly controlled by the receptor tyrosine protein kinase ERBB2 [16]. Considering the different structural complexity, oxygen availability, and workload of the mammalian versus

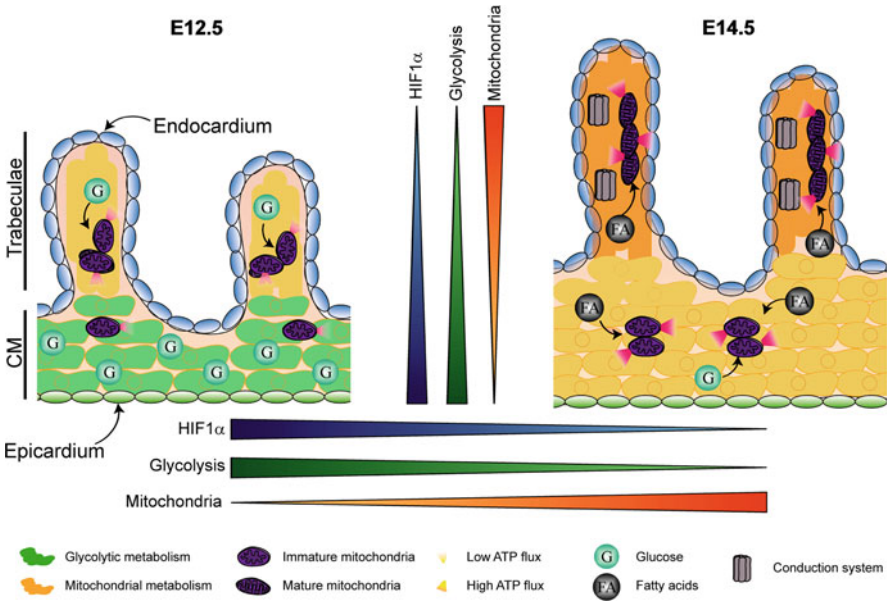

Fig. 19.1 Myocardial metabolism by midgestation. Schematic representation of a mouse embryonic ventricular chamber at E12.5 (left) and E14.5 (right). By E12.5, the compact myocardium (CM) metabolism is mainly based on glucose (G) consumption, while trabeculae display reduced expression of glycolytic enzymes and an immature mitochondrial network. By E14.5, CM metabolism switch to mitochondrial oxidation of fatty acids (FA) and trabeculae display a more mature and active mitochondrial network. This metabolic change is associated with higher ATP production and establishment of cardiac conduction system. Color triangles represent temporal (landscape) and spatial (portrait) gradients for HIF1 signaling (blue), glycolysis (green), and mitochondrial metabolism (orange). Higher color intensities indicate higher levels

the zebrafish heart, a full correlation of all the metabolic requirements needed for proper cardiac development may not be conserved.

It is important to note that there are some discrepancies in the literature about the outcomes of *Hif1a* deletion in embryonic cardiomyocytes. Some works reported embryonic lethality upon deletion and loss of HIF1 signaling [8, 17]. However, in these reports, the authors used a *Hif1a* floxed allele in combination with a germline *Hif1a* null allele. This global heterozygosity could explain the phenotypical differences in terms of embryonic lethality. Nevertheless, the transcriptional characterization of a heterozygous *Hif1a* null model in cardiac progenitors also revealed HIF1 dependency for the induction of glycolytic genes, as well as upregulation of amino acid transporters and the stress-induced transcription factor ATF4 [8], a master regulator of amino acid transport and metabolism [18].

From a developmental point of view, glucose is not only important as a source of energy through glycolysis when oxygen levels are low but also provides metabolic intermediates required for macromolecular biosynthesis. Indeed, glucose-6-

phosphate can be shunted to the pentose-phosphate pathway (PPP), a critical pathway for generating redox balance and influencing anabolism through the control of NADPH pool and providing carbon precursors for nucleotide synthesis required for proliferation [19]. Despite the exquisite spatiotemporal control of glycolytic enzyme expression during development, glucose has been shown to inhibit cardiomyocyte maturation and to promote cardiomyocyte proliferation through the PPP in human-ESC-derived cardiomyocytes [20]. In this way, the progressive decrease in glucose uptake in the fetal heart allows for the decrease in proliferation by nucleotide deprivation, gradually inducing cardiomyocyte maturation. This observation is also consistent with the fact that sustained glucose uptake and glycolysis upon *Vhl* loss result in maturation defects, especially at the level of cardiac conduction system development [9]. In this regard, sustained HIF1 signaling upon *Vhl* elimination is accompanied with a drastic reduction of the marker of early differentiating conduction system Connexin 40 [21] in the trabeculae of mutant embryos. Interestingly, Connexin 40 KO mice show delayed activation of the ventricles, which is in agreement with the decreased contractility observed in E14.5 *Vhl*-deficient embryos [9]. However, whether deficient establishment of the functional conduction system in *Vhl* mutant heart is due to altered HIF1 signaling, or sustained glycolysis remains uncertain, and further research will be needed to evaluate the direct role of metabolism during cardiac conduction system establishment.

19.3 Metabolic Switch at Postnatal Stages

The adult heart has high ATP demand to sustain the contractile activity. Ninety-five percent of the ATP in the adult heart is achieved by mitochondrial oxidative phosphorylation (OXPHOS), with FA as the main source of energy (60% of mitochondria-derived ATP, although this percentage varies with the time of the day, the nutritional status, and the energetic needs), together with glucose, lactate, and ketones [22]. This energetic demand requires a metabolic adaptation in the early stages of postnatal life, when the heart rapidly adapts from anaerobic glucose utilization to more efficient mitochondrial OXPHOS. For instance, in isolated rabbit hearts, glycolysis decreases from 44% to 5% contribution to ATP production in the first week of life, while following an opposite pattern, FAO increases from 13 to 39% [23].

A recent multiomics analysis confirmed these observations, and by means of proteomics, transcriptomics, and metabolomics characterization, Lalowski and coworkers confirmed that the postnatal day 1 (P1) murine heart largely relies on glycolysis, mostly through a fructose-induced mechanism. In contrast, during the first postnatal week of live, the number of metabolites involved in FAO and FA synthesis is coordinately increased, consistent with an elevation in mitochondrial oxidative metabolism and increased ROS production [24].

This transition from anaerobic glucose utilization to mitochondrial OXPHOS of glucose-derived pyruvate and FA not only influences the energy production capacity of the neonatal heart but also impacts on cardiomyocyte biology. While this

metabolic switch ensures the massive ATP production required to sustain effective cardiac function, it also has negative effects, such as increased DNA damage and reduction of cardiomyocyte proliferative capacity [25]. This is due, at least in part, to higher ROS production and increased nuclear oxidation upon FAO, which ultimately enhances DNA damage and promotes cell growth arrest [26].

19.4 Cardiac Regeneration and Metabolic Rewiring

19.4.1 General Considerations

Adult mammalian hearts lack the capacity of an effective regenerative response exhibited by other vertebrates like zebrafish that can fully repair their hearts upon injury [27] through proliferation of preexisting cardiomyocytes. Neonatal mammals, like mice and pigs, also display the ability to regenerate the heart after a myocardial insult, although just for few days right after birth [28–30]. During this short regenerative window, new cardiac muscle also arises from proliferation of preexisting cardiomyocytes though hyperplasia as it occurs in the zebrafish [31–33]. Cardiomyocyte proliferation at later stages in mice is achieved by a hypertrophic mechanism and implies polyploidization [34, 35]. This type of organ growth and the minimal turnover of adult mammalian cardiomyocytes [36] limit the capacity to replace the large amount of damaged tissue and huge cell death upon myocardial infarction. Therefore, there is an urgent need to develop alternative regenerative therapies for cardiac replacement upon cardiac damage. Considering the difficulties of obtaining full maturation of cardiomyocytes derived from pluripotent stem cells, as well as functional limitations of cellular-based therapies, like arrhythmia or coupling complications, a new trend in the cardiac regeneration field is focused on uncovering the endogenous cardiomyocyte proliferation strategies during the early postnatal window in order to reactivate them in the setting of cardiac injury.

Metabolism controls numerous biological processes and in the heart plays a crucial role in producing sufficient energy to sustain cardiac function. Nevertheless, our understanding about the influence of metabolism during cardiac repair and regeneration remains poorly understood. Indeed, metabolism has emerged as a novel line of investigation connecting embryonic, postnatal, and adult life with cardiomyocyte proliferation and heart repair capacity. Although less studied, novel evidences highlight the importance of non-myocyte metabolism during cardiac regeneration [37]. Therefore, metabolic modulation of different cardiac components could represent a novel opportunity for therapeutic intervention to improve heart tissue repair after injury in adult stages. In this section, we review our current knowledge on cardiac metabolism during homeostasis and in regeneration and discuss potential strategies based on the metabolic control of different cardiac populations with special focus on cardiomyocytes.

19.4.2 Hypoxia and Metabolism

HIFs are key transcriptional regulators controlling cellular adaptation to low oxygen availability. One of the most common adaptive responses to hypoxia consists of the coordinated expression of glycolytic enzymes to favor glucose uptake and ATP production in the cytoplasm instead of through the electron transport chain (ETC) which requires oxygen as an electron acceptor in the last steps of oxidative metabolism. Under hypoxic conditions, HIFs mediate the expression of all glycolytic enzymes and pyruvate dehydrogenase kinase 1 (PDK1), which phosphorylates pyruvate dehydrogenase (PDH) preventing oxidation of pyruvate into the mitochondria. In addition, through the induction of lactate dehydrogenase a (LDHa), HIFs favor the reduction of pyruvate into lactate, establishing a mitochondrial alternative for energy production [38]. This type of metabolic reprograming is common in cancer cells that need to grow under low oxygen conditions and was described by Otto Warburg in the 1920s [39].

As discussed in the former section of *cardiac metabolism during heart development*, the role of HIF signaling in cardiac metabolic control has been well characterized during cardiogenesis, when HIF1 expression mediates the metabolic compartmentalization of the growing myocardium and regulates the expression of key glycolytic enzymes (GLUT1, PDK1, and LDHa) in the proliferative compact myocardium [9]. One important aspect to keep in consideration is the fact that not all the hypoxia-induced responses are mediated by the transcriptional activity of HIF. For instance, several genes like Tank binding protein (TBK1) [40], Cyclin D1 [41], Thrombospondin-1 (TSP-1) [42], or heme-oxygenase 1 (HO-1) [43], which is part of an endogenous defense system against oxidative stress, are induced by low oxygen or PHD inhibition independently of HIF. Most of the current findings related to the role of hypoxia on cardiac regeneration have been performed exposing the embryos, pups, or adult animals to low oxygen concentrations, or high glucose, while genetic characterization of the direct influence of HIF signaling on cardiomyocyte regeneration or heart repair awaits future investigation. Interestingly, exposure of neonatal mouse pups to hypoxia extends the regenerative ability of the heart beyond 7 days after birth, reducing the DNA-damage response and increasing cardiomyocyte proliferation through hyperplasia [25]. However, the definitive role of HIFs and HIF-mediated metabolic reprogramming of cardiomyocytes on the perinatal/postnatal window requires further analysis using genetic models. Regarding mature cardiomyocytes at later stages, fate mapping analysis has demonstrated that the adult mammalian heart contains clusters of $HIF1^+$ cardiomyocytes that display features of neonatal mononuclear cardiomyocytes, with smaller size, enhanced proliferative ability, reduced ROS-mediated DNA-damage, and enhanced glycolytic signature [44], strongly suggesting that local metabolic reprograming governed by HIF1 might be related to the residual cardiomyocyte turnover of the adult heart [36]. Hypoxia is required for heart regeneration in the zebrafish, participating in cardiomyocyte dedifferentiation and subsequent proliferation [31, 45], pointing to HIF signaling as a potential shared mechanism essential for heart repair between mammals and lower vertebrates with full cardiac regenerative capacity. Furthermore,

progressive oxygen dropping after myocardial infarction has been reported to reduce infarct scar size, promote cardiomyocyte proliferation, and enhance cardiac function, further reinforcing the importance of hypoxia-driven responses during mammalian heart repair [46].

Therefore, hypoxia exposure and modulation of HIFs could be considered attractive therapeutic targets for heart regeneration and cardiomyocyte proliferation, while further understanding of the mechanism behind metabolic regulation by hypoxia/HIFs during cardiac repair is needed.

19.4.3 Metabolic Programs and Cardiac Regeneration

Work from different laboratories has demonstrated the capacity of the heart to metabolize different fuels depending on the maturation state and pathophysiological condition [47]. Adult cardiomyocytes are energetically very demanding and require a constant metabolic flux to produce ATP. The myocardium is enriched in mitochondria not only through OXPHOS, especially from FA (60–70%) and glucose (30–40%), but also using a variety of alternative fuels, like lactate, ketones, or amino acids, which can feed the TCA cycle, produce sufficient energy to enable the costly process of cardiac contraction [48, 49]. While FAO results in higher ATP production than anaerobic glycolysis [19], FAO is associated with higher oxidative stress due to enhanced mitochondrial ROS production in the ETC [26, 50], which as discussed above, could favor a DNA-damage response and impair cardiomyocyte proliferation [25]. Following different types of cardiac insult like ischemia or pressure overload, the mammalian heart undergoes a metabolic reprogramming toward anaerobic glycolysis [51], which might be partially due to HIF induction in poorly oxygenated tissues after cardiac damage [52, 53].

Interestingly, it has been recently reported that the adult zebrafish heart contains higher levels of FAO enzymes than juvenile fish [54] and that after cardiac injury there is a metabolic reprograming of a subset of cardiomyocytes close to the border zone, which switch from mitochondrial OXPHOS to anaerobic glycolysis and pyruvate reduction to lactate compared to the metabolic program of cardiomyocytes from the remote area that is based in FAO [54, 55]. This pool of cardiomyocytes of the border zone acquired an embryonic-like phenotype and is capable to proliferate and contribute to the regeneration of the damaged tissue. In this work, the authors propose that this metabolic reprograming might be independent of HIF1, as they did not observe any correlation between a GFP reporter for the HIF1-target *prolyl hydroxylase 3* (*phd3*) and instead described a novel role for the Neuregulin-1 (Nrg1)/Erbb2 pathway in the metabolic reprograming required for cardiac regeneration [55]. This new function of Nrg1/Erbb2 signaling controlling bioenergetics in the setting of cardiac regeneration contributes to a better understanding of the positive effect of this pathway during heart repair previously reported in murine hearts [56] and demonstrates the critical importance of metabolism in the physiological and pathological responses of cardiac tissue. Nevertheless, the potential participation of HIF1 signaling in the local metabolic reprograming of border zone cardiomyocytes

in the zebrafish upon cryoinjury cannot be fully excluded, as there are 2 additional *phd* genes—*phd1* and *phd2*—that could be induced in response to cardiac damage and because *phd1* is another established HIF1 target [57]. In addition, it is important to keep in mind that in murine hearts, HIF1 controls the expression of glycolytic enzymes like PDK1, LDHa, or GLUT1 in the developing compact myocardium [8–10]. Furthermore, hypoxia is important to promote cardiomyocyte proliferation in response to cardiac damage, both in mammals [44, 46] and in zebrafish [45], while the definitive relevance of HIF1 signaling in cardiac regeneration and injury-induced metabolic reprograming awaits future experiments with genetic models.

In mammals, induction of glucose metabolism through overexpression of the main embryonic glucose transporter GLUT1 improves the regenerative capacity of the neonatal heart, increasing cardiomyocyte proliferation and reducing scar size [58]. In vivo administration of the non-metabolizable glucose analogue 2-deoxy-D-glucose (2-DG)—a hexokinase 2 inhibitor broadly used to block glycolysis—to postnatal day 1 old (P1) pups immediately after induction of myocardial infarction significantly impairs the cardiac functional recovery of the neonatal mouse heart [59]. Moreover, repeated injections with 2DG substantially impairs cardiomyocyte proliferation at the border zone of adult zebrafish after cryoinjury [54, 55]. Another line of evidence supports that increased conversion of pyruvate into lactate by elimination of the master regulator of mitochondrial biogenesis and oxidative metabolism, peroxisome proliferator-activated receptor gamma coactivator 1 alpha (PPARGC1a/PGC1a), enhances cardiomyocyte proliferation and dedifferentiation in adult zebrafish [54]. Altogether, these results suggest that promoting glucose metabolism is important for both mammalian and zebrafish cardiomyocyte cell cycle reentry in response to acute cardiac damage.

Despite the important role of glucose-based metabolism during cardiac regeneration, sustained glycolytic activity during heart development is deleterious, impairing mammalian cardiomyocyte maturation and causing different types of congenital cardiac defects [9, 20]. In addition, although a metabolic switch toward glycolysis is initially beneficial and provides acute protection to cardiac damage in the adulthood, during the progression to heart failure [60, 61], there is a gradual mitochondrial damage and hence an increasing reliance on anaerobic glycolysis that contributes to contractile dysfunction and adverse remodeling [61, 62].

An important fact to consider is that reactivation of glucose metabolism upon cardiac injury not only provides an alternative source of ATP production to mitochondrial respiration but also contributes to diminishing oxidative stress by reducing mitochondrial ROS generation at the ETC. Furthermore, glucose is supplied to the cells with metabolic intermediates and building blocks required for cell growth and repairs such as nucleotides, amino acids, or lipids through the PPP and one carbon metabolism, which are indeed more limiting factors than ATP for cell proliferation [5]. Recent findings demonstrate that Krüppel-like factor 1 (KLF1), which is upregulated in the adult zebrafish heart upon injury, has a damage-independent capacity to stimulate cardiomyocyte proliferation and dedifferentiation by means of epigenetic mechanisms that promote cell cycle reentry, favoring sarcomere disassembly and modulating cardiac metabolism [63]. This metabolic rewiring

consists not only in the downregulation of genes involved in mitochondrial biogenesis like *pgc1a* or genes participating in OXPHOS/TCA cycle but also in a marked reduction of glycolytic genes and intermediates. These results suggest that instead of acquiring a glycolytic program toward lactate production during cardiac regeneration, alternative metabolic pathways might be involved in the regenerative response of adult zebrafish. In fact, KLF1-mediated metabolic reprogramming involves the increased expression of genes of the PPP and serine synthesis pathways [63] that act as glycolytic shunts for macromolecule production and anabolic reactions, at the time that contribute to the production of antioxidant capacity through the generation of NADPH, an important contributor of anabolism. A similar observation has been recently confirmed in murine hearts, where cardiac cryoinjury of cardiomyocytes overexpressing GLUT1 increases metabolites of the PPP [58]. Whether this metabolic reprogramming toward PPP occurs during the endogenous regenerative response awaits future research.

Based on observations of endogenous programs directed to decrease mitochondrial OXPHOS to enhance the cardiomyogenic potential, different strategies oriented toward metabolic rewiring in this line have been recently explored in the mammalian heart. Elimination of dietary FA during early postnatal life contributes to expand cardiomyocyte proliferative capacity beyond P7. However, sustaining this free FA diet up to adult stages does not contribute to further cardiomyocyte renewal but instead favors the development of liver steatosis due to enhanced FA synthesis as a compensatory response [64]. Similarly, inhibition of the long-chain FA (LCFA) mitochondrial transporter carnitine palmitoyl transferase I (CPT1) by etoxomir impairs LCFA oxidation and promotes neonatal cardiomyocyte proliferation [65], although this metabolic tuning is not sufficient to induce adult cardiomyocyte cell cycle reentry [66]. A genetic approach to favor mitochondrial oxidation of glycolytic-derived pyruvate rather than LCFA is based on cardiomyocyte-specific deletion of pyruvate dehydrogenase kinase 4 (PDK4). This deletion results in pyruvate dehydrogenase (PDH) activation and leads to increased glucose oxidation relative to FAO promoting cardiomyocyte proliferation and number, as well as to the reduction in oxidative stress-associated DNA-damage response, together with functional improvement and enhanced cardiac repair upon injury [64]. In contrast, a parallel approach in zebrafish based on the use of a Pdk-insensitive constitutive active form of the pyruvate dehydrogenase orthologue *Pdha1a* leads to the reduction of proliferating cardiomyocytes after injury, consistent with decreased cell cycle reentry of zebrafish cardiomyocytes treated with the PDK inhibitor dichloroacetate (DCA) [54]. These important discrepancies on the regenerative responses between zebrafish and mammals when genetically manipulating pyruvate metabolism might reflect the complexity of PDK/PDH enzymes family, and the potential compensatory role of the variety of isoforms found in the cardiac tissue. Nevertheless, further investigation on the metabolic modulation between zebrafish and mammals might uncover interesting regenerative differences between both species.

The direct inhibition of the mitochondrial enzyme succinate dehydrogenase (SDH) has been recently proposed as another strategy to reprogram cardiac metabolism. Treatment with the SDH inhibitors dimethyl malonate or atpenin A5 extends

the regenerative window of mammalian pups beyond the first week after birth. In contrast, succinate promotes cardiomyocyte DNA-damage response and impairs the regenerative capacity of the neonatal heart by reducing cardiomyocyte proliferative capacity and preventing fibrotic scar resolution and functional recovery. More importantly, malonate, a reversible inhibitor of SHD, restores cardiac structure and function after adult myocardial infarction [67]. During the endogenous regenerative response in adult zebrafish, there is a remarkable reduction of SDH activity (~40%) in cardiomyocytes of the border zone relative to remote zone cardiomyocytes [55], suggesting that local reduction of TCA cycle and ETC flux is an essential step for an effective cardiac repair response. The reported changes in cardiac metabolism after SDH inhibition resemble similar mechanisms of metabolic reprogramming from OXPHOS toward glycolysis previously described in certain type of cancers such as paraganglioma or pheochromocytoma, where succinate accumulation leads to inhibition of PHDs, resulting in HIF1α stabilization, and subsequently, in the induction of glycolytic enzymes [68, 69]. Whether PHD inhibition and HIF1 stabilization play an active role in malonate-induced metabolic reprogramming of neonatal or adult mammalian hearts remains elusive and needs to be further investigated.

An alternative approach toward metabolic reprogramming to favor cardiovascular regeneration is based on the application of advanced modified-RNA (mod-RNA) technology, which allows a transient and local gene expression delivery to cardiomyocytes. It has been recently reported that transient overexpression of pyruvate kinase muscle isozyme 2 (PKM2) increases cardiomyocyte proliferation, functional recovery, and long-term survival after myocardial infarction in neonatal and adult mice [70]. Mammals have four isoforms of PK (L, R, M1, and M2), which are present in different cell types. Both PKL and PKR are encoded by the PKLR gene and are expressed in the liver and red blood cells, respectively [71]. The PK in other tissues is produced from the PKM gene, through a pre-mRNA that is alternatively spliced to yield the PKM1 or PKM2 isoform, which contains exon 9 or 10, respectively [72]. Pyruvate kinase M1 is expressed in most differentiated tissues, whereas PKM2 is found primarily in embryonic tissues and tumor cells [73]. Pyruvate kinase (PK) catalyzes the last step of glycolysis, favoring the dephosphorylation of phosphoenolpyruvate to pyruvate, contributing to mitochondrial-independent ATP production. While PKL, R, and M1 PK types are present as highly enzymatically active tetrameric forms, PKM2 can exist as either active tetramer or inactive dimer, which display higher and lower affinity for the substrate phosphoenolpyruvate, respectively [74]. In cancer cells, the less active dimeric form of PKM2 slows the glycolytic flux and favors the accumulation of glycolytic intermediates above pyruvate, redirecting them toward the PPP for anabolic biosynthetic reactions [74, 75]. In addition, PKM2 has a nuclear localization signal and has been described to interact with several proteins including HIF1 transcription factor [76] and β-catenin [77]. Transient expression of PKM2 by cardiomyocyte-specific mod-RNA delivery results in the elevation of the limiting enzyme of the PPP glucose-6-phosphate dehydrogenase (G6PD)-enhanced antioxidant capacity, as shown by raised NADPH and reduced glutathione pools, together with diminished levels of superoxide and other ROS, as well as decreased signs of DNA oxidative stress.

Moreover, elevated levels of PKM2 delivered by mod-RNA directly interacts with β-catenin in cardiomyocytes nuclei, inducing the upregulation of the cell cycle regulators Cyclins D1 and D2 or c-Myc among others [70]. Under conditions of cardiac disease, such as ischemia and heart failure, mammalian cardiomyocytes return to glucose-based metabolism and increase glycolytic enzymes, including PKM2 [78, 79]. However, endogenous raise of glycolytic enzymes after cardiac injury in mammals might be limited, as it does not lead to cardiomyocyte proliferation. The PKM2 orthologue in zebrafish *Pkma* is induced in the damaged heart upon injury and, when blocked, reduces the ability of cardiomyocytes to reenter cell cycle after injury [54], pointing to the important role of pyruvate metabolism in cardiac regeneration. Hence, PKM2 appears as a promising therapeutic target related to the cardiac metabolism that controls cardiomyocytes survival and proliferation upon an insult.

All these results demonstrate that metabolic rewiring in response to cardiac injury leads to a blockage of oxidative metabolism and enhancement of anaerobic pathways, including the activation of anabolism and antioxidant responses that appear key modulators for effective cardiac regeneration (Table 19.1 and Fig. 19.2). The metabolic adaptations to cardiac SDH inhibition in mammalian hearts involve a decrease in TCA cycle intermediates except for succinate, which rises, and a parallel elevation of several glycolytic metabolic intermediates albeit lack of lactate increase [67]. Interestingly, metabolomics analysis of malonate-treated hearts also shows a significant increase of several PPP intermediates like 6-phosphogluconate, sedoheptulose-7-phosphate or its glycolytic precursor, dihydroxyacetone phosphate, raising the attractive possibility of anabolic and antioxidant stimulation as important effectors of cardiac regeneration upon SDH inhibition. Furthermore, transient upregulation of PKM2 in mammalian cardiomyocytes also favors the generation of macromolecular precursors and contributes to reduce oxidative stress of cardiomyocytes, due to the slower enzymatic activity of PKM2 over PKM1, which reduces PK activity and promotes the anabolic branch toward PPP. Moreover, cardiomyocyte-specific G6PD mod-RNA delivery seems to be sufficient to induce cell cycle reentry through PPP [70], highlighting the importance of this glycolytic branch during cardiac regeneration. The results from Cardoso and collaborators indicate that despite utilizing mitochondrial machinery for energy production, the fuel oxidized within the mitochondria could directly influence the capacity of cardiomyocytes to reenter cell cycle at postnatal/adult stages [64]. Cardiac-PDK4 KO mice show a reduced DNA-damage response despite enhanced pyruvate oxidation over pyruvate reduction, suggesting that in vivo FAO metabolism is associated with increased oxidative stress. This observation is in agreement with recent findings, indicating that indeed FAO yields higher ROS production than glucose consumption in neonatal rat ventricular cardiomyocytes [26]. It would be interesting to investigate into further metabolic adaptations leading to lesser extend of oxidative stress in PDK4 KO mice and whether there is any connection with the PPP that is involved in cardiac regeneration in mammals and zebrafish [55, 67, 70]. Future investigations centered on direct regulation of PPP and other carbon branches of glycolysis for regenerative purposes are guaranteed.

Table 19.1 Table of genetic and pharmacological approaches for modulation of cardiac metabolism

Pathway	Effect	Model	Specie	Impact on the heart	References
Glycolysis	Inhibited	ERBB2 KO	Mouse	Reduced cardiomyocyte proliferation at birth and compensatory hypertrophy	D'Uva et al. [56]
Glycolysis	Increased	ERBB2 OE	Mouse	Increased cardiomyocyte dedifferentiation and proliferation and cardiomegaly	D'Uva et al. [56]
Glycolysis	Increased	Erbb2 OE	Zebrafish	Enhanced cardiomyocyte proliferation and improved regeneration	Honkoop et al. [55]
Glycolysis	Increased	GLUT1 OE	Mouse	Increased proliferation of neonatal cardiomyocytes and reduced scar size after injury	Fajardo et al. [58]
Glycolysis	Inhibited	2DG administration	Mouse	Impaired neonatal heart regeneration	Wang et al. [59]
Glycolysis	Inhibited	2DG administration	Zebrafish	Impaired cardiomyocyte proliferation after cryoinjury	Honkoop et al. [55]
Glycolysis	Increased	Ppargc1a KO	Zebrafish	Increased proliferation and dedifferentiation of neonatal cardiomyocytes	Fukuda et al. [54]
Glycolysis	Inhibited	Pkm2a/Pkmb dKO	Zebrafish	Larger scar size after cryoinjury	Fukuda et al. [54]
Glycolysis	Inhibited	Pdha1aSTA OE	Zebrafish	Decreased proliferation after injury	Fukuda et al. [54]
Glycolysis	Increased	Pdk3b OE	Zebrafish	Increased proliferation injury	Fukuda et al. [54]
PPP	Increased	Klf1 KO (ZF)	Zebrafish	Increased proliferation, decreased differentiation	Ogawa et al. [63]
PPP	Increased	GLUT1 OE	Mouse	Increased proliferation, reduced scar size	Fajardo et al. [58]
PPP	Increased	PKM2 mod-RNA	Mouse	Increased cardiomyocyte proliferation and functional recovery	Magadum et al. [70]
PPP	Increased	G6PD mod-RNA	Mouse	Cell cycle reentry	Magadum et al. [70]

(continued)

Table 19.1 (continued)

Pathway	Effect	Model	Specie	Impact on the heart	References
FAO	Inhibited	Fat free diet	Mouse	Expanded neonatal proliferation, liver steatosis, no effect in adult proliferation	Cardosco et al. [64]
FAO	Inhibited	PDK4 KO	Mouse	Increased proliferation and regeneration, reduced oxidative stress	Cardosco et al. [64]
FAO	Inhibited	Etoxomir administration	Mouse	Increased neonatal proliferation	Cao et al. [65]
TCA/ OXPHOS	Inhibited	Atpenin A5/malonate administration	Mouse	Extended neonatal proliferation window, restored cardiac function in the adult	Bae et al. [67]
TCA/ OXPHOS	Inhibited	Succinate administration	Mouse	Increased DNA damage response and prevented fibrotic scar resolution	Bae et al. [67]
Amino acid	Increased	Proline administration		Reduced scar size, decreased oxidative stress	Wang et al. [80]
BCAAs	Inhibited	PP2Cm KO		Increased failure in pressure overload	Lu et al. [81]

Different genetic models of loss of function (KO) or overexpression (OE) of different proteins as well as chemical treatment or special diet are depicted. The metabolic program modulated (Pathway) and whether it is activated or inhibited (Effect) are shown for each animal model either in mouse or zebrafish (Specie). The impact on cardiac proliferation and recovery is also indicated
PPP, pentose phosphate pathway; *FAO*, fatty acid oxidation; *TCA*, tricarboxylic acid; *OXPHOS*, oxidative phosphorylation; *BCAA*, branches amino acids; *2DG*, 2-deoxy-D-glucose

Our growing knowledge on the biological and functional implications of metabolic rewiring on adult hearts opens a new door within the cardiac regenerative field for therapeutic intervention based on metabolic modulators. Nevertheless, the long-term impact of metabolic rewiring in cardiomyocytes mitochondrial biology and contractile capacity might need to be evaluated in detail prior translational attempts, as it has been previously reported that sustained glycolysis could lead to mitochondrial dysfunction and sarcomeric disassembly [9, 20]. In this regard, the use of chemical inhibitors might have the important advantage of reversible modulation and temporal metabolic reprogramming, without taking on the risks of prolonged activation of certain pathways that might have long-term deleterious outcomes, while systemic administration of such drugs might lead to undesirable and unpredictable effects in non-cardiac tissues. An attractive alternative would be based on the transient regulation of gene expression through the use of recently developed advanced cardiomyocyte-specific delivery of mod-RNAs of critical metabolic enzymes [70].

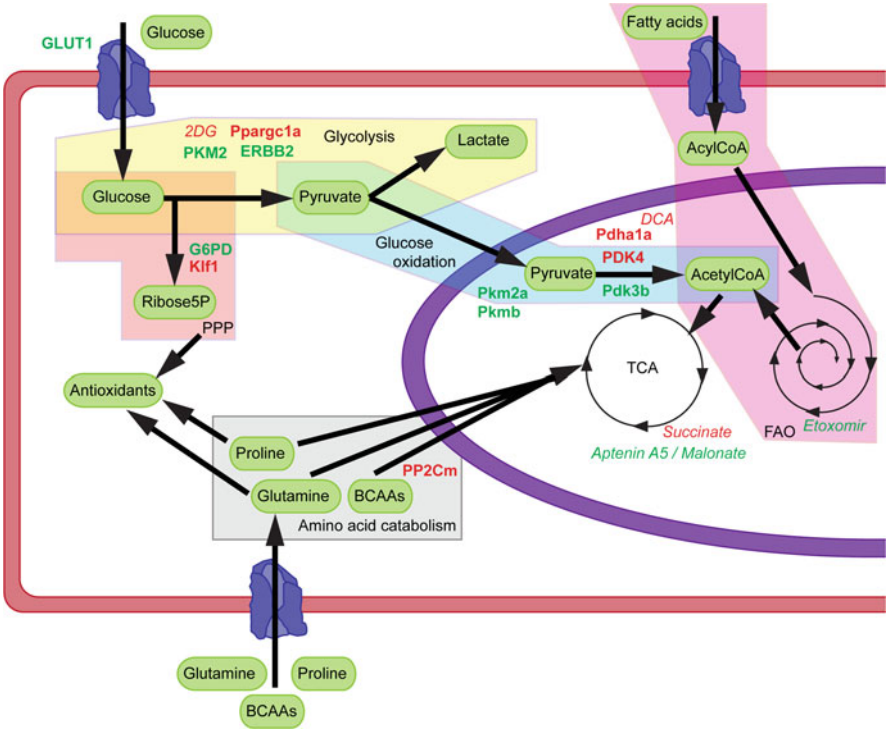

Fig. 19.2 Crosstalk of main cardiac metabolic pathways and strategies to modulate bioenergetic fluxes. Schematic representation of central cardiac metabolic pathways. The colored boxes represent core programs: glycolysis (yellow), pentose phosphate pathway (PPP, red), fatty acid oxidation (FAO, pink), amino acid catabolism (gray), and glucose oxidation (blue). Approaches to modulate metabolic signatures are indicated in bold (genetic model) or italic (drug administration). Green indicates upregulation of the pathway, while red indicates downregulation. Plasma and mitochondrial membrane are depicted in red and purple, respectively. 2DG, 2-deoxy-D-glucose; PKM2, Pyruvate kinase muscle isozyme 2; DCA, Dichloroacetate; Pdha1a, Pyruvate dehydrogenase 1a; PDK4, Pyruvate dehydrogenase kinase 4; Pdk3b, Pyruvate dehydrogenase kinase 3b; Ppargc1a, Peroxisome proliferator-activated receptor gamma coactivator 1 alpha; Klf1, Krüppel-like factor 1; ERBB2, erb-b2 receptor tyrosine kinase 2

Another important metabolic player to be discussed in the setting of cardiac regeneration are amino acids. While amino acids are always taken as protein building blocks, their ability to get incorporated into the TCA cycle through anaplerosis makes them an alternative source of energy and anabolic intermediates. The normal heart does not use amino acids as a metabolic source in a large extent. However, under stress situations, such as cardiac injury and heart failure, amino acid metabolism becomes an important alternative cardiac metabolic fuel [82].

Glutamine is the most abundant amino acid in the body and plays a pivotal function in nitrogen exchange between different tissues and in the regulation of pH through ammonia generation. Metabolically, glutamine participates in protein,

purines, pyrimidines, lipid, NADP, and antioxidant synthesis. In the heart, glutamine is mainly metabolized through glutaminase (GLS), which converts glutamine into glutamate and ammonia. Glutamine-derived glutamate can be used, for instance, to promote glutathione synthesis. Interestingly, glutamine starvation causes oxidative stress by depletion of endogenous glutathione levels [83]. On the other hand, glutamine administration decreases ROS production and reduces apoptosis in response to hypoxia-reoxygenation [84]. Glutamine-derived glutamate can also be transformed into α-ketoglutarate through the action of glutamate dehydrogenase (GDH) or several aminotransferases. Moreover, α-ketoglutarate can enter the TCA cycle, acting as a source of ATP and carbons for the synthesis of other biomolecules, such as non-essential amino acids or lipids. In addition, glutamine plays important roles in cardiovascular disease. For example, glutamine accumulation influences macrophage polarization and high glutamine uptake by macrophages is associated with M2 anti-inflammatory polarization [85], reducing the progression of atherosclerotic lesions.

Another amino acid that recently has attracted attention for its implications in cardiovascular pathophysiology is proline. In vitro, proline reduces ROS production in cells upon H_2O_2 treatment, while in vivo, proline administration reduces infarct size and decreases oxidative stress in injured hearts in mice [80]. Furthermore, another report recently showed that exercise-induced proline dehydrogenase (PRODH) expression, which catalyzes the first step of proline degradation, improves cardiac function after heart injury [86], supporting the idea that proline catabolism is beneficial in a context of cardiac injury.

Finally, branched-chain amino acid (BCAA) (leucine, valine, and isoleucine) metabolism is also important in the heart. BCAAs play three different roles in the cardiac tissue. First, functioning as a metabolic fuel source through their catabolism in the TCA. Second, being utilized as building blocks for protein synthesis. Third, balancing cell growth and autophagy, and uncoupling insulin signaling by activation of mTOR pathway [87]. BCAA metabolism has been described to be altered during pathological cardiac remodeling in response to injury or pressure overload [88, 89]. Interestingly, pharmacological activation of BCAA catabolism increased cardiac function in a mouse model of pressure overload [90]. However, this effect is not mediated by a metabolic rewiring toward oxidation of BCAAs to obtain an alternative source of energy. Instead, BCAA oxidation decreases total cardiac BCAA levels, improving cardiac insulin sensitivity. Indeed, impaired BCAA oxidation contributes to cardiac insulin resistance in heart failure [89]. Likewise, deletion of the branched-chain alpha-ketoacid dehydrogenase phosphatase (PP2CM), a positive regulator of BCAA metabolism, resulted in BCAA accumulation, earlier functional defects of cardiac aging and increased heart failure upon pressure overload, highlighting the importance of proper BCAA catabolism for cardiac homeostasis [81]. Similarly, to PP2CM deletion and subsequent BCAA elevation, chronic accumulation of BCAAs also makes the heart more sensitive to ischemia-reperfusion injury by increased lipid peroxidation toxicity due to transcriptional regulation of PPAR-alpha [91]. These data support the notion that BCAA lowering methods might be potentially effective cardioprotective strategies. On the other hand, the

concentration of BCAAs in cardiac tissue transiently increases from P1 to P9, after which they decrease to baseline levels by P23. Moreover, almost all enzymes involved in BCAA degradation are upregulated by P23 versus P1 [24]. Interestingly, the growth of cardiomyocytes that occurs during the early neonatal window requires accumulation of BCAAs, with subsequent mTOR activation to promote hypertrophy [92].

In conclusion, despite our growing understanding about the importance of amino acid metabolism in cardiomyocyte development, maturation, and dysfunction, and their potential as oxidative fuel in the failing heart [93], the role of amino acid metabolism in cardiac regeneration has only recently gained attention and ensures an exciting field for future research.

19.4.4 Nonmyocytes Metabolism and Cardiac Regeneration

The heart is a structurally and functionally complex organ formed by a diverse cellular collection that relies in cell–cell contact as well as paracrine signals for proper homeostasis. During cardiac injury, apart from the huge loss of millions of cardiomyocytes, which represent the contractile apparatus of the working myocardium, other heart components like epicardial, endothelial, or cardiac-resident immune cells are exposed to the damaging signals and hence react to the adverse microenvironment. Moreover, these and other cardiac populations like fibroblasts are essential in cardiac remodeling after injury and might significantly influence organ functional recovery. Metabolism is a key regulator of cellular homeostasis and functional competence not only of cardiomyocytes but also of all these additional cellular components participating in cardiac renewal and injury responses. While relevant advances about the impact of metabolism in cell cycle reentry and dedifferentiation of cardiomyocytes have been achieved as described above, little is known about the influence of metabolic programs in nonmyocytes during the course of cardiac regeneration. Therefore, deeper knowledge on this topic will be critical in order to evaluate novel therapeutic strategies for heart repair based on cardiometabolic modulation.

19.4.4.1 Metabolism of Cardiac Endothelial Cells

Endothelial cells represent the most abundant population of the heart and comprise vascular, microvascular, and endocardial endothelium [94]. Upon cardiac injury, there is a massive response of endothelial cells to contribute to the neovascularization of the damaged/necrotic tissue though angiogenesis, highlighting the communication between endothelial compartment and other cardiac cells. In high contrast to most cardiac cells, the endothelium largely relies on glucose metabolism and glycolysis is essential for endothelial cell proliferation and angiogenesis [95]. Indeed, shifting glycolysis toward OXPHOS by elimination of Sirtuin-3 leads to impaired angiogenesis, rarefaction of capillaries, and cardiac dysfunction [96], showing how alterations on endothelial metabolism can directly impact on cardiac homeostasis and performance (Fig. 19.3). A recent report describes the

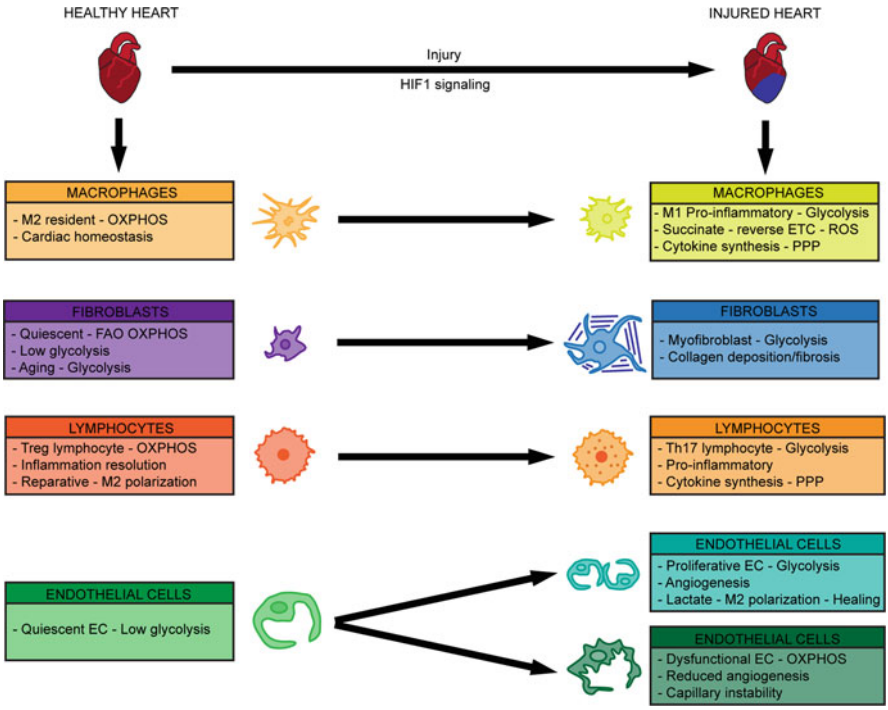

Fig. 19.3 Influence of cardiac injury and HIF signaling in non-myocyte populations of the heart. Summary of representative non-myocyte cardiac populations in healthy and pathological conditions, indicating their metabolic signature and function of the heart. The left boxes indicate the predominant subpopulation, as well as the preferential metabolic program in homeostatic conditions. The right boxes show the prevalent subpopulation under injury and the metabolic reprogramming that takes place in response to HIF activation and bioenergetic rewiring. OXPHOS, oxidative phosphorylation; ETC, electron transport chain; ROS, reactive oxygen species; PPP, pentose phosphate pathway; FAO, fatty acid oxidation; EC, endothelial cells

ability of endothelial-derived lactate to promote muscle regeneration by inducing M2 macrophage polarization [97]. However, our knowledge about metabolic adaptations of different pools of cardiac endothelium in response to cardiac injury, and the interplay of endothelial bioenergetics and inflammatory responses, or cardiomyocyte proliferation capacity in the setting of cardiac regeneration, remains largely unexplored. Therefore, further research on the crosstalk between endothelial metabolism and heart repair is needed for an integrative view of cardiovascular metabolic modulation and exploitation of novel therapeutic opportunities.

19.4.4.2 Bioenergetics of Cardiac Fibroblasts

Cardiac fibroblasts heterogeneity has been well established, reflecting distinct developmental origins for discrete pools of this population and the complexity of understanding their differential role in the setting of cardiovascular diseases [98]. In

response to acute injury after myocardial infarction, cardiac fibroblasts proliferate and differentiate into myofibroblasts. In the border zone, myofibroblasts contribute to reparative fibrosis through the secretion of collagen and other extracellular matrix components, playing a beneficial role to prevent cardiac rupture due to severe dilation of the ventricular wall. In contrast, excessive fibrosis on the remote area can enhance cardiac dysfunction and worse evolution after acute damage [99]. Furthermore, the importance of cardiac fibroblasts in response to cardiac damage is beyond its secretory function, as they also play an essential role in modulating inflammation and angiogenesis, as well as cardiomyocyte survival [100]. Although the direct role of cardiac fibroblasts metabolic adaptations in the setting of cardiac regeneration has not been extensively addressed, the influence of metabolism on fibroblasts differentiation toward a pro-secretory myofibroblast phenotype might have obvious consequences on the evolution of heart repair. In addition, the known crosstalk between cardiac fibroblasts and inflammatory cells, like resident macrophages, further highlights the important role of metabolic responses in cardiac fibroblasts in the global healing capacity of the heart. Indeed, metabolic changes in this population of the heart have been related to progression of cardiac diseases such as pulmonary arterial hypertension, where impaired OXPHOS and increased glycolysis, through a HIF1-dependent mechanism, favor enhanced right ventricular fibrosis [101]. In addition, the genetic conditional deletion of mitochondrial calcium uniporter (MCU) after myocardial infarction or Angiotensin II treatment contributes to a metabolic reprogramming toward glycolysis, which in fact favors a myofibroblasts phenotype and exacerbated fibrosis [102] (Fig. 19.3). Therefore, the metabolic signature of cardiac fibroblasts, in response to either chronic or acute injury, significantly impacts on the disease outcome and might be an attractive therapeutic target for cardiac regeneration.

19.4.4.3 Immunometabolism and Cardiac Repair

Although the influence of metabolism in modulating migration, differentiation, or effector functions of different immune populations is highly complex and beyond the scope of this chapter, it is important to briefly mention the general regulation of main metabolic pathways in immune populations toward an integrative view of cardiometabolism. Around 10% of non-cardiac muscle cells are represented by immune cells, mostly resident macrophages [94, 98], which provide defense against pathogens and are essential to control the extent of fibrosis [103], favoring electrical transmission throughout the atrioventricular node [104], and eliminating cardiac waste, including damaged mitochondria from cardiomyocytes [105], overall contributing to cardiac homeostasis. After cardiac injury, immune cells respond to the insult and play important roles in cardiac repair by modulating inflammation, revascularization, impacting cardiomyocyte dedifferentiation, and replenishment, as well as regulating the remodeling of the fibrotic scar. In particular, upon acute heart damage like myocardial infarction, resident cardiac macrophages are lost and replaced by infiltrating bone marrow-derived monocytes that polarize toward an M1-like pro-inflammatory phenotype, and together with other immune cells mobilized to the heart, mainly neutrophils, act as a first line of action after cardiac

damage to eliminate dead cells and debris [103, 106, 107]. Although neutrophils are the first immune responders to cardiac damage, they have a short life span and rapidly undergo apoptosis after contributing to a reparative phase by inducing macrophage polarization back to M2 phenotype [108]. Then, M2 macrophages contribute to neutrophil apoptosis, promoting inflammation resolution and favoring tissue remodeling and healing of the injured area [103, 106]. Macrophages are essential for cardiac repair and regeneration [109], and the importance of metabolism in balancing macrophage function and differentiation is well known, highlighting the importance of cardiometabolic modulation on the global response to heart damage. While the complexity of macrophage phenotypes is way beyond the simplistic view of M1/M2 polarization, it is clear that glycolysis supports proinflammatory functions in M1 macrophages, while OXPHOS-based metabolism is predominant in M2-like macrophages [110] (Fig. 19.3). Moreover, it has been recently proposed that a similar neutrophil N1/N2 metabolic-dependent polarization state might also exist as a dynamic reflect of the plasticity of phagocytes in response to acute cardiac injury and later reparative phases [97]. Mature neutrophils are mostly devoid of mitochondria, and glycolysis is important for their inflammatory functions, including NETosis [111], while OXPHOS metabolism is essential during neutrophil differentiation [112]. Glycolysis is also crucial for the M1-like phenotype, not only for energy production but also to generate biosynthetic intermediates through the PPP in order to synthesize proinflammatory mediators, such as cytokines, important for phagocytosis. In addition, proinflammatory M1-like macrophages have an uncoupled OXPHOS metabolism through interruptions on the TCA cycle at different levels, which ultimately contribute to reverse electron transport (RET) and enhanced ROS production, important for phagocytic and bacteria killing functions [113]. HIF1 signaling is essential in regulating this metabolic reprogramming of macrophages even in normal oxygen conditions [114] (Fig. 19.3). The oxygen-independent stabilization of HIF1a in macrophages has been described to be controlled mainly by NFκB and mTOR, which become activated by pro-inflammatory cytokines, growth factors, like GM-CSF, or ROS, together with the activation of PHD by TCA-derived succinate [110]. In addition to the shift between OXPHOS metabolism and aerobic glycolysis during innate immune response, amino acids are utilized in several anabolic reactions and are needed for effective migration, maturation, and effector functions. Moreover, amino acids control several signaling pathways essential for macrophage biology like mTOR or NO. Arginine, tryptophan, isoleucine, or glutamine are some examples of the importance of amino acids in controlling M1/M2 polarization, proliferation, and global immune response by regulation of macrophage and T-cell phenotype and interaction [97, 110].

Despite the relative scarce existence of resident cardiac T lymphocytes, and their delayed action after the initiation of a cardiac event, it is known that this pool of immune cells is important on the onset of cardiac diseases such as dilated cardiomyopathy [115] or myocardial infarction [116] (revised in [37]). The influence of metabolism in T-cell polarization has also been described, and the role of HIF1 in promoting a more glycolytic proinflammatory Th17 phenotype in T-cells is well

established [117]. Highly glycolytic Th17 cells are found in circulation of patients with dilated cardiomyopathy [115], while treatment with the glycolytic inhibitor 2DG of mice with dilated cardiomyopathy reverts the proinflammatory Th17 profile toward a basal T regulatory metabolism, restoring cardiac function [118]. In contrast, T regulatory cells play an essential role during the reparative phase after myocardial infarction by modulating the resolution of inflammation through the polarization of monocytes toward M2-like macrophages after the acute injury response [116] (Fig. 19.3). Nevertheless, further investigation on the direct role of T-cells immunometabolism during neonatal and adult cardiac repair is needed for a holistic view toward designing novel cardiac repair strategies.

19.5 Final Considerations and Future Perspectives

The development of novel strategies oriented to improve heart repair based on metabolic modulation requires a deep knowledge on the particular bioenergetic programs of all cardiac cells in both homeostatic and pathological conditions and needs to consider potential non-direct effects related to the crosstalk between different cardiovascular populations. Furthermore, the metabolic adaptations of cardiac cells might significantly differ depending on the pathological scenario, and acute versus chronic cardiovascular diseases could display different metabolic signatures and rewiring. Moreover, it is important to consider that many comorbidities like obesity, diabetes, or atherosclerosis are associated with immune imbalanced toward M1-like polarization and hence more proinflammatory status, which could influence the global response of cardiomyocytes and other cardiac cells to tissue damage [37]. Therefore, increasing our knowledge about the metabolic signature of immune populations, as well as other cardiovascular lineages, in homeostatic and different range of pathological conditions will contribute to an integrative view that might facilitate successful therapeutic interventions toward cardiac regeneration.

Certain drugs could be applied toward a global beneficial outcome upon cardiac injury and might present true therapeutic potential as cardiac metabolic modulators. A recent report indicates that dimethyl fumarate contributes to preserve left ventricular integrity after myocardial infarction through the modulation of OXPHOS metabolism of cardiac fibroblasts and macrophages [119]. Curiously, dimethyl fumarate treatment has a different effect on the bioenergetics of macrophages and fibroblasts, favoring or blocking OXPHOS metabolism in each cell type, respectively. Increased oxygen consumption rate in cardiac macrophages in the early response to acute injury is associated with reduced expression of proinflammatory cytokines like Il1β or Tnf and also decreased levels of the master regulator of metabolic rewiring HIF1α, and the protector against oxidative stress Nrf2. In contrast, dimethyl fumarate reduces OXPHOS in cardiac fibroblasts after MI and results in enhanced myofibroblast phenotype, promoting the expression of several extracellular matrix genes and reducing chemokines, overall favoring an anti-inflammatory pro-reparative phenotype of cardiac fibroblasts after MI [119]. These

results are in line with a former work describing the cardioprotective effect of fumarate on cardiomyocytes against ischemia reperfusion injury, through a metabolic reprogramming to amino acid anaplerosis and the activation of a Nrf2-mediated antioxidant response [120]. All in all, these findings suggest that despite the diverse metabolic rewiring observed in different cell types, some pharmacological treatments could be used to globally influence cardiac metabolism toward an improvement and renewal.

Increasing evidence suggests that epigenetic modifying enzymes can sense and respond to metabolic cues [121]. Therefore, an exciting field of research in order to gain further mechanistic insights connecting metabolism and cell differentiation, proliferation, or survival will be to investigate the transcriptional changes associated with metabolic rewiring in different cardiac populations. In this regard, the known function of certain metabolic intermediates regulating enzymes with epigenetic activity have begun to be elucidated in the setting of cardiac regeneration. For instance, in zebrafish, it has been recently reported that the transcription factor KLF1 coordinates the repression of transcriptional networks controlling myocardial differentiation and mitochondrial metabolism, with upregulation of cell proliferation genes, overall contributing to cardiomyogenesis during cardiac regeneration through epigenetic mechanisms [63]. Another example of the connection between metabolism and epigenome control of cell survival, differentiation, and organ homeostasis was reported in cardiac fibroblasts. In this cell population, the blockage of the mitochondrial calcium uniporter leads to a metabolic reprogramming that includes enhanced glycolysis and anabolic pathways, as well as increased glutamine catabolism that results in the accumulation of 2-alphaketoglurate, which modulating histone demethylases, enhances chromatin accessibility for loci of the myofibroblast gene program [102]. Finally, mutations in SDH have been shown to promote DNA methylation and modulate disease progression in familial paraganglioma [121–123]. Whether endogenous inhibition of SDH activity in border zone cardiomyocytes in zebrafish [55] or blockade by pharmacological administration of dimethyl malonate or atpenin 5 in mice that leads to enhanced regenerative capacity linked to epigenetic mechanisms has not been elucidated and opens an exciting field of future research. Another interesting axis connecting metabolism with epigenetics might be the relative generation of Acetyl-CoA from FAO versus glucose oxidation, which could vary the degree of DNA acetylation. Therefore, increasing our knowledge about epigenetic mechanisms linked to specific metabolic signatures in cardiac cells, regulating gene expression programs of proliferation or differentiation, will contribute to the development of novel therapeutic approaches for cardiac regeneration.

In order to increase our understanding of the influence of metabolism in cardiac regeneration, it would be important to further investigate the metabolic programs linked to signaling pathways participating in cardiomyocyte proliferation or heart repair. In this regard, the role of hypoxia/HIF signaling in metabolic control and its connection with cardiac regeneration has been reported [25, 44, 46], while the direct role of HIF1 in metabolic rewiring and cardiac regeneration awaits genetic confirmation. Nrg1 and its co-receptor Erbb2 are known regulators of cardiomyocyte

proliferation during development and can reactivate cardiomyocyte proliferation and heart regeneration [56, 124]. It has been reported that Nrg1β enhances glucose uptake in neonatal rat cardiomyocytes via ErbB2/ErbB4 heterodimers, PI3Kα, and Akt signaling [125]. Furthermore, the metabolic reprogramming from OXPHOS to glycolytic metabolism occurring in border zone cardiomyocytes in adult zebrafish is induced by Nrg1/ErbB2 signaling pathway and linked to cardiomyocyte proliferation [55].

Another essential signaling controlling organ growth and cardiomyocyte proliferation is the Hippo/YAP pathway, and increasing evidences show how metabolites might influence Hippo/YAP signaling and in turn, how the pathway can control gene expression of metabolic genes as well. Indeed, there are multiple metabolites that impact Hippo/YAP signaling, highlighting its central role in cell/organ growth and cell fate [126]. While many of the studies connecting Hippo/YAP and metabolism have been performed in the setting of tumor growth, the important interplay between Hippo/YAP and metabolism is emerging as well in the context of cardiovascular diseases [127]. YAP/TAZ stimulates glycolysis and nucleotide biosynthesis in different types of cancers, and phosphofructokinase 1 (PFK1) activates YAP/TAZ [128], offering a positive feedback loop mechanism. In cancer cells, YAP can also promote amino acid metabolism by increasing the expression levels of different amino acid transporters like Slc1a5, Slc7a5, and Slc38A1, together with mTOR activation [126]. Recent findings describe the activation of YAP by Erbb2 during cardiac regeneration [129], yielding the question of whether the metabolic switch from OXPHOS to glycolytic activation by Nrg1/Erbb2 during cardiac regeneration could be somehow mediated by YAP. In conclusion, the crosstalk between YAP signaling and metabolism in the onset of cardiac regeneration needs to be further characterized and might reveal interesting novel functions of YAP as a key element in coordinating nutrients and energy availability with anabolic pathways, cell proliferation, and organ metabolic control.

19.6 Conclusions

Metabolism is an essential process governing cardiac homeostasis as well as disease progression. During early stages of development, the embryonic myocardium mostly relies on anaerobic glycolysis for growth, while a progressive switch toward oxidative metabolism is required for myocardial maturation and effective cardiac performance [1, 9]. Changes in oxygen availability right after birth contribute to a further metabolic shift to oxidative metabolism of fatty acids and glucose-derived pyruvate in the mitochondria, which provides larger amount of energy in the form of ATP but at the same time increases oxidative risk through ROS production, limiting cardiomyocyte proliferation postnatally [25]. Interestingly, the myocardium can consume different types of substrates depending on nutrient availability, environmental factors, and developmental/pathological stages, demonstrating the high metabolic flexibility of the heart. Genetic or pharmacological manipulation of bioenergetic programs in the heart represent emerging approaches to improve

cardiac regeneration or disease control [64, 67, 70]. The reduction on FAO and activation of non-oxidative shunts of glycolysis toward the PPP in the adult heart recapitulate the embryonic metabolic signature, promoting cardiomyocyte cell cycle reentry and contributing to cardiac regeneration by activation of biosynthetic anabolic pathways and increasing cardiac antioxidant capacity [55, 63, 70]. The heterogeneous composition of cardiac tissue and the tight intercellular communication between different heart populations add an extra level of complexity when considering metabolic rewiring as a reparative opportunity, since each cell type likely depends on or responds differently to a specific bioenergetic signature. Expanding our knowledge on the metabolic programs of cardiomyocytes and non-myocytes compartments of the heart in homeostasis and disease and uncovering the molecular mechanisms participating in cardiac metabolic rewiring will enable the development of novel therapeutic strategies based on integrative cardiometabolic modulation.

Acknowledgements We would like to deeply acknowledge Dr. Luke Szweda and Dr. Hesham Sadek for critical revision of this chapter.

References

1. Lopaschuk GD, Jaswal JS. Energy metabolic phenotype of the cardiomyocyte during development, differentiation, and postnatal maturation. J Cardiovasc Pharmacol. 2010;56(2):130–40. https://doi.org/10.1097/FJC.0b013e3181e74a14.
2. Lee YM, Jeong CH, Koo SY, Son MJ, Song HS, Bae SK, et al. Determination of hypoxic region by hypoxia marker in developing mouse embryos in vivo: a possible signal for vessel development. Dev Dyn. 2001;220(2):175–86. https://doi.org/10.1002/1097-0177(20010201)220:2<175::AID-DVDY1101>3.0.CO;2-F.
3. Ferre P, Decaux JF, Issad T, Girard J. Changes in energy metabolism during the suckling and weaning period in the newborn. Reprod Nutr Dev. 1986;26(2B):619–31. https://doi.org/10.1051/rnd:19860413.
4. Ostadal B, Ostadalova I, Dhalla NS. Development of cardiac sensitivity to oxygen deficiency: comparative and ontogenetic aspects. Physiol Rev. 1999;79(3):635–59. https://doi.org/10.1152/physrev.1999.79.3.635.
5. Vander Heiden MG, Cantley LC, Thompson CB. Understanding the Warburg effect: the metabolic requirements of cell proliferation. Science. 2009;324(5930):1029–33. https://doi.org/10.1126/science.1160809.
6. Calmettes G, John SA, Weiss JN, Ribalet B. Hexokinase-mitochondrial interactions regulate glucose metabolism differentially in adult and neonatal cardiac myocytes. J Gen Physiol. 2013;142(4):425–36. https://doi.org/10.1085/jgp.201310968.
7. Chung S, Dzeja PP, Faustino RS, Perez-Terzic C, Behfar A, Terzic A. Mitochondrial oxidative metabolism is required for the cardiac differentiation of stem cells. Nat Clin Pract Cardiovasc Med. 2007;4(Suppl 1):S60–7. https://doi.org/10.1038/ncpcardio0766.
8. Guimaraes-Camboa N, Stowe J, Aneas I, Sakabe N, Cattaneo P, Henderson L, et al. HIF1alpha represses cell stress pathways to allow proliferation of hypoxic fetal cardiomyocytes. Dev Cell. 2015;33(5):507–21. https://doi.org/10.1016/j.devcel.2015.04.021.
9. Menendez-Montes I, Escobar B, Palacios B, Gomez MJ, Izquierdo-Garcia JL, Flores L, et al. Myocardial VHL-HIF signaling controls an embryonic metabolic switch essential for cardiac maturation. Dev Cell. 2016;39(6):724–39. https://doi.org/10.1016/j.devcel.2016.11.012.

10. Menendez-Montes I, Escobar B, Gomez MJ, Albendea-Gomez T, Palacios B, Bonzon-Kulichenko E, et al. Activation of amino acid metabolic program in cardiac HIF1-alpha-deficient mice. iScience. 2021b;24(2):102124. https://doi.org/10.1016/j.isci.2021.102124.
11. Breckenridge RA, Piotrowska I, Ng KE, Ragan TJ, West JA, Kotecha S, et al. Hypoxic regulation of hand1 controls the fetal-neonatal switch in cardiac metabolism. PLoS Biol. 2013;11(9):e1001666. https://doi.org/10.1371/journal.pbio.1001666.
12. Hom JR, Quintanilla RA, Hoffman DL, de Mesy Bentley KL, Molkentin JD, Sheu SS, Porter GA Jr. The permeability transition pore controls cardiac mitochondrial maturation and myocyte differentiation. Dev Cell. 2011;21(3):469–78. https://doi.org/10.1016/j.devcel.2011.08.008.
13. Kim HD, Kim DJ, Lee IJ, Rah BJ, Sawa Y, Schaper J. Human fetal heart development after mid-term: morphometry and ultrastructural study. J Mol Cell Cardiol. 1992;24(9):949–65. https://doi.org/10.1016/0022-2828(92)91862-y.
14. Shepard TH, Muffley LA, Smith LT. Ultrastructural study of mitochondria and their cristae in embryonic rats and primate (N. nemistrina). Anat Rec. 1998;252(3):383–92. https://doi.org/10.1002/(SICI)1097-0185(199811)252:3<383::AID-AR6>3.0.CO;2-Z.
15. Sybers HD, Ingwall JS, De Luca MA. Fetal mouse heart in organ structure: ultrastructure. Lab Investig. 1975;32(6):713–9. Retrieved from https://www.ncbi.nlm.nih.gov/pubmed/1171338
16. Fukuda R, Aharonov A, Ong YT, Stone OA, El-Brolosy M, Maischein HM, et al. Metabolic modulation regulates cardiac wall morphogenesis in zebrafish. Elife. 2019;8:e50161. https://doi.org/10.7554/eLife.50161.
17. Krishnan J, Ahuja P, Bodenmann S, Knapik D, Perriard E, Krek W, Perriard JC. Essential role of developmentally activated hypoxia-inducible factor 1alpha for cardiac morphogenesis and function. Circ Res. 2008;103(10):1139–46. https://doi.org/10.1161/01.RES.0000338613.89841.c1.
18. Harding HP, Zhang Y, Zeng H, Novoa I, Lu PD, Calfon M, et al. An integrated stress response regulates amino acid metabolism and resistance to oxidative stress. Mol Cell. 2003;11(3):619–33. https://doi.org/10.1016/s1097-2765(03)00105-9.
19. Lehninger AL, Nelson DL, Cox MM. Principles of biochemistry. New York: Worth Publishers; 1993.
20. Nakano H, Minami I, Braas D, Pappoe H, Wu X, Sagadevan A, et al. Glucose inhibits cardiac muscle maturation through nucleotide biosynthesis. Elife. 2017;6:e29330. https://doi.org/10.7554/eLife.29330.
21. Delorme B, Dahl E, Jarry-Guichard T, Marics I, Briand JP, Willecke K, et al. Developmental regulation of connexin 40 gene expression in mouse heart correlates with the differentiation of the conduction system. Dev Dyn. 1995;204(4):358–71. https://doi.org/10.1002/aja.1002040403.
22. Lopaschuk GD, Karwi QG, Tian R, Wende AR, Abel ED. Cardiac energy metabolism in heart failure. Circ Res. 2021;128(10):1487–513. https://doi.org/10.1161/CIRCRESAHA.121.318241.
23. Lopaschuk GD, Collins-Nakai RL, Itoi T. Developmental changes in energy substrate use by the heart. Cardiovasc Res. 1992;26(12):1172–80. https://doi.org/10.1093/cvr/26.12.1172.
24. Lalowski MM, Bjork S, Finckenberg P, Soliymani R, Tarkia M, Calza G, et al. Characterizing the key metabolic pathways of the neonatal mouse heart using a quantitative combinatorial omics approach. Front Physiol. 2018;9:365. https://doi.org/10.3389/fphys.2018.00365.
25. Puente BN, Kimura W, Muralidhar SA, Moon J, Amatruda JF, Phelps KL, et al. The oxygen-rich postnatal environment induces cardiomyocyte cell-cycle arrest through DNA damage response. Cell. 2014;157(3):565–79. https://doi.org/10.1016/j.cell.2014.03.032.
26. Menendez-Montes I, Abdisalaam S, Xiao F, Lam NT, Mukherjee S, Szweda LI, et al. Mitochondrial fatty acid utilization increases chromatin oxidative stress in cardiomyocytes. Proc Natl Acad Sci U S A. 2021a;118(34):e2101674118. https://doi.org/10.1073/pnas.2101674118.
27. Poss KD, Wilson LG, Keating MT. Heart regeneration in zebrafish. Science. 2002;298(5601):2188–90. https://doi.org/10.1126/science.1077857.

28. Porrello ER, Mahmoud AI, Simpson E, Hill JA, Richardson JA, Olson EN, Sadek HA. Transient regenerative potential of the neonatal mouse heart. Science. 2011;331(6020):1078–80. https://doi.org/10.1126/science.1200708.
29. Ye L, D'Agostino G, Loo SJ, Wang CX, Su LP, Tan SH, et al. Early regenerative capacity in the porcine heart. Circulation. 2018;138(24):2798–808. https://doi.org/10.1161/CIRCULATIONAHA.117.031542.
30. Zhu W, Zhang E, Zhao M, Chong Z, Fan C, Tang Y, et al. Regenerative potential of neonatal porcine hearts. Circulation. 2018;138(24):2809–16. https://doi.org/10.1161/CIRCULATIONAHA.118.034886.
31. Jopling C, Sleep E, Raya M, Marti M, Raya A, Izpisua Belmonte JC. Zebrafish heart regeneration occurs by cardiomyocyte dedifferentiation and proliferation. Nature. 2010;464(7288):606–9. https://doi.org/10.1038/nature08899.
32. Kikuchi K, Holdway JE, Werdich AA, Anderson RM, Fang Y, Egnaczyk GF, et al. Primary contribution to zebrafish heart regeneration by gata4(+) cardiomyocytes. Nature. 2010;464(7288):601–5. https://doi.org/10.1038/nature08804.
33. Senyo SE, Steinhauser ML, Pizzimenti CL, Yang VK, Cai L, Wang M, et al. Mammalian heart renewal by pre-existing cardiomyocytes. Nature. 2013;493(7432):433–6. https://doi.org/10.1038/nature11682.
34. Li F, Wang X, Capasso JM, Gerdes AM. Rapid transition of cardiac myocytes from hyperplasia to hypertrophy during postnatal development. J Mol Cell Cardiol. 1996;28(8):1737–46. https://doi.org/10.1006/jmcc.1996.0163.
35. Soonpaa MH, Kim KK, Pajak L, Franklin M, Field LJ. Cardiomyocyte DNA synthesis and binucleation during murine development. Am J Phys. 1996;271(5 Pt 2):H2183–9. https://doi.org/10.1152/ajpheart.1996.271.5.H2183.
36. Bergmann O, Zdunek S, Felker A, Salehpour M, Alkass K, Bernard S, et al. Dynamics of cell generation and turnover in the human heart. Cell. 2015;161(7):1566–75. https://doi.org/10.1016/j.cell.2015.05.026.
37. Mouton AJ, Hall JE. Novel roles of immunometabolism and nonmyocyte metabolism in cardiac remodeling and injury. Am J Physiol Regul Integr Comp Physiol. 2020;319(4):R476–84. https://doi.org/10.1152/ajpregu.00188.2020.
38. Kierans SJ, Taylor CT. Regulation of glycolysis by the hypoxia-inducible factor (HIF): implications for cellular physiology. J Physiol. 2021;599(1):23–37. https://doi.org/10.1113/JP280572.
39. Warburg O. Iron, the oxygen-carrier of respiration-ferment. Science. 1925;61(1588):575–82. https://doi.org/10.1126/science.61.1588.575.
40. Hu L, Xie H, Liu X, Potjewyd F, James LI, Wilkerson EM, et al. TBK1 is a synthetic lethal target in cancer with VHL loss. Cancer Discov. 2020;10(3):460–75. https://doi.org/10.1158/2159-8290.CD-19-0837.
41. Zhang Q, Gu J, Li L, Liu J, Luo B, Cheung HW, et al. Control of cyclin D1 and breast tumorigenesis by the EglN2 prolyl hydroxylase. Cancer Cell. 2009;16(5):413–24. https://doi.org/10.1016/j.ccr.2009.09.029.
42. Bienes-Martinez R, Ordonez A, Feijoo-Cuaresma M, Corral-Escariz M, Mateo G, Stenina O, et al. Autocrine stimulation of clear-cell renal carcinoma cell migration in hypoxia via HIF-independent suppression of thrombospondin-1. Sci Rep. 2012;2:788. https://doi.org/10.1038/srep00788.
43. Wood SM, Wiesener MS, Yeates KM, Okada N, Pugh CW, Maxwell PH, Ratcliffe PJ. Selection and analysis of a mutant cell line defective in the hypoxia-inducible factor-1 alpha-subunit (HIF-1alpha). Characterization of hif-1alpha-dependent and -independent hypoxia-inducible gene expression. J Biol Chem. 1998;273(14):8360–8. https://doi.org/10.1074/jbc.273.14.8360.
44. Kimura W, Xiao F, Canseco DC, Muralidhar S, Thet S, Zhang HM, et al. Hypoxia fate mapping identifies cycling cardiomyocytes in the adult heart. Nature. 2015;523(7559):226–30. https://doi.org/10.1038/nature14582.

45. Jopling C, Sune G, Faucherre A, Fabregat C, Izpisua Belmonte JC. Hypoxia induces myocardial regeneration in zebrafish. Circulation. 2012;126(25):3017–27. https://doi.org/10.1161/CIRCULATIONAHA.112.107888.
46. Nakada Y, Canseco DC, Thet S, Abdisalaam S, Asaithamby A, Santos CX, et al. Hypoxia induces heart regeneration in adult mice. Nature. 2017;541(7636):222–7. https://doi.org/10.1038/nature20173.
47. Bae J, Paltzer WG, Mahmoud AI. The role of metabolism in heart failure and regeneration. Front Cardiovasc Med. 2021a;8:702920. https://doi.org/10.3389/fcvm.2021.702920.
48. Harris DA, Das AM. Control of mitochondrial ATP synthesis in the heart. Biochem J. 1991;280(Pt 3):561–73. https://doi.org/10.1042/bj2800561.
49. Taegtmeyer H, Young ME, Lopaschuk GD, Abel ED, Brunengraber H, Darley-Usmar V, American Heart Association Council on Basic Cardiovascular Sciences, et al. Assessing cardiac metabolism: a scientific statement from the American Heart Association. Circ Res. 2016;118(10):1659–701. https://doi.org/10.1161/RES.0000000000000097.
50. Lopaschuk GD, Ussher JR, Folmes CD, Jaswal JS, Stanley WC. Myocardial fatty acid metabolism in health and disease. Physiol Rev. 2010;90(1):207–58. https://doi.org/10.1152/physrev.00015.2009.
51. Lehman JJ, Kelly DP. Gene regulatory mechanisms governing energy metabolism during cardiac hypertrophic growth. Heart Fail Rev. 2002;7(2):175–85. https://doi.org/10.1023/a:1015332726303.
52. Krishnan J, Suter M, Windak R, Krebs T, Felley A, Montessuit C, et al. Activation of a HIF1alpha-PPARgamma axis underlies the integration of glycolytic and lipid anabolic pathways in pathologic cardiac hypertrophy. Cell Metab. 2009;9(6):512–24. https://doi.org/10.1016/j.cmet.2009.05.005.
53. MacLellan WR, Schneider MD. Genetic dissection of cardiac growth control pathways. Annu Rev Physiol. 2000;62:289–319. https://doi.org/10.1146/annurev.physiol.62.1.289.
54. Fukuda R, Marin-Juez R, El-Sammak H, Beisaw A, Ramadass R, Kuenne C, et al. Stimulation of glycolysis promotes cardiomyocyte proliferation after injury in adult zebrafish. EMBO Rep. 2020;21(8):e49752. https://doi.org/10.15252/embr.201949752.
55. Honkoop H, de Bakker DE, Aharonov A, Kruse F, Shakked A, Nguyen PD, et al. Single-cell analysis uncovers that metabolic reprogramming by ErbB2 signaling is essential for cardiomyocyte proliferation in the regenerating heart. Elife. 2019;8:e50163. https://doi.org/10.7554/eLife.50163.
56. D'Uva G, Aharonov A, Lauriola M, Kain D, Yahalom-Ronen Y, Carvalho S, et al. ERBB2 triggers mammalian heart regeneration by promoting cardiomyocyte dedifferentiation and proliferation. Nat Cell Biol. 2015;17(5):627–38. https://doi.org/10.1038/ncb3149.
57. del Peso L, Castellanos MC, Temes E, Martin-Puig S, Cuevas Y, Olmos G, Landazuri MO. The von Hippel Lindau/hypoxia-inducible factor (HIF) pathway regulates the transcription of the HIF-proline hydroxylase genes in response to low oxygen. J Biol Chem. 2003;278(49):48690–5. https://doi.org/10.1074/jbc.M308862200.
58. Fajardo VM, Feng I, Chen BY, Perez-Ramirez CA, Shi B, Clark P, et al. GLUT1 overexpression enhances glucose metabolism and promotes neonatal heart regeneration. Sci Rep. 2021;11(1):8669. https://doi.org/10.1038/s41598-021-88159-x.
59. Wang X, Ha T, Liu L, Hu Y, Kao R, Kalbfleisch J, et al. TLR3 mediates repair and regeneration of damaged neonatal heart through glycolysis dependent YAP1 regulated miR-152 expression. Cell Death Differ. 2018;25(5):966–82. https://doi.org/10.1038/s41418-017-0036-9.
60. Karwi QG, Uddin GM, Ho KL, Lopaschuk GD. Loss of metabolic flexibility in the failing heart. Front Cardiovasc Med. 2018;5:68. https://doi.org/10.3389/fcvm.2018.00068.
61. Tran DH, Wang ZV. Glucose metabolism in cardiac hypertrophy and heart failure. J Am Heart Assoc. 2019;8(12):e012673. https://doi.org/10.1161/JAHA.119.012673.

62. Young LH, Russell RR 3rd, Yin R, Caplan MJ, Ren J, Bergeron R, et al. Regulation of myocardial glucose uptake and transport during ischemia and energetic stress. Am J Cardiol. 1999;83(12A):25H–30H. https://doi.org/10.1016/s0002-9149(99)00253-2.
63. Ogawa M, Geng FS, Humphreys DT, Kristianto E, Sheng DZ, Hui SP, et al. Kruppel-like factor 1 is a core cardiomyogenic trigger in zebrafish. Science. 2021;372(6538):201–5. https://doi.org/10.1126/science.abe2762.
64. Cardoso AC, Lam NT, Savla JJ, Nakada Y, Pereira AHM, Elnwasany A, et al. Mitochondrial substrate utilization regulates cardiomyocyte cell cycle progression. Nat Metab. 2020a;2(2):167–78. Retrieved from https://www.ncbi.nlm.nih.gov/pubmed/32617517
65. Cao T, Liccardo D, LaCanna R, Zhang X, Lu R, Finck BN, et al. Fatty acid oxidation promotes cardiomyocyte proliferation rate but does not change cardiomyocyte number in infant mice. Front Cell Dev Biol. 2019;7:42. https://doi.org/10.3389/fcell.2019.00042.
66. Roy R, Leigh T, Gao E, Zhang X, Tian Y. Activation or inhibition of PPARa-mediated fatty acid b-oxidation does not active cardiomyocyte proliferation in normal or infarcted adult mice. bioRxiv. 2019;2019:667964.
67. Bae J, Salamon RJ, Brandt EB, Paltzer WG, Zhang Z, Britt EC, et al. Malonate promotes adult cardiomyocyte proliferation and heart regeneration. Circulation. 2021b;143(20):1973–86. https://doi.org/10.1161/CIRCULATIONAHA.120.049952.
68. Hadrava Vanova K, Yang C, Meuter L, Neuzil J, Pacak K. Reactive oxygen species: a promising therapeutic target for SDHx-mutated Pheochromocytoma and Paraganglioma. Cancers (Basel). 2021;13(15):3769. https://doi.org/10.3390/cancers13153769.
69. Tseng PL, Wu WH, Hu TH, Chen CW, Cheng HC, Li CF, et al. Decreased succinate dehydrogenase B in human hepatocellular carcinoma accelerates tumor malignancy by inducing the Warburg effect. Sci Rep. 2018;8(1):3081. https://doi.org/10.1038/s41598-018-21361-6.
70. Magadum A, Singh N, Kurian AA, Munir I, Mehmood T, Brown K, et al. Pkm2 regulates cardiomyocyte cell cycle and promotes cardiac regeneration. Circulation. 2020;141(15):1249–65. https://doi.org/10.1161/CIRCULATIONAHA.119.043067.
71. Noguchi T, Yamada K, Inoue H, Matsuda T, Tanaka T. The L- and R-type isozymes of rat pyruvate kinase are produced from a single gene by use of different promoters. J Biol Chem. 1987;262(29):14366–71. Retrieved from https://www.ncbi.nlm.nih.gov/pubmed/3654663
72. Clower CV, Chatterjee D, Wang Z, Cantley LC, Vander Heiden MG, Krainer AR. The alternative splicing repressors hnRNP A1/A2 and PTB influence pyruvate kinase isoform expression and cell metabolism. Proc Natl Acad Sci U S A. 2010;107(5):1894–9. https://doi.org/10.1073/pnas.0914845107.
73. Mazurek S, Boschek CB, Hugo F, Eigenbrodt E. Pyruvate kinase type M2 and its role in tumor growth and spreading. Semin Cancer Biol. 2005;15(4):300–8. https://doi.org/10.1016/j.semcancer.2005.04.009.
74. Eigenbrodt E, Reinacher M, Scheefers-Borchel U, Scheefers H, Friis R. Double role for pyruvate kinase type M2 in the expansion of phosphometabolite pools found in tumor cells. Crit Rev Oncog. 1992;3(1–2):91–115. Retrieved from https://www.ncbi.nlm.nih.gov/pubmed/1532331
75. Boros LG, Torday JS, Lim S, Bassilian S, Cascante M, Lee WN. Transforming growth factor beta2 promotes glucose carbon incorporation into nucleic acid ribose through the nonoxidative pentose cycle in lung epithelial carcinoma cells. Cancer Res. 2000;60(5):1183–5. Retrieved from https://www.ncbi.nlm.nih.gov/pubmed/10728670
76. Luo W, Semenza GL. Pyruvate kinase M2 regulates glucose metabolism by functioning as a coactivator for hypoxia-inducible factor 1 in cancer cells. Oncotarget. 2011;2(7):551–6. https://doi.org/10.18632/oncotarget.299.
77. Yang W, Zheng Y, Xia Y, Ji H, Chen X, Guo F, et al. ERK1/2-dependent phosphorylation and nuclear translocation of PKM2 promotes the Warburg effect. Nat Cell Biol. 2012;14(12):1295–304. https://doi.org/10.1038/ncb2629.
78. Das DK, Engelman RM, Rousou JA, Breyer RH. Aerobic vs anaerobic metabolism during ischemia in heart muscle. Ann Chir Gynaecol. 1987;76(1):68–76. Retrieved from https://www.ncbi.nlm.nih.gov/pubmed/3592561

79. Doenst T, Nguyen TD, Abel ED. Cardiac metabolism in heart failure: implications beyond ATP production. Circ Res. 2013;113(6):709–24. https://doi.org/10.1161/CIRCRESAHA.113.300376.
80. Wang J, Xue Z, Lin J, Wang Y, Ying H, Lv Q, et al. Proline improves cardiac remodeling following myocardial infarction and attenuates cardiomyocyte apoptosis via redox regulation. Biochem Pharmacol. 2020;178:114065. https://doi.org/10.1016/j.bcp.2020.114065.
81. Lu G, Sun H, She P, Youn JY, Warburton S, Ping P, et al. Protein phosphatase 2Cm is a critical regulator of branched-chain amino acid catabolism in mice and cultured cells. J Clin Invest. 2009;119(6):1678–87. https://doi.org/10.1172/JCI38151.
82. Drake KJ, Sidorov VY, McGuinness OP, Wasserman DH, Wikswo JP. Amino acids as metabolic substrates during cardiac ischemia. Exp Biol Med (Maywood). 2012;237(12):1369–78. https://doi.org/10.1258/ebm.2012.012025.
83. Yuneva M, Zamboni N, Oefner P, Sachidanandam R, Lazebnik Y. Deficiency in glutamine but not glucose induces MYC-dependent apoptosis in human cells. J Cell Biol. 2007;178(1):93–105. https://doi.org/10.1083/jcb.200703099.
84. Li K, Cui YC, Zhang H, Liu XP, Zhang D, Wu AL, et al. Glutamine reduces the apoptosis of H9C2 cells treated with high-glucose and reperfusion through an oxidation-related mechanism. PLoS One. 2015;10(7):e0132402. https://doi.org/10.1371/journal.pone.0132402.
85. Tavakoli S, Downs K, Short JD, Nguyen HN, Lai Y, Jerabek PA, et al. Characterization of macrophage polarization states using combined measurement of 2-deoxyglucose and glutamine accumulation: implications for imaging of atherosclerosis. Arterioscler Thromb Vasc Biol. 2017;37(10):1840–8. https://doi.org/10.1161/ATVBAHA.117.308848.
86. Moreira JBN, Wohlwend M, Fenk S, Amellem I, Flatberg A, Kraljevic J, et al. Exercise reveals proline dehydrogenase as a potential target in heart failure. Prog Cardiovasc Dis. 2019;62(2):193–202. https://doi.org/10.1016/j.pcad.2019.03.002.
87. Zhang ZY, Monleon D, Verhamme P, Staessen JA. Branched-chain amino acids as critical switches in health and disease. Hypertension. 2018;72(5):1012–22. https://doi.org/10.1161/HYPERTENSIONAHA.118.10919.
88. Sansbury BE, DeMartino AM, Xie Z, Brooks AC, Brainard RE, Watson LJ, et al. Metabolomic analysis of pressure-overloaded and infarcted mouse hearts. Circ Heart Fail. 2014;7(4):634–42. https://doi.org/10.1161/CIRCHEARTFAILURE.114.001151.
89. Uddin GM, Zhang L, Shah S, Fukushima A, Wagg CS, Gopal K, et al. Impaired branched chain amino acid oxidation contributes to cardiac insulin resistance in heart failure. Cardiovasc Diabetol. 2019;18(1):86. https://doi.org/10.1186/s12933-019-0892-3.
90. Chen M, Gao C, Yu J, Ren S, Wang M, Wynn RM, et al. Therapeutic effect of targeting branched-chain amino acid catabolic flux in pressure-overload induced heart failure. J Am Heart Assoc. 2019;8(11):e011625. https://doi.org/10.1161/JAHA.118.011625.
91. Li Y, Xiong Z, Yan W, Gao E, Cheng H, Wu G, et al. Branched chain amino acids exacerbate myocardial ischemia/reperfusion vulnerability via enhancing GCN2/ATF6/PPAR-alpha pathway-dependent fatty acid oxidation. Theranostics. 2020;10(12):5623–40. https://doi.org/10.7150/thno.44836.
92. Shao D, Villet O, Zhang Z, Choi SW, Yan J, Ritterhoff J, et al. Glucose promotes cell growth by suppressing branched-chain amino acid degradation. Nat Commun. 2018;9(1):2935. https://doi.org/10.1038/s41467-018-05362-7.
93. Cardoso AC, Pereira AHM, Sadek HA. Mechanisms of neonatal heart regeneration. Curr Cardiol Rep. 2020b;22(5):33. https://doi.org/10.1007/s11886-020-01282-5.
94. Pinto AR, Ilinykh A, Ivey MJ, Kuwabara JT, D'Antoni ML, Debuque R, et al. Revisiting cardiac cellular composition. Circ Res. 2016;118(3):400–9. https://doi.org/10.1161/CIRCRESAHA.115.307778.
95. De Bock K, Georgiadou M, Schoors S, Kuchnio A, Wong BW, Cantelmo AR, et al. Role of PFKFB3-driven glycolysis in vessel sprouting. Cell. 2013;154(3):651–63. https://doi.org/10.1016/j.cell.2013.06.037.

96. He X, Zeng H, Chen ST, Roman RJ, Aschner JL, Didion S, Chen JX. Endothelial specific SIRT3 deletion impairs glycolysis and angiogenesis and causes diastolic dysfunction. J Mol Cell Cardiol. 2017;112:104–13. https://doi.org/10.1016/j.yjmcc.2017.09.007.
97. Zhang J, Muri J, Fitzgerald G, Gorski T, Gianni-Barrera R, Masschelein E, et al. Endothelial lactate controls muscle regeneration from ischemia by inducing M2-like macrophage polarization. Cell Metab. 2020;31(6):1136–1153 e1137. https://doi.org/10.1016/j.cmet.2020.05.004.
98. Tallquist MD, Molkentin JD. Redefining the identity of cardiac fibroblasts. Nat Rev Cardiol. 2017;14(8):484–91. https://doi.org/10.1038/nrcardio.2017.57.
99. Travers JG, Kamal FA, Robbins J, Yutzey KE, Blaxall BC. Cardiac fibrosis: the fibroblast awakens. Circ Res. 2016;118(6):1021–40. https://doi.org/10.1161/CIRCRESAHA.115.306565.
100. Humeres C, Frangogiannis NG. Fibroblasts in the infarcted, remodeling, and failing heart. JACC Basic Transl Sci. 2019;4(3):449–67. https://doi.org/10.1016/j.jacbts.2019.02.006.
101. Tian L, Wu D, Dasgupta A, Chen KH, Mewburn J, Potus F, et al. Epigenetic metabolic reprogramming of right ventricular fibroblasts in pulmonary arterial hypertension: a pyruvate dehydrogenase kinase-dependent shift in mitochondrial metabolism promotes right ventricular fibrosis. Circ Res. 2020;126(12):1723–45. https://doi.org/10.1161/CIRCRESAHA.120.316443.
102. Lombardi AA, Gibb AA, Arif E, Kolmetzky DW, Tomar D, Luongo TS, et al. Mitochondrial calcium exchange links metabolism with the epigenome to control cellular differentiation. Nat Commun. 2019;10(1):4509. https://doi.org/10.1038/s41467-019-12103-x.
103. Ma Y, Mouton AJ, Lindsey ML. Cardiac macrophage biology in the steady-state heart, the aging heart, and following myocardial infarction. Transl Res. 2018;191:15–28. https://doi.org/10.1016/j.trsl.2017.10.001.
104. Hulsmans M, Clauss S, Xiao L, Aguirre AD, King KR, Hanley A, et al. Macrophages facilitate electrical conduction in the heart. Cell. 2017;169(3):510–522.e520. https://doi.org/10.1016/j.cell.2017.03.050.
105. Nicolas-Avila JA, Lechuga-Vieco AV, Esteban-Martinez L, Sanchez-Diaz M, Diaz-Garcia E, Santiago DJ, et al. A network of macrophages supports mitochondrial homeostasis in the heart. Cell. 2020;183(1):94–109 e123. https://doi.org/10.1016/j.cell.2020.08.031.
106. Ma Y, Yabluchanskiy A, Iyer RP, Cannon PL, Flynn ER, Jung M, et al. Temporal neutrophil polarization following myocardial infarction. Cardiovasc Res. 2016;110(1):51–61.
107. Yan X, Anzai A, Katsumata Y, Matsuhashi T, Ito K, Endo J, et al. Temporal dynamics of cardiac immune cell accumulation following acute myocardial infarction. J Mol Cell Cardiol. 2013;62:24–35. https://doi.org/10.1016/j.yjmcc.2013.04.023.
108. Horckmans M, Ring L, Duchene J, Santovito D, Schloss MJ, Drechsler M, et al. Neutrophils orchestrate post-myocardial infarction healing by polarizing macrophages towards a reparative phenotype. Eur Heart J. 2017;38(3):187–97. https://doi.org/10.1093/eurheartj/ehw002.
109. Aurora AB, Porrello ER, Tan W, Mahmoud AI, Hill JA, Bassel-Duby R, et al. Macrophages are required for neonatal heart regeneration. J Clin Invest. 2014;124(3):1382–92. https://doi.org/10.1172/JCI72181.
110. Viola A, Munari F, Sanchez-Rodriguez R, Scolaro T, Castegna A. The metabolic signature of macrophage responses. Front Immunol. 2019;10:1462. https://doi.org/10.3389/fimmu.2019.01462.
111. Fossati G, Moulding DA, Spiller DG, Moots RJ, White MR, Edwards SW. The mitochondrial network of human neutrophils: role in chemotaxis, phagocytosis, respiratory burst activation, and commitment to apoptosis. J Immunol. 2003;170(4):1964–72. https://doi.org/10.4049/jimmunol.170.4.1964.
112. Tanimura A, Miyoshi K, Horiguchi T, Hagita H, Fujisawa K, Noma T. Mitochondrial activity and unfolded protein response are required for neutrophil differentiation. Cell Physiol Biochem. 2018;47(5):1936–50. https://doi.org/10.1159/000491464.

113. Ahmed D, Roy D, Jaworski A, Edwards A, Abizaid A, Kumar A, et al. Differential remodeling of the electron transport chain is required to support TLR3 and TLR4 signaling and cytokine production in macrophages. Sci Rep. 2019;9(1):18801. https://doi.org/10.1038/s41598-019-55295-4.
114. Wang T, Liu H, Lian G, Zhang SY, Wang X, Jiang C. HIF1alpha-induced glycolysis metabolism is essential to the activation of inflammatory macrophages. Mediat Inflamm. 2017;2017:9029327. https://doi.org/10.1155/2017/9029327.
115. Wu J, Sun P, Chen Q, Sun Y, Shi M, Mang G, et al. Metabolic reprogramming orchestrates CD4(+) T-cell immunological status and restores cardiac dysfunction in autoimmune induced-dilated cardiomyopathy mice. J Mol Cell Cardiol. 2019;135:134–48. https://doi.org/10.1016/j.yjmcc.2019.08.002.
116. Weirather J, Hofmann UD, Beyersdorf N, Ramos GC, Vogel B, Frey A, et al. Foxp3+ CD4+ T cells improve healing after myocardial infarction by modulating monocyte/macrophage differentiation. Circ Res. 2014;115(1):55–67. https://doi.org/10.1161/CIRCRESAHA.115.303895.
117. Dang EV, Barbi J, Yang HY, Jinasena D, Yu H, Zheng Y, et al. Control of T(H)17/T(reg) balance by hypoxia-inducible factor 1. Cell. 2011;146(5):772–84. https://doi.org/10.1016/j.cell.2011.07.033.
118. Corcoran SE, O'Neill LA. HIF1alpha and metabolic reprogramming in inflammation. J Clin Invest. 2016;126(10):3699–707. https://doi.org/10.1172/JCI84431.
119. Mouton AJ, Flynn ER, Moak SP, Aitken NM, Omoto ACM, Li X, et al. Dimethyl fumarate preserves left ventricular infarct integrity following myocardial infarction via modulation of cardiac macrophage and fibroblast oxidative metabolism. J Mol Cell Cardiol. 2021;158:38–48. https://doi.org/10.1016/j.yjmcc.2021.05.008.
120. Ashrafian H, Czibik G, Bellahcene M, Aksentijevic D, Smith AC, Mitchell SJ, et al. Fumarate is cardioprotective via activation of the Nrf2 antioxidant pathway. Cell Metab. 2012;15(3):361–71. https://doi.org/10.1016/j.cmet.2012.01.017.
121. Kaelin WG Jr, McKnight SL. Influence of metabolism on epigenetics and disease. Cell. 2013;153(1):56–69. https://doi.org/10.1016/j.cell.2013.03.004.
122. Her YF, Maher LJ 3rd. Succinate dehydrogenase loss in familial Paraganglioma: biochemistry, genetics, and epigenetics. Int J Endocrinol. 2015;2015:296167. https://doi.org/10.1155/2015/296167.
123. Letouze E, Martinelli C, Loriot C, Burnichon N, Abermil N, Ottolenghi C, et al. SDH mutations establish a hypermethylator phenotype in paraganglioma. Cancer Cell. 2013;23(6):739–52. https://doi.org/10.1016/j.ccr.2013.04.018.
124. Bersell K, Arab S, Haring B, Kuhn B. Neuregulin1/ErbB4 signaling induces cardiomyocyte proliferation and repair of heart injury. Cell. 2009;138(2):257–70. https://doi.org/10.1016/j.cell.2009.04.060.
125. Pentassuglia L, Heim P, Lebboukh S, Morandi C, Xu L, Brink M. Neuregulin-1beta promotes glucose uptake via PI3K/Akt in neonatal rat cardiomyocytes. Am J Physiol Endocrinol Metab. 2016;310(9):E782–94. https://doi.org/10.1152/ajpendo.00259.2015.
126. Ibar C, Irvine KD. Integration of hippo-YAP signaling with metabolism. Dev Cell. 2020;54(2):256–67. https://doi.org/10.1016/j.devcel.2020.06.025.
127. Kashihara T, Sadoshima J. Role of YAP/TAZ in energy metabolism in the heart. J Cardiovasc Pharmacol. 2019;74(6):483–90. https://doi.org/10.1097/FJC.0000000000000736.
128. Enzo E, Santinon G, Pocaterra A, Aragona M, Bresolin S, Forcato M, et al. Aerobic glycolysis tunes YAP/TAZ transcriptional activity. EMBO J. 2015;34(10):1349–70. https://doi.org/10.15252/embj.201490379.
129. Aharonov A, Shakked A, Umansky KB, Savidor A, Genzelinakh A, Kain D, et al. ERBB2 drives YAP activation and EMT-like processes during cardiac regeneration. Nat Cell Biol. 2020;22(11):1346–56. https://doi.org/10.1038/s41556-020-00588-4.

Environmental Signals

20

George A. Porter, Jr

Abstract

Environmental factors have long been known to play a role in the pathogenesis of congenital heart disease (CHD), but this has not been a major focus of research in the modern era. Studies of human exposures and animal models demonstrate that demographics (age, race, socioeconomic status), diseases (e.g., diabetes, hypertension, obesity, stress, infection, high altitude), recreational and therapeutic drug use, and chemical exposures are associated with an increased risk for CHD. Unfortunately, although studies suggest that exposures to these factors may cause CHD, in most cases, the data are not strong, are inconclusive, or are contradictory. Although most studies concentrate on the effects of maternal exposure, paternal exposure to some agents can also modify this risk. From a mechanistic standpoint, recent delineation of signaling and genetic controls of cardiac development has revealed molecular pathways that may explain the effects of environmental signals on cardiac morphogenesis and may provide further tools to study the effects of environmental stimuli on cardiac development. For example, environmental factors likely regulate cellular signaling pathways, transcriptional and epigenetic regulation, proliferation, and physiologic processes that can control the development of the heart and other organs. However, understanding of the epidemiology and risk of these exposures and the mechanistic basis for any effects on cardiac development remains incomplete. Further studies defining the relationship between environmental exposures and human CHD and the mechanisms involved should reveal strategies to prevent, diagnose, and treat CHD induced by environmental signals.

G. A. Porter, Jr (✉)
Departments of Pediatrics (Cardiology), Pharmacology and Physiology, and Medicine (Aab Cardiovascular Research Institute), University of Rochester Medical Center, Rochester, NY, USA
e-mail: george_porter@urmc.rochester.edu

© The Author(s), under exclusive license to Springer Nature Switzerland AG 2024

S. Rickert-Sperling et al. (eds.), *Congenital Heart Diseases: The Broken Heart*,
Advances in Experimental Medicine and Biology 1441,
https://doi.org/10.1007/978-3-031-44087-8_20

Keywords

Alcohol · Congenital heart defects · Chemical exposure · Congenital heart disease · Diabetes · Environmental factors · Folate deficiency · Human demographics · Hypoxia · Hypoxia signaling pathways · Maternal exposure · Maternal infections · Maternal stress · Medications · Mitochondria · Noncoding RNA · Obesity · Oxidative stress · Paternal exposure · Retinoic acid · Rubella infections · Smoke · Teratogens · Thalidomide

20.1 Introduction

Since the beginning of the modern, molecular era of developmental biology, it has become commonplace to investigate the role of signaling pathways and genetics in human disease and in animal models. However, genetic influences on developmental processes cannot explain all CHD [1–3]. Single-gene mutations in humans and animal models can cause heterogeneous phenotypes, suggesting that other factors regulate normal and abnormal morphogenesis. Genetic background explains some of this variation, but much of it may be due to environmental signals. Indeed, it has been estimated that nongenetic factors may play a role in up to 30% of CHD [4], and recent data are revealing the mechanisms by which environmental factors might regulate signaling pathways and gene transcription to cause various forms of CHD (Fig. 20.1).

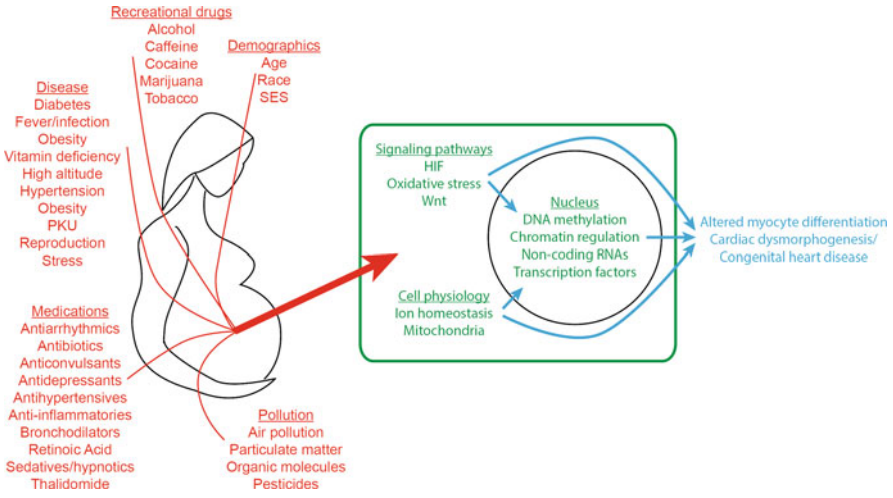

Fig. 20.1 Environmental factors can cause congenital heart disease. Exposure to various types of environmental factors (red) during pregnancy can affect multiple intracellular signaling pathways, cell physiologic process, and nuclear regulation of gene expression (green) to disrupt myocyte differentiation and cardiac morphogenesis to yield an infant with congenital heart disease

Cardiac morphogenesis is a complex process that extends from early gestation until well after birth, although the embryonic period (day 18–60 of human gestation) is generally the critical window for cardiac teratogenesis. Over the last 30 years, it has become apparent that the integration of numerous signaling pathways regulates an array of transcriptional regulatory factors to control cardiac morphogenesis, and mutations in many of these pathways cause CHD in animals and humans. More recent research has defined a role for epigenetic regulation of cardiac morphogenesis and also linked cardiac developmental abnormalities to structural and functional brain defects [5, 6]. These pathways are the subject of Part III of this book. However, environmental factors may modulate all of these processes to influence cardiac development. This chapter will summarize the evidence for the role of and potential mechanism by which environmental factors may control cardiac morphogenesis.

20.2 Role of Environmental Signals During Cardiac Development

20.2.1 General Evidence and Clinical Studies

Cardiac teratogens are environmental or physiologic factors that cause cardiac dysmorphogenesis and CHD. Generally, teratogens are thought to be environmental toxins, to which the mother and fetus are exposed, but human conditions, such as different demographic categories and maternal diseases, may also be considered teratogenic.

Prior to the 1980s, anecdotal evidence suggested that environmental factors played a role in the development of CHD. For example, the association of congenital rubella infection and CHD was reported in 1941 [7], and thalidomide use was associated with CHD in the 1950s and 1960s. These and other findings prompted large-scale epidemiologic studies to investigate the association of environmental factors and CHD. Two of the most important were case–control studies in Maryland and Virginia (the Baltimore Washington Infant Study [BWIS]) and in Finland [8, 9]. Additional reviews and more recent, large-scale, epidemiologic, and meta-analysis studies of multiple environmental factors [1, 10–15] are summarized below with additional citation of recent, more focused analyses of individual environmental agents; specific details can be found in these manuscripts. Many of these newer reports are from epidemiologic data from China and from the National Birth Defects Prevention Study in the United States.

The lack of clear data supporting the cardiac teratogenic potential of environmental factors is striking. In comparing data from various studies, the significance of individual environmental factors often is quite variable. For example, multiple medium/large studies show the relative risk (RR) or odds ratio (OR) of 0.9–1.3 for having a child with CHD after using selective serotonin reuptake inhibitors (SSRIs) during pregnancy, but in only one was there statistically significant risk [2, 13, 16]. Adding to this lack of definitive answers are smaller case reports and series without adequate controls. Finally, these studies are complicated by the presence of

overlapping risk factors in the population, which makes choosing appropriate controls and comparing individual studies difficult.

20.2.2 FDA Drug Risk Categories

Animal models are an excellent method to examine cardiac teratogenesis, but these studies can be difficult to interpret when the concentrations of reagents used in these studies are not consistent with human exposures or when data from human studies are lacking or inconsistent with results from these models. In 1979, the Food and Drug Administration (FDA) developed five Risk Categories (Table 20.1) that reflect the results of animal and human studies and the potential risks and benefits to the fetus and mother for each drug. However, in 2014, the FDA dramatically revised its rule for labeling of drugs for risk during pregnancy and lactation (https://www.fda.gov/drugs/labeling-information-drug-products/pregnancy-and-lactation-labeling-drugs-final-rule). The Pregnancy and Lactation Labeling (Drugs) Final Rule (PRLL) states that the previous categories should not be used. Instead, label information should include reference to a drug registry if available for that drug, a summary of relevant data about the pregnancy risks, and relevant information for health care providers to make prescribing decisions and counsel patients.

This newer FDA guidance has been partially adopted in that drug label information does contain the information described above to help patients and providers make prescribing decisions. However, many drug labels continue to refer to the Risk Categories described in Table 20.1, and these categories are useful to summarize the known data on the teratogenic risk of a particular agent. Therefore, the FDA Risk

Table 20.1 Definition of FDA Risk Categories for birth defects[a]

Risk category	Description
A	Adequate and well-controlled studies have failed to demonstrate a risk to the fetus in the first trimester of pregnancy (and there is no evidence of risk in later trimesters).
B	Animal reproduction studies have failed to demonstrate a risk to the fetus and there are no adequate and well-controlled studies in pregnant women.
C	Animal reproduction studies have shown an adverse effect on the fetus and there are no adequate and well-controlled studies in humans, but potential benefits may warrant use of the drug in pregnant women despite potential risks.
D	There is positive evidence of human fetal risk based on adverse reaction data from investigational or marketing experience or studies in humans, but potential benefits may warrant use of the drug in pregnant women despite potential risks.
X	Studies in animals or humans have demonstrated fetal abnormalities and/or there is positive evidence of human fetal risk based on adverse reaction data from investigational or marketing experience, and the risks involved in use of the drug in pregnant women clearly outweigh potential benefits.
N	Not classified.

[a]Source: http://chemm.nlm.nih.gov/pregnancycategories.htm

Table 20.2 FDA Risk Categories of various potentially cardio-teratogenic drugs[a]

Risk category	Drugs
A	Folate
B	Amoxicillin (±clavulanic acid), ampicillin, Cefotaxime, metronidazole
C	Acetaminophen, beta-carotene, bupropion, caffeine, cocaine (topical), codeine, diazepam, dofetilide, fluoxetine, ibuprofen, marinol, naproxen, rifampicin, sertraline, sotalol, sulfamethoxazole/trimethoprim, theophylline, tretinoin topical, zidovudine
D	Amiodarone, aspirin (in third trimester), carbamazepine, fluconazole, lithium, paroxetine, phenytoin, valproic acid
X	Retinoic acid agents (alitretinoin, etretinate, isotretinoin), thalidomide
N	Acetaminophen, aspirin, marijuana

[a]Sources include recent and past drug information inserts

Categories of the pharmacologic agents listed in the following section are presented in Table 20.2 for reference although note that this classification is not specific for cardiac teratogenesis.

20.2.3 Risk Assessment

The risk of developing CHD after different exposures can be defined in a number of ways depending on the methods. Generally, odds ratios (OR) are derived from case-control studies, while relative risks (RR) are derived from randomized control trials or cohort studies. As the following sections will summarize data from various studies, OR and RR will be sometimes be reported as OR/RR without confidence intervals, and the reader is referred to the individual references for details.

The relative importance of any particular environmental factor is a combination of the prevalence of exposure, the relative risk of associated CHD, and the clinical severity of the CHD. For example, the extremely low prevalence of uncontrolled phenylketonuria during pregnancy mitigates the high risk of CHD in these pregnancies. By contrast, although the risk for CHD after in utero exposure to diabetes, fever, tobacco smoking, ethanol ingestion, seizures, or obesity may (or may not) be low, the relative importance to society may be high due to the high prevalence of these exposures. From a global health care perspective, such factors guide investigations of these risks and the development of therapies to mitigate their effects.

20.3 Environmental Signals During Cardiac Development

The following sections review data from human studies of potential cardiac teratogens. Note that studies of the risk and etiology of congenital defects in conditions such as those listed below are complicated by the association of some

of these conditions with each other, making accurate assignment of any single risk factor difficult. One example of such a combination is the association of maternal fever, exposure to infectious agents, and the use of antibiotic and anti-inflammatory agents. Other combinations have been studied showing that there are interactions between the effects of folate supplementation and other exposures [17] and socioeconomic status and air pollution [14].

20.3.1 Human Demographics

20.3.1.1 Age

Younger and older age in both parents is associated with increased risk for all CHD or specific types of CHD, although these associations are inconsistent between studies [11, 13–15, 18–20]. Men older than 25 years and women older than 30 years and both men and women younger than 20 years may have increased risk.

20.3.1.2 Race

Race may alter the risk for CHD [14]. Some studies suggest that Caucasian infants are more likely to have left-sided obstructive lesions, septal defects, Ebstein's anomaly, and some conotruncal defects and are less likely to have atrial septal defect (ASD) and valvular pulmonary stenosis (PS) than African-American infants. One study showed equal risk for Hispanic women compared to Caucasian women. Eastern Asian infants are also more likely to have supracristal/outlet ventricular septal defect (VSD).

20.3.1.3 Socioeconomic Status

Lower socioeconomic status, perhaps associated with lower education levels, may be associated with increased risk for CHD, with the significant OR/RR of 1.1–3.4 [11, 13, 14, 19, 20].

20.3.2 Human Conditions and Diseases

20.3.2.1 Connective Tissue Disorders

Maternal connective tissue disorder has been associated with offspring CHD, particularly heterotaxy disorders, with an OR of 3 [18].

20.3.2.2 Diabetes

Pregestational and gestational maternal diabetes can cause many cardiac and noncardiac dysmorphology, particularly when it is uncontrolled in the early stages of pregnancy. Cardiac abnormalities include laterality defects, conotruncal defects, atrioventricular septal defect (AVSD), VSDs, and left-sided obstructive lesions. The OR/RR of any form of CHD in infants of diabetic mothers ranges from 1.8 to 18 [1, 2, 11, 13, 14, 18, 20–22]. This risk decreases with good glycemic control. In addition, gestational diabetes can lead to obstructive and nonobstructive

hypertrophic cardiomyopathy in infants. At any risk above baseline, the increasing rate of diabetes in the general population has worrisome implications for the global incidence of CHD.

20.3.2.3 Fever/Maternal Infections

Maternal fever is teratogenic in animal models. Although data are inconsistent among human studies (OR/RR = 1.8–2.9), meta-analyses suggest that human gestational fever in the first trimester increases the risk for CHD [1, 11, 13, 15, 17]. A variety of CHD types may be associated with fever, but conotruncal defects are the most common. However, interpreting data in humans are complicated by the effects of the infectious sources of and the therapies for fever [17]. For example, the relationship between maternal rubella infection and patent ductus arteriosus (PDA), PS, peripheral pulmonic stenosis (PPS), and VSDs is well documented, while some studies show that common treatments, such as multivitamins, may mitigate the risk of fevers. Influenza exposure during pregnancy may also increase the risk for CHD (OR/RR = 1.5–2.1) [1, 11, 13], and gestational HIV exposure increases the risk for dilated cardiomyopathy [1]. Zika virus causes congenital malformations and may increase the risk for minor cardiac defects, such as ASDs, VSDs, and PDAs, but there are very little published data on this [23, 24]. There are currently no data in the literature that suggest that the recent outbreaks of coronavirus infections, such as severe acute respiratory syndrome (SARS), middle east respiratory syndrome (MERS), and severe acute respiratory syndrome–related coronavirus 2 (SARSr-CoV-2), lead to CHD.

20.3.2.4 Folate Deficiency

Data supporting a risk for CHD in pregnancies complicated by folate (vitamin B9) deficiency are largely derived from studies showing that folate supplementation during early stage of pregnancy decreases the risk for CHD (OR/RR = 0.5–0.8) that is supported by meta-analyses [1, 11, 13, 15, 17]. Although the results of these studies are inconsistent, the potential benefit of folate supplementation during pregnancy on the risk of CHD strengthens the recommendation for this therapy. Additional studies suggest that hyperhomocysteinemia, which can result from folate and vitamin B12 deficiency, may also increase the risk for CHD [13]. Finally, multivitamin/folate use may ameliorate the effects of fever, alcohol, lithium, and hyperhomocysteinemia on the risk for CHD [25].

20.3.2.5 High Altitude/Hypoxia

Being born at high altitude causes maternal hypoxia and increases the risk for ASDs and PDAs, and this risk increases with increasing altitude [26, 27].

20.3.2.6 Hypertension and Hypercholesterolemia

Hypertension may increase the risk of CHD (OR/RR = 1.4–2.8), with perhaps a higher incidence of ASDs, VSDs, and conotruncal defects [13, 17, 18]. Some studies have also shown an association of CHD with maternal hypercholesterolemia [13].

20.3.2.7 Maternal Stress

Increased maternal stress has been associated with a risk (OR/RR = 1.4–2.7) for CHD, particularly conotruncal defects, in some studies [13].

20.3.2.8 Nutrients and Vitamins

Deficiency of some nutrients and vitamins may increase the risk for CHD. For example, lower intake of carbohydrates, folate, fructose, linoleic acid, niacin, riboflavin, and vitamins B12, A (retinoic acid), and E may increase the risk for offspring with D-transposition of the great arteries, while low intake of total protein and methionine may provide protection against tetralogy of Fallot (ToF) [2, 28].

20.3.2.9 Obesity

The association of obesity with CHD has been inconsistent among various studies, and OR/RR ranges between <1 and 3, but meta-analyses suggests that there is increased risk for CHD [11, 13–15, 20, 21]. These studies also suggest that increased risk is observed with increasing levels of obesity.

20.3.2.10 Phenylketonuria

There is a strong association of phenylketonuria with CHD, with a RR of >6 and a rate of up to 14% of pregnancies with high levels of phenylketonuria having newborns with CHD. However, good dietary control can reduce or eliminate this risk. The most likely CHD lesions to be seen are left-sided obstructive lesions, ToF, VSDs, and PDAs.

20.3.2.11 Reproductive History

Multiparous women are more likely to have children with CHD, while nulliparous women may have increased risk for children with ASDs, ToF, and VSDs [13, 18, 19]. A history of reproductive problems carries increased risk for ASDs, AVSDs, Ebstein's anomaly, and ToF. Assisted reproductive technology is associated with increased risk for congenital lesions (OR/RR = 1.2–1.6), including CHD such as aortic valve stenosis, ASDs, coarctation of the aorta (CoA), ToF, and VSDs [11, 13, 15].

20.3.2.12 Thyroid Disease

Maternal thyroid disease has been associated with CHD with an OR of 3 [18]. In addition, thyroid replacement therapy may increase the risk for CHD [13].

20.3.3 Recreational Drug Exposures

20.3.3.1 Alcohol

The original description of fetal alcohol syndrome included CHD. The data on this are inconsistent, but higher maternal alcohol consumption during pregnancy is associated with CHD, particularly ASDs, conotruncal defects, and VSDs (OR/RR = 1.1–3.0) [1, 13, 15, 17, 19–21]. However, although it is likely that

there is increased risk with increased alcohol consumption during pregnancy, the exact level of exposure required to increase the risk of CHD is difficult to determine.

20.3.3.2 Caffeine

Caffeine has not been shown to cause CHD in humans, although animal models of in utero exposure to caffeine may alter cardiac function in adults [1, 29, 30].

20.3.3.3 Tobacco Smoke

Active and passive exposure to tobacco smoking appears to increase the risk for CHD, particularly ASDs, VSDs, and conotruncal defects, although the risk is relatively low and inconsistent in a number of studies (OR/RR = 1.1–2.8) [1, 13, 17, 21]. Interestingly, meta-analyses confirmed that there is risk with tobacco smoke exposure, but paternal smoking and secondhand exposure appeared to be more significant than maternal smoking [11, 15]. It is too early to tell if vaping will be a cardiac teratogen in humans.

20.3.3.4 Other Recreational Drugs

Maternal cocaine use may increase the risk for CHD, such as ASDs, AVSDs, looping defects, PPS, and VSDs [1, 13]. Marijuana use by the mother may increase the risk for Ebstein's anomaly, tricuspid atresia, and VSDs [1, 13]. Paternal cocaine use increases the risk for ASDs, looping defects, VSDs, and/or tricuspid atresia, and paternal marijuana use increased the risk for VSDs in the BWIS [8, 13, 31].

20.3.4 Medications

20.3.4.1 Antiarrhythmic Medications

Type III antiarrhythmics (e.g., amiodarone, dofetilide, sotalol), which inhibit potassium channels, have been shown to cause heart defects in animal models, but no human studies have definitively shown an association with CHD. Most antiarrhythmics are considered to be in Risk Category C, although amiodarone is in Risk Category D due to teratogenicity in other organs [32]. Also note that other cardiovascular medications, such as those for heart failure, thrombosis, and pulmonary hypertension, are generally in Risk Categories B and C, with some notable exceptions [32].

20.3.4.2 Antibiotics

In general, antibiotic use during pregnancy is not thought to increase the risk for CHD. However, sulfonamide-containing antibiotics inhibit folate metabolism and may increase the risk for CHD (OR/RR = no risk or 1.8–3.4 depending on the study), such as CoA and hypoplastic left heart syndrome (HLHS), and this risk may be decreased by folate supplementation [1, 13]. In addition, metronidazole was associated with CHD in the BWIS, but this finding has not been validated by other studies [33]. By contrast, a meta-analysis recently showed fluconazole use during pregnancy increased the risk of CHD (OR ~ 1.9) [34]. The risk of antiretroviral

therapy (e.g., zidovudine) during pregnancy appears to be low for causing CHD. Antibiotics are generally listed under FDA Risk Category B or C, and a few common antibiotics are listed in Table 20.2.

20.3.4.3 Anticonvulsant Medications

Epilepsy may increase the risk for CHD due to the disease itself, comorbid conditions, or increased detection of CHD with increased surveillance [1, 18]. As a class, anticonvulsants may or may not increase the risk for CHD, but some individual agents, such as phenytoin, carbamazepine, and valproic acid (ASDs), increase this risk [1, 13].

20.3.4.4 Antidepressant Medications

The BWIS suggested that antidepressant medications may increase the risk of CHD if used during pregnancy (OR/RR = 3.0, range 1.2–7.6), but other studies do not necessarily confirm this. For example, studies on the risk of SSRI and serotonin-norepinephrine reuptake inhibitor use during pregnancy produced very mixed results [1, 13]. Fluoxetine (VSDs), paroxetine (ASDs, VSDs, right ventricular outflow tract obstruction [RVOTO]), and sertraline (ASDs, VSDs) have been found to cause CHD in some studies, but many other studies have not demonstrated significant risk. Some large-scale studies have found no significant risk of CHD in women taking antidepressants during the first trimester of pregnancy compared to other women with depression who did not take these drugs [16]. A meta-analysis suggests that SSRI use during pregnancy increases the risk for CHD [15], and inserts for some SSRIs do warn that there is a higher risk for cardiac malformations (2%) if these agents are used during the first trimester of pregnancy.

The association of tricyclic antidepressant use during pregnancy with CHD is also inconsistent. In addition, lithium use during pregnancy increases the risk for CHD, particularly Ebstein's anomaly (RR = 1.65), despite lingering questions about the magnitude of this risk [35]. Finally, maternal depression itself may increase the risk of delivering a child with CHD [18] for reasons discussed in the last section.

20.3.4.5 Antihypertensive Medications

Studies of the association between various antihypertensive medications, including angiotensin-converting enzyme inhibitors and beta-blockers, during pregnancy and CHD give inconsistent results, and any CHD associated with these agents could be due to the underlying hypertension [1, 13].

20.3.4.6 Anti-Inflammatory Agents

Reports on the risk of CHD when mothers have taken aspirin, ibuprofen, and other nonsteroidal anti-inflammatory drugs (NSAIDs) have been inconsistent, although associations with AVSDs, bicuspid aortic valves, conotruncal defects, HLHS, interrupted aortic arch, and VSDs have been reported (OR/RR = 0.9–1.9) [1, 13, 36]. In addition, the use of a number of NSAIDs in late pregnancy has been associated with premature closure of the ductus arteriosus and conversely with the persistence of PDAs, and thus, these agents should be avoided in the third trimester

of pregnancy. Neither maternal acetaminophen nor corticosteroid use appears to increase the risk for CHD [1, 36].

20.3.4.7 Bronchodilators

There is a relationship between the use of bronchodilators, but not inhaled anti-inflammatory agents, during early pregnancy and some forms of CHD (OR/RR = 1.1–2.5) [13, 37], while worse maternal asthma status/control may predispose to CHD in offspring [38].

20.3.4.8 Retinoic Acid/Vitamin A

Animal and human studies demonstrate that vitamin A analogs affect cardiac development and cause a variety of defects, particularly conotruncal defects (RR = 0–9.2) [1]. Retinoic acid agents, even most topical formulations that may be used to treat acne, are listed in FDA Risk Category X. However, beta-carotene use seems to be safe during pregnancy. By contrast, low intake of vitamin A may be associated with CHD [28].

20.3.4.9 Sedatives/Hypnotics

The small amount of data available on the effects of sedatives and narcotics during pregnancy on CHD risk is inconsistent [1], but a more recent report suggests that opioid use increases the risk for CHD (OR = 1.9) and specifically for ToF [36].

20.3.4.10 Thalidomide

The use of this agent as an antiemetic in the 1960s led to congenital heart defects in up to 30%, particularly ASDs, conotruncal defects, and VSDs. Its use is contraindicated during pregnancy.

20.3.5 Chemical Exposures

Exposure to various environmental pollutants is known to affect human development, including the heart [1, 10, 13, 14]. Furthermore, studies have shown that low socioeconomic status is associated with higher levels of pollution [14]. Determining the extent of this problem and the specific substances that cause cardiac teratogenesis has been aided in recent years by large epidemiologic studies.

20.3.5.1 Air Pollution

The risk of developing CHD in the children of women exposed to air pollution could be due to the molecules in the polluted air (carbon monoxide, nitrogen dioxide, ozone, sulfur dioxide) or the particulate matter, to which the molecules can bind ($PM_{2.5}$ and PM_{10}, particulate matter less than 2.5 and 10 microns, respectively). Recent studies and meta-analyses from throughout the world suggest that air pollution is associated with CHD, but the effect size is relatively low and there is great variability regarding the causative molecules and particles [1, 10–13, 15, 19, 39–46].

20.3.5.2 Organic Molecules and Solvents

A variety of other environmental agents that may be cardiac teratogens. Chlorinated molecules, heavy metals, hazardous waste, organic solvents, radiation, and xenoestrogens are inconsistently associated with the development of CHD [1, 10, 13, 19, 21, 47, 48]. For example, organic compounds may increase the risk for ASDs, coarctation of the aorta, conotruncal defects, and VSDs, but this risk has not been seen in all studies. Some manuscripts report more risk after paternal exposure compared to maternal exposure.

20.3.5.3 Pesticides

Gestational exposure to pesticides may increase the risk of CHD, but the results are inconsistent and, in some cases, required secondary analysis to find significance [1, 10, 19, 20]. Associated lesions include ASDs, conotruncal defects, HLHS, total anomalous pulmonary venous return, and VSDs.

20.4 Potential Signaling Pathways Affected by Environmental Agents

Understanding how the environmental agents discussed above can affect cardiac morphogenesis to cause CHD is currently problematic due to a lack of both basic knowledge about the effects of these factors on the processes that control cardiac development and clinical confirmation of these effects. Over the last 30 years, extensive research has defined many molecular mechanisms that control heart morphogenesis, and each year new mechanisms are discovered, but linking these vital pathways to environment signals has not been a major focus of research. The following sections briefly summarize how cardiac regulatory pathways may be regulated by environmental factors, with some examples of recent investigations into this subject.

20.4.1 Extracellular and Intracellular Signaling Pathways and Cardiac Transcription Factors

Even before the heart fields form in the early gastrulating embryo, extracellular and intracellular signaling pathways feed into transcription factor networks to regulate the specification, proliferation, differentiation, migration, and function of cells in the heart (see other chapters in Part. III for reviews of these pathways). Although effects of environmental stimuli on these pathways during cardiac development have received little attention, some published data in animal models suggest that these cascades can be regulated by environmental factors to cause CHD. At least one report in humans shows such an interaction between maternal diabetes and variants of the cardiac transcription factor NKX2-5 [22], while expression of a number of important signaling pathway and transcription factor genes is altered in diabetic rodent models of gestational diabetes [49]. Additional studies suggest that the

organic pollutant, perfluorooctane sulfonate (PFOS), and xenoestrogens/phthalates alter the expression of transcription factors such as NKX2-5, PCG-1α, and TBX5 in differentiating cardiac myocytes and the developing zebrafish heart [47, 50–52]. For further details on the role of these pathways during cardiac development, see the other chapters in this section, while the perspective by Kalisch-Smith gives an excellent and more detailed review of the interaction of environmental agents and these pathways [2].

20.4.1.1 Hypoxia Signaling Pathways

Altered oxygen content (hypoxia, hyperoxia) has been shown to control cardiac morphogenesis, proliferation, and differentiation from early development to the postnatal period via a number of signaling pathways, the most well-known being hypoxia-inducible factor (HIF) signaling [53, 54]. Hypoxia and hyperoxia can also increase oxidative stress, which also feels back to control the HIF pathway (see below). Pregnancy at high altitude may directly control hypoxia signaling, while secondary effects on these pathways may occur due to environmental factors that alter oxidative stress or mitochondrial function. For example, HIF signaling and the expression of HIF gene targets are increased in rodent models of gestational diabetes, while haploinsufficiency of HIF1A increases cardiac malformations in these models [49].

20.4.1.2 Oxidative Stress Pathways

There are little specific human data on environmental control of reactive oxygen species (ROS) signaling in the developing heart, but treatment with antioxidants during diabetic pregnancies can prevent CHD [1]. Many environmental factors, including alcohol, diabetes, therapeutic drugs (e.g., phenytoin, thalidomide, valproic acid), heavy metals, hyperhomocysteinemia, pesticides, pollution, tobacco smoke, and xenoestrogens, may cause oxidative stress in utero by increasing ROS production or decreasing antioxidant defenses [49, 50]. These changes could affect the activity of cardiac transcription factors, such HIFs, GATA-binding protein 4 (GATA4), myocyte enhancer factor 2C (MEF2C), and NK2 homeobox 5 (NKX2-5) [55].

20.4.1.3 Retinoic Acid Receptor Signaling

Retinoic acid/vitamin A deficiency or abundance can affect retinoic acid receptor nuclear transcription factors that control laterality signaling pathways involving left-right determination factors (LEFTY), nodal growth differentiation factor (NODAL), and paired-like homeodomain 2 (PITX2) as well as pathways that control myocyte patterning, proliferation, and differentiation [56].

20.4.1.4 Wnt Signaling

Alcohol, folate, lithium, and homocysteine may work via Wnt (Wingless and Int-1) signaling to regulate/disrupt the expression of genes involved in early cardiac development [25]. Gestational diabetes in animal models alters canonical and noncanonical Wnt signaling pathways [49].

20.4.1.5 Miscellaneous Pathways

Caffeine may affect adenosine and phosphodiesterase signaling to alter cardiac development [57]. Xenoestrogens and other pollutants may regulate hormone signaling pathways in the early heart [55]. Furthermore, stress or exogenous steroid treatment during pregnancy may alter maternal glucocorticoid levels, while maternal diabetes could affect embryonic/fetal insulin signaling to affect the developing heart. SSRIs could affect serotonin signaling pathways in developing myocardium and cardiac neural crest cells. NSAIDs inhibit cyclooxygenases to close the PDA and could affect other aspects of cardiac development via this pathway.

20.4.2 Epigenetics: DNA and Histone Modifications and Noncoding RNAs

Epigenetics is the study of heritable mechanisms that regulate gene transcription without modifying the sequence of the deoxyribonucleic acid (DNA). The three epigenetic processes (DNA methylation, histone modification, and noncoding ribonucleic acids (RNAs)) control chromatin remodeling and mRNA processing and can regulate cardiac morphogenesis, metabolism, and myocyte differentiation (see also Chaps. 17 and 18). For example, human mutations in histone methylation pathways are associated with CHD [6]. Published data from other systems or work in the mature heart suggest that many of the factors listed in Sect. 20.3 control epigenetic mechanisms, and some recent reports suggest that this also occurs in the developing heart. For example, in utero exposure to $PM_{2.5}$ in mice decreased the binding of acetylated histone 3 (H3K9ac) to the GATA4 promoter, decreasing its expression and causing changes in myocyte structure [58].

20.4.2.1 DNA Methylation

Methylation of DNA in utero can be affected by environmental factors [43]. Folate deficiency and hyperhomocysteinemia may affect DNA methylation as these molecules are essential to the DNA methylation pathway. In utero exposure to alcohol, caffeine, and hypoxia alters DNA methylation [25, 30, 59]. DNA methylation in the developing heart has also been shown to be altered by air pollution-, diabetes-, heavy metal-, phthalate-induced oxidative stress, isotretinoin, and thalidomide [51, 60–62].

20.4.2.2 Chromatin and Histone Modification

As with DNA methylation, epigenetic chromatin and histone modulation can be disrupted by environmental factors [43]. For example, valproic acid inhibition of a histone deacetylase may explain some of its teratogenicity [62]. Diabetes and antidepressants (SSRI and tricyclic) also affect chromatin remodeling via effects on histone modifying enzymes [49, 60, 62].

20.4.2.3 Noncoding RNAs

Data suggest that air pollution, alcohol, diabetes, heavy metals, and xenoestrogens affect the expression of a number of microRNAs [43, 60, 61]. Little is known about environmental regulation of long noncoding RNAs in the developing heart.

20.4.3 Physiologic Factors

20.4.3.1 Ion Homeostasis

Lithium inhibits various channels and exchangers, and other environmental agents may regulate ion homeostasis to control cellular physiology. For example, diabetes and caffeine can modify calcium release from the sarcoplasmic reticulum to alter myocyte contractility and calcium signaling pathways [57, 60]. In addition, PFOS decreases intracellular calcium signaling in embryonic stem cell-cardiac myocytes [52].

20.4.3.2 Mitochondria

Mitochondria regulate myocyte physiology, differentiation, and embryonic survival. Hypoxia may regulate mitochondrial function as low oxygen concentrations limit oxidative phosphorylation. In addition, hypoxia may paradoxically increase oxidative stress, which can affect mitochondrial function. Disruption of canonical Wnt signaling, via glycogen synthase kinase-3β or other pathways, could also affect mitochondrial activity. These changes in mitochondrial function can regulate ROS signaling pathways that control cardiac myocyte differentiation [63]. In addition, environmental signals converging on mitochondria may affect stress, apoptotic, and necrotic pathways centered on mitochondria. Finally, teratogens could disrupt the production of metabolites derived from mitochondria and bioenergetic pathways, which are essential for epigenetic regulation of gene expression [64]. One example of environmental agent-mediated mitochondrial effects during cardiac development is the ability of PFOS to alter mitochondrial structure and decrease mitochondrial function, ATP production, and peroxisome proliferator-activated receptor-gamma coactivator-1α (PCG-1α) expression in embryonic stem cell-derived cardiac myocytes [52]. Furthermore, PFOS and phthalates can increase apoptosis in cardiac myocytes and the developing zebrafish heart [50, 51].

20.4.4 Multiple Pathways May Be Involved

Finally, as should be apparent in the previous sections, a single environmental agent may affect multiple pathways that can modulate developmental processes in the heart. Two examples discussed above include (1) the effects of PFOS on intracellular calcium signaling, mitochondrial function, ATP production, apoptosis, and expression of various molecules and transcriptional regulators in differentiating cardiac myocytes [50, 52]; and (2) the effects of diabetes on intracellular signals (Wnt, HIF), gene transcription, and epigenetic mechanisms in the rodent heart [49]. Thus, the

signaling pathways and physiologic processes affected by environmental agents likely contribute to their epigenetic effects to create a complex cascade that disrupts cardiac development.

20.5 Conclusion

Every cellular pathway that regulates metabolism, proliferation, differentiation, and cell death can be affected by many environmental factors. However, although studies in humans and animals support a role for these factors in CHD, in many cases, data are insufficient to draw definitive conclusions about the magnitude of and mechanisms of action by which most environmental factors cause CHD. Further studies of the causative role of human environmental exposures in the pathogenesis of CHD and of the cellular mechanisms by which these factors exert these effects should be undertaken to design strategies to prevent, diagnose, and treat CHD induced by environmental signals.

References

1. Jenkins KJ, Correa A, Feinstein JA, Botto L, Britt AE, Daniels SR, Elixson M, Warnes CA, Webb CL. Noninherited risk factors and congenital cardiovascular defects: current knowledge: a scientific statement from the American Heart Association Council on Cardiovascular Disease in the Young: endorsed by the American Academy of Pediatrics. Circulation. 2007;115(23): 2995–3014.
2. Kalisch-Smith JI, Ved N, Sparrow DB. Environmental risk factors for congenital heart disease. Cold Spring Harb Perspect Biol. 2020;12(3):a037234. https://doi.org/10.1101/cshperspect.a037234.
3. Nees SN, Chung WK. Genetic basis of human congenital heart disease. Cold Spring Harb Perspect Biol. 2020;12(9):a036749. https://doi.org/10.1101/cshperspect.a036749.
4. Wilson PD, Loffredo CA, Correa-Villasenor A, Ferencz C. Attributable fraction for cardiac malformations. Am J Epidemiol. 1998;148(5):414–23.
5. Homsy J, Zaidi S, Shen Y, Ware JS, Samocha KE, Karczewski KJ, DePalma SR, McKean D, Wakimoto H, Gorham J, Jin SC, Deanfield J, Giardini A, Porter GA Jr, Kim R, Bilguvar K, Lopez-Giraldez F, Tikhonova I, Mane S, Romano-Adesman A, Qi H, Vardarajan B, Ma L, Daly M, Roberts AE, Russell MW, Mital S, Newburger JW, Gaynor JW, Breitbart RE, Iossifov I, Ronemus M, Sanders SJ, Kaltman JR, Seidman JG, Brueckner M, Gelb BD, Goldmuntz E, Lifton RP, Seidman CE, Chung WK. De novo mutations in congenital heart disease with neurodevelopmental and other congenital anomalies. Science. 2015;350(6265): 1262–6. https://doi.org/10.1126/science.aac9396.
6. Zaidi S, Choi M, Wakimoto H, Ma L, Jiang J, Overton JD, Romano-Adesman A, Bjornson RD, Breitbart RE, Brown KK, Carriero NJ, Cheung YH, Deanfield J, DePalma S, Fakhro KA, Glessner J, Hakonarson H, Italia MJ, Kaltman JR, Kaski J, Kim R, Kline JK, Lee T, Leipzig J, Lopez A, Mane SM, Mitchell LE, Newburger JW, Parfenov M, Pe'er I, Porter G, Roberts AE, Sachidanandam R, Sanders SJ, Seiden HS, State MW, Subramanian S, Tikhonova IR, Wang W, Warburton D, White PS, Williams IA, Zhao H, Seidman JG, Brueckner M, Chung WK, Gelb BD, Goldmuntz E, Seidman CE, Lifton RP. De novo mutations in histone-modifying genes in congenital heart disease. Nature. 2013;498(7453):220–3. https://doi.org/10.1038/nature12141.
7. Forrest JM, Turnbull FM, Sholler GF, Hawker RE, Martin FJ, Doran TT, Burgess MA. Gregg's congenital rubella patients 60 years later. Med J Aust. 2002;177(11–12):664–7.

8. Ferencz C, Loffredo CA, Correa-Villasenor A, Wilson PD. Genetic and environmental risk factors of major cardiovascular malformations: the Baltimore-Washington Infant Study: 1981-1989, vol 5. Perspectives in pediatric cardiology. Armonk, NY: Futura Publishing Company; 1997.
9. Tikkanen J, Heinonen OP. Risk factors for cardiovascular malformations in Finland. Eur J Epidemiol. 1990;6(4):348–56.
10. Gorini F, Chiappa E, Gargani L, Picano E. Potential effects of environmental chemical contamination in congenital heart disease. Pediatr Cardiol. 2014;35(4):559–68. https://doi.org/10.1007/s00246-014-0870-1.
11. Lee KS, Choi YJ, Cho J, Lee H, Lee H, Park SJ, Park JS, Hong YC. Environmental and genetic risk factors of congenital anomalies: an umbrella review of systematic reviews and meta-analyses. J Korean Med Sci. 2021;36(28):e183. https://doi.org/10.3346/jkms.2021.36.e183.
12. Ma Z, Cao X, Chang Y, Li W, Chen X, Tang NJ. Association between gestational exposure and risk of congenital heart disease: a systematic review and meta-analysis. Environ Res. 2021;197:111014. https://doi.org/10.1016/j.envres.2021.111014.
13. Patel SS, Burns TL. Nongenetic risk factors and congenital heart defects. Pediatr Cardiol. 2013;34(7):1535–55. https://doi.org/10.1007/s00246-013-0775-4.
14. Peyvandi S, Baer RJ, Chambers CD, Norton ME, Rajagopal S, Ryckman KK, Moon-Grady A, Jelliffe-Pawlowski LL, Steurer MA. Environmental and socioeconomic factors influence the live-born incidence of congenital heart disease: a population-based study in California. J Am Heart Assoc. 2020;9(8):e015255. https://doi.org/10.1161/JAHA.119.015255.
15. Zhang TN, Wu QJ, Liu YS, Lv JL, Sun H, Chang Q, Liu CF, Zhao YH. Environmental risk factors and congenital heart disease: an umbrella review of 165 systematic reviews and meta-analyses with more than 120 million participants. Front Cardiovasc Med. 2021;8:640729. https://doi.org/10.3389/fcvm.2021.640729.
16. Huybrechts KF, Palmsten K, Avorn J, Cohen LS, Holmes LB, Franklin JM, Mogun H, Levin R, Kowal M, Setoguchi S, Hernandez-Diaz S. Antidepressant use in pregnancy and the risk of cardiac defects. N Engl J Med. 2014;370(25):2397–407. https://doi.org/10.1056/NEJMoa1312828.
17. Qu Y, Lin S, Bloom MS, Wang X, Nie Z, Ou Y, Mai J, Gao X, Wu Y, Chen J, Justino J, Tan H, Zhuang J, Liu X. First-trimester maternal folic acid supplementation modifies the effects of risk factors exposures on congenital heart disease in offspring. Life (Basel). 2021;11(8):724. https://doi.org/10.3390/life11080724.
18. Liu S, Joseph KS, Lisonkova S, Rouleau J, Van den Hof M, Sauve R, Kramer MS, Canadian Perinatal Surveillance System. Association between maternal chronic conditions and congenital heart defects: a population-based cohort study. Circulation. 2013;128(6):583–9. https://doi.org/10.1161/CIRCULATIONAHA.112.001054.
19. Liu X, Nie Z, Chen J, Guo X, Ou Y, Chen G, Mai J, Gong W, Wu Y, Gao X, Qu Y, Bell EM, Lin S, Zhuang J. Does maternal environmental tobacco smoke interact with social-demographics and environmental factors on congenital heart defects? Environ Pollut. 2018;234:214–22. https://doi.org/10.1016/j.envpol.2017.11.023.
20. Rocheleau CM, Bertke SJ, Lawson CC, Romitti PA, Sanderson WT, Malik S, Lupo PJ, Desrosiers TA, Bell E, Druschel C, Correa A, Reefhuis J, National Birth Defects Prevention Study. Maternal occupational pesticide exposure and risk of congenital heart defects in the National Birth Defects Prevention Study. Birth Defects Res. 2015;103(10):823–33. https://doi.org/10.1002/bdra.23351.
21. Patel J, Nembhard WN, Politis MD, Rocheleau CM, Langlois PH, Shaw GM, Romitti PA, Gilboa SM, Desrosiers TA, Insaf T, Lupo PJ, National Birth Defects Prevention Study. Maternal occupational exposure to polycyclic aromatic hydrocarbons and the risk of isolated congenital heart defects among offspring. Environ Res. 2020;186:109550. https://doi.org/10.1016/j.envres.2020.109550.
22. Zhao M, Diao J, Huang P, Li J, Li Y, Yang Y, Luo L, Zhang S, Chen L, Wang T, Zhu P, Qin J. Association of Maternal Diabetes Mellitus and Polymorphisms of the NKX2.5 gene in

children with congenital heart disease: a single centre-based case-control study. J Diabetes Res. 2020;2020:3854630. https://doi.org/10.1155/2020/3854630.
23. Cavalcanti DD, Alves LV, Furtado GJ, Santos CC, Feitosa FG, Ribeiro MC, Menge P, Lira IM, Alves JG. Echocardiographic findings in infants with presumed congenital Zika syndrome: retrospective case series study. PLoS One. 2017;12(4):e0175065. https://doi.org/10.1371/journal.pone.0175065.
24. Orofino DHG, Passos SRL, de Oliveira RVC, Farias CVB, Leite M, Pone SM, Pone M, Teixeira Mendes HAR, Moreira MEL, Nielsen-Saines K. Cardiac findings in infants with in utero exposure to Zika virus- a cross sectional study. PLoS Negl Trop Dis. 2018;12(3):e0006362. https://doi.org/10.1371/journal.pntd.0006362.
25. Linask KK, Huhta J. Folate protection from congenital heart defects linked with canonical Wnt signaling and epigenetics. Curr Opin Pediatr. 2010;22(5):561–6. https://doi.org/10.1097/MOP.0b013e32833e2723.
26. Gonzalez-Andrade F. High altitude as a cause of congenital heart defects: a medical hypothesis rediscovered in Ecuador. High Alt Med Biol. 2020;21(2):126–34. https://doi.org/10.1089/ham.2019.0110.
27. Chun H, Yue Y, Wang Y, Dawa Z, Zhen P, La Q, Zong Y, Qu Y, Mu D. High prevalence of congenital heart disease at high altitudes in Tibet. Eur J Prev Cardiol. 2019;26(7):756–9. https://doi.org/10.1177/2047487318812502.
28. Shaw GM, Carmichael SL, Yang W, Lammer EJ. Periconceptional nutrient intakes and risks of conotruncal heart defects. Birth Defects Res. 2010;88(3):144–51. https://doi.org/10.1002/bdra.20648.
29. Browne ML, Bell EM, Druschel CM, Gensburg LJ, Mitchell AA, Lin AE, Romitti PA, Correa A, National Birth Defects Prevention Study. Maternal caffeine consumption and risk of cardiovascular malformations. Birth Defects Res. 2007;79(7):533–43. https://doi.org/10.1002/bdra.20365.
30. Buscariollo DL, Breuer GA, Wendler CC, Rivkees SA. Caffeine acts via A1 adenosine receptors to disrupt embryonic cardiac function. PLoS One. 2011;6(12):e28296. https://doi.org/10.1371/journal.pone.0028296.
31. Ewing CK, Loffredo CA, Beaty TH. Paternal risk factors for isolated membranous ventricular septal defects. Am J Med Genet. 1997;71(1):42–6.
32. Halpern DG, Weinberg CR, Pinnelas R, Mehta-Lee S, Economy KE, Valente AM. Use of medication for cardiovascular disease during pregnancy: JACC State-of-the-art review. J Am Coll Cardiol. 2019;73(4):457–76. https://doi.org/10.1016/j.jacc.2018.10.075.
33. Nwosu OC, Bloom K. The safety of metronidazole in pregnancy. Health Care Women Int. 2021;42(4–6):726–38. https://doi.org/10.1080/07399332.2021.1882462.
34. Budani MC, Fensore S, Di Marzio M, Tiboni GM. Maternal use of fluconazole and congenital malformations in the progeny: a meta-analysis of the literature. Reprod Toxicol. 2021;100:42–51. https://doi.org/10.1016/j.reprotox.2020.12.018.
35. Patorno E, Huybrechts KF, Bateman BT, Cohen JM, Desai RJ, Mogun H, Cohen LS, Hernandez-Diaz S. Lithium use in pregnancy and the risk of cardiac malformations. N Engl J Med. 2017;376(23):2245–54. https://doi.org/10.1056/NEJMoa1612222.
36. Interrante JD, Ailes EC, Lind JN, Anderka M, Feldkamp ML, Werler MM, Taylor LG, Trinidad J, Gilboa SM, Broussard CS, National Birth Defects Prevention Study. Risk comparison for prenatal use of analgesics and selected birth defects, National Birth Defects Prevention Study 1997-2011. Ann Epidemiol. 2017;27(10):645–653.e642. https://doi.org/10.1016/j.annepidem.2017.09.003.
37. Howley MM, Papadopoulos EA, Van Bennekom CM, Van Zutphen AR, Carmichael SL, Munsie JW, Herdt ML, Browne ML, National Birth Defects Prevention Study. Asthma medication use and risk of birth defects: National Birth Defects Prevention Study, 1997-2011. J Allergy Clin Immunol Pract. 2020;8(10):3490–3499.e3499. https://doi.org/10.1016/j.jaip.2020.07.033.

38. Lin S, Herdt-Losavio M, Gensburg L, Marshall E, Druschel C. Maternal asthma, asthma medication use, and the risk of congenital heart defects. Birth Defects Res. 2009;85(2):161–8. https://doi.org/10.1002/bdra.20523.
39. Huang CC, Chen BY, Pan SC, Ho YL, Guo YL. Prenatal exposure to PM2.5 and congenital heart diseases in Taiwan. Sci Total Environ. 2019;655:880–6. https://doi.org/10.1016/j.scitotenv.2018.11.284.
40. Huang C, Li J, Qin G, Liew Z, Hu J, Laszlo KD, Tao F, Obel C, Olsen J, Yu Y. Maternal hypertensive disorder of pregnancy and offspring early-onset cardiovascular disease in childhood, adolescence, and young adulthood: a national population-based cohort study. PLoS Med. 2021;18(9):e1003805. https://doi.org/10.1371/journal.pmed.1003805.
41. Parkes B, Hansell AL, Ghosh RE, Douglas P, Fecht D, Wellesley D, Kurinczuk JJ, Rankin J, de Hoogh K, Fuller GW, Elliott P, Toledano MB. Risk of congenital anomalies near municipal waste incinerators in England and Scotland: retrospective population-based cohort study. Environ Int. 2020;134:104845. https://doi.org/10.1016/j.envint.2019.05.039.
42. Stingone JA, Luben TJ, Sheridan SC, Langlois PH, Shaw GM, Reefhuis J, Romitti PA, Feldkamp ML, Nembhard WN, Browne ML, Lin S, National Birth Defects Prevention Study. Associations between fine particulate matter, extreme heat events, and congenital heart defects. Environ Epidemiol. 2019;3(6):e071. https://doi.org/10.1097/EE9.0000000000000071.
43. Vecoli C, Pulignani S, Andreassi MG. Genetic and epigenetic mechanisms linking air pollution and congenital heart disease. J Cardiovasc Dev Dis. 2016;3(4):32. https://doi.org/10.3390/jcdd3040032.
44. Wang L, Xiang X, Mi B, Song H, Dong M, Zhang S, Bi Y, Zhao Y, Li Q, Zhang Q, Zhang L, Yan H, Wang D, Dang S. Association between early prenatal exposure to ambient air pollution and birth defects: evidence from newborns in Xi'an, China. J Public Health (Oxf). 2019;41(3):494–501. https://doi.org/10.1093/pubmed/fdy137.
45. Yu G, Chen Y, Tang J, Lin Z, Zheng F, Zheng C, Zhou J, Su Q, Wu S, Li H. Meta-analyses of maternal exposure to atmospheric particulate matter and risk of congenital anomalies in offspring. Environ Sci Pollut Res Int. 2021;28(40):55869–87. https://doi.org/10.1007/s11356-021-16200-7.
46. Zhang Q, Sun S, Sui X, Ding L, Yang M, Li C, Zhang C, Zhang X, Hao J, Xu Y, Lin S, Ding R, Cao J. Associations between weekly air pollution exposure and congenital heart disease. Sci Total Environ. 2021;757:143821. https://doi.org/10.1016/j.scitotenv.2020.143821.
47. Ou Y, Zeng X, Lin S, Bloom MS, Han F, Xiao X, Wang H, Matala R, Li X, Qu Y, Nie Z, Dong G, Liu X. Gestational exposure to perfluoroalkyl substances and congenital heart defects: a nested case-control pilot study. Environ Int. 2021;154:106567. https://doi.org/10.1016/j.envint.2021.106567.
48. Snijder CA, Vlot IJ, Burdorf A, Obermann-Borst SA, Helbing WA, Wildhagen MF, Steegers EA, Steegers-Theunissen RP. Congenital heart defects and parental occupational exposure to chemicals. Hum Reprod. 2012;27(5):1510–7. https://doi.org/10.1093/humrep/des043.
49. Basu M, Garg V. Maternal hyperglycemia and fetal cardiac development: clinical impact and underlying mechanisms. Birth Defects Res. 2018;110(20):1504–16. https://doi.org/10.1002/bdr2.1435.
50. Cheng W, Yu Z, Feng L, Wang Y. Perfluorooctane sulfonate (PFOS) induced embryotoxicity and disruption of cardiogenesis. Toxicol In Vitro. 2013;27(5):1503–12. https://doi.org/10.1016/j.tiv.2013.03.014.
51. Mu X, Chen X, Liu J, Yuan L, Wang D, Qian L, Qian Y, Shen G, Huang Y, Li X, Li Y, Lin X. A multi-omics approach reveals molecular mechanisms by which phthalates induce cardiac defects in zebrafish (Danio rerio). Environ Pollut. 2020;265(Pt B):113876. https://doi.org/10.1016/j.envpol.2019.113876.
52. Tang LL, Wang JD, Xu TT, Zhao Z, Zheng JJ, Ge RS, Zhu DY. Mitochondrial toxicity of perfluorooctane sulfonate in mouse embryonic stem cell-derived cardiomyocytes. Toxicology. 2017;382:108–16. https://doi.org/10.1016/j.tox.2017.03.011.

53. O'Reilly VC, Lopes Floro K, Shi H, Chapman BE, Preis JI, James AC, Chapman G, Harvey RP, Johnson RS, Grieve SM, Sparrow DB, Dunwoodie SL. Gene-environment interaction demonstrates the vulnerability of the embryonic heart. Dev Biol. 2014;391(1):99–110. https://doi.org/10.1016/j.ydbio.2014.03.005.
54. Puente BN, Kimura W, Muralidhar SA, Moon J, Amatruda JF, Phelps KL, Grinsfelder D, Rothermel BA, Chen R, Garcia JA, Santos CX, Thet S, Mori E, Kinter MT, Rindler PM, Zacchigna S, Mukherjee S, Chen DJ, Mahmoud AI, Giacca M, Rabinovitch PS, Aroumougame A, Shah AM, Szweda LI, Sadek HA. The oxygen-rich postnatal environment induces cardiomyocyte cell-cycle arrest through DNA damage response. Cell. 2014;157(3):565–79. https://doi.org/10.1016/j.cell.2014.03.032.
55. Al-Gubory KH. Environmental pollutants and lifestyle factors induce oxidative stress and poor prenatal development. Reprod Biomed Online. 2014;29:17. https://doi.org/10.1016/j.rbmo.2014.03.002.
56. Wagner M, Siddiqui MA. Signal transduction in early heart development (II): ventricular chamber specification, trabeculation, and heart valve formation. Exp Biol Med (Maywood). 2007;232(7):866–80.
57. Buscariollo DL, Fang X, Greenwood V, Xue H, Rivkees SA, Wendler CC. Embryonic caffeine exposure acts via A1 adenosine receptors to alter adult cardiac function and DNA methylation in mice. PLoS One. 2014;9(1):e87547. https://doi.org/10.1371/journal.pone.0087547.
58. Li R, Zhao Y, Shi J, Zhao C, Xie P, Huang W, Yong T, Cai Z. Effects of PM2.5 exposure in utero on heart injury, histone acetylation and GATA4 expression in offspring mice. Chemosphere. 2020;256:127133. https://doi.org/10.1016/j.chemosphere.2020.127133.
59. Patterson AJ, Chen M, Xue Q, Xiao D, Zhang L. Chronic prenatal hypoxia induces epigenetic programming of PKCε gene repression in rat hearts. Circ Res. 2010;107(3):365–73. https://doi.org/10.1161/CIRCRESAHA.110.221259.
60. Asrih M, Steffens S. Emerging role of epigenetics and miRNA in diabetic cardiomyopathy. Cardiovasc Pathol. 2013;22(2):117–25. https://doi.org/10.1016/j.carpath.2012.07.004.
61. Baccarelli A, Ghosh S. Environmental exposures, epigenetics and cardiovascular disease. Curr Opin Clin Nutr Metab Care. 2012;15(4):323–9. https://doi.org/10.1097/MCO.0b013e328354bf5c.
62. Csoka AB, Szyf M. Epigenetic side-effects of common pharmaceuticals: a potential new field in medicine and pharmacology. Med Hypotheses. 2009;73(5):770–80. https://doi.org/10.1016/j.mehy.2008.10.039.
63. Hom JR, Quintanilla RA, Hoffman DL, de Mesy Bentley KL, Molkentin JD, Sheu SS, Porter GA Jr. The permeability transition pore controls cardiac mitochondrial maturation and myocyte differentiation. Dev Cell. 2011;21(3):469–78. https://doi.org/10.1016/j.devcel.2011.08.008.
64. Ly CH, Lynch GS, Ryall JG. A metabolic roadmap for somatic stem cell fate. Cell Metab. 2020;31(6):1052–67. https://doi.org/10.1016/j.cmet.2020.04.022.

The Contractile Machines of the Heart

21

Ingo Morano

Abstract

This chapter will describe basic structural and functional features of the contractile apparatus of muscle cells of the heart, namely, cardiomyocytes and smooth muscle cells. Cardiomyocytes form the contractile myocardium of the heart, while smooth muscle cells form the contractile coronary vessels. Both muscle types have distinct properties and will be considered with respect to their cellular appearance (brick-like cross-striated versus spindle-like smooth), arrangement of contractile proteins (sarcomeric versus non-sarcomeric organization), calcium activation mechanisms (thin-filament versus thick-filament regulation), contractile features (fast and phasic versus slow and tonic), energy metabolism (high oxygen versus low oxygen demand), molecular motors (type II myosin isoenzymes with high adenosine diphosphate [ADP]-release rate versus myosin isoenzymes with low ADP-release rates), chemomechanical energy conversion (high adenosine triphosphate [ATP] consumption and short duty ratio versus low ATP consumption and high duty ratio of myosin II cross-bridges [XBs]), and excitation-contraction coupling (calcium-induced calcium release versus pharmacomechanical coupling). Part of the work has been published (Neuroscience – From Molecules to Behavior", Chap. 22, Galizia and Lledo eds 2013, Springer-Verlag; with kind permission from Springer Science + Business Media).

I. Morano (✉)
Max-Delbrück Center for Molecular Medicine and University Medicine Charité Berlin, Berlin, Germany
e-mail: imorano@mdc-berlin.de

© The Author(s), under exclusive license to Springer Nature Switzerland AG 2024

S. Rickert-Sperling et al. (eds.), *Congenital Heart Diseases: The Broken Heart*,
Advances in Experimental Medicine and Biology 1441,
https://doi.org/10.1007/978-3-031-44087-8_21

Keywords

Contractile proteins · Muscle · Sarcomere · Oxygen · Calcium · Epicardium · Endocardium · Myocardium · Cardiomyocytes · Cell-cell junctions · Heartbeat · Systole · Diastole · Sarcoplasmic reticulum · Calsequestrin · Ryanodine receptor · Calcium channel · Myofibrils · Thin filament · Thick filament · Titin · Actin · Troponin · Tropomyosin · Myosin · Myosin-binding protein C · Adenylate cyclase · ATP · ADP · Oxygen consumption · Isometric contraction · Frank-Starling mechanism · Isotonic contraction · Excitation-contraction coupling · PKA · SERCA · Chronotropy · Inotropy · Smooth muscle cells · Coronary vessels · Cross-striation · Gap junctions · Phosphorylation · Myosin heavy chain · MYH · IP3 receptor · IP3R

21.1 Introduction

The heart is a permanently contractile muscular organ, with around 60 beats per minute in humans at rest. Each day, the human heart, which has the size of a fist, therefore contracts more than 86,000 times, pumping about 3500–4500 l of blood through the body performing about 100 kJ of work. The tone of coronary arteries regulates the perfusion of the heart with blood.

21.2 The Myocardium

The heart consists of the epicardium, which covers the outer surface, and the endocardium, which covers the inner surfaces, with the myocardium in between. The myocardium consists of sheets of contractile cells, the cardiomyocytes, which are interconnected by electron-dense specialized cell-cell junctions, the intercalated disks, providing mechanical stability and electrical communication between neighboring cardiomyocytes [1]. The right and left coronary arteries, which arise at the root of the aorta, course as epicardial blood vessels and provide the blood supply to the myocardium of the right and left atria and ventricles, respectively. The venous effluent is collected in veins that parallel the epicardial coronary arteries. The main venous drainage of the left ventricle enters the coronary sinus, emptying into the right atrium. The main venous drainage of the right (and some of the left) ventricle reaches the right atrium by the anterior coronary veins [1].

A heartbeat, or cardiac cycle, consists of a contraction period (systole) and a relaxation period (diastole) of the myocardium that generates ejection of blood from the heart and filling of the heart, respectively. Cardiomyocytes are cross-striated, longitudinally arranged cells (around 150 μm long and 20 μm wide). They contain a well-developed sarcoplasmic reticulum (SR), forming longitudinal vesicles and terminal cisternae that store large amounts (mM concentrations) of Ca^{2+}, buffered by specific Ca^{2+}-binding proteins, in particular calsequestrin [2]. Invaginations of the sarcolemma, the T-tubules, communicate with terminal cisternae of the SR to

form dyads, i.e., a single T-tubule associated with one terminal cisternae (cf. triads in skeletal muscle fibers). Calcium release channels (ryanodine receptors, RyR) are inserted into the terminal cisternae of the SR. Three RyR isoforms are expressed: RyR2 in the cardiomyocytes and all three, RyR1, RyR2, and RyR3, in the smooth muscle. The RyR is a homotetramer that forms a macromolecular complex with multiple interacting partners, including anchoring proteins, protein kinases, phosphatases, and accessory regulatory proteins (triadin, junction, calsequestrin). Specific voltage-gated L-type calcium channels (dihydropyridine receptors, DHPR) are located mainly in the T-tubular membrane of the sarcolemma. DHPR comprise a voltage-sensing and pore-forming α1s subunit and four accessory subunits called α2/δ, ß, and γ. In contrast to skeletal muscle fibers, DHPR do not directly bind to RyR2 in the terminal cisternae of the SR. There is a small space of 0.05–0.2 μm between DHPR and RYR2 called the dyadic cleft [1, 3].

Cardiomyocytes contain myofibrils, i.e., tubular cross-striated contractile structures about 1 μm in diameter that extend along the length of the cardiomyocyte (around 150 μm). In the phase contrast microscope, myofibrils show regions with high birefringence (dark anisotropic "A-bands") and regions with lower birefringence, i.e., bright isotropic "I-bands." Hence, similar to skeletal muscle fibers, cardiomyocytes present as cross-striated muscle type. Electron microscopic analysis shows Z-lines in the middle of the I-bands and "H-bands" and "H-zones" in the middle of the A-bands, while M-lines locate in the middle of the H-zones. The distance between Z-lines is called a sarcomere with a length of approximately 2 μm in the resting cardiomyocyte [1, 3] (Fig. 21.1).

Sarcomeres consist mainly of three types of longitudinally arranged filaments: (i) thin (or actin) filaments (around 1 μm in length, 50 nm thick) formed by polymerized G-actin molecules; (ii) thick (or myosin) filaments (around 1.6 μm in length, 100 nm thick) formed by polymerized myosin II molecules; and (iii) filaments formed mainly by titin (TTN; also called connectin) (around 1 μm in length and 5 nm thick) (Fig. 21.1). Actin filaments are anchored vertically into the Z-lines of the sarcomeres while the most terminal actin filaments of the sarcomeres anchor into the fascia adherens of the intercalated disks by binding to cytosolic catenins (e.g., plakoglobin). This provides a contractile continuity of neighboring cardiomyocytes. Myosin filaments are centered within the sarcomeres, vertically interconnected by the central M-line. Titin is spanning a half sarcomere: It anchors with its N-terminus into the Z-line, spans through the half I-band, running over the thick filament, and anchors with its C-terminus into the M-line [3] (Fig. 21.1). The Z-line with its characteristic zigzag structure (Fig. 21.1) is predominantly composed of globular α-actinin but contains many additional structural and regulatory proteins (e.g., CapZ, desmin, myotilin, telethonin, obscurin, and muscle lim protein). Z-lines of adjacent myofibrils are interconnected by networks of the intermediate filament desmin. Z-lines of subsarcolemmal myofibrils connect with the sarcolemma through binding to costameres via desmin filament networks and cytoskeletal actin filaments, which bind to the large rod-shaped protein dystrophin of the costameres. Costameres are multi-protein complexes located around the sarcolemma, each consisting of a dystrophin-cytoplasmic syntrophin complex, a transmembrane sarcoglycan

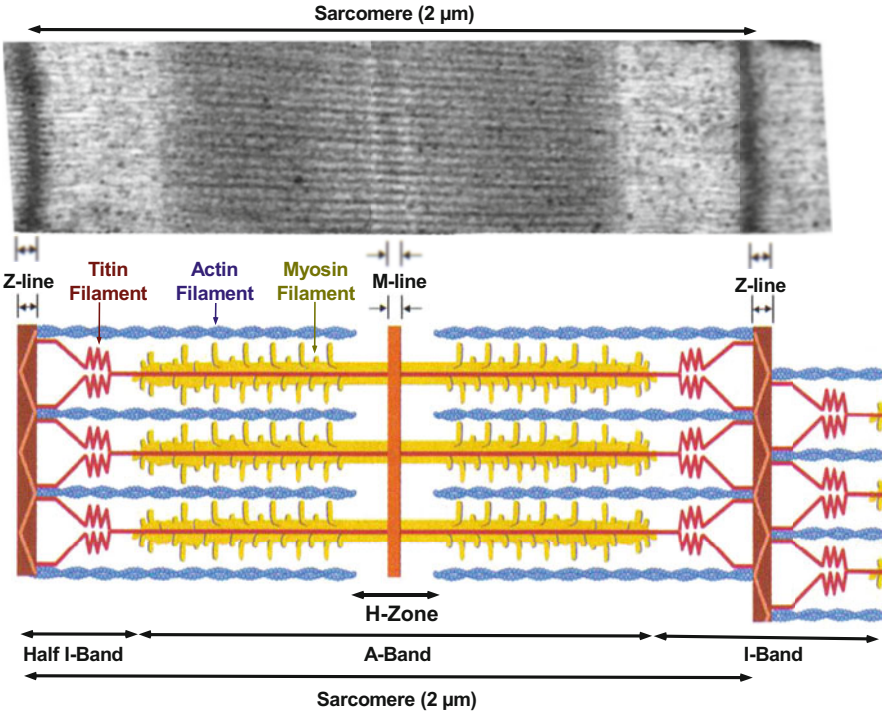

Fig. 21.1 Structure of a cardiac sarcomere. *Top*: electron microscopy of a cardiomyocyte sarcomere (Photograph Dr. Mahmoodzadeh 2014, with permission). *Bottom*: schematic interpretation (from: Chapter 6 "Kontraktionsmechanismen", Linke and Pfitzer; in: "Physiologie des Menschen" 2011; Schmidt, Robert F., Lang, Florian, Heckmann, Manfred (eds); Springer-Verlag, with kind permission from Springer Science + Business Media). *Abbreviations*: *A-band* anisotropic band, *I-band* isotropic band, *H-zone* "helle Zone" (bright zone), *M-band* middle band

complex, and a transmembrane/extracellular dystroglycan complex, which binds to the extracellular matrix protein laminin. Thus, costameres couple force generation of myofibrils with the sarcolemma in the striated muscle. The main proteins forming the M-line are muscle-specific creatine kinase, myomesin 2 (M-protein), and myomesin 1. M-lines of subsarcolemmal myofibrils are linked to costameres by keratins [3].

21.3 The Myosin Filament

According to the sequence of their motor domain, myosins were classified into 35 classes [4]. Those myosins that form dimers and assemble into thick filaments are called conventional or type II myosins and were first roughly prepared and named by W. Kühne in 1863 [5].

Type II myosins (constituting around 35% of the total skeletal muscle protein) are the motor proteins of all muscle types. They are composed of two heavy chains (myosin-HC) with around 200 kDa (around 1950 aa) each. Myosin-HC associates with two different light chains (MLC), the essential light chains (ELC) and regulatory light chains (RLC). Two genes coding for myosin heavy chains are expressed in the adult cardiomyocytes, MYH7 and MYH6, coding for myosinHC-ß and myosin-HC-α with low and high ATPase activities, respectively. MYH7 is predominantly expressed in ventricular, while MYH6 is predominantly expressed in atrial cardiomyocytes of the human heart [1, 2].

Experimentally, the myosin-HC can be proteolytically cleaved into a C-terminal 150 nm alpha-helical rod domain and a pear-shaped ≈ 20 nm N-terminal head domain with associated MLC, called subfragment 1 or S-1. Proteolytic cleavage of the myosin rod domain yields subfragment 2 (S-2) and light meromyosin (LMM). They contain multiple heptad-repeat sequences, allowing dimerization to form a coiled-coil superstructure. S-1 and S-2 together are termed heavy meromyosin (HMM) [1, 3].

Limited proteolysis of S-1 produces (from N-terminus to C-terminus) three domains: (i) a 25 K domain, (ii) a 50 K domain with a large cleft and specific actin-binding sites, and (iii) a 20 K domain with the converter and the α-helical lever arm. The ATPase binding site forms a cleft at the 25 K/50 K interface. The lever arm contains two IQ motifs in tandem, IQ1 for ELC binding and IQ2 for RLC binding [1, 3, 6].

Two genes coding for RLC, MYL2 and MYL7, exist which are predominantly expressed in the human ventricle and atrium, respectively. RLC are four EF-hand domain proteins with 18–19 kDa. RLC are phosphorylated mainly by MLCK3, the cardiac-specific Ca^{2+}-calmodulin-dependent myosin light chain kinase isoform (and, to a minor extent, by MLCK2), and dephosphorylated by a cardiac-specific phosphatase (cMLCP). cMLCP is a PP1 phosphatase composed of three subunits: the 38 kDa catalytic subunit (PP1c), the 110 kDa myosin phosphatase target subunit (MYPT2) that plays an important role in targeting cMLCP to myosin, and the small subunit hHS-M_{21}. In vivo, around 40% of the ventricular RLC are phosphorylated at serine-15 which remain stable independent from the systole/diastole rhythm or inotropic interventions. Normal phosphorylation levels of the RLC are important for proper force generation and sarcomere organization [3].

Two genes coding for ELC, MYL3 and MYL4, exist which are predominantly expressed in the human ventricle and atrium, respectively. They have around 25–28 kDa and are designated as alkali 1 (A1). Nota bene, only in skeletal muscle N-terminally spliced ELC forms alkali 2 (A2). The C-terminus of A1 with its four EF-hand domains binds to the myosin lever arm, while its antenna-like N-terminus binds to the actin filament. ELCs modulate stiffness, working stroke, and force generating properties of the single myosin motor protein [7].

The coiled-coil rod domains of myosin associate to form end-polar myosin filaments in striated muscles or side-polar myosin filaments in the smooth muscle. Each end-polar myosin filament (≈1.6 μm in length, 100 nm in diameter) contains

about 300 myosin molecules and is associated with myosin-binding protein C (C-protein) at regular intervals [1, 3].

The myosin head domains of end-polar thick filament project in a helical array with a periodicity of 42.9 nm and an axial interval of 14.3 nm—except for a 0.15 μm bare zone, where there are only overlapping myosin rods. The myosin head domains bind as "cross-bridges" (XBs) to specific sites on the actin filament for contraction generation. Purified HMM forms arrowhead complexes with actin filaments that point to the minus end (i.e., toward the center of the sarcomere). Hence, type II myosin is termed a minus-end-directed motor protein [1, 3].

21.4 The Actin Filament

Actin (which comprises about 19% of total skeletal muscle protein) is a globular protein (G-actin) with a diameter of 5.5 nm and molecular weight of 42 kDa. G-actin can be divided into four subdomains with a central ATP bound. G-actin molecules polymerize under physiological conditions to form a polarized helical filamentous structure, called F-actin, while the central ATP of G-actin hydrolyzes into ADP. F-actin with a length of 1 μm and diameter of 50 nm (thin filament) shows a plus-end and a minus-end, i.e., the sites of preferential G-actin attachment and detachment, respectively. Plus and minus ends of F-actin are also called barbed and pointed ends, respectively, according to the arrowhead structure that appears when F-actin is mixed with HMM. Subdomain 1 of G-actin containing both the N- and C-termini is located at the periphery of the thin filament available for myosin interactions. F-actin appears in the electron microscope as two twisting strands with axial separation of the crossover points of about 35 nm; thus, every seventh actin has the same orientation [1, 3].

F-actin is anchored into the Z-line by its barbed end and binds to the capping protein tropomodulin at its pointed end that directs into the center of the sarcomere. The final thin filament contains about 200 actin monomers associated with regulatory troponin-tropomyosin complexes (ca. 30 tropomyosin [Tm] molecules and ca. 30 troponin [Tn] complexes) regularly spaced along the thin filament. Furthermore, F-actin associates with the filamentous protein nebulette (~100 kDa), the small cardiac homolog of the larger nebulin filament of skeletal muscle (~700 kDa). Nebulette is anchored with its C-terminus to the Z-disk and may act as a molecular ruler to determine thin filament length and Z-line integrity [3].

Tropomyosin (Tm) consists of two α-helical polypeptide chains, each of ca. 35 kDa, forming a ≈42-nm-long coiled coil. Tm molecules aggregate end to end to form continuous strands running along the actin filament. Interactions between tropomyosin and actin are electrostatic [1, 3].

The troponin (Tn) complex consists of three components, TnI, TnT, and TnC, with a total molecular weight of ≈80 kDa. Tn complexes are located every 35 nm on F-actin (i.e., every seven actins along the long pitch helix), probably at the sites of overlap between neighboring tropomyosin molecules. TnT (≈36 kDa) is a rod-like protein (18.5 nm long) that binds with its C-terminal half to both TnI and TnC and

with its N-terminal half to both Tm and actin. TnI (≈24 kDa) holds the Tn complex together by binding to both TnC and actin. Cardiac TnI has a ≈30 aa N-terminal extension with several phosphorylation sites. TnC (≈18 kDa) is the Ca^{2+} sensor of the contractile apparatus. It has a dumbbell-like shape with an N-terminal lobe and a C-terminal lobe. Binding of Ca^{2+} to TnC at the low-affinity sites at the N-lobe (two sites in skeletal, one site in cardiac TnC) represents the physiological trigger regulating contraction. The C-lobe of TnC (containing two high-affinity Ca^{2+}/Mg^{2+} binding sites) interacts with TnI and TnT [1, 3].

21.5 The Titin Filament

The titin (TTN) gene is encoded by 364 exons expressing the giant elastic titin protein molecule with around 3900 kDa [3, 8]. Titin's A-band region is non-elastic and composed of immunoglobulin (Ig)- and fibronectin-like domains anchored to the thick filament and most C-terminal to the M-line of the sarcomere. Ttitin's I-band region, which inserts with its N-terminus into the Z-line, consists of spring-like elements, i.e., tandem segments consisting of serially linked Ig-like domains, a PEVK sequence (rich in proline, glutamate, valine, and lysine residues), and the N2B and N2A elements. Thus, titin plays a critical role in passive elastic properties of cardiomyocytes. Low forces stretch serially linked Ig domains, and high forces stretch the elastic PEVK and then N2B, the element with the highest stiffness. Resting tension curve, i.e., passive force generated upon increasing stretch amplitudes during rest, a main determinant of the diastolic ventricular filling volume, mainly depends on the spring-like properties of titin filaments. Stored energy in stretched titin spring elements provides the passive forces necessary to recoil the stretched cardiomyocyte into resting length [3, 8]. Furthermore, titin spring elements may provide the passive restoring force that sets the sarcomere length to resting levels after isotonic shortening when activation ceases. TTN is alternatively spliced in a tissue and developmental manner. Alternative splicing of titin in the I-band region in cardiomyocytes causes the expression of a fetal and several adult titin isoforms. Adult cardiomyocytes express two main isoforms with different elasticities, namely, titin-N2B, with minor Ig domains, has a smaller PEVK domain and is less elastic than the titin-N2BA (that contains both the N2B and N2A sequences) isoform [3, 8]. Nota bene, two more splice variants closely resembling titin-N2B, called novex-1 titin and novex-2 titin, as well as a "tiny titin" (novex-3 titin) with 625 kDa, could be demonstrated in adult cardiomyocytes. In the atria of adult human hearts, the N2BA isoform dominates, while in the ventricles the titin-N2BA/N2B ratio is 0.4–0.6. Changing the expression ratio of titin isoforms, which could be observed in patients with dilative cardiomyopathy, therefore could alter the stiffness of the cardiac tissue [8]. Besides its role in passive elasticity, titin filaments regulate sarcomere assembly and act as a stretch sensor for adaptation of protein turnover and gene expression to cardiomyocyte activity [3, 8].

21.6 Cardiomyocyte Contraction

Cardiomyocytes have passive and active properties. The active state of the cardiomyocyte is determined by the level of myoplasmic free Ca^{2+} and interaction of the XBs of the myosin with the actin filament. High myoplasmic Ca^{2+} concentrations cause contraction (systole) while low myoplasmic Ca^{2+} levels cause relaxation (diastole) of the cardiomyocytes. At resting Ca^{2+} levels during diastole, the actin filament-Tn-Tm complexes are in the "off-state," blocking actomyosin interactions while allowing some non-force-generating electrostatic actomyosin interactions. Activating Ca^{2+} levels during systole binds to the regulatory sites of TnC located at its N-terminal lobe. This strengthens the TnC-TnI and TnC-TnT interactions, thereby weakening the binding of TnI to actin. The subsequent changes of conformation and location of the Tn-Tm complex on the thin filament relieve myosin-binding sites on actin and turn the thin filament into the "on state," which allows force-generating stereospecific interactions of the thin filaments with the XBs (steric block model [1, 3, 9, 10]).

An activated cardiomyocyte generates force and shortens with a load. Force generation without shortening is termed isometric and shortening at constant load/force generation, isotonic. The energy for muscle contraction comes from the hydrolysis of ATP at the ATPase site of the myosin-S1. Hydrolyzed ATP could effectively be resynthesized by the transfer of P_i from phosphocreatine to ADP through the activity of creatine kinase (Lohmann reaction). Adenylate kinase (or myokinase) produces ATP by conversion of two ADP molecules to one ATP and one AMP molecule, which is removed by AMP deaminase to form inosine monophosphate and NH_4. In the heart, ATP is mainly synthesized through aerobic metabolism, i.e., conversion of glucose, fatty acids, and lactate to acetyl CoA and subsequent oxidation to CO_2 and H_2O in the mitochondria (Krebs cycle, electron transport chain) [1, 3]. Hence, oxygen consumption of the heart (around 0.1 ml/g/min) is high, accounting for approximately 10% of the total oxygen consumption of the body.

Mechanochemical energy transformation is accomplished by cyclic interaction of the cross-bridges (XBs) with the thin filament. During this process, the XBs bind independently to the thin filament, generate force through a conformational change (the power stroke) while extending an elastic spring element, and detach from the thick filaments [1, 3, 11]. Recent X-ray crystallographic 3D analysis of myosin-S1 fixed at different states of the XB cycle revealed the domain movements. According to a recent model [3, 6, 12] (Fig. 21.2), ATP binds to the ATP-binding cleft of the myosin XB (M), which causes the rapid detachment of the XB from the actin (A) filament (A + M-ATP). ATP is hydrolyzed, forming the M-ADP-Pi state (pre-power-stroke state, lever arm up, 50 K-cleft open). The M-ADP-Pi state weakly attaches to actin through ionic interactions (A-M-ADP-P_i). Releasing Pi then forms a strong stereospecific actin-binding state required for the power stroke of the XB (A-M-ADP). The power stroke is executed by movement of the myosin lever arm by ≈10 nm (lever arm down, 50 K-cleft closed). Detachment of the force-generating XB from the actin filament is achieved by the release of ADP and binding of ATP

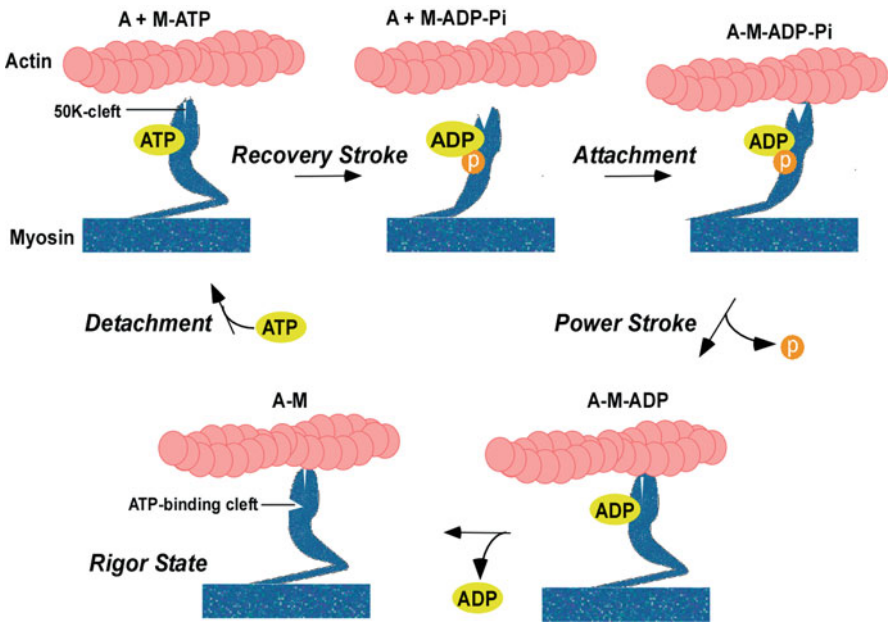

Fig. 21.2 Simplified scheme of chemomechanical coupling. A–M: The myosin cross-bridge is bound in a nucleotide-free force-generating state to actin (rigor position; lever arm "down," 50 K-cleft closed). A+M-ATP: ATP binds to myosin which detaches from actin. A+M–ADP–Pi: ATP is quickly hydrolyzed moving the lever arm "up," 50 K-cleft open (recovery stroke). A–M–ADP–P_i: Myosin attaches to actin in a non-force-generating pre-power-stroke state (lever arm up, 50 K-cleft open). A–M–ADP: Upon release of P_i, myosin is shifting into its force-generating state (power stroke), with the lever arm "down," 50 K-cleft closed. A–M: Release of ADP forms the transient rigor state; rapid binding of ATP to the active site of the myosin cross-bridge then causes the rapid detachment of the A–M into the A+M–ATP state. *Abbreviations*: *A* actin, *M* myosin, P_i inorganic phosphate, *ATP* adenosine triphosphate, *ADP* adenosine diphosphate

and then restoration of the lever arm of the XB to its non-force-generating position (recovery stroke). In the absence of ATP, the nucleotide-free XBs remain strongly bound to the actin filament producing a rigor mortis state (A-M; lever arm down, 50 K-cleft closed; the swinging lever arm model) [13]. Crystal structures have also shown that a small conformational change in the ATP-binding domain of the XB (movement of 0.5 nm) is amplified into the ≈10 nm movement of the lever arm.

21.6.1 Isometric Contraction

Isometric force generation of a muscle cell (F_0) during steady-state contraction depends on the number of XBs in the force-generating state and the force a XB can exert (F', ≈6 pN). Since XBs independently interact with the thin filament during muscle activation, only a fraction "n" of the total amount of actively cycling

XBs (n_{tot}) generates force at any one time. "n" therefore depends on the XB kinetics, i.e., the rates of transitions of XBs from force- into non-force-generating states (detachment rate; g_{app}) and the rate of transitions of XBs from non-force- into force-generating states (attachment rate; f_{app}), namely:

$$n = f_{app} / \left(f_{app} + g_{app} \right)$$

[7, 10] and therefore

$$F_0 = F' \cdot n_{tot} \cdot \left[f_{app} / \left(f_{app} + g_{app} \right) \right]$$

[11, 14].

There is a bell-shaped dependency of isometric force generation on the muscle/sarcomere length. The optimal force of cardiomyocytes is elicited at sarcomere length around 2 μm, while smaller or larger sarcomere lengths gradually decrease force generation. The level of thick and thin filaments overlaps, and the resulting different amounts of force-generating XBs provide the structural basis for this observation [14, 15]. The heart is working on the ascending limb of the length-tension curve. An increased filling volume of the heart could therefore be acutely compensated by an increased force generation and stroke volume since the sarcomeres are set into a more optimal filament overlap zone (Frank-Starling mechanism). In addition, Ca^{2+} sensitivity of the myofilaments increases upon stretching the sarcomeres, supporting the increased force and ejection volume after increased diastolic filling.

21.6.2 Isotonic Contraction

Cardiomyocytes shorten by the relative sliding of thick and thin filaments, and the distance between Z-lines (the sarcomere length) decreases (the sliding filament model; [16]. The velocity of shortening declines with increasing loads in a characteristic hyperbolic mode [17]. Power and efficiency curves can be calculated from the force-velocity relationship, showing a bell-shaped function with maximal efficiency at around one third of maximal shortening velocity and zero efficiency at maximal isometric force generation or maximal shortening velocity.

If an isometrically contracting muscle is allowed to shorten quickly (1 ms; "quick release"), there is an instantaneous decline of tension due to the discharge of the elastic spring element of the force-generating XB. A quick release of roughly 1% of muscle length at optimal overlap (which equals a step size of around 10 nm per half-sarcomere) causes a complete drop to zero force. Larger shortening distances then compress elastic spring elements of the XBs, generating force in the reverse direction. Thus, with increasing shortening velocities, the fraction of compressed ("negative") XBs increases while pulling ("positive") force-generating XBs decreases. To allow fast shortening, the detachment rate of negative XBs ("g2")—and consequently ADP release rate and ATP consumption—should be higher during

shortening than during isometric contraction. As a consequence, the maximal shortening velocity (V_{max}) of a muscle depends on "g2." In fact, the different V_{max} values of fast and slow muscles types result from distinct gene expression of myosin isoenzymes with higher and lower ADP release rates, respectively. Attenuated force-bearing capacity and increased ATP consumption during muscle shortening could explain both the hyperbolic force-velocity relationship and the increased heat released during shortening (Fenn effect) [11, 14].

Activated muscles produce heat and work. The work performed by an XB is around 22 kJ/mol. Since the free energy change of ATP splitting is about 50 kJ/mol, the mechanical efficiency of an XB is roughly 50%. The lower efficiency of the whole muscle (around 30%) is due to additional ATP consumption processes, mainly Ca^{2+} sequestration into the SR by ATP-driven SERCA, sarcolemmal Ca^{2+} pumps, and Na^+/K^+ ATPase (cf. below).

21.7 Excitation-Contraction Coupling of Cardiomyocytes

Action potentials of cardiomyocytes start with a rapid depolarization caused by gating of the voltage-operated Na^+ channels and a subsequent characteristic long-lasting plateau phase due to a slow Ca^{2+} inward current through the α1ca subunit of voltage-operated L-type Ca^{2+} channels (DHPR). Compared to nerve fibers or skeletal muscle fibers, the action potential of a cardiomyocyte is long, roughly 200–300 ms, almost the duration of a twitch contraction. Hence, the cardiomyocyte cannot readily generate tetanic contractions.

Roughly 20–40 DHPR and 100–200 RyR2s are clustered, forming functional couplons. The small Ca^{2+} inward current during the action potential passes the dyadic cleft and triggers the release of large amounts of Ca^{2+} from the SR through RyR2 into the myoplasm (Ca^{2+}-induced Ca^{2+} release; CICR) [18]. CICR occurs upon binding of low Ca^{2+} concentration (pCa 6.25) to high-affinity sites of the RyR2; inactivation occurs by high Ca^{2+} (pCa 5.5) through binding of Ca^{2+} to low-affinity site of RyR2. Inactivation of Ca^{2+} release is also facilitated by calmodulin, which increases RyR2 channel close times. Phosphorylation of RyR2s by Ca^{2+}/calmodulin-dependent protein kinase II (CaMKII) and by cAMP-dependent protein kinase (PKA), i.e., upon sympathetic stimulation, increases Ca^{2+} release from RyR2 [3, 19].

Activation of the heart by depolarization and generation of action potentials starts in specialized pacemaker cells of the sinoatrial node (SA). SA cells express a specific type of a cAMP-gated Na^+ channel that opens at resting membrane potentials ("funny channel," HCN channel) and a T-type Ca^{2+} channel that opens at more negative membrane potentials than the L-type Ca^{2+} channel. Those channel activities slowly depolarize the resting membrane potential up to the threshold potential, thus spontaneously eliciting an action potential. Electrical impulses then propagate between cardiomyocytes by a special class of ion channels, connexons, each made up of 6 connexin molecules (gap junctions or nexus) of the intercalated disks. Therefore, the heart represents a functional syncytium [1, 3, 19].

During systole, free cytosolic Ca^{2+} rises to about 600 nM, which only half maximally activates the myofilaments, generating half-maximal force (for ventricular pressure) and shortening (for blood ejection). Thus, there is a large contractile reserve that could be recruited by increasing activating Ca^{2+} concentrations, e.g., via sympathetic stimulation (cf. below). This induces a more intense activation of the myofilaments by increasing the amount of troponin-tropomyosin units in the "on-state," the amount of cycling XBs interacting with the thin filament, and consequently the amount of XBs in the force-generating state. Repolarization of the sarcolemma upon Na^+-channel inactivation and increased K^+-outward conductance inactivates the couplons. Eliminating Ca^{2+} from the myoplasm then elicits diastolic relaxation. In particular, the sarcoplasmic-endoplasmic reticulum Ca^{2+} ATPase (SERCA), a Ca^{2+}-regulated ATP-dependent Ca^{2+} pump, sequesters myoplasmic Ca^{2+} into the SR. In addition, a Na^+/Ca^{2+} exchanger (NCX) in the sarcolemma and sarcolemmal Ca^{2+} pumps (PMCA) eliminates activating Ca^{2+} from the myoplasm into the extracellular space. Decreased free cytoplasmic Ca^{2+} inactivates the myofilaments and the heart relaxes [3, 19].

The contractile reserve of the myocardium may be recruited by its sympathetic innervation, which originates from the stellate ganglia and cardiac plexus, innervated predominantly from the 4th and 5th thoracic segments of the spinal cord. Binding of norepinephrine to its seven-membrane-spanning Gs-coupled ß1-adrenergic receptor activates adenylyl cyclase which rises the myoplasmic level of the second messenger cyclic adenosine monophosphate (cAMP). cAMP activates cAMP-dependent protein kinase (PKA) that phosphorylates DHPR and RyR, thus increasing their open probabilities and consequently increasing myoplasmic Ca^{2+}. Higher myoplasmic Ca^{2+} levels increase the contractile force of the cardiomyocyte (positive inotropy). Increased cAMP levels activate the funny channels of pacemaker cells, thus increasing diastolic depolarization velocity to threshold potential causing an increased frequency of action potentials (positive chronotropy). Higher frequencies can raise myoplasmic free Ca^{2+} and myocardial contraction (frequency inotropy). Activated PKA phosphorylates gap junctions, which increases their open probabilities, thus improving action potential propagation (positive dromotropy) [19]. PKA-dependent phosphorylation inactivates phospholamban, a potent SERCA inhibitor, and the cardiac-specific N-terminal extension of TnI. This accelerates Ca^{2+} sequestration from the myoplasm into the sarcoplasmic reticulum and Ca^{2+} dissociation from TnC, respectively, accelerating the relaxation rate (positive lusitropy). The contractile reserve may be conserved by raising the parasympathetic vagal tone. Vagal nerve fibers originate in the dorsal efferent nuclei of the medulla oblongata and principally innervate sinoatrial node cells. Acetylcholine binds to muscarinic G_i-coupled GPCRs of SA cells, thus decreasing myoplasmic cAMP levels via inhibition of adenylyl cyclase activity. Hence, funny channel activity is reduced, thus decreasing diastolic depolarization velocity, resulting in a decreased action potential frequency (negative chronotropy) and lower myoplasmic Ca^{2+} activation levels of myocardial cells (negative inotropy) [19].

Besides the level of myoplasmic free Ca^{2+}, sympathetic activation modulates the responsiveness of myofibrils to Ca^{2+} (calcium sensitivity) by phosphorylation of

regulatory and structural proteins of cardiac myofibrils. Activation of PKA upon sympathetic stimulation phosphorylates TnI at Ser23/24, which reduces myofibrillar calcium sensitivity, i.e., decreases isometric force generation at given Ca^{2+} activation level, by reducing the affinity of cTnC for Ca^{2+}. This may support Ca^{2+} dissociation from cTnC during diastole and fasten relaxation (lusitropic effect). Although titin showed a variety of phosphorylation sites targeted by a multitude of protein kinases, phosphorylation of the N2B segment by PKA reduced titin stiffness as well as passive tension of the sarcomere and cardiomyocyte, supporting diastolic filling of the ventricle upon sympathetic activation [3, 19].

21.8 Smooth Muscle Cells of Coronary Blood Vessels

The tone of coronary arteries defines the perfusion rate of the heart and directly corresponds to the contractile state of the smooth muscle cells of the tunica media of the coronary arteries. Smooth muscle cells are spindle shaped, 5–10 μm wide, and 50–200 μm long. They show no cross-striations since the thin and thick filaments of their myofibrils are not arranged in sarcomeres. Instead, actin filaments are anchored to the sarcolemma by dense (adhesion) plaques and fixed by dense bodies, a Z-band analog, which contain α-actinin within the smooth muscle cells. Thin filaments of smooth muscle associate with tropomyosin and caldesmon and/or calponin, while troponins are completely absent. In contrast to the striated muscle, which forms end-polar thick filaments, myosins in smooth muscle myosins assemble into side-polar thick filaments. An alternatively spliced small titin isoform with around 500 kDa (sm-titin, also called smitin) with around 500 kDa, which shares some N-terminal titin domains, is expressed in smooth muscle cells.

Coronary vessels are composed of multi-unit smooth muscle types that have no pacemaker cells and are only sparsely interconnected by gap junctions but are densely innervated by sympathetic nerve fibers. Each smooth muscle cell is activated independently upon nerve stimulation (neurogenic regulation). This is in contrast to "single-unit" (or "unitary") smooth muscle. Organs composed of single-unit smooth muscle cells (e.g., intestine, urinary bladder, and uterus) have specialized smooth muscle cells that act as pacemaker cells, i.e., they spontaneously and rhythmically generate depolarizations (myogenic regulation). Electrical impulses of single-unit smooth muscle cells then propagate between smooth muscle cells by gap junctions electrically connecting the neighboring smooth muscle cells. Therefore, the single-unit type is syncytial, and its contractile state is modulated by sympathetic and parasympathetic nerve fibers [20].

21.9 Activation of Smooth Muscle Contraction

Contraction of smooth muscle cells generally operates by Ca^{2+}-dependent activation and sliding filament mechanisms but shows distinct activation properties when compared to striated muscles.

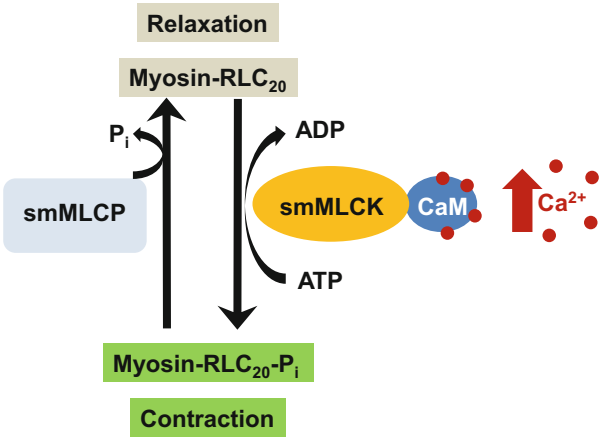

Fig. 21.3 Simplified scheme of contraction activation of smooth muscle. The active smMLCK-Ca^{2+}-calmodulin complex phosphorylates RLC_{20} of myosin, thus activating myosin ATPase activity and actomyosin interaction, leading to smooth muscle contraction. Dephosphorylation of RLC_{20} by smMLCP inactivates smooth muscle myosin causing relaxation of smooth muscle cells. *Abbreviations*: *CaM* calmodulin, *sm* smooth muscle, *MLCK* myosin light chain kinase, *MLCP* myosin light chain phosphatase, *Ca^{2+}* calcium ions, *RLC20* regulatory light chain with 20 kDa, *Pi* inorganic phosphate, *ATP* adenosine triphosphate, *ADP* adenosine diphosphate

Although a rise of free myoplasmic Ca^{2+} triggers smooth muscle contraction, the Ca^{2+} receptor is calmodulin rather than troponin C in the striated muscle. The Ca^{2+}-calmodulin complex activates myosin light chain kinase 1 (MLCK1), which specifically phosphorylates Ser19 of the regulatory myosin light chain (RLC) with 20 kDa (RLC_{20}) of the myosin II isoforms expressed in smooth muscle cells. In contrast to myosin II isoforms expressed in cardiomyocytes and skeletal muscle fibers, the two myosin-S1 heads of smooth muscle myosin with unphosphorylated RLC_{20} show an intense asymmetric interaction in which the ATPase and actin-binding domains of one head are blocked and could only weakly be activated by actin. It adopts a compact, soluble 10S form (S = Svedberg units) ("tonomyosin"). Phosphorylation of RLC_{20} converts the smooth muscle myosin into an open, less-soluble 6S conformation with high ATPase activity that could be activated by actin and assembles into thick filaments for contraction generation. Dephosphorylation of RLC_{20} by a smooth muscle-specific phosphatase (smMLCP) enforces the relaxation of smooth muscle cells. Most probably, smMLCP is a PP1 phosphatase composed of three subunits: a 38 kDa catalytic subunit (PP1c), the 110 kDa myosin phosphatase target subunit (MYPT1) that plays an important role in targeting smMLCP to myosin, and the 20 kDa (M20) subunit [21–23]. Thus, smooth muscle activation is elicited by a thick-filament activation mechanism (phosphorylation of the regulatory myosin light chains) rather than by the troponin/tropomyosin-bound thin-filament activation (steric block) mechanism of the striated muscle (Fig. 21.3.)

Three myosin heavy chain genes are expressed in smooth muscle cells, MYH9, MYH10, and MYC11, coding for NMA (non-muscle myosin-HC A), NMB

(non-muscle myosin-HC B, also called smooth muscle embryonic myosin-HC or NMemb), and SM (smooth-muscle myosin-HC), respectively. They form a large number of different isoenzymes by alternative splicing mechanisms. Thus, the MYH11 gene product is alternatively spliced at both the head and tail domains, forming four different myosin-HC isoenzymes. MYH10 is alternatively spliced at two sites of the head domain expressing additional four different myosin-HC isoforms. The biological functions of this variety of myosin isoforms in smooth muscle cells are not yet clarified, but they may contribute to the large variety of contractile features of distinct smooth muscle cells.

In contrast to cardiomyocytes that periodically contract and relax, smooth muscle cells of coronary vessels generate a permanent energy-consuming contractile tone. This is facilitated because during sustained activation, smooth muscle cells generate a unique state of high-efficiency contraction, referred to as the "latch state" [21]. Intracellular Ca^{2+}, RLC_{20} phosphorylation, oxygen and ATP consumption, and maximal shortening velocity significantly decrease during latch, while force is maintained. A number of mechanisms, including the formation of slowly cycling dephosphorylated cross-bridges and activation of non-muscle myosin-HC upon prolonged activation [24], have been proposed as putative latch mechanisms.

All myosin II isoforms expressed in smooth muscle cells bind ADP with stronger affinities than striated muscle myosins. Therefore, the detachment rate, g_{app}, of myosin II isoforms in smooth muscles is lower than those myosin II isoforms expressed in the striated muscle. Smooth muscle myosins thus remain for a longer fraction of their XB cycle time in the force-generating state (the duty cycle is high). Hence, the fraction of actively cycling XBs in the force-generating state increases, explaining the high force generation with little myosin expression. In fact, although smooth muscle cells contain only 1/3 of the myosin concentration found in the striated muscle, they generate similar forces. Another consequence of the high ADP affinity and small g_{app} of smooth muscle myosins is that maximal shortening velocity becomes very low, roughly 1/10 of the maximal shortening velocity of the striated muscle.

21.10 Excitation-Contraction Coupling of Mammalian Smooth Muscle

Smooth muscle cells may be activated by electromechanical and/or pharmacomechanical coupling, which access distinct intracellular pathways for raising activating free myoplasmic Ca^{2+}.

During electromechanical coupling, the entry of extracellular Ca^{2+} through the L-type Ca^{2+} channels directly activates the contractile machinery and elicits Ca^{2+} release from the sarcoplasmic reticulum by a Ca^{2+}-induced Ca^{2+} release mechanism, which opens the RyRs (predominantly RyR2).

Pharmacomechanical coupling occurs upon neurohumoral stimulation and comprises distinct mechanisms that regulate myoplasmic Ca^{2+} of smooth muscle independently of the membrane potential. Binding of norepinephrine to its alpha-

adrenergic receptor at the sarcolemma of smooth muscle cells activates heterotrimeric Gq/11-proteins that in turn stimulate phospholipase C-ß activity and phosphatidylinositol turnover. This leads to the formation of two second messengers: (i) inositol trisphosphate (IP3), which triggers Ca^{2+} release from the sarcoplasmic reticulum by binding to IP3 receptors (IP3R), and (ii) diacylglycerol (DAG), which activates PKC. PKC phosphorylates a variety of proteins involved in signal transduction, contraction, and membrane polarization. For example, PKC phosphorylates CPI-17, a 17 kDa phosphatase inhibitor, which inhibits the catalytic subunit of smMLCP. Inhibition of smMLCP activity leads to an increase of the fraction of force-generating myosin with phosphorylated RLC_{20}, therefore increasing force generation. Since inhibition of smMLCP activity increases force without affecting Ca^{2+} activation levels, it acts as a Ca^{2+} sensitizing mechanism. Inhibition of smMLCP can also be achieved by activation of Rho-kinase through the small monomeric G-protein Rho-A. Active Rho-kinase inhibits smMLCP activity by phosphorylation of its regulatory subunit [25].

21.11 Conclusion

Contraction regulations of cardiomyocytes and smooth muscle cells of the heart present as Ca^{2+}-driven interactomes of a variety of protein complexes in distinct cellular compartments. Thus, the contractile apparatus of the smooth muscle is regulated by a thick-filament activation mechanism in contrast to the thin-filament activation (steric block) mechanism of cardiomyocytes. Understanding the contractile interaction networks of muscle cells provide the prerequisite for rational therapeutic interventions of cardiac diseases. Thus, familial cardiomyopathies are mainly associated with mutations affecting genes coding for proteins involved in contraction regulation of cardiomyocytes, i.e., myofibrillar, plasmalemmal, or Ca^{2+} handling proteins. Intense future work is required to understand the molecular pathomechanisms of these disease-causing mutations in the genesis of familial cardiomyopathies. Those investigations will eventually lead to the development of novel molecular therapies and biomarkers in patient-based clinical research.

References

1. Squire JM. Muscle: design, diversity, and disease. Menlo Park: The Benjamin/Cummings Publishing Co; 1986.
2. Franzini-Armstrong C. Studies of the triad. I. Structure of the junction in frog twitch fibers. J Cell Biol. 1970;47:488–9.
3. Sweeney HL, Hammers DW. Muscle Contraction (2018). Cold Spring Harb Perspect Biol. 2018;10(2)
4. Odronitz F, Kollmar M. Drawing the tree of eukaryotic life based on the analysis of 2,269 manually annotated myosins from 328 species. Genome Biol. 2007;8:R196.
5. Kühne W. Über das Protoplasma und die Contractilität. Leipzig: Verlag von Wilhelm Engelmann; 1864.

6. Rayment I, Rypniewski WR, Schmidt-Bäse K, et al. Three-dimensional structure of myosin subfragment-1: a molecular motor. Science. 1993;261:50–8.
7. Morano I. Essential myosin light chains regulate myosin function and muscle contraction. In: Sugi H, editor. Muscle contraction and cell motility. Pan Stanford Publishing; 2016. p. 273–88.
8. Tharp CA, Haywood ME, Sbaizero O, et al. Giant protein Titin's role in cardiomyopathy: genetic, transcriptional, and post-translational modifications of TTN and their contribution to cardiac disease. Front Physiol. 2019;10:1436.
9. Huxley HE. Structural changes of the actin- and myosin-containing filaments during contraction. In: The mechanism of muscle contraction, Cold Spring Harbor symposia on quantitative biology, vol. XXXVII; 1973. p. 361–76.
10. Haselgrove JC. Evidence for a conformational change in the actin-containing filaments of vertebrate striated muscle. In: The mechanism of muscle contraction, Cold Spring Harbor symposia on quantitative biology, vol. XXXVII; 1973. p. 341–53.
11. Huxley AF. Muscle structure and theories of contraction. Prog Biophys Chem. 1957;7:255–318.
12. Lymn RW, Taylor EW. Mechanism of adenosine triphosphate hydrolysis by actomyosin. Biochemistry. 1971;10:4617–24.
13. Geeves MA, Holmes KC. The molecular mechanism of muscle contraction. Adv Protein Chem. 2005;71:161–93.
14. Brenner B. Effects of Ca^{2+} on cross-bridge turnover kinetics in skinned single rabbit psoas fibers: implications for regulation of muscle contraction. Proc Natl Acad Sci U S A. 1988;85:3265–9.
15. Gordon AM, Huxley AF, Julian FJ. The variation in isometric tension with sarcomere length in vertebrate muscle fibers. J Physiol. 1966;184:170–92.
16. Huxley H, Hanson J. Changes in the cross-striations of muscle during contraction and stretch and their structural interpretation. Nature. 1953;173:973–6.
17. Hill AV. The heat of shortening and the dynamic constants of muscle. Proc R Soc Lond B Biol Sci. 1938;126:136–95.
18. Fabiato A. Calcium-induced release of calcium from the cardiac sarcoplasmic reticulum. Am J Physiol Cell Physiol. 1983;245:C1–C14.
19. Bers DM. Cardiac excitation-contraction coupling. Nature. 2002;415:198–205.
20. Bozler E. Action potentials and conduction of excitation in muscle. Biol Symp. 1941;3:95–109.
21. Dillon PF, Aksoy MO, Driska SP, et al. Myosin phosphorylation and the cross-bridge cycle in arterial smooth muscle. Science. 1981;211:495–7.
22. Rüegg JC. Calcium in muscle contraction. Heidelberg: Springer; 1992.
23. Somlyo AP, Somlyo AV. Ca^{2+} sensitivity of smooth muscle and nonmuscle myosin II: modulated by G proteins, kinases, and myosin phosphatase. Physiol Rev. 2003;834:1325–58.
24. Arner A, Löfgren M, Morano I. Smooth, slow and smart muscle motors. J Muscle Res Cell Motil. 2003;24:165–73.
25. Somlyo AP, Somlyo AV. Signal transduction by G-proteins, rho-kinase and protein phosphatase to smooth muscle and non-muscle myosin II. J Physiol. 2000;522:177–85.

Technologies to Study Genetics and Molecular Pathways

22

Marcel Grunert, Cornelia Dorn, Ana Dopazo, Fátima Sánchez-Cabo, Jésus Vázquez, Silke Rickert-Sperling, and Enrique Lara-Pezzi

Abstract

Over the last few decades, the study of congenital heart disease (CHD) has benefited from various model systems and the development of molecular biological techniques enabling the analysis of single gene as well as global effects. In this chapter, we first describe different models including CHD patients and their families, animal models ranging from invertebrates to mammals, and various cell culture systems. Moreover, techniques to experimentally manipulate these models are discussed. Second, we introduce cardiac phenotyping technologies comprising the analysis of mouse and cell culture models, live imaging of cardiogenesis, and histological methods for fixed hearts. Finally, the most important and latest molecular biotechniques are described. These include

M. Grunert
Cardiovascular Genetics, Charité – Universitätsmedizin Berlin, Berlin, Germany

DiNAQOR AG, Schlieren, Switzerland

C. Dorn · S. Rickert-Sperling (✉)
Cardiovascular Genetics, Charité – Universitätsmedizin Berlin, Berlin, Germany
e-mail: silke.sperling@charite.de

A. Dopazo
Genomics Unit, Centro Nacional de Investigaciones Cardiovasculares, Madrid, Spain

F. Sánchez-Cabo
Bioinformatics Unit, Centro Nacional de Investigaciones Cardiovasculares, Madrid, Spain

J. Vázquez
Proteomics Unit, Centro Nacional de Investigaciones Cardiovasculares, Madrid, Spain

E. Lara-Pezzi (✉)
Myocardial Homeostasis and Cardiac Injury Programme, Centro Nacional de Investigaciones Cardiovasculares, Madrid, Spain
e-mail: elara@cnic.es

© The Author(s), under exclusive license to Springer Nature Switzerland AG 2024

S. Rickert-Sperling et al. (eds.), *Congenital Heart Diseases: The Broken Heart*,
Advances in Experimental Medicine and Biology 1441,
https://doi.org/10.1007/978-3-031-44087-8_22

genotyping technologies, different applications of next-generation sequencing, and the analysis of transcriptome, epigenome, proteome, and metabolome. In summary, the models and technologies presented in this chapter are essential to study the function and development of the heart and to understand the molecular pathways underlying CHD.

Keywords

Genotyping technologies · Next-generation sequencing · Transcriptome · Epigenome · Proteome · Metabolome · Animal models · Nematode · *Caenorhabditis elegans* · Fruit fly · *Drosophila melanogaster* · Mouse · *Mus musculus* · Rat · *Rattus norvegicus* · Zebrafish · NKX2-5 · Clawed frog · *Xenopus laevis* · Chicken · *Gallus gallus* · Embryonic stem cells · ES cells · Cell culture · Cardiomyocytes · Induced pluripotent ES cells · iPSCs · Transcription activator-like effector nucleases · TALENs · Zinc finger nucleases · ZFN · CRISPR · Morpholino oligonucleotides · Imaging · Phenotyping · Micro-computed tomography · Micro-CT · Magnetic resonance imaging · MRI · Histological analysis · In situ hybridization · Immunohistochemistry · Fluorescence-activated cell sorting · FACS · Single-nucleotide polymorphisms · SNPs · Sanger sequencing · Fluorescence in situ hybridization · FISH · Array comparative genomic hybridization · Array-CGH · NGS · Genome-wide association studies · GWAS · RNA-seq · Chromatin immunoprecipitation · ChIP · ChIP-seq · DNA methylation · MBD · ATAC-seq · CLIP · PAR-CLIP · Mass spectrometry · MS · Nuclear magnetic resonance spectroscopy · NMR · SILAC · Yeast-two-hybrid

22.1 Introduction

Understanding the genetic alterations and molecular pathways underlying congenital heart disease (CHD) is essential to develop novel therapeutic strategies. Besides genomic mutations, CHD is characterized by multiple changes in epigenetic marks as well as in the expression and modification of RNAs and proteins. Some of these changes have strong effects on the protein structure, function, or localization, while others result in more subtle differences. Over the last decade, advanced high-throughput technologies have been developed that allow the study of CHD from single-locus effects to the global level. Here, we describe the most important model systems and techniques to explore the changes in the different regulatory layers affecting cardiac function and development.

22.2 Model Systems

22.2.1 Animal Models

A large variety of animal models are used in cardiovascular research ranging from invertebrates such as the nematode *Caenorhabditis elegans* and the fruit fly *Drosophila melanogaster* to mammals such as the mouse *Mus musculus* and the

laboratory rat *Rattus norvegicus*. Although it has no heart or vascular system, *C. elegans* has become a useful model that is easy to culture and manipulate by RNA interference (RNAi) or mutation. Its body wall muscle cells are well-suited to gain insights into human cardiomyocytes; as they form, striated muscle and many structures and proteins such as sarcomeric components are highly conserved [1]. The fruit fly is characterized by a simple tube-shaped heart, also called the dorsal vessel, which consists of a single layer of cardiomyocytes and pumps the hemolymph around the body. *Drosophila* can be used easily for genetic screens and for crossing experiments, for which several large collections of mutant stocks are available. Due to few genetic redundancies, it is a widely used model of regulatory pathways and essential players of heart development [2, 3]. For example, the important role of the cardiac transcription factor NKX2-5 (tinman) was first demonstrated in *Drosophila* [4]. However, the fly might not be well-suited for studies of buffering effects, which are essential for the understanding of human cardiac disease [3].

The zebrafish (*Danio rerio*) has a two-chambered heart, and the transparency of the developing embryo allows the *in vivo* study of heart size, shape, and function [5]. Due to its small size, fecundity, and brief generation time, the zebrafish can easily be used for forward genetic perturbation screens [6] and moreover allows the study of otherwise lethal disturbances because no functional cardiovascular system is required during embryogenesis [3]. In addition, the zebrafish represents a valuable model for cardiac muscle regeneration, as it has the ability to replace massive sections of damaged myocardium [7]. In contrast to the zebrafish, the African clawed frog (*Xenopus laevis*) has a three-chambered heart with two atria and one ventricle. Its large embryo allows surgical manipulations of the developing heart and is useful for genetic screens [8]. Like the human, the chicken (*Gallus gallus*) develops a four-chambered heart and is a powerful model for experimental embryology as its imaging during development requires no surgical procedures [9].

The two essential mammalian animal models are the mouse and the laboratory rat. The cardiovascular system of the latter shares a high similarity to human physiology and is widely used for pharmaceutical testing [10]. Recently, the genetic manipulation limits for the rat have been overcome by the development of gene-targeting approaches for gene knockout and replacement [3]. However, the mouse remains the most important model for genetic studies, and transgenic mice have become a valuable human CHD pathology model [11]. The International Knockout Mouse Consortium aims to generate a major resource of knockout mouse embryonic stem (ES) cells. So far, more than 17,400 mutant murine embryonic stem cell clones have been generated, which provides the opportunity of systematic screens of gene functions [12]. Currently, more than 500 genes are known to be causative for heart defects when mutated in mice, while only about 50 CHD genes are known in humans [13]. In addition, mouse strains with different genetic backgrounds offer the opportunity to study genetic buffering effects, as recently shown for NKX2-5 [14]. Finally, the mouse is also a useful model for gene expression studies, and several large-scale projects aim to systematically determine gene expression patterns during mouse embryogenesis [15].

22.2.2 Cell Culture Models

The heart comprises a mixture of different cell types including cardiac fibroblasts and cardiomyocytes. *In vitro* studies using largely homogeneous cell populations enable the analysis of spatiotemporal changes and distinct molecular pathways. Moreover, cell culture models are easier to manipulate than animal models, can be sorted for surface markers, and provide the opportunity to produce enough material for downstream experiments.

Isolated cardiomyocytes cultured in primary cell culture are one of the established models to investigate cardiac function and closely reflect *in vivo* physiology. In addition, several stable, immortalized cell lines have been generated. The HL-1 cell line, derived from mouse atrial cardiomyocytes, maintains the ability to contract, shows a gene expression pattern similar to adult cardiomyocytes [16], and can be used in tissue engineering applications (3D cell culture) [17]. By contrast, the H9C2 cell line, which was established from the embryonic rat heart tissue, shows cardiac and skeletal muscle properties [18]. To study myogenesis, the mouse myogenic cell line C2C12 is frequently used since it is capable of differentiation into myotubes [19]. Furthermore, embryonic cell lines such as the mouse P19 embryonic stem (ES) cells [20] and the human H1 or hES2 ES cells [21] can be differentiated into mesodermal cells, including cardiac and skeletal muscle cells, and have been used for the quantification of cardiomyocyte differentiation [22]. Finally, the generation of cardiomyocytes from induced pluripotent stem cells (iPSCs) and the direct conversion of fibroblasts into cardiomyocytes have been established as additional approaches that enable the study of patient-specific cells and provide novel perspectives for regenerative medicine [23, 24].

22.2.3 Patients with CHD

Patients with CHD and their families are a unique resource to gain insights into cardiac functional properties and molecular pathways. For example, linkage analysis in CHD families has led to the identification of single-gene defects such as mutations in *NKX2-5* [25] and *GATA4* (GATA binding protein 4) [26]. Several national registries such as the CONCOR registry of the Netherlands or the National Register for Congenital Heart Defects in Germany aim to establish comprehensive collections of biomaterial like blood or cardiac biopsies. While genomic DNA isolated from blood can be used for genetic studies, cardiac biopsies offer the opportunity to study gene expression profiles and epigenetic mechanisms, providing insights into regulatory relationships. Besides the direct analysis of patient material, the generation of patient-specific iPSCs present a powerful tool to study human diseases. In addition, differentiation of iPSCs into more complex, three-dimensional, multicellular systems, such as organoids, allows transfer to tissue and organ levels, enabling the modeling of human diseases including CHD [27, 28].

22.2.4 Techniques to Induce Perturbations

To enable the study of cause–effect relationships in different model systems, *in vivo* gene targeting techniques play an essential role. For example, the generation of designed mouse mutants relies on gene targeting in ES cells. Representing appropriate genetic models of inherited diseases, knockout mice with a null allele in their germline often exhibit embryonic or early postnatal lethality [29]. To study cell type or stage-specific gene functions, a system based on the DNA recombinase Cre and its recognition sites (loxP) has been established [29]. Other faster methods for targeted genome editing, which are also used in cell culture models, include transcription activator-like effector nucleases (TALENs), zinc finger nucleases (ZFN), and clustered regulatory interspaced short palindromic repeat (CRISPR)/Cas-based RNA-guided DNA endonucleases [30]. Besides the targeted perturbation of selected genes in a reverse genetics approach, random mutation screens enable the discovery of novel gene functions in an unbiased manner. For example, treatment with the supermutagen *N*-ethyl-*N*-nitrosourea (ENU) is the most potent method to induce random point mutations throughout the mouse genome. The offspring of treated animals can then be screened for autosomal dominant or recessive phenotypes and used for the identification of the causal mutation in a forward genetics approach [31].

In addition to the perturbation of the genomic DNA sequence, knockdown of a gene at the transcriptional level provides another valuable approach for studying gene functions and can be used for large genome-scale high-throughput screens. RNA interference (RNAi) is a widely used approach for screens in cell culture systems, *C. elegans* and *Drosophila* [32], while the most common antisense knockdown technique in zebrafish are morpholino oligonucleotides (MOs) [33]. Moreover, the overexpression of genes, for example, by the transfection of expression vectors, not only allows the study of wild-type gene function but also enables the analysis of mutant alleles. Finally, knockdown in combination with overexpression can be applied to perform rescue experiments to demonstrate the specificity of the observed phenotype.

Besides genetic alterations, environmental influences also play an important role in the etiology of CHD. Thus, a variety of stress models have been established to analyze gene–environment interactions. For example, a maternal high-fat diet increases the penetrance of CHD in heterozygous *Cited2* knockout mice [34]. Moreover, a commonly used experimental model to induce hemodynamic stress in the mouse heart is the transverse aortic constriction (TAC), which results in a pressure overload-induced cardiac hypertrophy [35]. In cell culture models, hypertrophic agents such as phenylephrine (PE) and endothelin 1 (ET1) are commonly used to study signaling pathways involved in cardiomyocyte hypertrophy [36].

22.3 Cardiac Phenotyping

22.3.1 Systematic Phenotyping of Mouse Models

The International Knockout Mouse Consortium has established thousands of mutant mouse models [12], whose characterization, archiving, and distribution are realized by phenotyping centers (mouse clinics) organized in large consortia such as the International Mouse Phenotyping Consortium (IMPC) [37] or its forerunner the European Mouse Disease Clinic (EUMODIC) [38]. The phenotyping pipelines systematically assess the stage of a potential embryonic lethality and a broad range of physiological parameters, such as metabolic functions, fertility, behavior, body composition, and immune function in adult animals. Cardiac phenotyping includes the measurement of heart weight, electrocardiography, and echocardiography as well as histological analysis [37, 39]. Until 2021, almost 7.9 thousand genes had been knockout by the IPMC generating 8.5 thousand phenotypes of which 3.5 affected the cardiovascular system.

22.3.2 Imaging Cardiogenesis in Live Animals

Embryogenesis is based on three fundamental processes, namely, growth, differentiation, and organization. Thus, in vivo imaging of these processes is important for understanding the structural formation and function of the heart and its molecular background. The main quantitative in vivo imaging techniques are optical imaging, ultrasound, micro-computed tomography (micro-CT), and magnetic resonance imaging (MRI) [40].

Confocal microscopy is a routine method to study the transparent zebrafish embryo, and multiple fluorescent transgenic lines have been established to label, for example, cardiac myocytes and endothelial cells [4]. Ultrasound is another inherently real-time imaging technique and is useful to analyze aberrant morphologies and hemodynamic phenotypes in developing embryos [40]. The small size and rapid motions of the embryo make ultrasound imaging challenging in mice, and thus, the hemodynamics of the dorsal aorta is often used as a surrogate for intracardiac hemodynamics. By contrast, avian embryos allow the direct measurement of chamber-specific blood flow and valve motions [40]. The highest possible imaging resolution is theoretically provided by micro-CT. However, x-rays are attenuated poorly by soft tissues and necessitate the application of contrast agents, which are mostly unsuitable for live embryonic imaging. Nevertheless, recent studies have evaluated different agents with a reduced toxicity [40]. Finally, MRI has mainly been used for the imaging of fixed murine embryos, as technical limitations hinder its application for live embryonic imaging. It offers excellent tissue contrast and the ability of three-dimensional image reconstruction [41], but high field strengths of 7–11 T and long acquisition times (6–24 h) are required for the high spatial resolution needed for embryonic imaging (25–50 μm) [40, 42]. Therefore, multiple embryos are often analyzed at once to increase the throughput of

phenotyping. Live imaging applications of MRI with a reduced spatial resolution include the study of mouse embryos in utero and chicken embryos in ovo [40].

22.3.3 Histological Analysis of Fixed Hearts

Classical methods for the histological assessment of fixed hearts are hematoxylin and eosin (HE) staining for morphological inspection, in situ hybridization for transcript expression, and immunohistochemistry for protein expression. For the visualization of subcellular structures, electron microscopy is the gold standard [3].

To identify cell nuclei and cytoplasm, HE staining is the most widely used method and provides a general overview of the sample. Moreover, a large variety of special stains is available to visualize, for example, polysaccharides, glycoproteins, and glycolipids (periodic acid–Schiff; PAS stain) or collagen fibers (trichome staining) [43]. In situ hybridization is based on the binding of an approximately 20-bp-long oligonucleotide probe, usually labeled with digoxigenin or fluorescent dyes, to the complementary mRNA. By contrast, immunohistochemistry is based on the application of labeled antibodies. To reconstruct the 3D structure of embryonic hearts and to visualize cardiac gene expression patterns, techniques such as high-resolution episcopic microscopy (HREM) and optical projection tomography (OPT) [44, 45] have proved to be very useful tools and enhance the phenotyping of mouse embryos. Finally, electron microscopes provide the highest resolution in the range of picometers [46], which is needed for studying the ultrastructure of a wide variety of biological and inorganic specimens.

22.3.4 Phenotyping of Cell Culture Models

The easy handling of cell culture models allows the application of various phenotyping techniques. Immunohistochemistry provides the opportunity to detect the subcellular localization of proteins within the cell under defined conditions. Moreover, co-staining with different antibodies allows visualization of protein–protein interactions and is thus a useful method to study molecular signaling pathways. Fluorescence-activated cell sorting (FACS) combines specific immunostaining and single-cell analysis using flow cytometry. For example, in a heterogeneous cell population like blood, distinct cell types can be distinguished based on their expressed surface markers [47]. Other cell-based assays include the measurement of proliferation, viability, apoptosis, autophagy, production of reactive oxygen species (ROS), mitochondrial function, cell migration, and cytotoxicity of chemical compounds. Finally, cultures of beating cardiomyocytes are an important model for electrophysiology studies, and the patch clamp technique enables the measurement of ionic currents on isolated cells down to the single-channel level [48].

22.4 Molecular Biological Techniques

22.4.1 Genotyping Techniques

One of the first methods to identify disease genes in affected families was the mapping of genes relative to known genetic markers by linkage analysis. This method is based on the recombination between homologous chromosomes, which occurs randomly. Thus, two genomic positions are less likely to undergo recombination if they are located in close proximity to each other. Different genetic markers including single-nucleotide polymorphisms (SNPs), microsatellites (short repeat sequences of variable length), or restriction fragment length polymorphisms (RFLPs) can be used for linkage analysis. RFLPs are sequence polymorphisms that cause differences in enzymatic cleavage sites between alleles, resulting in DNA fragments of unequal lengths that can be detected by probe hybridization [49]. For the genotyping of SNPs, microsatellites, and other short variations, direct sequencing or denaturing high-performance liquid chromatography (DHPLC) has been frequently used. DHPLC is based on the formation of heteroduplexes between chromosomes and can identify the presence but not the exact position and nature of a mismatch [50].

The gold standard for direct DNA sequencing is the Sanger method, reaching read lengths of up to 1000 bp and a per-base sequencing accuracy as high as 99.999% [51]. It is based on the incorporation of dideoxynucleotides (ddNTPs) into the DNA that act as specific chain-terminating inhibitors of the DNA polymerase [52]. The introduction of shotgun sequencing, fluorescent labeling, and capillary gel electrophoresis significantly increased the throughput of Sanger sequencing and enabled the deciphering of the complete human genome in 2001 [53, 54]. The sequencing biochemistry is performed in a cycle sequencing reaction, which is stochastically terminated by the incorporation of fluorescently labeled ddNTPs. This results in a mixture of end-labeled products, and the final sequence is determined by electrophoretic separation of the products and laser excitation of the four different fluorescent labels [51] (Fig. 22.1a).

A variety of methods have also been developed for the detection of chromosomal abnormalities. Giemsa staining is a simple and rapid technique for conventional karyotyping and can identify many chromosomal changes, including balanced chromosomal aberrations [56]. A higher resolution from tens of kilobases up to several megabases is offered by fluorescence in situ hybridization (FISH), which uses fluorescently labeled probes that hybridize to their complementary chromosomal sequences [56]. As an alternative to these microscopy-based methods, multiplex ligation-dependent probe amplification (MLPA) can be applied, which is based on a multiplexed PCR and can detect copy number changes of up to 50 different loci in parallel [56].

New possibilities for the analysis of genetic variations were provided by microarray-based genotyping, which offers high-resolution genome-wide variation detection and is based on the hybridization of a DNA sample to oligonucleotide probes that have been immobilized on a glass or silicon surface [57]. Array

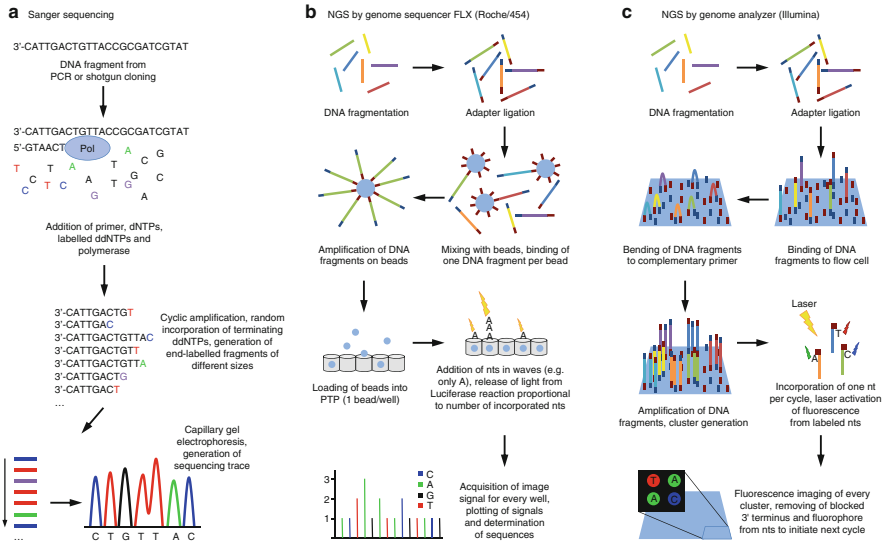
a Sanger sequencing
3'-CATTGACTGTTACCGCGATCGTAT
DNA fragment from PCR or shotgun cloning
3'-CATTGACTGTTACCGCGATCGTAT
5'-GTAACT
Pol
Addition of primer, dNTPs, labelled ddNTPs and polymerase
3'-CATTGACTGT
3'-CATTGAC
3'-CATTGACTGTTAC
3'-CATTGACTGTT
3'-CATTGACTGTTA
3'-CATTGACTG
3'-CATTGACT
Cyclic amplification, random incorporation of terminating ddNTPs, generation of end-labelled fragments of different sizes
Capillary gel electrophoresis, generation of sequencing trace
C T G T T A C
b NGS by genome sequencer FLX (Roche/454)
DNA fragmentation
Adapter ligation
Amplification of DNA fragments on beads
Mixing with beads, binding of one DNA fragment per bead
Loading of beads into PTP (1 bead/well)
Addition of nts in waves (e.g. only A), release of light from Luciferase reaction proportional to number of incorporated nts
Acquisition of image signal for every well, plotting of signals and determination of sequences
C
A
G
T
c NGS by genome analyzer (Illumina)
DNA fragmentation
Adapter ligation
Bending of DNA fragments to complementary primer
Binding of DNA fragments to flow cell
Amplification of DNA fragments, cluster generation
Laser
Incorporation of one nt per cycle, laser activation of fluorescence from labeled nts
Fluorescence imaging of every cluster, removing of blocked 3' terminus and fluorophore from nts to initiate next cycle

Fig. 22.1 Workflow of Sanger sequencing and two next-generation sequencing platforms. (**a**) Sanger sequencing. (**b**) Genome Sequencer FLX from Roche/454. (**c**) Genome Analyzer from Illumina. *dNTP* deoxynucleotide, *ddNTP* dideoxynucleotides, *NGS* next-generation sequencing, *nts* nucleotides, *Pol* DNA polymerase (Figure adapted from Shendure and Ji [51], and Mardis [55])

comparative genomic hybridization (array-CGH) is used to identify chromosomal aberrations by comparing a DNA sample to a reference sample. Moreover, DNA microarrays enable the analysis of disease-specific or even genome-wide SNP panels (SNP arrays) [56]. Thus, they allow the detection of known disease-causing mutations in individual patients or the identification of novel associations between SNPs and complex traits in genome-wide association studies (GWAS) [58].

22.4.2 Next-Generation Sequencing

Since its emergence, genomic sequencing has led to exceptional achievements in biomedical research. The evolution of DNA sequencing during the last few decades has been breathtaking: from Maxam–Gilbert and Sanger—the first-generation sequencing technologies developed in the 1970s and recognized with the 1980 Nobel Prize in Chemistry—to today's widely used high-throughput short-read second-generation sequencing technologies, to the powerful yet challenging latest developments of long-read third-generation technologies.

Sanger sequencing dominated the research landscape until the early twenty-first century and allowed the generation of the first "reference" human genome sequence under the framework of the Human Genome Project (HGP). This first genome costed about $300 million and took 13 years to be achieved [53, 54]. Following the end of

the HGP, genomic research continued to refine sequencing methodologies enabling the development of massively parallel sequencing techniques, the so-called next-generation sequencing (NGS) or second-generation sequencing technologies [59, 60]. The advent of these NGS technologies represented a major step change in affordability and set the stage for revolutionary advances in DNA sequencing technologies, including time and cost reductions that continued until recently. Most importantly, NGS does not require prior knowledge of sequence information.

Among the most important NGS platforms that were initially established by the companies Roche/454, Illumina, and Life Technologies, the Solexa sequencing by the synthesis method of Illumina [61, 62] has undoubtedly been the most successful one to the point of near monopoly [63, 64]. Illumina has probably made the greatest contribution to the second generation of DNA sequencers, also reflected in the amount of sequencing data generated so far. While the first Illumina Genome Analyzer (GA) machines were initially only capable of producing very short reads (up to 35 bp long), they could produce paired-end data, in which the sequence at both ends of each DNA cluster is recorded, benefiting subsequent bioinformatics data analysis. The GA was later followed by the HiSeq sequencing systems, capable of greater read length and depth. Continuous improvements of next-generation DNA sequencers, in terms of lowering genome-sequencing costs [65], led to achieve the expected "1000 dollar human genome" goal around 2017–2018 [66]. Today, the use of Illumina's NovaSeq system, with a scalable output that can generate up to 6 Tb and 20 billion reads, probably represents the most cost-effective way to perform whole genome sequencing (pending details of the DNBseq™ sequencing technology developed by the Chinese Beijing Genomics Institute, BGI).

In 2009, the third-generation of DNA sequencing technologies [67, 68] began to emerge. Unlike second-generation sequencing, which produces short reads with a few hundred base-pairs, third-generation single-molecule technologies generate over 10,000 bp reads or map over 100,000 bp molecules. These fundamentally different techniques are capable of sequencing single molecules without the need for DNA amplification shared by all previous technologies. This is a very interesting feature that allows modifications (such as methylation) to be detected. Furthermore, longer read length circumvents the inherent limitations of short-read methods. By spanning more repetitive elements and thus producing more contiguous reconstructions of the genome, this approach allows for the analysis of some very interesting parts of the genome.

The two major players in long-read sequencing are the companies Pacific Biosciences (PacBio), with its single-molecule real-time sequencing (SMRT-seq) and Oxford Nanopore Technologies (ONT) with nanopore sequencing using the small MinION device. Although these technologies are undergoing active development and sequencing data have much higher error rates than previous technologies [69], expected improvements might facilitate numerous possibilities. Very recent publications report the first human genome assembled de novo from ultra-long (>100 kb) nanopore reads [70], nanopore sequencing of the human transcriptome [71], and first gapless assembly of a human chromosome achieved by a combination of the latest developments in nanopore and PacBio sequencing and ad hoc assembly algorithms [72].

NGS platforms are the dominant type of sequencing technology used today in research and clinical diagnostics. The use of NGS to identify genetic characteristics associated with CHD started quite a few years ago by performing targeted resequencing (gene panels) and whole exome sequencing (WES) in several large cohorts of CHD patients [73]. Given the complex genetic structure of CHD, WES has contributed to the identification of the genetic etiology of a significant fraction of CHD, including coding inherited and the novo variants [74]. Over time, not only have the cohorts grown (increasing the statistical power of the studies) but also have the continuously expanding NGS applications used. The Pediatric Cardiac Genomics Consortium of the Bench to Bassinet Program supported by the National Heart, Lung, and Blood Institute (NHLBI) has enrolled by now more than 13,300 patients with a diverse range of CHD and over 19,000 relatives (21). Recent genomic analyses using whole genome sequencing (WGS) from parent-child trios have implicated non-coding de novo variants in CHD [75], highlighting the potential of WGS to improve the CHD diagnostic yields and promoting the discovery of new molecular mechanisms of CHD development [76]. WGS significantly expands genome coverage and enables the detection of all types of genetic variations throughout the genome, including single-nucleotide variants, small insertion/deletions, CNVs, and structural variations [77]. With NGS prices dropping, WGS is increasingly being used in research and in clinical practice for patients with CHD.

22.4.3 Transcriptome and Epigenome Analysis

Both NGS and array-based technologies are extensively used for transcriptome and epigenome analysis. In addition, quantitative real-time PCR is a useful low- to medium-throughput application. The study of gene expression was revolutionized by RNA sequencing (RNA-seq), which enables the discovery, profiling, and quantification of RNA transcripts across the entire transcriptome without prior knowledge about the probed sequences. Applications of RNA-seq comprise total RNA-seq (coding and non-coding RNA above a certain size), mRNA-seq (including mRNAs and long non-coding RNAs with a poly-A tail), and small RNA-seq (including microRNAs and other small non-coding RNAs). Applications of RNA-seq include de novo transcriptome assembly [78] and tomography sequencing to determine spatially resolved transcription profiles in whole embryos or isolated organs [79]. Furthermore, the so-called third-generation RNA-seq now allows sequencing very long RNA molecules. This approach uses the PacBio and Nanopore technologies described above and is essential for accurate transcript quantification, including alternative splicing and alternative polyadenylation analyses [80, 81].

A major highlight in the field was the development of single-cell RNA-seq (scRNA-seq), which allows studying transcription in a given tissue in all its complexity by analyzing each cell separately. scRNA-seq combines RNA-seq with microfluidics, which enables the accurate control of very small volumes (nano or femtoliter), in such a way that each isolated cell in the sample is held separately in a droplet where the sequencing takes place [82]. scRNA-seq can be applied to whole

cells or to isolated nuclei, which is sometimes convenient if the cells is too large, as with a cardiomyocyte. scRNA-seq has made it possible to produce full cell profiles, particularly in the fields of immunology [83, 84] and oncology [85, 86]. In the cardiovascular field, a catalog of cells in the adult heart was recently reported [87]. Using the single-cell technology and profiling half a million cells and nuclei from six anatomical cardiac regions within the Human Cell Atlas revealed 11 major cardiac cell types and 62 different cell states in the human heart [87].

In addition to hardware, this new sequencing technology has fueled the development of hundreds of new analytical algorithms [88, 89]. The field is moving fast, and new protocols to identify where each sequenced cell was have been developed. This technique, known as spatial transcriptome sequencing or spatially resolved transcriptomics, combines RNA-seq with fluorescence in situ hybridization (FISH), which was named "method of the year" in 2020 [90–92].

A powerful technique for the genome-wide identification of protein–DNA interactions such as transcription factor binding sites or chromatin histone marks is chromatin immunoprecipitation (ChIP). In ChIP, the protein of interest is cross-linked to the DNA, either in cultured cells or in tissue samples. After cross-linking, the chromatin is sheared and an antibody is used to enrich for DNA fragments bound to the protein. Immunoprecipitation and reverse cross-linking isolate the DNA enriched in the binding sites, and finally, the enriched DNA fragments can further be analyzed by hybridization to microarrays (ChIP-chip) or NGS (ChIP-seq) [93, 94] (Fig. 22.2). If candidate target genes or potential sites are available, ChIP-qPCR represents an alternative strategy. To investigate the co-localization of proteins on the DNA, ChIP-reChIP (sequential ChIP) has been developed using two independent rounds of immunoprecipitation [95]. An alternative method used to map protein–genome interactions is DamID, which does not require the use of antibodies. This technique is based on the fusion of the protein of interest to *Escherichia coli* DNA adenine methyltransferase (dam) and the resulting methylation of adenines in DNA surrounding the native binding sites of the dam fusion partner. In most eukaryotes, adenine methylation does not occur endogenously. Thus, it provides a unique tag to mark protein interaction sites, which can further be identified by array hybridization or NGS [96].

In addition to histone modifications, DNA methylation occurring on cytosine residues in the context of CpG dinucleotides is also an important epigenetic mark. Altered DNA methylation has been shown to play a role in various diseases, including CHD [98]. Three methods are commonly used to detect genome-wide DNA methylation levels. Two techniques are based on the isolation of methylated DNA fragments by methylated DNA immunoprecipitation (MeDIP) or methyl-CpG binding domain-based (MBD) proteins. Subsequently, the enriched DNA fragments can be detected by arrays or NGS [99]. The third technique applies the treatment of DNA with sodium bisulfite, which converts all non-methylated cytosines to uracil. These will finally be detected as thymine residues, analogous to a C to T SNP, by, for example, pyrosequencing [100] or NGS.

Several techniques are available to assess chromatin structure and regulatory interactions. Chromatin that has lost its condensed structure is sensitive to cleavage

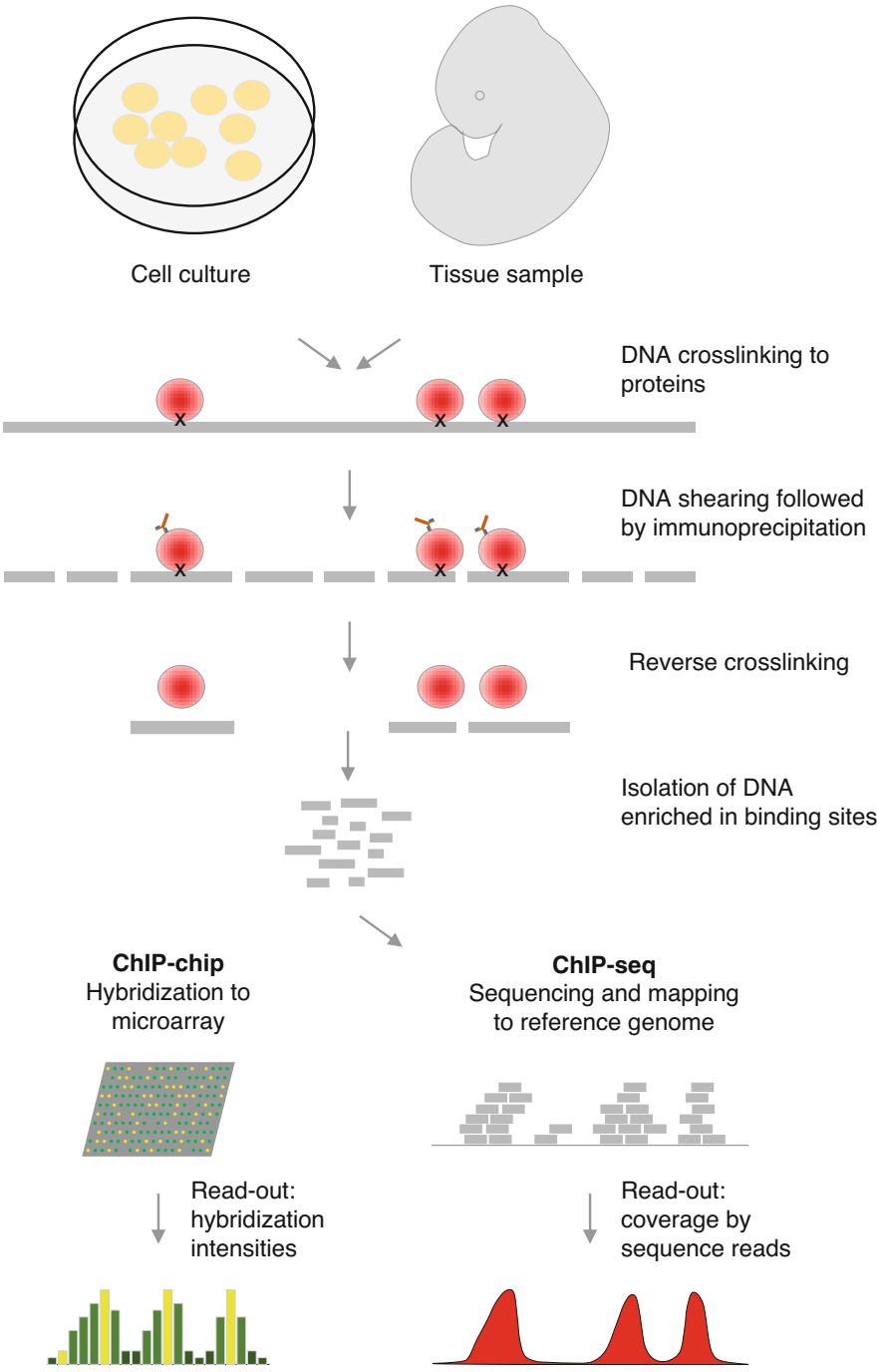

Fig. 22.2 Schematic representation of a chromatin immunoprecipitation (ChIP) experiment followed by microarray detection (ChIP-chip) or next-generation sequencing (ChIP-seq) (Figure adapted from Visel et al. [97])

by the DNase I enzyme (DNase I hypersensitive sites). Thus, the enzymatic degradation of DNA can be used to identify regions of open chromatin, representing cis-regulatory elements including promoters, enhancers, insulators, and silencers [101]. An alternative method to DNase-seq is the assay of transposase-accessible chromatin (ATAC-seq), which uses an engineered Tn5 transposase to cleave DNA in open chromatin and to integrate primer DNA sequences into the cleaved genomic DNA. Modifications to the protocol also allow the analysis based on single-cell resolution (scATAC-seq). Microfluidics can be used to isolate single nuclei and perform ATAC-seq individually [102]. Furthermore, a commonly used method to identify the exact positions of nucleosomes is the treatment with micrococcal nuclease (MNase), an endo-exonuclease that processively digests DNA until it is blocked, for example, by a nucleosome [103]. To study interactions between regulatory elements, including long-range interactions between different chromosomes, the chromosome conformation capture (3C) and various derivatives (4C, 5C, and Hi-C) have been developed. They are all based on the cross-linking of interacting DNA fragments and their subsequent restriction digest [104]. Using an additional ChIP step, chromatin analysis by paired-end tag sequencing (ChIA-PET) allows the identification of long-range interactions mediated by target proteins of interest [105].

The interaction of RNAs and proteins is also an important layer for the co-transcriptional and posttranscriptional regulation of gene expression. Genome-wide protein–RNA interaction can be identified based on ultraviolet cross-linking and immunoprecipitation (CLIP). To reach a base-pair resolution, this method was further developed to photoactivatable ribonucleoside-enhanced CLIP (PAR-CLIP), which relies on the incorporation of photoactivatable nucleotide analogs into the RNA. Here, reverse transcription results in a T to C base transition at the cross-link site, detectable as SNPs in the subsequent NGS analysis. However, the need to incorporate photoactivatable nucleotides restricts PAR-CLIP to cultured cells [106]. Finally, a highly sensitive method for the general profiling of RNA-induced silencing complexes (RISC) and individual microRNA target identification is RISC-seq [107].

22.4.4 Proteome and Metabolome Analysis

The quantitative and qualitative large-scale study of proteins (proteomics) has undergone great developments over the last few years. The majority of proteomics analysis is performed by subjecting proteins to enzymatic digestion followed by analysis of the peptides generated by liquid chromatography in tandem with mass spectrometry (MS-based proteomics). The development of isotope labeling techniques, including metabolic [108] and 4-plex iTRAQ [109] or 6-plex TMT isobaric labeling [110], has allowed producing relative quantitative information with improved accuracy. More recently, multiplexing has been increased to allow 10-plex [111] and even 18-plex [112], and label-free methods are becoming increasingly available [113]. Robust statistical methods have also been developed to systematically analyze the quantitative information produced by mass spectrometry

[114–116]. Despite these developments, MS-based proteomics still suffers from a lack of sensitivity that impedes its application to the analysis of the small amounts of tissue usually available from embryonic heart or to the analysis of specific heart regions or cell populations isolated by sorting methods. Hence, these techniques have not still exploited its full potential in the field of CHD research. For these reasons, researchers have applied MS-based proteomics using enrichment techniques such as affinity purification in tandem with MS analysis (AP-MS). This technique has allowed the identification of binding partners of Nkx2.5, a transcription factor that regulates cardiomyogenesis and is a common target in CHD, revealing that myosin phosphatase modulates cardiac cell fate through the Wnt/ROCK-dependent pathway [117]. A similar approach was followed to identify TBX5 transcriptional coregulators, demonstrating that the interaction of TBX5 with the NuRD (nucleosome remodeling and deacetylase) transcriptional repressor complex is essential to cardiac development [118]. Other works have used an approach to enrich the N-terminal acetylome, defining a set of human proteins that requires a full NAA15 complement for normal synthesis and development [119]. Other authors have used a high-throughput *Xenopus tropicalis* model together with label-free unbiased proteomics to discover a critical role for the endoplasmic reticulum membrane protein complex 1 (EMC1), a protein involved in CHD, in Wnt signaling [120]. Further developments in MS-proteomics have recently increased throughput and chromatography robustness and stability [121], as well as sensitivity [122] [123], allowing some authors to perform singe-cell proteomics [124]. We foresee that the application of these front-end technologies will considerable boost our knowledge of molecular processes undergoing congenital diseases.

The high-throughput analysis of small-molecule metabolites such as alcohols, amino acids, nucleotides, and lipids, also called metabolomics, has similarly manifested a strong development in recent years. Metabolomics, like proteomics, also uses liquid chromatography in tandem with MS, but gas chromatography in tandem with MS (GC-MS) has also been extensively used for the analysis of small polar metabolites [125, 126]. As occurs with proteomics, these approaches require large amounts of biological material, and for this reason, metabolomics has mostly been applied in the CHD field to analyze circulating metabolites in biological fluids. Thus, some authors have investigated plasma metabolism association with CHD in offspring [127], and metabolomics has also been used to analyze plasma [128] and urine [129] in children undergoing surgery for CHD. Finally, nuclear magnetic resonance spectroscopy (NMR) offers the ability of analyzing metabolites directly in tissue samples, and this technique has been used to study tissue cerebral white matter energy metabolism in neonates with CHD [130].

An overview of the various molecular biological techniques to study the different regulatory layers that control the gene and protein expression is given in Fig. 22.3.

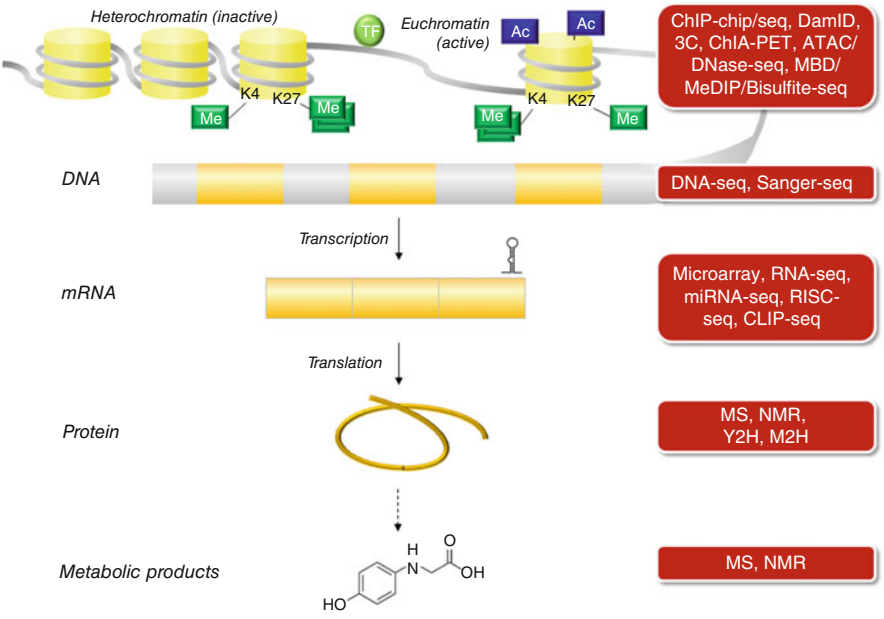

Fig. 22.3 Overview of various molecular biological techniques to study the different regulatory layers controlling gene and protein expression (Figure adapted from Lara-Pezzi et al. [131])

22.4.5 Integration of Omics Data for Studying CHD

Congenital heart disease is a multifaceted disease in which data at different molecular levels need to be integrated to shed light into its etiology and possible treatments. In general, CHD is believed to be sporadic and non-syndromic [132]. Genetic studies of a large number of patients have identified rare variants [74, 133] and differences in copy number [134] that could partially explain some of the diseases. However, the proportion of cases explained by the genetic structure of the individuals is limited, suggesting that other molecular mechanisms might also contribute to the prevalence of different types of CHD. scRNA-seq data are emerging as a valuable source of information in this regard [135].

After 20 years of using *omics* technologies to separately understand each layer of molecular information, we currently face the challenge to integrate all available information to unravel many of the open questions in CHD. The key is to integrate molecular and clinical information mainly extracted from electronic health records. Also, the number of individuals who needs to be included in this type of integrative studies needs to be large and validation cohorts need to be available in order to make the results reproducible and general. In general, data integration has two main aspects [136]: (a) the "physical" integration of the data in dedicated data warehouses/data lakes and (b) the development of algorithms to extract the relevant information and produce predictive models:

Data warehousing: Data integration of high-dimensional molecular data (*omics* data) and clinical information from a large number of individuals requires databases that allow to keep data traceability, to ensure data integrity, and to allow performing simple data analysis routines to standardize and explore the data [137]. These systems need also to provide an environment to query and subset the data in a rapid and intuitive manner. Relational databases, such as Oracle [138], SQL, and postgres [139], have reached their limit, and big data platforms, such as Hail, BigQuery, and Dataproc [140], are being used to this aim. These powerful technologies, coupled with front-end solutions for easy use by life scientists and clinicians, are being successfully applied in biomedical research.

Algorithms for data integration: Once the data are collected, preprocessed, and physically integrated, two types of mathematical models can be built: Predictive models use the minimum possible number of predictors, which can be clinical or molecular variables or both, to predict a given outcome (i.e., a particular type of CHD) while explanatory models try to identify the variables that are more relevant for this outcome. Among predictive models, machine learning algorithms are becoming very popular in biomedical research and, in particular, in cardiology, with an increase of 80% in articles in *PubMed* including the words "Machine Learning" and "Cardiovascular" between 2019 and 2020 and a similar trend for 2021 [141, 142]. While multivariate analysis is often used for explanatory models, once the number of predictors to consider have been reduced through univariate analysis, methods such as deep learning do not need a feature selection step. Regularization is also very useful tool to build predictive models without the need to prefilter the predictor variables: lasso (L2) regression will automatically select the set of most relevant features and give a zero weight to those not so relevant, while ridge regression (L1) estimates a homogeneous weight to all variables. In between, elastic net, for which the trade-off between L1 and L2 penalization can be optimized as a hyperparameter. This methodology is being largely used in studies for outcome prediction in cardiology [143] due to the small number of predictors needed per case vs other machine learning algorithms [144]. Notably, the performance of traditional machine (deep) learning algorithms is strongly dependent on quality and in particular size of training data.

Although the integrative use of data in CHD is still limited, some studies are in place to predict adverse outcomes after CHD surgery using machine learning in heterogeneous data [145]. Still, data integration is the only way to learn more from the heterogeneity and complexity of CHD and the interplay between modifiable and non-modifiable CV risk factors and unknown variables [28].

22.5 Conclusion

In this chapter, we described various model systems and biotechniques to study the different regulatory levels affecting congenital heart defects. In particular, the application of NGS techniques has revolutionized biomedical research and is still rapidly developing, enabling its application to a wide range of scientific questions.

Thus, these high-throughput techniques will enhance our understanding of CHD and will hopefully accelerate the development of novel therapeutic and preventive strategies.

References

1. Benian GM, Epstein HF. Caenorhabditis elegans muscle: a genetic and molecular model for protein interactions in the heart. Circ Res. 2011;109(9):1082–95.
2. Reim I, Frasch M. Genetic and genomic dissection of cardiogenesis in the Drosophila model. Pediatr Cardiol. 2010;31(3):325–34.
3. Sperling SR. Systems biology approaches to heart development and congenital heart disease. Cardiovasc Res. 2011;91(2):269–78.
4. Bodmer R. The gene tinman is required for specification of the heart and visceral muscles in Drosophila. Development. 1993;118(3):719–29.
5. Schoenebeck JJ, Yelon D. Illuminating cardiac development: advances in imaging add new dimensions to the utility of zebrafish genetics. Semin Cell Dev Biol. 2007;18(1):27–35.
6. Molina G, Vogt A, Bakan A, Dai W, Queiroz de Oliveira P, Znosko W, et al. Zebrafish chemical screening reveals an inhibitor of Dusp6 that expands cardiac cell lineages. Nat Chem Biol. 2009;5(9):680–7.
7. Major RJ, Poss KD. Zebrafish heart regeneration as a model for cardiac tissue repair. Drug Discov Today Dis Models. 2007;4(4):219–25.
8. Warkman AS, Krieg PA. Xenopus as a model system for vertebrate heart development. Semin Cell Dev Biol. 2007;18(1):46–53.
9. Kain KH, Miller JW, Jones-Paris CR, Thomason RT, Lewis JD, Bader DM, et al. The chick embryo as an expanding experimental model for cancer and cardiovascular research. Dev Dyn. 2014;243(2):216–28.
10. Gill TJ 3rd, Smith GJ, Wissler RW, Kunz HW. The rat as an experimental animal. Science. 1989;245(4915):269–76.
11. Snider P, Conway SJ. Probing human cardiovascular congenital disease using transgenic mouse models. Prog Mol Biol Transl Sci. 2011;100:83–110.
12. Bradley A, Anastassiadis K, Ayadi A, Battey JF, Bell C, Birling MC, et al. The mammalian gene function resource: the International Knockout Mouse Consortium. Mamm Genome. 2012;23(9–10):580–6.
13. Andersen TA, Troelsen Kde L, Larsen LA. Of mice and men: molecular genetics of congenital heart disease. Cell Mol Life Sci. 2014;71(8):1327–52.
14. Winston JB, Erlich JM, Green CA, Aluko A, Kaiser KA, Takematsu M, et al. Heterogeneity of genetic modifiers ensures normal cardiac development. Circulation. 2010;121(11):1313–21.
15. Siddiqui AS, Khattra J, Delaney AD, Zhao Y, Astell C, Asano J, et al. A mouse atlas of gene expression: large-scale digital gene-expression profiles from precisely defined developing C57BL/6J mouse tissues and cells. Proc Natl Acad Sci U S A. 2005;102(51):18485–90.
16. Claycomb WC, Lanson NA Jr, Stallworth BS, Egeland DB, Delcarpio JB, Bahinski A, et al. HL-1 cells: a cardiac muscle cell line that contracts and retains phenotypic characteristics of the adult cardiomyocyte. Proc Natl Acad Sci U S A. 1998;95(6):2979–84.
17. Gonnerman EA, Kelkhoff DO, McGregor LM, Harley BA. The promotion of HL-1 cardiomyocyte beating using anisotropic collagen-GAG scaffolds. Biomaterials. 2012;33 (34):8812–21.
18. Kimes BW, Brandt BL. Properties of a clonal muscle cell line from rat heart. Exp Cell Res. 1976;98(2):367–81.
19. Yaffe D, Saxel O. Serial passaging and differentiation of myogenic cells isolated from dystrophic mouse muscle. Nature. 1977;270(5639):725–7.

20. McBurney MW, Jones-Villeneuve EM, Edwards MK, Anderson PJ. Control of muscle and neuronal differentiation in a cultured embryonal carcinoma cell line. Nature. 1982;299(5879):165–7.
21. Yang L, Soonpaa MH, Adler ED, Roepke TK, Kattman SJ, Kennedy M, et al. Human cardiovascular progenitor cells develop from a KDR+ embryonic-stem-cell-derived population. Nature. 2008;453(7194):524–8.
22. Moore JC, Spijker R, Martens AC, de Boer T, Rook MB, van der Heyden MA, et al. A P19Cl6 GFP reporter line to quantify cardiomyocyte differentiation of stem cells. Int J Dev Biol. 2004;48(1):47–55.
23. Dambrot C, Passier R, Atsma D, Mummery CL. Cardiomyocyte differentiation of pluripotent stem cells and their use as cardiac disease models. Biochem J. 2011;434(1):25–35.
24. Wada R, Muraoka N, Inagawa K, Yamakawa H, Miyamoto K, Sadahiro T, et al. Induction of human cardiomyocyte-like cells from fibroblasts by defined factors. Proc Natl Acad Sci U S A. 2013;110(31):12667–72.
25. Schott JJ, Benson DW, Basson CT, Pease W, Silberbach GM, Moak JP, et al. Congenital heart disease caused by mutations in the transcription factor NKX2-5. Science. 1998;281(5373):108–11.
26. Garg V, Kathiriya IS, Barnes R, Schluterman MK, King IN, Butler CA, et al. GATA4 mutations cause human congenital heart defects and reveal an interaction with TBX5. Nature. 2003;424(6947):443–7.
27. Rowe RG, Daley GQ. Induced pluripotent stem cells in disease modelling and drug discovery. Nat Rev Genet. 2019;20(7):377–88.
28. Mullen M, Zhang A, Lui GK, Romfh AW, Rhee JW, Wu JC. Race and genetics in congenital heart disease: application of iPSCs, omics, and machine learning technologies. Front Cardiovasc Med. 2021;8:635280.
29. Friedel RH, Wurst W, Wefers B, Kuhn R. Generating conditional knockout mice. Methods Mol Biol. 2011;693:205–31.
30. Gaj T, Gersbach CA, Barbas CF 3rd. ZFN, TALEN, and CRISPR/Cas-based methods for genome engineering. Trends Biotechnol. 2013;31(7):397–405.
31. Probst FJ, Justice MJ. Mouse mutagenesis with the chemical supermutagen ENU. Methods Enzymol. 2010;477:297–312.
32. Mohr SE, Perrimon N. RNAi screening: new approaches, understandings, and organisms. Wiley Interdiscip Rev RNA. 2012;3(2):145–58.
33. Bedell VM, Westcot SE, Ekker SC. Lessons from morpholino-based screening in zebrafish. Brief Funct Genomics. 2011;10(4):181–8.
34. Bentham J, Michell AC, Lockstone H, Andrew D, Schneider JE, Brown NA, et al. Maternal high-fat diet interacts with embryonic Cited2 genotype to reduce Pitx2c expression and enhance penetrance of left-right patterning defects. Hum Mol Genet. 2010;19(17):3394–401.
35. Rockman HA, Ross RS, Harris AN, Knowlton KU, Steinhelper ME, Field LJ, et al. Segregation of atrial-specific and inducible expression of an atrial natriuretic factor transgene in an in vivo murine model of cardiac hypertrophy. Proc Natl Acad Sci U S A. 1991;88(18):8277–81.
36. Yue TL, Gu JL, Wang C, Reith AD, Lee JC, Mirabile RC, et al. Extracellular signal-regulated kinase plays an essential role in hypertrophic agonists, endothelin-1 and phenylephrine-induced cardiomyocyte hypertrophy. J Biol Chem. 2000;275(48):37895–901.
37. Brown SD, Moore MW. The International Mouse Phenotyping Consortium: past and future perspectives on mouse phenotyping. Mamm Genome. 2012;23(9–10):632–40.
38. Ayadi A, Birling MC, Bottomley J, Bussell J, Fuchs H, Fray M, et al. Mouse large-scale phenotyping initiatives: overview of the European Mouse Disease Clinic (EUMODIC) and of the Wellcome Trust Sanger Institute Mouse Genetics Project. Mamm Genome. 2012;23(9–10):600–10.
39. Gates H, Mallon AM, Brown SD, Consortium E. High-throughput mouse phenotyping. Methods. 2011;53(4):394–404.

40. Gregg CL, Butcher JT. Quantitative in vivo imaging of embryonic development: opportunities and challenges. Differentiation. 2012;84(1):149–62.
41. Bamforth SD, Schneider JE, Bhattacharya S. High-throughput analysis of mouse embryos by magnetic resonance imaging. Cold Spring Harb Protoc. 2012;2012(1):93–101.
42. Phoon CK. Imaging tools for the developmental biologist: ultrasound biomicroscopy of mouse embryonic development. Pediatr Res. 2006;60(1):14–21.
43. Veuthey T, Herrera G, Dodero VI. Dyes and stains: from molecular structure to histological application. Front Biosci (Landmark Ed). 2014;19:91–112.
44. Mohun TJ, Weninger WJ. Imaging heart development using high-resolution episcopic microscopy. Curr Opin Genet Dev. 2011;21(5):573–8.
45. Norris FC, Wong MD, Greene ND, Scambler PJ, Weaver T, Weninger WJ, et al. A coming of age: advanced imaging technologies for characterising the developing mouse. Trends Genet. 2013;29(12):700–11.
46. Erni R, Rossell MD, Kisielowski C, Dahmen U. Atomic-resolution imaging with a sub-50-pm electron probe. Phys Rev Lett. 2009;102(9):096101.
47. Herzenberg LA, Parks D, Sahaf B, Perez O, Roederer M, Herzenberg LA. The history and future of the fluorescence activated cell sorter and flow cytometry: a view from Stanford. Clin Chem. 2002;48(10):1819–27.
48. Bebarova M. Advances in patch clamp technique: towards higher quality and quantity. Gen Physiol Biophys. 2012;31(2):131–40.
49. Botstein D, White RL, Skolnick M, Davis RW. Construction of a genetic linkage map in man using restriction fragment length polymorphisms. Am J Hum Genet. 1980;32(3):314–31.
50. Xiao W, Oefner PJ. Denaturing high-performance liquid chromatography: a review. Hum Mutat. 2001;17(6):439–74.
51. Shendure J, Ji H. Next-generation DNA sequencing. Nat Biotechnol. 2008;26(10):1135–45.
52. Sanger F, Nicklen S, Coulson AR. DNA sequencing with chain-terminating inhibitors. Proc Natl Acad Sci U S A. 1977;74(12):5463–7.
53. Lander ES, Linton LM, Birren B, Nusbaum C, Zody MC, Baldwin J, et al. Initial sequencing and analysis of the human genome. Nature. 2001;409(6822):860–921.
54. Venter JC, Adams MD, Myers EW, Li PW, Mural RJ, Sutton GG, et al. The sequence of the human genome. Science. 2001;291(5507):1304–51.
55. Mardis ER. The impact of next-generation sequencing technology on genetics. Trends Genet. 2008;24(3):133–41.
56. Gijsbers AC, Ruivenkamp CA. Molecular karyotyping: from microscope to SNP arrays. Horm Res Paediatr. 2011;76(3):208–13.
57. Maskos U, Southern EM. Oligonucleotide hybridizations on glass supports: a novel linker for oligonucleotide synthesis and hybridization properties of oligonucleotides synthesised in situ. Nucleic Acids Res. 1992;20(7):1679–84.
58. Visscher PM, Brown MA, McCarthy MI, Yang J. Five years of GWAS discovery. Am J Hum Genet. 2012;90(1):7–24.
59. Margulies M, Egholm M, Altman WE, Attiya S, Bader JS, Bemben LA, et al. Genome sequencing in microfabricated high-density picolitre reactors. Nature. 2005;437(7057):376–80.
60. Shendure J, Porreca GJ, Reppas NB, Lin X, McCutcheon JP, Rosenbaum AM, et al. Accurate multiplex polony sequencing of an evolved bacterial genome. Science. 2005;309(5741):1728–32.
61. Mitra RD, Shendure J, Olejnik J, Edyta Krzymanska O, Church GM. Fluorescent in situ sequencing on polymerase colonies. Anal Biochem. 2003;320(1):55–65.
62. Ley TJ, Mardis ER, Ding L, Fulton B, McLellan MD, Chen K, et al. DNA sequencing of a cytogenetically normal acute myeloid leukaemia genome. Nature. 2008;456(7218):66–72.
63. Greenleaf WJ, Sidow A. The future of sequencing: convergence of intelligent design and market Darwinism. Genome Biol. 2014;15(3):303.
64. Zimmerman E. Illumina. MIT Technology Review. 2014.

65. Wetterstrand K. DNA sequencing costs: data from the NHGRI Genome Sequencing Program (GSP). 2020.
66. Mardis ER. The $1,000 genome, the $100,000 analysis? Genome Med. 2010;2(11):84.
67. Eid J, Fehr A, Gray J, Luong K, Lyle J, Otto G, et al. Real-time DNA sequencing from single polymerase molecules. Science. 2009;323(5910):133–8.
68. Clarke J, Wu H-C, Jayasinghe L, Patel A, Reid S, Bayley H. Continuous base identification for single-molecule nanopore DNA sequencing. Nat Nanotech. 2009;4(4):265–70.
69. Gupta PK. Single-molecule DNA sequencing technologies for future genomics research. Trends Biotech. 2008;26(11):602–11.
70. Jain M, Koren S, Miga KH, Quick J, Rand AC, Sasani TA, et al. Nanopore sequencing and assembly of a human genome with ultra-long reads. Nat Biotech. 2018;36(4):338–45.
71. Workman RE, Tang AD, Tang PS, Jain M, Tyson JR, Razaghi R, et al. Nanopore native RNA sequencing of a human poly(A) transcriptome. Nat Methods. 2019;16(12):1297–305.
72. Miga KH, Koren S, Rhie A, Vollger MR, Gershman A, Bzikadze A, et al. Telomere-to-telomere assembly of a complete human X chromosome. Nature. 2020;585(7823):79–84.
73. Dorn C, Grunert M, Sperling SR. Application of high-throughput sequencing for studying genomic variations in congenital heart disease. Brief Funct Genomics. 2013;13(1):51–65.
74. Jin SC, Homsy J, Zaidi S, Lu Q, Morton S, DePalma SR, et al. Contribution of rare inherited and de novo variants in 2,871 congenital heart disease probands. Nat Genet. 2017;49(11):1593–601.
75. Richter F, Morton SU, Kim SW, Kitaygorodsky A, Wasson LK, Chen KM, et al. Genomic analyses implicate noncoding de novo variants in congenital heart disease. Nat Genet. 2020;52(8):769–77.
76. Reuter MS, Chaturvedi RR, Liston E, Manshaei R, Aul RB, Bowdin S, et al. The Cardiac Genome Clinic: implementing genome sequencing in pediatric heart disease. Genet Med. 2020;22(6):1015–24.
77. Meienberg J, Bruggmann R, Oexle K, Matyas G. Clinical sequencing: is WGS the better WES? Hum Genet. 2016;135(3):359–62.
78. Martin JA, Wang Z. Next-generation transcriptome assembly. Nat Rev Genet. 2011;12(10):671–82.
79. Junker JP, Noël ES, Guryev V, Peterson KA, Shah G, Huisken J, et al. Genome-wide RNA tomography in the zebrafish embryo. Cell. 2014;159(3):662–75.
80. Byrne A, Beaudin AE, Olsen HE, Jain M, Cole C, Palmer T, et al. Nanopore long-read RNAseq reveals widespread transcriptional variation among the surface receptors of individual B cells. Nat Commun. 2017;8(1):16027.
81. Tang AD, Soulette CM, van Baren MJ, Hart K, Hrabeta-Robinson E, Wu CJ, et al. Full-length transcript characterization of SF3B1 mutation in chronic lymphocytic leukemia reveals downregulation of retained introns. Nat Commun. 2020;11(1):1438.
82. Jammes FC, Maerkl SJ. How single-cell immunology is benefiting from microfluidic technologies. Microsyst Nanoeng. 2020;6(1):45.
83. Chen H, Ye F, Guo G. Revolutionizing immunology with single-cell RNA sequencing. Cell Mol Immunol. 2019;16(3):242–9.
84. Papalexi E, Satija R. Single-cell RNA sequencing to explore immune cell heterogeneity. Nat Rev Immunol. 2018;18(1):35–45.
85. Wu F, Fan J, He Y, Xiong A, Yu J, Li Y, et al. Single-cell profiling of tumor heterogeneity and the microenvironment in advanced non-small cell lung cancer. Nat Commun. 2021;12(1):2540.
86. Sun G, Li Z, Rong D, Zhang H, Shi X, Yang W, et al. Single-cell RNA sequencing in cancer: applications, advances, and emerging challenges. Mol Ther Oncolytics. 2021;21:183–206.
87. Litviňuková M, Talavera-López C, Maatz H, Reichart D, Worth CL, Lindberg EL, et al. Cells of the adult human heart. Nature. 2020;588(7838):466–72.
88. Hie B, Peters J, Nyquist SK, Shalek AK, Berger B, Bryson BD. Computational methods for single-cell RNA sequencing. Annu Rev Biomed Data Sci. 2020;3(1):339–64.

89. Slovin S, Carissimo A, Panariello F, Grimaldi A, Bouché V, Gambardella G, et al. Single-cell RNA sequencing analysis: a step-by-step overview. In: Picardi E, editor. RNA bioinformatics. New York: Springer US; 2021. p. 343–65.
90. Marx V. Method of the year: spatially resolved transcriptomics. Nat Methods. 2021;18(1): 9–14.
91. Eng C-HL, Lawson M, Zhu Q, Dries R, Koulena N, Takei Y, et al. Transcriptome-scale super-resolved imaging in tissues by RNA seqFISH+. Nature. 2019;568(7751):235–9.
92. Rodriques SG, Stickels RR, Goeva A, Martin CA, Murray E, Vanderburg CR, et al. Slide-seq: a scalable technology for measuring genome-wide expression at high spatial resolution. Science. 2019;363(6434):1463–7.
93. Johnson DS, Mortazavi A, Myers RM, Wold B. Genome-wide mapping of in vivo protein-DNA interactions. Science. 2007;316(5830):1497–502.
94. Han Y, Garcia BA. Combining genomic and proteomic approaches for epigenetics research. Epigenomics. 2013;5(4):439–52.
95. Furlan-Magaril M, Rincon-Arano H, Recillas-Targa F. Sequential chromatin immunoprecipitation protocol: ChIP-reChIP. Methods Mol Biol. 2009;543:253–66.
96. Greil F, Moorman C, van Steensel B. DamID: mapping of in vivo protein-genome interactions using tethered DNA adenine methyltransferase. Methods Enzymol. 2006;410:342–59.
97. Visel A, Rubin EM, Pennacchio LA. Genomic views of distant-acting enhancers. Nature. 2009;461(7261):199–205.
98. Serra-Juhe C, Cusco I, Homs A, Flores R, Toran N, Perez-Jurado LA. DNA methylation abnormalities in congenital heart disease. Epigenetics. 2015;10(2):167–77.
99. Hsu HK, Weng YI, Hsu PY, Huang TH, Huang YW. Detection of DNA methylation by MeDIP and MBDCap assays: an overview of techniques. Methods Mol Biol. 2014;1105:61–70.
100. Ronaghi M, Uhlen M, Nyren P. A sequencing method based on real-time pyrophosphate. Science. 1998;281(5375):363, 5.
101. Thurman RE, Rynes E, Humbert R, Vierstra J, Maurano MT, Haugen E, et al. The accessible chromatin landscape of the human genome. Nature. 2012;489(7414):75–82.
102. Buenrostro JD, Wu B, Litzenburger UM, Ruff D, Gonzales ML, Snyder MP, et al. Single-cell chromatin accessibility reveals principles of regulatory variation. Nature. 2015;523(7561): 486–90.
103. Meyer CA, Liu XS. Identifying and mitigating bias in next-generation sequencing methods for chromatin biology. Nat Rev Genet. 2014;15(11):709–21.
104. Belmont AS. Large-scale chromatin organization: the good, the surprising, and the still perplexing. Curr Opin Cell Biol. 2014;26:69–78.
105. Fullwood MJ, Liu MH, Pan YF, Liu J, Xu H, Mohamed YB, et al. An oestrogen-receptor-alpha-bound human chromatin interactome. Nature. 2009;462(7269):58–64.
106. Konig J, Zarnack K, Luscombe NM, Ule J. Protein-RNA interactions: new genomic technologies and perspectives. Nat Rev Genet. 2012;13(2):77–83.
107. Matkovich SJ, Van Booven DJ, Eschenbacher WH, Dorn GW 2nd. RISC RNA sequencing for context-specific identification of in vivo microRNA targets. Circ Res. 2011;108(1):18–26.
108. Ong SE, Blagoev B, Kratchmarova I, Kristensen DB, Steen H, Pandey A, et al. Stable isotope labeling by amino acids in cell culture, SILAC, as a simple and accurate approach to expression proteomics. Mol Cell Proteomics. 2002;1(5):376–86.
109. Ross PL, Huang YN, Marchese JN, Williamson B, Parker K, Hattan S, et al. Multiplexed protein quantitation in Saccharomyces cerevisiae using amine-reactive isobaric tagging reagents. Mol Cell Proteomics. 2004;3(12):1154–69.
110. Thompson A, Schafer J, Kuhn K, Kienle S, Schwarz J, Schmidt G, et al. Tandem mass tags: a novel quantification strategy for comparative analysis of complex protein mixtures by MS/MS. Anal Chem. 2003;75(8):1895–904.
111. Increasing the Multiplexing Capacity of TMTs Using Reporter Ion Isotopologues with Isobaric Masses, (2012).

112. Li J, Cai Z, Bomgarden RD, Pike I, Kuhn K, Rogers JC, et al. TMTpro-18plex: the expanded and complete set of TMTpro reagents for sample multiplexing. J Proteome Res. 2021.
113. Bache N, Geyer PE, Bekker-Jensen DB, Hoerning O, Falkenby L, Treit PV, et al. A novel LC system embeds analytes in pre-formed gradients for rapid, ultra-robust proteomics. Mol Cell Proteomics. 2018;17(11):2284–96.
114. Navarro P, Trevisan-Herraz M, Bonzon-Kulichenko E, Nunez E, Martinez-Acedo P, Perez-Hernandez D, et al. General statistical framework for quantitative proteomics by stable isotope labeling. J Proteome Res. 2014;13(3):1234–47.
115. Garcia-Marques F, Trevisan-Herraz M, Martinez-Martinez S, Camafeita E, Jorge I, Lopez JA, et al. A novel systems-biology algorithm for the analysis of coordinated protein responses using quantitative proteomics. Mol Cell Proteomics. 2016;15(5):1740–60.
116. Trevisan-Herraz M, Bagwan N, García-Marqués F, Rodriguez JM, Jorge I, Ezkurdia I, et al. SanXoT: a modular and versatile package for the quantitative analysis of high-throughput proteomics experiments. Bioinformatics (Oxford, England). 2019;35(9):1594–6.
117. Ryan T, Shelton M, Lambert JP, Malecova B, Boisvenue S, Ruel M, et al. Myosin phosphatase modulates the cardiac cell fate by regulating the subcellular localization of Nkx2.5 in a Wnt/Rho-associated protein kinase-dependent pathway. Circ Res. 2013;112(2):257–66.
118. Waldron L, Steimle JD, Greco TM, Gomez NC, Dorr KM, Kweon J, et al. The cardiac TBX5 interactome reveals a chromatin remodeling network essential for cardiac septation. Dev Cell. 2016;36(3):262–75.
119. Ward T, Tai W, Morton S, Impens F, Van Damme P, Van Haver D, et al. Mechanisms of congenital heart disease caused by NAA15 haploinsufficiency. Circ Res. 2021;128(8):1156–69.
120. Marquez J, Criscione J, Charney RM, Prasad MS, Hwang WY, Mis EK, et al. Disrupted ER membrane protein complex-mediated topogenesis drives congenital neural crest defects. J Clin Invest. 2020;130(2):813–26.
121. Krieger JR, Wybenga-Groot LE, Tong J, Bache N, Tsao MS, Moran MF. Evosep one enables robust deep proteome coverage using tandem mass tags while significantly reducing instrument time. J Proteome Res. 2019;18(5):2346–53.
122. Bekker-Jensen DB, Martinez-Val A, Steigerwald S, Ruther P, Fort KL, Arrey TN, et al. A compact quadrupole-orbitrap mass spectrometer with FAIMS interface improves proteome coverage in short LC gradients. Mol Cell Proteomics. 2020;19(4):716–29.
123. Yu Q, Paulo JA, Naverrete-Perea J, McAlister GC, Canterbury JD, Bailey DJ, et al. Benchmarking the orbitrap tribrid eclipse for next generation multiplexed proteomics. Anal Chem. 2020;92(9):6478–85.
124. Cong Y, Liang Y, Motamedchaboki K, Huguet R, Truong T, Zhao R, et al. Improved single-cell proteome coverage using narrow-bore packed NanoLC columns and ultrasensitive mass spectrometry. Anal Chem. 2020;92(3):2665–71.
125. Ferrarini A, Di Poto C, He S, Tu C, Varghese RS, Kara Balla A, et al. Metabolomic analysis of liver tissues for characterization of hepatocellular carcinoma. J Proteome Res. 2019;18(8):3067–76.
126. Mastrangelo A, Ferrarini A, Rey-Stolle F, Garcia A, Barbas C. From sample treatment to biomarker discovery: a tutorial for untargeted metabolomics based on GC-(EI)-Q-MS. Anal Chim Acta. 2015;900:21–35.
127. Wang T, Chen L, Huang P, Yang T, Zhang S, Zhao L, et al. Association of maternal gut microbiota and plasma metabolism with congenital heart disease in offspring: a multi-omic analysis. Sci Rep. 2021;11(1):5339.
128. Correia GD, Wooi Ng K, Wijeyesekera A, Gala-Peralta S, Williams R, MacCarthy-Morrogh S, et al. Metabolic profiling of children undergoing surgery for congenital heart disease. Crit Care Med. 2015;43(7):1467–76.
129. Vedovelli L, Cogo P, Cainelli E, Suppiej A, Padalino M, Tassini M, et al. Pre-surgery urine metabolomics may predict late neurodevelopmental outcome in children with congenital heart disease. Heliyon. 2019;5(10):e02547.

130. Gertsvolf N, Votava-Smith JK, Ceschin R, Del Castillo S, Lee V, Lai HA, et al. Association between subcortical morphology and cerebral white matter energy metabolism in neonates with congenital heart disease. Sci Rep. 2018;8(1):14057.
131. Lara-Pezzi E, Dopazo A, Manzanares M. Understanding cardiovascular disease: a journey through the genome (and what we found there). Dis Model Mech. 2012;5(4):434–43.
132. Fotiou E, Williams S, Martin-Geary A, Robertson DL, Tenin G, Hentges KE, et al. Integration of large-scale genomic data sources with evolutionary history reveals novel genetic loci for congenital heart disease. Circ Genom Precis Med. 2019;12(10):e002694.
133. Cordell HJ, Bentham J, Topf A, Zelenika D, Heath S, Mamasoula C, et al. Genome-wide association study of multiple congenital heart disease phenotypes identifies a susceptibility locus for atrial septal defect at chromosome 4p16. Nat Genet. 2013;45(7):822–4.
134. Soemedi R, Wilson IJ, Bentham J, Darlay R, Töpf A, Zelenika D, et al. Contribution of global rare copy-number variants to the risk of sporadic congenital heart disease. Am J Hum Genet. 2012;91(3):489–501.
135. Friedman CE, Nguyen Q, Lukowski SW, Helfer A, Chiu HS, Miklas J, et al. Single-cell transcriptomic analysis of cardiac differentiation from human PSCs reveals HOPX-dependent cardiomyocyte maturation. Cell Stem Cell. 2018;23(4):586–98.e8.
136. Mlecnik B, Sanchez-Cabo F, Charoentong P, Bindea G, Pagès F, Berger A, et al. Data integration and exploration for the identification of molecular mechanisms in tumor-immune cells interaction. BMC Genomics. 2010;11(1):S7.
137. Klann JG, Abend A, Raghavan VA, Mandl KD, Murphy SN. Data interchange using i2b2. J Am Med Inform Assoc: JAMIA. 2016;23(5):909–15.
138. Maurer M, Molidor R, Sturn A, Hartler J, Hackl H, Stocker G, et al. MARS: microarray analysis, retrieval, and storage system. BMC Bioinform. 2005;6(1):101.
139. Athey BD, Braxenthaler M, Haas M, Guo Y. tranSMART: an open source and community-driven informatics and data sharing platform for clinical and translational research. AMIA Jt Summits Transl Sci Proc. 2013;2013:6–8.
140. Anon H. Genomics analysis with Hail, BigQuery, and Dataproc. https://cloudgooglecom/blog/products/data-analytics/genomics-data-analytics-with-cloud-pt2. 2020.
141. Shameer K, Johnson KW, Glicksberg BS, Dudley JT, Sengupta PP. Machine learning in cardiovascular medicine: are we there yet? Heart (British Cardiac Society). 2018;104(14):1156–64.
142. Johnson KW, Torres Soto J, Glicksberg BS, Shameer K, Miotto R, Ali M, et al. Artificial intelligence in cardiology. J Am Coll Cardiol. 2018;71(23):2668–79.
143. Sánchez-Cabo F, Rossello X, Fuster V, Benito F, Manzano JP, Silla JC, et al. Machine learning improves cardiovascular risk definition for young, asymptomatic individuals: EN-PESA. J Am Coll Cardiol. 2020;76(14):1674-1685.
144. van der Ploeg T, Austin PC, Steyerberg EW. Modern modelling techniques are data hungry: a simulation study for predicting dichotomous endpoints. BMC Med Res Methodol. 2014;14(1):137.
145. Bertsimas D, Zhuo D, Dunn J, Levine J, Zuccarelli E, Smyrnakis N, et al. Adverse outcomes prediction for congenital heart surgery: a machine learning approach. World J Pediatr Congenit Heart Surg. 2021;12(4):453–60.

Part IV

Atrial Septal Defect

Clinical Presentation and Therapy of Atrial Septal Defect

23

Nikolaus A. Haas, David J. Driscoll, and Silke Rickert-Sperling

23.1 Introduction

Atrial septal defects (ASDs) occur in 1 of 1500 live births and constitute 6–10% of congenital heart defects. There is a female-to-male predominance of 2 to 1. According to their embryological origins, we can differentiate five different types of ASDs (see Fig. 23.1):

The most common form of ASD is the *ostium secundum ASD* or *ASD II*. This occurs in the region of the fossa ovalis. This results from excessive absorption of the septum primum or insufficient development of the septum secundum or both.

Ostium primum ASD or *ASD I* is a type of atrioventricular sepal defect (formerly known as "endocardial cushion defects"). It is located in the inferior aspect of the atrial septum contiguous with the tricuspid and mitral valves and will be discussed further in Chap. 25.

Superior sinus venosus ASDs occur in the posterosuperior aspect of the atrial septum. Frequently, there is associated partial anomalous drainage of the right upper pulmonary vein. This vein can drain into the superior vena cava or the right atrium. Resorption of the wall between the vena cava and pulmonary vein results in this type

N. A. Haas (✉)
Department of Pediatric Cardiology and Intensive Care, Ludwig Maximilians University, Munich, Germany
e-mail: Nikolaus.haas@med.uni-muenchen.de

D. J. Driscoll
Division of Pediatric Cardiology, Department of Pediatrics, Mayo Clinic College of Medicine, Rochester, MN, USA
e-mail: driscoll.david@mayo.edu

S. Rickert-Sperling
Cardiovascular Genetics, Charité – Universitätsmedizin Berlin, Berlin, Germany
e-mail: silke.sperling@charite.de

© The Author(s), under exclusive license to Springer Nature Switzerland AG 2024

S. Rickert-Sperling et al. (eds.), *Congenital Heart Diseases: The Broken Heart*,
Advances in Experimental Medicine and Biology 1441,
https://doi.org/10.1007/978-3-031-44087-8_23

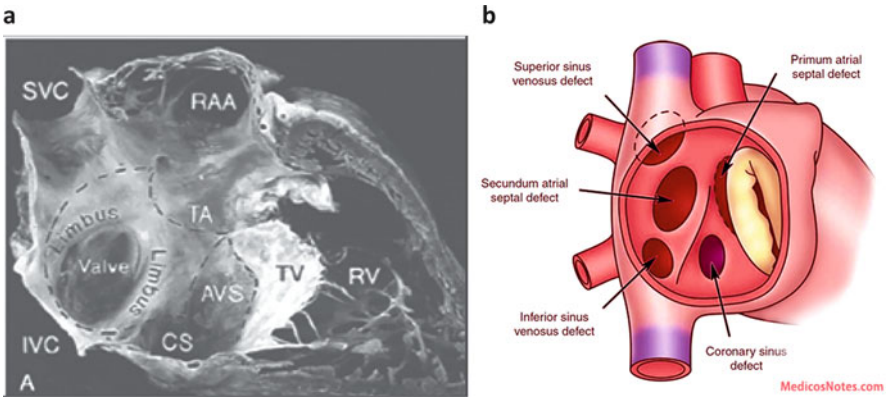

Fig. 23.1 An illustration of the location of atrial septal defects (ASD). (**a**) Pathological specimen of a normal heart with the anterior surface of the heart removed. Viewed from the right atrium, the atrial septum is enclosed within the dotted line. (**b**) Diagrammatic representation of the relative locations of different types of ASDs: ostium secundum defect (ASD II), ostium primum defect (ASD I), superior or inferior sinus venosus defect, and unroofed coronary sinus

of atrial septal defect. This also explains the anomalous drainage of the right upper pulmonary vein into the right atrium or superior vena cava (SVC) commonly associated with sinus venous atrial septal defects. In fact, technically the atrial septum is not defective, but rather the roof of the pulmonary vein is defective. Inferior sinus venosus defects are located in the inferior posterior region of the atrial septum in the area where the inferior vena cava drains into the right atrium.

The most uncommon form of ASD is *the unroofed coronary sinus* or *coronary sinus defect*. The coronary sinus is apposed to the posterior aspect of the left atrium, but the orifice is in the right atrium. If a hole exists in the roof of the coronary sinus, the coronary sinus and the left atrium will be in continuity, and therefore, the right and left atria will be in communication with each other (Fig. 23.2).

In a secundum type defect, there is a real defect or continuous connection between the two atria. A patent foramen ovale (PFO), however, describes the fact that the foramen ovale with its different layers has not closed completely and may be probed or crossed. This can be found in about 20–25% of the general population and usually has no clinical relevance. Based on the trap-door mechanism, there is no shunt across this PFO.

23.2 Pathologic Physiology

In uncomplicated atrial septal defects, the flow of blood is from the left to the right atrium through the defect (i.e., a left-to-right shunt). The flow is in this direction because the right ventricle (and right atrium) is more compliant than the left ventricle (and left atrium). This results in an excess volume of blood transiting the right

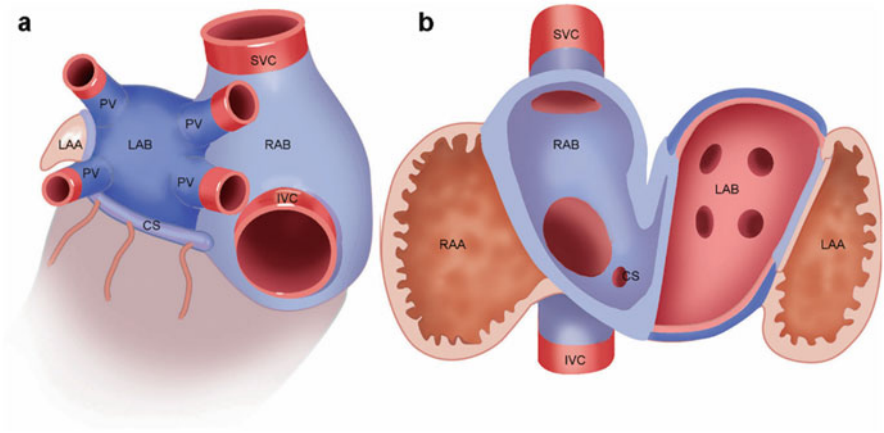

Fig. 23.2 (**a**) Schematic representation of the outside of the atrial chambers with the pulmonary veins (*PV*) and systemic veins (superior caval vein [*SCV*], inferior caval vein [*IVC*], coronary sinus [*CS*]). The left atrial body (*LAB*) and right atrial body (*RAB*) are covered with a smooth-walled myocardium (*blue*), extending to the extracardiac segments of the PV and over a small peripheral part of the systemic veins. The left atrial appendage (*LAA*) and right atrial appendage (*RAA*) consist of trabeculated myocardium (*brown*). A small area of myocardium at the junction of the LAB to the LAA resembles the right-sided sinus venosus myocardium. (**b**) Schematic representation of different tissue types in the left and right atria as observed from the inside of the atria. Vessel wall tissue (*red*), myocardial tissue with a smooth-walled inner aspect (*blue*), primary atrial segment tissue (*brown*), and sinus venosus-like tissue (*light blue*, between LAA and LAB), which is smooth-walled, lacking vessel wall tissue. *CS*, coronary sinus; *IVC*, inferior caval vein; *SVC*, superior caval vein (Source: Reproduced with permission (Douglas YL, Jongbloed MR, Gittenberger-de Groot AC, Evers D, Dion RA, Voigt P, Bartelings MM, Schalij MJ, Ebels T, DeRuiter MC (2006) Histology of vascular myocardial wall of left atrial body after pulmonary venous incorporation. Am J Cardiol 97:662–670))

atrium, the tricuspid valve, the right ventricle, the pulmonary valve, and the pulmonary circulation. This explains why a systolic murmur is present from excess flow through the pulmonary valve (relative pulmonary stenosis), and a diastolic murmur may be present from excess flow through the tricuspid valve. Long-standing volume load of the RV may lead to a significant tricuspid regurgitation, and so a systolic murmur at the right side of the sternum may be present.

Anything that results in decreased compliance of the right ventricle can alter the direction of flow through the atrial septal defect, such as development of pulmonary hypertension. In this case, the patient may exhibit cyanosis. Cyanosis may also occur in patients with a very large atrial septal defect.

23.3 Clinical Presentation

Most children with an ASD are asymptomatic and come to medical attention because a heart murmur is detected. In fewer than 10% of patients with ASD, symptoms of recurrent pulmonary infections, rarely congestive heart failure, and growth failure can occur in infancy. In adults however, ASDs often become symptomatic with reduced exercise capacity, early onset of atrial arrhythmias usually linked to an older age (such as atrial fibrillation or atrial flutter), clinical signs of pulmonary affections (for example, asthma-like symptoms), pulmonary hypertension, or right heart failure or paradoxical embolism. These symptoms present earlier when additional partial anomalous venous drainage exists.

23.4 Physical Examination

In patients with an ASD, the right ventricular impulse felt along the lower left sternal border or the subxiphoid area may be more forceful than normal (i.e., hyperactivity or right ventricular parasternal heave). The first heart sound will be normal. The second heart sound will be more widely split than normal and does not become single with expiration, the so-called "fixed splitting" of S2. Patients with an ASD usually have a systolic ejection murmur which is best heard along the left sternal border and is loudest at the upper left sternal border. This murmur is created by excessive blood flow through the pulmonary valve (i.e., relative pulmonary stenosis). This murmur is similar to an "innocent pulmonary flow murmur" and probably explains why many patients with ASD are not diagnosed until several years of age. With moderate- and large-size defects, a mid-diastolic murmur can be heard along the lower right or left sternal border. In some patients, this murmur is best heard over the xiphoid. This murmur is created by excessive blood flow through the tricuspid valve.

Patients with ostium primum ASD, in addition to the murmurs described above, may have a murmur of mitral insufficiency because of the cleft in the septal leaflet of the mitral valve associated with this defect.

In older patients, clinical signs of right-sided heart failure, such as enlargement of the liver, edema, and prominent jugular vein pulses, may be evident. In patients with a large ASD or impaired right ventricular compliance (diastolic dysfunction), clinical signs of cyanosis may be visible (low saturation, clubbing).

23.5 Diagnostic Imaging

Echocardiography is the primary method for diagnosing ASD (atrial septal defect) and determining the specific type. Transesophageal echo is typically used in adults with inadequate transthoracic echo windows. This allows for better visualization of the heart structures. Echocardiography also enables the assessment of right atrial and right ventricular enlargement and hypertrophy. Doppler techniques can be employed

to estimate pulmonary artery pressure by evaluating blood flow velocity across the tricuspid and pulmonary valves.

Sinus venosus defects can be challenging to diagnose with transthoracic echocardiography, and transesophageal echocardiography may be required for confirmation, especially in adolescent and adult patients.

Cardiac catheterization is now rarely necessary for ASD diagnosis due to advances in echocardiography. However, it is still crucial in cases of severe pulmonary hypertension. Catheterization allows for the assessment of pulmonary vascular pressure and resistance, including a stepwise test protocol to evaluate the vasoreactivity of elevated pulmonary vascular resistance. Ideally, these investigations should coincide with interventional cardiac catheterization to facilitate the closure of secundum ASDs using devices, eliminating the need for open-heart surgery.

Magnetic resonance imaging (MRI) is useful in adults and teenagers when echocardiography results are inconclusive or when precise measurements of cardiac flow and shunt fraction are required to determine the indication for ASD closure. MRI accurately measures flow, shunt fraction, right ventricle size, and the exact location of the connection of the pulmonary veins.

Computed tomography (CT) scan provides similar anatomical details to MRI and is rarely necessary for ASD diagnosis. It can be considered in patients with contraindications for MRI.

23.6 Treatment

The treatment of ASD is surgical or device closure when there is significant shunt across the septum. This shunt fraction can be assessed indirectly by the amount of right ventricular volume load; therefore, it is commonly agreed that the ASD should be closed when there is evidence of right ventricular enlargement. For secundum ASD, closure can be accomplished surgically by direct suture for small defects or patch closure for larger defects. Currently, device closure using cardiac catheterization techniques is the preferred method to close secundum ASD in appropriately selected patients. The procedural morbidity and mortality as well as the actual procedural costs are clearly in favor of the interventional techniques. In addition, the long-term outcomes of these treatment modalities do not seem to be different to surgical closure.

For ostium primum ASD, patch closure is invariably used, and in most cases, the cleft in the mitral valve leaflet is repaired. For superior sinus venosus ASD, the anomalous drainage of the right upper pulmonary vein is corrected by patch placement and the ASD is closed by the same path. In carefully selected patients, the used of a covered stent may reroute the partial anomalous pulmonary venous return (PAPVR) and close the sinus venosus defect (SVD). Inferior sinus venosus defects are also managed by patch closure. In patients with a coronary sinus defect, surgical correction consists of opening the atrial septum and patch closure of the roof of the coronary sinus followed by closure of the atrial septum.

The usual age for closure of an uncomplicated ASD is before school age, at about 4 years, when the defects are detected early. Otherwise the defects should be closed in the year of detection without any significant delay to reduce the duration of right ventricular volume load. In a rare infant with ASD and clinical signs of heart failure, closure should be performed in infancy and can be performed safely with minimal morbidity.

In patients with significant elevated pulmonary artery pressure or pulmonary vascular resistance, or in those with significant diastolic left ventricular impairment, partial closure of the large ASDs by the use of a surgical patch or dedicated ASD device with fenestration may be an option.

23.7 Outcome

The periprocedural mortality for device or surgical closure of a secundum atrial septal defect in childhood is usually less than 1%, and the long-term outcome is excellent. Patients will only rarely require reoperation for a residual atrial septal defect or to deal with a prior surgical misadventure. In adults, the perioperative morbidity and mortality may be higher due to concomitant diseases such as pulmonary hypertension, overt right heart failure, arrhythmias, diastolic left heart failure, or other problems such as pulmonary disease. Interventional treatment is associated with less risks than surgery.

The periprocedural mortality for closure of an ostium primum atrial septal defect is also low, but there is an 8–10% chance that a future reoperation will be need to deal with mitral insufficiency or left ventricular outflow tract obstruction. Even after successful treatment in infancy, these patients require lifelong follow-up due to the potential risk of atrial arrhythmias caused by atrial scar tissue, right ventricular dysfunction, and pulmonary hypertension in cases of late closure.

Human Genetics of Atrial Septal Defect

24

Lars A. Larsen and Marc-Phillip Hitz

Abstract

Although atrial septal defects (ASD) can be subdivided based on their anatomical location, an essential aspect of human genetics and genetic counseling is distinguishing between isolated and familiar cases without extracardiac features and syndromic cases with the co-occurrence of extracardiac abnormalities, such as developmental delay. Isolated or familial cases tend to show genetic alterations in genes related to important cardiac transcription factors and genes encoding for sarcomeric proteins. By contrast, the spectrum of genes with genetic alterations observed in syndromic cases is diverse. Currently, it points to different pathways and gene networks relevant to the dysregulation of cardiomyogenesis and ASD pathogenesis. Therefore, this chapter reflects the current knowledge and highlights stable associations observed in human genetics studies. It gives an overview of the different types of genetic alterations in these subtypes, including common associations based on genome-wide association studies (GWAS), and it highlights the most frequently observed syndromes associated with ASD pathogenesis.

Keywords

Atrial septal defect · ASD · Patent foramen ovale · PFO · Secundum atrial septal defects · ASD 2 · Primum atrial septal defects · Atrioventricular septum defects ·

L. A. Larsen
Department of Cellular and Molecular Medicine, University of Copenhagen, Copenhagen, Denmark

M.-P. Hitz (✉)
Institute of Medical Genetics, University Medicine Oldenburg, Oldenburg, Germany

Department for Paediatric Cardiology, University Hospital Kiel, Kiel, Germany
e-mail: Hitz.Marc-Phillip@klinikum-oldenburg.de

© The Author(s), under exclusive license to Springer Nature Switzerland AG 2024

S. Rickert-Sperling et al. (eds.), *Congenital Heart Diseases: The Broken Heart*,
Advances in Experimental Medicine and Biology 1441,
https://doi.org/10.1007/978-3-031-44087-8_24

Sinus venosus defects · Sporadic ASD · Familial ASD · Isolated ASD · Syndromic ASD · *NKX2-5* · *GATA4* · *MYH6* · *ACTC1* · *TBX20* · Genome-wide association studies · Holt-Oram syndrome · *TBX5* · TARP syndrome · *RBM10* · Mowat-Wilson syndrome · *ZEB2* · Noonan syndrome · *PTPN11* · Cardio-facio-cutaneous syndrome · *BRAF* · *MAP2K1* · *MAP2K2* · *CDK13* · CHARGE syndrome · *CHD7* · Kabuki syndrome · *KMT2D* · Smith–Lemli–Opitz syndrome · *DHCR7* · Sifrim-Hitz-Weiss syndrome · *CHD4* · *G6PC3* · Rhizomelic chondrodysplasia punctata · *PEX7* · Cardiomyogenesis · endoMT

24.1 Introduction

Atrial septal defect (ASD) is the second most common malformation in congenital heart disease (CHD), occurring in 13% of CHD patients [1]. Anatomically, ASDs can be divided into four types: patent foramen ovale, secundum atrial septal defects (ASD2), primum atrial septal defects (atrioventricular septum defects), and sinus venosus defects [2]. ASD2, the most common type of ASD, is characterized by defects within the fossa ovalis part of the atrial septum.

From a genetic point of view, ASD may present as "sporadic," where no other ASD or CHD cases are known in the family, or in "multiplex families," where at least two family members have ASD or another type of CHD. Most multiplex ASD families are small, with two to three affected individuals [3], but large families with a pronounced monogenic autosomal dominant inheritance pattern have been reported [4–7]. In approximately one-third of multiplex ASD families, the heart malformation of all affected family members is an isolated ASD. In the other two-thirds of multiplex ASD families, one or more family members present with other types of CHD [3]. In particular, Ebstein's anomaly, mitral valve atresia and stenosis, tricuspid valve stenosis, and patent foramen ovale co-occur with ASD in families, suggesting a shared genetic etiology [3].

Genetic analysis of familial cases, sporadic ASD patients, and patients with ASD as part of a well-defined genetic syndrome have led to identifying several genes associated with ASD. In this chapter, we provide an overview of the human genes associated with ASD and outline experimental data, which support the underlying genetic origin and, to some extent, provide functional insight into the pathophysiological mechanisms of ASD.

24.2 Genes Associated with ASD in Isolated CHD

Linkage analysis of multiplex ASD families revealed that mutations of the genes *NKX2-5* (*NK2 homeobox 5*) and *GATA4* (*GATA binding protein 4*) encode cardiac transcription factors. The genes *MYH6* (*myosin heavy chain 6*) and *ACTC1* (*actin alpha cardiac muscle 1*), encoding cardiac sarcomeric proteins, can cause ASD [4–7]. Additional independent family studies have confirmed that rare variants in these

four genes can cause monogenic ASD [8–18], and functional studies in animal models confirm the role of these four genes in heart and ASD development [4, 6, 19–22].

In addition to ASD, mutation of *NKX2-5* and *ACTC1* can cause severe cardiac comorbidities. Familial ASD, caused by rare variants in *NKX2-5*, is often accompanied by cardiac conduction defects and the mutation carriers are at increased risk of sudden death [23, 24]. Recently, late-onset dilated cardiomyopathy was associated with ASD and mutation of *ACTC1* [10].

Three independent studies have reported an association between heterozygous carriers of rare variants in *TBX20* (*T-box transcription factor 20*) and ASD [25–27]. In total, 14 heterozygous carriers were identified in four families. All 14 carriers had heart malformation (CHD and cardiomyopathy). Six of these carriers (43%) presented with ASD. *TBX20* encodes a T-box transcription factor involved in cardiac morphogenesis [28, 29]. In mice, *Tbx20* is expressed in the developing atrial septum, and 16% of $Tbx20^{+/-}/NKX2\text{-}5^{+/-}$ double heterozygous mice present with ASD, while single heterozygotes for both genes are normal [29]. Experiments using mouse models thus suggest a functional interaction between *Nkx2-5* and *Tbx20* during atrial septation and thus support an association between *TBX20* and ASD.

Cordell and colleagues performed a genome-wide association study (GWAS) using a cohort of 340 ASD cases and 5159 controls [30]. They identified an association between the risk of ASD and the markers rs6824295, s16835979, and rs870142, near *MSX1*, *STX18*, and the non-coding RNA *STX18-AS*. The association was replicated in several cohorts of European and Asian ancestry [31–35], but the exact causal gene(s) remains to be identified. Lahm and colleagues recently identified an association between the risk of ASD type II and the markers rs145619574 and rs72917381 located in an intron of *WDR7* and rs187369228 located in an intron of *LEPREL1* [32].

An overview of genes associated with ASD in isolated CHD is shown in Table 24.1.

24.3 Genes Associated with ASD in Syndromic CHD

Mutations in *TBX5* (*T-box transcription factor 5*) cause Holt-Oram syndrome (HOS, OMIM #142900), a rare autosomal dominant disorder characterized by upper limb defects, CHD, and conduction defects [36, 37]. CHD is found in 71/78 (91%) of HOS probands carrying pathogenic variants in *TBX5* [38]. The most prevalent heart malformation in HOS is ASD, found in 48/78 (62%) patients with pathogenic *TBX5* variants. *TBX5* encodes a T-box transcription factor with critical roles in heart development and cardiomyogenesis [39]. TBX5 interacts with NKX2-5 and GATA4 to activate cardiac developmental programs [5, 39, 40], and haploinsufficiency of *Tbx5* causes limb anomalies, conduction defects, and ASD in mice [40]. Thus, functional analyses of *TBX5* support a role in the developing atrial septum.

Table 24.1 Genes associated with isolated ASD. Genes with strong evidence of association are shown in bold

Gene(s)	Genetic evidence[a]	Markers	Experimental evidence	References
NKX2-5	Linkage (LS = 3.9)	D5S1456	Yes	[7, 12, 13, 15, 16]
GATA4	Linkage (LS = 5.7)	D8S264-D8S1827	Yes	[5, 8, 9]
MYH6	Linkage (LS = 4.2)	D14S990	Yes	[4, 14, 17]
ACTC1	Linkage (LS = 4.8)	*ACTC1*	Yes	[6, 10, 11]
TBX20	Segregation[b]	n/a	Yes	[25–27]
MSX1, *STX18*, *STX18-AS*	Association ($P = 9.5 \times 10^{-7}$)	rs870142	No	[30–35]
WDR7	Association ($P = 2.6 \times 10^{-8}$)	rs145619574	No	[32]
LEPREL1	Association ($P = 1.7 \times 10^{-8}$)	rs187369228	No	[32]

[a] Evidence in the form of LOD score (LS) or *P*-value
[b] Three independent reports of segregation in small families

TARP syndrome (TARPS, OMIM #311900) is a rare X-linked recessive disorder characterized by Atrial septal defect, Talipes equinovarus, Robin sequence, and Persistent left superior vena cava (PLSVC). TARPS is caused by mutation of *RBM10* (*RNA binding motif protein 10*) [41]. More than 90% of TARPS patients have CHD. The most common heart malformations are ASD and PLSVC, which are observed in 13/23 (57%) and 11/20 (55%) of patients, respectively [42]. *RBM10* encodes an RNA binding protein regulating alternative splicing [43]. A role of RBM10 in heart development has not been established.

Mowat-Wilson syndrome (MOWS, OMIM #235730) is characterized by a distinctive facial appearance, moderate to severe intellectual disability (ID), microcephaly, seizures, Hirschsprung disease, and several congenital anomalies, including CHD, which is found in 61% (52/85) of patients [44, 45]. The most prevalent heart malformations in MOWS patients are PDA (30%), VSD (27%), ASD (26%), and PS (20%), but a diverse spectrum of heart malformations have been observed [44]. MOWS is caused by haploinsufficiency of *ZEB2* (*zinc finger E-box binding homeobox 2*) [46, 47]. *ZEB2* encodes a multifunctional zinc-finger E-box transcription factor, which can interact with Smad proteins to regulate BMP/TGFβ signaling and with the corepressor CtBP to repress transcription [48–50]. ZEB2 is a driver of epithelial-mesenchymal transition (EMT) [51, 52]. BMP/TGFβ signaling forms the mesenchymal cap on the leading edge of the primary atrial septum, possibly by the regulation of endothelial-mesenchymal transition (endoMT) [53]. Given the role of ZEB2 in EMT, it is tempting to speculate that ZEB2 may be involved in the regulation of the formation of the mesenchymal cap and that haploinsufficiency of *ZEB2* could cause ASD by dysregulation of this process. However, more research is needed to evaluate the exact functional role of ZEB2 in ASD.

Noonan syndrome (NS, OMIM #163950) is an autosomal dominant inherited disorder that affects 1 in 1000–2500 live births [54]. NS is a multisystem disorder with variable degrees of clinical characteristics, including distinctive facial features, developmental delay, short stature, skeletal malformations, cardiac malformations, and hypertrophic cardiomyopathy (HCM). CHD is observed in more than 80% of NS patients, with valvar pulmonary stenosis being the most common malformation (57%), followed by ASD (32%) [55]. NS is caused by mutations in genes involved in RAS-mitogen activated protein kinase (MAPK) signaling [54]. Approximately 50% of NS patients are heterozygotes for gain-of-function mutations in *PTPN11* (*protein tyrosine phosphatase non-receptor type 11*) [56, 57], and a significant genotype-phenotype association between *PTPN11* and ASD has been established [55]. *PTPN11* encodes the protein tyrosine phosphatase SHP2. Analysis of knock-in mice for NS-associated *Ptpn11* mutations suggests that most NS's cardiac defects are caused by enhanced activation of RAS-MAPK signaling in the endocardium, leading to dysregulated endoMT in the endocardial cushions [58]. The mechanism of ASD in NS remains unresolved, but considering the role of NS genes in endoMT in the endocardial cushions, a possible role in establishing the mesenchymal cap could be speculated.

Cardio-facio-cutaneous syndrome (CFC, #115150) is a distinct syndrome with many features overlapping with Noonan syndrome [59]. Approximately 75% of CFC patients have structural heart disease, often in the form of PVS [59]. Between 18% and 33% of patients have septum defects, most commonly ASDs [60, 61]. CFC is caused by mutation of *BRAF*, *MAP2K1* (*MEK1*), and *MAP2K2* (*MEK2*), which cause dysregulation of the RAS-MAPK pathway; thus, we find it likely that the pathophysiological mechanism of ASD in CFC patients may be similar to the mechanism in Noonan syndrome.

Exome sequencing of a large cohort of CHD patients led to the identification of a small group of patients presenting with CHD in addition to extra-cardiac manifestations (distinctive facial features, developmental delay, and microcephaly), with rare de novo variants in *CDK13* (*cyclin-dependent kinase 13*) [62]. Recent studies have confirmed that mutation of *CDK13* is associated cause congenital heart disease, dysmorphic facial features, and intellectual developmental disorder (CHDFIDD, OMIM #617360), also known as CDK13-related disorder (CDK13-RD) [63–65]. Forty-six percent (18/51) of CDK13-RD patients have CHD. The most common cardiac malformation is ASD, which is found in 31% (18/58) of patients, followed by pulmonary artery stenosis (14%) and VSD (9%) [64]. A recently developed hypomorphic mouse model with targeted deletion of *Cdk13* shows that the gene is essential for normal craniofacial development and development of the heart, lung, liver, kidneys, and brain [66]. Homozygous deletion of *Cdk13* is embryonic lethal and results in developmental delay. The hearts of homozygous mutant mice have reduced and non-compact myocardium and exhibit dramatic heart failure at E14.5-E15.5, suggesting that CDK13 is necessary for myocardial development. CDK13 is involved in regulating the elongation rate and processivity of RNA polymerase II and modulates the selection of transcription termination sites [67]; thus, we find it likely that mutation of *CDK13* results in dysregulated expression of

specific genes involved in cardiomyogenesis, but this hypothesis remains to be shown.

CHARGE syndrome (CHS, OMIM #214800), also known as *CHD7* disorder, is characterized by a variable combination of congenital malformations. The acronym CHARGE is generated from the phenotypes ocular coloboma (C), heart defects (H), atresia of the choanae (A), retardation of growth (R), genital hypoplasia (G), and ear abnormalities (E) of which CAE together with cranial nerve anomalies are defined as major diagnostic criteria. In addition, the clinical spectrum may include a range of additional anomalies [68]. Three-fourths (74%) of CHS patients present with cardiac malformation, of which conotruncal anomalies are the most prevalent subtypes. Nevertheless, 15% (31/202) of cardiac malformations observed in patients are ASD [69]. CHS is caused by mutation of *CHD7* (*chromodomain helicase DNA binding protein 7*), which encodes an ATP-dependent helicase involved in chromatin remodeling [70]. A recent study using a conditional mouse model with targeted deletion of *CHD7*, specifically in neural crest cells (NCC), strongly implicates that CHD7 regulates cardiac NCC development and that dysregulation of these processes causes conotruncal defects in CHS patients [71]. Another mechanism must be responsible for the ASDs observed in a smaller proportion of patients since NCC does not appear to contribute to the development of the atrial septum [72]. However, Liu and colleagues identified an interaction between CHD7 and BMP signaling mediators SMAD1/5/8. They showed that depletion of CHD7 negatively affects the expression of the SMAD target gene *Nkx2-5* in cardiomyocytes in vitro and in vivo [73]. Considering that *NKX2-5* is a well-known ASD disease gene, it is tempting to speculate that dysregulation of *Nkx2-5* could cause ASD in CHS patients.

Kabuki syndrome (KS, OMIM #147920) is a rare multisystem disorder with variable clinical features, including distinctive facial features, postnatal growth retardation, mild-to-moderate ID, skeletal abnormalities, and organ dysfunction malformations. CHD is found in 40–70% of KS patients, with a wide spectrum of malformation types [74, 75]. A recent study reported ASD in 16% (3/19) of KS cases with CHD [75]. The majority of KS is caused by haploinsufficiency of *KMT2D* (*lysine methyltransferase 2D*) and *KDM6A* (*lysine-specific demethylase 6A*) [76, 77]. *KMT2D* encodes a H3K4 methyltransferase, while *KDM6A* encodes a H3K27 demethylase. Both proteins are part of the KMT2D COMPASS-like complex, which plays a significant role in the de novo activation of enhancers during cellular differentiation [78]. KMT2D is expressed in cardiomyocytes and endocardial cells within the developing heart [79]. Conditional deletion of *Kmt2d* in cardiac progenitors (ΔCP) and cardiomyocytes (ΔCM) causes disorganized ventricular septum and thin, compact myocardium (only ΔCM) [79]. Further analysis of mutant mice suggested that loss of *Kmt2d* causes dysregulation of ion transport genes, calcium signaling, hypoxia signaling, and cell cycle regulation in the developing heart, concomitant with changes in the H3K4 methylation level in a subset of dysregulated genes [79]. In summary, experimental studies in mouse models support the role of KMT2D as a critical regulator of transcriptional programs during cardiogenesis, but the specific role in atrial septation is currently unknown.

Mutation of *DHCR7* (*7-dehydrocholesterol reductase*) cause Smith–Lemli–Opitz syndrome (SLOS; OMIM #270400) [80–82]. SLOS is an autosomal recessive variable multisystem disorder characterized by distinctive facial features, growth retardation, moderate-to-severe ID, autism, and multiple congenital malformations, including microcephaly, cleft palate, digit malformations, and CHD [83]. A wide range of cardiac malformations are observed in 44% (95/215) of patients, with atrioventricular canal defects (27%), ASD (21%), and PDA (16%) being the most common subtypes [84]. The role of DHCR7 in heart development and the pathophysiological mechanism of DHCR7 deficiency in CHD are currently unknown.

Sifrim-Hitz-Weiss syndrome (SHWS, OMIM #617159) is a neurodevelopmental disorder characterized by mild-to-moderate ID, speech and motor delay [85]. Patients may also present with a range of additional defects, including abnormalities of the eyes, heart, ears, gonads, skeletal, and limbs [86]. CHD is found in 65% (19/29) of patients. Many cardiac malformations have been identified in patients with ASD as the most common malformation identified in 58% (11/19) of patients with CHD [86]. SHWS is caused by de novo variants in CHD4 (chromodomain helicase DNA binding protein 4) [62]. CHD4 encodes a core subunit of the ATP-dependent chromatin remodeling complex NuRD [87]. NuRD complexes play significant roles in controlling gene transcription programs during human development [88]. Analysis of mouse models with conditional deletion of *Chd4* in cardiomyocytes shows that CHD4 regulates the expression of sarcomere genes in the developing heart and that CHD4 is critical for the assembly of cardiac myofibrils and the development of the myocardium [89].

G6PC3 deficiency (G6D, OMIM #612541) is a rare autosomal recessive disorder characterized by severe congenital neutropenia, accompanied by a wide spectrum of comorbidities, including cardiovascular, urogenital, skeletal, and thymic anomalies [90]. Congenital heart diseases are found in 77% (44/57) of patients, with ASD as the predominant malformation, observed in 84% (37/44) of the patients with CHD. G6D is caused by variants in *G6PC3* (*glucose-6-phosphatase catalytic subunit 3*), abolishing the enzymatic activity of glucose-6-phosphatase [91]. The pathophysiological mechanism that causes ASD in G6D patients is currently unknown.

Rhizomelic chondrodysplasia punctata (RCDP, OMIM #215100) is a rare autosomal recessive syndrome characterized by skeletal abnormalities, cataracts, growth retardation, and ID [92]. Two recent studies have revealed that CHD is found more often in RCDP than previously anticipated [93, 94]. In a population of 32 RCP patients with available cardiac data, CHD was observed in 21 individuals (65%). ASD was the most prevalent cardiac malformation found in 66% (14/21) of patients with CHD. Rare variants in *PEX7* (*peroxisomal biogenesis factor 7*) were causative in 13/14 (93%) of RCDP cases with ASD. Peroxisomes are subcellular organelles with essential metabolic functions [95], but the pathophysiological mechanism that causes ASD in RCDP patients is currently unknown.

An overview of genes associated with ASD in syndromic CHD is shown in Table 24.2.

Table 24.2 Genes associated with ASD in syndromic CHD. Only genes where ASD is found in more than 10% of CHD patients are included

Gene(s)	Syndrome	CHD prevalence	ASD prevalence	References
G6PD	G6PC3 deficiency	77% (44/57)	84% (37/44)	[90]
PEX7	Rhizomelic chondrodysplasia punctata	65% (21/32)	66% (14/21)	[94, 95]
TBX5	Holt-Oram	91% (71/78)	62% (48/78)	[36–38]
CHD4	Sifrim-Hitz-Weiss syndrome	65% (19/29)	58% (11/19)	[86]
RBM10	TARP syndrome	92% (22/24)	57% (13/23)	[41, 42]
PTPN11,[a] *CBL*, *LZTR1*, *KRAS*, *NRAS*, *RRAS*, *RAF1*, *RIT1*, *PPP1CB*, *SOS1*, *SOS2*, *RASA2* *SHOC2*	Noonan syndrome	81% (237/293)	32% (94/237)[b]	[54–57]
BRAF, *MEK1*, *MEK2*	Cardio-facio-cutaneous syndrome	75%	18–33%	[59–61]
CDK13	CDK13-related disorder	46% (18/51)	31% (18/58)	[62–65]
ZEB2	Mowat-Wilson syndrome	61% (52/85)	26% (21/82)	[44–46]
DHCR7	Smith-Lemli-Opitz syndrome	44% (95/215)	21% (19/91)[b]	[84]
DHCR7	Smith–Lemli–Opitz syndrome	44% (95/215)	21% (19/91)	[84]
KMT2D, *KMD6A*	Kabuki syndrome	40–70%	16% (3/19)[b]	[74, 75]
CHD7	CHARGE association	74% (220/299)	15% (31/202)[b]	[69]

[a] *PTPN11* genotypes are significantly associated with ASD ($P = 0.001$)
[b] Prevalence among patients with CHD

24.4 Conclusion and Future Directions

A large proportion of the genes associated with ASD encodes proteins involved in the development of the myocardium, suggesting that dysregulation of cardiomyogenesis is a major pathophysiological factor in ASD. In addition, a few ASD disease genes encode proteins involved in endoMT, which could suggest that defects of the mesenchymal cap are another factor.

The number of known ASD disease genes is currently relatively low. To gain deeper insight into the genetic and molecular mechanisms involved in human ASD

pathogenesis, identification of additional disease genes and a thorough understanding of these interplay during critical time points during ASD pathogenesis is necessary. The majority of known disease genes are associated with syndromes, where ASD is part of the clinical spectrum; thus, genetic analyses of cohorts of patients with isolated ASD, combined with functional analyses in experimental models, are warranted.

References

1. van der Linde D, Konings EE, Slager MA, Witsenburg M, Helbing WA, Takkenberg JJ, Roos-Hesselink JW. Birth prevalence of congenital heart disease worldwide: a systematic review and meta-analysis. J Am Coll Cardiol. 2011;58:2241–7.
2. Geva T, Martins JD, Wald RM. Atrial septal defects. Lancet. 2014;383:1921–32.
3. Ellesøe SG, Workman CT, Bouvagnet P, Loffredo CA, McBride KL, Hinton RB, van Engelen K, Gertsen EC, Mulder BJM, Postma AV, et al. Familial co-occurrence of congenital heart defects follows distinct patterns. Eur Heart J. 2018;39:1015–22.
4. Ching YH, Ghosh TK, Cross SJ, Packham EA, Honeyman L, Loughna S, Robinson TE, Dearlove AM, Ribas G, Bonser AJ, et al. Mutation in myosin heavy chain 6 causes atrial septal defect. Nat Genet. 2005;37:423–8.
5. Garg V, Kathiriya IS, Barnes R, Schluterman MK, King IN, Butler CA, Rothrock CR, Eapen RS, Hirayama-Yamada K, Joo K, et al. GATA4 mutations cause human congenital heart defects and reveal an interaction with TBX5. Nature. 2003;424:443–7.
6. Matsson H, Eason J, Bookwalter CS, Klar J, Gustavsson P, Sunnegardh J, Enell H, Jonzon A, Vikkula M, Gutierrez I, et al. Alpha-cardiac actin mutations produce atrial septal defects. Hum Mol Genet. 2008;17:256–65.
7. Schott JJ, Benson DW, Basson CT, Pease W, Silberbach GM, Moak JP, Maron BJ, Seidman CE, Seidman JG. Congenital heart disease caused by mutations in the transcription factor NKX2-5. Science. 1998;281:108–11.
8. Chen J, Qi B, Zhao J, Liu W, Duan R, Zhang M. A novel mutation of GATA4 (K300T) associated with familial atrial septal defect. Gene. 2016;575:473–7.
9. Chen Y, Han ZQ, Yan WD, Tang CZ, Xie JY, Chen H, Hu DY. A novel mutation in GATA4 gene associated with dominant inherited familial atrial septal defect. J Thorac Cardiovasc Surg. 2010;140:684–7.
10. Frank D, Yusuf Rangrez A, Friedrich C, Dittmann S, Stallmeyer B, Yadav P, Bernt A, Schulze-Bahr E, Borlepawar A, Zimmermann WH, et al. Cardiac alpha-Actin (ACTC1) gene mutation causes atrial-septal defects associated with late-onset dilated cardiomyopathy. Circ Genom Precis Med. 2019;12:e002491.
11. Greenway SC, McLeod R, Hume S, Roslin NM, Alvarez N, Giuffre M, Zhan SH, Shen Y, Preuss C, Andelfinger G, et al. Exome sequencing identifies a novel variant in ACTC1 associated with familial atrial septal defect. Can J Cardiol. 2014;30:181–7.
12. Gutierrez-Roelens I, De Roy L, Ovaert C, Sluysmans T, Devriendt K, Brunner HG, Vikkula M. A novel CSX/NKX2-5 mutation causes autosomal-dominant AV block: are atrial fibrillation and syncopes part of the phenotype? Eur J Hum Genet. 2006;14:1313–6.
13. Gutierrez-Roelens I, Sluysmans T, Gewillig M, Devriendt K, Vikkula M. Progressive AV-block and anomalous venous return among cardiac anomalies associated with two novel missense mutations in the CSX/NKX2-5 gene. Hum Mutat. 2002;20:75–6.
14. Huang S, Wu Y, Chen S, Yang Y, Wang Y, Wang H, Li P, Zhuang J, Xia Y. Novel insertion mutation (Arg1822_Glu1823dup) in MYH6 coiled-coil domain causing familial atrial septal defect. Eur J Med Genet. 2021;64:104314.
15. Pabst S, Wollnik B, Rohmann E, Hintz Y, Glänzer K, Vetter H, Nickenig G, Grohé C. A novel stop mutation truncating critical regions of the cardiac transcription factor NKX2-5 in a large

family with autosomal-dominant inherited congenital heart disease. Clin Res Cardiol. 2008;97:39–42.
16. Perera JL, Johnson NM, Judge DP, Crosson JE. Novel and highly lethal NKX2.5 missense mutation in a family with sudden death and ventricular arrhythmia. Pediatr Cardiol. 2014;35:1206–12.
17. Posch MG, Waldmuller S, Muller M, Scheffold T, Fournier D, Andrade-Navarro MA, De Geeter B, Guillaumont S, Dauphin C, Yousseff D, et al. Cardiac alpha-myosin (MYH6) is the predominant sarcomeric disease gene for familial atrial septal defects. PLoS One. 2011;6:e28872.
18. Zhang X, Wang J, Wang B, Chen S, Fu Q, Sun K. A novel missense mutation of GATA4 in a Chinese family with congenital heart disease. PLoS One. 2016;11:e0158904.
19. Nakashima Y, Yanez DA, Touma M, Nakano H, Jaroszewicz A, Jordan MC, Pellegrini M, Roos KP, Nakano A. Nkx2-5 suppresses the proliferation of atrial myocytes and conduction system. Circ Res. 2014;114:1103–13.
20. Rajagopal SK, Ma Q, Obler D, Shen J, Manichaikul A, Tomita-Mitchell A, Boardman K, Briggs C, Garg V, Srivastava D, et al. Spectrum of heart disease associated with murine and human GATA4 mutation. J Mol Cell Cardiol. 2007;43:677–85.
21. Tanaka M, Chen Z, Bartunkova S, Yamasaki N, Izumo S. The cardiac homeobox gene Csx/Nkx2.5 lies genetically upstream of multiple genes essential for heart development. Development. 1999;126:1269–80.
22. Zakariyah AF, Rajgara RF, Veinot JP, Skerjanc IS, Burgon PG. Congenital heart defect causing mutation in Nkx2.5 displays in vivo functional deficit. J Mol Cell Cardiol. 2017;105:89–98.
23. Abou Hassan OK, Fahed AC, Batrawi M, Arabi M, Refaat MM, DePalma SR, Seidman JG, Seidman CE, Bitar FF, Nemer GM. NKX2-5 mutations in an inbred consanguineous population: genetic and phenotypic diversity. Sci Rep. 2015;5:8848.
24. Ellesoe SG, Johansen MM, Bjerre JV, Hjortdal VE, Brunak S, Larsen LA. Familial atrial septal defect and sudden cardiac death: identification of a novel NKX2-5 mutation and a review of the literature. Congenit Heart Dis. 2016;11:283–90.
25. Kirk EP, Sunde M, Costa MW, Rankin SA, Wolstein O, Castro ML, Butler TL, Hyun C, Guo G, Otway R, et al. Mutations in cardiac T-box factor gene TBX20 are associated with diverse cardiac pathologies, including defects of septation and valvulogenesis and cardiomyopathy. Am J Hum Genet. 2007;81:280–91.
26. Posch MG, Gramlich M, Sunde M, Schmitt KR, Lee SH, Richter S, Kersten A, Perrot A, Panek AN, Al-Khatib IH, et al. A gain-of-function TBX20 mutation causes congenital atrial septal defects, patent foramen ovale and cardiac valve defects. J Med Genet. 2010;47:230–5.
27. Zhou YM, Dai XY, Huang RT, Xue S, Xu YJ, Qiu XB, Yang YQ. A novel TBX20 lossoffunction mutation contributes to adult-onset dilated cardiomyopathy or congenital atrial septal defect. Mol Med Rep. 2016;14:3307–14.
28. Singh MK, Christoffels VM, Dias JM, Trowe MO, Petry M, Schuster-Gossler K, Bürger A, Ericson J, Kispert A. Tbx20 is essential for cardiac chamber differentiation and repression of Tbx2. Development. 2005;132:2697–707.
29. Stennard FA, Costa MW, Lai D, Biben C, Furtado MB, Solloway MJ, McCulley DJ, Leimena C, Preis JI, Dunwoodie SL, et al. Murine T-box transcription factor Tbx20 acts as a repressor during heart development, and is essential for adult heart integrity, function and adaptation. Development. 2005;132:2451–62.
30. Cordell HJ, Bentham J, Topf A, Zelenika D, Heath S, Mamasoula C, Cosgrove C, Blue G, Granados-Riveron J, Setchfield K, et al. Genome-wide association study of multiple congenital heart disease phenotypes identifies a susceptibility locus for atrial septal defect at chromosome 4p16. Nat Genet. 2013;45:822–4.
31. Córdova-Palomera A, Priest JR. Association between the 4p16 genomic locus and different types of congenital heart disease: results from adult survivors in the UK Biobank. Sci Rep. 2019;9:16515.

32. Lahm H, Jia M, Dreßen M, Wirth F, Puluca N, Gilsbach R, Keavney BD, Cleuziou J, Beck N, Bondareva O, et al. Congenital heart disease risk loci identified by genome-wide association study in European patients. J Clin Invest. 2021;131
33. Pei K, Huang Q, Zhang G, Lu C, Yu B, Yang L. Association between the 4p16 susceptibility locus and the risk of atrial septal defect in population from southeast China. Pediatr Cardiol. 2016;37:120–4.
34. Zhao B, Lin Y, Xu J, Ni B, Da M, Ding C, Hu Y, Zhang K, Yang S, Wang X, et al. Replication of the 4p16 susceptibility locus in congenital heart disease in Han Chinese populations. PLoS One. 2014;9:e107411.
35. Zhao L, Li B, Dian K, Ying B, Lu X, Hu X, An Q, Chen C, Huang C, Tan B, et al. Association between the European GWAS-identified susceptibility locus at chromosome 4p16 and the risk of atrial septal defect: a case-control study in Southwest China and a meta-analysis. PLoS One. 2015;10:e0123959.
36. Basson CT, Bachinsky DR, Lin RC, Levi T, Elkins JA, Soults J, Grayzel D, Kroumpouzou E, Traill TA, Leblanc-Straceski J, et al. Mutations in human TBX5 [corrected] cause limb and cardiac malformation in Holt-Oram syndrome. Nat Genet. 1997;15:30–5.
37. Li QY, Newbury-Ecob RA, Terrett JA, Wilson DI, Curtis AR, Yi CH, Gebuhr T, Bullen PJ, Robson SC, Strachan T, et al. Holt-Oram syndrome is caused by mutations in TBX5, a member of the Brachyury (T) gene family. Nat Genet. 1997;15:21–9.
38. Vanlerberghe C, Jourdain AS, Ghoumid J, Frenois F, Mezel A, Vaksmann G, Lenne B, Delobel B, Porchet N, Cormier-Daire V, et al. Holt-Oram syndrome: clinical and molecular description of 78 patients with TBX5 variants. Eur J Hum Genet. 2019;27:360–8.
39. Steimle JD, Moskowitz IP. TBX5: a key regulator of heart development. Curr Top Dev Biol. 2017;122:195–221.
40. Bruneau BG, Nemer G, Schmitt JP, Charron F, Robitaille L, Caron S, Conner DA, Gessler M, Nemer M, Seidman CE, et al. A murine model of Holt-Oram syndrome defines roles of the T-box transcription factor Tbx5 in cardiogenesis and disease. Cell. 2001;106:709–21.
41. Johnston JJ, Teer JK, Cherukuri PF, Hansen NF, Loftus SK, Chong K, Mullikin JC, Biesecker LG. Massively parallel sequencing of exons on the X chromosome identifies RBM10 as the gene that causes a syndromic form of cleft palate. Am J Hum Genet. 2010;86:743–8.
42. Kump's C, D'Haenens E, Vergult S, Lee J, van Coster R, Jansen A, Devriendt K, Oostra A, Vanakker OM. Phenotypic spectrum of the RBM10-mediated intellectual disability and congenital malformation syndrome beyond classic TARP syndrome features. Clin Genet. 2021;99:449–56.
43. Inoue A. RBM10: structure, functions, and associated diseases. Gene. 2021;783:145463.
44. Ivanovski I, Djuric O, Caraffi SG, Santodirocco D, Pollazzon M, Rosato S, Cordelli DM, Abdalla E, Accorsi P, Adam MP, et al. Phenotype and genotype of 87 patients with Mowat-Wilson syndrome and recommendations for care. Genet Med. 2018;20:965–75.
45. Mowat DR, Croaker GD, Cass DT, Kerr BA, Chaitow J, Adès LC, Chia NL, Wilson MJ. Hirschsprung disease, microcephaly, mental retardation, and characteristic facial features: delineation of a new syndrome and identification of a locus at chromosome 2q22-q23. J Med Genet. 1998;35:617–23.
46. Cacheux V, Dastot-Le Moal F, Kääriäinen H, Bondurand N, Rintala R, Boissier B, Wilson M, Mowat D, Goossens M. Loss-of-function mutations in SIP1 Smad interacting protein 1 result in a syndromic Hirschsprung disease. Hum Mol Genet. 2001;10:1503–10.
47. Wakamatsu N, Yamada Y, Yamada K, Ono T, Nomura N, Taniguchi H, Kitoh H, Mutoh N, Yamanaka T, Mushiake K, et al. Mutations in SIP1, encoding Smad interacting protein-1, cause a form of Hirschsprung disease. Nat Genet. 2001;27:369–70.
48. Postigo AA, Dean DC. ZEB represses transcription through interaction with the corepressor CtBP. Proc Natl Acad Sci U S A. 1999;96:6683–8.
49. Postigo AA, Depp JL, Taylor JJ, Kroll KL. Regulation of Smad signaling through a differential recruitment of coactivators and corepressors by ZEB proteins. Embo J. 2003;22:2453–62.

50. Verschueren K, Remacle JE, Collart C, Kraft H, Baker BS, Tylzanowski P, Nelles L, Wuytens G, Su MT, Bodmer R, et al. SIP1, a novel zinc finger/homeodomain repressor, interacts with Smad proteins and binds to 5'-CACCT sequences in candidate target genes. J Biol Chem. 1999;274:20489–98.
51. Comijn J, Berx G, Vermassen P, Verschueren K, van Grunsven L, Bruyneel E, Mareel M, Huylebroeck D, van Roy F. The two-handed E box binding zinc finger protein SIP1 downregulates E-cadherin and induces invasion. Mol Cell. 2001;7:1267–78.
52. Vandewalle C, Comijn J, De Craene B, Vermassen P, Bruyneel E, Andersen H, Tulchinsky E, Van Roy F, Berx G. SIP1/ZEB2 induces EMT by repressing genes of different epithelial cell-cell junctions. Nucleic Acids Res. 2005;33:6566–78.
53. Deepe R, Fitzgerald E, Wolters R, Drummond J, Guzman K, Hoff M, Wessels A. The mesenchymal cap of the atrial septum and atrial and atrioventricular septation. J Cardiovasc Dev Dis. 2020;7
54. Roberts AE, Allanson JE, Tartaglia M, Gelb BD. Noonan syndrome. Lancet. 2013;381:333–42.
55. Prendiville TW, Gauvreau K, Tworog-Dube E, Patkin L, Kucherlapati RS, Roberts AE, Lacro RV. Cardiovascular disease in Noonan syndrome. Arch Dis Child. 2014;99:629–34.
56. Tartaglia M, Mehler EL, Goldberg R, Zampino G, Brunner HG, Kremer H, van der Burgt I, Crosby AH, Ion A, Jeffery S, et al. Mutations in PTPN11, encoding the protein tyrosine phosphatase SHP-2, cause Noonan syndrome. Nat Genet. 2001;29:465–8.
57. Tartaglia M, Kalidas K, Shaw A, Song X, Musat DL, van der Burgt I, Brunner HG, Bertola DR, Crosby A, Ion A, et al. PTPN11 mutations in Noonan syndrome: molecular spectrum, genotype-phenotype correlation, and phenotypic heterogeneity. Am J Hum Genet. 2002;70:1555–63.
58. Araki T, Chan G, Newbigging S, Morikawa L, Bronson RT, Neel BG. Noonan syndrome cardiac defects are caused by PTPN11 acting in endocardium to enhance endocardial-mesenchymal transformation. Proc Natl Acad Sci U S A. 2009;106:4736–41.
59. Pierpont ME, Magoulas PL, Adi S, Kavamura MI, Neri G, Noonan J, Pierpont EI, Reinker K, Roberts AE, Shankar S, et al. Cardio-facio-cutaneous syndrome: clinical features, diagnosis, and management guidelines. Pediatrics. 2014;134:e1149–62.
60. Dentici ML, Sarkozy A, Pantaleoni F, Carta C, Lepri F, Ferese R, Cordeddu V, Martinelli S, Briuglia S, Digilio MC, et al. Spectrum of MEK1 and MEK2 gene mutations in cardio-facio-cutaneous syndrome and genotype-phenotype correlations. Eur J Hum Genet. 2009;17:733–40.
61. Lee Y, Choi Y, Seo GH, Kim GH, Choi IH, Keum C, Ko JM, Cheon CK, Jeon J, Choi JH, et al. Clinical and molecular spectra of BRAF-associated RASopathy. J Hum Genet. 2021;66:389–99.
62. Sifrim A, Hitz MP, Wilsdon A, Breckpot J, Turki SH, Thienpont B, McRae J, Fitzgerald TW, Singh T, Swaminathan GJ, et al. Distinct genetic architectures for syndromic and nonsyndromic congenital heart defects identified by exome sequencing. Nat Genet. 2016;48:1060–5.
63. Bostwick BL, McLean S, Posey JE, Streff HE, Gripp KW, Blesson A, Powell-Hamilton N, Tusi J, Stevenson DA, Farrelly E, et al. Phenotypic and molecular characterization of CDK13-related congenital heart defects, dysmorphic facial features and intellectual developmental disorders. Genome Med. 2017;9:73.
64. Rouxel F, Relator R, Kerkhof J, McConkey H, Levy M, Dias P, Barat-Houari M, Bednarek N, Boute O, Chatron N, et al. CDK13-related disorder: report of a series of 18 previously unpublished individuals and description of an epigenetic signature. Genet Med. 2022.
65. van den Akker WMR, Brummelman I, Martis LM, Timmermans RN, Pfundt R, Kleefstra T, Willemsen MH, Gerkes EH, Herkert JC, van Essen AJ, et al. De novo variants in CDK13 associated with syndromic ID/DD: molecular and clinical delineation of 15 individuals and a further review. Clin Genet. 2018;93:1000–7.
66. Nováková M, Hampl M, Vrábel D, Procházka J, Petrezselyová S, Procházková M, Sedláček R, Kavková M, Zikmund T, Kaiser J, et al. Mouse model of congenital heart defects, dysmorphic facial features and intellectual developmental disorders as a result of non-functional CDK13. Front Cell Dev Biol. 2019;7:155.

67. Fan Z, Devlin JR, Hogg SJ, Doyle MA, Harrison PF, Todorovski I, Cluse LA, Knight DA, Sandow JJ, Gregory G, et al. CDK13 cooperates with CDK12 to control global RNA polymerase II processivity. Sci Adv. 2020;6
68. Meisner JK, Martin DM. Congenital heart defects in CHARGE: the molecular role of CHD7 and effects on cardiac phenotype and clinical outcomes. Am J Med Genet C Semin Med Genet. 2020;184:81–9.
69. Corsten-Janssen N, Kerstjens-Frederikse WS, du Marchie Sarvaas GJ, Baardman ME, Bakker MK, Bergman JE, Hove HD, Heimdal KR, Rustad CF, Hennekam RC, et al. The cardiac phenotype in patients with a CHD7 mutation. Circ Cardiovasc Genet. 2013;6:248–54.
70. Vissers LE, van Ravenswaaij CM, Admiraal R, Hurst JA, de Vries BB, Janssen IM, van der Vliet WA, Huys EH, de Jong PJ, Hamel BC, et al. Mutations in a new member of the chromodomain gene family cause CHARGE syndrome. Nat Genet. 2004;36:955–7.
71. Yan S, Thienthanasit R, Chen D, Engelen E, Brühl J, Crossman DK, Kesterson R, Wang Q, Bouazoune K, Jiao K. CHD7 regulates cardiovascular development through ATP-dependent and -independent activities. Proc Natl Acad Sci U S A. 2020;117:28847–58.
72. Erhardt S, Zheng M, Zhao X, Le TP, Findley TO, Wang J. The cardiac neural crest cells in heart development and congenital heart defects. J Cardiovasc Dev Dis. 2021;8
73. Liu Y, Harmelink C, Peng Y, Chen Y, Wang Q, Jiao K. CHD7 interacts with BMP R-SMADs to epigenetically regulate cardiogenesis in mice. Hum Mol Genet. 2014;23:2145–56.
74. Bogershausen N, Gatinois V, Riehmer V, Kayserili H, Becker J, Thoenes M, Simsek-Kiper PO, Barat-Houari M, Elcioglu NH, Wieczorek D, et al. Mutation update for Kabuki syndrome genes KMT2D and KDM6A and further delineation of X-linked Kabuki syndrome subtype 2. Hum Mutat. 2016;37:847–64.
75. Digilio MC, Gnazzo M, Lepri F, Dentici ML, Pisaneschi E, Baban A, Passarelli C, Capolino R, Angioni A, Novelli A, et al. Congenital heart defects in molecularly proven Kabuki syndrome patients. Am J Med Genet A. 2017;173:2912–22.
76. Miyake N, Koshimizu E, Okamoto N, Mizuno S, Ogata T, Nagai T, Kosho T, Ohashi H, Kato M, Sasaki G, et al. MLL2 and KDM6A mutations in patients with Kabuki syndrome. Am J Med Genet A. 2013;161a:2234–43.
77. Lederer D, Grisart B, Digilio MC, Benoit V, Crespin M, Ghariani SC, Maystadt I, Dallapiccola B, Verellen-Dumoulin C. Deletion of KDM6A, a histone demethylase interacting with MLL2, in three patients with Kabuki syndrome. Am J Hum Genet. 2012;90:119–24.
78. Lavery WJ, Barski A, Wiley S, Schorry EK, Lindsley AW. KMT2C/D COMPASS complex-associated diseases [K(CD)COM-ADs]: an emerging class of congenital regulopathies. Clin Epigenetics. 2020;12:10.
79. Ang SY, Uebersohn A, Spencer CI, Huang Y, Lee JE, Ge K, Bruneau BG. KMT2D regulates specific programs in heart development via histone H3 lysine 4 di-methylation. Development. 2016;143:810–21.
80. Waterham HR, Wijburg FA, Hennekam RC, Vreken P, Poll-The BT, Dorland L, Duran M, Jira PE, Smeitink JA, Wevers RA, et al. Smith-Lemli-Opitz syndrome is caused by mutations in the 7-dehydrocholesterol reductase gene. Am J Hum Genet. 1998;63:329–38.
81. Wassif CA, Maslen C, Kachilele-Linjewile S, Lin D, Linck LM, Connor WE, Steiner RD, Porter FD. Mutations in the human sterol delta7-reductase gene at 11q12-13 cause Smith-Lemli-Opitz syndrome. Am J Hum Genet. 1998;63:55–62.
82. Fitzky BU, Witsch-Baumgartner M, Erdel M, Lee JN, Paik YK, Glossmann H, Utermann G, Moebius FF. Mutations in the Delta7-sterol reductase gene in patients with the Smith-Lemli-Opitz syndrome. Proc Natl Acad Sci U S A. 1998;95:8181–6.
83. Nowaczyk MJM, Wassif CA. Smith-Lemli-Opitz Syndrome. In: Adam MP, Ardinger HH, Pagon RA, Wallace SE, Bean LJH, Gripp KW, Mirza GM, Amemiya A, editors. GeneReviews ((R)). Seattle (WA); 1993.
84. Lin AE, Ardinger HH, Ardinger RH Jr, Cunniff C, Kelley RI. Cardiovascular malformations in Smith-Lemli-Opitz syndrome. Am J Med Genet. 1997;68:270–8.

85. Weiss K, Terhal PA, Cohen L, Bruccoleri M, Irving M, Martinez AF, Rosenfeld JA, Machol K, Yang Y, Liu P, et al. De novo mutations in CHD4, an ATP-dependent chromatin remodeler gene, cause an intellectual disability syndrome with distinctive dysmorphisms. Am J Hum Genet. 2016;99:934–41.
86. Weiss K, Lazar HP, Kurolap A, Martinez AF, Paperna T, Cohen L, Smeland MF, Whalen S, Heide S, Keren B, et al. The CHD4-related syndrome: a comprehensive investigation of the clinical spectrum, genotype-phenotype correlations, and molecular basis. Genet Med. 2020;22: 389–97.
87. Lai AY, Wade PA. Cancer biology and NuRD: a multifaceted chromatin remodelling complex. Nat Rev Cancer. 2011;11:588–96.
88. Hoffmann A, Spengler D. Chromatin remodeling complex NuRD in neurodevelopment and neurodevelopmental disorders. Front Genet. 2019;10:682.
89. Wilczewski CM, Hepperla AJ, Shimbo T, Wasson L, Robbe ZL, Davis IJ, Wade PA, Conlon FL. CHD4 and the NuRD complex directly control cardiac sarcomere formation. Proc Natl Acad Sci U S A. 2018;115:6727–32.
90. Banka S, Newman WG. A clinical and molecular review of ubiquitous glucose-6-phosphatase deficiency caused by G6PC3 mutations. Orphanet J Rare Dis. 2013;8:84.
91. Boztug K, Appaswamy G, Ashikov A, Schäffer AA, Salzer U, Diestelhorst J, Germeshausen M, Brandes G, Lee-Gossler J, Noyan F, et al. A syndrome with congenital neutropenia and mutations in G6PC3. N Engl J Med. 2009;360:32–43.
92. Braverman NE, Steinberg SJ, Fallatah W, Duker A, Bober M. Rhizomelic Chondrodysplasia Punctata Type 1. In: Adam MP, Ardinger HH, Pagon RA, Wallace SE, Bean LJH, Gripp KW, Mirza GM, Amemiya A, editors. GeneReviews(®). Seattle (WA): University of Washington, Seattle Copyright © 1993-2022, University of Washington, Seattle. GeneReviews is a registered trademark of the University of Washington, Seattle. All rights reserved.; 1993.
93. Huffnagel IC, Clur SA, Bams-Mengerink AM, Blom NA, Wanders RJ, Waterham HR, Poll-The BT. Rhizomelic chondrodysplasia punctata and cardiac pathology. J Med Genet. 2013;50: 419–24.
94. Duker AL, Eldridge G, Braverman NE, Bober MB. Congenital heart defects common in rhizomelic chondrodysplasia punctata. Am J Med Genet A. 2016;170a:270–2.
95. Wanders RJ. Metabolic functions of peroxisomes in health and disease. Biochimie. 2014;98: 36–44.

Molecular Pathways and Animal Models of Atrial Septal Defect

25

Rachel A. Magnan, Lillian Kang, Karl R. Degenhardt, Robert H. Anderson, and Patrick Y. Jay

Abstract

The relative simplicity of the clinical presentation and management of an atrial septal defect belies the complexity of the developmental pathogenesis. Here, we describe the anatomic development of the atrial septum and the venous return to the atrial chambers. Experimental models suggest how mutations and naturally occurring genetic variation could affect developmental steps to cause a defect within the oval fossa, the so-called secundum defect, or other interatrial communications, such as the sinus venosus defect or ostium primum defect.

Keywords

Atrial septal defect · ASD · Atrioventricular septal defect · AVSD · Sinus venosus defect · Ostium secundum defect · Ostium primum defect · Atrial septation · Second heart field · Dorsal mesocardium · Dorsal mesenchymal protrusion · Common atrium · Coronary sinus · Endocardium · Mesenchymal cap · Endocardial cushions · Primary atrial foramen · Primary atrial septum · ACTC1 ·

R. A. Magnan
Department of Pediatrics, Goryeb Children's Hospital, Morristown, NJ, USA

L. Kang
Department of Surgery, Duke University, Durham, NC, USA

K. R. Degenhardt
Division of Cardiology, Department of Pediatrics, Children's Hospital of Philadelphia, Perelman School of Medicine at the University of Pennsylvania, Philadelphia, PA, USA

R. H. Anderson
Cardiovascular Research Center, Biosciences Institute, Newcastle University, Newcastle upon Tyne, UK

P. Y. Jay (✉)
Alnylam Pharmaceuticals, Cambridge, MA, USA

© The Author(s), under exclusive license to Springer Nature Switzerland AG 2024

S. Rickert-Sperling et al. (eds.), *Congenital Heart Diseases: The Broken Heart*,
Advances in Experimental Medicine and Biology 1441,
https://doi.org/10.1007/978-3-031-44087-8_25

TBX5 · Knockout · GATA4 · NOS3 · Hox transcription factors · Down syndrome · Semaphorin · Sema3d · MGRN1

25.1 Introduction

The term “atrial septal defect” (ASD) is commonly used to describe any abnormal communication between the atrial chambers. The hemodynamic consequences of atrial septal defects as loosely defined are similar, but their developmental bases are not. To be clear, we define a component of the atrial septum as one in which a defect through it will produce a direct communication between the two atrial cavities [1]. By this definition, the primary atrial septum and its ventral buttress are the only structures that comprise the atrial septum. The primary atrial septum acts as a flap valve over the foramen ovale. An ostium secundum defect, often referred to as a secundum ASD, is a direct communication in which deficiency of the primary atrial septum permits shunting across the oval fossa. The ostium primum defect represents the persistence of the primary atrial foramen, a direct communication that existed in the embryo in the setting of the initially common atrioventricular junction. When existing in the postnatal heart, it provides an atrioventricular septal defect. Indirect communications involve anomalous venous connections. Sinus venosus defects involve an anomalous pulmonary venous connection to the superior or inferior caval vein. Coronary sinus defects involve an anomalous connection between the venous channel and the left atrium. Such veno-venous and veno-atrial connections are outside the true atrial septum.

This chapter provides an overview of the mechanisms pertinent to the secundum ASD and anomalous venous connections as well as our experimental observations pertinent to ostium primum defects. The discussion focuses on mouse models, in which most experiments have been performed. Some experiments have been done in chick [2], but the system is not as amenable to genetic dissection. Frogs have a rudimentary primary atrial septum and can be useful for visualizing atrial septation in a living embryo [3, 4]. Despite certain anatomic differences between the human and mouse, the similarities of development and mutant phenotypes suggest that the genetic pathways are conserved.

25.2 Synopsis of Normal Atrial Septation

On mouse embryonic day (E) 8, the heart is a linear tube, oriented along the anterior–posterior or rostral–caudal axis. Developmental biologists refer to the embryonic head–tail axis by the former terminology, whereas human anatomists prefer the latter. “Anterior–posterior” in the human anatomic frame of reference is synonymous with “ventral–dorsal.” The arterial and venous poles are rostral and caudal, respectively. Each pole is connected to the splanchnic mesoderm by the dorsal mesocardium. Second heart field progenitors from the mesoderm migrate through

the dorsal mesocardium to contribute to the right ventricle, the outflow tract, and the ventricular septum at the arterial pole and to the atrial chambers, including the primary atrial septum and the vestibular spine, at the venous pole [5].

At E9, the right and left sinus horns enter the common atrial cavity on either side of the midline dorsal mesocardium. Just rostral to the confluence of the sinus horns, the pulmonary pit can be seen at the site of the dorsal mesocardium. The sinus horns are the precursors of the systemic venous return to the heart. The pulmonary pit provides the eventual site of entrance of the pulmonary venous return. It is flanked at this early stage by the right and left pulmonary ridges (Fig. 25.1a). Second heart field progenitors migrate through the dorsal mesocardium to contribute to the growth of the right pulmonary ridge, also referred to as the dorsal mesenchymal protrusion, which ultimately forms the vestibular spine (Fig. 25.1b). At E10, growth at the right pulmonary ridge partitions the pulmonary vein to the left atrium, while the sinus horns rotate to the right atrium (Fig. 25.1a).

The right superior and inferior caval veins will drain to the right sinus horn, while the left superior caval vein will drain through the left sinus horn, opening to the right atrium as the coronary sinus. The left superior caval vein persists in the mouse but normally regresses in humans. Rotation of the sinus horns ultimately places the coronary sinus in the left atrioventricular groove. Although the coronary sinus runs adjacent to the left atrium, each has its own wall from the beginning of development (Fig. 25.1a) [6].

In humans, the solitary pulmonary vein that initially opens through the pulmonary pit becomes incorporated into the roof of the left atrium, eventually achieving four discrete orifices [7]. This does not occur in the mouse: the right and left pulmonary veins connect to a common vein to the left atrium adjacent to the dorsal atrioventricular groove [8].

At E10, the primary atrial septum, which develops from second heart field progenitors, is first seen growing from the dorsal roof of the common atrium toward the endocardial cushions of the atrioventricular canal (Fig. 25.1c). The leading edge of the primary atrial septum has a mesenchymal cap, which is derived from the endocardium [9]. The mesenchymal cap is continuous with the developing vestibular spine at the caudal end of the primary atrial septum (Fig. 25.1d). The primary atrial foramen, or ostium primum, is thus bounded by the edge of the primary atrial septum with its mesenchymal cap, the vestibular spine, and the atrial surface of the endocardial cushions. By E12, fusion of the mesenchymal cap, vestibular spine, and endocardial cushions closes the primary atrial foramen. Persistence of the primary atrial foramen, in other words an ostium primum defect, is commonly associated with failure of the development of the vestibular spine, but disruption of any of the steps required to close the primary atrial foramen can also cause an ostium primum defect (Fig. 25.1e, f) [9–11]. The essential feature of this defect is the commonality of the atrioventricular junction, making it an atrioventricular, rather than an atrial, septal defect [12].

At E10.5, fenestrations appear at the origin of the primary atrial septum at the atrial roof as the septum grows toward the atrioventricular canal. The fenestrations coalesce to form the secondary atrial foramen, which is essential during fetal life for

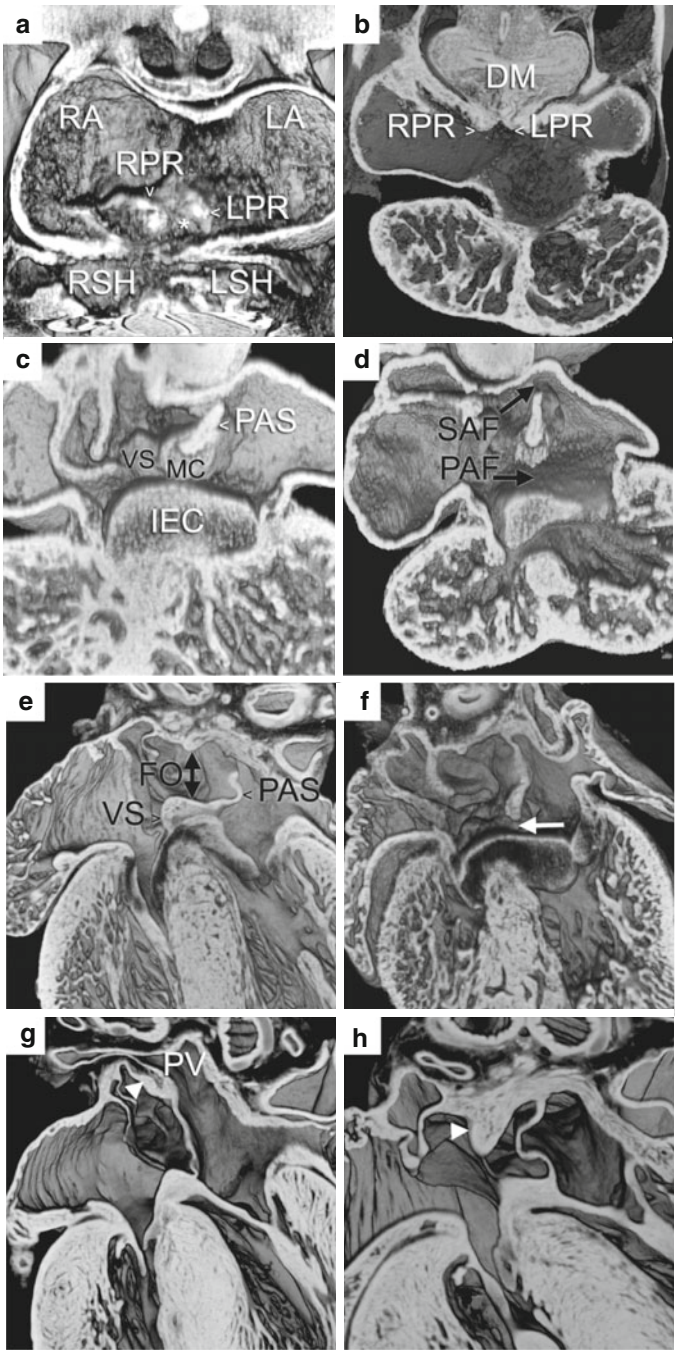

Fig. 25.1 Details of atrial septation and venous return in the developing mouse heart are shown in a series of episcopic images. (**a**, **b**) Images of an E10.5 heart are shown in the frontal (**a**) and transverse (**b**) planes. The right and left sinus horns (*RSH*, *LSH*) drain into to the right atrium (*RA*). The left sinus horn, which gives rise to the coronary sinus, never shares a common wall with the left

right-to-left shunting of oxygenated blood after closure of the primary atrial foramen (Fig. 25.1c). The primary atrial septum thus becomes the flap valve of the foramen ovale (Fig. 25.1e). At E13, the dorsal rim of the foramen ovale forms by the infolding of the atrial wall between the pulmonary vein and wall of the developing right atrial chamber to the left of the left venous valve (Fig. 25.1g). The cranial rim is a muscular ridge that remains at the site of breakdown at the atrial roof of the primary septum (Fig. 25.1h). Infolding is a consequence of the incorporation of the pulmonary vein into the left atrium. The infolded rim of the foramen is commonly referred to as the secondary atrial septum or septum secundum, but it is not a true septum, since a hole through it will enter a potential space outside the heart. The ventral–caudal rim of the foramen, which buttresses the flap valve to the atrioventricular junctions, is formed by muscularization of the mesenchymal cap of the primary atrial septum and vestibular spine (Fig. 25.1e–h) [9–11]. This rim is a true septum, as illustrated by a rare vestibular defect in a newborn *Nkx2-5*$^{+/-}$ mouse (Fig. 25.2a). Vestibular defects have also been described in fetal mice [13].

The embryologic relationship between the systemic and pulmonary venous return was hotly debated in the past, but multiple studies in human and mouse now clearly establish their separate development. An analysis on the chick embryo demonstrates this elegantly with three-dimensional reconstructions. The pulmonary veins in the lungs develop from a plexus within the splanchnic mesoderm. They subsequently connect to the solitary pulmonary vein that develops within the pharyngeal mesenchyme adjacent to the pulmonary pit. The systemic venous sinus originates from the junction between the splanchnic and somatic mesoderm. The systemic veins develop in the splanchnic mesoderm caudal to the pulmonary venous plexus. There are no anastomoses between the two venous systems in the normal embryo [14]. Studies of developing human hearts also support the separate developmental origins of the systemic and pulmonary veins [15].

Fig. 25.1 (continued) atrium (*LA*) during development. The pulmonary pit (*) is situated between the right and left pulmonary ridges (*RPR*, *LPR*). Second heart field progenitors migrate through the dorsal mesocardium (*DM*) into the right pulmonary ridge to form the vestibular spine. (**c**, **d**) In two E11.5 hearts, the relationships are shown between the primary atrial septum (*PAS*), its mesenchymal cap (*MC*), the developing vestibular spine (*VS*), and the inferior endocardial cushion (*IEC*). The primary and secondary atrial foramina are noted (*PAF*, *SAF*). (**c**) is cranial to (**d**). (**e**) In this E14.5 heart, fusion of the mesenchymal cap of the primary atrial septum, the vestibular spine, and the endocardial cushions has closed the primary atrial foramen. The primary atrial septum acts as a flap valve on the foramen ovale (*FO*). (**f**) An ostium primum defect (*arrow*) in this E18.5 heart results from persistence of the primary atrial foramen in the setting of a common atrioventricular junction. (**g**, **h**) In this E18.5 heart, the atrial septum is shown (**g**) at the level of the pulmonary vein and (**h**) more cranially. Incorporation of the pulmonary vein (PV) into the left atrium causes infolding of the dorsal atrial wall (*arrowhead*, **g**). A muscular rim, not present in humans, exists at the site of breakdown at the atrial roof of the primary septum (*arrowhead*, **h**) (Dr. Timothy Mohun prepared the episcopic image datasets)

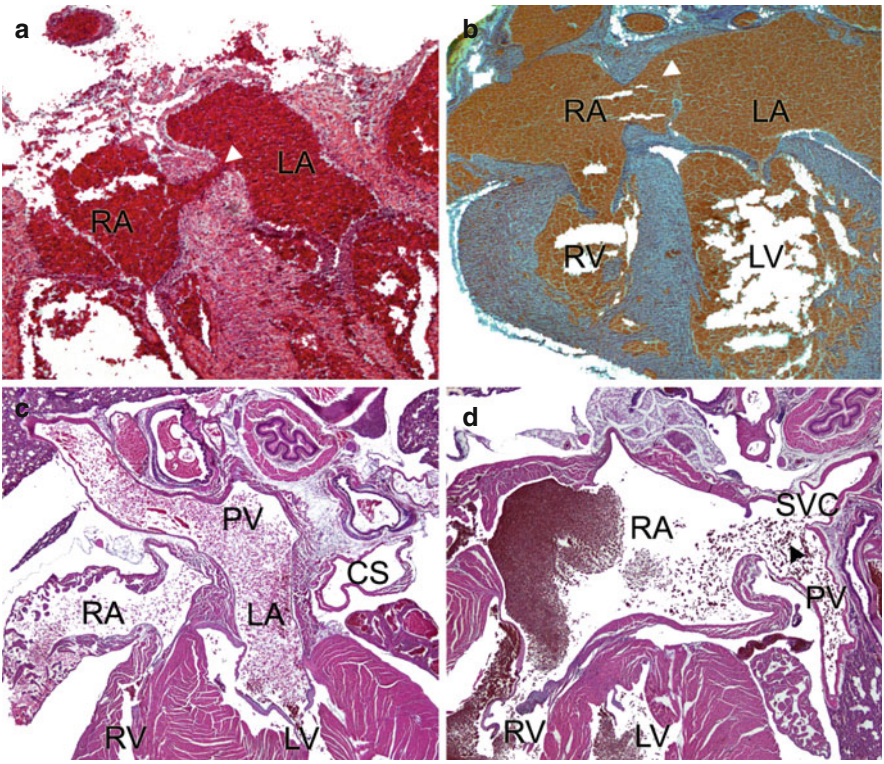

Fig. 25.2 Examples of atrial septal defects and an anomalous veno-venous communication. (**a**) A vestibular defect and (**b**) a secundum ASD in newborn *Nkx2-5*$^{+/-}$ mice. (**c**) Normal pulmonary venous drainage is shown into the left atrium of a mouse. (**d**) The pulmonary vein communicates anomalously with the superior caval vein in a *Sema3d*$^{-/-}$ mouse. *Arrowheads* indicate the defects. (Mr. Suk Dev Regmi prepared the sections shown in **a**, **b** and in Fig. 25.3.) *CS* coronary sinus, *PV* pulmonary vein, *RA*, *LA* right, left atrium, *RV*, *LV* right, left ventricle, *SVC* superior caval vein

25.3 Pathways to a Defect Within the Oval Fossa (Secundum ASD)

Most experimental studies of atrial septation to date pertain to the pathogenesis of the primum rather than secundum defect. Developmental biologists often do not distinguish between the two defects, describing mutant phenotypes merely as "ASDs." A secundum ASD is the consequence of deficiency of the primary atrial septum, such that it cannot cover the complete area of the foramen ovale because of incomplete overlap with the infolded rim of the foramen (Fig. 25.2b). Fenestrations in the primary atrial septum also occur but are less common. Of note, the vestibular spine and the mesenchymal cap, forming the buttress of the foramen, have developed and muscularized normally, which is not necessarily the case in the primum defect.

An appreciation of normal development and the morphology of defects within the oval fossa can help to circumscribe the pathogenic mechanisms. While the molecular pathways that lead to a secundum ASD have not been as thoroughly studied as, say, outflow tract defects, excessive myocyte apoptosis in the primary atrial septum during the development of the secondary atrial foramen may be the final common result of disparate genetic mutations, as demonstrated in studies of the transcription factors, *TBX5* and *GATA4*, endothelial nitric oxide synthase, *NOS3*, and cardiac actin, *ACTC1*.

Human and mouse *TBX5* and *GATA4* mutations are commonly associated with secundum ASD, although other malformations, such as AVSD, are also seen [16–19]. Independent functions of *Tbx5* in the endocardium and the second heart field can explain the pathogenesis of both secundum and primum defects, respectively. These functions have been explored in a series of conditional deletion experiments, in which one or both copies of a gene are deleted in a specific cell type or developmental period. In the embryo, *Tbx5* is expressed by the endothelial cells lining the primary atrial septum. Conditional knockout of *Tbx5* in endothelial cells increased the number of apoptotic cells in the developing primary septum. The adult conditional knockout mice had near-complete absence of the primary atrial septum, while the conditional heterozygotes had a high incidence of patency of the foramen ovale. Endothelial knockout of *Tbx5* did not affect the vestibular spine [20]. The diminished activity of *Tbx5* in the endothelium thus causes defects within the oval fossa, or the forme fruste as seen in persistent patency of the foramen ovale. On the other hand, conditional deletion of *Tbx5* in the second heart field prevented the development of the vestibular spine, resulting in primum defects with a common atrioventricular junction [21].

In an endocardial cell culture model, TBX5 upregulated the expression of *NOS3*. In the same cell culture system, TBX5 and GATA4 independently and cooperatively transactivated a *Nos3* promoter construct [20]. *Nos3*-null-mutant mice have a high incidence of defects within the oval fossa. The thinness of the primary atrial septum may make it more susceptible to apoptosis caused by the loss of *Nos3* [22]. Furthermore, compound heterozygotes, in which one allele of *Tbx5* is deleted in the endothelium and one allele of *Nos3* in the germline, have a higher incidence of secundum defects than either single heterozygote. *Nos3* is expressed in both the endocardial cells and myocytes, so its activity in one or both cell types may be necessary to prevent myocyte apoptosis. Taken together, the results suggest that *Tbx5*, *Gata4*, and *Nos3* operate in a molecular pathway involving an endocardial signal that inhibits myocyte apoptosis.

Mutations of *ACTC1*, an uncommon cause of secundum ASDs, have been described in large pedigrees [23, 24]. Two reports suggest that *ACTC1* mutation can cause cardiac myocyte apoptosis as well as myofibrillar disarray. In one study, apoptosis and myofibrillar disarray were found in the myocardium of *ACTC1*-null-mutant mice just before and after birth. Anatomical development of the heart was reportedly normal, but the atrial septum was not specifically described [25]. In another study, the ventricular myocardium of a patient with a missense mutation of *ACTC1* that caused familial ASD and dilated cardiomyopathy also showed

increased apoptosis and myofibrillar disarray. Forced expression of the mutant, but not the wild-type protein in cultured neonatal rat cardiomyocytes reproduced the phenotypes [23]. Whether myofibrillar disarray causes apoptosis or the two phenotypes are separate consequences of *ACTC1* mutation is unknown. Careful studies of apoptosis in the developing primary atrial septum seem worthwhile to understand the basis of secundum ASD.

25.4 Pathways to Sinus Venosus and Coronary Sinus Defects

With regard to the developmental pathogenesis of sinus venosus and coronary sinus defects, we assert that the salient anatomic feature is the anomalous communication between a vein and an adjacent structure, with the vein itself continuing on its normal course. In a sinus venosus defect, a pulmonary vein communicates with the superior or inferior caval veins while retaining its own left atrial connection. The most common defect is between the right upper pulmonary vein and the superior caval vein. The normal connections of the caval veins and the pulmonary vein to their respective atrial chambers permit the interatrial shunting of blood. In a coronary sinus defect, the anomalous communication is with the left atrium as the vessel courses within the left atrioventricular groove. The shunt then flows from the cavity of the left atrium to the right atrium through the mouth of the coronary sinus.

The morphology of sinus venosus defects with the separate development of the systemic and pulmonic venous returns makes certain pathogenic mechanisms unlikely. The anomalous communication cannot be due to the persistence of a transient anastomosis in the embryo. The failure of development of a common wall, or its dissolution between two veins, is also implausible. On the other hand, a semaphorin 3d (*Sema3d*) knockout mouse model of anomalous pulmonary venous return suggests that the basis is the development of an ectopic communication [26].

Semaphorins are secreted ligands. First discovered as mediators of axonal guidance by repulsion or attraction, semaphorins and their receptors, the plexins and neuropilins, have broad functions in cardiovascular development [27, 28]. In the embryonic mouse heart, *Sema3d* expression marks an avascular border region in the splanchnic mesoderm between the pulmonary and systemic venous plexuses, with the latter developing more caudally in the splanchnic mesoderm. Pulmonary venous endothelial cells express the neuropilin-1 receptor for *Sema3d*. In *Sema3d* knockout embryos, pulmonary venous endothelial cells cross the border and form connections with the systemic veins, while the main pulmonary vein still uses the pulmonary pit to enter the atrial cavity to the left of the primary atrial septum [26]. In the *Sema3d* knockout mutant, abnormal veno-venous communications arise because of a failure of repulsion. The mechanism that directs the common pulmonary vein to the left atrium remains intact. We hypothesize that sinus venosus defects arise by a similar failure of repulsion. As a pulmonary vein passes by the superior or inferior sinus horn on its way to the left atrium, it forms the anomalous communication (Fig. 25.2c, d).

The morphology of a coronary sinus defect, when considered relative to normal development, also makes certain mechanisms unlikely. There is never a common wall between the coronary sinus and left atrium in the embryo, so the failure of its development or its dissolution is implausible. The development of an anomalous veno-atrial communication, similar to the mechanism hypothesized for a sinus venosus defect, seems more plausible, but affirmative evidence remains lacking. No gene has been associated with an isolated coronary sinus defect in humans or mice. In the only report of such a defect in the mouse, the authors suggest that a knockout of *mahogunin ring finger*-1 (*MGRN1*) caused a coronary sinus defect, albeit in association with a cardiac phenotype suggestive of isomerism, or heterotaxy [29]. Genes that affect embryonic left–right patterning might be candidates for screening in isolated coronary sinus defects.

25.5 Pathways to Ostium Primum Defects

The ostium primum defect is usually discussed in the context of AVSDs. That said, we briefly discuss our experimental observations that point to developmental pathways specific to atrial structures involved in closure of the primary atrial foramen.

The hallmark of an AVSD is a common atrioventricular junction in which the superior and inferior leaflets of the common valve bridge the atrioventricular septum (Fig. 25.3a–e). AVSDs are hence often referred to as common atrioventricular canal defects. Persistence of the primary atrial foramen and the absence of a vestibular spine are typical, but not essential, features of the defect, as demonstrated by defects that have only a ventricular component, with absence of shunting at atrial level, or completely intact atrial and ventricular septae [30, 31]. The anatomic variants of AVSDs have also been observed in mouse models of trisomy 21 [32] and *Nkx2-5* mutation, as shown by a newborn *Nkx2-5*$^{+/-}$ mouse with a common atrioventricular junction and an intact atrioventricular septum (Fig. 25.3c, d).

To investigate the multifactorial basis of congenital heart disease, we have performed inbred strain crosses with the *Nkx2-5*$^{+/-}$ mouse [33]. The genetic variation introduced by the crosses permitted the mapping of genes that modify the risk of secundum ASD, perimembranous and muscular VSDs, and AVSD [34]. The genes mapped within a cross as well as the variation in the incidence of a defect between crosses point to pathways in the development of the affected cardiac structure. Polymorphisms of genes within the pathways affect the robustness of specific developmental processes to the *Nkx2-5* mutation.

We analyzed 255 AVSDs collected from >14,000 *Nkx2-5*$^{+/-}$ hearts across four inbred strain crosses. Not only is there variation in the incidence of AVSDs between the crosses (Fig. 25.3f), but there is variation in the incidence of AVSD subtypes that have a vestibular spine or an intact atrial septum (Fig. 25.3g, h). The incidences between strains of any AVSD or of AVSDs with the particular atrial septal variants are unequal or tend to be unequal. The genetic background appears to influence whether a cross is more or less susceptible to an AVSD or of a subtype. Furthermore,

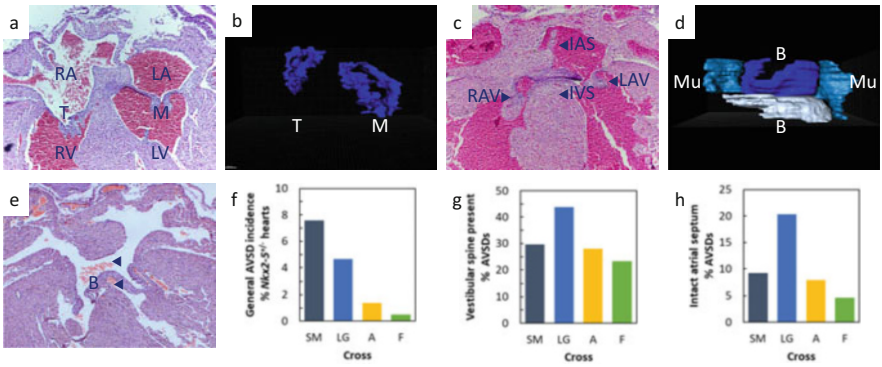

Fig. 25.3 (**a**) A structurally normal *Nkx2-5*$^{+/-}$ heart with intact atrial and ventricular septae and separate tricuspid and mitral valves. (**b**) 3-dimensional reconstruction of the separate tricuspid and mitral valves. (**c**) An *Nkx2-5*$^{+/-}$ heart with an AVSD consisting of a common atrioventricular valve but intact atrial and ventricular septal structures. (**d**) 3-dimensional reconstruction of the common valve with superior and inferior bridging leaflets and mural leaflets. (**e**) An *Nkx2-5*$^{+/-}$ heart with a common atrioventricular canal guarded by a common valve with a common orifice. The atrial and ventricular communications are seen above and below the bridging leaflet (arrowheads). (**f**) Incidences of any type of AVSD from four different inbred strain crosses ($N = 1293$, 1372, 3652, and 8406 *Nkx2-5*$^{+/-}$ hearts from the SM, LG, F and A crosses). (**g**, **h**) Percentage of AVSDs that have a vestibular spine or an intact atrial septum. The percentages of AVSD or of the subtypes are unequal or tend to be between the crosses ($P < 1 \times 10^{-10}$, $= 0.10$, and $= 0.04$ in f, g, and h). The percentage of AVSDs with a vestibular spine or an intact atrial septum is not related to the incidence of AVSDs in a cross ($P < 1 \times 10^{-8}$ for both comparisons). *RA*, *LA* right, left atrium, *RV*, *LV* right, left ventricle, *M*, *T*, *LAV*, *RAV*, mitral, tricuspid, left, right atrioventricular valve, *B*, *Mu*, bridging and mural leaflets of the common valve

there is no correlation between the incidences of AVSD and AVSD subtypes. For example, while the LG cross has an intermediate incidence of AVSD compared to the other three crosses, it has the highest percentage of AVSDs with a vestibular spine or an intact atrial septum. Thus, genes that modify the risk of a common atrioventricular junction caused by the *Nkx2-5* mutation may not directly affect the development of the atrial septal components, and vice versa.

Taking the clinical and experimental observations together, we propose that the anatomic subtypes of AVSD arise from different combinations of missteps in a series of developmental pathways. The first, essential misstep causes a common atrioventricular junction. One or more subsequent missteps in the development of the vestibular spine or primary atrial septum or in fusion of the atrial septal components with the endocardial cushions then lead to an ostium primum defect. (Likewise, a misstep in ventricular septal development would produce the interventricular communication.) Given this framework, one may consider in which pathway a gene acts. Mutations that cause AVSD may disrupt a pathway common to the development of the atrioventricular junction and septal structures, such as a progenitor cell population. For example, perturbation of a second heart field subdomain that contributes cells to the subpulmonary myocardium, primary atrial septum, and vestibular spine has been postulated to explain the co-occurrence of tetralogy of Fallot and AVSD in

persons with Down syndrome [35, 36]. Modifier genes could act either in the common pathway to modulate the risk of an AVSD or in a pathway specific to a septal structure to determine the risk of an AVSD subtype. Embryos possess remarkable mechanisms to correct development that goes awry. Elegant examples include pattern formation in flies and left-right patterning and craniofacial development in frogs [37–39]. Thus, the alleles of modifier genes could either weaken or strengthen corrective mechanisms in cardiac development, leading to a complete common AV canal or the anatomic variants of AVSDs after an embryo has committed to form a common atrioventricular junction.

25.6 Conclusion

While the physiological consequences of atrial septal defects and interatrial communications are relatively simple to understand, their development and genetics are just as complicated and arguably less well understood than defects like tetralogy of Fallot. What little is known suggests that their investigation in animal models will yield novel insights into interactions between the endocardium and myocytes, vascular patterning, and second heart field development. We suggest that a clear understanding of the developmental morphogenesis is as important as any advances in experimental genetics to elucidate the mechanisms.

References

1. Anderson RH, Brown NA. The anatomy of the heart revisited. Anat Rec. 1996;246:1–7.
2. Rutland C, Warner L, Thorpe A, et al. Knockdown of alpha myosin heavy chain disrupts the cytoskeleton and leads to multiple defects during chick cardiogenesis. J Anat. 2009;214:905–15.
3. Deniz E, Jonas S, Khokha M, et al. Endogenous contrast blood flow imaging in embryonic hearts using hemoglobin contrast subtraction angiography. Opt Lett. 2012;37:2979–81.
4. Jahr M, Manner J. Development of the venous pole of the heart in the frog Xenopus laevis: a morphological study with special focus on the development of the venoatrial connections. Dev Dyn. 2011;240:1518–27.
5. Kelly RG. The second heart field. Curr Top Dev Biol. 2012;100:33–65.
6. Webb S, Brown NA, Anderson RH. Formation of the atrioventricular septal structures in the normal mouse. Circ Res. 1998;82:645–56.
7. Webb S, Kanani M, Anderson RH, et al. Development of the human pulmonary vein and its incorporation in the morphologically left atrium. Cardiol Young. 2001;11:632–42.
8. Webb S, Brown NA, Wessels A, et al. Development of the murine pulmonary vein and its relationship to the embryonic venous sinus. Anat Rec. 1998;250:325–34.
9. Mommersteeg MT, Soufan AT, de Lange FJ, et al. Two distinct pools of mesenchyme contribute to the development of the atrial septum. Circ Res. 2006;99:351–3.
10. Snarr BS, O'Neal JL, Chintalapudi MR, et al. Isl1 expression at the venous pole identifies a novel role for the second heart field in cardiac development. Circ Res. 2007;101:971–4.
11. Snarr BS, Wirrig EE, Phelps AL, et al. A spatiotemporal evaluation of the contribution of the dorsal mesenchymal protrusion to cardiac development. Dev Dyn. 2007;236:1287–94.
12. Anderson RH, Mohun TJ, Brown NA. Clarifying the morphology of the ostium primum defect. J Anat. 2015;226:244–57.

13. Loomba RS, Tretter JT, Mohun TJ, et al. Identification and morphogenesis of vestibular atrial septal defects. J Cardiovasc Dev Dis. 2020;7
14. van den Berg G, Moorman AF. Development of the pulmonary vein and the systemic venous sinus: an interactive 3D overview. PLoS One. 2011;6:e22055.
15. Sizarov A, Anderson RH, Christoffels VM, et al. Three-dimensional and molecular analysis of the venous pole of the developing human heart. Circulation. 2010;122:798–807.
16. Basson CT, Bachinsky DR, Lin RC, et al. Mutations in human TBX5 cause limb and cardiac malformation in Holt-Oram syndrome. Nat Genet. 1997;15:30–5.
17. Garg V, Kathiriya IS, Barnes R, et al. GATA4 mutations cause human congenital heart defects and reveal an interaction with TBX5. Nature. 2003;424:443–7.
18. Jay PY, Bielinska M, Erlich JM, et al. Impaired mesenchymal cell function in Gata4 mutant mice leads to diaphragmatic hernias and primary lung defects. Dev Biol. 2007;301:602–14.
19. Li QY, Newbury-Ecob RA, Terrett JA, et al. Holt-Oram syndrome is caused by mutations in TBX5, a member of the Brachyury (T) gene family. Nat Genet. 1997;15:21–9.
20. Nadeau M, Georges RO, Laforest B, et al. An endocardial pathway involving Tbx5, Gata4, and Nos3 required for atrial septum formation. Proc Natl Acad Sci U S A. 2010;107:19356–61.
21. Xie L, Hoffmann AD, Burnicka-Turek O, et al. Tbx5-hedgehog molecular networks are essential in the second heart field for atrial septation. Dev Cell. 2012;23:280–91.
22. Feng Q, Song W, Lu X, et al. Development of heart failure and congenital septal defects in mice lacking endothelial nitric oxide synthase. Circulation. 2002;106:873–9.
23. Frank D, Yusuf Rangrez A, Friedrich C, et al. Cardiac alpha-Actin (ACTC1) gene mutation causes atrial-septal defects associated with late-onset dilated cardiomyopathy. Circ Genom Precis Med. 2019;12:e002491.
24. Matsson H, Eason J, Bookwalter CS, et al. Alpha-cardiac actin mutations produce atrial septal defects. Hum Mol Genet. 2008;17:256–65.
25. Abdelwahid E, Pelliniemi LJ, Szucsik JC, et al. Cellular disorganization and extensive apoptosis in the developing heart of mice that lack cardiac muscle alpha-actin: apparent cause of perinatal death. Pediatr Res. 2004;55:197–204.
26. Degenhardt K, Singh MK, Aghajanian H, et al. Semaphorin 3d signaling defects are associated with anomalous pulmonary venous connections. Nat Med. 2013;19:760–5.
27. Epstein JA, Aghajanian H, Singh MK. Semaphorin signaling in cardiovascular development. Cell Metab. 2015;21:163–73.
28. He Z, Wang KC, Koprivica V, et al. Knowing how to navigate: mechanisms of semaphorin signaling in the nervous system. Sci STKE. 2002;2002:re1.
29. Cota CD, Bagher P, Pelc P, et al. Mice with mutations in Mahogunin ring finger-1 (Mgrn1) exhibit abnormal patterning of the left-right axis. Dev Dyn. 2006;235:3438–47.
30. Anderson RH, Wessels A, Vettukattil JJ. Morphology and morphogenesis of atrioventricular septal defect with common atrioventricular junction. World J Pediatr Congenit Heart Surg. 2010;1:59–67.
31. Kaski JP, Wolfenden J, Josen M, et al. Can atrioventricular septal defects exist with intact septal structures? Heart. 2006;92:832–5.
32. Lana-Elola E, Watson-Scales S, Slender A, et al. Genetic dissection of Down syndrome-associated congenital heart defects using a new mouse mapping panel. Elife. 2016;5
33. Jay PY, Akhirome E, Magnan RA, et al. Transgenerational cardiology: One way to a baby's heart is through the mother. Mol Cell Endocrinol. 2016;435:94–102.
34. Akhirome E, Regmi SD, Magnan RA, et al. The genetic architecture of a congenital heart defect is related to its fitness cost. Genes (Basel). 2021;12
35. Bertrand N, Roux M, Ryckebusch L, et al. Hox genes define distinct progenitor sub-domains within the second heart field. Dev Biol. 2011;353:266–74.
36. Nguyen HH, Jay PY. A single misstep in cardiac development explains the co-occurrence of tetralogy of fallot and complete atrioventricular septal defect in Down syndrome. J Pediatr. 2014;165:194–6.

37. Eldar A, Dorfman R, Weiss D, et al. Robustness of the BMP morphogen gradient in Drosophila embryonic patterning. Nature. 2002;419:304–8.
38. McDowell GS, Lemire JM, Pare JF, et al. Conserved roles for cytoskeletal components in determining laterality. Integr Biol (Camb). 2016;8:267–86.
39. Vandenberg LN, Adams DS, Levin M. Normalized shape and location of perturbed craniofacial structures in the Xenopus tadpole reveal an innate ability to achieve correct morphology. Dev Dyn. 2012;241:863–78.

Part V

Ventricular Septal Defect

Clinical Presentation and Therapy of Ventricular Septal Defect

26

Nikolaus A. Haas, David J. Driscoll, and Silke Rickert-Sperling

Abstract

Ventricular septal defects (VSDs) occur in 1.5–3.5 of 1000 live births and constitutes 20 % of congenital cardiac defects. There is no gender predominance.

Keywords

Ventricular septal defect · VSD · Perimembranous VSD · Supracristal VSD · Inlet VSD · Muscular VSD · Gerbode type VSD · Cyanosis · Pulmonary artery hypertension · Left-to-right shunt · Left ventricle · Congestive heart failure

26.1 Introduction

Ventricular septal defects (VSDs) occur in 1.5–3.5 of 1000 live births and constitute 20% of congenital cardiac defects. There is no gender predominance. A VSD can present in isolation or be part of complex heart defects.

According to their location, there are five types of VSD (Fig. 26.1):

N. A. Haas (✉)
Department of Pediatric Cardiology and Intensive Care, Ludwig Maximilians University, Munich, Germany
e-mail: Nikolaus.haas@med.uni-muenchen.de

D. J. Driscoll
Division of Pediatric Cardiology, Department of Pediatrics, Mayo Clinic College of Medicine, Rochester, MN, USA
e-mail: driscoll.david@mayo.edu

S. Rickert-Sperling
Cardiovascular Genetics, Charité – Universitätsmedizin Berlin, Berlin, Germany
e-mail: silke.sperling@charite.de

© The Author(s), under exclusive license to Springer Nature Switzerland AG 2024

S. Rickert-Sperling et al. (eds.), *Congenital Heart Diseases: The Broken Heart*,
Advances in Experimental Medicine and Biology 1441,
https://doi.org/10.1007/978-3-031-44087-8_26

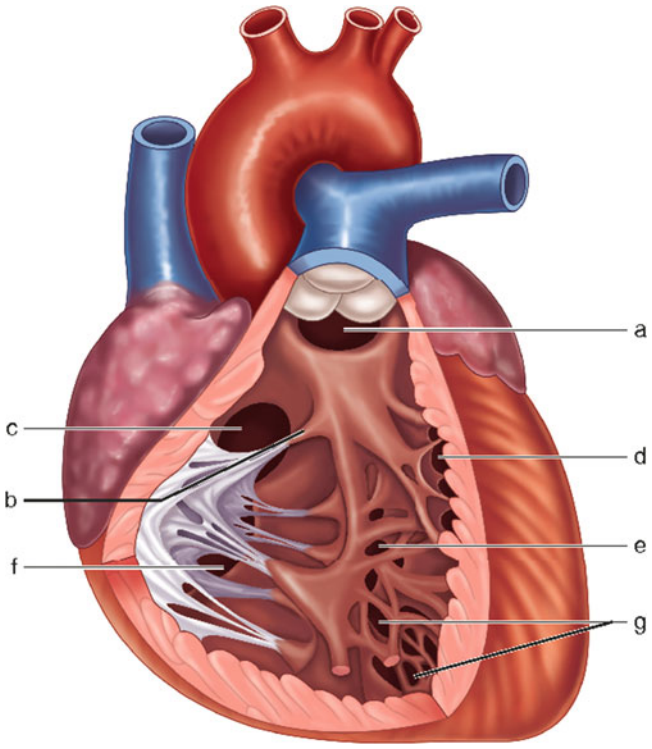

Fig. 26.1 Diagrammatic representation of the types and locations of VSDs. The anterior surface of the heart has been removed, revealing the ventricular septum as viewed from the right side. *Abbreviations*: *a* outlet or supracristal VSD, *b* septal papillary muscle of the tricuspid valve, *c* perimembranous VSD, *d* right ventricular muscle bundle, *e* muscular VSD, *f* inlet VSD, *g* muscular VSDs

1. Perimembranous VSD (also: membranous, subaortic, infracristal VSD)
2. Supracristal (also infundibular, outlet, or subpulmonary VSD)
3. Inlet VSD (VSD of the atrioventricular canal type)
4. Muscular
5. Gerbode type VSD (direct connection between the left ventricle and the right atrium above the tricuspid valve)

A *perimembranous VSD* is in the area of the membranous septum. This places it in the outflow tract of the left ventricle and immediately under the aortic valve. A *supracristal VSD* is located superior to the crista supraventricularis which places it in the right ventricular outflow tract and immediately below the right cusp of the aortic valve. An *inlet VSD* is located posteriorly in the septum just inferior to the tricuspid and mitral valves. This is a type of endocardial cushion defect. A *muscular VSD* is located in the muscular ventricular septum. Patients can have more than one muscular VSD. The Gerbode defect is very rare and a special form of a perimembranous

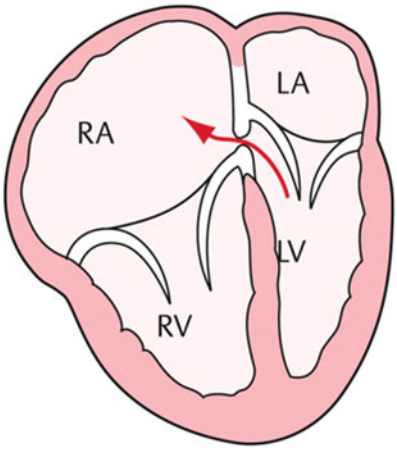

Fig. 26.2 Gerbode defect. The tricuspid valve extends more apically (towards the apex) into the ventricle compared to the mitral valve. As a result, a portion of the left ventricle comes into direct contact with the right atrium. A defect in this region leads to an abnormal communication or shunt between the left ventricle and right atrium. The defect is named after Dr. Frank Gerbode, who first described this condition in 1958. Reproduced from Kinderkardiologie, Georg Thieme Verlag, N. Haas, U. Kleideiter, 2011

VSD; it consists of a direct connection between the left ventricle and the right atrium above the tricuspid valve (Fig. 26.2). When multiple VSDs come together in one patient, the term "Swiss cheese VSD" is used. Typically, these patients show a large perimembranous VSD and multiple muscular VSDs. In addition, there are malalignment VSDs where there is an abnormal displacement of the outflow tract septum with the result that the semilunar valves override the VSD (for example in Tetralogy of Fallot).

26.2 Pathologic Physiology

According to hemodynamic relevance and size, VSDs are clinically classified in three categories: large VSDs, where the size of the VSD is larger than the size of the aorta and there is unrestricted flow and pressure transduction to the right ventricle; mid-sized VSDs, with a size of 50–100% of the aorta and pressure reduction (restriction) but still substantial left-to-right shunt; and small VSDs, with a size of less than 50% of the aorta. These latter VSDs are restrictive and show no substantial or clinically relevant shunt.

The vast majority of VSDs are small VSDs. In uncomplicated VSD, the typical flow hemodynamics shows blood flow according to the pressure gradients from the left ventricle through the VSD traversing the right ventricle and into the pulmonary artery. This results in volume overload of the pulmonary circulation, the left atrium, and the left ventricle. When there is a large VSD without pressure reduction, the right side of the heart is additionally exposed to a pressure load. Over time, secondary changes in the pulmonary vasculature may develop according to the amount of shunt and pressure load. These patients develop pulmonary vascular obstructive disease, i.e., pulmonary hypertension with secondary increase of pulmonary vascular

resistance. Thereafter, the direction of flow of blood can reverse such that desaturated blood from the right ventricle will traverse the VSD into the left ventricle and exit through the aorta. These patients may exhibit cyanosis. This clinical picture is named Eisenmenger syndrome.

Flow acceleration through the restriction will create a systolic murmur by blood flowing through the VSD or through the pulmonary valve (for unrestrictive VSDs). In patients with very large VSDs, no murmur may be present.

26.3 Clinical Presentation

The clinical presentation of patients with VSD depends primarily upon the size of the VSD, the secondary flow across the VSD, and, to a much lesser extent, upon the type of VSD. Typically, if the VSD itself is unrestrictive to blood flow, then the downstream resistance of the right ventricular outflow tract or the pulmonary microcirculation will determine the volume of pulmonary blood flow.

Patients with a small- or moderate-sized VSD may present only with a cardiac murmur. If there is a substantial amount of left-to-right shunt, clinical signs of increased cardiac workload and additional pulmonary volume transfer may become evident, such as tachycardia, sweating, tachypnea, wheezing, and failure to thrive.

Infants with a large VSD may, initially, present only with a murmur. As pulmonary resistance declines within the first three months of life, however, they will develop signs and symptoms of pulmonary edema, pulmonary venous hypertension, and congestive heart failure. This is manifested by tachypnea, tachycardia, pallor, poor feeding, and poor weight gain. When these children develop significant pulmonary hypertension (at ages greater than 1–2 years), the clinical symptoms may disappear because the left-to-right shunts will decrease on account of increased pulmonary vascular resistance.

In addition, the type of VSD may influence the clinical presentation. For example, a patient with a small perimembranous VSD may present primarily with aortic valve insufficiency caused by flow characteristics of a left-to-right shunt.

26.4 Physical Examination

The physical findings for a patient with a VSD depend upon the size of the VSD, the magnitude of the left-to-right shunt, and the level of right ventricular and pulmonary artery hypertension.

A small VSD and normal or only slightly elevated right ventricular and pulmonary artery pressure is characterized by normal precordial impulses and normal first and second heart sounds. The murmur is holosystolic. For moderate and large VSDs, the right ventricular impulse, felt at the lower left sternal border or the subxiphoid region, is prominent. In addition, the left ventricular impulse will be displaced laterally and have increased activity. The first heart sound will be normal. As the degree of pulmonary hypertension increases, the intensity of the pulmonary

component of S2 will increase. There will be a holosystolic mid-frequency murmur. In patients with Qp/Qs >2 (ratio of pulmonary to systemic blood flow greater than 2), in addition to the systolic murmur, there will be a mid-diastolic mitral flow murmur (this produces the so-called "gallop rhythm") as a result of increased volume of blood flowing from the left atrium to the left ventricle.

In patients with shunt reversal and elevated pulmonary vascular resistance, there will be a very loud and split second heart sound and, due to the right-to-left shunt, cyanosis with clubbing.

26.5 Diagnostic Imaging

Echocardiography is the primary diagnostic tool for confirming a ventricular septal defect (VSD). It allows for the precise identification of the defect's location, anatomical classification, and size, as well as the detection of associated anomalies. In children, transthoracic echocardiography is typically sufficient for diagnosis, while adults with inadequate echocardiographic windows may require transesophageal echocardiography. Echocardiography also enables the assessment of left atrial and left ventricular enlargement, right ventricular hypertrophy, and estimation of pulmonary artery pressure through Doppler techniques, including measuring blood flow velocity across the tricuspid and pulmonary valves or directly across the VSD. Additionally, it provides an approximation of the shunt fraction.

Diagnostic cardiac catheterization is rarely necessary for VSD diagnosis in the era of echocardiography. It may be reserved for patients with severe pulmonary hypertension, where catheterization helps assess pulmonary vascular pressure and resistance, as well as to determine the patient's candidacy for VSD closure. In selected cases of perimembranous, subpulmonary, and most muscular VSDs, interventional VSD closure can be performed during catheterization.

Magnetic resonance imaging (MRI) is an alternative imaging modality that can be used in adults and teenagers when echocardiography is inconclusive or when cardiac flow and shunt fraction assessment are required to define the indication for VSD closure. MRI provides accurate measurements of flow and shunt fraction, as well as precise assessment of left atrial and ventricular size.

Computer tomography (CT) can offer similar anatomical details as MRI but is rarely necessary for VSD diagnosis. It may be considered in cases where MRI is contraindicated.

26.6 Treatment

The treatment goals for ventricular septal defects (VSDs) are to ensure adequate patient growth, prevent the development of pulmonary vascular obstructive disease, avoid chronic dysfunction of the right and left ventricles, and prevent bacterial endocarditis.

Small VSDs typically do not require closure unless they cause aortic regurgitation. However, cultural influences, particularly in Asian countries, may lead to the closure of even small VSDs that have no clinical significance but generate a loud murmur. Social factors such as marriage restrictions for women with cardiac defects or military service and insurance limitations for men may contribute to this practice.

Infants with moderate VSDs may appear clinically normal. However, if the shunt fraction exceeds 1.5:1 or if there are significant signs of left-sided volume overload, closure is recommended. For moderate to large VSDs associated with congestive heart failure, medical treatment with betablockers, ACE inhibitors, and diuretics is initially employed. High-caloric formula can be used to optimize growth in cases where failure to thrive results from congestive heart failure. If growth failure persists despite medical management, closure of the defect is indicated. In infants with pulmonary hypertension, VSD closure should be performed before the age of 1 to prevent the development of irreversible pulmonary vascular obstructive disease. In patients with syndromic VSDs, such as Trisomy 21, closure should be considered earlier due to a higher probability of developing pulmonary hypertension.

Surgical closure using cardiopulmonary bypass is the standard treatment for many VSDs in children older than 1 year, especially for large perimembranous VSDs and all inlet VSDs. In cases where surgery is contraindicated, such as very low birth weight, complex VSD anatomy, concomitant diseases, or specific genetic syndromes like Trisomy 13 or 18, placement of a pulmonary band may be used as a palliative measure or preparation for corrective surgery. The pulmonary band helps reduce pressure and volume load on the heart, improving symptoms of heart failure. Typically, after a period of several months, surgical debanding and VSD closure are performed under improved clinical conditions.

Over the past 20 years, interventional closure using dedicated VSD closure devices such as coils, plugs, or discs has been developed. Interventional VSD closure has become the standard of care for selected patients, especially for muscular VSDs, small to moderate perimembranous or subpulmonary VSDs.

26.7 Outcome

In small ventricular septal defects (VSDs), regular clinical follow-up is sufficient, and these patients do not require intervention. However, in some cases of small VSDs with a low shunt fraction (<1.5:1), even this small volume load may lead to the development of atrial arrhythmias (such as atrial flutter or fibrillation) in young adulthood. In such situations, VSD closure may be indicated to prevent these arrhythmias.

For mid-sized and large VSDs, closure is generally recommended. When closure is performed before the onset of pulmonary vascular obstructive disease, the surgical mortality rate is now less than 1%, and the long-term prognosis is excellent. However, long-term follow-up studies have shown that older patients (over 40 years of age) who underwent surgical VSD closure in early childhood (before 2 years of age) may have an increased incidence of relevant arrhythmias. Therefore,

a lifelong surveillance strategy is important to monitor and manage any potential complications.

Patients with Eisenmenger syndrome, a specific condition characterized by a reversal of the shunt flow due to severe pulmonary hypertension, require special attention and care in dedicated departments for grown-up congenital heart (GUCH) patients. These specialized units ensure comprehensive management and follow-up for individuals with complex congenital heart defects, including VSDs associated with Eisenmenger syndrome.

Human Genetics of Ventricular Septal Defect

27

Andreas Perrot and Silke Rickert-Sperling

Abstract

Ventricular septal defects (VSDs) are recognized as one of the commonest congenital heart diseases (CHD), accounting for up to 40% of all cardiac malformations, and occur as isolated CHDs as well as together with other cardiac and extracardiac congenital malformations in individual patients and families. The genetic etiology of VSD is complex and extraordinarily heterogeneous. Chromosomal abnormalities such as aneuploidy and structural variations as well as rare point mutations in various genes have been reported to be associated with this cardiac defect. This includes both well-defined syndromes with known genetic cause (e.g., DiGeorge syndrome and Holt–Oram syndrome) and so far undefined syndromic forms characterized by unspecific symptoms. Mutations in genes encoding cardiac transcription factors (e.g., *NKX2-5* and *GATA4*) and signaling molecules (e.g., *CFC1*) have been most frequently found in VSD cases. Moreover, new high-resolution methods such as comparative genomic hybridization enabled the discovery of a high number of different copy number variations, leading to gain or loss of chromosomal regions often containing multiple genes, in patients with VSD. In this chapter, we will describe the broad genetic heterogeneity observed in VSD patients considering recent advances in this field.

A. Perrot
Experimental and Clinical Research Center, a Cooperation Between the Max Delbrück Center for Molecular Medicine in the Helmholtz Association and Charité Universitätsmedizin Berlin, Berlin, Germany

S. Rickert-Sperling (✉)
Cardiovascular Genetics, Charité – Universitätsmedizin Berlin, Berlin, Germany
e-mail: silke.sperling@charite.de

© The Author(s), under exclusive license to Springer Nature Switzerland AG 2024

S. Rickert-Sperling et al. (eds.), *Congenital Heart Diseases: The Broken Heart*,
Advances in Experimental Medicine and Biology 1441,
https://doi.org/10.1007/978-3-031-44087-8_27

Keywords

Ventricular septal defect · VSD · Atrial septal defect · ASD · Ventricular septum · Whole exome sequencing · WES · Down syndrome · Trisomy 21 · Patau syndrome · Trisomy 13 · Edwards syndrome · Trisomy 18 · Pallister–Killian syndrome · 22q11 deletion syndrome · DiGeorge syndrome · Velocardiofacial syndrome · Wolf–Hirschhorn syndrome · Cri-du-chat syndrome · Sotos syndrome · Williams–Beuren syndrome · Kleefstra syndrome · Jacobsen syndrome · Potocki–Lupski syndrome · Copy number variation · CNV · TBX1 · CRKL · PRKAB2 · FMO5 · CHD1 · BCL9 · ACP6 · GJA5 · GATA4 · SOX7 · NTRK3 · TBX5 · Holt–Oram syndrome · TBX3 · Ulnar–mammary syndrome · Townes–Brock syndrome · SALL1 · Okihiro syndrome · SALL4 · Char syndrome · TFAP2B · Oculofaciocardiodental syndrome · BCOR · Ellis–van Creveld syndrome · EVC1 · EVC2 · Blepharophimosis syndrome · FOXL2 · GATA6 · Diaphragmatic hernia · Mowat–Wilson syndrome · ZFHX1B · Pelger–Huet anomaly · LBR · Alagille syndrome · NOTCH1 · NOTCH2 · JAG1 · Adams–Oliver syndrome · Ras/MAPK · Noonan syndrome · PTPN11 · Noonan-like syndrome · SHOC2 · Costello syndrome · HRAS · Robinow syndrome · WNT5A · DVL1 · ROR2 · Muenke syndrome · FGFR3 · Cornelia de Lange syndrome · NIPBL · Opitz syndrome · MID1 · CHARGE syndrome · CHD7 · Sotos syndrome · NSD1 · Kabuki syndrome · MLL2 · Frank–ter Haar syndrome · SH3PXD2B · Simpson–Golabi–Behmel syndrome · GPC3 · Marfan syndrome · Hypophosphatemia · FBN1 · Peters plus syndrome · B3GALTL · Larsen-like syndrome · NKX2-5 · NKX2-6 · TBX20 · ZIC3 · IRX4 · CITED2 · PITX2 · TGFβμ CRYPTIC · CFC1 · GDF3 · Nodal · NF1 · MYH6 · MYH7 · Noncompaction · LVNC · TNNI3 · MKRN2 · HAS2 · GWAS · TBX15 · MAML3 · TDGF1 · MESP1 · ISL1 · ADCY2 · CACNA1D · CACNA1S · CACNA1F · PLCB2 · ACTC1 · KMT2A · SCN5A · Brugada syndrome · MYBPC3 · SMAD2 · HEY2 · MEIS2 · NF1 · Neurofibromatosis · GWAS

27.1 Introduction

Ventricular septal defects are recognized as one of the commonest congenital heart defects, accounting for up to 40% of all cardiac malformations [1, 2]. They can be classified according to their location, either within the muscular septum (muscular defects) at its margins (perimembranous and supracristal defects) or in the inflow portion (inlet ventricular septal defect) (see Chap. 22) [1]. Further, ventricular septal defect (VSD) is not only a common isolated congenital heart disease (CHD) but is often associated with other congenital cardiac defects, either in an individual or within a family. This heart defect also exists as an intrinsic component of several complex malformations, including tetralogy of Fallot (see Chap. 31) and univentricular hearts (see Chap. 49) [1].

Epidemiologic studies strongly suggest that genetic factors play an important role in CHD etiology, although environmental exposures are also relevant (see Chap. 16)

[3]. In a nation-wide population-based study, Oyen et al. reported that CHDs in general show highly variable familial clustering in first degree relatives and indicated a threefold recurrence risk for isolated VSD [4]. In the following chapter, we will focus on the role of genetic factors associated with ventricular septal defects and describe their various genetic causes including chromosomal aberrations, structural variants, and single disease genes and mutations.

27.2 Isolated VSD

A number of studies have shown that isolated VSDs (without further cardiac and/or extracardiac congenital defects) can be associated with copy-number variations as well as single-gene mutations in patients and related families. Of note, the affected families often comprise individuals showing isolated VSDs as well as individuals with VSD and other CHDs (the latter will be presented in Sect. 3).

27.2.1 Copy Number Variation in Isolated VSD

A copy number variation (CNV) is a structural genomic variant that results in confined copy-number changes in a specific chromosomal region that often contains multiple contiguous genes [5]. This leads to altered dosage of such genes encompassed by the CNV. Commonly, CNVs are defined as any submicroscopic chromosomal changes affecting more than 1,000 bases [6]. CNVs can occur *de novo*, or be inherited. Frequently, microdeletions and microduplications are identified by high-resolution comparative genomic hybridization (array CGH) as changes of DNA quantity (see Chap. 18) [5].

Studies analyzing CNVs commonly used cohorts of patients with a broad range of different CHDs [7–11]. To date, in five studies analyzing a range of CHDs including isolated VSDs, a total of eight affected loci have been identified with the chromosomal region 22q11.2 and 8p23.1 being most frequently affected. At the 22q11.2 locus, the *TBX1* gene (transcription factor T-box 1) known to be implicated in DiGeorge syndrome (see Sect. 4.2) was duplicated in one familial case [7], while the protein kinase *CRKL* gene (V-Crk avian sarcoma virus CT10 oncogene homolog-like) was affected in two independent patients [10, 11]. The locus 8p23.1 contains the candidate genes *GATA4* (transcription factor GATA-binding protein 4), playing an important role in cardiac development (see Sect. 2.2.1), and *SOX7* (SRY (sex-determining region Y)-box 7) [9, 10]. Rare copy-number gains at the locus 11q25 were found in two patients but not associated with known risk genes [7, 8]. A summary of all CNVs found in isolated VSD cases is given in Table 27.1.

Table 27.1 Copy-number variation in isolated VSD

Cytoband	CNV start (hg18)	CNV end (hg18)	Size	Copy number	Candidate genes	References
1q21.1 22q11.2	144723763 19389671		1574 kb 406 kb	Deletion Duplication	*ACP6, BCL9, CHD1L, FMO5, GJA5, PRKAB2* *CRKL*	[10]
2p22.3	32.51 Mb	33.21 Mb	0.70 Mb	Duplication	*LTBP1*	[7]
3p14.2				Deletion		[9]
3p22.1				Deletion		[9]
3q25				Deletion		[9]
3q29				Duplication		[9]
5q31.3				Deletion		[9]
6p12.1	55356489	55493937	137 kb	Deletion		[11]
6q24.1	142187041	142290373	103 kb	Deletion		[11]
8p23.1				Deletion	*GATA4*	[9]
8p23.1				Duplication		[9]
8p23.1	8027361		4456 kb	Deletion	*GATA4, SOX7*	[10]
9p24.1	6770364	6953533	183 kb	Deletion		[11]
9q33.2	124774046	125024684	251 kb	Duplication		[11]
11p13	34458230[a]	34460862[a]	2.6 kb	Deletion		[8]
11p15.4				Deletion		[9]
11q25	134598043[a]	134617838[a]	19.8 kb	Duplication		[8]
11q25	132.23 Mb	132.76 Mb	0.53 Mb	Duplication		[7]
14q32.12	92475603	92709736	234 kb	Duplication		[11]
15q11.2	20384417		251,468 bp	Deletion		[9]
15q13.3				Duplication		[9]
16p13.11				Duplication		[9]
17q12				Duplication		[9]
18q11.1-11.2	16795645		6118 kb	Duplication	*GATA6*	[10]
18q22.1				Duplication		[9]

18q23	75996798	75076224	921 kb	Duplication	*NFATC1*	[11]
20p12.3				Duplication		[9]
20q13.2				Duplication		[9]
22q11.2	17.39 Mb	19.74 Mb	2.35 Mb	Duplication	*TBX1, CRKL*	[7]
22q11.2				Deletion		[9]
22q11.2	19051034	19825156	774 kb	Deletion		[11]
Xq28	153436333	154895334	1.5 Mb	Deletion		[11]

Each row refers to one case
hg18 human reference genome (full sequence) version 18, *kb* kilobases, *Mb* megabases, *bp* basepairs
[a] Genomic coordinates refer to hg19

27.2.2 Single-Gene Defects in Isolated VSD

In patients with isolated VSD, a number of different mutations have been found in genes encoding for transcription factors, signaling molecules, and proteins of other functions (see Table 27.2).

27.2.2.1 Transcription Factors

The development of the heart is orchestrated by transcription factor (TF) networks including members of the NK2 homeobox, T-box, and GATA-binding families (see Chap. 12) [31]. GATA-binding protein 4 (GATA4) is a transcriptional activator found to be affected in sporadic and familial cases of isolated VSD. Three different missense mutations in the *GATA4* gene (p.Pro407Val, p.Ser175Cys, and p. Ala411Val) have been reported in sporadic cases [13–15]. In addition, two families carrying *GATA4* missense mutations (p.Arg43Trp and p.Gly296Arg) were discovered in a follow-up analysis of index patients that participated in a screen of unrelated individuals (see also Sect. 3.2.1) [16, 17]. In the follow-up of affected family members, two and four additional cases of isolated VSD were found in the studies by Wang et al. [16] and Yang et al. [17], respectively.

So far, mutations affecting three members of the T-box family, namely, TBX1, TBX5, and TBX20, have been associated with isolated VSDs. Pan et al. screened 230 CHD cases and observed a heterozygous nonsense mutation (p.Gln277X) in the DNA-binding domain of *TBX1* in one patient with double outlet right ventricle who had one affected relative with isolated VSD carrying the same mutation (see also

Table 27.2 Single-gene defects in isolated VSD

Gene	Protein function	References
Transcription factors (TF)		
CITED2	Transcriptional coactivator	[12]
GATA4	GATA-binding TF	[13–17]
IRX4	Iroquois homeobox TF	[18]
NKX2-6	Homeobox TF	[16]
PITX2	Homeodomain TF	[19]
TBX1	T-box TF	[20]
TBX5	T-box TF	[21]
TBX20	T-box TF	[22]
MESP1	Basic helix-loop-helix TF	[23]
ISL1	Homeodomain TF	[24]
Signaling molecules		
CFC1	Ligand (TGFβ signaling)	[25]
GDF3	Ligand (TGFβ signaling)	[26]
TDGF1	Coreceptor (TGFβ signaling)	[27]
ADCY2	Adenylate cyclase (cAMP signaling)	[28]
Other genes		
HAS2	Hyaluronan synthase	[29]
MYH6	Myosin heavy chain	[30]

Sect. 3.2.1) [20]. A missense mutation (p.Ile152Met) in *TBX20* causing impaired DNA binding was found in a family affected by multiple septal defects including isolated VSD, atrial septal defect (ASD), and a large patent foramen ovale in different relatives [22].

A study focusing on the analysis of *PITX2* (paired-like homeodomain 2) in a cohort of 170 unrelated neonates with CHD found two missense mutations (p.Arg91Gln and p.Thr129Ser) in two affected families [18]. Four mutation carriers presented with isolated VSD whereas two other relatives showed transposition of the great arteries (TGA) with VSD (see Sect. 3.2.1) [19].

Mutations have also been identified in the TF genes *NKX2-6*, *CITED2*, and *IRX4* [12, 18, 32]. Screening a CHD cohort including 66 isolated VSD cases, Wang et al. identified a missense mutation (p.Lys152Gln) in the homeodomain of *NKX2-6* (NK2 homeobox 6) [32]. Subsequent analysis identified the mutation in two further family members with isolated VSDs [32]. In a cohort of nearly 400 sporadic CHD cases, a nine amino acid deletion (p.Ser170_Gly178del) in *CITED2* (Cbp/P300-interacting transactivator, with Glu/Asp-rich carboxy-terminal domain, 2), resulting in impaired activity, was detected in one patient with isolated perimembranous VSD [12]. For the ventricle-specific TF *IRX4* (Iroquois homeobox 4), two missense mutations (p.Asn85Tyr and p.Glu92Gly) were reported in two unrelated patients with isolated VSD by direct sequencing of the gene in a cohort of about 700 CHD patients [18]. The two mutations affected the interaction with retinoid X receptor alpha, a nuclear receptor of the vitamin A signaling pathway important in cardiac morphogenesis.

Werner et al. found four pathologic variants (two missense mutations, one duplication, and one loss-of-function frameshift mutation) in four unrelated patients with isolated VSD in the TF gene *MESP1* (encoding mesoderm posterior basic helix-loop-helix transcription factor 1), an early regulator of cardiac development [23].

Finally, the prominent role of transcriptional regulation in CHD predicts that mutations affecting regulatory elements may contribute to septal defects [33]. There are two interesting studies concerning VSD cases. Screening 200 patients with isolated and sporadic VSD, Zheng et al. identified three variants in the promoter of *ISL1* (encoding ISL LIM homeobox 1) which significantly altered the expression of the *ISL1* gene and affected the binding of other TFs [24]. The encoded protein binds to the enhancer region of the insulin gene, among others; it marks cardiac progenitor cells and is involved in a variety of multipotent cardiac cell lineages [24]. In the case of *TBX5*, a noncoding variant in one of its enhancers was suggested to impact on the development of VSD [21]. The variant was found homozygous in a case of isolated VSD with unaffected heterozygous parents and was supported by functional evidence based on transgenic expression studies in mouse and zebrafish [21].

27.2.2.2 Signaling Molecules

Various cellular processes in both the embryonic and adult organism are regulated via transforming growth factor beta (TGFβ) signaling pathways. Important developmental steps, such as the establishment of left–right asymmetry, are driven by the NODAL signaling pathway, which is named after the TGFβ superfamily member of

the same name (see Chap. 7). Two genes encoding cofactors of the NODAL signaling pathway, *TDGF1* (teratocarcinoma-derived growth factor 1 also known as CRIPTO) and *CFC1* (Cripto, FRL-1, Cryptic family 1 also known as CRYPTIC), have been analyzed in a cohort of 500 CHD cases [25, 27]. Three missense mutations, p.Arg41Gly in *TDGF1* [27] as well as p.Leu219Phe and p.Gly169Val in *CFC1* [25], were identified in three patients with isolated VSD (see also Sect. 3.2.2). Another member of the NODAL signaling pathway, *GDF3* (growth differentiation factor 3), was analyzed by Xiao et al. [26]. Direct sequencing of *GDF3* in a cohort of 200 CHD patients led to the identification of a missense mutation (p.Ser212Leu) in a patient with isolated muscular VSD [26].

Izarzugaza et al. used WES to analyze 32 Danish families with recurrent CHD [28]. They identified a small family with two patients with isolated VSD carrying a splice site variant in *ADCY2* encoding adenylate cyclase 2, a membrane-associated enzyme catalyzing the formation of the secondary messenger cyclic adenosine monophosphate (cAMP). Functional investigation of the zebrafish ortholog of *ADCY2* verified a role in cardiac development [28].

27.2.2.3 Other Genes

The gene *HAS2* encodes hyaluronan synthase 2, an enzyme that synthesizes hyaluronic acid (a major component of the extracellular matrix) during embryogenesis [29]. Among 100 nonsyndromic VSD cases, Zhu et al. detected a *HAS2* missense mutation (p.Glu499Val) in one patient. The synthesis of hyaluronic acid was significantly impaired in the mutant enzyme as shown by *in vitro* assays [29].

Screening 16 CHD genes via a targeted gene panel on an Illumina platform, Pulignani et al. analyzed a cohort of 68 CHD patients excluding syndromic forms [30]. They identified three different missense mutations in three cases with isolated VSD in the gene *MYH6* encoding myosin heavy chain 6, a sarcomeric motor protein expressed in cardiac muscle [30]. Interestingly, this gene is a validated disease gene for another common septal defect, i.e., ASD (see Chap. 20).

27.3 Nonsyndromic VSD

VSDs do not only occur as isolated malformations but most frequently are part of a more complex malformation. In the absence of extracardiac malformations, these VSDs are classified as "nonsyndromic" (in contrast to syndromic VSD; see Sect. 4). Of note, VSD is an intrinsic component of complex malformations such as tetralogy of Fallot and double outlet right ventricle as well as univentricular hearts (see Chaps. 31 and 49, respectively).

27.3.1 Copy-Number Variation in Nonsyndromic VSD

Two microduplications and two microdeletions were described in four cases of VSD with additional cardiac malformations (see Table 27.3) [7, 10]. Tomita-Mitchell

Table 27.3 Copy-number variation in nonsyndromic VSD

Cytoband	CNV start (hg18)	CNV end (hg18)	Size	Copy number	Candidate genes	References
1q21.1	144812585		1480 kb	Duplication	*ACP6, BCL9, CHD1L, FMO5, GJA5, PRKAB2*	[10]
4q32.3	167.52 Mb	169.28 Mb	1.76 Mb	Duplication		[7]
17p11.2	16.47 Mb	16.47 Mb	3.98 Mb	Deletion		[7]
22q11.2	17.39 Mb	20.00 Mb	2.61 Mb	Deletion	*TBX1*	[7]

Each row refers to one case
hg18 human reference genome (full sequence) version 18, *kb* kilobases, *Mb* megabases

et al. analyzed a cohort of several hundred CHD cases and identified among others one patient with VSD and pulmonary atresia who carried a duplication at the locus 1q21.1 comprising candidate genes such as *CHD1* (chromodomain helicase DNA-binding protein 1) and *GJA5* (gap junction protein alpha 5, 40 kDa; also known as connexin 40) [10]. Screening a cohort of 105 CHD patients by array CGH, Erdogan et al. found a deletion at the 22q11.2 locus (including *TBX1*) in a case of VSD and aortic coarctation [7]. Further, they detected a duplication at chromosome 4q32.3 in one patient with VSD and persistent ductus arteriosus (PDA) and a large 4 megabase deletion at chromosome 17p11.2 in a patient with VSD and ASD. No evident candidate genes have been identified in either of these regions [7].

27.3.2 Single-Gene Defects in Nonsyndromic VSD

Mutations have been reported in transcription factors, signaling molecules, sarcomeric proteins, Calcium signaling proteins, and other proteins in patients and families with nonsyndromic VSD (see Table 27.4).

27.3.2.1 Transcription Factors

The evolutionary highly conserved homeobox factor *NKX2-5* controls the expression of various cardiac genes during heart development [31]. Frameshift and missense mutations in the DNA-binding domain of *NKX2-5* have been described in six families mainly affected by ASD and atrioventricular conduction block, but also showing other CHDs [35–38]. In total, 11 affected mutation carriers from those families showed additional VSDs [35–38]. Moreover, screening of 135 sporadic CHD cases revealed an *NKX2-5* missense mutation (p.Pro283Gln) in a patient characterized by VSD, ASD, and PDA [13].

Direct interaction partners of NK2 homeobox 5 include the cardiac TFs T-box 5 and GATA-binding protein 4. In a large pedigree with familial ASD, Garg et al. described a *GATA4* missense mutation (p.Gly296Ser) located between the nuclear

Table 27.4 Single-gene defects in nonsyndromic VSD

Gene	Protein function	References
Transcription factors (TF)		
GATA4	GATA-binding TF	[16, 17, 34]
NKX2-5	Homeobox TF	[13, 35–38]
PITX2	Homeodomain TF	[19]
TBX1	T-box TF	[20]
TBX5	T-box TF	[39]
ZIC3	Zink finger TF	[40]
HEY2	Transcriptional repressor	[41]
NR2F2	Nuclear receptor TF	[42, 43]
MESP1	Basic helix-loop-helix TF	[23]
Signaling molecules		
NF1	RAS signaling	[44]
NOTCH1	Notch signaling	[45, 46]
SMAD2	TGFβ signaling	[47]
Sarcomere genes		
MYH7	Thick filament	[48, 49]
MYH6	Thick filament	[50]
MYBPC3	Thin filament	[51]
TNNI3	Thin filament	[52]
ACTC1	Thin filament	[53]
Calcium signaling genes		
CACNA1D	Calcium voltage-gated channel subunit	[28]
CACNA1S	Calcium voltage-gated channel subunit	[28]
CACNA1F	Calcium voltage-gated channel subunit	[28]
Other genes		
PLCB2	Phosphodiesterase	[28]
KMT2A	Methyltransferase	[53]
PLD1	Phospholipase	[54]
SCN5A	Ion channel (sodium)	[55]

localization sequence and one of two *GATA4* zinc fingers, which altered the interaction between *GATA4* and *TBX5* [34]. Three affected mutation carriers in that family presented with an additional VSD [34]. Furthermore, sequencing of *GATA4* in two VSD cohorts revealed two missense mutations (p.Arg43Trp and p.Gly296Arg) in two families [16, 17]. Besides isolated VSDs, affected family members presented VSDs in combination with ASD in three cases and with PDA in one case (see also Sect. 2.2.1) [16, 17]. A dominantly inherited novel *TBX5* stopgain variant (p. Tyr407*) segregating with all six affecteds was identified in a family with atrial and ventricular septal defects by Szot et al. using WES [38]. A nonsense mutation (p. Gln277X) in another T-box TF, meaning *TBX1,* has been found in a family including relatives with isolated VSD as well as one individual with VSD and PDA (see Sect. 2.2.1) [20].

Additional cardiac TF genes mutated in patients with nonsyndromic VSD comprise *ZIC3* (Zic family member 3) and *PITX2*. *ZIC3*, a zinc finger TF known for its association with laterality defects (see Chap. 38), was mutated in one sporadic heterotaxy case showing VSD in combination with ASD, pulmonary stenosis, and TGA [40]. Wei et al. identified two subjects with VSD and TGA from two affected families who carried *PITX2* missense mutations (see also Sect. 2.2.1) [19].

Van Walree et al. presented a large family affected by CHD, thoracic aortic aneurysm, noncompaction, and valve abnormalities [40]. The authors identified a loss-of-function variant (p.Gly108*) in HEY2 (Hes related family BHLH transcription factor with YRPW motif 2), a transcriptional repressor that regulates cardiogenesis in vertebrates. All homozygous mutation carriers showed a VSD (besides other cardiac lesions), whereas only 15% of heterozygous carriers had a VSD [41].

Two studies showed mutations in the pleiotropic TF *NR2F2* (nuclear receptor subfamily 2 group F member 2) required for normal cardiovascular development [42, 43]. First, Al-Turki et al. identified a small family with an in-frame duplication (p.Gln75dup) in a family member with VSD and aortic stenosis and showed that the variant altered the activity of NR2F2 on target promoters [42]. Second, Qiao et al. found the novel p.Gly83X mutation in a patient with VSD as well as double outlet right ventricle; the mutant protein showed no transcriptional activity using a dual-luciferase reporter assay [43].

Mutations in *MESP1* (encoding mesoderm posterior basic helix-loop-helix transcription factor 1) were detected in patients with isolated VSD (see Sect. 2.2.1) as well as in a patient with VSD, coarctation of the aorta, and aortic atresia by Werner et al. [23].

27.3.2.2 Signaling Molecules

As described before, various signaling pathways are active during cardiac development such as the NODAL signaling pathway (see Sect. 2.2.2), the Notch signaling pathway, and the TGFβsignaling pathway.

In a cohort of 362 severe CHD cases, the *NF1* gene encoding neurofibromin 1, a negative regulator of the RAS signaling pathway, was found to be mutated in one case with VSD accompanied by pulmonary atresia and multiple aorticopulmonary collaterals [44].

Two studies could identify pathogenic variants in *NOTCH1* encoding Notch receptor 1 involved in the Notch signaling pathway important for cardiac cell fate regulation and morphogenesis of cardiac chambers and valves [45, 46]. Using familial based WES, Preuss et al. found two highly conserved missense mutations in cis (p.Gly578Ala and p.Arg1287His) which segregated with CHD on the same haplotype in relatives of one family with tetralogy of Fallot or VSD [45]. The *NOTCH1* gene was sequenced in 428 patients with left-sided CHD by Kerstjens-Frederikse et al. [46]. Among 14 families, they identified three individuals as mutation carriers who showed a VSD and valve defects; these individuals presented with a splice site mutation (c.865+2C>A), a truncating mutation (p.Tyr550*), and a frameshift mutation (p.Gly557fs), respectively [46].

Granadillo et al. used WES in four patients with complex CHD to find pathogenic variants in *SMAD2* (SMAD family member 2), a downstream effector in the TGFβμ signaling pathway which is important for pattern formation and tissue differentiation [47]. Three patients carrying a *SMAD2* mutation showed VSD and ASD, among other features; two were further characterized by PDA, double outlet right ventricle and valve abnormalities [47].

27.3.2.3 Sarcomere Genes

Contraction of the heart involves the shortening of sarcomeres by the ATP-dependent interaction between thin (actin) and thick (myosin) filaments (see Chap. 17). Mutations in genes encoding sarcomeric proteins have been well established as disease-causing for ASD (see Chap. 20) and different forms of cardiomyopathy (see Chap. 59).

For *MYH7* encoding cardiac specific β-myosin heavy chain, two mutations (p.Met362Arg and p.Glu1220del, respectively) in two families characterized by Ebstein's anomaly (EA), left ventricular noncompaction cardiomyopathy (LVNC), and VSD were reported [48, 49]. Two mutation carriers from each family showed the phenotype with the combination of EA, LVNC, and VSD [48, 49]. The other important cardiac heavy chain gene is *MYH6* encoding α-myosin, which is highly expressed in embryonic heart. Jin et al. identified a rare missense mutation (p.Arg1610Cys) in *MYH6* in a patient with VSD and ASD [50].

Of note, two further patients with sarcomeric mutations showed VSD in combination with LVNC [51, 53]. The study by Wessels et al. described a neonate with feeding problems and dyspnea with compound heterozygosity for the pathogenic p.Trp792fs and p.Arg943* mutations in *MYBPC3*, the cardiac myosin-binding protein C-binding thick filaments and titin [51]. WES was performed in a cohort of 98 CHD patients from Nigeria by Ekure et al. [53]. They identified one patient with the missense mutation p.Ser235Phe in ACTC1 encoding cardiac α-actin 1, a major constituent of the thin filament [53].

Troponin I (encoded by *TNNI3*) is a cardiac specific thin filament component important for Calcium sensing during contraction of the heart muscle. Yang et al. detected a *de novo* missense mutation in *TNNI3* (p.Arg204His) in a patient first diagnosed with perimembranous VSD who then gradually developed restrictive cardiomyopathy [52].

27.3.2.4 Calcium Signaling Genes

Voltage-dependent calcium channels mediate the entry of calcium ions into excitable cells; intracellular calcium plays essential roles in physiology and pathophysiology of the heart. Although mutations in calcium handling genes mainly cause arrhythmia, Izarzugaza et al. were the first to describe pathogenic variants in the calcium voltage-gated channel subunits alpha1 D (*CACNA1D*), alpha1 F (*CACNA1F*), and alpha1 S (*CACNA1S*) in CHD patients (see also Sect. 2.2.2) [28]. They detected the *CACNA1D* mutation p.Ala376Val in a patient with VSD and ASD, the *CACNA1F* mutation p.Thr59Ala in a patient with VSD, ASD and pulmonary valve stenosis, and the *CACNA1S* mutation p.Pro1767Thr in a patient with VSD and AVSD [28].

27.3.2.5 Other Genes

The gene *PLCB2* (phospholipase C beta 2) belongs to the phospholipase family of enzymes that hydrolyze phospholipids into fatty acids and other lipophilic molecules. Izarzugaza et al. identified a family member with VSD and PDA of a CHD family carrying a *PLCB2* missense mutation [28]. Functional validation of *PLCB2* in a zebrafish model confirmed a critical role during embryonic heart development; defects in cardiac morphology and laterality in a significant proportion of fish embryos injected with morpholinos targeting plcb2 were detected [28].

A female patient with the same phenotype was found by Ekure et al. [53]. She carried a *de novo* duplication leading to a frame shift (p.Met1009Profs*11) in *KMT2A* encoding lysine methyltransferase 2A, a transcriptional coactivator involved in methylation of lysine residues on histones that plays an essential role in regulating gene expression during early development [53].

Lahrouchi et al. identified 30 patients from 21 unrelated families of different ancestries with biallelic phospholipase D1 (*PLD1*) variants who presented predominantly with congenital cardiac valve defects. Among these patients were two individuals also having a VSD; they carried the recessive missense variants p.Gly826Arg and p.His442Pro, respectively [54]. The authors observed a strong reduction in enzymatic activity for most of the mutant proteins and further showed that *PLD1* is required for endocardial cell endothelial-mesenchymal transition [54].

Finally, the case report by Liu et al. presented a grown-up patient with conduction disease and syncope diagnosed with Brugada syndrome combined with a VSD [55]. Brugada syndrome is an inherited disorder confined to the heart characterized by a specific electrocardiogram pattern and increased risk of sudden cardiac death. Subsequently, the variant p.Glu654X in the established Brugada syndrome gene *SCN5A* encoding Sodium voltage-gated channel alpha subunit 5 was identified by WES and variant filtering [55]. This protein is found primarily in cardiac muscle and is responsible for the initial upstroke of the action potential in an electrocardiogram.

27.4 Syndromic VSD

In the following section, we describe VSDs observed in patients showing additional congenital malformations in other organs. Those so-called syndromic forms include well-defined syndromes with known genetic cause (e.g., DiGeorge syndrome) as well as so far undefined syndromic forms with unspecific symptoms such as mental retardation and dysmorphic features of unknown genetic etiology. For further reading, the scientific statement “Genetic Basis for Congenital Heart Disease: Revisited” of the American Heart Association provided an extensive table of syndromes associated with CHD and described in detail common clinical features of most of these syndromes [56].

27.4.1 Aneuploidy Syndromes

Chromosomal aneuploidy is the presence of an abnormal number of chromosomes in the cell leading to various syndromic genetic disorders. Aneuploidies that commonly survive to term include trisomy 21, 18, and 13 and sex chromosome aneuploidies such as Turner syndrome. Aneuploidy syndromes can occur with almost any cardiac malformation [57]. The large number of genes that are dysregulated in the setting of aneuploidy results in effects in development that are often pleiotropic and severe; 98% of fetuses with cytogenetic abnormalities and CHD have at least one extracardiac abnormality [33].

CHD occurs in about 45–50% of patients with Down syndrome (trisomy 21), the most common aneuploidy syndrome [58, 59]. Källen et al. showed in a large epidemiologic study with more than 5,000 patients with trisomy 21 that VSD was present in 28% of individuals with cardiac malformation [60]. In the National Down Syndrome Project cohort, Freeman et al. found a VSD rate of 19% regarding all registered infants (65% were membranous and 35% were muscular VSDs) [59]. A retrospective cohort study including about 4300 Down syndrome patients undergoing CHD surgery was performed by Fudge et al. to examine postoperative outcomes [61]. VSD closure of any type was the second most common procedure (19%) performed for patients with Down syndrome [61].

Further, CHD occurs in about 35% of cases of Patau syndrome (trisomy 13) and about 45% of cases with Edwards syndrome (trisomy 18) as Pont et al. described in a large epidemiologic study of hospitalizations of live-born infants with chromosomal abnormalities [62]. VSD was the most common heart defect in trisomy 13 (18%) and in trisomy 18 (31%) [62]. Pallister–Killian syndrome, a sporadic multisystem developmental disorder, is typically caused by the presence of a supernumerary isochromosome composed of the short arms of chromosome 12 resulting in tetrasomy 12p [63]. Tilton et al. evaluated 30 patients with this syndrome and CHD and found a VSD in 10% of those [63].

27.4.2 Copy-Number Variation in Syndromic VSD

A number of studies have shown the importance of CNVs, mainly microdeletions and microduplications, in syndromic CHD [57, 64]. Those studies reported subjects with well-known syndromes as well as so far undefined syndromic forms. CNVs that encompass multiple genes can have a wide range of phenotypic effects because of the additive impact of individual genes on individual phenotypes or the pleiotropic effects of single genes on multiple phenotypes [56].

Table 27.5 includes clinically delineated microdeletion and microduplication syndromes, where a specific association to VSD was described. Of note, the most frequent genomic disorder associated with CHD is DiGeorge syndrome (DGS; 22q11 deletion or velocardiofacial syndrome) (see, e.g., Chap. 38). Cardiovascular anomalies are present in about 80% of neonates with DGS [65]. Ryan et al. evaluated a cohort of 545 DGS patients and could show that VSDs were observed in 14% of

Table 27.5 Copy-number variation in well-defined syndromic VSD

Cytoband	Copy number	Syndrome	Candidate genes[a]	References
4p16.3	Deletion	Wolf–Hirschhorn	*WHSC1, FGFRL1*	[69]
5p15.2	Deletion	Cri-du-chat	*TERT*	[70]
5q35.2-q35.3	Deletion	Sotos	*NSD1*	[71]
7q11.23	Deletion	Williams–Beuren	*ELN*	[67]
9q34.3	Deletion	Kleefstra	*EHMT1*	[72]
11q23	Deletion	Jacobsen	Not specified	[73]
17p11.2	Deletion	Smith–Magenis	*RAI1*	[74]
17p11.2	Duplication	Potocki–Lupski	*MAPK7*	[68]
22q11.2	Deletion	DiGeorge	*TBX1*	[64, 66]

Abbreviations: *WHSC1* Wolf–Hirschhorn syndrome candidate 1, *FGFRL1* fibroblast growth factor receptor-like 1, *TERT* telomerase reverse transcriptase, *NSD1* nuclear receptor-binding SET domain protein 1, *ELN* elastin, *EHMT1* euchromatic histone-lysine *N*-methyltransferase 1, *RAI1* retinoic acid induced 1, *MAPK7* mitogen-activated protein kinase 7, *TBX1* T-box 1

[a] These include known disease genes (such as TBX1 and ELN) as well as genes causing heart defects when deleted in mice and/or by mutations in CHD patients

these patients (among other heart defects) [66]. Momma described in his review of several studies of DGS cohorts (ranging from 100 up to 222 patients) quite similar VSD rates [65]. All other syndromes show lower VSD rates. For example, in Williams–Beuren syndrome (caused by a deletion of about 1.5 megabases in chromosome 7q11.23), VSDs, mainly muscular ones (75%), are present in 4–9% of all patients [67]. A similar VSD rate (8%) was described by Jefferies et al. in patients with Potocki–Lupski syndrome whereby most individuals harbor a common 3.7 megabase duplication within chromosome 17q11.2 [68].

Besides well-known syndromes, there are a number of studies describing syndromic patients with VSD who present different unspecific symptoms (see Table 27.6).

Using array-based CGH, Syrmou et al. screened a cohort of 55 syndromic CHD patients and detected CNVs in 37 of them [75]. They found five patients with VSD showing either one CNV or a combination of up to three different deletions and duplications (ranging from 0.023 to 6.6 megabases) [75]. Through a genome-wide survey of two independent cohorts of CHD subjects with extracardiac abnormalities (700 subjects in total), Lalani et al. identified 16 CNV regions, present in two or more cases and absent in about 3000 controls [76]. Interestingly, one of the most frequent CNVs they found was a *de novo* copy-number loss of 16q24.3 (affecting *ANKRD11* encoding ankyrin repeat domain 11) in five subjects of whom four presented with VSD together with other CHDs (two with perimembranous and one each with muscular and conoventricular VSD) [76].

Screening a cohort of 60 syndromic CHD cases by array CGH, Thienpont et al. identified among others one patient with muscular VSD and various extracardiac manifestations showing a 3.8 megabase duplication at locus 19p13.12-13.11 [77]. Using the same detection method, a similar cohort of 90 patients was analyzed by Breckpot et al. [78]. They found two deletions at locus 1p36.33 (ranging from 3.5

Table 27.6 Copy-number variation in syndromic VSD with unspecific symptoms

Cytoband	CNV start (hg18)	CNV end (hg18)	Size	Copy number	Candidate genes	References
1p36.33	1 kb	4608–5866 kb	4.61–5.87 Mb	Deletion		[78]
1p36.33	1 kb	3514–3519 kb	3.51–3.52 Mb	Deletion		[78]
1q41 Xp11.3 Xq21.31			0.37 Mb 0.042 Mb 0.118 Mb	Duplication Deletion Deletion	*DISP1*	[75]
3p24.1-23	29,757 kb		1488 kb	Deletion		[80]
3q13.32 10q26.3 16p12.1			0.074 Mb 0.043 Mb 0.023 Mb	Duplication Deletion Duplication		[75]
4q34.1	185603346[b]	185638397[b]	35.1 kb	Deletion		[8]
5q21.1-21.2	100934417[a]	103557609[a]	2.6 Mb	Duplication		[79]
6p24.1-22.3			6.64 Mb	Deletion	*EDN1, DTNBP1, MYLIP*	[75]
6q24.2-25.1	143649–143708 kb	150253–150271 kb	6.62 Mb	Deletion		[78]
9p23	9163303[a]	9606645[a]	0.44 Mb	Deletion		[79]
10p12.1-11.21	28728683[a]	35905297[a]	7.1 Mb	Deletion	*NRP1*	[79]
15q26.1	86439405[a]	90753814[a]	4.3 Mb	Deletion	*NTRK3, MESP1*	[79]
16q24.3	86406011–86406037	87962518–87962533	1.58 Mb	Deletion	*ANKRD11*	[76]
16q24.3	86051611	88133224	2.07 Mb	Deletion	*ANKRD11*	[76]
16q24.3	87822867–87862929	88001859–88011936	139 kb	Deletion	*ANKRD11*	[76]
16q24.3			1.8 Mb	Deletion	*ANKRD11*	[76]
18p11.32	284494[a]	918189[a]	0.64 Mb	Duplication		[79]
19p13.12-13.11			3.86 Mb	Duplication		[76]
20p12.2 21q21.3			0.219 Mb 0.095 Mb	Duplication Duplication	*ADAMTS, ADAMTS5*	[75]
22q11.21	18351387[a]	20306802[a]	1.96 Mb	Deletion		[79]

Each row refers to one case
hg18 human reference genome (full sequence) version 18, *kb* kilobases, *Mb* megabases
[a] Genomic coordinates refer to hg17
[b] Genomic coordinates refer to hg19

to 5.9 megabases) in two patients with VSD and minor extracardiac malformations, one subject with additional hypertrophic cardiomyopathy and one with microcephaly [78].

Goldmuntz et al. analyzed 58 syndromic CHD cases and reported six different CNVs in six patients characterized by VSD and further congenital abnormalities and dysmorphic features such as cleft palate [79]. They detected copy-number gains at loci 5q21.1-21.2 and 18p11.32, whereas losses were detected for the loci 9p23, 10p12.1-11.21, 15q26.1, and 22q11.21 (ranging from 0.4 to 7.1 megabases in length) [79]. Analyzing several hundred CHD trios (nonsyndromic and syndromic cases) by SNP arrays and whole exome sequencing, a paternally inherited deletion of 35 kilobases at chromosome 4q34.1 was detected in a patient with VSD, TGA, and extracardiac manifestations [8]. Fakhro et al. genotyped a cohort of more than 250 heterotaxy cases by SNP arrays: they identified a heterozygous 1.5 megabase deletion at locus 3p24.1-23 (affecting *TGFBR2* encoding TGFβμreceptor II) in a patient characterized by VSD, ASD, partial anomalous pulmonary venous return, and situs inversus (see Chap. 38) [80].

27.4.3 Single-Gene Defects in Syndromic VSD

In addition to structural genomic variations, syndromic CHD can be caused by point mutations influencing the dosage of genes functioning in developmental pathways that are broadly used in organogenesis and therefore affecting many organs. As the patients covered in Sect. 4.2, the cases presented in the following section are also characterized by a variety of extracardiac manifestations. All described single-gene syndromes are summarized in Table 27.7.

27.4.3.1 Transcription Factors

Mutations in the transcription factor *TBX5* (T-box 5) cause Holt–Oram syndrome (HOS), which is characterized by upper-extremity malformations and cardiac defects including VSD [126] (see Chap. 20). Septal defects (VSD and ASD) are the most common cardiac malformations observed in HOS as Al-Qattan et al. showed in their meta-analysis of 16 different studies [126]. In total, 13 different TBX5 mutations (mostly missense ones) were associated with VSDs as part of complex cardiac malformations [126]. Borozdin et al. described VSDs in five out of 23 HOS patients with *TBX5* mutations of which four were accompanied by ASD [94]. Another T-box gene, *TBX3*, is causative to ulnar–mammary syndrome characterized by limb malformations and sporadically associated with VSDs [92, 93].

Cardiac malformations, in particular VSDs, are described in about 14% of Townes–Brocks syndrome patients, which are further characterized by hand and ear abnormalities and are caused by mutations in *SALL1* encoding spalt-like transcription factor, a zinc finger TF [89]. In contrast, mutations of *SALL4* (spalt-like transcription factor 4) cause Okihiro syndrome that is characterized by forearm and renal malformations (also known as Duane-radial ray syndrome) and rarely associated with VSD [90, 91].

Table 27.7 Single-gene defects in well-defined syndromic VSD

Gene	Protein function	Syndrome	References
Transcription factors			
BCOR	Transcriptional corepressor	Oculofaciocardiodental (OFCD) (X)	[81, 82]
EVC1, EVC2	Leucine zipper proteins	Ellis–van Creveld	[83, 84]
FOXL2	Forkhead TF	Blepharophimosis (AD)	[85, 86]
GATA6	GATA-binding TF	Diaphragmatic hernia	[87, 88]
SALL1	Spalt-like TF	Townes–Brocks	[89]
SALL4	Spalt-like TF	Okihiro	[90, 91]
TBX3	T-box TF	Ulnar–mammary	[92, 93]
TBX5	T-box TF	Holt–Oram	[94]
TFAB2B	AP-2 TF	Char	[95]
ZEB2/ ZFHX1B	Zinc finger homeobox TF	Mowat–Wilson	[96]
MEIS2	TALE homeobox TF	Chromosome 15q14 deletion	[97]
Signaling molecules			
FGFR3	Fibroblast growth factor	Muenke	[98]
HRAS	Ras/MAPK signaling	Costello	[99]
KRAS	Ras/MAPK signaling	Noonan 3	[100]
SOS1	Ras/MAPK signaling	Noonan 4	[101]
SHOC2	Ras/MAPK signaling	Noonan-like	[102]
NF1	Ras/MAPK signaling	Neurofibromatosis, type 1	[53]
JAG1, NOTCH2	Notch ligand, Notch signaling	Alagille	[103]
NOTCH1	Notch signaling	Adams–Oliver 5	[104]
PTPN11	Protein tyrosine phosphatase	Noonan 1	[105, 106]
ROR2	Receptor protein tyrosine kinase	Robinow (AR)	[107]
WNT5A, DVL1	Wnt signaling	Robinow (AD)	[108, 109]
Chromatin regulators			
CHD7	DNA helicase	CHARGE	[110]
MLL2	Methyltransferase	Kabuki	[111, 112]
NIPBL	Sister chromatid cohesin	Cornelia de Lange 1	[113, 114]
NSD1	Methyltransferase	Sotos (AD)	[115]
LBR	Chromatin binding	Pelger–Huet	[116]
Structural and cell adhesion molecules			
FBN1	Fibrillin	Marfan with hypophosphatemia (X)	[117]
GPC3	Proteoglycan	Simpson–Golabi–Behmel (X)	[118]
SH3PXD2B	Adapter protein	Frank–ter Haar (AR)	[119]
Enzymes for posttranslational modification			
B3GALTL	Glycosyltransferase	Peters plus	[120–122]
B3GAT3	Glucuronyltransferase	Larsen-like	[123]
Other			

(continued)

Table 27.7 (continued)

Gene	Protein function	Syndrome	References
DNAI1, DNAH5	Ciliary dynein arm proteins	Kartagener	[124]
MID1	RING finger ubiquitin ligase	Opitz (X)	[125]
MKRN2	E3 ubiquitin ligase	Heterotaxy	[44]

AD autosomal recessive, *AR* autosomal recessive, *X* X linked, *TF* transcription factor

VSDs are frequently seen in syndromes such as oculofaciocardiodental (OFCD), Ellis–van Creveld, Mowat–Wilson, and congenital diaphragmatic hernia with CHD. OFCD syndrome is an inherited X-linked dominant disorder caused by mutations in *BCOR* (BCL6 corepressor), a key transcriptional regulator during embryogenesis [81]. Ng et al. were the first to describe three OFCD patients who showed a VSD (one perimembranous, one subpulmonary, and one not further characterized VSD) [81]. In a later study, Hilton et al. presented six OFCD patients with VSD from 21 families showing that VSD was the second most common CHD in these patients [82].

Mutations in *EVC1* and *EVC2* (two leucine zipper transcription factors) lead to Ellis–van Creveld syndrome, which is mainly associated with atrioventricular septal defect and more sporadically with VSDs [83, 84] Mowat–Wilson syndrome is caused by mutations in *ZEB2 (ZFHX1B)* encoding a zinc finger E-box-binding factor and is frequently accompanied by cardiac malformations including VSD and ASD [96]. Mutations in *GATA6* have been found in familial cases of congenital diaphragmatic hernia accompanied by VSD [87, 88].

Char and blepharophimosis syndrome infrequently present with VSD. Char syndrome is caused by mutations in the gene *TFAP2B* (transcription factor AP-2 beta) and associates with PDA [94]. However, in one case, Char syndrome was accompanied by VSD [95]. Blepharophimosis syndrome is an autosomal dominant disorder that is characterized by a malformation of the eyelids and is caused by loss-of-function mutations in the forkhead TF *FOXL2* (forkhead box L2) [85, 86]. VSDs are rare (about 1%) in patients with this syndrome [85, 86].

Microdeletions on chromosome 15q14 are a known cause of cleft palate, typically co-occurring with intellectual disability, facial dysmorphism, and CHD [97]. The identification of patients with loss-of-function variants in *MEIS2*, a gene within this deletion, suggests that these features are attributed to haploinsufficiency of *MEIS2* (encoding Meis homeobox 2) belonging to the TALE ("three amino acid loop extension") family of homeodomain-containing TFs. Using WES, Verheije et al. identified three syndromic patients with VSD carrying the *MEIS2* mutations p. Trp326*, p.Leu312Argfs*11, and p.Arg333Lys, respectively [97].

27.4.3.2 Signaling Molecules

Inter- and intracellular communication via signaling molecules coordinates heart development, as has been shown, for example, for the Notch signaling pathway (see Chap. 11). Alagille syndrome, an autosomal dominant multisystem disorder, is

associated with CHD in about 25% of patients [103]. This syndrome is caused by mutations in either *JAG1* or *NOTCH2*, with Jagged 1 being a ligand of the membranous Notch 2 receptor. Emerick et al. showed in a cohort of 73 Alagille syndrome patients a frequent association with cardiac malformation of which 32% showed VSDs [103]. A further NOTCH signaling driven syndrome is Adams–Oliver syndrome characterized by limb defects and less frequent cardiac malformations including VSDs [104]. A study based on 11 familiar cases identified truncating mutations in *NOTCH1* of which three cases showed VSDs [104].

Mutations of genes of the Ras/MAPK (Ras/mitogen-activated protein kinase) signaling pathway are involved in a number of syndromic forms. They represent a frequent cause of Noonan syndrome, which is after Down syndrome the most common syndromic disorder involving cardiac malformations [105]. Noonan syndrome is genetically heterogeneous and characterized by short stature, facial dysmorphism, and cardiac defects of different nature such as pulmonary stenosis, hypertrophic cardiomyopathy, ASD, and at a lower rate VSDs. *PTPN11* (protein tyrosine phosphatase nonreceptor type 11) causing Noonan syndrome 1 was described being mutated in about 50% of cases [105]. Snayer et al. reported an incidence of 7% of VSDs in Noonan syndrome 1 patients [106]. Single case reports showed VSDs in the less frequent Noonan syndrome 3 caused by mutations in KRAS (Kirsten rat sarcoma viral oncogene homolog) [101] and Noonan syndrome 4 caused by mutations in SOS1 (son of sevenless homolog 1) [100]. In 25 patients with a phenotype termed Noonan-like syndrome with anagen hair, the missense mutation p.Ser2Gly in *SHOC2* (Soc-2 suppressor of clear homolog), a leucine-rich repeat-containing protein, was detected by Cordeddu et al. [102]. While the majority of patients have cardiac malformations, VSDs were found only in two cases [102]. Mutations in another member of the Ras/MAPK pathway, *HRAS* (Harvey rat sarcoma viral oncogene homolog), cause Costello syndrome, a disorder phenotypically closely related to Noonan syndrome. For Costello syndrome, one case report with VSD has been published [99]. Finally, a *de novo* mutation in *NF1* (encoding neurofibromin 1), a negative regulator of the Ras signaling pathway, was found in a patient with neurofibromatosis type 1 and VSD (see also Sect. 3.2.2) [53]. Neurofibromatosis is a neurocutaneous disorder characterized by tumors in the nervous system and skin.

Robinow syndrome is a rare skeletal dysplasia, inherited either in an autosomal dominant or recessive manner. Autosomal dominant Robinow syndrome, either caused by pathogenic variants in *WNT5A* (wingless-type MMTV integration site family member 5A) or *DVL1* (dishevelled segment polarity protein 1), is frequently accompanied by VSDs [108, 109]. In contrast, VSDs are rarely present in autosomal recessive Robinow syndrome, caused by biallelic pathogenic variants in *ROR2* (receptor tyrosine kinase-like orphan receptor 2) [107]. A further rare case with VSD has been documented for Muenke syndrome, which is characterized by fusion of cranial bones and is caused by mutations of *FGFR3* encoding fibroblast growth factor receptor 3 [98].

27.4.3.3 Chromatin Regulators

In syndromes related to chromatin regulators, the VSD rates greatly vary ranging from about 40% in Cornelia de Lange syndrome to about 4% in Sotos syndrome. Cornelia de Lange syndrome 1 is caused by mutations in *NIPBL* encoding Nipped-B homolog with putative sister chromatid cohesion function [113, 114]. From a cohort of 24 typical Sotos cases, Cecconi et al. observed one individual with VSD [115]. Sotos syndrome is caused by haploinsufficiency of the *NSD1* gene encoding a histone methyltransferase [115]. Microdeletions involving this gene are the major cause of the syndrome in Japanese patients (see Sect. 3) [71], whereas intragenic mutations are more frequent in non-Japanese patients [115].

About two-thirds of patients with CHARGE syndrome show cardiac malformations including 12% with VSDs [110]. Genetically CHARGE syndrome is caused by mutations in *CHD7* encoding a chromodomain helicase DNA-binding protein. A far less frequent association of VSDs is given in Pelger–Huet anomaly, where one case was described in a cohort of 20 families harboring mutations in *LBR* encoding for the lamin B receptor, which mediates the interaction of chromatin and lamin B [116].

Finally, mutations in *MLL2* encoding a DNA methyltransferase have been found in cases of Kabuki syndrome [111]. Half of these patients present with VSDs often accompanied by an ASD. In a meta-analysis, Yuan examined the cardiac phenotype of 76 published Kabuki cases and showed that about 20% presented a VSD either isolated or as part of a complex cardiac malformation [112].

27.4.3.4 Structural and Cell Molecules

The integrity of the cell is maintained by structural proteins while cell adhesion factors are crucial for cell–cell contacts in a respective tissue. There are three different syndromes associated with VSD caused by mutations in structural and cell adhesion proteins. Mutations in *SH3PXD2B* (SH3 and PX domains 2B, involved in cell adhesion and migration of numerous cell types) cause Frank–ter Haar syndrome, an autosomal recessive skeletal dysplasia characterized among others by cardiovascular malformations [119]. VSD is commonly seen in patients with this syndrome (in 50% of mutation carriers) as Iqbal et al. showed in their study [119]. Lin et al. reviewed 26 patients with genetically confirmed Simpson–Golabi–Behmel syndrome, a disorder characterized by high birth weight and length, which is caused by mutations in *GPC3* encoding glypican 3, a cell surface proteoglycan [118]. A VSD in association with other CHDs was present in five of them (19%) [118]. One case with Marfan syndrome (with the typical cardiovascular feature of aortic aneurysm) combined with X-linked hypophosphatemia showing VSD and ASD was described by Sheng et al. [117]. They found a *de novo* missense mutation in *FBN1* encoding fibrillin 1, a large extracellular matrix glycoprotein, using whole exome sequencing [117].

27.4.3.5 Enzymes for Posttranslational Modification

Enzymes involved in posttranslational modifications of proteins such as glycosylation play a role in two syndromes associated with VSDs. Peters plus syndrome

(named after the Peters anomaly, an eye-chamber defect) is caused by mutations in *B3GALTL* encoding a glycosyltransferase involved in addition of glycans to proteins and is associated with VSDs in about one-third of cases [120–122]. The rare Larsen-like syndrome is caused by mutations in *B3GAT3* coding for glucuronyltransferase-I and is characterized by joint dislocations, short stature, craniofacial dysmorphism, and heart defects including VSDs [123].

27.4.3.6 Other Genes

Defects in ciliary structure cause Kartagener syndrome that is characterized by primary ciliary dyskinesia leading to situs inversus, the mirror image arrangement of all internal organs. It is caused by mutations in a number of genes encoding dynein arm components (see more details in Chap. 38). Kennedy et al. examined 21 Kartagener patients and found VSDs among other CHDs in three individuals (14%) [124]. Zaidi et al. searched for *de novo* mutations in 362 severe CHD cases [44]. In one heterotaxy patient with abdominal situs inversus and CHD including VSD, they identified a missense mutation (p.Ala251Val) in *MKRN2* (encoding makorin ring finger protein 2, a putative E3 ubiquitin ligase) [44]. The gene implicated in the X-linked form of Opitz syndrome, *MID1* (midline 1), encodes a RING finger protein and is involved in the formation of multiprotein structures acting as anchor points to microtubules [125]. In a meta-analysis of several studies, Fontanella et al. showed that about 22% of cases have heart defects with a high incidence of VSDs and ASDs [125].

27.5 Associations with Common Variations

Genome-wide associations studies (GWAS) look for associations between DNA sequence variants and phenotypes of interest [127]. They do so by studying many hundreds of individuals (affecteds and nonaffecteds) and determining their genotype at the positions of hundreds of thousands of single-nucleotide polymorphisms (SNPs) followed by statistical analysis and subsequent confirmation experiments in replication cohorts [127].

A small case–control association study genotyped 58 SNPs in the TBX5 region in 192 VSD cases and matched controls of Han Chinese origin and identified a significant association of SNP rs11067075 within intron eight of the TBX5 gene with VSD [128]. Hu et al. performed a large GWAS in 945 cases with septation defects (ASD, VSD, and ASD/VSD) and 1,246 controls of Han Chinese ancestry followed by two-stage validation with further 2,160 cases and 3,866 controls [129]. They identified a highly significant association of two SNPs at chromosome 1p12 (SNP rs2474937 near *TBX15*) and 4q31.1 (SNP rs1531070 near *MAML3* encoding mastermind like three involved in Notch signaling) [129]. A GWAS with 1,995 CHD cases (including VSD) and 5,159 controls of European Caucasian origin was carried out by Cordell et al. and failed to identify any SNPs with genome-wide significance [130]. A further replication study focusing on a subgroup analysis of about 200 VSD cases also did not find any significant association [130]. Lahm

et al. performed a GWAS of 4,034 unrelated White CHD patients (including about 1,000 patients with septal defects) and 8,486 controls and identified one SNP on chromosome 5q22.2 (rs185531658) which reached genome-wide significance across all CHD phenotypes and was also indicative for septal defects including VSD [131].

The above mentioned associations could be highly significant from a statistical perspective but, unfortunately, have limited clinical relevance [132]. Further limitations of GWAS are the inability to transfer findings to other populations and the problem which variants in close proximity to the marker SNP have a causal role. As a result, although contributing to our overall understanding of CHD genomics, GWAS have failed to explain the majority of genetic variation in complex diseases such as CHD [132].

27.6 Conclusion

VSDs, one of the most common cardiac malformations in the general population, are commonly associated with a high number of well-known genetic syndromes caused by chromosomal aberrations or by smaller deletions and duplications as well as by single point mutations. Moreover, so far undefined syndromic disorders are often accompanied by VSDs.

As shown by a number of studies, genetic variants perturb multicellular interactions that are crucial for cardiogenesis. The complex developmental processes of cardiogenesis seem to be quite sensitive to changes in gene expression and dosage. Mutations in genes encoding cardiac transcription factors (e.g., *NKX2-5*, *GATA4*, and *TBX5*) and signaling molecules (e.g., *CFC1*) have been most frequently found in VSD cases and families. This holds true for isolated VSD as well as for syndromic and nonsyndromic forms. Of note, there is a great overlap of genes associated with other CHDs such as ASD (see Chap. 20), atrioventricular septal defect (see Chap. 26), tetralogy of Fallot, and double outlet right ventricle (see Chap. 32), as well as defects of the situs (see Chap. 38).

Over the last decade, tremendous effort has been made in the area of genetic technologies such as calling of CNVs and next-generation sequencing of whole exomes and genomes [132, 133]. Advances in these technologies have discovered the genetic causes of a significant fraction of VSD cases, while at the same time pointing to remarkable complexity in genetics of VSD and CHD in general. However, future studies are still required to unravel the effects of altered gene dosage or loss of function on formation of VSD. In addition, the interpretation of complex patterns of inheritance and phenotypic heterogeneity remains a difficult obstacle in individual VSD cases and families [64, 132].

Nevertheless, these new technologies hold the potential to improve patient care. Especially in VSD cases with a growing number of surviving adults after successful cardiac surgery or intervention, the urgency for a better characterization of the CHD-related morbidities and mortality occurring late after surgery is evident [134]. Menting et al. reported on the outcomes in about hundred late survivors up to 40 years after VSD closure and demonstrated the ongoing clinical problems in this

patient cohort such as arrhythmias and heart failure [135]. In fact, it is distinctly possible that some of the course of VSD cases is influenced by the underlying genetics. This observation drives the hope that identification of genetic causes of VSD may allow more tailored clinical management of patients, with respect to the many comorbidities of ventricular septal defects.

References

1. Penny DJ, Vick GW 3rd. Ventricular septal defect. Lancet. 2011;377:1103–12.
2. Lindinger A, Schwedler G, Hense HW for the participants of the PAN study. Prevalence of congenital heart defects in newborns in Germany: results of the first registration year of the PAN study (July 2006 to June 2007). Klin Padiatr. 2010;222:321–6.
3. Gelb BD, Chung WK. Complex genetics and the etiology of human congenital heart disease. Cold Spring Harb Perspect Med. 2014;4:a013953.
4. Oyen N, Poulsen G, Boyd HA, et al. Recurrence of congenital heart defects in families. Circulation. 2009;120:295–301.
5. Pollex RL, Hegele RA. Copy number variation in the human genome and its implications for cardiovascular disease. Circulation. 2007;115:3130–8.
6. Redon R, Ishikawa S, Fitch KR, et al. Global variation in copy number in the human genome. Nature. 2006;444:444–54.
7. Erdogan F, Larsen LA, Zhang L, et al. High frequency of submicroscopic genomic aberrations detected by tiling path array comparative genome hybridisation in patients with isolated congenital heart disease. J Med Genet. 2008;45:704–9.
8. Glessner JT, Bick AG, Ito K, et al. Increased frequency of de novo copy number variants in congenital heart disease by integrative analysis of single nucleotide polymorphism array and exome sequence data. Circ Res. 2014;115:884–96.
9. Soemedi R, Wilson IJ, Bentham J, et al. Contribution of global rare copy-number variants to the risk of sporadic congenital heart disease. Am J Hum Genet. 2012;91:489–501.
10. Tomita-Mitchell A, Mahnke DK, Struble CA, et al. Human gene copy number spectra analysis in congenital heart malformations. Physiol Genomics. 2012;44:518–41.
11. Zhao W, Niu G, Shen B, et al. High-resolution analysis of copy number variants in adults with simple-to-moderate congenital heart disease. Am J Med Genet A. 2013;161:3087–94.
12. Sperling S, Grimm CH, Dunkel I, et al. Identification and functional analysis of CITED2 mutations in patients with congenital heart defects. Hum Mutat. 2005;26:575–82.
13. Peng T, Wang L, Zhou SF, et al. Mutations of the GATA4 and NKX2.5 genes in Chinese pediatric patients with non-familial congenital heart disease. Genetica. 2010;138:1231–40.
14. Salazar M, Consoli F, Villegas V, et al. Search of somatic GATA4 and NKX2.5 gene mutations in sporadic septal heart defects. Eur J Med Genet. 2011;54:306–9.
15. Tomita-Mitchell A, Maslen CL, Morris CD, et al. GATA4 sequence variants in patients with congenital heart disease. J Med Genet. 2007;44:779–83.
16. Wang J, Fang M, Liu XY, et al. A novel GATA4 mutation responsible for congenital ventricular septal defects. Int J Mol Med. 2011;28:557–64.
17. Yang YQ, Li L, Wang J, et al. A novel GATA4 loss-of-function mutation associated with congenital ventricular septal defect. Pediatr Cardiol. 2012;33:539–46.
18. Cheng Z, Wang J, Su D, et al. Two novel mutations of the IRX4 gene in patients with congenital heart disease. Hum Genet. 2011;130:657–62.
19. Wei D, Gong XH, Qiu G, et al. Novel PITX2 loss-of-function mutations associated with complex congenital heart disease. Int J Mol Med. 2014;33:1201–8.
20. Pan Y, Wang ZG, Liu XY, et al. A novel TBX1 loss-of-function mutation associated with congenital heart disease. Pediatr Cardiol. 2015;36:1400–10.

21. Smemo S, Campos LC, Moskowitz IP, et al. Regulatory variation in a TBX5 enhancer leads to isolated congenital heart disease. Hum Mol Genet. 2012;21:3255–63.
22. Kirk EP, Sunde M, Costa MW, et al. Mutations in cardiac T-box factor gene TBX20 are associated with diverse cardiac pathologies, including defects of septation and valvulogenesis and cardiomyopathy. Am J Hum Genet. 2007;81:280–91.
23. Werner P, Latney B, Deardorff MA, Goldmuntz E. MESP1 mutations in patients with congenital heart defects. Hum Mutat. 2016;37:308–14.
24. Zheng SQ, Chen HX, Liu XC, Yang Q, He GW. Identification of variants of ISL1 gene promoter and cellular functions in isolated ventricular septal defects. Am J Physiol Cell Physiol. 2021;321:C443–52.
25. Wang B, Wang J, Liu S, et al. CFC1 mutations in Chinese children with congenital heart disease. Int J Cardiol. 2011;146:86–8.
26. Xiao J, Kang G, Wang J, et al. A novel variation of GDF3 in Chinese Han children with a broad phenotypic spectrum of non-syndromic CHDs. Cardiol Young. 2014;5:1–5.
27. Wang B, Yan J, Peng Z, et al. Teratocarcinoma-derived growth factor 1 (TDGF1) sequence variants in patients with congenital heart defect. Int J Cardiol. 2011;146:225–7.
28. Izarzugaza JMG, Ellesøe SG, Doganli C, et al. Systems genetics analysis identifies calcium-signaling defects as novel cause of congenital heart disease. Genome Med. 2020;12:76.
29. Zhu X, Deng X, Huang G, et al. A novel mutation of Hyaluronan synthase 2 gene in Chinese children with ventricular septal defect. PLoS One. 2014;9:e87437.
30. Pulignani S, Vecoli C, Borghini A, et al. Targeted next-generation sequencing in patients with non-syndromic congenital heart disease. Pediatr Cardiol. 2018;39:682–9.
31. Olson EN. Gene regulatory networks in the evolution and development of the heart. Science. 2006;313:1922–7.
32. Wang J, Mao JH, Ding KK, et al. A novel NKX2.6 mutation associated with congenital ventricular septal defect. Pediatr Cardiol. 2015;36:646–56.
33. Zaidi S, Brueckner M. Genetics and genomics of congenital heart disease. Circ Res. 2017;120:923–40.
34. Garg V, Kathiriya IS, Barnes R, et al. GATA4 mutations cause human congenital heart defects and reveal an interaction with TBX5. Nature. 2003;424:443–7.
35. Benson DW, Silberbach GM, Kavanaugh-McHugh A, et al. Mutations in the cardiac transcription factor NKX2.5 affect diverse cardiac developmental pathways. J Clin Invest. 1999;104:1567–73.
36. Gutierrez-Roelens I, Sluysmans T, Gewillig M, et al. Progressive AV-block and anomalous venous return among cardiac anomalies associated with two novel missense mutations in the CSX/NKX2-5 gene. Hum Mutat. 2002;20:75–6.
37. Pabst S, Wollnik B, Rohmann E, et al. A novel stop mutation truncating critical regions of the cardiac transcription factor NKX2-5 in a large family with autosomal-dominant inherited congenital heart disease. Clin Res Cardiol. 2008;97:39–42.
38. Sarkozy A, Conti E, Neri C, et al. Spectrum of atrial septal defects associated with mutations of NKX2. 5 and GATA4 transcription factors. J Med Genet. 2005;42:e16.
39. Szot JO, Cuny H, Blue GM, et al. A screening approach to identify clinically actionable variants causing congenital heart disease in exome data. Circ Genom Precis Med. 2018;11:e001978.
40. Ware SM, Peng J, Zhu L, et al. Identification and functional analysis of ZIC3 mutations in heterotaxy and related congenital heart defects. Am J Hum Genet. 2004;74:93–105.
41. van Walree ES, Dombrowsky G, Jansen IE, et al. Germline variants in HEY2 functional domains lead to congenital heart defects and thoracic aortic aneurysms. Genet Med. 2021;23:103–10.
42. Al Turki S, Manickaraj AK, Mercer CL, et al. Rare variants in NR2F2 cause congenital heart defects in humans. Am J Hum Genet. 2014;94:574–85.
43. Qiao XH, Wang Q, Wang J, et al. A novel NR2F2 loss-of-function mutation predisposes to congenital heart defect. Eur J Med Genet. 2018;61:197–203.

44. Zaidi S, Choi M, Wakimoto H, et al. De novo mutations in histone-modifying genes in congenital heart disease. Nature. 2013;498:220–3.
45. Preuss C, Capredon M, Wünnemann F, et al. Family based whole exome sequencing reveals the multifaceted role of Notch signaling in congenital heart disease. PLoS Genet. 2016;12: e1006335.
46. Kerstjens-Frederikse WS, van de Laar IM, Vos YJ, et al. Cardiovascular malformations caused by NOTCH1 mutations do not keep left: data on 428 probands with left-sided CHD and their families. Genet Med. 2016;18:914–23.
47. Granadillo JL, Chung WK, Hecht L, et al. Variable cardiovascular phenotypes associated with SMAD2 pathogenic variants. Hum Mutat. 2018;39:1875–84.
48. Hirono K, Hata Y, Ibuki K, et al. Familial Ebstein's anomaly, left ventricular noncompaction, and ventricular septal defect associated with an MYH7 mutation. J Thorac Cardiovasc Surg. 2014;148:e223–6.
49. Bettinelli AL, Mulder TJ, Funke BH, et al. Familial ebstein anomaly, left ventricular hypertrabeculation, and ventricular septal defect associated with a MYH7 mutation. Am J Med Genet A. 2013;161A:3187–90.
50. Jin SC, Homsy J, Zaidi S, et al. Contribution of rare inherited and de novo variants in 2,871 congenital heart disease probands. Nat Genet. 2017;49:1593–601.
51. Wessels MW, Herkert JC, Frohn-Mulder IM, et al. Compound heterozygous or homozygous truncating MYBPC3 mutations cause lethal cardiomyopathy with features of noncompaction and septal defects. Eur J Hum Genet. 2015;23:922–8.
52. Yang SW, Hitz MP, Andelfinger G. Ventricular septal defect and restrictive cardiomyopathy in a paediatric TNNI3 mutation carrier. Cardiol Young. 2010;20:574–6.
53. Ekure EN, Adeyemo A, Liu H, et al. Exome sequencing and congenital heart disease in sub-saharan Africa. Circ Genom Precis Med. 2021;14:e003108.
54. Lahrouchi N, Postma AV, Salazar CM, et al. Biallelic loss-of-function variants in PLD1 cause congenital right-sided cardiac valve defects and neonatal cardiomyopathy. J Clin Invest. 2021;131:e142148.
55. Liu X, Zheng J, Fan Z, Rao L. Case report: an unusual case of Brugada syndrome combined with a ventricular septal defect: a case report. Medicine (Baltimore). 2017;96:e8695.
56. Pierpont ME, Brueckner M, Chung WK, et al. Genetic basis for congenital heart disease: revisited: a scientific statement from the American Heart Association. Circulation. 2018;138: e653–711.
57. Andersen TA, Troelsen Kde LL, Larsen LA. Of mice and men: molecular genetics of congenital heart disease. Cell Mol Life Sci. 2014;71:1327–52.
58. Vis JC, Duffels MG, Winter MM, et al. Down syndrome: a cardiovascular perspective. J Intellect Disabil Res. 2009;53:419–25.
59. Freeman SB, Bean LH, Allen EG, et al. Ethnicity, sex, and the incidence of congenital heart defects: a report from the National Down Syndrome Project. Genet Med. 2008;10:173–80.
60. Källen B, Mastroiacovo P, Robert E. Major congenital malformations in Down syndrome. Am J Med Genet. 1996;65:160–6.
61. Fudge JC Jr, Li S, Jaggers J, et al. Congenital heart surgery outcomes in Down syndrome: analysis of a national clinical database. Pediatrics. 2010;126:315–22.
62. Pont SJ, Robbins JM, Bird TM, et al. Congenital malformations among liveborn infants with trisomies 18 and 13. Am J Med Genet A. 2006;140:1749–56.
63. Tilton RK, Wilkens A, Krantz ID, et al. Cardiac manifestations of Pallister–Killian syndrome. Am J Med Genet A. 2014;164A:1130–5.
64. Lalani SR, Belmont JW. Genetic basis of congenital cardiovascular malformations. Eur J Med Genet. 2014;57:402–13.
65. Momma K. Cardiovascular anomalies associated with chromosome 22q11.2 deletion syndrome. Am J Cardiol. 2010;105:1617–24.

66. Ryan AK, Goodship JA, Wilson DI, et al. Spectrum of clinical features associated with interstitial chromosome 22q11 deletions: a European collaborative study. J Med Genet. 1997;34:798–804.
67. Collins RT 2nd. Cardiovascular disease in Williams syndrome. Circulation. 2013;127:2125–34.
68. Jefferies JL, Pignatelli RH, Martinez HR, et al. Cardiovascular findings in duplication 17p11.2 syndrome. Genet Med. 2012;14:90–4.
69. Battaglia A, Filippi T, Carey JC. Update on the clinical features and natural history of Wolf-Hirschhorn (4p) syndrome: experience with 87 patients and recommendations for routine health supervision. Am J Med Genet C Semin Med Genet. 2008;148C:246–51.
70. Hills C, Moller JH, Finkelstein M, et al. Cri du chat syndrome and congenital heart disease: a review of previously reported cases and presentation of an additional 21 cases from the Pediatric Cardiac Care Consortium. Pediatrics. 2006;117:924–7.
71. Kaneko H, Tsukahara M, Tachibana H, et al. Congenital heart defects in Sotos sequence. Am J Med Genet. 1987;26:569–76.
72. Stewart DR, Kleefstra T. The chromosome 9q subtelomere deletion syndrome. Am J Med Genet C Semin Med Genet. 2007;145C:383–92.
73. Mattina T, Perrotta CS, Grossfeld P. Jacobsen syndrome. Orphanet J Rare Dis. 2009;4:9.
74. Girirajan S, Vlangos CN, Szomju BB, et al. Genotype-phenotype correlation in Smith-Magenis syndrome: evidence that multiple genes in 17p11.2 contribute to the clinical spectrum. Genet Med. 2006;8:417–27.
75. Syrmou A, Tzetis M, Fryssira H, et al. Array comparative genomic hybridization as a clinical diagnostic tool in syndromic and nonsyndromic congenital heart disease. Pediatr Res. 2013;73:772–6.
76. Lalani SR, Shaw C, Wang X, et al. Rare DNA copy number variants in cardiovascular malformations with extracardiac abnormalities. Eur J Hum Genet. 2013;21:173–81.
77. Thienpont B, Mertens L, de Ravel T, et al. Submicroscopic chromosomal imbalances detected by array-CGH are a frequent cause of congenital heart defects in selected patients. Eur Heart J. 2007;28:2778–84.
78. Breckpot J, Thienpont B, Peeters H, et al. Array comparative genomic hybridization as a diagnostic tool for syndromic heart defects. J Pediatr. 2010;156:810–7.
79. Goldmuntz E, Paluru P, Glessner J, et al. Microdeletions and microduplications in patients with congenital heart disease and multiple congenital anomalies. Congenit Heart Dis. 2011;6:592–602.
80. Fakhro KA, Choi M, Ware SM, et al. Rare copy number variations in congenital heart disease patients identify unique genes in left-right patterning. Proc Natl Acad Sci U S A. 2011;108:2915–20.
81. Ng D, Thakker N, Corcoran CM, et al. Oculofaciocardiodental and Lenz microphthalmia syndromes result from distinct classes of mutations in BCOR. Nat Genet. 2004;36:411–6.
82. Hilton E, Johnston J, Whalen S, et al. BCOR analysis in patients with OFCD and Lenz microphthalmia syndromes, mental retardation with ocular anomalies, and cardiac laterality defects. Eur J Hum Genet. 2009;17:1325–35.
83. Digilio MC, Marino B, Ammirati A, et al. Cardiac malformations in patients with oral-facial-skeletal syndromes: clinical similarities with heterotaxia. Am J Med Genet. 1999;84:350–6.
84. Ruiz-Perez VL, Tompson SW, Blair HJ, et al. Mutations in two nonhomologous genes in a head-to-head configuration cause Ellis-van Creveld syndrome. Am J Hum Genet. 2003;72:728–32.
85. Beysen D, Raes J, Leroy BP, et al. Deletions involving long-range conserved nongenic sequences upstream and downstream of FOXL2 as a novel disease-causing mechanism in blepharophimosis syndrome. Am J Hum Genet. 2005;77:205–18.
86. Beysen D, De Jaegere S, Amor D, et al. Identification of 34 novel and 56 known FOXL2 mutations in patients with Blepharophimosis syndrome. Hum Mutat. 2008;29:E205–19.

87. Yu L, Bennett JT, Wynn J, et al. Whole exome sequencing identifies de novo mutations in GATA6 associated with congenital diaphragmatic hernia. J Med Genet. 2014;51:197–202.
88. Suzuki S, Nakao A, Sarhat AR, et al. A case of pancreatic agenesis and congenital heart defects with a novel GATA6 nonsense mutation: evidence of haploinsufficiency due to nonsense-mediated mRNA decay. Am J Med Genet A. 2014;164A:476–9.
89. Surka WS, Kohlhase J, Neunert CE, et al. Unique family with Townes-Brocks syndrome, SALL1 mutation, and cardiac defects. Am J Med Genet. 2001;102:250–7.
90. Kohlhase J, Heinrich M, Schubert L, et al. Okihiro syndrome is caused by SALL4 mutations. Hum Mol Genet. 2002;11:2979–87.
91. Kohlhase J, Schubert L, Liebers M, et al. Mutations at the SALL4 locus on chromosome 20 result in a range of clinically overlapping phenotypes, including Okihiro syndrome, Holt-Oram syndrome, acro-renal-ocular syndrome, and patients previously reported to represent thalidomide embryopathy. J Med Genet. 2003;40:473–8.
92. Linden H, Williams R, King J, et al. Ulnar mammary syndrome and TBX3: expanding the phenotype. Am J Med Genet A. 2009;149A:2809–12.
93. Meneghini V, Odent S, Platonova N, et al. Novel TBX3 mutation data in families with ulnar-mammary syndrome indicate a genotype-phenotype relationship: mutations that do not disrupt the T-domain are associated with less severe limb defects. Eur J Med Genet. 2006;49:151–8.
94. Borozdin W, Bravo Ferrer Acosta AM, Bramshad MJ, et al. Expanding the spectrum of TBX5 mutations in Holt-Oram syndrome: detection of two intragenic deletions by quantitative real time PCR, and report of eight novel point mutations. Hum Mutat. 2006;27:975–6.
95. Satoda M, Pierpont ME, Diaz GA, et al. Char syndrome, an inherited disorder with patent ductus arteriosus, maps to chromosome 6p12-p21. Circulation. 1999;99:3036–42.
96. Mowat DR, Wilson MJ, Goossens M. Mowat-Wilson syndrome. J Med Genet. 2003;40:305–10.
97. Verheije R, Kupchik GS, Isidor B, et al. Heterozygous loss-of-function variants of MEIS2 cause a triad of palatal defects, congenital heart defects, and intellectual disability. Eur J Hum Genet. 2019;27:278–90.
98. Escobar LF, Hiett AK, Marnocha A. Significant phenotypic variability of Muenke syndrome in identical twins. Am J Med Genet A. 2009;149A:1273–6.
99. Zampino G, Pantaleoni F, Carta C, et al. Diversity, parental germline origin, and phenotypic spectrum of de novo HRAS missense changes in Costello syndrome. Hum Mutat. 2007;28:265–72.
100. Roberts AE, Araki T, Swanson KD, et al. Germline gain-of-function mutations in SOS1 cause Noonan syndrome. Nat Genet. 2007;39:70–4.
101. Schubbert S, Zenker M, Rowe SL, et al. Germline KRAS mutations cause Noonan syndrome. Nat Genet. 2006;38:331–6.
102. Cordeddu V, Di Schiavi E, Pennacchio LA, et al. Mutation of SHOC2 promotes aberrant protein N-myristoylation and causes Noonan-like syndrome with loose anagen hair. Nat Genet. 2009;41:1022–6.
103. Emerick KM, Rand EB, Goldmuntz E, et al. Features of Alagille syndrome in 92 patients: frequency and relation to prognosis. Hepatology. 1999;29:822–9.
104. Southgate L, Sukalo M, Karountzos ASV, et al. Haploinsufficiency of the NOTCH1 receptor as a cause of Adams–Oliver syndrome with variable cardiac anomalies. Circ Cardiovasc Genet. 2015;8:572–81.
105. Roberts AE, Allanson JE, Tartaglia M, et al. Noonan syndrome. Lancet. 2013;381:333–42.
106. Sznajer Y, Keren B, Baumann C, et al. The spectrum of cardiac anomalies in Noonan syndrome as a result of mutations in the PTPN11 gene. Pediatrics. 2007;119:e1325–31.
107. Schwabe GC, Tinschert S, Buschow C, et al. Distinct mutations in the receptor tyrosine kinase gene ROR2 cause brachydactyly type B. Am J Hum Genet. 2000;67:822–31.
108. Al-Ata J, Paquet M, Teebi AS. Congenital heart disease in Robinow syndrome. Am J Med Genet. 1998;77:332–3.

109. Webber SA, Wargowski DS, Chitayat D, et al. Congenital heart disease and Robinow syndrome: coincidence or an additional component of the syndrome? Am J Med Genet. 1990;37:519–21.
110. Jongmans MC, Admiraal RJ, van der Donk KP, et al. CHARGE syndrome: the phenotypic spectrum of mutations in the CHD7 gene. J Med Genet. 2006;43:306–14.
111. Ng SB, Bigham AW, Buckingham KJ, et al. Exome sequencing identifies MLL2 mutations as a cause of Kabuki syndrome. Nat Genet. 2010;42:790–3.
112. Yuan SM. Congenital heart defects in Kabuki syndrome. Cardiol J. 2013;20:121–4.
113. Jackson L, Kline AD, Barr MA, et al. De Lange syndrome: a clinical review of 310 individuals. Am J Med Genet. 1993;47:940–6.
114. Tsukahara M, Okamoto N, Ohashi H, et al. Brachmann-de Lange syndrome and congenital heart disease. Am J Med Genet. 1998;75:441–2.
115. Cecconi M, Forzano F, Milani D, et al. Mutation analysis of the NSD1 gene in a group of 59 patients with congenital overgrowth. Am J Med Genet A. 2005;134:247–53.
116. Hoffmann K, Dreger CK, Olins AL, et al. Mutations in the gene encoding the lamin B receptor produce an altered nuclear morphology in granulocytes (Pelger-Huët anomaly). Nat Genet. 2002;31:410–4.
117. Sheng X, Chen X, Lei B, et al. Whole exome sequencing confirms the clinical diagnosis of Marfan syndrome combined with X-linked hypophosphatemia. J Transl Med. 2015;13:179.
118. Lin AE, Neri G, Hughes-Benzie R, et al. Cardiac anomalies in the Simpson-Golabi-Behmel syndrome. Am J Med Genet. 1999;83:378–81.
119. Iqbal Z, Cejudo-Martin P, de Brouwer A, et al. Disruption of the podosome adaptor protein TKS4 (SH3PXD2B) causes the skeletal dysplasia, eye, and cardiac abnormalities of Frank-Ter Haar syndrome. Am J Hum Genet. 2010;86:254–61.
120. Lesnik Oberstein SA, Kriek M, White SJ, et al. Peters Plus syndrome is caused by mutations in B3GALTL, a putative glycosyltransferase. Am J Hum Genet. 2006;79:562–6.
121. Hennekam RC, Van Schooneveld MJ, Ardinger HH. The Peters'-Plus syndrome: description of 16 patients and review of the literature. Clin Dysmorphol. 1993;2:283–300.
122. Maillette de Buy Wenniger-Prick LJ, Hennekam RC. The Peters' plus syndrome: a review. Ann Genet. 2002;45:97–103.
123. Baasanjav S, Al-Gazali L, Hashiguchi T, et al. Faulty initiation of proteoglycan synthesis causes cardiac and joint defects. Am J Hum Genet. 2011;89:15–27.
124. Kennedy MP, Omran H, Leigh MW, et al. Congenital heart disease and other heterotaxic defects in a large cohort of patients with primary ciliary dyskinesia. Circulation. 2007;115:2814–21.
125. Fontanella B, Russolillo G, Meroni G. MID1 mutations in patients with X-linked Opitz G/BBB syndrome. Hum Mutat. 2008;29:584–94.
126. Al-Qattan MM, Abou Al-Shaar H. Molecular basis of the clinical features of Holt-Oram syndrome resulting from missense and extended protein mutations of the TBX5 gene as well as TBX5 intragenic duplications. Gene. 2015;560:129–36.
127. Donelly P. Progress and challenges in genome-wide association studies in humans. Nature. 2008;456:728–31.
128. Liu CX, Shen AD, Li XF, et al. Association of TBX5 gene polymorphism with ventricular septal defect in the Chinese Han population. Chin Med J (Engl). 2009;122:30–4.
129. Hu Z, Shi Y, Mo X, et al. A genome-wide association study identifies two risk loci for congenital heart malformations in Han Chinese populations. Nat Genet. 2013;45:818–21.
130. Cordell HJ, Bentham J, Topf A, et al. Genome-wide association study of multiple congenital heart disease phenotypes identifies a susceptibility locus for atrial septal defect at chromosome 4p16. Nat Genet. 2013;45:822–4.
131. Lahm H, Jia M, Dreßen M, et al. Congenital heart disease risk loci identified by genome-wide association study in European patients. J Clin Invest. 2021;131:e141837.
132. Blue GM, Kirk EP, Giannoulatou E, et al. Advances in the genetics of congenital heart disease: a clinician's guide. J Am Coll Cardiol. 2017;69:859–70.

133. Andelfinger G. Next-generation sequencing in congenital heart disease: do new brooms sweep clean? J Am Coll Cardiol. 2014;64:2507–9.
134. Hsu DT. Closure is not correction: late outcomes of ventricular septal defect surgery. J Am Coll Cardiol. 2015;65:1952–3.
135. Menting ME, Cuypers JAAE, Opić P, et al. The unnatural history of the ventricular septal defect: outcome up to 40 years after surgical closure. J Am Coll Cardiol. 2015;65:1941–51.

Ventricular Septal Defects: Molecular Pathways and Animal Models

28

Lucile Houyel

Abstract

Ventricular septation is a complex process which involves the major genes of cardiac development, acting on myocardial cells from first and second heart fields, and on mesenchymal cells from endocardial cushions. These genes, coding for transcription factors, interact with each other, and their differential expression conditions the severity of the phenotype. In this chapter, we will describe the formation of the ventricular septum in the normal heart, as well as the molecular mechanisms leading to the four main anatomic types of ventricular septal defects: outlet, inlet, muscular, and central perimembranous, resulting from failure of development of the different parts of the ventricular septum. Experiments on animal models, particularly transgenic mouse lines, have helped us to decipher the molecular determinants of ventricular septation. However, a precise description of the anatomic phenotypes found in these models is mandatory to achieve a better comprehension of the complex mechanisms responsible for the various types of VSDs.

Keywords

Ventricular septal defect · VSD · Interventricular communication · Outlet · Inlet · Muscular · Central perimembranous · First heart field · Second heart field · Endocardial cushions · Tbx5 · Tbx1 · GATA4 · Shh · Hand1/eHand

L. Houyel (✉)
Pediatric and Congenital Cardiology Unit, Necker-Enfants Malades Hospital – M3C, University of Paris, Paris, France
e-mail: lucile.houyel@aphp.fr

© The Author(s), under exclusive license to Springer Nature Switzerland AG 2024

S. Rickert-Sperling et al. (eds.), *Congenital Heart Diseases: The Broken Heart*,
Advances in Experimental Medicine and Biology 1441,
https://doi.org/10.1007/978-3-031-44087-8_28

28.1 Introduction

Isolated ventricular septal defects are the most frequent congenital heart defects in children [1], and are also an integral part of a large number of congenital heart malformations. The term "ventricular septal defect" is widely used to describe any type of hole, or channel, or communication, between the two ventricles [2, 3]. However, it is possible to make a distinction between the "true" ventricular septal defects (VSD) which represent holes, or channels, within the ventricular septum itself, and the interventricular communications, which are the space between two components of the ventricular septum which did not fuse properly during embryonic life [2, 3].

Many classifications have been used to describe the communications between the ventricular chambers. In 2018, the International Society for Nomenclature of Paediatric and Congenital Heart Disease (ISNPCHD) has proposed a classification based both on their geographic location on the right ventricular septal surface and the borders of the defect, with further subclassification based on the presence or absence of septal malalignment [4]. The four main anatomic types of VSD retained in this classification are (Fig. 28.1):

- Muscular defects
- Defects opening into the outlet of the ventricles (outlet defects)
- Defects opening into the inlet of the ventricles (inlet defects)
- Central perimembranous defects

The anatomic characteristics of these defects and their assumed embryologic origin are depicted in Table 28.1.

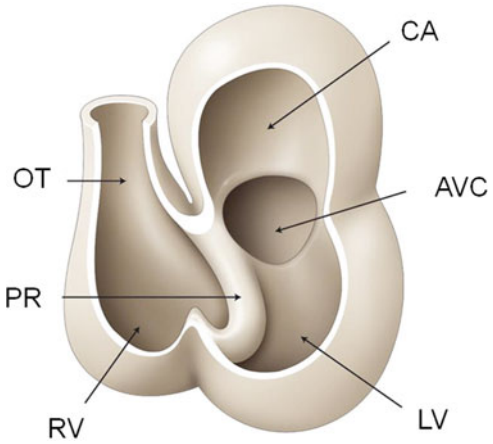

Fig. 28.1 The embryonic heart just after cardiac looping. The common atrium (CA) communicates with the left ventricle (LV) only, via the atrioventricular canal (AVC). The primary ring (PR) marks the boundary between the left ventricle, derived from the first heart field (straight heart tube), and the developing right ventricle (RV), derived from the anterior part of the second heart field. The outflow tract (OFT) is entirely above the developing right ventricle

Table 28.1 The four main anatomic types of ventricular septal defect with their anatomic characteristics, and their presumably embryologic origin

Type of defect			Fibrous continuity	Embryologic origin
Central perimembranous			Yes (*septal* tricuspid leaflet/aortic leaflets)	Formation of membranous septum (AV cushions)
Outflow tract (Outlet) defects	Malalignment defects (aortic overriding)	With aortic-tricuspid fibrous continuity (membranous extension)	Yes (*anterior* tricuspid leaflet/aortic leaflets)	Cardiac neural crest and anterior second heart field Outflow tract cushions
		Muscular borders	No (muscular borders)	
	Juxta-arterial defects (fibrous continuity Ao/pulm valves)	With aortic-tricuspid fibrous continuity (membranous extension)	Yes (*anterior* tricuspid leaflet/aortic leaflets)	
		Muscular borders	No (muscular borders)	
Inflow tract (Inlet) defects	Common atrioventricular junction (isolated ventricular component)		Yes (tricuspid/mitral)	Posterior second heart field, AV cushions
	Straddling tricuspid valve (malalignment atrial/ventricular septum)			Convergence formation of AV junction
Muscular	Muscular trabecular		No	Myocardial compaction, coalescence of trabeculations
	Bulboventricular foramen			Early looping

Ventricular septation, as a crucial step in heart development, was studied first in human embryos from a purely morphologic point of view, then on chick and mouse. Recent techniques such as high-resolution episcopic microscopy and high-resolution MRI have been used in mouse and human embryos to better analyze the development of the atrial and ventricular septa [5–7]. Despite these recent advances, the precise mechanisms leading to normal ventricular septation are not fully understood and controversies still exist. Some of them are due to some developmental differences in the chick and in the mouse. On the other hand, despite some minor differences, the steps of cardiac development are very similar in mouse and human [8].

28.2 Normal Ventricular Septation

Ventricular septation is a complex process starting from the onset of cardiac looping to its final steps which are the formation of the membranous septum and later on, during fetal life, compaction of the ventricular myocardium.

Immediately after cardiac looping (early looping stage), the inlet segment (atria and atrioventricular canal) is located entirely above the future left ventricle, and the outlet segment (the conotruncus or outflow tract) is located entirely above the future right ventricle, leading to both double-inlet left ventricle and double-outlet right ventricle types of atrioventricular (AV) and ventriculoarterial connection (Fig. 28.2). From this stage on, the heart continues to grow by addition of myocardial cells from two cellular populations: the first heart field or primitive linear heart tube will form the left ventricle and a small part of the atria above the AV valves including the atrial appendages; the second heart field (SHF) is essential for the development of the right ventricle and the OFT (anterior SHF), and also the venous pole, including the major part of the atria (posterior SHF or dorsal mesocardium).

Ventricular septation involves not only myocardial cells of the two heart fields, but also mesenchymal cells of the endocardial cushions, most of those will be secondarily muscularized. Proper ventricular septation can be achieved normally only if all elements of the definitive four-chambered heart are correctly aligned.

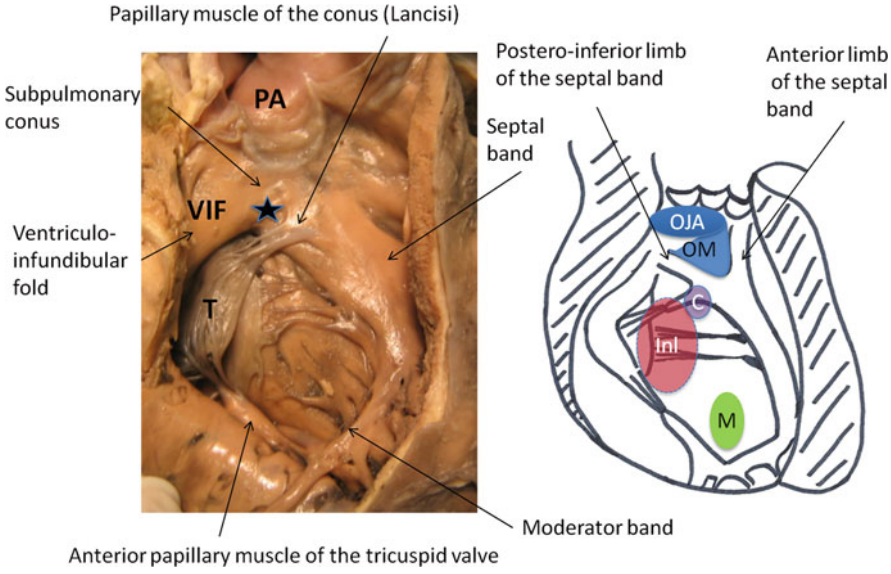

Fig. 28.2 The right ventricle in the normal heart, and the four main anatomic types of ventricular septal defect, viewed from the right ventricle. C = central perimembranous; Inl = inlet; OJA: outlet, juxta-arterial; OM: outlet, malalignment; PA, pulmonary artery. M, muscular; T, tricuspid valve; VIF: ventriculoinfundibular fold

The interventricular septum first appears immediately after the cardiac loop, as a myocardial ridge developed at the posterior part and at the apex of the primitive heart, the primary ring (Fig. 28.2). Cardiac looping creates an outer curvature, formed by the ventral surface of the straight heart tube, and an inner curvature, between the outflow and the inflow parts of the heart. The outer curvature will take part to the growth of the ventricles, by ballooning of the cavities with formation of multiple trabeculations [9], while the remodeling of the inner curvature controls the alignment between the inlet and outlet segments [10]. The right ventricle develops later than the left ventricle [11], by addition of the cardiomyocytes of the anterior SHF [12]. This differential growth contributes to the alignment of the developing atrial and ventricular septa. The formation of the interventricular septum would thus be both passive (ballooning) and active [13–15].

The embryonic interventricular communication or "primary interventricular foramen," between the inlet and outlet components of the developing heart, will undergo extensive remodeling, leading to its final closure [7]. Immediately after cardiac looping, the borders of the primary interventricular foramen are exclusively muscular. This corresponds to the "bulboventricular foramen" found in tricuspid atresia and double-inlet left ventricle. The remodeling of this primitive communication into secondary interventricular foramen permits the establishment of the right atrioventricular connection, leading to the alignment between the atria and the ventricles. Any interruption in this process leads to an inlet VSD without a common AV junction but with malalignment of atrial and ventricular septa, associated with a straddling tricuspid valve. The remodeling of the secondary foramen into tertiary interventricular foramen permits the formation of the outlet for the left ventricle, by the transfer of the aortic valve above the left ventricle. When this process is achieved, the tertiary interventricular foramen will be closed by the membranous part of the interventricular septum, derived from the endocardial cushions [7]. The secondary interventricular foramen corresponds thus to the channel between the ventricles found in double-outlet right ventricle with subaortic VSD, and can evolve toward outlet VSD with anteriorly malaligned outlet septum. Persisting tertiary foramen will correspond to central perimembranous VSD [7].

The ventricular septum can be divided in several components, each one having a different embryologic origin.

- The muscular trabeculated septum is constituted by the myocytes of both left and right ventricles [13] and thus originates from both first and second heart fields.
- The origin of the inlet septum is still controversial. What is commonly called the inlet septum is the posteroinferior, or caudal, part of the ventricular septum [14, 16], but for some authors it does not exist in the normal heart [6, 17]. Experimental studies in the mouse embryo demonstrate that the larger part of the central mesenchymal mass created by the fusion of the mesenchymal tissues of the vestibular spine, the mesenchymal cap of the primitive atrial septum and the AV cushions becomes muscularized to form the inferior margin of the oval fossa [18]. Whether muscularization occurs or not in the posteroinferior part of the mass (the part which is lacking in hearts with a common AV junction, forming the

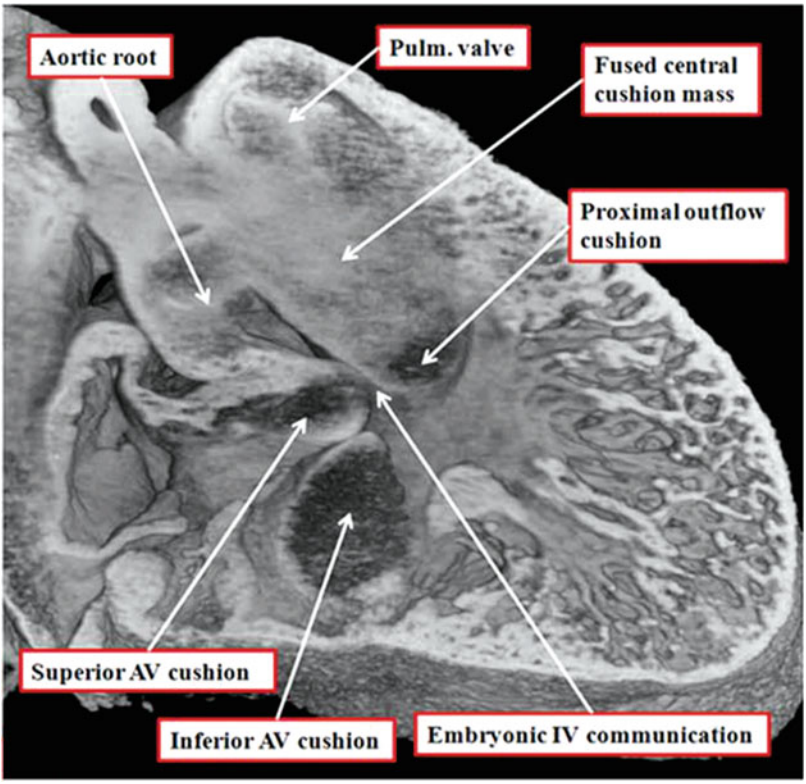

Fig. 28.3 Episcopic section from a developing mouse heart at E13.5. The aortic root is still above the right ventricle. The proximal outflow cushions have fused but have not yet muscularized. The embryonic interventricular communication lies at the confluence of the outflow tract cushions and the superior and inferior atrioventricular cushions (Courtesy of Pr R.H. Anderson)

inlet VSD) has been demonstrated in the chick embryo [19] but not in mammals, in which the posterior–inferior part of the ventricular septum would be part of the developing trabeculated muscular septum [20].

– The outlet septum develops by fusion and muscularization of the proximal part of the endocardial cushions of the OFT [21], and is taken along leftward by the rotation of the developing aortic valve, to fuse with the upper primitive ventricular septum between the two limbs of the septal band or septomarginal trabeculation (Fig. 28.3), itself derived from the primary fold [22]. This rotation depends on the proper growth of the OFT by addition of myocardial cells from the anterior heart field, in response to the migration of cardiac neural crest cells toward the OFT [23]. The rotation of the aortic valve permits its transfer toward

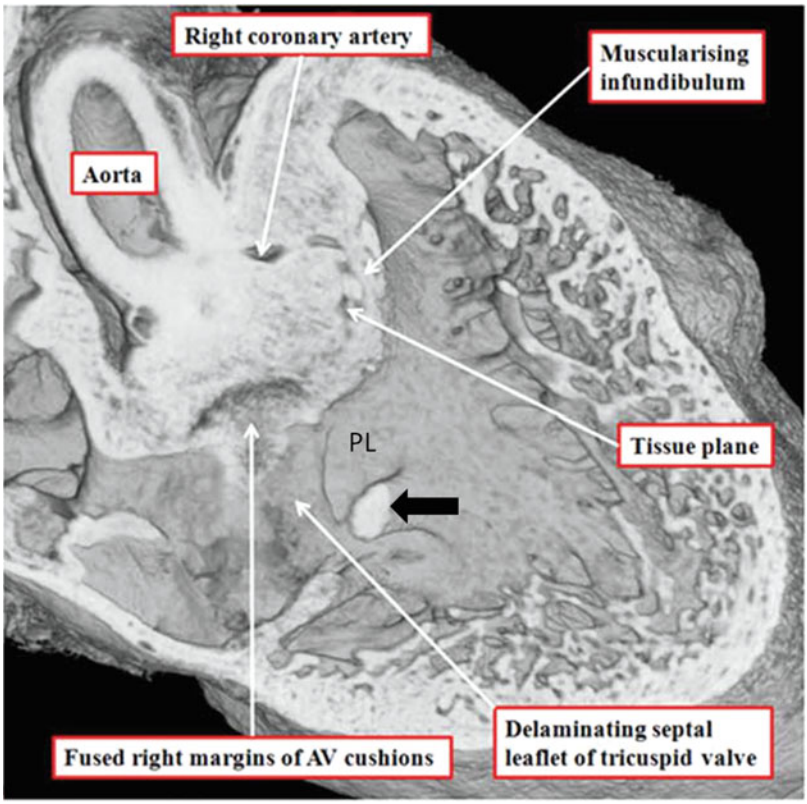

Fig. 28.4 Episcopic section from a developing mouse heart at E14.5. The fused central cushion mass is inserted between the two limbs of the septomarginal trabeculation (septal band) and has begun to muscularize. It will be transformed into the outlet septum and into the free-standing muscular subpulmonary infundibulum. The aorta has achieved its transfer towards the left ventricle. The rightward margins of the atrioventricular endocardial cushions fuse to close the right ventricular entrance to the subaortic vestibule, completing the process of ventricular septation. The membranous septum which results from this fusion is visible under the posterior limb (PL) of the septal band (black arrow) (Courtesy of Pr R.H. Anderson)

the left ventricle, and its wedging between the tricuspid and mitral valves, establishing fibrous mitral-aortic continuity [24–26].

– The membranous septum (Fig. 28.4) completes cardiac septation by closing the residual central defect (tertiary interventricular foramen), by fusion of the AV canal cushions with the left outflow tract cushion [2].

Any failure of development of these different parts (the limits of which are barely recognizable in the normal heart) leads to a corresponding phenotype of VSD.

28.3 Pathways to the Different Anatomic Types of Ventricular Septal Defects

The molecular determinants of the complex events leading to ventricular septation are not fully understood yet [27]. This is due in part to the uncertainties relative to the normal development of the ventricular septum, and also to the difficulties in assessing the precise anatomic phenotype in animal models. In addition, few animal models exhibit isolated VSDs.

A lot of genes coding for transcription factors have been recognized as playing a role in ventricular septation [28, 29]. However, the major ones (Tbx5, GATA4, Nkx2.5, Tbx20, GATA6), when deleted in mouse or mutated in human, produce VSDs but also atrial septal defects (ASDs) and atrioventricular septal defects (AVSD). An explanation for this could be that several genes act on cells from both parts of SHF, anterior and posterior. For example, Shh signaling has been found essential for the contribution of the anterior heart field to the developing outflow tract in mice [30], and regulates the expression of Tbx1 and the semaphorin receptor Neuropilin 2 in the SHF [31]. Shh signaling has also been demonstrated to play a crucial role in the formation of the vestibular spine, which originates from the posterior SHF, loss of Shh from the pharyngeal endoderm resulting in AVSD in mice [32]. It also governs the formation of the muscular trabeculated septum [33]. In the vertebrates, Shh pathway is mediated by primary (immotile) cilia, and VSD at various sites, as well as atrioventricular septal defects, are part of the phenotype of many mouse mutants for genes encoding Hedgehog signaling components [33].

28.3.1 Pathways to the Outlet VSDs

All outflow tract defects share the same anatomic type of VSD, opening to the outlet of the right ventricle and located between the two limbs of the septal band (except transposition of the great arteries, in which this type of VSD is not constant, and double outlet right ventricle with noncommitted VSD) [34]. The phenotypic differences observed, especially regarding the posteroinferior rim of the VSD (fibrous, with fibrous continuity between the anterior leaflet of the tricuspid valve and the aortic valve, or muscular, due to the fusion of the posterior limb of the septal band with the ventriculoinfundibular fold) are related to the degree of rotation of the aortic valve during heart development [34]. Separation of the posterior limb of the septal band from the ventriculoinfundibular fold (so-called outlet VSD with perimembranous extension or “outlet perimembranous VSD”) would indicate a higher degree of rotation of the aortic valve, by analogy with the normal heart [34]. Therefore, the molecular pathways that lead to an outlet VSD have to be the same that those leading to so-called conotruncal, or cardiac neural crest, defects, which include tetralogy of Fallot and its anatomic variants, common arterial trunk, interrupted aortic arch type B, isolated outlet VSDs, and double-outlet right ventricle with subaortic or doubly committed VSD. The genetic background of these anomalies is well known, because of their frequent association with 22q11

microdeletion or Di George syndrome. The major candidate gene for Di George syndrome is Tbx1, which is expressed in the anterior part of the SHF [31] and is a key regulator of SHF development. Mice Tbx1+/− have defects of the aortic arches (especially the 4th aortic arch) and great arteries, while mice Tbx1−/− have outflow tract defects, with variable severity according to the dosage of the gene [35]. This dosage effect, interacting with the complex molecular pathways affecting the anterior SHF, could explain the phenotypic differences observed between the various outflow tract defects, and within a same malformation. Other animal experiments have shown that Tbx1 is expressed in a particular SHF subdomain, which contributes to the subpulmonary myocardium [31]. In Tbx1 mutant mice, the outflow tract is shorter and narrower, due to reduction of the future subpulmonary myocardial domain [36].

28.3.1.1 Malalignment Type Outlet VSDs

These defects are due to a malalignment between the developing outflow tract and the ventricles, due to lack of rotation of the aortic valve, and result in a failure of fusion of the outlet septum with the primitive ventricular septum between the two limbs of the septal band. This is due to a lack of addition of myocardial cells by the anterior SHF, in interaction with neural crest cells, to the developing outflow tract [37], resulting in an underdevelopment of the subpulmonary myocardium [31]. All the genes involved in regulation of anterior SHF, when mutated in animals and in humans, can determine, in addition to so-called conotruncal defects, isolated malalignment outlet VSDs.

28.3.1.2 Doubly Committed and Juxta-arterial Outlet VSDs

This particular type of outlet VSD is due to a failure of fusion and muscularization of the proximal part of the endocardial cushions of the outflow tract, resulting in absent or fibrous outlet septum [4]. The genetic background is different whether this type of VSD is found in isolation (with a particular frequency in populations of Asian origin) or in the setting of a common arterial trunk. Common arterial trunk results from a complete failure of septation of the outflow tract, involving a defect of migration of the neural crest cells [38]. Several animal models exhibit a common arterial trunk (Tbx1, Sema3c, Splotch, Raldh2), with various phenotypes according to the position of the pulmonary branches originating from the common arterial trunk.

28.3.2 Pathways to the Inlet VSDs

The majority of the defects in the posterior, or caudal, part of the ventricular septum are part of an AVSD, in the setting of a common AV junction.

28.3.2.1 Inlet VSD in the Setting of a Common Atrioventricular Junction

Many experiments have recognized as the major mechanism leading to abnormal AV septation a deficient growth of the vestibular spine, or dorsal mesenchymal protrusion [18, 32, 39]. This mechanism was confirmed in human T21 embryos with

AVSD [40]. Thus, the vestibular spine would participate in the normal septation of the AV canal, and presumably to the posteroinferior part of the ventricular septum. Mutant mice heterozygous for GATA4 exhibit a common AV junction phenotype, including hearts with an isolated inlet VSD [38]. Indeed, a defect of the posteroinferior part of the ventricular septum is found anatomically in all hearts with a common atrioventricular junction, even if the shunt through this defect may disappear because of fusion of the valvar leaflets with the crest of the ventricular septum. Other experiments on mice have found a dose effect for various genes, which could explain the occurrence of the different forms of common AV junction [41, 42], and also the frequent association with outlet defects such as DORV.

28.3.2.2 Inlet VSD Associated with Straddling Tricuspid Valve

TGF-β2 knockout mice exhibit as part of their phenotype an inlet VSD, associated in 2/3 of cases with a straddling tricuspid valve. This anomaly was associated in most embryos with a double outlet right ventricle [43]. These defects could be due to a lack of myocardialization of the endocardial cushions, with altered neural crest cell migration and excessive apoptosis [43]. This would alter the final phase of wedging, resulting in a malalignment between atrial and ventricular septa which precludes normal closure of the posterior part of the primitive interventricular foramen, and impairs the normal rotation of the outflow tract.

28.3.3 Pathways to the Muscular VSD

In an experimental study using two different transgenic mouse lines (Mlc1v, expressed in the outflow tract and RV myocardium, and Mlc3f, expressed in LV myocardium and the atrial appendages), Franco et al. [13] demonstrated that cells contributing to the trabeculated ventricular septum originate from both first and second heart fields. During the early stages of development, the expression of the two transgenes is symmetrical in the developing interventricular septum in the mouse. Then the left ventricular cardiomyocytes become progressively predominant, particularly in the dorsal part of the septum. A third population of cardiomyocytes could be added by the inner curvature of the heart at the upper part of the muscular trabeculated septum. Some muscular VSDs could occur at the zones of junction of these different cell populations.

Several transcriptions factors, like TBX5, GATA4, Nkx 2.5 are involved in the development of the primitive ventricular septum and seem to interact at some stages of cardiac development [44]. Some of these genes exhibit gradients of expression along the ventricular septum, which are critical for ventricular septation [45]. Tbx18 was expressed on both sides of the dorsal aspect of the developing ventricular septum in mice, but was restricted to the left side in its ventral aspect [13]. In the mouse, Tbx5 expression is stronger in the LV, weaker in the RV inlet, and almost negative in the RV outflow tract [46]. When Tbx5 is deleted from all or part of the ventricular myocardium, ventricular septation is deficient [47]. Hand1/eHand knock-out mouse embryos exhibited normal morphology of the inner curvature, the AV

junction and the outflow tract, but the interventricular septum failed to form and the compact myocardium was thinner than normal, leading to embryonic lethality [48]. Takeuchi et al. demonstrated in chicken and mouse embryo that Tbx5 may control Hand1/eHand expression and that the boundary of Tbx5 and Tbx20 expression may determine the position of the ventricular septum [49]. The absence of Tbx5 and Hand1/eHand expression in the region between the two developing ventricles may be necessary for normal development of the ventricular septum [48].

Compaction of the primary trabeculated myocardium may play a major role in the formation of the ventricular septum, and could be mediated by epicardial-derived cells [46]. Podoplanin-mutant mice exhibit an underdeveloped epicardium, a thin muscular septum with few epicardial cells, spongy inlet septum, and septal defects including AVSDs [50]. Multiple muscular VSDs could be related to a certain degree of noncompaction of the trabeculated ventricular septum [50]. More recently, a transmembrane protein in the dystrophin–glycoprotein complex, Sarcospan (Sspn), has been identified as a candidate modifier gene for muscular VSD in $Nkx2.5^{+/-}$ mice [51]. A malalignment of myofibers in the ventricular septum has been observed around these muscular VSDs. This malalignment could lead to a defective coalescence of the ventricular trabeculae, which has been recognized as one of the mechanisms responsible for muscular VSD [5, 52].

28.3.4 Pathways to the Central Membranous VSD

Central perimembranous VSD must be differentiated from malalignment outlet defects with perimembranous extension [34]. The latter also exhibit a fibrous continuity between the tricuspid and the aortic valve, but this continuity involves the anterior leaflet of the tricuspid valve and not the septal leaflet as in central perimembranous VSD [34]. The central perimembranous defect is located below the posterior limb of the septal band, and under the ventriculoinfundibular fold, while the malalignment outlet defect is located between the two limbs of the septal band. This is extremely important because the genetic and molecular pathways are different: central perimembranous defects depend on the AV cushions, while outlet defects depend on cardiac neural crest [43]. The main phenotype associated with trisomy 18 is a central membranous VSD. However, the phenotypic distinction is rarely made on animal models such as mouse and chick.

Likewise malalignment outlet defects can extend posteriorly and have a perimembranous extension, central perimembranous defects can extend posteriorly toward the inlet. This underlines the common origin of central perimembranous and inlet defects, namely the mesenchyme of the AV endocardial cushions.

28.4 Conclusions

Ventricular septation is a complex phenomenon which involves the major genes of cardiac development, acting on myocardial cells from first and second heart field, and mesenchymal cells from endocardial cushions. These genes, coding for transcription factors, interact with each other, and their differential expression conditions the severity of the phenotype. Gene deletion experiments in animal models have helped to decipher their role in heart development, although heterozygous models are probably closer to human phenotypes. The complexity of the molecular determinants of ventricular septation, and the distinct origin of each part of the ventricular septum, underline the extreme importance for developmental biologists of being able to determine the exact anatomic phenotype in their animal models, and not to refer only to "VSDs."

References

1. Khoshnood B, Lelong N, Houyel L, Thieulin AC, Jouannic JM, Magnier S, Delezoide AL, Magny JF, Rambaud C, Bonnet D, Goffinet F, on behalf of the Epicard study group. Prevalence, timing of diagnosis and mortality of newborns with congenital heart defects: a population-based study. Heart. 2012;98:1667–73.
2. Bailliard F, Spicer DE, Mohun TJ, Henry GW, Anderson RH. The problems that exist when considering the anatomic variability between the channels that permit interventricular shunting. Cardiol Young. 2015;25:15–28.
3. Crucean A, Brawn WJ, Spicer DE, Franklin RC, Anderson RH. Holes and channels between the ventricles revisited. Cardiol Young. 2015;25:1099–110.
4. Lopez L, Houyel L, Colan SD, Anderson RH, Béland MJ, Aiello VD, Bailliard F, Cohen MS, Jacobs JP, Kurosawa H, Sanders SP, Walters HL III, Weinberg PM, Boris JR, Cook AC, Crucean A, Everett AD, Gaynor W, Giroud J, Guluserian KJ, Hughes M, Juraszek AL, Krogmann ON, Maruszewski BJ, St. Louis JD, Seslar SP, Spicer DE, Srivastava S, Stellin G, Tchervenkov CI, Wang L, Franklin RCG. Classification of ventricular septal defects for the Eleventh Iteration of the International classification of Diseases – striving for consensus: A report from the International Society for Nomenclature of Paediatric and Congenital Heart Disease. Ann Thorac Surg. 2018;106:1578–89.
5. Anderson RH, Spicer DE, Brown NA, Mohun TJ. The development of septation in the four-chambered heart. Anat Rec. 2014;297:1414–29.
6. Dhanantwari P, Lee E, Krishnan A, Samtani R, Yamada S, Anderson S, Lockett E, Donofrio M, Shiota K, Leatherbury L, Lo CW. Human cardiac development in the first trimester: a high resolution MRI and episcopic fluorescence image capture atlas. Circulation. 2009;120:343–51.
7. Anderson RH, Spicer DE, Mohun TJ, Hikspoors JPJM, Lamers WH. Remodeling of the embryonic interventricular communication in regard to the description and classification of ventricular septal defects. Anat Rec. 2019;302:19–31.
8. Krishnan A, Samtani R, Dhanantwari P, Lee E, Yamada S, Shiota K, Donofrio MT, Leatherbury L, Lo CW. A detailed comparison of mouse and human cardiac development. Pediatr Res. 2014;76:500–7.
9. Christoffels VM, Habets PE, Franco D, Campione M, de Jong F, Lamers WH, Bao ZZ, Palmer S, Biben C, Harvey RP, Moorman AF. Chamber formation and morphogenesis in the developing mammalian heart. Dev Biol. 2000;223:266–78.
10. Srivastava D. Making or breaking the heart: from lineage determination to morphogenesis. Cell. 2006;126:1037–48.

11. Moorman AFM, Christoffels VM. Cardiac chamber formation: development, genes, and evolution. Physiol Rev. 2003;83:1223–67.
12. Zaffran S, Kelly RG, Meilhac SM, Buckingham ME, Brown NA. Right ventricular myocardium derives from the anterior heart field. Circ Res. 2004;95:261–8.
13. Franco D, Meilhac SM, Christoffels VM, Kispert A, Buckingham M, Kelly RG. Left and right ventricular contributions to the formation of the interventricular septum in the mouse heart. Dev Biol. 2006;294:366–75.
14. Van Mierop LHS, Kutsche LM. Development of the ventricular septum of the heart. Heart Vessels. 1985;1:114–9.
15. Patten BM. The heart. Foundation of embryology. New York: McGraw Hill; 1954. p. 545–69.
16. Goor DA, Edwards JE, Lillehei CW. The development of the interventricular septum of the human heart: correlative morphogenetic study.
17. Lamers WH, Wessels A, Verbeek FJ, Moorman AFM, Viragh S, Wenink ACG, Gittenberger-de Groot AC, Anderson RH. New findings concerning ventricular septation in the human heart. Circulation. 1992;86:1194–205.
18. Webb S, Brown NA, Anderson RH. Formation of the atrioventricular septal structures in the normal mouse. Circ Res. 1998;82:645–56.
19. De la Cruz MV, Castillo MM, Villavicencio GL, Valencia A, Moreno-Rodriguez RA. Primitive interventricular septum, its primordium, and its contribution in the definitive interventricular septum: in vivo labeling study in the chick embryo heart. Anat Rec. 1997;247:512–20.
20. Anderson RH, Webb S, Brown NA, Lamers W, Moorman A. Development of the heart: (2) Septation of the atriums and ventricles. Heart. 2003;89:949–58.
21. Mjaatvedt CH, Yamamura H, Wessels A, Ramsdell A, Turner D, Markwald R. Mechanisms of segmentation, septation, and remodeling of the tubular heart: endocardial cushion fate and cardiac looping. In: Harvey RP, Rosenthal N, editors. Heart development. San Diego: Academic Press; 1999. p. 159–77.
22. Gittenberger-De Groot AC. The quintessence of the making of the heart. Cardiol Young. 2003;13:175–83.
23. Waldo KL, Hutson MR, Ward CC, et al. Secondary heart field contributes myocardium and smooth muscle to the arterial pole of the developing heart. Dev Biol. 2005;281:78–90.
24. Ward C, Stadt H, Hutson M, Kirby ML. Ablation of the secondary heart field leads to tetralogy of Fallot and pulmonary atresia. Dev Biol. 2005;284:72–83.
25. Yelbuz TM, Waldo KL, Kumiski DH, et al. Shortened outflow tract leads to altered cardiac looping after neural crest ablation. Circ. 2002;106:504–10.
26. Bajolle F, Zaffran S, Kelly RG, et al. Rotation of the myocardial wall of the outflow tract is implicated in the normal positioning of the great arteries. Circ Res. 2006;98:421–8.
27. Bruneau BG. Signaling and transcriptional networks in heart development and regeneration. Cold Spring Harb Perspect. 2013;5:a008292.
28. Clark KL, Yutzey KE, Benson DW. Transcription factors and congenital heart defects. Annu Rev Physiol. 2006;68:97–121.
29. Gittenberger-de Groot AC, Calkoen EE, Poelmann RE, Bartelings MM, Jongbloed MRM. Morphogenesis and molecular consideration on congenital septal defects. Ann Med. 2014;46:640–52.
30. Goddeeris MM, Schwartz R, Klingensmith J, Meyers EN. Independent requirements for Hedgehog signaling by both the anterior heart field and neural crest cells for outflow tract development. Development. 2007;134:1593–604.
31. Parisot P, Mesbah K, Théveniau-Ruissy M, Kelly RG. Tbx1, subpulmonary myocardium and conotruncal congenital heart defects. Birth Defects Res. 2011;91(Part A):477–84.
32. Goddeeris MM, Rho S, Petiet A, Davenport CL, Johnson GA, Meyers EN, Klingensmith J. Intracardiac septation requires hedgehog-dependent cellular contributions from outside the heart. Development. 2008;135:1887–95.
33. Wiegering A, Rüther U, Gerhardt C. The role of hedgehog signalling in the formation of the ventricular septum. J Dev Biol. 2017;5(4):17. https://doi.org/10.3390/jdb5040017.

34. Mostefa-Kara M, Bonnet D, Belli E, Fadel E, Houyel L. Anatomy of the ventricular septal defect in outflow tract defects: similarities and differences. J Thorac Cardiovasc Surg. 2015;149:682–8.
35. Baldini A. The 22q11.2 deletion syndrome: a gene dosage perspective. Sci World J. 2006;6: 1881–7.
36. Theveniau-Ruissy M, Dandonneau M, Mesbah K, Ghez O, Mattei MG, Miquerol L, Kelly RG. The del22q11.2 candidate gene Tbx1 controls regional outflow tract identity and coronary artery patterning. Circ Res. 2008;103:142–8.
37. Waldo KL, Hutson MR, Stadt HA, Zdanowicz M, Zdanovic J, Kirby ML. Cardiac neural crest is necessary for normal addition of the myocardium to the arterial pole from the secondary heart field. Dev Biol. 2005;281:66–77.
38. Kirby ML. Pulmonary atresia or persistent truncus arteriosus: is it important to make the distinction and how do we do it? Circ Res. 2008;103:337–9.
39. Snarr BS, Wirrig EE, Phelps AL, Trusk TC, Wessels A. A spatiotemporal evaluation of the contribution of the dorsal mesenchymal protrusion to cardiac development. Dev Dyn. 2007: 2361287–94.
40. Blom NA, Ottenkamp J, Wenink AG, Gittenberger-de Groot AC. Deficiency of the vestibular spine in atrioventricular septal defects in human fetuses with Down syndrome. Am J Cardiol. 2003:91180–4.
41. Rajagopal SK, Ma Q, Obler D, Shen J, Manichaikul A, Tomita-Mitchell A, Boardman K, Briggs C, Garg V, Srivastava D, Goldmuntz E, Broman KW, Benson DW, Smoot LB, Pu WT. Spectrum of heart disease associated with murine and human GATA4 mutation. J Mol Cell Cardiol. 2007;43:677–85.
42. Jiao K. An essential role of Bmp4 in the atrioventricular septation of the mouse heart. Genes Dev. 2003;17:2362–7.
43. Bartram U, Molin DGM, Wisse LJ, Mohamad A, Sanford LP, Doetschman T, Speer C, Poelmann RE, Gittenberger-de Groot AC. Double outlet right ventricle and overriding tricuspid valve reflect disturbances of looping, myocardialization, endocardial cushion differentiation, and apoptosis in TGFβ2 knockout mice. Circulation. 2001;103:2745–52.
44. Bruneau BG, Srivastava D. Congenital heart disease: entering a new era of human genetics. Circ Res. 2014;114:598–9.
45. Greulich F, Rudat C, Kispert A. Mechanisms of T-box function in the developing heart. Circ Res. 2011;91:212–22.
46. Poelmann RE, Gittenberger-de Groot AC, Vicente-Steijn R, Wisse LJ, Bartelings MM, Everts S, Hoppenbrouwers T, Kruithof BP, Jensen B, de Bruin PW, Hirasawa T, Kuratani S, Vonk F, van de Put JM, de Bakker MA, Richardson MK. Evolution and development of ventricular septation in the amniote heart. Plos One. 2014;9:e106569.
47. Koshiba-Takeuchi K, Mori AD, Kaynak B, Cebra-Thomas J, Sukonnik T, George RO, Latham S, Beck L, Henkelman RM, Black BL, et al. Reptilian heart development and the molecular basis of cardiac chamber evolution. Nature. 2009;461:95–8.
48. Togi K, Kawamoto T, Yamauchi R, Yoshida Y, Kita T, Tanaka M. Role of Hand1/eHand in the dorso-ventral patterning and interventricular septum formation in the embryonic heart. Mol Cell Biol. 2004;24:4627–35.
49. Takeuchi JK, Ohgi M, Koshiba-Takeuchi K, Shiratori H, Sakaki I, Ogura K, Saijoh Y, Ogura T. Tbx5 specifies the left/right ventricles and ventricular septum position during cardiogenesis. Development. 2003;130:5953–64.
50. Mahtab EAF, Wijffels MCEF, van den Akker NMS, Hahurij ND, Lie-Venema H, et al. Cardiac malformations and myocardial abnormalities in podoplanin knockout mouse embryos: correlation with abnormal epicardial development. Dev Dyn. 2008;237:847–57.

51. Panzer AA, Regmi SD, Cormier D, Danzo MT, Chen ID, Winston JB, Hutchinson AK, Salm D, Schulkey CE, Cochran RS, Wilson DB, Jay PY. Nkx2.5 and Sarcospan genetically interact in the development of the muscular ventricular septum of the heart. Sci Rep. 2017;7:46438. https://doi.org/10.1038/srep46438.
52. Captur G, Lopes LR, Patel V, Li C, Bassett P, Syrris P, Sado DM, Maestrini V, Mohun TJ, McKenna WJ, Muthurangu V, Elliott PM, Moon JC. Abnormal cardiac formation in hypertrophic cardiomyopathy: fractal analysis of trabeculae and preclinical gene expression. Circ Cardiovasc Genet. 2014;7(3):241–8. https://doi.org/10.1161/CIRCGENETICS.113.000362.

Part VI

Atrioventricular Septal Defect

Clinical Presentation and Therapy of Atrioventricular Septal Defect

29

Nikolaus A. Haas, David J. Driscoll, and Silke Rickert-Sperling

Abstract

Atrioventricular septal defects (AVSDs) consist of a number of cardiac malformations that result from abnormal development of the endocardial cushions. AVSDs occur in 0.19 of 1000 live births and constitute 4–5 % of congenital heart defects. AVSDs can be categorized as incomplete (or partial) or complete, and intermediate or transitional.

Keywords

Atrioventricular septal defect · AVSD · Endocardial cushions · Ostium primum ASD · Mitral insufficiency · Right atrial shunt · Common atrium

N. A. Haas (✉)
Department of Pediatric Cardiology and Intensive Care, Ludwig Maximilians University, Munich, Germany
e-mail: Nikolaus.haas@med.uni-muenchen.de

D. J. Driscoll
Division of Pediatric Cardiology, Department of Pediatrics, Mayo Clinic College of Medicine, Rochester, MN, USA
e-mail: driscoll.david@mayo.edu

S. Rickert-Sperling
Cardiovascular Genetics, Charité – Universitätsmedizin Berlin, Berlin, Germany
e-mail: silke.sperling@charite.de

© The Author(s), under exclusive license to Springer Nature Switzerland AG 2024

S. Rickert-Sperling et al. (eds.), *Congenital Heart Diseases: The Broken Heart*,
Advances in Experimental Medicine and Biology 1441,
https://doi.org/10.1007/978-3-031-44087-8_29

29.1 Introduction

Atrioventricular septal defects (AVSDs) result from abnormal development of the endocardial cushions with an abnormality of the segments of the atrial and/or ventricular septum near the AV valves. These defects can affect the atrial septum, the ventricular septum, and the AV valves including the papillary muscles, chordae, and valve leaflets. AVSDs occur in 0.19 of 1000 live births and constitute 4–5% of congenital heart defects. According to the cardiac structures involved, AVSDs can be categorized as incomplete (or partial), intermediate, or transitional and complete (Fig. 29.1).

Instead of two separate AV valves, in AVSD, only a single AV valve develops which can however have two different openings. This AV valve usually has five leaflets, whereas two leaflets start from one side of heart and reach out to the other side across the septal defects—i.e., bridging leaflets. There is an anterior and a posterior bridging leaflet, and these leaflets play a role when classifying the AVSDs.

Partial or incomplete AVSDs include an ostium primum ASD (or sometimes a very large ASD called common atrium) and a cleft in the mitral valve. There is no connection at the ventricular septum level, i.e., no VSD. Anatomically, there will be bridging leaflets; there is however tissue that seals off the ventricular part of the defect. Ostium primum ASD results from lack of closure of the ostium primum by the endocardial cushions. Since the endocardial cushions also form major portions of the mitral and tricuspid valves, abnormalities of the atrioventricular valves are associated with ostium primum ASDs. A cleft in the septal leaflet of the mitral valve is invariably associated with ostium primum ASDs. In some cases, there may be an additional defect of the atrioventricular septum producing a left ventricular to right atrial shunt (Gerbode defect). There are also very rare cases where there is only a cleft in the mitral valve but no ASD.

Intermediate or transitional AVSDs consist of an ostium primum ASD and a mostly restrictive posterior VSD but two complete atrioventricular valve rings and thereby two separate openings in a common AV valve. Thus, the ASD and VSD are not contiguous. There is however a primum ASD just above the bridging leaflet and an inlet VSD just below the bridging leaflets.

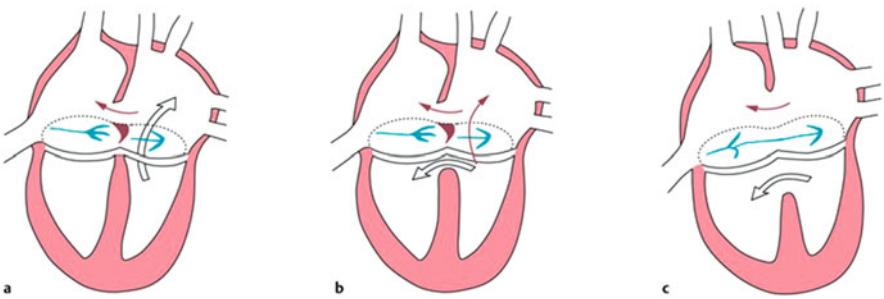

Fig. 29.1 Classification and schematic representation of partial (**a**), intermediate (**b**), and complete (**c**) AVSD. Reproduced from Kinderkardiologie, Georg Thieme Verlag, N. Haas, U. Kleideiter, 2011

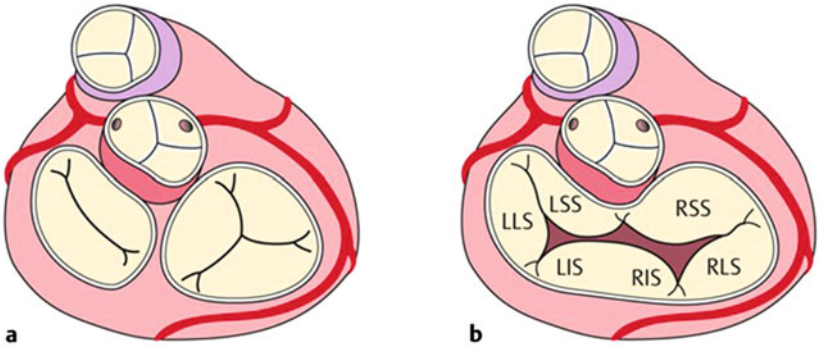

Fig. 29.2 Schematic representation of complete AVSD. Atrioventricular (AV) and semilunar valves in a normal heart (**a**) and in complete AVSD (**b**). Reproduced from Kinderkardiologie, Georg Thieme Verlag, N. Haas, U. Kleideiter, 2011

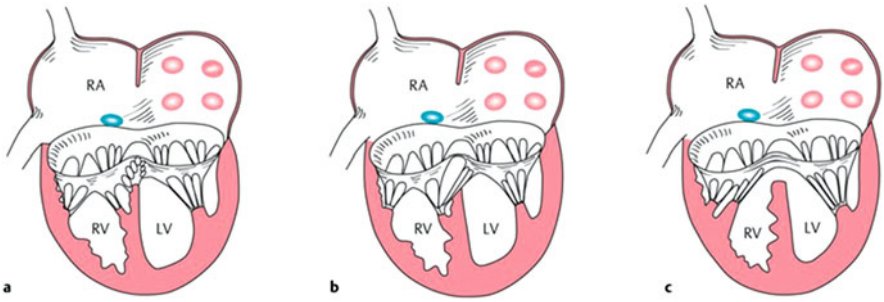

Fig. 29.3 Rastelli classification of AVSD. (**a**) Type A: In this type of AVSD, there is a large ventricular septal defect (VSD) located closer to the apex of the heart. The common AV valve is usually large and positioned toward the apex as well. The left ventricle is usually hypoplastic (underdeveloped) or small in size. (**b**) Type B: Type B AVSD also involves a large VSD, but it is positioned higher in the ventricular septum compared to Type A. The common AV valve is usually more centrally located. The left ventricle is typically larger in size compared to Type A. (**c**) Type C: This type of AVSD is characterized by a small or restrictive VSD located near the base of the heart. The common AV valve is usually smaller and located closer to the atrioventricular septum. The left ventricle is well-developed and typically of normal size. Reproduced from Kinderkardiologie, Georg Thieme Verlag, N. Haas, U. Kleideiter, 2011

Finally, complete AVSD initially is a condition in which the inferior portion of the atrial septum and the posterior portion of the ventricular septum are absent, i.e., a large primum ASD and a large, nonrestrictive inlet VSD. These two defects are contiguous. In addition, instead of two separate atrioventricular valve openings, there is one large common atrioventricular valve with free bridging leaflets. Hence, the entire central portion of the heart is missing (Fig. 29.2). Complete AVSDs are further divided into the Rastelli classifications Type A, B, and C (Fig. 29.3). Here, the attachment and chordae of the anterior bridging leaflet are

used to classify the defects for surgical purposes. Type A and C are easily correctable, whereas the VSD in Type B cannot be closed without damaging the AV valve and is often found in combination with an imbalanced AVSD. The Rastelli classification provides a framework for understanding the anatomical variations seen in AVSD. The specific type of AVSD observed in a patient will influence the surgical approach and treatment options chosen by the cardiac surgical team. In an imbalanced AVSD, one of the two ventricles is hypoplastic so that a biventricular repair cannot be achieved. These patients will be managed by the univentricular "Fontan" pathway.

29.2 Pathologic Physiology

The pathologic physiology of atrioventricular septal defects varies substantially according to the presentation. Partial AVSDs often present with a simple ASD hemodynamics as discussed previously (see Chap. 19). The degree of mitral valve regurgitation adds to the clinical picture by increasing the left atrial and ventricular volume load. Intermediate type AVSDs basically show the same hemodynamics; in most cases, the VSD is small and does not contribute to the clinical picture. Again, the amount of mitral or tricuspid valve regurgitation will add a substantial volume load to the ventricles. Similarly, the pathologic physiology for AVSD involving the ventricular septum is the same as for large ventricular septal defects as discussed previously (Chap. 22). Many children affected show additional mitral and tricuspid regurgitation and will show signs of severe additional cardiac work load due to ventricular regurgitation. In patients with complete AVSD and large shunts, pulmonary hypertension may develop earlier than in simple large VSDs.

29.3 Clinical Presentation and Physical Examination

The presentation and clinical examination of patients with ostium primum ASD and common atrium are the same as ASD as discussed in Chap. 19. However, because of the associated cleft of the septal leaflet of the mitral valve associated with ostium primum ASD, there can be a systolic murmur of mitral insufficiency and, if the leakage is severe, there can be a diastolic mitral flow murmur. Clinically, these children may present earlier based on the amount of regurgitation and some even in overt heart failure due to severe mitral regurgitation (showing failure to thrive, dyspnea, tachycardia, etc.). The presentation and clinical examination of patients with complete AVSDs are similar to patients with a large VSD and are discussed in Chap. 22. Many children affected show however additional mitral and tricuspid regurgitation and will present with clinical signs of heart failure earlier in life. Based on the embryology of the AV node and the conduction system, there is always a typical left axis deviation in patients with AVSD; therefore, a left axis deviation in the ECG should always make one think of an AVSD.

29.4 Diagnostic Imaging

Echocardiography is a valuable tool for accurately diagnosing atrioventricular septal defects (AVSD) and determining the type of AVSD (partial, intermediate, or complete), as well as assessing other associated malformations. Transthoracic echocardiography is usually sufficient for diagnosis in children, while adults with inadequate echocardiographic windows may require transesophageal echocardiography. Echocardiography also allows for the evaluation of atrial and ventricular dilatation, as well as the degree of mitral and/or tricuspid regurgitation. Doppler techniques can be utilized to estimate pulmonary artery pressure by assessing blood flow velocities across the tricuspid and pulmonary valves via tricuspid and pulmonary regurgitation. In some cases, particularly adolescents and adults, transesophageal echocardiography may be necessary to confirm the diagnosis.

Diagnostic cardiac catheterization is generally unnecessary for AVSD diagnosis in the era of echocardiography. However, in patients with severe pulmonary hypertension, diagnostic catheterization may be required to assess pulmonary vascular pressure and resistance, including a stepwise test protocol to evaluate vasoreactivity of elevated pulmonary vascular resistance.

Magnetic resonance imaging (MRI) can be employed in adults and teenagers when echocardiography results remain unclear or when cardiac flow and shunt/regurgitation fraction assessment is needed to determine the indication for AVSD closure in partial or intermediate AVSDs. MRI provides accurate measurements of flow, shunt/regurgitation fraction, and ventricular size, and can also aid in the evaluation of additional cardiac malformations.

Computer tomography (CT) can offer similar anatomical details as MRI but is rarely necessary for AVSD diagnosis. It may be used in patients with contraindications for MRI.

29.5 Treatment

The same management guidelines for treatment of ASD can be applied to patients with incomplete or partial AVSDs. Whereas in simple secundum type ASDs interventional management is feasible in most cases, interventional treatment of ASDs in AVSDs is not possible. In patients with complete AVSDs, the same treatment guidelines for VSD can be applied; however, the degree of mitral regurgitation needs to be considered.

Surgical treatment consists of patch closure of the ASD and VSD together with a surgical closure of the cleft in the mitral valve and/or tricuspid valve. As the AV valves are very thin and delicate structures earlier in life, surgery is usually postponed until the children have reached about 6 months of age whenever possible. To reach this, medical management for heart failure and high caloric input via a nasogastric tube may be necessary. In selected cases, a transient pulmonary band may be necessary (see Chap. 22).

In patients with a late presentation or severe pulmonary hypertension with elevated pulmonary vascular resistance, surgical repair is not possible. These patients will develop right-to-left shunt (Eisenmenger's syndrome).

29.6 Outcome

For partial atrioventricular septal defects of the ostium primum type, the surgical mortality rate is low, typically below 2%, and the long-term prognosis is generally favorable. However, there is an approximately 8% chance that a second operation may be necessary to address subaortic stenosis or mitral valve abnormalities.

For complete forms of atrioventricular septal defects, the surgical mortality rate is 5% or less. However, there is a risk of later reoperation due to complications such as mitral valve or tricuspid valve insufficiency, as well as left ventricular outflow tract obstruction. Even after successful treatment in infancy, patients with complete AVSDs require lifelong follow-up due to the potential risk of deterioration in mitral valve integrity. Additionally, some patients may develop significant mitral regurgitation, atrial arrhythmias, and pulmonary hypertension, particularly in cases where closure is performed at a later stage.

Patients with Eisenmenger syndrome require special care and attention in dedicated departments for grown-up congenital heart (GUCH) patients.

Human Genetics of Atrioventricular Septal Defect

30

Cheryl L. Maslen

Abstract

Atrioventricular septal defects (AVSD), also known as a common atrioventricular canal (CAVC), are clinically severe heart malformations that affect about 1 out of every 2100 live births. AVSD makes up about 5% of all congenital heart defects. AVSD is associated with cytogenetic disorders such as Down syndrome and numerous other rare genetic syndromes, but also occurs as a simplex trait. Studies in mouse models have identified over 100 genetic mutations that have the potential to cause an AVSD. However, studies in humans indicate that AVSD is genetically heterogeneous, and that the cause in humans is very rarely a single-gene defect. Familial cases do occur albeit rarely, usually with autosomal dominant inheritance and variable expression. In addition, the frequent occurrence of AVSD in some syndromes with known genetic causes such as heterotaxy syndrome points to additional genes/pathways that increase AVSD risk. Accordingly, while the genetic underpinnings for most AVSD remain unknown, there have been advances in identifying genetic risk factors for AVSD in both syndromic and nonsyndromic cases. This chapter summarizes the current knowledge of the genetic basis for AVSD.

30.1 Introduction

Atrioventricular septal defects (AVSD) are a group of phenotypically and genetically heterogeneous heart malformations (see Chap. 25). The most commonly occurring genetic association for AVSD is trisomy 21, which causes Down

C. L. Maslen (✉)
Knight Cardiovascular Institute, Oregon Health & Science University, Portland, OR, USA
e-mail: maslenc@ohsu.edu

© The Author(s), under exclusive license to Springer Nature Switzerland AG 2024

S. Rickert-Sperling et al. (eds.), *Congenital Heart Diseases: The Broken Heart*,
Advances in Experimental Medicine and Biology 1441,
https://doi.org/10.1007/978-3-031-44087-8_30

syndrome. An estimated 65% of all cases of complete AVSD occur in individuals with Down syndrome. However, only about 25% of trisomy 21 cases have a complete AVSD, indicating that an extra copy of chromosome 21 is not sufficient to cause the heart defect. However, individuals with trisomy 21 have about a 2000-fold increase in risk for AVSD compared to euploid individuals, so having an extra copy of chromosome 21 is of a very large effect size. Much effort has been focused on finding the gene(s) on chromosome 21 that contribute to the increased risk. Advances in understanding this increased risk are described below.

Individuals with heterotaxy syndrome (HTX) also frequently have a complete AVSD or related heart malformation. Heterotaxy syndrome is caused by mutations in genes that control left-right patterning of the body during development. The premise that AVSD itself is a heterotaxy has been proposed, based on the recognition that improper folding of the heart during development which requires proper left-right patterning would result in an AVSD. However, not all individuals with HTX have an AVSD, so other risk factors must be involved.

Other rare syndromes that sometimes include AVSD as part of the phenotypic spectrum include syndromes such as Ellis-van Creveld (*EVC*, *EVC2*), CHARGE (*CHD7*), Ivemark, and Kaufman-McKusick (*MKKS*), Noonan (*MRAS, SPRED2, RRAS2, PTPN11, CBL, SOS1, KRAS, RAF1, NRAS, RIT1, LZTR1, RASA2, SOS2*), and Holt–Oram (*TBX5*) syndromes. Although uncommon, holoprosencephaly, RASopathies (including Noonan syndrome), and alveolar capillary dysplasia have an increased rate of AVSD occurrence. Rare chromosome deficiencies such as del2q13, del 3p25 (3p syndrome; *CRELD1*), and del 8p23 are also associated with a high rate of AVSD in affected individuals. Families with isolated AVSD inherited in an autosomal dominant pattern with incomplete penetrance have also been described [1, 2]. However, apart from Down syndrome most cases of AVSD occur sporadically and do not have a clear familial component or syndromic association. These are referred to as "simplex AVSD." The complete clinical spectrum of AVSD is presented in Chap. 25, but in euploid individuals with simplex AVSD the most common form is an incomplete or partial AVSD, whereas in Down syndrome complete AVSD is the most common form.

30.2 Disease Threshold Model

AVSD is a complex trait that can be described using a threshold model, where otherwise risk factors of insufficient effect size may occur in combination to breach the disease threshold resulting in a heart defect (Fig. 30.1). The number of required risk factors likely varies depending on an individual's genetic background and could include multiple factors each of small effect size, a combination of large and small effect size variants, or a single variant of very large effect size sufficient to cause the defect (dominant inheritance). Risk factors may be genetic, epigenetic, environmental, or a combination of factors. In the case of Down syndrome there is a clear, but poorly defined contribution of trisomy 21 that greatly increases risk, but alone is not sufficient to cause the defect. This is likely true in general for other syndromes,

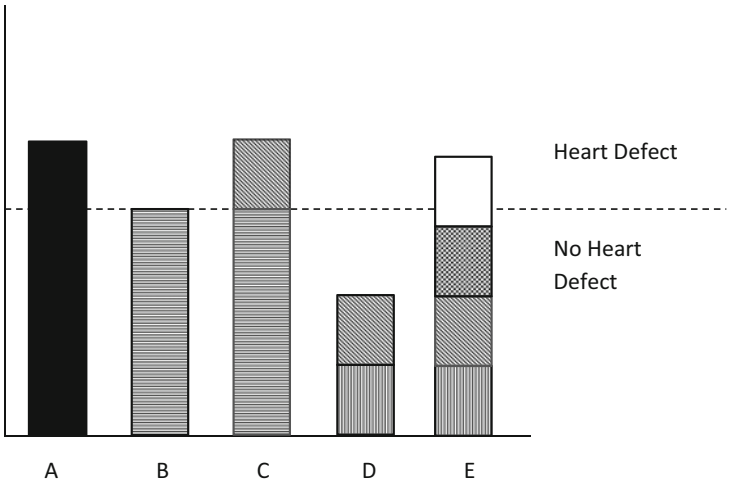

Fig. 30.1 Bar graph demonstrating the genetic disease threshold model. A, Fully penetrant gene mutation causing a heart defect. B, Risk factor with a large effect size, but insufficient to alone cause a heart defect (e.g., trisomy 21). C, Risk factor with a large effect size, but insufficient to alone cause a heart defect plus a genetic mutation in combination causing the heart defect (e.g., trisomy 21 and a *CRELD1* mutation). D, Risk factors with small effect size insufficient to cause a heart defect. E, Combination of small effect size risk factors that in combination cause a heart defect (genetic, epigenetic, environmental, or various combinations including multiple risk alleles)

where the primary cause of the syndrome increases risk, but additional factors push past the disease threshold resulting in a heart defect.

Since trisomy 21 is such an important contributor to AVSD pathogenesis there has been considerable effort over several decades to try and determine which genes on chromosome 21 are causative for AVSD in Down syndrome based on the assumption that there is altered chromosome 21 gene expression due to trisomy. However, the most successful studies have identified association with genes on other chromosomes that somehow interact with trisomy 21 to raise the risk of developing an AVSD, as described below.

30.3 AVSD Genes and Pathways

30.3.1 *CRELD1* Mutations

Cysteine-rich protein with EGF-like domains 1 (CRELD1) was first identified through a study of infants with the cytogenetic disorder, 3p syndrome. These children are missing the distal portion of the short arm of chromosome 3 and have a variable phenotype with AVSD found in those with a more proximal breakpoint. This defined a "critical region" of 3p that encompassed the *AVSD2* locus, which presumably included a gene, or genes, that when deleted caused the heart defect

[3]. Molecular mapping identified a previously unrecognized gene, *CRELD1*, in that interval [4]. Expressed in the developing heart, *CRELD1* became a candidate for the *AVSD2* locus. Further studies determined that missense mutations in *CRELD1* were associated with simplex AVSD [5], which have been confirmed in multiple populations around the world, occurring in about 5% of simplex cases [6–10]. Family studies showed that *CRELD1* missense mutations are incompletely penetrant, which is consistent with the proposed disease threshold model for AVSD [5]. Additional studies demonstrated that missense mutations in *CRELD1* were also associated with AVSD in Down syndrome [11] and heterotaxy syndrome [12], demonstrating a specificity of the mutations for AVSD regardless of genetic background. The association of *CRELD1* mutations and AVSD in Down syndrome has now been validated in additional studies in different populations [13–15]. The outcomes suggest that there may be population differences in the incidence of *CRELD1* mutations associated with AVSD. Two studies performed in India showed that a relatively high percentage of individuals with Down syndrome and AVSD carry a heterozygous damaging *CRELD1* missense variant occurring in up to 30% of cases studied. These included both novel and recurrent variants specifically associated with AVSD. Two recurrent variants have been reported in multiple studies and are clearly specific to the diagnosis of AVSD regardless of the genetic background. These predominant variants, p.Arg329Cys (R329C) and p.Glu325Lys (E325K), are emerging as a major contributors to AVSD etiology. R329C has been found in simplex AVSD, AVSD in Down syndrome, and AVSD in heterotaxy syndrome. E325K alters protein folding and disrupts calcium binding and is found in about 5% of Down syndrome AVSD cases and has also been seen in simplex AVSD.

In contrast to the findings from studies in India and the United States (including samples from Scotland), a study performed in Mexico including 148 subjects with Down syndrome and AVSD did not find any *CRELD1* variants that were not also seen in Down syndrome individuals with healthy hearts [14]. This suggests that there might be differences in the incidence of damaging *CRELD1* variants between racial/ethnic groups.

The contribution of CRELD1 defects to the risk of heart malformations was confirmed in an innovative study using the Ts65Dn mouse model as a sensitized genetic background for heart defects [16]. This mouse model of Down syndrome has an incidence of cardiac septal defects at birth of approximately 4.7%. However, when crossed with a *Creld1* heterozygous null mouse the incidence of heart defects at birth increased to 33.3%, indicating that deficiency of Creld1 does indeed contribute to the risk of heart defects.

Mouse models also have helped define CRELD1 function and the mechanism of disease when there are mutations. The *Creld1* knockout mouse model demonstrated that Creld1 function is essential for heart development and that absence of Creld1 interferes with VEGFA-dependent proliferation of endocardial cells [17]. CRELD1 activates calcineurin/NFATc1 signaling under the control of VEGFA thereby promoting the expression of NFATc1 targets, which is required for the endocardial cushions to remodel into valves. Two *CRELD1* missense mutations associated with AVSD in humans, the recurrent p.R329C mutation and another mutation, p.R107H,

have been shown to directly interfere with activation of the calcineurin/NFATc1 signaling cascade thereby impairing valve formation [18]. Although the specific mechanistic action for other *CRELD1* mutations is unknown protein structure is altered, which would likely impair activation of NFATc1.

30.3.2 *NFATc1* Mutations

The recognition that CRELD1 activates NFATc1 signaling resulted in the recognition of *NFATc1* as a viable candidate gene for AVSD. This prompted an international candidate gene study to test this hypothesis [19]. The study cohort included confirmed simplex AVSD and AVSD with heterotaxy. All had previously been genotyped for variants in *CRELD1*, *GATA4*, *PTPN11* and *NR2F2* to rule out other causative mutations. Of the 60 study subjects three (5%) were positive for heterozygous missense variants predicted to be high-impact damaging mutations. Ectopic expression of the mutant alleles in zebrafish demonstrated that they caused abnormal heart looping and atrioventricular canal development consistent with AVSD formation. This important finding indicates that the CRELD1/NFATc1 pathway genes are major contributors to the pathogenesis of AVSD regardless of the underlying genetic background.

30.3.3 *NR2F2* Mutations

Another transcription factor gene, nuclear receptor subfamily2/group F (NR2F2), has been shown to have AVSD-associated mutations in simplex AVSD cases and familial cases of mixed heart malformations including AVSD. *NR2F2* was identified as an AVSD candidate gene based on a finding of enrichment of *de novo* mutations in cases compared to controls in a whole exome sequencing study [20]. The premise of the study was that *de novo* variants are likely to be the most damaging variants, thereby providing a strategy for filtering the exome data. Targeted gene sequencing identified additional *NR2F2* mutations in more simplex cases and identified inherited mutations in families with multigenerational congenital heart disease. Cosegregation of those mutations with the heart defects indicates that *NR2F2* mutations can be causal. There appeared to be a possible genotype–phenotype correlation, with loss-of-function variants biased toward left ventricular outflow tract obstruction and functional missense mutations most often associated with septal defects.

30.3.4 VEGFA Pathway Gene Mutations

Vascular endothelial growth factor A (VEGFA) has long been known to play a key role in heart valve development, and the demonstrated interaction between CRELD1 and VEGF (Redig) suggested that mutations in other VEGFA pathway genes might be additional risk factors for AVSD. Using a candidate gene exome sequencing

approach, it was demonstrated that there is an excess of damaging missense mutations in VEGFA pathway genes in individuals with Down syndrome-associated AVSD, including several recurrent mutations in *GATA5* that altered transcriptional activity [21]. Although individually rare, recurrent missense mutations in these genes were identified in 10% of cases studied, indicating a significant contribution to risk of AVSD in Down syndrome. Further study is needed to determine if this phenomenon specific to Down syndrome or if it extends to simplex AVSD.

30.3.5 Association of Additional Genetic Risk Factors with AVSD

There are several isolated reports of single-gene mutations associated with AVSD (Table 30.1), including *PTPN11*, *GATA4*, *GATA6*, *ALK2*, and *FOXP1* that likely represent rare or family-specific events that may be important in understanding AVSD biology but do not account for the majority of cases [22, 24, 25, 29–31]. More recently, targeted exome sequencing of 112 candidate genes showed a significant enrichment of rare damaging variants in individuals with simplex AVSD compared to a non-AVSD control cohort [32]. The candidate genes were selected from several sources, including association with human syndromes that include AVSD, animal models with AVSD, literature overlap for genes implicated in AVSD in both humans and animals, reported AVSD genes in isolated human cases, and reported cardiac modifiers in Down syndrome. In total, seven genes of the 112 genes had an enrichment of rare variants associated with AVSD. Of these genes, *NIPBL*, *CHD7*, *CEP152*, *BMPR1a*, *ZFPM2,* and *MDM4* had novel associations with the AVSD phenotype in humans. There was also enrichment of rare variants in *NR2F2*, which has been previously reported. Three of the genes, *NIPBL*, *CHD7*, *CEP152*, have been associated with syndromes. These cases were clinically evaluated to rule out an undiagnosed syndrome, so the association with simplex AVSD is new. Eight individuals had more than one rare or rare/damaging variant in more than one gene, suggesting that there may be a compound effect, consistent with the disease threshold model presented above. These studies underscore the substantial genetic heterogeneity in AVSD and may point to biochemical pathways or biological functions that are central to the cause of this defect. For instance, the greatly increased incidence of AVSD in heterotaxy syndrome (60–70%) implicates genes involved in left-right patterning of the embryo in the pathogenesis of AVSD. This includes genes such as *ACVR2B*, *CFC1*, *FOXP1*, *LEFTY2*, *NODAL,* and *ZIC3* [23, 24, 27, 28]. Mutations in these genes clearly cause heterotaxy syndrome and significantly increase risk for AVSD and related heart malformations. Heterotaxy syndrome is one of the many disorders that are classified as ciliopathies, or diseases that occur due to dysfunction of primary and/or motile cilia. AVSD also occurs in association with other ciliopathies such as Bardet–Biedl and Meckel–Gruber syndromes. It is notable that defects in cilia-related genes disrupt second heart field development in mice, leading to AVSD. In addition, a study of children with Down syndrome showed that rare, large genetic deletions involving genes encoding components of the cilia were enriched in the children with

Table 30.1 Genetic variants associated with AVSD

Gene	Protein variant	Function	Phenotypes	Reference
ALK2	p.His286Asp	Reduced BMP signaling	pAVSD, DS	[22]
CFC1	p.Ala145Thr	Reduced Nodal signaling	AVSD, HPE	[23]
CRELD1	p.Arg107His	Reduced calcineurin/ NFATc1 signaling	pAVSD, HTX	[5]
	p.Pro162Ala	Misfolding	AVSD	[10]
	p.Pro286Arg	Misfolding	pAVSD	[6]
	p.Glu325Lys[a]	Disruption of calcium binding	pAVSD, DS	[6]
	p.Thr311Ile	Misfolding	pAVSD	[5]
	p.Arg329Cys[a]	Misfolding, reduced calcineurin/NFATc1 signaling	pAVSD	[5, 7, 18]
	p.Arg329Cys[a]		cAVSD, DS	[11]
	p.Arg329Cys[a]		cAVSD, HTX	[12]
	p.Glu414Lys	Misfolding, reduced calcineurin/NFATc1 signaling	cAVSD, DS	[11]
	p.Met379Thr[a]	Altered protein structure	cAVSD, DS	[13]
	p. Met339Asnfs*7	Frameshift, Premature termination codon	cAVSD, DS	[15]
	p.Val344Val	Exon splicing enhancer disruption	cAVSD, DS	
	p. Asp137Argfs*34	Frameshift, Premature termination codon	cAVSD, DS	
	p.Gly149Gly	Exon splicing enhancer disruption	cAVSD, DS	
	p. Lys233Argfs*15	Frameshift, Premature termination codon	cAVSD, DS	
	p. Lys319Serfs*26	Frameshift, Premature termination codon	cAVSD, DS	
	p.Glu325Lys[a]	Disruption of calcium binding	cAVSD, DS	
	p.Ser374Leufs*4	Frameshift, Premature termination codon	cAVSD, DS	
	p.His373His	Exon splicing enhancer disruption	cAVSD, DS	
	p.Met379Thr[a]	Altered protein structure	cAVSD, DS	
FOXP1	p. Pro568Ser	Decreased transcriptional activity	ubAVSD, PA, single ventricle, HTX	[24]
GATA4	p.Gly296Ser	Decreased transcriptional activity	Familial CHD, including AVSD	[25]
GATA5	p.Gln3Arg	Increased transcriptional activity	cAVSD, DS	[21]
	p.Tyr142His	Increased transcriptional activity	cAVSD, DS	

(continued)

Table 30.1 (continued)

Gene	Protein variant	Function	Phenotypes	Reference
	p.Phe159Leu	Decreased transcriptional activity	cAVSD, DS	
GATA6	p.A178V	Increased transcriptional activity	AVSD, HLH, VSD	[26]
LEFTY2	p.S342K	Disruption of L/R axis determination	AVSD, HLH, AV shunt, HTX	[27]
	p.R314[b]	Disruption of L/R axis determination	AVSD, HLV, AV shunt, HTX	
NFATc1	p.Val210Met	Disruption of atrioventricular canal specification domains	pAVSD, HTX	[19]
	p.Ala696Thr	Disruption of atrioventricular canal specification domains	pAVSD, HTX	
	p.Ala367Val	Disruption of atrioventricular canal specification domains	pAVSD	
NODAL	p.Arg275Cys	Decreased transactivation of NODAL targets	cAVSD, d-TGA, HTX	[28]
NR2F2	p.Gln75dup	Increased transcriptional activity	cAVSD	[20]
	p.Asp179Val	No change in transcriptional activity	pAVSD	
	p.Asn205Ile	Increased transcriptional activity	iAVSD	
	p.Glu251Asp	Decreased transcriptional activity	ubAVSD	
	p.Ser341Tyr	Decreased transcriptional activity	cAVSD	
	p.Ala412Ser	No change in transcriptional activity	cAVSD	
PTPN11	p.Leu43Phe	Altered phosphotyrosine binding	cAVSD	[29]
ZIC3	p.Ser402Pro	Disruption of L/R axis determination	AVSD, HTX	

AVSD, atrioventricular septal defects; cAVSD, complete AVDS; iAVSD, intermediate AVSD; pAVSD, partial AVSD (ostium primum ASD); ubAVSD, unbalanced AVSD; CVM, complex cardiac vascular abnormalities; DS, Down syndrome; HLH, hypoplastic left heart; HLV, hypoplastic left ventricle; HPE, holoprosencephaly; HTX, heterotaxy syndrome; N.D., not determined; PA, pulmonary atresia; TGA, transposition of the great arteries; *dup*, duplication

[a] Recurrent variant

[b] Translation termination (stop) codon

an AVSD [33]. Collectively, these data suggest that defects in cilia may be a primary pathogenic event in AVSD, although this is yet to be shown for AVSD not associated with heterotaxy.

Meta-analysis of genetic data from the Down Syndrome Heart Project, including whole-genome, whole-exome, and array-based imputation generated polygenic risk scores that indicated that the NOTCH pathway, with a focus on *NOTCH4*, and genes involved in the ciliome, particularly *CEP290*, may play a role in the cause of AVSD in Down syndrome albeit as a small contribution of approximately 1% [34]. Further studies are needed to confirm these associations.

Other potential contributing factors include rare copy-number variants [35] and other chromosome abnormalities [36]. However, like most of the single-gene defects, these are rare and unlikely to contribute significantly to the incidence of AVSD. Indeed, in a study of copy-number variants on chromosome 21 in Down syndrome individuals with and without AVSD showed no specific association between any CNV and AVSD [37].

Environmental factors may also contribute to the cause of AVSD, including gene × environment interactions such as genetic variants that affect folate metabolism [38], and epigenetics [39]. This may be particularly true in Down syndrome, where it has been shown that there is differential DNA methylation compared to euploid individuals [40]. However, these areas are largely unexplored at this point and deserve further attention.

Genetic mutations with demonstrated functional consequences with a direct link to heart development are summarized in Table 30.1.

30.4 Conclusions

AVSD is a phenotypically and genetically heterogeneous heart defect. Numerous genes have been associated with AVSD, although few have been confirmed by additional studies and are either very rare mutations or spurious associations that may not contribute to the pathogenesis of the heart defect. For the most part, simplex AVSD is associated with deleterious rare coding variants in at least 25 genes to date. In addition, there is enrichment of damaging variants in genes within the VEGFA pathway, and in a cluster of additional candidate genes derived from circumstantial associations. With a couple of exceptions, the pattern of genotypic burden is unknown. It appears certain that the VEGFA pathway is a source of causative AVSD mutations. Indeed, the three most frequently mutated genes *CRELD1* *NFATc1*, and *N2RF2*, are all part of the VEGFA pathway. Mutations in these genes have been identified in numerous unrelated affected individuals with confirmed pathogenicity in animal models. However, mutations in these genes contribute to only a small percentage of simplex AVSD cases.

Syndromes play a significant role in the incidence of AVSD, mostly due to Down syndrome, which accounts for 45% of all AVSD. *CRELD1* mutations are seen in 10–30% of Down syndrome AVSD cases, indicating that it is a major contributor to AVSD pathogenesis when expressed on the trisomy 21 background. All other syndromes that include AVSD as part of the phenotype are extremely rare. However, Digilio and colleagues have proposed that there is a unifying role for sonic hedgehog (SHH) for genetic syndromes that have AVSD as part of their phenotypic spectrum

(Digilio et al. 2019). This is supported by data from Down syndrome sequencing studies that indicates that ciliome gene mutations and the NOTCH pathway contribute to the pathogenesis of AVSD, as these are elements of SHH signaling. Indeed, studies in mouse models have demonstrated that cilia gene mutations cause AVSD via multiple mechanisms [41].

Combining all reported known and potential risk factors still falls short of accounting for the incidence of AVSD, indicating that additional discovery is still needed. Epigenetic analyses may provide additional insight into the overall etiology AVSD.

References

1. Sheffield VC, Pierpont ME, Nishimura D, Beck JS, Burns TL, Berg MA, Stone EM, Patil SR, Lauer RM. Identification of a complex congenital heart defect susceptibility locus by using DNA pooling and shared segment analysis. Hum Mol Genet. 1997;6:117–21.
2. Wilson L, Curtis A, Korenberg JR, Schipper RD, Allan L, Chenevix-Trench G, Stephenson A, Goodship J, Burn J. A large, dominant pedigree of atrioventricular septal defect (AVSD): exclusion from the Down syndrome critical region on chromosome 21. Am J Hum Genet. 1993;53:1262–8.
3. Green EK, Priestley MD, Waters J, Maliszewska C, Latif F, Maher ER. Detailed mapping of a congenital heart disease gene in chromosome 3p25. J Med Genet. 2000;37:581–7.
4. Rupp PA, Fouad GT, Egelston CA, Reifsteck CA, Olson SB, Knosp WM, Glanville RW, Thornburg KL, Robinson SW, Maslen CL. Identification, genomic organization and mRNA expression of CRELD1, the founding member of a unique family of matricellular proteins. Gene. 2002;293:47–57.
5. Robinson SW, Morris CD, Goldmuntz E, Reller MD, Jones MA, Steiner RD, Maslen CL. Missense mutations in CRELD1 are associated with cardiac atrioventricular septal defects. Am J Hum Genet. 2003;72:1047–52.
6. Guo Y, Shen J, Yuan L, Li F, Wang J, Sun K. Novel CRELD1 gene mutations in patients with atrioventricular septal defect. World J Pediatr. 2010;6:348–52.
7. Kusuma L, Dinesh SM, Savitha MR, Krishnamurthy B, Narayanappa D, Ramachandra NB. A maiden report on CRELD1 single-nucleotide polymorphism association in congenital heart disease patients of Mysore, South India. Genet Test Mol Biomarkers. 2011;15:483–7.
8. Posch MG, Perrot A, Schmitt K, Mittelhaus S, Esenwein EM, Stiller B, Geier C, Dietz R, Gessner R, Ozcelik C, Berger F. Mutations in GATA4, NKX2.5, CRELD1, and BMP4 are infrequently found in patients with congenital cardiac septal defects. Am J Med Genet A. 2008;146A:251–3.
9. Sarkozy A, Esposito G, Conti E, Digilio MC, Marino B, Calabro R, Pizzuti A, Dallapiccola B. CRELD1 and GATA4 gene analysis in patients with nonsyndromic atrioventricular canal defects. Am J Med Genet A. 2005;139:236–8.
10. Zatyka M, Priestley M, Ladusans EJ, Fryer AE, Mason J, Latif F, Maher ER. Analysis of CRELD1 as a candidate 3p25 atrioventicular septal defect locus (AVSD2). Clin Genet. 2005;67:526–8.
11. Maslen CL, Babcock D, Robinson SW, Bean LJ, Dooley KJ, Willour VL, Sherman SL. CRELD1 mutations contribute to the occurrence of cardiac atrioventricular septal defects in Down syndrome. Am J Med Genet A. 2006;140:2501–5.
12. Zhian S, Belmont J, Maslen CL. Specific association of missense mutations in CRELD1 with cardiac atrioventricular septal defects in heterotaxy syndrome. Am J Med Genet A. 2012;158A:2047–9.

13. Ghosh P, Bhaumik P, Ghosh S, Ozbek U, Feingold E, Maslen C, Sarkar B, Pramanik V, Biswas P, Bandyopadhyay B, Dey SK. Polymorphic haplotypes of CRELD1 differentially predispose Down syndrome and euploids individuals to atrioventricular septal defect. Am J Med Genet A. 2012;158A(11):2843–8. https://doi.org/10.1002/ajmg.a.35626. Epub 2012 Sep 14
14. Alcántara-Ortigoza MA, De Rubens-Figueroa J, Reyna-Fabian ME, Estandía-Ortega B, González-del Angel A, Molina-Álvarez B, Velázquez-Aragón JA, Villagómez-Martínez S, Pereira-López GI, Martínez-Cruz V, Álvarez-Gómez RM, Díaz-García L. Germline mutations in NKX2-5, GATA4, and CRELD1 are rare in a Mexican sample of Down syndrome patients with endocardial cushion and septal heart defects. Pediatr Cardiol. 2015;36(4):802–8.
15. Asim A, Agarwal S, Panigrahi I, Sarangi AN, Muthuswamy S, Kapoor A. CRELD1 gene variants and atrioventricular septal defects in Down syndrome. Gene. 2018;641:180–5. https://doi.org/10.1016/j.gene.2017.10.044. Epub 2017 Oct 18
16. Li H, Cherry S, Klinedinst D, DeLeon V, Redig J, Reshey B, Chin MT, Sherman SL, Maslen CL, Reeves RH. Genetic modifiers predisposing to congenital heart disease in the sensitized Down syndrome population. Circ Cardiovasc Genet. 2012;5:301–8.
17. Redig JK, Fouad GT, Babcock D, Reshey B, Feingold E, Reeves RH, Maslen CL. Allelic interaction between CRELD1 and VEGFA in the pathogenesis of cardiac atrioventricular septal defects. AIMS Genet. 2014;1:1–19.
18. Mass E, Wachten D, Aschenbrenner AC, Voelzmann A, Hoch M. Murine Creld1 controls cardiac development through activation of calcineurin/NFATc1 signaling. Dev Cell. 2014;28:711–26.
19. Ferese R, Bonetti M, Consoli F, Guida V, Sarkozy A, Lepri FR, Versacci P, Gambardella S, Calcagni G, Margiotti K, Piceci Sparascio F, Hozhabri H, Mazza T, Digilio MC, Dallapiccola B, Tartaglia M, Marino B, Hertog JD, De Luca A. Heterozygous missense mutations in NFATC1 are associated with atrioventricular septal defect. Hum Mutat. 2018;39(10):1428–41.
20. Al Turki S, Manickaraj AK, Mercer CL, Gerety SS, Hitz MP, Lindsay S, D'Alessandro LC, Swaminathan GJ, Bentham J, Arndt AK, Low J, Breckpot J, Gewillig M, Thienpont B, Abdul-Khaliq H, Harnack C, Hoff K, Kramer HH, Schubert S, Siebert R, Toka O, Cosgrove C, Watkins H, Lucassen AM, O'Kelly IM, Salmon AP, Bu'lock FA, Granados-Riveron J, Setchfield K, Thornborough C, Brook JD, Mulder B, Klaassen S, Bhattacharya S, Devriendt K, Fitzpatrick DF, Consortium UK, Wilson DI, Mital S, Hurles ME. Rare variants in NR2F2 cause congenital heart defects in humans. Am J Hum Genet. 2014;94:574–85.
21. Ackerman C, Locke AE, Feingold E, Reshey B, Espana K, Thusberg J, Mooney S, Bean LJ, Dooley KJ, Cua CL, Reeves RH, Sherman SL, Maslen CL. An excess of deleterious variants in VEGF-A pathway genes in Down-syndrome-associated atrioventricular septal defects. Am J Hum Genet. 2012;91:646–59.
22. Joziasse IC, Smith KA, Chocron S, van Dinther M, Guryev V, van de Smagt JJ, Cuppen E, Ten Dijke P, Mulder BJ, Maslen CL, Reshey B, Doevendans PA, Bakkers J. ALK2 mutation in a patient with Down's syndrome and a congenital heart defect. Eur J Hum Genet. 2011;19:389–93.
23. Roessler E, Ouspenskaia MV, Karkera JD, Velez JI, Kantipong A, Lacbawan F, Bowers P, Belmont JW, Towbin JA, Goldmuntz E, Feldman B, Muenke M. Reduced NODAL signaling strength via mutation of several pathway members including FOXH1 is linked to human heart defects and holoprosencephaly. Am J Hum Genet. 2008;83:18–29.
24. Chang SW, Mislankar M, Misra C, Huang N, Dajusta DG, Harrison SM, McBride KL, Baker LA, Garg V. Genetic abnormalities in FOXP1 are associated with congenital heart defects. Hum Mutat. 2013;34:1226–30.
25. Garg V, Kathiriya IS, Barnes R, Schluterman MK, King IN, Butler CA, Rothrock CR, Eapen RS, Hirayama-Yamada K, Joo K, Matsuoka R, Cohen JC, Srivastava D. GATA4 mutations cause human congenital heart defects and reveal an interaction with TBX5. Nature. 2003;424:443–7.

26. Maitra M, Schluterman MK, Nichols HA, Richardson JA, Lo CW, Srivastava D, Garg V. Interaction of Gata4 and Gata6 with Tbx5 is critical for normal cardiac development. Dev Biol. 2009;326:368–77.
27. Kosaki K, Bassi MT, Kosaki R, Lewin M, Belmont J, Schauer G, Casey B. Characterization and mutation analysis of human LEFTY A and LEFTY B, homologues of murine genes implicated in left-right axis development. Am J Hum Genet. 1999;64:712–21.
28. Mohapatra B, Casey B, Li H, Ho-Dawson T, Smith L, Fernbach SD, Molinari L, Niesh SR, Jefferies JL, Craigen WJ, Towbin JA, Belmont JW, Ware SM. Identification and functional characterization of NODAL rare variants in heterotaxy and isolated cardiovascular malformations. Hum Mol Genet. 2009;18:861–71.
29. Weismann CG, Hager A, Kaemmerer H, Maslen CL, Morris CD, Schranz D, Kreuder J, Gelb BD. PTPN11 mutations play a minor role in isolated congenital heart disease. Am J Med Genet A. 2005;136:146–51.
30. Tomita-Mitchell A, Maslen CL, Morris CD, Garg V, Goldmuntz E. GATA4 sequence variants in patients with congenital heart disease. J Med Genet. 2007;44:779–83.
31. Rajagopal SK, Ma Q, Obler D, Shen J, Manichaikul A, Tomita-Mitchell A, Boardman K, Briggs C, Garg V, Srivastava D, Goldmuntz E, Broman KW, Benson DW, Smoot LB, Pu WT. Spectrum of heart disease associated with murine and human GATA4 mutation. J Mol Cell Cardiol. 2007;43:677–85.
32. D'Alessandro LC, Al Turki S, Manickaraj AK, Manase D, Mulder BJ, Bergin L, Rosenberg HC, Mondal T, Gordon E, Lougheed J, Smythe J, Devriendt K, Bhattacharya S, Watkins H, Bentham J, Bowdin S, Hurles ME, Mital S. Exome sequencing identifies rare variants in multiple genes in atrioventricular septal defect. Genet Med. 2016;18(2):189–98.
33. Ramachandran D, Mulle J, Locke A, Bean L, Rosser T, Bose P, Dooley K, Cua C, Capone G, Reeves R, Maslen C, Cutler D, Sherman S, Zwick M. Contribution of copy-number variation to Down syndrome-associated atrioventricular septal defects. Genet Med. 2014.
34. Trevino CE, Holleman AM, Corbitt H, Maslen CL, Rosser TC, Cutler DJ, Johnston HR, Rambo-Martin BL, Oberoi J, Dooley KJ, Capone GT, Reeves RH, Cordell HJ, Keavney BD, Agopian AJ, Goldmuntz E, Gruber PJ, O'Brien JE Jr, Bittel DC, Wadhwa L, Cua CL, Moskowitz IP, Mulle JG, Epstein MP, Sherman SL, Zwick ME. Identifying genetic factors that contribute to the increased risk of congenital heart defects in infants with Down syndrome. Sci Rep. 2020;10(1):18051.
35. Priest JR, Girirajan S, Vu TH, Olson A, Eichler EE, Portman MA. Rare copy number variants in isolated sporadic and syndromic atrioventricular septal defects. Am J Med Genet A. 2012;158A:1279–84.
36. Maslen CL. Molecular genetics of atrioventricular septal defects. Curr Opin Cardiol. 2004;19:205–10.
37. Rambo-Martin BL, Mulle JG, Cutler DJ, Bean LJH, Rosser TC, Dooley KJ, Cua C, Capone G, Maslen CL, Reeves RH, Sherman SL, Zwick ME. Analysis of copy number variants on chromosome 21 in Down syndrome-associated congenital heart defects. G3 (Bethesda). 2018;8(1):105–11.
38. Locke AE, Dooley KJ, Tinker SW, Cheong SY, Feingold E, Allen EG, Freeman SB, Torfs CP, Cua CL, Epstein MP, Wu MC, Lin X, Capone G, Sherman SL, Bean LJ. Variation in folate pathway genes contributes to risk of congenital heart defects among individuals with Down syndrome. Genet Epidemiol. 2010;34:613–23.
39. Chang CP, Bruneau BG. Epigenetics and cardiovascular development. Annu Rev Physiol. 2012;74:41–68.
40. Kerkel K, Schupf N, Hatta K, Pang D, Salas M, Kratz A, Minden M, Murty V, Zigman WB, Mayeux RP, Jenkins EC, Torkamani A, Schork NJ, Silverman W, Croy BA, Tycko B. Altered DNA methylation in leukocytes with trisomy 21. PLoS Genet. 2010;6(11):e1001212. https://doi.org/10.1371/journal.pgen.1001212.

41. Burnicka-Turek O, Steimle JD, Huang W, Felker L, Kamp A, Kweon J, Peterson M, Reeves RH, Maslen CL, Gruber PJ, Yang XH, Shendure J, Moskowitz IP. Cilia gene mutations cause atrioventricular septal defects by multiple mechanisms. Hum Mol Genet. 2016;25(14):3011–28. https://doi.org/10.1093/hmg/ddw155. Epub 2016 Jun 23
42. Digilio MC, Pugnaloni F, De Luca A, Calcagni G, Baban A, Dentici ML, Versacci P, Dallapiccola B, Tartaglia M, Marino B. Atrioventricular canal defect and genetic syndromes: The unifying role of sonic hedgehog. Clin Genet. 2019;95(2):268–76. https://doi.org/10.1111/cge.13375.

Molecular Pathways and Animal Models of Atrioventricular Septal Defect

31

Andy Wessels

Abstract

The development of a fully functional four-chambered heart is critically dependent on the correct formation of the structures that separate the atrial and ventricular chambers. Perturbation of this process typically results in defects that allow mixing of oxygenated and deoxygenated blood. Atrioventricular septal defects (AVSD) form a class of congenital heart malformations that are characterized by the presence of a primary atrial septal defect (pASD), a common atrioventricular valve (cAVV), and frequently also a ventricular septal defect (VSD). While AVSD were historically considered to result from failure of the endocardial atrioventricular cushions to properly develop and fuse, more recent studies have determined that inhibition of the development of other components of the atrioventricular mesenchymal complex can lead to AVSDs as well. The role of the dorsal mesenchymal protrusion (DMP) in AVSD pathogenesis has been well-documented in studies using animal models for AVSDs, and in addition, preliminary data suggest that the mesenchymal cap situated on the leading edge of the primary atrial septum may be involved in certain situations as well. In this chapter, we review what is currently known about the molecular mechanisms and animal models that are associated with the pathogenesis of AVSD.

Keywords

Atrioventricular septal defects · AVSD · Congenital · Septation · Regulation · Pathways · Dorsal mesenchymal protrusion · Mesenchymal cap · Atrial septum

A. Wessels (✉)
Department of Regenerative Medicine and Cell Biology, Medical University of South Carolina, Charleston, SC, USA
e-mail: wesselsa@musc.edu

© The Author(s), under exclusive license to Springer Nature Switzerland AG 2024

S. Rickert-Sperling et al. (eds.), *Congenital Heart Diseases: The Broken Heart*, Advances in Experimental Medicine and Biology 1441,
https://doi.org/10.1007/978-3-031-44087-8_31

31.1 Introduction

31.1.1 Atrioventricular Septal Defects

Atrioventricular septal defects (AVSDs) are complex heart malformations found in approximately 5% of individuals with congenital heart disease (CHD). Based on the potential for shunting between the left and right side of the heart, two major AVSD subtypes can be distinguished [1]. In the case of "incomplete or partial" AVSDs, shunting is restricted to the atrial level via a primary atrial septal defect (pASD) or *ostium primum defect*. In "complete" AVSDs, we find, in addition to a pASD, also an inlet-type ventricular septal defect (VSD). In complete AVSDs, shunting can occur at both atrial and ventricular level. For many years, it was believed that perturbation of proper development of the endocardial AV cushions (the mesenchymal precursor tissues for the AV valves) was the only mechanism leading to AVSD (hence the frequently used term "endocardial cushion defect" as a synonym for AVSD). However, a number of observations in the human heart [2, 3] as well as a growing number of experimental studies in recent years, have revealed that abnormal development of another mesenchymal tissue, the posterior second heart field (pSHF)-derived dorsal mesenchymal protrusion (DMP), may play an even more critical role in the pathogenesis of AVSDs [4–6]. In addition, unpublished and ongoing studies suggest that a third component of the AV mesenchymal complex, the mesenchymal cap on the leading edge of the primary atrial septum [7], could be involved in the pathogenesis of AVSDs as well. In this chapter we will discuss several conditions and models in which AVSDs are observed. Unless we specifically mention "complete" or "incomplete," the term AVSD refers to either form.

31.1.2 AVSDs and Human Genetics

In the human population, AVSDs are found as part of a variety of genetic syndromes, but also in association with nonsyndromic single-gene mutations. Down syndrome (trisomy 21), the most common genetic syndrome in humans, is strongly associated with AVSDs: approximately 1/4 of children with Down syndrome have an AVSD and roughly 2/3 of cases of complete AVSD are found in patients with trisomy 21 [8]. That not all individuals with Down syndrome have an AVSD indicates that the pathogenesis of AVSD in Down syndrome may involve multiple genetic modifiers and/or environmental components. Other syndromes in which AVSDs are frequently observed include CHARGE syndrome [9], Smith–Lemli–Opitz syndrome (SLOS) [10], Ellis–van Creveld syndrome [11], Noonan syndrome [12], and Heterotaxy syndrome [13]. Elsewhere in this publication, a chapter can be found in which information is provided about genetic variants that are found in association with AVSDs.

31.1.3 The Dorsal Mesenchymal Protrusion (DMP) and the Mesenchymal Cap and the Pathogenesis of AVSDs

The DMP, sometimes referred to as the "vestibular spine" [2, 3, 14, 15] or "spina vestibuli" [16, 17], plays an essential role in atrial and atrioventricular septation [18–20]. The window in which the DMP develops is relatively narrow. Virtually all our insight into how the DMP develops comes from studies in the mouse. The development of the DMP starts around E9–9.5 of development when high proliferative activity of the pSHF cells that are located ventral to the foregut, leads to a rapid expansion of the pSHF cell population. Around E10–10.5 the expanded pSHF-derived cell population protrudes into the common atrium as the DMP, using the dorsal mesocardium as its portal of entry [17, 19]. Here the DMP becomes a critical player in the septation process. As described in Chap. 4 ("Development of the Venous Pole"), atrial septation starts when the myocardial primary atrial septum (or *septum primum*) descends from the atrial roof into the common atrium [21]. On the leading edge of this septum is located an endocardially-derived mesenchymal cap (or ridge). Although this mesenchymal cap and the DMP have different origins, the two mesenchymal tissues are contiguous with each other. The space located under the primary atrial septum, through which the left and right atriums are in open communication with each other, is the primary foramen (or *ostium primum*). During normal development, the mesenchymal cap, the DMP, and the major AV cushions will eventually fuse and close the primary foramen [18]. The body of mesenchyme formed after the fusion of the cap, the DMP, and the AV cushions is known as the AV mesenchymal complex [20]. Eventually, the mesenchyme of the DMP, but not the mesenchyme of the cap and cushions, undergoes a myocardial differentiation. In the formed heart, the muscularized DMP can be recognized as the inferior muscular rim at base of the atrial septum [21, 22, 20]. As described above, an important event in the development of the DMP is the expansion of the pSHF cell population resulting from its high proliferative activity. When cell proliferation is inhibited/impaired, the pSHF precursor population does not expand, the DMP fails to develop (or is severely truncated) and will, as a result, not be able to participate in atrioventricular septation. In this case, the AV mesenchymal complex will not form properly and the primary foramen will not be closed. This results in a common AV valve (cAVV) and a primary atrial septal defect (pASD). The development of the DMP also involves cell migration [5]. Cell migration is important for organogenesis as well as numerous other developmental processes. Extracellular components, including growth factors, cytokines and/or extracellular matrix (ECM) proteins, are typically required for the initiation and progression of cell migration [23]. These components may be produced by neighboring cells and/or are present in the extracellular matrix and can be involved in the regulation of intracellular signaling pathway factors, including Rho, Rac, and other members of the small GTPase family that facilitate migration by stimulating extension of lamellipodia, turnover of cell–substrate adhesion, and cell body contraction [24–26]. Perturbation of SHF cell migration has been proposed to be a mechanism that can lead to inhibition of DMP formation, resulting in failure of the AV mesenchymal complex to form [5]. That the

cap is an integral part of the AV mesenchymal complex, and that it is involved in the fusion of the primary atrial septum with the AV cushions, is well-documented [18]. Relatively little is known about how the mechanisms that regulate the development of the cap, about the molecular features of the cap mesenchyme, or whether perturbation of its development can play a role in AVSD pathogenesis. In line with studies that have revealed the role of the DMP in AV valvuloseptal development, ongoing studies are now looking into the role of the cap in the formation of the AV mesenchymal cap in more detail. In the context of this chapter we will focus on what is known about the DMP.

31.1.4 Emerging Insights into the Molecular Pathways That Are Involved in DMP Development

Insights into the cellular and molecular mechanisms that govern proper DMP development and its maturation are slowly emerging. Below, we will discuss a number of studies, performed in recent years on mouse models with AVSDs, that have increased our understanding of how the development and growth of the pSHF and DMP are regulated and have provided insights into the etiology of AVSDs.

31.1.4.1 The BMP Signaling Pathway and AVSDs

Bone morphogenetic proteins (BMPs) play an important role in cardiovascular development. At least six BMP isoforms are expressed in the heart (BMP2,4,5,6,7,10). Of these isoforms, BMP2 has been most frequently studied. BMP2 is highly expressed in the myocardium of the AV junction at early stages of development [27]. Here it plays a crucial role in regulating the endocardial-to-mesenchymal transformation necessary for formation of the AV cushions [28]. Mice that do not express BMP2 (BMP2 knockout mice) die before E12.5. Embryos isolated at this stage show severe defects in AV cushion development [28, 29]. BMP4 is also very important for heart formation [30–32]. Mice deficient for this isoform also die early in development [33]. However, transgenic BMP4 hypomorphic mice (i.e., mice that express a severely reduced amount of BMP4) survive until after birth but die within 1 week. Histological examination of BMP4 hypomorphic mice shows a 100% penetrance of AVSD [34]. Furthermore, when BMP4 is specifically deleted from the myocardium, the offspring also have AVSDs [34]. In this context it is important to note that BMP4 is abundantly expressed in the myocardial walls of the dorsal mesocardium (a.k.a. the mesocardial reflections) but that BMP4 is not expressed in the myocardial AV junction [4]. The mesocardial reflections flank the space through which the expanding pSHF protrudes into the common atrial cavity [1, 18]. In a recent study it was shown that the pSHF population that eventually will form the DMP expresses BmpR1A/Alk3, a BMP receptor known to interact with BMP4. Furthermore, positive staining for activated pSmad1,5,8 in this cell population indicates ongoing BMP signaling. The importance of BmpR1A/Alk3-dependent BMP signaling for the formation of the DMP and atrioventricular septation was demonstrated in experiments in which BmpR1A/Alk3

was conditionally deleted from the SHF using the myocyte enhancer factor 2C (*Mef2C)-AHF-Cre* mouse line. SHF-specific deletion of Alk3 resulted in impaired formation of the DMP and a completely penetrant incomplete AVSD (*ostium primum defect*) phenotype at stages ED13.5 to 15.5. Analysis of *Mef2C-AHF-Cre*; $Alk3^{fl/fl}$ mutants at E10–10.5 revealed decreased proliferative index of SHF cells and, consequently, a reduced number of pSHF cells at the cardiac venous pole [4].

31.1.4.2 The (Sonic) Hedgehog Signaling Pathway and AVSDs

Sonic hedgehog (Shh) is a secreted morphogen that plays an important role in the development of the heart. Specifically, Shh is crucial for regulating SHF contributions to the cardiac inflow tract, to the cardiac outflow tract, and to cardiac septation [5, 35, 36]. Interestingly, while Shh knockout mice have severe cardiac defects [37, 38], Shh is not expressed within the heart itself. This indicates that extracardiac sources are involved in Shh-dependent regulation of heart development. One of the tissues secreting Shh is the ventral pharyngeal endoderm [35]. Conditional deletion of Shh with a NK2 homeobox 5 (*Nkx2–5)-Cre* mouse, driving expression in a number of tissues including the pharyngeal endoderm, leads to a fully penetrant AVSD phenotype [35]. Shh signaling involves two coreceptors. Smoothened (Smo) is a G-protein-coupled like receptor acting downstream of Patched (Ptch1) to confer Shh signaling; when secreted Shh binds to Ptch1 it abolishes an inhibitory effect on Smo, allowing Smo to transduce signals via Gli transcription factors. Shh expressing ventral pharyngeal endoderm is juxtaposed to the SHF/DMP-precursor cell population located between the foregut and the heart. Conditionally deleting Smo from the SHF/DMP-precursor cell with the *Mef2c-AHF-Cre* mouse (*Mef2c-AHF-Cre;* $Smo^{fl/-}$) inhibits Shh signaling in these cells, perturbs DMP formation, and results in a fully penetrant AVSD phenotype [5]. Thus interaction between Shh (expressed in, and secreted from pharyngeal endoderm) and the Shh receptor Smo (expressed in the SHF/DMP-precursor cell population) is essential for development of the DMP and, hence, for proper AV septation.

31.1.4.3 The Wnt/β-Catenin Signaling Pathway and AVSDs

The wingless-type MMTV integration site family (Wnt)/β-catenin signaling pathway is involved in many developmental events. In the heart, Wnt/β-catenin signaling has been shown to regulate the development of the outflow tract and right ventricle, components of the heart that are derived from the SHF [39, 40]. In addition, the Wnt/β-catenin signaling pathway is also of importance for the development of the venous pole of the heart. Deletion of β-catenin with the islet 1 (*Isl1)-Cre* mouse (like the *Mef2c-AHF-Cre* mouse driving Cre-expression in the SHF) results in embryonic lethality, pharyngeal arch defects, and cardiac malformations including AVSD (pASD) [41]. Conditional deletion of β-catenin results in reduction of proliferation of SHF-derived cardiac progenitor cells and significant downregulation of a number of downstream genes including Isl1, T-box (Tbx) 3, Wnt11, and Shh [41]. One specific Wnt variant found to be directly associated with the development of the posterior SHF and the DMP, and therefore with atrioventricular septation, is Wnt2 [6]. At the critical stages of DMP development (ED9.5–10.5), Wnt2 and Lef-1, a

central transcription mediator of Wnt/β-catenin signaling, are expressed in the SHF mesodermal cell population and the DMP. Wnt2 and lymphoid enhancer-binding factor 1 (Lef-1) are, however, not expressed in the ventricles, AV canal, or AV cushions [6, 42]. Mice that do not express Wnt2 (Wnt2-null mutants) show reduced expression of axin2, Isl1, Lef1, and fibroblast growth factor 10 (Fgf10), a direct target of Wnt/β-catenin signaling [6, 40]. Staining for Ki67 shows a decrease in proliferative activity of the SHF/DMP-precursor population and histological analysis reveals severe inhibition of DMP development. The proliferation defect and associated failure of the DMP to properly develop resembles what is observed in the conditional SHF-Alk3 knock-out mouse [4] (see also above). Approximately 85% of Wnt2-null mutants die at birth and histological analysis of Wnt2-null specimens reveals the presence of AVSDs. LiCl is a pharmacological inhibitor of Gsk-3b and a strong activator of Wnt/β-catenin signaling. Administration of LiCl to pregnant female mice carrying ED8–10 mutant Wnt2 embryos, leads to an elevation of Lef1 expression in the posterior SHF, restores SHF cell proliferation, rescues the AVSD phenotype, and increases the survival rate of Wnt2-null mutant offspring. Another member of the Wnt family associated with the development of the DMP is *Wnt11*. *Wnt11*-null mice die embryonically and demonstrate hypoplasia of the DMP, a phenotype that is recapitulated when Wnt11 is deleted in a SHF-specific manner with an *Isl1*-cre mouse [43].

31.1.4.4 Pdgf and Pdgf Receptors and AVSDs

Platelet-derived growth factors (*Pdgf's*) play major roles in cardiac development. Knockout mice for *Pdgf* ligands and their receptors (*Pdgfr's*) present with a spectrum of cardiac malformations, including abnormalities of the outflow tract [44, 45]. AVSDs are found in *Pdgfrα* and *Pdgfrβ* mutant mice. While *Pdgfrβ* knockout mice only show sporadic AVSDs, the malformations are more common in *Pdgfrα* knockout mice, where the presence of an AVSD has been associated with hypoplasia of the DMP [46]. *Pdgfrα* is expressed in the pSHF and in the pSHF-derived DMP. During the analysis of *Pdgfrα* knockout mice significantly elevated levels of the transcription factor Nkx2–5 were found. Nkx2–5 is a transcription factor expressed in embryonic and differentiated cardiomyocytes and during normal development, Nkx2–5 is switched on in cells of the DMP as they undergo mesenchymal-to-myocardial differentiation around E14 [19]. If the gradual increase in *Nkx2–5* expression in the DMP is the driving force behind the muscular differentiation of the DMP mesenchyme after the formation of the AV mesenchymal complex, and if *Nkx2–5* expression is indeed elevated in the pSHF of the *Pdgfrα* knockout mouse, then premature and ectopic myocardial differentiation of the pSHF cell population should be considered as a possible mechanism involved in inhibiting normal DMP formation and causing AVSD. In this context it is interesting to note that premature myocardial differentiation of pSHF has also been suggested to be involved in the pathogenesis of AVSDs in *Mef2c-AHF-cre;Smo*$^{fl/-}$ embryos [5].

31.1.4.5 Tbx5 and AVSD

Haploinsufficiency of *TBX5* causes Holt–Oram syndrome [47, 48]. Patients with Holt–Oram syndrome have a spectrum of congenital malformations, including limb and cardiac defects. In the *Tbx5* mutant mouse, ASD and AVSDs are found in approximately 40% of *Tbx5* haploinsufficient offspring [49]. Within the pSHF, *Tbx5* is coexpressed with *Gli1*, a member of a transcription factor family responsible for *Shh* signal transduction [49]. That *Tbx5* expression in the pSHF is critical to the development of the DMP was demonstrated by deleting *Tbx5* from the SHF with two SHF Cre-mouse models; *Mef2c-AHF-Cre* and *Gli1-Cre-ERT2* mice [49]. Both approaches resulted in fully penetrant incomplete AVSD (*ostium primum defect*). Quantitative analysis of markers for Shh signaling in the *Mef2c-AHF-Cre;Tbx5* embryos revealed a significant reduction in the expression of the *Shh* receptor *Ptch1* (see 25.5.3) and *Gli1*, suggesting that *Shh* signaling is downstream of *Tbx5* in the regulation of pSHF and DMP development. Furthermore, the gene encoding *Odd-skipped related-1* (*Osr1*), a zinc finger transcription factor, was identified as a direct downstream target of Tbx5 in the SHF. Given the fact that *Osr1* knockout mice also develop AVSDs [50], and in combination with additional data, implicating *Tbx5* in promoting pSHF proliferation by directly regulating cell-cycle gene transcription through the cyclin-dependent kinase *Cdk6*, these results shows that *Tbx5* plays a critical role within the pSHF.

31.1.4.6 Cilia and AVSDs

Primary cilia are organelles that protrude from the cell surface. The core structure of primary cilia is composed of microtubule bundles (the ciliary axoneme), which extends, via a transition zone, from a microtubule-based basal body. The formation, maintenance and function of cilia are dependent largely on trafficking of particles along the axoneme by the intraflagellar transport (IFT) machinery. Proteins of the IFT-B complex are required for anterograde trafficking from the base to the tip of the cilium, whereas the IFT-A complex is believed to be involved in controlling retrograde ciliary trafficking. Primary cilia are found on almost all mammalian cell types and a growing body of evidence shows their significance in the development of a variety of organs. Cilia "dysfunction" has been associated with a spectrum of human congenital malformations, including cardiac defects. For instance, a recent publication reports atrial and ventricular septal defects in humans with mutations in nimA-related kinase 8 (NEK8), a primary cilium-associated protein [51] while another recent study suggests that AVSDs and other congenital heart malformations found in Down syndrome patients may be associated with an altered ciliome [52]. A comprehensive study of the avc1 mouse mutant, a mouse carrying a hypomorphic mutation of intraflagellar transport protein *Ift172* ($Ift172^{avc1}/Ift172^{avc1}$), showed AVSDs in 100% of avc1 mutants analyzed [53]. Another mouse model with impaired cilia formation is the cobblestone (*cbs*) mutant, carrying a hypomorphic allele for *Ift88* (a.k.a. *Polaris*). Analysis of *cbs/cbs* mutants also showed a 100% penetrance of complete AVSD [54]. Cilia are important in a number of signal transduction and molecular pathways associated with the development of the pSHF/DMP, in particular the *Shh* pathway. *Shh* signaling is initiated when secreted

Shh binds to the membrane receptor *Patched* (*Ptc1*) localized on the distal end of the axoneme. This interaction alleviates inhibition of the transmembrane protein *Smoothened* (*Smo*; see 25.5.2) by *Ptc1*. *Smo* then activates the transcriptional activator *Gli2,* thereby transmitting the *Shh* signal to the nucleus. The *Shh* signaling pathway is critically dependent on intraflagellar transport which acts downstream of *Ptc1* and *Smo* but upstream of the *Gli* transcriptional activity. Thus, primary cilia present on the cells of the posterior SHF, may play a pivotal role in atrioventricular septation through the regulation of the *Shh* pathway and associated molecular and cellular mechanisms.

31.1.5 Conclusion

The studies described in this chapter show that compromised proliferation of the pSHF/DMP precursor cell population is the most common mechanism underlying the pathogenesis of AVSD [4, 6, 49]. In addition, some observations suggest that premature myocardial differentiation of pSHF cells and/or altered migration characteristics of these cells also contribute to the pathogenesis of this cardiac defect [5, 46]. The LiCl embryonic rescue experiment in the *Wnt2* knockout mouse [6] that resulted in lowering the penetrance of the AVSD phenotype in the *Wnt2* knockout offspring, provides hope that in the foreseeable future pharmacological (or other) approaches may be developed which, in specific situations, can lower the risk of developing this congenital heart defect.

References

1. Briggs LE, Kakarla J, Wessels A. The pathogenesis of atrial and atrioventricular septal defects with special emphasis on the role of the dorsal mesenchymal protrusion. Differentiation. 2012;84(1):117–30. https://doi.org/10.1016/j.diff.2012.05.006.
2. Blom NA, Ottenkamp J, Wenink AG, Gittenberger-de Groot AC. Deficiency of the vestibular spine in atrioventricular septal defects in human fetuses with down syndrome. Am J Cardiol. 2003;91(2):180–4.
3. Sharratt GP, Webb S, Anderson RH. The vestibular defect: an interatrial communication due to a deficiency in the atrial septal component derived from the vestibular spine. Cardiol Young. 2003;13(2):184–90.
4. Briggs LE, Phelps AL, Brown E, Kakarla J, Anderson RH, van den Hoff MJ, Wessels A. Expression of the BMP receptor Alk3 in the second heart field is essential for development of the dorsal mesenchymal protrusion and atrioventricular Septation. Circ Res. 2013;112(11):1420–32. https://doi.org/10.1161/CIRCRESAHA.112.300821.
5. Goddeeris MM, Rho S, Petiet A, Davenport CL, Johnson GA, Meyers EN, Klingensmith J. Intracardiac septation requires hedgehog-dependent cellular contributions from outside the heart. Development. 2008;135(10):1887–95.
6. Tian Y, Yuan L, Goss AM, Wang T, Yang J, Lepore JJ, Zhou D, Schwartz RJ, Patel V, Cohen ED, Morrisey EE. Characterization and in vivo pharmacological rescue of a Wnt2-Gata6 pathway required for cardiac inflow tract development. Dev Cell. 2010;18(2):275–87.

7. Deepe R, Fitzgerald E, Wolters R, Drummond J, Guzman K, Hoff M, Wessels A. The mesenchymal cap of the atrial septum and atrial and atrioventricular Septation. J Cardiovasc Dev Dis. 2020;7(4) https://doi.org/10.3390/jcdd7040050.
8. Barlow GM, Chen XN, Shi ZY, Lyons GE, Kurnit DM, Celle L, Spinner NB, Zackai E, Pettenati MJ, Van Riper AJ, Vekemans MJ, Mjaatvedt CH, Korenberg JR. Down syndrome congenital heart disease: a narrowed region and a candidate gene. Genet Med. 2001;3(2): 91–101.
9. Corsten-Janssen N, Kerstjens-Frederikse WS, du Marchie Sarvaas GJ, Baardman ME, Bakker MK, Bergman JE, Hove HD, Heimdal KR, Rustad CF, Hennekam RC, Hofstra RM, Hoefsloot LH, Van Ravenswaaij-Arts CM, Kapusta L. The cardiac phenotype in patients with a CHD7 mutation. Circ Cardiovasc Genet. 2013;6(3):248–54. https://doi.org/10.1161/CIRCGENETICS.113.000054.
10. Digilio MC, Marino B, Giannotti A, Dallapiccola B, Opitz JM. Specific congenital heart defects in RSH/Smith-Lemli-Opitz syndrome: postulated involvement of the sonic hedgehog pathway in syndromes with postaxial polydactyly or heterotaxia. Birth Defects Res A Clin Mol Teratol. 2003;67(3):149–53. https://doi.org/10.1002/bdra.10010.
11. Hills CB, Kochilas L, Schimmenti LA, Moller JH. Ellis-van Creveld syndrome and congenital heart defects: presentation of an additional 32 cases. Pediatr Cardiol. 2011;32(7):977–82. https://doi.org/10.1007/s00246-011-0006-9.
12. Digilio MC, Romana Lepri F, Dentici ML, Henderson A, Baban A, Roberti MC, Capolino R, Versacci P, Surace C, Angioni A, Tartaglia M, Marino B, Dallapiccola B. Atrioventricular canal defect in patients with RASopathies. Eur J Hum Genet. 2013;21(2):200–4. https://doi.org/10.1038/ejhg.2012.145.
13. Degenhardt K, Rychik J. Fetal situs, isomerism, Heterotaxy syndrome: diagnostic evaluation and implication for postnatal management. Curr Treat Options Cardiovasc Med. 2016;18(12): 77. https://doi.org/10.1007/s11936-016-0494-2.
14. Kim JS, Viragh S, Moorman AF, Anderson RH, Lamers WH. Development of the myocardium of the atrioventricular canal and the vestibular spine in the human heart. Circ Res. 2001;88(4): 395–402.
15. Mommersteeg MT, Soufan AT, de Lange FJ, van den Hoff MJ, Anderson RH, Christoffels VM, Moorman AF. Two distinct pools of mesenchyme contribute to the development of the atrial septum. Circ Res. 2006;99(4):351–3. https://doi.org/10.1161/01.RES.0000238360.33284.a0.
16. Webb S, Anderson RH, Lamers WH, Brown NA. Mechanisms of deficient cardiac septation in the mouse with trisomy 16. Circ Res. 1999;84(8):897–905.
17. Webb S, Brown NA, Anderson RH. Formation of the atrioventricular septal structures in the normal mouse. Circ Res. 1998;82(6):645–56.
18. Snarr BS, Kern CB, Wessels A. Origin and fate of cardiac mesenchyme. Dev Dyn. 2008;237 (10):2804–19.
19. Snarr BS, O'Neal JL, Chintalapudi MR, Wirrig EE, Phelps AL, Kubalak SW, Wessels A. Isl1 expression at the venous pole identifies a novel role for the second heart field in cardiac development. Circ Res. 2007a;101(10):971–4. https://doi.org/10.1161/CIRCRESAHA.107.162206.
20. Snarr BS, Wirrig EE, Phelps AL, Trusk TC, Wessels A. A spatiotemporal evaluation of the contribution of the dorsal mesenchymal protrusion to cardiac development. Dev Dyn. 2007c;236(5):1287–94. https://doi.org/10.1002/dvdy.21074.
21. Wessels A, Anderson RH, Markwald RR, Webb S, Brown NA, Viragh S, Moorman AF, Lamers WH. Atrial development in the human heart: an immunohistochemical study with emphasis on the role of mesenchymal tissues. Anat Rec. 2000;259(3):288–300.
22. Anderson RH, Brown NA, Webb S. Development and structure of the atrial septum. Heart. 2002;88(1):104–10.
23. Affolter M, Weijer CJ. Signaling to cytoskeletal dynamics during chemotaxis. Dev Cell. 2005;9 (1):19–34. https://doi.org/10.1016/j.devcel.2005.06.003.

24. Allen WE, Jones GE, Pollard JW, Ridley AJ. Rho, Rac and Cdc42 regulate actin organization and cell adhesion in macrophages. J Cell Sci. 1997;110(Pt 6):707–20.
25. Nobes CD, Hall A. Rho, rac, and cdc42 GTPases regulate the assembly of multimolecular focal complexes associated with actin stress fibers, lamellipodia, and filopodia. Cell. 1995;81(1): 53–62.
26. Zhao ZS, Manser E, Loo TH, Lim L. Coupling of PAK-interacting exchange factor PIX to GIT1 promotes focal complex disassembly. Mol Cell Biol. 2000;20(17):6354–63.
27. Somi S, Buffing AA, Moorman AF, Van Den Hoff MJ. Dynamic patterns of expression of BMP isoforms 2, 4, 5, 6, and 7 during chicken heart development. Anat Rec A Discov Mol Cell Evol Biol. 2004;279(1):636–51.
28. Sugi Y, Yamamura H, Okagawa H, Markwald RR. Bone morphogenetic protein-2 can mediate myocardial regulation of atrioventricular cushion mesenchymal cell formation in mice. Dev Biol. 2004;269(2):505–18.
29. Ma L, Lu MF, Schwartz RJ, Martin JF. Bmp2 is essential for cardiac cushion epithelial-mesenchymal transition and myocardial patterning. Development. 2005;132(24):5601–11. https://doi.org/10.1242/dev.02156.
30. Liu W, Selever J, Wang D, Lu MF, Moses KA, Schwartz RJ, Martin JF. Bmp4 signaling is required for outflow-tract septation and branchial-arch artery remodeling. Proc Natl Acad Sci U S A. 2004;101(13):4489–94.
31. McCulley DJ, Kang JO, Martin JF, Black BL. BMP4 is required in the anterior heart field and its derivatives for endocardial cushion remodeling, outflow tract septation, and semilunar valve development. Dev Dyn. 2008;237(11):3200–9.
32. Uchimura T, Komatsu Y, Tanaka M, McCann KL, Mishina Y. Bmp2 and Bmp4 genetically interact to support multiple aspects of mouse development including functional heart development. Genesis. 2009;47(6):374–84. https://doi.org/10.1002/dvg.20511.
33. Fujiwara T, Dehart DB, Sulik KK, Hogan BL. Distinct requirements for extra-embryonic and embryonic bone morphogenetic protein 4 in the formation of the node and primitive streak and coordination of left-right asymmetry in the mouse. Development. 2002;129(20):4685–96.
34. Jiao K, Kulessa H, Tompkins K, Zhou Y, Batts L, Baldwin HS, Hogan BL. An essential role of Bmp4 in the atrioventricular septation of the mouse heart. Genes Dev. 2003;17(19):2362–7.
35. Goddeeris MM, Schwartz R, Klingensmith J, Meyers EN. Independent requirements for hedgehog signaling by both the anterior heart field and neural crest cells for outflow tract development. Development. 2007;134(8):1593–604. https://doi.org/10.1242/dev.02824.
36. Hoffmann AD, Peterson MA, Friedland-Little JM, Anderson SA, Moskowitz IP. Sonic hedgehog is required in pulmonary endoderm for atrial septation. Development. 2009;136(10): 1761–70.
37. Hildreth V, Webb S, Chaudhry B, Peat JD, Phillips HM, Brown N, Anderson RH, Henderson DJ. Left cardiac isomerism in the sonic hedgehog null mouse. J Anat. 2009;214(6):894–904. https://doi.org/10.1111/j.1469-7580.2009.01087.x.
38. Washington Smoak I, Byrd NA, Abu-Issa R, Goddeeris MM, Anderson R, Morris J, Yamamura K, Klingensmith J, Meyers EN. Sonic hedgehog is required for cardiac outflow tract and neural crest cell development. Dev Biol. 2005;283(2):357–72. https://doi.org/10.1016/j.ydbio.2005.04.029.
39. Ai D, Fu X, Wang J, Lu MF, Chen L, Baldini A, Klein WH, Martin JF. Canonical Wnt signaling functions in second heart field to promote right ventricular growth. Proc Natl Acad Sci U S A. 2007;104(22):9319–24. https://doi.org/10.1073/pnas.0701212104.
40. Cohen ED, Wang Z, Lepore JJ, Lu MM, Taketo MM, Epstein DJ, Morrisey EE. Wnt/beta-catenin signaling promotes expansion of Isl-1-positive cardiac progenitor cells through regulation of FGF signaling. J Clin Invest. 2007;117(7):1794–804. https://doi.org/10.1172/jci31731.
41. Lin L, Cui L, Zhou W, Dufort D, Zhang X, Cai CL, Bu L, Yang L, Martin J, Kemler R, Rosenfeld MG, Chen J, Evans SM. Beta-catenin directly regulates Islet1 expression in cardiovascular progenitors and is required for multiple aspects of cardiogenesis. Proc Natl Acad Sci U S A. 2007;104(22):9313–8. https://doi.org/10.1073/pnas.0700923104.

42. Watanabe Y, Kokubo H, Miyagawa-Tomita S, Endo M, Igarashi K, Aisaki K, Kanno J, Saga Y. Activation of Notch1 signaling in cardiogenic mesoderm induces abnormal heart morphogenesis in mouse. Development. 2006;133(9):1625–34. https://doi.org/10.1242/dev.02344.
43. van Vliet PP, Lin L, Boogerd CJ, Martin JF, Andelfinger G, Grossfeld PD, Evans SM. Tissue specific requirements for WNT11 in developing outflow tract and dorsal mesenchymal protrusion. Dev Biol. 2017;429(1):249–59. https://doi.org/10.1016/j.ydbio.2017.06.021.
44. Soriano P. The PDGF alpha receptor is required for neural crest cell development and for normal patterning of the somites. Development. 1997;124(14):2691–700.
45. Tallquist MD, Soriano P. Cell autonomous requirement for PDGFRalpha in populations of cranial and cardiac neural crest cells. Development. 2003;130(3):507–18.
46. Bax NA, Bleyl SB, Gallini R, Wisse LJ, Hunter J, Van Oorschot AA, Mahtab EA, Lie-Venema H, Goumans MJ, Betsholtz C, Gittenberger-de Groot AC. Cardiac malformations in Pdgfralpha mutant embryos are associated with increased expression of WT1 and Nkx2.5 in the second heart field. Dev Dyn. 2010;239(8):2307–17. https://doi.org/10.1002/dvdy.22363.
47. Basson CT, Bachinsky DR, Lin RC, Levi T, Elkins JA, Soults J, Grayzel D, Kroumpouzou E, Traill TA, Leblanc-Straceski J, Renault B, Kucherlapati R, Seidman JG, Seidman CE. Mutations in human TBX5 [corrected] cause limb and cardiac malformation in Holt-Oram syndrome. Nat Genet. 1997;15(1):30–5. https://doi.org/10.1038/ng0197-30.
48. Li QY, Newbury-Ecob RA, Terrett JA, Wilson DI, Curtis AR, Yi CH, Gebuhr T, Bullen PJ, Robson SC, Strachan T, Bonnet D, Lyonnet S, Young ID, Raeburn JA, Buckler AJ, Law DJ, Brook JD. Holt-Oram syndrome is caused by mutations in TBX5, a member of the Brachyury (T) gene family. Nat Genet. 1997;15(1):21–9. https://doi.org/10.1038/ng0197-21.
49. Xie L, Hoffmann AD, Burnicka-Turek O, Friedland-Little JM, Zhang K, Moskowitz IP. Tbx5-hedgehog molecular networks are essential in the second heart field for atrial septation. Dev Cell. 2012;23(2):280–91. https://doi.org/10.1016/j.devcel.2012.06.006.
50. Wang Q, Lan Y, Cho ES, Maltby KM, Jiang R. Odd-skipped related 1 (odd 1) is an essential regulator of heart and urogenital development. Dev Biol. 2005;288(2):582–94.
51. Frank V, Habbig S, Bartram MP, Eisenberger T, Veenstra-Knol HE, Decker C, Boorsma RA, Gobel H, Nurnberg G, Griessmann A, Franke M, Borgal L, Kohli P, Volker LA, Dotsch J, Nurnberg P, Benzing T, Bolz HJ, Johnson C, Gerkes EH, Schermer B, Bergmann C. Mutations in NEK8 link multiple organ dysplasia with altered hippo signalling and increased c-MYC expression. Hum Mol Genet. 2013;22(11):2177–85. https://doi.org/10.1093/hmg/ddt070.
52. Ripoll C, Rivals I, Ait Yahya-Graison E, Dauphinot L, Paly E, Mircher C, Ravel A, Grattau Y, Blehaut H, Megarbane A, Dembour G, de Freminville B, Touraine R, Creau N, Potier MC, Delabar JM. Molecular signatures of cardiac defects in down syndrome lymphoblastoid cell lines suggest altered ciliome and hedgehog pathways. PLoS One. 2012;7(8):e41616. https://doi.org/10.1371/journal.pone.0041616.
53. Friedland-Little JM, Hoffmann AD, Ocbina PJ, Peterson MA, Bosman JD, Chen Y, Cheng SY, Anderson KV, Moskowitz IP. A novel murine allele of Intraflagellar transport protein 172 causes a syndrome including VACTERL-like features with hydrocephalus. Hum Mol Genet. 2011;20(19):3725–37. https://doi.org/10.1093/hmg/ddr241.
54. Willaredt MA, Gorgas K, Gardner HA, Tucker KL. Multiple essential roles for primary cilia in heart development. Cilia. 2012;1(1):23. https://doi.org/10.1186/2046-2530-1-23.

Part VII

Total Anomalous Pulmonary Venous Return

Clinical Presentation and Therapy of Total Anomalous Pulmonary Venous Return

32

Nikolaus A. Haas, David J. Driscoll, and Silke Rickert-Sperling

Keywords

Total anomalous pulmonary venous return · TAPVR · Partial anomalous venous return · Pulmonary veins · Pulmonary artery · Cyanosis · Pulmonary edema · Right atrium · Left atrium · Right ventricle · Left ventricle · Systolic murmur · Obstruction

32.1 Introduction

Total anomalous pulmonary venous return (TAPVR) is rare (accounting for about 1% of all CHD) and can occur as a single lesion or in combination with other types of CHD (such as heterotaxy or HLHS). TAPVR is defined as an abnormal connection where all pulmonary veins do not drain into the left atrium but into the right atrium either directly or through a vein that is connected to the right atrium. TAPVR can be divided into four anatomic groups (Fig. 32.1): (1) supracardiac (about 55%), (2) cardiac (about 30%), (3) infracardiac (about 13%), and (4) mixed (very rare). In addition, it can be divided into two physiological types: nonobstructed and

N. A. Haas (✉)
Department of Pediatric Cardiology and Intensive Care, Ludwig Maximilians University, Munich, Germany
e-mail: Nikolaus.haas@med.uni-muenchen.de

D. J. Driscoll
Division of Pediatric Cardiology, Department of Pediatrics, Mayo Clinic College of Medicine, Rochester, MN, USA
e-mail: driscoll.david@mayo.edu

S. Rickert-Sperling
Cardiovascular Genetics, Charité–Universitätsmedizin Berlin, Berlin, Germany
e-mail: silke.sperling@charite.de

© The Author(s), under exclusive license to Springer Nature Switzerland AG 2024

S. Rickert-Sperling et al. (eds.), *Congenital Heart Diseases: The Broken Heart*,
Advances in Experimental Medicine and Biology 1441,
https://doi.org/10.1007/978-3-031-44087-8_32

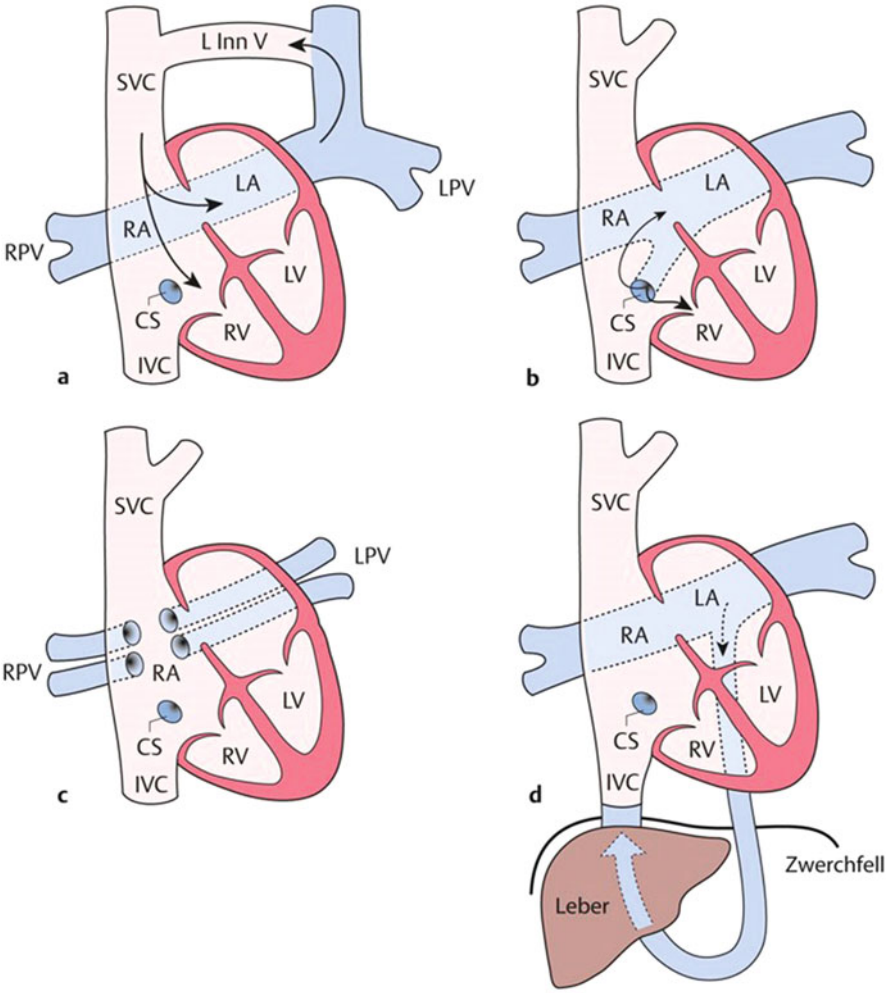

Fig. 32.1 The four types of TAPVR are illustrated: (**a**) Supracardiac TAPVR: The pulmonary veins drain into a confluence behind the heart and then connect to a systemic vein, usually the superior vena cava; (**b**) Cardiac TAPVR: The pulmonary veins drain (**b**) directly into the right atrium or (**c**) in a confluence draining directly into the right atrium; (**d**) Infracardiac TAPVR: The pulmonary veins drain into a confluence below the diaphragm and then connect to a systemic vein, usually the portal vein (not shown) or the hepatic vein (shown). Reproduced from Kinderkardiologie, Georg Thieme Verlag, N. Haas, U. Kleideiter, 2011

obstructed. Embryologically, all pulmonary veins usually connect to a pulmonary venous confluence that connects to the left atrium. If this connection does not occur, the pulmonary venous confluence connects to a systemic vein instead.

32.2 Pathologic Physiology

Instead of connecting to the left atrium, the pulmonary veins connect to the systemic venous system or directly into the right atrium. Consequently, pulmonary venous blood returns to the right atrium instead of to the left atrium. The locations of the connection of the pulmonary veins to the systemic veins (in order of decreasing frequency) are: supracardiac TAPVR: the left vertical vein, innominate vein, and superior vena cava; intracardiac TAPVR: coronary sinus, right atrium; infracardiac TAPVR: umbilicovitelline system (portal vein, ductus venosus, inferior vena cava, hepatic vein). In "mixed" total anomalous pulmonary venous return, a combination of the above might occur. For example, the left pulmonary veins may connect to the left vertical vein and the right pulmonary veins directly to the right atrium. Because there is no direct communication between the pulmonary veins and the left atrium, a communication must exist between the right atrium and left atrium to allow blood to reach the left atrium and the left ventricle. Relatively complete mixing of the systemic and pulmonary venous returns occurs in the right atrium such that blood oxygen saturations in the right atrium, left atrium, right ventricle, pulmonary artery, left ventricle, and aorta are similar. Hemodynamically, there is a substantial volume load of the right ventricle that appears to be enlarged; the left ventricle seems small and underfilled.

32.3 Clinical Presentation

The clinical presentation depends upon whether there is partial or total anomalous venous return and whether or not there is obstruction to the venous return. In unobstructed forms with an interatrial communication, the physiology is similar to a large atrial septal defect. These patients may present with a murmur or signs of pulmonary overcirculation or right heart failure. As there is complete mixing of the venous and arterial blood, these babies may be picked up by a general pulse oximetry screening due to saturations below 94%. There are reports of unobstructed supracardiac TAPVR detected incidentally in adults. Patients with obstructed forms (mostly infracardiac TAPVR) are one of the few true emergencies that warrant cardiac surgery immediately upon diagnosis. These babies will present with cyanosis and increasing pulmonary edema immediately after birth.

32.4 Physical Examination

If there is an adequate interatrial communication and no significant obstruction to pulmonary venous return, the infant has mild cyanosis and evidence of increased pulmonary blood flow. There will be a systolic murmur and saturations below 94%. The clinical picture is completely different if there is an obstruction to pulmonary venous return. Characteristically, obstruction to pulmonary venous return occurs with infradiaphragmatic forms of TAPVR. Some cases of obstructed TAPVR in

supracardiac forms may exist. In these cases, there is pulmonary edema, severe respiratory distress, and a typical picture on chest X-ray.

32.5 Diagnostic Imaging

Echocardiography is an essential tool for accurately diagnosing the type of total anomalous pulmonary venous return (TAPVR), whether it is supracardiac, cardiac, infracardiac, or mixed, along with identifying any additional malformations. Transthoracic echocardiography is typically sufficient for diagnosis in neonates and children. Echocardiography allows for the assessment of any obstruction in the connecting or draining vessels. Even in cases of unobstructed TAPVR detected later in life, echocardiography remains the primary diagnostic tool. Pathognomonic signs on echocardiography include an enlarged right ventricle, a small left ventricle, an atrial septal defect with right-to-left shunting, and the absence of pulmonary venous drainage to the left atrium.

Diagnostic cardiac catheterization is generally not necessary in the era of echocardiography for TAPVR diagnosis. However, in cases of severe pulmonary venous obstruction, interventional dilatation and/or stenting may be chosen as the palliative treatment when immediate surgery is not available or the patient is in a critical condition. In selected cases where TAPVR is part of a more complex congenital heart defect, diagnostic cardiac catheterization may be required.

Magnetic resonance imaging (MRI) can be used in adults and teenagers who present later in life with unobstructed forms of TAPVR. MRI is particularly helpful in defining the exact anatomy of pulmonary venous drainage, especially in mixed forms, to aid in surgical planning for corrective procedures.

Computer tomography (CT) can provide the same detailed anatomical information as MRI and may be necessary, especially in cases of mixed forms of TAPVR, to precisely define the anatomy of all pulmonary venous drainage in preparation for corrective surgery. CT scans are generally faster compared to cardiac catheterization procedures in these cases.

32.6 Treatment

Treatment is surgical correction with anastomosis of the pulmonary veins to the left atrium. In unobstructed (mostly supracardiac) forms, surgical repair may be postponed from neonatal age to infancy. Infants with obstructed totally anomalous pulmonary venous return represent a surgical emergency, and immediate repair is indicated upon diagnosis. In selected cases, interventional palliation with stent implantation into the obstructed vessel may be helpful to improve the patient's condition in preparation for surgery.

32.7 Outcome

The outcome of total anomalous pulmonary venous return depends primarily on the presence or absence of pulmonary vein obstruction and the overall health status of the infant prior to the operation. The highest mortality rates are observed in infants with obstructed pulmonary venous return who are critically ill. In such cases, preoperative palliation measures may be beneficial.

For all other cases, the operative mortality is very low, particularly when selective surgery is performed in unobstructed cases beyond the neonatal period. The long-term prognosis for TAPVR patients is generally excellent. However, some patients may require reoperation due to stenosis at the anastomosis site between the common pulmonary venous chamber and the left atrium. This can typically be managed through surgical intervention.

Unfortunately, there are rare cases where patients develop progressive pulmonary venous obstruction despite multiple surgeries or interventional treatments for stenosis. These patients have a very poor prognosis.

Total Anomalous Pulmonary Venous Connections, Human Genetics

33

R. E. Poelmann, M. R. M. Jongbloed, and M. C. DeRuiter

Abstract

Partial anomalous pulmonary venous connections (PAVC) have been found after abnormal gene expressions involving several syndromes. Total anomalous pulmonary venous connection (TAPVC) is found in conjunction with heterotaxia syndrome as well as several other syndromes. It has been reported with an autosomal dominance with variable expression and incomplete penetrance. The occurrence is also related to environmental factors which may superimpose on a familial susceptibility for TAPVC. Many pathways are involved in the normal development of the pulmonary venous connections and as a consequence disturbance of many genetic and epigenetic pathways lead to partial or total pulmonary venous misconnections. In this chapter, an overview of current knowledge regarding human genetics of anomalous venous connections is provided

R. E. Poelmann
Institute of Biology Leiden, Leiden University, Leiden, The Netherlands

M. R. M. Jongbloed
Department Cardiology, Leiden University Medical Center, Leiden, The Netherlands

Department Anatomy & Embryology, Leiden University Medical Center, Leiden, The Netherlands

M. C. DeRuiter (✉)
Department Anatomy & Embryology, Leiden University Medical Center, Leiden, The Netherlands
e-mail: m.c.deruiter@lumc.nl

© The Author(s), under exclusive license to Springer Nature Switzerland AG 2024

S. Rickert-Sperling et al. (eds.), *Congenital Heart Diseases: The Broken Heart*,
Advances in Experimental Medicine and Biology 1441,
https://doi.org/10.1007/978-3-031-44087-8_33

33.1 Introduction

As all congenital malformations have a developmental background, there is no exception for total anomalous pulmonary venous connections [1]. A short overview of events during embryology is necessary to understand its genesis. The cellular players will be introduced including the time windows for their interactions to provide a scaffold for the genetic and inheritance aspects of the anomalies.

The venous pole of the heart encompasses the sinus venosus and the atrium [2, 3]. In the fourth week of development, the sinus venosus consists of a left and a right part receiving blood from the common cardinal veins, the omphalomesenteric and umbilical veins. The sinuatrial fold marks the border with the common atrium. Asymmetrical expansion of the common atrium corresponds with a rightward shift of the connection of the sinus to the atrium. The right-sided part of the sinus venosus including its tributing cardinal veins enlarges to form the venae cava that will incorporate into the right atrium [4]. In human development, but not in mouse, the left-sided part largely obliterates and remodels to form the coronary sinus in adults.

In approximately the same time window (4th–5th weeks), a splanchnic vascular plexus surrounds the developing lung buds (putative lungs) with a twofold connection. The first connection is from this pulmonary vascular plexus to the systemic veins (mostly the cardinal veins). The second connection is to the sinus venosus via the so-called "mid-pharyngeal endothelial strand" or MPES, the Anlage of the plexus from which the pulmonary vein develops, and this is initially not lumenized [5–7]. This means that during early developmental stages, the primary route of drainage from the pulmonary is toward the systemic veins and not to the heart. After lumenization of the MPES, the common pulmonary vein can be observed in the dorsal mesocardium, and the primary route of drainage will gradually change toward a cardiac drainage. The splanchnic pulmonary venous connections with the systemic cardinal veins will gradually disappear during normal development (Fig. 33.1). In case of absence or atresia of the MPES, the pulmonary to systemic connections will persist, clinically resulting in TAPVC [1].

Clinically, it is of importance to know that in hearts with TAPVC, the myocardial sleeve surrounding the pulmonary vein is missing, while the left atrial dorsal wall is hypoplastic [8]. The accompanying sinus node dysfunction in some of these patients [9, 10] points to an abnormal contribution of the so-called posterior heart field (part of the second heart field, which is also evident in the patient group with total absence of the myocardial sleeve presenting with a low incidence of atrial arrhythmias [10]. We have to keep in mind that many other patterns of pulmonary venous return are encountered including partial anomalous pulmonary venous return, cor triatriatum, primary and acquired stenosis, sinus venosus defects, and variant numbers of pulmonary veins [1], which may complicate an adequate diagnosis [11].

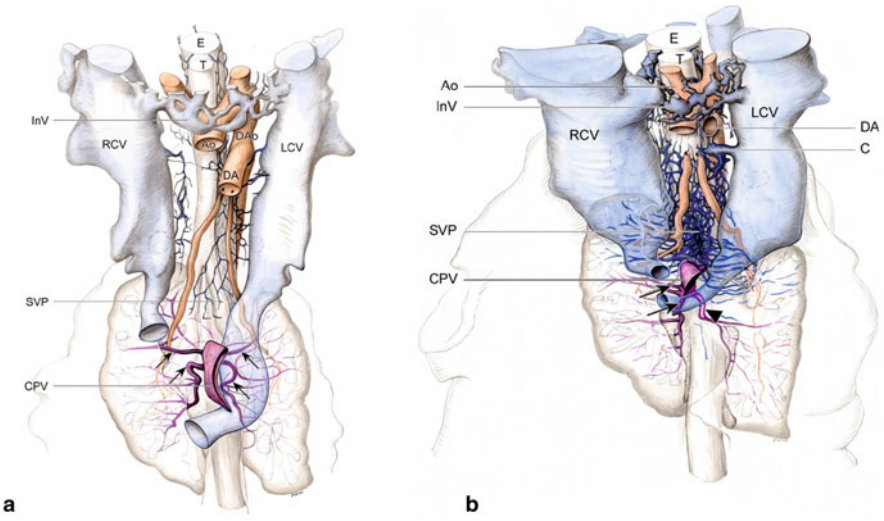

Fig. 33.1 3D reconstructions of human embryos. Approximate gestational age 8 weeks (crown-rump length 18 m, Carnegie stage 14). Frontal views. The heart and part of the left atrial dorsal walls have been resected. (**a**) Normal embryo. *Arrows* indicate 4 pulmonary veins that drain the lung toward the left atrium (*LA*). There are no pulmonary-to-systemic connections anymore via the splanchnic venous plexus (*SVP*), although small communications of this plexus into the right and left cardinal veins (*RCV* and *LCV*) can still be observed. (**b**) Embryo with abnormal pulmonary venous connection. The *black arrows* point at 2 right-sided pulmonary veins normally draining toward the LA. The left superior pulmonary vein is lacking (*open arrow*), and the left inferior pulmonary vein is devoid of blood (*black arrowhead*). Note the extensive SVP, with numerous connections to both lungs. Also, a large connection (*C*) is present between the SVP and the LCV. Abbreviations: *AO* aorta, *DA* ductus arteriosus, *DAO* descending aorta, *E* esophagus, *INV* innominate vein, *T* trachea (Source: Modified after [31]

33.2 TAPVC and Genetics

Cardiac development is the result of many interactions between morphogens and transcription factors [12]. Mismatches in signaling are at the base of about 30% of the known congenital cardiac malformations. TAPVC is found in conjunction with genetic syndromes including heterotaxia syndrome, craniofacial and skeletal dysmorphia, Holt–Oram syndrome, ciliary genes, and cat eye syndrome [13–16], and was reported with an autosomal dominance with variable expression and incomplete penetrance [13]. The occurrence is also related to environmental factors such as exposure to lead, solvents, and pesticides, which may superimpose on a familial susceptibility for TAPVC [17]. Survey of families with high frequency of TAPVC revealed several candidate genes: TAPVR1, ANKRD1/CARP, Semaphorin 3d/Plexin, RNF20, and TBX5.

TAPVR1 maps to chromosome 4q12, the centromeric region containing kinase domain receptor (KDR), and this gene plays a role in vasculogenesis [18]. Disturbed

vasculogenesis may potentially lead to deficient development of the MPES, causing PAPVC with persisting pulmonary-to-systemic connections, although the exact developmental mechanism has not been elucidated. More recently, the region has been narrowed down to the intergenic locus between PDGFRA and KIT [19] . Mutation analysis of the *PDGFRA* gene in TAPVR patients revealed a rare sequence variant pointing toward a presumptive TAPVR gene. Mouse models with deficient PDGFr alpha show a small DMP and abnormal drainage of the systemic and pulmonary veins, although a phenotype of PAPVC was not observed [20].

Furthermore, the ANKRD1/CARP gene encoding a muscle specific protein is implicated in cardiac transcriptional regulation and myofibrillar assay [21]. It is localized to chromosome 10 proximal to a previously found translocation point [22, 23]. The ANKRD1/CARP gene is regulated by GATA4, and disruption of this signaling axis *in vitro* leads to sarcomere disarray [24]. Ankyrin repeat proteins are stress inducible that are thought to be involved in mechanosensing in response to pressure overload [25]. Therefore, the mechanism of the occurrence of TAPVC may relate to atresia caused by dysregulated flow through the MPES during embryology, although this remains speculative at this point.

As described above, pulmonary vein development starts with the early embryonic connection of the mid-pharyngeal endothelial strand (MPES) to the heart [26]. TAPVC occurs in Semaphorin 3d mutant mice [5] despite normal formation of the MPES. In 35% of mutant mouse embryos, the developing splanchnic plexus surrounding the lung buds does not anastomose uniquely with the MPES. Normally, Sema3d provides a migration repulsive signal to endothelial cells in early stages of development (E9.5 in mouse), establishing a boundary between the pulmonary plexus and the systemic circulation, whereas in the mutants endothelial tubes form aberrant connections traversing this normally vascular-free area. Furthermore, atrial septation is impaired in these mutants, providing further evidence for the codevelopment of the atrial septum and the pulmonary vein. Sequencing of *SEMA3D* in patients with TAPVC revealed a substitution (phenylalanine>leucine) that affects SEMA3D function. Whole-exome sequencing in patient cohorts revealed rare genetic variants in PLXND1 encoding a receptor for semaphorins. All variants displayed an anomalous drainage to the right atrium [27].

Mutations in the RNF20 complex are identified in patients with complex CHD including dextrocardia, complete AV-canal, atrial isomerism, and pulmonary atresia [16]. This complex affects ciliary motility and development of left–right asymmetry. Its effect is through histone H2B ubiquitinization, hence epigenetically controlled cilia genes.

TBX5 mutants are implicated in Holt–Oram syndrome, known for heart and upper limb malformations [28, 29], and nonsyndromic cardiac defects [30]. Furthermore, a multigenerational family has been investigated with autosomal dominant congenital heart defects with variability of manifestations and severity including Holt–Oram syndrome. The proband had a lethal mixed type TAPVR with a variant in the T-box domain of *TBX5* [15].

In conclusion, several mutations have been described in the human population that affects the formation of the pulmonary venous drainage. The perturbed genes are

involved in ciliary function, left–right asymmetry, PDGF signaling, sarcomere formation, and endothelial migration, thereby regulating various phases of differentiation. In view of the complexity of the interactions, it will be no surprise to welcome other involved signaling pathways in the near future.

References

1. Douglas YL, Jongbloed MR, Deruiter MC, Gittenberger-de Groot AC. Normal and abnormal development of pulmonary veins: state of the art and correlation with clinical entities. Int J Cardiol. 2011;147(1):13–24.
2. Snarr BS, O'Neal JL, Chintalapudi MR, Wirrig EE, Phelps AL, Kubalak SW, et al. Isl1 expression at the venous pole identifies a novel role for the second heart field in cardiac development. Circ Res. 2007;101(10):971–4.
3. Hikspoors J, Kruepunga N, Mommen GMC, Kohler SE, Anderson RH, Lamers WH. A pictorial account of the human embryonic heart between 3.5 and 8 weeks of development. Commun Biol. 2022;5(1):226.
4. Blom NA, Gittenberger-de Groot AC, Jongeneel TH, DeRuiter MC, Poelmann RE, Ottenkamp J. Normal development of the pulmonary veins in human embryos and formulation of a morphogenetic concept for sinus venosus defects. Am J Cardiol. 2001;87(3):305–9.
5. Degenhardt K, Singh MK, Aghajanian H, Massera D, Wang Q, Li J, et al. Semaphorin 3d signaling defects are associated with anomalous pulmonary venous connections. Nat Med. 2013;19(6):760–5.
6. DeRuiter MC, Gittenberger-De Groot AC, Wenink AC, Poelmann RE, Mentink MM. In normal development pulmonary veins are connected to the sinus venosus segment in the left atrium. Anat Rec. 1995;243(1):84–92.
7. Gittenberger-de Groot AC, Peterson JC, Wisse LJ, Roest AAW, Poelmann RE, Bokenkamp R, et al. Pulmonary ductal coarctation and left pulmonary artery interruption; pathology and role of neural crest and second heart field during development. PLoS One. 2020;15(5):e0228478.
8. Douglas YL, Jongbloed MR, den Hartog WC, Bartelings MM, Bogers AJ, Ebels T, et al. Pulmonary vein and atrial wall pathology in human total anomalous pulmonary venous connection. Int J Cardiol. 2009;134(3):302–12.
9. Korbmacher B, Buttgen S, Schulte HD, Hoffmann M, Krogmann ON, Rammos S, et al. Long-term results after repair of total anomalous pulmonary venous connection. Thorac Cardiovasc Surg. 2001;49(2):101–6.
10. Tanel RE, Kirshbom PM, Paridon SM, Hartman DM, Burnham NB, McBride MG, et al. Long-term noninvasive arrhythmia assessment after total anomalous pulmonary venous connection repair. Am Heart J. 2007;153(2):267–74.
11. Laux D, Fermont L, Bajolle F, Boudjemline Y, Stirnemann J, Bonnet D. Prenatal diagnosis of isolated total anomalous pulmonary venous connection: a series of 10 cases. Ultrasound Obstet Gynecol. 2013;41(3):291–7.
12. Lim TB, Foo SYR, Chen CK. The role of epigenetics in congenital heart disease. Genes (Basel). 2021;12(3)
13. Correa-Villasenor A, Ferencz C, Boughman JA, Neill CA. Total anomalous pulmonary venous return: familial and environmental factors. The Baltimore-Washington Infant Study Group. Teratology. 1991;44(4):415–28.
14. Devriendt K, Casaer A, Van Cauter A, de Zegher F, Dumoulin M, Gewillig M, et al. Asplenia syndrome and isolated total anomalous pulmonary venous connection in siblings. Eur J Pediatr. 1994;153(10):712–4.
15. Azab B, Aburizeg D, Ji W, Jeffries L, Isbeih NJ, Al-Akily AS, et al. TBX5 variant with the novel phenotype of mixedtype total anomalous pulmonary venous return in HoltOram syndrome and variable intrafamilial heart defects. Mol Med Rep. 2022;25(6)

16. Robson A, Makova SZ, Barish S, Zaidi S, Mehta S, Drozd J, et al. Histone H2B monoubiquitination regulates heart development via epigenetic control of cilia motility. Proc Natl Acad Sci U S A. 2019;116(28):14049–54.
17. Jackson LW, Correa-Villasenor A, Lees PS, Dominici F, Stewart PA, Breysse PN, et al. Parental lead exposure and total anomalous pulmonary venous return. Birth Defects Res A Clin Mol Teratol. 2004;70(4):185–93.
18. Bleyl SB, Botto LD, Carey JC, Young LT, Bamshad MJ, Leppert MF, et al. Analysis of a Scottish founder effect narrows the TAPVR-1 gene interval to chromosome 4q12. Am J Med Genet A. 2006;140(21):2368–73.
19. Bleyl SB, Saijoh Y, Bax NA, Gittenberger-de Groot AC, Wisse LJ, Chapman SC, et al. Dysregulation of the PDGFRA gene causes inflow tract anomalies including TAPVR: integrating evidence from human genetics and model organisms. Hum Mol Genet. 2010;19 (7):1286–301.
20. Bax NA, Bleyl SB, Gallini R, Wisse LJ, Hunter J, Van Oorschot AA, et al. Cardiac malformations in Pdgfralpha mutant embryos are associated with increased expression of WT1 and Nkx2.5 in the second heart field. Dev Dyn. 2010;239(8):2307–17.
21. Badi I, Cinquetti R, Frascoli M, Parolini C, Chiesa G, Taramelli R, et al. Intracellular ANKRD1 protein levels are regulated by 26S proteasome-mediated degradation. FEBS Lett. 2009;583 (15):2486–92.
22. Acquati F, Russo A, Taramelli R, Tibiletti MG, Taborelli M, Camesasca C, et al. Nonsyndromic total anomalous venous return associated with a de novo translocation inolving chromosomes 10 and 21 t(10;21)(q23.1;q11.2). Am J Med Genet. 2000;95(3):285–6.
23. Cinquetti R, Badi I, Campione M, Bortoletto E, Chiesa G, Parolini C, et al. Transcriptional deregulation and a missense mutation define ANKRD1 as a candidate gene for total anomalous pulmonary venous return. Hum Mutat. 2008;29(4):468–74.
24. Chen B, Zhong L, Roush SF, Pentassuglia L, Peng X, Samaras S, et al. Disruption of a GATA4/Ankrd1 signaling axis in cardiomyocytes leads to sarcomere disarray: implications for anthracycline cardiomyopathy. PLoS One. 2012;7(4):e35743.
25. Bang ML, Gu Y, Dalton ND, Peterson KL, Chien KR, Chen J. The muscle ankyrin repeat proteins CARP, Ankrd2, and DARP are not essential for normal cardiac development and function at basal conditions and in response to pressure overload. PLoS One. 2014;9(4):e93638.
26. DeRuiter MC, Poelmann RE, Mentink MM, Vaniperen L, Gittenberger-De Groot AC. Early formation of the vascular system in quail embryos. Anat Rec. 1993;235(2):261–74.
27. Zhou WZ, Zeng Z, Shen H, Chen W, Li T, Ma B, et al. Association of PLXND1 with a novel subtype of anomalous pulmonary venous return. Hum Mol Genet. 2022;31(9):1443–52.
28. Basson CT, Cowley GS, Solomon SD, Weissman B, Poznanski AK, Traill TA, et al. The clinical and genetic spectrum of the Holt-Oram syndrome (heart-hand syndrome). N Engl J Med. 1994;330(13):885–91.
29. Mori AD, Bruneau BG. TBX5 mutations and congenital heart disease: Holt-Oram syndrome revealed. Curr Opin Cardiol. 2004;19(3):211–5.
30. Yoshida A, Morisaki H, Nakaji M, Kitano M, Kim KS, Sagawa K, et al. Genetic mutation analysis in Japanese patients with non-syndromic congenital heart disease. J Hum Genet. 2016;61(2):157–62.
31. Rammos S, Gittenberger-de Groot AC, Oppenheimer-Dekker A. The abnormal pulmonary venous connexion: a developmental approach. Int J Cardiol. 1990;29(3):285–95.

TAPVR: Molecular Pathways and Animal Models

34

Robert E. Poelmann, Monique R. M. Jongbloed, and Marco C. DeRuiter

Abstract

The venous pole of the heart where the pulmonary veins will develop encompasses the sinus venosus and the atrium. In the fourth week of development, the sinus venosus consists of a left and a right part receiving blood from the common cardinal vein, the omphalomesenteric and umbilical veins. Asymmetrical expansion of the common atrium corresponds with a rightward shift of the connection of the sinus to the atrium. The right-sided part of the sinus venosus including its tributing cardinal veins enlarges to form the right superior and inferior vena cava that will incorporate into the right atrium. The left-sided part in human development largely obliterates and remodels to form the coronary sinus in adults. In approximately the same time window (4th–fifth weeks), a splanchnic vascular plexus surrounds the developing lung buds (putative lungs) with a twofold connection. Of note, during early developmental stages, the primary route of drainage from the pulmonary plexus is toward the systemic veins and not to the heart. After lumenization of the so-called mid-pharyngeal endothelial strand (MPES), the first anlage of the pulmonary vein, the common

R. E. Poelmann
Department of Integrative Zoology, Institute of Biology, University of Leiden, Leiden, The Netherlands

M. R. M. Jongbloed
Department Cardiology, Leiden University Medical Center, Leiden, The Netherlands

Department Anatomy and Embryology, Leiden University Medical Center, Leiden, The Netherlands

M. C. DeRuiter (✉)
Department Anatomy and Embryology, Leiden University Medical Center, Leiden, The Netherlands
e-mail: m.c.deruiter@lumc.nl

© The Author(s), under exclusive license to Springer Nature Switzerland AG 2024

S. Rickert-Sperling et al. (eds.), *Congenital Heart Diseases: The Broken Heart*,
Advances in Experimental Medicine and Biology 1441,
https://doi.org/10.1007/978-3-031-44087-8_34

pulmonary vein can be observed in the dorsal mesocardium, and the primary route of drainage will gradually change toward a cardiac drainage. The splanchnic pulmonary venous connections with the systemic cardinal veins will gradually disappear during normal development. In case of absence or atresia of the MPES, the pulmonary-to-systemic connections will persist, clinically resulting in total anomalous pulmonary venous return (TAPVR). This chapter describes the developmental processes and molecular pathways underlying anomalous pulmonary venous connections.

34.1 Introduction to Cardiac Development

The primary heart tube develops from the bilateral cardiogenic plates as part of the splanchnic mesoderm. After midline fusion of the plates, together comprising the first heart field, the primary heart tube is formed. It is connected anteriorly to the aortic sac that feeds the pharyngeal arch arteries and caudally to the omphalomesenteric veins collecting the returning blood. The venous pole of the heart encompasses the sinus venosus and the atrium [1]. In the fourth week of development, the sinus venosus consists of a left and a right part receiving blood from the common cardinal, omphalomesenteric and umbilical veins. The sinoatrial fold marks the border with the common atrium. Asymmetrical expansion of the common atrium corresponds with a rightward shift of the connection of the sinus to the atrium. The right-sided part of the sinus venosus including its tributing cardinal veins enlarge to form the superior and inferior vena cava that will incorporate into the right atrium [2]. The left-sided part in human development largely obliterates and remodels to form the coronary sinus in adults (Fig. 34.1). The inner lining of the myocardial tube consists of endocardial cells that are continuous with the endothelium of the blood vessels. As a consequence of left–right patterning, the heart tube is asymmetric and loops to the right in normal development. Major parts of both the arterial and venous pole are derived from the splanchnic mesoderm behind the heart during development, referred to as contributions from the second heart field (SHF). The primitive heart tube thus expands by intrinsic growth patterns of the cardiac tube, but also by extrinsic additions at both the arterial and the venous pole at expense of the SHF splanchnic mesoderm, as shown by expression patterns of, e.g., Tbx (T-box) 5, GATA (GATA binding protein) 4–6 and NKX2–5 (NK2 homeobox 5) [3], Islet1 (ISL LIM homeobox 1) [4], and Id2 (inhibitor of DNA binding 2) [5]. During heart development, cardiac chambers and transitional zones appear, the latter involved in septation, valvulogenesis and formation of the conduction system. The future atrial and ventricular components are separated by the atrioventricular canal. At the venous pole, recruitment of myocardium has been reported to depend on Pitx2c (paired-like homeodomain 2), Nkx2–5, Tbx18, Shox2 (short-stature homeobox 2), and Pdpn (podoplanin) [6–10]. This region located posterior to the primary heart tube, as part of the SHF is referred to as the posterior

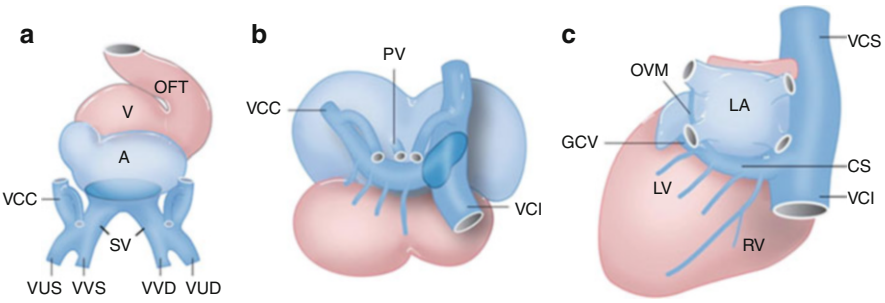

Fig. 34.1 Schematic representation of subsequent stages of cardiac development. (**a**) The venous pole of the heart encompasses the sinus venosus (*SV*) and the atrium (*A*). Initially, the SV consists of, more or less symmetrical, *left* and *right* horns that receive blood from the common cardinal vein (*VCC*), the *left* and *right* vitellin veins (*VVS* and *VVD*, resp.) and the *left* and *right* umbilical veins (*VUS* and *VUD*, resp.). (**b**, **c**) Due to an asymmetrical expansion of the common atrium, a rightward shift of the connection of the sinus to the atrium occurs. The right-sided cardinal vein will form the superior caval vein (*VCS*). The *left side* in human will largely obliterate, the remaining part will form the coronary sinus (*CS*) and the vein of Marshall (*OVM*, remnant of the *left* cardinal vein). Initially, the single pulmonary vein Anlage will drain rather central in the atrium. After septation, the pulmonary veins (*PV*) will drain into the *left* atrium. *GCV* great cardiac vein, *LV* left ventricle, *OFT* outflow tract, *OVM* oblique vein of Marshall, *RV* right ventricle, *V* common ventricle, *VCI* inferior caval vein (Source: 41)

second heart field being involved in addition of myocardium to the sinus venosus, the pulmonary veins, the cardinal veins, as well as to the body of the atria.

34.2 Pulmonary Plexus and Vein Development

During the 4th week of embryonic human development, the primary lung buds appear at the apex of the endodermal respiratory diverticulum, surrounded by splanchnic mesoderm (Fig. 34.2). The lung buds differentiate into the bronchial system and their bifurcations in the future lungs. The splanchnic mesoderm provides the pulmonary vascular smooth muscle and connective tissues as well as the capillaries, the latter developing into a splanchnic plexus by which the primitive lungs drain into the systemic circulation. The splanchnic plexus is connected to the venous pole of the primitive heart tube by a strand of endothelial cells, the so-called mid-pharyngeal endothelial strand that becomes the common pulmonary vein (Fig. 34.2a, g). The MPES is initially not lumenized, and the main route of drainage to the venous pole of the heart is via connections of the pulmonary splanchnic plexus to the embryonic systemic veins (cardinal, umbilical, and vitellin veins). This early drainage pattern has also been referred to as a *peripheral* drainage pattern.

Upon lumenization of the MPES, the lungs initially drain both centrally to the atrium and peripherally to the systemic veins, the so-called *intermediate* drainage period (Fig. 34.2b). After atrial septation, the pulmonary–systemic connections are lost and regress (Fig. 34.2c), the beginning of the *central* drainage period [11]

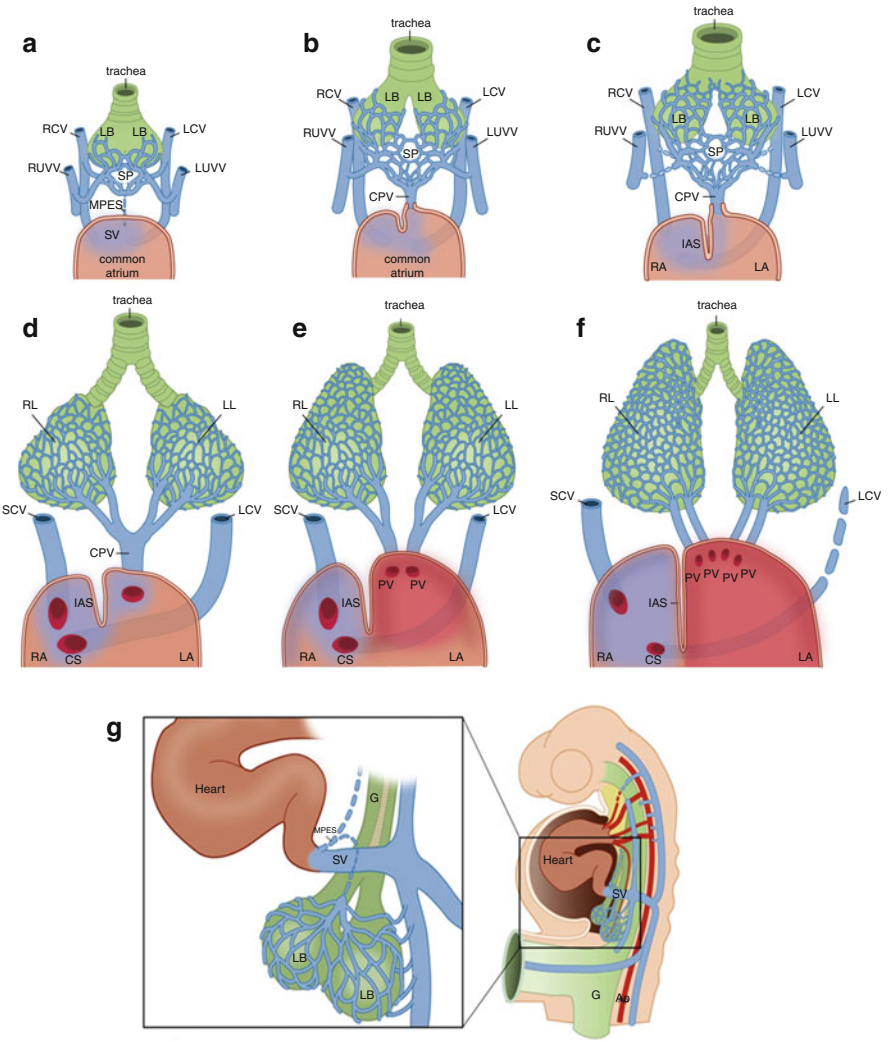

Fig. 34.2 Schematic overview of pulmonary vein development, frontal views. (**a**) Peripheral draining period. During the fourth week of embryonic development, 2 lung buds (*LB*) can be discriminated at the caudal end of the respiratory diverticulum of the foregut. These lung buds into the bronchi and their bifurcations in the future lungs. The splanchnic mesenchyme forms a splanchnic plexus (*SP*) of veins that is already connected to the endocardium of the primitive heart tube, by means of a strand of endothelial cells, the mid-pharyngeal endothelial strand (*MPES*), the Anlage of the common pulmonary vein. Initially this strand is not lumenized yet; during early embryology, the normal route of drainage is from the pulmonary venous plexus to the systemic veins via pulmonary-to-systemic venous connections. (**b**) Intermediate draining period. At this stage, the MPES has lumenized to become the common pulmonary vein (*CPV*), allowing drainage of the splanchnic plexus not only to the systemic veins but also into heart. (**c**) As the CPV grows and dilates and becomes the main route of drainage of the pulmonary venous blood, the primitive pulmonary-to-systemic connections will gradually regress. (**d**) Central drainage period. During

(Fig. 34.2d–g). Persistence of early pulmonary-to-systemic connections is likely the substrate for anomalous pulmonary venous connections. Several forms of anomalous pulmonary venous connections can be attributed to a deficiency in development toward the establishment of a central drainage pattern (Table 34.1).

Table 34.1 Abnormal pulmonary vein development in relation to anatomical level, time and clinical entities

Anatomical level	Anomaly	Developmental impairment	Time relation (in relation to atrial septation)	Pulmonary-to-systemic connections	Clinical entity
Common PV/MPES	Absence	Absent connection PV-LA (absent MPES)	Before	Will persist	TAPVC (extracardiac type)
	Atresia	Non-lumenization of the MPES (PV Anlage)	Before	Will persist	TAPVC (extracardiac type)
	Stenosis	Secondary stenosis of an initially lumenized common PV	Before/ during	Will disappear	Cor triatriatum
	Atresia	Secondary obliteration of an initially lumenized PV	After	Have disappeared	TAPVC (lethal)

(continued)

Fig. 34.2 (continued) normal development, the primitive pulmonary-to-venous connections will regress completely, and the only route of drainage of the pulmonary venous blood is now directly into the heart. (**e**, **f**) During further development, bifurcations of the CPV will be incorporated into the left atrium (*LA*), usually to an extent that four separate pulmonary venous ostia (*2 right sided* and *2 left sided*) can be distinguished, although variations occur [17]. The right cardinal vein (*RCV*) has become the superior caval vein (*SCV*), and the left cardinal vein (*LCV*) will partly become the coronary sinus (*CS*), whereas the extracardiac part of the LCV will regress to become the ligament of Marshall. (**g**) Lateral view of the embryo with a magnification of the boxed area. A splanchnic vascular network surrounds the lung buds (*LB*) that grow out from the foregut (*G*). *G* foregut, *IAS* interatrial septum, *LB* lung buds, *LL* left lung, *LUVV* left umbilical and vitellin veins, *RA* right atrium, *RL* right lung, *RUVV* right umbilical and vitellin veins, *SV* sinus venosus

Table 34.1 (continued)

Anatomical level	Anomaly	Developmental impairment	Time relation (in relation to atrial septation)	Pulmonary-to-systemic connections	Clinical entity
First or second PV bifurcation	Atresia	Non-lumenization of 1 or more individual PV (s)/tributaries	During	Will persist	PAPVC (extracardiac type)
	Stenosis	Secondary stenosis of an initially lumenized individual PV	Before/ during After	Will disappear Have disappeared	Congenital PV stenosis Acquired PV stenosis
	Atresia	Obliteration of 1 or more initially lumenized PVs	After	Have disappeared	(Solitary) PV atresia
Veno-atrial junction	Variant number of PVs	Abnormal PV incorporation	After	Have disappeared	Unilateral common
	<4	Incomplete			PV ostium[a]
	>4	Extreme			>4 PV ostia[a]
Dorsal mesenchymal protrusion	Hypoplasia	Abnormal mesenchymal contribution from SHF	During	Will disappear	Sinus venosus defect with PAPVC (cardiac type) A(V)SD
	Absence	Absent mesenchymal contribution from SHF	During	Will mostly disappear	TAPVC (cardiac type) A(V)SD

Source: Reproduced with permission from [23]
MPES mid-pharyngeal endothelial strand, *PAPVC* partial anomalous, PV connection, *PV(s)* pulmonary vein(s), *TAPVC* total anomalous PV connection, *SHF* second heart field
[a]Not regarded as pathological but rather as anatomical variations

34.3 Myocardialization of the Pulmonary Veins

The entrance of the common pulmonary vein to the sinus venosus is bordered by two muscular ridges (Fig. 34.3). The right-sided pulmonary ridge merges with the so-called dorsal mesenchymal protrusion (DMP), important for formation of the base of the atrial septum [12, 13]. As a consequence, the pulmonary vein between the two muscularized ridges will at the left side be incorporated in the posterior wall of the left atrium, thereby contributing to the histological characteristics of the left atrial

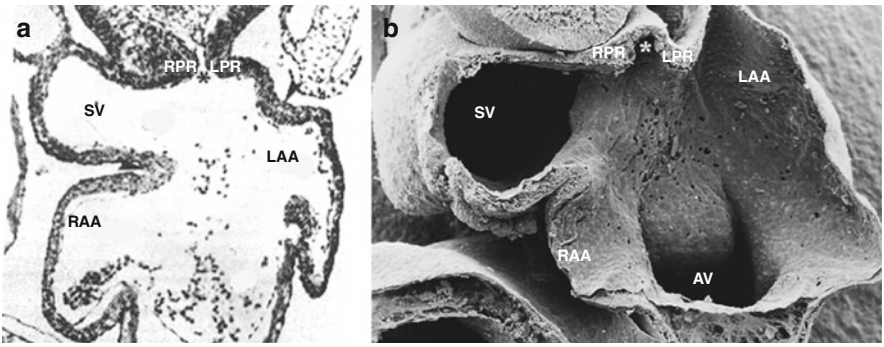

Fig. 34.3 Transverse light microscopic section (**a**) and electron microscopic (**b**) section at the level of the sinus venosus (*SV*) and atrial appendages (*RAA* and *LAA*) of a chick embryo. The entrance of the common pulmonary vein (*asterisk*) to the SV is bordered by two muscular ridges, the *left* (*LPR*) and *right* pulmonary ridge (*RPR*). The latter merges with the so-called dorsal mesenchymal protrusion (not shown), at the base of the interatrial septum, causing the pulmonary vein to be located at the *left side* after atrial septation (Source: Panel a adapted from 42)

body, consisting partly of vascular smooth muscle cells and partly of myocardium [13]. The DMP is derived from the embryonic second heart field that comprises an area of mesenchyme behind the heart that will contribute to the embryonic heart during further development [3].

The common pulmonary vein becomes myocardialized and gives rise to separate venous orifices in the posterior left atrial wall. The degree of incorporation is variable, and not all individuals have four distinct pulmonary venous ostia, while common ostia of particularly the left pulmonary veins as well as additional pulmonary venous ostia are often observed [14–16].

The wall of the pulmonary veins will develop a myocardial sleeve as is the case with the cardinal (cava) veins. The myocardial continuity of the atrial and venous walls, varying in different species, has been thoroughly investigated by several groups and has led to different opinions regarding the origin and differentiation of the involved cell populations [7, 13, 17–19].

34.4 Histological Characterization During Normal Development

Pulmonary vein development in human embryos takes place between 7 and 22 weeks (crown rump length 19–170 mm). Using various specific antibodies for muscle actins, alpha-smooth muscle actin, and atrial myosin light chain, three different areas can be distinguished in the posterior left atrial wall: [1] the smooth-walled atrial body with incorporated pulmonary vein smooth muscle cells, [2] the trabeculated appendage without vascular smooth muscle cells, and [3] the transitional zone between body and appendage (see Fig. 34.2). The transitional zone histologically resembles the sinus venosus and presents with a very thin and even absent myocardium, from which it was hypothesized that during incorporation of the

pulmonary vein into the body of the left atrium, the area of the sinus venosus myocardium was reduced to the narrow zone encircling the entrance to the atrial appendage [13]. These observations are relevant for interpreting the definition of the sinoatrial transition and the sinus venosus, but also for the interpretation of areas of preferential induction of arrhythmias in later life. Interestingly, the body of the right atrium, the right atrial appendage and the right-sided face of the atrial septum are not lined by vascular smooth muscle cells.

34.5 Origin and Incorporation into the Left Atrium

The origin and incorporation of myocardium and smooth muscle cells into the pulmonary vein and left atrium has been investigated using various approaches. Based on overlapping gene expression patterns in the SHF of Pitx2c, Islet1, Tbx18, and Nkx2–5, clues are provided to the origin of myocardial cells enveloping the cava and pulmonary veins together with segments of the atrium (elegantly summarized by Lescroart et al. [18]. The topic of connection of the pulmonary vein to the sinus venosus and subsequent incorporation into the left atrium is debated [20–24]. It is noteworthy that myocardium associated with the left-sided veins (pulmonary vein and left cardinal vein, including the dorsal left atrium) shares a common lineage, as does myocardium associated with the right-sided veins including the dorsal right atrium [18]. Therefore, we favor an original left-sided connection of the common pulmonary vein to that part of the sinus venosus that will be incorporated in the dorsal wall of the left atrium. We must realize, however, that patterning of the various developmental actors (second heart field, DMP, myocardium, smooth muscle cells) will be reflected by the (epi)genetic regulation networks and in case of TAPVC by misregulation. It is evident that different areas of gene expression can be recognized, as Pitx2c is expressed in the myocardium of the pulmonary vein, left superior vena cava and (left) part of the atrium, Nkx2–5 in the pulmonary vein myocardium/mesenchyme and atrial myocardium, Tbx18 only in the myocardium surrounding the vena cava and Nppa (natriuretic peptide A) only in the atrial wall. Podoplanin is expressed in the myocardium and smooth muscle cells of the pulmonary veins, as well as in the left atrial dorsal wall including the left and right venous valves. The temporospatial expression pattern of these genes in SHF progenitors based on the use of reporters and transgenes in mice is intricate [7, 9, 10, 25]. An approach by Buckingham [26] exploits retrospective clonal analysis based on rare random events of recombination of a nonfunctional *nLaacz* sequence into functional *nLacZ,* targeted to the alpha cardiac actin gene [18], the recombination event being independent of gene expression. They conclude that there are left and right myocardial sublineages at the venous pole of the heart. The pulmonary and left superior vena cava share common progenitors with the dorsal left atrial myocardium (Fig. 34.4), whereas the right superior vena cava and dorsal right atrial myocardium share their own common progenitors, illustrating the difference between genetic tracing experiments and lineage analysis. Furthermore, these results suggest that the vena cava myocardium does not have a separate clonal origin from the pulmonary myocardium.

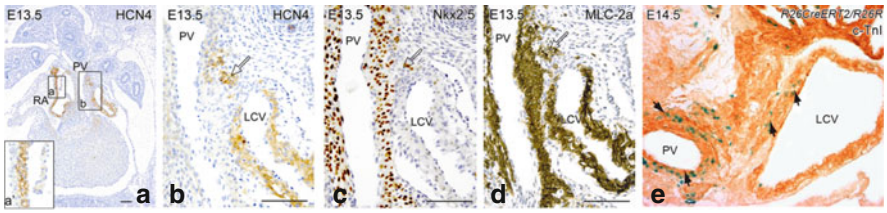

Fig. 34.4 Cellular continuity between myocardium forms the left cardinal vein (*LCV*) that includes a transient left sinoatrial node (SAN) and pulmonary veins (*PV*). (**a**–**d**) Cells from the region of the left-sided SAN can be traced section to section toward the myocardium surrounding the pulmonary veins (*PV*). (**a**) Overview section of an E13.5 heart, showing expression of the marker HCN4 at the level of the sinus venosus. (**b**, **c** and **d**) are enlargements of the boxed area in (**a**). Expression of HCN4 (**b**) is observed as the cluster of cells (*open arrows* in **b**–**d**) that can be followed section to section from the *left* SAN region toward the PV myocardium. These cells also express the myocardial marker MLC-2a (**d**) and mostly lacking expression of Nkx2.5 (**c**). (**e**) Section of an E14.5 heart of a *R26CreERT2/R26R* embryo showing a clone of β-galactosidase-positive cells in the LSCV, PV, and LA. A c-TnI antibody was used to stain the myocardium (Source: Panels **a**–**d** are reproduced with permission from [49]. Source: Panel **e** is modified with permission from [19])

34.6 Total Anomalous Pulmonary Venous Connection (TAPVC)

At the end of the fifth week in human development, the common pulmonary vein has established the connection of the lungs with the atrium allowing regression of the earlier splanchnic connections and the MPES to the systemic circulation (Fig. 34.2). In hearts with TAPVC, a connection between the splanchnic plexus and the left atrium is lacking, leading to persistence of pulmonary drainage via (one of) the cardinal veins. This can be distinguished clinically in infracardiac, cardiac, and supracardiac connections. The left atrial wall lacks vessel wall tissue as incorporation of the pulmonary vein has not been established in neonate and adult patients [27] (Fig. 34.5a–d). In mouse embryos, the differentiation of the sinus venosus and pulmonary myocardium has been investigated showing that both share expression of podoplanin (expressed in the posterior second heart field) and the cation channel protein HCN4 (hyperpolarization-activated cyclic nucleotide-gated potassium channel 4) but lack Nkx2–5 [8, 28]. During subsequent development, Nkx2–5 becomes upregulated and HCN4 (a conduction-related gene) downregulated in the pulmonary vein until the latter becomes restricted to the sinus node, suggesting that early conduction properties may relate to the enhanced susceptibility of this area for arrhythmias later in life. The low incidence of arrhythmias in patients with TAPVC might be explained by impaired myocardial sleeve formation surrounding the pulmonary veins [27]. Furthermore, as a consequence of impaired pulmonary vein incorporation, resulting probably in diminished flow and hemodynamics, the left atrium is hypoplastic (Fig. 34.5e). Optimizing results of TAPVC correction is often accompanied by surgical augmentation of left atrial function [29].

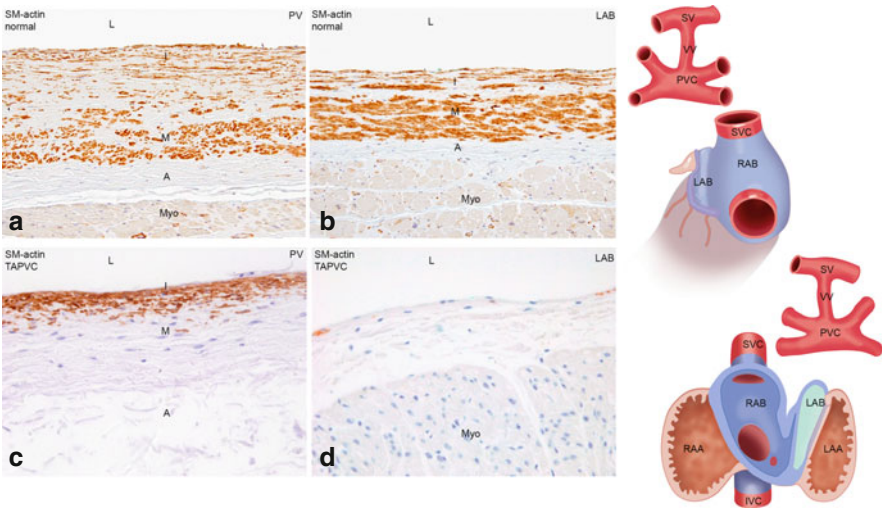

Fig. 34.5 Histology of total anomalous pulmonary venous connection (*TAPVC*). (**a**, **b**) Sections of a normal adult heart stained with alpha SM actin, showing the histological structure of pulmonary venous and *left* atrial wall. In the PV (**a**) as well as in the LAB (**b**), an identical and characteristic vessel wall, with myocardial covering (*myo*) is found. Profound intimal thickening (*I*) is observed most obviously in the PV in this adult heart. (**c**, **d**) Sections of neonatal heart–lung specimens stained with 1A4 against alpha-smooth muscle actin (*SM actin*), showing the histological structure of pulmonary venous and *left* atrial wall in hearts with total anomalous pulmonary venous connection (*TAPVC*). (**c**) Pulmonary venous confluence representative for TAPVC showing vessel wall consisting of a tunica intima (*I*), media (*M*) and a tunica adventitia (*A*) without myocardial covering. (**d**) Smooth-walled *left* atrial body (*LAB*) with a slightly thickened (sub)endocardial layer of collagen, elastic fibers and occasional smooth muscle cells covered by myocardium (*Myo*). No vessel wall tissue was found. (**e**) Schematic depiction of outer (**a**) and inner (**b**) side of atrial chambers and pulmonary veins (*PV*) in hearts with extracardiac type of TAPVC. The pulmonary veins (*PV*) drain via a vertical vein (*VV*) into a systemic vein (*SV*) and are not covered by myocardium. The *left* atrium body (*LAB*) consists of smooth-walled primary myocardium, without secondary addition of myocardium from the posterior heart field. Because of the absence of PV connection and incorporation into the LA, the LAB is small and does not contain vessel wall tissue. *CS* coronary sinus, *IVC* inferior caval vein, *L* lumen, *PVC* pulmonary venous confluence, *SVC* superior caval vein (Source: Modified with permission [28])

34.7 Animal Models

Several reporter and transgenic mouse models have been employed to study the development of the venous pole of the heart, focusing on the left (pulmonary) side. Only conditional deletion and transgenesis of transcription factors governing many aspects of cardiogenesis including Islet1, GATA4–6, BMPs (bone morphogenic proteins), Nkx2–5, SRF (serum response factor), Tbx family members, and others can address the function of these genes in specific parts of heart development. Reporter models rely heavily upon specific expression patterns in defined time

windows and as such have their limitations. Nevertheless, in this field, much evidence has been gained. In this chapter, specific animal models for pulmonary venous development will be high-lighted. Genes involved in the formation of the posterior heart field and subsequent recruitment of myocytes to the venous pole of the heart will often result in a phenotype when mutated. The sinus venous myocardium forms a horseshoe-shaped band lining the base of the left and right cardinal veins. It is unique in that it does not express the precardiac marker Nkx2–5 in early developmental stages [7, 8]. The PDGF (platelet-derived growth factor) family of growth factors comprises regulators involved in various stages of cardiac development. In the posterior heart field and venous pole, expression of PDGF-receptor alpha and the ligands PDGF-A and PDGF-C has been shown in, e.g., chicken [30] and mouse embryos [31] showing temporal and spatial patterns consistent with a role in pulmonary vein development. Knockdown of PDGFRA function in a mouse model may result in a spectrum of cardiac inflow defects including TAPVR in humans [31]. Loss of PDGFRA function causes TAPVR with low penetrance (∼7%) reminiscent of that observed in the human population. Mutation analysis of the PDGFRA gene in TAPVR patients revealed a sequence variant on human chromosome 4q12 suggestive for a putative TAPVR gene. An important component of the atrium is the posterior heart field-derived dorsal mesenchymal protrusion (DMP), involved in development of the dorsal wall of the atrium and more specifically in atrial septation. Furthermore, the DMP is essential for partitioning the vein from the systemic venous system as shown in the abovementioned Pdgf signaling [31]. In a cohort of patients with TAPVR, the retinol binding protein5 (*rbp5*) was mutated [32]. In a subsequent project the zebrafish ortholog *rbp7,* as a TAPVR susceptibility gene, showed deleterious variants in retinoic acid signaling including *NODAL* and retinol dehydrogenase10. Morpholino-induced *rbp7a* morphants showed that cilia in the early embryonic Kuppfer's vesicle were significantly shorter, indicating a role in left-right asymmetry [32]. It is evident that ciliar length is involved in mechanosensing of fluid flow [33, 34]. Retinoic acid-related FGF-signaling for ciliation is also involved in abnormal SHF differentiation [35]. In Xenopus chromatin modification (histone 2B ubiquitination) also points to ciliary involvement in TAPVR via *RNF20* mutation, while H2Bub1 marks are enriched on the cilia transcription factor *Rfx3* [36]. Both genes are involved in cardiac left-right patterning. Cilia-associated cardiovascular anomalies include high penetrance of TAPV as revealed by abnormal development of the DMP and pulmonary return after mutation of the flagellar transport protein ift88 in a mouse model [37]. Abnormal developing DMP from impaired podoplanin signaling results in atrioventricular septum defects, combined with a diminished incorporation of the vascular smooth muscle cells, but also in deficient pulmonary vein myocardium and connection [25, 31] (Fig. 34.6). Furthermore, sonic hedgehog [32] and the Tbx5-hedgehog molecular network [38] are essential for second heart field, atrial septation and DMP formation. Nevertheless, pulmonary vein differentiation is unaffected when DMP formation is hampered in Tbx5 mutants [38] suggesting that the DMP and pulmonary vein develop independently and in parallel from the SHF.

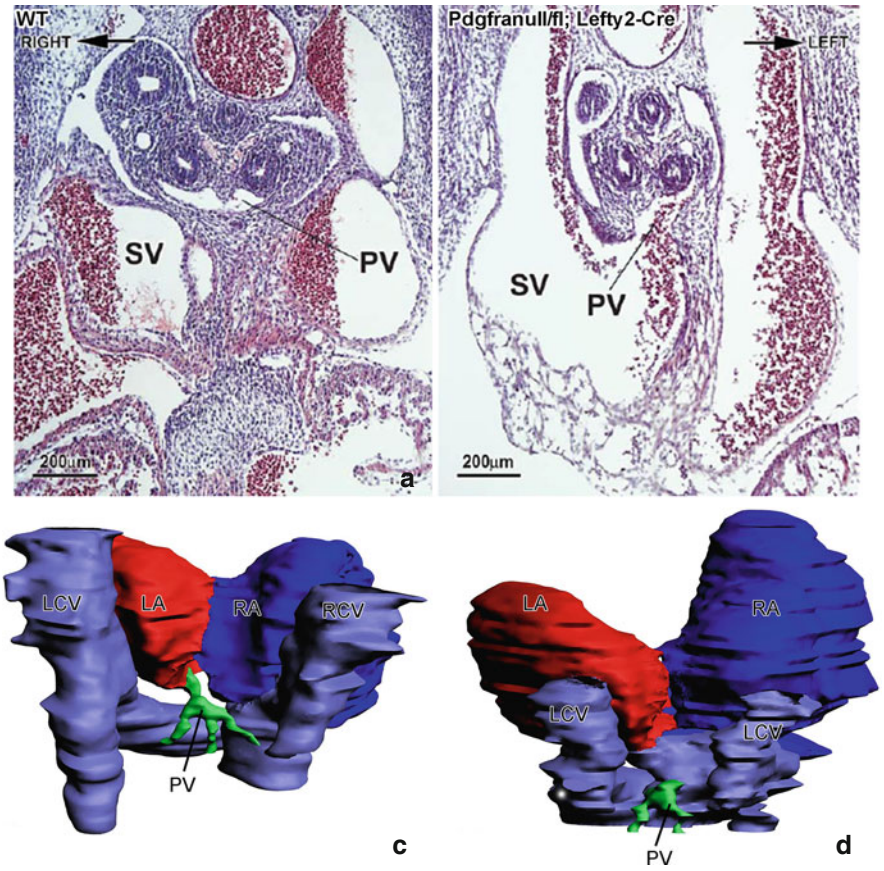

Fig. 34.6 TAPVR in the Pdgfra mouse mutant. A restricted deficiency of PDGFRA was achieved here in Pdgfra$^{flox/flox}$; H Lefty 2-Cre embryos, to avoid the confounding effects of earlier PDGFRA deficiency during gastrulation or early cardiogenesis [32]. Transverse section (**a**) and dorsal view of a 3D reconstruction (**b**) of a wild-type E11.5 mouse embryo. The primitive pulmonary vein (indicated in green in the 3D reconstruction) with its tributaries connects to the *left* atrium (red area in b). (**c**, **d**) Similar levels in the Pdgfra $^{null/fl}$. Lefty 2-Cre embryo. The PV (indicated in green in the 3D reconstruction) connects to the sinus venosus, consisting of the *right* and *left* cardinal veins (*RPV* and *LCV*, resp.) and their confluence (indicated in purple in the 3D reconstruction). The *right* atrium (*RA*) is indicated in blue (Source: Modified with permission after [32])

Shox2, homologous to *SHOX*, involved in short-stature syndrome in humans, is expressed in the sinus venosus myocardium. *Shox2* knockout mice showed embryonic lethality between 11.5 and 13.5 dpc, and sinus venosus myocardium was markedly hypoplastic. Although primarily investigated for the anomalies at the right side of the venous pole including the sinoatrial node, the left-sided pulmonary vein was also diminished in size [6]. As this mouse model did not survive beyond E13.5, further development of the pulmonary vein could not be investigated.

The role of Id2 (inhibitor of differentiation/inhibitor of DNA binding) in chicken, Xenopus and mouse has been described in the second heart field [28]. Id2 proteins are negative regulators of basic loop–helix proteins, promoting cell proliferation and keeping the cells in an undifferentiated state [39] dependent on GATA4 and NKX2–5. Knockout mouse embryos (embryonic day, ED 11.5) present with severe abnormalities including dilated cardinal veins and an underdeveloped sinus venosus resulting in displaced venous drainage. The pulmonary veins are connected to the atrium caudally to that of the left cardinal vein into the sinus venosus. At ED 12.5, a less well-developed interatrial septum is present, while the cardinal and pulmonary veins hardly show any myocardial layer. Furthermore, the intracardiac part of the pulmonary vein is surrounded by differentiated atrial myocardium lacking the transitional zone characteristic for wild-type embryos. In ED 13.5 and 14.5, the left atrium appears smaller, reminiscent of human patients with TAPVC. However, the DMP does not seem to be affected in the Id2 mutant which is in line with the observation that atrioventricular defects have not been found. Remarkably, the myocardialization of the DMP appears more advanced than in the wild type after loss of Id2 control. Nevertheless, myocardialization of the systemic veins was diminished from which may be concluded that in Id2 mutants the balance between differentiated and undifferentiated cells is lost [28].

In animal models, it has been shown that many genes are involved in atrial and venous return development. Myocardial progenitor cells in the left or right posterior heart field contribute to the left or right atrium, respectively [18]. Manipulation of Pitx2c [35] demonstrates repression of either right atrial identity or of proliferation of the left sinus venosus. Isl1 is an important regulator in the posterior heart field [4]. The Isl1 SHF enhancer contains three consensus binding sites suggestive for regulation by Forkhead transcription factors [40] and is part of a more complex regulative network also including sonic hedgehog, Fgf8 (fibroblast growth factor 8), Tbx1, and retinoic acid [41]. The pulmonary vein gains access to the Isl1 expressing medial dorsal side of the caudal heart tube that is no longer Tbx18 positive. As the remainder of the venous pole expresses Tbx18, it has been suggested [10] that the ancestors to the pulmonary and systemic veins are strictly separated. This gene expression-based evidence contrasts strongly with the findings of Galli [42] and Lescroart [18] who describe distinct left- and right-sided lineages in contrast to systemic and pulmonary lineages.

TAPVC occurs in Semaphorin 3d (Sema3d) mutant mice [43], despite normal formation of the MPES. In 35% of mutant mouse embryos, the developing splanchnic plexus surrounding the lung buds does not anastomose uniquely with the MPES. Normally, Sema3d provides a migration repulsive signal to endothelial cells in early stages of development (E9.5 in mouse), establishing a boundary between the pulmonary plexus and the systemic circulation, whereas in the mutants, endothelial tubes form aberrant connections traversing this normally vascular-free area. Furthermore, atrial septation is impaired in these mutants providing further evidence for the codevelopment of the atrial septum and the pulmonary vein (Fig. 34.7).

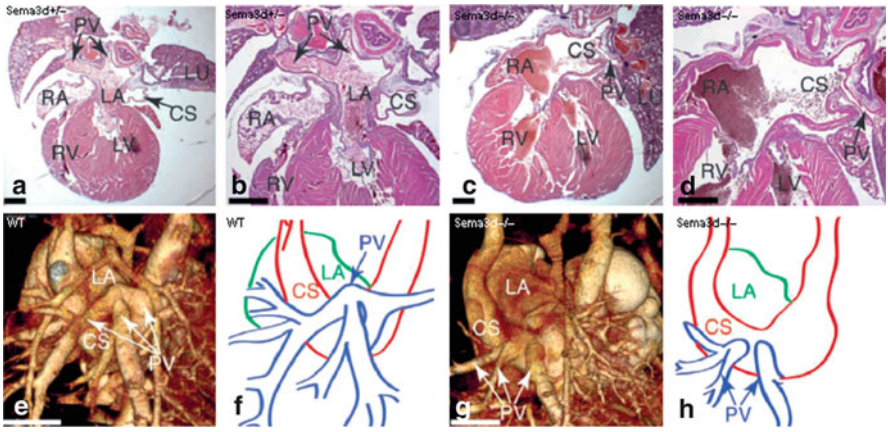

Fig. 34.7 Pulmonary venous connections in Semaphorin 3d heterozygous ($Sema3d^{+/-}$) and Semaphorin 3d mutant ($Sema3d^{-/-}$) adult mice. The pulmonary veins (*PV*) normally connect to the *left* atrium (*LA*) in the $Sema3d^{+/-}$ mouse (**a**, **b**). In the mutant mouse, an (**c**, **d**) anomalous pulmonary venous connections to the coronary sinus is observed (**e**–**h**). Volume-rendered microcomputed tomography (microCT) images (**e**, **g**, dorsal views) and schematic drawings of the pulmonary venous connections (**f**, **h**). The pulmonary veins normally enter the LA in a newborn wild-type (*WT*) mouse (**e**, **f**) and connect to the coronary sinus in a newborn mutant mouse (**g**, **h**) (Source: Adapted with permission [47])

34.8 Conclusion

In summary, it is evident that several gene networks act in the differentiation of the pulmonary veins, starting already early in development before formation of the myocardial and smooth muscle sleeves. The formation of the myocardial wall of the pulmonary vein is accompanied by incorporation into the dorsal wall of the right atrium, a differentiation that can be followed during development. Maldevelopment of the connection between pulmonary vein and left atrium may result in persisting connections to the systemic circulation as seen in patients with TAPVC.

References

1. Snarr BS, O'Neal JL, Chintalapudi MR, Wirrig EE, Phelps AL, Kubalak SW, et al. Isl1 expression at the venous pole identifies a novel role for the second heart field in cardiac development. Circ Res. 2007;101(10):971–4.
2. Blom NA, Gittenberger-de Groot AC, Jongeneel TH, DeRuiter MC, Poelmann RE, Ottenkamp J. Normal development of the pulmonary veins in human embryos and formulation of a morphogenetic concept for sinus venosus defects. Am J Cardiol. 2001;87(3):305–9.
3. Kelly RG. The second heart field. Curr Top Dev Biol. 2012;100:33–65.
4. Cai CL, Liang X, Shi Y, Chu PH, Pfaff SL, Chen J, et al. Isl1 identifies a cardiac progenitor population that proliferates prior to differentiation and contributes a majority of cells to the heart. Dev Cell. 2003;5(6):877–89.

5. Martinsen BJ, Frasier AJ, Baker CV, Lohr JL. Cardiac neural crest ablation alters Id2 gene expression in the developing heart. Dev Biol. 2004;272(1):176–90.
6. Blaschke RJ, Hahurij ND, Kuijper S, Just S, Wisse LJ, Deissler K, et al. Targeted mutation reveals essential functions of the homeodomain transcription factor Shox2 in sinoatrial and pacemaking development. Circulation. 2007;115(14):1830–8.
7. Christoffels VM, Mommersteeg MT, Trowe MO, Prall OW, de Gier-de VC, Soufan AT, et al. Formation of the venous pole of the heart from an Nkx2-5-negative precursor population requires Tbx18. Circ Res. 2006;98(12):1555–63.
8. Gittenberger-de Groot AC, Mahtab EA, Hahurij ND, Wisse LJ, Deruiter MC, Wijffels MC, et al. Nkx2.5-negative myocardium of the posterior heart field and its correlation with podoplanin expression in cells from the developing cardiac pacemaking and conduction system. Anat Rec (Hoboken). 2007;290(1):115–22.
9. Mahtab EA, Vicente-Steijn R, Hahurij ND, Jongbloed MR, Wisse LJ, DeRuiter MC, et al. Podoplanin deficient mice show a RhoA-related hypoplasia of the sinus venosus myocardium including the sinoatrial node. Dev Dyn. 2009;238(1):183–93.
10. Mommersteeg MT, Dominguez JN, Wiese C, Norden J, de Gier-de VC, Burch JB, et al. The sinus venosus progenitors separate and diversify from the first and second heart fields early in development. Cardiovasc Res. 2010;87(1):92–101.
11. Rammos S, Gittenberger-de Groot AC, Oppenheimer-Dekker A. The abnormal pulmonary venous connexion: a developmental approach. Int J Cardiol. 1990;29(3):285–95.
12. Snarr BS, Kern CB, Wessels A. Origin and fate of cardiac mesenchyme. Dev Dyn. 2008;237 (10):2804–19.
13. Douglas YL, Jongbloed MR, Gittenberger-de Groot AC, Evers D, Dion RA, Voigt P, et al. Histology of vascular myocardial wall of left atrial body after pulmonary venous incorporation. Am J Cardiol. 2006;97(5):662–70.
14. Haissaguerre M, Jais P, Shah DC, Takahashi A, Hocini M, Quiniou G, et al. Spontaneous initiation of atrial fibrillation by ectopic beats originating in the pulmonary veins. N Engl J Med. 1998;339(10):659–66.
15. Ho SY, Cabrera JA, Tran VH, Farre J, Anderson RH, Sanchez-Quintana D. Architecture of the pulmonary veins: relevance to radiofrequency ablation. Heart. 2001;86(3):265–70.
16. Jongbloed MR, Dirksen MS, Bax JJ, Boersma E, Geleijns K, Lamb HJ, et al. Atrial fibrillation: multi-detector row CT of pulmonary vein anatomy prior to radiofrequency catheter ablation–initial experience. Radiology. 2005;234(3):702–9.
17. DeRuiter MC, Gittenberger-de Groot AC, Poelmann RE, VanIperen L, Mentink MM. Development of the pharyngeal arch system related to the pulmonary and bronchial vessels in the avian embryo. With a concept on systemic-pulmonary collateral artery formation. Circulation. 1993;87(4):1306–19.
18. Lescroart F, Mohun T, Meilhac SM, Bennett M, Buckingham M. Lineage tree for the venous pole of the heart: clonal analysis clarifies controversial genealogy based on genetic tracing. Circ Res. 2012;111(10):1313–22.
19. van den Berg G, Moorman AF. Development of the pulmonary vein and the systemic venous sinus: an interactive 3D overview. PLoS One. 2011;6(7):e22055.
20. Manner J, Merkel N. Early morphogenesis of the sinuatrial region of the chick heart: a contribution to the understanding of the pathogenesis of direct pulmonary venous connections to the right atrium and atrial septal defects in hearts with right isomerism of the atrial appendages. Anat Rec (Hoboken). 2007;290(2):168–80.
21. Moorman AF, Anderson RH. Development of the pulmonary vein. Anat Rec (Hoboken). 2007;290(9):1046–9.
22. Douglas YL, Jongbloed MR, Deruiter MC, Gittenberger-de Groot AC. Normal and abnormal development of pulmonary veins: state of the art and correlation with clinical entities. Int J Cardiol. 2011;147(1):13–24.
23. Moorman AF, Anderson RH. Development of the pulmonary vein. Int J Cardiol. 2011;147(1): 182.

24. Gittenberger-de Groot AC. The development of the pulmonary vein revisited. Int J Cardiol. 2011;147(3):463–4.
25. Douglas YL, Mahtab EA, Jongbloed MR, Uhrin P, Zaujec J, Binder BR, et al. Pulmonary vein, dorsal atrial wall and atrial septum abnormalities in podoplanin knockout mice with disturbed posterior heart field contribution. Pediatr Res. 2009;65(1):27–32.
26. Buckingham ME, Meilhac SM. Tracing cells for tracking cell lineage and clonal behavior. Dev Cell. 2011;21(3):394–409.
27. Douglas YL, Jongbloed MR, den Hartog WC, Bartelings MM, Bogers AJ, Ebels T, et al. Pulmonary vein and atrial wall pathology in human total anomalous pulmonary venous connection. Int J Cardiol. 2009;134(3):302–12.
28. Jongbloed MR, Vicente-Steijn R, Douglas YL, Wisse LJ, Mori K, Yokota Y, et al. Expression of Id2 in the second heart field and cardiac defects in Id2 knock-out mice. Dev Dyn. 2011;240 (11):2561–77.
29. Ricci M, Elliott M, Cohen GA, Catalan G, Stark J, de Leval MR, et al. Management of pulmonary venous obstruction after correction of TAPVC: risk factors for adverse outcome. Eur J Cardiothorac Surg. 2003;24(1):28–36. discussion
30. Bax NA, Lie-Venema H, Vicente-Steijn R, Bleyl SB, Van Den Akker NM, Maas S, et al. Platelet-derived growth factor is involved in the differentiation of second heart field-derived cardiac structures in chicken embryos. Dev Dyn. 2009;238(10):2658–69.
31. Bleyl SB, Saijoh Y, Bax NA, Gittenberger-de Groot AC, Wisse LJ, Chapman SC, et al. Dysregulation of the PDGFRA gene causes inflow tract anomalies including TAPVR: integrating evidence from human genetics and model organisms. Hum Mol Genet. 2010;19 (7):1286–301.
32. Nash D, Arrington CB, Kennedy BJ, Yandell M, Wu W, Zhang W, et al. Shared segment analysis and next-generation sequencing implicates the retinoic acid signaling pathway in Total anomalous pulmonary venous return (TAPVR). PLoS One. 2015;10(6):e0131514.
33. Dummer A, Poelma C, DeRuiter MC, Goumans MJ, Hierck BP. Measuring the primary cilium length: improved method for unbiased high-throughput analysis. Cilia. 2016;5:7.
34. Egorova AD, Khedoe PP, Goumans MJ, Yoder BK, Nauli SM, ten Dijke P, et al. Lack of primary cilia primes shear-induced endothelial-to-mesenchymal transition. Circ Res. 2011;108 (9):1093–101.
35. Franco D, Campione M. The role of Pitx2 during cardiac development. Linking left-right signaling and congenital heart diseases. Trends Cardiovasc Med. 2003;13(4):157–63.
36. Robson A, Makova SZ, Barish S, Zaidi S, Mehta S, Drozd J, et al. Histone H2B monoubiquitination regulates heart development via epigenetic control of cilia motility. Proc Natl Acad Sci U S A. 2019;116(28):14049–54.
37. Burns TA, Deepe RN, Bullard J, Phelps AL, Toomer KA, Hiriart E, et al. A novel mouse model for cilia-associated cardiovascular anomalies with a high penetrance of Total anomalous pulmonary venous return. Anat Rec (Hoboken). 2019;302(1):136–45.
38. Xie L, Hoffmann AD, Burnicka-Turek O, Friedland-Little JM, Zhang K, Moskowitz IP. Tbx5-hedgehog molecular networks are essential in the second heart field for atrial septation. Dev Cell. 2012;23(2):280–91.
39. Lim JY, Kim WH, Kim J, Park SI. Induction of Id2 expression by cardiac transcription factors GATA4 and Nkx2.5. J Cell Biochem. 2008;103(1):182–94.
40. Kang J, Nathan E, Xu SM, Tzahor E, Black BL. Isl1 is a direct transcriptional target of Forkhead transcription factors in second-heart-field-derived mesoderm. Dev Biol. 2009;334(2):513–22.
41. Pandur P, Sirbu IO, Kuhl SJ, Philipp M, Kuhl M. Islet1-expressing cardiac progenitor cells: a comparison across species. Dev Genes Evol. 2013;223(1–2):117–29.
42. Galli D, Dominguez JN, Zaffran S, Munk A, Brown NA, Buckingham ME. Atrial myocardium derives from the posterior region of the second heart field, which acquires left-right identity as Pitx2c is expressed. Development. 2008;135(6):1157–67.
43. Degenhardt K, Singh MK, Aghajanian H, Massera D, Wang Q, Li J, et al. Semaphorin 3d signaling defects are associated with anomalous pulmonary venous connections. Nat Med. 2013;19(6):760–5.

Part VIII

Tetralogy of Fallot and Double Outlet Right Ventricle

Clinical Presentation and Therapy of Tetralogy of Fallot and Double-Outlet Right Ventricle

35

Nikolaus A. Haas, David J. Driscoll, and Silke Rickert-Sperling

35.1 Tetralogy of Fallot and Pulmonary Atresia with Ventricular Septal Defect

Tetralogy of Fallot (TOF) is the most common cyanotic heart defect. TOF consists of the combination of four anomalies (Fig. 35.1): (1) a large malalignment ventricular septal defect, (2) an obstruction of the right ventricular outflow tract (usually infundibular and valvular pulmonary stenosis with a small pulmonary valve annulus and supravalvular stenosis, (3) an aorta that "overrides" the ventricular septal defect, and (4) right ventricular hypertrophy. TOF represents 4–8% of congenital heart defects. Specific variations of TOF include all forms of pulmonary atresia with VSD and absent pulmonary valve syndrome. In addition, the left and right main pulmonary arteries may be stenotic or hypoplastic. In these cases, there may be major aortopulmonary collateral arteries (MAPCAs) which are vessels arising from the aorta or the subclavian arteries that supply segments of the pulmonary arterial tree. Additional variations include an ASD (Pentalogy of Fallot), a right aortic arch, and coronary abnormalities.

N. A. Haas (✉)
Department of Pediatric Cardiology and Intensive Care, Ludwig Maximilians University, Munich, Germany
e-mail: Nikolaus.haas@med.uni-muenchen.de

D. J. Driscoll
Division of Pediatric Cardiology, Department of Pediatrics, Mayo Clinic College of Medicine, Rochester, MN, USA
e-mail: driscoll.david@mayo.edu

S. Rickert-Sperling
Cardiovascular Genetics, Charité–Universitätsmedizin Berlin, Berlin, Germany
e-mail: silke.sperling@charite.de

© The Author(s), under exclusive license to Springer Nature Switzerland AG 2024

S. Rickert-Sperling et al. (eds.), *Congenital Heart Diseases: The Broken Heart*,
Advances in Experimental Medicine and Biology 1441,
https://doi.org/10.1007/978-3-031-44087-8_35

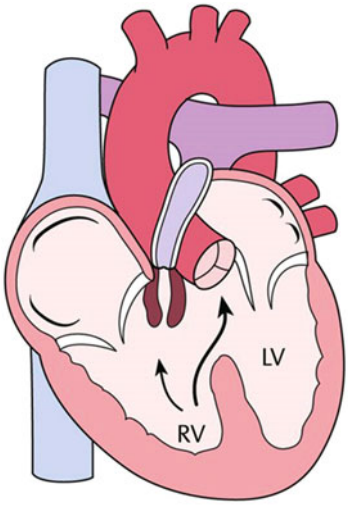

Fig. 35.1 Anatomical features of tetralogy of Fallot. *LV* left ventricle; *RV* right ventricle. Reproduced from Kinderkardiologie, Georg Thieme Verlag, N. Haas, U. Kleideiter, 2011

Pulmonary Atresia with VSD (PA/VSD)

Pulmonary atresia with ventricular septal defect (PA/VSD) is often considered a more severe form of TOF. The main difference between the two conditions lies in the absence of a hemodynamic outlet from the right ventricle in PA/VSD, while in TOF, there is a stenotic outlet. In PA/VSD, the anatomical right ventricular outlet is present but hypoplastic, leading to the atresia. The atresia in PA/VSD can occur at the valve level, infundibular level, involve only a short segment of the main pulmonary artery, or in severe cases, encompass the entire main pulmonary artery. In the most complex cases, the atresia can extend to both the central and distal pulmonary arteries (Fig. 35.2).

TOF with Agenesis of the Pulmonary Valve

Miller–Lev–Paul syndrome, also known as pulmonary valve agenesis, is a rare form of tetralogy of Fallot (TOF) accounting for approximately 2% of cases. In this condition, the pulmonary valve is absent, and instead, patients have a rudimentary ring or membrane that serves as a substitute "valve." Due to the absence of a functional pulmonary valve, there is both regurgitation and stenosis of blood flow into the main pulmonary artery.

The turbulent flow resulting from these abnormalities leads to significant dilation of the central pulmonary arteries. This dilation can be so pronounced that it causes compression of the trachea and bronchi, potentially leading to respiratory difficulties shortly after birth.

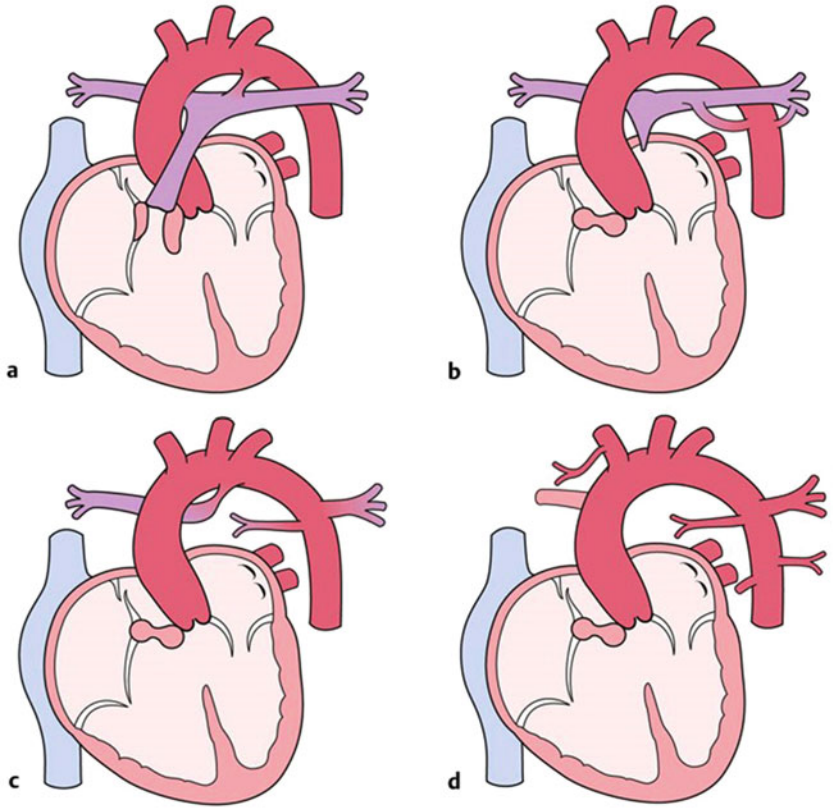

Fig. 35.2 The classification of PA/VSD. (**a**) Type I: normal development of central and peripheral pulmonary arteries, but the main pulmonary artery is very narrow or hypoplastic (underdeveloped). (**b**) Type II: normal development of central and peripheral pulmonary arteries, but the main pulmonary artery is missing. In this case, blood supply to the lung occurs through collateral blood vessels. (**c**) Type III: the central pulmonary arteries are narrow and hypoplastic. The blood supply to the lungs primarily occurs through aortopulmonary collaterals (additional blood vessels that form between the aorta and the pulmonary arteries). The ductus arteriosus (connection between the aorta and pulmonary artery before birth) may be absent or very narrow. (**d**) Type IV: there are no central pulmonary arteries, and the entire lung blood supply occurs exclusively through mostly multifocal (occurring at multiple locations) aortopulmonary collaterals. Reproduced from Kinderkardiologie, Georg Thieme Verlag, N. Haas, U. Kleideiter, 2011

35.1.1 Pathologic Physiology

Newborns and infants with tetralogy of Fallot (TOF) typically present with cyanosis due to a right-to-left shunt through the ventricular septal defect and decreased pulmonary blood flow. The severity of hypoxemia is directly related to the volume of pulmonary blood flow, which is influenced by the degree of right ventricular outflow tract obstruction (RVOTO) and the presence of other sources of pulmonary

blood flow, such as a patent ductus arteriosus and systemic-to-pulmonary artery collateral vessels. In cases where pulmonary blood flow is sufficient, normal oxygen saturation levels may be achieved, resulting in a condition known as "Pink Fallot."

However, in severe forms of TOF with significantly reduced pulmonary blood flow, these children may rely on the pulmonary blood flow provided by a patent ductus arteriosus. They may also depend on major aortopulmonary collateral arteries (MAPCAs) for additional pulmonary blood flow. In the case of pulmonary atresia with ventricular septal defect (PA/VSD), there is no forward blood flow from the right ventricle into the pulmonary artery. Therefore, survival in these patients is entirely dependent on pulmonary blood flow from a patent ductus arteriosus and/or MAPCAs.

In cases of TOF with agenesis of the pulmonary valve, affected children typically exhibit the hemodynamic characteristics of TOF. Additionally, there may be associated pulmonary anomalies and, in some cases, respiratory failure may occur if there is compression of the trachea or bronchi.

35.1.2 Clinical Presentation

If not detected prenatally, infants with tetralogy of Fallot, PA/VSD or absent pulmonary valve syndrome come to medical attention because of cyanosis or a murmur soon after birth or even respiratory distress. When a neonatal pulse oximetry screening is in place, they should be picked up by lower than normal saturations.

Hypercyanotic or "tetralogy" spells can occur in all forms of congenital heart disease in which there is obstruction to pulmonary blood flow and a communication between the subpulmonary and subaortic ventricles. These are much more common in TOF than in PA/VSD. These spells initially were associated with tetralogy of Fallot, hence, the name. Hypercyanotic spells consist of the abrupt onset of increased cyanosis, hypoxemia, dyspnea, and agitation. If left untreated, they can lead to profound hypoxemia, acidosis, seizures, and death. They rarely occur before the age of 2 months. Pathophysiologically, there are two main explanations: first, an increase of agitation and catecholamine effect, the infundibular (muscular) stenosis aggravates and this will be intensified by crying and elevated pressure in the chest. The effect is a massively reduced pulmonary blood flow and consequent hypoxia. Second, many "Tet-spells" may occur after feeding in a more quiet situation. Peripheral vasodilation and blood flow distribution to the gut will distribute blood flow from the right heart to the low resistance systemic circulation; the effect is the same. Acute management consists of various measures to optimize pulmonary perfusion (i.e., volume administration, sedation, etc.). For chronic management, betablockers are usually used to reduce infundibular spasms. If the "Tet spells" persist, interventional or surgical measures are required.

35.1.3 Physical Examination

Most patients with Tetralogy of Fallot (TOF) or Pulmonary Atresia with Ventricular Septal Defect (PA/VSD) will exhibit cyanosis. However, in some cases, the degree of cyanosis may be minimal, leading to the term "pink tetralogy." On physical examination, an increased right ventricular impulse can be palpated at the right lower sternal border. The first heart sound is typically normal, but the second heart sound is intensified and often single. Along the left sternal border, there is a systolic ejection murmur in the case of TOF. However, in PA/VSD, where there is no patent right ventricular outflow tract, there is no systolic ejection murmur. Instead, a systolic murmur or systolic–diastolic continuous murmur may be heard, which is created by the flow through a patent ductus arteriosus (PDA) or the MAPCAs.

35.1.4 Diagnostic Imaging

Echocardiography is the primary imaging modality for diagnosing Tetralogy of Fallot (TOF), Pulmonary Atresia with Ventricular Septal Defect (PA/VSD), and Absent Pulmonary Valve Syndrome. It allows for accurate assessment of the malformations, detection of associated abnormalities, and evaluation of the severity and location of obstruction within the right ventricular outflow tract. Transthoracic echocardiography is usually sufficient for diagnosis in neonates and children. In the case of multiple Aortopulmonary Collateral Arteries (MAPCAs), additional imaging modalities may be required.

Chest radiographs may show a right aortic arch in approximately 25% of patients. The cardiac silhouette may exhibit a "boot-shaped" appearance due to hypoplasia of the main pulmonary artery and right ventricular hypertrophy. In cases of absent pulmonary valve syndrome, enlarged pulmonary arteries and bronchial obstruction may be visible. However, chest radiographs have limited diagnostic value in infants.

Diagnostic cardiac catheterization is generally unnecessary for the diagnosis of simple cases of TOF, absent pulmonary valve syndrome, or uncomplicated PA/VSD, as echocardiography provides sufficient information. However, in patients with MAPCAs, cardiac catheterization may still be required to characterize the pulmonary blood supply, assess peripheral pulmonary arteries, evaluate the presence of stenosis or additional ventricular septal defects, and determine the need for interventional palliation before surgery.

Magnetic resonance imaging (MRI) is useful for older patients to assess the pulmonary vascular bed, especially in the presence of MAPCAs. It is also the standard for follow-up after surgical repair, providing information on right ventricular size and function, pulmonary stenosis and regurgitation, and guiding decisions regarding the timing and type of pulmonary valve replacement. In children, MRI can help define the anatomy of coronary arteries and MAPCAs prior to surgical intervention.

Computer tomography (CT) can provide detailed anatomical information similar to MRI but with higher resolution for smaller vessels. CT scans are often utilized in

patients with multiple MAPCAs for comprehensive preoperative planning. Three-dimensional models can be created to optimize treatment strategies.

35.1.5 Treatment

The initial management of patients with Tetralogy of Fallot (TOF) and Pulmonary Atresia with Ventricular Septal Defect (PA/VSD) focuses on addressing the specific cardiac abnormalities and managing the associated hypoxemia and acidosis. Here is an optimized summary of the management approach:

1. Establish anatomic diagnosis: Detailed evaluation and imaging studies, such as echocardiography and cardiac catheterization, are conducted to confirm the specific diagnosis and assess the extent of the cardiac abnormalities.
2. Address hypoxemia and acidosis: If the infant is severely hypoxemic, measures should be taken to improve oxygenation and correct acidosis. Infusion of prostaglandin E1 (PGE1) is used to reopen the ductus arteriosus or maintain its patency, ensuring adequate pulmonary blood flow.
3. Surgical intervention for inadequate pulmonary blood flow: If the pulmonary blood flow is insufficient, a systemic-to-pulmonary artery anastomosis is established surgically. The preferred procedures are the Blalock–Taussig shunt (connecting the subclavian artery to the pulmonary artery) or modified Blalock–Taussig shunt (using a Gore-Tex tube as an interposition graft).
4. Intracardiac repair: Intracardiac repair of TOF or PA/VSD is typically performed between the ages of 3 and 12 months. The procedure involves closure of the ventricular septal defect and relief of the right ventricular outflow tract obstruction or atresia. This may require patch enlargement of the right ventricular outflow tract, pulmonary annulus, or both, and the insertion of a valve-containing conduit from the right ventricle to the pulmonary artery.

Following intracardiac repair, close postoperative monitoring and regular follow-up visits are necessary to assess the patient's cardiac function, development, and potential complications. Medications may be prescribed to manage symptoms and prevent arrhythmias, as needed.

35.1.6 Outcome

The long-term outcome of treatment of TOF or PA/VSD depends primarily on the size and anatomy of the pulmonary arteries and whether or not a competent native pulmonary valve remains after operation. Patients with normal size pulmonary arteries that are normally distributed and a competent pulmonary valve postoperatively have an excellent long-term prognosis. For patients who require insertion of a right ventricle to pulmonary conduit (which includes all patients with PA/VSD), the conduits will eventually fail and require replacement several times during the

patient's lifetime. Patients with TOF who, after operation, have pulmonary valve insufficiency may require insertion of a prosthetic valve later in life.

The long-term outcome is mainly dependent on the performance of the right ventricle. Mild residual stenosis (i.e., < 30 mmHg) is usually well tolerated, pulmonary regurgitation however will lead to right ventricular dilatation and ultimately failure and the risk of sudden cardiac death. These patients require permanent and lifelong surveillance in dedicated centers. Repeat objective determination of exercise capacity will measure the cardiocirculatory function objectively. Repeat MRI is the key point in assessment of RV size and function. There is an ongoing risk of arrhythmias and late sudden death for patients with repaired tetralogy of Fallot or PA/VSD. The highest risk is in patients with residual VSD, residual RVOTO, poor ventricular function, and a QRS duration >180 msec.

Patients with hypoplastic pulmonary arteries (i.e., complex forms of PA/VSD) will suffer from elevated pulmonary vascular resistance, reduced cardiac output, inadequately compensated right heart even at rest, show clinically relevant reduced exercise capacity at mild exercise and have reduced quality of life and life expectancy.

35.2 Double-Outlet Right Ventricle

As the name indicates, in double-outlet right ventricle (DORV), both great arteries arise totally or primarily from the right ventricle; it represents about 1–15% of all CHD and in most cases the presentation and pathophysiology is similar to TOF. Invariably, there is a ventricular septal defect (VSD) that is then the only outlet of the left ventricle; its location in relation to the great vessels is the basis for the classification. If there is no VSD, the left ventricle would be hypoplastic and then the anomaly would be considered a form of functional single ventricle which will not be discussed in this chapter (Fig. 35.3).

The classification of DORV is not always consistent and various definitions are used. Traditionally a DORV was defined when one artery originates from the RV and if at least 51% of the other vessel is committed to the right ventricle. This classification is today often used by surgeons, because it is more difficult to repair a DORV as compared to a simple TOF. This classification is however not correct from an embryological point of view. The correct definition has to include the fact that there must be an infundibulum in the right ventricle below the pulmonary artery. Therefore, in DORV there must be a muscular infundibulum below both arteries and muscle tissue between the two arteries (a conus septum). With regard to the left side of the heart, there must be some muscular tissue between the mitral valve and the aorta (or pulmonary valve). This contrasts with normal hearts where there is a fibrous continuity between the mitral valve and the aorta. In DORV there is no mitral annular fibrous continuity with the annulus of the nearest semilunar valve, that is instead separated by muscular tissue.

Regarding the relationships between the ventricular septal defect (VSD) and the great arteries, there are four types (Fig. 35.4):

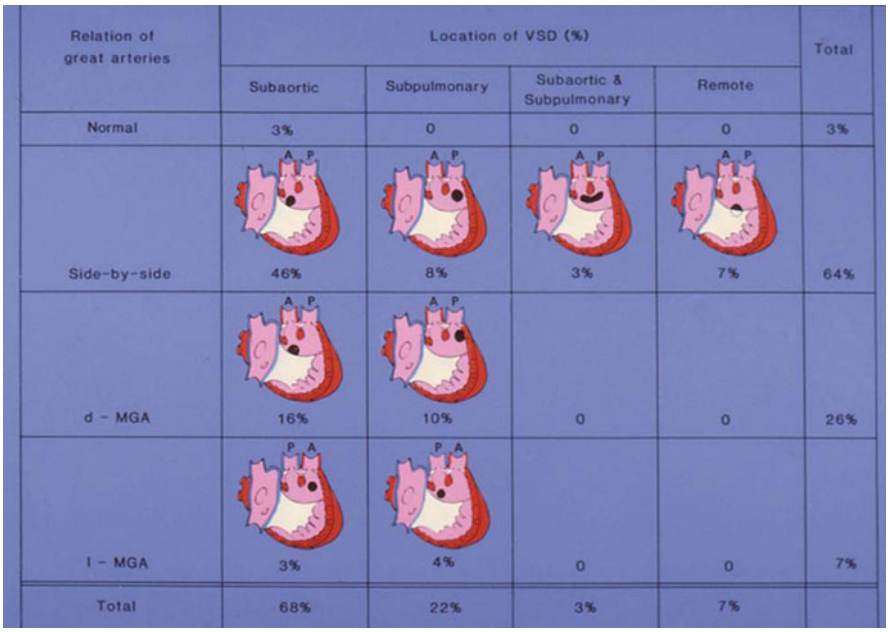

Relation of great arteries	Location of VSD (%)				Total
	Subaortic	Subpulmonary	Subaortic & Subpulmonary	Remote	
Normal	3%	0	0	0	3%
Side-by-side	46%	8%	3%	7%	64%
d – MGA	16%	10%	0	0	26%
l – MGA	3%	4%	0	0	7%
Total	68%	22%	3%	7%	

Fig. 35.3 Table of the various types of double-outlet right ventricle (Reproduced or adapted from Hagler, D., Double-Outlet Right Ventricle and Double-Outlet Left Ventricle, in *Moss and Adams' Heart Disease in Infants, Children, and Adolescents*, 7th edition 2008, Lippincott Williams & Wilkins, 2006, with permission of the author and publisher)

1. DORV with subaortic VSD (approximately 50%–70% of cases): This is sometimes referred to as Fallot-type DORV and often includes right ventricular outflow tract stenosis (conus septum) and typical Tetralogy of Fallot hemodynamics.
2. DORV with subpulmonary VSD (20–25% of cases): Known as Taussig-Bing anomaly, this condition involves a subaortic stenosis caused by the conus septum. There may also be additional abnormalities such as hypoplasia, coarctation, or interruption of the aortic arch.
3. DORV with doubly committed VSD (approximately 5% of cases): The VSD is related to both great arteries, and significant obstruction is rare.
4. DORV with remote (uncommitted) VSD (7–20% of cases): In this scenario, the VSD has no relationship to the great arteries and may be muscular in nature.

The great arteries in DORV can be either in a normal relationship or malposed relative to each other. However, DORV should not be classified as "d-transposition" or "l-transposition." The arteries can be side-by-side, and the classification should reflect l-malposition or d-malposition, with both arteries arising from the correct ventricle.

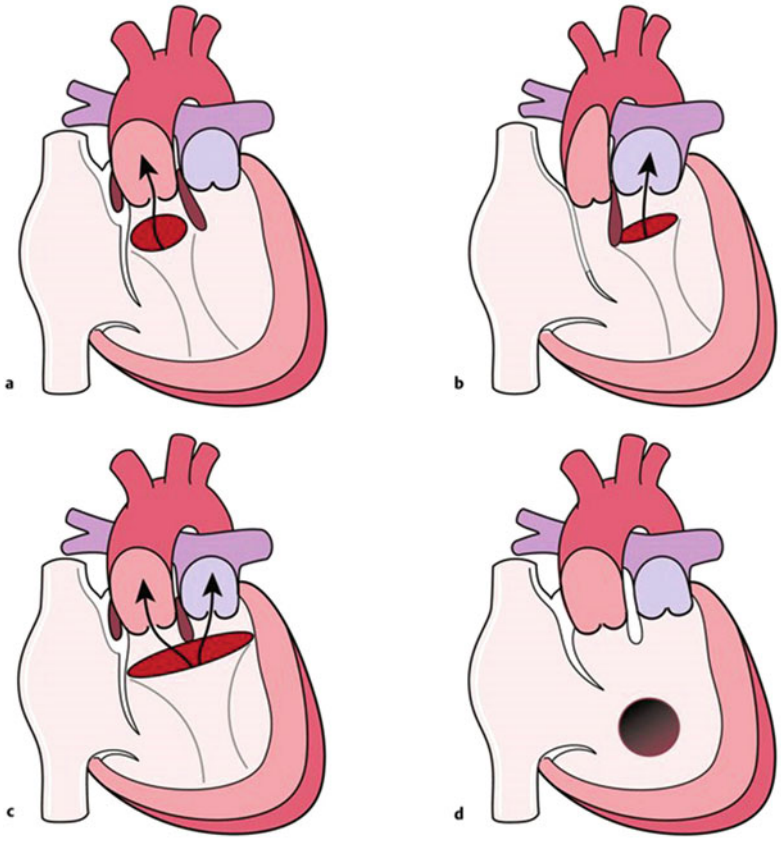

Fig. 35.4 Double-outlet right ventricle. (**a**) DORV with subaortic VSD, (**b**) DORV with subpulmonary VSD, (**c**) DORV with doubly committed VSD, (**d**) DORV with remote (uncommitted) VSD. Reproduced from Kinderkardiologie, Georg Thieme Verlag, N. Haas, U. Kleideiter, 2011

35.2.1 Pathologic Physiology

The pathophysiology of DORV varies depending on the specific VSD and arterial positions, as well as the presence of subarterial stenosis. The physiology of the defect can be divided into three forms:

1. DORV with Tetralogy of Fallot hemodynamics: If the aorta is committed to the VSD and there is pulmonary stenosis, the physiology and operative repair resemble those of Tetralogy of Fallot. Cyanosis is the predominant symptom.
2. DORV with VSD hemodynamics: If the aorta is committed to the VSD and there is no pulmonary stenosis, the physiology and operative repair resemble those of a

VSD. Excessive pulmonary blood flow and heart failure are the primary symptoms.

3. DORV with Transposition of the Great Arteries (TGA) hemodynamics: If the pulmonary artery is committed to the VSD, the physiology and operative approach resemble those of d-transposition of the great arteries, either with or without pulmonary stenosis. This form is also known as "Taussig-Bing anomaly." The primary symptoms include severe cyanosis and excessive pulmonary blood flow, which can lead to secondary heart failure.

35.2.2 Physical Examination

Since the physiology of DORV depends upon the relative position of the great arteries to the VSD, the physical findings also will depend upon the position of the great arteries and the presence or absence of pulmonary stenosis. In DORV with Fallot hemodynamics, the main symptoms are a murmur and cyanosis; in DORV with VSD hemodynamics, the leading symptoms are excessive blood flow, respiratory distress and clinical signs of heart failure. In DORV with TGA hemodynamics, the main symptoms are excessive pulmonary blood flow with respiratory distress, clinical signs of heart failure, and additional severe cyanosis (see Sect. 31.1.3 above for examination of TOF and Chap. 34 for findings with d-TGA).

35.2.3 Diagnostic Imaging

Echocardiography is the primary imaging modality for diagnosing various forms of double-outlet right ventricle (DORV). It allows for the identification of the relationship between the great arteries and the ventricular septal defect (VSD), malposition of the great arteries, the presence and severity of pulmonary stenosis or atresia, subpulmonary or subaortic stenosis, the anatomy of the aortic arch, and the presence and size of the patent ductus arteriosus. Echocardiography can also detect the important embryological difference between Tetralogy of Fallot (TOF) and DORV, such as the presence or absence of fibrous continuity between the mitral valve and the adjacent vessel. Additionally, echocardiography can identify other important malformations, including abnormalities of the AV valves that can impact surgical strategies.

In the current era of echocardiography, diagnostic cardiac catheterization is typically unnecessary for the diagnosis of DORV. However, in cases where there is inadequate mixing of blood or for interventional purposes, cardiac catheterization may be required.

Magnetic resonance imaging (MRI) is often used in adults and teenagers with DORV who present later in life. It is the standard of care for follow-up after surgical repair to assess the aortic arch anatomy, right ventricular size and function, the degree of pulmonary stenosis and regurgitation, and for discussions regarding the timing and form of pulmonary valve replacement.

Computer tomography (CT) can provide similar anatomical details as MRI but offers higher resolution for smaller vessels. CT scans are sometimes used in patients with complex anatomy prior to surgery to facilitate detailed planning. Three-dimensional models can be created from CT scans to optimize treatment strategies.

35.2.4 Treatment

The management approach for patients with double-outlet right ventricle (DORV) depends on factors such as the amount of pulmonary perfusion (i.e., saturation) and respiratory impairment. The overall approach is similar to that of other congenital heart defects like Tetralogy of Fallot (TOF), Ventricular Septal Defect (VSD), or Transposition of the Great Arteries (TGA).

In patients with uncomplicated DORV of Fallot-Type, where there is moderate cyanosis (i.e., saturations >80%) and no respiratory distress, outpatient monitoring is typically sufficient. Corrective surgery is usually performed between 6 and 12 months of age. The intracardiac repair involves closure of the ventricular septal defect and relief of the right ventricular outflow tract obstruction (RVOTO) or atresia. This may involve procedures such as patch enlargement of the right ventricular outflow tract, pulmonary annulus, or both, or the insertion of a valve-containing conduit from the right ventricle to the pulmonary artery.

35.2.5 Outcome

The surgical approach for double-outlet right ventricle (DORV) is similar to that of other congenital heart defects such as TOF, VSD, or Transposition of the Great Arteries (TGA). Consequently, the overall outcome of DORV is comparable to these defects.

However, in cases where the aorta is located at a considerable distance from the VSD, a more complex surgical approach is required. This involves creating a baffled pathway within the right ventricle to direct blood from the left ventricle through the VSD and into the aorta. Over time, these baffled pathways can become narrow, necessitating reoperation to address the obstruction.

It's important to note that the long-term outcome and potential complications of DORV are influenced by the specific anatomical features and surgical procedures performed. In cases where biventricular repair is not possible, univentricular palliation becomes necessary. This approach, although providing some degree of functional improvement, is associated with reduced overall outcome, long-term complications, and a lower life expectancy compared to biventricular repair.

Human Genetics of Tetralogy of Fallot and Double-Outlet Right Ventricle

36

Cornelia Dorn, Andreas Perrot, Marcel Grunert, and Silke Rickert-Sperling

Abstract

Tetralogy of Fallot (TOF) and double-outlet right ventricle (DORV) are conotruncal defects resulting from disturbances of the second heart field and the neural crest, which can occur as isolated malformations or as part of multiorgan syndromes. Their etiology is multifactorial and characterized by overlapping genetic causes. In this chapter, we present the different genetic alterations underlying the two diseases, which range from chromosomal abnormalities like aneuploidies and structural mutations to rare single nucleotide variations affecting distinct genes. For example, mutations in the cardiac transcription factors *NKX2–5*, *GATA4*, and *HAND2* have been identified in isolated TOF cases, while mutations of *TBX5* and 22q11 deletion, leading to haploinsufficiency of *TBX1*, cause Holt–Oram and DiGeorge syndrome, respectively. Moreover, genes involved in signaling pathways, laterality determination, and epigenetic mechanisms have also been found mutated in TOF and/or DORV patients. Finally, genome-wide association studies identified common single nucleotide polymorphisms associated with the risk for TOF.

Keywords

Tetralogy of Fallot · TOF · Double-outlet right ventricle · DORV · NKX2–5 · GATA4 · HAND2 · TBX5 · 22q11 deletion · TBX1 · Holt–Oram syndrome ·

C. Dorn · A. Perrot · S. Rickert-Sperling (✉)
Cardiovascular Genetics, Charité Universitätsmedizin Berlin, Berlin, Germany
e-mail: silke.sperling@charite.de

M. Grunert
Cardiovascular Genetics, Charité Universitätsmedizin Berlin, Berlin, Germany

DiNAQOR AG, Schlieren, Switzerland

© The Author(s), under exclusive license to Springer Nature Switzerland AG 2024

S. Rickert-Sperling et al. (eds.), *Congenital Heart Diseases: The Broken Heart*,
Advances in Experimental Medicine and Biology 1441,
https://doi.org/10.1007/978-3-031-44087-8_36

DiGeorge syndrome · Copy number variations · CNVs · Single nucleotide polymorphisms · SNPs · Down syndrome · Patau syndrome · Trisomy · Edwards syndrome · 22q11 deletion syndrome · Velocardiofacial syndrome · Cri du chat syndrome · Cat eye syndrome · Williams–Beuren syndrome · Jacobsen syndrome · JAG1 · FOG2 · Laterality defects · Heterotaxy · NOTCH2 · LEOPARD syndrome · CHARGE syndrome · Genome-wide association studies · CHD7 · GDF1 · CFC1

36.1 Introduction

Tetralogy of Fallot (TOF) is the most common form of cyanotic congenital heart disease (CHD) and affects about 0.28 children per 1,000 live births [1, 2], while double-outlet right ventricle (DORV) is diagnosed in approximately 0.03–0.09 of 1,000 live births [3]. Both malformations are conotruncal defects, which result from disturbances of the second heart field and the neural crest, and show overlapping genetic causes. The etiology of TOF is multifactorial, with about 25% of cases occurring in the context of chromosomal abnormalities and syndromic disorders [4]. Genetic causes for isolated TOF include rare single-gene defects, copy number variations (CNVs), as well as associations with common single nucleotide polymorphisms (SNPs). The majority of cases probably have a multigenic background, with individual combinations of risk alleles occurring in each patient [5, 6]. For DORV, the proportion of cases with chromosomal abnormalities is higher (>40%), and the majority of patients show additional extracardiac symptoms [3]. Furthermore, epigenetic and environmental factors including DNA methylation, exposure to teratogens, and insufficient folate supply can also impact on the etiology of cardiac malformations like TOF and DORV [7, 8].

36.2 Recurrence Risk in Affected Families

The genetic basis of CHD has been demonstrated by the study of affected families and by an increased recurrence risk in siblings and offspring of CHD patients. In 1972, one of the first large studies for TOF determined a recurrence risk of 1% for TOF and 2% for any form of CHD in the siblings of 100 index patients [9]. In 2014, a significant reduction in reproductive fitness was observed in a large cohort of 543 adult TOF patients. Moreover, the offspring had a recurrence risk of 4.8% for any form of CHD and of 2.3% for severe cardiac malformations [10]. Familial recurrence of DORV was reported in 5% (7/149) of cases [3]. Finally, both TOF and DORV have been demonstrated to be associated with parental consanguinity [11].

36.3 Chromosomal Abnormalities in TOF and DORV

36.3.1 Aneuploidies

Chromosomal aneuploidies were the first recognized genetic cause of CHD and represent a major pathogenic burden. Trisomy 21 (Down syndrome) is present in 5% of TOF cases, usually associated with atrioventricular canal defect [12, 13], and in 4% of DORV patients [3]. CHD is also a common feature of trisomy 13 (Patau syndrome), with more than 90% of patients affected by cardiac malformations (among them 11% DORV and 6% TOF) and trisomy 18 (Edwards syndrome) with 85% of patients with CHD (among them 13% DORV and 9% TOF) [14]. Moreover, TOF has been reported in several cases of monosomy X (Turner syndrome) [15], while DORV has been diagnosed in a patient with a 47, XYY genotype [16].

36.3.2 Chromosomal Structural Mutations

Besides numerical chromosomal changes, structural aberrations like deletions, duplications, and inversions play a major role in the etiology of CHD. 22q11 deletion syndrome (DiGeorge/velocardiofacial syndrome) is the most common cause of TOF and can be detected in up to 16% of patients [17]. Moreover, it is present in 7% of DORV cases [3]. The cardiac phenotype is caused by hemizygosity of the cardiac transcription factor T-box protein 1 (*TBX1*) [18], which has also been found to be mutated in affected patients without the 22q11 deletion [12, 19]. Another major cause of CHD are abnormalities of chromosome 8, which have been detected in 10% of DORV patients [3] and can also result in TOF [20]. Moreover, the malformations have been identified in cases of cri du chat syndrome (5p15.2 deletion, with TOF and DORV [21]), cat eye syndrome (22q11 inversion/duplication, with TOF [22]), Williams–Beuren syndrome (7q11.23 deletion, with TOF [23]), Jacobsen syndrome (11q terminal deletion, with TOF and DORV [24, 25]), and 1p36 deletion syndrome (with TOF [26]).

36.3.3 Copy Number Variations

Submicroscopic structural variations changing the genomic copy number (copy number variation, CNV) have been studied in several large cohorts of isolated TOF patients or broad panels of CHD cases using SNP arrays and whole exome sequencing. The estimated burden of rare de novo CNVs (5–10%) was significantly higher than in healthy controls [27–30]. Different gene prioritization approaches were used to identify novel candidate genes located in the CNV regions, and moreover, well-known CHD genes including jagged 1 (*JAG1*) [27], GATA-binding protein (*GATA*) *4* [28], and *TBX1* [27, 29] were found affected by copy number changes. Furthermore, a study of nearly 2,500 patients with CHD showed a strong association of 1q21.1 microduplications with sporadic isolated TOF, implicating the *GJA5* gene

encoding connexin 40 in the pathology of cardiac malformations [31]. In general, the overlap of CNVs identified in the patients is very low, demonstrating the genetic heterogeneity of TOF [32].

36.4 Single-Gene Defects

Over the last decades, more than 50 human genes involved in isolated or syndromic forms of CHD have been identified [6]. Most CHD gene mutations cause haploinsufficiency or a dosage reduction of the encoded protein, while mutations increasing gene activity or dosage are less common [8]. Genes playing a role in the pathogenesis of TOF and DORV encode cardiac transcription factors, components of signaling cascades, or other regulatory proteins such as epigenetic regulators. A detailed overview of the genes and studies can be found in Table 36.1. Here, we only list those genes for which a clear genetic diagnosis could be made in a patient with TOF or DORV. However, mutations in additional genes might be causative in the respective syndromic disorders.

36.4.1 Cardiac Transcription Factors

Cardiac development is a finely tuned process regulated by transcriptional networks that are governed by a core set of cardiac transcription factors, many of which are associated with isolated CHD [6]. The gene *NKX2–5* encoding the transcription factor NK2 homeobox 5 is found mutated in about 4% of TOF patients [87] and also rarely in DORV patients. Mutations in GATA4, which interacts with NKX2–5 at cardiac promoters, primarily cause septal defects [6, 87] but have also been identified in several cohorts of sporadic TOF patients as well as one study of familial TOF [88]. Moreover, mutations in TOF patients have also been reported for the *GATA6* gene [41] and *HAND2* encoding heart and neural crest derivatives expressed 2 protein [44], a downstream target of GATA4. The activity of GATA proteins is modulated by the FOG family of transcription factors and mutations in the zinc finger protein FOG family member 2 (*ZFPM2*/*FOG2*) have been found in various studies on TOF and DORV patients [61, 62]. Furthermore, T-box transcription factors also play an important role in cardiac developmental processes. Haploinsufficiency of *TBX1* is the primary cause of CHD in DiGeorge syndrome, and mutations in this gene have also been identified in patients without the 22q11 deletion [12, 19]. Furthermore, mutations in *TBX5* cause Holt–Oram syndrome, for which 20 cases with TOF have been described so far [56] and which can also present with DORV. ISL1 functions during cardiogenesis by transactivating MEF2C alone or together with TBX20 and loss-of-function mutations in *ISL1* have been identified in CHD patients [89], including DORV [47].

Table 36.1 Single-gene defects involved in isolated or syndromic TOF and/or DORV

Gene	Protein function	Phenotype	Status	References
Transcription factors and cofactors				
BCOR	Transcriptional corepressor	OFCD syndrome (with DORV)	2 or more independent reports	[33, 34]
FOXC1	Forkhead TF	TOF	2 or more patients	[35]
FOXC2	Forkhead TF	TOF	Single case report	[35]
FOXH1	Forkhead TF	TOF	2 or more patients	[36]
GATA4	GATA-binding TF	TOF	2 or more independent reports	[37–40]
GATA6	GATA-binding TF	TOF	2 or more independent reports	[41–43]
HAND2	Helix-loop-helix TF	TOF	2 or more independent reports	[35, 44]
HOXA1	Homeobox TF	BSAS (with TOF), ABDS (with TOF)	2 or more independent reports	[45, 46]
ISL1	Homeobox TF	DORV	Single case report	[47]
NKX2–5	Homeobox TF	TOF	2 or more independent reports	[12, 48–50]
		DORV, heterotaxy (with DORV)	2 or more independent reports	[49–51]
NKX2–6	Homeobox TF	TOF	Single case report	[52]
		DORV	Single case report	[52]
PITX2	Homeobox TF	DORV	Single case report	[53]
SALL4	Zinc finger TF	Okihiro syndrome (with TOF)	Single case report	[54]
TBX1	T-box TF	TOF, DiGeorge syndrome (with TOF)	2 or more independent reports	[12, 19, 35, 55]
TBX5	T-box TF	Holt–Oram syndrome (with TOF)	2 or more independent reports	[56, 57]
		Holt–Oram syndrome (with DORV)	Single case report	[58]
TBX20	T-box TF	TOF	Single case report	[59]
TFAP2B	AP-2 TF	TOF	Single case report	[60]
ZFMP2	Zink finger TF	TOF	2 or more independent reports	[61–63]

(continued)

Table 36.1 (continued)

Gene	Protein function	Phenotype	Status	References
		DORV	2 or more independent reports	[62–64]
ZIC3	Zink finger TF	DORV, heterotaxy (with DORV)	2 or more independent reports	[65, 66]
Genes involved in signaling pathways				
ACVR2B	Activin receptor	Heterotaxy (with DORV)	Single case report	[67]
ALDH1A2	Aldehyde dehydrogenase	TOF	2 or more patients	[68]
BRAF	Serine/threonine protein kinase	LEOPARD syndrome (with TOF)	Single case report	[69]
CFC1	Ligand (EGF family)	TOF	2 or more patients	[36]
		DORV	Single case report	[70]
FLT4	Tyrosine kinase	TOF	2 or more patients	[71–73]
GDF1	Ligand (BMP/TGF-beta family)	TOF	2 or more patients	[74]
		DORV	Single case report	[74]
JAG1	Notch ligand	TOF, Alagille syndrome (with TOF)	2 or more independent reports	[13, 75–78]
MAP2K1	MAP kinase kinase	CFC syndrome (with TOF)	Single case report	[79]
NODAL	Ligand (TGF-beta family)	TOF	2 or more patients	[80]
		DORV	2 or more independent reports	[80, 81]
NOTCH1	Notch receptor	TOF	2 or more patients	[71–73]
NOTCH2	Notch receptor	Alagille syndrome (with TOF)	Single case report	[82]
RAF1	Serine/threonine protein kinase	Noonan syndrome (with TOF)	Single case report	[83]
TDGF1	Coreceptor (TGF-beta signaling)	TOF	2 or more patients	[36]
Other genes				
CHD7	DNA helicase	CHARGE syndrome (with TOF)	2 or more patients	[84]
		CHARGE syndrome (with DORV)	2 or more patients	[84]

(continued)

Table 36.1 (continued)

Gene	Protein function	Phenotype	Status	References
GJA5	Gap junction protein	TOF	2 or more patients	[31]
NPHP4	Ciliary protein	DORV, heterotaxy (with DORV)	2 or more patients	[85]
SH3PXD2B	Adapter protein	FTHS (incl. DORV)	2 or more patients	[86]

Only those genes are listed, for which a clear genetic diagnosis was made in the respective case(s). *ABDS* Athabascan brainstem dysgenesis syndrome, *BSAS* Bosley–Salih–Alorainy syndrome, *CFC syndrome* cardiofasciocutaneous syndrome, *DORV* double-outlet right ventricle, *FTHS* Frank–Ter Haar syndrome, *OFCD syndrome* oculofasciocardiodental syndrome, *TF* transcription factor, *TOF* tetralogy of Fallot

36.4.2 Genes Associated with Laterality Determination

The bilateral symmetry of the developing embryo is first broken during cardiac development, and left-right patterning is established during early embryogenesis by the interplay of different signaling pathways and by the action of nodal cilia [6]. Components of the Nodal signaling pathway are critical in determining organ laterality, and disruption of these genes causes a wide variety of cardiac malformations, often associated with laterality defects [6]. Many DORV patients show laterality defects such as heterotaxy, and a number of mutations have been identified in the Nodal pathway [3]. Nodal growth differentiation factor (*NODAL*) mutations were reported in two studies on DORV patients and could also be identified in TOF patients [80]. The *CFC1* gene, encoding the CRYPTIC protein (a co-receptor in Nodal signaling), was found to be mutated in isolated TOF and DORV cases. Moreover, non-synonymous variants that could act as susceptibility alleles were identified in patients with DORV and heterotaxy [90, 91]. Further genes encoding signaling molecules of the Nodal pathway that have been found mutated in DORV and/or TOF patients are growth differentiation factor 1 (*GDF1*), teratocarcinoma-derived growth factor 1 (*TDGF1*), and activin A receptor, type IIB (*ACVR2B*). Furthermore, mutations in the transcription factors Zic family member 3 (*ZIC3*; acting upstream of Nodal signaling) and forkhead box H1 (*FOXH1*; a possible link between the BMP and Nodal pathways) could be found in several DORV and TOF patients, respectively [36, 65]. Finally, the cilia-related gene *NPHP4* encoding nephronophthisis 4 protein was identified in a linkage analysis of a consanguineous family with laterality defects and DORV and was subsequently found mutated in further DORV patients [85].

36.4.3 Genes Involved in Signaling Pathways

Several signaling pathways are involved in the coordination of cardiac development, and mutations of signaling molecules have been identified in isolated and syndromic

forms of CHD [6, 8]. Notch signaling is required for patterning of the cardiac chambers and valves and moreover regulates cardiomyocyte proliferation and differentiation [92]. Mutations in the Notch ligand gene *JAG1* cause the multisystem disorder Alagille syndrome (AGS), which includes CHD in about 90% of patients [6]. Approximately 10% of AGS patients present with TOF [75], and moreover, *JAG1* mutations have also been identified in isolated TOF cases [76] and in one study on familial TOF [77]. Interestingly, a *JAG1* mutation also was found in a patient with DiGeorge syndrome and TOF, indicating that it might act as a modifier of the phenotype [93]. About 1% of AGS cases are caused by mutations in *NOTCH2* [6], which has been shown for one TOF patient so far. Large-scale sequencing studies revealed a negative effect of mutations in *NOTCH1* on the Notch signaling pathway in TOF patients. In addition to *NOTCH1*, *FLT4* mutations account for 2.3–2.4% of TOF [71–73]. *FLT4* encodes a receptor tyrosine kinase known as vascular endothelial growth factor (VEGF) expressed in lymphatics and the vasculature. Mutations in the rat sarcoma viral oncogene homolog/mitogen-activated protein kinase (Ras/MAPK) pathway, which regulates cell proliferation, differentiation, and survival, cause Noonan syndrome (NS) and other distinct but overlapping syndromes. NS presents with TOF in about 4% of patients [8, 94], and a microduplication encompassing v-raf-1 murine leukemia viral oncogene homolog 1 (*RAF1*) has been identified in a patient with NS phenotype including TOF [83]. Moreover, mitogen-activated protein kinase kinase 1 (*MAP 2 K1*) and v-raf murine sarcoma viral oncogene homolog B (*BRAF*) mutations were reported in one TOF patient with cardiofasciocutaneous syndrome and one with LEOPARD syndrome, respectively. Finally, retinoic acid (RA) signaling is both a regulator and target of TBX1, thus playing a role in pharyngeal arch development [6]. Mutations in *ALDH1A2*, encoding an aldehyde dehydrogenase involved in RA signaling, were identified in two non-syndromic TOF patients.

36.4.4 Epigenetic Regulators

Epigenetic mechanisms represent an important layer of transcriptional regulation and play a central role in cardiac development [95]. Mutations in the *CHD7* gene, encoding chromodomain helicase DNA-binding protein 7 whose binding correlates with H3K4 methylation, cause CHARGE syndrome. Cardiac malformations occur in 75–80% of the patients, with TOF being the most common defect. Moreover, DORV with atrioventricular canal is also frequently seen in CHARGE patients [84, 96]. Furthermore, an enrichment of de novo mutations in histone-modifying enzymes could recently be demonstrated in a large CHD cohort including TOF and DORV patients and their parents [97]. Recent studies on monozygotic twins discordant for TOF and DORV showed epigenetic alterations given by DNA methylation changes in regulatory regions of cardiac-relevant genes [98, 99].

36.5 Oligogenic Defects

The majority of TOF cases are isolated, non-syndromic cases—the precise causes of which are yet to be discovered. This is true for the majority of CHDs and many serious non-Mendelian diseases with a clear genetic component. It has been assumed that CHDs might also be caused by rare autosomal recessive variations in concert with private variations [8, 100], which might individually show minor functional impairment but in combination could be disease causing [101]. In this concept, multiple mutations in different genes can lead to disturbances of a molecular network that result in a common phenotypic expression. TOF was the first CHD for which this concept was discovered to be correct [5]. Rare and private mutations in neural crest, apoptotic, and sarcomeric genes were shown to define the genetic background of isolated, non-syndromic TOF (see Fig. 36.1). A great challenge, however, is the discrimination of causative genes. This challenge was successfully addressed using a burden analysis approach named GMF (gene mutation frequency), which considers

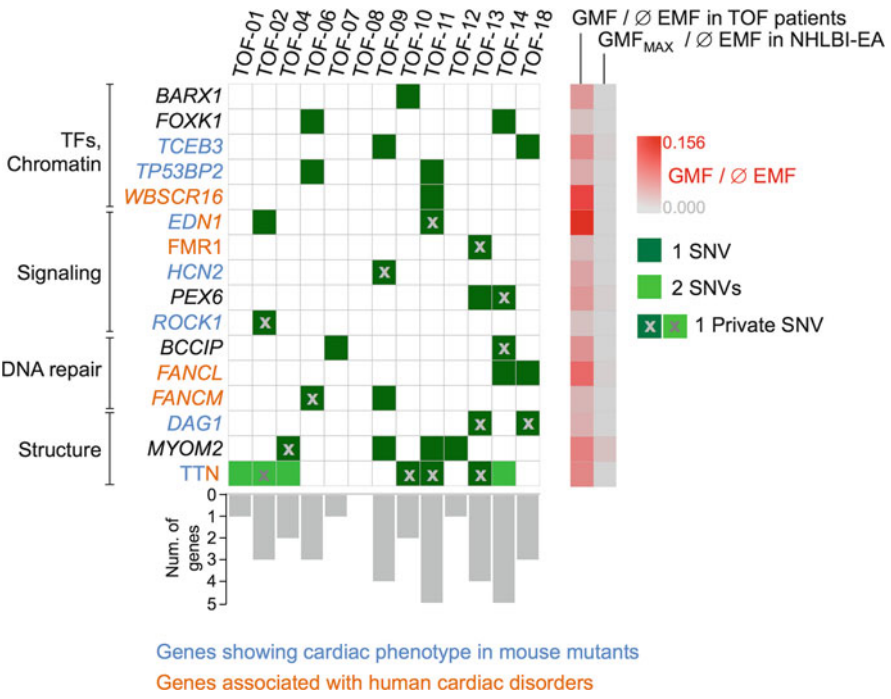

Fig. 36.1 Distribution of mutations found in 16 significantly affected genes ($P > 0.05$) in TOF patients. Private mutations are marked by "*x*." Gene-wise frequencies of mutations are represented by *gray bars*. Gene mutation frequency (GMF) in TOF cases and European-American controls (NHLBI-EA) are indicated by a gray-to-red gradient. For titin (TTN), the average exon-mutation frequency (EMF) over all significantly over-mutated exons is given. *EMF* exon mutation frequency, *GMF* gene mutation frequency, *SNV* single nucleotide variation (adapted from Grunert et al. [5])

the frequency at which a gene is affected by selected deleterious variations in a cohort [5]. Interestingly, besides known developmental genes, cardiomyopathy genes have been confirmed to form part of the genetic basis of TOF. This discovery harbors the possibility that the genetic background of TOF might be correlated to its clinical long-term outcome. The concept of burden analysis was further used in large-scale sequencing projects with thousands of CHD patients [71–73].

36.6 Associations with Common Variations

Besides rare damaging mutations in cardiac regulators and signaling pathways, common SNPs have also been found associated with CHD in several genome-wide association studies (GWAS). Two associated loci (12q24 and 13q32) could be identified in a two-stage study of more than 1,600 TOF patients, demonstrating that common genetic variation influences the risk of TOF [102]. However, the majority of CHD-associated variants are individually unique, which results in allelic heterogeneity and reduces the power of GWAS for CHD [103].

36.7 Conclusion

Huge advances have been made in understanding the etiology of congenital heart malformations. However, the underlying causes for the majority of CHDs still remain unclear. Estimates suggest that 80% of cardiac malformations are caused by the interaction of various genetic, epigenetic, and environmental factors [104], which complicates studies aiming to identify single contributors. About 25% of TOF patients have chromosomal abnormalities such as trisomy 21 or 22q11 deletion, while the majority are isolated cases caused by mutations in cardiac transcription factors, signaling pathways, or most likely combinations of different genes. For DORV, the proportion of patients with chromosomal abnormalities is higher. Moreover, the malformation often occurs in combination with laterality defects like heterotaxy, which is also reflected by the high number of DORV-associated genes playing a role in laterality determination. Taken together, further studies will be required for a deeper understanding of CHD etiology, which will hopefully offer novel preventive and therapeutic strategies and help to improve genetic counseling for affected families.

References

1. Ferencz C, Rubin JD, McCarter RJ, Brenner JI, Neill CA, Perry LW, et al. Congenital heart disease: prevalence at livebirth. The Baltimore-Washington Infant Study. Am J Epidemiol. 1985;121(1):31–6.
2. Apitz C, Webb GD, Redington AN. Tetralogy of Fallot. Lancet. 2009;374(9699):1462–71.
3. Obler D, Juraszek AL, Smoot LB, Natowicz MR. Double outlet right ventricle: aetiologies and associations. J Med Genet. 2008;45(8):481–97.

4. Villafane J, Feinstein JA, Jenkins KJ, Vincent RN, Walsh EP, Dubin AM, et al. Hot topics in tetralogy of Fallot. J Am Coll Cardiol. 2013;62(23):2155–66.
5. Grunert M, Dorn C, Schueler M, Dunkel I, Schlesinger J, Mebus S, et al. Rare and private variations in neural crest, apoptosis and sarcomere genes define the polygenic background of isolated tetralogy of Fallot. Hum Mol Genet. 2014;23(12):3115–28.
6. Andersen TA, Troelsen Kde L, Larsen LA. Of mice and men: molecular genetics of congenital heart disease. Cell Mol Life Sci. 2014;71(8):1327–52.
7. Sheng W, Qian Y, Zhang P, Wu Y, Wang H, Ma X, et al. Association of promoter methylation statuses of congenital heart defect candidate genes with tetralogy of Fallot. J Transl Med. 2014;12:31.
8. Fahed AC, Gelb BD, Seidman JG, Seidman CE. Genetics of congenital heart disease: the glass half empty. Circ Res. 2013;112(4):707–20.
9. Boon AR, Farmer MB, Roberts DF. A family study of Fallot's tetralogy. J Med Genet. 1972;9 (2):179–92.
10. Chin-Yee NJ, Costain G, Swaby JA, Silversides CK, Bassett AS. Reproductive fitness and genetic transmission of tetralogy of Fallot in the molecular age. Circ Cardiovasc Genet. 2014;7 (2):102–9.
11. Nabulsi MM, Tamim H, Sabbagh M, Obeid MY, Yunis KA, Bitar FF. Parental consanguinity and congenital heart malformations in a developing country. Am J Med Genet A. 2003;116A (4):342–7.
12. Rauch R, Hofbeck M, Zweier C, Koch A, Zink S, Trautmann U, et al. Comprehensive genotype-phenotype analysis in 230 patients with tetralogy of Fallot. J Med Genet. 2010;47 (5):321–31.
13. Vergara P, Digilio MC, De Zorzi A, Di Carlo D, Capolino R, Rimini A, et al. Genetic heterogeneity and phenotypic anomalies in children with atrioventricular canal defect and tetralogy of Fallot. Clin Dysmorphol. 2006;15(2):65–70.
14. Maeda J, Yamagishi H, Furutani Y, Kamisago M, Waragai T, Oana S, et al. The impact of cardiac surgery in patients with trisomy 18 and trisomy 13 in Japan. Am J Med Genet A. 2011;155A(11):2641–6.
15. Papp C, Beke A, Mezei G, Szigeti Z, Ban Z, Papp Z. Prenatal diagnosis of turner syndrome: report on 69 cases. J Ultrasound Med. 2006;25(6):711–7. quiz 8–20
16. Kim N, Friedberg MK, Silverman NH. Diagnosis and prognosis of fetuses with double outlet right ventricle. Prenat Diagn. 2006;26(8):740–5.
17. Goldmuntz E, Clark BJ, Mitchell LE, Jawad AF, Cuneo BF, Reed L, et al. Frequency of 22q11 deletions in patients with conotruncal defects. J Am Coll Cardiol. 1998;32(2):492–8.
18. Merscher S, Funke B, Epstein JA, Heyer J, Puech A, Lu MM, et al. TBX1 is responsible for cardiovascular defects in velo-cardio-facial/DiGeorge syndrome. Cell. 2001;104(4):619–29.
19. Yagi H, Furutani Y, Hamada H, Sasaki T, Asakawa S, Minoshima S, et al. Role of TBX1 in human del22q11.2 syndrome. Lancet. 2003;362(9393):1366–73.
20. Wat MJ, Shchelochkov OA, Holder AM, Breman AM, Dagli A, Bacino C, et al. Chromosome 8p23.1 deletions as a cause of complex congenital heart defects and diaphragmatic hernia. Am J Med Genet A. 2009;149A(8):1661–77.
21. Hills C, Moller JH, Finkelstein M, Lohr J, Schimmenti L. Cri du chat syndrome and congenital heart disease: a review of previously reported cases and presentation of an additional 21 cases from the pediatric cardiac care consortium. Pediatrics. 2006;117(5):e924–7.
22. Rosa RF, Mombach R, Zen PR, Graziadio C, Paskulin GA. Clinical characteristics of a sample of patients with cat eye syndrome. Rev Assoc Med Bras (1992). 2010;56(4):462–5.
23. Del Pasqua A, Rinelli G, Toscano A, Iacobelli R, Digilio C, Marino B, et al. New findings concerning cardiovascular manifestations emerging from long-term follow-up of 150 patients with the Williams-Beuren-Beuren syndrome. Cardiol Young. 2009;19(6):563–7.
24. Podraza J, Fleenor J, Grossfeld P. An 11q terminal deletion and tetralogy of Fallot. Am J Med Genet A. 2007;143A(10):1126–8.

25. Grossfeld PD, Mattina T, Lai Z, Favier R, Jones KL, Cotter F, et al. The 11q terminal deletion disorder: a prospective study of 110 cases. Am J Med Genet A. 2004;129A(1):51–61.
26. Battaglia A, Hoyme HE, Dallapiccola B, Zackai E, Hudgins L, McDonald-McGinn D, et al. Further delineation of deletion 1p36 syndrome in 60 patients: a recognizable phenotype and common cause of developmental delay and mental retardation. Pediatrics. 2008;121(2): 404–10.
27. Greenway SC, Pereira AC, Lin JC, DePalma SR, Israel SJ, Mesquita SM, et al. De novo copy number variants identify new genes and loci in isolated sporadic tetralogy of Fallot. Nat Genet. 2009;41(8):931–5.
28. Soemedi R, Wilson IJ, Bentham J, Darlay R, Topf A, Zelenika D, et al. Contribution of global rare copy-number variants to the risk of sporadic congenital heart disease. Am J Hum Genet. 2012;91(3):489–501.
29. Silversides CK, Lionel AC, Costain G, Merico D, Migita O, Liu B, et al. Rare copy number variations in adults with tetralogy of Fallot implicate novel risk gene pathways. PLoS Genet. 2012;8(8):e1002843.
30. Glessner JT, Bick AG, Ito K, Homsy J, Rodriguez-Murillo L, Fromer M, et al. Increased frequency of de novo copy number variants in congenital heart disease by integrative analysis of single nucleotide polymorphism array and exome sequence data. Circ Res. 2014;115(10): 884–96.
31. Soemedi R, Topf A, Wilson IJ, Darlay R, Rahman T, Glen E, et al. Phenotype-specific effect of chromosome 1q21.1 rearrangements and GJA5 duplications in 2436 congenital heart disease patients and 6760 controls. Hum Mol Genet. 2012;21(7):1513–20.
32. Bansal V, Dorn C, Grunert M, Klaassen S, Hetzer R, Berger F, et al. Outlier-based identification of copy number variations using targeted resequencing in a small cohort of patients with tetralogy of Fallot. PLoS One. 2014;9(1):e85375.
33. Hilton E, Johnston J, Whalen S, Okamoto N, Hatsukawa Y, Nishio J, et al. BCOR analysis in patients with OFCD and Lenz microphthalmia syndromes, mental retardation with ocular anomalies, and cardiac laterality defects. Eur J Hum Genet. 2009;17(10):1325–35.
34. Ng D, Thakker N, Corcoran CM, Donnai D, Perveen R, Schneider A, et al. Oculofaciocardiodental and Lenz microphthalmia syndromes result from distinct classes of mutations in BCOR. Nat Genet. 2004;36(4):411–6.
35. Topf A, Griffin HR, Glen E, Soemedi R, Brown DL, Hall D, et al. Functionally significant, rare transcription factor variants in tetralogy of Fallot. PLoS One. 2014;9(8):e95453.
36. Roessler E, Ouspenskaia MV, Karkera JD, Velez JI, Kantipong A, Lacbawan F, et al. Reduced NODAL signaling strength via mutation of several pathway members including FOXH1 is linked to human heart defects and holoprosencephaly. Am J Hum Genet. 2008;83(1):18–29.
37. Nemer G, Fadlalah F, Usta J, Nemer M, Dbaibo G, Obeid M, et al. A novel mutation in the GATA4 gene in patients with tetralogy of Fallot. Hum Mutat. 2006;27(3):293–4.
38. Tomita-Mitchell A, Maslen CL, Morris CD, Garg V, Goldmuntz E. GATA4 sequence variants in patients with congenital heart disease. J Med Genet. 2007;44(12):779–83.
39. Peng T, Wang L, Zhou SF, Li X. Mutations of the GATA4 and NKX2.5 genes in Chinese pediatric patients with non-familial congenital heart disease. Genetica. 2010;138(11–12): 1231–40.
40. Zhang WM, Li XF, Ma ZY, Zhang J, Zhou SH, Li T, et al. GATA4 and NKX2.5 gene analysis in Chinese Uygur patients with congenital heart disease. Chin Med J. 2009;122(4):416–9.
41. Maitra M, Koenig SN, Srivastava D, Garg V. Identification of GATA6 sequence variants in patients with congenital heart defects. Pediatr Res. 2010;68(4):281–5.
42. Lin X, Huo Z, Liu X, Zhang Y, Li L, Zhao H, et al. A novel GATA6 mutation in patients with tetralogy of Fallot or atrial septal defect. J Hum Genet. 2010;55(10):662–7.
43. Wang J, Luo XJ, Xin YF, Liu Y, Liu ZM, Wang Q, et al. Novel GATA6 mutations associated with congenital ventricular septal defect or tetralogy of fallot. DNA Cell Biol. 2012;31(11): 1610–7.

44. Shen L, Li XF, Shen AD, Wang Q, Liu CX, Guo YJ, et al. Transcription factor HAND2 mutations in sporadic Chinese patients with congenital heart disease. Chin Med J. 2010;123 (13):1623–7.
45. Tischfield MA, Bosley TM, Salih MA, Alorainy IA, Sener EC, Nester MJ, et al. Homozygous HOXA1 mutations disrupt human brainstem, inner ear, cardiovascular and cognitive development. Nat Genet. 2005;37(10):1035–7.
46. Holve S, Friedman B, Hoyme HE, Tarby TJ, Johnstone SJ, Erickson RP, et al. Athabascan brainstem dysgenesis syndrome. Am J Med Genet A. 2003;120A(2):169–73.
47. Wang Z, Song HM, Wang F, Zhao CM, Huang RT, Xue S, et al. A new ISL1 loss-of-function mutation predisposes to congenital double outlet right ventricle. Int Heart J. 2019;60(5): 1113–22.
48. Goldmuntz E, Geiger E, Benson DW. NKX2.5 mutations in patients with tetralogy of fallot. Circulation. 2001;104(21):2565–8.
49. McElhinney DB, Geiger E, Blinder J, Benson DW, Goldmuntz E. NKX2.5 mutations in patients with congenital heart disease. J Am Coll Cardiol. 2003;42(9):1650–5.
50. Benson DW, Silberbach GM, Kavanaugh-McHugh A, Cottrill C, Zhang Y, Riggs S, et al. Mutations in the cardiac transcription factor NKX2.5 affect diverse cardiac developmental pathways. J Clin Invest. 1999;104(11):1567–73.
51. Izumi K, Noon S, Wilkens A, Krantz ID. NKX2.5 mutation identification on exome sequencing in a patient with heterotaxy. Eur J Med Genet. 2014;57(10):558–61.
52. Zhao L, Ni SH, Liu XY, Wei D, Yuan F, Xu L, et al. Prevalence and spectrum of Nkx2.6 mutations in patients with congenital heart disease. Eur J Med Genet. 2014;57(10):579–86.
53. Wang J, Xin YF, Xu WJ, Liu ZM, Qiu XB, Qu XK, et al. Prevalence and spectrum of PITX2c mutations associated with congenital heart disease. DNA Cell Biol. 2013;32(12):708–16.
54. Borozdin W, Wright MJ, Hennekam RC, Hannibal MC, Crow YJ, Neumann TE, et al. Novel mutations in the gene SALL4 provide further evidence for acro-renal-ocular and Okihiro syndromes being allelic entities, and extend the phenotypic spectrum. J Med Genet. 2004;41 (8):e102.
55. Paylor R, Glaser B, Mupo A, Ataliotis P, Spencer C, Sobotka A, et al. Tbx1 haploinsufficiency is linked to behavioral disorders in mice and humans: implications for 22q11 deletion syndrome. Proc Natl Acad Sci U S A. 2006;103(20):7729–34.
56. Baban A, Postma AV, Marini M, Trocchio G, Santilli A, Pelegrini M, et al. Identification of TBX5 mutations in a series of 94 patients with tetralogy of Fallot. Am J Med Genet A. 2014;164A(12):3100–7.
57. McDermott DA, Bressan MC, He J, Lee JS, Aftimos S, Brueckner M, et al. TBX5 genetic testing validates strict clinical criteria for Holt-Oram syndrome. Pediatr Res. 2005;58(5): 981–6.
58. Brassington AM, Sung SS, Toydemir RM, Le T, Roeder AD, Rutherford AE, et al. Expressivity of Holt-Oram syndrome is not predicted by TBX5 genotype. Am J Hum Genet. 2003;73 (1):74–85.
59. Liu C, Shen A, Li X, Jiao W, Zhang X, Li Z. T-box transcription factor TBX20 mutations in Chinese patients with congenital heart disease. Eur J Med Genet. 2008;51(6):580–7.
60. Xiong F, Li Q, Zhang C, Chen Y, Li P, Wei X, et al. Analyses of GATA4, NKX2.5, and TFAP2B genes in subjects from southern China with sporadic congenital heart disease. Cardiovasc Pathol. 2013;22(2):141–5.
61. Pizzuti A, Sarkozy A, Newton AL, Conti E, Flex E, Digilio MC, et al. Mutations of ZFPM2/ FOG2 gene in sporadic cases of tetralogy of Fallot. Hum Mutat. 2003;22(5):372–7.
62. De Luca A, Sarkozy A, Ferese R, Consoli F, Lepri F, Dentici ML, et al. New mutations in ZFPM2/FOG2 gene in tetralogy of Fallot and double outlet right ventricle. Clin Genet. 2011;80(2):184–90.
63. Huang X, Niu W, Zhang Z, Zhou C, Xu Z, Liu J, et al. Identification of novel significant variants of ZFPM2/FOG2 in non-syndromic tetralogy of Fallot and double outlet right ventricle in a Chinese Han population. Mol Biol Rep. 2014;41(4):2671–7.

64. Tan ZP, Huang C, Xu ZB, Yang JF, Yang YF. Novel ZFPM2/FOG2 variants in patients with double outlet right ventricle. Clin Genet. 2012;82(5):466–71.
65. Ware SM, Peng J, Zhu L, Fernbach S, Colicos S, Casey B, et al. Identification and functional analysis of ZIC3 mutations in heterotaxy and related congenital heart defects. Am J Hum Genet. 2004;74(1):93–105.
66. D'Alessandro LC, Latney BC, Paluru PC, Goldmuntz E. The phenotypic spectrum of ZIC3 mutations includes isolated d-transposition of the great arteries and double outlet right ventricle. Am J Med Genet A. 2013;161A(4):792–802.
67. Kosaki R, Gebbia M, Kosaki K, Lewin M, Bowers P, Towbin JA, et al. Left-right axis malformations associated with mutations in ACVR2B, the gene for human activin receptor type IIB. Am J Med Genet. 1999;82(1):70–6.
68. Pavan M, Ruiz VF, Silva FA, Sobreira TJ, Cravo RM, Vasconcelos M, et al. ALDH1A2 (RALDH2) genetic variation in human congenital heart disease. BMC Med Genet. 2009;10: 113.
69. Koudova M, Seemanova E, Zenker M. Novel BRAF mutation in a patient with LEOPARD syndrome and normal intelligence. Eur J Med Genet. 2009;52(5):337–40.
70. Goldmuntz E, Bamford R, Karkera JD, dela Cruz J, Roessler E, Muenke M. CFC1 mutations in patients with transposition of the great arteries and double-outlet right ventricle. Am J Hum Genet. 2002;70(3):776–80.
71. Jin SC, Homsy J, Zaidi S, Lu Q, Morton S, DePalma SR, et al. Contribution of rare inherited and de novo variants in 2,871 congenital heart disease probands. Nat Genet. 2017;49(11): 1593–601.
72. Page DJ, Miossec MJ, Williams SG, Monaghan RM, Fotiou E, Cordell HJ, et al. Whole exome sequencing reveals the major genetic contributors to nonsyndromic tetralogy of Fallot. Circ Res. 2019;124(4):553–63.
73. Manshaei R, Merico D, Reuter MS, Engchuan W, Mojarad BA, Chaturvedi R, et al. Genes and pathways implicated in tetralogy of Fallot revealed by ultra-rare variant burden analysis in 231 genome sequences. Front Genet. 2020;11:957.
74. Karkera JD, Lee JS, Roessler E, Banerjee-Basu S, Ouspenskaia MV, Mez J, et al. Loss-of-function mutations in growth differentiation factor-1 (GDF1) are associated with congenital heart defects in humans. Am J Hum Genet. 2007;81(5):987–94.
75. McElhinney DB, Krantz ID, Bason L, Piccoli DA, Emerick KM, Spinner NB, et al. Analysis of cardiovascular phenotype and genotype-phenotype correlation in individuals with a JAG1 mutation and/or Alagille syndrome. Circulation. 2002;106(20):2567–74.
76. Kola S, Koneti NR, Golla JP, Akka J, Gundimeda SD, Mundluru HP. Mutational analysis of JAG1 gene in non-syndromic tetralogy of Fallot children. Clin Chim Acta. 2011;412(23–24): 2232–6.
77. Eldadah ZA, Hamosh A, Biery NJ, Montgomery RA, Duke M, Elkins R, et al. Familial tetralogy of Fallot caused by mutation in the jagged1 gene. Hum Mol Genet. 2001;10(2): 163–9.
78. Bauer RC, Laney AO, Smith R, Gerfen J, Morrissette JJ, Woyciechowski S, et al. Jagged1 (JAG1) mutations in patients with tetralogy of Fallot or pulmonic stenosis. Hum Mutat. 2010;31(5):594–601.
79. Dentici ML, Sarkozy A, Pantaleoni F, Carta C, Lepri F, Ferese R, et al. Spectrum of MEK1 and MEK2 gene mutations in cardio-facio-cutaneous syndrome and genotype-phenotype correlations. Eur J Hum Genet. 2009;17(6):733–40.
80. Roessler E, Pei W, Ouspenskaia MV, Karkera JD, Velez JI, Banerjee-Basu S, et al. Cumulative ligand activity of NODAL mutations and modifiers are linked to human heart defects and holoprosencephaly. Mol Genet Metab. 2009;98(1–2):225–34.
81. Mohapatra B, Casey B, Li H, Ho-Dawson T, Smith L, Fernbach SD, et al. Identification and functional characterization of NODAL rare variants in heterotaxy and isolated cardiovascular malformations. Hum Mol Genet. 2009;18(5):861–71.

82. McDaniell R, Warthen DM, Sanchez-Lara PA, Pai A, Krantz ID, Piccoli DA, et al. NOTCH2 mutations cause Alagille syndrome, a heterogeneous disorder of the NOTCH signaling pathway. Am J Hum Genet. 2006;79(1):169–73.
83. Luo C, Yang YF, Yin BL, Chen JL, Huang C, Zhang WZ, et al. Microduplication of 3p25.2 encompassing RAF1 associated with congenital heart disease suggestive of Noonan syndrome. Am J Med Genet A. 2012;158A(8):1918–23.
84. Jongmans MC, Admiraal RJ, van der Donk KP, Vissers LE, Baas AF, Kapusta L, et al. CHARGE syndrome: the phenotypic spectrum of mutations in the CHD7 gene. J Med Genet. 2006;43(4):306–14.
85. French VM, van de Laar IM, Wessels MW, Rohe C, Roos-Hesselink JW, Wang G, et al. NPHP4 variants are associated with pleiotropic heart malformations. Circ Res. 2012;110(12):1564–74.
86. Iqbal Z, Cejudo-Martin P, de Brouwer A, van der Zwaag B, Ruiz-Lozano P, Scimia MC, et al. Disruption of the podosome adaptor protein TKS4 (SH3PXD2B) causes the skeletal dysplasia, eye, and cardiac abnormalities of Frank-Ter Haar syndrome. Am J Hum Genet. 2010;86(2):254–61.
87. Di Felice V, Zummo G. Tetralogy of fallot as a model to study cardiac progenitor cell migration and differentiation during heart development. Trends Cardiovasc Med. 2009;19(4):130–5.
88. Yang YQ, Gharibeh L, Li RG, Xin YF, Wang J, Liu ZM, et al. GATA4 loss-of-function mutations underlie familial tetralogy of fallot. Hum Mutat. 2013;34(12):1662–71.
89. Ma L, Wang J, Li L, Qiao Q, Di RM, Li XM, et al. ISL1 loss-of-function mutation contributes to congenital heart defects. Heart Vessel. 2019;34(4):658–68.
90. Bamford RN, Roessler E, Burdine RD, Saplakoglu U, dela Cruz J, Splitt M, et al. Loss-of-function mutations in the EGF-CFC gene CFC1 are associated with human left-right laterality defects. Nat Genet. 2000;26(3):365–9.
91. Selamet Tierney ES, Marans Z, Rutkin MB, Chung WK. Variants of the CFC1 gene in patients with laterality defects associated with congenital cardiac disease. Cardiol Young. 2007;17(3):268–74.
92. de la Pompa JL, Epstein JA. Coordinating tissue interactions: notch signaling in cardiac development and disease. Dev Cell. 2012;22(2):244–54.
93. Digilio MC, Luca AD, Lepri F, Guida V, Ferese R, Dentici ML, et al. JAG1 mutation in a patient with deletion 22q11.2 syndrome and tetralogy of Fallot. Am J Med Genet A. 2013;161A(12):3133–6.
94. Marino B, Digilio MC, Toscano A, Giannotti A, Dallapiccola B. Congenital heart diseases in children with Noonan syndrome: an expanded cardiac spectrum with high prevalence of atrioventricular canal. J Pediatr. 1999;135(6):703–6.
95. Chang CP, Bruneau BG. Epigenetics and cardiovascular development. Annu Rev Physiol. 2012;74:41–68.
96. Blake KD, Prasad C. CHARGE syndrome. Orphanet J Rare Dis. 2006;1:34.
97. Zaidi S, Choi M, Wakimoto H, Ma L, Jiang J, Overton JD, et al. De novo mutations in histone-modifying genes in congenital heart disease. Nature. 2013;498(7453):220–3.
98. Grunert M, Appelt S, Grossfeld P, Sperling SR. The needle in the haystack-searching for genetic and epigenetic differences in monozygotic twins discordant for tetralogy of Fallot. J Cardiovasc Dev Dis. 2020;7(4)
99. Lyu G, Zhang C, Ling T, Liu R, Zong L, Guan Y, et al. Genome and epigenome analysis of monozygotic twins discordant for congenital heart disease. BMC Genomics. 2018;19(1):428.
100. Sperling SR. Systems biology approaches to heart development and congenital heart disease. Cardiovasc Res. 2011;91(2):269–78.
101. Cohen JC, Kiss RS, Pertsemlidis A, Marcel YL, McPherson R, Hobbs HH. Multiple rare alleles contribute to low plasma levels of HDL cholesterol. Science. 2004;305(5685):869–72.

102. Cordell HJ, Topf A, Mamasoula C, Postma AV, Bentham J, Zelenika D, et al. Genome-wide association study identifies loci on 12q24 and 13q32 associated with tetralogy of Fallot. Hum Mol Genet. 2013;22(7):1473–81.
103. Bentham J, Bhattacharya S. Genetic mechanisms controlling cardiovascular development. Ann N Y Acad Sci. 2008;1123:10–9.
104. Blue GM, Kirk EP, Sholler GF, Harvey RP, Winlaw DS. Congenital heart disease: current knowledge about causes and inheritance. Med J Aust. 2012;197(3):155–9.

Molecular Pathways and Animal Models of Tetralogy of Fallot and Double Outlet Right Ventricle

37

Robert G. Kelly

Abstract

Tetralogy of Fallot and double-outlet right ventricle are outflow tract (OFT) alignment defects situated on a continuous disease spectrum. A myriad of upstream causes can impact on ventriculoarterial alignment that can be summarized as defects in either i) OFT elongation during looping morphogenesis or ii) OFT remodeling during cardiac septation. Embryological processes underlying these two developmental steps include deployment of second heart field cardiac progenitor cells, establishment and transmission of embryonic left/right information driving OFT rotation and OFT cushion and valve morphogenesis. The formation and remodeling of pulmonary trunk infundibular myocardium is a critical component of both steps. Defects in myocardial, endocardial, or neural crest cell lineages can result in alignment defects, reflecting the complex intercellular signaling events that coordinate arterial pole development. Importantly, however, OFT alignment is mechanistically distinct from neural crest-driven OFT septation, although neural crest cells impact indirectly on alignment through their role in modulating signaling during SHF development. As yet poorly understood nongenetic causes of alignment defects that impact the above processes include hemodynamic changes, maternal exposure to environmental teratogens, and stochastic events. The heterogeneity of causes converging on alignment defects characterizes the OFT as a hotspot of congenital heart defects.

R. G. Kelly (✉)
Aix Marseille Université, Institut de Biologie du Dévelopment de Marseille, Marseille, France
e-mail: Robert.Kelly@univ-amu.fr

© The Author(s), under exclusive license to Springer Nature Switzerland AG 2024

S. Rickert-Sperling et al. (eds.), *Congenital Heart Diseases: The Broken Heart*,
Advances in Experimental Medicine and Biology 1441,
https://doi.org/10.1007/978-3-031-44087-8_37

37.1 Introduction

Division of the embryonic outflow tract (OFT) during cardiac septation creates an exclusive connection between the ascending aorta and left ventricle that is essential to isolate the pulmonary and systemic circulatory systems at birth. Tetralogy of Fallot (TOF) and double-outlet right ventricle (DORV) are OFT (or conotruncal) congenital heart defects (CHDs) resulting from defects in correct alignment of the ascending aorta and pulmonary trunk with the left and right ventricles. In the unseptated embryonic heart, the OFT is aligned with the future right ventricle. Subsequent remodeling events associated with cardiac septation, including rotation of the dividing OFT, cushion and valve morphogenesis, regional cell death and a leftward shift of the OFT, align the ascending aorta and pulmonary trunk and with the left and right ventricles to create independent left and right ventriculoarterial connections. Defects in initial elongation of the OFT, by addition of myocardial progenitor cells from the second heart field (SHF), that creates the template for OFT division, and/or in subsequent remodeling events, lead to a failure of the ascending aorta to make an exclusive connection with the left ventricle (Fig. 37.1). Thus defects in a wide range of underlying morphogenetic processes converge on alignment defects. These processes include progenitor cell specification and deployment, embryonic laterality pathways, cushion morphogenesis and epithelial to mesenchymal transition (EMT), planar cell polarity and nongenetic factors such as the uterine environment and stochastic events that may impact on hemodynamics in the developing heart. A spectrum of morphological variation is commonly seen in animal

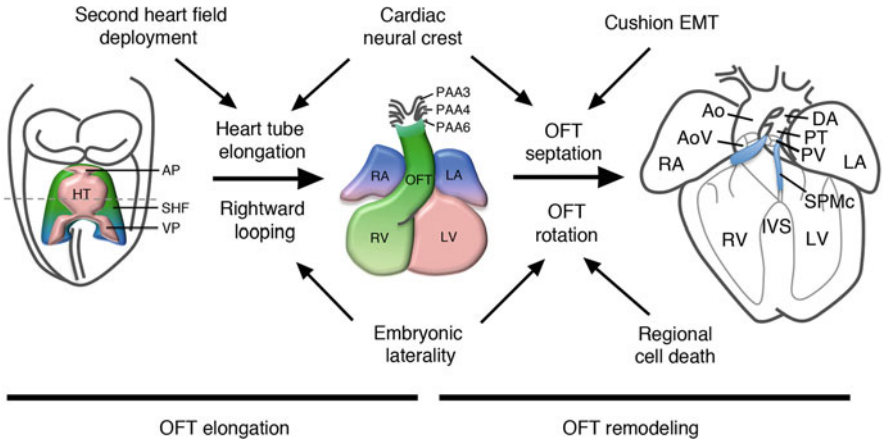

Fig. 37.1 Schema illustrating the progressive developmental steps during formation and remodeling of the outflow tract (OFT), together with the major cell types and developmental processes involved. *HT* heart; *AP* arterial pole; *VP* venous pole; *SHF* second heart field; *PAA* pharyngeal arch artery; *RA* right atrium; *LA* left atrium; *RV* right ventricle; *LV* left ventricle; *Ao* aorta; *AoV* aortic valve; *DA* ductus arteriosus; *PT* pulmonary trunk; *PV* pulmonary valve; *SPMc* subpulmonary myocardium; *IVS* interventricular septum

models of alignment defects extending from overriding aorta to transposition of the great arteries (TGA). Furthermore, TOF and DORV are associated with other forms of CHD including an obligatory ventricular septal defect (VSD), as well as aortic arch and atrioventricular septal defects. This complexity of etiology and phenotype is reflected in the frequency of alignment defects in human CHD patients and in the wide range of genes and pathways that have been implicated in TOF and DORV in patients and animal models. In this chapter we will first consider the relationship between TOF and DORV and then review examples of current knowledge about the molecular pathways driving the sequential processes of OFT elongation and OFT remodeling.

37.2 TOF and DORV Are Part of a Spectrum of Outflow Tract Alignment Defects

Addition of cardiac progenitor cells from the SHF in pharyngeal mesoderm to the elongating poles of the heart drives heart tube elongation during looping morphogenesis [1]. The entire OFT is derived from the SHF and direct or indirect impairment of SHF deployment results in OFT shortening [2]. Maximal OFT extension creates the template for subsequent septation and is critical for correct ventriculoarterial alignment. Septation is driven by coincident cushion morphogenesis and influx of neural crest derived mesenchyme that together divide the OFT into the ascending aorta and pulmonary trunk [3]. During this process, the OFT rotates in a counterclockwise direction (with respect to the direction of blood flow) and the future pulmonary trunk is positioned in a ventral position above the right ventricle, the ascending aorta becoming wedged between the atrioventricular valves and aligned with the left ventricle (Fig. 37.2). Extensive evidence suggests that septation and alignment are distinct, though coincident, processes: failure of OFT septation will result in common arterial trunk (or persistent truncus arteriosus), while failure of alignment will result in a spectrum of alignment defects, ranging from mild to severe [4, 5]. At the mild end of the spectrum, failure of the aorta to make an exclusive connection with the left ventricle results in overriding aorta (OA), where the aorta connects with both ventricles above a membranous VSD. The VSD arises due to malalignment of ventricular and outflow tract septa. When associated with pulmonary stenosis or atresia, overriding aorta results in a TOF phenotype. If >50% of the aorta lies over the right ventricle, overriding aorta becomes DORV, with a subaortic VSD. Total failure of OFT rotation, in the absence of a leftward shift of the OFT, results in a dextraposed aorta that connects with the right ventricle in a side-by-side configuration with the pulmonary trunk (Fig. 37.2). This defect, DORV with a subpulmonary VSD, is known as Taussig–Bing syndrome and is a configuration hemodynamically related to TGA. TOF and DORV thus lie within a disease spectrum of alignment defects and are distinguished by the degree of aortic dextraposition.

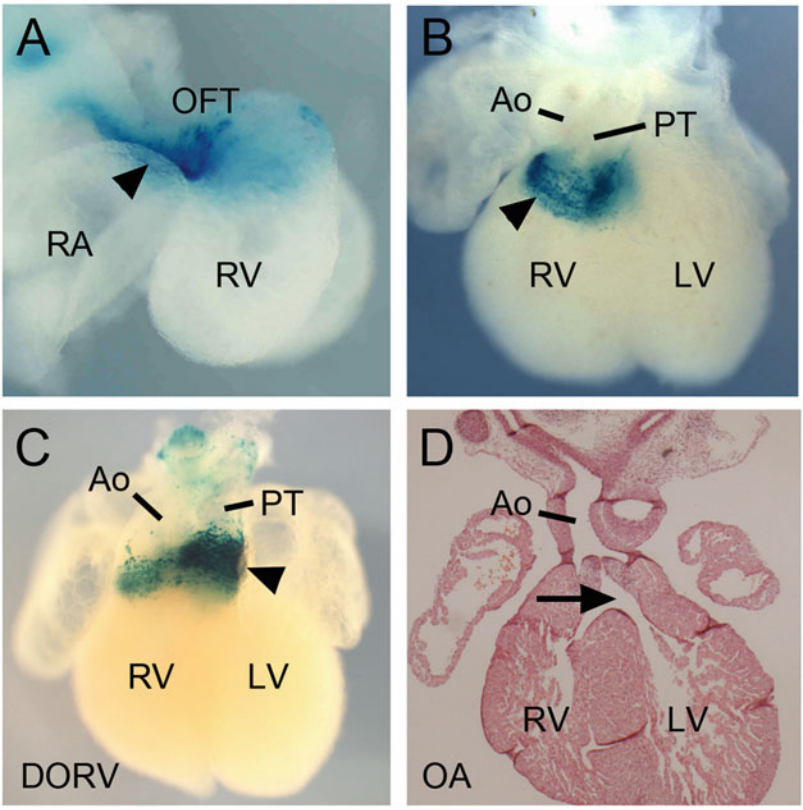

Fig. 37.2 Mouse hearts illustrating rotation of the myocardial OFT wall using a transgene enhancer trap (line y96-*Myf5-nlacZ-16*) expressed in the inferior wall of the midgestation OFT (**a**) and in subpulmonary myocardium after septation (**b**). Transgene-driven β-galactosidase activity is visible (arrowheads) in blue after incubation in X-gal solution. Expression of the *y96-Myf5-nlacZ-16* transgene in a fetal $Tbx3^{-/-}$ heart (**c**) with double-outlet right ventricle (DORV) and a leftward positioned pulmonary trunk (arrowhead). Histological section through an $Fgfr2IIIb^{-/-}$ heart (**d**) with overriding aorta (OA), showing the aorta aligned with a ventricular septal defect (arrow). *RA* right atrium; *RV* right ventricle; *OFT* outflow tract, *Ao* aorta; *PT* pulmonary trunk; *LV* left ventricle

37.3 The Second Heart Field and Outflow Tract Elongation

Failure to maximally elongate the embryonic OFT results in an OFT that is too short to make an exclusive connection between the ascending aorta and left ventricle. Defects in SHF progenitor cell deployment extend from defects in addition of cells to the distal OFT to total failure to extend the linear heart tube, producing a consequent spectrum of mild to severe OFT defects, spanning from ventriculoarterial alignment defects to early gestational lethality [2, 6]. Addition of cells giving rise to

myocardium at the base of the pulmonary trunk, known as subpulmonary (or infundibular) myocardium, is of particular importance for alignment defects. Indeed, underdevelopment of subpulmonary myocardium is thought to be a primary cause of TOF [7]. Ablation of the SHF in chick embryos results in a reduction of subpulmonary myocardium and OA with pulmonary stenosis (TOF) [8]. Future subpulmonary myocardium is the last myocardial derivative of the SHF to be added to the OFT, giving rise to the inferior wall of the embryonic OFT [9]. Subpulmonary myocardium originates in the posterior SHF, adjacent to progenitor cells that contribute to the venous pole of the heart and are critical for atrioventricular septation [10, 11]. Clonal analysis and lineage experiments have shown that subpulmonary and venous pole myocardium are clonally related, identifying a common progenitor cell population in the SHF that segregates to the cardiac poles to give rise to parts of the heart affected in common forms of CHD [12–14].

Many transcriptional regulators and signaling pathways have been implicated in the control of proliferation and progressive differentiation of epithelial SHF progenitor cells [2, 15, 16]. In mouse embryos, addition of subpulmonary myocardium is dependent on the T-box containing transcription factor Tbx1, encoded by the major gene implicated in del22q11.2 (or DiGeorge) syndrome [17]. Haploinsufficiency for *TBX1* in human patients is the most common known genetic cause of TOF, accounting for 15% of TOF [6, 18]. Tbx1 is required for proliferation and delayed differentiation in the SHF, as well as regulating dynamic cell extensions and focal adhesions within the progenitor cell epithelium [19–22]. Whereas homozygous *Tbx1*-null mouse embryos have common arterial trunk with failure of subpulmonary myocardial addition, mice carrying hypomorphic *Tbx1* alleles with <25% of normal *Tbx1* levels have a range of alignment defects including DORV and OA [23]. Among other transcriptional regulators of SHF development, NK2 homeobox 5 (*Nkx2–5)* is essential for elongation of the early heart tube. As in the case of *Tbx1*, hypomorphic embryos with <25% of normal *Nkx2–5* levels display alignment defects including DORV and OA, preceded by a shortened OFT and decreased proliferation in the SHF [24]. Embryos doubly heterozygous for GATA binding protein (*Gata)* 4 or *Gata6* plus *Gata5* also display DORV and overriding aorta [25, 26]}. *Gata3* mutant embryos also have a shortened OFT and DORV and common arterial trunk phenotypes [27]. Loss of function of the Gata cofactor friend of GATA 2 (Fog2; or zinc finger protein, FOG family member; ZFPM2), or the domain of Gata4 that interacts with Fog2, also result in CHD, including OA and DORV phenotypes [28, 29]. Mutation of homeobox A1 (*Hoxa1)*, expressed in subpulmonary myocardial progenitors in the SHF, has also been shown to result in an OA phenotype [12, 30].

Intercellular signaling pathways play an important role in SHF development. Fibroblast growth factor (FGF) signaling controls SHF proliferation downstream of Tbx1 [18]. Mouse embryos lacking components of the FGF signaling pathway display OFT shortening and alignment defects, including Fgf receptor *Fgfr2IIIb*-null embryos, mesodermal conditional *Fgfr1* and *Fgfr2*-null embryos and *Fgf8* hypomorphic and mesodermal conditional mutant embryos [31–34]. The incidence of alignment defects in mesodermal *Fgf8* mutant embryos is increased when alleles

of *Fgf10* are additionally removed [35]. *Fgf15*-null embryos also display DORV and OA [36]. In chick embryos, treatment with Fgf8-blocking antibodies or an FGF receptor antagonist results in DORV and OA phenotypes with pulmonary stenosis or atresia [37]. Additional intercellular signaling pathways regulating SHF development include Notch signaling: conditional Notch mutant embryos and embryos lacking the Notch target genes Hes family bHLH transcription factor 1 (*Hes1)* and Hes-related family bHLH transcription factor with YRPW motif 1 (*Hey1)* display OFT shortening, DORV and OA with pulmonary stenosis and are associated with impaired FGF signaling and proliferation in the SHF [38–40]. Deletion of *Jag1*, encoding a Notch ligand, in the SHF results in DORV (in addition to common arterial trunk and atrial septal defects) and *Jag1 Notch2* compound heterozygous embryos display OA with pulmonary stenosis [40, 41]. A second Notch ligand, Dll4, is also expressed in the SHF where it regulates progenitor cell pool size through controlling proliferation and survival, acting upstream of Fgf8 [42]. A spectrum of OFT defects, including DORV, was observed both on loss of Dll4 function in the SHF and in compound heterozygous embryos carrying mutations in *Dll4* and *Fgf8* [42]. Endothelial specific *Jag1* deletion also results in OA, highlighting the multiplicity of roles intercellular signaling pathways play during OFT development [43]. DORV is also observed in embryos lacking an enzyme encoded by the gene Presenilin 1 (*Psen1),* required to activate the Notch receptor [44]. Mice heterozygous for both *Notch1* and *Nos3* display valve defects and TOF; transcriptional profiling of mutant OFTs has revealed that differentially expressed genes are enriched in de novo variants in TOF patients, showing how mouse models can be used to prioritize candidate CHD genes emerging from human genetic studies [45].

Proliferation in the SHF is also regulated by canonical Wnt and hedgehog signaling pathways [2, 15]. Indeed, mouse embryos cultured in the presence of an activator of the canonical Wnt signaling pathway have elongated OFTs and expanded numbers of SHF cells; conditional loos of function of canonical Wnt signaling leads to a reduction in progenitor cell numbers [46]. Chick embryos cultured in the presence of the Shh antagonist cyclopamine have decreased proliferation in the SHF resulting in OA [47]. Genetic tracing in the mouse has shown that SHF cells exposed to Shh signaling contribute to subpulmonary myocardium [48]. Mouse embryos lacking Shh display a single ventricular outlet, corresponding to total pulmonary atresia [49]. Hedgehog signaling has been shown to act downstream of Gata4 in the SHF for OFT alignment [26]. Retinoic acid signaling is also active in future subpulmonary myocardial progenitor cells. Analysis of retinoic acid receptor mutant embryos have revealed a role in renewal of SHF cells during OFT elongation leading to DORV and OA phenotypes [50]. Exposure of mouse embryos to retinoic acid also results in DORV (together with common trunk and TGA) phenotypes, revealing critical RA dosage requirements for SHF deployment [51, 52]. The planar cell polarity pathway regulates polarized cell movements and has also been implicated in the regulation of SHF deployment and OFT alignment [16, 53, 54]. Mouse embryos lacking components of this pathway encoded by genes such as disheveled segment polarity protein 2 (*Dvl2)*, VANGL planar cell polarity protein 2 (*Vangl2)* or Scribble (*Scrb)* have shorter OFTs and consequent alignment

defects [53, 55, 56]. Double heterozygous *Vangl2*$^{+/-}$;*Scrb*$^{+/-}$ mutant mice also have DORV [57]. Planar cell polarity plays an important role in epithelial SHF cells during their deployment to the elongating OFT [55]. *Vangl2* mutant mice display altered epithelial properties in a region known as the transition zone in the distal OFT, where myocardial differentiation initiates, that may be essential for maximal OFT elongation [56]. The noncanonical wingless-type MMTV integration site family (Wnt) ligand encoding genes *Wnt5a* and *Wnt11* have been implicated upstream of PCP during SHF deployment and OFT morphogenesis [55, 58, 59]. Embryos lacking either of these genes display DORV, as well as common arterial trunk and TGA phenotypes; double mutant mice have a severe reduction of SHF progenitors [60]. *Wnt5a* is a direct target of Tbx1 in the SHF and has been shown to phenocopy the subpulmonary myocardial deficit of *Tbx1*-null embryos [61, 62]. Analysis of loss and gain of *Wnt5a* function in transgenic mice suggests that *Wnt5a* drives future subpulmonary myocardial development by complementary pushing and pulling forces generated by epithelial cell intercalation in the posterior SHF and increased cell cohesion in the anterior SHF associated with Wnt5a downregulation [63]. A number of these genes have been implicated in human TOF patients through ultrarare variant burden analysis following genomic sequencing, including WNT5A, NOTCH1, as well as VEGF signaling pathway genes [64].

Intercellular signals controlling SHF development are both autocrine in origin, as in the case of Notch and FGF signaling, and from surrounding cell types in the pharyngeal region, including pharyngeal endoderm and ectoderm and neural crest-derived mesenchyme [2, 15]. Together, these signals define and regulate the niche of these progenitor cells during heart tube extension. Experiments in chick embryos have revealed the critical requirement for neural crest-derived cells in SHF deployment. Ablation of the cardiac neural crest results not only in common arterial trunk due to failure of formation of the outflow tract septum, but also to alignment defects such as TOF and DORV. These arise due to perturbation of critical signal exchange between crest and SHF cells in the pharyngeal region prior to the addition of these cell populations to the heart [4]. Neural crest cells have been shown to modulate FGF signaling in the pharyngeal region, thus decreasing SHF proliferation during the terminal stages of heart tube elongation [37]. Neural crest ablation rescues the alignment defects observed in embryos cultured in the presence of Fgf8-blocking antibodies [37]. The precise regulation of proliferation in the SHF is a critical step in progenitor cell deployment and loss of cardiac neural crest cells perturbs the balance between proliferation and differentiation leading to decreased SHF incorporation and a shorter OFT that fails to wedge and align correctly [5]. Consistent with these findings, mutations in genes affecting cardiac neural crest development in the mouse result in a spectrum of OFT defects that include both septation (direct) and alignment (indirect) defects. Mouse embryos lacking paired box 3 (*Pax3)*, expressed early in the neural crest lineage, for example, display a range of OFT defects including septation defects (common arterial trunk) and alignment defects (DORV) [65]. Mice lacking *Tbx3*, expressed in different cell types in the pharyngeal region including neural crest derived mesenchyme, also have a high incidence of DORV [66, 67]. Mutation of pre-B-cell leukemia homeobox (*Pbx)* 1–3 result in OA,

possibly through *Pax3* regulation [68, 69]. Neural crest-specific mutation of the cytoplasmic adaptor protein Crk results in DORV; combined loss of *Crk* and the related gene *Crkl* in neural crest cells leads to a more severe phenotype accompanied by pharyngeal arch artery defects and altered Notch signaling [70]. Together these experiments reveal how perturbation of any of a large number of convergent pathways leads to OFT alignment defects through impaired SHF deployment.

37.4 OFT Remodeling and Alignment

OFT elongation is clearly not the only prerequisite for correct ventriculoarterial alignment. Maximal elongation of the OFT by addition of SHF progenitor cells creates the template for a series of coincident processes that remodel the OFT into separate right and left ventricular outlets. These processes include OFT rotation, cushion morphogenesis and differential growth and cell death. Evidence from analysis of developing mouse, chick and human hearts has shown that the OFT wall rotates in a counter-clockwise direction during the septation process and that this is essential for the correct positioning of the great arteries [71–74]. Maximal OFT elongation appears to be required for normal OFT rotation to occur. During the rotation process the superior and inferior myocardial walls of the OFT give rise to subaortic and subpulmonary myocardium, respectively [75]. Subpulmonary myocardium assumes a ventral position at the base of the pulmonary trunk (Fig. 37.2). Different degrees of perturbation of OFT rotation result in arrest of this process and lead to positioning of the aortic valve over the right ventricle or to the right of the pulmonary valve, generating alignment defects including OA, DORV and TGA.

Counterclockwise OFT rotation is driven by the embryonic left–right laterality pathway. Left–right laterality is initiated in the early embryo by cilia-driven flow of signaling molecules to the left side of the node at the anterior end of the primitive streak [76]. Mutation of genes involved in cilia morphogenesis and function result in a range of CHD including alignment defects. These include dynein, axonemal, heavy chain 11 (*Dnah11),* encoding a dynein molecule mutant in *iv/iv* mice, together with *inv* mutant mice, which display DORV, OA and TGA [77, 78]. Cbp/p300-interacting transactivator, with Glu/Asp-rich carboxy-terminal domain, 2 (*Cited2)* also regulates early establishment of laterality and loss of function leads to a range of laterality and alignment defects including DORV and TGA, together with common arterial trunk [79, 80]. Genes involved in ciliogenesis have been identified from mutation screens in mice with alignment defects and TOF patients [81, 82]. Conditional mutagenesis will reveal the extent to which cilia also contribute to alignment defects through direct later roles in SHF deployment or in flow detection in the developing heart. The failure to establish embryonic laterality results in heterotaxy phenotypes by which independent laterality decisions are made by different components of the heart, leading to a large spectrum of CHD including alignment defects. Asymmetric growth factor signaling at the node establishes distinct left and right domains of gene expression in lateral mesoderm, including left-sided expression of genes encoding the Nodal ligand and the transcription factor paired-like

homeodomain 2 (Pitx2) [76]. Pitx2 confers laterality to organs that develop asymmetrically, including the heart. Although not the driver of rightward looping, *Pitx2* is expressed in the left side of the SHF and controls OFT rotation [83]. Indeed, *Pitx2* mutant embryos are characterized by DORV and TGA, together with common trunk, and subpulmonary myocardium is malpositioned in the absence of *Pitx2* [73]. The gene encoding the Nodal coreceptor Tdgf1 has been identified as a critical target of the transcription factor Me2fc; loss of Mef2c in the SHF results in a spectrum of OFT alignment defects ranging from OA to DORV and TGA, illustrating how a range of alignment defects can be associated with a single genetic lesion [84]. The terminal stages of SHF addition have been shown to be asymmetric and left-sided addition of subpulmonary myocardial progenitors expressing *Nkx2–5* has been identified as a potential driving force in OFT rotation, through a process termed the pulmonary push [85]. This promotes counter-clockwise rotation of the pulmonary trunk around the aorta. Interestingly, this process is impaired in embryos lacking the Vegf164 isoform: insufficient addition of subpulmonary myocardium in these embryos is likely to account for subsequent DORV and pulmonary hypoplasia phenotypes [85]. Furthermore, compound heterozygosity for *Pitx2* and *Tbx1* results in alignment defects including DORV and pulmonary stenosis, further indicating how SHF deployment and laterality pathways intersect during OFT morphogenesis [86].

Multiple mechanisms intervene in OFT remodeling and impact on alignment. Rotation of the OFT myocardial wall is accompanied by spiraling of the underlying endocardial cushions that contribute to aortic and pulmonary valve leaflets. OFT cushions contain mesenchyme derived from endocardial EMT in the proximal OFT and neural crest cell influx in the distal OFT; SHF cells may also directly contribute to cushion mesenchyme [3]. Fusion of endocardial cushions plays an essential role in division of the OFT into the ascending aorta and pulmonary trunk. Defects in EMT are thought also to lead to alignment defects through disruption of cushion growth. Diverse signaling pathways are involved in cushion EMT and valve morphogenesis, including bone morphogenetic protein (BMP), transforming growth factor beta (TGFβ), PDGF, and Notch signaling pathways [87]. A gradient of BMP signaling, regulated by the nuclear phosphatase Dullard, has been shown to control the pattern of neural crest condensation during OFT septation [88]. OFT cushion defects are observed in TGFβ2 mutant mice characterized by DORV and TGA phenotypes [89]. *Pdgra* is required in the endothelial lineage for correct neural crest cell migration and OFT alignment, highlighting the importance of crosstalk between different cell types during arterial pole development [90]. Hemodynamics is also an important contributor to cushion remodeling: altered blood flow patterns lead to alignment defects including DORV, OA and TGA [91]. Flow also impacts on aortic arch remodeling downstream of Pitx2 function in the OFT, suggesting that OFT rotation itself may be genetically determined rather than flow driven [92]. Differential growth of subaortic and subpulmonary myocardium has also been proposed to be essential for OFT alignment. Accordingly, either deficiency of subpulmonary myocardium or overgrowth of subaortic myocardium after progenitor cell addition to the heart would lead to a side-by-side configuration of the ascending aorta and pulmonary trunk [7, 93]. Analysis of genes differentially expressed in subaortic versus

subpulmonary myocardium may generate new insights into the remodeling processes [10]. Independently of OFT rotation, a leftward shift of the OFT has been proposed to play an important, although poorly understood, role in aligning the ascending aorta with the left ventricle [94, 95]. The absence of such a leftward shift would distinguish DORV from TGA in the context of a lack of OFT rotation. Myocardial cell shape defects have also been proposed to potentially contribute to alignment defects [53]. For example, altered cell polarity in the remodeling OFT has been observed in *Wnt11*-null embryos and mutation of the gene encoding nonmuscle myosin IIB results in an OA phenotype associated with myocardial hypertrophy [59, 96]. Finally, programmed cell death also plays a major role in the remodeling step, in particular at the base of the ascending aorta, where patterned apoptosis is required to align the aorta with the left ventricle [97]. Blocking cell death in chick embryos using caspase inhibitors or by expression of an inhibitor of apoptosis results in DORV (TGA type) and TGA phenotypes [98].

The generation and remodeling of OFT myocardium are thus both essential for correct ventriculoarterial alignment. It is important to point out that the range of OFT phenotypes observed in mouse models and human CHD patients reveal the importance of genetic modifiers of mutant phenotypes. In addition, nongenetic factors, including teratogens, maternal iron deficiency, maternal diabetes or illness, epigenetic factors and even stochastic events, can impact on either or both steps of OFT elongation and remodeling and result in alignment defects such as DORV and TOF [99–101]. In a recent study prenatal alcohol exposure in mice has been shown to significantly increase the incidence of OFT alignment defects, an effect that is further enhanced by concomitant heterozygous mutation of the Notch ligand Dll4 [102]. This study illustrates the complex mechanisms upstream of OFT alignment defects and highlights the interaction between environmental and genetic factors in the etiology of CHD.

37.5 Conclusion

In conclusion, DORV and TOF are part of a disease spectrum of OFT alignment defects arising through multiple upstream causes, reflecting the diversity of cell types, genes and embryological processes involved in OFT extension and remodeling. While OFT alignment is distinct from neural crest driven OFT septation the two processes are coincident and together ensure the separation of systemic and pulmonary circulatory systems at birth. The mechanistic complexity underlying these processes is reflected in the range of associated CHDs and genetic heterogeneity observed in human patients.

Acknowledgments Research in the author's laboratory is supported by the Agence Nationale pour la Recherche, Fondation pour la Recherche Médicale and Association Françiase contre les Myopathies.

References

1. Kelly RG. The second heart field. Curr Top Dev Biol. 2012;100:33–65.
2. Dyer LA, Kirby ML. The role of secondary heart field in cardiac development. Dev Biol. 2009;336(2):137–44.
3. Miquerol L, Kelly RG. Organogenesis of the vertebrate heart. Wiley Interdiscip Rev Dev Biol. 2013;2(1):17–29.
4. Hutson MR, Kirby ML. Neural crest and cardiovascular development: a 20-year perspective. Birth Defects Res C Embryo Today. 2003;69(1):2–13.
5. Yelbuz TM, Waldo KL, Kumiski DH, Stadt HA, Wolfe RR, Leatherbury L, et al. Shortened outflow tract leads to altered cardiac looping after neural crest ablation. Circulation. 2002;106 (4):504–10.
6. Di Felice V, Zummo G. Tetralogy of fallot as a model to study cardiac progenitor cell migration and differentiation during heart development. Trends Cardiovasc Med. 2009;19 (4):130–5.
7. Van Praagh R. The first Stella van Praagh memorial lecture: the history and anatomy of tetralogy of Fallot. Semin Thorac Cardiovasc Surg Pediatr Card Surg Annu. 2009;19-38:19.
8. Ward C, Stadt H, Hutson M, Kirby ML. Ablation of the secondary heart field leads to tetralogy of Fallot and pulmonary atresia. Dev Biol. 2005;284(1):72–83.
9. Parisot P, Mesbah K, Theveniau-Ruissy M, Kelly RG. Tbx1, subpulmonary myocardium and conotruncal congenital heart defects. Birth Defects Res A Clin Mol Teratol. 2011;91(6): 477–84.
10. Rana MS, Theveniau-Ruissy M, De Bono C, Mesbah K, Francou A, Rammah M, et al. Tbx1 coordinates addition of posterior second heart field progenitor cells to the arterial and venous poles of the heart. Circ Res. 2014;115(9):790–9.
11. De Bono C, Thellier C, Bertrand N, Sturny R, Jullian E, Cortes C, et al. T-box genes and retinoic acid signaling regulate the segregation of arterial and venous pole progenitor cells in the murine second heart field. Hum Mol Genet. 2018;27(21):3747–60.
12. Bertrand N, Roux M, Ryckebusch L, Niederreither K, Dolle P, Moon A, et al. Hox genes define distinct progenitor sub-domains within the second heart field. Dev Biol. 2011;353(2): 266–74.
13. Dominguez JN, Meilhac SM, Bland YS, Buckingham ME, Brown NA. Asymmetric fate of the posterior part of the second heart field results in unexpected left/right contributions to both poles of the heart. Circ Res. 2012;111(10):1323–35.
14. Lescroart F, Mohun T, Meilhac SM, Bennett M, Buckingham M. Lineage tree for the venous pole of the heart: clonal analysis clarifies controversial genealogy based on genetic tracing. Circ Res. 2012;111(10):1313–22.
15. Rochais F, Mesbah K, Kelly RG. Signaling pathways controlling second heart field development. Circ Res. 2009;104(8):933–42.
16. Cortes C, Francou A, De Bono C, Kelly RG. Epithelial properties of the second heart field. Circ Res. 2018;122(1):142–54.
17. Theveniau-Ruissy M, Dandonneau M, Mesbah K, Ghez O, Mattei MG, Miquerol L, et al. The del22q11.2 candidate gene Tbx1 controls regional outflow tract identity and coronary artery patterning. Circ Res. 2008;103(2):142–8.
18. Baldini A. Dissecting contiguous gene defects: TBX1. Curr Opin Genet Dev. 2005;15(3): 279–84.
19. Chen L, Fulcoli FG, Tang S, Baldini A. Tbx1 regulates proliferation and differentiation of multipotent heart progenitors. Circ Res. 2009;105(9):842–51.
20. Liao J, Aggarwal VS, Nowotschin S, Bondarev A, Lipner S, Morrow BE. Identification of downstream genetic pathways of Tbx1 in the second heart field. Dev Biol. 2008;316(2): 524–37.
21. Francou A, Saint-Michel E, Mesbah K, Kelly RG. TBX1 regulates epithelial polarity and dynamic basal filopodia in the second heart field. Development. 2014;141(22):4320–31.

22. Alfano D, Altomonte A, Cortes C, Bilio M, Kelly RG, Baldini A. Tbx1 regulates extracellular matrix-cell interactions in the second heart field. Hum Mol Genet. 2019;28(14):2295–308.
23. Zhang Z, Baldini A. In vivo response to high-resolution variation of Tbx1 mRNA dosage. Hum Mol Genet. 2008;17(1):150–7.
24. Prall OW, Menon MK, Solloway MJ, Watanabe Y, Zaffran S, Bajolle F, et al. An Nkx2-5/Bmp2/Smad1 negative feedback loop controls heart progenitor specification and proliferation. Cell. 2007;128(5):947–59.
25. Laforest B, Nemer M. GATA5 interacts with GATA4 and GATA6 in outflow tract development. Dev Biol. 2011;358(2):368–78.
26. Liu J, Cheng H, Xiang M, Zhou L, Wu B, Moskowitz IP, et al. Gata4 regulates hedgehog signaling and Gata6 expression for outflow tract development. PLoS Genet. 2019;15(5):e1007711.
27. Raid R, Krinka D, Bakhoff L, Abdelwahid E, Jokinen E, Karner M, et al. Lack of Gata3 results in conotruncal heart anomalies in mouse. Mech Dev. 2009;126(1–2):80–9.
28. Tevosian SG, Deconinck AE, Tanaka M, Schinke M, Litovsky SH, Izumo S, et al. FOG-2, a cofactor for GATA transcription factors, is essential for heart morphogenesis and development of coronary vessels from epicardium. Cell. 2000;101(7):729–39.
29. Crispino JD, Lodish MB, Thurberg BL, Litovsky SH, Collins T, Molkentin JD, et al. Proper coronary vascular development and heart morphogenesis depend on interaction of GATA-4 with FOG cofactors. Genes Dev. 2001;15(7):839–44.
30. Makki N, Capecchi MR. Cardiovascular defects in a mouse model of HOXA1 syndrome. Hum Mol Genet. 2012;21(1):26–31.
31. Ilagan R, Abu-Issa R, Brown D, Yang YP, Jiao K, Schwartz RJ, et al. Fgf8 is required for anterior heart field development. Development. 2006;133(12):2435–45.
32. Marguerie A, Bajolle F, Zaffran S, Brown NA, Dickson C, Buckingham ME, et al. Congenital heart defects in Fgfr2-IIIb and Fgf10 mutant mice. Cardiovasc Res. 2006;71(1):50–60.
33. Park EJ, Ogden LA, Talbot A, Evans S, Cai CL, Black BL, et al. Required, tissue-specific roles for Fgf8 in outflow tract formation and remodeling. Development. 2006;133(12):2419–33.
34. Park EJ, Watanabe Y, Smyth G, Miyagawa-Tomita S, Meyers E, Klingensmith J, et al. An FGF autocrine loop initiated in second heart field mesoderm regulates morphogenesis at the arterial pole of the heart. Development. 2008;135(21):3599–610.
35. Watanabe Y, Miyagawa-Tomita S, Vincent SD, Kelly RG, Moon AM, Buckingham ME. Role of mesodermal FGF8 and FGF10 overlaps in the development of the arterial pole of the heart and pharyngeal arch arteries. Circ Res. 2010;106(3):495–503.
36. Vincentz JW, McWhirter JR, Murre C, Baldini A, Furuta Y. Fgf15 is required for proper morphogenesis of the mouse cardiac outflow tract. Genesis. 2005;41(4):192–201.
37. Hutson MR, Zhang P, Stadt HA, Sato AK, Li YX, Burch J, et al. Cardiac arterial pole alignment is sensitive to FGF8 signaling in the pharynx. Dev Biol. 2006;295(2):486–97.
38. Donovan J, Kordylewska A, Jan YN, Utset MF. Tetralogy of fallot and other congenital heart defects in Hey2 mutant mice. Curr Biol. 2002;12(18):1605–10.
39. Rochais F, Dandonneau M, Mesbah K, Jarry T, Mattei MG, Kelly RG. Hes1 is expressed in the second heart field and is required for outflow tract development. PLoS One. 2009;4(7):e6267.
40. High FA, Jain R, Stoller JZ, Antonucci NB, Lu MM, Loomes KM, et al. Murine Jagged1/notch signaling in the second heart field orchestrates Fgf8 expression and tissue-tissue interactions during outflow tract development. J Clin Invest. 2009;119(7):1986–96.
41. McCright B, Lozier J, Gridley T. A mouse model of Alagille syndrome: Notch2 as a genetic modifier of Jag1 haploinsufficiency. Development. 2002;129(4):1075–82.
42. De Zoysa P, Liu J, Toubat O, Choi J, Moon A, Gill PS, et al. Delta-like ligand 4-mediated notch signaling controls proliferation of second heart field progenitor cells by regulating Fgf8 expression. Development. 2020;147(17)
43. High FA, Lu MM, Pear WS, Loomes KM, Kaestner KH, Epstein JA. Endothelial expression of the notch ligand Jagged1 is required for vascular smooth muscle development. Proc Natl Acad Sci U S A. 2008;105(6):1955–9.

44. Nakajima M, Moriizumi E, Koseki H, Shirasawa T. Presenilin 1 is essential for cardiac morphogenesis. Dev Dyn. 2004;230(4):795–9.
45. Matos-Nieves A, Manivannan S, Majumdar U, McBride KL, White P, Garg V. A multi-omics approach using a mouse model of cardiac malformations for prioritization of human congenital heart disease contributing genes. Front Cardiovasc Med. 2021;8:683074.
46. Cohen ED, Wang Z, Lepore JJ, Lu MM, Taketo MM, Epstein DJ, et al. Wnt/beta-catenin signaling promotes expansion of Isl-1-positive cardiac progenitor cells through regulation of FGF signaling. J Clin Invest. 2007;117(7):1794–804.
47. Dyer LA, Kirby ML. Sonic hedgehog maintains proliferation in secondary heart field progenitors and is required for normal arterial pole formation. Dev Biol. 2009;330(2):305–17.
48. Hoffmann AD, Peterson MA, Friedland-Little JM, Anderson SA, Moskowitz IP. Sonic hedgehog is required in pulmonary endoderm for atrial septation. Development. 2009;136(10):1761–70.
49. Washington Smoak I, Byrd NA, Abu-Issa R, Goddeeris MM, Anderson R, Morris J, et al. Sonic hedgehog is required for cardiac outflow tract and neural crest cell development. Dev Biol. 2005;283(2):357–72.
50. Li P, Pashmforoush M, Sucov HM. Retinoic acid regulates differentiation of the secondary heart field and TGFbeta-mediated outflow tract septation. Dev Cell. 2010;18(3):480–5.
51. Yasui H, Morishima M, Nakazawa M, Ando M, Aikawa E. Developmental spectrum of cardiac outflow tract anomalies encompassing transposition of the great arteries and dextroposition of the aorta: pathogenic effect of extrinsic retinoic acid in the mouse embryo. Anat Rec. 1999;254(2):253–60.
52. Ratajska A, Zlotorowicz R, Blazejczyk M, Wasiutynski A. Coronary artery embryogenesis in cardiac defects induced by retinoic acid in mice. Birth Defects Res A Clin Mol Teratol. 2005;73(12):966–79.
53. Henderson DJ, Phillips HM, Chaudhry B. Vang-like 2 and noncanonical Wnt signaling in outflow tract development. Trends Cardiovasc Med. 2006;16(2):38–45.
54. Li D, Wang J. Planar cell polarity signaling in mammalian cardiac morphogenesis. Pediatr Cardiol. 2018;39(5):1052–62.
55. Sinha T, Wang B, Evans S, Wynshaw-Boris A, Wang J. Disheveled mediated planar cell polarity signaling is required in the second heart field lineage for outflow tract morphogenesis. Dev Biol. 2012;370(1):135–44.
56. Ramsbottom SA, Sharma V, Rhee HJ, Eley L, Phillips HM, Rigby HF, et al. Vangl2-regulated polarisation of second heart field-derived cells is required for outflow tract lengthening during cardiac development. PLoS Genet. 2014;10(12):e1004871.
57. Phillips HM, Rhee HJ, Murdoch JN, Hildreth V, Peat JD, Anderson RH, et al. Disruption of planar cell polarity signaling results in congenital heart defects and cardiomyopathy attributable to early cardiomyocyte disorganization. Circ Res. 2007;101(2):137–45.
58. Schleiffarth JR, Person AD, Martinsen BJ, Sukovich DJ, Neumann A, Baker CV, et al. Wnt5a is required for cardiac outflow tract septation in mice. Pediatr Res. 2007;61(4):386–91.
59. Zhou W, Lin L, Majumdar A, Li X, Zhang X, Liu W, et al. Modulation of morphogenesis by noncanonical Wnt signaling requires ATF/CREB family-mediated transcriptional activation of TGFbeta2. Nat Genet. 2007;39(10):1225–34.
60. Cohen ED, Miller MF, Wang Z, Moon RT, Morrisey EE. Wnt5a and Wnt11 are essential for second heart field progenitor development. Development. 2012;139(11):1931–40.
61. Chen L, Fulcoli FG, Ferrentino R, Martucciello S, Illingworth EA, Baldini A. Transcriptional control in cardiac progenitors: Tbx1 interacts with the BAF chromatin remodeling complex and regulates Wnt5a. PLoS Genet. 2012;8(3):e1002571.
62. Sinha T, Li D, Theveniau-Ruissy M, Hutson MR, Kelly RG, Wang J. Loss of Wnt5a disrupts second heart field cell deployment and may contribute to OFT malformations in DiGeorge syndrome. Hum Mol Genet. 2014;24:1704.
63. Li D, Sinha T, Ajima R, Seo HS, Yamaguchi TP, Wang J. Spatial regulation of cell cohesion by Wnt5a during second heart field progenitor deployment. Dev Biol. 2016;412(1):18–31.

64. Manshaei R, Merico D, Reuter MS, Engchuan W, Mojarad BA, Chaturvedi R, et al. Genes and pathways implicated in tetralogy of Fallot revealed by ultra-rare variant burden analysis in 231 genome sequences. Front Genet. 2020;11:957.
65. Conway SJ, Henderson DJ, Kirby ML, Anderson RH, Copp AJ. Development of a lethal congenital heart defect in the splotch (Pax3) mutant mouse. Cardiovasc Res. 1997;36(2): 163–73.
66. Mesbah K, Harrelson Z, Theveniau-Ruissy M, Papaioannou VE, Kelly RG. Tbx3 is required for outflow tract development. Circ Res. 2008;103(7):743–50.
67. Bakker ML, Boukens BJ, Mommersteeg MT, Brons JF, Wakker V, Moorman AF, et al. Transcription factor Tbx3 is required for the specification of the atrioventricular conduction system. Circ Res. 2008;102(11):1340–9.
68. Stankunas K, Shang C, Twu KY, Kao SC, Jenkins NA, Copeland NG, et al. Pbx/Meis deficiencies demonstrate multigenetic origins of congenital heart disease. Circ Res. 2008;103(7):702–9.
69. Chang CP, Stankunas K, Shang C, Kao SC, Twu KY, Cleary ML. Pbx1 functions in distinct regulatory networks to pattern the great arteries and cardiac outflow tract. Development. 2008;135(21):3577–86.
70. Shi L, Racedo SE, Diacou A, Park T, Zhou B, Morrow BE. Crk and Crkl have shared functions in neural crest cells for cardiac outflow tract septation and vascular smooth muscle differentiation. Hum Mol Genet. 2022;31(8):1197–215.
71. Bostrom MP, Hutchins GM. Arrested rotation of the outflow tract may explain double-outlet right ventricle. Circulation. 1988;77(6):1258–65.
72. Lomonico MP, Bostrom MP, Moore GW, Hutchins GM. Arrested rotation of the outflow tract may explain tetralogy of Fallot and transposition of the great arteries. Pediatr Pathol. 1988;8 (3):267–81.
73. Bajolle F, Zaffran S, Kelly RG, Hadchouel J, Bonnet D, Brown NA, et al. Rotation of the myocardial wall of the outflow tract is implicated in the normal positioning of the great arteries. Circ Res. 2006;98(3):421–8.
74. Thompson RP, Abercrombie V, Wong M. Morphogenesis of the truncus arteriosus of the chick embryo heart: movements of autoradiographic tattoos during septation. Anat Rec. 1987;218(4):434–40. 394–5
75. Bajolle F, Zaffran S, Meilhac SM, Dandonneau M, Chang T, Kelly RG, et al. Myocardium at the base of the aorta and pulmonary trunk is prefigured in the outflow tract of the heart and in subdomains of the second heart field. Dev Biol. 2008;313(1):25–34.
76. Vandenberg LN, Levin M. A unified model for left-right asymmetry? Comparison and synthesis of molecular models of embryonic laterality. Dev Biol. 2013;379(1):1–15.
77. Icardo JM, Sanchez de Vega MJ. Spectrum of heart malformations in mice with situs solitus, situs inversus, and associated visceral heterotaxy. Circulation. 1991;84(6):2547–58.
78. Morishima M, Yasui H, Nakazawa M, Ando M, Ishibashi M, Takao A. Situs variation and cardiovascular anomalies in the transgenic mouse insertional mutation, inv. Teratology. 1998;57(6):302–9.
79. Bamforth SD, Braganca J, Farthing CR, Schneider JE, Broadbent C, Michell AC, et al. Cited2 controls left-right patterning and heart development through a nodal-Pitx2c pathway. Nat Genet. 2004;36(11):1189–96.
80. Weninger WJ, Lopes Floro K, Bennett MB, Withington SL, Preis JI, Barbera JP, et al. Cited2 is required both for heart morphogenesis and establishment of the left-right axis in mouse development. Development. 2005;132(6):1337–48.
81. Tan SY, Rosenthal J, Zhao XQ, Francis RJ, Chatterjee B, Sabol SL, et al. Heterotaxy and complex structural heart defects in a mutant mouse model of primary ciliary dyskinesia. J Clin Invest. 2007;117(12):3742–52.
82. Willaredt MA, Gorgas K, Gardner HA, Tucker KL. Multiple essential roles for primary cilia in heart development. Cilia. 2012;1(1):23.
83. Franco D, Christoffels VM, Campione M. Homeobox transcription factor Pitx2: the rise of an asymmetry gene in cardiogenesis and arrhythmogenesis. Trends Cardiovasc Med. 2014;24(1): 23–31.

84. Barnes RM, Harris IS, Jaehnig EJ, Sauls K, Sinha T, Rojas A, et al. MEF2C regulates outflow tract alignment and transcriptional control of Tdgf1. Development. 2016;143(5):774–9.
85. Scherptong RW, Jongbloed MR, Wisse LJ, Vicente-Steijn R, Bartelings MM, Poelmann RE, et al. Morphogenesis of outflow tract rotation during cardiac development: the pulmonary push concept. Dev Dyn. 2012;241(9):1413–22.
86. Nowotschin S, Liao J, Gage PJ, Epstein JA, Campione M, Morrow BE. Tbx1 affects asymmetric cardiac morphogenesis by regulating Pitx2 in the secondary heart field. Development. 2006;133(8):1565–73.
87. Garside VC, Chang AC, Karsan A, Hoodless PA. Co-ordinating notch, BMP, and TGF-beta signaling during heart valve development. Cell Mol Life Sci. 2013;70(16):2899–917.
88. Darrigrand JF, Valente M, Comai G, Martinez P, Petit M, Nishinakamura R, et al. Dullard-mediated Smad1/5/8 inhibition controls mouse cardiac neural crest cells condensation and outflow tract septation. elife. 2020;9:9.
89. Bartram U, Molin DG, Wisse LJ, Mohamad A, Sanford LP, Doetschman T, et al. Double-outlet right ventricle and overriding tricuspid valve reflect disturbances of looping, myocardialization, endocardial cushion differentiation, and apoptosis in TGF-beta(2)-knock-out mice. Circulation. 2001;103(22):2745–52.
90. Aghajanian H, Cho YK, Rizer NW, Wang Q, Li L, Degenhardt K, et al. Pdgfralpha functions in endothelial-derived cells to regulate neural crest cells and the development of the great arteries. Dis Model Mech. 2017;10(9):1101–8.
91. Midgett M, Rugonyi S. Congenital heart malformations induced by hemodynamic altering surgical interventions. Front Physiol. 2014;5:287.
92. Yashiro K, Shiratori H, Hamada H. Haemodynamics determined by a genetic programme govern asymmetric development of the aortic arch. Nature. 2007;450(7167):285–8.
93. Van Praagh R, Van Praagh S, Isolated ventricular inversion. A consideration of the morphogenesis, definition and diagnosis of nontransposed and transposed great arteries. Am J Cardiol. 1966;17(3):395–406.
94. Goor DA, Edwards JE. The spectrum of transposition of the great arteries: with specific reference to developmental anatomy of the conus. Circulation. 1973;48(2):406–15.
95. Restivo A, Piacentini G, Placidi S, Saffirio C, Marino B. Cardiac outflow tract: a review of some embryogenetic aspects of the conotruncal region of the heart. Anat Rec A Discov Mol Cell Evol Biol. 2006;288(9):936–43.
96. Tullio AN, Accili D, Ferrans VJ, Yu ZX, Takeda K, Grinberg A, et al. Nonmuscle myosin II-B is required for normal development of the mouse heart. Proc Natl Acad Sci U S A. 1997;94(23):12407–12.
97. Schaefer KS, Doughman YQ, Fisher SA, Watanabe M. Dynamic patterns of apoptosis in the developing chicken heart. Dev Dyn. 2004;229(3):489–99.
98. Watanabe M, Jafri A, Fisher SA. Apoptosis is required for the proper formation of the ventriculo-arterial connections. Dev Biol. 2001;240(1):274–88.
99. Molin DG, Roest PA, Nordstrand H, Wisse LJ, Poelmann RE, Eriksson UJ, et al. Disturbed morphogenesis of cardiac outflow tract and increased rate of aortic arch anomalies in the offspring of diabetic rats. Birth Defects Res A Clin Mol Teratol. 2004;70(12):927–38.
100. Kalisch-Smith JI, Ved N, Sparrow DB. Environmental risk factors for congenital heart disease. Cold Spring Harb Perspect Biol. 2020;12(3)
101. Kalisch-Smith JI, Ved N, Szumska D, Munro J, Troup M, Harris SE, et al. Maternal iron deficiency perturbs embryonic cardiovascular development in mice. Nat Commun. 2021;12(1):3447.
102. Harvey DC, De Zoysa P, Toubat O, Choi J, Kishore J, Tsukamoto H, et al. Concomitant genetic defects potentiate the adverse impact of prenatal alcohol exposure on cardiac outflow tract maturation. Birth Defects Res. 2022;114(3–4):105–15.

Part IX

d-Transposition of the Great Arteries

Clinical Presentation and Therapy of d-Transposition of the Great Arteries

38

Nikolaus A. Haas, David J. Driscoll, and Silke Rickert-Sperling

38.1 Introduction

d-Transposition of the great arteries (d-TGA) is the most common form of congenital heart disease that presents with cyanosis in a newborn. The aorta arises from the right ventricle and the pulmonary artery arises from the left ventricle. It constitutes 3–5% of all congenital heart defects. In a simple d-TGA (about two-thirds of patients), there is no other cardiac abnormality other than a patent foramen ovale (PFO) and a patent ductus arteriosus (PDA). In a complex d-TGA additional cardiac abnormalities such as VSD, pulmonary stenosis or coronary abnormalities are present. About one-third to 40% of patients with d-TGA have an associated ventricular septal defect. Among patients with d-TGA, 6% of those with intact ventricular septum and 31% of those with ventricular septal defect have associated pulmonary stenosis. Coronary abnormalities are of importance with regard to the complexity of surgical repair.

N. A. Haas (✉)
Department of Pediatric Cardiology and Intensive Care, Ludwig Maximilians University, Munich, Germany
e-mail: Nikolaus.haas@med.uni-muenchen.de

D. J. Driscoll
Division of Pediatric Cardiology, Department of Pediatrics, Mayo Clinic College of Medicine, Rochester, MN, USA
e-mail: driscoll.david@mayo.edu

S. Rickert-Sperling
Cardiovascular Genetics, Charité–Universitätsmedizin Berlin, Berlin, Germany
e-mail: silke.sperling@charite.de

© The Author(s), under exclusive license to Springer Nature Switzerland AG 2024

S. Rickert-Sperling et al. (eds.), *Congenital Heart Diseases: The Broken Heart*,
Advances in Experimental Medicine and Biology 1441,
https://doi.org/10.1007/978-3-031-44087-8_38

38.2 Pathologic Physiology

The pathophysiology of transposition is unique and the two circulations run in parallel without or only poor mixing; many other defects with a similar blood flow pattern are referred to as having "TGA physiology" (see DORV with subpulmonary VSD). In d-TGA, systemic venous return (blood with low oxygen content) returns to the right ventricle and then is pumped to the body via the aorta without passing through the lungs for gas exchange (Fig. 38.1). The aorta lies anterior and to the left, and the coronary arteries arise from there. Pulmonary venous return (oxygenated blood) returns to the left ventricle and then is pumped back to the lungs (Fig. 38.1) via the pulmonary artery. This vessel lies more to the left and posterior. The effective pulmonary blood flow (the volume of deoxygenated blood that participates in gas exchange in the lungs) is low, albeit total pulmonary blood flow is increased mainly due to a left-to-right shunt across the patent ductus arteriosus.

d-TGA is incompatible with life unless a communication exists between the two circuits to allow mixture of oxygenated and deoxygenated blood. This mixture occurs mainly at the patent foramen ovale (or atrial septal defect), the ductus arteriosus (if patent), and the ventricular septal defect (if present). This is a tenuous situation for a patient with an intact ventricular septum and no true atrial septal defect

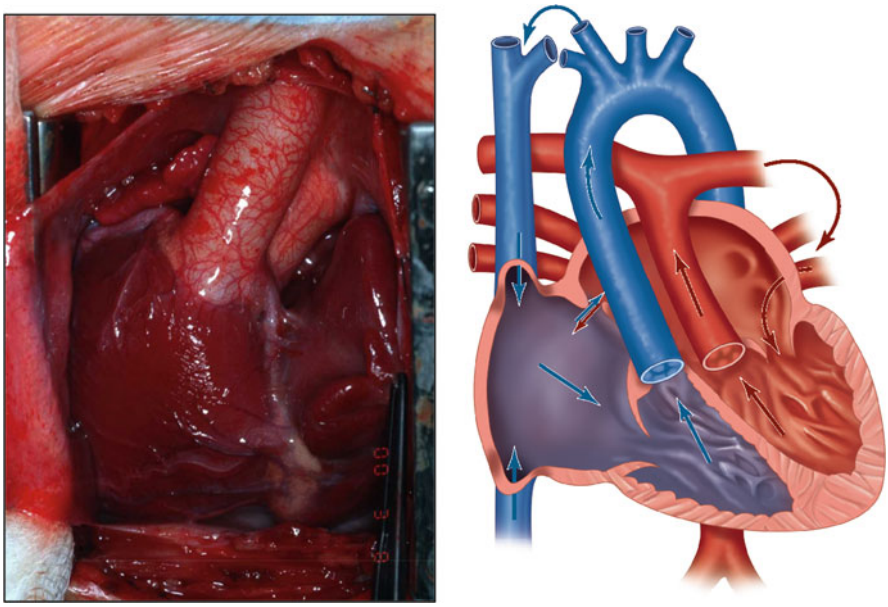

Fig. 38.1 Illustration of transposition of the great arteries. The left panel shows an intraoperative view and right panel a schematic representation. Note that the aorta arises from the right ventricle and the pulmonary artery arises from the left ventricle. If there are no communications between the left and right side of the heart, it would be impossible to supply oxygenated blood to the body which is incompatible with life

because mixing of the two circuits will decrease as the ductus arteriosus closes and the patent foramen ovale becomes sealed. Without intervention, these children succumb rapidly in the first days of life. Additional cardiac defects may exist such as subaortic stenosis, aortic arch hypoplasia and coarctation of the aorta; a simple d-TGA is rarely combined with other genetic syndromes or extracardiac malformations.

38.3 Clinical Presentation

A newborn with a simple d-TGA represents a medical emergency and profound cyanosis. It is critical to establish or exclude this diagnosis and to document and to insure adequate sites for mixing between the systemic and pulmonary circuits which, in d-TGA, are in parallel rather than in series. In d-TGA with a large ASD or VSD, cyanosis may be less prominent. When a neonatal pulse oximetry screening is in place, these patients should be picked up by lower than normal saturations. In patients with a VSD or pulmonary stenosis, a murmur may be the first presentation.

38.4 Physical Examination

The primary physical finding is cyanosis. The right ventricular impulse will be increased. Depending upon the associated defects, there may or may not be a murmur. If a VSD or pulmonary stenosis is present, there will be a systolic murmur. If there is associated coarctation of the aorta, the femoral pulses will be weak or absent. Pulse oximetry may reveal a differential cyanosis, i.e., different saturations at the level of the hands/fingers (cyanotic) and feet/toes (pink).

38.5 Diagnostic Imaging

Echocardiography is the primary diagnostic tool for accurately diagnosing d-transposition of the great arteries (d-TGA) in neonates and children. It allows for the detection of other associated malformations and anomalies such as arch abnormalities and coarctation. Echocardiography can visualize the parallel arrangement of the two vessels in the long-axis view, with the vessel from the left ventricle showing bifurcation and the aorta positioned anteriorly and to the right in the short-axis view. Assessment of the interatrial communication is crucial, and the need for a Rashkind procedure should be determined. The presence of a patent ductus arteriosus (PDA) can be determined, but it should not be relied upon as a stable source of mixing as it is likely to close. In cases where the baby is extremely hypoxemic, acidotic, or requires transfer to another institution, maintaining PDA patency through prostaglandin E-1 infusion is recommended. Preoperative definition of the coronary artery anatomy is helpful for surgical repair.

Cardiac catheterization is typically unnecessary for the diagnostic evaluation of simple d-TGA or d-TGA with ventricular septal defect (VSD) due to the availability of echocardiography. Angiography may be considered in rare cases where the coronary anatomy cannot be adequately visualized or at the discretion of the surgeons. Interventional catheterization is commonly performed in cases with inadequate mixing at the atrial level.

Magnetic resonance imaging (MRI) is not the primary diagnostic modality for d-TGA but is valuable for follow-up evaluations after surgical repair. MRI is particularly useful for assessing pulmonary artery anatomy, flow distribution to the lungs, coronary perfusion after repair, and aortic arch anatomy in adults.

Computer tomography (CT) can provide similar anatomical details as MRI but offers higher resolution for smaller vessels. CT scans may be utilized in cases where the coronary distribution pattern is unclear or for postsurgical assessment.

38.6 Treatment: Management of d-TGA with Intact Ventricular Septum

38.6.1 Neonatal Management

In neonates with adequate mixing at the atrial level, the only management may consist of the administration of a low to moderate doses of prostaglandin E1 to maintain ductal patency and keep the saturations at a level above 80%.

In neonates with inadequate mixing, balloon septostomy has to be performed (i.e., Rashkind procedure). This is usually done at the bed side in the neonatal unit. A balloon catheter is advanced via the umbilical or femoral vein under echocardiographing guidance across the PFO in the left atrium. There the balloon is filled with saline until a maximum volume can be achieved and the balloon nearly fills the complete left atrium. Then this balloon is pulled back in a rapid movement to the right atrium thereby destroying the interatrial septum. This leads to a wide communication and better mixing. Usually, the saturations improve immediately.

In neonates with concomitant coarctation, prostaglandin is also used, as much of the narrowing of the coarctation is caused by ductal tissue. Ductal patency is then required for abdominal perfusion.

In the second week of life, surgical repair is planned. Today, an arterial switch operation is the standard of care. Historically, an atrial switch operation was performed and so many adult patients alive today have had this form of surgical treatment.

38.6.2 Arterial Switch (Jatene) Procedure

The Jatene operation, also known as the arterial switch operation, represents the best option for managing infants with d-TGA, intact ventricular septum or a VSD, and a normal pulmonary valve (Fig. 38.2). This operation has been performed since the

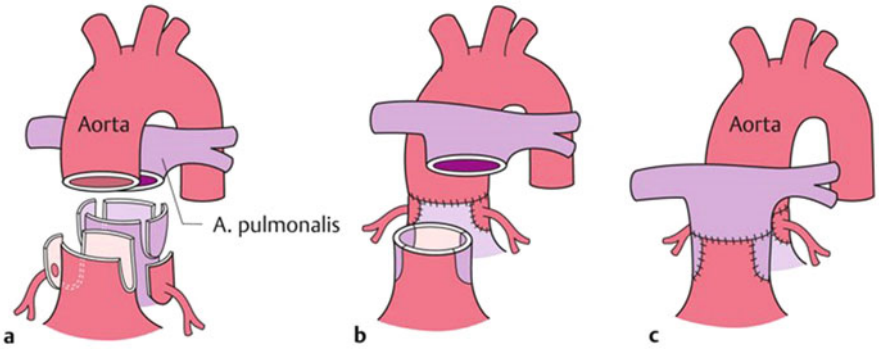

Fig. 38.2 Arterial switch operation (Jatene). (**a**) The pulmonary artery and the aorta are disconnected from their respective ventricles. The coronary arteries, which supply blood to the heart muscle, are also detached from their original positions. (**b**) The next step involves transferring the coronary arteries to the appropriate positions and the aorta is connected to the right ventricle. (**c**) The pulmonary artery is then connected to the left ventricle. Reproduced from Kinderkardiologie, Georg Thieme Verlag, N. Haas, U. Kleideiter, 2011

1980s, and the aorta and pulmonary artery are transected cephalad to their respective valves. The ostia of the coronary arteries are removed from the stump of the aorta and sewed to the stump of the pulmonary artery (the neoaorta). The distal portion of the aorta is anastomosed to the proximal stump of the pulmonary artery, and the distal portion of the pulmonary artery is anastomosed to the stump of the aorta. For anatomical reasons, the aorta is placed posterior to the pulmonary artery (the LeCompte maneuver). In addition, the coronary arteries have to be transferred (coronary transfer, see picture). The ASD and the PDA will be closed and the VSD will be repaired if there is no pulmonary stenosis.

The mortality after this procedure is 2% or less and the long-term results are quite good. This procedure must be done early (<4 weeks of age), before the thickened left ventricular walls involute as pulmonary arterial resistance decreases. Today, in nearly all institutions, the operation is performed without preoperative cardiac catheterization. Prostaglandin E_1 is infused preoperatively to maintain patency of the ductus arteriosus and preserve the acid–base stability of the patient.

38.6.3 Rastelli Procedure

This surgical approach is used in patients with a large perimembranous VSD and a severe pulmonary stenosis. A simple switch operation would leave a severe aortic stenosis and so the pulmonary artery is transected and the VSD closed with a patch so that the blood of the LV drains to the aorta. No coronary transfer is necessary. The RV is then connected to the pulmonary artery with a valved extracardiac conduit.

38.6.4 Atrial Switch (Senning or Mustard) Procedure

The Senning and Mustard operations were described in the 1960s and predate the arterial switch operation. These are alternatives to the arterial switch procedure. They are used if the pulmonary valve is abnormal such that it would not work as the neoaortic valve following a Jatene (arterial switch) procedure. With these procedures systemic and pulmonary venous returns are rerouted in the atria. This is accomplished by sewing a baffle in the atrium (Mustard, Fig. 38.3) or by using intrinsic atrial tissue (Senning). That systemic venous return from the superior and inferior venae cavae is thereby directed through the mitral valve and into the left ventricle (and subsequently to the pulmonary artery). The pulmonary venous return is directed through the tricuspid valve (and subsequently to the aorta). In essence, transposition of the great arteries is treated by creating "transposition" of the venous return to the heart. The result is a rerouting of the venous blood to the pulmonary artery and the arterialized blood to the systemic circulation; the right ventricle has however to support the systemic circulation and the left ventricle the pulmonary circulation.

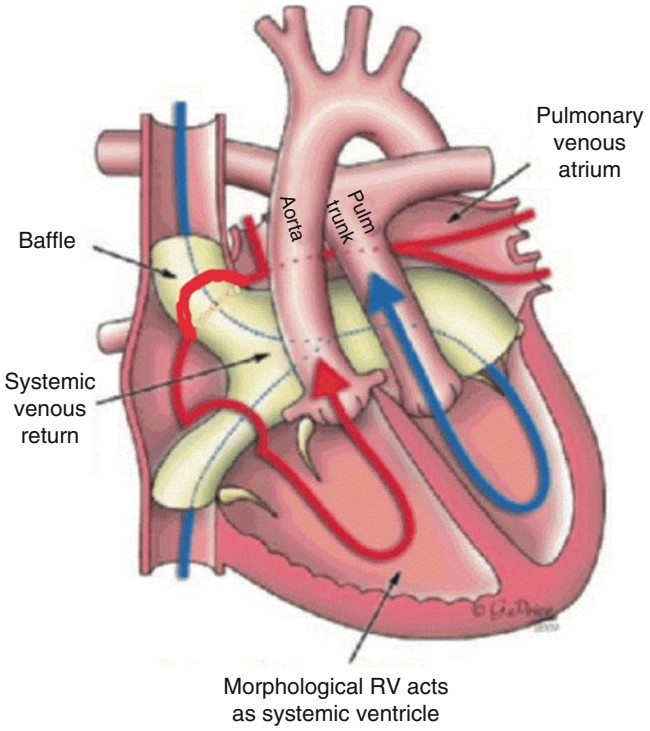

Fig. 38.3 The Mustard procedure involves redirecting the blood flow in the heart by creating baffles or tunnels within the atria. The surgeon creates an atrial septal defect (ASD) by removing a portion of the atrial septum and then uses a patch to redirect the blood flow. The deoxygenated blood from the systemic circulation (venous blood) is directed to the right atrium, then to the left atrium through the ASD, and finally to the left ventricle and aorta

The Senning and Mustard operations have a low operative mortality but significant intermediate and long-term problems. These include obstruction of systemic and pulmonary venous returns by the baffle, atrial arrhythmias, tricuspid insufficiency, and right ventricular failure. The Senning and Mustard operations usually are performed in patients 6 months to 1 year of age but some surgeons will perform the operation in the newborn period. If one of these methods of operation is to be utilized, an adequate interatrial communication must be established in the newborn period. This is accomplished by doing a Rashkind balloon atrial septostomy.

38.7 Outcome

Besides the surgical results**,** brain injury, impaired brain growth, and long-term neurodevelopmental problems such as slower language development are common in children with transposition of the great arteries. Although the mechanisms underlying this association are still unclear, extended periods of cyanosis and pulmonary overcirculation may adversely impact brain growth and subsequent neurodevelopment.

38.7.1 Arterial Switch (Jatene) Procedure

The operative mortality for the arterial switch is in the range of about 2–5%. The long-term outcome is excellent. Some patients will require reoperation for pulmonary artery stenosis. However this has become less common with the introduction of the LeCompte maneuver. Adults after the switch operation may require aortic root and valve surgery, as the neoaortic valve, that genetically is a pulmonary valve, may show regurgitation and the aortic root may dilate. Some patients show obliteration of transposed coronary arteries and collateral blood flow from the contralateral arteries will develop; the long term outcome seems promising.

38.7.2 Rastelli Procedure

After the Rastelli procedure the operative results are satisfactory and the mortality is below 10%. The long term outcome is mainly dominated by the degeneration of the RV-to-PA conduits that require interventional management (i.e., balloon dilatation, stent implantation) or interventional or surgical valve replacement. This may be necessary on several occasions throughout life.

38.7.3 Atrial Switch (Senning or Mustard) Procedure

The operative mortality for the atrial switch operation is in the range of 1–5%. There are numerous long-term problems with the atrial switch procedure. Since the right ventricle remains the systemic ventricle after this operation, late right ventricular failure occurs, necessitating cardiac transplantation. Because of the extensive suturing in the atria, late stenosis of the pathways as well as sick sinus syndromes, atrial arrhythmias and sudden death occur.

Human Genetics of d-Transposition of Great Arteries

39

Lucile Houyel

Abstract

Although several genes underlying occurrence of transposition of the great arteries have been found in the mouse, human genetics of the most frequent cyanotic congenital heart defect diagnosed in neonates is still largely unknown. Development of the outflow tract is a complex process which involves the major genes of cardiac development, acting on myocardial cells from the anterior second heart field, and on mesenchymal cells from endocardial cushions. These genes, coding for transcription factors, interact with each other, and their differential expression conditions the severity of the phenotype. A precise description of the anatomic phenotypes is mandatory to achieve a better comprehension of the complex mechanisms responsible for transposition of the great arteries.

Keywords

Transposition of great arteries · TGA · Outflow tract rotation · Second heart field · Endocardial cushions · Laterality · Cilia · Heterotaxy

39.1 Introduction

Transposition of the great arteries (TGA) is defined as "a congenital cardiovascular malformation in which the morphologically right ventricle connects to the aorta and the morphologically left ventricle connects to the pulmonary trunk," which implies

L. Houyel (✉)
Department of Congenital and Pediatric Cardiology, Necker-Enfants Malades Hospital–M3C, APHP, Paris, France

Université Paris Cité, Paris, France
e-mail: lucile.houyel@aphp.fr

© The Author(s), under exclusive license to Springer Nature Switzerland AG 2024

S. Rickert-Sperling et al. (eds.), *Congenital Heart Diseases: The Broken Heart*, Advances in Experimental Medicine and Biology 1441,
https://doi.org/10.1007/978-3-031-44087-8_39

discordant ventriculoarterial connections [1]. The term "d-TGA" refers to the most usual form of the disease, characterized by atrial situs solitus, concordant atrioventricular connections, and usually parallel great arteries with aorta to the right of the pulmonary artery. Segmental analysis according to Van Praagh is in this case {S,D, D} [2].

Pathogenesis of d-TGA is still largely unknown. Over the last decade, several genetic studies using new techniques of whole-genome or -exome sequencing in patients have been published. As in previous studies, the problem is complexified by the frequent inclusion of patients with two other types of congenital heart defects (CHD) [3, 4]: congenitally corrected TGA (ccTGA), and double-outlet right ventricle with subpulmonary ventricular septal defect (TGA-type DORV). Congenitally corrected TGA is a complex CHD associating discordant atrioventricular connections and discordant ventriculoarterial connections (double discordance). Double-outlet right ventricle with subpulmonary ventricular septal defect (VSD) shares the same physiology with TGA but the two great arteries originate from the right ventricle and thus are not strictly transposed. These distinctions are important, because the embryologic mechanisms leading to these malformations are not exactly the same for each of the 3 phenotypes. For example, it has been confirmed that ccTGA, in which an inverted ventricular loop is the major determinant of the CHD, may result from a more severe perturbation in left–right patterning pathways during heart development [4].

Children with TGA undergo corrective surgery in the first week of life, and more than 90% survive now until the adult age. Genetic counseling has therefore gained increasing importance, especially since the publication of several familial cases of TGA, prompting basic scientists to try to decipher the pathogenesis and genetic background of this cardiac malformation.

39.2 Epidemiology

The majority of cases are isolated and sporadic, and the recurrence rate of TGA is one of the lowest among all CHD: null in the English multicentric series by Burns et al. [5], 1.7% in the Italian multicentric study by Digilio in 2001 [6].

The first case of familial recurrence of TGA was published in 1997 [7]. Since, several studies have confirmed that in some families, there were not only several patients with TGA but also with ccTGA, suggesting monogenic inheritance (autosomal dominant or autosomal recessive) with a variable phenotypic expression [8]. In some of these families, multiple mutations in laterality genes were found, including Nodal and ZIC3 [8].

Male dominance is well known in TGA, with a ratio M/F of 2.32, although no X-linked heredity could be demonstrated in humans [4].

39.3 Morphogenesis of TGA

Etiology and morphogenesis of TGA are still not fully elucidated. From the developmental point of view, TGA is a total departure from the normal outflow tract development, in other terms an "ontogenic impossibility" [9].

The embryonic OT has three components: proximal, intermediate and distal [10]. These three components will give rise respectively to the subarterial outflow tracts, the arterial valves and the intrapericardial great arteries (ascending aorta and pulmonary trunk). Transposition of the great arteries belongs to the large group of outflow tract defects, and is often included in the group of so-called conotruncal defects, also called cardiac neural crest-anterior second heart field (CNC-ASHF)-related defects [11]. However, TGA is by some aspects morphologically distinct from so-called "conotruncal defects." Half of hearts with TGA have an intact ventricular septum, and when a ventricular septal defect (VSD) is present, it can be of any morphological type, while in CNC-ASHF-related defects, the VSD is always an outlet VSD [12, 13]. Cardiac neural crest and anterior second heart field-related outflow tract defects are commonly associated with micro-deletion 22q11.1, while it is exceptionally found in association with TGA. In addition, extracardiac anomalies have been reported to be less frequent in TGA that in other outflow tract defects [14]. Taken together, all these elements are in favor of different pathogenetic mechanisms for TGA and CNC-ASHF-related CHD.

Anatomically, the outflow tract of TGA is abnormal. The aortic valve has retained its original position over the right ventricle, above a subaortic conus, and the pulmonary valve has been transferred toward the left ventricle, with mitral-to-pulmonary fibrous continuity. As a consequence, the outflow portion of the ventricular septum is straight and not directed obliquely from right to left as in the normal right ventricle. This was confirmed by an anatomic study in which the orientation of the septal band on the right ventricular surface is similar in normal heart and in ccTGA, compared to hearts with TGA [15].

Two hypotheses have historically been proposed for the morphogenesis of TGA. The first one, developed by Goor and Edwards, is the absence of rotation of the outflow tract during heart development, due to abnormal resorption of the subpulmonary part of the conus, with abnormal persistence of the subaortic conus [16]. This theory would place TGA at the extremity of the spectrum of the outflow tract defects, underlining one of the major features common to almost all these anomalies except for interrupted aortic arch, namely the complete or partial position of the aorta above the right ventricle (Fig. 39.1). The second one, developed by de la Cruz, is the lack of spiralization of the endocardial cushions of the outflow tract during heart development [17, 18]. This theory however does not take into account the straight appearance of the subarterial regions in isolated TGA and the great variety of infundibular anatomy in complex TGA [9, 19]. Due to the paucity of animal models of TGA, none of these hypotheses could be really confirmed or infirmed. A recent echocardiographic study in children with TGA showed that they had a shorter ascending aorta, while the length of the pulmonary trunk was not different from that observed in control patients [20]. This could be explained by a

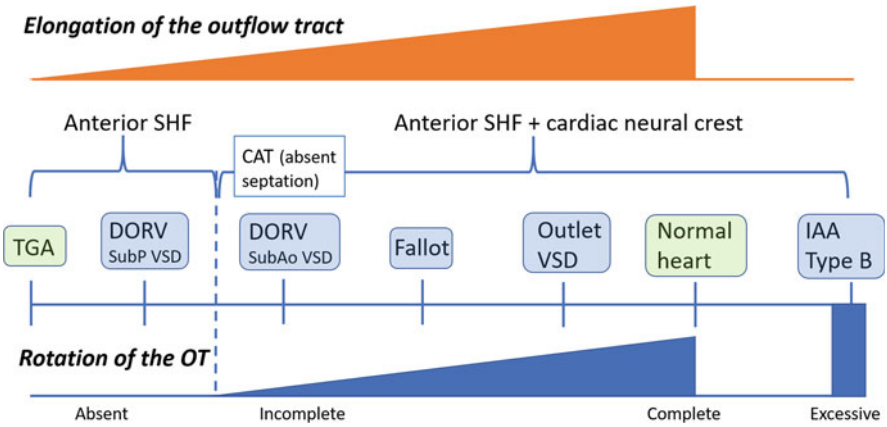

Fig. 39.1 The spectrum of the outflow tract defects, according to the proposed mechanisms of elongation and rotation of the outflow tract. *CAT* common arterial trunk; *DORV* double-outlet right ventricle; *IAA* interruption of the aortic arch; *OT* outflow tract; *SHF* second heart field; *TGA* transposition of the great arteries; *VSD* ventricular septal defect

lack of addition of the first wave of progenitor cells to the developing outflow tract by the "aortic subdomain" of the anterior second heart field [21], which would prevent "spiraling" of the outflow tract, confirming in part Goor's hypothesis (Fig. 39.1).

39.4 Chromosomal Abnormalities

(a) *Aneuploidies*
Transposition of the great arteries is exceptionally associated with common genetic syndromes such as Turner, Noonan, and Marfan syndromes [22], and is extremely rare in Down syndrome, with only a few isolated cases reported [23, 24].

(b) *Chromosomal structural mutations and copy-number variations*
Copy-number variation (CNV) refers to structural aberrations in both coding and noncoding regions of the genome, consisting of deletions or duplications of variable extent and leading to altered dosage of genes present in the region concerned by the CNV [25]. The most frequent CNV associated with CHD is 22q11 microdeletion, responsible for DiGeorge syndrome, which is associated with TGA in less than 1% of patients, contrarily to CNC-ASHF-related CHD [26].

Overall, CNV could be involved in 10% to 15% of CHD [27]. Costain et al., using high-resolution genome-wide microarrays in 83 adult patients with TGA, found 9 CNV, 4 of them having already been found in patients with tetralogy of Fallot and 1 with unspecified CHD [28]. The same team published the case of an individual patient with TGA associated with mental retardation and dysmorphic

facial features, with two rare CNV, one of them having been implied in Timothy syndrome [29]. In a recent whole-genome study about 100 patients with isolated TGA, Blue et al. find 6 CNVs, among them 2 were already described [30].

(c) *De novo mutations*

De novo mutations associated with the occurrence of CHD involve in majority chromatin modifiers [31], which account for 2.3% of all CHD [32]. Two further studies have demonstrated that de novo mutations in chromatin modifiers account for 28% of syndromic CHD [33, 34]. A mutation in a chromatin-regulating gene, MED13L (PROSIT240), has been reported in a patient with a polymalformative syndrome associating TGA, dysmorphic facial features and mental retardation [35]. A case-control genome-wide association study about 1237 patients with simple (66%) or complex (33%) TGA has recently identified the gene WNT5A on the locus 3p14.3 as a causative gene for TGA [36]. WNT5A activates the planar cell polarity signaling pathway, which is involved in development of left/right patterning, in cardiac looping and in the normal elongation of the outflow tract [37, 38]. WNT5A plays a role in cohesion of cells in the second heart field and may participate to the elongation of the outflow tract during heart development. Dysregulation of WNT5A may affect normal development of the outflow tract and increase the susceptibility to TGA [36].

39.5 Laterality and TGA

Mutations in several laterality genes, known for their role in heterotaxy, have been reported in some individuals with isolated TGA, like ZIC-3, FOXH1, and CFC1 [3, 8, 37]. These observations have led to the hypothesis that TGA could be part of the same disease spectrum as other laterality defects such as heterotaxy and ccTGA, and may be considered as a disturbance in left–right patterning expressed at the level of the outflow tract only [3, 8]. However, TGA in situs solitus and D-loop is actually rare among heterotaxy patients, compared to TGA in situs inversus and L-looped ventricles, and to ccTGA. In addition, the most frequent outflow tract anomaly associated with heterotaxy is DORV rather than TGA.

Mutations of ZIC-3, a transcription factor, have been reported in three patients with TGA, but only one of them had an isolated TGA, one having heterotaxy and the third one a ccTGA [39]. Heterozygous mutations of Nodal and GDF1, two TGFβ members involved in left–right axis establishment in the mouse [40] have been described in cases of familial TGA [41, 42]. Another gene involved in left–right signaling, MEGF8, has been associated with TGA in patients with Carpenter syndrome [43]. However, no causal mutations of PITX2, a gene involved in left–right patterning and associated with TGA in mice, could be found in 96 patients with isolated TGA, although several SNPs in coding and noncoding regions were found [44]. Two other studies found Pitx2 loss-of-function mutations in patients with TGA but also in healthy probands, suggesting an incomplete penetrance [45, 46]. All these results suggest that the hypothesis of a laterality anomaly at the origin of TGA may

not be the predominant mechanism involved in pathogenesis of TGA {S,D,D} but be one of the mechanisms involved in pathogenesis of TGA {I,D,D} and in ccTGA [40].

39.6 Cilia and TGA

Mutations in ciliary genes are increasingly recognized as a cause of congenital heart defects, leading to anomalies of both primary (nonmotile) cilia and motile cilia. In a recent study, Liu et al. performed whole-exome sequencing in 249 patients and 66 family trios including isolated TGA (60.2%), ccTGA (23.3%) and DORV TGA-type (16.5%) [4]. A total of 82 core candidate genes harboring potentially damaging de novo (11), loss of function (60), compound heterozygous (4), or X-linked recessive (7) variants were found [4]. Among them, 23% were ciliary genes, underlining the role of ciliary genes in CHD pathogenesis and particularly in TGA. This study proposes a new candidate gene for TGA, DYNC2LI1, but fails to identify potentially clinically significant variants in primary cilia dyskinesia (PCD) genes in this population.

Blue et al. performed whole-genome sequencing in 100 patients with isolated TGA, in order to look for clinically relevant genetic variants in key developmental heart expressing genes (CHD), in laterality genes involved in heterotaxy and PCD, and in key brain expressing genes which could be responsible for neurodevelopmental disorders (NDD) observed in TGA patients after switch operation [30]. After filtering and prioritization, the authors identified 24 candidate variants in CHD genes, 188 in NDD genes, and 15 variants in laterality genes. Case-control analysis revealed that TGA cases had significantly more predicted-damaging variants per proband than controls in CHD and NDD genes, but not in laterality genes. However, especially for NDD genes, most of these variants require to be biallelic to be clinically significant and, coupled to the fact that no pathogenic variants were identified in the 38 genes associated with both cardiac and neurodevelopmental issues, it is therefore unlikely that NDD associated with TGA would be due to one or several variants of these genes. Patients with TGA had also more protein-altering and silent variants in CHD and NDD genes, but less in laterality genes compared to controls [30].

Although TGA has been described in association with airway ciliary dysfunction in some patients [47], the authors did not find any biallelic causal variants in known PCD genes, and conclude that "TGA may constitute a different form of ciliary dysfunction, distinct from classic autosomal recessive PCD" [30]. A heterozygous mutation of DNAH1, a gene associated with PCD, has been described in one patient with TGA in situs solitus [48]. However, the association between TGA and genes related with PCD has been demonstrated mostly in patients with situs inversus or heterotaxy [49]. In addition, animal models knockout for ciliary genes rarely display TGA but rather atrioventricular septal defects [40].

39.7 Epigenetic Regulators

Epigenetic regulation by modifiers affecting the expression of the genes is increasingly recognized as a major determinant of various CHD, especially in syndromic forms [50]. Transposition of the great arteries is not usually associated with extracardiac abnormalities. However, a significant number of patients with TGA develop neurodevelopmental disorders [51], and the first de novo mutation found in association with TGA, involving a chromatin-regulating gene, MED13L (PROSIT240), was reported in a patient with a polymalformative syndrome associating TGA, dysmorphic facial features and mental retardation [35]. Other epigenetic alterations have not yet been reported in association with TGA, probably because TGA is rarely syndromic, and epigenetic modifiers might be mostly associated with syndromic CHD.

A recent study has compared induced pluripotent stem cells (iPSC) lines in two patients with TGA and two healthy subjects, and has differentiated them into endothelial cells (iPSC-EC) [52]. RNA sequencing and bioinformatics analysis were performed 20 days after differentiation into iPSC-EC. Of the 4672 genes identified in the two groups, 201 (4.3%) were differently expressed between TGA and normal patients, of which 62 were upregulated, and 139 were downregulated in the TGA group. The main upregulated genes included genes associated with extracellular matrix (COL1A1 and 2, LAMA4), transcription factors involved in heart morphogenesis (SIX1, TBX2 (involved in heart looping, and related to retinoic acid)), FOXC1, which plays an important role in vascular development, and two members of the histone family, HIST1H3C and HIST1H2BB. The main downregulated genes included specific endothelial markers (PECAM1, CDH5, TIE1, VEGF receptor 2 KDR), genes involved in Notch signaling (JAG2, DLL4), genes involved in gap junctions (GJA4 and 5), vascular stabilizing genes related to extracellular matrix (COL4A1 and 2, HSPG2). Some of these findings are reminiscent of some mechanisms suggested in mouse models with TGA, like an alteration of extracellular matrix of the endocardial cushions in Perlecan-null mice, and the role of retinoic acid [53, 54]. Taken as a whole, the modifications observed in the endothelial cells of TGA patients affect biological processes related to vascular development and may help to decipher the pathogenesis of TGA.

Pregestational diabetes leads to a three-fold increased risk of CHD in the fetus due to prolonged hyperglycemia during organogenesis [55]. Transposition of the great arteries as well as common arterial trunk, heterotaxy or univentricular hearts, has been reported in the offspring of affected mothers [56].

39.8 Conclusions

The genetic substrate for TGA is still far from being elucidated. It involves several intricate pathways including laterality, cilia, anterior second heart field development, and vascular development. TGA is most often an isolated and sporadic lesion, and it must be underlined that in recent studies with whole-genome or -exome sequencing

in patients with isolated TGA [30], as well in previous studies [57], no variation in one of the candidate genes reported in familial cases of TGA was found [30]. This is in favor of an oligogenic and/or polygenic etiology in the majority of TGA cases, rather than monogenic.

The difficulties of establishing the genetic determinants of pathogenesis of TGA underline, as for other CHD, the extreme importance of determining the exact phenotype of the lesion, in order not to bring additional confusion to already complex mechanisms [58].

References

1. Jacobs JP, Franklin RCG, Béland MJ, Spicer DE, Colan SD, Walters HL, Bailliard F, Houyel L, St Louis JD, Lopez L, Aiello VD, Gaynor JW, Krogmann ON, Kurosawa H, Maruszewski BJ, Stellin G, Weinberg PM, Jacobs ML, Boris JR, Cohen MS, Everett AD, Giroud JM, Guleserian KJ, Hughes ML, Juraszek AL, Seslar SP, Shepard CW, Srivastava S, Cook AC, Crucean A, Hernandez LE, Loomba RS, Rogers LS, Sanders SP, Savla JJ, Tierney ESS, Tretter JT, Wang L, Elliott MJ, Mavroudis C, Tchervenkov CI. Nomenclature for pediatric and congenital cardiac care: unification of clinical and administrative nomenclature–the 2021 international Paediatric and congenital cardiac code (IPCCC) and the eleventh revision of the international classification of diseases (ICD-11). Cardiol Young. 2021 Jul;31(7):1057–188. https://doi.org/10.1017/S104795112100281X.
2. Van Praagh R. The segmental approach to diagnosis in congenital heart disease. Birth Defects Orig Art Ser. 1972;8:4–23.
3. Goldmuntz E, Bamford R, Karkera D, de la Cruz J, Roessler E, Muenke M. CFC1 mutations in patients with transposition of the great arteries and double-outlet right ventricle. Am J Human Genet. 2002;70:776–80.
4. Liu X, Chen W, Priest JR, Fu Y, Pang K, Ma B, Liu X, Hu S, Zhou Z. Exome-based case-control analysis highlights the pathogenic role of ciliary genes in transposition of the great arteries. Circ Res. 2020;126:811–21.
5. Burn J, Brennan P, Little J, Holloway S, Coffey R, Somerville J, et al. Recurrence risks in offspring of adults with major heart defects: results from first cohort of British collaborative study. Lancet. 1998;351:311–6. https://doi.org/10.1016/S0140-6736(97)06486-6.
6. Digilio MC, Casey B, Toscano A, Calabrò R, Pacileo G, Marasini M, et al. Complete transposition of the great arteries. Patterns of congenital heart disease in familial precurrence. Circulation. 2001;104:2809–14.
7. Digilio MC, Marino B, Giannotti A, Dallapiccola B. Familial recurrence of transposition of the great arteries and intact ventricular septum. Am J Med Genet. 1997;73:93–4. https://doi.org/10.1002/(SICI)1096-8628(19971128)73:1<93:AID-AJMG20>3.3.CO;2-9.
8. De Luca A, Sarkozy A, Consoli F, Ferese R, Guida V, Dentici ML, et al. Familial transposition of great arteries caused by multiple mutations in laterality genes. Heart. 2010;96:673–7. https://doi.org/10.1136/hrt.2009.181685.
9. Unolt M, Putotto C, Silvestri LM, Marino D, Scarabotti A, Massaccesi V, Caiaro A, Versacci P, Marino B. Transposition of great arteries: new insights into the pathogenesis. Front Pediatr. 2013;1:1–7.
10. Anderson RH, Mori S, Spicer DE, Brown NA, Mohun TJ. Development and morphology of the ventricular outflow tracts. World J Pediatr Congenit Heart Surg. 2016 Sep;7(5):561–77. https://doi.org/10.1177/2150135116651114.
11. Botto LD, Lin AE, Riehl-Colarusso T, Malik S, Correa A. Seeking causes: classifying and evaluating congenital heart defects in etiologic studies. Birth Defects Res (Part A). 2007;79:714–27.

12. Mostefa-Kara M, Houyel L, Bonnet D. Anatomy of the ventricular septal defect in congenital heart defects: a random association? Orphanet J Rare Dis. 2018;13:118.
13. Mostefa-Kara M, Bonnet D, Belli E, Fadel E, Houyel L. Anatomy of the ventricular septal defect in outflow tract defects: similarities and differences. J Thorac Cardiovasc Surg. 2015;149 (682):8.
14. Ferencz C, Brenner JI, Loffredo C, Kappetein AP, Wilson PD. Transposition of great arteries: etiologic distinctions of outflow tract defects in a case-control study of risk factors. In: Clark EB, Markwald RR, Takao A, editors. Developmental mechanism of heart disease. Armonk, NY: Futura Publishing; 1995. p. 639–53.
15. Arribard N, Mostefa Kara M, Hascoët S, Bessières B, Bonnet D, Houyel L. Congenitally corrected transposition of the great arteries: is it really a transposition? An anatomical study of the right ventricular septal surface. J Anat. 2020 Feb;236(2):325–33. https://doi.org/10.1111/joa.13097.
16. Goor DA, Edwards JP. The spectrum of transposition of the great arteries: with special reference to developmental anatomy of the conus. Circulation. 1973;48:406–15.
17. De la Cruz MV, Sánchez Gómez C, Arteaga MM, Argüello C. Experimental study of the development of the truncus and the conus in the chicken embryo. J Anat. 1977;123:661.
18. De la Cruz MV, Arteaga M, Espino-Vela J, Quero-Jiménez M, Anderson RH, Diaz GF. Complete transposition of the great arteries: types and morphogenesis of ventriculoarterial discordance. Am Heart J. 1981;102:271–81.
19. Versacci P, Pugnaloni F, Digilio MC, Putotto C, Unolt M, Calcagni G, Baban A, Marino B. Some isolated cardiac malformations can be related to laterality defects. J Cardiovasc Dev Dis. 2018;5(2):24. https://doi.org/10.3390/jcdd5020024.
20. Omer SO, Alhabshan FM, Jijeh AMZ, Caimbon NC, Enriauez CC, Männer J, Yelbuz TM. Is transposition of the great arteries associated with shortening of the intrapericardial portions of the great arterial trunks? An echocardiographic analysis on newborn infants with simple transposition of the great arteries to explore an animal model-based hypothesis on human beings. J Am Heart Assoc. 2021;10:e019334. https://doi.org/10.1161/JAHA.120.019334.
21. Hikspoors JPJM, Kruepunga N, Mommen GMC, Köhler SE, Anderson RH, Lamers WH. A pictorial account of the human embryonic heart between 3.5 and 8 weeks of development. Commun Biol. 2022;5(1):226. https://doi.org/10.1038/s42003-022-03153-x.
22. Marino B. Patterns of congenital heart disease and associated cardiac anomalies in children with down syndrome. In: Marino B, Pueschel SM, editors. Heart disease in persons with down syndrome. Baltimore, MD: Paul H Brookes Publishing; 1996. p. 133–40.
23. McCay N, McCrossan B. Down syndrome and transposition of the great arteries. Cardiol Young. 2017;27(8):1630–2. https://doi.org/10.1017/S1047951117000774.
24. Mishra C, Kadiyani L, Ramakrishnan S, Sehgal T. Trisomy 21, transposition of the great arteries and abnormal myelopoiesis. Cardiol Young. 2022;32(1):142–3. https://doi.org/10.1017/S1047951121002444.
25. Zaidi S, Brueckner M. Genetics and genomics of congenital heart disease. Circ Res. 2017;120: 923–40. https://doi.org/10.1161/CIRCRESAHA.116.309140.
26. Van Mierop LHS, Kutsche LM. Cardiovascular anomalies in Di George syndrome and importance of neural crest as a possible pathogenetic factor. Am J Cardiol. 1986;58:133–7.
27. Kim DS, Kim JH, Burt AA, et al. Burden of potentially pathologic copy number variants is higher in children with isolated congenital heart disease and significantly impairs covariate-adjusted transplant-free survival. J Thorac Cardiovasc Surg. 2016;151:1147.e4–51.e4. https://doi.org/10.1016/j.jtcvs.2015.09.136.
28. Costain G, Lionel AC, Ogura L, Marshall CR, Scherer SW, Silversides CK, Bassett AS. Genome-wide rare copy number variations contribute to genetic risk for transposition of the great arteries. Int J Cardiol. 2016;204:115–21. https://doi.org/10.1016/j.ijcard.2015.11.127.
29. Costain G, Roche SL, Scherer SW, Silversides CK, Bassett AS. Rare copy number variations in an adult with transposition of the great arteries emphasize the importance of updated genetic

assessments in syndromic congenital cardiac disease. Int J Cardiol. 2016;203:516–8. https://doi.org/10.1016/j.ijcard.2015.10.216.
30. Blue GM, Mekel M, Das D, Troup M, Rath E, Ip E, et al. Whole genome sequencing in transposition of the great arteries and associations with clinically relevant heart, brain and laterality genes. Am Heart J. 2022 Feb;244:1–13. https://doi.org/10.1016/j.ahj.2021.10.185.
31. Diab NS, Barish S, Dong W, Zhao S, Allington G, Yu X, Kahle KT, Brueckner M, Jin SC. Molecular genetics and complex inheritance of congenital heart disease. Genes (Basel). 2021;12(7):1020. https://doi.org/10.3390/genes12071020.2021.
32. Zaidi S, Choi M, Wakimoto H, Ma L, Jiang J, Overton JD, Romano-Adesman A, Bjornson RD, Breitbart RE, Brown KK, et al. De novo mutations in histone-modifying genes in congenital heart disease. Nature. 2013;498:220–3.
33. Homsy J, Zaidi S, Shen Y, Ware JS, Samocha KE, Karczewski KJ, DePalma SR, McKean D, Wakimoto H, Gorham J, et al. De novo mutations in congenital heart disease with neurodevelopmental and other congenital anomalies. Science. 2015;350:1262–6.
34. Jin SC, Homsy J, Zaidi S, Lu Q, Morton S, DePalma SR, Zeng X, Qi H, Chang W, Sierant MC, et al. Contribution of rare inherited and de novo variants in 2871 congenital heart disease probands. Nat Genet. 2017;49:1593–601.
35. Muncke N, Jung C, Rüdige H, Ulmer H, Roeth R, Hubert A, Goldmuntz E, Driscoll D, Goodship J, Schön G, et al. References missense mutations and gene interruption in PROSIT240, a novel TRAP240-like gene, in patients with congenital heart defect (transposition of the great arteries). Circulation. 2003;108:2843–50.
36. Škorić-Milosavljević D, Tadros R, Bosada FM, Tessadori F, van Weerd JH, Woudstra OI, et al. Common genetic variants contribute to risk of transposition of the great arteries. Circ Res. 2022 Jan 21;130(2):166–80. https://doi.org/10.1161/CIRCRESAHA.120.317107.
37. Axelrod JD. Planar cell polarity signaling in the development of left-right asymmetry. Curr Opin Cell Biol. 2020;62:61–9. https://doi.org/10.1016/j.ceb.2019.09.002.
38. Li D, Wang J. Planar cell polarity singling in mammalian cardiac morphogenesis. Pediatr Cardiol. 2018;39:1052–62. https://doi.org/10.1007/s0024.6-018-1860-5.
39. D'Alessandro LC, Latney BC, Paluru PC, Goldmuntz E. The phenotypic spectrum of ZIC3 mutations includes isolated d-transposition of the great arteries and double outlet right ventricle. Am J Med Genet A. 2013 Apr;161A(4):792–802. https://doi.org/10.1002/ajmg.a.35849.
40. De Ita M, Cisneros B, Rosas-Vargas H. Genetics of transposition of great arteries: between laterality abnormality and outflow tract defect. J Cardiovasc Transl Res. 2021 Jun;14(3):390–9. https://doi.org/10.1007/s12265-020-10064-x.
41. Mohapatra B, Casey B, Li H, Ho-Dawson T, Smith L, Fernbach SD, et al. Identification and functional characterization of NODAL rare variants in heterotaxy and isolated cardiovascular malformations. Hum Mol Genet. 2009;18:861–71. https://doi.org/10.1093/hmg/ddn411.
42. Luca D, Karkera JD, Lee JS, Roessler E, Banerjee-Basu S, Ouspenskaia MV, Mez J, et al. Loss-of-function mutations in growth differentiation factor-1 (GDF1) are associated with congenital heart defects in humans. Am J Hum Genet. 2007;81(5):987–94. https://doi.org/10.1086/522890.
43. Twigg SR, Lloyd D, Jenkins D, Elcioglu NE, Cooper CD, Al-Sannaa N, et al. Mutations in multidomain protein MEGF8 identify a carpenter syndrome subtype associated with defective lateralization. Am J Hum Genet. 2012;91(5):897–905. https://doi.org/10.1016/j.ajhg.2012.08.027.
44. Muncke N, Niesler B, Roeth R, Schön K, Rüdiger HJ, Goldmuntz E, Goodship J, Rappold G. Mutational analysis of the PITX2 coding region revealed no common cause for transposition of the great arteries (dTGA). BMC Med Genet. 2005;6:20. https://doi.org/10.1186/1471-2350-6-20.2005.
45. Wei D, Gong XH, Qiu G, Wang J, Yang YQ. Novel PITX2c loss-of-function mutations associated with complex congenital heart disease. Int J Mol Med. 2014;33(5):1201–8. https://doi.org/10.3892/ijmm.2014.1689.

46. Zhao CM, Peng LY, Li L, Liu XY, Wang J, Zhang XL, et al. PITX2 loss-of-function mutation contributes to congenital endocardial cushion defect and Axenfeld-Rieger syndrome. PLoS One. 2015;10(4):e0124409. https://doi.org/10.1371/journal.pone.0124409.
47. Zahid M, Bais A, Tian X, et al. Airway ciliary dysfunction and respiratory symptoms in patients with transposition of the great arteries. PLoS One. 2018;13:e0191605.
48. Kurtz JD, Boucek K, Kavarana M, Atz AM. Two brothers with dextro-transposition of the great arteries. World J Pediatr Congenit Heart Surg. 2020;11:NP155–7. https://doi.org/10.1177/2150135118768718.
49. Bitar FF, Shbaro R, Mroueh S, Yunis K, Obeid M. Dextrocardia and corrected transposition of the great arteries (I,D,D) in a case of Kartagener's syndrome: a unique association. Clin Cardiol. 1998;21:298–9.
50. Moore-Morris T, van Vliet PP, Andelfinger G, Puceat M. Role of epigenetics in cardiac development and congenital diseases. Physiol Rev. 2018 Oct 1;98(4):2453–75. https://doi.org/10.1152/physrev.00048.2017.
51. Kasmi L, Bonnet D, Montreuil M, Kalfa D, Geronikola N, Bellinger DC, Calderon J. Neuropsychological and psychiatric outcomes in dextro-transposition of the great arteries across the lifespan: a state-of-the-art review. Front Pediatr. 2017;5:59. https://doi.org/10.3389/fped.2017.00059. eCollection 2017
52. Ontoria-Oviedo I, Földes G, Tejedor S, Panadero J, Kitani T, Vázquez A, Wu JC, Harding SE, Sepúlveda P. Modeling transposition of the great arteries with patient-specific induced pluripotent stem cells. Int J Mol Sci. 2021 Dec 9;22(24):13270. https://doi.org/10.3390/ijms222413270.
53. Costell M, Carmona R, Gustafsson E, González-Iriarte M, Fässler R, Muñoz-Chápuli R. Hyperplastic Conotruncal endocardial cushions and transposition of great arteries in Perlecan-null mice. Circ Res. 2002;91:158–64.
54. Yasui H, Nakazawa M, Morishima M, Miyagawa-Tomita S, Momma K. Morphological observations on the pathogenetic process of transposition of the great arteries induced by retinoic acid in mice. Circulation. 1995;91:2478–86.
55. Leirgul E, Brodwall K, Greve G, Vollset SE, Holmstrøm H, Tell GS, Øyen N. Maternal diabetes, birth weight, and neonatal risk of congenital heart defects in Norway, 1994–2009. Obstet Gynecol. 2016;128:1116–25.
56. Lisowski LA, Verheijen PM, Copel JA, Kleinman CS, Wassink S, Visser GHA, Meijboom E-J. Congenital heart disease in pregnancies complicated by maternal diabetes mellitus. An international clinical collaboration, literature review, and meta-analysis. Herz. 2010;35:19–26.
57. Lei LM, Lin HM, Zhong SL, et al. Analysis of mutations in 7 candidate genes for dextro-transposition of the great arteries in Chinese population. J Thorac Dis. 2014;6:491–6.
58. Silvestri LM, Scarabotti A, Marino B. Challenges of classifying double outlet right ventricle: importance for genotype-phenotype analyses. Am J Med Gen Part A. 2014;164A:1340. https://doi.org/10.1002/ajmg.a.36448.

Molecular Pathways and Animal Models of d-Transposition of the Great Arteries

40

Eleanor Gill and Simon D. Bamforth

Abstract

During normal cardiovascular development, the outflow tract becomes septated and rotates so that the separate aorta and pulmonary trunk are correctly aligned with the left and right ventricles, respectively. However, when this process goes wrong, the aorta and pulmonary trunk are incorrectly positioned, resulting in oxygenated blood being directly returned to the lungs, with deoxygenated blood being delivered to the systemic circulation. This is termed transposition of the great arteries (TGA). The precise etiology of TGA is not known, but the use of animal models has elucidated that genes involved in determination of the left–embryonic body axis play key roles. Other factors such as retinoic acid levels are also crucial. This chapter reviews the animal models presenting with TGA that have been generated by genetic manipulation or with exogenous agents.

Keywords

Transposition of the great arteries · Left–right patterning · Congenital heart defects · Model organisms · Heterotaxy · Genetics · Nodal signaling pathway · Neural crest cells · Retinoic acid · Diabetes

40.1 Introduction

Transposition of the great arteries (TGA), also known as discordant ventriculoarterial connections, is a congenital heart defect affecting the emergence of the aorta and pulmonary trunk from the heart. In the normal configuration, the

E. Gill · S. D. Bamforth (✉)
Newcastle University Biosciences Institute, Newcastle, UK
e-mail: simon.bamforth@newcastle.ac.uk

© The Author(s), under exclusive license to Springer Nature Switzerland AG 2024

S. Rickert-Sperling et al. (eds.), *Congenital Heart Diseases: The Broken Heart*,
Advances in Experimental Medicine and Biology 1441,
https://doi.org/10.1007/978-3-031-44087-8_40

aorta will arise from the left ventricle to deliver oxygenated blood to the systemic circulation, while the pulmonary trunk will arise from the right ventricle to take blood to the lungs for oxygenation. However, in TGA these major vessels have been transposed so that the aorta and pulmonary trunk are situated above the right and left ventricles, respectively. Consequently, the aorta takes deoxygenated blood from the right ventricle to the systemic circulation, while the pulmonary trunk shuttles oxygenated blood to the lungs and back to the left atrium. This is therefore a serious heart defect and survival is dependent on the mixing of blood within the heart, usually by septal defects. TGA appears to be caused by a failure of the outflow tract to rotate so the aorta and pulmonary trunk do not spiral and form two parallel vessels that are aligned to the incorrect ventricles.

Animal models have been produced that mimic TGA (Fig. 40.1), and these are restricted to the mouse and chick as the anatomy of the cardiac outflow tract is analogous to that of the human. However, the development of TGA is often not highly penetrant and not seen consistently within the same animal model. This makes the molecular pathways underlying the cause of TGA very difficult to identify. A number of causes for TGA in animal models have been proposed, including environmental factors such as those affecting retinoic acid (RA) and glucose levels, and genetic mutations affecting the left–right patterning pathway.

40.2 Genetic Causes of TGA

40.2.1 Heterotaxy

Despite many human syndromes presenting with some form of cardiovascular defect, TGA is extremely rare in any syndrome except for heterotaxy [2]. TGA, however, may be sporadically associated with VACTERL syndrome [3]. Mutant mice with a deletion of a gene associated with this syndrome, *Pcsk5,* have TGA and double-outlet right ventricle (DORV) [4]. Heterotaxy is a rare congenital defect where the major organs are positioned abnormally within the body (see Chaps. 37 and 38). In the normal body, the position of the organs is called *situs solitus*, but when the organs are found in a mirror image configuration it is known as *situs inversus*. When the reversal of organs is incomplete, however, this is known as *situs ambiguous* and can have profound effects on the formation of the heart and lungs. For example, in a mutant mouse line known as *iv/iv* (*inversus viscerum*), half of all mutant mice present with *situs inversus*, associated with complex cardiac malformations, including TGA [5]. Indeed, it is considered that defects in the establishment of the left–right axis almost always result in complex congenital heart malformations [6].

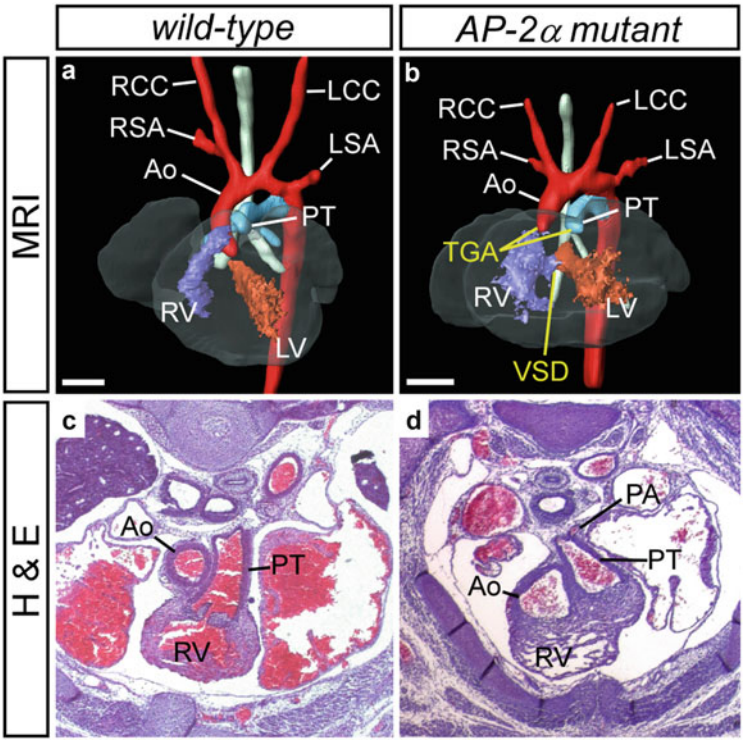

Fig. 40.1 Mutant mouse model displaying transposition of the great arteries (TGA)**.** 3-D reconstructions from MRI datasets (**a, b**) and H&E sections (**c, d**) of E15.5 fetuses. **a, c,** By E15.5, the heart and its associated great vessels have developed into the mature configuration with the aorta (Ao) arising from the left ventricle (LV) and the pulmonary trunk (PT) arising from the right ventricle (RV). **b, d,** The heart of a fetus mutated for AP-2α presents with TGA [1], whereby the Ao arises from the RV and the PT arises from the LV. Note how the two arteries lie in parallel (**b**) rather than spiral around each other (as shown in **a**). The presence of a pulmonary artery (PA) joining the PT is indicated (**d**) as is a VSD (**b**). Other abbreviations: LCC, left common carotid; LSA, left subclavian artery; RCC, right common carotid; RSA, right subclavian artery. Scale, 500 μm

40.2.2 Dysregulation of Left–Right Patterning Genes

The establishment of laterality in the embryo is conducted through the asymmetric and transient expression of TGFβ-related proteins that are both positively and negatively regulated (Fig. 40.2). This pathway begins in the node, a pit at the end of the primitive streak containing cells with posterior-tilting cilia whose clockwise rotation initiates left–right determination [8]. The cilia are localized on the posterior portion of the apical surface of each nodal cell and display a morphological planar polarization. Planar cell polarity (PCP) regulates the polarity of epithelial cells in relation to their apical–basal axis [9], and PCP proteins are responsible for regulating planar polarity within the node [10]. As the polarity and function of nodal cilia is

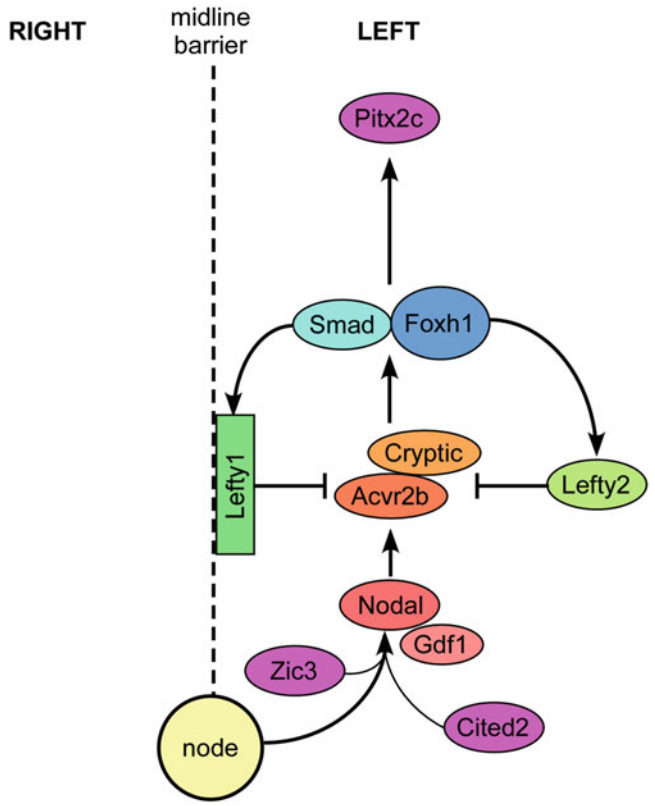

Fig. 40.2 Signaling molecules involved in the establishment of laterality. Nodal is expressed in the node from where it is transferred to the left lateral plate mesoderm (LLPM) by Cited2 and Zic3, forming a Gdf1-Nodal heterodimer. Nodal signals through type I and type II TGFβ receptors (e.g., *Acvr2b*) and the coreceptor Cryptic. Smad proteins, along with Foxh1, transduce the Nodal signal, and in response Lefty1 and Lefty2 are expressed asymmetrically in the LLPM. The Lefty proteins inhibit Nodal signaling by competitively interacting with Cryptic and the type II TGFβ receptor, thereby acting as antagonists of Nodal, and restricting its expression to the LLPM. The Nodal signaling pathway results in the induction of genes involved in left–right patterning, e.g., *Pitx2c*. Adapted from [7]

critical for establishing the left–right signaling pathway, it is perhaps not surprising that left–right patterning defects leading to TGA can be found in some mutant mouse models mutated for PCP genes. For example, half of all mice deficient for the PCP gene *Disheveled 2* (*Dvl2*) die from defects in outflow tract development that include TGA, DORV and common arterial trunk [11, 12]. (More information on common arterial trunk is provided in Chap. 52) The defects observed in *Dvl2* mutant mice are more penetrant in mice doubly homozygous for *Disheveled 1* and *Dvl2*. Cardiac outflow tract defects are also seen in mice mutated for *Scrib* (*Circletail, Crc*), another PCP gene [13]. The defects observed include TGA, as well as DORV, aberrant right

subclavian artery and atrioventricular septal defect. These studies highlight the importance of PCP in establishing the localization of cilia on nodal cells.

In the early mouse embryo (around E7.5 of gestation), cilia in the center of the pit, known as nodal cilia, rotate in a clockwise manner to induce a leftward nodal flow, initiating the left–right axis determination process. Mutations in genes involved in ciliary rotation can prevent left–right determination and therefore contribute to TGA. In *iv/iv* embryos, the nodal cilia are immotile because of a mutation in the gene encoding the motor protein left–right dynein (*Dnah11*) [14–16]. This corresponds with human studies, in which the high mutation rate of *DNAH11* is associated with heterotaxy and congenital heart defects [17]. While these *Dnah11*-positive nodal cilia are critical for rotating and initiating the left–right determination process, peripheral nodal cells, known as "crown cells" possess immotile *Dnah11*-negative cilia that respond to mechanical stimuli such as flow to regulate laterality [18, 19]. *Nodal* is expressed on the left side of the perinodal crown cells and is important in left determination. In mutant mice specifically lacking *Nodal* activity within the node, left–right patterning defects include the improper localization of the stomach, right pulmonary isomerism and randomization of heart looping resulting in TGA [18]. Nodal is therefore critical for left–right determination in the node, and its activity is greatly increased through coexpression with growth differentiation factor-1 (*Gdf1*). *Gdf1*-null embryos die before birth or in the immediate perinatal period, and present with aberrant ciliogenesis, incorrect formation of the left–right axis and cardiovascular defects including TGA [20, 21]. Expression of Gdf1 in perinodal cells requires Sonic hedgehog (Shh) signaling, and mice with a mutation in the hedgehog gene *Smoothened* (*Smo*) exhibit loss of Gdf1 expression and TGA [22]. Additionally, *Cerl2*, a *Nodal* antagonist, is expressed in a horseshoe pattern on the right side of the perinodal crown cells, where it inhibits Nodal signaling and leftward determination, possibly by inhibiting the interaction between Nodal and Gdf1 [23]. *Cerl2* mRNA is degraded in left crown cells following activation of the Hedgehog protein Wnt3 by leftward nodal flow [24]. Interestingly, in *iv/iv* embryos, the asymmetric expression of *Nodal* is reversed: *Nodal* is expressed on the right while *Cerl2* is expressed on the left [23, 25, 26]. Moreover, *Cerl2*-null mice exhibit randomized left–right asymmetry and TGA [23]. These mouse models demonstrate that immotile peripheral nodal cells are important in determining left–right signaling during embryogenesis, while genetic mutations in perinodal genes contribute to TGA.

Following expression in the node, Nodal is subsequently transferred to the left lateral plate mesoderm (LLPM), where it further promotes *Nodal* expression [18, 27]. Nodal dimerizes with Gdf1 in the LLPM to induce downstream gene expression, and in *Smo*-deficient mice *Gdf1* is undetectable in the node, and Nodal itself is not expressed in the LLPM [21, 22]. Cited2 is a transcriptional coactivator that controls expression of left–right determining genes, and *Cited2*-null mice lack *Nodal* expression in the LLPM and present with left–right patterning defects and cardiovascular abnormalities including TGA [28, 29]. Cited2 binds to the *Nodal* asymmetric enhancer element to drive *Nodal* transcription to the LLPM, and this expression may be enhanced by Cited2 forming a complex with FoxH1 and Smad

proteins [30]. Conditional deletion of *Cited2* from the mesoderm and epiblast causes laterality defects and TGA [31]. *Zic3* is expressed in the mesoderm, and when deleted in mice, the transfer of Nodal from the node to the LLPM is inhibited, resulting in randomized expression of left–right determining genes and TGA [32].

While in the LLPM, Nodal signaling results in the induction of genes that, when mutated in mice, result in left–right patterning defects including TGA. Nodal signals through type I and type II TGFβ receptors such as the type II receptor *Acvr2b*. Mice lacking *Acvr2b* have left–right patterning defects and TGA [33]. Cryptic is an EGF-CFC (epidermal growth factor–Cripto-FRL1-Cryptic) family protein that acts as a coreceptor for Nodal that allows phosphorylation and activation of type I TGFβ receptors, and mice lacking Cryptic also exhibit left–right patterning defects and TGA [34]. Functional type I and II TGFβ receptors also phosphorylate Smad proteins, which transduce the Nodal signal. Mutant mice lacking *Smad2* die early in development from defects in gastrulation [35], and mice heterozygous for both *Smad2* and *Nodal* (i.e., $Smad2^{+/-};Nodal^{+/-}$), display TGA associated with right pulmonary isomerism of the lung, in more than 50% of cases [35]. Together this demonstrates that Nodal receptor activation and signal transduction by Smad proteins is critical in maintaining leftward expression, dysregulation of which contributes to TGA.

In response to Smad2 signaling, Foxh1 induces asymmetric Lefty1 and Lefty2 expression in the LLPM. The Lefty proteins inhibit Nodal signaling by competitively interacting with Cryptic and Acvr2b, thereby acting as antagonists of Nodal, and restricting its expression to the LLPM. Lefty1 is expressed at the midline and is thought to act as a physical barrier preventing the movement of left-sided proteins across to the right LPM. *Foxh1*-null mice present with a hypoplastic outflow tract, and any surviving mice present with DORV or TGA [36]. Mutant mice lacking *Lefty1* have left–right patterning defects, such as left pulmonary isomerism and misalignment of the cardiac outflow tract resulting in TGA, as well as DORV [37]. Other cardiovascular malformations include VSD, ASD and common atrioventricular canal. Mice null for *Lefty2* die early during embryogenesis, but this can be overcome through the creation of an alternative allele in mutant mice. Deletion of the *Lefty2* asymmetric enhancer element prevents these early gastrulation defects, but also prevents the asymmetric expression of Lefty2 in the LLPM at the early somite stage [38]. In these mutant mice, visceral *situs* abnormalities were identified along with cardiovascular defects including TGA, as well as DORV and aberrant great arteries. The *Lefty* genes are therefore important in maintaining leftward expression, and improper leftward expression contributes to TGA.

One of the last genes in the left–right determination cascade is *Pitx2c*. The paired-like homeobox transcription factor gene, *Pitx2* has four known isoforms: *Pitx2a* and *Pitx2b* are expressed symmetrically in the brain, whereas the *Pitx2c* isoform is expressed asymmetrically in the LLPM [39]. *PITX2D* has only been identified in humans [40]. *Pitx2c*, a direct target of Nodal, is expressed at the end of the cascade of laterality genes and therefore the last effector for transmitting positional information from the LLPM to distinct organs, such as the heart, that develop asymmetrically *[7, 41, 42]*. Transgenic mice null for *Pitx2c* display conotruncal defects with rotational

anomalies, leading to TGA [43]. Unlike previous leftward genes, *Pitx2c* expression is maintained throughout development and it is still present in the outflow tract and is therefore critical in ensuring correct positioning of the great vessels.

40.2.3 Gene Expression in the Heart Fields

Asymmetric gene expression in precardiogenic cells is maintained as the LPM splits into the dorsal somatic mesoderm and the ventral splanchnic mesoderm, from which the first heart field (FHF) and second heart field (SHF) derive. The left ventricle derives from the FHF, which initially forms as the heart tube which is structurally symmetrical although it becomes asymmetrical as it bends ventrally and to the right. The SHF lies medially and dorsally to the FHF and consists of pharyngeal mesoderm-derived cardiac progenitor cells that contribute to the formation of the right ventricle, outflow tract and atria [44]. Progenitor cells from the SHF, particularly in the anterior region of the second heart field (AHF), are therefore critical in outflow tract formation. Mouse mutants in which genes are crucial for conotruncal development have been conditionally deleted from the SHF, may display TGA. For example, *Wnt11* is involved in proliferation and cell patterning, and both global and SHF-specific *Wnt11* deletion results in TGA, likely due to reduced cellular proliferation within the SHF [45, 46]. *Mef2c* is a transcription factor that promotes cardiomyocyte differentiation, and conditional deletion of *Mef2c* from the AHF results in TGA. [47]. *Prdm1* is a transcriptional repressor expressed in the pharyngeal arches, and removal of *Prdm1* from the mesoderm, which encompasses the SHF, is associated with improper formation of the pharyngeal arch arteries and the appearance of TGA [48]. *Fgf8* is critical at many stages of cardiac development, and mutant mice hypomorphic for *Fgf8* display TGA [49]. Conditional deletion of *Fgf8* from the AHF mesoderm also prevents correct alignment of the outflow tract and ventricles leading to TGA [50]. In the chick, TGA can be induced by blocking Fgf8 signaling with an Fgf8 receptor antibody [51]. This prevents adequate myocardium being added to the outflow tract resulting in a malalignment of the arterial pole. These mouse models, therefore, demonstrate how perturbation of SHF development prevents correct alignment of the outflow tract resulting in TGA.

40.2.4 TGA without Left–Right Patterning Defects

Model organisms may also display the TGA phenotype in the absence of overt laterality defects. For example, mice mutated for AP-2α also display TGA coincident with increased ectodermal apoptosis in the caudal pharyngeal arches and incorrect rotation of the outflow tract cushions [1] (Fig. 40.1). Additionally, fetuses from mice mutated for *Perlecan* present with a high incidence of TGA in the absence of other laterality defects [52]. It appears that TGA in this model is a consequence of excess mesenchyme preventing proper outflow tract rotation and thereby producing discordant ventriculoarterial alignment.

40.2.5 Neural Crest Cells

Cardiac neural crest cells (NCCs) migrate to the distal part of the outflow tract from the pharyngeal arches where they participate in septation of the arterial and pulmonary trunks. Although NCCs appear to regulate pharyngeal arch growth factor availability which affects addition of myocardium from the SHF to the outflow tract, some mutant mouse models affecting NCC migration do present with TGA.

Endothelin promotes migration of cardiac NCCs to the outflow tract, and mutant mice null for the endothelin A receptor (*Ednra*) display craniofacial, aortic arch and outflow tract defects, which include TGA [53]. Deletion of *Fgf8* from the ectoderm also prevents cardiac neural crest cell migration, which contributes to TGA [54]. Pdgfrα signaling in endothelial-derived mesenchyme influences neural crest behavior, and when *Pdgfrα* is conditionally deleted from endothelial and endocardial lineages using *Tie2Cre*, conotruncal defects including TGA are observed [55].

40.3 Environmental Causes of TGA

40.3.1 Retinoic Acid

It appears that the most reliable method of causing TGA in a mouse model is to administer pregnant mice with retinoic acid (RA) or with RA inhibitors [2]. RA is a very important molecule during development, and disruptions in the amounts produced, whether increased or decreased, can be severely teratogenic. The cardiovascular system is particularly sensitive to RA levels and a range of phenotypes affecting the heart and great arteries can be observed in affected mouse embryos. However, as discussed above, TGA is only seen in patients with heterotaxy, but mouse models with disrupted RA levels do not appear to show any other aspects of a heterotaxy-like phenotype. The administration of all-*trans* RA to pregnant females at E8.5 of gestation has been demonstrated to result in three-quarters of the fetuses presenting with TGA [56]. A smaller proportion had DORV and defects in the great arteries were also observed. RA contributes to TGA by impairing the development of the AHF in mouse embryos, resulting in reduced expression of critical genes such as *Fgf8* and *Isl1* [57]. TGA is also produced by a reduction in RA levels through the administration of the retinoic acid antagonist BMS-189453 to pregnant females [58]. This is a synthetic retinoid that acts as an antagonist of the RA receptors alpha, beta, and gamma. Following administration of this compound to pregnant females at E7.5, cardiovascular malformations were identified in three-quarters of the embryos, with two-thirds of these displaying TGA. The transposition phenotype is much more prevalent than DORV. This suggests that RA depletion is a key factor in the misalignment of the outflow tract. Timing of the administration of BMS-189453 appears to be critical as exposure earlier or later than ~E7.5 results in much lower rates of TGA. Interestingly, of those embryos with TGA, the aorta was displaced to a right-sided, anterior position in comparison to the pulmonary

trunk in the majority of embryos (60%), while a smaller proportion showed the great arteries positioned side-by-side (40%) [58].

Treating pregnant females with folic acid (FA) during pregnancy was found to reduce the teratogenic effects of BMS-189453 [59]. Cardiovascular malformations, including the incidence of TGA, were significantly reduced in embryos collected from the FA-treated pregnant females compared to BMS-treated controls. Additionally, a substantial reduction in the levels of neural tube defects and thymus defects was also observed. To further understand the genetic changes induced by varying the levels of RA signaling during development, a microarray experiment was designed to analyze the genes that were differentially expressed between wild type and BMS-treated embryos, and between BMS-treated offspring and those from females that were treated with FA during pregnancy [60]. *Hif1α* was found to be down-regulated in BMS-treated embryos, compared to wild type, but up-regulated in those embryos pretreated with FA. Additionally, an RA response element (RARE) was identified in the promoter region of mouse *Hif1α*, suggesting that this is a downstream target of RA signaling, which can be rescued by FA treatment [60]. In a separate study, mice null for *Folr1,* a folate-binding protein gene, died at mid-embryogenesis from extensive cell death. However, FA supplementation of pregnant females greatly reduced this early embryonic lethality and allowed for *Folr1*-null mice to be born and bred [61]. Examination of $Folr1^{-/-}$ fetuses from matings between *Folr1*-null mice identified cardiovascular defects including TGA. In a further study, the outflow tract myocardium in RA treated embryos was found to have downregulation of the *Tbx2-Tgfb2* signaling pathway [62]. This is thought to impact on the development of the outflow tract cushions, through the impaired migration of mesenchymal cells, preventing the establishment of normal ventriculoarterial connections.

40.3.2 Diabetes

Glucose is the most important nutrient for heart growth in the developing embryo, and its uptake is synonymous with maternal blood glucose levels [63]. Its continuous uptake is enabled through expression of the insulin-independent glucose transporter GLUT1 on the fetal basement membrane and maternal microvillus [63]. While this is critical in ensuring adequate glucose supply to the developing fetus, maternal diabetes is associated with a three-fold increase in fetal Glut1 expression, associated with fetal hyperglycemia and a two to five-fold increase in congenital heart defects [63, 64]. Moreover, *Glut1* expression is usually downregulated in the fetal heart after E10.5, while Glut1 expression remains high in the fetal heart in of diabetic mothers [65]. The consequent intracellular hyperglycemia in the fetal heart is associated with increased superoxide (O_2^-) production and oxidative stress, which is associated with TGA [66].

Diabetes can be induced in mice through injection of streptozotocin (STZ), a drug that destroys pancreatic β-cells to prevent insulin release. STZ-induced diabetes promotes fetal hyperglycemia and this is sufficient to promote birth defects in

embryos, including TGA [67, 68]. This is in part due to dysregulation of laterality genes: rodent models of maternal diabetes are associated with knockdown of *Gdf1* and *Nodal* in the node, as well as *Nodal*, *Cited2* and *Pitx2c* in the LLPM [69–71]. Moreover, rodent fetal hearts exposed to maternal diabetes exhibit decreased Dvl2 phosphorylation and decreased Wnt5a activity [72]. Treatment of diabetic rodents with vitamin E prevented hyperglycemia-induced TGA in their fetuses [70, 73].

40.4 Concluding Remarks

TGA occurs in the developing mammalian heart when the outflow tract fails to rotate correctly resulting in the great arteries becoming misaligned with the correct ventricles. Experimental models have demonstrated that the developing embryo is extremely sensitive to RA levels; an excess of, or too little, RA results in a high incidence of TGA. Moreover, maternal diabetes promotes fetal hyperglycemia, associated with congenital heart defects including TGA. In mutant mouse models, the genetic manipulation of factors necessary for establishing the left–right asymmetry pathway often results in a malrotation of the developing outflow tract resulting in TGA. As some mutant mouse models also display TGA without heterotaxy, however, this suggests that the manifestation of TGA may be the only phenotype seen that is typical of an overt left-right patterning defect.

Acknowledgments We thank the British Heart Foundation for funding our research.

References

1. Johnson AL, Schneider JE, Mohun TJ, Williams T, Bhattacharya S, Henderson DJ, et al. Early Embryonic Expression of AP-2α Is Critical for Cardiovascular Development. J Cardiovasc Dev Dis. 2020;7(3)
2. Unolt M, Putotto C, Silvestri LM, Marino D, Scarabotti A, Valerio M, et al. Transposition of great arteries: new insights into the pathogenesis. Frontiers in pediatrics. 2013;1:1–11.
3. Debost-Legrand A, Goumy C, Laurichesse-Delmas H, Déchelotte P, Perthus I, Francannet C, et al. Prenatal diagnosis of the VACTERL association using routine ultrasound examination. Birth Defects Research Part A: Clinical and Molecular Teratology. 2015;103(10):880–6.
4. Szumska D, Pieles G, Essalmani R, Bilski M, Mesnard D, Kaur K, et al. VACTERL/caudal regression/Currarino syndrome-like malformations in mice with mutation in the proprotein convertase Pcsk5. Genes Dev. 2008;22(11):1465–77.
5. Icardo JM, Sanchez de Vega MJ. Spectrum of heart malformations in mice with situs solitus, situs inversus, and associated visceral heterotaxy. Circulation. 1991;84(6):2547–58.
6. Ramsdell AF. Left-right asymmetry and congenital cardiac defects: getting to the heart of the matter in vertebrate left-right axis determination. Dev Biol. 2005;288(1):1–20.
7. Shiratori H, Hamada H. TGFbeta signaling in establishing left-right asymmetry. Seminars in cell & developmental biology. 2014;32:80–4.
8. Nonaka S, Yoshiba S, Watanabe D, Ikeuchi S, Goto T, Marshall WF, et al. De novo formation of left-right asymmetry by posterior tilt of nodal cilia. PLoS Biol. 2005;3(8):e268.

9. Axelrod JD. Progress and challenges in understanding planar cell polarity signaling. Seminars in cell & developmental biology. 2009;20(8):964–71.
10. Antic D, Stubbs JL, Suyama K, Kintner C, Scott MP, Axelrod JD. Planar cell polarity enables posterior localization of nodal cilia and left-right axis determination during mouse and Xenopus embryogenesis. PloS one. 2010;5(2):e8999.
11. Hamblet NS, Lijam N, Ruiz-Lozano P, Wang J, Yang Y, Luo Z, et al. Dishevelled 2 is essential for cardiac outflow tract development, somite segmentation and neural tube closure. Development. 2002;129(24):5827–38.
12. Sinha T, Wang B, Evans S, Wynshaw-Boris A, Wang J. Disheveled mediated planar cell polarity signaling is required in the second heart field lineage for outflow tract morphogenesis. Dev Biol. 2012;370(1):135–44.
13. Phillips HM, Rhee HJ, Murdoch JN, Hildreth V, Peat JD, Anderson RH, et al. Disruption of planar cell polarity signaling results in congenital heart defects and cardiomyopathy attributable to early cardiomyocyte disorganization. Circ Res. 2007;101(2):137–45.
14. Nonaka S, Shiratori H, Saijoh Y, Hamada H. Determination of left-right patterning of the mouse embryo by artificial nodal flow. Nature. 2002;418(6893):96–9.
15. Okada Y, Nonaka S, Tanaka Y, Saijoh Y, Hamada H, Hirokawa N. Abnormal nodal flow precedes situs inversus in iv and inv. mice. Molecular cell. 1999;4(4):459–68.
16. Supp DM, Witte DP, Potter SS, Brueckner M. Mutation of an axonemal dynein affects left-right asymmetry in inversus viscerum mice. Nature. 1997;389(6654):963–6.
17. Liu S, Chen W, Zhan Y, Li S, Ma X, Ma D, et al. DNAH11 variants and its association with congenital heart disease and heterotaxy syndrome. Sci Rep. 2019;9(1):6683.
18. Brennan J, Norris DP, Robertson EJ. Nodal activity in the node governs left-right asymmetry. Genes Dev. 2002;16(18):2339–44.
19. Goetz SC, Anderson KV. The primary cilium: a signalling centre during vertebrate development. Nat Rev. Genet. 2010;11(5):331–44.
20. Botilde Y, Yoshiba S, Shinohara K, Hasegawa T, Nishimura H, Shiratori H, et al. Cluap1 localizes preferentially to the base and tip of cilia and is required for ciliogenesis in the mouse embryo. Dev Biol. 2013;381(1):203–12.
21. Rankin CT, Bunton T, Lawler AM, Lee S-J. Regulation of left-right patterning in mice by growth/differentiation factor-1. Nat Genet. 2000;24(3):262–5.
22. Zhang XM, Ramalho-Santos M, McMahon AP. Smoothened mutants reveal redundant roles for Shh and Ihh signaling including regulation of L/R asymmetry by the mouse node. Cell. 2001;105(6):781–92.
23. Marques S, Borges AC, Silva AC, Freitas S, Cordenonsi M, Belo JA. The activity of the Nodal antagonist Cerl-2 in the mouse node is required for correct L/R body axis. Genes Dev. 2004;18 (19):2342–7.
24. Nakamura T, Saito D, Kawasumi A, Shinohara K, Asai Y, Takaoka K, et al. Fluid flow and interlinked feedback loops establish left-right asymmetric decay of Cerl2 mRNA. Nat Commun. 2012;3:1322.
25. Collignon J, Varlet I, Robertson EJ. Relationship between asymmetric nodal expression and the direction of embryonic turning. Nature. 1996;381(6578):155–8.
26. Oki S, Kitajima K, Marques S, Belo JA, Yokoyama T, Hamada H, et al. Reversal of left-right asymmetry induced by aberrant Nodal signaling in the node of mouse embryos. Development. 2009;136(23):3917–25.
27. Saijoh Y, Oki S, Ohishi S, Hamada H. Left-right patterning of the mouse lateral plate requires nodal produced in the node. Dev Biol. 2003;256(1):160–72.
28. Bamforth SD, Braganca J, Eloranta JJ, Murdoch JN, Marques FI, Kranc KR, et al. Cardiac malformations, adrenal agenesis, neural crest defects and exencephaly in mice lacking Cited2, a new Tfap2 co-activator. Nat Genet. 2001;29(4):469–74.
29. Bamforth SD, Braganca J, Farthing CR, Schneider JE, Broadbent C, Michell AC, et al. Cited2 controls left-right patterning and heart development through a Nodal-Pitx2c pathway. Nat Genet. 2004;36(11):1189–96.

30. Lopes Floro K, Artap ST, Preis JI, Fatkin D, Chapman G, Furtado MB, et al. Loss of Cited2 causes congenital heart disease by perturbing left-right patterning of the body axis. Human molecular genetics. 2011;20(6):1097–110.
31. MacDonald ST, Bamforth SD, Chen CM, Farthing CR, Franklyn A, Broadbent C, et al. Epiblastic Cited2 deficiency results in cardiac phenotypic heterogeneity and provides a mechanism for haploinsufficiency. Cardiovasc Res. 2008;79(3):448–57.
32. Purandare SM, Ware SM, Kwan KM, Gebbia M, Bassi MT, Deng JM, et al. A complex syndrome of left-right axis, central nervous system and axial skeleton defects in Zic3 mutant mice. Development. 2002;129(9):2293–302.
33. Oh SP, Li E. The signaling pathway mediated by the type IIB activin receptor controls axial patterning and lateral asymmetry in the mouse. Genes Dev. 1997;11(14):1812–26.
34. Gaio U, Schweickert A, Fischer A, Garratt AN, Muller T, Ozcelik C, et al. A role of the cryptic gene in the correct establishment of the left-right axis. Curr Biol. 1999;9(22):1339–42.
35. Nomura M, Li E. Smad2 role in mesoderm formation, left-right patterning and craniofacial development. Nature. 1998;393(6687):786–90.
36. Yamamoto M, Mine N, Mochida K, Sakai Y, Saijoh Y, Meno C, et al. Nodal signaling induces the midline barrier by activating Nodal expression in the lateral plate. Development. 2003;130 (9):1795–804.
37. Meno C, Shimono A, Saijoh Y, Yashiro K, Mochida K, Ohishi S, et al. lefty-1 is required for left-right determination as a regulator of lefty-2 and nodal. Cell. 1998;94(3):287–97.
38. Meno C, Takeuchi J, Sakuma R, Koshiba-Takeuchi K, Ohishi S, Saijoh Y, et al. Diffusion of nodal signaling activity in the absence of the feedback inhibitor Lefty2. Developmental cell. 2001;1(1):127–38.
39. Kitamura K, Miura H, Miyagawa-Tomita S, Yanazawa M, Katoh-Fukui Y, Suzuki R, et al. Mouse Pitx2 deficiency leads to anomalies of the ventral body wall, heart, extra- and periocular mesoderm and right pulmonary isomerism. Development. 1999;126(24):5749–58.
40. Cox CJ, Espinoza HM, McWilliams B, Chappell K, Morton L, Hjalt TA, et al. Differential regulation of gene expression by PITX2 isoforms. The Journal of biological chemistry. 2002;277(28):25001–10.
41. Schweickert A, Campione M, Steinbeisser H, Blum M. Pitx2 isoforms: involvement of Pitx2c but not Pitx2a or Pitx2b in vertebrate left-right asymmetry. Mech Dev. 2000;90(1):41–51.
42. Franco D, Sedmera D, Lozano-Velasco E. Multiple Roles of Pitx2 in Cardiac Development and Disease. J Cardiovasc Dev Dis. 2017;4(4)
43. Bajolle F, Zaffran S, Kelly RG, Hadchouel J, Bonnet D, Brown NA, et al. Rotation of the myocardial wall of the outflow tract is implicated in the normal positioning of the great arteries. Circ Res. 2006;98(3):421–8.
44. Kelly RG. The second heart field. Curr Top Dev Biol. 2012;100:33–65.
45. van Vliet PP, Lin L, Boogerd CJ, Martin JF, Andelfinger G, Grossfeld PD, et al. Tissue specific requirements for WNT11 in developing outflow tract and dorsal mesenchymal protrusion. Dev Biol. 2017;429(1):249–59.
46. Zhou W, Lin L, Majumdar A, Li X, Zhang X, Liu W, et al. Modulation of morphogenesis by noncanonical Wnt signaling requires ATF/CREB family-mediated transcriptional activation of TGFbeta2. Nat Genet. 2007;39(10):1225–34.
47. Barnes RM, Harris IS, Jaehnig EJ, Sauls K, Sinha T, Rojas A, et al. MEF2C regulates outflow tract alignment and transcriptional control of Tdgf1. Development. 2016;143(5):774–9.
48. Vincent SD, Mayeuf-Louchart A, Watanabe Y, Brzezinski J, Miyagawa-Tomita S, Kelly RG, et al. Prdm1 functions in the mesoderm of the second heart field, where it interacts genetically with Tbx1, during outflow tract morphogenesis in the mouse embryo. Human molecular genetics. 2014;23(19):5087–101.
49. Abu-Issa R, Smyth G, Smoak I, Yamamura K, Meyers EN. Fgf8 is required for pharyngeal arch and cardiovascular development in the mouse. Development. 2002;129(19):4613–25.
50. Park EJ, Ogden LA, Talbot A, Evans S, Cai CL, Black BL, et al. Required, tissue-specific roles for Fgf8 in outflow tract formation and remodeling. Development. 2006;133(12):2419–33.

51. Hutson MR, Zhang P, Stadt HA, Sato AK, Li YX, Burch J, et al. Cardiac arterial pole alignment is sensitive to FGF8 signaling in the pharynx. Dev Biol. 2006;295(2):486–97.
52. Costell M, Carmona R, Gustafsson E, Gonzalez-Iriarte M, Fassler R, Munoz-Chapuli R. Hyperplastic conotruncal endocardial cushions and transposition of great arteries in perlecan-null mice. Circ Res. 2002;91(2):158–64.
53. Clouthier DE, Hosoda K, Richardson JA, Williams SC, Yanagisawa H, Kuwaki T, et al. Cranial and cardiac neural crest defects in endothelin-A receptor-deficient mice. Development. 1998;125(5):813–24.
54. Watanabe Y, Miyagawa-Tomita S, Vincent SD, Kelly RG, Moon AM, Buckingham ME. Role of mesodermal FGF8 and FGF10 overlaps in the development of the arterial pole of the heart and pharyngeal arch arteries. Circ Res. 2010;106(3):495–503.
55. Aghajanian H, Cho YK, Rizer NW, Wang Q, Li L, Degenhardt K, et al. Pdgfrα functions in endothelial-derived cells to regulate neural crest cells and the development of the great arteries. Disease Models & Mechanisms. 2017;10(9):1101–8.
56. Yasui H, Nakazawa M, Morishima M, Miyagawa-Tomita S, Momma K. Morphological observations on the pathogenetic process of transposition of the great arteries induced by retinoic acid in mice. Circulation. 1995;91(9):2478–86.
57. Narematsu M, Kamimura T, Yamagishi T, Fukui M, Nakajima Y. Impaired development of left anterior heart field by ectopic retinoic acid causes transposition of the great arteries. J Am Heart Assoc. 2015;4(5)
58. Cipollone D, Amati F, Carsetti R, Placidi S, Biancolella M, D'Amati G, et al. A multiple retinoic acid antagonist induces conotruncal anomalies, including transposition of the great arteries, in mice. Cardiovascular Pathology. 2006;15(4):194–202.
59. Cipollone D, Carsetti R, Tagliani A, Rosado MM, Borgiani P, Novelli G, et al. Folic acid and methionine in the prevention of teratogen-induced congenital defects in mice. Cardiovascular pathology: the official journal of the Society for Cardiovascular Pathology. 2009;18(2):100–9.
60. Amati F, Diano L, Campagnolo L, Vecchione L, Cipollone D, Bueno S, et al. Hif1alpha down-regulation is associated with transposition of great arteries in mice treated with a retinoic acid antagonist. BMC Genomics. 2010;11:497.
61. Zhu H, Wlodarczyk BJ, Scott M, Yu W, Merriweather M, Gelineau-van Waes J, et al. Cardiovascular abnormalities in Folr1 knockout mice and folate rescue. Birth defects research Part A, Clinical and molecular teratology. 2007;79(4):257–68.
62. Sakabe M, Kokubo H, Nakajima Y, Saga Y. Ectopic retinoic acid signaling affects outflow tract cushion development through suppression of the myocardial Tbx2-Tgfbeta2 pathway. Development. 2012;139(2):385–95.
63. Barros LF, Yudilevich DL, Jarvis SM, Beaumont N, Baldwin SA. Quantitation and immunolocalization of glucose transporters in the human placenta. Placenta. 1995;16(7):623–33.
64. Simeone RM, Devine OJ, Marcinkevage JA, Gilboa SM, Razzaghi H, Bardenheier BH, et al. Diabetes and congenital heart defects: a systematic review, meta-analysis, and modeling project. Am J Prev Med. 2015;48(2):195–204.
65. Shao D, Tian R. Glucose Transporters in Cardiac Metabolism and Hypertrophy. Compr Physiol. 2015;6(1):331–51.
66. Yaribeygi H, Atkin SL, Sahebkar A. A review of the molecular mechanisms of hyperglycemia-induced free radical generation leading to oxidative stress. J Cell Physiol. 2019;234(2):1300–12.
67. Pitkin RM, Van Orden DE. Fetal effects of maternal streptozotocin-diabetes. Endocrinology. 1974;94(5):1247–53.
68. Rousseau-Ralliard D, Couturier-Tarrade A, Thieme R, Brat R, Rolland A, Boileau P, et al. A short periconceptional exposure to maternal type-1 diabetes is sufficient to disrupt the feto-placental phenotype in a rabbit model. Mol Cell Endocrinol. 2019;480:42–53.

69. Hachisuga M, Oki S, Kitajima K, Ikuta S, Sumi T, Kato K, et al. Hyperglycemia impairs left-right axis formation and thereby disturbs heart morphogenesis in mouse embryos. Proc Natl Acad Sci U S A. 2015;112(38):E5300–7.
70. Morgan SC, Relaix F, Sandell LL, Loeken MR. Oxidative stress during diabetic pregnancy disrupts cardiac neural crest migration and causes outflow tract defects. Birth Defects Res A Clin Mol Teratol. 2008;82(6):453–63.
71. Su D, Song JX, Gao Q, Guan L, Li Q, Shi C, et al. Cited2 participates in cardiomyocyte apoptosis and maternal diabetes-induced congenital heart abnormality. Biochem Biophys Res Commun. 2016;479(4):887–92.
72. Wang F, Fisher SA, Zhong J, Wu Y, Yang P. Superoxide Dismutase 1 In Vivo Ameliorates Maternal Diabetes Mellitus-Induced Apoptosis and Heart Defects Through Restoration of Impaired Wnt Signaling. Circ Cardiovasc Genet. 2015;8(5):665–76.
73. Siman CM, Gittenberger-De Groot AC, Wisse B, Eriksson UJ. Malformations in offspring of diabetic rats: morphometric analysis of neural crest-derived organs and effects of maternal vitamin E treatment. Teratology. 2000;61(5):355–67.

Part X

Defects of Situs

Clinical Presentation and Therapy of Anomalies of the Situs

41

Nikolaus A. Haas, David J. Driscoll, and Silke Rickert-Sperling

41.1 Introduction

Situs abnormalities may occur in many and most often more complex congenital cardiac malformations. These conditions are collectively referred to as heterotaxy syndromes, derived from the Greek words "heteros" meaning different and "taxos" meaning orientation or arrangement. Clinically, heterotaxy spectrum encompasses defects in the left–right laterality and arrangement of visceral organs. "Situs" is derived from Latin and is the place where something exists or originates. In human anatomy, situs can be solitus (derived from Latin, meaning "normal"), inversus, or ambiguus. Heterotaxy syndrome represents an intermediate arrangement of internal organs between situs solitus and situs inversus, also known as "situs ambiguous." Situs ambiguus describes an abnormal distribution of major visceral organs within the chest and abdomen. The determination of situs as normal, inversus, or ambiguus is primarily based on the location of unpaired organs such as the spleen, liver, stomach, and intestines. Diagnosis is made by clinical examination, echocardiography, a chest X-ray (position of the heart, stomach, and liver), and ultrasound of the abdominal organs. Situs is considered solitus if the left atrium, spleen, stomach, and

N. A. Haas (✉)
Department of Pediatric Cardiology and Intensive Care, Ludwig Maximilians University, Munich, Germany
e-mail: Nikolaus.haas@med.uni-muenchen.de

D. J. Driscoll
Division of Pediatric Cardiology, Department of Pediatrics, Mayo Clinic College of Medicine, Rochester, MN, USA
e-mail: driscoll.david@mayo.edu

S. Rickert-Sperling
Cardiovascular Genetics, Charité–Universitätsmedizin Berlin, Berlin, Germany
e-mail: silke.sperling@charite.de

© The Author(s), under exclusive license to Springer Nature Switzerland AG 2024

S. Rickert-Sperling et al. (eds.), *Congenital Heart Diseases: The Broken Heart*,
Advances in Experimental Medicine and Biology 1441,
https://doi.org/10.1007/978-3-031-44087-8_41

the trilobed lung are on the left side and the liver and bilobed lung are on the right side. Situs ambiguus is present if the location of unpaired structures is random or indeterminate even after detailed and appropriate imaging. Situs inversus results when the arrangement of the thoracic and abdominal organs is mirrored. Individuals with situs inversus or situs solitus do not experience fatal dysfunction of their organ systems, as general anatomy and morphology of the abdominothoracic organ-vessel systems are conserved.

Two types of heterotaxia include polysplenia and asplenia. Polysplenia sometimes is referred to as bilateral left sidedness and asplenia is sometimes referred to as bilateral right sidedness. Another term describing sidedness is "isomerism." The term left-sided isomerism indicates that both atria are morphologically like a left atrium. This is associated with polysplenia and bilateral bilobed lungs. The term right-sided isomerism implies that both atria are morphologically like a right atrium. This is associated with asplenia and bilateral trilobed lungs. The sidedness of lungs is best determined by the relationship of the pulmonary arteries to their respective bronchi. Normally, for the morphologic right lung, the pulmonary artery travels anterior to the upper and intermediate bronchi. For the morphologic left lung, the left pulmonary artery courses over the main bronchus and posterior to the upper lobe bronchus. Also, the mainstem bronchus of the morphologically left lung is 1.5–2 times longer than the mainstem bronchus of the right lung. This frequently can be appreciated on a chest radiogram. With bilateral right or bilateral left sidedness, the mainstem bronchi will be equal in length.

41.2 Dextrocardia

In addition to heterotaxy syndromes, it is important to differentiate various forms of dextrocardia, such as mirror image dextrocardia, dextroposition, and dextroversio cordis, which involve normal organ distribution but with the heart positioned differently. Dextrocardia is a situation where the heart is located on the right side of the thorax**.** The different forms of dextrocardia can occur as an anatomical variant without congenital heart defects (CHD) but can also be related to specific forms of CHD (Fig. 41.1).

41.3 Heterotaxy Syndromes, Isomerism, and Situs Ambiguus

Heterotaxy syndrome, also known as situs ambiguus, is a rare condition occurring in approximately 1 out of every 10,000 live births. It is associated with around 3% of CHD. In heterotaxy syndromes, there can be abnormal positioning of the heart, including left-sided (levocardia, 50–70%), right-sided (dextrocardia, 25–30%), or central (mesocardia, 5–10%) location. In situs ambiguus, the characteristic features of thoracic organs are as follows: the right atrium has openings for the vena cava and a broad-based, pyramid-shaped atrial appendage. The left atrium exhibits a finger-

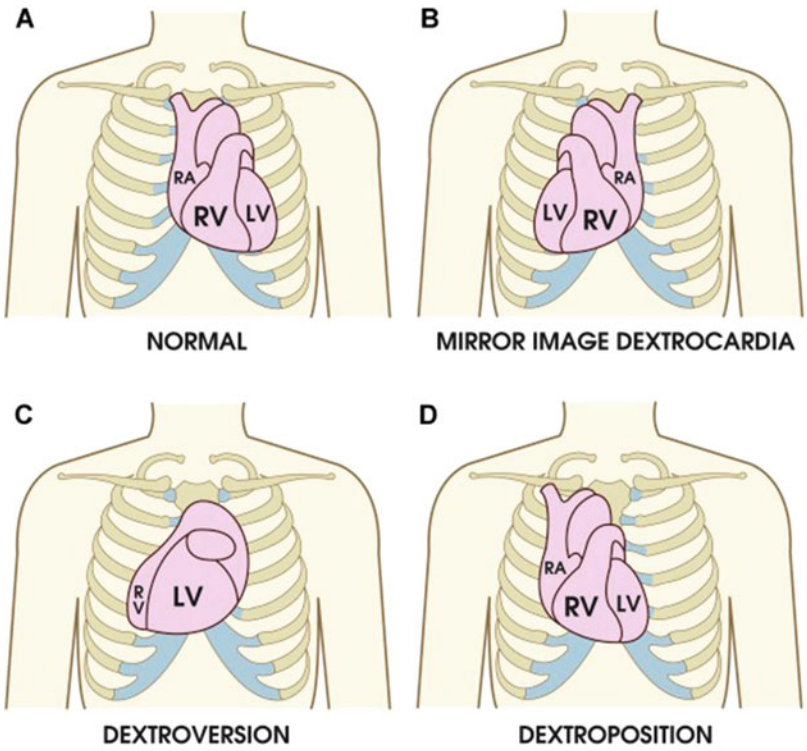

Fig. 41.1 Different types of dextrocardia. (**a**) Normal situs: The cardiac anatomy is in its typical arrangement, with the apex pointing to the left. The right ventricle is anterior, and the left ventricle is posterior. (**b**) Mirror-Image Dextrocardia: In this type, the cardiac anatomy is a mirror image of the normal anatomy. The apex points to the right, the right ventricle is anterior, and the left ventricle is posterior. A significant percentage of these patients may have Kartagener's syndrome. (**c**) Dextroversion of the heart: The heart is rotated to the right, resulting in the apex pointing to the right. The right ventricle is rotated posteriorly, while the left ventricle is positioned just behind the sternum and lies anteriorly. This anomaly is often associated with complex heart diseases such as ccTGA (congenitally corrected transposition of the great arteries) or TAPVR (total anomalous pulmonary venous return). (**d**) Dextroposition of the heart: The apex of the heart points to the left, but the entire heart appears displaced to the right side of the chest. The right ventricle is located anteriorly and behind the right rib cage, while the left ventricle is posterior but situated on the left side of the chest. Dextroposition may occur in conditions such as right-sided pulmonary hypoplasia, for example in Scimitar syndrome

shaped atrial appendage. The right lung typically has three lobes and an eparterial main bronchus, while the left lung has two lobes and a hyparterial main bronchus. The aorta is located on the left side of the spine, and the vena cava is on the right side.

Due to the abnormal arrangement of organs in situs ambiguus, early disruptions in fetal development occur, leading to severely impaired cardiac development and function in 50–80% of cases. There are also complications in the development of systemic and pulmonary blood vessels. Patients with situs ambiguus often develop

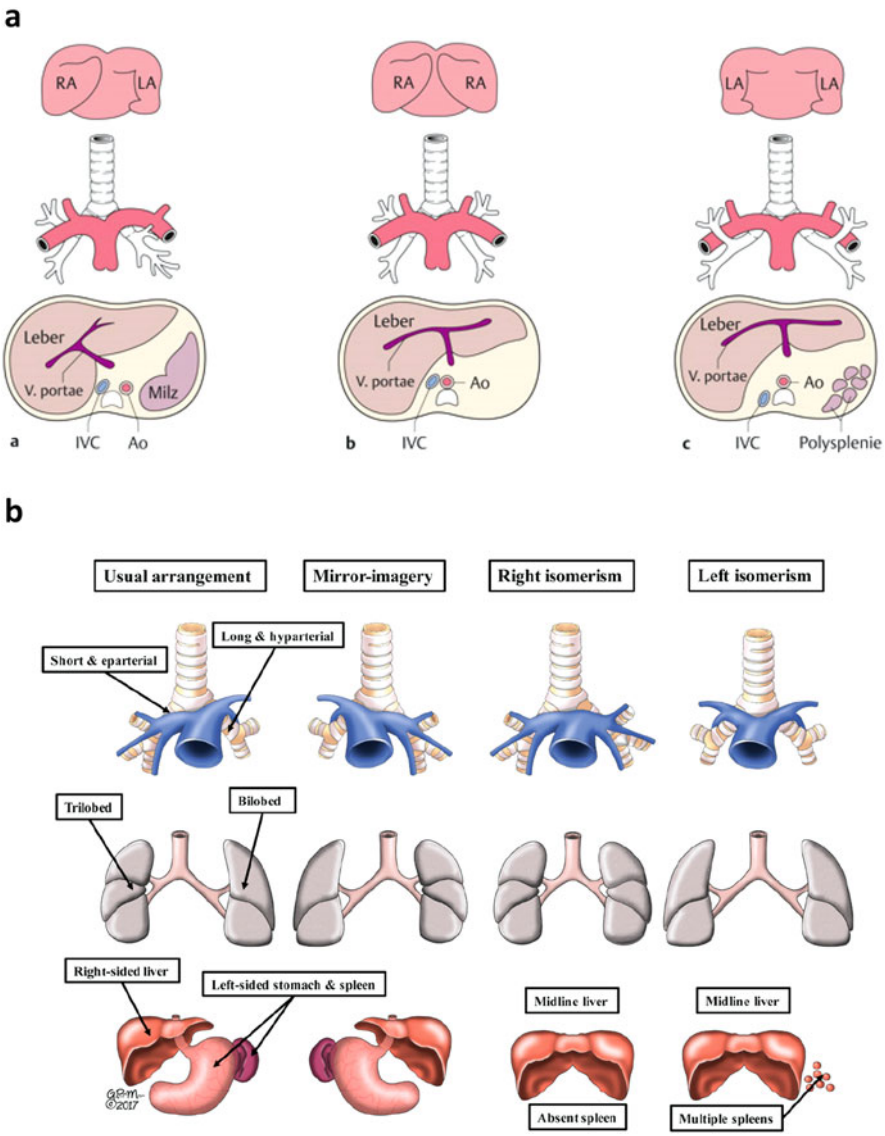

Fig. 41.2 Anatomical characteristics of (**a**) situs solitus, (**b**) right atrial isomerism (Asplenia syndrome), and (**c**) left atrial isomerism (polysplenia syndrome). Reproduced from Kinderkardiologie, Georg Thieme Verlag, N. Haas, U. Kleideiter, 2011

right atrial isomerism, characterized by two bilaterally paired right atria, or left atrial isomerism, characterized by two bilaterally paired left atria (Fig. 41.2). Intestinal malrotation is commonly observed, with unpaired abdominal organs being in mirror image position (situs abdominalis inversus), normal position (situs abdominalis solitus), or a more random arrangement (situs abdominalis ambiguus). The spleen

is always affected, with asplenia usually associated with right atrial isomerism and polysplenia with left atrial isomerism. Polysplenia is often linked with dextrocardia, atrial situs ambiguus, ventricular inversion, ventriculoarterial concordance with a left posterior aorta, partial anomalous pulmonary venous return, atrioventricular septal defects (approximately 1/3 of cases), and interruption of the inferior vena cava with azygos continuation to the superior vena cava. While certain defects may have a tendency to occur more frequently in either asplenia or polysplenia, there can be considerable overlap between the two conditions.

41.3.1 Right Atrial Isomerism

Right atrial isomerism, also known as right atrial appendage isomerism, asplenia syndrome or Ivemark syndrome, is a congenital malformation characterized by the presence of two right-sided atria. This condition is associated with a tendency toward bilateral right-sidedness. Asplenia, or the absence of a spleen, is commonly seen in individuals with right atrial isomerism.

In general, asplenia syndrome is accompanied by anomalies in systemic and pulmonary venous return, including bilateral superior vena cavae, bilateral hepatic venous connections, complete atrioventricular septal defects (approximately two-third of cases), transposition of the great arteries, double-outlet right ventricle, pulmonary stenosis, and pulmonary atresia. Additionally, there are typically two sinus nodes in the heart. The presence of two right lungs, each with three lobes and eparterial bronchi, is another characteristic feature.

One of the major risks associated with asplenia syndrome is the susceptibility to overwhelming bacterial infections due to the absence of a functioning spleen. Cardiac malformations often observed in this condition include a bilateral superior vena cava, right-sided aortic arch, inferior vena cava located behind the aorta, a single atrioventricular valve (atrioventricular septal defect), and a functional univentricular heart in most cases. Transposition of the great arteries with pulmonary stenosis or atresia is also commonly seen. Since there is no left atrium, total anomalous pulmonary venous return (TAPVR) is frequently present. Atrial arrhythmias are common due to the presence of two sinus nodes.

41.3.2 Left Atrial Isomerism

Left atrial isomerism, also known as left atrial appendage isomerism, is a rare congenital heart defect, accounting for less than 1% of all cases of congenital heart disease (CHD). This condition is characterized by a tendency toward bilateral left-sidedness, with both atria exhibiting features typical of left atria.

In individuals with left atrial isomerism, both lungs are left-sided, consisting of two lobes each, and hyparterial main bronchi. Polysplenia, or the presence of multiple spleens, is common in this condition, although functional asplenia may also occur. An interrupted inferior vena cava (IVC) with azygos vein continuation is

typically observed, while pulmonary venous connections are normal. The atrioventricular (AV) valves are usually normal, with two ventricles in most cases, although ventricular septal defects (VSD) or double-outlet right ventricle (DORV) can also be present. The great vessels are in their normal positions, and pulmonary stenosis is rarely seen. One notable feature of left atrial isomerism is the absence of a sinus node, which can result in bradycardia and occasionally atrioventricular (AV) block in affected individual.

41.4 Management

The wide range of cardiac malformations associated with abnormal situs demonstrates their diverse nature. Instead of delving into the details of pathologic physiology, clinical presentation, physical examination, echocardiographic and cardiac catheterization considerations, treatment, and outcomes for each specific defect in this chapter, it is recommended that readers refer to the relevant chapters dedicated to those specific defects for a comprehensive understanding.

Human Genetics of Defects of Situs

42

Andreas Perrot and Silke Rickert-Sperling

Abstract

Defects of situs are associated with complex sets of congenital heart defects in which the normal concordance of asymmetric thoracic and abdominal organs is disturbed. The cellular and molecular mechanisms underlying the formation of the embryonic left–right axis have been investigated extensively in the past decade. This has led to the identification of mutations in at least 33 different genes in humans with heterotaxy and situs defects. Those mutations affect a broad range of molecular components, from transcription factors, signaling molecules, and chromatin modifiers to ciliary proteins. A substantial overlap of these genes is observed with genes associated with other congenital heart diseases such as tetralogy of Fallot and double-outlet right ventricle, d-transposition of the great arteries, and atrioventricular septal defects. In this chapter, we present the broad genetic heterogeneity of situs defects including recent human genomics efforts.

Keywords

Situs inversus · Situs ambiguus · Situs defects · Heterotaxy · Dextrocardia · Tetralogy of Fallot · Double-outlet right ventricle · d-Transposition of the great arteries · Atrioventricular septal defects · Copy-number variations · CNVs · Cardiac transcription factors · NKX2–5 · GATA4 · ZIC3 · Signaling pathways · ACVR2B · GDF1 · CFC1 · LEFTY2 · NODAL · Histone-modifying genes ·

A. Perrot
Experimental and Clinical Research Center, a cooperation between the Max Delbrück Center for Molecular Medicine in the Helmholtz Association and Charité Universitätsmedizin Berlin, Berlin, Germany

S. Rickert-Sperling (✉)
Cardiovascular Genetics, Charité Universitätsmedizin Berlin, Berlin, Germany
e-mail: silke.sperling@charite.de

© The Author(s), under exclusive license to Springer Nature Switzerland AG 2024

S. Rickert-Sperling et al. (eds.), *Congenital Heart Diseases: The Broken Heart*,
Advances in Experimental Medicine and Biology 1441,
https://doi.org/10.1007/978-3-031-44087-8_42

Ciliary genes · Primary cilia · Motile cilia · Kartagener syndrome · DNAH5 · DNAI1 · DNAH6 · DNAH11 · Primary ciliary dyskinesia · PCD · Nephronophthisis · NPHP · NPHP2 · NPHP3 · NPHP4 · PKD2 · CRELD1 · SHROOM3 · WDR16 · MMP21 · MNS1 · NME7 · PKD1L1 · NUP205 · NUP210 · Whole-exome sequencing

42.1 Introduction

Situs inversus is found in about 0.01% of the population, or about 1 person in 10,000. In the most common situation, the relationship between the organs is unchanged, and most people with situs inversus have no medical symptoms or complications [1]. In cases of situs ambiguus, the arrangement of the thoracoabdominal organs across the left–right (LR) axis of the body is variable. Frequently, the term heterotaxy is used synonymously for situs ambiguus. This broad term includes patients with a wide variety of very complex cardiac lesions. A right-sided heart position is called dextroposition. If the apex of the heart points to the right, it is called dextrocardia.

Heterotaxy shows a high 79% recurrence risk ratio among first-degree relatives, which underlines a strong genetic basis of the disease [2]. Recent studies concerning its etiology have yielded new insights into the genetic architecture and will be summarized here [3]. A number of specific gene studies in patients were based on insights obtained by the study of left–right patterning in the early embryo of model organisms. However, multiple genetic variations, RNA and protein expression, and the interaction of these molecules impacts on the ultimate phenotype. Furthermore, this individual-specific mix of genes and expression patterns collides with the environment (teratogens, maternal exposures, and infectious agents; see Chap. 16). We will focus on the genetic causes and provide insight into the extensive genetic heterogeneity of situs defects.

42.2 Copy-Number Variations

Copy-number variations (CNVs) are subchromosomal changes in genome structure and generally comprise structural variants of intermediate size that range from about 1000 to 5×10^6 bases of DNA [3, 4]. These deletions, duplications, and inversions lead to gain or loss of chromosomal segments often containing multiple genes. CNVs can occur *de novo*, or be inherited. Pathogenic CNVs tend to be *de novo*, large, and disrupt parts of genes, mostly coding regions, that are dosage sensitive. Recent studies have identified multiple CNVs that contribute to nonsyndromic CHD [3].

Fakhro et al. analyzed more than 250 patients with heterotaxy with high-resolution genotyping and estimated from these data copy-number frequencies. They found 45 CNVs in 39 cases of which five where further assessed and confirmed

by Morpholino knockdown in *Xenopus tropicalis*, the clawed frog [5]. Knockdown of these genes, *NEK2* (NIMA-related kinase 2), *ROCK2* (Rho-associated, coiled-coil containing protein kinase 2), *TGFBR2* (transforming growth factor, beta receptor II), *GALNT11* (polypeptide N-acetylgalactosaminyltransferase 11), and *NUP188* (nucleoporin 188 kDa), leads to strongly disrupted morphological LR development and altered expression of Pitx2 (paired-like homeodomain 2), a molecular marker of LR patterning [5].

Glessner et al. studied several hundred CHD trios with two complementary high-resolution techniques, single-nucleotide polymorphism (SNP) arrays, and whole-exome sequencing (WES) [6]. A significant increase in CNV burden was observed when comparing CHD trios with healthy trios. Rare *de novo* CNVs were identified in 51 probands, among them three patients with heterotaxy. The CNVs of these patients were located on chromosomes 6q21.2, 17p11.2, and 22q13.2, and size ranged between 5 and 680 kilobases. They affected genes such as *CDKN1A* (cyclin-dependent kinase inhibitor 1A), *FAM27L* (family with sequence similarity 27-like), and *CYP2D6* (cytochrome P450, family 2, subfamily D, polypeptide 6), respectively [6].

A further study examined 63 sporadic heterotaxy patients using Affymetrix microarrays [7]. Liu et al. identified 19 rare CNVs, comprising 5 heterozygous genic deletions, 4 internal genic deletions, and 10 complete duplications of at least one gene. Further analyses revealed 5 novel candidate genes (*NUMB, PACRG, TCTN2, DANH10,* and *RNF115)*. Functional testing in zebrafish showed that these genes were early expressed in development and disrupted cardiac looping as well as disturbed expression of the L-R patterning markers *lefty2* and *pitx2* [7].

42.3 Single-Gene Defects

A number of different genes have been implicated in situs defects indicating that there is an extensive genetic heterogeneity. Here, we present a list of 33 genes involved in situs abnormalities; but this number should be seen as preliminary and is likely to rise with future genetic studies. Genes playing a role in heterotaxy frequently encode cardiac transcription factors, components of signaling pathways, ciliary proteins, histone-modifying proteins, along with other proteins (Table 42.1 lists all known genes).

42.3.1 Cardiac Transcription Factors

The expression of cardiac transcription factors occurs in highly specified temporal-spatial patterns throughout development [3] (see Chap. 12). Transcription factors orchestrate heart development, and many of them are associated with isolated CHD [3, 42] (see, e.g., Chap. 30). Transcriptional focal points include NK2 homeobox 5 (*NKX2–5*) and GATA-binding protein 4 (*GATA 4*) which are known to be involved in situs defects.

Table 42.1 Genes where mutations in patients with heterotaxy and situs defects have been described

Gene	Protein function	Phenotype	Status	References
Transcription factors (TF)				
NKX2–5	Homeobox TF	HTX, s. inversus	2 or more ind. Rep.	[8, 9]
GATA4	GATA-binding TF	Dextrocardia	Single case report	[10]
ZIC3	Zink finger TF	HTX, s.ambiguus, s. inversus, dextrocardia	2 or more ind. Rep.	[11–13]
Genes involved in signaling pathways				
ACVR2B	Activin receptor (TGFbeta fam.)	HTX, dextrocardia	2 or more ind. Rep.	[14, 15]
GDF1	Ligand (TGFbeta fam.)	S.Inversus, s.ambiguus, dextrocardia	2 or more pat.	[16]
CFC1	Ligand (EGF-CFC fam.)	HTX, dextrocardia	2 or more ind. Rep.	[17–19]
LEFTY A	Ligand (TGFbeta fam.)	Dextrocardia	2 or more pat.	[20]
NODAL	Ligand (TGFbeta fam.)	S. Inversus, dextrocardia	2 or more ind. Rep.	[15, 21]
Histone-modifying genes				
RNF20	Histone-modifying protein	HTX, dextrocardia	Single case	[22]
SMAD2	Histone-modifying protein	HTX, dextrocardia	2 or more ind. Rep.	[15, 22]
MED20	Histone-modifying protein	HTX, dextrocardia	Single case rep.	[22]
NAA15	Histone-modifying protein	HTX, dextrocardia	Single case rep.	[22]
Ciliary genes				
DNAI1	Dynein arm	S.Inversus	2 or more ind. Rep.	[15, 23, 24]
DNAH5	Dynein arm	S.Inversus	2 or more ind. Rep.	[15, 25]
DNAH6 *DNAH11* *NPHP2*	Dynein arm Dynein arm Ciliary protein	HTX HTX S.Inversus	2 or more pat. 2 or more pat. 2 or more pat.	[26] [27] [25]
NPHP3	Ciliary protein	S.Inversus	2 or more pat.	[28]
NPHP4	Ciliary protein	S.Inversus, dextrocardia	2 or more pat.	[29]
CCDC11 *WDR16* *MNS1*	Ciliary protein Cilia-related signaling Cilia-related signaling	S.Inversus HTX, s. inversus S. Inversus, dextrocardia	2 or more ind. Rep. 2 or more pat. 2 or more pat.	[30, 31] [32] [33]

(continued)

Table 42.1 (continued)

Gene	Protein function	Phenotype	Status	References
Other genes				
PKD2 *PKD1L1*	Polycystin 2 Polycystin-like protein	S. Inversus, dextrocardia HTX, s.inversus	2 or more ind. Rep. 2 or more ind. Rep.	[34, 35] [15, 36]
SHROOM3	Cytoskeletal protein	S. Inversus, dextrocardia	2 or more pat.	[37]
CRELD1 *MMP21* *NME7* *NUP205* *NUP210*	Cell adhesion protein Matrix metalloproteinase Tubulin ring complex Nucleoporin Nucleoporin	HTX HTX, s.inversus, dextrocardia S. Inversus S. Inversus HTX, s. inversus	2 or more pat. 2 or more ind. Rep. 2 or more pat. Single case rep. 2 or more pat.	[38] [15, 39] [40] [41] [41]
MKRN2	E3 ubiquitin ligase	S.Inversus	Single case rep.	[22]
OBSCN	Sarcomeric protein	HTX, dextrocardia	Single case rep.	[22]
UMODL1	Urinary protein	HTX, dextrocardia	Single case rep.	[22]

Abbreviations: *ind.* Independent, *rep.* Report, *pat.* Patients, *s.* situs, *HTX* heterotaxy, *fam.* family

Watanabe et al. identified a deletion frameshift mutation in *NKX2–5* in a familiar CHD case with heterotaxy as well as atrial septal defect (ASD) [8]. Izumi et al. described a further deletion frameshift mutation in *NKX2–5* (along with three other variants of unknown significance in genes associated with ciliary disease; see Sect. 42.3.4) in a patient with complex CHD including heterotaxy using clinical exome sequencing [9]. In *GATA4*, a frameshift mutation was identified by Hirayama-Yamada et al. in a family with multiple ASD cases of which one showed additional dextrocardia [10]. However, affection of other contributing genes might be likely in this case.

The X-linked form of heterotaxy is caused by mutations in the zinc finger transcription factor *ZIC3* (Zic family member 3) and affects approximately 1% of sporadic heterotaxy cases [1]. Mutations often cause loss of function and, in some cases, result in abnormal subcellular localization and trafficking [1]. *ZIC3* was the first gene unequivocally associated with human situs abnormalities [43, 44]. To date, a number of different *ZIC3* point mutations (missense, nonsense, and frameshift) have been described in X-linked familial heterotaxy cases as well as in sporadic heterotaxy and isolated CHD cases [11–13, 43, 45]. Patients from these studies show the whole spectrum of situs defects such as situs inversus, heterotaxy (situs ambiguus including asplenia and polysplenia), and dextrocardia. In summary, *ZIC3* is the most frequent disease gene for laterality defects.

42.3.2 Genes Involved in TGFβ Signaling Pathways

Heart development involves coordination of a number of signaling pathways [42]. Several mutations in signaling molecules have been detected in different forms of CHD associated with situs defects.

Activins and their receptors are members of the transforming growth factor beta (TGFβ) family of signaling molecules. Two missense mutations in *ACVR2B* encoding the activin receptor type II B were found in three patients showing heterotaxy and complex CHD [14]. Performing WES in 323 cases with laterality defects, Li et al. could confirm a number of genes known to cause heterotaxy including *ACVVR2B* as well as *NODAL, DNAI1, DNAH5, MMP21, SMAD2,* and *PKD1L1* [15].

Kaasinen et al. described a family with right atrial isomerism associated with situs inversus, situs ambiguus, dextrocardia, and asplenia showing mutations in the growth differentiation factor 1 (*GDF1*) [16]. Two truncating mutations of *GDF1* were observed to segregate with the phenotype in an autosomal recessive manner [16]. Of note, this study also identified 11 carriers of heterozygous truncating mutations in *GDF1* in control subjects without CHD indicating a high frequency and compatibility with normal development and health.

CFC1 encoding CRYPTIC protein is a member of the EGF (epidermal growth factor)-CFC (Cripto, Frl1, and Cryptic) family encoding extracellular proteins important for intercellular signaling pathways during vertebrate embryogenesis. Bamford et al. were the first to describe loss-of-function mutations in human *CFC1* in patients with heterotaxic phenotypes [17]. They identified nine patients carrying four different missense mutations and one deletion with various forms of heterotaxy associated with CHDs such as d-transposition of the great arteries (d-TGA), ventricular septal defect (VSD), and ASD; five of the patients showed dextrocardia. The mutant proteins had aberrant cellular localization in transfected cells and showed functional effects in a zebrafish model [17]. Selamet Tierney et al. found three nonsynonymous variants in *CFC1* in patients with laterality defects and CHD and suggested that these may act as susceptibility alleles in conjunction with other genes and/or environmental factors [18]. Further, Roessler et al. screened *CFC1* in a cohort of 251 patents with laterality defects and identified two mutations [19].

A further member of the TGFβ family, the left–right determination factor 2 (*LEFTY2*, also known as *LEFTY A*), was shown to be mutated in heterotaxy patients and is well known for its role in left–right patterning during mouse development [20]. Kosaki et al. found one nonsense and one missense mutation in *LEFTY A* in two patients with LR-axis malformations and CHD [20]. However, they stated that the *LEFTY A* mutant alleles may be necessary, but not sufficient, to give an LR phenotype in these affected individuals, because each mutation was found to be carried by one of the parents [20].

Analysis of a cohort of 269 patients with heterotaxy and/or isolated cardiovascular malformations revealed four different missense mutations in *NODAL* (Nodal growth differentiation factor) [21]. *NODAL* mutations were found in 14 unrelated

subjects consisting of one in-frame insertion/deletion and two conserved splice site mutations. About one third of these patients showed dextrocardia and situs inversus (as well as asplenia in some cases) associated with a wide spectrum of CHD including pulmonary atresia, d-TGA, ASD, and VSD.

42.3.3 Histone-Modifying Genes

Histone proteins package chromosomal DNA into structural units called nucleosomes. They act as "spools" around which DNA winds and play an important role in gene regulation. Histone-modifying proteins have been identified for a number of distinct forms of modifications such as acetylation and methylation/demethylation.

Zaidi et al. used exome sequencing in parent–offspring trios to determine and compare the incidence of *de novo* mutations in 362 severe CHD cases (including heterotaxy) and 264 controls [22]. They found an excess of *de novo* mutations in genes involved in the production, removal, and reading of histone 3 lysine 4 (H3K4) methylation, an activating chromatin mark, and H3K27 methylation, an inactivating chromatin mark [22]. In heterotaxy or dextrocardiac patients, they found mutations in *SMAD2* (SMAD family member 2), *MED20* encoding mediator complex subunit 20, and *RNF20* encoding RING finger protein 20, an E3 ubiquitin ligase that regulates chromosome structure by monoubiquitinating histone H2B. The latter case showed additional asplenia as also seen in a further case with a frameshift mutation in *NAA15* (N-alpha-acetyltransferase 15, NatA auxiliary subunit) [22].

42.3.4 Ciliary Genes

Cilia are hair-like organelles found on the surface of most vertebrate cell types; there are two general types of cilia, namely, primary cilia serving as sensory organelles and motile cilia exerting mechanical force. Motile cilia are critical to the development of proper organ laterality in the developing embryo and represent a central pathway disturbed in heterotaxy [46]. Primary ciliary dyskinesia (PCD), a sinopulmonary disease with dyskinetic cilia in the airway, is a monogenic recessive disorder resulting from loss of function of different parts of the primary ciliary apparatus, often components of the dynein motor complex [1] (see Chap. 39). In cases where dextrocardia, situs ambiguus, or situs inversus are present in the infant, PCD should be considered as a highly possible diagnosis [47]. To date, PCD-causative mutations in about 35 genes are known, and the number of causative genes is bound to rise (as reviewed by Kurkowiak et al. [47]). It remains unknown how many of the PCD genes cause CHD, since a diagnosis of PCD in CHD patients is challenging, due to the difficulty differentiating whether respiratory symptoms are primary or secondary to the underlying cardiac pathology [48]. In this section, we will present a selection of important PCD genes associated with situs defects.

Kartagener syndrome is characterized by the combination of PCD and situs inversus and occurs in approximately 20% of patients with PCD [46]. The absence of normal ciliary movement results in a lack of definitive patterning; thus whether the viscera take up the normal or reversed left–right position during embryogenesis is driven by stochasticity [1]. The syndrome is caused by mutations in *DNAI1* encoding axonemal dynein intermediate chain 1, an outer dynein arm component that is essential for ciliary function at the node [23]. Guichard et al. identified compound heterozygous DNAI1 gene defects in three independent patients from a cohort of 34 patients with Kartagener syndrome [23]. A further study in more than 300 PCD patients showed that half of them had situs inversus and at least 6% of patients with PCD have heterotaxy, and most of those have CHDs such as systemic vein abnormalities, aortic coarctation, atrioventricular septal defect (AVSD), and double-outlet right ventricle [24]. Further, the patients carried more mutations in ciliary outer dynein arm genes (*DNAI1* and *DNAH5* encoding axonemal dynein heavy chain 5) as compared with PCD patients with situs solitus [24]. Li et al. carried out targeted exome sequencing of 25 CHD/heterotaxy patients and identified 6 individuals with heterozygous mutations in the dynein axonemal heavy chain gene *DNAH6* who also carried mutations in *DNAH5* or other PCD genes [26]. A similar study performed by Liu et al. analyzed 42 heterotaxy patients with CHD and detected 14 disease-causing mutations in the dynein axonemal heavy chain gene *DNAH11*. Six different compound heterozygous mutations could be validated in six small families [27].

Nephronophthisis (NPHP), an autosomal recessive cystic kidney disease, belongs to the ciliopathies and is characterized by cilia-related defects. Mutations in *nephronophthisis-2 (NPHP2* also named *INVS* for inversin) can result in NPHP with situs inversus and mild cardiac defects [25]. Bergmann et al. showed that *NPHP3* (also named nephrocystin-3) mutations can cause a broad clinical spectrum of early embryonic patterning defects comprising situs inversus and structural heart defects as well as kidney disease [28]. Interestingly, a genome-wide linkage analysis identified *nephronophthisis-4 (NPHP4)* mutations in patients with cardiac laterality defects but without NPHP from a consanguineous family [29]. Further sequencing of this gene identified eight additional missense mutations in a cohort of unrelated patients with dextrocardia, situs inversus, and asplenia/polysplenia [29].

Performing homozygosity mapping in a consanguineous family with laterality defects, Perles et al. identified a homozygous splice site mutation in *CCDC11* encoding coiled-coil domain containing 11 protein which is preferentially expressed in ciliated cells [30]. The patient carrying the mutation was characterized by situs inversus and severe cardiac malformations [30]. This finding could be confirmed by Narasimhan et al. who found homozygous loss-of-function mutations in *CCDC11* in a patient with situs inversus without any discernible effect on respiratory function descending from consanguineous parents [31].

Using WES in consanguineous families, two genes involved in cilia-related signaling were found to play a role in the pathogenicity of situs defects. Ta-Shma et al. identified a homozygous deletion in *WDR16* (also known as *CFAP52* encoding cilia and flagella associated protein 52) in a family characterized with heterotaxy and

situs inversus and without PCD [32]. Later on, the same group was able to describe two recessive loss-of-function mutations in *MNS1* encoding meiosis specific nuclear structural 1 protein. These variants were detected in five individuals of four families with laterality defects such as situs inversus and dextrocardia [33].

Finally, it is worth to mention that cilia-related genes are significantly enriched for damaging rare recessive genotypes, but comparatively depleted for *de novo* variants in general CHD as Watkins et al. showed by performing a gene burden analysis in about 2400 whole-exome trios with CHD [49].

42.3.5 Other Genes

PKD2, encoding polycystin 2 and belonging to the superfamily of transient receptor potential channels, causes autosomal dominant polycystic kidney disease. Bataille et al. reported an association of that disease resulting from *PKD2* mutations with left–right laterality defects [34]. One large gene deletion, one single-exon duplication, and one in-frame duplication, respectively, were found in three unrelated patients characterized by dextrocardia or situs inversus in addition to kidney disease [34]. Another patient with complete situs inversus and autosomal dominant polycystic kidney disease caused by a *PKD2* missense mutation (leading to a premature truncation of polycystin 2) was identified by Oka et al. [35]. Via WES, Vetrini et al. found two homozygous mutations in a polycystin-related gene, i.e., *PKD1L1* encoding polycystin-1-like protein 1. They detected one splicing and one missense mutation in three infants from two families who were characterized by heterotaxy, situs inversus, dextrocardia/levocardia, and complex CHD [36].

Using WES, Tariq et al. found mutations in *SHROOM3* (Shroom family member 3), an actin-binding protein, which is responsible for early cell shape during morphogenesis through a myosin II-dependent pathway [37]. They first identified a mutation in a patient with complex heterotaxy phenotype (including dextrocardia and situs inversus) by exome sequencing and subsequently analyzed a cohort of sporadic heterotaxy patients in *SHROOM3* leading to the identification of further two mutations that were predicted to be pathogenic [37].

CRELD1 encoding the cell adhesion molecule cysteine-rich with EGF-like domains 1 was analyzed in a cohort of 11 patients with AVSD and heterotaxy [38]. One missense mutation was detected in a patient characterized by dextrocardia, right ventricle aorta with pulmonary atresia, and a right aortic arch in addition to partial AVSD [38]. However, Robinson et al. suggested that *CRELD1* mutations might increase the risk of developing a heart defect, rather than being directly causative [38].

Perles et al. performed WES in a consanguineous family with heterotaxia, situs inversus, and dextrocardia [39]. They identified a homozygous deletion in *MMP21* encoding matrix metalloproteinase 21 as the sole coding mutation segregating with the phenotype and confirmed functional effects in a zebrafish model [39].

A homozygous deletion of an exon causing an in-frame deletion of 34 amino acids in *NME7* (encoding NME/NM23 family member 7 protein) was detected in

two siblings with situs inversus of an consanguineous family [40]. The NME7 protein is a component of the gamma-tubulin ring complex.

Screening of 61 family trios with heterotaxy or situs inversus by whole-exome and -genome sequencing revealed eight bi-allelic missense mutations in two nucleoporin genes, NUP205 and NUP210, in four trios [41]. Both proteins comprise components of the nuclear pore complex.

Besides alterations in histone-modifying enzymes, the study of Zaidi et al. (see Sect. 42.3.3) identified three *de novo* mutations in *MKRN2* (encoding makorin RING finger protein 2, a probable E3 ubiquitin ligase), in *OBSCN* (encoding obscurin, a giant sarcomeric protein important for myofibrillogenesis), and in *UMODL1* (encoding uromodulin-like 1, a protein similar to uromodulin which is associated with various kidney diseases). Interestingly, Zaidi et al. also described a second *de novo* missense mutation in all of the three genes in a CHD patient without heterotaxy or situs defect [22].

42.4 Conclusion

As observed in other forms of congenital heart disease, defects of the situs and heterotaxy have a complex genetic architecture, spanning several single-gene inheritance models, potential multilocus contributions, and other putative disease mechanisms [15]. The findings from the mentioned studies in this chapter are entirely consistent with a complex, oligogenic disease model. One can speculate that rare heterozygous mutations identified in the sporadic cases have probably an epistatic effect with additional genetic modifiers within other developmental pathways. Even in consanguineous families, there may exist other genetic variants that lead to the phenotype [29, 30]. It is well known that there is an increase of all CHD in consanguineous populations. But heterotaxy and situs defects are observed at a higher frequency in such populations [48]. Pedigrees of consanguineous families with heterotaxy identified recessively inherited mutations in genes including *NPHP4, MMP21, MNS1, WDR16, SHROOM3, CCDC11,* and *NME7*. Further, the observed variety in the phenotype in combination with ciliopathies and kidney disease as well as other CHDs supports this notion.

Point mutations in at least 33 different genes have been described in patients with heterotaxy and situs defects (see Table 42.1). There is a wide genetic heterogeneity including genes encoding for transcription factors, signaling molecules, ciliary proteins, histone-modifying proteins, and others. There is no doubt that additional genes will be identified based on the technical advances [1, 3, 46]. A substantial overlap of situs genes is observed with genes associated with other CHDs such as tetralogy of Fallot and double-outlet right ventricle (see Chap. 32), d-transposition of the great arteries (see Chap. 35), and atrioventricular septal defects (see Chap. 26). To date, there are only a few data pointing to an important role of subchromosomal changes such as copy-number variation in the etiology of situs defects.

Although there is a strong genetic contribution to situs defects, the majority of situs defects are idiopathic indicating the need for better utilization of novel

approaches such as whole-exome/genome sequencing to find the genetic variations contributing to this severe congenital heart disease.

References

1. Sutherland MJ, Ware SM. Disorders of left-right asymmetry: heterotaxy and situs inversus. Am J Med Genet C Semin Med Genet. 2009;151C:307–17.
2. Oyen N, Poulsen G, Boyd HA, et al. Recurrence of congenital heart defects in families. Circulation. 2009;120:295–301.
3. Fahed AC, Gelb BD, Seidman JG, et al. Genetics of congenital heart disease: the glass half empty. Circ Res. 2013;112:707–20.
4. Pollex RL, Hegele RA. Copy number variation in the human genome and its implications for cardiovascular disease. Circulation. 2007;115:3130–8.
5. Fakhro KA, Choi M, Ware SM, et al. Rare copy number variations in congenital heart disease patients identify unique genes in left-right patterning. Proc Natl Acad Sci U S A. 2011;108: 2915–20.
6. Glessner JT, Bick AG, Ito K, et al. Increased frequency of de novo copy number variants in congenital heart disease by integrative analysis of single nucleotide polymorphism array and exome sequence data. Circ Res. 2014;115:884–96.
7. Liu C, Cao R, Xu Y, et al. Rare copy number variants analysis identifies novel candidate genes in heterotaxy syndrome patients with congenital heart defects. Genome Med. 2018;10:40.
8. Watanabe Y, Benson DW, Yano S, et al. Two novel frameshift mutations in NKX2.5 result in novel features including visceral inversus and sinus venosus type ASD. J Med Genet. 2001;39: 807–11.
9. Izumi K, Noon S, Wilkens A, et al. NKX2.5 mutation identification on exome sequencing in a patient with heterotaxy. Eur J Med Genet. 2014;57:558–61.
10. Hirayama-Yamada K, Kamisago M, et al. Phenotypes with GATA4 or NKX2.5 mutations in familial atrial septal defect. Am J Med Genet A. 2005;135:47–52.
11. Ware SM, Peng J, Zhu L, et al. Identification and functional analysis of ZIC3 mutations in heterotaxy and related congenital heart defects. Am J Hum Genet. 2004;74:93–105.
12. Ma L, Selamet Tierney ES, Lee T, et al. Mutations in ZIC3 and ACVR2B are a common cause of heterotaxy and associated cardiovascular anomalies. Cardiol Young. 2012;22:194–201.
13. D'Alessandro LC, Casey B, Siu VM. Situs inversus totalis and a novel ZIC3 mutation in a family with X-linked heterotaxy. Congenit Heart Dis. 2013;8:E36–40.
14. Kosaki R, Gebbia M, Kosaki K, et al. Left-right axis malformations associated with mutations in ACVR2B, the gene for human activin receptor type IIB. Am J Med Genet. 1999;82:70–6.
15. Li AH, Hanchard NA, Azamain M, et al. Genetic architecture of laterality defects revealed by whole exome sequencing. Eur J Hum Genet. 2019;27:563–73.
16. Kaasinen E, Aittomäki K, Eronen M, et al. Recessively inherited right atrial isomerism caused by mutations in growth/differentiation factor 1 (GDF1). Hum Mol Genet. 2010;19:2747–53.
17. Bamford RN, Roessler E, Burdine RD, et al. Loss-of-function mutations in the EGF-CFC gene CFC1 are associated with human left-right laterality defects. Nat Genet. 2000;26:365–9.
18. Selamet Tierney ES, Marans Z, Rutkin MB, et al. Variants of the CFC1 gene in patients with laterality defects associated with congenital cardiac disease. Cardiol Young. 2007;17:268–74.
19. Roessler E, Ouspenskaia MV, Karkera JD, et al. Reduced NODAL signaling strength via mutation of several pathway members including FOXH1 is linked to human heart defects and holoprosencephaly. Am J Hum Genet. 2008;83:18–29.
20. Kosaki K, Bassi MT, Kosaki R, et al. Characterization and mutation analysis of human LEFTY a and LEFTY B, homologues of murine genes implicated in left-right axis development. Am J Hum Genet. 1999;64:712–21.

21. Mohapatra B, Casey B, Li H, et al. Identification and functional characterization of NODAL rare variants in heterotaxy and isolated cardiovascular malformations. Hum Mol Genet. 2009;18:861–71.
22. Zaidi S, Choi M, Wakimoto H, et al. De novo mutations in histone-modifying genes in congenital heart disease. Nature. 2013;498:220–3.
23. Guichard C, Harricane MC, Lafitte JJ, et al. Axonemal dynein intermediate-chain gene (DNAI1) mutations result in situs inversus and primary ciliary dyskinesia (Kartagener syndrome). Am J Hum Genet. 2001;68:1030–5.
24. Kennedy MP, Omran H, Leigh MW, et al. Congenital heart disease and other heterotaxic defects in a large cohort of patients with primary ciliary dyskinesia. Circulation. 2007;115: 2814–21.
25. Otto EA, Schermer B, Obara T, et al. Mutations in INVS encoding inversin cause nephronophthisis type 2, linking renal cystic disease to the function of primary cilia and left-right axis determination. Nat Genet. 2003;34:413–20.
26. Li Y, Yagi H, Obi Onuoha E, a. DNAH6 and its interactions with PCD genes in heterotaxy and primary ciliary dyskinesia. PLoS Genet. 2016;12:e1005821.
27. Liu S, Chen W, Zhan Y, et al. DNAH11 variants and its association with congenital heart disease and heterotaxy syndrome. Sci Rep. 2019;9(1):6683.
28. Bergmann C, Fliegauf M, Bruchle NO, et al. Loss of nephrocystin-3 function can cause embryonic lethality, Meckel-Gruber-like syndrome, situs inversus, and renal-hepatic-pancreatic dysplasia. Am J Hum Genet. 2008;82:959–70.
29. French VM, van de Laar IMBH, Wessels MW, et al. NPHP4 variants are associated with pleiotropic heart malformations. Circ Res. 2012;110:1564–74.
30. Perles Z, Cinnamon Y, Ta-Shma A, et al. A human laterality disorder associated with recessive CCDC11 mutation. J Med Genet. 2012;49:386–90.
31. Narasimhan V, Hjeij R, Vij S, et al. Mutations in CCDC11, which encodes a coiled-coil containing ciliary protein, causes situs inversus due to dysmotility of monocilia in the left-right organizer. Hum Mutat. 2015;36:307–18.
32. Ta-Shma A, Perles Z, Yaacov B, et al. A human laterality disorder associated with a homozygous WDR16 deletion. Eur J Hum Genet. 2015;23:1262–5.
33. Ta-Shma A, Hjeij R, Perles Z, et al. Homozygous loss-of-function mutations in MNS1 cause laterality defects and likely male infertility. PLoS Genet. 2018;14:e1007602.
34. Bataille S, Demoulin N, Devuyst O, et al. Association of PKD2 (polycystin 2) mutations with left-right laterality defects. Am J Kidney Dis. 2011;58:456–60.
35. Oka M, Mochizuki T, Kobayashi S. A novel mutation of the PKD2 gene in a Japanese patient with autosomal dominant polycystic kidney disease and complete situs inversus. Am J Kidney Dis. 2014;64:660.
36. Vetrini F, D'Alessandro LC, Akdemir ZC, et al. Bi-allelic mutations in PKD1L1 are associated with laterality defects in humans. Am J Hum Genet. 2016;99(4):886–93.
37. Tariq M, Belmont JW, Lalani S, et al. SHROOM3 is a novel candidate for heterotaxy identified by whole exome sequencing. Genome Biol. 2011;12:R91.
38. Robinson SW, Morris CD, Goldmuntz E, et al. Missense mutations in CRELD1 are associated with cardiac atrioventricular septal defects. Am J Hum Genet. 2003;72:1047–52.
39. Perles Z, Moon S, Ta-Shma A, et al. A human laterality disorder caused by a homozygous deleterious mutation in MMP21. J Med Genet. 2015;52:840–7.
40. Reish O, Aspit L, Zouella A, et al. A homozygous Nme7 mutation is associated with situs inversus totalis. Hum Mutat. 2016;37:727–31.
41. Chen W, Zhang Y, Yang S, et al. Bi-allelic mutations in NUP205 and NUP210 are associated with abnormal cardiac left-right patterning. Circ Genom Precis Med. 2019;12:e002492.
42. Andersen TA, Troelsen Kde LL, Larsen LA. Of mice and men: molecular genetics of congenital heart disease. Cell Mol Life Sci. 2014;71:1327–52.
43. Gebbia M, Ferrero GB, Pilia G, et al. X-linked situs abnormalities result from mutations in ZIC3. Nat Genet. 1997;17:305–8.

44. Casey B, Devoto M, Jones K, et al. Mapping a gene for familial situs abnormalities to human chromosome Xq24–q27.1. Nat Genet. 1993;5:403–7.
45. Ferrero GB, Gebbia M, Pilia G, et al. A submicroscopic deletion in Xq26 associated with familial situs ambiguus. Am J Hum Genet. 1997;61:395–401.
46. Belmont JW, Mohapatra B, Towbin JA, et al. Molecular genetics of heterotaxy syndromes. Curr Opin Cardiol. 2004;19:216–20.
47. Kurkowiak M, Zietkiewicz E, Witt M. Recent advances in primary cilia dyskinesia. J Med Genet. 2015;52:1–9.
48. Zaidi S, Brueckner M. Genetics and genomics of congenital heart disease. Circ Res. 2017;120: 923–40.
49. Watkins WS, Hernandez EJ, Wesolowski S, et al. De novo and recessive forms of congenital heart disease have distinct genetic and phenotypic landscapes. Nat Commun. 2019;10:4722.

Molecular Pathways and Animal Models of Defects in Situs

43

George C. Gabriel and Cecilia W. Lo

Abstract

Left–right patterning is among the least well understood of the three axes defining the body plan, and yet it is no less important, with left–right patterning defects causing structural birth defects with high morbidity and mortality, such as complex congenital heart disease, biliary atresia, or intestinal malrotation. The cell signaling pathways governing left–right asymmetry are highly conserved and involve multiple components of the TGF-β superfamily of cell signaling molecules. Central to left–right patterning is the differential activation of Nodal on the left, and BMP signaling on the right. In addition, a plethora of other cell signaling pathways including Shh, FGF, and Notch also contribute to the regulation of left–right patterning. In vertebrate embryos such as the mouse, frog, or zebrafish, the specification of left–right identity requires the left–right organizer (LRO) containing cells with motile and primary cilia that mediate the left-sided propagation of Nodal signaling, followed by left-sided activation of *Lefty* and then *Pitx2*, a transcription factor that specifies visceral organ asymmetry. While this overall scheme is well conserved, there are striking species differences, including the finding that motile cilia do not play a role in left–right patterning in some vertebrates. Surprisingly, the direction of heart looping, one of the first signs of organ left–right asymmetry, was recently shown to be specified by intrinsic cell chirality, not Nodal signaling, possibly a reflection of the early origin of Nodal signaling in radially symmetric organisms. How this intrinsic chirality interacts with downstream molecular pathways regulating visceral organ

G. C. Gabriel · C. W. Lo (✉)
Department of Developmental Biology, University of Pittsburgh School of Medicine, Pittsburgh, PA, USA
e-mail: gcg9@pitt.edu; cel36@pitt.edu

© The Author(s), under exclusive license to Springer Nature Switzerland AG 2024

S. Rickert-Sperling et al. (eds.), *Congenital Heart Diseases: The Broken Heart*,
Advances in Experimental Medicine and Biology 1441,
https://doi.org/10.1007/978-3-031-44087-8_43

asymmetry will need to be further investigated to elucidate how disturbance in left–right patterning may contribute to complex CHD.

Keywords

Left–right patterning · Situs inversus · Heterotaxy · Dextrocardia · Primary ciliary dyskinesia · Laterality defects · Kartagener syndrome · Motile cilia · Sonic hedgehog · Pitx2 · Dand5 · FoxJ1 · Nodal, Chirality

43.1 Introduction

The developmental regulation of anteroposterior and dorsoventral body axes are well described, while the mechanisms specifying left–right asymmetry are much less understood, but no less important [1, 2]. The establishment of left–right (L-R) asymmetry in the embryo is essential for developmental patterning of normal visceral organ asymmetry, referred to as situs solitis [Fig. 43.1]. Laterality defects can involve either complete mirror symmetric positioning of all visceral organs, referred to as situs inversus, or the randomized left–right patterning of visceral organ situs, referred to as heterotaxy [Fig. 43.1]. Individuals with situs inversus generally have no clinical presentations, and often are not discovered until a clinic visit uncovers abnormal right-sided position of the heart, also known as dextrocardia. However, patients with heterotaxy can present with life threatening birth defects, especially those associated with the cardiovascular system [3].

CHD patients with heterotaxy usually have complex structural heart defects with anomalous left–right atrioventricular and ventriculoarterial connections that disrupt systemic vs. pulmonary circulation. This causes high morbidity and mortality, as it prevents efficient oxygenation of blood from air in the lung. Left–right patterning defects also can disrupt development of the biliary duct causing biliary atresia [4]. In the absence of a functional bile duct, bile backs into the liver, causing liver cirrhosis, one of the most common reasons for pediatric liver transplantation. Left–right patterning defects also can cause bowel obstruction due to gut malrotation and formation of a volvulus, a life-threatening condition that requires surgical remediation [5]. Together these findings show disruptions in left–right patterning have important clinical consequences, and only with more mechanistic insights into the developmental regulation of left–right patterning can we hope to improve the management of heterotaxy patient care.

43.2 Nodal and TGFβ Signaling in the Embryonic Node

Studies using different model organisms have identified multiple evolutionarily conserved signaling pathways contributing to the specification of left–right asymmetry. In many vertebrate embryos, the specification of left–right patterning involves a specialized tissue referred to as the L-R organizer, also known as the

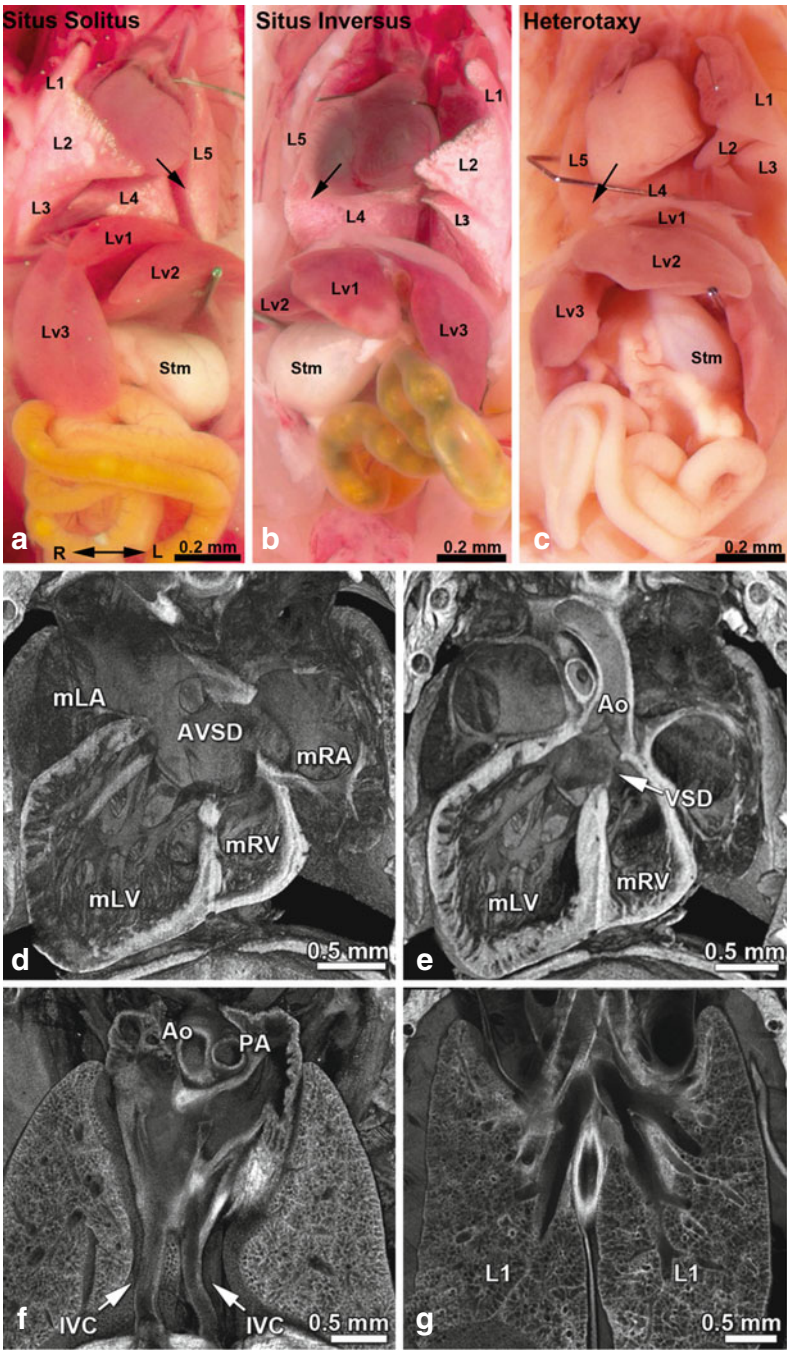

Fig. 43.1 Laterality defects in mutant mouse models. *Ap1b1*$^{m/m}$ mutants can exhibit a spectrum of laterality phenotypes spanning from normal situs solitus (**a**) to complete mirror symmetric situs inversus (**b**), or randomized visceral organ situs referred to as heterotaxy (**c**). In situs solitus, the heart apex (arrow) points to the left (levocardia), four lung lobes are on the right and one on the left,

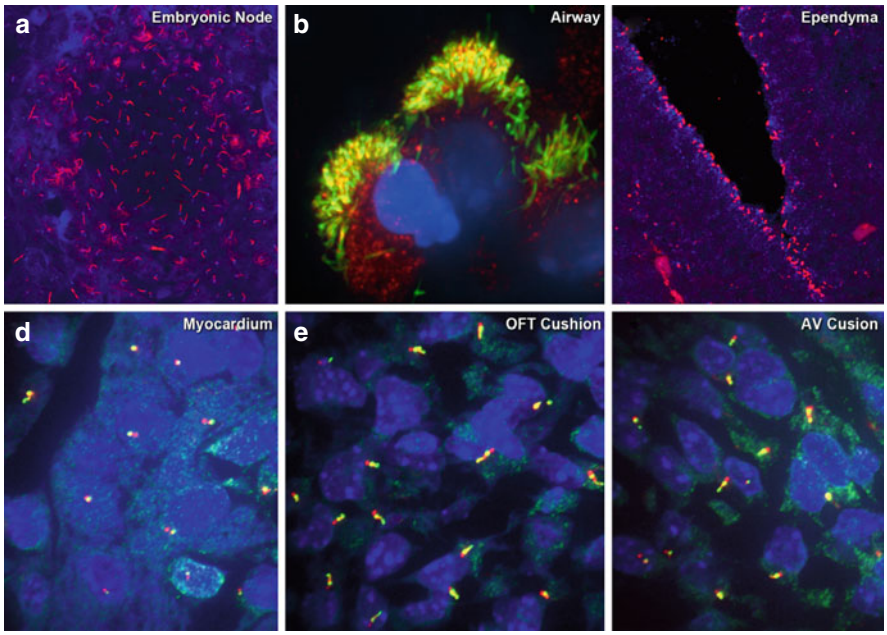

Fig. 43.2 Motile and primary cilia in different tissues of the mouse embryo. (**a**). Immunostaining with antibodies to acetylated tubulin (red) and γ-tubulin (blue) was used to visualize motile cilia in the E7.75 mouse embryonic node. (**b**–**f**) Immunostaining with antibodies to acetylated tubulin and IFT88 visualized cilia in the newborn mouse tracheal airway epithelia (**b**), in E12.5 brain ependyma (**c**), and primary cilia in the myocardium (**d**), outflow tract cushion (**e**), and atrioventricular cushion (**f**) of the E12.5 mouse embryonic heart

embryonic node in mice [Fig. 43.2], Kupffer's vesicle in zebrafish, the gastrocoel roof plate [GRP] in *Xenopus*, or Hensen's node in the chick. The asymmetric expression of genes in the embryonic node provides some of the earliest molecular signatures showing the evolving specification of visceral organ asymmetry [Fig. 43.3]. One such gene, *Nodal*, a TGFβ family member, is initially expressed bilaterally symmetric in the perinodal crown cells, but as development progresses, expression becomes elevated on the left side of the node [Fig. 43.3].

This left dominant expression of *Nodal* is propagated to the left lateral plate mesoderm (LPM) [Fig. 43.3], causing the induction of *Lefty2,* another TGFβ family member, and also the transcription factor *Pitx2,* the master regulator of left-sided tissue morphogenesis. Lefty2 is a diffusible competitive inhibitor of Nodal, and being monomeric, it diffuses more rapidly than the functionally active dimeric

Fig. 43.1 (continued) stomach is to the left, and the dominant liver lobe is on the right. With situs inversus, complete mirror reversal of organ situs is observed with both the heart and stomach on the right, while heterotaxy involves randomized visceral organ situs such as dextrocardia with levogastria shown in (**c**). From Li et al. [15]

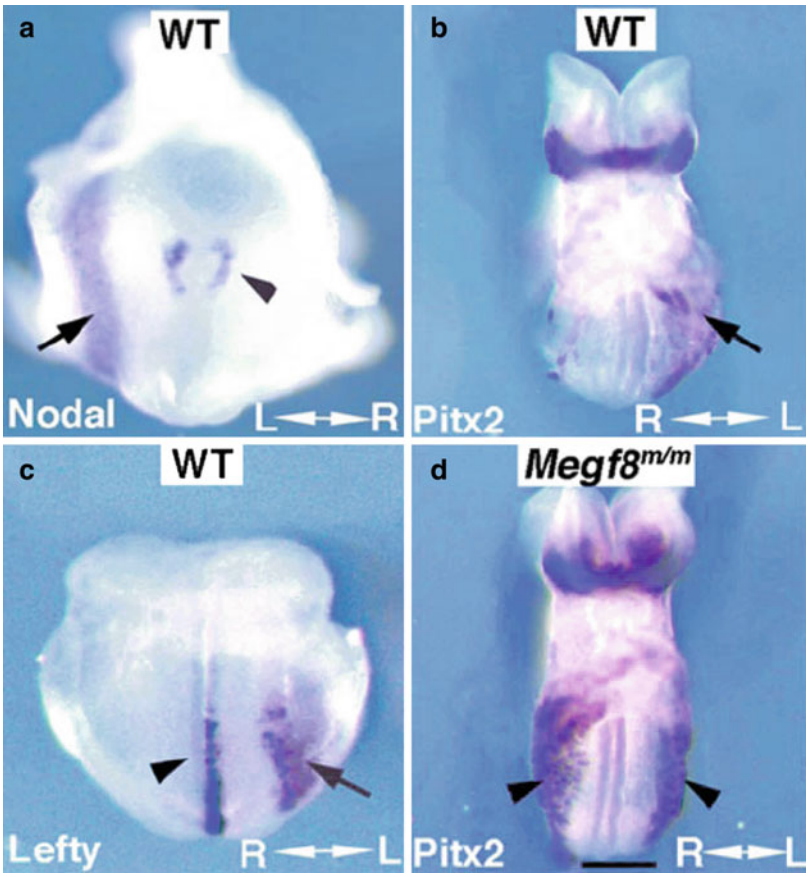

Fig. 43.3 Left-sided expression of left–determinant genes in mouse embryos. In situ hybridization analysis showed (***a*** and ***b***) left-sided expression of *Nodal* (**a**), Lefty (**b**), and Pitx2 (**c**) in wild type embryos. Note Nodal expression is reduced in the right (see arrowhead) vs. the opposing left side of the node (**a**). Lefty panel (**b**) shows expression Lefty1 expression (arrowhead) on the left side of the floor plate, while Lefty2 expression (arrow) is seen in the left LPM. PItx2 expression was observed in the left LPM and bilaterally in the head fold (**c**). In contrast, embryo with *Megf8*$^{m/m}$ mutation known to cause laterality defects (**d**), shows bilateral Pitx2 expression in the right and left LPM. From Zhang et al. 2009 [32]

Nodal, allowing it to repress Nodal signaling in the right LPM. A recent study in Zebrafish showed that this *Nodal/Lefty* feedback loop stabilized *Nodal* signaling ensuring robustness of signal propagation [6]. Additionally, expression of the related family member, *Lefty1,* along the axial midline, provides a barrier function that further ensures Nodal signaling is restricted to the embryo's right side. Ultimately, it is the Nodal activated expression of *Pitx2* on the embryo's left side that drives left-sided visceral organ morphogenesis.

43.3 Complex Regulation of Nodal

Nodal plays an important role not only in left–right patterning, but also in specification of the anterior–posterior axis, indicating the integration of left–right patterning with anterior posterior axis specification. The winged-helix transcription factor *FoxH1* acts upstream of Nodal [Fig. 43.4], with *FoxH1*-deficient mice exhibiting defects including anterior–posterior patterning defects, and failure of the node to form, phenotypes recapitulated by the loss of Nodal signaling [7]. *Nodal* and *FoxH1* also show overlapping expression in the node [8], and expression of *FoxH1* can induce *Lefty2* expression asymmetrically in both the *Xenopus* and mouse embryos [8, 9]. Nodal expression at the node is also subject to regulation by Notch signaling [10]. This is indicated by the finding of several binding sites for RBP-J, the main transcription factor mediating Notch signaling, in the Nodal enhancer. In addition, mice homozygote null for the Notch ligand *Dll1*, or doubly null for *Notch1/Notch2* are observed to have left–right patterning defects [10].

Recent work in zebrafish has also demonstrated the necessity of a Nodal coreceptor, one eyed pinhead (oep), for both the capture of the *Nodal* ligand and also in sensitizing receiving cells to the *Nodal* signal [11]. Furthermore, Nodal has also been shown to be subject to positive and negative regulation by other TGF-β family members. Thus, GDF1 is highly expressed in the node and is an upstream positive regulator of the Nodal signaling cascade on the embryo's left side. *Gdf1* knockout mouse embryos exhibit left–right patterning defects, such as situs inversus totalis or heterotaxy with congenital heart defects and right pulmonary isomerism [12]. This is associated with absence of *Lefty1* and *2* expression and failure in Nodal propagation to the left LPM.

Nodal expression mediating left–right patterning is also subject to negative regulation by various components of the TGF-β signaling pathways. In mouse embryos, *Cerberus-2 (Cerl2)*, also known as *Dand5,* or *Coco* in the Xenopus embryo, is a TGF-β antagonist expressed on the embryo's right side, causing *Nodal* repression on the right. However, beyond the 3-somite stage, Cerl2 protein shows nodal flow dependent accumulation on the embryo's left side, while *Cerl2* transcript expression remains right-sided. This translocation of Cerl2 protein to the left may serve to shut down Nodal expression on the left as the left–right axis is established [13]. Interestingly, flow-responsive post-transcriptional repression of *Dand5* was shown to be mediated through the binding of its 3'UTR by Bicc1, a RNA binding protein. This *Bicc1* repression of *Dand5* is induced by calcium currents generated by leftward fluid flow, accounting for the degradation of *Dand5* transcript*s* on the left side of the embryonic node [14]. Accordingly, mutation in *Bicc1* can cause left–right patterning defects in mice, Xenopus, and zebrafish [14, 15].

Thus, the combined observations from multiple model systems show *Nodal* acts as a morphogen diffusing from the embryonic node to the left lateral plate mesoderm to specify the left–right axis, a complex biological process involving many cofactors and complex feedback mechanisms. However, it is worth noting that recent work has shown the direction of heart tube looping, one of the first signs of visceral organ

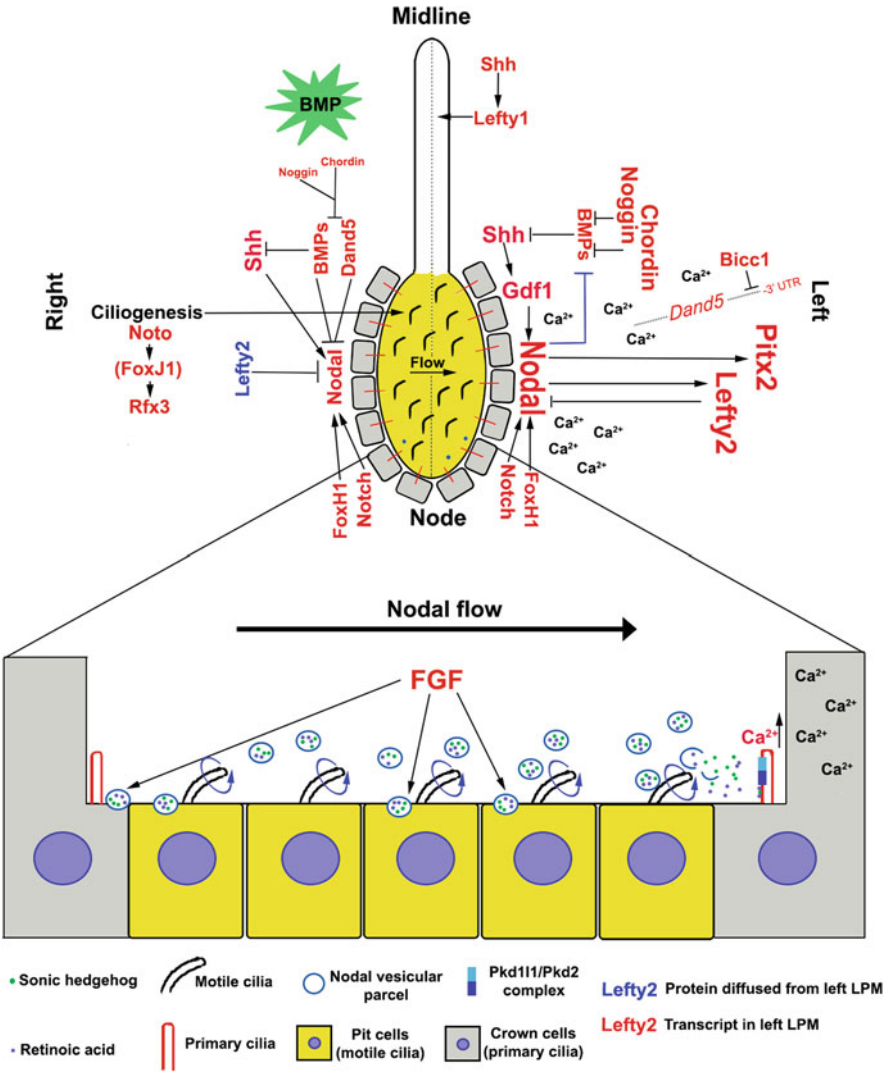

Fig. 43.4 Signaling pathways specifying left–right asymmetry. Schematic summary of cell signaling pathways contributing to the specification of laterality based on work in the mouse model. Left–right patterning requires cilia in the embryonic node. Indicated are pit cells (yellow) in the embryonic node with motile cilia driving unidirectional fluid flow. This causes mechanosensory transduction of primary cilia in the left perinodal crown cells and the elevation of calcium. A cascade of molecular signals help to propagate Nodal signaling on the embryo's left side, defining left identity. In contrast, Nodal signaling is repressed on the embryo's right, and together with high levels of BMP signaling, help define right identity. Unlike *Lefty2, Bmp* expression is bilaterally symmetric, but the green star serves to indicate high level of BMP signaling only on the right

asymmetry, is in fact not regulated by Nodal, but rather is encoded by intrinsic cell chirality ([16, 17]; also see Chap. 7). This surprising finding has been suggested to reflect the early origin of Nodal signaling in radially symmetric organisms [18]. How intrinsic cell chirality interacts with the molecular pathways of left–right patterning to establish cardiac left–right asymmetry will need to be further investigated, as only then can we hope to elucidate how defects in intrinsic chirality may contribute to complex CHD.

43.4 BMP Regulation of Nodal Signaling and Right-Sided Identity

BMP signaling is another pathway that plays an essential role in left–right patterning, exerting both positive and negative regulation on Nodal signaling. Thus, deficiency in BMP type II or type I receptors, *AcvrIIb* [19] and *Acvr1* [20], respectively, causes left–right patterning defects. Expression of the BMP ligand, BMP-4, is required for left–right patterning, but surprisingly its expression is actually bilaterally symmetric. This apparent discordance is explained by the higher left-sided expression of the BMP antagonists, *Noggin (Nog)* and *Chordin (Chrd)*, which represses BMP signaling on the embryo's left side, allowing left-sided Nodal propagation in the LPM [21, 22]. While these and other studies clearly show BMP signaling plays important roles in restricting Nodal activation in the right LPM, its right-sided activation may also help define right-sided identity.

43.5 Sonic Hedgehog Signaling and Left–Right Patterning

Sonic hedgehog (SHH) signaling, which is cilia transduced, is also required for left–right patterning. Canonical SHH signaling occurs when SHH binds to the receptor *Patched (Ptch)*, resulting in disinhibition and translocation of *Smoothened* (*Smo)* to the primary cilia where it activates a downstream signaling cascade. SHH was first identified to be involved in left–right axis determination in the chick embryo, where it is expressed on the left side of Hensen's node. Disturbance of this restricted expression in the node can result in heterotaxy with heart looping defects and gut malrotation [23, 24]. Interestingly, in mouse embryos this asymmetric expression of SHH is not observed. Nevertheless, SHH, and the related ligand *Indian hedgehog,* do contribute to left–right patterning, and also midline formation, and the establishment of the left-sided gene expression profile [25, 26]. Similarly, in *Smo* knock-out mice, left-sided activation of *Nodal* and *Lefty* is lost, resulting in failure of heart looping [26, 27]. These findings indicate the loss of SHH signaling can result in left–right patterning defects and impaired heart looping.

Additionally, mutations in genes identified as negative regulators of SHH signaling have also been associated with left–right patterning defects. Recent CRISPR screens have identified *Megf8*, *Mgrn1*, and *Mosmo* as negative regulators of SHH signaling [28, 29]. These proteins physically interact to form a membrane-tethered

ubiquitin complex, termed the MMM complex, that negatively regulates SHH signaling strength by promoting degradation of *Smo* [30, 31]. Loss of function mutations in *Megf8* cause heterotaxy with congenital heart disease including transposition of the great arteries (TGA), as do loss of function mutations in *Mgrn1*, though with a reduced penetrance [32, 33]. These mutations are associated with increased SHH signaling and accumulation of *Smo* in the cilia. Interestingly, in mice heterozygous for both *Megf8* and *Mgrn1* loss of function mutations, laterality defects were also observed, with 15% of animals showing dextrocardia and 36% of animals showing abnormal lung patterning [30]. Mutations in *Mosmo* were also found to result in laterality defects associated with elevated SHH signaling activity [31]. In addition to laterality defects, the *Megf8, Mgrn1,* and *Mosmo* mutant mice also were observed to exhibit transposition of the great arteries, an outflow tract malalignment defect often seen in conjunction with disturbance of laterality. Interestingly, detailed analysis of the *Megf8* mutant mice showed D vs. L-TGA can be observed with similar incidence, indicating dextro vs. levo outflow tract rotation represent randomization in left–right patterning [34]. This stands in marked contrast to the common consideration in the clinical context, that L-TGA but not D-TGA is a CHD phenotype associated with the disturbance of laterality. Overall, findings from the *Megf8*, *Mgrn1* and *Mosmo* mutant mice would suggest the precise level of SHH signaling is critical for proper-left right patterning and that disturbances in SHH signaling can result in complex CHD associated with other laterality defects.

43.6 Embryonic Node and Left–Right Patterning

The important role of Nodal signaling in patterning left–right visceral organ morphogenesis is unequivocal, but how the Nodal signaling cascade brings about the left–right asymmetric patterning of visceral organ morphogenesis is not well understood. The embryonic node has been the focal point of such studies. In the mouse embryo, it is formed at the anterior tip of the primitive streak at the future posterior side of the embryo. While it is often said that breaking of left–right symmetry occurs with asymmetric activation of nodal signaling at the embryonic node, left–right symmetry is already established earlier. Thus with formation of an anterior–posterior and dorsoventral axes in the pregastrulating mouse embryo, a left–right axis is defined by default [35]. The node subsequently forms at the anterior tip of the primitive streak, playing a critical role in the differential propagation of the Nodal signaling cascade to specify left identity. This regulation involves motile cilia that exhibit clockwise rotation creating a leftward fluid flow. In addition, there are also nonmotile primary cilia in cells at the node periphery referred to as perinodal crown cells. These have been shown to have a mechanosensory function in flow sensing and may help relay calcium signaling to propagate Nodal signaling.

43.7 Motile Cilia in Left–Right Patterning

The requirement for motile cilia in left–right patterning is suggested by the finding of laterality defects in mutants with disruption of motile cilia function. Insights first came from observations of mutations in two genes encoding kinesins, *Kif3a,* and *Kif3b* [36, 37]. Kinesins are molecular motors which traffic cargo along microtubule tracks, and importantly, are required for the assembly of cilia through intraflagellar transport. These kinesin mutant mice not only failed to form cilia and showed no nodal fluid flow, approximately 50% displayed laterality defects.

In reality, the connection between motile cilia and abnormalities of the situs has long been known clinically through observations of patients with Kartagener syndrome [38], a condition in which patients can exhibit situs inversus totalis together with sinopulmonary disease and male infertility due to motile cilia dysfunction, a condition referred to as primary ciliary dyskinesia, or PCD. While the mechanism by which motile cilia defect caused laterality defects in PCD patients was unknown at the time, the requirement for motile cilia function in left–right patterning was clearly indicated by these findings.

Corroborating these clinical findings with PCD patients were observation of the *inversus viserum (iv)* mutant mice. This mutant was later shown to harbor a mutation in the dynein gene, *Dnah11,* a gene now demonstrated to be a common cause of PCD [39]. In *iv* mutant mice, nodal cilia are formed, but are rendered immotile by the *Dnah11* deficiency, causing the disruption in left–right patterning. Such motile cilia defects underlie the sinopulmonary disease associated with PCD. Thus, *Dnah11* is required for motile cilia function mediating mucus clearance in the airway and in left–right patterning in the embryonic node.

Since these early studies, many motile cilia related genes have now been identified to cause PCD and laterality defects, including genes encoding other motor dyneins such as *DNAH5* [40, 41], and *DNAI1* [42, 43], as well as other cilia related genes [15]. These studies established a clear link between motile cilia defects and defects in left–right patterning. Two transcription factors, *FoxJ1* and *Rfx3*, are observed to play important roles in ciliogenesis at the node, with *Foxj1* also referred to as a master regulator of ciliogenesis [44]. While *Foxj1* knockout mice and morpholino knockdown of *foxj1* show loss of cilia [45–47], ciliogenesis was not affected in a *Foxj1* mouse mutant harboring a missense mutation in the conserved DNA binding domain [25]. Cilia were observed both in the airway and in the embryonic node of this mutant, although ciliary motion was dyskinetic in the node. These findings suggest the intriguing possibility that *Foxj1* may also have a nontranscriptional role in the regulation of cilia function.

It is notable that many if not all of the PCD genes also are known to cause complex CHD. This is observed in conjunction with heterotaxy. While many of the PCD genes can yield three phenotypic outcomes, situs solitus, situs inversus or heterotaxy, CHD is only observed with heterotaxy. Exactly how motile cilia regulate left–right patterning is still not well understood. Currently there are two predominant models, one referred to as a "morphogen" hypothesis that suggests motile cilia play a role in transporting a morphogen to the embryo's left side to specify left identity,

while a second model referred to as the "two cilia" hypothesis proposes motile cilia generated nodal flow propagates Nodal signaling via mechanosensory transduction of primary cilia in the perinodal crown cells. Below we briefly discuss evidence in support of these two models.

43.8 The "Morphogen" Hypothesis

The "morphogen" hypothesis proposes cilia generated flow in the node provides leftward transport of a secreted morphogen that establishes left identity [48]. This model builds on the observation of leftward transport of membrane vesicles up to 5 um in size termed nodal vesicular parcels (NVPs) in the node. These NVPs, released from microvilli, are swept across the node by cilia generated flow. Upon coming into contact with the rotating cilia, the NVPs undergo fragmentation, releasing smaller particles that accumulate along the left wall of the node. Significantly, these NVPs contain sonic hedgehog (SHH) and retinoic acid (RA), both known to play essential roles in left–right patterning (Fig. 43.4) [49, 50]. This left-sided concentration of morphogens from the NVPs is further proposed to trigger left-sided signal transduction mediated by sensory cilia in the perinodal crown cells, resulting in left-sided elevation of Ca^{2+}, and the propagation of *Nodal* expression, and asymmetric organ patterning.

Consistent with this NVP model, *Kif3a*-deficient embryos with no nodal cilia were observed to have significantly more NVPs [48]. Similarly, in *Dnah5* mutant embryos with paralyzed nodal cilia, we observed a similar accumulation of large vesicles, suggesting NVPs may fail to undergo fragmentation in *Dnah5* mutant embryos with paralyzed cilia (Fig. 43.5) [40]. Also of interest is our recent recovery of a mutant mouse harboring a mutation in an adaptin protein required for vesicular trafficking, *Ap1b1*. This mutant has laterality defects that precisely phenocopies

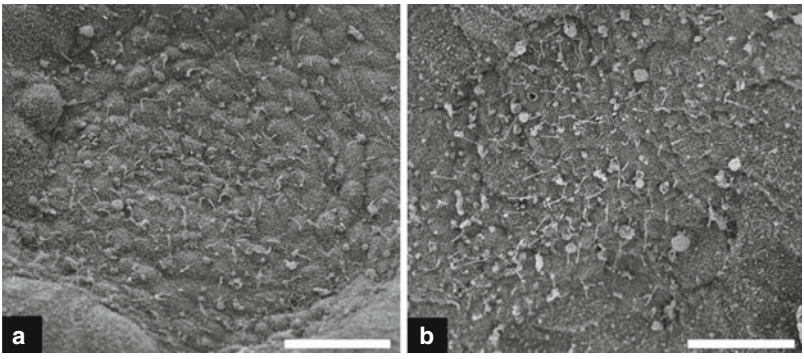

Fig. 43.5 Scanning electron microscopy images of mouse node. Scanning EM showing monociliated cells in the embryonic node of a wild-type (**a**) and Dnah5 mutant (**b**) mouse embryo. Note the markedly higher abundance of large vesicles that may correspond to an accumulation of NVPs in the *Dnah5* mutant node. From Tan et al. [40]

those observed in the *Dnah5* mutants [15]. Given the known roles of AP1B1 in recycling cargo destined for the membrane, and in regulating post-translational modifications of secreted proteins, this suggests the intriguing possibility of a role for *Ap1b1* in regulating NVP release at the node.

43.9 Role of Cilia in Left–Right Patterning

Two Cilia Hypothesis Another model that can account for the role of nodal flow in left–right patterning suggests motile and primary cilia are both involved in the specification of left–right patterning. This model proposes primary cilia in the perinodal crown cells on the left side of the node are deflected by nodal flow resulting in mechanosensory transduction and the elevation of Ca^{2+} to the left of the node. The notion that primary cilia may mediate flow sensing was first uncovered in the context of renal cells [51, 52], and its potential role in flow sensing in left–right patterning emerged with analysis of polycystin-2 (*Pkd2*) mutant mice [53], an ion channel protein known to be associated with polycystic kidney disease. Pkd2 is localized in nodal cilia (Fig. 43.6) [54] and *Pkd2* mutant mice failed to show Ca^{2+} elevation with nodal flow, while the *iv Dnah11* mutant mice with immotile cilia displayed left–right randomized calcium elevation. Together these observations support a role for polycystin-2 in mediating Ca^{2+} signaling upstream of Nodal signaling.

As polycystin-2 is known to form a complex with polycsytin-1 encoded by *Pkd1* in the primary cilia of renal cells to initiate calcium signaling, it was surprising that *Pkd1* mutants did not manifest any left–right patterning defects [55]. However, subsequent studies showed *Pkd1* is actually not expressed in the node [55]. Instead, node expression was observed for a *Pkd1* paralog, *Pkd1l1,* and *Pkd1l1* deficiency disrupted the propagation of Nodal signaling and resulted in left–right patterning defects [56]. PKD1L1 was shown to bind PKD2, an interaction required for ciliary localization of both proteins [57]. Together these observations provide further

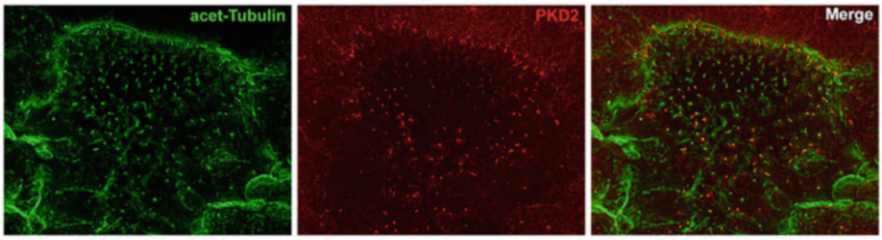

Fig. 43.6 Pkd2 is expressed in cilia at the mouse embryonic node. Cilia at the mouse embryonic node was visualized with antibodies to acetylated tubulin (green). Double immunostaining with a Pkd2 antibody showed Pkd2 (red) localization in a subset of cilia, including presumptive primary cilia in the crown cells at the node periphery and motile cilia within the pit of the node

evidence supporting the two-cilia hypothesis and the essential role of calcium signaling in left–right patterning.

Ciliogenesis Planar Cell Polarity Effector Network and Left–Right Patterning Genes mediating planar cell polarity (PCP), a highly conserved pathway that regulates epithelial cell polarity and also cilia transduced cell signaling (Wallingford paper). Proteomic analysis showed many of the PCP proteins physically interact forming a network of proteins referred to as the ciliogenesis planar cell polarity effector (CPLANE) network. The PCP genes are well described to mediate PCP signaling in *Drosophila*. In vertebrates, PCP signaling is essential for proper positioning of basal body required for establishing cilia orientation mediating leftward fluid flow required for left–right patterning. Thus, defects in proper basal body positioning in the mouse embryonic node can impair nodal flow and cause defects in left–right patterning [58–62].

The CPLANE network also has important roles in regulating ciliogenesis, actin dynamics, intraflagellar transport (IFT) and cilia transduced cell signaling. Importance of this CPLANE network is highlighted by the finding that five of the core genes in this network are highly evolutionarily conserved from sea anemone to man. Interestingly, at least 31 genes in the CPLANE network are identified to cause left–right patterning defects in mice. Moreover, many of the genes recovered from a large-scale mouse mutagenesis screen for mutations causing CHD are found in the CPLANE network ([15]; Gabriel and Lo, unpublished observations). Together these findings point to the CPLANE network playing a significant role both in cilia mediated regulation of left–right patterning and CHD pathogenesis.

43.10 Specification of Visceral Organ Asymmetry

The ultimate driver of left–right patterning of visceral organs is the left-sided expression of *Pitx2*. Loss of function in genes downstream of *Pitx2* in progenitor cells of the heart, lungs, liver, brain and other tissues can cause regionalized laterality defects [63], confirming the importance of *Pitx2* in visceral organ patterning. It is presumed the downstream response to *Pitx2* expression helps orchestrate patterning of visceral organ left–right asymmetry, but precisely how this is translated to visceral organ asymmetry is not well understood.

Left–Right Asymmetry of the Heart *Pitx2* has been shown to regulate the left–right asymmetry of the heart through patterning myocardium derived from the second heart field [64]. A conditional knockout of *Pitx2* in the secondary heart field perturbed outflow tract expansion and caused various outflow tract anomalies [64]. Interestingly, a nodal-independent pathway for determining the orientation of heart looping has been described in zebrafish. This involves intrinsic cardiomyocyte chirality regulated by actin polymerization and requiring myosin II activity [65]. While Nodal signaling initiates the actomyosin polymerization that drives

dextral heart looping, actomyosin dynamics were shown to be sufficient in driving dextral looping even in the absence of Nodal signaling. Conversely, Nodal signaling alone could not overcome the dextral heart looping defects caused by loss of actomyosin activity. Together these findings suggest the intrinsic chirality of actin polymerization and the resulting tissue tension may determine heart looping orientation, a mechanism similar to that proposed for cellular flow in establishing tissue polarity in the *Drosophilia* wing [66]. This cell intrinsic and Nodal independent specification of heart looping orientation has been suggested to reflect the early origin of Nodal signaling in radially symmetric organisms.

Left–Right Asymmetry of the Gut Asymmetry of the developing gut is also regulated by *Pitx2* in conjunction with expression of the transcription factors *Isl1* on the left vs. *Tbx18* on the right side of the dorsal mesentery (DM) [67]. This transcriptional cascade results in left-sided condensation of cells in the DM, forming a trapezoidal shape that causes a leftward tilt that drives stereotypical looping of the primitive gut tube. This involves downstream activation of *Daam2*, a GTPase-binding protein regulating the actin cytoskeleton, and is mediated through Pitx2 modulation of noncanonical Wnt signaling components Gpc3 and Frz [68]. Binding of activated Daam2 to α-catenin and N-Cadherin modulates cell adhesion to promote cell condensation in the left DM, driving orderly L-R asymmetric looping of the gut [68].

Left–Right Asymmetry of the Lung *Pitx2* also plays an important role in left–right asymmetric lung lobation. Typically, there are 3 lung lobes on the right and 2 on the left in the mouse and humans. However, it should be noted the pattern of mouse lung lobation is often referred to as four on the left and one on the right, as the left lower lung lobe is actually connected to the right bronchus. With disruption of left–right patterning, lung lobation may exhibit left isomerism with a single or two lung lobes observed bilaterally, or right isomerism with bilateral three or four lung lobes. Interestingly, knockout of all three isoforms of *Pitx2 (a,b,c)* causes right lung isomerism [69–71]. Deficiency in *FGF8*, which acts upstream of *Nodal*, also causes right pulmonary isomerism [72]. Mutation in *Mmp21*, an uncharacterized matrix metalloproteinase, is observed to cause heterotaxy with fully penetrant right pulmonary isomerism [15], indicating a role for the extracellular matrix in specification of lung asymmetry. The spleen is found along the curvature of the stomach on the left side of the abdomen, but perturbations in Nodal signaling and left-specific asymmetry pathways can result in polysplenia with several smaller, punctate spleens, asplenia, or hypoplastic spleen [8].

Brain Laterality An area much less studied is lateralization of the brain. In zebrafish, Nodal signaling has been shown to regulate the asymmetry of the epithalamus [73], a major division of the diencephalon that functions in photoreception and communication. Interestingly, morpholino knockdown of the *nodal*-related gene *southpaw* in zebrafish causes diencephalic and pancreatic left–right patterning defects in addition to disruption of cardiac looping [74], demonstrating coordination

in the patterning of visceral organ and brain left–right asymmetry. Additionally, a clinical study using MRI showed individuals with situs inversus have reversed frontal and occipital petalia, while left hemisphere dominance for language and handedness remained unchanged [75]. Overall, there is a paucity of information on lateralization of the brain, making it difficult to ascertain its potential importance in neurobehavioral and neurocognitive function.

43.11 Conserved Yet Divergent Mechanisms Regulating Left–Right Patterning

The developmental pathways regulating left–right patterning are largely conserved in evolution, but there are some notable differences observed. Thus the essential role of motile cilia driven flow in left–right patterning has been well demonstrated in most vertebrates such as the mouse, zebrafish, or Xenopus, but unexpectedly, motile cilia do not appear to play a role in left–right patterning in the chick or pig embryos [76]. Furthermore, the "two cilia hypothesis" does not appear to be applicable to zebrafish or Medaka fish, as only motile cilia are observed in Kupffer's vesicle, the mouse embryonic node equivalent [57].

The overall molecular mechanism governing L-R asymmetry with Nodal signaling is largely conserved, but some species-specific differences have been noted downstream of *Nodal*. For example, the asymmetric expression of *activin-BB*, *activin receptor IIA*, and *Shh* in Hensen's node of the chick is not observed in the mouse, *Xenopus*, or zebrafish. In the chick embryo, *Shh* expression is asymmetrically expressed in the left LPM, a pattern not observed in the mouse or other vertebrate species. In chick embryos, *Shh* signaling is observed to mediate L-R asymmetry by inducing the Cer-like protein Caronte (Car) [77]. Car then activates *Nodal* expression by antagonizing Notch repression mediated by BMP signaling. This complex molecular cascade involving Shh, Caronte, BMP, and FGF8 appears to be unique to the chick embryo.

Also notable is the finding in *Xenopus*, of early specification of left–right asymmetries mediated by differential expression of $H^{+/}K^{+}$ dependent ATPase transcript and protein at the two-cell stage [78]. Ablation of H^{+} and K^{+} dependent ATPase causes heterotaxy not only in *Xenopus* embryos, but also in the zebrafish and chick embryos [79]. Its loss disrupts the normal pattern of asymmetric Shh expression in Hensen's node of the chick [78]. In *Xenopus* embryos, the asymmetric expression of the $H^{+/}K^{+}$ dependent ATPase together with gap junction mediated cell-cell communication is proposed to specify asymmetric expression of the neurotransmitter serotonin in the 32-cell stage embryo. Its importance in left–right patterning is indicated by the finding of heterotaxy with loss of serotonin receptors R3 and R4 [80]. To date, the role of serotonin in the regulation of left–right patterning has not been studied in other species.

43.12 Summary

Left–right patterning is regulated by a conserved pathway involving a complex cascade of positive and negative regulation of Nodal signaling. This involves cross regulation by a plethora of other cell signaling pathways including Shh, Bmp, and Fgf. This culminates in the left-sided expression of *Pitx2* specifying left identity, while BMP signaling contributes to right identity. Both motile and primary cilia play important roles in laterality specification. This likely involves the downstream modulation of calcium signaling. The requirement for motile cilia in left–right patterning is not universal, nor the mechanosensory transduction by primary cilia. As yet, precisely how *Pitx2* expression translates to a pattern of visceral organ asymmetry is not well understood, but regulation of cytoskeletal organization, and cell migration may contribute to the patterning of tissue asymmetries. The recent identification of intrinsic chirality specifying heart looping orientation independent of Nodal signaling indicates an additional layer of complexity in the regulation of heart organ laterality that will require further investigation. Insights into how intrinsic cell chirality interacts with downstream pathways to regulate cardiac laterality will be needed to elucidate the developmental etiology of complex CHD.

Acknowledgment This work is supported by funding from NIH HL142788 and HL132024 (to CWL) and HD097967 (to GCG).

References

1. Huelsken J, Vogel R, Brinkmann V, Erdmann B, Birchmeier C, Birchmeier W. Requirement for beta-catenin in anterior-posterior axis formation in mice. J Cell Biol. 2000;148(3):567–78.
2. Zeng L, Fagotto F, Zhang T, Hsu W, Vasicek TJ, Perry WL 3rd, et al. The mouse fused locus encodes Axin, an inhibitor of the Wnt signaling pathway that regulates embryonic axis formation. Cell. 1997;90(1):181–92.
3. Ware SM, Jefferies JL. New genetic insights into congenital heart disease. J Clin Exp Cardiol. 2012:S8. https://doi.org/10.4172/2155-9880.S8-003.
4. Mack CL, Sokol RJ. Unraveling the pathogenesis and etiology of biliary atresia. Pediatr Res. 2005;57(5 Pt 2):87R–94R. https://doi.org/10.1203/01.PDR.0000159569.57354.47.
5. Martin V, Shaw-Smith C. Review of genetic factors in intestinal malrotation. Pediatr Surg Int. 2010;26(8):769–81. https://doi.org/10.1007/s00383-010-2622-5.
6. Rogers KW, Lord ND, Gagnon JA, Pauli A, Zimmerman S, Aksel DC, et al. Nodal patterning without lefty inhibitory feedback is functional but fragile. Elife. 2017;6:e28785.
7. Yamamoto M, Meno C, Sakai Y, Shiratori H, Mochida K, Ikawa Y, et al. The transcription factor FoxH1 (FAST) mediates nodal signaling during anterior-posterior patterning and node formation in the mouse. Genes Dev. 2001;15(10):1242–56. https://doi.org/10.1101/gad.883901.
8. Saijoh Y, Adachi H, Sakuma R, Yeo CY, Yashiro K, Watanabe M, et al. Left-right asymmetric expression of lefty2 and nodal is induced by a signaling pathway that includes the transcription factor FAST2. Mol Cell. 2000;5(1):35–47.
9. Osada SI, Saijoh Y, Frisch A, Yeo CY, Adachi H, Watanabe M, et al. Activin/nodal responsiveness and asymmetric expression of a Xenopus nodal-related gene converge on a FAST-regulated module in intron 1. Development. 2000;127(11):2503–14.

10. Krebs LT, Iwai N, Nonaka S, Welsh IC, Lan Y, Jiang R, et al. Notch signaling regulates left-right asymmetry determination by inducing nodal expression. Genes Dev. 2003;17(10):1207–12. https://doi.org/10.1101/gad.1084703.
11. Lord ND, Carte AN, Abitua PB, Schier AF. The pattern of nodal morphogen signaling is shaped by co-receptor expression. elife. 2021;10:e54894.
12. Rankin CT, Bunton T, Lawler AM, Lee SJ. Regulation of left-right patterning in mice by growth/differentiation factor-1. Nat Genet. 2000;24(3):262–5. https://doi.org/10.1038/73472.
13. Inacio JM, Marques S, Nakamura T, Shinohara K, Meno C, Hamada H, et al. The dynamic right-to-left translocation of Cerl2 is involved in the regulation and termination of nodal activity in the mouse node. PLoS One. 2013;8(3):e60406. https://doi.org/10.1371/journal.pone.0060406.
14. Minegishi K, Rothé B, Komatsu KR, Ono H, Ikawa Y, Nishimura H, et al. Fluid flow-induced left-right asymmetric decay of Dand5 mRNA in the mouse embryo requires a Bicc1-Ccr4 RNA degradation complex. Nat Commun. 2021;12(1):4071. https://doi.org/10.1038/s41467-021-24295-2.
15. Li Y, Klena NT, Gabriel GC, Liu X, Kim AJ, Lemke K, et al. Global genetic analysis in mice unveils central role for cilia in congenital heart disease. Nature. 2015;521(7553):520–4. https://doi.org/10.1038/nature14269.
16. Noël ES, Verhoeven M, Lagendijk AK, Tessadori F, Smith K, Choorapoikayil S, et al. A nodal-independent and tissue-intrinsic mechanism controls heart-looping chirality. Nat Commun. 2013;4(1):2754. https://doi.org/10.1038/ncomms3754.
17. Ray P, Chin AS, Worley KE, Fan J, Kaur G, Wu M, et al. Intrinsic cellular chirality regulates left–right symmetry breaking during cardiac looping. Proc Natl Acad Sci. 2018;115(50):E11568–E77. https://doi.org/10.1073/pnas.1808052115.
18. Blum M, Feistel K, Thumberger T, Schweickert A. The evolution and conservation of left-right patterning mechanisms. Development. 2014;141(8):1603–13. https://doi.org/10.1242/dev.100560.
19. Oh SP, Li E. The signaling pathway mediated by the type IIB activin receptor controls axial patterning and lateral asymmetry in the mouse. Genes Dev. 1997;11(14):1812–26.
20. Kishigami S, Yoshikawa S, Castranio T, Okazaki K, Furuta Y, Mishina Y. BMP signaling through ACVRI is required for left-right patterning in the early mouse embryo. Dev Biol. 2004;276(1):185–93. https://doi.org/10.1016/j.ydbio.2004.08.042.
21. Mine N, Anderson RM, Klingensmith J. BMP antagonism is required in both the node and lateral plate mesoderm for mammalian left-right axis establishment. Development. 2008;135(14):2425–34. https://doi.org/10.1242/dev.018986.
22. Veerkamp J, Rudolph F, Cseresnyes Z, Priller F, Otten C, Renz M, et al. Unilateral dampening of Bmp activity by nodal generates cardiac left-right asymmetry. Dev Cell. 2013;24(6):660–7. https://doi.org/10.1016/j.devcel.2013.01.026.
23. Levin M, Johnson RL, Sterna CD, Kuehn M, Tabin C. A molecular pathway determining left-right asymmetry in chick embryogenesis. Cell. 1995;82(5):803–14. https://doi.org/10.1016/0092-8674(95)90477-8.
24. Levin M, Pagan S, Roberts DJ, Cooke J, Kuehn MR, Tabin CJ. Left/right patterning signals and the independent regulation of different aspects of Situsin the Chick Embryo. Dev Biol. 1997;189(1):57–67. https://doi.org/10.1006/dbio.1997.8662.
25. Tsukui T, Capdevila J, Tamura K, Ruiz-Lozano P, Rodriguez-Esteban C, Yonei-Tamura S, et al. Multiple left-right asymmetry defects in Shh(−/−) mutant mice unveil a convergence of the Shh and retinoic acid pathways in the control of Lefty-1. Proc Natl Acad Sci. 1999;96(20):11376–81. https://doi.org/10.1073/pnas.96.20.11376.
26. Zhang XM, Ramalho-Santos M, McMahon AP. Smoothened mutants reveal redundant roles for Shh and Ihh signaling including regulation of L/R asymmetry by the mouse node. Cell. 2001;105(6):781–92.
27. Tsiairis CD, McMahon AP. An Hh-dependent pathway in lateral plate mesoderm enables the generation of left/right asymmetry. Curr Biol. 2009;19(22):1912–7.

28. Breslow DK, Hoogendoorn S, Kopp AR, Morgens DW, Vu BK, Kennedy MC, et al. A CRISPR-based screen for hedgehog signaling provides insights into ciliary function and ciliopathies. Nat Genet. 2018;50(3):460–71.
29. Pusapati GV, Kong JH, Patel BB, Krishnan A, Sagner A, Kinnebrew M, et al. CRISPR screens uncover genes that regulate target cell sensitivity to the morphogen sonic hedgehog. Dev Cell. 2018;44(1):113–29. e8
30. Kong JH, Young CB, Pusapati GV, Patel CB, Ho S, Krishnan A, et al. A membrane-tethered ubiquitination pathway regulates hedgehog signaling and heart development. Dev Cell. 2020;55 (4):432–49.e12. https://doi.org/10.1016/j.devcel.2020.08.012.
31. Kong JH, Young CB, Pusapati GV, Espinoza FH, Patel CB, Beckert F, et al. Gene-teratogen interactions influence the penetrance of birth defects by altering Hedgehog signaling strength. Development. 2021;148(19) https://doi.org/10.1242/dev.199867.
32. Zhang Z, Alpert D, Francis R, Chatterjee B, Yu Q, Tansey T, et al. Massively parallel sequencing identifies the gene Megf8 with ENU-induced mutation causing heterotaxy. Proc Natl Acad Sci. 2009;106(9):3219–24.
33. Cota CD, Bagher P, Pelc P, Smith CO, Bodner CR, Gunn TM. Mice with mutations in Mahogunin ring finger-1 (Mgrn1) exhibit abnormal patterning of the left–right axis. Dev Dyn. 2006;235(12):3438–47. https://doi.org/10.1002/dvdy.20992.
34. Aune CN, Chatterjee B, Zhao X-Q, Francis R, Bracero L, Yu Q, et al. Mouse model of heterotaxy with single ventricle spectrum of cardiac anomalies. Pediatr Res. 2008;63(1):9–14.
35. Tam PP, Behringer RR. Mouse gastrulation: the formation of a mammalian body plan. Mech Dev. 1997;68(1–2):3–25.
36. Nonaka S, Tanaka Y, Okada Y, Takeda S, Harada A, Kanai Y, et al. Randomization of left-right asymmetry due to loss of nodal cilia generating leftward flow of extraembryonic fluid in mice lacking KIF3B motor protein. Cell. 1998;95(6):829–37.
37. Takeda S, Yonekawa Y, Tanaka Y, Okada Y, Nonaka S, Hirokawa N. Left-right asymmetry and kinesin superfamily protein KIF3A: new insights in determination of laterality and mesoderm induction by kif3A−/− mice analysis. J Cell Biol. 1999;145(4):825–36.
38. Afzelius BA. A human syndrome caused by immotile cilia. Science. 1976;193(4250):317–9.
39. Supp DM, Witte DP, Potter SS, Brueckner M. Mutation of an axonemal dynein affects left-right asymmetry in inversus viscerum mice. Nature. 1997;389(6654):963–6. https://doi.org/10.1038/40140.
40. Tan SY, Rosenthal J, Zhao XQ, Francis RJ, Chatterjee B, Sabol SL, et al. Heterotaxy and complex structural heart defects in a mutant mouse model of primary ciliary dyskinesia. J Clin Invest. 2007;117(12):3742–52. https://doi.org/10.1172/JCI33284.
41. Hornef N, Olbrich H, Horvath J, Zariwala MA, Fliegauf M, Loges NT, et al. DNAH5 mutations are a common cause of primary ciliary dyskinesia with outer dynein arm defects. Am J Respir Crit Care Med. 2006;174(2):120–6. https://doi.org/10.1164/rccm.200601-084OC.
42. Nakhleh N, Francis R, Giese RA, Tian X, Li Y, Zariwala MA, et al. High prevalence of respiratory ciliary dysfunction in congenital heart disease patients with heterotaxy. Circulation. 2012;125(18):2232–42. https://doi.org/10.1161/CIRCULATIONAHA.111.079780.
43. Zariwala M, Noone PG, Sannuti A, Minnix S, Zhou Z, Leigh MW, et al. Germline mutations in an intermediate chain dynein cause primary ciliary dyskinesia. Am J Respir Cell Mol Biol. 2001;25(5):577–83. https://doi.org/10.1165/ajrcmb.25.5.4619.
44. Yu X, Ng CP, Habacher H, Roy S. Foxj1 transcription factors are master regulators of the motile ciliogenic program. Nat Genet. 2008;40(12):1445–53. https://doi.org/10.1038/ng.263.
45. Chen J, Knowles HJ, Hebert JL, Hackett BP. Mutation of the mouse hepatocyte nuclear factor/forkhead homologue 4 gene results in an absence of cilia and random left-right asymmetry. J Clin Invest. 1998;102(6):1077–82. https://doi.org/10.1172/JCI4786.
46. Brody SL, Yan XH, Wuerffel MK, Song SK, Shapiro SD. Ciliogenesis and left-right axis defects in forkhead factor HFH-4-null mice. Am J Respir Cell Mol Biol. 2000;23(1):45–51. https://doi.org/10.1165/ajrcmb.23.1.4070.

47. Stubbs JL, Oishi I, Izpisua Belmonte JC, Kintner C. The forkhead protein Foxj1 specifies node-like cilia in Xenopus and zebrafish embryos. Nat Genet. 2008;40(12):1454–60. https://doi.org/10.1038/ng.267.
48. Tanaka Y, Okada Y, Hirokawa N. FGF-induced vesicular release of sonic hedgehog and retinoic acid in leftward nodal flow is critical for left-right determination. Nature. 2005;435(7039):172–7. https://doi.org/10.1038/nature03494.
49. Levin M, Pagan S, Roberts DJ, Cooke J, Kuehn MR, Tabin CJ. Left/right patterning signals and the independent regulation of different aspects of situs in the chick embryo. Dev Biol. 1997;189(1):57–67. https://doi.org/10.1006/dbio.1997.8662.
50. Kawakami Y, Raya A, Raya RM, Rodriguez-Esteban C, Izpisua Belmonte JC. Retinoic acid signalling links left-right asymmetric patterning and bilaterally symmetric somitogenesis in the zebrafish embryo. Nature. 2005;435(7039):165–71. https://doi.org/10.1038/nature03512.
51. Praetorius H, Spring K. Bending the MDCK cell primary cilium increases intracellular calcium. J Membr Biol. 2001;184(1):71–9.
52. Praetorius H, Spring K. Removal of the MDCK cell primary cilium abolishes flow sensing. J Membr Biol. 2003;191(1):69–76.
53. Pennekamp P, Karcher C, Fischer A, Schweickert A, Skryabin B, Horst J, et al. The ion channel polycystin-2 is required for left-right axis determination in mice. Curr Biol. 2002;12(11):938–43.
54. McGrath J, Somlo S, Makova S, Tian X, Brueckner M. Two populations of node monocilia initiate left-right asymmetry in the mouse. Cell. 2003;114(1):61–73.
55. Karcher C, Fischer A, Schweickert A, Bitzer E, Horie S, Witzgall R, et al. Lack of a laterality phenotype in Pkd1 knock-out embryos correlates with absence of polycystin-1 in nodal cilia. Differ Res Biol Diver. 2005;73(8):425–32. https://doi.org/10.1111/j.1432-0436.2005.00048.x.
56. Field S, Riley KL, Grimes DT, Hilton H, Simon M, Powles-Glover N, et al. Pkd1l1 establishes left-right asymmetry and physically interacts with Pkd2. Development. 2011;138(6):1131–42. https://doi.org/10.1242/dev.058149.
57. Kamura K, Kobayashi D, Uehara Y, Koshida S, Iijima N, Kudo A, et al. Pkd1l1 complexes with Pkd2 on motile cilia and functions to establish the left-right axis. Development. 2011;138(6):1121–9. https://doi.org/10.1242/dev.058271.
58. Hashimoto M, Shinohara K, Wang J, Ikeuchi S, Yoshiba S, Meno C, et al. Planar polarization of node cells determines the rotational axis of node cilia. Nat Cell Biol. 2010;12(2):170–6. https://doi.org/10.1038/ncb2020.
59. Antic D, Stubbs JL, Suyama K, Kintner C, Scott MP, Axelrod JD. Planar cell polarity enables posterior localization of nodal cilia and left-right axis determination during mouse and Xenopus embryogenesis. PLoS One. 2010;5(2):e8999.
60. Song H, Hu J, Chen W, Elliott G, Andre P, Gao B, et al. Planar cell polarity breaks bilateral symmetry by controlling ciliary positioning. Nature. 2010;466(7304):378–82.
61. Borovina A, Superina S, Voskas D, Ciruna B. Vangl2 directs the posterior tilting and asymmetric localization of motile primary cilia. Nat Cell Biol. 2010;12(4):407–12.
62. Toriyama M, Lee C, Taylor SP, Duran I, Cohn DH, Bruel A-L, et al. The ciliopathy-associated CPLANE proteins direct basal body recruitment of intraflagellar transport machinery. Nat Genet. 2016;48(6):648–56. https://doi.org/10.1038/ng.3558.
63. Piedra ME, Icardo JM, Albajar M, Rodriguez-Rey JC, Ros MA. Pitx2 participates in the late phase of the pathway controlling left-right asymmetry. Cell. 1998;94(3):319–24.
64. Ai D, Liu W, Ma L, Dong F, Lu MF, Wang D, et al. Pitx2 regulates cardiac left-right asymmetry by patterning second cardiac lineage-derived myocardium. Dev Biol. 2006;296(2):437–49. https://doi.org/10.1016/j.ydbio.2006.06.009.
65. Noel ES, Verhoeven M, Lagendijk AK, Tessadori F, Smith K, Choorapoikayil S, et al. A nodal-independent and tissue-intrinsic mechanism controls heart-looping chirality. Nat Commun. 2013;4:2754. https://doi.org/10.1038/ncomms3754.

66. Major RJ, Irvine KD. Localization and requirement for myosin II at the dorsal-ventral compartment boundary of the *Drosophila* wing. Dev Dyn. 2006;235(11):3051–8. https://doi.org/10.1002/dvdy.20966.
67. Davis NM, Kurpios NA, Sun X, Gros J, Martin JF, Tabin CJ. The chirality of gut rotation derives from left-right asymmetric changes in the architecture of the dorsal mesentery. Dev Cell. 2008;15(1):134–45. https://doi.org/10.1016/j.devcel.2008.05.001.
68. Welsh IC, Thomsen M, Gludish DW, Alfonso-Parra C, Bai Y, Martin JF, et al. Integration of left-right Pitx2 transcription and Wnt signaling drives asymmetric gut morphogenesis via Daam2. Dev Cell. 2013;26(6):629–44. https://doi.org/10.1016/j.devcel.2013.07.019.
69. Gage PJ, Suh H, Camper SA. Dosage requirement of Pitx2 for development of multiple organs. Development. 1999;126(20):4643–51.
70. Kitamura K, Miura H, Miyagawa-Tomita S, Yanazawa M, Katoh-Fukui Y, Suzuki R, et al. Mouse Pitx2 deficiency leads to anomalies of the ventral body wall, heart, extra- and periocular mesoderm and right pulmonary isomerism. Development. 1999;126(24):5749–58.
71. Liu S, Cheung E, Rajopadhye M, Williams NE, Overoye KL, Edwards DS. Isomerism and solution dynamics of (90)Y-labeled DTPA--biomolecule conjugates. Bioconjug Chem 2001;12(1):84–91
72. Fischer A, Viebahn C, Blum M. FGF8 acts as a right determinant during establishment of the left-right axis in the rabbit. Curr Biol. 2002;12(21):1807–16.
73. Concha ML, Wilson SW. Asymmetry in the epithalamus of vertebrates. J Anat. 2001;199(Pt 1–2):63–84.
74. Long S, Ahmad N, Rebagliati M. The zebrafish nodal-related gene southpaw is required for visceral and diencephalic left-right asymmetry. Development. 2003;130(11):2303–16.
75. Kennedy DN, O'Craven KM, Ticho BS, Goldstein AM, Makris N, Henson JW. Structural and functional brain asymmetries in human situs inversus totalis. Neurology. 1999;53(6):1260–5.
76. Gros J, Feistel K, Viebahn C, Blum M, Tabin CJ. Cell movements at Hensen's node establish left/right asymmetric gene expression in the chick. Science. 2009;324(5929):941–4. https://doi.org/10.1126/science.1172478.
77. Rodriguez Esteban C, Capdevila J, Economides AN, Pascual J, Ortiz A, Izpisua Belmonte JC. The novel Cer-like protein Caronte mediates the establishment of embryonic left-right asymmetry. Nature. 1999;401(6750):243–51. https://doi.org/10.1038/45738.
78. Aw S, Adams DS, Qiu D, Levin M. H,K-ATPase protein localization and Kir4.1 function reveal concordance of three axes during early determination of left-right asymmetry. Mech Dev. 2008;125(3–4):353–72. https://doi.org/10.1016/j.mod.2007.10.011.
79. Adams DS, Robinson KR, Fukumoto T, Yuan S, Albertson RC, Yelick P, et al. Early, H+-V-ATPase-dependent proton flux is necessary for consistent left-right patterning of non-mammalian vertebrates. Development. 2006;133(9):1657–71. https://doi.org/10.1242/dev.02341.
80. Fukumoto T, Kema IP, Levin M. Serotonin signaling is a very early step in patterning of the left-right axis in chick and frog embryos. Curr Biol. 2005;15(9):794–803. https://doi.org/10.1016/j.cub.2005.03.044.

Part XI

Semilunar Valve and Aortic Arch Anomalies

Clinical Presentation and Therapy of Semilunar Valve and Aortic Arch Anomalies

44

Nikolaus A. Haas, David J. Driscoll, and Silke Rickert-Sperling

44.1 Introduction

The following semilunar valve defects and aortic arch anomalies are called simple defects because there is a single problem that can be well described. Based on the degree of malformation and hemodynamic consequence, these simple lesions can however be life threatening immediately after birth. They all affect either the left or right outflow tract or the aortic arch.

There are three types of congenital aortic stenosis that all share as common hemodynamics a pressure load of the left ventricle. The most common is aortic valve stenosis and this comprises approximately 5% of congenital heart defects. The aortic valve cusps or leaflets are congenitally malformed. The second type of aortic stenosis is supravalvar aortic stenosis, involving a narrowing of the ascending aorta just above the sinotubular junction. The third type of aortic stenosis is subvalvar aortic stenosis. Some forms may be linked to a malformed aortic valve with additional stenosis and will lead to a significant volume load of the LV.

Coarctation of the aorta consists of a ledge-shaped protrusion of tissue into the aorta immediately opposite the insertion of the ductus or ligamentum arteriosus. An interrupted aortic arch can be seen as the maximum form of coarctation. Frequently,

N. A. Haas (✉)
Department of Pediatric Cardiology and Intensive Care, Ludwig Maximilians University, Munich, Germany
e-mail: Nikolaus.haas@med.uni-muenchen.de

D. J. Driscoll
Division of Pediatric Cardiology, Department of Pediatrics, Mayo Clinic College of Medicine, Rochester, MN, USA
e-mail: driscoll.david@mayo.edu

S. Rickert-Sperling
Cardiovascular Genetics, Charité – Universitätsmedizin Berlin, Berlin, Germany
e-mail: silke.sperling@charite.de

© The Author(s), under exclusive license to Springer Nature Switzerland AG 2024

S. Rickert-Sperling et al. (eds.), *Congenital Heart Diseases: The Broken Heart*,
https://doi.org/10.1007/978-3-031-44087-8_44

there is an associated bicuspid aortic valve or other variations of the aortic vessels, including rings and slings that may cause compression of the trachea and/or esophagus.

Pulmonary valve stenosis (with intact ventricular septum) usually occurs sporadically and may be combined with supravalvular and/or infundibular stenoses. In extreme cases, there is pulmonary atresia with intact ventricular septum. Isolated pulmonary valve insufficiency is rare. It can accompany idiopathic dilation of the pulmonary artery and pulmonary vascular obstructive disease.

44.2 Aortic Stenosis and Insufficiency

44.2.1 Pathologic Physiology

There are three types of congenital aortic stenosis that all share as common hemodynamics a pressure load of the left ventricle. The most common is aortic valve stenosis and this comprises approximately 5% of congenital heart defects. The aortic valve cusps or leaflets are congenitally malformed. They may be thickened and the raphe may be fused. Usually, these valves are bicuspid. One to 2% of the general population has a bicuspid aortic valve that may or may not be stenotic or insufficient. However, over time these valves may develop stenosis or insufficiency. In addition, even in the absence of stenosis or insufficiency, they can be associated with ascending aortic aneurysm formation.

The second type of aortic stenosis is supravalvar aortic stenosis. This involves a narrowing of the ascending aorta just above the sinotubular junction. This form is often linked to specific syndromes of the elastin pathway, such as Williams (Beuren) Syndrome and the stenosis may be short and circular or long and tubular.

The third type of aortic stenosis is subvalvar aortic stenosis. In this condition, there is a fibromuscular ridge or tunnel that causes obstruction a short distance below the valve. In those cases with a tunnel, this usually presents immediately after birth whereas those cases with a fibromuscular ridge often develop over time and present later during infancy and childhood. This type is associated with AVSDs.

Aortic regurgitation is rarely a single congenital problem; aortic insufficiency frequently occurs in conjunction with aortic valve stenosis especially if the valve is bicuspid (Fig. 44.1). However, aortic insufficiency can occur because of a bicuspid aortic valve even in the absence of aortic stenosis. Aortic insufficiency is frequently a complication of surgical or balloon procedures to treat aortic valve stenosis by balloon valvuloplasty. Some forms may be linked to a malformed aortic valve with additional stenosis and will lead to a significant volume load of the left ventricle.

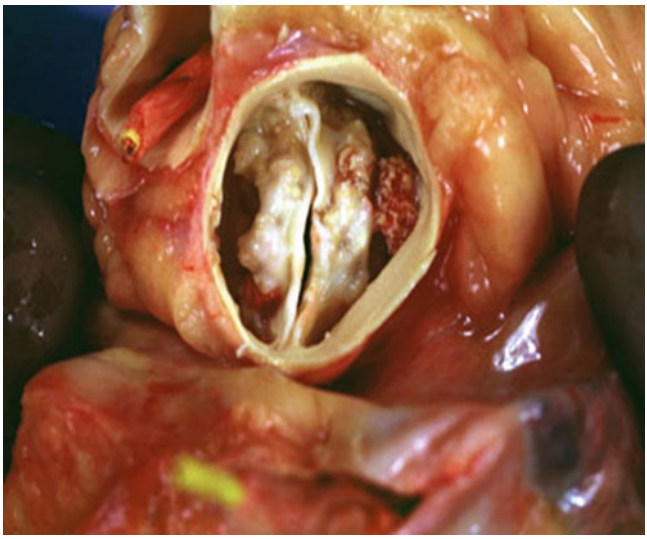

Fig. 44.1 Pathologic specimen of a bicuspid stenotic calcified aortic valve

44.2.2 Clinical Presentation

The clinical presentation of aortic valve stenosis depends upon the severity of the obstruction. The measure of severity of the obstruction is based upon the pressure drop across the valve during systole. In trivial aortic stenosis, the pressure difference is 0–25 mmHg; in mild stenosis, it is 26–50 mmHg. In moderate stenosis, the pressure difference is 51–79 mmHg, while it is >80 mmHg in severe stenosis.

Most patients with aortic stenosis are asymptomatic and are diagnosed because of the presence of a cardiac murmur. Rarely, syncope is the presenting sign of aortic stenosis. There are cases of severe aortic stenosis where the first presentation is acute cardiac death during exercise or similar situations. A critical aortic stenosis describes the situation in newborns when systemic perfusion cannot be maintained via transaortic blood flow; this may be because of the severe narrowing of the valve orifice or the dramatically reduced left ventricular function. In these circumstances systemic perfusion must be maintained by the right ventricle and a patent ductus arteriosus (i.e., duct dependent systemic perfusion or circulation). Infants with severe aortic stenosis can present with low cardiac output, severely reduced ejection fraction, shock, and/or congestive heart failure. Aortic insufficiency usually presents with a diastolic murmur. Severe or progressive aortic insufficiency may present with fatigue, shortness of breath, exercise intolerance, orthopnea, and/or paroxysmal nocturnal dyspnea.

44.2.3 Physical Examination

The apical impulse may be increased for patients with moderate or severe stenosis. There may be a thrill palpable at the base of the heart and over the carotid arteries. The first heart sound is normal and the second heart sound is normal. With aortic valve stenosis (but not with supravalvar or subvalvar stenosis) an ejection click will be heard immediately after the first heart sound.

The murmur of aortic stenosis is systolic and crescendo decrescendo or "diamond shaped." It is best heard along the left sternal border and radiates to the right upper sternal border. Some patients with aortic stenosis have associated aortic insufficiency, and, if that is the case, a decrescendo diastolic murmur will be audible.

Aortic insufficiency is characterized by a decrescendo murmur that begins immediately after S2 that is best heard at the left sternal border. In severe aortic regurgitation, there is a high pulse amplitude.

44.2.4 Diagnostic Imaging

Transthoracic echocardiography is an accurate diagnostic tool for evaluating all forms of aortic stenosis and regurgitation, as well as detecting other possible associated malformations. Using echo/Doppler techniques, it is possible to estimate the transaortic pressure gradient noninvasively, providing important information about the severity of the stenosis. Additionally, echocardiography allows for the assessment of left ventricular wall thickness, which is reflective of the severity of the stenosis.

Echocardiography and Doppler can also confirm the presence of aortic insufficiency and are useful in determining the severity of the regurgitation. In cases of severe regurgitation, diastolic backward flow into the abdominal aorta or cerebral vessels may be observed in neonates. These techniques enable the determination of regurgitant fraction, left ventricular systolic and diastolic dimensions, and left ventricular ejection fraction, providing valuable information about the impact of the regurgitation on cardiac function.

In some cases, transesophageal echocardiography may be necessary in teenagers and adult patients to clarify the exact anatomy of the aortic valve and provide additional information for surgical repair.

In the era of echocardiography, it is today usually not necessary to perform diagnostic cardiac catheterization for the diagnosis of aortic stenosis or regurgitation.

Magnetic resonance imaging (MRI) can be used in adults and teenagers to assess the left ventricular mass in aortic stenosis and/or left ventricular volume in aortic regurgitation. Serial assessment can help in defining the indication for therapeutic intervention.

Computer tomography (CAT-Scan) can provide the same anatomic details as MRI and is rarely necessary for the diagnosis of AS/AI in children. It can be used however in patients with contraindications for MRI.

44.2.5 Treatment

In the management of valvular aortic stenosis, various treatment options are available to alleviate the stenosis. These include:

1. Trantransvascular Balloon Dilation: This procedure involves inserting a catheter with a balloon tip into the narrowed valve and inflating the balloon to stretch the valve open. It is a minimally invasive approach.
2. Surgical Valvotomy, Repair, or Reconstruction: Open-heart surgery may be performed to directly manipulate the valve. This can involve techniques such as valvotomy (incising the valve to widen the opening), valve repair (reconstructing the valve to improve its function), or valve replacement.
3. Valve Replacement: In cases where the valve cannot be repaired, it may need to be replaced. Several options are available, including homograft valves (from human donors), porcine valves (from pigs), or mechanical valves. The choice depends on factors such as the patient's age, condition, and preference.
4. Transcatheter Aortic Valve Implantation (TAVI): This procedure, commonly performed in elderly patients, involves inserting a new valve through a catheter and implanting it within the diseased valve. TAVI is less invasive than open-heart surgery and is suitable for certain patients, however, for the time beeing not for children or younger patients.

In infants, children, and small teenagers, commercially available valves may not be suitable due to their size. Alternative approaches, such as the Ross procedure, may be considered. The Ross procedure involves using the patient's own pulmonary valve to replace the stenotic aortic valve, with a homograft valve used in the pulmonary position. Additional procedures such as resection of fibromuscular tissue or patch augmentation of the left ventricular outflow tract (LVOT) may be necessary in some cases.

For significant aortic insufficiency, valve reconstruction or replacement options are similar to those for aortic stenosis. In selected cases, the surgeon may attempt to repair the valve. If bicuspid aortic valve or aortic stenosis is associated with an ascending aneurysm, repair of the aneurysm may also be necessary.

44.2.6 Outcome

Patients with aortic stenosis generally have an excellent long-term prognosis and maintain a normal quality of life and exercise capacity. However, aortic stenosis remains a lifelong condition despite treatment. It is important to note the following considerations:

1. Likelihood of additional surgery: After balloon dilation or surgical valvotomy, there is a 40% chance that additional surgery will be required over the next

25 years. This is typically due to the development of aortic regurgitation (leakage of the aortic valve).
2. Lifelong anticoagulation: If aortic valve replacement is performed using a mechanical prosthesis, the patient will need to take lifelong anticoagulation therapy to prevent blood clots. This therapy helps reduce the risk of valve thrombosis, but it requires regular monitoring and medication adherence.
3. Tissue valve replacement: Alternatively, a tissue valve may be used for aortic valve replacement. However, it is important to note that tissue valves have a limited lifespan. On average, the half-life of a tissue valve is approximately 10–20 years, depending on factors such as the type of valve used, the age of the patient, and the patient's size. Eventually, the tissue valve may need to be replaced.
4. Treatment of Aortic Valve Insufficiency: In cases of primary aortic valve insufficiency (leakage of the aortic valve), repair of the valve may be possible in some instances. However, in most cases, valve replacement will be necessary.
5. Periprocedural Mortality: The risk of mortality associated with aortic valve interventions, including both repair and replacement, is generally low, with periprocedural mortality rates reported to be less than 5%.

44.3 Coarctation of the Aorta

44.3.1 Pathologic Physiology

Coarctation of the aorta is a condition characterized by a narrowing or protrusion of tissue in the aorta, specifically at the aortic isthmus, which is the segment just opposite the insertion of the ductus arteriosus or ligamentum arteriosus (Fig. 44.2). This narrowing can lead to significant obstruction of blood flow through the aorta, resulting in decreased blood supply to the lower body.

In response to the obstruction caused by coarctation of the aorta, collateral vessels may develop as a compensatory mechanism (Fig. 44.3). These collateral vessels serve to bypass the narrowed segment of the aorta and ensure an adequate blood supply to the abdominal organs and lower extremities. The collateral vessels can

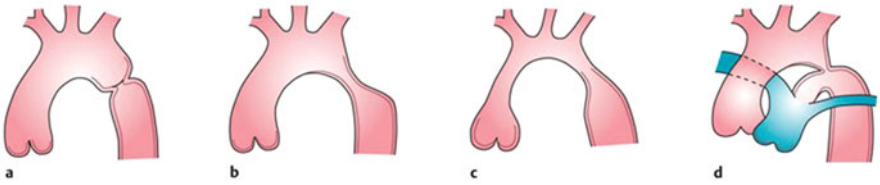

Fig. 44.2 Cartoon showing different variants of coarctation of the aorta: (**a**) localized aortic isthmus stenosis, (**b**) tubular aortic isthmus stenosis, (**c**) aortic isthmus stenosis with hypoplasia of the entire aortic arch, (**d**) critical aortic isthmus stenosis with duct-dependent systemic perfusion. Reproduced from Kinderkardiologie, Georg Thieme Verlag, N. Haas, U. Kleideiter, 2011

Fig. 44.3 Pathological specimen of severe coarctation of the aorta and compensatory collateral vessels

arise from various sources, such as intercostal arteries, internal mammary arteries, or subclavian arteries, and their development helps maintain blood flow to the areas downstream of the coarctation.

The narrowing of the aorta leads to increased pressure proximal to the stenosis and reduced blood flow and pressure distal to the stenosis. This results in a noticeable difference in blood pressure and pulse between the arms and legs, known as an arm-to-leg blood pressure gradient and pulse deficit. However, in some cases, the coarctation may also affect the orifice of the left subclavian artery. In these instances, the blood pressure discrepancy may be between the right arm and leg rather than the left arm and leg. Similarly, if the right subclavian artery has an aberrant origin from the descending aorta distal to the coarctation, there may not be a significant difference in blood pressure or pulses between the right arm and leg. To accurately diagnose coarctation of the aorta, it is crucial to measure blood pressure in both arms and at least one leg. This helps ensure the correct identification of any discrepancies. Additionally, coarctation of the aorta is often accompanied by varying degrees of hypoplasia (underdevelopment) of the aortic arch proximal to the

stenosis. This combination of coarctation and arch hypoplasia further contributes to the hemodynamic changes and clinical presentation of the condition.

44.3.2 Clinical Presentation

The clinical presentation of coarctation of the aorta depends upon the severity of the obstruction and the associated anomalies. Very severe coarctation of the aorta may become apparent at 2–5 days of life when the ductus arteriosus closes and congestive heart failure occurs. These forms are defined as critical.

A critical coarctation describes the situation in newborns when the systemic perfusion cannot be maintained via the usual transaortic blood flow; this may be because of the severe narrowing of the vessel and sometimes in combination with a dramatically reduced left ventricular function. In these circumstances systemic perfusion must be maintained by the right ventricle and a patent ductus arteriosus (i.e., duct dependent systemic perfusion or circulation).

If the coarctation is not severe enough to cause heart failure in infancy, the patient usually remains asymptomatic. The presence of the defect may be heralded by the presence of a heart murmur or systemic hypertension. The simple pulse palpation and the measurement of blood pressure at all four extremities will lead to the diagnosis. Unfortunately, in some instances the presence of a coarctation is not appreciated until adolescence. As there is a significant prestenotic permanent hypertension, rarely, with previously undetected coarctation of the aorta, a cerebral vascular accident may be the presenting event.

44.3.3 Physical Examination

Newborns with critical Coarctation or infants with severe coarctation of the aorta may have the usual signs of congestive heart failure including tachycardia, poor perfusion, grunting, tachypnea, and hepatomegaly. Low amplitude or absent pulses in the lower extremities as compared to the upper extremities is the sine quo non of coarctation of the aorta. In places where a pulse oximetry screening is in place, these children should be picked up by low saturations at the feet/toes.

Since many patients with coarctation of the aorta have an associated bicuspid aortic valve, an aortic ejection click frequently is heard shortly after the first heart sound.

Turbulent blood flow through the area of coarctation produces a systolic ejection murmur that is best heard at the cardiac apex and below the left scapula. Because many patients with coarctation of the aorta have subtle or important abnormalities of the mitral valve, a diastolic murmur may be heard at the apex of the heart.

The formation of collateral vessels can affect the physical findings. Parascapular collateral vessels can produce a continuous murmur in the region of the scapula, and, in some patients, these vessels can be palpated. As collateral vessels form, the pressure gradient across the coarctation can decrease making the arm-to-leg blood

pressure gradient a less reliable measure of severity of the coarctation. The typical finding however is a reduced femoral pulse and this is a pathognomonic sign for coarctation and implemented in most pediatric screening programs. In addition there will be a blood pressure gradient between the arms and legs.

44.3.4 Diagnostic Imaging

44.3.4.1 Echocardiography

The presence of coarctation of the aorta is ascertained by clinical examination. Although the vast majority of coarctations are located opposite the aortic insertion of the ductus or ligamentum arteriosus, rarely the lesion may be located more distally in the aorta (i.e., midaortic syndrome). Thus, transthoracic echocardiography or some other form of imaging is necessary to localize the area of coarctation and to establish the length of the narrow segment. Using echo/Doppler techniques, it is possible, noninvasively, to estimate the transaortic pressure gradient. A typical indirect sign is the reduced flow in the abdominal aorta. In addition, associated lesions such as aortic stenosis, VSD, or mitral valve disease can be identified and quantified. The severity of the coarctation can be estimated by the degree of left ventricular hypertrophy and wall thickness, which also is a reflection of the severity of the stenosis. In some cases, measuring the cross-sectional area or the diameter of the coarctation site may be feasible.

44.3.4.2 Cardiac Catheterization

In the era of echocardiography, it is today usually not necessary to perform diagnostic cardiac catheterization for the diagnosis of coarctation of the aorta. It is however used to treat coarctation interventionally.

44.3.4.3 Magnetic Resonance Imaging

Magnetic resonance imaging (MRI) can be used in children, adults and teenagers to assess the exact localization and anatomy of the coarctation, and assessing its severity. MRI allows detailed imaging of the entire aorta in multiple planes and views as well as a 3D reconstruction. It also allows identification of collateral vessels. This may be helpful for the planning of surgery or intervention, as well as for the follow-up. Serial assessment by MRI can help in defining the indication for therapeutic intervention.

44.3.4.4 Computer Tomography

Computer tomography (CAT-Scan) can provide the same anatomic details as MRI and is rarely necessary for the diagnosis of coarctation in children. It can be used however in patients with contraindications for MRI.

44.3.4.5 Prenatal Detection

Usually coarctations will not be picked up in routine prenatal scans due to the patency of the large ductus arteriosus and the related flow patterns. Indirect signs

that may lead to an early postnatal assessment may be a hypoplastic distal aortic arch or a bicuspid aortic valve.

44.3.5 Treatment

The treatment approach for coarctation of the aorta involves the removal or elimination of the obstruction, aiming to create an adequately sized aorta. This is typically determined by comparing the size of the coarctation site to the minimum diameter of the aorta at the level of the diaphragm, known as the coarctation gradient (normal: >1).

In infants with critical coarctation, it is important to provide a prostaglandin E1 infusion until surgical repair can be performed. Surgery, specifically extended end-to-end resection, is the preferred treatment for all patients below the age of 6–-12 months. After this age, interventional measures such as balloon dilatation and/or stent implantation have shown comparable results and can be considered. In cases of recurrent coarctation, interventional management is the preferred treatment option.

44.3.5.1 Prenatal Management

Prenatal management of coarctation of the aorta involves specific considerations. If coarctation is detected as a single cardiac malformation during prenatal screening, it does not typically warrant termination of the pregnancy. These children generally have favorable clinical outcomes, normal exercise capacity, and a normal life expectancy. Spontaneous vaginal delivery is recommended, and there is no medical indication for a cesarean section solely due to coarctation of the aorta. However, if a critical coarctation is anticipated, delivery should be planned in a medical center equipped with the necessary resources, including prostaglandin E infusion, pediatric cardiologists, pediatric cardiac intensive care, and surgical services.

44.3.6 Outcome

Today with the widespread use of prostaglandin, preprocedure mortality is less than 5% for the management of coarctation of the aorta. This is mainly caused by undetected patients with abdominal malperfusion and the development of necrotizing enterocolitis, sepsis, and/or cardiogenic shock.

However, long-term problems persist even after excellent primary repair. Recurrent or persistent coarctation occurs in a significant number of patients and can be as high as 30% if operation or balloon dilation is necessary in the first 6 weeks of life. Since 50–80% of patients with coarctation of the aorta have associated bicuspid aortic valve, eventual treatment of aortic stenosis or insufficiency may be necessary. Also, even for patients with repaired coarctation of the aorta, persistent hypertension may be present and require long-term follow-up and treatment, especially in those where an insufficient anatomical result persists (i.e., with a coarctation index below 0.9).

44.4 Aortic Arch Abnormalities: Rings and Slings

There is a great variation of vascular abnormalities that will impair the trachea and the esophagus and lead to a variability of the anatomy with or without compression of the esophagus and trachea. There are some well described forms of these variations that will be described here.

44.4.1 Aberrant Origin of the Right Subclavian Artery (ARSA, Lusorian Artery)

Normally the first branch of the aorta (subsequent to the coronary arteries) is the right innominate artery which gives rise to the subclavian and the right carotid arteries. However, the right subclavian artery can arise directly from the aorta distal to the origin of the left subclavian artery In this instance, the right subclavian artery travels behind the esophagus to reach the right arm. This anatomical variant is also called Lusorian artery, and it is the most common variant of the aortic arch; sometimes there is an enlargement or dilatation of the origin of this artery that is called the diverticulum of Kommerell. In most cases, this anomaly is of no clinical significance and, contrary to some belief, does *not* result in a vascular ring. It may however cause dysphagia or in rare cases stridor, dyspnea, and even chest pain. This clinical picture is termed as dysphagia lusoria. In very rare cases a Lusorian artery with a diverticulum of Kommerell may compress the recurrent laryngeal nerve causing a palsy (i.e., hoarseness); this is termed Ortner's syndrome. If clinically relevant, the artery may be dissected and transposed. The presence of an ARSA is more common in fetuses with Trisomy 21 and other chromosomal defects (22q11.1 microdeletion or duplication) than in healthy fetuses. It is a weak prenatal marker and should prompt a detailed search for additional "soft markers" and structural defects.

44.4.2 Double Aortic Arch

This malformation represents about one third of all congenital vascular rings. Usually during embryonic life, the right-sided aortic arch obliterates, but if both sides persist, a true double arch results. These two arches include the esophagus as well as the trachea and may cause tracheal obstruction with stridor and stenosis, pulmonary infections and chocking as well as esophageal obstruction with dysphagia, feeding difficulties and/or recurrent aspirations.

In many cases, there is a dominant (i.e., larger) right arch and a hypoplastic (i.e., smaller) left-sided arch. The two arches join and form the descending aorta. Complete double aortic arch can usually be detected by simple echocardiography, barium esophagogram, and tracheoscopy. The latter may reveal various forms of tracheal stenoses and/or tracheomalacia.

When one side—usually the smaller left side—obliterates and forms a fibrous band, it is called an incomplete double arch; the term vascular ring is however

accepted in these cases. MRI and CT may be helpful to visualize the exact anatomy before surgical intervention.

In all symptomatic patients, surgical repair is needed. This consists of resection of the hypoplastic left-sided arch and all ligaments including the PDA, and sometimes even tracheal surgery and/or aortopexia or tracheopexia to improve the space for the respiratory pathways. Nevertheless, tracheobronchomalacia may persist for several years.

44.4.3 Pulmonary Artery Sling

A pulmonary artery sling (or pulmonary sling or aberrant left pulmonary artery) is another form of vascular ring. Usually the left pulmonary artery and the right pulmonary artery both originate at the end of the main pulmonary artery in front of the trachea and the esophagus. In a pulmonary sling however, the left pulmonary artery arises from the right pulmonary artery and is usually much smaller. It runs above and anterior to the right main bronchus and then turns backward behind the trachea and in front of the esophagus to the left side and then enters the hilum of the left lung.

Depending on its size a pulmonary artery sling can lead to significant tracheobronchial compression, a tracheal cartilage ring with stenosis and tracheobronchomalacia, hyperinflation and/or migrating atelectasis. Typically this congenital heart defect presents in the neonatal period with severe stridor, cough, apneic spells, hypoxia, and ventilator dependency. Infants may suffer from acute life threatening events (ALTE). Ultimately, all patients with a pulmonary sling will become symptomatic, however some patients may present late in life. Age at presentation is typically determined by the degree of tracheal stenosis. Congenital heart defects such as septal defects, TOF, PDA, AVSD, and aortic arch abnormalities are observed in 30–40% of the cases. Repair is recommended in all patients with PAS and tracheal stenosis at the time of diagnosis. The principles of surgical repair consist of translocation of the aberrant left pulmonary artery and reconstruction of the abnormal trachea (i.e., slide tracheostomy).

44.4.4 Right Aortic Arch with Aberrant Left Subclavian Artery and Left Ductus Arteriosus or Ligamentum Arteriosum

This is another abnormality that is responsible for about one third of congenital vascular rings, Even though it is not really a vascular ring, as most of the anatomical structures are fibrous, the hemodynamic result is identical. The right aortic arch descends right of the trachea and crosses behind the trachea and esophagus to the left side of the chest. The left common carotid crosses from anterior to the left side. The left subclavian artery originates (similarly to a Lusorian artery) with a diverticulum (of Kommerell) and provides the origin of the PDA or ligamentum arteriosum Thus, the trachea and esophagus are completely encircled. Clinically, tracheomalacia and

or esophageal obstruction and even acute life-threatening events (ALTE) may occur depending on the size of the left subclavian artery and diverticulum of Kommerell and the size of the fibrous ring. Surgical relief is recommended in all symptomatic patients as well as in all other patients with congenital heart defects at the time of their surgical repair.

44.5 Interrupted Aortic Arch

Interrupted aortic arch (IAA) implies discontinuity between the ascending aorta and the descending aorta. Between the two parts there is usually fibrous tissue but no true vascular lumen. The perfusion of the lower part of the body depends on patency of the ductus arteriosus. There are three types of IAA. Type A occurs distal to the left subclavian artery and comprises about one third of cases. It may well be regarded as the most severe form of coarctation of the aorta. The most common is type B which occurs between the left carotid artery and the left subclavian artery. It comprises about two thirds of cases. Type C occurs between the right and left carotid artery and is the least common type.

IAA occurs between 19 and 66 per million live births. It is very unusual for IAA to occur as an isolated anomaly. Type A frequently is associated with aortopulmonary window with an intact ventricular septum. Type B frequently is associated with conotruncal defects and is frequently associated with 22q11 microdeletion (about 75%). A VSD is present in 90% of cases. Subaortic stenosis caused by left-sided malalignment is common. Ten to 20% of cases of truncus arteriosus are associated with IAA.

44.5.1 Pathologic Physiology

With IAA perfusion of the descending aorta is dependent upon the presence of a patent ductus arteriosus. Hence, newborns with IAA need to be maintained on a prostaglandin infusion until continuity of the ascending and descending aorta can be established surgically. Perfusion of the lower body may be possible by collateral blood flow in certain cases of type A. When the PDA closes, these children become acutely symptomatic with cardiogenic shock.

44.5.2 Clinical Presentation

Newborns with interrupted aortic arch may exhibit a murmur caused by the associated ventricular septal defect (VSD) shortly after birth. In settings where general pulse oximetry screening is implemented, these infants may be identified by differential cyanosis, characterized by higher oxygen saturations in the arms/fingers and lower saturations in the feet/toes. The closure of the patent ductus arteriosus (PDA) can lead to the sudden onset of symptoms, including cardiogenic shock.

44.5.3 Physical Examination

Newborns with interrupted aortic arch may exhibit typical signs of congestive heart failure, such as tachycardia, poor perfusion, grunting, tachypnea, and hepatomegaly. A notable characteristic is the presence of lower extremity pulses with lower amplitude or weakness compared to pulses in the upper extremities. In settings where pulse oximetry screening is conducted, these infants may be identified by low oxygen saturations in the feet/toes.

44.5.4 Diagnostic Imaging

44.5.4.1 Echocardiography

Echocardiography is a reliable method for accurately diagnosing interrupted aortic arch in neonates and children, along with the detection of other potential malformations. It can identify abnormalities in the aortic arch, coarctation, coronary variations, and the presence of a patent ductus arteriosus (PDA). Echocardiography allows for the visualization of the subaortic narrowing caused by a ventricular septal defect (VSD) with malalignment, as well as the examination of carotid and subclavian artery anatomy. Additionally, it can confirm the presence of other defects such as aortopulmonary window. The PDA must be kept patent through the infusion of prostaglandin E1.

44.5.4.2 Cardiac Catheterization

Diagnostic cardiac catheterization is typically unnecessary in the current era of echocardiography for the diagnosis of interrupted aortic arch.

44.5.4.3 Magnetic Resonance Imaging

Magnetic resonance imaging (MRI) is a valuable tool for follow-up assessments in children, adults, and teenagers. Serial MRI evaluations can assist in determining the need for therapeutic interventions.

44.5.4.4 Computer Tomography

Computer tomography (CAT-Scan) can provide similar anatomical details as MRI but is rarely required for the diagnosis of interrupted aortic arch in children. It may be utilized in cases where MRI is contraindicated.

44.5.4.5 Prenatal Detection

Routine prenatal scans may have difficulty detecting interrupted aortic arch and detailed vascular anatomy due to the presence of a large patent ductus arteriosus and related flow patterns. However, indirect signs such as a hypoplastic or small ascending aorta and a VSD with septum malalignment can provide clues for prenatal detection of the condition.

44.5.5 Treatment

Surgical repair of IAA is usually performed in neonatal life and continuous infusion of prostaglandin E1 is used to maintain PDA patency until surgery. Today, a single stage surgery is preferred. If complex other malformations exist, it may be favorable to repair the aortic arch first and band the pulmonary artery at neonatal age and address the remaining problems at a later stage.

44.5.5.1 Prenatal Management

The prenatal detection of an interrupted arch as single cardiac malformation without other malformations and/or syndromes is no indication for the termination of pregnancy. These children have a good clinical outcome, normal exercise capacity and as far as we know normal life expectancy. There is no indication for prenatal interventions. Spontaneous vaginal delivery is recommended, there is no medical indication for a cesarean section due to IAA. As many patients with IAA—mainly type B—are related to syndromes (i.e., 22q11 deletion syndrome) or also present other malformations, this may change the overall judgment; then, the complex forms of these cardiac defects can influence the judgment in favor of termination. As ductal patency is crucial, delivery should be planned in a center with prostaglandin E infusion prepared and on site availability of pediatric cardiologists, pediatric cardiac intensive care and surgery.

44.5.6 Outcome

Today with the widespread use of prostaglandin, the preprocedure mortality is low and surgical mortality is reported between 10 and 30% according to the related other CHD. If the patients survive the immediate postoperative period, the long-term outcome is however good. Long-term follow-up resembles those for patients with coarctation of the aorta.

44.6 Pulmonary Valve Stenosis and Insufficiency

Pulmonary valve stenosis (with intact ventricular septum) usually occurs sporadically and may be combined with supravalvular and/or infundibular stenoses. In its extreme case, there is pulmonary atresia with intact ventricular septum. It is an incomplete obstruction of the blood flow from the right ventricle to the pulmonary arteries. Isolated pulmonary valve insufficiency is rare. It can accompany idiopathic dilation of the pulmonary artery and pulmonary vascular obstructive disease. Most cases of pulmonary insufficiency result from surgical or balloon procedures to treat pulmonary valve stenosis.

44.6.1 Pathologic Physiology

Pulmonary stenosis is a relatively common congenital heart defect characterized by obstruction of blood flow from the right ventricle to the pulmonary artery. There are different types of pulmonary stenosis, including valvular pulmonary stenosis, supravalvular stenosis, and subvalvular or infundibular stenosis. Valvular pulmonary stenosis is the most common form, accounting for about 80–90% of cases. It is characterized by a bicuspid pulmonary valve with thickened and fused leaflets. The valve may also have a hypoplastic annulus. In some cases, the valve leaflets are dysplastic and have a cauliflower-like appearance. These dysplastic forms are often seen in patients with Noonan syndrome. Supravalvular stenosis can occur centrally, affecting the main pulmonary artery, or peripherally, involving the branches of the pulmonary vascular tree. Multiple supravalvular stenoses are often seen in patients with Williams syndrome or those with tetralogy of Fallot. Subvalvular stenosis, also known as infundibular stenosis, refers to the thickening and hypercontractility of the muscles beneath the pulmonary valve annulus. This can result in obstruction of blood flow from the right ventricle to the pulmonary artery, as seen in tetralogy of Fallot. All forms of pulmonary stenosis lead to increased pressure load on the right ventricle, causing right ventricular hypertrophy, reduced cardiac output, and diastolic impairment of the right ventricle.

Isolated pulmonary valve insufficiency is rare and is usually associated with a dysplastic pulmonary valve. It can occur in conditions such as idiopathic dilation of the pulmonary artery or pulmonary vascular obstructive disease. Pulmonary insufficiency can also result from surgical or balloon procedures performed to treat pulmonary valve stenosis or after right-sided endocarditis. It may be seen in patients with repaired tetralogy of Fallot. Pulmonary insufficiency leads to volume overload of the right ventricle, ventricular dilation, secondary tricuspid regurgitation, reduced ejection fraction, and an increased risk of ventricular arrhythmias.

44.6.2 Clinical Presentation

Mild and moderate pulmonary stenosis (PS) or pulmonary insufficiency is generally well tolerated, and most patients are asymptomatic, with the condition often detected through a cardiac murmur. In cases of severe PS, patients may experience reduced exercise capacity and symptoms of right heart failure, such as an enlarged liver, ascites, and distended jugular veins.

Critical pulmonary stenosis refers to a severe narrowing of the valve orifice in newborns, leading to inadequate systemic perfusion through normal transpulmonary blood flow. This results in cyanosis due to a right-to-left shunt across the patent foramen ovale (PFO). Infants with critical pulmonary stenosis rely on a patent ductus arteriosus to maintain pulmonary perfusion and oxygenation. These infants may present with low cardiac output, significantly reduced oxygen saturation, shock, congestive heart failure, and acidosis.

Pulmonary insufficiency that occurs as a result of surgical or balloon procedures to relieve right ventricular outflow tract obstruction was once thought to have minimal long-term consequences. However, it is now recognized that long-standing pulmonary valve insufficiency and right ventricular volume overload can lead to right ventricular failure and tricuspid regurgitation. Patients in this situation may experience symptoms such as fatigue, exercise intolerance, arrhythmias, and even sudden cardiac death.

44.6.3 Physical Examination

Infants with critical pulmonary stenosis present as severely sick neonates with cyanosis, low cardiac output, and even shock. When a general neonatal pulse oximetry screening is available, these children will be picked up by low saturations.

Patients with simple pulmonary valve stenosis are usually acyanotic. Careful palpation at the lower left sternal border will reveal an increased right ventricular impulse. The first sound is normal and is followed by a click. The click is best heard at the upper left sternal border. The second heart sound may be normal, widely split, or single depending on the severity of the pulmonary stenosis. In very mild cases, S2 can be normally split. As the severity increases, S2 becomes more widely split. With severe stenosis, the second heart sound becomes single (it is still widely split but closure of the pulmonary valve becomes inaudible). The murmur of pulmonary stenosis is an ejection murmur (crescendo decrescendo or "diamond shaped"), and the peak intensity of the murmur occurs later as the severity of the stenosis increases. If ventricular failure occurs, a prominent fourth sound may be heard. Pulmonary insufficiency is characterized by a mid- to high-frequency decrescendo murmur that begins immediately after S2. In contrast to the murmur of aortic insufficiency, the murmur is louder when the patient is supine than when sitting. With significant pulmonary insufficiency, the right ventricular impulse, felt at the lower left sternal border in the xiphoid area may be prominent.

44.6.4 Diagnostic Imaging

44.6.4.1 Echocardiography

Echocardiography is a reliable tool for diagnosing all types of pulmonary stenosis and regurgitation, as well as assessing associated malformations. It allows for the determination of valve morphology (e.g., bicuspid or tricuspid valves), evaluation of valve thickness, dysplasia, and cusp mobility. The maximum instantaneous Doppler gradient helps estimate the right ventricular to pulmonary artery pressure gradient. Additionally, echocardiography can assess right ventricular size, wall thickness, and function, providing insights into the severity of stenosis.

The presence and severity of pulmonary regurgitation can be confirmed using echocardiography by observing the degree of right ventricular and atrial enlargement, right ventricular function, and the degree of tricuspid regurgitation.

44.6.4.2 Cardiac Catheterization

Diagnostic cardiac catheterization is generally not necessary for the diagnosis of pulmonary stenosis or regurgitation in the era of echocardiography.

44.6.4.3 Magnetic Resonance Imaging

Magnetic resonance imaging (MRI) is the preferred method for assessing the severity of pulmonary regurgitation, right ventricular volumes and function, and the anatomy of the right ventricular outflow tract (RVOT). It is commonly used after initial procedures, and serial assessments with MRI are preferred to determine the need for therapeutic intervention.

44.6.4.4 Computer Tomography

Computer tomography (CT) can provide similar anatomical details as MRI but is rarely required for diagnosing pulmonary stenosis or regurgitation in children. It may be used in cases where MRI is contraindicated.

44.6.4.5 Prenatal Detection

Moderate and severe forms of pulmonary stenosis are typically detected during routine prenatal scans due to turbulent flow across the valve or flow reversal during diastole. However, supravalvular pulmonary stenosis may be missed. Severe valvular pulmonary stenosis may be associated with reduced right ventricular function and additional tricuspid regurgitation.

44.6.5 Treatment

The currently accepted best method of treatment of significant pulmonary valve stenosis is balloon pulmonary valvuloplasty. Most cardiologists agree that valvuloplasty should be performed if the transpulmonary gradient exceeds 40 mmHg or if there is evidence of right ventricular hypertrophy on the electrocardiogram, increasing tricuspid regurgitation or clinical factors such as impaired exercise capacity, shortness of breath or arrhythmias.

In critical pulmonary stenosis, the gradient is irrelevant and valvotomy is indicted regardless of the gradient. Usually, balloon dilatation is the treatment of choice and with excellent results. In some forms of supravalvular PS, stent implantation is an ideal solution. In subvalvular PS, or supravalvular PS unsuitable for interventional treatment, or in patients with failed balloon dilatation (i.e., myxomatoid pulmonary valves), surgical repair is the method of choice.

Today, the timing and optimum treatment for pulmonary insufficiency is much better defined than in the past. It is generally accepted that treatment, surgical or interventional, to restore a competent valve in the pulmonary position should be performed if there is progressive right ventricular enlargement and/or tricuspid regurgitation especially in the setting of ventricular arrhythmias and/or progressive exercise intolerance. Unfortunately, the treatment for pulmonary insufficiency is valve replacement, and none of the current implantable valves last for an extended

time. Current recommendations take into consideration the size of the right ventricle (i.e., diastolic size more than 150 ml/m^2), the amount of regurgitation, the development of tricuspid regurgitation, the ECG (QRS width), ventricular arrhythmias and/or other clinical signs.

It is commonly agreed that biological valves should be implanted only in the pulmonary position. Surgically this can be performed by valved xenografts or homografts or bioprosthesis. Interventionally percutaneous pulmonary valve implantation (PPVI) has been possible for about 20 years with excellent long-term results.

44.6.5.1 Prenatal Management

The prenatal detection of valvular pulmonary stenosis (PS) as a single cardiac malformation, without any other malformations or syndromes, is not a reason to consider terminating the pregnancy. These children typically have a favorable clinical outcome, normal exercise capacity, and normal life expectancy. Spontaneous vaginal delivery is recommended, and there is no medical indication for a cesarean section solely due to PS. In cases where critical PS is anticipated, delivery should be planned in a center equipped with prostaglandin E infusion, and with pediatric cardiologists, pediatric cardiac intensive care, and surgical services readily available.

Prenatal counseling may differ when there are associated syndromic defects, although this is rare. In such cases, the cardiac diagnosis should not automatically influence the decision in favor of termination, considering the generally favorable cardiac prognosis.

Prenatal intervention for PS is rarely indicated. The prenatal diagnosis of severe PS accompanied by impaired right ventricular function and progressive tricuspid regurgitation may warrant early cesarean delivery with the possibility of early intervention. Prenatal balloon valvuloplasty is another option, but its effectiveness in improving long-term outcomes for affected babies is currently inconclusive, and the procedure carries significant risks.

44.6.6 Outcome

The outcome of balloon dilation or surgical valvotomy for pulmonary valve stenosis is excellent with 25-year survival not different from that of the general population. Pulmonary valve insufficiency is well tolerated in the long term. However, some patients may develop progressive right ventricular dilation and reduced function secondary to chronic pulmonary insufficiency and require late valve replacement. In a patient with pulmonary regurgitation as the leading hemodynamic problem, regular yearly follow up and repeat MRI assessments are required to minimize the risk of severe RV enlargement and subsequent sudden cardiac death.

Human Genetics of Semilunar Valve and Aortic Arch Anomalies

45

Matina Prapa and Siew Yen Ho

Abstract

Lesions of the semilunar valve and the aortic arch can occur either in isolation or as part of well-described clinical syndromes. The polygenic cause of calcific aortic valve disease will be discussed including the key role of *NOTCH1* mutations. In addition, the complex trait of bicuspid aortic valve disease will be outlined, both in sporadic/familial cases and in the context of associated syndromes, such as Alagille, Williams, and Kabuki syndromes. Aortic arch abnormalities particularly coarctation of the aorta and interrupted aortic arch, including their association with syndromes such as Turner and 22q11 deletion, respectively, are also discussed. Finally, the genetic basis of congenital pulmonary valve stenosis is summarized, with particular note to Ras-/mitogen-activated protein kinase (Ras/MAPK) pathway syndromes and other less common associations, such as Holt–Oram syndrome.

Keywords

Semilunar valve · Aortic arch · Alagille syndrome · Williams syndrome · Kabuki syndrome · NOTCH1 · Turner syndrome · 22q11 deletion syndrome · Holt–Oram syndrome · Ras–MAPK pathway · Aortic valve stenosis · Bicuspid aortic valve · BAV · Supravalvar aortic stenosis · Elastin · ELN · Vascular smooth muscle cells · Aortic coarctation · JAG1 · MLL2 · NKX2–5 · BMP · SMAD · Interrupted aortic arch · IAA · CHD7 · DiGeorge syndrome · Velocardiofacial syndrome · TBX1 ·

M. Prapa (✉)
Department of Clinical Genetics, St George's University Hospitals NHS Foundation Trust, London, UK
e-mail: s.prapa09@alumni.imperial.ac.uk

S. Y. Ho
Cardiac Morphology, Royal Brompton & Harefield Hospitals, London, UK

© The Author(s), under exclusive license to Springer Nature Switzerland AG 2024

S. Rickert-Sperling et al. (eds.), *Congenital Heart Diseases: The Broken Heart*,
Advances in Experimental Medicine and Biology 1441,
https://doi.org/10.1007/978-3-031-44087-8_45

Pulmonary stenosis · PTPN11 · Noonan syndrome · SOS1 · Costello syndrome · TBX5 · GATA4

45.1 Introduction

Congenital malformations of the arterial valves and of the aortic arch can occur separately, in isolation, or as part of well-defined clinical syndromes, many of which now have established genetic causes. The process of semilunar valvulogenesis has been well described in animal models with a number of key pathways involved in endocardial cushion formation and subsequent migration of neural crest cells to the distal outflow tract contributing to aorticopulmonary septation [1]. The following sections will focus on our current knowlegde of genes implicated in semilunar valve and aortic arch abnormalities, summarised below (see Table 45.1).

45.2 Aortic Valve Stenosis

Calcific aortic valve disease traditionally has been regarded as a degenerative process involving passive wear and tear of the valve leaflets. On the contrary, current evidence points to a continuum disease process similar to that of atherosclerosis with active cell proliferation and chronic inflammation resulting in leaflet calcification [2].

Familial predisposition to aortic valve sclerosis has been shown by the Hypertension Genetic Epidemiology Network (HyperGEN) Study Group reporting a sibling recurrence risk ratio of 2.3 with several associated chromosomal regions identified by genome-wide association (GWAS) studies [3]. A different study in Western France focused on the more advanced disease trait of calcified aortic valve stenosis requiring surgical replacement to identify clusters of large families segregating aortic stenosis [4]. Together with clinical risk factors, a number of established susceptibility loci involved in lipid metabolism and inflammatory processes can be combined into a polygenic risk score to provide individual risk measures for aortic stenosis [5]. Genetic variation in the *LPA* locus, determining the circulating levels of the atherogenic lipoprotein(a), has been strongly associated with calcific aortic valve stenosis disease and progression, including familial risk of microcalcification [6]. Antisense oligonucleotide therapy specifically targeting Lp(a) levels was shown to be potent in randomized clinical trials and may be beneficial in mitigating disease progression [7].

Congenital malformation of the aortic valve is an additional major risk factor for aortic stenosis [8]. In 2005, Garg et al. performed a genome-wide association study in two kindreds affected by congenital heart disease (CHD) and aortic valve calcification [9]. The first pedigree was a five-generation European-American family in which nine affected members had aortic valve disease (six had bicuspid aortic valve

Table 45.1 Genetic basis of syndromic and nonsyndromic forms of arterial valve and aortic arch abnormalities

Phenotype	Genetic cause (nonsyndromic) and inheritance mode	Associated syndrome & extracardiac features	Genetic cause (syndromic) and inheritance mode
Calcific aortic stenosis	*NOTCH1*, AD Polygenic risk score including *LPA* locus	–	–
Supravalvar aortic stenosis	*ELN*, AD	Williams—Elfin facies, intellectual disability, overly friendly personality, connective tissue abnormalities, growth & endocrine abnormalities	Recurrent chromosome 7q11.23 deletion encompassing *ELN* gene, AD
Bicuspid aortic valve	*NOTCH1* *NKX2–5* *SMAD6* *GATA5* (AD, likely multifactorial)	Williams—detailed above Alagille—jaundice in early infancy, characteristic facies, butterfly vertebrae, ocular anomalies Kabuki—typical facial features, intellectual disability, skeletal abnormalities, postnatal growth deficiency	*JAG1, NOTCH2* (both AD) *KMT2D,* AD *KDM6A,* X-linked
Aortic coarctation	*NKX2–5* *SMAD6*	Turner—ovarian failure, short stature, neck webbing, thyroid disease, hearing loss Kabuki—detailed above	45, XO (sporadic)
Interrupted aortic arch	–	22q11 deletion—hypocalcemia, immunodeficiency, characteristic facial features, learning difficulties, palatal abnormalities CHARGE—Coloboma, heart disease, atresia choanae, retarded growth and development and/or CNS anomalies, genital hypoplasia, and ear anomalies and/or deafness	Recurrent chromosome 22q11.2 deletion including *TBX1* gene, AD *CHD7,* AD
Pulmonary stenosis	*GATA4,* AD	Noonan—renal and hematological abnormalities, developmental delay, short stature, characteristic facies NFNS—overlap of neurofibromatosis and Noonan syndrome features Holt–Oram—abnormalities of upper extremities, thumb anomalies	*PTPN11, SOS1, RAF1, RIT1, KRAS* (AD) *NF1,* AD *TBX5,* AD

Abbreviations: *AD* autosomal dominant, *CNS* central nervous system, *NFNS* neurofibromatosis–Noonan syndrome

and seven had calcific aortic stenosis). Other cardiac malformations included ventricular septal defect, tetralogy of Fallot, and mitral stenosis. A genome-wide scan in all available family members revealed linkage to a single locus on chromosome 9q34–35 including *NOTCH1* gene with a nonsense mutation in affected individuals. Additional screening of a smaller kindred of Hispanic origin revealed a frameshift *NOTCH1* mutation in three affected members with bicuspid aortic valve (BAV) [9]. *NOTCH1* gene encodes a transmembrane protein regulating cell fate decisions involved in the development of the atrioventricular canal, ventricular myocardium, and cardiac outflow tract [10]. *NOTCH1* signaling pathway also represses Runx2 (runt-related transcription factor 2), a critical transcription factor involved in osteoblast differentiation, which is upregulated in human calcified aortic valves [2]. Thus, mutations in *NOTCH1* may have a key role in aortic stenosis, resulting in an early developmental defect and a later derepression of calcium deposition in the aortic valve [11].

Following these findings, Mohamed et al. investigated the role of *NOTCH1* gene mutations in 48 German patients with sporadic BAV leading to identification of two mutations (p.Thr596Met and p.Pro1797His); both patients had calcification of the aortic valve and concomitant aneurysms of the ascending aorta [12]. Subsequently, a number of mutations in the *NOTCH1* coding region have been reported as segregating in families with mainly left-sided nonsyndromic congenital heart disease but also in association with sporadic tricuspid aortic valve calcification [13, 14]. Additional *NOTCH1* non-coding (deep intronic) variants may confer significant risk for left-ventricular outflow tract obstruction defects although further work, including functional studies, will be needed to assess whether these should be included in clinical screenings [15].

45.3 Supravalvar Aortic Stenosis

Congenital supravalvar aortic stenosis (SVAS) belongs to a different disease spectrum of diffuse arteriopathy characterized by medial and/or intimal thickening of the aortic wall with narrowing of its lumen [16]. SVAS is commonly a feature of Williams syndrome with an estimated prevalence of approximately 70% but can also occur in nonsyndromic forms [17]. Both syndromic and nonsyndromic SVAS are caused by disruptions in the elastin (*ELN*) gene with reduced ELN expression found in vascular smooth muscle cells (VSMCs) of affected patients [18]. Reductions in elastin, a key structural protein of the extracellular matrix, lead to elastic fragmentation with increased collagen and VSMC hypertrophy in the media of SVAS patients [16].

45.4 Aortic Coarctation and Bicuspid Aortic Valve

Aortic coarctation accounts for 5–7% of CHD lesions [19]. More than 50% of patients with coarctation of the aorta are also found to have a BAV [19, 20] (Fig. 45.1). The latter is the commonest congenital heart lesion affecting 0.5–2% of the general population and is a more complex trait than initially thought, with coexistence of defective valvulogenesis and an additive effect on structural properties of the aortic wall [21, 22].

Aortic coarctation and BAV disease can occur in isolation or as part of genetic syndromes, with their underlying genetic basis under ongoing investigation. Both defects frequently can be found in females with Turner syndrome (45,XO) characterized by the presence of webbed neck, short stature, and gonadal dysgenesis [23]. Cardiovascular abnormalities are found in up to 45% of Turner patients, with BAV and aortic coarctation in 30% and 12%, respectively [23, 24]. Bileaflet aortic valve can also be a component part of familial thoracic aortic aneurysm or hypoplastic left heart syndrome [25, 26]. Genes located on the short arm of chromosome X are considered key to aortic valve and arch development with haploinsufficiency for Xp associated with higher prevalence of BAV and coarctation in Turner syndrome [24]. A maldevelopment of neural crest cells, which give rise to the outflow tract of the heart, the aortic arch system, and the cervicocephalic arteries, may also underlie development of these lesions in nonsyndromic cases [27].

The presence of BAV can comprise a feature of a number of additional syndromes, such as Alagille, Williams, and Kabuki syndromes. Alagille syndrome (AGS) consists of jaundice in early infancy, characteristic facies, butterfly vertebrae, ocular anomalies, and a wide spectrum of cardiovascular anomalies, the most common of which being stenosis or hypoplasia of the branch pulmonary arteries. Mutations in the jagged 1 (*JAG1*) gene, encoding a NOTCH receptor ligand, are

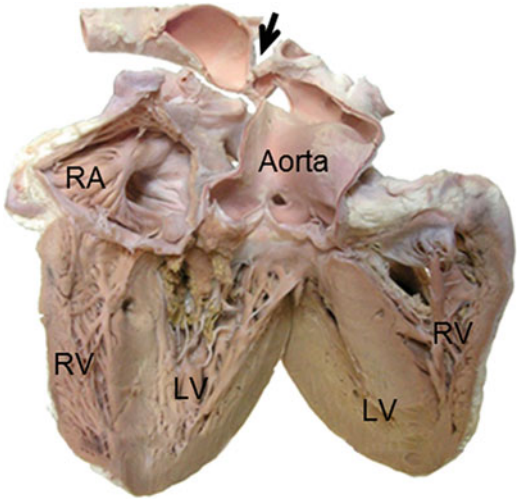

Fig. 45.1 The left ventricle (*LV*) has been opened longitudinally through the outflow tract and the aortic valve. There is a bicuspid aortic valve with dilatation of the ascending aorta and coarctation (*arrow*) where the arch narrows discretely. *RA* right atrium, *RV* right ventricle (Leon Gerlis Museum, Royal Brompton Hospital, London, UK)

present in the majority of individuals (94.3%) with a clinical diagnosis of AGS, with a smaller subset (2.6%) harboring mutations in the *NOTCH2* gene, and a proportion of individuals (3.2%) having no detected pathogenic variants in either gene [28]. In 2002, McElhinney et al. reviewed the cardiac phenotype of 200 individuals with AGS or a *JAG1* mutation [29]. Two of the probands had BAV disease as a primary cardiovascular anomaly and another two as a secondary anomaly, with *JAG1* mutations present in three of the BAV patients. Coarctation of the aorta was also present in four subjects with *JAG1* mutations found in two of these. Isolated reports of systemic vascular abnormalities in AGS patients exist in the literature, including intracranial aneurysms as well as coarctation of the thoracic and abdominal aorta, with presence of *JAG1* mutations in the latter [30, 31]. Expression of *JAG1* has been previously shown to contribute to angiogenesis, both in in vitro models as well as in animal studies, with disruption of the mouse *JAG1* gene leading to lethal diffuse hemorrhages [32, 33].

Notably, bileaflet aortic valve has also been reported in up to 12% of patients with a clinical diagnosis of Williams syndrome [34] and in 25–39% of patients with SVAS [35, 36]. Sugayama et al. used fluorescence in situ hybridization (FISH) methods to detect microdeletions in the elastin gene in 20 WBS patients [37]. All FISH-positive patients (85%) had cardiovascular malformations, out of which 18% had combined BAV and SVAS. Another syndromic association of both BAV disease and coarctation of the aorta is that of Kabuki syndrome, characterized by typical facial dysmorphology, mild–moderate intellectual disability, postnatal growth deficiency, and various congenital defects present to a variable degree including genitourinary anomalies and cleft lip/palate. Approximately 70% of affected individuals have a molecularly proven diagnosis with pathogenic variants in *KMT2D* in the vast majority and less frequently, *KDM6A* [38]. Congenital heart disease is present in 70% of individuals with *KMT2D* pathogenic variants; coarctation of the aorta is the commonest defect (21%) and can occur alone or in combination with other lesions including BAV [39]. *KMT2D* (also known as *MLL2*) encodes a histone methyltransferase, lysine (K)-specific methyltransferase 2D, regulating the transcription of a diverse group of genes with murine studies of *MLL2* loss-of-function phenotype exhibiting increased apoptosis and retarded development [40, 41].

The cardiac homeobox gene *NKX2–5* has a major role in cardiac development with mutations in this gene associated with a range of cardiac malformations [42–44]. Targeted sequencing of *NKX2–5* in 608 subjects with conotruncal anomalies, left-sided lesions, atrial septal defect, and Ebstein's anomaly resulted in identification of 12 distinct mutations in 3% of the studied population, including a single (out of 59) patient with coarctation of the aorta [45]. Moreover, previous murine studies have exhibited that heterozygous *NKX2–5* ablation results in an eightfold increase in the prevalence of stenotic BAV [42]. Following these findings, Majumdar et al. performed a targeted mutational analysis of the protein coding sequence of *NKX2–5* gene in 19 patients with BAV and ascending aortic aneurysm [46]. DNA was extracted from peripheral blood leukocytes and diseased aortic tissue. Three subjects with normal aortic valves and isolated ascending aortic aneurysm were used as

controls. Sequence analysis of leukocyte DNA demonstrated a single known polymorphic alteration in the 3′ untranslated region adjacent to exon 2 in four BAV and two control subjects. The same polymorphism was detected following DNA sequencing from aortic tissue samples, in six BAV and one control subject. Interestingly, in four of the BAV patients (and none of the controls), the mutation was only present in the DNA extracted from the aortic tissue suggesting somatically acquired mutation and clonal expansion during aortogenesis. More recently, a novel *NKX2–5* loss-of-function mutation (p.K192X) was implicated in isolated BAV transmitted in an autosomal dominant manner in a Han Chinese family [47].

Aside from the association of calcific BAV disease with *NOTCH1* mutations, the latter have also been reported in patients with BAV and thoracic aortic aneurysms [48, 49]. Lack of another cardiac transcription factor, Gata5, results in partial BAV penetrance with a prevalence of 26% in null mice [50]. Screening of 78 individuals for *GATA5* sequence variants via Sanger sequencing (50 with isolated BAV and 28 with concomitant coarctation of the aorta) led to identification of 2 rare heterozygous missense variants, p.Gln3Arg and p.Leu233Pro, with a frequency of 2.6% (2/78) [51]. Bone morphogenetic protein (*BMP*) signaling also has a pivotal role in cardiac morphogenesis with mice genetically disrupted for *BMP* exhibiting hypoplastic cardiac cushion formation [52, 53]. SMAD family member 6 (*SMAD6*) is an important intracellular inhibitor of the BMP pathway, with its genetic disruption in mice resulting in heart valve defects and aortic ossification [54]. Nonsynonymous mutations in *SMAD6* gene have been reported in 3 out of 436 individuals with a wide range of CHD lesions, out of which two had a BAV: a 30-year-old male with aortic stenosis, coarctation, and calcification of the aorta and an infant with moderate aortic stenosis [55].

Importantly, BAV disease with thoracic aortic aneurysm formation can be part of a connective tissue syndromic diagnosis with mutations in *ACTA2*, *TGFBR2,* and *TGFB2* genes [56, 57]. *FBN1* gene mutations have also been identified in two patients with BAV and aortic root dilatation not fulfilling clinical diagnostic criteria for Marfan syndrome [58]. Increasing availability of high-throughput sequencing technologies allows simultaneous screening for sequence variants in the above genes in a clinical setting, usually as part of a panel test for thoracic aortic aneurysm and dissection. In contrast, the diagnostic yield of genetic testing for isolated BAV remains low likely owing to its multifactorial nature involving multiple gene-hits as well as environmental factors [56, 59].

45.5 Interrupted Aortic Arch

Interrupted aortic arch (IAA) accounts for approximately 0.2–1.4% of all congenital heart defects and is commonly associated with other cardiac lesions, such as ventricular septal defect, patent arterial duct, BAV, truncus arteriosus, and complete transposition of the great arteries [60, 61]. IAA can occur in the context of coloboma, heart disease, atresia choanae, retarded growth and development and/or CNS anomalies, genital hypoplasia, and ear anomalies and/or deafness (CHARGE)

syndrome, with a frequency of 3/299 in a study population carrying pathogenic *CHD7* mutations for CHARGE syndrome [62]. However, its commonest association is with 22q11 deletion syndrome with 50% of IAA patients testing positive for a deletion [63].

The 22q11 deletion syndrome has a wide spectrum of clinical features, including the phenotypes of DiGeorge and velocardiofacial syndrome (DGS/VCFS) [64]. The syndrome is characterized by cardiovascular defects, hypocalcemia, immunodeficiency, characteristic facial features, and learning difficulties. Common associated cardiac malformations include tetralogy of Fallot, IAA, and truncus arteriosus [65]. Most DGS/VCFS patients are hemizygous for a 1.5–3.0 Mb 22q11.2 deletion encompassing up to 40 genes, including TBX (T-box) 1 with development of conotruncal defects in heterozygous mice for a null *TBX1* mutation [66, 67]. Interestingly, the incidence of 22q11 deletions varies significantly between different types of IAA, with approximately half of type B patients (interruption between the left carotid and left subclavian artery) and none of the type A patients (interruption distal to the left subclavian artery) having a deletion, suggestive of differential underlying pathologies [63, 68].

45.6 Pulmonary Stenosis

Congenital pulmonary stenosis can occur in isolation (Fig. 45.2), in combination with other congenital heart lesions, such as tetralogy of Fallot, or as part of genetic syndromes with cardiac involvement. A characteristic example of the latter is Noonan syndrome, the second commonest syndromic cause of congenital heart disease (CHD) after trisomy 21 [69]. Noonan syndrome is an autosomal dominant trait affecting multiple systems, including renal and hematological abnormalities,

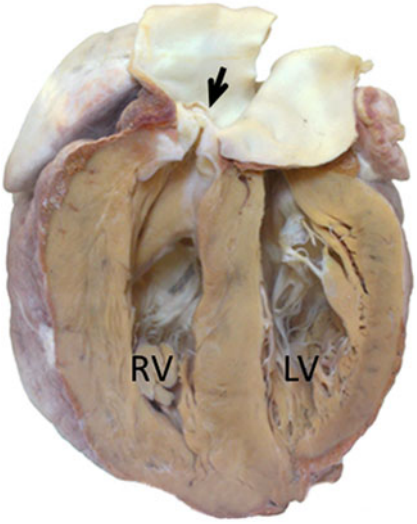

Fig. 45.2 The heart has been cut longitudinally through the right ventricular outflow tract. There is a thickened dome-shaped pulmonary valve (*arrow*) causing pulmonary stenosis. Flow is through a small orifice. Consequently there is remarkable hypertrophy of the right ventricular wall. *RV* right ventricle, *LV* left ventricle (Leon Gerlis Museum, Royal Brompton Hospital, London, UK)

developmental delay, short stature, and characteristic facial features. Pulmonary stenosis is found in up to 60% of affected patients with other associated heart lesions including hypertrophic cardiomyopathy, ventricular and atrial septal defect, aortic and mitral valve lesions, and aortic coarctation [70].

Noonan syndrome has been linked to *PTPN11* gene mutations encoding for SHP-2, a protein tyrosine phosphatase with signaling roles in semilunar valvulogenesis [71]. The prevalence of *PTN11* mutations in Noonan syndrome is approximately 50% with affected patients having a significantly higher frequency of pulmonary stenosis and a lower frequency of hypertrophic cardiomyopathy [72]. *PTPN11* gene belongs to the Ras-/mitogen-activated protein kinase (MAPK) signaling cascade with a number of additional integral genes implicated in Noonan syndrome (see Table). The Ras/MAPK pathway is a well-recognized signaling pathway which via a series of phosphorylation events in the cytoplasm results in entry of activated ERK (extracellular signal-regulated kinase) in the nucleus and appropriate response to the initial stimulus. Noonan syndrome-causing mutations in respective genes usually enhance signaling via the Ras/MAPK pathway, with detected variants in *SOS1* in approximately 10% of cases, *RAF1* and *RIT1* in 5% each, and *KRAS* in less than 5% [70]. Phenotypic correlations include smaller incidence of atrial septal defect in patients harboring *SOS1* mutations and higher incidence of hypertrophic cardiomyopathy in those with *RAF1* mutations [70].

In a Dutch genotype–phenotype study undertaken in 33 patients with a clinical diagnosis of Noonan syndrome who tested negative for *PTPN11* mutations, 42% of cases had mutations in genes involved in RASopathies with a higher prevalence of heart defects (79% versus 56%) and pulmonary stenosis (69% versus 39%) compared to mutation-negative patients [73]. The genetically heterogeneous Noonan syndrome overlaps clinically with a number of other Ras/MAPK pathway syndromes, such as cardio-facio-cutaneous (CFC), multiple lentigines (previously known as LEOPARD), and Costello syndrome. The frequency of pulmonary stenosis in the setting of Costello syndrome (*HRAS*) appears to be relatively rare (20%) and nonprogressive in nature in comparison with CFC syndrome (*BRAF*) and Noonan syndrome with multiple lentigines (*PTPN11)* with a frequency of approximately 40% based on a systematic literature review [74]. In another RASopathy, neurofibromatosis type 1 (NF1), pulmonary stenosis has an estimated frequency of 1.1% with a 20 times higher prevalence in patients with Neurofibromatosis-Noonan syndrome (NFNS); in both conditions, pulmonary stenosis was associated with nontruncating (missense/in-frame) *NF1* variants which may have a specific effect on the cardiac phenotype [75]. A recent multicenter observational study of 371 patients with molecularly confirmed RASopathy reported cardiac involvement in 80.3%, most commonly pulmonary stenosis (59%), with a higher risk of required early intervention in individuals with Noonan syndrome and *PTPN11* mutations, and an overall good cumulative survival (94.3% estimated survival at 20 years) [76].

Pulmonary stenosis can also occur in other less prevalent familial and syndromic forms. An example is that of Holt–Oram syndrome, a rare heart–hand syndrome characterized by mutations in the *TBX5* transcription factor. Associated heart defects commonly include atrial septal defect and conduction abnormalities, with the less

typical finding of pulmonary stenosis reported in a five-generation family carrying a novel intragenic *TBX5* duplication segregating with the disease phenotype [77]. Interestingly, *TBX5* is known to interact with transcription factor *GATA4* (GATA binding protein 4) with an increasing number of familial studies reporting *GATA4* mutations segregating with atrial septal defect and pulmonary stenosis [78–80].

45.7 Conclusion

Although there is increasing evidence of genetic involvement in outflow malformations that include the arterial valves as well as the great arteries, other factors, such as hemodynamic changes, are likely at play. In both isolated and syndromic forms, there may be common causative genes affecting the valvar and the arterial parts of the outflow. Co-ordinated detailed phenotyping, including hemodynamic imaging, together with molecular studies will help distinguish cases in which genetic factors play the dominant role and lead to further advances in clinical management.

References

1. Armstrong EJ, Bischoff J. Heart valve development: endothelial cell signaling and differentiation. Circ Res. 2004;95(5):459–70. https://doi.org/10.1161/01.RES.0000141146.95728.da.
2. Garg V. Molecular genetics of aortic valve disease. Curr Opin Cardiol. 2006;21(3):180–4. https://doi.org/10.1097/01.hco.0000221578.18254.70.
3. Bella JN, Tang W, Kraja A, Rao DC, Hunt SC, Miller MB, et al. Genome-wide linkage mapping for valve calcification susceptibility loci in hypertensive sibships: the Hypertension Genetic Epidemiology Network Study. Hypertension. 2007;49(3):453–60. https://doi.org/10.1161/01.HYP.0000256957.10242.75.
4. Probst V, Le Scouarnec S, Legendre A, Jousseaume V, Jaafar P, Nguyen JM, et al. Familial aggregation of calcific aortic valve stenosis in the western part of France. Circulation. 2006;113(6):856–60. https://doi.org/10.1161/CIRCULATIONAHA.105.569467.
5. Chen HY, Small AM, Dina C, Cairns BJ, Whitmer RA, Lathrop M, et al. Genome-wide association meta-analysis in 652,134 participants identifies 9 novel susceptibility loci for aortic stenosis. Eur Heart J. 2020;41(Supplement_2):ehaa946-1862. https://doi.org/10.1093/ehjci/ehaa946.1862.
6. Perrot N, Thériault S, Dina C, Chen HY, Boekholdt SM, Rigade S, et al. Genetic variation in LPA, calcific aortic valve stenosis in patients undergoing cardiac surgery, and familial risk of aortic valve microcalcification. JAMA Cardiol. 2019;4(7):620–7. https://doi.org/10.1001/jamacardio.2019.1581.
7. Viney NJ, van Capelleveen JC, Geary RS, Xia S, Tami JA, Yu RZ, et al. Antisense oligonucleotides targeting apolipoprotein(a) in people with raised lipoprotein(a): two randomised, double-blind, placebo-controlled, dose-ranging trials. Lancet. 2016;388(10057):2239–53. https://doi.org/10.1016/S0140-6736(16)31009-1.
8. Otto CM. Calcification of bicuspid aortic valves. Heart. 2002;88(4):321–2.
9. Garg V, Muth AN, Ransom JF, Schluterman MK, Barnes R, King IN, et al. Mutations in NOTCH1 cause aortic valve disease. Nature. 2005;437(7056):270–4. https://doi.org/10.1038/nature03940.

10. Niessen K, Karsan A. Notch signaling in cardiac development. Circ Res. 2008;102(10):1169–81. https://doi.org/10.1161/CIRCRESAHA.108.174318.
11. Wang Y, Fang Y, Lu P, Wu B, Zhou B. NOTCH signaling in aortic valve development and calcific aortic valve disease. Front Cardiovasc Med. 2021;8:682298. https://doi.org/10.3389/fcvm.2021.682298.
12. Mohamed SA, Aherrahrou Z, Liptau H, Erasmi AW, Hagemann C, Wrobel S, et al. Novel missense mutations (p.T596M and p.P1797H) in NOTCH1 in patients with bicuspid aortic valve. Biochem Biophys Res Commun. 2006;345(4):1460–5. https://doi.org/10.1016/j.bbrc.2006.05.046.
13. Kerstjens-Frederikse WS, van de Laar IM, Vos YJ, Verhagen JM, Berger RM, Lichtenbelt KD, et al. Cardiovascular malformations caused by NOTCH1 mutations do not keep left: data on 428 probands with left-sided CHD and their families. Genet Med. 2016;18(9):914–23. https://doi.org/10.1038/gim.2015.193.
14. Ducharme V, Guauque-Olarte S, Gaudreault N, Pibarot P, Mathieu P, Bosse Y. NOTCH1 genetic variants in patients with tricuspid calcific aortic valve stenosis. J Heart Valve Dis. 2013;22(2):142–9.
15. Helle E, Cordova-Palomera A, Ojala T, Saha P, Potiny P, Gustafsson S, et al. Loss of function, missense, and intronic variants in NOTCH1 confer different risks for left ventricular outflow tract obstructive heart defects in two European cohorts. Genet Epidemiol. 2019;43(2):215–26. https://doi.org/10.1002/gepi.22176.
16. Merla G, Brunetti-Pierri N, Piccolo P, Micale L, Loviglio MN. Supravalvular aortic stenosis: elastin arteriopathy. Circ Cardiovasc Genet. 2012;5(6):692–6. https://doi.org/10.1161/CIRCGENETICS.112.962860.
17. Pober BR, Johnson M, Urban Z. Mechanisms and treatment of cardiovascular disease in Williams-Beuren syndrome. J Clin Invest. 2008;118(5):1606–15. https://doi.org/10.1172/JCI35309.
18. Urban Z, Zhang J, Davis EC, Maeda GK, Kumar A, Stalker H, et al. Supravalvular aortic stenosis: genetic and molecular dissection of a complex mutation in the elastin gene. Hum Genet. 2001;109(5):512–20. https://doi.org/10.1007/s00439-001-0608-z.
19. Mitchell SC, Korones SB, Berendes HW. Congenital heart disease in 56,109 births. Incidence and natural history. Circulation. 1971;43(3):323–32.
20. Rosenthal E. Coarctation of the aorta from fetus to adult: curable condition or life long disease process? Heart. 2005;91(11):1495–502. https://doi.org/10.1136/hrt.2004.057182.
21. Braverman AC, Guven H, Beardslee MA, Makan M, Kates AM, Moon MR. The bicuspid aortic valve. Curr Probl Cardiol. 2005;30(9):470–522. https://doi.org/10.1016/j.cpcardiol.2005.06.002.
22. Prapa M, Ho SY. Risk stratification in bicuspid aortic valve disease: still more work to do. Eur J Cardiothorac Surg. 2012;41(2):327–8. https://doi.org/10.1016/j.ejcts.2011.06.023.
23. Ho VB, Bakalov VK, Cooley M, Van PL, Hood MN, Burklow TR, et al. Major vascular anomalies in turner syndrome. Circulation. 2004;110(12):1694–700. https://doi.org/10.1161/01.CIR.0000142290.35842.B0.
24. Bondy C, Bakalov VK, Cheng C, Olivieri L, Rosing DR, Arai AE. Bicuspid aortic valve and aortic coarctation are linked to deletion of the X chromosome short arm in Turner syndrome. J Med Genet. 2013;50(10):662–5. https://doi.org/10.1136/jmedgenet-2013-101720.
25. Loffredo CA, Chokkalingam A, Sill AM, Boughman JA, Clark EB, Scheel J, et al. Prevalence of congenital cardiovascular malformations among relatives of infants with hypoplastic left heart, coarctation of the aorta, and d-transposition of the great arteries. Am J Med Genet A. 2004;124A(3):225–30. https://doi.org/10.1002/ajmg.a.20366.
26. Loscalzo ML, Goh DL, Loeys B, Kent KC, Spevak PJ, Dietz HC. Familial thoracic aortic dilation and bicommissural aortic valve: a prospective analysis of natural history and inheritance. Am J Med Genet A. 2007;143A(17):1960–7. https://doi.org/10.1002/ajmg.a.31872.

27. Kappetein AP, Gittenberger-de Groot AC, Zwinderman AH, Rohmer J, Poelmann RE, Huysmans HA. The neural crest as a possible pathogenetic factor in coarctation of the aorta and bicuspid aortic valve. J Thorac Cardiovasc Surg. 1991;102(6):830–6.
28. Gilbert MA, Bauer RC, Rajagopalan R, Grochowski CM, Chao G, McEldrew D, et al. Alagille syndrome mutation update: comprehensive overview of JAG1 and NOTCH2 mutation frequencies and insight into missense variant classification. Hum Mutat. 2019;40(12): 2197–220. https://doi.org/10.1002/humu.23879.
29. McElhinney DB, Krantz ID, Bason L, Piccoli DA, Emerick KM, Spinner NB, et al. Analysis of cardiovascular phenotype and genotype-phenotype correlation in individuals with a JAG1 mutation and/or Alagille syndrome. Circulation. 2002;106(20):2567–74.
30. Raas-Rothschild A, Shteyer E, Lerer I, Nir A, Granot E, Rein AJ. Jagged1 gene mutation for abdominal coarctation of the aorta in Alagille syndrome. Am J Med Genet. 2002;112(1):75–8. https://doi.org/10.1002/ajmg.10652.
31. Kamath BM, Spinner NB, Emerick KM, Chudley AE, Booth C, Piccoli DA, et al. Vascular anomalies in Alagille syndrome: a significant cause of morbidity and mortality. Circulation. 2004;109(11):1354–8. https://doi.org/10.1161/01.CIR.0000121361.01862.A4.
32. Zimrin AB, Pepper MS, McMahon GA, Nguyen F, Montesano R, Maciag T. An antisense oligonucleotide to the notch ligand jagged enhances fibroblast growth factor-induced angiogenesis in vitro. J Biol Chem. 1996;271(51):32499–502.
33. Xue Y, Gao X, Lindsell CE, Norton CR, Chang B, Hicks C, et al. Embryonic lethality and vascular defects in mice lacking the Notch ligand Jagged1. Hum Mol Genet. 1999;8(5):723–30.
34. Hallidie-Smith KA, Karas S. Cardiac anomalies in Williams-Beuren syndrome. Arch Dis Child. 1988;63(7):809–13.
35. Sharma BK, Fujiwara H, Hallman GL, Ott DA, Reul GJ, Cooley DA. Supravalvar aortic stenosis: a 29-year review of surgical experience. Ann Thorac Surg. 1991;51(6):1031–9. https://doi.org/10.1016/0003-4975(91)91045-w.
36. McElhinney DB, Petrossian E, Tworetzky W, Silverman NH, Hanley FL. Issues and outcomes in the management of supravalvar aortic stenosis. Ann Thorac Surg. 2000;69(2):562–7. https://doi.org/10.1016/s0003-4975(99)01293-x.
37. Sugayama SM, Moises RL, Wagenfur J, Ikari NM, Abe KT, Leone C, et al. Williams-Beuren syndrome: cardiovascular abnormalities in 20 patients diagnosed with fluorescence in situ hybridization. Arq Bras Cardiol. 2003;81(5):462–73.
38. Bogershausen N, Gatinois V, Riehmer V, Kayserili H, Becker J, Thoenes M, et al. Mutation update for Kabuki syndrome genes KMT2D and KDM6A and further delineation of X-linked Kabuki syndrome subtype 2. Hum Mutat. 2016;37(9):847–64. https://doi.org/10.1002/humu.23026.
39. Digilio MC, Gnazzo M, Lepri F, Dentici ML, Pisaneschi E, Baban A, et al. Congenital heart defects in molecularly proven Kabuki syndrome patients. Am J Med Genet A. 2017;173(11): 2912–22. https://doi.org/10.1002/ajmg.a.38417.
40. Issaeva I, Zonis Y, Rozovskaia T, Orlovsky K, Croce CM, Nakamura T, et al. Knockdown of ALR (MLL2) reveals ALR target genes and leads to alterations in cell adhesion and growth. Mol Cell Biol. 2007;27(5):1889–903. https://doi.org/10.1128/MCB.01506-06.
41. Glaser S, Schaft J, Lubitz S, Vintersten K, van der Hoeven F, Tufteland KR, et al. Multiple epigenetic maintenance factors implicated by the loss of Mll2 in mouse development. Development. 2006;133(8):1423–32. https://doi.org/10.1242/dev.02302.
42. Biben C, Weber R, Kesteven S, Stanley E, McDonald L, Elliott DA, et al. Cardiac septal and valvular dysmorphogenesis in mice heterozygous for mutations in the homeobox gene Nkx2-5. Circ Res. 2000;87(10):888–95.
43. Schott JJ, Benson DW, Basson CT, Pease W, Silberbach GM, Moak JP, et al. Congenital heart disease caused by mutations in the transcription factor NKX2-5. Science. 1998;281(5373): 108–11.

44. Benson DW, Silberbach GM, Kavanaugh-McHugh A, Cottrill C, Zhang Y, Riggs S, et al. Mutations in the cardiac transcription factor NKX2.5 affect diverse cardiac developmental pathways. J Clin Invest. 1999;104(11):1567–73. https://doi.org/10.1172/JCI8154.
45. McElhinney DB, Geiger E, Blinder J, Benson DW, Goldmuntz E. NKX2.5 mutations in patients with congenital heart disease. J Am Coll Cardiol. 2003;42(9):1650–5.
46. Majumdar R, Yagubyan M, Sarkar G, Bolander ME, Sundt TM 3rd. Bicuspid aortic valve and ascending aortic aneurysm are not associated with germline or somatic homeobox NKX2-5 gene polymorphism in 19 patients. J Thorac Cardiovasc Surg. 2006;131(6):1301–5. https://doi.org/10.1016/j.jtcvs.2006.01.039.
47. Qu XK, Qiu XB, Yuan F, Wang J, Zhao CM, Liu XY, et al. A novel NKX2.5 loss-of-function mutation associated with congenital bicuspid aortic valve. Am J Cardiol. 2014;114(12):1891–5. https://doi.org/10.1016/j.amjcard.2014.09.028.
48. Proost D, Vandeweyer G, Meester JA, Salemink S, Kempers M, Ingram C, et al. Performant mutation identification using targeted next-generation sequencing of 14 thoracic aortic aneurysm genes. Hum Mutat. 2015;36(8):808–14. https://doi.org/10.1002/humu.22802.
49. McKellar SH, Tester DJ, Yagubyan M, Majumdar R, Ackerman MJ, Sundt TM 3rd. Novel NOTCH1 mutations in patients with bicuspid aortic valve disease and thoracic aortic aneurysms. J Thorac Cardiovasc Surg. 2007;134(2):290–6. https://doi.org/10.1016/j.jtcvs.2007.02.041.
50. Laforest B, Andelfinger G, Nemer M. Loss of Gata5 in mice leads to bicuspid aortic valve. J Clin Invest. 2011;121(7):2876–87. https://doi.org/10.1172/JCI44555.
51. Bonachea EM, Chang SW, Zender G, LaHaye S, Fitzgerald-Butt S, McBride KL, et al. Rare GATA5 sequence variants identified in individuals with bicuspid aortic valve. Pediatr Res. 2014;76(2):211–6. https://doi.org/10.1038/pr.2014.67.
52. Gaussin V, Van de Putte T, Mishina Y, Hanks MC, Zwijsen A, Huylebroeck D, et al. Endocardial cushion and myocardial defects after cardiac myocyte-specific conditional deletion of the bone morphogenetic protein receptor ALK3. Proc Natl Acad Sci U S A. 2002;99(5):2878–83. https://doi.org/10.1073/pnas.042390499.
53. Kim RY, Robertson EJ, Solloway MJ. Bmp6 and Bmp7 are required for cushion formation and septation in the developing mouse heart. Dev Biol. 2001;235(2):449–66. https://doi.org/10.1006/dbio.2001.0284.
54. Galvin KM, Donovan MJ, Lynch CA, Meyer RI, Paul RJ, Lorenz JN, et al. A role for smad6 in development and homeostasis of the cardiovascular system. Nat Genet. 2000;24(2):171–4. https://doi.org/10.1038/72835.
55. Tan HL, Glen E, Topf A, Hall D, O'Sullivan JJ, Sneddon L, et al. Nonsynonymous variants in the SMAD6 gene predispose to congenital cardiovascular malformation. Hum Mutat. 2012;33(4):720–7. https://doi.org/10.1002/humu.22030.
56. Giusti B, Sticchi E, De Cario R, Magi A, Nistri S, Pepe G. Genetic bases of bicuspid aortic valve: the contribution of traditional and high-throughput sequencing approaches on research and diagnosis. Front Physiol. 2017;8:612. https://doi.org/10.3389/fphys.2017.00612.
57. Lindsay ME, Schepers D, Bolar NA, Doyle JJ, Gallo E, Fert-Bober J, et al. Loss-of-function mutations in TGFB2 cause a syndromic presentation of thoracic aortic aneurysm. Nat Genet. 2012;44(8):922–7. https://doi.org/10.1038/ng.2349.
58. Pepe G, Nistri S, Giusti B, Sticchi E, Attanasio M, Porciani C, et al. Identification of fibrillin 1 gene mutations in patients with bicuspid aortic valve (BAV) without Marfan syndrome. BMC Med Genet. 2014;15:23. https://doi.org/10.1186/1471-2350-15-23.
59. Freeze SL, Landis BJ, Ware SM, Helm BM. Bicuspid aortic valve: a review with recommendations for genetic counseling. J Genet Couns. 2016;25(6):1171–8. https://doi.org/10.1007/s10897-016-0002-6.
60. Powell CB, Stone FM, Atkins DL, Watson DG, Moller JH. Operative mortality and frequency of coexistent anomalies in interruption of the aortic arch. Am J Cardiol. 1997;79(8):1147–8.
61. Gruber PJ, Epstein JA. Development gone awry: congenital heart disease. Circ Res. 2004;94(3):273–83. https://doi.org/10.1161/01.RES.0000116144.43797.3B.

62. Corsten-Janssen N, Kerstjens-Frederikse WS, du Marchie Sarvaas GJ, Baardman ME, Bakker MK, Bergman JE, et al. The cardiac phenotype in patients with a CHD7 mutation. Circ Cardiovasc Genet. 2013;6(3):248–54. https://doi.org/10.1161/CIRCGENETICS.113.000054.
63. Goldmuntz E, Clark BJ, Mitchell LE, Jawad AF, Cuneo BF, Reed L, et al. Frequency of 22q11 deletions in patients with conotruncal defects. J Am Coll Cardiol. 1998;32(2):492–8.
64. Ryan AK, Goodship JA, Wilson DI, Philip N, Levy A, Seidel H, et al. Spectrum of clinical features associated with interstitial chromosome 22q11 deletions: a European collaborative study. J Med Genet. 1997;34(10):798–804.
65. Marino B, Digilio MC, Toscano A, Anaclerio S, Giannotti A, Feltri C, et al. Anatomic patterns of conotruncal defects associated with deletion 22q11. Genet Med. 2001;3(1):45–8. https://doi.org/10.1097/00125817-200101000-00010.
66. Gao S, Li X, Amendt BA. Understanding the role of Tbx1 as a candidate gene for 22q11.2 deletion syndrome. Curr Allergy Asthma Rep. 2013;13(6):613–21. https://doi.org/10.1007/s11882-013-0384-6.
67. Merscher S, Funke B, Epstein JA, Heyer J, Puech A, Lu MM, et al. TBX1 is responsible for cardiovascular defects in velo-cardio-facial/DiGeorge syndrome. Cell. 2001;104(4):619–29.
68. Marino B, Digilio MC, Persiani M, Di Donato R, Toscano A, Giannotti A, et al. Deletion 22q11 in patients with interrupted aortic arch. Am J Cardiol. 1999;84(3):360–1. A9
69. Marino B, Digilio MC, Toscano A, Giannotti A, Dallapiccola B. Congenital heart diseases in children with Noonan syndrome: an expanded cardiac spectrum with high prevalence of atrioventricular canal. J Pediatr. 1999;135(6):703–6.
70. Roberts AE, Allanson JE, Tartaglia M, Gelb BD. Noonan syndrome. Lancet. 2013;381(9863):333–42. https://doi.org/10.1016/S0140-6736(12)61023-X.
71. Tartaglia M, Kalidas K, Shaw A, Song X, Musat DL, van der Burgt I, et al. PTPN11 mutations in Noonan syndrome: molecular spectrum, genotype-phenotype correlation, and phenotypic heterogeneity. Am J Hum Genet. 2002;70(6):1555–63. https://doi.org/10.1086/340847.
72. Tartaglia M, Mehler EL, Goldberg R, Zampino G, Brunner HG, Kremer H, et al. Mutations in PTPN11, encoding the protein tyrosine phosphatase SHP-2, cause Noonan syndrome. Nat Genet. 2001;29(4):465–8. https://doi.org/10.1038/ng772.
73. Croonen EA, Nillesen W, Schrander C, Jongmans M, Scheffer H, Noordam C, et al. Noonan syndrome: comparing mutation-positive with mutation-negative dutch patients. Mol Syndromol. 2013;4(5):227–34. https://doi.org/10.1159/000350686.
74. Lin AE, Alexander ME, Colan SD, Kerr B, Rauen KA, Noonan J, et al. Clinical, pathological, and molecular analyses of cardiovascular abnormalities in Costello syndrome: a Ras/MAPK pathway syndrome. Am J Med Genet A. 2011;155A(3):486–507. https://doi.org/10.1002/ajmg.a.33857.
75. Ben-Shachar S, Constantini S, Hallevi H, Sach EK, Upadhyaya M, Evans GD, et al. Increased rate of missense/in-frame mutations in individuals with NF1-related pulmonary stenosis: a novel genotype-phenotype correlation. Eur J Hum Genet. 2013;21(5):535–9. https://doi.org/10.1038/ejhg.2012.221.
76. Calcagni G, Limongelli G, D'Ambrosio A, Gesualdo F, Digilio MC, Baban A, et al. Cardiac defects, morbidity and mortality in patients affected by RASopathies. CARNET study results. Int J Cardiol. 2017;245:92–8. https://doi.org/10.1016/j.ijcard.2017.07.068.
77. Patel C, Silcock L, McMullan D, Brueton L, Cox H. TBX5 intragenic duplication: a family with an atypical Holt-Oram syndrome phenotype. Eur J Hum Genet. 2012;20(8):863–9. https://doi.org/10.1038/ejhg.2012.16.
78. Xiang R, Fan LL, Huang H, Cao BB, Li XP, Peng DQ, et al. A novel mutation of GATA4 (K319E) is responsible for familial atrial septal defect and pulmonary valve stenosis. Gene. 2013;534:320. https://doi.org/10.1016/j.gene.2013.10.028.

79. Garg V, Kathiriya IS, Barnes R, Schluterman MK, King IN, Butler CA, et al. GATA4 mutations cause human congenital heart defects and reveal an interaction with TBX5. Nature. 2003;424 (6947):443–7. https://doi.org/10.1038/nature01827.
80. Okubo A, Miyoshi O, Baba K, Takagi M, Tsukamoto K, Kinoshita A, et al. A novel GATA4 mutation completely segregated with atrial septal defect in a large Japanese family. J Med Genet. 2004;41(7):e97.

Molecular Pathways and Animal Models of Semilunar Valve and Aortic Arch Anomalies

46

Eleanor Gill and Simon D. Bamforth

Abstract

The great arteries of the vertebrate carry blood from the heart to the systemic circulation and are derived from the pharyngeal arch arteries. In higher vertebrates, the pharyngeal arch arteries are a symmetrical series of blood vessels that rapidly remodel during development to become the asymmetric aortic arch arteries carrying oxygenated blood from the left ventricle via the outflow tract. At the base of the aorta, as well as the pulmonary trunk, are the semilunar valves. These valves each have three leaflets and prevent the backflow of blood into the heart. During development, the process of aortic arch and valve formation may go wrong, resulting in cardiovascular defects, and these may, at least in part, be caused by genetic mutations. In this chapter, we will review models harboring genetic mutations that result in cardiovascular defects affecting the great arteries and the semilunar valves.

Keywords

Aortic arch arteries · Interruption of the aortic arch · Semilunar valves · Bicuspid aortic valve · Coarctation · Stenosis · Congenital heart defects · Model organisms · Genetics · Extracellular matrix · *TBX1* · *GBX2* · *TGFβ* · *FGF8* · Neural crest cells

E. Gill · S. D. Bamforth (✉)
Newcastle University Biosciences Institute, Newcastle upon Tyne, UK
e-mail: simon.bamforth@newcastle.ac.uk

© The Author(s), under exclusive license to Springer Nature Switzerland AG 2024

S. Rickert-Sperling et al. (eds.), *Congenital Heart Diseases: The Broken Heart*,
Advances in Experimental Medicine and Biology 1441,
https://doi.org/10.1007/978-3-031-44087-8_46

46.1 Introduction

The great arteries of the human heart are derived from the pharyngeal arch arteries (PAAs) [1, 2]. The PAAs form symmetrically and sequentially during early embryogenesis in a cranial to caudal sequence and are rapidly remodeled over an approximately 3-week period in human embryonic development to form the asymmetric great arteries seen in the adult, namely the aorta, carotid and subclavian arteries. Initially the PAAs are derived from endothelial cell precursors and form the five pairs of vessels traditionally known as PAAs 1–4 and 6. The first two pairs of PAA (numbered 1 and 2) become interrupted early in development and contribute to the vascular plexus within the forming jaw. The asymmetric remodeling process that will result in the formation of the mature aorta, carotid and subclavian arteries involves PAAs 2, 3 and 4. The proximal part of the second PAAs, on both the right and the left, form the external carotid arteries while the third PAAs form the common carotid arteries and the stem of the internal carotid arteries [3]. The fourth PAA persists on the right as the proximal region of the subclavian artery, while on the left, it contributes to the section of the mature aortic arch between the origins of the left common carotid artery and the left subclavian artery. The right sixth PAA regresses, while the left sixth PAA forms the arterial duct (also known as the ductus arteriosus).

Each PAA is housed within a pharyngeal arch, a series of transient structures important for the development of the jaw, ears, cartilages of the throat and the pharyngeal glands [4]. The pharyngeal arches, and the PAAs formed within them, are typically numbered in a cranial to caudal sequence as 1–4 and 6. The reason for the missing 5 is attributed to a transient fifth arch artery formed during development but we have recently argued against this numbering strategy as it is based on a hypothetical 6 arch model from the 1880s [5]. All amniotes, however, only develop five arch arteries so we have proposed that the arches and the PAAs should be named based on the anatomical location of the artery: mandibular (1st), hyoid (2nd), carotid (3rd), aortic (4th) and pulmonary (most caudal) [5–7]. The pharyngeal arches are bordered on the outside by ectoderm and the inside by endoderm, and within is a mesodermal core surrounded by neural crest-derived mesenchyme. Neural crest cells will differentiate into the smooth muscle cells that surround the arch arteries, as well as migrating into the outflow tract to septate the single vessel into the separate aorta and pulmonary trunk. Each tissue plays a role in creating the great arteries of the heart, and consequently many molecular pathways are important for the establishment and patterning of the PAAs into the great arteries found in the adult.

The semilunar, or arterial, valves are found at the base of the aorta and pulmonary trunk, each comprising of three leaflets, and prevent the back-flow of blood into the heart following ventricular systole. Whereas it is the extrapericardial components of the arterial trunks that are derived from the PAAs, the intrapericardial arterial trunks are derived from the distal part of the outflow tract, subsequent to growth from the second heart field, with the arterial valves formed in the intermediate component [8]. When the three leaflets of the aortic valve fail to form correctly, only two leaflets are seen giving rise to the condition known as bicuspid aortic valve. This is the commonest form of congenital heart disease and results in regurgitation of blood

from the aorta back into the ventricle. Although this may be a mild phenotype, and is often asymptomatic at birth and in childhood, it is thought to predispose an affected individual to more severe heart disease in later life [9].

Animal models are useful to investigate the roles of individual genes in the process of semilunar valve and PAA formation and remodeling. Cardiovascular development in the mouse closely mimics that seen in the human, albeit at a more rapid pace (total gestation time in the mouse is approximately 19 days). Moreover, current scientific knowledge and tools mean that genetic modification in mice is a relatively straightforward process. The chicken is also a useful animal model for PAA development as it has many similarities to mammals although the development of the aortic arch arteries varies somewhat; the chicken develops a right-sided aortic arch, with two brachiocephalic arteries and an arterial duct on each side. The chicken embryo is directly accessible through a window made in the eggshell, allowing for the application of substances or genetic material to modify development. The zebrafish is also utilized as an animal model for the formation of the PAAs due to its ability to be genetically manipulated, but the more evolutionary primitive body plan and lack of cardiac septation mean that the PAAs mostly remain as symmetric and paired blood vessels and do not remodel as in mammals.

In this chapter, we will review several molecular pathways that are known to play a role in the formation and development of the great arteries and semilunar valves, predominantly focusing on the mouse as a model organism and the genetic or chemical manipulation of this model that results in a number of congenital defects seen in infants, including interruption of the aortic arch (IAA), aberrant right subclavian artery (A-RSA), coarctation of the aorta, bicuspid aortic valve, and aortic and pulmonary stenosis.

46.2 Aortic Arch Anomalies

A review of the published literature on mutant mouse models presenting with cardiovascular defects, including the aortic arch arteries, reveals that many genes from different molecular pathways can result in similar heart defects (Table 46.1).

46.3 T-Box 1

The major gene thought to be responsible for the cardiovascular defects seen in 22q11 deletion syndrome (22q11DS, also known as DiGeorge, velocardiofacial, or Shprintzen syndrome) is *TBX1*. Although clinically rare, 50% of all cases of IAA occur in this syndrome [58]. Mice null for *Tbx1* die in the perinatal period with common arterial trunk [59] (see Chap. 48). Mice lacking one copy of *Tbx1* (i.e., heterozygous, $Tbx1^{+/-}$), however, are generally healthy and fertile, but, importantly, a proportion do display fourth PAA defects such as IAA (which is lethal) and A-RSA (which may be tolerated) (Fig. 46.1) [26]. This heterozygous phenotype makes the $Tbx1^{+/-}$ mouse a relatively good clinical model for 22q11DS. The IAA and A-RSA

Table 46.1 Genes when mutated in mice give rise to defects affecting the development of the pharyngeal arch arteries which subsequently result in defects such as IAA and A-RSA. Other congenital cardiovascular malformations are also seen in some of these mutants (e.g., common arterial trunk—see Chap. 48, and transposition of the great arteries—see Chap. 36)

Class	Gene	Reference
Transcription factor	*Cited2*	[10]
	Eya1	[11]
	Foxc1, Foxc2	[12]
	Foxi3	[13]
	Foxp1	[14]
	Gata3	[15]
	Gata6	[16]
	Gbx2	[17]
	Hand2	[18]
	Hoxa1;Hoxb1	[19]
	Hrt1;Hey1	[20]
	Pax9	[21]
	Pbx1	[22]
	Prdm1	[23]
	Prdm3	[24]
	Prrx1;Prrx2	[25]
	Tbx1	[26]
	Tcfap2a	[27]
	Zic3	[28]
Transcriptional regulator	*Hdac3*	[29]
Signaling molecule	*Notch*	[30]
	Scrib	[31]
	Sema3c	[32]
Growth factor	*Fgf8*	[33]
	Tgfb2	[34]
	Vegfa	[35]
Protein binding	*Bmp4*	[36]
	Chrd	[37]
	Crkl	[38]
	Edn1	[39]
	Ednra	[40]
	Flna	[41]
	Fn1	[42]
	Ltbp1l	[43]
	Vangl2	[44]
Receptor	*Acvr1*	[45]
	Bmpr2	[46]
	Folr1	[47]
	Itga5	[42]
	Itgb1	[48]

(continued)

Table 46.1 (continued)

Class	Gene	Reference
	Pdgfra	[49]
	Plxnd1	[50]
	Rara;Rarb, Rara;Rarc	[51]
	Ryk	[52]
	Tgfbr2	[53]
Enzyme	*Aldh1a2*	[54]
	Chd7	[55]
	Ece1	[56]

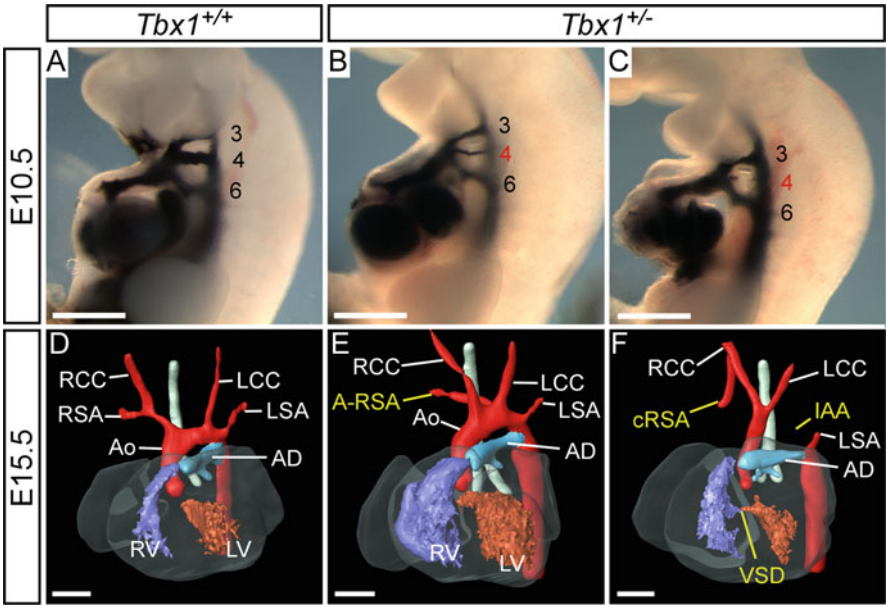

Fig. 46.1 Cardiovascular defects in *Tbx1*-heterozygous (*Tbx1*$^{+/-}$) mouse embryos and fetuses. **(a–c)** Injection of India ink into the heart of E10.5 embryos. **(a)** In the wild-type embryo (*Tbx1*$^{+/+}$) three bilaterally symmetrical PAA are present (here numbered 3, 4 and 6) which are fully patent to ink. **(b, c)** In *Tbx1*$^{+/-}$ embryos the fourth PAA may either be hypoplastic (b) or nonpatent to ink (**c**) revealing that this PAA has failed to form properly. **(d–f)** 3-D reconstructions from MRI datasets [57] of E15.5 fetuses. **(d)** By E15.5 the heart and its associated great vessels have developed into the mature configuration. **(e, f)** The hearts of *Tbx1*$^{+/-}$ fetuses present with great artery defects related to the failure of the fourth PAA to form correctly: A-RSA (**e**) and IAA (f) which, in this case, is accompanied by cervical origin of the RSA (cRSA) and a VSD. Abbreviations: Ao, aorta; AD, arterial duct; LCC, left common carotid; LSA, left subclavian artery; LV, left ventricle; RCC, right common carotid; RSA, right subclavian artery; RV, right ventricle. Scale, 500 μm. Figure adapted from [21]

Table 46.2 Penetrance of fourth PAA defects in *Tbx1*$^{+/-}$ mutant embryos assessed from published data

Stage	N	% Defects (mean with 95% confidence intervals)	Reference
E10.5–E11.0	127	87% (63–100%)	[21, 26, 55, 60–63]
E11.5	76	62% (50–74%)	[26, 62, 64]
Fetal (E14.5–P2)	215	34% (18–49%)	[21, 55, 60–63, 65, 66]

phenotypes are caused by a failure of the fourth PAAs to form correctly during embryonic development. In *Tbx1*$^{+/-}$ embryos the symmetric PAAs are commonly visualized through intracardiac ink injection and the patency of the PAAs can be scored as a measure of how well developed the PAAs are. *Tbx1*$^{+/-}$ embryos typically have fourth PAAs that are either hypoplastic or nonpatent to ink so are thus considered to be absent, and the frequency of this varies between studies (Table 46.2). It is well documented, however, that the *Tbx1*$^{+/-}$ fourth PAA phenotype recovers during development and fewer fetuses display fourth PAA-derived defects than would be expected from the defects observed at mid-gestation (Table 46.2).

Mutant embryos have been produced to investigate the tissue-specific requirements in PAA morphogenesis in the *Tbx1* heterozygous state. Hypoplasia of the fourth PAA was achieved by removing *Tbx1* from the second heart field, mesoderm, ectoderm and endoderm using *Foxg1Cre* mutant mice [67]. As conditional deletion from the mesoderm using *Mesp1Cre* mutant mice does not result in PAA defects, this seems to exclude the role of Tbx1 in the mesoderm for fourth PAA morphogenesis [67]. Additional evidence for this is provided from pharyngeal epithelial deletion using *Sox17iCre* and *AP-2α-IRESCre* to conditionally delete *Tbx1* from the endoderm and ectoderm, respectively [55, 68]. Although fourth PAA defects observed are relatively mild, the simultaneous conditional deletion of *Tbx1* from both pharyngeal epithelia using *Fgf15Cre* resulted in PAA defects similar to the endoderm and ectoderm specific deletions [69]. This suggests that the role of the pharyngeal endoderm and ectoderm are linked in PAA morphogenesis, and the removal of *Tbx1* from one domain can affect the other.

In the zebrafish, mutant alleles of *tbx1* have been generated through the DNA damaging agent ENU [70, 71]. The two separately identified alleles cause a complete loss of function of *tbx1*. These *tbx1* mutant zebrafish have small otic vesicles and show defects in the segmentation of the posterior pharyngeal arches. Whereas in mice or humans the PAAs become asymmetrically remodeled, in zebrafish the four posterior PAAs persist into adulthood and only the two anterior PAAs become remodeled [72]. In all *tbx1*-mutant larvae, however, the PAAs are highly reduced in number, with only one or two PAAs formed which are capable of carrying blood. This is comparable to the *Tbx1*-null mouse, where segmentation of the caudal pharyngeal arches fails and only the first and second arches form. As the caudal arches are missing, the third, fourth, and sixth PAAs do not develop, resulting in a

common arterial trunk [3, 59, 73]. Similarly to the mouse model of *Tbx1* loss, the neural crest defects are secondary to endodermal defects in the zebrafish [70]. A genetic interaction between *tbx1* and *vegfa* has been demonstrated in the zebrafish through coinjection of morpholinos to knock down each gene simultaneously [35].

Direct targets of *Tbx1* have been identified, either through microarray analysis or genetic interaction studies in vivo. For example, microarray analyses comparing *Tbx1* null embryo tissue with wild-type controls have generated many potential downstream targets of *Tbx1* [74, 75], although not all will directly affect PAA development. Studies in vivo have shown that *Tbx1* is in epistasis, or able to genetically interact, with a number of other genes and pathways, including a *Bmp-Smad* pathway [76], *Chd7* [55], *Crkl* [38], *Fgf8* [63], *Fgf-Six1* signaling [11], *Gbx2* [60], *Hes1* [77], *Pitx2* [78], *Prdm1* [79], *Smad7* [64], and *Wnt5a* signaling [80]. *Tbx1* also functionally interacts with *Pax9*, a transcription factor with various roles in embryonic development, in the pharyngeal endoderm. A high proportion of mice double heterozygous for both genes (i.e., $Tbx1^{+/-};Pax9^{+/-}$) die neonatally with IAA [21].

46.4 Fibroblast Growth Factor 8

As mentioned above, *Fgf8* is in epistasis with *Tbx1*. *Fgf8* is an important signaling factor in PAA development, and the *Fgf8* gene is expressed in the ectoderm and endoderm of the pharyngeal arch region. Mice null for *Fgf8* die early in embryogenesis [81] but mice expressing a *Fgf8* hypomorphic allele present with IAA, right-sided aortic arch and A-RSA, as well as other intracardiac and outflow tract defects such as common arterial trunk and double-outlet right ventricle [82, 83]. Mice doubly heterozygous for *Tbx1* and *Fgf8* have a higher penetrance of fourth PAA-derived defects than *Tbx1* heterozygotes [63]. The PAA defects were attributed to the loss or hypoplasia of the fourth PAAs as a result of neural crest cell disruption, suggesting that *Fgf8* is essential in neural crest cell survival [82]. Interestingly, an expanded expression pattern of *Hand2* in *Fgf8* hypomorphs was observed, which could suggest a complex regulatory loop between these two genes [82].

Tissue-specific removal of *Fgf8* from pharyngeal epithelia (ectoderm and endoderm) has revealed that ectodermal expression of the gene is required for PAA development [33]. Removal of *Fgf8* from the pharyngeal ectoderm using *AP-2-α-IRESCre* resulted in 95% penetrance of fourth PAA malformations at E18.5, of which 30% were IAA. Other defects included abnormalities of the subclavian arteries, circumflex RAA with or without a right-sided arterial duct, and malformations of the coronary arteries. Overall, the levels of PAA malformation mirror that of hypomorphic mutants, suggesting that the pharyngeal ectoderm is the important expression domain of *Fgf8* for fourth PAA development. Early differentiation and migration of endothelial cells was unaffected in these mutant embryos, however, these cells failed to organize correctly into vascular tubes. Additionally, removal of *Fgf8* from the ectoderm and endoderm using *Hoxa3-IREScre*, revealed a comparable number of PAA malformations to those seen in the ectoderm-specific

deletion. Thymus and parathyroid malformations, in addition to bicuspid aortic valve, were uniquely identified in these mutants, suggesting that endodermal *Fgf8* expression is key in gland and valve development. Apoptosis of neural crest cells was identified within the third pharyngeal arch mesenchyme and that of the forming fourth and sixth pharyngeal arches. It appears that the ectodermal expression of *Fgf8* is crucial for the formation of the fourth pharyngeal arch, however, the defects observed in *Fgf8*;*Hoxa3-IRESCre* mutants are perhaps the result of a synergistic effect of *Fgf8* removal from both the ectoderm and endoderm simultaneously. A signaling pathway between the neural crest-derived mesenchyme and endothelial cells is apparently required for correct formation of the PAA, at a time prior to differentiation of neural crest cells into vascular smooth muscle cells [33].

46.5 Gastrulation Brain Homeobox 2

Another gene that has been linked to *Tbx1*, as a potential downstream target is the transcription factor gastrulation brain homeobox 2 (*Gbx2*) [74]. Mice null for *Gbx2* present with a range of cardiovascular malformations including IAA and A-RSA, as well as outflow tract defects, such as over-riding aorta and DORV [17, 60, 84]. Reminiscent of the *Tbx1*-null phenotype, these malformations appear to be related to disrupted neural crest cell migration at E8.0–9.5 of mouse embryonic development. However, as *Gbx2* is not expressed in neural crest cells, it was determined that *Gbx2* expression within the pharyngeal epithelia is responsible for the activation of signaling pathways required in neural crest cell migration into the pharyngeal arches [60]. Conditional deletion of *Gbx2* from the pharyngeal ectoderm, using *AP-2-α-IRESCre*, resulted in a comparable level of fourth PAA defects as seen in $Gbx2^{-/-}$ embryos, when examined at E10.5 by ink injection. This suggests that ectodermal expression of *Gbx2* is key to the neural crest cell migration defects observed in $Gbx2^{-/-}$ embryos. A fusion of the neural crest cell streams as they entered the pharyngeal arches was also observed. These defects were found to be the result of disruption of the Slit/Robo pathway, involved in migration of the neural crest cells to the pharyngeal arches [60].

The penetrance of cardiovascular defects in *Gbx2*-null embryos is significantly increased when *Pax9* is hemizygous, suggesting epistasis between these two genes [84]. Additionally, there is evidence to support a potential genetic interaction between *Gbx2* and *Tbx1* [60]. Double heterozygous mutant embryos (i.e., $Tbx1^{+/-}$;$Gbx2^{+/-}$) showed a statistically significant increase in fourth PAA malformation at E10.5 than that observed in *Tbx1*-heterozygous mutant embryos (i.e., $Tbx1^{+/-}$;$Gbx2^{+/+}$), although this effect was not observed in $Tbx1^{+/-}$;$Gbx2^{+/-}$ embryos later in development at E15.5 [84]. Reduced expression of *Slit2* was also observed in $Tbx1^{+/-}$ mutant embryos, and those with a pharyngeal ectoderm specific deletion, to a greater extent than that seen in *Gbx2* mutants [60]. This suggests that *Tbx1* may also be capable of regulating *Slit2*, independent of *Gbx2*.

A further genetic interaction has been proposed between *Gbx2* and *Fgf8*. The expression patterns of both *Gbx2* and *Fgf8* overlap, suggesting that the two genes

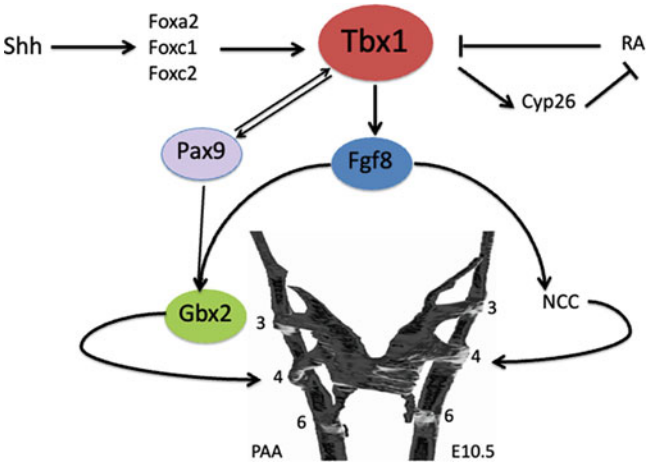

Fig. 46.2 Schematic model of some of the genes discussed in this chapter and their involvement in regulating *Tbx1* and the development of the fourth PAA. Figure adapted from [17, 85, 86]

may be interlinked, although there is no change in the expression levels of *Fgf8* in *Gbx2* mutant embryos [17]. However, *Gbx2* can be induced by ectopic FGF8 expression, and *Gbx2* expression in E8.5 *Fgf8* hypomorphs was found to be reduced in the region overlying the future fourth PAA. This, therefore, suggests that *Gbx2* is a downstream effector of *Fgf8* signaling (Fig. 46.2). This notion was confirmed by changes in the number of PAA defects in complex mutant embryos. Double heterozygous embryos (i.e., $Gbx2^{+/-};Fgf8^{+/-}$) showed an increase in the incidence of A-RSA and RAA, while no defects were observed in either of the single heterozygotes. Generating embryos homozygous null for *Gbx2* and heterozygous for *Fgf8* (i.e., $Gbx2^{-/-};Fgf8^{+/-}$) resulted in a significant increase in the number of PAA malformations, compared to those seen in $Gbx2^{-/-}$ embryos. It is proposed that *Tbx1* is upstream of *Fgf8*, which then activates *Gbx2* and results in correct PAA development. It is also postulated that *Fgf8* is capable of acting independently, through a parallel pathway which controls neural crest cell survival, in forming the PAA, as neural crest cell apoptosis is observed in *Fgf8* mutants, but not in *Gbx2*-null embryos [17, 33].

46.6 *Transforming Growth Factor-β* Signaling

Transforming growth factor (TGF)-β signaling is crucial for regulating basic cell responses, including proliferation, migration and apoptosis, and has been shown to be important for embryonic development in mouse models. The TGFβ signaling pathway is initiated by the binding of TGFβ ligand to the cell surface TGFβ type II receptor (TGFBR2), which activates the TGFβ type I receptor, TGFBR1 (also known as ALK5), and phosphorylates SMAD2 and SMAD3 proteins, allowing

association with SMAD4 and translocation to the nucleus to regulate downstream gene expression.

Mice null for the TGFβ2 ligand (*Tgfb2*) die perinatally with cardiovascular defects, including IAA and A-RSA, as well as VSD, DORV and CAT [34, 87]. Aberrant apoptosis within the fourth PAA was observed, without any defects in neural crest cell migration, which may contribute to the IAA phenotype as well as causing problems with its innervation [87, 88]. The TGFβ receptor *Tgfbr2* is essential for embryogenesis, as mice lacking this gene die around mid-gestation [89, 90]. The conditional deletion of *Tgfbr2* from the neural crest results in IAA [53]. Disruption of the *Ltbp1* gene, which encodes for the long form of latent TGF-β binding protein 1, and is required for correct storage of TGFβ ligands in the extracellular matrix, also results in embryos with IAA [43].

46.7 The Extracellular Matrix

The extracellular matrix (ECM) is a three-dimensional network of extracellular macromolecules, such as collagen, enzymes and glycoproteins, and provides structural and biochemical support to surrounding cells. Common functions of the ECM are cell adhesion, cell-to-cell communication and differentiation, mediated through focal adhesion with interacting cells via integrins and their ligands. Recent evidence has been presented that shows the importance of the ECM in cardiovascular development [91], and perturbations in key gene expression related to the ECM can lead to arch artery anomalies. For example, the integrin α5β1 heterodimer binds to fibronectin 1 (*Fn1*) which is a major component of the ECM. Conditional deletion from the SHF of either integrin α5 (*Itga5*) or *Fn1* results in fourth PAA-derived defects such as IAA and A-RSA in mutant mouse embryos [42], and this is caused by defective α5β1-Fn1-mediated cell–ECM interactions in the SHF which are essential for fourth PAA remodeling [92]. Deletion of *Fn1* conditionally from neural crest cells also causes IAA [93], and loss of another ECM protein, *Fibulin-1*, causes cardiovascular defects including A-RSA [94].

46.8 Coarctation

Coarctation of the aorta is defined as a narrowing of a section of the aorta that will restrict the flow of blood from the heart. This defect has been recognized in mouse models with heart and great vessel defects, but rarely as an isolated phenotype. It is much more commonly seen within the context of complex cardiovascular malformations.

Aortic coarctation is present within the spectrum of cardiovascular phenotypes seen in 22q11DS patients, and coarctation has also been seen in mouse models genetically connected to *Tbx1*. The expression of *Tbx1* is induced and sustained by Sonic hedgehog (Shh) in the pharyngeal endoderm [95]. However, the Forkhead transcription factors *Foxa2*, *Foxc1* and *Foxc2,* have been shown to recognize and

bind to cis-regulatory elements in the *Tbx1* promoter, and to directly promote the expression of Tbx1 [96, 97]. It is proposed that Tbx1 is a direct transcriptional target of Fox proteins, which play an intermediary role in the regulation of Tbx1 by Shh (Fig. 46.2). It should be noted, however, that mutation of *Tbx1* regulatory regions, and the deletion of the putative Fox binding site in transgenic mice, have illustrated the complex nature of Tbx1 regulation and expression [98]. Mice null for *Foxc1* have coarctation and aortic and pulmonary valve dysplasia, as well as IAA-B and patent arterial duct [12] and mice null for *Foxc2* have IAA-A and IAA-B [12, 99]. The different descriptions for IAA reflect the location of the interruption: IAA type A is found when the segment of the aortic arch distal to the left subclavian artery is interrupted; IAA type B occurs when the segment of the aortic arch between the left common carotid and left subclavian artery is missing; and type C is when the aortic arch between the right and left common carotid arteries is absent. Mice doubly heterozygous for *Foxc1* and *Foxc2* (i.e., $Foxc1^{+/-};Foxc2^{+/-}$) also present with coarctation and aortic and pulmonary valve dysplasia, and also have IAA-A and IAA-B [12] whereas individual heterozygotes do not.

Folr1 is a folate-binding protein gene, and mice null for *Folr1* die at mid-embryogenesis from extensive cell death. However, folic acid supplementation of pregnant females greatly reduces this early embryonic lethality and allows for *Folr1*-null mice to be born and bred [47]. A small proportion of these *Folr1*-null fetuses had coarctation of the aortic arch or IAA, as well as a right-sided aortic arch and A-RSA. In these fetuses, coarctation was found proximal to the arterial duct.

Coarctation has also been described in mice double homozygous for the retinoic acid receptors alpha and beta ($Rara^{-/-}$; $Rarb^{-/-}$), and additionally these mice present with CAT, right-sided aortic arch and A-RSA [51]. Also, mice null for *Vangl2*, a membrane protein involved in the regulation of planar cell polarity, and the gene mutated in the Loop-tail mouse, die from complex cardiovascular defects that includes preductal coarctation as well as IAA, DORV, VSD and right-sided aortic arch [44].

46.9 Bicuspid Aortic Valve

The semilunar, or arterial, valves form the three leaflets of the aorta and pulmonary trunk that prevent the backflow of blood to the heart. When only two leaflets of the aortic semilunar valves are formed, this is known as bicuspid aortic valve (BAV). Although BAV is frequently seen in patients, it is infrequently described in mutant mouse models with cardiovascular malformation. This is either because the mouse is resilient to forming this phenotype, or more likely, its presentation is under-reported due to the technical difficulties in identifying it. Patients with Down's, 22q11 deletion, and Turner's syndromes have been reported to have BAV [100]. In Turner Syndrome patients with a specific deletion of the short arm of the X chromosome, BAV and coarctation are seen [101]. One of the genes in the deleted region, which will therefore be predicted to be haploinsufficient, is *USP9X*, a ubiquitinase involved in TGFβ-Smad signaling and which is expressed in the heart. Genes within the TGFβ

superfamily of structurally related signaling proteins may therefore be important for the correct formation of the arterial valves. A mouse model of deficient signaling via the activin A receptor, type I (*Acvr1*) presents with BAV [102]. Activins are dimeric growth and differentiation factors which belong to the TGFβ superfamily. Moreover, mutant mice lacking the bone morphogenetic receptor *Bmpr2* present with absent arterial valves, as well as CAT, IAA and VSD [46]. The ligands of this receptor are BMPs, which are also members of the TGFβ superfamily. Mice deficient in *Adamts5* (A Disintegrin-like And Metalloprotease domain with ThromboSpondin-type 1 motifs) display myxomatous valve disease where the arterial valves are enlarged [103]. This is linked to an accumulation within the valves of uncleaved versican, a large chondroitin sulfate proteoglycan. When mice null for *Adamts5* are complexed with *Smad2* heterozygosity (i.e., $Adamts5^{-/-};Smad2^{+/-}$) a highly penetrant BAV phenotype occurs, concomitant with insufficient cleavage of versican as well as Smad2 phosphorylation [104]. This suggests that a reduction in TGFβ signaling exacerbates the *Adamts5* valve phenotype.

As described in Chap. 48, mice null for the homeodomain transcription factor *Pbx1* have CAT, but the other Pbx family members, *Pbx2* and *Pbx3*, when deleted have normal cardiovascular development [22, 105]. However, complex alleles of these three genes (homozygous and heterozygous) reveal their importance in the development of the arterial valves. Mice triply heterozygous for all three Pbx alleles (i.e., $Pbx1^{+/-};Pbx2^{+/-};Pbx3^{+/-}$) display BAV [105], as do $Pbx1^{+/-};Pbx2^{-/-};Pbx3^{+/-}$ embryos who also present with a tetralogy of Fallot type phenotype.

The transcription factor *Gata5* is required for the development of the heart and endoderm in zebrafish [106]. In the mouse, *Gata5* is expressed in the developing heart [107], and the Gata family (*Gata4*, *Gata5,* and *Gata6*) may function in endoderm induction in the mouse [108]. Mouse embryos null for *Gata5* present with BAV [109], and *GATA5* has been suggested to be a candidate modifier gene for congenital heart disease [110].

Conditional deletions of *Fgf8* have revealed that this gene is implicated in correct development of the arterial valves. BAV has been described in mutant mice with a mesoderm-specific deletion of *Fgf8* [111], and when *Fgf8* was deleted from the pharyngeal epithelia [33]. In mice null for endothelial nitric oxide synthase (*Nos3*), a bicuspid valve is observed where it is the nonadjacent and right coronary leaflets that form the conjoined leaflet [112]. Mice lacking the transcriptional regulator *Krox20* conditionally from neural crest cells develop BAV which is possibly caused by an aberrant increase in neural crest cells in the noncoronary leaflet [113]. Interestingly, *Krox20* can regulate *Nos3* expression, and mice double heterozygous for each gene have BAV, indicating a genetic interaction between these two genes [114].

Disturbing the regulation of signaling pathways in mutant mice also gives rise to the BAV phenotype, for example, with mutation in genes of the Slit-Robo [115, 116], Notch [117], and Rho kinase [118] signaling pathways. BAV also occurs alongside the complex cardiovascular defects seen in *Pax9*-deficient mice [21].

Although the majority of great artery and valve defects have been described as a result of a genetic manipulation, it is sometimes possible to discover a phenotype within a wild-type animal model. This is the case with BAV seen in the Syrian

hamster [119, 120]. In this model, a significant proportion of hamster embryos present with a fusion of the leaflets associated with the coronary arteries to produce a bicuspid valve [121].

46.10 Aortic and Pulmonary Stenosis

Stenosis of the aortic and/or pulmonary outflow tract has been described in several mutant mouse models. These include mutations in *Acvr1* [102], *Hand2* [18], *Hey2* [122], *Msx1;Msx2* [123], *Prdm1* [79], and *Tcfap2a* [124]. In the majority of cases, the stenosis is seen in combination with other cardiovascular defects such as CAT, IAA, A-RSA, DORV and VSD. Most of these genes are expressed in the neural crest and the second heart field, underlying the importance of these cell populations in the formation of the vessels of the outflow tract. Maternal diabetes has also been shown to cause complex abnormalities in the outflow tracts, including aortic and pulmonary stenosis and CAT [125].

46.11 Concluding Remarks

As discussed in this chapter, there are many genes that appear to play a role in the formation and development of the semilunar valves and the great arteries, and when mutated or misexpressed in animal models will result in blood vessel and valve defects. That different genes coding for a variety of transcription factors, growth factors, and other types of molecules, can give rise to similar defects to each other when mutated, illustrates the complexity of genetic networks and signaling pathways that control and orchestrate a very complex morphogenetic pathway that results in a functioning cardiovascular system. Also of interest is the apparent sensitivity of the fourth PAA to developmental defects, and raises questions as to why this vessel is so vulnerable to genetic or environmental insult with devastating clinical implications when affecting the left fourth PAA in particular which leads to IAA. Various explanations have been postulated including its particular morphogenetic characteristics, blood flow during remodeling, interaction with the ECM, and gene expression.

Acknowledgments We thank the British Heart Foundation for supporting our research.

References

1. Bamforth SD, Chaudhry B, Bennett M, Wilson R, Mohun TJ, Van Mierop LH, et al. Clarification of the identity of the mammalian fifth pharyngeal arch artery. Clin Anat. 2013;26(2):173–82.
2. Gupta SK, Bamforth SD, Anderson RH. How frequent is the fifth arch artery? Cardiol Young. 2014;25(4):1–19.

3. Anderson RH, Bamforth SD. Morphogenesis of the Mammalian Aortic Arch Arteries. Front Cell Dev Biol. 2022;10:892900.
4. Graham A. Development of the pharyngeal arches. Am J Med Genet A. 2003;119A(3):251–6.
5. Graham A, Hikspoors JPJM, Lamers WH, Anderson RH, Bamforth SD. Morphogenetic processes in the development and evolution of the arteries of the pharyngeal arches: their relations to congenital cardiovascular malformations. Front Cell Dev Biol. 2023;11
6. Graham A, Hikspoors JPJM, Anderson RH, Lamers WH, Bamforth SD. A revised terminology for the pharyngeal arches and the arch arteries. J Anat. 2023.
7. Anderson RH, Graham A, Hikspoors JPJM, Lamers WH, Bamforth SD. The advantages of naming rather than numbering the arteries of the pharyngeal arches. Cardiol Young. 2023:1–9.
8. Anderson RH, Chaudhry B, Mohun TJ, Bamforth SD, Hoyland D, Phillips HM, et al. Normal and abnormal development of the intrapericardial arterial trunks in humans and mice. Cardiovasc Res. 2012;95(1):108–15.
9. Siu SC, Silversides CK. Bicuspid aortic valve disease. J Am Coll Cardiol. 2010;55(25): 2789–800.
10. Bamforth SD, Braganca J, Eloranta JJ, Murdoch JN, Marques FI, Kranc KR, et al. Cardiac malformations, adrenal agenesis, neural crest defects and exencephaly in mice lacking Cited2, a new Tfap2 co-activator. Nat Genet. 2001;29(4):469–74.
11. Guo C, Sun Y, Zhou B, Adam RM, Li X, Pu WT, et al. A Tbx1-Six1/Eya1-Fgf8 genetic pathway controls mammalian cardiovascular and craniofacial morphogenesis. J Clin Invest. 2011;121(4):1585–95.
12. Winnier GE, Kume T, Deng K, Rogers R, Bundy J, Raines C, et al. Roles for the winged helix transcription factors MF1 and MFH1 in cardiovascular development revealed by nonallelic noncomplementation of null alleles. Dev Biol. 1999;213(2):418–31.
13. Hasten E, Morrow BE. Tbx1 and Foxi3 genetically interact in the pharyngeal pouch endoderm in a mouse model for 22q11.2 deletion syndrome. PLoS Genet. 2019;15(8):e1008301.
14. Wang B, Weidenfeld J, Lu MM, Maika S, Kuziel WA, Morrisey EE, et al. Foxp1 regulates cardiac outflow tract, endocardial cushion morphogenesis and myocyte proliferation and maturation. Development. 2004;131(18):4477–87.
15. Raid R, Krinka D, Bakhoff L, Abdelwahid E, Jokinen E, Karner M, et al. Lack of Gata3 results in conotruncal heart anomalies in mouse. Mech Dev. 2008;126(1–2):80–9.
16. Lepore JJ, Mericko PA, Cheng L, Lu MM, Morrisey EE, Parmacek MS. GATA-6 regulates semaphorin 3C and is required in cardiac neural crest for cardiovascular morphogenesis. J Clin Invest. 2006;116(4):929–39.
17. Byrd NA, Meyers EN. Loss of Gbx2 results in neural crest cell patterning and pharyngeal arch artery defects in the mouse embryo. Dev Biol. 2005;284(1):233–45.
18. Morikawa Y, Cserjesi P. Cardiac neural crest expression of Hand2 regulates outflow and second heart field development. Circ Res. 2008;103(12):1422–9.
19. Roux M, Laforest B, Eudes N, Bertrand N, Stefanovic S, Zaffran S. Hoxa1 and Hoxb1 are required for pharyngeal arch artery development. Mech Dev. 2017;143:1–8.
20. Fujita M, Sakabe M, Ioka T, Watanabe Y, Kinugasa-Katayama Y, Tsuchihashi T, et al. Pharyngeal arch artery defects and lethal malformations of the aortic arch and its branches in mice deficient for the Hrt1/Hey1 transcription factor. Mech Dev. 2016;139:65–73.
21. Phillips HM, Stothard CA, Shaikh Qureshi WM, Kousa AI, Briones-Leon JA, Khasawneh RR, et al. Pax9 is required for cardiovascular development and interacts with Tbx1 in the pharyngeal endoderm to control 4th pharyngeal arch artery morphogenesis. Development. 2019;146 (18):dev177618.
22. Chang CP, Stankunas K, Shang C, Kao SC, Twu KY, Cleary ML. Pbx1 functions in distinct regulatory networks to pattern the great arteries and cardiac outflow tract. Development. 2008;135(21):3577–86.
23. Robertson EJ, Charatsi I, Joyner CJ, Koonce CH, Morgan M, Islam A, et al. Blimp1 regulates development of the posterior forelimb, caudal pharyngeal arches, heart and sensory vibrissae in mice. Development. 2007;134(24):4335–45.

24. Bard-Chapeau EA, Szumska D, Jacob B, Chua BQL, Chatterjee GC, Zhang Y, et al. Mice carrying a Hypomorphic Evi1 allele are embryonic viable but exhibit severe congenital heart defects. PLoS One. 2014;9(2):e89397.
25. Bergwerff M, Gittenberger-de Groot AC, Wisse LJ, DeRuiter MC, Wessels A, Martin JF, et al. Loss of function of the Prx1 and Prx2 homeobox genes alters architecture of the great elastic arteries and ductus arteriosus. Virchows Arch. 2000;436(1):12–9.
26. Lindsay EA, Vitelli F, Su H, Morishima M, Huynh T, Pramparo T, et al. Tbx1 haploinsufficieny in the DiGeorge syndrome region causes aortic arch defects in mice. Nature. 2001;410(6824):97–101.
27. Johnson AL, Schneider JE, Mohun TJ, Williams T, Bhattacharya S, Henderson DJ, et al. Early embryonic expression of AP-2α is critical for cardiovascular development. J Cardiovasc Dev Dis. 2020;7(3):27.
28. Purandare SM, Ware SM, Kwan KM, Gebbia M, Bassi MT, Deng JM, et al. A complex syndrome of left-right axis, central nervous system and axial skeleton defects in Zic3 mutant mice. Development. 2002;129(9):2293–302.
29. Singh N, Trivedi CM, Lu M, Mullican SE, Lazar MA, Epstein JA. Histone deacetylase 3 regulates smooth muscle differentiation in neural crest cells and development of the cardiac outflow tract. Circ Res. 2011;109(11):1240–9.
30. High FA, Zhang M, Proweller A, Tu L, Parmacek MS, Pear WS, et al. An essential role for notch in neural crest during cardiovascular development and smooth muscle differentiation. J Clin Invest. 2007;117(2):353–63.
31. Phillips HM, Rhee HJ, Murdoch JN, Hildreth V, Peat JD, Anderson RH, et al. Disruption of planar cell polarity signaling results in congenital heart defects and cardiomyopathy attributable to early cardiomyocyte disorganization. Circ Res. 2007;101(2):137–45.
32. Feiner L, Webber AL, Brown CB, Lu MM, Jia L, Feinstein P, et al. Targeted disruption of semaphorin 3C leads to persistent truncus arteriosus and aortic arch interruption. Development. 2001;128(16):3061–70.
33. Macatee TL, Hammond BP, Arenkiel BR, Francis L, Frank DU, Moon AM. Ablation of specific expression domains reveals discrete functions of ectoderm- and endoderm-derived FGF8 during cardiovascular and pharyngeal development. Development. 2003;130(25):6361–74.
34. Bartram U, Molin DG, Wisse LJ, Mohamad A, Sanford LP, Doetschman T, et al. Double-outlet right ventricle and overriding tricuspid valve reflect disturbances of looping, myocardialization, endocardial cushion differentiation, and apoptosis in TGF-beta(2)-knockout mice. Circulation. 2001;103(22):2745–52.
35. Stalmans I, Lambrechts D, De Smet F, Jansen S, Wang J, Maity S, et al. VEGF: a modifier of the del22q11 (DiGeorge) syndrome? Nat Med. 2003;9(2):173–82.
36. Liu W, Selever J, Wang D, Lu MF, Moses KA, Schwartz RJ, et al. Bmp4 signaling is required for outflow-tract septation and branchial-arch artery remodeling. Proc Natl Acad Sci U S A. 2004;101(13):4489–4.
37. Bachiller D, Klingensmith J, Shneyder N, Tran U, Anderson R, Rossant J, et al. The role of chordin/bmp signals in mammalian pharyngeal development and DiGeorge syndrome. Development. 2003;130(15):3567–78.
38. Guris DL, Fantes J, Tara D, Druker BJ, Imamoto A. Mice lacking the homologue of the human 22q11.2 gene CRKL phenocopy neurocristopathies of DiGeorge syndrome. Nat Genet. 2001;27(3):293–8.
39. Kurihara Y, Kurihara H, Oda H, Maemura K, Nagai R, Ishikawa T, et al. Aortic arch malformations and ventricular septal defect in mice deficient in endothelin-1. J Clin Invest. 1995;96(1):293–300.
40. Yanagisawa H, Hammer RE, Richardson JA, Williams SC, Clouthier DE, Yanagisawa M. Role of Endothelin-1/Endothelin-a receptor-mediated signaling pathway in the aortic arch patterning in mice. J Clin Invest. 1998;102(1):22–33.

41. Feng Y, Chen MH, Moskowitz IP, Mendonza AM, Vidali L, Nakamura F, et al. Filamin a (FLNA) is required for cell–cell contact in vascular development and cardiac morphogenesis. Proc Natl Acad Sci. 2006;103(52):19836–41.
42. Chen D, Wang X, Liang D, Gordon J, Mittal A, Manley N, et al. Fibronectin signals through integrin α5β1 to regulate cardiovascular development in a cell type-specific manner. Dev Biol. 2015;407(2):195–210.
43. Todorovic V, Frendewey D, Gutstein DE, Chen Y, Freyer L, Finnegan E, et al. Long form of latent TGF-beta binding protein 1 (Ltbp1L) is essential for cardiac outflow tract septation and remodeling. Development. 2007;134(20):3723–32.
44. Henderson DJ, Conway SJ, Greene ND, Gerrelli D, Murdoch JN, Anderson RH, et al. Cardiovascular defects associated with abnormalities in midline development in the loop-tail mouse mutant. Circ Res. 2001;89(1):6–12.
45. Kaartinen V, Dudas M, Nagy A, Sridurongrit S, Lu MM, Epstein JA. Cardiac outflow tract defects in mice lacking ALK2 in neural crest cells. Development. 2004;131(14):3481–90.
46. Delot EC, Bahamonde ME, Zhao M, Lyons KM. BMP signaling is required for septation of the outflow tract of the mammalian heart. Development. 2003;130(1):209–20.
47. Zhu H, Wlodarczyk BJ, Scott M, Yu W, Merriweather M, Gelineau-van Waes J, et al. Cardiovascular abnormalities in Folr1 knockout mice and folate rescue. Birth Defects Res A Clin Mol Teratol. 2007;79(4):257–68.
48. Turlo KA, Noel OD, Vora R, LaRussa M, Fassler R, Hall-Glenn F, et al. An essential requirement for beta1 integrin in the assembly of extracellular matrix proteins within the vascular wall. Dev Biol. 2012;365(1):23–35.
49. Tallquist MD, Soriano P. Cell autonomous requirement for PDGFRalpha in populations of cranial and cardiac neural crest cells. Development. 2003;130(3):507–18.
50. Gitler AD, Lu MM, Epstein JA. PlexinD1 and semaphorin signaling are required in endothelial cells for cardiovascular development. Dev Cell. 2004;7(1):107–16.
51. Mendelsohn C, Lohnes D, Decimo D, Lufkin T, LeMeur M, Chambon P, et al. Function of the retinoic acid receptors (RARs) during development (II). Multiple abnormalities at various stages of organogenesis in RAR double mutants. Development. 1994;120(10):2749–71.
52. Kugathasan K, Halford MM, Farlie PG, Bates D, Smith DP, Zhang YF, et al. Deficiency of the Wnt receptor Ryk causes multiple cardiac and outflow tract defects. Growth Factors. 2018;36 (1–2):58–68.
53. Choudhary B, Ito Y, Makita T, Sasaki T, Chai Y, Sucov HM. Cardiovascular malformations with normal smooth muscle differentiation in neural crest-specific type II TGFbeta receptor (Tgfbr2) mutant mice. Dev Biol. 2006;289(2):420–9.
54. Niederreither K, Vermot J, Le Roux I, Schuhbaur B, Chambon P, Dolle P. The regional pattern of retinoic acid synthesis by RALDH2 is essential for the development of posterior pharyngeal arches and the enteric nervous system. Development. 2003;130(11):2525–34.
55. Randall V, McCue K, Roberts C, Kyriakopoulou V, Beddow S, Barrett AN, et al. Great vessel development requires biallelic expression of Chd7 and Tbx1 in pharyngeal ectoderm in mice. J Clin Invest. 2009;119(11):3301–10.
56. Yanagisawa H, Yanagisawa M, Kapur RP, Richardson JA, Williams SC, Clouthier DE, et al. Dual genetic pathways of endothelin-mediated intercellular signaling revealed by targeted disruption of endothelin converting enzyme-1 gene. Development. 1998;125(5):825–36.
57. Bamforth SD, Schneider JE, Bhattacharya S. High-throughput analysis of mouse embryos by magnetic resonance imaging. Cold Spring Harb Protoc. 2012;2012(1):93–101.
58. Lewin MB, Lindsay EA, Jurecic V, Goytia V, Towbin JA, Baldini A. A genetic etiology for interruption of the aortic arch type B. Am J Cardiol. 1997;80(4):493–7.
59. Jerome LA, Papaioannou VE. DiGeorge syndrome phenotype in mice mutant for the T-box gene, Tbx1. Nat Genet. 2001;27(3):286–91.
60. Calmont A, Ivins S, Van Bueren KL, Papangeli I, Kyriakopoulou V, Andrews WD, et al. Tbx1 controls cardiac neural crest cell migration during arch artery development by regulating Gbx2 expression in the pharyngeal ectoderm. Development. 2009;136(18):3173–83.

61. Guris DL, Duester G, Papaioannou VE, Imamoto A. Dose-dependent interaction of Tbx1 and Crkl and locally aberrant RA signaling in a model of del22q11 syndrome. Dev Cell. 2006;10 (1):81–92.
62. Ryckebusch L, Bertrand N, Mesbah K, Bajolle F, Niederreither K, Kelly RG, et al. Decreased levels of embryonic retinoic acid synthesis accelerate recovery from arterial growth delay in a mouse model of DiGeorge syndrome. Circ Res. 2010;106(4):686–94.
63. Vitelli F, Taddei I, Morishima M, Meyers EN, Lindsay EA, Baldini A. A genetic link between Tbx1 and fibroblast growth factor signaling. Development. 2002;129(19):4605–11.
64. Papangeli I, Scambler PJ. Tbx1 genetically interacts with the transforming growth factor-beta/bone morphogenetic protein inhibitor Smad7 during great vessel remodeling. Circ Res. 2013;112(1):90–102.
65. Zhang Z, Baldini A. In vivo response to high-resolution variation of Tbx1 mRNA dosage. Hum Mol Genet. 2008;17(1):150–7.
66. Aggarwal VS, Liao J, Bondarev A, Schimmang T, Lewandoski M, Locker J, et al. Dissection of Tbx1 and Fgf interactions in mouse models of 22q11DS suggests functional redundancy. Hum Mol Genet. 2006;15(21):3219–28.
67. Zhang Z, Cerrato F, Xu H, Vitelli F, Morishima M, Vincentz J, et al. Tbx1 expression in pharyngeal epithelia is necessary for pharyngeal arch artery development. Development. 2005;132(23):5307–15.
68. Jackson A, Kasah S, Mansour SL, Morrow B, Basson MA. Endoderm-specific deletion of Tbx1 reveals an FGF-independent role for Tbx1 in pharyngeal apparatus morphogenesis. Dev Dyn. 2014;243(9):1143–51.
69. Wei L, Wang W, Yang J, Huang X, Baldini A, Zhang Z. Pharyngeal epithelial deletion of Tbx1 causes caudal pharyngeal arch defect but not cardiac conotruncal anomaly. Biochem Biophys Res Commun. 2020;533(4):1315–22.
70. Piotrowski T, Ahn DG, Schilling TF, Nair S, Ruvinsky I, Geisler R, et al. The zebrafish van gogh mutation disrupts tbx1, which is involved in the DiGeorge deletion syndrome in humans. Development. 2003;130(20):5043–52.
71. Piotrowski T, Nusslein-Volhard C. The endoderm plays an important role in patterning the segmented pharyngeal region in zebrafish (Danio rerio). Dev Biol. 2000;225(2):339–56.
72. Isogai S, Horiguchi M, Weinstein BM. The vascular anatomy of the developing zebrafish: an atlas of embryonic and early larval development. Dev Biol. 2001;230(2):278–301.
73. Merscher S, Funke B, Epstein JA, Heyer J, Puech A, Lu MM, et al. TBX1 is responsible for cardiovascular defects in velo-cardio-facial/DiGeorge syndrome. Cell. 2001;104(4):619–29.
74. Ivins S, Lammerts van Beuren K, Roberts C, James C, Lindsay E, Baldini A, et al. Microarray analysis detects differentially expressed genes in the pharyngeal region of mice lacking Tbx1. Dev Biol. 2005;285(2):554–69.
75. Liao J, Aggarwal VS, Nowotschin S, Bondarev A, Lipner S, Morrow BE. Identification of downstream genetic pathways of Tbx1 in the second heart field. Dev Biol. 2008;316(2): 524–37.
76. Fulcoli FG, Huynh T, Scambler PJ, Baldini A. Tbx1 regulates the BMP-Smad1 pathway in a transcription independent manner. PLoS One. 2009;4(6):e6049.
77. van Bueren KL, Papangeli I, Rochais F, Pearce K, Roberts C, Calmont A, et al. Hes1 expression is reduced in Tbx1 null cells and is required for the development of structures affected in 22q11 deletion syndrome. Dev Biol. 2010;340(2):369–80.
78. Nowotschin S, Liao J, Gage PJ, Epstein JA, Campione M, Morrow BE. Tbx1 affects asymmetric cardiac morphogenesis by regulating Pitx2 in the secondary heart field. Development. 2006;133(8):1565–73.
79. Vincent SD, Mayeuf-Louchart A, Watanabe Y, Brzezinski JAT, Miyagawa-Tomita S, Kelly RG, et al. Prdm1 functions in the mesoderm of the second heart field, where it interacts genetically with Tbx1, during outflow tract morphogenesis in the mouse embryo. Hum Mol Genet. 2014;23(19):5087–101.

80. Chen L, Fulcoli FG, Ferrentino R, Martucciello S, Illingworth EA, Baldini A. Transcriptional control in cardiac progenitors: Tbx1 interacts with the BAF chromatin remodeling complex and regulates Wnt5a. PLoS Genet. 2012;8(3):e1002571.
81. Meyers EN, Lewandoski M, Martin GR. An Fgf8 mutant allelic series generated by Cre- and Flp-mediated recombination. Nat Genet. 1998;18(2):136–41.
82. Abu-Issa R, Smyth G, Smoak I, Yamamura K, Meyers EN. Fgf8 is required for pharyngeal arch and cardiovascular development in the mouse. Development. 2002;129(19):4613–25.
83. Frank DU, Fotheringham LK, Brewer JA, Muglia LJ, Tristani-Firouzi M, Capecchi MR, et al. An Fgf8 mouse mutant phenocopies human 22q11 deletion syndrome. Development. 2002;129(19):4591–603.
84. Stothard CA, Mazzotta S, Vyas A, Schneider JE, Mohun TJ, Henderson DJ, et al. Pax9 and Gbx2 interact in the pharyngeal endoderm to control cardiovascular development. J Cardiovasc Dev Dis. 2020;7(2):20.
85. Fernandez B, Duran AC, Fernandez-Gallego T, Fernandez MC, Such M, Arque JM, et al. Bicuspid aortic valves with different spatial orientations of the leaflets are distinct etiological entities. J Am Coll Cardiol. 2009;54(24):2312–8.
86. Greulich F, Rudat C, Kispert A. Mechanisms of T-box gene function in the developing heart. Cardiovasc Res. 2011;91(2):212–22.
87. Molin DG, DeRuiter MC, Wisse LJ, Azhar M, Doetschman T, Poelmann RE, et al. Altered apoptosis pattern during pharyngeal arch artery remodelling is associated with aortic arch malformations in Tgfbeta2 knock-out mice. Cardiovasc Res. 2002;56(2):312–22.
88. Molin DG, Poelmann RE, DeRuiter MC, Azhar M, Doetschman T, Gittenberger-de Groot AC. Transforming growth factor beta-SMAD2 signaling regulates aortic arch innervation and development. Circ Res. 2004;95(11):1109–17.
89. Larsson J, Goumans MJ, Sjostrand LJ, van Rooijen MA, Ward D, Leveen P, et al. Abnormal angiogenesis but intact hematopoietic potential in TGF-beta type I receptor-deficient mice. EMBO J. 2001;20(7):1663–73.
90. Oshima M, Oshima H, Taketo MM. TGF-beta receptor type II deficiency results in defects of yolk sac hematopoiesis and vasculogenesis. Dev Biol. 1996;179(1):297–302.
91. Derrick CJ, Noël ES. The ECM as a driver of heart development and repair. Development. 2021;148(5):dev191320.
92. Warkala M, Chen D, Ramirez A, Jubran A, Schonning M, Wang X, et al. Cell-extracellular matrix interactions play multiple essential roles in aortic arch development. Circ Res. 2021;128(3):e27–44.
93. Wang X, Astrof S. Neural crest cell-autonomous roles of fibronectin in cardiovascular development. Development. 2016;143(1):88–100.
94. Cooley MA, Kern CB, Fresco VM, Wessels A, Thompson RP, McQuinn TC, et al. Fibulin-1 is required for morphogenesis of neural crest-derived structures. Dev Biol. 2008;319(2):336–45.
95. Garg V, Yamagishi C, Hu T, Kathiriya IS, Yamagishi H, Srivastava D. Tbx1, a DiGeorge syndrome candidate gene, is regulated by sonic hedgehog during pharyngeal arch development. Dev Biol. 2001;235(1):62–73.
96. Hu T, Yamagishi H, Maeda J, McAnally J, Yamagishi C, Srivastava D. Tbx1 regulates fibroblast growth factors in the anterior heart field through a reinforcing autoregulatory loop involving forkhead transcription factors. Development. 2004;131(21):5491–502.
97. Yamagishi H, Maeda J, Hu T, McAnally J, Conway SJ, Kume T, et al. Tbx1 is regulated by tissue-specific forkhead proteins through a common sonic hedgehog-responsive enhancer. Genes Dev. 2003;17(2):269–81.
98. Zhang Z, Baldini A. Manipulation of endogenous regulatory elements and transgenic analyses of the Tbx1 gene. Mamm Genome. 2010;21(11–12):556–64.
99. Iida K, Koseki H, Kakinuma H, Kato N, Mizutani-Koseki Y, Ohuchi H, et al. Essential roles of the winged helix transcription factor MFH-1 in aortic arch patterning and skeletogenesis. Development. 1997;124(22):4627–38.

100. Niaz T, Poterucha JT, Olson TM, Johnson JN, Craviari C, Nienaber T, et al. Characteristic morphologies of the bicuspid aortic valve in patients with genetic syndromes. J Am Soc Echocardiogr. 2018;31(2):194–200.
101. Bondy C, Bakalov VK, Cheng C, Olivieri L, Rosing DR, Arai AE. Bicuspid aortic valve and aortic coarctation are linked to deletion of the X chromosome short arm in turner syndrome. J Med Genet. 2013;50(10):662–5.
102. Thomas PS, Sridurongrit S, Ruiz-Lozano P, Kaartinen V. Deficient signaling via Alk2 (Acvr1) leads to bicuspid aortic valve development. PLoS One. 2012;7(4):e35539.
103. Dupuis LE, McCulloch DR, McGarity JD, Bahan A, Wessels A, Weber D, et al. Altered versican cleavage in ADAMTS5 deficient mice; a novel etiology of myxomatous valve disease. Dev Biol. 2011;357(1):152–64.
104. Dupuis LE, Osinska H, Weinstein MB, Hinton RB, Kern CB. Insufficient versican cleavage and Smad2 phosphorylation results in bicuspid aortic and pulmonary valves. J Mol Cell Cardiol. 2013;60(0):50–9.
105. Stankunas K, Shang C, Twu KY, Kao SC, Jenkins NA, Copeland NG, et al. Pbx/Meis deficiencies demonstrate multigenetic origins of congenital heart disease. Circ Res. 2008;103(7):702–9.
106. Reiter JF, Alexander J, Rodaway A, Yelon D, Patient R, Holder N, et al. Gata5 is required for the development of the heart and endoderm in zebrafish. Genes Dev. 1999;13(22):2983–95.
107. Morrisey EE, Ip HS, Tang Z, Lu MM, Parmacek MS. GATA-5: a transcriptional activator expressed in a novel temporally and spatially-restricted pattern during embryonic development. Dev Biol. 1997;183(1):21–36.
108. Molkentin JD. The zinc finger-containing transcription factors GATA-4, −5, and −6. Ubiquitously expressed regulators of tissue-specific gene expression. J Biol Chem. 2000;275(50):38949–52.
109. Laforest B, Andelfinger G, Nemer M. Loss of Gata5 in mice leads to bicuspid aortic valve. J Clin Invest. 2011;121(7):2876–87.
110. Singh MK, Li Y, Li S, Cobb RM, Zhou D, Lu MM, et al. Gata4 and Gata5 cooperatively regulate cardiac myocyte proliferation in mice. J Biol Chem. 2010;285(3):1765–72.
111. Park EJ, Ogden LA, Talbot A, Evans S, Cai CL, Black BL, et al. Required, tissue-specific roles for Fgf8 in outflow tract formation and remodeling. Development. 2006;133(12):2419–33.
112. Lee TC, Zhao YD, Courtman DW, Stewart DJ. Abnormal aortic valve development in mice lacking endothelial nitric oxide synthase. Circulation. 2000;101(20):2345–8.
113. Odelin G, Faure E, Coulpier F, Di Bonito M, Bajolle F, Studer M, et al. Krox20 defines a subpopulation of cardiac neural crest cells contributing to arterial valves and bicuspid aortic valve. Development. 2018;145(1):dev151944.
114. Odelin G, Faure E, Maurel-Zaffran C, Zaffran S. Krox20 regulates endothelial nitric oxide signaling in aortic valve development and disease. J Cardiovasc Dev Dis. 2019;6(4):39.
115. Gould RA, Aziz H, Woods CE, Seman-Senderos MA, Sparks E, Preuss C, et al. ROBO4 variants predispose individuals to bicuspid aortic valve and thoracic aortic aneurysm. Nat Genet. 2019;51(1):42–50.
116. Mommersteeg MT, Yeh ML, Parnavelas JG, Andrews WD. Disrupted slit-Robo signalling results in membranous ventricular septum defects and bicuspid aortic valves. Cardiovasc Res. 2015;106(1):55–66.
117. MacGrogan D, D'Amato G, Travisano S, Martinez-Poveda B, Luxan G, Del Monte-Nieto G, et al. Sequential ligand-dependent notch signaling activation regulates valve primordium formation and morphogenesis. Circ Res. 2016;118(10):1480–97.
118. Phillips HM, Mahendran P, Singh E, Anderson RH, Chaudhry B, Henderson DJ. Neural crest cells are required for correct positioning of the developing outflow cushions and pattern the arterial valve leaflets. Cardiovasc Res. 2013;99(3):452–60.
119. Sans-Coma V, Arque JM, Duran AC, Cardo M, Fernandez B. Coronary artery anomalies and bicuspid aortic valves in the Syrian hamster. Basic Res Cardiol. 1991;86(2):148–53.

120. Fernandez B, Soto-Navarrete MT, Lopez-Garcia A, Lopez-Unzu MA, Duran AC, Fernandez MC. Bicuspid aortic valve in 2 model species and review of the literature. Vet Pathol. 2020;57 (2):321–31.
121. Sans-Coma V, Fernandez B, Duran AC, Thiene G, Arque JM, Munoz-Chapuli R, et al. Fusion of valve cushions as a key factor in the formation of congenital bicuspid aortic valves in Syrian hamsters. Anat Rec. 1996;244(4):490–8.
122. Donovan J, Kordylewska A, Jan YN, Utset MF. Tetralogy of fallot and other congenital heart defects in Hey2 mutant mice. Curr Biol. 2002;12(18):1605–10.
123. Chen YH, Ishii M, Sun J, Sucov HM, Maxson RE Jr. Msx1 and Msx2 regulate survival of secondary heart field precursors and post-migratory proliferation of cardiac neural crest in the outflow tract. Dev Biol. 2007;308(2):421–37.
124. Brewer S, Jiang X, Donaldson S, Williams T, Sucov HM. Requirement for AP-2alpha in cardiac outflow tract morphogenesis. Mech Dev. 2002;110(1–2):139–49.
125. Zhao Z. TGFbeta and Wnt in cardiac outflow tract defects in offspring of diabetic pregnancies. Birth Defects Res B Dev Reprod Toxicol. 2014;101(5):364–70.

Part XII

Coronary Artery Anomalies

Clinical Presentation and Therapy of Coronary Artery Anomalies

47

Nikolaus A. Haas, David J. Driscoll, and Silke Rickert-Sperling

47.1 Normal Coronary Artery Anatomy

There are two major coronary arteries that arise normally directly above the aortic valve in the sinus. The left main coronary artery (LCA or LMCA) arises from the left coronary sinus and divides shortly after its origin into the left anterior descending and the circumflex coronary arteries (LCX). Branches of the left anterior descending (LAD) coronary artery include the left conus, septal, and diagonal arteries. Branches of the circumflex coronary artery may include the sinus node artery, Kugel's artery, marginal arteries, and the left atrial circumflex artery (Fig. 47.1). The LAD follows the interventricular septum to the apex, the LCX turns posterior, follows the atrioventricular groove between the left atrium and ventricle to the coronary sinus. Branches of the right coronary artery (RCX) include the conal branch, the sinus node artery, an atrial branch, the right ventricular muscle branches (including the acute marginal branch), the posterior descending coronary artery, the atrioventricular node artery, and septal branches (Fig. 47.2). The RCX follows the atrioventricular groove between the right atrium and ventricle. The "dominant coronary artery" is the

N. A. Haas (✉)
Department of Pediatric Cardiology and Intensive Care, Ludwig Maximilians University, Munich, Germany
e-mail: Nikolaus.haas@med.uni-muenchen.de

D. J. Driscoll
Division of Pediatric Cardiology, Department of Pediatrics, Mayo Clinic College of Medicine, Rochester, MN, USA
e-mail: driscoll.david@mayo.edu

S. Rickert-Sperling
Cardiovascular Genetics, Charité – Universitätsmedizin Berlin, Berlin, Germany
e-mail: silke.sperling@charite.de

© The Author(s), under exclusive license to Springer Nature Switzerland AG 2024

S. Rickert-Sperling et al. (eds.), *Congenital Heart Diseases: The Broken Heart*,
Advances in Experimental Medicine and Biology 1441,
https://doi.org/10.1007/978-3-031-44087-8_47

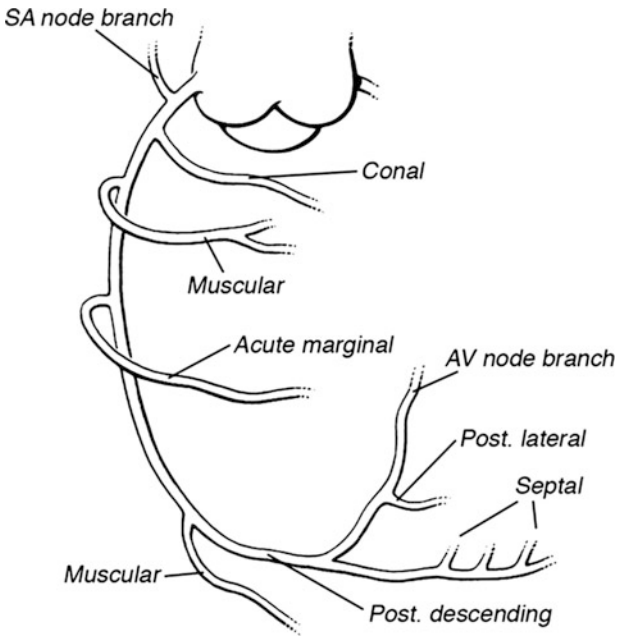

Fig. 47.1 Normal left coronary artery system

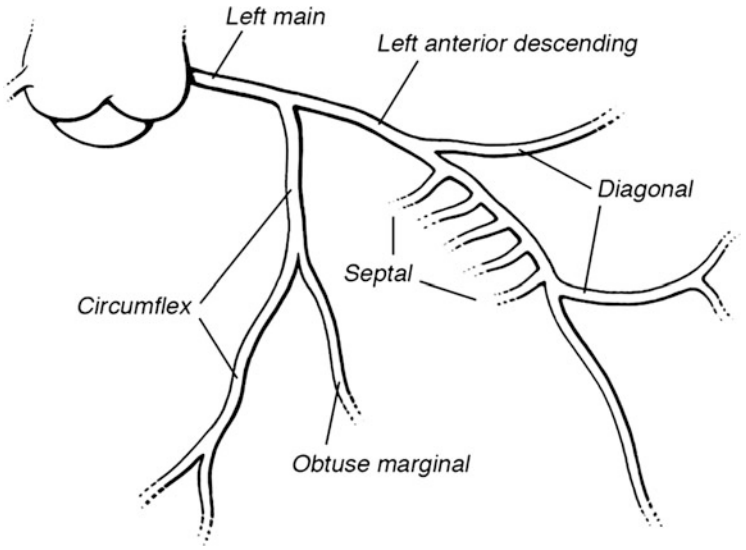

Fig. 47.2 Normal right coronary artery system

one giving rise to the posterior descending coronary artery. It originates from the right coronary artery in 80% of people.

Kugel's artery is a relatively rare variant of the coronary arteries, characterized by a preformed anastomotic connection between the branches of the proximal left circumflex artery (LCX) and the distal right coronary artery (RCX). This arterial connection traverses the atrial septum, linking the anterior coronary septum to the posterior ventricular coronary tree. The incidence of Kugel's artery is reported to be up to 6% in the population. It is important to note that none of the coronary artery variants, including Kugel's artery, can be detected through prenatal examinations.

47.2 Anomalous Origin of the Left Coronary Artery from the Pulmonary Artery

Anomalous origin of the Left Coronary Artery from the Pulmonary Artery (ALCAPA), also known as Bland–White–Garland syndrome, is a rare coronary abnormality that occurs in less than 1% of all congenital heart defects. It has an incidence of approximately 1 in 20,000 to 30,000 live births. There is also a variant called Anomalous origin of the Right Coronary Artery from the Pulmonary Artery (ARCAPA).

47.2.1 Pathophysiology

In the fetal and immediate postnatal period, individuals with ALCAPA are typically asymptomatic. However, as pulmonary vascular resistance decreases over the following months, a low-resistance pulmonary vascular bed develops where blood from the coronary circulation can drain. Collaterals form, redirecting blood flow from the right coronary artery to supply the myocardium of the left coronary artery territory. This leads to a significant "steal phenomenon" and ischemia, primarily affecting the posterior wall of the left ventricle and the papillary muscles. The cause of ischemia is not deoxygenated blood from the pulmonary artery, but rather the coronary steal effect.

47.2.2 Presentation

Infants with ALCAPA typically present with signs and symptoms of myocardial infarction and congestive heart failure at around 4–6 months of age. However, in rare cases, when there is a stenosis at the ostium into the pulmonary artery, the condition may remain asymptomatic or be incidentally detected in adulthood or at autopsy.

47.2.3 Management

The ideal treatment for ALCAPA is early detection of the anomaly before significant myocardial ischemia or infarction occurs, and establishing a coronary system that prevents myocardial infarction. However, most cases are diagnosed after myocardial ischemia and infarction have already occurred. These infants often have severe heart failure and frequently present with severe mitral regurgitation, requiring intensive care management.

Diagnosis of ALCAPA is typically made using echocardiography, which can reveal poor left ventricular function, a white (ischemic) papillary muscle, and a large right coronary ostium. The left ostium may not be visualized, and occasionally, a jet into the main pulmonary artery can be observed. In cases where the diagnosis is unclear, selective right coronary angiography can provide further clarification of the anatomy. Surgical intervention aims to establish a two-coronary-artery system and involves direct reimplantation of the left coronary ostium into the aorta.

47.2.4 Outcome

The recovery of myocardium following surgical correction of ALCAPA may take several months. In cases of severe myocardial failure, left ventricular assist device support or cardiac transplantation may be necessary. Patients detected later in life typically have better myocardial performance, less ischemia, and a more favorable prognosis compared to those diagnosed in infancy.

47.3 Anomalous Origin of the Left Coronary Artery from the Right Sinus of Valsalva

Anomalous origin of the left coronary artery from the right sinus of Valsalva, also known as anomalous coronary artery from the opposite sinus (ACAOS), is a rare but significant malformation. In this condition, the left coronary artery (LCA) takes a course between the aorta and the pulmonary artery, and its ostium may have an elliptical, oblique, or slit-like shape.

47.3.1 Pathophysiology

During infancy, at rest and under normal conditions, ACAOS does not typically play a significant role. However, as the aorta and pulmonary artery grow in size over time, and the pressure in the aorta increases, exercise or exertion can lead to increased pressure on the LCA. This compromised flow in a situation where additional flow is required can result in myocardial ischemia. The risk of sudden death is significant due to compression of the left coronary artery between the aorta and the pulmonary artery, the noncircular shape of the LCA ostium, and acute angulation near its origin.

47.3.2 Presentation

Some children with ACAOS may report chest pain during or after exercise and exhibit symptoms of angina or coronary insufficiency. Standardized exercise testing can reveal signs of ischemia. Symptoms may also include exercise-associated syncope or light-headedness. However, most patients with ACAOS are usually asymptomatic until sudden death occurs. Diagnosis is typically made through coronary angiography or CT scans. Angiography can be performed under pharmacological stress in cases where exercise simulation is needed. High-resolution CT scans allow for 3D reconstruction and visualization of the slit-like ostium.

47.3.3 Management

When ACAOS is detected and clinical hints suggest a problem, surgical intervention is indicated. The surgical options include augmentation of the coronary ostium (unroofing) with or without coronary transfer. Surgery involves direct implantation of the anomalous artery, unroofing the intramural segment of the vessel within the aortic wall to create a new ostium, osteoplasty, reimplantation of the right coronary artery (RCA) to the aorta, and, in older patients, bypass graft to the distal RCA with proximal ligation.

47.3.4 Outcome

When ACAOS is detected early, surgical outcomes are excellent, with favorable prognosis and resolution of symptoms. Early intervention is crucial to prevent the risk of sudden death associated with this condition.

47.4 Anomalous Origin of the Right Coronary Artery from the Left Sinus of Valsalva

Anomalous origin of the right coronary artery from the left sinus of Valsalva, coursing between the aorta and pulmonary artery, is a rare congenital abnormality, accounting for less than 3% of congenital coronary anomalies. It is also known as anomalous coronary artery from the opposite sinus (ACAOS). In this condition, the right coronary artery (RCA) originates from the left sinus of Valsalva and takes a course between the two large vessels, and the ostium may have a slit-like shape (Fig. 47.3).

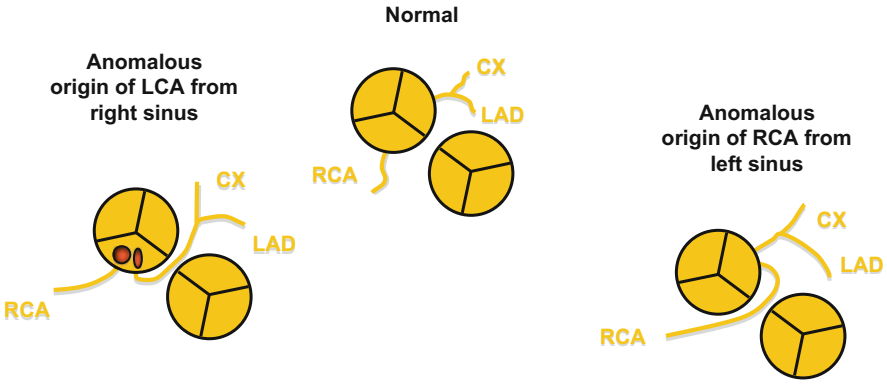

Fig. 47.3 Origin of left coronary artery from the right aortic sinus of Valsalva (*left panel*). Origin of the right coronary artery from the left sinus of Valsalva (*right panel*). Normal coronary origin (*center panel*). Abbreviations: *CX* circumflex coronary artery, *LAD* left anterior descending coronary artery, *RCA* right coronary artery (Reproduced or adapted from Driscoll, David, *Fundamentals of Pediatric Cardiology*, Lippincott Williams & Wilkins, 2006, with permission of the author and publisher)

47.4.1 Pathophysiology

It remains unclear whether anomalous origin of the right coronary artery from the left sinus of Valsalva is associated with sudden death in infancy. The lower pressure in the right ventricle during exercise may reduce the likelihood of significant ischemia, which could explain the lower risk compared to other coronary anomalies.

47.4.2 Presentation

Most patients with this anomaly are asymptomatic during childhood. However, some adult patients may present with myocardial ischemia, arrhythmias, or sudden cardiac death. It is important to suspect this diagnosis in young patients without risk factors for coronary artery disease.

47.4.3 Management

The indications for operative repair of this anomaly are less clear compared to cases where the left coronary artery arises anomalously from the right sinus of Valsalva. Diagnosis can be easily confirmed using 64-slice MDCT angiography, which visualizes the slit-like origin of the coronary artery. Most clinicians recommend surgery for symptomatic patients, while conservative management is often considered for asymptomatic patients.

Surgery involves surgical augmentation of the coronary ostium (unroofing) with or without coronary transfer, similar to the management of other anomalous coronary artery anomalies.

47.4.4 Outcome

When detected early, surgical results are generally excellent. Early detection and intervention are crucial in preventing complications and ensuring favorable outcomes for patients with anomalous origin of the right coronary artery from the left sinus of Valsalva.

47.5 Single Coronary Artery

Single coronary artery (SCA) is a rare anomaly in which the entire myocardium is supplied by a single coronary artery. Its incidence is reported to be between 0.024% and 0.27%, and it is often associated with other cardiac congenital abnormalities. SCA occurs in approximately two out of every 1000 patients and is commonly found in conjunction with conditions such as transposition of the great arteries, coronary artery fistula, and bicuspid aortic valve.

The presentation of SCA can vary, with some individuals experiencing mild nonspecific symptoms, while others may be asymptomatic. In children, SCA typically does not have significant consequences. However, in cases where the coronary artery takes an interarterial course, SCA may be associated with a higher risk of sudden cardiac death. Unfortunately, the exact quantification of this risk is challenging due to limited specific studies on the topic.

It is important to note that further evaluation and assessment are required to determine the specific implications and management strategies for individuals diagnosed with SCA. The presence of SCA should prompt a thorough evaluation for associated cardiac abnormalities and consideration of potential risks, particularly when the coronary artery takes an interarterial course.

47.6 Coronary Artery Fistula

Coronary artery fistulas are abnormal connections between the high-pressure coronary system and, in approximately 90% of cases, the low-pressure system of the right side of the heart. They account for about 0.2% to 0.4% of congenital cardiac defects and are typically formed during abnormal embryological development. Acquired coronary artery fistulas, on the other hand, are most commonly caused by traumatic events such as gunshot wounds or stab injuries. Iatrogenic causes include interventional cardiac procedures like biopsies, cardiac angiography, coronary artery bypass grafting, valve replacements, or device implantations.

Coronary artery fistulas can originate equally from the right and left coronary arteries, with the fistula typically connecting to the right ventricular cavity. The right atrium is the second most common termination point, and around two-thirds of fistulas draining into the right atrium originate from the right coronary artery. Other potential termination points include the pulmonary artery, left atrium, left ventricle, superior vena cava, coronary sinus, or a persistent left superior vena cava. The involved coronary artery often shows dilation, and the chamber into which the fistula drains may also be enlarged.

Small fistulas are typically asymptomatic and may cause a murmur. They usually result in a left-to-right shunt. In contrast, large fistulas can cause symptoms such as a systolic-diastolic murmur, coronary steal phenomenon, significant shunting, and heart failure. Echocardiography can detect a large ostium of the affected coronary artery and the drainage of the shunt, although it may not provide detailed information about the course of the fistula. In such cases, cardiac catheterization, MRI, or multislice CT imaging can be helpful for anatomical classification, quantification of the shunt, and treatment planning.

Large or clinically significant fistulas with a significant shunt should be closed either through interventional procedures or surgery as soon as possible after the diagnosis is made. Following closure, life expectancy is usually normal.

47.7 Coronary Artery Patterns Associated with Congenital Heart Defects

Coronary artery variations and abnormalities are frequently observed in congenital heart defects, particularly in cases involving imbalanced ventricles, single ventricles (DILV), or ventricular inversion. These abnormalities play a significant clinical role in conditions such as tetralogy of Fallot, double outlet right ventricle (DORV), truncus arteriosus, and transposition of the great arteries, as they can pose challenges during surgical repair or catheter interventions.

Variations in coronary anatomy are common and can be related to the position of the coronary ostium relative to the aortic sinus, the angle at which the coronary arteries arise, or the course of the coronary arterial branches. Several classification systems have been proposed to categorize these anatomical patterns, but they often lack a simple rationale that can be universally applied, regardless of the relative position of the great arteries or the presence of a bicuspid aortic valve.

One modification of a relatively simple system introduced in the early 1980s is known as the “Leiden Convention.” The Leiden Convention coronary coding system (Fig. 47.4.) provides a structured approach to categorize the wide range of coronary anatomical patterns. It can be used in cases with normally related great arteries, cases with single sinus coronary arteries, and cases with bicuspid aortic valves. The Leiden Convention is a straightforward and broadly applicable coronary coding system that helps standardize the classification of coronary variations and abnormalities.

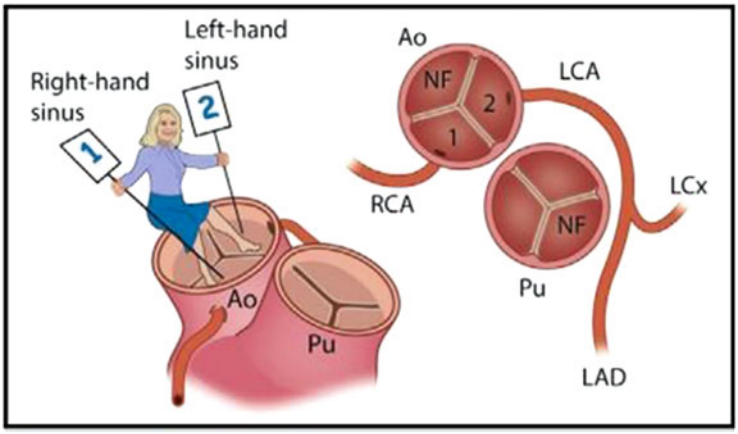

Fig. 47.4 The Leiden Convention coronary coding system is a classification system used to describe the anatomical patterns of coronary arteries. R—right, L—left, NF—nonfacing, Cx—circumflex

47.7.1 Tetralogy of Fallot

In patients with tetralogy of Fallot, only 5–10% of cases are associated with coronary artery anomalies. However, it is crucial to identify these abnormalities to prevent damage to essential coronary arteries during surgical repair. Among the various variations observed, those involving large vessels crossing the right ventricular outflow tract are particularly clinically significant, as modifications to this structure are often necessary during surgical procedures such as patch augmentation or the insertion of a valved conduit.

Approximately 75% of patients with an anomalous coronary artery have the anomalous vessel crossing the right ventricular outflow tract. The combined risk of encountering either an anomalous coronary artery or a large conus artery crossing the right ventricular outflow tract is around 10%.

In some cases, a large conus branch may be observed and occasionally labeled as a second left anterior descending coronary artery (LAD). Additionally, about 4% of patients with tetralogy of Fallot may have the left anterior descending coronary artery originating from the right coronary artery. The second most common coronary anomaly associated with tetralogy of Fallot is a single coronary artery.

Before surgery, it is important to define the coronary anatomy and adapt the surgical approach accordingly. This ensures that any potential anomalies or variations are taken into account during the procedure, minimizing the risk of complications and optimizing patient outcomes.

47.7.2 d-Transposition of the Great Arteries

In transposition of the great arteries, the variation of the coronary arteries is of clinical importance due to the necessity of coronary transfer during the arterial switch operation, which is the standard surgical procedure for treating this condition. Normally, the coronary arteries arise from the sinuses opposite to the pulmonary artery, which will become the aorta after the switch. These sinuses are referred to as the facing sinuses.

There is a wide variation in coronary anatomy, and different surgical classifications exist to categorize these variations. In rare cases, certain anatomical variations may make an arterial switch operation impossible, and an atrial switch procedure may need to be performed instead.

In the usual anatomy, the right coronary artery arises from the posterior aortic sinus, and the left coronary artery arises from the left coronary sinus, dividing into a circumflex coronary artery and an anterior descending coronary artery. The right aortic sinus of Valsalva serves as the noncoronary cusp.

Alternatively, in some cases, the right coronary artery may arise from the posterior aortic sinus and give rise to the circumflex coronary artery, which passes posterior to the pulmonary artery. The anterior descending coronary artery may then arise from the left coronary sinus, and the right aortic sinus of Valsalva serves as the noncoronary sinus.

Understanding the specific coronary anatomy is crucial for planning and performing the arterial switch operation successfully. The surgical team will assess the individual patient's coronary variation and adapt the surgical approach accordingly to ensure optimal outcomes.

47.7.3 l-Transposition of the Great Arteries

In l-transposition of the great arteries (l-TGA), also known as congenitally corrected transposition of the great arteries (cc-TGA) or ventricular inversion, the aorta is positioned anteriorly and to the left of the pulmonary artery. In most cases of l-TGA, surgical intervention involving the coronaries is not required, and the coronary anatomy is primarily of scientific interest. However, with the introduction of double switch procedures for the treatment of cc-TGA, understanding the coronary artery anatomy has become important.

Previous studies have indicated a consistently inverted coronary arterial pattern in l-TGA. There are three aortic sinuses of Valsalva: one oriented anteriorly (anterior sinus of Valsalva), one posterior and rightward (right sinus of Valsalva), and one posterior and leftward (left sinus of Valsalva). The right coronary artery originates from the right aortic sinus of Valsalva and gives rise to an anterior descending branch that follows the course of the interventricular sulcus. The right coronary artery then continues its course in the right atrioventricular sulcus. The left coronary artery originates from the left aortic sinus of Valsalva and follows the course of the circumflex coronary artery in the left atrioventricular sulcus. The left (circumflex)

coronary artery gives off a marginal branch and further extends as the posterior descending coronary artery.

Although many patients with l-TGA exhibit the same coronary artery pattern as the usual pattern seen in transposition of the great arteries, variations can occur, such as single coronary arteries or the left anterior descending (LAD) artery arising from the right coronary artery (RCA), and the coronary artery and circumflex artery arising from the right-hand facing sinus. In most cases, an arterial switch operation is feasible if necessary. Understanding the coronary artery anatomy in l-TGA is important for surgical planning, especially in cases where double switch procedures are performed.

The Genetics of Human Congenital Coronary Vascular Anomalies

48

Almudena Ortiz Garrido, Beatriz Picazo, Juan Antonio Guadix, Adrián Ruiz-Villalba, and José M. Pérez-Pomares

Abstract

The genetics of human congenital coronary vascular anomalies (hCCVA) remains largely underresearched. This is surprising, because although coronary vascular defects represent a relatively small proportion of human congenital heart disease (CHD), hCCVAs are clinically significant conditions. Indeed, hCCVA frequently associate to other congenital cardiac structural defects and may even result in sudden cardiac death in the adult. In this brief chapter, we will attempt to summarize our current knowledge on the topic, also proposing a rationale for the development of novel approaches to the genetics of hCCVA.

48.1 Congenital Coronary Vascular Defects: An Isolated Pathology?

Like the majority of CHDs, hCCVA do not seem to segregate in Mendelian ratios. However, some familial cases have been reported for this type of congenital malformations [1, 2]. This has been historically overlooked by the application of standard CHD diagnostic methods [3]. Regardless of our perception on the heritability of hCCVA, these should not be considered as isolated conditions only, as they strongly correlate with the malformation of other cardiac structures like heart valves

A. O. Garrido · B. Picazo
Hospital Materno Infantil-Hospital Carlos de Haya, Málaga, Spain

J. A. Guadix · A. Ruiz-Villalba · J. M. Pérez-Pomares (✉)
Department of Animal Biology, Faculty of Sciences, University of Málaga, Málaga, Spain

Instituto de Biomedicina de Málaga (IBIMA)-Plataforma BIONAND, Málaga, Spain
e-mail: jmperezp@uma.es

© The Author(s), under exclusive license to Springer Nature Switzerland AG 2024

S. Rickert-Sperling et al. (eds.), *Congenital Heart Diseases: The Broken Heart*,
Advances in Experimental Medicine and Biology 1441,
https://doi.org/10.1007/978-3-031-44087-8_48

and chamber myocardial walls. Furthermore, hCCVA can form part of the phenotype of well-characterized and complex CHDs like transposition of the great arteries, tetralogy of Fallot, or double-outlet right ventricle [4], although in these cases, it is difficult to assess whether coronary vascular anomalies are a direct consequence of the genetic defect or secondary to the disrupted mechanics of embryonic development. The tight relationship existing between hCCVA and other pathological cardiac entities is nonetheless emphasized by the classification proposed by the International Pediatric and Congenital Cardiac Code (IPCCC, www.ipccc.net), that pools together in the same category developmentally related abnormalities such arteriovenous fistulae, defects in the patterning of coronary arteries, and anomalies of the arterial duct and the pericardium.

48.2 Congenital Coronary Anomalies in the Context of Adult Cardiac Disease

Congenital coronary vascular anomalies have been found in cases of ventricular fibrillation, cardiomyopathy, myocardial infarction, and sudden death, among other severe cardiac conditions [5]. The latter one can be regarded as a showcase for the clinical significance of hCCVA, since 11–19% of sudden deaths in American athletes were reported to involve coronary malformations [6]. Accordingly, attempts to classify forms of hCCVA have been frequently based on the severity of the clinical outcome of the malformation [7] rather than on comprehensive, anatomic, and/or developmental criteria [8]. This has resulted in a biased, incomplete understanding of hCCVA which first precluded the identification of the embryological origin of these defects, and then the establishment of a causal association between defined genes and morphogenetic mechanisms.

Congenital anomalies of the heart are important, but it is also true that most CHD patients survive to adulthood [9]. However, a negative counterpart of this positive clinical outcome is that the potential genetic substrates for congenital cardiac ailments are progressively increasing their chances to be transmitted to the next generation. This unambiguously points to the necessity of planning new diagnostic routines for hCCVA in the near future.

48.3 Candidate Genes for Human Coronary Blood Vessel Congenital Defects

Given the clinical relevance of hCCVA, it is surprising to discover that our knowledge on the genetics of these ailments is extremely poor. Association of multiple gene variants with coronary atherosclerosis (simply referred to as "coronary disease") is common in the literature [10], but the number of systematic studies on the genetics of hCCVA is very low. In humans, several genetic-wide association studies (GWAS) have identified specific regions (e.g., 12q24 locus) which are related to distinct CHD forms, namely tetralogy of Fallot, Noonan, and LEOPARD

syndromes; deletions at this locus have also been associated to atherosclerotic coronary disease, but no specific reference to hCCVAs were made in this study [11]. Other pieces of work have identified a role for gene copy-number variants (CNVs) in several forms of CHD, but not coronary artery congenital anomalies [12].

Considering these results at a glance might not seem encouraging to those interested in the genetics of hCCVA, but then we would like to suggest a strategy to re-evaluate data from previously existing genetic screenings. This strategy is based in the known association of hCCVA with increased risk of atherosclerosis, deficient myocardial perfusion and myocardial infarction [13], and tries to apply our knowledge on coronary blood vessel embryonic development to the identification of genetic variants in regions close to genes important for coronary vascular morphogenesis. We should therefore focus in studies aiming at the identification of genetic factors for coronary atherosclerotic disease (see [14]), and search for genes related to cellular and molecular mechanisms involved in blood vessel development. Following this rationale, two good candidates are to be found for variations at regions 11q22.3 [15] and 6q23.2 [16], close to PDGF and TCF21, respectively, which are key genes in epicardial and coronary blood vessel embryonic development [17, 18]. In particular, TCF21, (together with SMAD3, that is part of the TGF-β signaling pathway) often appears identified as a "coronary disease gene" in different studies [19–21]. Schunkert and colleagues [16] also identified variations at 13q34, close to the COL4A1 gene, reported to be required for vascular formation in the embryo [22]. Mutations in the ELN gene may result in coronary stenosis [23]. This same anomaly is also frequently found in recurrent 1q21.1 microdeletion. In this latter case, although the deleted chromosomal region is known to encode relevant genes such as PRKAB2, CHD1L, BCL9, GJA5, and GJA8, none of them could be directly linked to coronary pathogenesis [23, 24]. Even more interesting is the case of variations identified at 10q11, close to the CXCL12/SDF1 gene [25], since the chemokine it encodes is necessary for the proper septation of the cardiac outflow tract [26], whose anomalous development often leads to coronary vascular defects [27]. In accordance with our proposed strategy, it also seems logical to reconsider previously described single-nucleotide polymorphisms (SNPs) in the vascular endothelial growth factor (VEGF) promoter (C2578A, G1154A, C634G) [28, 29] as potential genetic substrates for hCCVA. This is supported by multiple studies highlighting the relevance of VEGF during blood vessel formation in general [30], and coronary vasculature morphogenesis in particular [31].

48.4 Does Coronary Blood Vessel Embryonic Morphogenesis Influence Adult Coronary Disease?

Besides the adult persistence of coronary blood vessel congenital anomalies, coronary disease is, in large part, regarded as a synonym for coronary blood vessel atherosclerotic disease (CAD). Generally considered as an "acquired" disease, CAD is a prevalent condition that could, at least in part, have a congenital substrate. This hypothesis is supported by the finding of early atherosclerotic traits like intimal

thickening and fatty streaks in fetuses and newborns [32], including coronary arteries [33]. It is not known whether factors related to the peculiarities of coronary artery embryonic development may impact the initiation of atherosclerotic disease in fetuses, newborns and children, and therefore the full progression of the disease in the adult. It is possible that sustained hyperlipidemia elicits an autonomous endothelial response to pathologic metabolic studies [32], but intrinsic differences in distinct populations of endothelial cells should also be considered. In this regard, it has been shown that arteries from different anatomical positions show a differential resistance to hypercholesterolemia-induced fatty streaks [34], and it is thus tempting to speculate with embryonic coronary vessel endothelial heterogeneity as a factor involved in the early susceptibility of these structures to atherosclerosis.

48.5 Conclusions

Systematic, continuous series of studies will be required to improve our knowledge on the genetics of coronary congenital anomalies. These studies should use criteria related to the embryonic development of coronary vasculature to filter data from homozygosity mapping, transcriptome, and array-comparative genomic hybridization (array-CGH) for linkage analyses, GWAS, and CNV approaches and identify potential candidates for hCCVA. This could be especially relevant if applied to samples from familial cases of hCCVA or selected cases of atherosclerotic coronary artery disease in which plaque formation relates to morphologically anomalous coronary blood vessels.

References

1. Laureti J, Singh K, Blankenship J. Anomalous coronary arteries : a familial clustering. Clin Cardiol. 2005;490:488–90.
2. Brothers JA, Stephens P, Gaynor JW, et al. Anomalous aortic origin of a coronary artery with an interarterial course: should family screening be routine? J Am Coll Cardiol. 2008;51:2062–4.
3. Cheitlin MD. Finding asymptomatic people with a coronary artery arising from the wrong sinus of valsalva: consequences arising from knowing the anomaly to be familial. J Am Coll Cardiol. 2008;51:2065–7.
4. Tomanek R. Coronary vasculature. Development, structure-function, and adaptations. New York: Springer Science; 2013.
5. Angelini P. Normal and anomalous coronary arteries in humans. In: Angelini P, editor. Coronary artery anomalies. Philadelphia: Lippincott, Williams and Wilkins; 1999. p. 27–150.
6. Maron B, Doerer J, Haas T, Tierney DM, Mueller F. Sudden deaths in young competitive athletes: analysis of 1866 deaths in the United States, 1980-2006. Circulation. 2009;119:1085–92.
7. Rigatelli G, Docali G, Rossi P, et al. Validation of a clinical-significance-based classification of coronary artery anomalies. Angiology. 2005;56:25–34.
8. Angelini P. Coronary artery anomalies: an entity in search of an identity. Circulation. 2007;115:1296–305.
9. Moodie D. Adult congenital heart disease. Curr Opin Cardiol. 1994;9:137–42.

10. Weber C, Noels H. Atherosclerosis: current pathogenesis and therapeutic options. Nat Med. 2011;17:1410–22.
11. Cordell HJ, Bentham J, Topf A, et al. Genome-wide association study of multiple congenital heart disease phenotypes identifies a susceptibility locus for atrial septal defect at chromosome 4p16. Nat Genet. 2013;45:822–4.
12. Tomita-Mitchell A, Mahnke DK, Struble CA, et al. Human gene copy number spectra analysis in congenital heart malformations. Physiol Genomics. 2012;44:518–41.
13. Hauser M. Congenital anomalies of the coronary arteries. Heart. 2005;91:1240–5.
14. Roberts R. Genetics of coronary artery disease: an update. Methodist Debakey Cardiovasc J. 2014;10:7–12.
15. Kathiresan S, Voight BF, Purcell S, et al. Genome-wide association of early-onset myocardial infarction with single nucleotide polymorphisms and copy number variants. Nat Genet. 2009;41:334–41.
16. Schunkert H, König IR, Kathiresan S, et al. Large-scale association analysis identifies 13 new susceptibility loci for coronary artery disease. Nat Genet. 2011;43:333–8.
17. Smith CL, Baek ST, Sung CY, Tallquist MD. Epicardial-derived cell epithelial-to-mesenchymal transition and fate specification require PDGF receptor signaling. Circ Res. 2011;108:e15–26.
18. Acharya A, Baek ST, Huang G, et al. The bHLH transcription factor Tcf21 is required for lineage-specific EMT of cardiac fibroblast progenitors. Development. 2012;139:2139–49.
19. Iyer D, Zhao Q, Wirka R, et al. Coronary artery disease genes SMAD3 and TCF21 promote opposing interactive genetic programs that regulate smooth muscle cell differentiation and disease risk. PLoS Genet. 2018;14:e1007681.
20. Wirka RC, Wagh D, Paik DT, et al. Atheroprotective roles of smooth muscle cell phenotypic modulation and the TCF21 disease gene as revealed by single-cell analysis. Nat Med. 2019;25:1280–9.
21. Nagao M, Lyu Q, Zhao Q, et al. Coronary disease-associated gene TCF21 inhibits smooth muscle cell differentiation by blocking the myocardin-serum response factor pathway. Circ Res. 2020;126:517–29.
22. Gould DB, Phalan FC, Breedveld GJ, et al. Mutations in Col4a1 cause perinatal cerebral hemorrhage and porencephaly. Science. 2005;308:1167–71.
23. Pierpont ME, Brueckner M, Chung WK, et al. Genetic basis for congenital heart disease: revisited: a scientific statement from the American Heart Association. Circulation. 2018;138:e653–711.
24. Busè M, Cuttaia HC, Palazzo D, et al. Expanding the phenotype of reciprocal 1q21.1 deletions and duplications: a case series. Ital. J Pediatr. 2017;43:61.
25. Samani N, Erdmann J, Hall A, et al. Genome wide association analysis of coronary artery disease. N Engl J Med. 2007;357:443–53.
26. Escot S, Blavet C, Härtle S, et al. Misregulation of SDF1-CXCR4 signaling impairs early cardiac neural crest cell migration leading to conotruncal defects. Circ Res. 2013;113:505–16.
27. Théveniau-Ruissy M, Dandonneau M, Mesbah K, et al. The del22q11.2 candidate gene Tbx1 controls regional outflow tract identity and coronary artery patterning. Circ Res. 2008;103:142–8.
28. Lambrechts D, Storkebaum E, Morimoto M, et al. VEGF is a modifier of amyotrophic lateral sclerosis in mice and humans and protects motoneurons against ischemic death. Nat Genet. 2003;34:383–94.
29. Stalmans I, Lambrechts D, De Smet F, et al. VEGF: a modifier of the del22q11 (DiGeorge) syndrome? Nat Med. 2003;9:173–82.
30. Risau W, Flamme I. Vasculogenesis. Annu Rev Cell Biol Dev Biol. 1995;11:73–91.
31. Wu B, Zhang Z, Lui W, et al. Endocardial cells form the coronary arteries by angiogenesis through myocardial-endocardial VEGF signaling. Cell. 2012;151:1083–96.
32. Napoli C, Armiento FPD, Mancini FP, et al. Fatty streak formation occurs in human fetal aortas and is greatly enhanced by maternal hypercholesterolemia. J Clin Invest. 1997;100:2680–90.

33. Velican C, Velican D. Coronary arteries in children up to the age of ten years II. Intimal thickening and its role in atherosclerotic involvement. Med Interne. 1976;14:17–24.
34. Napoli C, Witztum J, de Nigris F, et al. Intracraneal arteries of human fetuses are more resistant to hypercholesterolemia-induced fatty streak formation than extracranial arteries. Circulation. 1999;99:2003–10.

49 Congenital Coronary Blood Vessel Anomalies: Animal Models and the Integration of Developmental Mechanisms

Juan Antonio Guadix, Adrián Ruiz-Villalba, and José M. Pérez-Pomares

Abstract

Coronary blood vessels are in charge of sustaining cardiac homeostasis. It is thus logical that coronary congenital anomalies (CCA) directly or indirectly associate with multiple cardiac conditions, including sudden death. The coronary vascular system is a sophisticated, highly patterned anatomical entity, and therefore a wide range of congenital malformations of the coronary vasculature have been described. Despite the clinical interest of CCA, very few attempts have been made to relate specific embryonic developmental mechanisms to the congenital anomalies of these blood vessels. This is so because developmental data on the morphogenesis of the coronary vascular system derive from complex studies carried out in animals (mostly transgenic mice), and are not often accessible to the clinician, who, in turn, possesses essential information on the significance of CCA. During the last decade, advances in our understanding of normal embryonic development of coronary blood vessels have provided insight into the cellular and molecular mechanisms underlying coronary arteries anomalies. These findings are the base for our attempt to offer plausible embryological explanations to a variety of CCA as based on the analysis of multiple animal models for the study of cardiac embryogenesis, and present them in an organized manner, offering to the reader developmental mechanistic explanations for the pathogenesis of these anomalies.

J. A. Guadix · A. Ruiz-Villalba · J. M. Pérez-Pomares (✉)
Department of Animal Biology, Faculty of Sciences, University of Málaga, Málaga, Spain

Instituto de Biomedicina de Málaga (IBIMA)—Plataforma BIONAND, Málaga, Spain
e-mail: jmperezp@uma.es

© The Author(s), under exclusive license to Springer Nature Switzerland AG 2024

S. Rickert-Sperling et al. (eds.), *Congenital Heart Diseases: The Broken Heart*,
Advances in Experimental Medicine and Biology 1441,
https://doi.org/10.1007/978-3-031-44087-8_49

49.1 Embryogenesis of the Coronary Vasculature

49.1.1 The Basic Elements of the Coronary Vascular System

To properly understand the origin complexity and clinical impact of CCA [1], it is important to be aware of some critical developmental anatomical features of this vascular system. As evidenced by a simple phylogenetic analysis of the Vertebrate clade, the coronary vasculature forms by the coalescence of two anatomical domains or elements. The first, proximal one is represented by aortic arch efferent vessels in fishes or the aortic root in most tetrapods (including the coronary ostia). The second, distal element includes the characteristic inverted crown-shaped network of blood vessels lying over the cardiac atrioventricular and ventricular surfaces. The connection of these two domains guarantees the provision of oxygenated blood to the working myocardium from the closest possible source. This connection is, however, a late event in avian and mammalian coronary vascular development, and therefore any mechanistic analysis of CCA has to take into account that these two components of the adult coronary vascular system form separately [2].

49.1.2 Coronary Arteries and Veins

The embryonic formation of coronary arteries and veins (the two main blood vessel types of the coronary vascular system) deserves attention of its own. Multiple recent studies have reported the origin of the arterial and venous endothelium from a variety of sources, suggesting coronary endothelium is a developmental mosaic [2–6], see part I, Chap. 5). Since the endothelium is the tissue scaffolding and guiding blood vessel development in all vertebrates, it is obvious that the origin of embryonic coronary endothelium is key point to understand coronary blood vessel development. The findings quoted above explain why arteries and veins, as reported by several authors along three decades of research on coronary embryonic development [4, 7, 8], form as two separate vascular plexuses which merge shortly before birth. The early uncoupling of coronary arterial and venous vascular networks during coronary development adds an additional layer of complexity to the identification of the cellular and molecular mechanisms accounting for CCA.

49.2 A Brief Classification of CCA

It is not the aim of this chapter to provide a detailed account of the current classifications of CCA. A simple, summarized description of the nature of these congenital anomalies is nevertheless necessary for the understanding of the following sections.

CCA are often classified, in accordance to their clinical impact, into "major" and "minor" ones [9]. This classification may be practical to the clinician, but neither does throw light on the specific developmental and/or genetic origin of the known spectrum of CCA, nor allows for the establishment of potential correlations between different cardiac and coronary blood vessel anomalies. We thus favor a simple classification which groups CCA following an embryological rationale [2]. This classification has three main categories:

A. Anomalies of coronary artery connection to the great arteries (CCA Group 1), including: (1) the anomalous connection to the pulmonary root; (2) to the noncoronary (posterior/dorsal) Valsalva sinus; (3) absence of the right, left or both coronary arteries; (4) and alteration of the position, form, size (width) of coronary *ostia*.
B. Anomalies of coronary anatomy (CCA Group 2), including coronary aneurisms and abnormal ramification of coronary blood vessels.
C. Anomalies of myocardial-coronary interaction (CCA Group 3), including: (1) the intramural or subendocardial course of coronary arteries, and (2) fistulae (abnormal connection of coronary arteries to the ventricular or atrial cavities, the sinus venosus, superior vena cava, aorta or pulmonary artery).

In the following section we will present and discuss animal models for, at least, part of the CCA groups listed above (graphically summarized in Fig. 49.1); animal models will be introduced as related with developmental mechanisms whose disruption is more likely to originate every anomaly.

49.3 Developmental Substrates of Coronary Congenital Anomalies

In principle, any gene required for proper blood vessel development could be a genetic substrate for CAA. However, animal models for these genes (mostly transgenic/mutant mice) often die before coronary blood vessels form, as they often display deficient yolk sac vascularization [10]. Therefore, in this chapter we will focus in mice whose phenotype includes defects in coronary blood vessels similar to those observed in humans.

49.3.1 Defective Outflow Tract Septation and Rotation

The majority of the known forms of congenital heart disease affect the outflow tract (arterial pole of the heart), and some of them include coronary anomalies as part of their phenotype. Several cellular mechanisms are in charge of coordinating outflow

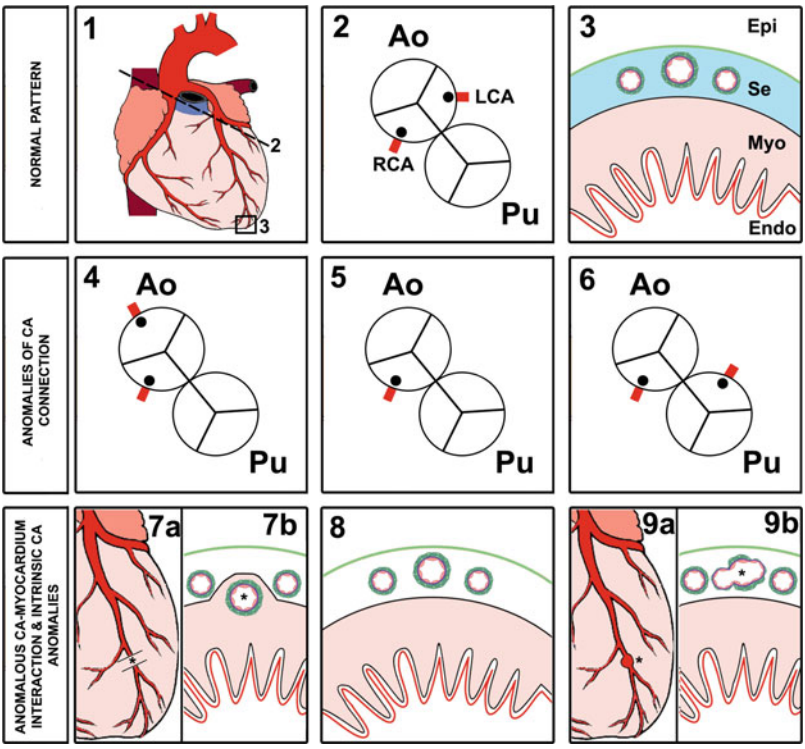

Fig. 49.1 Normal and abnormal coronary anatomy. Cartoons illustrate normal (1–3) coronary anatomy and relevant cases of coronary congenital anomalies (4–9)

tract transformation into mature aorta and pulmonary arteries and valves. The first one is the septation of the embryonic outflow tract of the heart (common truncus arteriosus), mostly driven by cardiac neural crest cells (NCC) [11, 12]. Persistent truncus arteriosus (PTA) is a severe congenital heart disease that results from restricted or absent outflow tract septation [13]; this anomaly also affects to the structure of arterial semilunar valves the relative position of the coronary *ostia*. PTA is characteristic of null mice for genes relevant to NCC development like *Pax3* [14] or *Pbx1* [15]. Abnormal NCC migration defects also relate to the Notch signaling pathway, which has been shown to be required for the proper development of outflow tract endocardial cushions, including arterial valve primordia [16]. This study emphasizes the importance of tissue interaction during outflow tract development, proving that NCC and secondary heart field progenitor interaction is necessary for endocardial-derived valvuloseptal mesenchyme formation via Notch signaling. Accordingly, mutant mice for the Notch target gene *Hes1* display outflow defects [17].

The best-known mouse model for outflow tract anomalies is that of the *Tbx1* knockout, a candidate gene for di George syndrome. *Tbx1* null mice display PTA with both right and left coronary ostia preferentially located at the right or ventral aortic Valsalva sinus, and present proximal coronary artery stems abnormally coursing ventrally and not laterally [18]. These authors suggest it is the loss of the subpulmonary myocardium, hypothesized to be refractory to blood vessels, the factor accounting for this coronary defect.

Proper rotation of the outflow tract is as important as correct outflow tract septation, and both phenomena are developmentally linked by the neural crest, and the genetic specification of outflow tract myocardial subpopulations [19, 20]. For example, the loss of the extracellular matrix component perlecan (*Hspg2*) first affects NCC migration and then outflow tract rotation, resulting in transposition of the great arteries [21], and in multiple defects in left and right coronary stem course [22]. These latter anomalies suggest that it is the location of the aortic root what determines the path followed by coronary blood vessels at the base of the heart, which can be quite variable [1, 23]. As a result of outflow tract malrotation coronary ostia frequently appear at wrong anatomical positions [24]. In summary, we suggest that the disruption of outflow tract septation and rotation, especially when combined with mispatterning of the unique antivascular properties of the subpulmonary myocardium [18] and the pro-vascular ones of the aortic myocardium (via Vegf-C, [25]), are enough to explain an important part of group 1 CAA.

49.3.2 Anomalous Epicardial Development

It has been proposed that the epicardium and embryonic coronary blood vessels are a developmental continuum [26]. The intricate relationship existing between these two structures can explain some CAA (groups 1–3) through the alteration of four basic developmental epicardial mechanisms:

1) Epicardial formation and EMT: The primitive epicardial epithelium forms after epicardial progenitor cells are transferred from the proepicardium to the myocardial surface [27, 28]. Abnormal primitive epicardium formation is known to affect ventricular myocardium growth and coronary vascular development [29]. Integrins are about the only type of adhesion molecule shown to be involved in this process [30], being the α4-integrin null mice the one displaying a more severe ventricular myocardial thinning and coronary phenotype [31]. Soon after the primitive epicardium forms, epicardial epithelial-to-mesenchymal transition (EMT) is initiated. Epicardial EMT a finely regulated process which supplies the heart with highly invasive mesenchymal epicardial-derived cells (EPDCs) [26]. Multiple molecules participate in the regulation of EMT by triggering the process. So far, TGFβ1–2 seem to be the stronger epicardial EMT inducers [32–34], as shown by the epicardial deletion of the Tgf-beta type I receptor Alk5, which disrupts epicardial EMT and coronary blood vessel development [35]. Epicardial transcription factors Wt1 and Tbx18, together with

canonical Wnt effectors like β-catenin and retinoic acid also participate as effectors for the EMT process modulating cell adhesion and motility [36, 37]. Potentially, genetic defects in any of the genes encoding for all these molecules (or participating in their biosynthesis) could give rise to CCAs, but due to the importance of primitive epicardial formation and EMT, individuals carrying the defect are likely to die during gestation. Still, experimental studies using the chick embryo as experimental animal model reveal that a simple delay in epicardial formation and EMT activation is enough to generate abnormal coronary patterning and arterioventricular connections or fistulae (CAA group 3) [38, 39], all of them anomalies which can reach adulthood.

2) Epicardial and myocardial instructive signaling: The epicardium does not only contribute cells to the developing coronary vascular system, but it also acts as a signaling center by secreting various morphogens; the list of these epicardial-secreted molecules includes retinoic acid, Fgf9,16,20 and Igf2 [26, 40]; retinoic acid itself seems to act in an autocrine fashion also, supporting the secretory activity of the epicardium [41] which in turn impacts on coronary development. Although the characterization of this secretome has been carried out with the main goal of identifying epicardial-secreted molecules regulating myocardial compact layer growth, many of these molecules are likely to affect coronary blood vessel development also. As a matter of fact, the thin myocardium that characterizes mice mutant for epicardial molecules frequently carries aberrant coronary blood vessels [31, 36, 42], mostly abnormal ventricular patterning and ramification of coronary blood vessels (group 2 CCA).
   The epicardium is also sensitive to widely distributed molecules like erythropoietin [43] and, accordingly, erythropoietin receptor knockouts have severe coronary dysmorphogenesis [44]. Interfering with embryonic epicardial transcriptional regulation, as shown by the molecular characterization of *Wt1* and *Tbx18* mouse mutants [36, 45], reveals anomalies in the expression of secreted molecules like VEGF-A and angiopoietin-1, and growth factor receptors or mediators like PDGFRα, β, smoothened and patched (part of the Hedgehog signal transduction machinery), all of which are known to be involved in coronary blood vessel development [5, 46–48].
   The developing myocardium also contributes to coronary development by providing a material substrate for blood vessel formation, as evidenced by the altered coronary pattering found in mice defective for myocardially-expressed *Vcam-1* and *Vangl-2*. Of these two genes, *Vcam1* encodes for a cell adhesion molecule which can act as ligand for α4 integrin-containing cell receptors [49], while Vangl-2 is a molecule involved in the planar cell polarity signaling pathway [50]. Genetic deletion of co-factors involved in the transcriptional regulation of the myocardium like Fog-2 also gives rise to anomalous coronary development [51].
3) Determination and differentiation of coronary progenitor cells: Misspecification of coronary cell types and/or poor deployment of epicardial-derived mesenchymal cells (EPDCs) can alter early coronary vascular formation. Knockout embryos for the gap junction connexin 43, which is expressed by epicardial

progenitor (proepicardial) cells, have severe defects in coronary vascular patterning [52]. Accordingly, *Wt1*-null mice present decreased coronary endothelial and ectopic smooth muscle differentiation, eventually impairing coronary formation at midgestation [36]. Abrogation of Notch1 signaling (a well-known cell fate determinant) in the epicardium severely impacts coronary morphogenesis [42, 53]. Some other genes like *Tcf21* have been reported to be involved in the early specification of fibroblasts from the epicardium, as shown by the epicardial EMT and coronary morphogenesis defects displayed by *Tcf21* mutants [54]. It is of particular interest to consider here that epicardial progenitor (proepicardial) cells seem to carefully balance their developmental fate as a response to local BMP2 and FGF2 levels [55], what suggests that genetic defects in any element of these signaling pathways could result in defects in coronary embryonic development.

4) Muscularization and stabilization of coronary artery anatomical pattern: The muscular fate of EPDCs is modulated by the subepicardial microenvironment and requires activation of Srf-dependent pool of characteristic smooth muscle genes [56] and p160 Rho-kinase activation [57]. Both Vegf-A and retinoic acid have been shown to act synergistically to favor early endothelial differentiation from EPDCs at the expenses of smooth muscle cell differentiation [58]. This study proposes, for the first time, a mechanism that explains the physiological delay in the muscularization of developing blood vessels, which is supposed to allow for the extensive remodeling of the primitive coronary vasculature before its maturation and stabilization is initiated. Therefore, premature muscularization of the developing coronary blood vessels may alter the ramification and complexity of adult coronary vasculature, whereas a delay in the formation of the vascular medial wall could result in the formation of aneurism-like defects (Group 2 CCA).

49.3.3 Outgrowth of Endocardial Cells

Defective endocardial incorporation to the coronary vascular system from both the outer (sinus venosus-derived) and inner (ventricle-derived) endocardium can impair coronary vascular patterning. In order to establish a functional vascular circuitry, independent coronary vascular plexuses have to connect growing through the ventricular chamber wall. Altered transmural vascular growth may originate abnormal coronary arteriovenous shunts, arterioventricular connections (fistulae), defects that are compatible with postnatal and adult life [2]. It is logical to think that *Vegf* is a good candidate gene to explain these developmental alterations, because epicardial-to-endocardial Vegf gradients (sensitive to the transmural changes in oxygen tension) are known to determine compact myocardium colonization by embryonic blood vessels [5], and developing vascular structures are known to be extremely sensitive to Vegf doses [59].

49.4 Using Animal Models to Explore Gene Interactions in Congenital Coronary Anomalies

Animal models are key tools to understand the genetic basis of congenital anomalies, including coronary ones. Candidate genes can be identified and the impact of their gain- or loss-of-function assessed. Mouse (*Mus musculus*) has been extensively used as experimental model for the understanding of human disease. Despite its small size, the mouse heart, like the human one, has a four-chambered heart with a septated outflow tract, left-sided great arteries, and parallel pulmonary and systemic circulations and in many aspects is very close to the human organ [60]. Furthermore, the mouse is a genetically-tractable animal, allowing for a large number of modifications including, among others, the generation of systemic or tissue-specific mutants for one or more gene or the addition of constructs for the tagging and tracing of cells. Relevant to this chapter, multiple mouse experimental genetic manipulations have been shown to result in the recapitulation of malformations similar to those observed in humans. Accordingly, those genes having a major role in mouse heart development are candidate genes for congenital heart diseases in humans (Table 49.1).

49.5 Conclusions

As a summary for this chapter, a list of genes involved in CAA is provided in Table 49.1. Please note that the selection of these molecules is based in its known involvement in coronary morphogenesis in mice. The functional properties of the molecules encoded by these genes have been experimentally tested by germ line (systemic mutants) or conditional (tissue-specific) gene deletion, but to know whether these genes also participate in human coronary development will require further, systematic genetic analysis of human CCAs.

Table 49.1 Genes required for coronary vascular development

Genes deleted or altered	Phenotype	References
Sema3c knock-out	Abnormal coronary artery position	[20]
Tbx1 knock-out	Abnormal proximal left coronary artery	[20]
Vegf-C knock-out	Inhibited dorsal and lateral coronary growth	[25]
α-4 integrin knock-out	Poor epicardial integrity; Abnormal coronary Development	[31]
Tgf-b type I receptor Alk5 epicardial deletion	Thin myocardium and defective coronary muscularization	[35]
Wt1 knock-out	Hypoplastic ventricular Myocardium; poor epicardial Integrity reduced EPDCs, And abnormal coronary Morphogenesis	[36, 61, 96]
Notch knock-out	Disrupts coronary artery differentiation, reduces myocardium wall thickness and myocyte proliferation. Smooth muscle differentiation impaired	[42, 53]
Erythropoietin Receptor knock-out	Hypoplastic ventricular Myocardium; epicardial Detachment and Underdeveloped Subepicardium; abnormal Coronary morphogenesis	[44]
Tbx18 knock-out	Perturbation of EPDCs; altered Coronary development	[45]
Pdgfrβ knock-out	Thin myocardium; fail to form coronary vessels on the ventral heart surface	[47, 62, 63]
Vcam knock-out	Hypoplastic ventricular Myocardium; poor epicardial Integrity and abnormal Coronary development	[49]
Vangl2 knock-out	Disrupted the organization of the cardiomyocytes and formation of the coronary vessel	[50]
Fof-2 knock-out Fog-2 function via Gata4 knock-in	Hypoplastic ventricular Myocardium; abnormal Coronary vessels	[51, 64]
Connexin 43 knock-out	Abnormal coronary patterning And presence of conal "Pouches"; reduction in the branching complexity of the distal coronary arteries	[52, 65]
Tcf21 knock-out	Hemorrhaging in the pericardial cavity and thin myocardium	[54]
Neuropilin Overexpression	Hypoplastic ventricular Myocardium; aberrant Coronary vasculature	[66]
Vegf-B knock-out	Dysfunctional coronary vasculature (coronary occlusion)	[67]

(continued)

Table 49.1 (continued)

Genes deleted or altered	Phenotype	References
RXRα epicardial deletion	Thin myocardium; abnormal epicardial epithelial-to-mesenchymal transformation; defects in coronary vascular formation	[61]
Coup-tfII endocardial and myocardial deletion	Atrioventricular septal defects; thin-walled myocardium; abnormal coronary morphogenesis	[68, 69]
Kcnj8 knock-out	Defects in coronary vascular development	[70]
Fgf9 knock-out.	Defects in growth of the coronary plexus; Defects in formation of the subepicardial mesenchyme; Failure of both subepicardial and intramyocardial vessel growth	[69]
Tgfbr3 knock-out	Poor coronary vessel development	[71, 72]
Syndecan-4 knock-out	Attenuation of coronary arteriole growth	[73]
Epicardial β-catenin deletion	Impaired coronary artery formation	[74]
A_{2A} receptor knock-out	Defects in coronary artery formation	[75]
Podoplanin knock-out	Hypoplastic and perforated compact and septal myocardium, hypoplastic atrioventricular cushions and coronary artery abnormalities	[76]
Glypican-3 knock-out	Formation of coronary fistulas	[77]
EphB4 knock-out	Reduced vascular coronary venosus endothelium	[77]
CHF1/Hey2 knock-out	Coronary vascular anomalies and thin compact ventricular myocardium	[78]
Tgfbr2 smooth muscle cell deletion	Anomalous epicardium, myocardium and coronary smooth muscle cell formation	[79]
Hand2	Defective epicardialization and failure to form coronary arteries	[80]
FAK smooth muscle cell deletion	Defective coronary smooth muscle cell formation	[81]
Nephrin knock-out	Abnormal epicardial cell morphology and a reduced number of coronary vessels	[82]
Vegf-a and Vegfr-2 knock-out	Failure to form coronary arteries	[83]
Vegfr1 knock-out	Excessive coronary angiogenesis	[84]
Myocardium Ang1 deletion	Defective formation of the subepicardial coronary veins; no significant effect on the formation of intramyocardial coronary arteries	[85]
Tbx5 proepicardial deletion	Epicardial and coronary blood vessel formation defects	[83]
Nitric oxide synthase-3 knock-out	Coronary artery hypoplasia	[86]
Cxcl12 knock-out	Lack of intra-ventricular coronary arteries and absent or misplaced coronary arteries stems	[87]
Notch3 knock-out	Defective coronary artery smooth muscle development	[63]

(continued)

Table 49.1 (continued)

Genes deleted or altered	Phenotype	References
Epicardial yap/Taz deletion	Reduction in epicardial cell proliferation and differentiation into coronary endothelial cells	[88]
Pofut1 knock-out	Development of anomalous coronary arteries	[89]
Dach1 knock-out	Small coronary arteries, decreased endothelial cell polarization	[90]
Systemic Smad4 deletion	Increased coronary arteries diameter	[91]
Myh10 knock-out (ENU mutagenesis)	Defects in the formation of the coronary vasculature	[92]
Apj knock-out	Defects in coronary growth	[93]
Ela knock-out	Defects in coronary growth	[93]
Ino80 knock-out	Defects in coronary vascularization	[94]
Endocardial Jag1 or Dll4 deletion	Disruption of coronary plexus formation	[95]

References

1. Angelini P. Coronary artery anomalies: an entity in search of an identity. Circulation. 2007;115:1296–305.
2. Pérez-Pomares JM, de la Pompa JL, Franco D, et al. Congenital coronary artery anomalies: a bridge from embryology to anatomy and pathophysiology – a position statement of the development, anatomy, and pathology ESC Working Group. Cardiovasc Res. 2016;109:204–16.
3. Red-Horse K, Ueno H, Weissman IL, Krasnow M. Coronary arteries form by developmental reprogramming of venous cells. Nature. 2010;464:549–53.
4. Palmquist-Gomes P, Guadix JA, Pérez-Pomares JM. Avian embryonic coronary arterio-venous patterning involves the contribution of different endothelial and endocardial cell populations. Dev Dyn. 2018;247:686–98.
5. Wu B, Zhang Z, Lui W, et al. Endocardial cells form the coronary arteries by angiogenesis through myocardial-endocardial VEGF signaling. Cell. 2012;151:1083–96.
6. Tian X, Hu T, Zhang H, et al. De novo formation of a distinct coronary vascular population in neonatal heart. Science. 2014;80(345):90–4.
7. Waldo K, Willner W, Kirby M. Origin of the proximal coronary artery stems and a review of ventricular vascularization in the chick embryo. Am J Anat. 1990;188:109–20.
8. Vrancken Peeters MP, Gittenberger-de Groot AC, Mentink MM, et al. Differences in development of coronary arteries and veins. Cardiovasc Res. 1997;36:101–10.
9. Roberts W. Major anomalies of coronary arterial origin seen in adulthood. Am Heart J. 1986;111:941–63.
10. Marcelo KL, Goldie LC, Hirschi KK. Regulation of endothelial cell differentiation and specification. Circ Res. 2013;112:1272–87.
11. Kirby ML, Waldo KL. Role of neural crest in congenital heart disease. Circulation. 1990;82:332–40.
12. Chai Y, Jiang X, Ito Y, et al. Fate of the mammalian cranial neural crest during tooth and mandibular morphogenesis. Development. 2000;127:1671–9.
13. Nishibatake M, Kirby ML, Van Mierop LH. Pathogenesis of persistent truncus arteriosus and dextroposed aorta in the chick embryo after neural crest ablation. Circulation. 1987;75:255–64.
14. Epstein JA. Pax3, neural crest and cardiovascular development. Trends in Cardiovasc Med. 1996;6:255–61.

15. Chang C-P, Stankunas K, Shang C, et al. Pbx1 functions in distinct regulatory networks to pattern the great arteries and cardiac outflow tract. Development. 2008;135:3577–86.
16. High F, Jain R, Stoller J, et al. Murine Jagged1/notch signaling in the second heart field orchestrates Fgf8 expression and tissue-tissue interactions during outflow tract development. J Clin Invest. 2009;119:1986–96.
17. Rochais F, Dandonneau M, Mesbah K, et al. Hes1 is expressed in the second heart field and is required for outflow tract development. PLoS One. 2009;4(7):e6267.
18. Théveniau-Ruissy M, Dandonneau M, Mesbah K, et al. The del22q11.2 candidate gene Tbx1 controls regional outflow tract identity and coronary artery patterning. Circ Res. 2008;103:142–8.
19. Bajolle F, Zaffran S, Kelly RG, et al. Rotation of the myocardial wall of the outflow tract is implicated in the normal positioning of the great arteries. Circ Res. 2006;98:421–8.
20. Théveniau-Ruissy M, Pérez-Pomares JM, Parisot P, et al. Coronary stem development in wild-type and Tbx1 null mouse hearts. Dev Dyn. 2016;245:445–59.
21. Costell M, Carmona R, Gustafsson E, et al. Hyperplastic conotruncal endocardial cushions and transposition of great arteries in perlecan-null mice. Circ Res. 2002;91:158–64.
22. Gonzalez-Iriarte M, Carmona R, Perez-Pomares JM, et al. Development of the coronary arteries in a murine model of transposition of great arteries. J Mol Cell Cardiol. 2003;35:795–802.
23. Chiu I, Chu S, Wang J, et al. Evolution of coronary artery pattern according to short-axis aortopulmonary rotation: a new categorization for complete transposition of the great arteries. J Am Coll Cardiol. 1995;26:250–8.
24. Houyel L, Bajolle F, Capderou A, et al. The pattern of the coronary arterial orifices in hearts with congenital malformations of the outflow tracts: a marker of rotation of the outflow tract during cardiac development? J Anat. 2013;222:349–57.
25. Chen HI, Poduri A, Numi H, et al. VEGF-C and aortic cardiomyocytes guide coronary artery stem development. J Clin Investig. 2014;124:4899–914.
26. Pérez-Pomares JM, de la Pompa JL. Signaling during epicardium and coronary vessel development. Circ Res. 2011;109:1429–42.
27. Männer J, Pérez-Pomares JM, Macías D, Muñoz-Chápuli R. The origin, formation and developmental significance of the epicardium: a review. Cells Tissues Organs. 2001;169:89–103.
28. Peralta M, Steed E, Harlepp S, et al. Heartbeat-driven pericardiac fluid forces contribute to epicardium morphogenesis. Curr Biol. 2013;23:1726–35.
29. Wessels A, Pérez-Pomares JM. The epicardium and epicardially derived cells (EPDCs) as cardiac stem cells. Anat Rec A Discov Mol Cell Evol Biol. 2004;276:43–57.
30. Pae SH, Dokic D, Dettman RW. Communication between integrin receptors facilitates epicardial cell adhesion and matrix organization. Dev Dyn. 2008;237:962–78.
31. Yang JT, Rayburn H, Hynes RO. Cell adhesion events mediated by alpha 4 integrins are essential in placental and cardiac development. Development. 1995;121:549–60.
32. Romano LA, Runyan RB. Slug is an essential target of TGFbeta2 signaling in the developing chicken heart. Dev Biol. 2000;223:91–102.
33. Takeichi M, Nimura K, Mori M, et al. The transcription factors Tbx18 and Wt1 control the Epicardial epithelial-Mesenchymal transition through bi-directional regulation of slug in murine primary Epicardial cells. PLoS One. 2013;8(2):e57829.
34. Trembley MA, Velasquez LS, de Mesy Bentley KL, Small EM. Myocardin-related transcription factors control the motility of epicardium-derived cells and the maturation of coronary vessels. Development. 2014;142:21–30.
35. Sridurongrit S, Larsson J, Schwarts R, et al. Signaling via the Tgf-β type I receptor Alk5 in heart development. Dev Biol. 2008;322:208–18.
36. Guadix JA, Ruiz-Villalba A, Lettice L, et al. Wt1 controls retinoic acid signalling in embryonic epicardium through transcriptional activation of Raldh2. Development. 2011;138:1093–7.
37. Von Gise A, Zhou B, Honor LB, et al. WT1 regulates epicardial epithelial to mesenchymal transition through β-catenin and retinoic acid signaling pathways. Dev Biol. 2011;356:421–31.

38. Pérez-Pomares JM, Phelps A, Sedmerova M, et al. Experimental studies on the spatiotemporal expression of WT1 and RALDH2 in the embryonic avian heart: a model for the regulation of myocardial and Valvuloseptal development by Epicardially derived cells (EPDCs). Dev Biol. 2002;247:307–26.
39. Eralp I, Lie-Venema H, DeRuiter MC, et al. Coronary artery and orifice development is associated with proper timing of epicardial outgrowth and correlated Fas ligand associated apoptosis patterns. Circ Res. 2005;96:526–34.
40. Lavine KJ, Ornitz DM. Fibroblast growth factors and hedgehogs: at the heart of the epicardial signaling center. Trends Genet. 2008;24:33–40.
41. Chen THP, Chang T-C, Kang J-O, et al. Epicardial induction of fetal cardiomyocyte proliferation via a retinoic acid-inducible trophic factor. Dev Biol. 2002;250:198–207.
42. Del Monte G, Casanova JC, Guadix JA, et al. Differential notch signaling in the epicardium is required for cardiac inflow development and coronary vessel morphogenesis. Circ Res. 2011;108:824–36.
43. Stuckmann I, Evans S, Lassar AB. Erythropoietin and retinoic acid, secreted from the epicardium, are required for cardiac myocyte proliferation. Dev Biol. 2003;255:334–49.
44. Wu H, Lee SH, Gao J, et al. Inactivation of erythropoietin leads to defects in cardiac morphogenesis. Development. 1999;126:3597–605.
45. Wu S, Dong X, Regan J, et al. Tbx18 regulates development of the epicardium and coronary vessels. Dev Biol. 2013;383:307–20.
46. Lavine KJ, White AC, Park C, et al. Fibroblast growth factor signals regulate a wave of hedgehog activation that is essential for coronary vascular development. Genes Dev. 2006;20:1651–66.
47. Smith CL, Baek ST, Sung CY, Tallquist MD. Epicardial-derived cell epithelial-to-mesenchymal transition and fate specification require PDGF receptor signaling. Circ Res. 2011;108: e15–26.
48. Jeansson M, Gawlik A, Anderson G, et al. Angiopoietin-1 is essential in mouse vasculature during development and in response to injury. J Clin Invest. 2011;121:2278–89.
49. Kwee L, Baldwin HS, Shen HM, et al. Defective development of the embryonic and extraembryonic circulatory systems in vascular cell adhesion molecule (VCAM-1) deficient mice. Development. 1995;121:489–503.
50. Phillips HM, Rhee HJ, Murdoch JN, et al. Disruption of planar cell polarity signaling results in congenital heart defects and cardiomyopathy attributable to early cardiomyocyte disorganization. Circ Res. 2007;101:137–45.
51. Tevosian SG, Deconinck AE, Tanaka M, et al. FOG-2, a cofactor for GATA transcription factors, is essential for heart morphogenesis and development of coronary vessels from epicardium. Cell. 2000;101:729–39.
52. Li WEI, Waldo K, Linask KL, et al. An essential role for connexin43 gap junctions in mouse coronary artery development. Development. 2002;129:2031–42.
53. Grieskamp T, Rudat C, Lüdtke TH-W, et al. Notch signaling regulates smooth muscle differentiation of epicardium-derived cells. Circ Res. 2011;108:813–23.
54. Acharya A, Baek ST, Huang G, et al. The bHLH transcription factor Tcf21 is required for lineage-specific EMT of cardiac fibroblast progenitors. Development. 2012;139:2139–49.
55. Van Wijk B, Van Den Berg G, Abu-Issa R, et al. Epicardium and myocardium separate from a common precursor pool by crosstalk between bone morphogenetic protein- and fibroblast growth factor-signaling pathways. Circ Res. 2009;105:431–41.
56. Landerholm TE, Dong XR, Lu J, et al. A role for serum response factor in coronary smooth muscle differentiation from proepicardial cells. Development. 1999;126:2053–62.
57. Lu J, Landerholm TE, Wei JS, et al. Coronary smooth muscle differentiation from proepicardial cells requires rhoA-mediated actin reorganization and p160 rho-kinase activity. Dev Biol. 2001;240:404–18.

58. Azambuja AP, Portillo-Sánchez V, Rodrigues M, et al. Retinoic acid and VEGF delay smooth muscle relative to endothelial differentiation to coordinate inner and outer coronary vessel wall morphogenesis. Circ Res. 2010;107:204–16.
59. Risau W, Flamme I. Vasculogenesis. Annu Rev Cell Biol Dev Biol. 1995;11:73–91.
60. Kent GC, Carr RK. Comparative anatomy of the vertebrates. 9th ed. Boston, MA: McGraw Hill; 2001.
61. Merki E, Zamora M, Raya A, et al. Epicardial retinoid X receptor alpha is required for myocardial growth and coronary artery formation. Proc Natl Acad Sci U S A. 2005;102: 18455–60.
62. Mellgren AM, Smith CL, Olsen GS, et al. Platelet-derived growth factor receptor beta signaling is required for efficient epicardial cell migration and development of two distinct coronary vascular smooth muscle cell populations. Circ Res. 2008;103:1393–401.
63. Volz KS, Jacobs AH, Chen HI, et al. Pericytes are progenitors for coronary artery smooth muscle. elife. 2015;4:e10036.
64. Crispino JD, Lodish MB, Thurberg BL, et al. Proper coronary vascular development and heart morphogenesis depend on interaction of GATA-4 with FOG cofactors. Genes Dev. 2001;15: 839–44.
65. Walker DL, Vacha SJ, Kirby ML, Lo CW. Connexin43 deficiency causes dysregulation of coronary vasculogenesis. Dev Biol. 2005;284:479–98.
66. Kitsukawa T, Shimono A, Kawakami A, et al. Overexpression of a membrane protein, neuropilin, in chimeric mice causes anomalies in the cardiovascular system, nervous system and limbs. Development. 1995;121:4309–18.
67. Bellomo D, Headrick JP, Silins GU, et al. Mice lacking the vascular endothelial growth factor-B gene (Vegfb) have smaller hearts, dysfunctional coronary vasculature, and impaired recovery from cardiac ischemia. Circ Res. 2000;86:e29–35.
68. You LR, Lin FJ, Lee CT, et al. Suppression of notch signalling by the COUP TFII transcription factor regulates vein identity. Nature. 2005;435:98–104.
69. Lin F-J, You L-R, Yu C-T, et al. Endocardial cushion morphogenesis and coronary vessel development require chicken ovalbumin upstream promoter-transcription factor II. Arterioscler Thromb Vasc Biol. 2012;32:e135–46.
70. Kane GC, Lam C-F, O'Cochlain F, et al. Gene knockout of the KCNJ8-encoded Kir6.1 K(ATP) channel imparts fatal susceptibility to endotoxemia. FASEB J. 2006;20:2271–80.
71. Compton LA, Potash DA, Brown CB, Barnett JV. Coronary vessel development is dependent on the Type III transforming growth factor _ receptor. Circ Res. 2007;101:784–91.
72. Sánchez N, Hill C, Love J, et al. The cytoplasmic domain of TGFβR3 through its interaction with the scaffolding protein, GIPC, directs epicardial cell behavior. Dev Biol. 2011;358:331–43.
73. Dedkov EI, Thomas MT, Sonka M, et al. Synectin/Syndecan-4 regulate coronary arteriolar growth during development. Dev Dyn. 2007;236:2004–10.
74. Zamora M, Manner J, Ruiz-Lozano P. Epicardium-derived progenitor cells require b-catenin for coronary artery formation. Proc Natl Acad Sci U S A. 2007;104:18109–14.
75. Teng B, Ledent C, Mustafa J. Up-regulation of A2B adenosine receptor in A2A adenosine receptor knockout mouse coronary artery. J Cell Mol Cardiol. 2008;44:905–14.
76. Mahtab EAF, Wijffels MCEF, Van den Akker NMS, et al. Cardiac malformations and myocardial abnormalities in podoplanin knockout mouse embryos: correlation with abnormal epicardial development. Dev Dyn. 2008;237:847–57.
77. Ng A, Wong M, Viviano B, et al. Loss of glypican-3 function causes growth factor-dependent defects in cardiac and coronary vascular development. Dev Biol. 2009;335:208–15.
78. Watanabe T, Koibuchi N, Chin MT. Transcription factor CHF1/Hey2 regulates coronary vascular maturation. Mech Dev. 2010;127:9–12.
79. Langlois D, Hneino M, Bouazza L, et al. Conditional inactivation of TGF-beta type II receptor in smooth muscle cells and epicardium causes lethal aortic and cardiac defects. Transgenic Res. 2010;19:1069–82.

80. Barnes RM, Firulli B, VanDusen J, et al. Hand2 loss-of-function in Hand1-expressing cells reveals distinct roles in epicardial and coronary vessel formation. Circ Res. 2011;108:940–9.
81. Cheng Z, Sundberg-Smith LJ, Mangiante LE, et al. Focal adhesion kinase regulates smooth muscle cell recruitment to the developing vasculature. Arterioscler Thromb Vasc Biol. 2011;31: 2193–202.
82. Wagner N, Morrison H, Pagnotta S, et al. The podocyte protein nephrin is required for cardiac vessel formation. Hum Mol Genet. 2011;20:2182–94.
83. Diman N, Brooks G, Kruithof B, et al. Tbx5 is required for avian and mammalian epicardial formation and coronary vasculogenesis. Circ Res. 2014;115:834–44.
84. Zhang Z, Zhou B. Accelerated coronary angiogenesis by Vegfr1-knockout endocardial cells. PLoS One. 2013;8:e70570.
85. Arita Y, Nakaoka Y, Matsunaga T, et al. Myocardium-derived angiopoietin-1 is essential for coronary vein formation in the developing heart. Nat Commun. 2014;5:4552.
86. Liu Y, Lu X, Xiang FL, et al. Nitric oxide synthase-3 deficiency results in hypoplastic coronary arteries and postnatal myocardial infarction. Eur Heart J. 2014;35:920–31.
87. Ivins S, Chappell J, Vernay B, et al. The CXCL12/CXCR4 axis plays a critical role in coronary artery development. Dev Cell. 2015;33:455–68.
88. Singh A, Ramesh S, Cibi DM, et al. Hippo signaling mediators yap and Taz are required in the epicardium for coronary vasculature development. Cell Rep. 2016;15:1384–93.
89. Wang Y, Wu B, Lu P, et al. Uncontrolled angiogenic precursor expansion causes coronary artery anomalies in mice lacking Pofut1. Nat Commun. 2017;8:578.
90. Chang AH, Raftrey BC, D'Amato G, et al. DACH1 stimulates shear stress-guided endothelial cell migration and coronary artery growth through the CXCL12– CXCR4 signaling axis. Genes Dev. 2017;31:1308–24.
91. Poduri A, Raftrey B, Chang AH, et al. Endothelial cells respond to the direction of mechanical stimuli through SMAD signaling to regulate coronary artery size. Development. 2017;144: 3241–52.
92. Ridge LA, Mitchell K, Al-Anbaki A, et al. Non-muscle myosin IIB (Myh10) is required for epicardial function and coronary vessel formation during mammalian development. PLoS Genet. 2017;13:e1007068.
93. Sharma B, Ho L, Ford GH, et al. Alternative progenitor cells compensate to rebuild the coronary vasculature in Elabela- and Apj-deficient hearts. Dev Cell. 2017;42:655–66.
94. Rhee S, Chung JI, King DA, et al. Endothelial deletion of Ino80 disrupts coronary angiogenesis and causes congenital heart disease. Nat Commun. 2018;9:368.
95. Travisano SI, Oliveira VL, Prados B, et al. Coronary arterial development is regulated by a Dll4-Jag1-EphrinB2 signaling cascade. elife. 2019;8:e49977.
96. Moore AW, McInnes L, Kreidberg J, et al. YAC complementation shows a requirement for Wt1 in the development of epicardium, adrenal gland and throughout nephrogenesis. Development. 1999;126:1845–57.

Part XIII

Truncus Arteriosus

Clinical Presentation and Therapy of Truncus Arteriosus

50

Nikolaus A. Haas, David J. Driscoll, and Silke Rickert-Sperling

50.1 Introduction

Truncus arteriosus (TA, also known as common arterial trunk) consists of only one great artery ("the truncus") with a semilunar valve (truncus valve) arising from the heart and an additional ventricular septal defect and (Fig. 50.1). This great artery is positioned above the ventricular septal defect and gives rise to the coronary arteries, the pulmonary arteries, and the aortic arch. Historically, TA has been classified by Collet and Edwards in three types, where in type I there was a common pulmonary artery truncus, in type II the left and right PA arise separately but close to each other, in type III both PA arise independently; in addition, there was a type IV that was later characterized as pulmonary atresia with VSD and major aortopulmonary collateral arteries arising from the descending aorta.

Today, the classification of Van Praagh is used, and TA is divided in four types (see Fig. 50.2). The Van Praagh classification categorizes according to the position of the great arteries (aorta and pulmonary artery) and their relationship to each other. In type 1 the right and left pulmonary arteries arise from a main pulmonary artery that arises from the aorta directly above the truncus valve. In type 2 the right and left

N. A. Haas (✉)
Department of Pediatric Cardiology and Intensive Care, Ludwig Maximilians University, Munich, Germany
e-mail: Nikolaus.haas@med.uni-muenchen.de

D. J. Driscoll
Division of Pediatric Cardiology, Department of Pediatrics, Mayo Clinic College of Medicine, Rochester, MN, USA
e-mail: driscoll.david@mayo.edu

S. Rickert-Sperling
Cardiovascular Genetics, Charité – Universitätsmedizin Berlin, Berlin, Germany
e-mail: silke.sperling@charite.de

© The Author(s), under exclusive license to Springer Nature Switzerland AG 2024

S. Rickert-Sperling et al. (eds.), *Congenital Heart Diseases: The Broken Heart*,
Advances in Experimental Medicine and Biology 1441,
https://doi.org/10.1007/978-3-031-44087-8_50

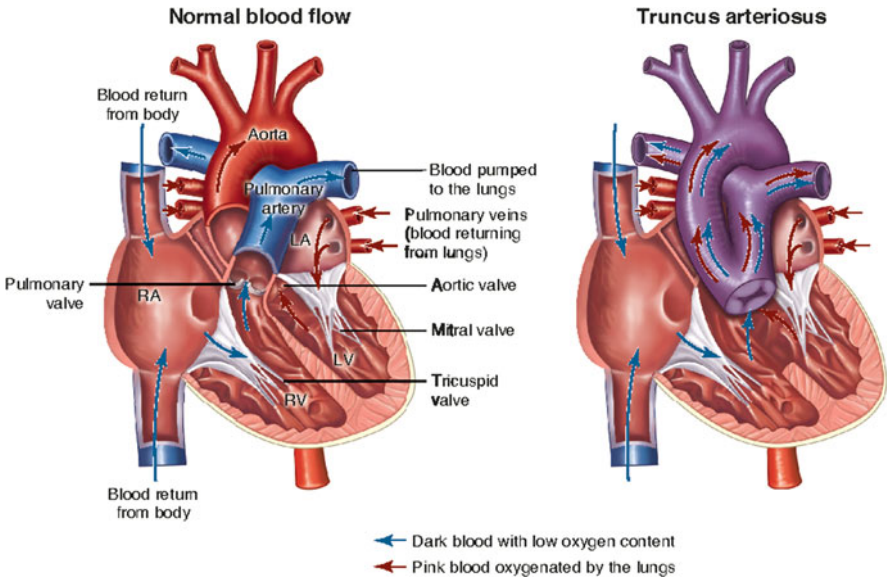

Fig. 50.1 Diagrammatic representation of normal circulation (*right panel*) and truncus arteriosus (*left panel*). Note that in truncus arteriosus, there is only one semilunar valve and this is referred to as the "truncal valve." It can be tricuspid or quadricuspid (as is shown in the diagram). Abbreviations: *RA* right atria, *LA* left atria, *RV* right ventricle, *LV* left atrium (Reproduced or adapted from Driscoll D (2006) Fundamentals of pediatric cardiology. Lippincott Williams & Wilkins, with permission of the author and publisher)

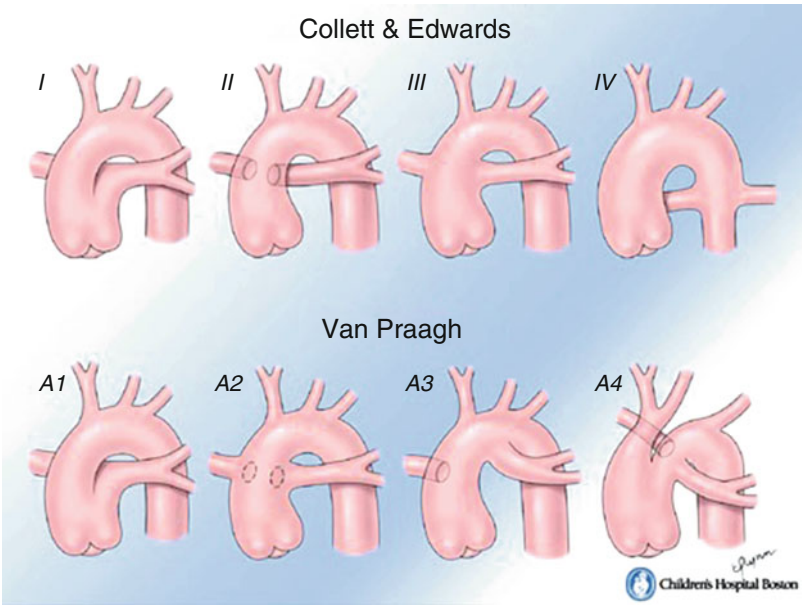

Fig. 50.2 Truncus arteriosus classification of Van Praagh. The Van Praagh classification provides a framework reflecting the position and relationship of the great arteries

pulmonary arteries arise from separate orifices positioned close together on the main vessel. In type 3 the pulmonary arteries arise separately and distant from each other. In type 4 there are additional abnormalities of the aortic arch, mainly an interrupted aortic arch type B. Significant associated anomalies include truncal valve insufficiency, stenosis, a right sided aortic arch and interrupted aortic arch. Clinically the most frequent form of TA is a mixture of types 1 and 2, commonly termed type 1.5. TA constitutes approximately 1–2% of all congenital heart defects. It results from abnormal conotruncal septation. There is a relatively common association between microdeletion 22q11.2 and truncus arteriosus, especially if there is interruption of the aortic arch.

The truncus valve may show many variations of the number and function of the cusps. In most cases, the truncal valve is quadricuspid, but all variations from 6 to 1 cusps have been reported. Some degree of truncus valve regurgitation is common, as is mild stenosis. Severe forms of regurgitation will affect outcome.

50.2 Pathologic Physiology

Cyanosis occurs because of a right-to-left shunt at the level of the unrestrictive ventricular septal defect and is dependent upon the volume of pulmonary blood flow through the pulmonary arteries. The relative volume of pulmonary and systemic blood flow depends on the relative resistance to flow into the pulmonary vascular bed and into the systemic vascular bed. Immediately after birth, there is physiologically elevated pulmonary vascular resistance (PVR) and so transpulmonary blood flow is limited. During the next weeks and first month in life, PVR will drop and transpulmonary blood flow will increase dramatically. The resistance to flow into the pulmonary vascular bed also will be effected by the presence or absence, as well as the severity, of pulmonary arterial stenosis. In addition, the degree of truncal valve regurgitation (or stenosis) will influence hemodynamics; moderate or severe reflux increases the likelihood of heart failure at neonatal age. Children who survive this stage will develop pulmonary hypertension and increased pulmonary vascular resistance that may make surgical repair impossible.

50.3 Clinical Presentation

As there is complete mixing of the venous and arterial blood, these babies may be picked up by a general pulse oximetry screening due to saturations below 94%. Infants with truncus arteriosus may present with a variable degree of cyanosis, a heart murmur or severe congestive heart failure. There are reports of TAC detected incidentally in adulthood.

50.4 Physical Examination

These patients have a prominent right ventricular impulse at the lower left sternal border. Usually, there is a systolic ejection murmur at the left sternal border. There may be an apical aortic ejection click and increased pulse pressure. If there is truncal valve insufficiency, there will be a decrescendo diastolic murmur. If there is associated interruption of the aortic arch, the femoral pulses may be decreased or absent.

50.5 Diagnostic Imaging

Echocardiography is a reliable diagnostic tool for accurately diagnosing truncus arteriosus (TA) and its different types, as well as detecting any associated malformations. Transthoracic echocardiography is usually sufficient for diagnosis in neonates and children. It allows for the assessment of the anatomy of the arch (right aortic arch, interrupted aortic arch) and the origin of the pulmonary arteries. The degree of truncal valve obstruction or regurgitation, as well as its exact anatomy, can also be evaluated. Differential diagnoses to consider include pulmonary atresia with ventricular septal defect (VSD) and aortopulmonary window.

In most cases, diagnostic cardiac catheterization is unnecessary for the diagnosis of TA due to the availability of echocardiography. However, cardiac catheterization may be necessary in older patients (over 1 yr of age) when knowledge of the pulmonary vascular resistance is required to determine operability.

Magnetic resonance imaging (MRI) can be utilized in adults and teenagers presenting later in life with unobstructed forms of TA. MRI is particularly valuable for long-term follow-up to assess surgical outcomes and evaluate right ventricular size and function.

Computer tomography (CT) can provide similar anatomical details as MRI and may be required, especially in patients who present at a later stage, to define the precise anatomy of the arch and pulmonary arteries. CT scans can help provide detailed information for surgical planning and assessment.

50.6 Treatment

In infancy, as pulmonary arteriolar resistance decreases, significant congestive heart failure develops, usually early and within the first month of life, and may be aggravated in cases with moderate or severe truncal valve regurgitation. The initial management consists of medical treatment of the congestive heart failure (betablockers, afterload-reducing agents and perhaps diuretics) as well as high caloric input (for example, nasogastric feeding). In neonates with type 4 TA, prostaglandin E1 has to be administered to prevent PDA closure until surgery.

Surgery to correct TA is necessary and should be performed before the age of 3 months but usually is necessary in the first month of life because of severe

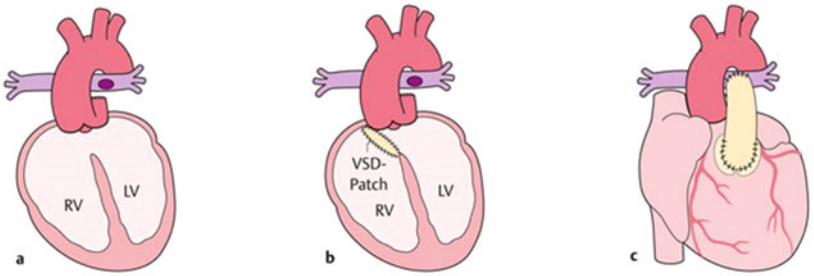

Fig. 50.3 Rastelli Operation. During the Rastelli operation, several steps are typically performed to correct TA (a): (b) Ventricular Septal Defect (VSD) Closure; (c) Creation of a Conduit: A conduit, typically made from a synthetic material or a segment of the patient's own tissue, is used to establish a connection between the right ventricle and the pulmonary artery. This conduit allows blood to flow from the right ventricle to the lungs. Reproduced from Kinderkardiologie, Georg Thieme Verlag, N. Haas, U. Kleideiter, 2011

congestive heart failure Surgical correction, named after its developer, Dr. Giancarlo Rastelli, involves closure of the ventricular septal defect, separation of the pulmonary arteries from the truncus, and establishing continuity between the right ventricle and pulmonary arteries with a valved biological conduit (Fig. 50.3). The truncal valve now becomes the new aortic valve. If necessary, repair of the aortic arch is performed at the same time. In selected cases (i.e., low birth weight, severe sepsis, etc.) a two-step approach may be favorable; this consists of a (bilateral) banding of the pulmonary arteries and additional procedures according to the type of TA. Early surgical correction is necessary to prevent the development of pulmonary vascular obstructive disease and to treat the congestive heart failure.

50.7 Outcome

Operative mortality depends on the associated problems in a patient with truncus arteriosus. In the absence of interrupted aortic arch and/or truncal valve stenosis/insufficiency, the surgical mortality is in the range of 5–10% and the 10 yrs survival is about 80%. Since the repair includes placement of a conduit from the right ventricle to the pulmonary artery and possibly a repair of the aortic arch, patients with TAC will require lifelong follow up and specialized management. The RV to PA conduit will have to be replaced as the patient outgrows it or it becomes stenotic or insufficient. For patients with interrupted aortic arch, reoperation or balloon dilatation may be necessary because of the recurrent narrowing of the aorta as the patient grows. In a considerable number of patients the truncal valve (i.e., the new aortic valve) may need replacement. In patients with 22q11 deletion syndrome, specialized follow-up programs are required.

Human Genetics of Truncus Arteriosus

51

Hiroyuki Yamagishi

Abstract

Integrated human genetics and molecular/developmental biology studies have revealed that truncus arteriosus is highly associated with 22q11.2 deletion syndrome. Other congenital malformation syndromes and variants in genes encoding TBX, GATA, and NKX transcription factors and some signaling proteins have also been reported as its etiology.

Keywords

Congenital heart disease · Diabetic mother · 22q11.2 deletion syndrome · DiGeorge syndrome · TBX1 · CHARGE syndrome · CHD7 · VACTERL syndrome · TBX transcript · NKX transcription factors · NKX2-5 · NKX2-6 · GATA transcription factors · GATA4 · GATA6 · SEMA3C · PLXNA2 · Tetralogy of Fallot · Second heart field · Neural crest cells

51.1 Introduction

Truncus arteriosus (TA) is an uncommon congenital heart defect (CHD) that results from complete failure of aorticopulmonary septum formation. Embryologically, ablation of cardiac neural crest cells (CNCC) leads to failure of partitioning the embryonic truncus arteriosus and disrupts conotruncal development by interfering with addition of the myocardium derived from the second heart field (SHF) (Fig. 51.1), resulting in TA [1].

H. Yamagishi (✉)
Division of Pediatric Cardiology, Department of Pediatrics, Keio University School of Medicine, Tokyo, Japan
e-mail: hyamag@keio.jp

© The Author(s), under exclusive license to Springer Nature Switzerland AG 2024

S. Rickert-Sperling et al. (eds.), *Congenital Heart Diseases: The Broken Heart*,
Advances in Experimental Medicine and Biology 1441,
https://doi.org/10.1007/978-3-031-44087-8_51

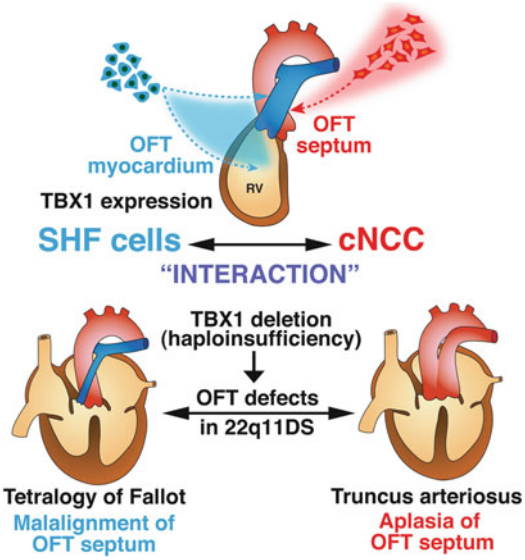

Fig. 51.1 Cellular and molecular basis for normal and abnormal outflow tract development of the heart. The interaction of progenitor cells derived from the second heart field (SHF cells) and the cardiac neural crest (*CNCC*) that give rise to the outflow tract (*OFT*) myocardium and septum, respectively, plays a key role in the development of the OFT. TBX1, a major genetic determinant of the 22q11.2 deletion syndrome (22q11DS), is exclusively expressed in the SHF cells. TBX1 deletion in 22q11DS may affect not only the SHF cells but also the interaction of the SHF cells and CNCC and result in OFT defects ranging from tetralogy of Fallot, which is characterized by malalignment of the OFT septum, to truncus arteriosus, which results from aplasia of the OFT septum

The etiology of most patients with TA is usually unknown, and it is considered to be heterogeneous and multifactorial in nature. Approximately 60% of TA occurs as an isolated cardiovascular malformation, while the remainder has additional extracardiac anomalies and is frequently syndromic [1]. A diabetic mother has an increased risk of developing TA compared with the infant of a nondiabetic mother [2, 3]. A typical pattern of malformation was reported in embryos exposed to retinoic acid involving conotruncal and aortic arch anomalies including TA [2, 3].

Several genes encoding transcription factors and signaling proteins highlight the importance of the CNCC and SHF along with their interaction [4]. Mice deficient for genes encoding these proteins result in TA. Syndromes with chromosome 22q11.2 microdeletion served as an entry to understanding the genetic basis for TA, and a gene encoding the transcription factor T-box 1 (TBX1) has been proposed as a major genetic determinant [5, 6]. To date, pathogenic variants of genes encoding TBX, GATA or NKX transcription factors, or some signaling proteins have been reported in patients with TA without 22q11.2 deletion.

51.2 Genetics

TA has no striking gender difference in frequency. Several reports describe families with one proband with TA and several relatives with CHD although most cases of TA occur sporadically. A recurrence risk for siblings of probands with TA is reported as 1.2% in a combined study [7] and 6.6% in a consecutive study of 49 families [8]. In some families, the affected relatives have concordant defects, namely, conotruncal or cardiac outflow tract defects, whereas in other families, the defects are morphologically discordant, suggesting that the recurrence risk is highly variable and dependent on the specific etiology in each family. Syndromes and genes associated with TA are summarized in Tables 51.1 and 51.2, respectively.

51.2.1 Syndromes and Chromosomal Anomalies

Approximately 40% of patients with TA are syndromic. TA accounts for approximately 10% of cardiovascular malformations associated with the 22q11.2 deletion syndrome (22q11DS). It was also reported that 2–3% of TA patients have chromosomal anomalies other than 22q11.2 deletion [1].

Table 51.1 Syndromes associated with truncus arteriosus

Syndrome	Gene/ Loci	Clinical feature	Refs.
22q11.2 deletion syndrome DiGeorge syndrome Velo-cardio-facial syndrome Conotruncal anomaly face syndrome	TBX1 22q11.2	CHD (74–85%): TOF, TA, IAA, VSD, etc. Others: characteristic facies, thymic hypoplasia/ immune deficit, velopharyngeal insufficiency, cleft palate, bifid uvula, hypocalcemia/ hypoparathyroidism, learning disability, psychiatric disorder, etc.	[5, 6], [10–13], [25–31]
CHARGE syndrome	CHD7 8q12.2 ? SEMA3E 7q21.11	CHD (75–85%): TOF, PDA, AVSD, VSD, TA, etc. Others: coloboma, choanal atresia, genital hypoplasia, ear anomalies, hearing loss, developmental delay, growth retardation, intellectual disability	[15, 16]
VACTERL association	? HOXD13 2q31.1	CHD (53–80%): VSD, ASD, PDA, TOF, HLHS, TGA, TA, etc. Others: vertebral anomalies, anal atresia, tracheoesophageal fistula, renal anomalies, radial dysplasia, thumb hypoplasia, single umbilical artery	[17]

AVSD, atrioventricular septal defect; CHD, congenital heart disease; HLHS, hypoplastic left heart syndrome; IAA, interrupted aortic arch; PDA, patent ductus arteriosus; TA, truncus arteriosus; TGA, transposition of great arteries; TOF, tetralogy of Fallot; VSD, ventricular septal defect

Table 51.2 Single-gene variants associated with truncus arteriosus

Gene	Loci	Function	Cardiac (other) defects	Refs.
Established				
TBX1	22q11.2	TF	TA, IAA, TOF, VSD (22q11.2 deletion syndrome)	[32]
GATA6	18q11.2	TF	TA, TOF (pancreas)	[35, 38–47]
Reported				
NKX2-5	5q35.1	TF	ASD, TOF, HLHS, TA	[57–60]
NKX2-6	8p21.2	TF	TA	[61, 62]
TBX20	7p14.2	TF	ASD, VSD, DCM, TA	[33]
GATA4	8p23.1	TF	ASD, VSD, AVSD, TOF, TA	[38, 49]
Reported pending confirmation				
PLXD1	3q22.1	SP (receptor)	TA	[36]
NRP1	10p11.22	SP (receptor)	TA	[63]
PRKD1	14q12	SP (kinase)	TA	[63]
PRDM1	6q21	TR	TA	[63]
TMEM260	14q22.3	unknown	TA, ASD, VSD (kidney)	[64, 65]

ASD, atrial septal defect; AVSD, atrioventricular septal defect; DCM; dilated cardiomyopathy; HLHS, hypoplastic left heart syndrome; IAA, interrupted aortic arch; PDA, patent ductus arteriosus; SP, signaling protein; TA, truncus arteriosus; TF, (DNA-binding) transcriptional factor; TOF, tetralogy of Fallot; TR: (DNA-binding) transcriptional repressor; VSD, ventricular septal defect

51.2.1.1 22q11.2 Deletion Syndrome (22q11DS)

Monoallelic microdeletion of chromosome 22q11.2 results in the most common human genetic deletion syndrome with an incidence of 1 in 4000–5000 live births [5, 6, 9]. Recognition that DiGeorge syndrome (DGS), velo-cardio-facial syndrome (VCFS), and conotruncal anomaly face syndrome (CAFS) have overlapping clinical presentations and share 22q11.2 deletion revealed a common etiology of these clinical entities.

The clinical findings associated with 22q11DS are highly variable. Approximately 80% of patients with 22q11DS are born with CHD. The types of CHD are variable, but characterized as conotruncal and aortic arch defects including tetralogy of Fallot (TOF) (~30%), interrupted aortic arch (IAA) type B (~15%), ventricular septal defect (VSD) (~15%), TA (~10%), and others (~5%) (Table 51.1). 22q11.2 deletion is the second most common genetic cause of CHD and is present in ~60% of patients with IAA type B, ~35% of patients with TA, and ~ 15% of patients with TOF (~55% of patients with TOF plus pulmonary atresia and major aortopulmonary collateral arteries) [10, 11].

22q11DS commonly involves 1.5 or 3 Mb microdeletion on chromosome 22q11.2, including the deletion of *TBX1* (see below). Despite the homogenous deletions, 22q11DS has individually variable penetrance and expressivity, suggesting that additional factors influence the clinical phenotype. Although these additional factors are largely unknown, some genetic modifiers influencing

conotruncal defects in 22q11DS have been proposed by genome-wide analyses [12, 13].

As for the type of TA associated with 22q11.2 deletion, Momma et al. reported that three had type A1 and two had type A3 with no other in their five consecutive patient types, according to the Van Praagh classification [14], while Goldmuntz et al. reported all four types in their largest series of consecutive patients with TA and 22q11.2 deletion [10]. They also found that patients with the additional finding of an aortic arch anomaly (such as a right aortic arch or aberrant subclavian artery) were more likely to have a 22q11.2 deletion than those with a normal left aortic arch.

A genetic test for 22q11.2 deletion would be recommended to screen all infants who are newly diagnosed with TA because the syndromic feature might be difficult to identify in the neonatal period and the finding of the deletion could facilitate the clinician to carefully detect the associated extracardiac features. It is also important to provide accurate recurrence risk and comprehensive genetic counseling for the family.

51.2.1.2 CHARGE Syndrome

CHARGE syndrome is an acronym characterized by a pattern of congenital anomalies including coloboma of the eye (C), heart anomaly (H), atresia of choanal (A), retardation of mental and somatic development (R), genital anomalies (G), and ear abnormalities and/or deafness (E). Variants of CHD7 on 8q12.1-q12.2 are found in approximately 60% of patients with CHARGE syndrome [15]. A variant of *SEMA3E* on 7q21.11 encoding semaphorin 3E was also reported, but not many cases [16]. Approximately 30–40% of CHD associated with CHARGE syndrome represents outflow tract defects including TA.

51.2.1.3 VACTERL Association

VACTERL association is an acronym for the nonrandom association of vertebral defects (V), anal atresia (A), cardiac malformations (C), tracheoesophageal fistula (T) with esophageal atresia (E), radial or renal dysplasia (R), and limb anomalies (L). A variant of *HOXD13* (homeobox D13) on 2q31.1 was reported in a patient with VACTERL association [17]. Up to 75% of patients with VACTERL association have CHDs. VSD, atrial septal defects (ASD), and TOF are commonly seen, whereas TA and transposition of the great arteries (TGA) are less common.

51.2.1.4 Other Syndromes

DGS is highly associated with TA and the common 22q11.2 deletion as mentioned above, but some cases have no detectable molecular defect of this region. Relatively rare cases of DGS can be caused by heterozygous deletion of 10p14-13 (DGS2 locus) [18]. We reported a unique patient with a de novo deletion beginning in the intron between exons 5 and 6 of *CDC* (cell division cycle) *45 L* and deleting exons 1–3 of *UFD* (ubiquitin fusion degradation) *1 L* on 22q11.2 critical region and typical features of the DGS including TA [19]. The *CDC45L* gene is situated immediately telomeric of *UFD1L* and is transcribed in the opposite direction through a common cis-acting element [20].

Association between TA and the following rare syndromes has also been cited in Online Mendelian Inheritance in Man (OMIM): cleft-limb-heart malformation [21]; fibuloulnar aplasia/hypoplasia with renal abnormalities [22]; microcephaly, congenital heart disease, unilateral renal agenesis, and hyposegmented lungs [23]; and renal-hepatic-pancreatic dysplasia 2 implicated with variant of *NEK8* (nimA-related kinase 8) on 17q11.2 [24].

51.2.2 Gene Variants

TBX1 and *GATA6* are established genes associated with TA. Recent advance in new genomic techniques have uncovered numerous gene variants that may be associated with CHD including TA.

51.2.2.1 TBX Transcription Factors

Because of the high incidence and association with CHD, including TA, 22q11DS has attracted attention as a model for investigating the genetic and developmental basis for TA. Although extensive gene searches have been successful in identifying more than 30 genes in the critical 22q11.2 locus, direct sequencing has failed to detect a responsible gene [5, 6, 25]. Elegant efforts to model 22q11DS in mice by creating orthologous chromosomal deletions were successful in reproducing aortic arch defects of 22q11DS, leading to identification of a T-box transcription factor, TBX1, as a major genetic determinant of CHD associated with 22q11DS [26, 27].

We and other groups found that Tbx1 was expressed in the SHF, but not in the CNCC [28–30]. This finding was surprising because CHD associated with 22q11DS had been considered primarily to be a result of developmental defects of CNCC [5, 6, 9, 25]. Cre-mediated murine transgenic system suggested that Tbx1-expressing descendants representing a subset of cells derived from the SHF contribute predominantly to the pulmonary infundibulum [31]. Developmental defects of this subset of cardiac progenitor cells may cause hypoplasia of the pulmonary infundibulum, resulting in TOF. A more severe decrease in number or absence of this subset of cells may affect development and/or migration of CNCC, resulting in TA. This hypothetical model is supported by the observation that outflow tract defects ranging from TOF to TA are highly associated with 22q11DS (Fig. 51.1).

There is a report of *TBX1* variants in three unrelated patients with CHD without the common 22q11.2 deletion [32]. Yagi et al. identified variants in the *TBX1* gene in heterozygous state in three patients with phenotypes related to the 22q11DS, including the characteristic conotruncal anomaly face.

In addition to *TBX1*, another family member, *TBX20*, was reported to be implicated in nonsyndromic CHD, including ASD, VSD, mitral valve stenosis and dilated cardiomyopathy (DCM), and variants in *TBX20* have subsequently been described in other familial and sporadic cardiac malformations, including TOF and TA [33].

51.2.2.2 GATA Transcription Factors

GATA transcription factors are characterized as zinc finger proteins and play roles in the differentiation and survival of many cell types, including cardiomyocytes [34]. Among six GATA transcription factors, GATA4, GATA5, and GATA6 are expressed in the precardiac mesoderm and are thought to play essential roles during development of the heart.

We identified two different *GATA6* variants in two probands with nonsyndromic TA [35]. Our subsequent biological analyses revealed that *SEMA3C* and plexin (*PLXN*) A2 were directly regulated by GATA6 and that both GATA6 mutant proteins failed to transactivate these genes. During development, SEMA3C and PLXNA2 mediate signal transduction essential for neurovascular guidance as a ligand and a receptor, respectively. Our data implicate variants in *GATA6* as genetic causes of TA, as a result of the disruption of the direct regulation of semaphorin-plexin signaling. In fact, a variant in the *PLXND1* which encodes another receptor for *SEMA3C* was reported to be associated with nonsyndromic TA [36]. A recent animal study suggested a model that proper spatiotemporal expression of *SEMA3C*, regulated positively by GATA6 and negatively by the TBX1-FGF8 signaling, respectively, is essential for the interaction between CNCC and the SHF that correctly navigates CNCC towards the outflow tract [37].

Other reports [38–43] came out on variants in *GATA6* that are associated with CHD including not only TA and TOF, but also atrioventricular septal defects (AVSD) and ASD. Intriguingly, the *GATA6* variants identified in humans are predominantly associated with outflow tract defects, whereas *GATA4* variants are commonly associated with ASD/VSD (see below), although there are some phenotypic overlaps likely to result from a redundant role of both genes.

It is of note that pancreatic agenesis and congenital heart defects (PACHD) could also be caused by heterozygous variant in the *GATA6* gene [44]. In the examination of 27 individuals with pancreatic agenesis by Allen et al., CHDs were present in 14 (93%) of the 15 patients with variants in the *GATA6* gene, whereas affected individuals in whom no *GATA6* variant was detected rarely had extrapancreatic features. In the report by Yorifuji et al., the dominantly inherited *GATA6* variant resulted in a variable degree of pancreatic hypoplasia, and similar intrafamilial variability was observed with regard to the types of CHD present in affected individuals [45]. A patient with PACHD associated with a *GATA6* variant who manifested a severe form of TA was also reported [46]. It is considered that distinct *GATA6* variants may be associated with the molecular mechanisms for diverse developmental defects, including cardiac outflow tract defects, pancreas and diaphragm dysgenesis [47].

As for *GATA4*, Garg et al. reported that sequence variants in *GATA4* caused ASD/VSD, probably as a result of disruptions to interactions with TBX5 [48]. A few reports have demonstrated an association between *GATA4* variants and outflow tract defects [49]. We identified a novel *GATA4* sequence variants in a patient with TA [38]. This variant (p.Thr330Arg) was located in a common basic region of the GATA transcription factors and resulted in disruption of the synergistic activity between *GATA4* and *NKX2-5* or *GATA6*. It has been reported that a reciprocal

regulation and a synergistic activity between *GATA4* and *NKX2-5* are essential for the expression of several cardiac-specific genes [50, 51]. Other studies have indicated that *GATA4* plays a role in cardiovascular development in collaboration with *GATA6* [52, 53] Taken together, a decrease in the synergistic and/or collaborative activity of *GATA4* with *NKX2-5* and/or *GATA6* may be implicated in TA.

51.2.2.3 NKX Transcription Factors

Homeobox-containing genes regulate tissue-specific gene expression and play roles in differentiation and patterning of tissues during development [54]. *NKX2-5*/*CSX* and *NKX2-6* were identified as vertebrate homologs of a Drosophila "tinman," a homeobox-containing gene essential for development of the heart-like dorsal vessel [55, 56].

Schott et al. reported that heterozygous variants of *NKX2-5* caused familial ASD with atrioventricular block [57]. This was the first report clearly showing that a single-gene variant could cause a nonsyndromic CHD. McElhinney et al. examined the *NKX2-5* gene in 474 patients with CHD and identified a heterozygous variant in 1 (4%) of 22 patients with TA [58]. A number of subsequent studies have indicated that variants in the homeodomain of *NKX2-5* are likely to cause ASD, whereas variants located outside the homeodomain may be associated with outflow tract defects including TA [59, 60].

By variant analyses for *NKX2-6*, Heathcote et al. identified homozygosity for a variant (F151L) in the *NKX2-6* gene in affected members of a large consanguineous Kuwaiti family with TA [61]. Ta-Shma et al. identified a homozygous truncating variant in the *NKX2-6* gene in three sibs, born of consanguineous Palestinian parents with TA [62]. These findings indicate that variants of *NKX2-5* or *NKX2-6* are the genetic cause of a minority of cases of TA.

51.2.2.4 Other Genes

To date, some genes other than *TBX*s, *GATA*s, or *NKX*s have been reported to be associated with TA, including *PLXND1*, *NRP1*, *PRKD1*, *PRDM1,* and *TMEM260* [36, 63–66]. *PLXND1* encodes a member of the plexin family of proteins that bind to semaphorins, a large family of extracellular secreted and membrane proteins. *NRP1* encodes a membrane-bound coreceptor to a tyrosine kinase receptor for both vascular endothelial growth factor and semaphorin family members. *PRKD1* encodes a serine/threonine kinase that regulates a variety of cellular functions. *PRDM1* encodes a DNA-binding transcriptional repressor. *TMEM260* encodes transmembrane protein with unknown function. Furthermore, a multicenter genome-wide study suggested de novo sequence variants of 19 genes including *TBX1*, *GATA6,* and *SEMA3C*, in 13 patients with TA [67].

51.3 Conclusion

Although human genetic studies have revealed frequent association of 22q11.2 microdeletion with TA, the etiology of most TA is still unknown. Recently, single-gene variants associated with TA are beginning to emerge. As a lesson from 22q11DS, it is important to consider the developmental spectrum of CHD and gene variants associated with other conotruncal defects, especially TOF, may also be associated with TA. Through the use of next-generation sequencing technique, we can now elucidate more genetic causes associated with TA, some of which might provide targets for prevention or genetic intervention of this CHD.

References

1. Yamagishi H, Fukuda K. Truncus arteriosus. In: Lang F, editor. Encyclopedia of molecular mechanisms of disease. Springer; 2009. Version: print (book), LXXXVI, 2270 p. 646 illus. In 3 volumes, not available separately. Hardcover ISBN: 978-3-540-67136-7.
2. Ferencz C, Correa-Villasenor A, Loffredo CA, editors. Genetic and environmental risk factors of major cardiovascular malformations: the Baltimore-Washington infant study: 1981–1989. Armonk: Futura Publishing Co; 1997.
3. Jenkins KJ, Correa A, Feinstein JA, et al. Noninherited risk factors and congenital cardiovascular defects: current knowledge: a scientific statement from the American Heart Association Council on cardiovascular disease in the young: endorsed by the American Academy of Pediatrics. Circulation. 2007;115:2995–3014.
4. Kodo K, Yamagishi H. A decade of advances in the molecular embryology and genetics underlying congenital heart defects. Circ J. 2011;75:2296–304.
5. Yamagishi H. The 22q11.2 deletion syndrome. Keio J Med. 2002;51:77–88.
6. Yamagishi H, Srivastava D. Unraveling the genetic and developmental mysteries of 22q11 deletion syndrome. Trends Mol Med. 2003;9:383–9.
7. Nora JJ, Nora AH. Update on counseling the family with a first degree relative with a congenital heart defect. Am J Med Genet. 1988;29:137–42.
8. Pierpont MEM, Gobel JW, Moller JH, et al. Cardiac malformations in relatives of children with truncus arteriosus or interruption of the aortic arch. Am J Cardiol. 1988;61:423–7.
9. Lindsay EA, Baldini A. Congenital heart defects and 22q11 deletions: which genes count? Mol Med Today. 1998;4:350–7.
10. Goldmuntz E, Clark BJ, Mitchell LE, et al. Frequency of 22q11 deletions in patients with conotruncal defects. J Am Coll Cardiol. 1988;32:492–8.
11. Maeda J, Yamagishi H, Matsuoka R, et al. Frequent association of 22q11.2 deletion with tetralogy of Fallot. Am J Med Genet. 2000;92:269–72.
12. Mlynarski EE, Xie M, Taylor D, et al. Rare copy number variants and congenital heart defects in the 22q11.2 deletion syndrome. Hum Genet. 2016;135:273–85.
13. Zhao Y, Diacou A, Johnston HR, et al. Complete sequence of the 22q11.2 allele in 1,053 subjects with 22q11.2 deletion syndrome reveals modifiers of Conotruncal heart defects. Am J Hum Genet. 2020;106:26–40.
14. Momma K, Ando M, Matsuoka R. Truncus arteriosus communis associated with chromosome 22q11 deletion. J Am Coll Cardiol. 1997;30:1067–71.
15. Lalani SR, Safiullah AM, Fernbach SD, et al. Spectrum of CHD7 variants in 110 individuals with CHARGE syndrome and genotype-phenotype correlation. Am J Hum Genet. 2006;78:303–14.
16. Lalani SR, Safiullah AM, Molinari LM, et al. SEMA3E variant in a patient with CHARGE syndrome. J Med Genet. 2004;41:e94.

17. Garcia-Barcelo M-M, Wong KK, Lui VC, et al. Identification of a HOXD13 variant in a VACTERL patient. Am J Med Genet. 2008;146A:3181–5.
18. Daw SCM, Taylor C, Kraman M, et al. A common region of 10p deleted in DiGeorge and velocardiofacial syndromes. Nat Genet. 1996;13:458–61.
19. Yamagishi H, Garg V, Matsuoka R, et al. A molecular pathway revealing a genetic basis for human cardiac and craniofacial defects. Science. 1999;283:1158–61.
20. Kunte A, Ivey C, Yamagishi C, et al. A common cis-acting sequence in the DiGeorge critical region regulates bi-directional transcription of UFD1L and CDC45L. Mech Dev. 2001;108:81–92.
21. Verloove-Vanhorick SP, Brubakk AM, Ruys JH. Extensive congenital malformations in two siblings: maternal pre-diabetes or a new syndrome? Acta Paediatr Scand. 1981;70:767–9.
22. Lewin SO, Opitz JM. Fibular a/hypoplasia: review and documentation of the fibular developmental field. Am J Med Genet. 1986;25(suppl 2):215–38.
23. Ellis IH, Yale C, Thomas R, et al. Three sibs with microcephaly, congenital heart disease, lung segmentation defects and unilateral absent kidney: a new recessive multiple congenital anomaly (MCA) syndrome? Clin Dysmorphol. 1996;5:129–34.
24. Frank V, Habbig S, Bartram MP, et al. Variants in NEK8 link multiple organ dysplasia with altered hippo signaling and increased c-MYC expression. Hum Mol Genet. 2013;22:2177–85.
25. Lindsay EA. Chromosome microdeletions: dissecting del22q11 syndrome. Nat Rev Genet. 2001;2:858–68.
26. Lindsay EA, Vitelli F, Su H, et al. Tbx1 haploinsufficiency in the DiGeorge syndrome region causes aortic arch defects in mice. Nature. 2001;410:97–101.
27. Merscher S, Funke B, Epstein JA, et al. TBX1 is responsible for cardiovascular defects in velo-cardio-facial/DiGeorge syndrome. Cell. 2001;104:619–29.
28. Garg V, Yamagishi C, Hu T, et al. Tbx1, a DiGeorge syndrome candidate gene, is regulated by sonic hedgehog during pharyngeal arch development. Dev Biol. 2001;235:62–73.
29. Yamagishi H, Maeda J, Hu T, et al. Tbx1 is regulated by tissue-specific forkhead proteins through a common sonic hedgehog-responsive enhancer. Genes Dev. 2003;17:269–81.
30. Xu H, Morishima M, Wylie JN, et al. Tbx1 has a dual role in the morphogenesis of the cardiac outflow tract. Development. 2004;131:3217–27.
31. Maeda J, Yamagishi H, McAnally J, et al. Tbx1 is regulated by forkhead proteins in the secondary heart field. Dev Dyn. 2006;235:701–10.
32. Yagi H, Furutani Y, Hamada H, et al. Role of TBX1 in human del22q11.2 syndrome. Lancet. 2003;362:1366–73.
33. Huang RT, Wang J, Xue S, et al. TBX20 loss-of-function mutation responsible for familial tetralogy of Fallot or sporadic persistent truncus arteriosus. Int J Med Sci. 2017;14:323–32.
34. Brewer A, Pizzey J. GATA factors in vertebrate heart development and disease. Expert Rev Mol Med. 2006;8:1–20.
35. Kodo K, Nishizawa T, Furutani M, et al. GATA6 variants cause human cardiac outflow tract defects by disrupting semaphoring-plexin signaling. Proc Natl Acad Sci U S A. 2009;106:13933–8.
36. Ta-Shma A, Pierri CL, Stepensky P, et al. Isolated truncus arteriosus associated with a variant in the plexin-D1 gene. Am J Med Genet A. 2013;161A:3115–20.
37. Kodo K, Shibata S, Miyagawa-Tomita S, et al. Regulation of Sema3c and the interaction between cardiac neural crest and second heart field during outflow tract development. Sci Rep. 2017;7:6771.
38. Kodo K, Nishizawa T, Furutani M, et al. Genetic analysis of essential cardiac transcription factors in 256 patients with non-syndromic congenital heart defects. Circ J. 2012;76:1703–11.
39. Maitra M, Koenig SN, Srivastava D, et al. Identification of GATA6 sequence variants in patients with congenital heart defects. Pediatr Res. 2010;68:281–5.
40. Lin X, Huo Z, Liu X, et al. A novel GATA6 variant in patients with tetralogy of Fallot or atrial septal defect. J Hum Genet. 2010;55:662–7.

41. Wang X, Ji W, Wang J, et al. Identification of two novel GATA6 mutations in patients with nonsyndromic conotruncal heart defects. Mol Med Rep. 2014;10:743–8.
42. Zhang E, Hong N, Chen S, et al. Targeted sequencing identifies novel GATA6 variants in a large cohort of patients with conotruncal heart defects. Gene. 2018;641:341–8.
43. Raghuram N, Marwaha A, Greer MC, et al. Congenital hypothyroidism, cardiac defects, and pancreatic agenesis in an infant with GATA6 mutation. Am J Med Genet A. 2020;182:1496–9.
44. Allen HL, Flanagan SE, Shaw-Smith C, et al. GATA6 haploinsufficiency causes pancreatic agenesis in humans. Nat Genet. 2011;44:20–2.
45. Yorifuji T, Kawakita R, Hosokawa Y, et al. Dominantly inherited diabetes mellitus caused by GATA6 haploinsufficiency: variable intrafamilial presentation. J Med Genet. 2012;49:642–3.
46. Stanescu DE, Hughes N, Patel P, et al. A novel variant in GATA6 causes pancreatic agenesis. Pediatr Diabetes. 2015;16:67–70.
47. Škorić-Milosavljević D, Tjong FVY, Barc J, et al. GATA6 mutations: characterization of two novel patients and a comprehensive overview of the GATA6 genotypic and phenotypic spectrum. Am J Med Genet A. 2019;179:1836–45.
48. Garg V, Kathiriya IS, Barnes R, et al. GATA4 variants cause human congenital heart defects and reveal an interaction with TBX5. Nature. 2003;424:443–7.
49. Nemer G, Fadlalah F, Usta J, et al. A novel variant in the GATA4 gene in patients with tetralogy of Fallot. Hum Mutat. 2006;27:293–4.
50. Lien CL, Wu C, Mercer B, et al. Control of early cardiac-specific transcription of Nkx2-5 by a GATA-dependent enhancer. Development. 1999;126:75–84.
51. Durocher D, Charron F, Warren R, et al. The cardiac transcription factors Nkx2-5 and GATA-4 are mutual cofactors. EMBO J. 1997;16:5687–96.
52. Charron F, Paradis P, Bronchain O, et al. Cooperative interaction between GATA-4 and GATA-6 regulates myocardial gene expression. Mol Cell Biol. 1999;19:4355–65.
53. Xin M, Davis CA, Molkentin JD, et al. A threshold of GATA4 and GATA6 expression is required for cardiovascular development. Proc Natl Acad Sci U S A. 2006;103:11189–94.
54. Shiojima I, Komuro I, Inazawa J, et al. Assignment of cardiac homeobox gene CSX to human chromosome 5q34. Genomics. 1995;27:204–6.
55. Komuro I, Izumo S. Csx a murine homeobox-containing gene specifically expressed in the developing heart. Proc Natl Acad Sci U S A. 1993;90:8145–9.
56. Newman CS, Krieg PA. Tinman-related genes expressed during heart development in Xenopus. Dev Genet. 1998;22:230–8.
57. Schott JJ, Benson DW, Basson CT, et al. Congenital heart disease caused by variants in the transcription factor NKX2-5. Science. 1998;281:108–11.
58. McElhinney DB, Geiger E, Blinder J, et al. NKX2.5 variants in patients with congenital heart disease. J Am Coll Cardiol. 2003;42:1650–5.
59. Benson DW, Silberbach GM, Kavanaugh-McHugh A, et al. Variants in the cardiac transcription factor NKX2.5 affect diverse cardiac developmental pathways. J Clin Invest. 1999;104:1567–73.
60. Akçaboy MI, Cengiz FB, Inceoğlu B, et al. The effect of p.Arg25Cys alteration in NKX2-5 on conotruncal heart anomalies: variant or polymorphism? Pediatr Cardiol. 2008;29:126–9.
61. Heathcote K, Braybrook C, Abushaban L, et al. Common arterial trunk associated with a homeodomain variant of NKX2.6. Hum Mol Genet. 2005;14:585–93.
62. Ta-Shma A, El-Lahham N, Edvardson S, et al. Conotruncal malformations and absent thymus due to a deleterious NKX2-6 variant. J Med Genet. 2014;51:268–70.
63. Shaheen R, Al Hashem A, Alghamdi MH, et al. Positional mapping of PRKD1, NRP1 and PRDM1 as novel candidate disease genes in truncus arteriosus. J Med Genet. 2015;52:322–9.
64. Ta-Shma A, Khan TN, Vivante A, et al. Mutations in TMEM260 cause a pediatric neurodevelopmental, cardiac, and renal syndrome. Am J Hum Genet. 2017;100:666–75.
65. Pagnamenta AT, Jackson A, Perveen R, et al. Biallelic TMEM260 variants cause truncus arteriosus, with or without renal defects. Clin Genet Online ahead of print. 2021;101(1):127–33.

66. Inoue T, Takase R, Uchida K, et al. The c.1617del variant of TMEM260 is identified as the most frequent single gene determinant for Japanese patients with a specific type of congenital heart disease. J Hum Genet. 2024; in press.
67. Jin SC, Homsy J, Zaidi S, et al. Contribution of rare inherited and de novo variants in 2,871 congenital heart disease probands. Nat Genet. 2017;49:1593–601.

Molecular Pathways and Animal Models of Truncus Arteriosus

52

Eleanor Gill and Simon D. Bamforth

Abstract

In normal cardiovascular development in birds and mammals, the outflow tract of the heart is divided into two distinct channels to separate the oxygenated systemic blood flow from the deoxygenated pulmonary circulation. When the process of outflow tract septation fails, a single common outflow vessel persists resulting in a serious clinical condition known as persistent truncus arteriosus or common arterial trunk. In this chapter, we will review molecular pathways and the cells that are known to play a role in the formation and development of the outflow tract and how genetic manipulation of these pathways in animal models can result in common arterial trunk.

Keywords

Persistent truncus arteriosus · Common arterial trunk · Congenital heart defects · Model organisms · Genetics · Extracellular matrix · *TBX1* · *TGFβ* · *FGF* · Neural crest cells

52.1 Introduction

The outflow tract (OFT) of the mammalian heart is formed at the arterial pole of the primary heart tube concomitant with additional contributions of cells from the second heart field (SHF). The newly formed tract interposes between the developing right ventricle and the aortic sac, the latter manifold giving rise to the pharyngeal arch arteries (PAA). Usually described as the "conotruncus," it is now recognized

E. Gill · S. D. Bamforth (✉)
Newcastle University Biosciences Institute, Newcastle, UK
e-mail: simon.bamforth@newcastle.ac.uk

© The Author(s), under exclusive license to Springer Nature Switzerland AG 2024

S. Rickert-Sperling et al. (eds.), *Congenital Heart Diseases: The Broken Heart*,
Advances in Experimental Medicine and Biology 1441,
https://doi.org/10.1007/978-3-031-44087-8_52

that it is preferable to consider the outflow tract as possessing distal, intermediate, and proximal components [1, 2]. When first formed, the OFT possesses a solitary lumen, which is then divided into the aortic and pulmonary pathways by fusion of the endocardial cushions, the precursors to the OFT valves, thus separating the intermediate and proximal components. Growth of a protrusion from the dorsal wall of the aortic sac separates the intrapericardial parts of the aortic and pulmonary trunks. The endocardial cushions and the protrusion are populated by cells migrating from the neural crest, known as neural crest cells (NCCs). Fusion between the cushions themselves, and then between the distal end of the fused cushions and the protrusion, is needed to produce complete separation of the aortic and pulmonary pathways. It is failure of fusion of the major outflow cushions that results in the persistence of a common outflow vessel, described as a common arterial trunk (CAT), but also frequently known as persistent truncus arteriosus. The intrapericardial arterial trunks themselves, however, can be well separated in some examples of CAT, indicating that growth of the protrusion from the dorsal wall of the aortic sac, which produces the aortopulmonary septum, is independent of fusion of the outflow cushions. Thus failure of fusion of the cushions provides the phenotypic feature of CAT, rather than failure of distal aortopulmonary septation. A review of the published literature on transgenic mouse models demonstrates that many genes from different molecular pathways can result in CAT (Table 52.1).

52.2 T-Box 1

Malformations of the great arteries are a major feature in 22q11 deletion syndrome (22q11DS, also known as DiGeorge, velocardiofacial, or Shprintzen syndrome). The transcription factor T-Box 1 (*TBX1)* is thought to be the main causative gene for the 22q11DS phenotype [17, 45, 46], and several animal models, including mouse and zebrafish, with mutant *Tbx1* alleles have been created, allowing this gene to be studied in great depth to understand its role in the formation and patterning of the cardiovascular system, including the PAAs (see Chap. 46). Transgenic mice null for *Tbx1* have a severe phenotype, and they die in the perinatal period with cardiovascular defects including CAT (Fig. 52.1). The segmentation of the caudal pharyngeal arches fails to proceed normally in *Tbx1*-null embryos which results in only the first and second PAAs forming. Without the caudal third and fourth PAAs the common carotid arteries and the aortic arch cannot form [48]. Although this phenotype was once assumed to be caused by a cell-autonomous role of *Tbx1* in NCCs, it was soon recognized that Tbx1 protein is not expressed within the neural crest itself. It is therefore believed that loss of *Tbx1* affects NCC migration [49–51] which leads to the failure in OFT septation in *Tbx1*-null mice.

Genetic modification of mice can be used to conditionally inactivate a gene in a temporal manner. When this is performed with *Tbx1*, the timing of expression within the developing embryo, and the consequences this has on cardiovascular development, can be ascertained. For example, when *Tbx1* is inactivated between E7.5 and E8.5 of embryonic development, PAA defects occur such as interruption of the

Table 52.1 Genes when mutated in mice, either constitutively or conditionally from neural crest cells (ΔNCC), the heart fields (ΔHF), or endothelial cells (ΔEC), that result in common arterial trunk (persistent truncus arteriosus). Other congenital cardiovascular malformations may also be seen in these mutants (e.g., interrupted aortic arch, aberrant right subclavian artery, double-outlet right ventricle)

Class	Gene	Reference
Transcription factor	*Cited2*	[3]
	Foxc1;Foxc2 (ΔNCC)	[4]
	Foxp1	[5]
	Gata3	[6]
	Gata4;Gata6	[7]
	Gata6 (ΔNCC)	[8]
	Gbx2;Pax9	[9]
	Jun	[10]
	Msx1;Msx2	[11]
	Pax3	[12]
	Pbx1	[13]
	Prdm1	[14]
	Prdm3	[15]
	Sox4	[16]
	Tbx1	[17]
	Tcfap2a	[18]
Signaling molecule	*Sema3c*	[19]
	Shh	[20]
	mTORC1(ΔNCC)	[21]
	Bcar1	[22]
Growth factor	*Fgf8*	[23]
	Vegfa	[24]
Protein binding	*Bmp4* (ΔHF)	[25]
	Chrd	[26]
	Ednra	[27]
	Flna	[28]
	Ltbp1l	[29]
	Pinch1 (ΔNCC)	[30]
Receptor	*Acvr1* (ΔNCC)	[31]
	Bmpr2	[32]
	Lrp2	[33]
	Nrp1 (ΔEC)	[34]
	Pdgfra (ΔNCC)	[35]
	Plxnd1	[36]
	Rara;Rarb, Rara;Rarc	[37]
	Rxra	[38]
	Smo (ΔSHF)	[39]
	Tgfbr1 (ΔNCC)	[40]
	Tgfbr2 (ΔNCC)	[41]
Enzyme	*Aldh1a2*	[42]
	Ece1	[43]
	Pcsk5	[44]

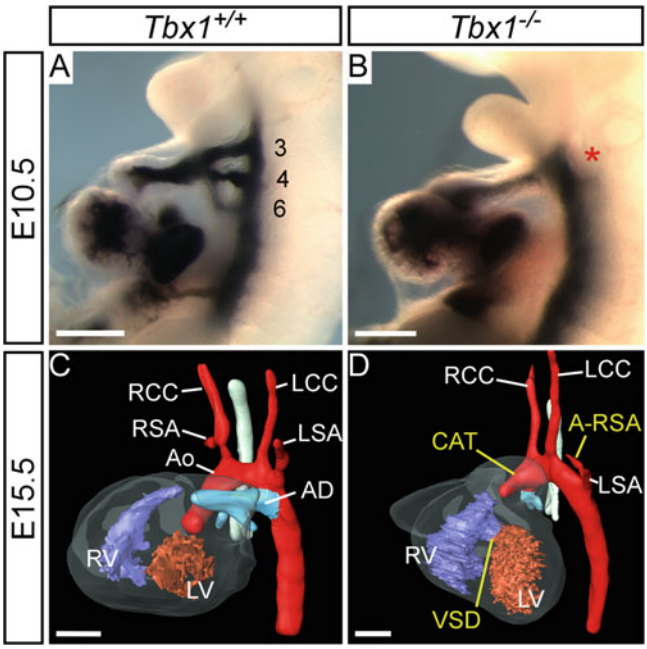

Fig. 52.1 Cardiovascular defects in *Tbx1*-null ($Tbx1^{-/-}$) mouse embryos and fetuses. **(a–b)** Injection of India ink into the heart of E10.5 embryos. **(a)** In the wild-type embryo ($Tbx1^{+/+}$) three bilaterally symmetrical PAAs are present (numbered 3, 4, and 6) which are fully patent to ink. **(b)** In the $Tbx1^{-/-}$ embryo a single outflow vessel is present (*asterisk*) revealing that the PAAs have failed to form properly. **(c–d)** 3-D reconstructions from MRI datasets [47] of E15.5 fetuses. **(c)** By E15.5 the heart and its associated great vessels have developed into the mature configuration. **(d)** The heart of a $Tbx1^{-/-}$ fetus presents with great artery defects related to the failure of the PAAs to form correctly: common arterial trunk (CAT) and aberrant right sublavian artery (A-RSA) as well as a ventricular septal defect (VSD). The heart in this fetus is abnormally rotated to the left. Abbreviations: Ao, aorta; AD, arterial duct; LCC, left common carotid; LSA, left subclavian artery; LV, left ventricle; RCC, right common carotid; RSA, right subclavian artery; RV, right ventricle. Scale, 500 μm

aortic arch (IAA) and aberrant right subclavian artery (A-RSA), but later deletion between E8.5 and E9.5 affects OFT septation, resulting in CAT [52]. Regulation of *Tbx1* gene dosage is also critical. *Tbx1* mRNA dosage levels can be controlled through a series of modified *Tbx1* alleles in mutant mice [53]. These hypomorphic alleles reveal that a critical threshold of *Tbx1* mRNA is required for correct formation of the PAAs. A reduction in *Tbx1* mRNA levels to ~20% of wild-type was sufficient to introduce the CAT phenotype. The overexpression of *Tbx1* in transgenic mice also results in cardiovascular abnormalities, including CAT and IAA [54].

As the *Tbx1*-null phenotype affects a wide range of tissues, including many of the embryonic structures derived from the pharyngeal arches and SHF, including the OFT, interventricular septum, PAAs, thymus, parathyroids, ears, and craniofacial development (reviewed in [55, 56]), it is possible that each expression domain may

contribute to different aspects of the phenotype. Therefore, conditional deletions of *Tbx1* have been used to investigate its tissue-specific requirements in the context of *Tbx1*-null embryos. Conditional deletion of *Tbx1* within the pharyngeal endoderm, ectoderm, and mesoderm, in addition to the SHF, through the use of *Nkx2.5Cre*, resulted in full recapitulation of the CAT and ventricular septal defect (VSD) phenotypes observed in $Tbx1^{-/-}$ mutants [57]. A reduced and disorganized smooth muscle cell layer surrounding the outflow tract was also observed, possibly due to the reduced proliferative activity in the SHF [57]. *Mesp1Cre*-mediated deletion of *Tbx1*, which removed the gene from all mesodermal derivatives, including the endothelium, also resulted in 100% penetrance of CAT, VSD and severe PAA malformations [51]. In addition, the segmentation of the pharynx is disrupted, resulting in the loss of the caudal pharyngeal arches, as is observed in $Tbx1^{-/-}$ mutant mice. Further defects affecting the migration of the NCCs into the pharyngeal arches, disruptions of the neural crest-derived cranial ganglia and reduced proliferation of the neural crest-derived pharyngeal arch mesenchyme, were also observed. Reactivation of *Tbx1* within the mesoderm of mutant embryos rescued the OFT and VSD phenotypes, but not the fourth PAA defects, suggesting other tissues are required in this aspect of the phenotype [51], most likely the epithelium. Deletion of *Tbx1* from the anterior component of the SHF using *Mef2c-AHF-Cre* also gives rise to the CAT phenotype, and this can be rescued by removing one allele of β-catenin in mutant mice [58]. This suggests that a negative feedback loop between canonical Wnt signaling and Tbx1 in the anterior heart field is important for OFT formation. Overexpression of *Tbx1* in the anterior heart field, however, also results in the development of the CAT phenotype [59].

Collectively, these studies demonstrate that precise *Tbx1* expression is required for correct cardiovascular development. Any perturbation to *Tbx1* mRNA levels, whether increased or decreased, and the timing of its expression, will result in defects in the OFT and aortic arch arteries. Moreover, the expression of *Tbx1* in the distinct embryonic compartments of the pharyngeal tissue and SHF control different aspects of cardiovascular development.

Sema3c mice display CAT, caused by disrupted migration of NCCs [19], and mice deficient for *Nrp1*, a transmembrane receptor for Sema3c, also present with CAT [60]. Furthermore, CAT is seen when *Nrp1* is conditionally deleted from endothelial cells [61]. Nrp1 is also a coreceptor of Vegfa, which is a genetic modifier of *Tbx1*, and *Vegfa* deficient mice also have CAT [24]. Although the CAT phenotype is seen in both *Tbx1* and *Nrp1* deficient mice, the developmental mechanisms underlying this defect in each case are distinct. The *Nrp1* mutant CAT phenotype is caused by aberrant endothelial cell and blood vessel organization, but NCC migration to the OFT is normal [34]. This is in contrast to the origins of the OFT septation defect in *Tbx1* mutants. Although *Tbx1* is expressed in the endothelium, conditional deletion from these cells does not cause any overt cardiovascular phenotype [50, 57]. The CAT defect is instead caused by failure of SHF progenitors being added to the arterial pole of the developing heart, combined with premature differentiation of the myocardial cells [62–64] resulting in a hypoplastic OFT.

Although NCC migration is also disrupted in *Tbx1*-null mice, this instead leads to arch artery defects [34, 65].

Other animal models have been employed to study the role of *Tbx1* in cardiovascular development, and Tbx1 is expressed throughout the pharyngeal regions of the frog [66], chicken [67], and zebrafish [68]. In the chicken, blocking *Cyp26a1*, a gene required for retinoic acid inactivation during embryogenesis, results in OFT defects, i.e., CAT and double-outlet right ventricle (DORV), and PAA defects similar to that seen in the mouse model of *Tbx1* loss [67]. *Tbx1* levels were downregulated, and the retinoic acid-synthesizing enzyme *Raldh2* was upregulated. Consistent with a role for Sonic hedgehog (Shh) in the regulation of Tbx1 (see Chap. 46), chick embryos exposed to Shh-soaked beads responded by upregulating Tbx1 expression in the pharyngeal arches [69].

52.3 Fibroblast Growth Factors

The fibroblast growth factors are a large group of secreted molecules with diverse roles in embryonic development and maintenance of tissues. Mice expressing a hypomorphic allele of *Fgf8* present with OFT defects such as CAT and DORV [23, 70]. The *Fgf8* receptors, *Fgfr1* and *Fgfr3*, are expressed within NCCs and are thought to be required in their migration. Plating NCCs in the presence of Fgf8 in vitro increased their migratory capacity, while inhibition of Fgfr1 both in vitro and in vivo reduced migration [71], indicating that Fgf8 signaling may therefore result in decreased NCC migration and survival within the pharyngeal arches causing DORV or, in more severe circumstances, CAT [71]. Overexpression of Fgf8 in NCCs causes these cells to be maintained in the endocardial cushions, and the mutant embryos develop CAT [72]. The fibroblast growth factors *Fgf3*, *Fgf8,* and *Fgf10* are all coexpressed with *Tbx1* and are downregulated in *Tbx1*-null mice [73–75]. Only *Fgf8*, however, appears to genetically interact with *Tbx1* in fourth PAA development [74], and within a larger genetic regulatory network involving *Six1* and *Eya1* [76]. Concomitant *Fgf3* or *Fgf10* mutation does not affect the *Tbx1* mutant cardiovascular phenotype [73].

52.4 Transforming Growth Factors

The signaling molecule transforming growth factor (TGF)-β is vital for regulating many basic cell responses and has been shown to be important for the development of the great arteries in mouse models (see Chap. 46). The TGFβ signaling pathway involves the binding of the TGFβ ligand to the cell surface TGFβ type II receptor (TGFBR2), which subsequently activates the TGFβ type I receptor, TGFBR1 (also known as ALK5). This results in the phosphorylation of SMAD2 and SMAD3 proteins, binding to SMAD4 and translocation to the nucleus to regulate downstream gene expression. Mutant mice null for the TGFβ2 ligand (*Tgfb2*) die perinatally with cardiovascular defects, which includes CAT [77, 78]. The TGFβ receptors *Tgfbr1*

and *Tgfbr2* are essential for embryogenesis as mice lacking these genes die around mid-gestation [79, 80]. Conditional alleles, however, allow for this early embryonic lethality to be avoided and the role of these genes in cardiovascular development dissected. When the *Tgfbr1* and *Tgfbr2* receptors are deleted from the neural crest using *Wnt1Cre* transgenic mice, the embryos present with CAT [40, 41, 81]. This suggests that TGFβ signaling is required for NCCs to control septation of the aorta and pulmonary trunk. CAT is also seen in embryos when the long form of latent TGF-β binding protein 1 gene (*Ltbp1*), is disrupted [29].

52.5 Additional Genes

The Pbx family of homeodomain transcription factors, *Pbx1*, *Pbx2,* and *Pbx3*, play an important role in cardiovascular development. Mice null for *Pbx1* have CAT, although *Pbx2*- and *Pbx3*-null mice do not have any cardiovascular defects [13, 82]. Mice lacking Sox4 have also been reported to display CAT [83].

52.6 Neural Crest Cells

The importance of NCCs per se in the septation of the OFT, rather than the genes expressed within them, has been demonstrated through the ablation of NCCs in the chick [84, 85]. The accessibility of this experimental model allowed for the manual removal, or ablation, of discrete segments of the embryo comprising the cardiac NCCs (cNCCs), that would result in cardiovascular defects. For example, it was found that the ablation of the cNCCs, either bilaterally or unilaterally, resulted in high proportions of embryos with CAT and VSD. In addition, smaller deletions—ablating only a single somite region unilaterally—also uncovered further, less severe OFT defects such as DORV and over-riding aorta. It was also found that bilateral deletion of a region encompassing just two somites (somites 1–2 or 2–3) resulted in 100% penetrance of CAT and VSD, while unilateral deletion of the same regions caused DORV in 40% of cases.

NCC ablation studies have also been achieved in the mouse using genetic modification allowing the specific expression of toxins (e.g., thymidine kinase and diphtheria toxin) to kill the NCCs. The first study investigating NCC ablation by inducing toxicity in those cells of the neural crest lineage utilized NCC-specific expression of the herpes simplex virus type 1 thymidine kinase suicide gene, which relies on the administration of the pro-drug ganciclovir in order to induce toxicity [86]. Thymidine kinase expression causes susceptibility to ganciclovir, which prevents the incorporation of guanosine residues into elongating DNA, which makes the cells incapable of DNA synthesis. They therefore undergo apoptosis, resulting in cell death but only in those cells having expressed thymidine kinase and also receiving ganciclovir. Administration of ganciclovir daily from E7.5 to E9.5 resulted in no embryos with normal cardiovascular development. The majority of the embryos (75%) had CAT, with the remainder presenting with DORV or over-riding

aorta. In addition, all embryos also displayed a PAA defect. A second study of NCC-ablation in the mouse used the diphtheria toxin fragment A to induce toxicity in NCCs by interfering with the RNA translation machinery and causing the cells to apoptose [87]. All affected mutant mice presented with CAT. NCCs interact with cells of the SHF as they migrate through the pharyngeal arches [88] and NCCs control the addition of SHF cells to the developing heart. When NCCs are ablated, the SHF cells proliferate excessively resulting in OFT abnormalities [89]. These studies demonstrate the direct and indirect effects of NCCs on cardiovascular development.

52.7 Environmental Effects

Exposure to environmental teratogens can also result in cardiovascular defects, with or without a genetic mutation to exacerbate the resulting phenotype. For example, when pregnant mice are exposed to hypoxia offspring with outflow tract defects are produced [90]. In support of this, when the alpha subunit of the hypoxia-inducible factor gene, *Hif-1α*, is conditionally inactivated in NCCs, embryos develop CAT [91]. Retinoic acid, the active derivative of Vitamin A, is a teratogen that can cause developmental defects. The morphogenesis of the outflow tract is sensitive to retinoic acid levels, and can result in the formation of CAT [92]. This is further supported by the finding that mouse embryos lacking the retinoic acid receptors *RARα1* and *RARβ* prevent NCC-dependent aorticopulmonary septation [93], potentially due to dysregulated *Tgfb2* expression [94]. The CAT phenotype is also seen in a mouse model of Down's syndrome combined with iron deficiency in pregnant mothers [95]. Maternal diabetes can cause complex cardiovascular abnormalities including CAT [96]. Embryos from female mice with streptozotocin (STZ)-induced diabetes present with CAT, associated with increased oxidative stress and reduced Wnt and TGFβ signaling [96].

52.8 Concluding Remarks

Correct cardiovascular development relies on a complex morphogenetic pathway to ensure that all the required tissue components are formed and remodeled precisely. When this process fails, either due to genetic or environmental consequences, cardiovascular malformations arise. Septation of the OFT is a vital component of heart development to separate the systemic and pulmonary circulations and a failure in this process results in a CAT. As described in this chapter, and demonstrated by animal models, it is clear that NCCs play a crucial role in OFT septation. The genes that are expressed within NCCs are also clearly important, but as are other genes, such as *Tbx1*, which are not expressed in NCCs. Tbx1 is expressed within the tissue layers of the pharyngeal arches, and it is through this structure that the NCC must pass to reach the OFT. This illustrates the requirement of other tissue types that are vital for controlling NCC migration to allow OFT septation to occur properly.

Acknowledgments We thank the British Heart Foundation for funding our research.

References

1. Anderson RH, Chaudhry B, Mohun TJ, Bamforth SD, Hoyland D, Phillips HM, et al. Normal and abnormal development of the intrapericardial arterial trunks in humans and mice. Cardiovasc Res. 2012;95(1):108–15.
2. Sizarov A, Lamers WH, Mohun TJ, Brown NA, Anderson RH, Moorman AF. Three-dimensional and molecular analysis of the arterial pole of the developing human heart. J Anat. 2012;220(4):336–49.
3. Bamforth SD, Braganca J, Eloranta JJ, Murdoch JN, Marques FI, Kranc KR, et al. Cardiac malformations, adrenal agenesis, neural crest defects and exencephaly in mice lacking Cited2, a new Tfap2 co-activator. Nat Genet. 2001;29(4):469–74.
4. Sanchez J, Miyake R, Cheng A, Liu T, Iseki S, Kume T. Conditional inactivation of Foxc1 and Foxc2 in neural crest cells leads to cardiac abnormalities. Genesis. 2020;58(7):e23364.
5. Wang B, Weidenfeld J, Lu MM, Maika S, Kuziel WA, Morrisey EE, et al. Foxp1 regulates cardiac outflow tract, endocardial cushion morphogenesis and myocyte proliferation and maturation. Development. 2004;131(18):4477–87.
6. Raid R, Krinka D, Bakhoff L, Abdelwahid E, Jokinen E, Karner M, et al. Lack of Gata3 results in conotruncal heart anomalies in mouse. Mech Dev. 2008;126(1–2):80–9.
7. Xin M, Davis CA, Molkentin JD, Lien CL, Duncan SA, Richardson JA, et al. A threshold of GATA4 and GATA6 expression is required for cardiovascular development. Proc Natl Acad Sci U S A. 2006;103(30):11189–94.
8. Lepore JJ, Mericko PA, Cheng L, Lu MM, Morrisey EE, Parmacek MS. GATA-6 regulates semaphorin 3C and is required in cardiac neural crest for cardiovascular morphogenesis. J Clin Invest. 2006;116(4):929–39.
9. Stothard CA, Mazzotta S, Vyas A, Schneider JE, Mohun TJ, Henderson DJ, et al. Pax9 and Gbx2 interact in the pharyngeal endoderm to control cardiovascular development. J Cardiovasc Dev Dis. 2020;7(2):20.
10. Eferl R, Sibilia M, Hilberg F, Fuchsbichler A, Kufferath I, Guertl B, et al. Functions of c-Jun in liver and heart development. J Cell Biol. 1999;145(5):1049–61.
11. Chen YH, Ishii M, Sun J, Sucov HM, Maxson RE Jr. Msx1 and Msx2 regulate survival of secondary heart field precursors and post-migratory proliferation of cardiac neural crest in the outflow tract. Dev Biol. 2007;308(2):421–37.
12. Franz T. Persistent truncus arteriosus in the splotch mutant mouse. Anat Embryol (Berl). 1989;180(5):457–64.
13. Chang CP, Stankunas K, Shang C, Kao SC, Twu KY, Cleary ML. Pbx1 functions in distinct regulatory networks to pattern the great arteries and cardiac outflow tract. Development. 2008;135(21):3577–86.
14. Robertson EJ, Charatsi I, Joyner CJ, Koonce CH, Morgan M, Islam A, et al. Blimp1 regulates development of the posterior forelimb, caudal pharyngeal arches, heart and sensory vibrissae in mice. Development. 2007;134(24):4335–45.
15. Bard-Chapeau EA, Szumska D, Jacob B, Chua BQL, Chatterjee GC, Zhang Y, et al. Mice carrying a Hypomorphic Evi1 allele are embryonic viable but exhibit severe congenital heart defects. PLoS One. 2014;9(2):e89397.
16. Schilham MW, Oosterwegel MA, Moerer P, Ya J, de Boer PAJ, van de Wetering M, et al. Defects in cardiac outflow tract formation and pro-B-lymphocyte expansion in mice lacking Sox-4. Nature. 1996;380(6576):711–4.
17. Jerome LA, Papaioannou VE. DiGeorge syndrome phenotype in mice mutant for the T-box gene, Tbx1. Nat Genet. 2001;27(3):286–91.
18. Brewer S, Jiang X, Donaldson S, Williams T, Sucov HM. Requirement for AP-2alpha in cardiac outflow tract morphogenesis. Mech Dev. 2002;110(1–2):139–49.

19. Feiner L, Webber AL, Brown CB, Lu MM, Jia L, Feinstein P, et al. Targeted disruption of semaphorin 3C leads to persistent truncus arteriosus and aortic arch interruption. Development. 2001;128(16):3061–70.
20. Washington Smoak I, Byrd NA, Abu-Issa R, Goddeeris MM, Anderson R, Morris J, et al. Sonic hedgehog is required for cardiac outflow tract and neural crest cell development. Dev Biol. 2005;283(2):357–72.
21. Nie X, Ricupero CL, Jiao K, Yang P, Mao JJ. mTOR deletion in neural crest cells disrupts cardiac outflow tract remodeling and causes a spectrum of cardiac defects through the mTORC1 pathway. Dev Biol. 2021;477:241–50.
22. Mahmoud M, Evans I, Wisniewski L, Tam Y, Walsh C, Walker-Samuel S, et al. Bcar1/p130Cas is essential for ventricular development and neural crest cell remodelling of the cardiac outflow tract. Cardiovasc Res. 2021;118(8):1993–2005.
23. Abu-Issa R, Smyth G, Smoak I, Yamamura K, Meyers EN. Fgf8 is required for pharyngeal arch and cardiovascular development in the mouse. Development. 2002;129(19):4613–25.
24. Stalmans I, Lambrechts D, De Smet F, Jansen S, Wang J, Maity S, et al. VEGF: a modifier of the del22q11 (DiGeorge) syndrome? Nat Med. 2003;9(2):173–82.
25. Liu W, Selever J, Wang D, Lu MF, Moses KA, Schwartz RJ, et al. Bmp4 signaling is required for outflow-tract septation and branchial-arch artery remodeling. Proc Natl Acad Sci U S A. 2004;101(13):4489–94.
26. Bachiller D, Klingensmith J, Shneyder N, Tran U, Anderson R, Rossant J, et al. The role of chordin/bmp signals in mammalian pharyngeal development and DiGeorge syndrome. Development. 2003;130(15):3567–78.
27. Yanagisawa H, Hammer RE, Richardson JA, Williams SC, Clouthier DE, Yanagisawa M. Role of Endothelin-1/Endothelin-a receptor-mediated signaling pathway in the aortic arch patterning in mice. J Clin Invest. 1998;102(1):22–33.
28. Feng Y, Chen MH, Moskowitz IP, Mendonza AM, Vidali L, Nakamura F, et al. Filamin a (FLNA) is required for cell–cell contact in vascular development and cardiac morphogenesis. Proc Natl Acad Sci. 2006;103(52):19836–41.
29. Todorovic V, Frendewey D, Gutstein DE, Chen Y, Freyer L, Finnegan E, et al. Long form of latent TGF-beta binding protein 1 (Ltbp1L) is essential for cardiac outflow tract septation and remodeling. Development. 2007;134(20):3723–32.
30. Liang X, Sun Y, Schneider J, Ding JH, Cheng H, Ye M, et al. Pinch1 is required for normal development of cranial and cardiac neural crest-derived structures. Circ Res. 2007;100(4):527–35.
31. Kaartinen V, Dudas M, Nagy A, Sridurongrit S, Lu MM, Epstein JA. Cardiac outflow tract defects in mice lacking ALK2 in neural crest cells. Development. 2004;131(14):3481–90.
32. Delot EC, Bahamonde ME, Zhao M, Lyons KM. BMP signaling is required for septation of the outflow tract of the mammalian heart. Development. 2003;130(1):209–20.
33. Baardman ME, Zwier MV, Wisse LJ, Gittenberger-de Groot AC, Kerstjens-Frederikse WS, Hofstra RMW, et al. Common arterial trunk and ventricular non-compaction in Lrp2 knockout mice indicate a crucial role of LRP2 in cardiac development. Dis Model Mech. 2016;9(4):413–25.
34. Zhou J, Pashmforoush M, Sucov HM. Endothelial neuropilin disruption in mice causes DiGeorge syndrome-like malformations via mechanisms distinct to those caused by loss of Tbx1. PLoS One. 2012;7(3):e32429.
35. Tallquist MD, Soriano P. Cell autonomous requirement for PDGFRalpha in populations of cranial and cardiac neural crest cells. Development. 2003;130(3):507–18.
36. Gitler AD, Lu MM, Epstein JA. PlexinD1 and semaphorin signaling are required in endothelial cells for cardiovascular development. Dev Cell. 2004;7(1):107–16.
37. Mendelsohn C, Lohnes D, Decimo D, Lufkin T, LeMeur M, Chambon P, et al. Function of the retinoic acid receptors (RARs) during development (II). Multiple abnormalities at various stages of organogenesis in RAR double mutants. Development. 1994;120(10):2749–71.

38. Gruber PJ, Kubalak SW, Pexieder T, Sucov HM, Evans RM, Chien KR. RXR alpha deficiency confers genetic susceptibility for aortic sac, conotruncal, atrioventricular cushion, and ventricular muscle defects in mice. J Clin Invest. 1996;98(6):1332–43.
39. Lin L, Bu L, Cai CL, Zhang X, Evans S. Isl1 is upstream of sonic hedgehog in a pathway required for cardiac morphogenesis. Dev Biol. 2006;295(2):756–63.
40. Wang J, Nagy A, Larsson J, Dudas M, Sucov HM, Kaartinen V. Defective ALK5 signaling in the neural crest leads to increased postmigratory neural crest cell apoptosis and severe outflow tract defects. BMC Dev Biol. 2006;6:51.
41. Choudhary B, Ito Y, Makita T, Sasaki T, Chai Y, Sucov HM. Cardiovascular malformations with normal smooth muscle differentiation in neural crest-specific type II TGFbeta receptor (Tgfbr2) mutant mice. Dev Biol. 2006;289(2):420–9.
42. Niederreither K, Vermot J, Le Roux I, Schuhbaur B, Chambon P, Dolle P. The regional pattern of retinoic acid synthesis by RALDH2 is essential for the development of posterior pharyngeal arches and the enteric nervous system. Development. 2003;130(11):2525–34.
43. Yanagisawa H, Yanagisawa M, Kapur RP, Richardson JA, Williams SC, Clouthier DE, et al. Dual genetic pathways of endothelin-mediated intercellular signaling revealed by targeted disruption of endothelin converting enzyme-1 gene. Development. 1998;125(5):825–36.
44. Szumska D, Pieles G, Essalmani R, Bilski M, Mesnard D, Kaur K, et al. VACTERL/caudal regression/Currarino syndrome-like malformations in mice with mutation in the proprotein convertase Pcsk5. Genes Dev. 2008;22(11):1465–77.
45. Lindsay EA, Vitelli F, Su H, Morishima M, Huynh T, Pramparo T, et al. Tbx1 haploinsufficieny in the DiGeorge syndrome region causes aortic arch defects in mice. Nature. 2001;410(6824):97–101.
46. Merscher S, Funke B, Epstein JA, Heyer J, Puech A, Lu MM, et al. TBX1 is responsible for cardiovascular defects in velo-cardio-facial/DiGeorge syndrome. Cell. 2001;104(4):619–29.
47. Bamforth SD, Schneider JE, Bhattacharya S. High-throughput analysis of mouse embryos by magnetic resonance imaging. Cold Spring Harb Protoc. 2012;2012(1):93–101.
48. Anderson RH, Bamforth SD. Morphogenesis of the mammalian aortic arch arteries. Front Cell Dev Biol. 2022;10:892900.
49. Calmont A, Ivins S, Van Bueren KL, Papangeli I, Kyriakopoulou V, Andrews WD, et al. Tbx1 controls cardiac neural crest cell migration during arch artery development by regulating Gbx2 expression in the pharyngeal ectoderm. Development. 2009;136(18):3173–83.
50. Zhang Z, Cerrato F, Xu H, Vitelli F, Morishima M, Vincentz J, et al. Tbx1 expression in pharyngeal epithelia is necessary for pharyngeal arch artery development. Development. 2005;132(23):5307–15.
51. Zhang Z, Huynh T, Baldini A. Mesodermal expression of Tbx1 is necessary and sufficient for pharyngeal arch and cardiac outflow tract development. Development. 2006;133(18):3587–95.
52. Xu H, Cerrato F, Baldini A. Timed mutation and cell-fate mapping reveal reiterated roles of Tbx1 during embryogenesis, and a crucial function during segmentation of the pharyngeal system via regulation of endoderm expansion. Development. 2005;132(19):4387–95.
53. Zhang Z, Baldini A. In vivo response to high-resolution variation of Tbx1 mRNA dosage. Hum Mol Genet. 2008;17(1):150–7.
54. Liao J, Kochilas L, Nowotschin S, Arnold JS, Aggarwal VS, Epstein JA, et al. Full spectrum of malformations in velo-cardio-facial syndrome/DiGeorge syndrome mouse models by altering Tbx1 dosage. Hum Mol Genet. 2004;13(15):1577–85.
55. Lindsay EA. Chromosomal microdeletions: dissecting del22q11 syndrome. Nat Rev Genet. 2001;2(11):858–68.
56. Scambler PJ. 22q11 deletion syndrome: a role for TBX1 in pharyngeal and cardiovascular development. Pediatr Cardiol. 2010;31(3):378–90.
57. Xu H, Morishima M, Wylie JN, Schwartz RJ, Bruneau BG, Lindsay EA, et al. Tbx1 has a dual role in the morphogenesis of the cardiac outflow tract. Development. 2004;131(13):3217–27.

58. Racedo SE, Hasten E, Lin M, Devakanmalai GS, Guo T, Ozbudak EM, et al. Reduced dosage of β-catenin provides significant rescue of cardiac outflow tract anomalies in a Tbx1 conditional null mouse model of 22q11.2 deletion syndrome. PLoS Genet. 2017;13(3):e1006687.
59. Hasten E, McDonald-McGinn DM, Crowley TB, Zackai E, Emanuel BS, Morrow BE, et al. Dysregulation of TBX1 dosage in the anterior heart field results in congenital heart disease resembling the 22q11.2 duplication syndrome. Hum Mol Genet. 2018;27(11):1847–57.
60. Kawasaki T, Kitsukawa T, Bekku Y, Matsuda Y, Sanbo M, Yagi T, et al. A requirement for neuropilin-1 in embryonic vessel formation. Development. 1999;126(21):4895–902.
61. Gu C, Rodriguez ER, Reimert DV, Shu T, Fritzsch B, Richards LJ, et al. Neuropilin-1 conveys semaphorin and VEGF signaling during neural and cardiovascular development. Dev Cell. 2003;5(1):45–57.
62. Liao J, Aggarwal VS, Nowotschin S, Bondarev A, Lipner S, Morrow BE. Identification of downstream genetic pathways of Tbx1 in the second heart field. Dev Biol. 2008;316(2):524–37.
63. Chen L, Fulcoli FG, Tang S, Baldini A. Tbx1 regulates proliferation and differentiation of multipotent heart progenitors. Circ Res. 2009;105(9):842–51. CIRCRESAHA.109.200295
64. Rana MS, Theveniau-Ruissy M, De Bono C, Mesbah K, Francou A, Rammah M, et al. Tbx1 coordinates addition of posterior second heart field progenitor cells to the arterial and venous poles of the heart. Circ Res. 2014;115(9):790–9.
65. Vitelli F, Morishima M, Taddei I, Lindsay EA, Baldini A. Tbx1 mutation causes multiple cardiovascular defects and disrupts neural crest and cranial nerve migratory pathways. Hum Mol Genet. 2002;11(8):915–22.
66. Ataliotis P, Ivins S, Mohun TJ, Scambler PJ. XTbx1 is a transcriptional activator involved in head and pharyngeal arch development in Xenopus laevis. Dev Dyn. 2005;232(4):979–91.
67. Roberts C, Ivins S, Cook AC, Baldini A, Scambler PJ. Cyp26 genes a1, b1 and c1 are down-regulated in Tbx1 null mice and inhibition of Cyp26 enzyme function produces a phenocopy of DiGeorge syndrome in the chick. Hum Mol Genet. 2006;15(23):3394–410.
68. Piotrowski T, Ahn DG, Schilling TF, Nair S, Ruvinsky I, Geisler R, et al. The zebrafish van gogh mutation disrupts tbx1, which is involved in the DiGeorge deletion syndrome in humans. Development. 2003;130(20):5043–52.
69. Garg V, Yamagishi C, Hu T, Kathiriya IS, Yamagishi H, Srivastava D. Tbx1, a DiGeorge syndrome candidate gene, is regulated by sonic hedgehog during pharyngeal arch development. Dev Biol. 2001;235(1):62–73.
70. Frank DU, Fotheringham LK, Brewer JA, Muglia LJ, Tristani-Firouzi M, Capecchi MR, et al. An Fgf8 mouse mutant phenocopies human 22q11 deletion syndrome. Development. 2002;129 (19):4591–603.
71. Tadros TM, Klein MD, Shapira OM. Ascending aortic dilatation associated with bicuspid aortic valve: pathophysiology, molecular biology, and clinical implications. Circulation. 2009;119(6): 880–90.
72. Tian A, Wang S, Wang H, Li N, Liu H, Zhou H, et al. Over-expression of Fgf8 in cardiac neural crest cells leads to persistent truncus arteriosus. J Mol Histol. 2021;52(2):351–61.
73. Aggarwal VS, Liao J, Bondarev A, Schimmang T, Lewandoski M, Locker J, et al. Dissection of Tbx1 and Fgf interactions in mouse models of 22q11DS suggests functional redundancy. Hum Mol Genet. 2006;15(21):3219–28.
74. Vitelli F, Taddei I, Morishima M, Meyers EN, Lindsay EA, Baldini A. A genetic link between Tbx1 and fibroblast growth factor signaling. Development. 2002;129(19):4605–11.
75. Arnold JS, Werling U, Braunstein EM, Liao J, Nowotschin S, Edelmann W, et al. Inactivation of Tbx1 in the pharyngeal endoderm results in 22q11DS malformations. Development. 2006;133(5):977–87.
76. Guo C, Sun Y, Zhou B, Adam RM, Li X, Pu WT, et al. A Tbx1-Six1/Eya1-Fgf8 genetic pathway controls mammalian cardiovascular and craniofacial morphogenesis. J Clin Invest. 2011;121(4):1585–95.
77. Bartram U, Molin DG, Wisse LJ, Mohamad A, Sanford LP, Doetschman T, et al. Double-outlet right ventricle and overriding tricuspid valve reflect disturbances of looping, myocardialization,

endocardial cushion differentiation, and apoptosis in TGF-beta(2)-knockout mice. Circulation. 2001;103(22):2745–52.
78. Molin DG, DeRuiter MC, Wisse LJ, Azhar M, Doetschman T, Poelmann RE, et al. Altered apoptosis pattern during pharyngeal arch artery remodelling is associated with aortic arch malformations in Tgfbeta2 knock-out mice. Cardiovasc Res. 2002;56(2):312–22.
79. Larsson J, Goumans MJ, Sjostrand LJ, van Rooijen MA, Ward D, Leveen P, et al. Abnormal angiogenesis but intact hematopoietic potential in TGF-beta type I receptor-deficient mice. EMBO J. 2001;20(7):1663–73.
80. Oshima M, Oshima H, Taketo MM. TGF-beta receptor type II deficiency results in defects of yolk sac hematopoiesis and vasculogenesis. Dev Biol. 1996;179(1):297–302.
81. Wurdak H, Ittner LM, Lang KS, Leveen P, Suter U, Fischer JA, et al. Inactivation of TGFbeta signaling in neural crest stem cells leads to multiple defects reminiscent of DiGeorge syndrome. Genes Dev. 2005;19(5):530–5.
82. Stankunas K, Shang C, Twu KY, Kao SC, Jenkins NA, Copeland NG, et al. Pbx/Meis deficiencies demonstrate multigenetic origins of congenital heart disease. Circ Res. 2008;103 (7):702–9.
83. Ya J, Schilham MW, de Boer PA, Moorman AF, Clevers H, Lamers WH. Sox4-deficiency syndrome in mice is an animal model for common trunk. Circ Res. 1998;83(10):986–94.
84. Kirby ML, Turnage KL 3rd, Hays BM. Characterization of conotruncal malformations following ablation of "cardiac" neural crest. Anat Rec. 1985;213(1):87–93.
85. Kirby ML, Waldo KL. Neural crest and cardiovascular patterning. Circ Res. 1995;77(2):211–5.
86. Porras D, Brown CB. Temporal-spatial ablation of neural crest in the mouse results in cardiovascular defects. Dev Dyn. 2008;237(1):153–62.
87. Olaopa M, Zhou H-m, Snider P, Wang J, Schwartz RJ, Moon AM, et al. Pax3 is essential for normal cardiac neural crest morphogenesis but is not required during migration nor outflow tract septation. Dev Biol. 2011;356(2):308–22.
88. Hutson MR, Kirby ML. Neural crest and cardiovascular development: a 20-year perspective. Birth Defects Res C Embryo Today. 2003;69(1):2–13.
89. Waldo KL, Hutson MR, Stadt HA, Zdanowicz M, Zdanowicz J, Kirby ML. Cardiac neural crest is necessary for normal addition of the myocardium to the arterial pole from the secondary heart field. Dev Biol. 2005;281(1):66–77.
90. Shi H, O'Reilly VC, Moreau JL, Bewes TR, Yam MX, Chapman BE, et al. Gestational stress induces the unfolded protein response, resulting in heart defects. Development. 2016;143(14): 2561–72.
91. Kenchegowda D, Liu H, Thompson K, Luo L, Martin SS, Fisher SA. Vulnerability of the developing heart to oxygen deprivation as a cause of congenital heart defects. J Am Heart Assoc. 2014;3(3):e000841.
92. Yasui H, Nakazawa M, Morishima M, Miyagawa-Tomita S, Momma K. Morphological observations on the pathogenetic process of transposition of the great arteries induced by retinoic acid in mice. Circulation. 1995;91(9):2478–86.
93. Jiang X, Choudhary B, Merki E, Chien KR, Maxson RE, Sucov HM. Normal fate and altered function of the cardiac neural crest cell lineage in retinoic acid receptor mutant embryos. Mech Dev. 2002;117(1–2):115–22.
94. Li P, Pashmforoush M, Sucov HM. Retinoic acid regulates differentiation of the secondary heart field and TGFbeta-mediated outflow tract septation. Dev Cell. 2010;18(3):480–5.
95. Kalisch-Smith JI, Ved N, Szumska D, Munro J, Troup M, Harris SE, et al. Maternal iron deficiency perturbs embryonic cardiovascular development in mice. Nat Commun. 2021;12(1): 3447.
96. Zhao Z. TGFbeta and Wnt in cardiac outflow tract defects in offspring of diabetic pregnancies. Birth Defects Res B Dev Reprod Toxicol. 2014;101(5):364–70.

Part XIV

Tricuspid Atresia and Univentricular Heart

Clinical Presentation and Therapy of Tricuspid Atresia and Univentricular Heart

53

Nikolaus A. Haas, David J. Driscoll, and Silke Rickert-Sperling

53.1 Introduction

Although the terms "single ventricle" and "univentricular heart" are frequently used to describe a variety of complex congenital heart defects, in fact, nearly all hearts have two ventricles, although one of the two may be too small to be functional. A better term for these hearts would therefore be "functional single ventricle."

Within the spectrum of "functional single ventricle," one could include tricuspid atresia, double-inlet left ventricle, common (single) ventricle, mitral atresia with ventricular septal defect, double-outlet right ventricle with straddling atrioventricular valve, imbalanced AVSDs, cc-TGA with hypoplastic LV, and hypoplastic left ventricle among others. In addition, there will be a large variety of the position and presence of the aorta and pulmonary arteries and the function of the valves. The principles outlined for the management of tricuspid atresia can be applied to the management of other forms of functional single ventricle.

N. A. Haas (✉)
Department of Pediatric Cardiology and Intensive Care, Ludwig Maximilians University, Munich, Germany
e-mail: Nikolaus.haas@med.uni-muenchen.de

D. J. Driscoll
Division of Pediatric Cardiology, Department of Pediatrics, Mayo Clinic College of Medicine, Rochester, MN, USA
e-mail: driscoll.david@mayo.edu

S. Rickert-Sperling
Cardiovascular Genetics, Charité – Universitätsmedizin Berlin, Berlin, Germany
e-mail: silke.sperling@charite.de

© The Author(s), under exclusive license to Springer Nature Switzerland AG 2024

S. Rickert-Sperling et al. (eds.), *Congenital Heart Diseases: The Broken Heart*,
Advances in Experimental Medicine and Biology 1441,
https://doi.org/10.1007/978-3-031-44087-8_53

53.2 Pathologic Physiology

In tricuspid atresia, there is no direct communication between the right atrium and the right ventricle (Fig. 53.1). The initial survival of infants with tricuspid atresia depends upon the presence of an interatrial communication to allow egress of blood from the right atrium to the left atrium. Tricuspid atresia occurs in combination with normally related or transposed great arteries and with or without pulmonary stenosis or atresia. In most forms, there is a VSD to allow blood flow to the hypoplastic RV.

The clinical presentation, physiologic manifestations, and treatment for all forms of Tricuspid atresia and other functional single ventricle defects depend, to a large extent, on the relationship of the great arteries (normal or transposed), the presence or absence of pulmonary stenosis or atresia, the presence or absence of adequate systemic circulation (coarctation) and the size of an interatrial communication.

53.3 Clinical Presentation

Infants with tricuspid atresia and functional single ventricle usually present with cyanosis and frequently have a murmur. However, the degree of cyanosis will be dependent upon the volume of pulmonary blood flow which, in turn, is related to the degree of pulmonary and/or subpulmonary obstruction. The greater the obstruction, the more severe will be the cyanosis. In patients with pulmonary atresia, there is a duct dependent pulmonary circulation. With unimpeded pulmonary blood flow, the patient can be quite pink but present with signs and symptoms of congestive heart failure. In patients with severe coarctation, the initial presentation may be sepsis like in cardiogenic shock.

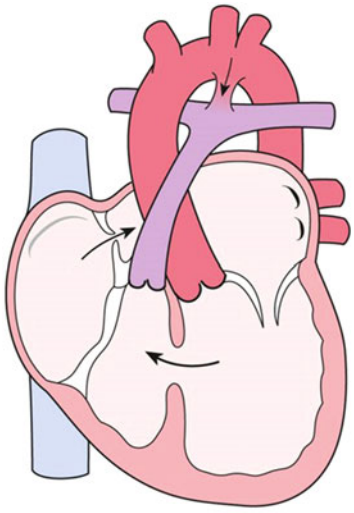

Fig. 53.1 Tricuspid atresia. Absence of the tricuspid valve showing blood flow through atrial and ventricular septal defects. Reproduced from Kinderkardiologie, Georg Thieme Verlag, N. Haas, U. Kleideiter, 2011

53.4 Physical Examination

The physical examination varies according to the underlying condition. In patients with an elevated pulmonary blood flow, cardiac precordial impulse may be overactive. The presence of a systolic ejection murmur can result from associated pulmonary or subpulmonary stenosis. One may hear a systolic murmur or systolic–diastolic continuous murmur created by flow through patent ductus arteriosus (PDA). A mid-diastolic apical cardiac murmur may be present, particularly if there is increased pulmonary blood flow and congestive heart failure. The pulses may be weak or absent in coarctation. If there is a general pulse oximetry screening in place, most children will be picked up by saturations below 94%. For patients with tricuspid atresia (TA) or hypoplastic left hearts (HLHS), the electrocardiogram is quite helpful in suggesting this diagnosis. It is characterized by left axis deviation (TA) or right axis deviation respectively (HLHS).

53.5 Diagnostic Imaging

Echocardiography is an accurate diagnostic tool for evaluating all variants of univentricular hearts in neonates and children, including the detection of other associated malformations. A segmental approach is used, systematically assessing the anatomy and position of the atria, atrioventricular valves, ventricles, septum, and great vessels. It allows for the assessment of the right ventricular outflow tract obstruction, size of pulmonary arteries, and exclusion of potential systemic circulation obstructions.

A chest radiograph can complement the evaluation by providing information on the position of the heart and assessing pulmonary perfusion. Unequal or inadequate lung perfusion may be visible in cases of severe pulmonary artery stenosis.

Diagnostic cardiac catheterization is generally unnecessary for the diagnosis of univentricular hearts, given the availability of echocardiography. However, it may be required for angiography to define the anatomy of abnormal pulmonary venous drainage and to perform interventional procedures for palliation prior to surgery.

While magnetic resonance imaging (MRI) is not typically used in the primary diagnosis or management of children with univentricular hearts, it can be helpful during follow-up management to assess the cardiac anatomy and function.

Computer tomography (CT) can provide detailed anatomical information similar to MRI but with higher resolution for smaller vessels. CT scans may be employed to define the anatomy of pulmonary venous drainage or major aortopulmonary collateral arteries in preparation for surgery, particularly when three-dimensional models are needed to optimize treatment strategies.

53.6 Treatment

The initial management of babies with tricuspid atresia or other forms of functional single ventricle depends strictly on the anatomical variant. In babies with duct dependent pulmonary blood supply, a continuous infusion of prostaglandin E1 has to be administered to maintain ductal patency. In those with duct-dependent systemic perfusion, the same principle applies. Those with unlimited systemic and pulmonary perfusion will require treatment for congestive heart failure, as pulmonary perfusion will increase over the next weeks due to the reduction of pulmonary vascular resistance. If present, afterload reduction, betablockers, digitalis and diuretics are used. Rarely, in tricuspid atresia or mitral atresia or hypoplastic left heart syndrome, the interatrial communication is too small for adequate egress of blood from the right atrium (for tricuspid atresia), or from the left atrium (for mitral atresia and hypoplastic left heart syndrome); a balloon atrial septostomy may be necessary to enlarge this communication.

After initial stabilization, extensive counseling is recommended for the families if further treatment is an option. Palliative care may be chosen for many forms of univentricular hearts because of the unfavorable long-term outcome.

If a therapeutic approach is decided, the next steps include a three step approach to establish the so called Fontan circulation as palliative management strategy for univentricular hearts. This includes:

A. At neonatal age: establishing an unobstructed systemic perfusion, balanced pulmonary perfusion and unobstructed pulmonary venous return. This includes a surgical shunt insertion or interventional PDA stenting in duct dependent pulmonary circulation, a PA banding in unobstructed pulmonary blood flow, an arch repair or coarctation repair if obstructed and redirection of total pulmonary venous return is present. As the univentricular heart has to supply the pulmonary circulation and the body (volume load), the saturation will be around 80–85% (cyanosis).
B. At the age of 3–6 months: surgical connection of the superior vena cava to the (right) pulmonary artery (i.e., so-called partial cavopulmonary connection, PCPC) bidirectional Glenn operation or Hemi-Fontan operation). This will lead to a complete unloading of the ventricle, the cyanosis will persist.
C. At the age of about 3 years: connection of the blood flow of the inferior vena cava to the pulmonary artery. This will reduce the cyanosis and create nearly normal saturations. This step is called total cavopulmonary connection (TCPC) or the Fontan operation in which GORE-TEX tube (extracardiac Fontan) or intracardiac patch (intracardiac Fontan) is used to accomplish this procedure.

Since its original description, the Fontan operation (Fig. 53.2) has undergone numerous modifications. The goal of the Fontan operation is to direct all of the systemic venous return (blue blood) to the pulmonary artery without passing through a ventricle. There will be a substantial rise in the central venous pressure as this now equals the pressure in the pulmonary artery. In some patients a small communication

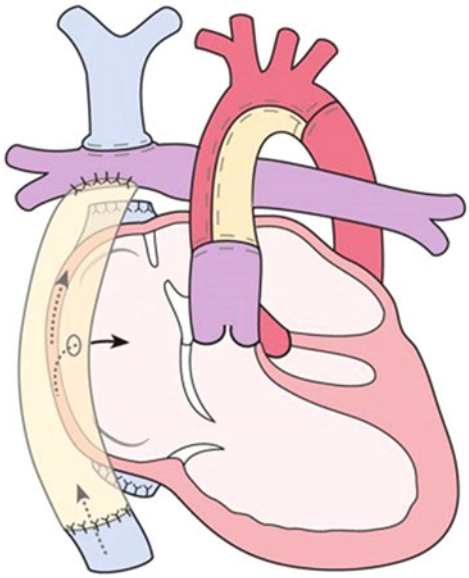

Fig. 53.2 Illustration of the modified extracardiac Fontan operation. The superior vena cava has been disconnected from the right atrium and anastomosed to the right pulmonary artery. A graft has been interposed between the inferior vena cava and the left pulmonary artery. This graft also has been anastomosed in a side-to-side fashion with the right pulmonary artery. Permanent pacemaker leads have been attached to the right atrial appendage and the ventricle. Reproduced from Kinderkardiologie, Georg Thieme Verlag, N. Haas, U. Kleideiter, 2011

("fenestration") is created between the inferior vena cava to pulmonary artery connection and the pulmonary venous atrium. Patients who have had a "fenestrated Fontan" operation continue to have a right-to-left shunt and are mildly cyanotic. The fenestration reduces some of the postoperative complications and may reduce the risk of late development of protein-losing enteropathy.

53.7 Outcome

The outcome after the various steps of the Fontan operation depends upon the number of disadvantageous factors for the Fontan operation that existed prior to the Fontan operation. Complex neonatal surgery has a mortality of up to 20–30%, there is some interstage mortality of about 5–10%, the surgical mortality in Glenn operation and Fontan completion is both about 5%.

From a hemodynamic point of view, there are some ideal preconditions for an optimal function of the Fontan circulation. Since patients with tricuspid atresia or single ventricle have only one functional ventricle, this ventricle is used to pump blood into the aorta. There is no ventricle to pump blood into the pulmonary artery. For blood to flow into the pulmonary artery, the pulmonary arteries have to be unobstructed and of normal size and there must be normal pulmonary arterial resistance. In addition, left ventricle filling pressure and ejection fraction must be normal, and there must be no significant mitral valve stenosis or insufficiency. It is preferable if there are no significant abnormalities of systemic and venous return. It is advantageous for these patients to have sinus rhythm.

The long-term survival for patients who are ideal candidates for the Fontan operation is excellent and may exceed 85% 10 years after operation, i.e., before they enter puberty. Thereafter exercise capacity continuously decreases and will reach a maximum of about 50% of normal in ideal candidates. As the number of disadvantageous factors for the Fontan operation increase, however, the long-term outcome worsens and most patients will suffer from heart failure and will be potential candidates for cardiac transplantation. There are numerous long-term complications after the Fontan operation; they include atrial arrhythmias, protein-losing enteropathy, liver cirrhosis, hepatocellular carcinoma, plastic bronchitis and left ventricular dysfunction.

In addition to the cardiovascular problems listed here, there is a large proportion of cerebral, psychiatric, psychosocial, and familiar problems associated with even "hemodynamically uncomplicated" Fontan patients that have to be addressed and play a role in parental counseling.

Human Genetics of Tricuspid Atresia and Univentricular Heart

54

Abdul-Karim Sleiman, Liane Sadder, and George Nemer

Abstract

Tricuspid atresia (TA) is a rare congenital heart condition that presents with a complete absence of the right atrioventricular valve. Because of the rarity of familial and/or isolated cases of TA, little is known about the potential genetic abnormalities contributing to this condition. Potential responsible chromosomal abnormalities were identified in exploratory studies and include deletions in 22q11, 4q31, 8p23, and 3p as well as trisomies 13 and 18. In parallel, potential culprit genes include the *ZFPM2*, *HEY2*, *NFATC1*, *NKX2-5*, *MYH6,* and *KLF13* genes. The aim of this chapter is to expose the genetic components that are potentially involved in the pathogenesis of TA in humans. The large variability in phenotypes and genotypes among cases of TA suggests a genetic network that involves many components yet to be unraveled.

Keywords

Tricuspid atresia · Univentricular heart · Atrioventricular valve · AV valve · ZFPM2 · FOG2 · HEY2 · NFATC1 · NKX2-5 · MYH6 · KLF13 · Alagille syndrome · Transposition of the great arteries · TGA · Ellis–van Creveld syndrome · Cardiac progenitor cells · Mesoderm · Endocardium · Epicardium · Myocardium · Endocardial cushions · 22q11 deletion · Trisomy 13 · Trisomy 18 · NFATC1 · Atrial septal defect · ASD · Ventricular septal defect · VSD

A.-K. Sleiman · L. Sadder
Faculty of Medicine, American University of Beirut, Beirut, Lebanon

G. Nemer (✉)
Faculty of Medicine, American University of Beirut, Beirut, Lebanon

College of Health and Life Sciences, Hamad bin Khalifa University, Doha, Qatar
e-mail: gn08@aub.edu.lb; gnemer@hbku.edu.qa

© The Author(s), under exclusive license to Springer Nature Switzerland AG 2024

S. Rickert-Sperling et al. (eds.), *Congenital Heart Diseases: The Broken Heart*,
Advances in Experimental Medicine and Biology 1441,
https://doi.org/10.1007/978-3-031-44087-8_54

54.1 Introduction

The evaluation of human genetics that characterize the pathogenesis of tricuspid atresia (TA) is ongoing, yet no single genetic or chromosomal defect has been singled out, and new candidate variants in genes are being discovered In this chapter, the embryological pathways of human heart valve development will be described and the different genetic and chromosomal abnormalities that may interrupt this intricate process will be highlighted.

54.2 Clinical Genetics

Tricuspid atresia (TA) constitutes 1–3% of all congenital heart defects [1]. A compilation of 11 studies revealed a mean incidence of TA of 0.079/1000 live births with an interquartile range of 0.024–0.118. TA has no sex predilection, and the recurrence risk for TA in siblings is relatively low (1%) and may be considered insignificant [2–4].

TA is classified into two types based on the presence or absence of transposed great arteries. Type I displays normally related great arteries and constitutes 66% of TA cases, whereas type II displays transposition of great arteries (dextro or levo) and comprises the remaining TA cases [5, 6]. Although TA can arise in an isolated form, it is also commonly associated with other cardiac anomalies, including atrial and ventricular septal defects (ASD/VSD) and patent ductus arteriosus (PDA). Less commonly associated conditions include Alagille syndrome and Ellis–van Creveld (EVC) syndrome. Transposition of the great arteries (TGA), on the other hand, is a condition where irregular twisting of the aorticopulmonary septum leads to an abnormal morphology, with the aorta originating from the right ventricle and the pulmonary artery from the left ventricle.

The reason behind concurrence of TGA with TA is still unclear. Alagille syndrome is an autosomal dominant disorder in which the renal, cardiac, hepatic, skeletal, and visual systems are affected [7]. It has been associated with TA due to a common involvement with *HEY2* mutations [8, 9]. Finally, EVC syndrome is an uncommon autosomal recessive condition that reflects a form of chondroectodermal dysplasia. The reasoning behind coexistence of EVC and TA has not yet been delineated. TA is also notably associated with other cardiac defects in siblings and relatives including Ebstein's anomaly, tetralogy of Fallot, truncus arteriosus communis, ASD, mitral valve prolapse, and unspecified cardiovascular malformations without TA.

54.3 Embryology

A review of the embryology of the heart is essential to the understanding of TA and the underlying molecular and genetic pathways. During the course of embryological heart development, bilateral cardiac progenitor cells originate from the mesoderm,

the fusion of which forms the primitive heart tube. This further differentiates into the endocardium and myocardium and is followed by formation of the epicardium from surrounding mesodermal tissue [10, 11].

Development of the atrioventricular valves is initiated by the formation of endocardial cushions. Mesenchymal proliferation from the anterior and posterior walls of the atrioventricular opening creates two elevations, referred to as endocardial cushions. Subsequently, these cushions will grow and fuse to form the definitive tricuspid and mitral valves, on the right and left side of the heart, respectively. Although the endocardial cushions play a large role in AV valve formation, myocardial remodeling also is implicated in the process [12, 13]. Specifically in TA, an endocardial-lined "dimple" marks the site of the absent tricuspid valve [14].

Notably, appropriate AV valve development is regulated by a large spectrum of genetic mechanisms and pathways, reflecting the susceptibility of this process to gene mutation and anomalous outcomes. The causes and predispositions of TA are numerous and complex. There is no indication of a single genetic, chromosomal, or environmental determinant for this condition. But specific genetic and chromosomal entities orchestrate the abnormal development of a fetal heart with TA.

54.4 Associated Chromosomal Defects

Although often demonstrated through single cases and small samples, the chromosomal defects implicated in TA are diverse, reflecting the intricacy of genotype–phenotype relationship in fetal heart development.

54.4.1 22q11 Deletions

Deletions on chromosome 22q11 can have adverse effects on any of the 30–40 genes present in that region, many of which are not studied yet. The diverse possibilities and combinations of resulting phenotypes led to the categorization of these syndromes into broader terms including DiGeorge syndrome, conotruncal anomaly face syndrome, and velocardiofacial syndrome. All anomalies fall under the more general umbrella term of 22q11 deletion syndrome—a condition of cardiac abnormality, craniofacial irregularity, thymic aplasia, and hypocalcemia/hypoparathyroidism [15, 16].

The first case reported with a microdeletion on chromosome 22q11 and TA with a common arterial trunk was in 2003 [16]. Recently, association was confirmed between deletions at chromosome 22q11 and TA phenotypes, the likelihood of 22q11 del. in TA being around 7%. Cases of sporadic hemizygous 22q11 microdeletion present with TA associated with other cardiac abnormalities such as VSD, TGA, PDA, and pulmonic stenosis have been reported [17, 18]. This indicates an overlap between 22q11 microdeletion genotypes and subsequent cardiac phenotypes. Del22q11.2 exhibits an increased risk of sibling recurrence, whereas congenital cardiac anomalies in general are not associated with an increased risk of

del22q11.2 in subsequent siblings. Although the pathogenesis of the TA phenotype due to 22q11 microdeletion has not been elucidated, there is significant indication of co-occurrence between the two.

54.4.2 Trisomies and Other Chromosomal Defects

TA has been reported with trisomies 13 and 18 [19]. Other chromosomal defects associated with TA include mutations on chromosomes 3, 4, and 8. Terminal deletions on the long arm of chromosome 4 at breakpoint 4q31—probably affecting the NFκB pathway—have been reported with congenital heart defects including left-sided vena cava, anomalous aortic arch, and TA [20]. Similarly, partial deletion of the short arm of chromosome 3 (3p)—possibly through affecting the transforming growth factor beta receptor TGFBR2—has been reported with double orifice mitral valve, complete atrioventricular canal, and TA [21]. Such relationships between chromosomal deletions and TA have been reported with interstitial deletions at chromosome 8p23.1, which harbors the GATA-binding protein 4 (*GATA4*) gene that plays a pivotal role in heart development [22].

54.5 Genes

Many of the genes involved in TA were identified thanks to the advances in prenatal diagnosis and whole-genome/exome sequencing [23, 24]. Most recently suggested is a common pathway that is based on subjects with nonsyndromic TA. The pathway begins with TGF-β (transforming growth factor beta) and RANKL (receptor activator of nuclear factor kappa-B ligand) signaling, involves the expression of NFATC1 via NFκB activity and NFATC1 transcription factor function regulation by a complex including TAB2 (TGF-beta activated kinase 1 (MAP 3 K7) binding protein 2) [25]. Whether TGF-β, RANKL, or TAB2 are directly involved in the development of TA is yet to be confirmed.

54.5.1 ZFPM2 (FOG2)

ZFPM2, also known as *FOG* (friend of GATA) family member 2, encodes a zinc finger protein; it maps to chromosome 8q22 and is mainly expressed in the human heart, brain, and testes. ZFPM2 presents significant modulation of cardiac GATA protein activity throughout development, interacting directly with the N-terminal zinc finger of these proteins, both in vivo and in vitro [26, 27]. A chief function of transcription factor GATA4 is the regulation of genes that are essential for complete myocardial differentiation, as indicated by its significant expression in the yolk sac endoderm and the mesodermal cells involved in heart development. Other functions of ZFPM2 include the maintenance of epithelial cell differentiation in the mammary gland, as well as interactions with GATA1, a transcriptional activator ensuring the

normal development of hematopoietic cell lineages, and with C-terminal binding protein 2 (*CTBP2*), a corepressor of diverse transcription factors [28].

ZFPM2 is co-expressed with GATA4 in the developing heart. Although *Zfpm2−/−* genotypes are implicated in the occurrence of TA in mice [29] (see Chap. 44), evaluation of the possible genetic mechanisms involved in human TA etiology is still underway. Some sequence variations in human *ZFPM2* (exon 8) are controversially associated with TA since they are also found in healthy individuals [30, 31].

54.5.2 HEY2

The *HEY* genes encode nuclear proteins of the hairy and enhancer-of-split related family with YRPW motif, which are known direct transcriptional targets of the Notch signaling pathways in *Drosophila* and vertebrates [32, 33]. The *HEY2* gene is a homologue of the zebrafish "gridlock gene," which is expressed during cardiac development prior to vessel formation and contributes to the arterial-venous cell fate decision. HEY2 is a suspected repressor of transcription downstream of Notch signaling in cardiac development. It is expressed in the embryonic heart, mainly in developing ventricles and arteries. Studies on *Hey2* mutant mice showed a weak association with TA (see Chap. 44). Still, there is potential correlation between TA and the specific single-nucleotide polymorphisms (SNPs) in the coding regions of *HEY2* [34].

54.5.3 NFATC1

NFATC1, also known as nuclear factor of activated T cells, is a DNA-binding protein which functions primarily in the regulation of T-cell activation and IL-2 expression alongside other heterologous transcription factors [35, 36]. It belongs to the Rel/NFkB family of transcription factors and is an essential player in endocardial cushion formation and remodeling as demonstrated by *Nfatc1−/−* knockout mice [37].

Two missense heterozygous SNPs in exons 2 (p.Pro66Leu) and 8 (p.Ile701Leu) of *NFATC1* have occurred in one patient with TA, concomitantly resulting in an 80% failure of NFATC1 translocation to the nucleus, while single mutations have no effect. Additionally, DNA-binding affinity and promoter activation is decreased in single and double mutant forms [38].

An unusual allele with 44 additional nucleotides bearing 6 SNPs contrasts the normal genotype that bears 4 SNPs repeated twice at 56 nucleotides downstream of the 3′ boundary of exon 7 with the intronic region [39]. However, the lack of homozygosity of this unique allele in TA subjects hinders the understanding of its contribution to the pathogenesis of TA.

Also, a single heterozygous SNP (p.Asp322Asn) was found in two nontwin sibling fetuses, aborted due to TA. The mutated *NFATC1* had lower expression

than the wild type and the transcriptional activity of NFATC1 was negatively impacted by the mutation [40].

54.5.4 NKX2-5

NKX2-5 is a human, homeobox-containing gene that is involved in regulating anatomical development and is exclusively expressed in cardiac cells. Homologues in Drosophila and mice have demonstrated major roles in cardiac differentiation in their respective species, suggesting a role of *NKX2-5* in human heart formation. It also was uncovered that *NKX2-5* has strong interactions with TBX5, a T-box containing transcription factor associated with Holt–Oram syndrome—an autosomal dominant disorder that affects the extremities and the heart. *NKX2-5* and *TBX5* synergistically activate the expression of a gene-encoding cardiac-specific natriuretic peptide precursor type A (*NPPA*) [41].

In mice, *Nkx2-5* serves an important role as a transcription factor, directing the expression of certain ion channel genes involved in cardiac conduction and contraction. It contributes to the AV node development and atrial septal formation. Numerous mutations in humans were identified as being the underlying cause for familial atrial septal defects. Two siblings with *NKX2-5* p.Arg190Leu recently were found to have TA in addition to ASD-II and VSD. Like other *NKX2-5* mutations at the same position, this mutation is suspected to reduce the DNA-binding activity of NKX2-5 but offers no clues as to its role in the malformation of the tricuspid valve [42].

A second mutation in *NKX2-5* in a patient with complex CHD including TA results in a premature stop codon and thus a truncated protein (255 amino acid residues rather than 292) but with an intact homeodomain indicates that the phenotype is likely due to a change in the affinity of the NKX2-5 protein to other transcriptional partners [42].

Evidently, the role of *NKX2-5* mutations in the abnormal development of the tricuspid valve elucidates the intricacy of this process, as we continue to explore the involvement of specific transcriptional factors it may interact with.

54.5.5 MYH6

MYH6 is a gene that codes for a potent ATPase represented by myosin alpha heavy chain subunits in cardiomyocytes. It is an important factor in heart development that is predominantly expressed in atrial muscle [43–45].

MYH6 p.Ala230Pro variant significantly contributes to the cardiac phenotype of several aberrant heart morphologies. The variant was identified in the concurrence of TA, valvular and supravalvular pulmonary stenosis, hypoplastic right ventricle, and ASD. The same allele was observed in family members with different cardiac malformations or none at all. The alanine at position 230 is located in the motor domain of MYH6 and consequently affects the kinetic coupling of nucleotide binding in muscle myosin molecules. This, in turn, results in an altered affinity

toward actin during the ATPase cycle. However, the effect this mutation has on the formation of the tricuspid vale is uncertain since MYH6 is restricted to the myocardium.

A MYH6 p.Glu501Stop variant has been identified in the presence of TA, restrictive ventricular septal defect, and hypoplastic right ventricle. It is a nonsense mutation thought to generate a truncated myosin peptide with missing lower domains (50 and 20 kDa) and neck and rod regions. The resulting protein retains most of the actin and nucleotide-binding capacities yet still exhibits other motor dysfunctions [44].

54.5.6 KLF13

Kruppel-like factor 13 (*KLF13*) maps to chromosome 15; it is a member of the KLF family of transcription factors that typically harbor three zinc finger DNA-binding domains. These domains activate or inhibit downstream target expression by preferential binding to GC/GT rich sequences in gene promoters and enhancer regions. KLF13 has been implicated as a cardiac transcription factor in association with other cardiac factors that are highly expressed in embryologic endocardial and myocardial tissues, including GATA4 and TBX5. KLF13 allele knockout studies in Xenopus embryos demonstrated valve immaturity, septal defects and hypotrabeculation, further implicating its role in cardiac development [46, 47].

Two heterozygous *KLF13* variants were characterized in patients with TA and TGA [48]; a study suggests that these variants may affect KLF13's transcriptional function and interaction with TBX5, alluding to a potential role in the development of CHD.

54.6 Conclusion

Most of the occurrences of tricuspid atresia that were identified with a genetic cause occurred as part of a multitude of congenital heart diseases. Genetic culprits ranged from extra chromosomes and chromosomal deletions to SNPs. The involvement of some genes such as *ZFPM2* and *NKX2-5* is certain. Other genes such as *HEY2* however are less likely to be involved. The heterogeneity of the observed phenotypes and reported genotypes, and hence of their relationship, diminishes the contribution of each report to the greater picture, allowing only very little to be known about the mechanism of development of TA and the molecular pathways involved therein. Since only a few mutations were found to be direct culprits in patients with tricuspid atresia so far, analysis of copy-number variation (CNV), yet to be undertaken to assess the genotypes of those patients, will provide an opportunity to discover new genes underlying tricuspid atresia.

References

1. Hoffman JI, Kaplan S. The incidence of congenital heart disease. J Am Coll Cardiol. 2002;39:1890–900.
2. Grant JW. Congenital malformations of the tricuspid valve in siblings. Pediatr Cardiol. 1996;17:327–9.
3. Lin AE, Rosti L. Tricuspid atresia in sibs. J Med Genet. 1998;35:1055–6.
4. Bonnet D, Fermont L, Kachaner J, et al. Tricuspid atresia and conotruncal malformations in five families. J Med Genet. 1999;36:349–50.
5. Rao PS. Consensus on timing of intervention for common congenital heart diseases: part II – cyanotic heart defects. Indian J Pediatr. 2013;80:663–74.
6. Rao PS. Consensus on timing of intervention for common congenital heart diseases: part I – acyanotic heart defects. Indian J Pediatr. 2013;80:32–8.
7. Benson DW, Basson CT, MacRae CA. New understandings in the genetics of congenital heart disease. Curr Opin Pediatr. 1996;8:505–11.
8. Fischer A, Klamt B, Schumacher N, et al. Phenotypic variability in Hey2 −/− mice and absence of HEY2 mutations in patients with congenital heart defects or Alagille syndrome. Mamm Genome. 2004;15:711–6.
9. El-Rassy I, Bou-Abdallah J, Al-Ghadban S, et al. Absence of NOTCH2 and Hey2 mutations in a familial Alagille syndrome case with a novel frameshift mutation in JAG1. Am J Med Genet A. 2008;146:937–9.
10. Wirrig EE, Yutzey KE. Transcriptional regulation of heart valve development and disease. Cardiovasc Pathol. 2011;20:162–7.
11. Garry DJ, Olson EN. A common progenitor at the heart of development. Cell. 2006;127:1101–4.
12. Chakraborty S, Combs MD, Yutzey KE. Transcriptional regulation of heart valve progenitor cells. Pediatr Cardiol. 2010;31:414–21.
13. Vaughan CJ, Basson CT. Molecular determinants of atrial and ventricular septal defects and patent ductus arteriosus. Am J Med Genet. 2000;97:304–9.
14. Thiene G, Anderson RH. The clinical morphology of tricuspid atresia. Atresia of the right atrioventricular valve. G Ital Cardiol. 1981;11:1845–59.
15. Hu P, Ji X, Yang C, et al. 22q11.2 microduplication in a family with recurrent fetal congenital heart disease. Eur J Med Genet. 2011;54:e433–6.
16. Alva C, David F, Hernandez M, et al. Tricuspid atresia associated with common arterial trunk and 22q11 chromosome deletion. Arch Cardiol Mex. 2003;73:271–4.
17. Miller GA, Paneth M, Lennox SC. Surgical management of pulmonary atresia with intact ventricular septum in first month of life. Br Heart J. 1973;35:554.
18. Trost D, Engels H, Bauriedel G, et al. Congenital cardiovascular malformations and chromosome microdeletions in 22q11.2. Dtsch Med Wochenschr. 1999;124:3–7.
19. Lizarraga MA, Mintegui S, Sanchez Echaniz J, et al. Heart malformations in trisomy 13 and trisomy 18. Rev Esp Cardiol. 1991;44:605–10.
20. Yu CW, Chen H, Baucum RW, et al. Terminal deletion of the long arm of chromosome 4. Report of a case of 46, XY, del(4)(q31) and review of 4q- syndrome. Ann Genet. 1981;24:158–61.
21. Brand A, Reifen RM, Armon Y, et al. Double mitral valve, complete atrioventricular canal, and tricuspid atresia in chromosomal 3P-syndrome. Pediatr Cardiol. 1987;8:55–6.
22. Wat MJ, Shchelochkov OA, Holder AM, et al. Chromosome 8p23.1 deletions as a cause of complex congenital heart defects and diaphragmatic hernia. Am J Med Genet A. 2009;149A:1661–77.
23. Wald RM, Tham EB, McCrindle BW, Goff DA, McAuliffe FM, Golding F, Jaeggi ET, Hornberger LK, Tworetzky W, Nield LE. Outcome after prenatal diagnosis of tricuspid atresia: a multicenter experience. Am Heart J. 2007;153(5):772–8. https://doi.org/10.1016/j.ahj.2007.02.030. PMID: 17452152

24. Morton SU, Quiat D, Seidman JG, Seidman CE. Genomic frontiers in congenital heart disease. Nat Rev Cardiol. 2021;19(1):26–42. https://doi.org/10.1038/s41569-021-00587-4. Epub ahead of print. PMID: 34272501
25. Hoggard, JA. Discovering pathogenic variants associated with tricuspid atresia through whole exome sequencing. Diss. 2019
26. Tevosian SG, Deconinck AE, Tanaka M, et al. FOG-2, a cofactor for GATA transcription factors, is essential for heart morphogenesis and development of coronary vessels from epicardium. Cell. 2000;101:729–39.
27. Lu JR, McKinsey TA, Xu H, et al. FOG-2, a heart- and brain-enriched cofactor for GATA transcription factors. Mol Cell Biol. 1999;19:4495–502.
28. Svensson EC, Huggins GS, Dardik FB, et al. A functionally conserved N-terminal domain of the friend of GATA-2 (FOG-2) protein represses GATA4-dependent transcription. J Biol Chem. 2000;275:20762–9.
29. Svensson EC, Huggins GS, Lin H, Clendenin C, Jiang F, Tufts R, Dardik FB, Leiden JM. A syndrome of tricuspid atresia in mice with a targeted mutation of the gene encoding fog-2. Nat Genet. 2000;25(3):353–6. https://doi.org/10.1038/77146. PMID: 10888889
30. Sarkozy A, Conti E, D'Agostino R, et al. ZFPM2/FOG2 and HEY2 genes analysis in nonsyndromic tricuspid atresia. Am J Med Genet A. 2005;133A:68–70.
31. Pizzuti A, Sarkozy A, Newton AL, et al. Mutations of ZFPM2/FOG2 gene in sporadic cases of tetralogy of Fallot. Hum Mutat. 2003;22:372–7.
32. Koibuchi N, Chin MT. CHF1/Hey2 plays a pivotal role in left ventricular maturation through suppression of ectopic atrial gene expression. Circ Res. 2007;100:850–5.
33. Fischer A, Schumacher N, Maier M, et al. The notch target genes Hey1 and Hey2 are required for embryonic vascular development. Genes Dev. 2004;18:901–11.
34. Reamon-Buettner SM, Borlak J. HEY2 mutations in malformed hearts. Hum Mutat. 2006;27:118.
35. Peng SL, Gerth AJ, Ranger AM, et al. NFATc1 and NFATc2 together control both T and B cell activation and differentiation. Immunity. 2001;14:13–20.
36. Zhou P, Sun LJ, Dotsch V, et al. Solution structure of the core NFATC1/DNA complex. Cell. 1998;92:687–96.
37. Ranger AM, Grusby MJ, Hodge MR, et al. The transcription factor NF-ATc is essential for cardiac valve formation. Nature. 1998;392:186–90.
38. Abdul-Sater Z, Yehya A, Beresian J, et al. Two heterozygous mutations in NFATC1 in a patient with tricuspid atresia. PLoS One. 2012;7:e49532.
39. Yehya A, Souki R, Bitar F, et al. Differential duplication of an intronic region in the NFATC1 gene in patients with congenital heart disease. Genome. 2006;49:1092–8.
40. Li B, Li T, Pu T, Liu C, Chen S, Sun K, Xu R. Genetic and functional analyses detect one pathological NFATC1 mutation in a Chinese tricuspid atresia family. Mol Genet Genomic Med. 2021;7:e1771. https://doi.org/10.1002/mgg3.1771. Epub ahead of print. PMID: 34363434
41. Bruneau BG, Nemer G, Schmitt JP, et al. A murine model of Holt-Oram syndrome defines roles of the T-box transcription factor Tbx5 in cardiogenesis and disease. Cell. 2001;106:709–21.
42. Stallmeyer B, Fenge H, Nowak-Gottl U, et al. Mutational spectrum in the cardiac transcription factor gene NKX2.5 (CSX) associated with congenital heart disease. Clin Genet. 2010;78:533–40.
43. Posch MG, Waldmuller S, Muller M, et al. Cardiac alpha-myosin (MYH6) is the predominant sarcomeric disease gene for familial atrial septal defects. PLoS One. 2011;6:e28872.
44. Granados-Riveron JT, Ghosh TK, Pope M, et al. Alpha-cardiac myosin heavy chain (MYH6) mutations affecting myofibril formation are associated with congenital heart defects. Hum Mol Genet. 2010;19:4007–16.
45. Ching YH, Ghosh TK, Cross SJ, et al. Mutation in myosin heavy chain 6 causes atrial septal defect. Nat Genet. 2005;37:423–8.

46. Nemer M, Horb ME. KLF family of transcriptional regulators in cardiomyocyte proliferation and differentiation. Cell Cycle. 2007;6(2):117–21. https://doi.org/10.4161/cc.6.2.3718. Epub 2007 Jan 13. PMID: 17245133
47. Li W, Li B, Li T, Zhang E, Wang Q, Chen S, Sun K. Identification and analysis of KLF13 variants in patients with congenital heart disease. BMC Med Genet. 2020;21(1):78. https://doi.org/10.1186/s12881-020-01009-x.
48. Darwich R, Li W, Yamak A, Komati H, Andelfinger G, Sun K, Nemer M. KLF13 is a genetic modifier of the Holt-Oram syndrome gene TBX5. Hum Mol Genet. 2017;26(5):942–54. https://doi.org/10.1093/hmg/ddx009. PMID: 28164238

Molecular Pathways and Animal Models of Tricuspid Atresia and Univentricular Heart

55

Kamel Shibbani and George Nemer

Abstract

The process of valve formation is a complex process that involves intricate interplay between various pathways at precise times. Although we have not completely elucidated the molecular pathways that lead to normal valve formation, we have identified a few major players in this process. We are now able to implicate TGF-ß, BMP, and NOTCH as suspects in tricuspid atresia (TA), as well as their downstream targets: NKX2-5, TBX5, NFATC1, GATA4, and SOX9. We know that the TGF-ß and the BMP pathways converge on the SMAD4 molecule, and we believe that this molecule plays a very important role to tie both pathways to TA. Similarly, we look at the NOTCH pathway and identify the HEY2 as a potential link between this pathway and TA. Another transcription factor that has been implicated in TA is NFATC1. While several mouse models exist that include part of the TA abnormality as their phenotype, no true mouse model can be said to represent TA. Bridging this gap will surely shed light on this complex molecular pathway and allow for better understanding of the disease process.

K. Shibbani
Division of Cardiology, Department of Pediatrics, University of Iowa Hospitals and Clinics, Iowa City, IA, USA

G. Nemer (✉)
Department of Biochemistry and Molecular Genetics, American University of Beirut, Beirut, Lebanon

Division of Genomics and Translational Biomedicine, Hamad Bin Khalifa University, Doha, Qatar
e-mail: gn08@aub.edu.lb; gnemer@hbku.edu.qa

© The Author(s), under exclusive license to Springer Nature Switzerland AG 2024

S. Rickert-Sperling et al. (eds.), *Congenital Heart Diseases: The Broken Heart*,
Advances in Experimental Medicine and Biology 1441,
https://doi.org/10.1007/978-3-031-44087-8_55

Keywords

Tricuspid atresia · TA · Univentricular heart · TGF-ß · BMP · NOTCH · NKX2-5 · TBX5 · NFATC1 · GATA4 · SOX9 · SMAD4 · HEY2 · VEGF · Transforming growth factor · Epithelial–mesenchymal transition · EMT · Atrioventricular canal · AV canal · Looping · Mesenchymal cells · Trisomy 16 · Mutant mice

55.1 Introduction

The process of valve formation is a tremendously complex process and involves a very intricate interplay between appropriate pathways at appropriate times. Although we have not completely elucidated the molecular pathways that lead to normal valve formation, we have identified a few major players in this process.

The transforming growth factor beta (TGF-ß) and bone morphogenetic protein (BMP) 4 pathways are critical in valve formation. They both require SMAD family member (SMAD) 4 molecules to propagate their intracellular message. SMAD4 is associated with GATA-binding protein 4 (GATA4) and zinc finger protein FOG family member 2 (ZFPM2), and mutations in either of these two transcription factors cause tricuspid atresia (TA).

Similarly, NOTCH is essential for normal valve formation, and its association with hes-related family bHLH transcription factor with YRPW motif 2 (HEY2) provides us with a possible link to TA. Other transcription factors like nuclear factor of activated T-cell, cytoplasmic, calcineurin-dependent 1 (NFATC1) should not be overlooked.

Mouse models for TA are far from being perfect, but the trisomy 16 mouse, the Hey2 mutant mouse, and the ZFPM2 mutant mouse all provide insight about the molecular pathways leading to TA. Despite these insights, our knowledge of the processes that lead to TA remains incomplete.

The tricuspid valve, like the mitral valve, becomes fully functional at mid-gestation following a process that requires an intimate interaction between endocardial and myocardial cells. Using genetic data in humans and animal models will allow us to understand the molecular pathways involved in normal valve formation and will afford us a better understanding of the molecular pathways involved in TA.

55.2 Normal Valve Development

Normal tricuspid valve development can be separated into three main events: inductive stimuli of endocardial cells, epithelial-to-mesenchymal transition (EMT), and maturation of the valves.

55.2.1 Inductive Stimuli

Studies performed in the mid-1980s using the collagen gel assay found that only a subset of the endocardial cells of the heart—those that line the atrioventricular (AV) canal and outflow tract—are capable of undergoing EMT. Indeed, when endocardial/myocardial cells were explanted from the (AV) canal region and placed on the gel assay, it was found that the endocardial cells underwent EMT, while the resulting mesenchymal cells migrated into the gel. If, however, explants of endocardial/myocardial cells from the ventricle were used, EMT would not occur. Furthermore, scientists mixed and matched endocardial and myocardial cells from different locations within the heart tube to find that only when both the endocardial and the myocardial explants originated from the AV canal region did EMT occur [1–3]. Such studies formed the bases of the belief that there must be a myocardial signal that primes the endocardium at the AV canal and allows it to undergo EMT. Certain extracellular matrix (ECM) components have been implicated in the inductive stimuli [2], as well as signals that include the TGF-ß superfamily of proteins [4].

55.2.2 Epithelial-to-Mesenchymal Transition

Following this initial inductive stimulus, the process of EMT begins. At this point, the developing heart has just finished looping [5]. Initially, the innermost endocardial layer is made up of cells that have an apical-basal polarity. Junctions on their lateral membranes connect them to each other, and they rest on a basement membrane. These characteristics define epithelial cells. As a result of the process of EMT, some of these cells will lose their polarity, change their morphology, dissociate from the endocardial layer, and migrate into the cardiac jelly. Once there, these, now mesenchymal cells, will play an integral part in tricuspid valve formation. Though much of EMT is still unclear, scientists have identified key regulators of this process. Two main growth factor pathways that act as upstream regulators of EMT are the TGF-ß/BMP pathway and the Notch pathway. Downstream targets of these pathways include transcription factors such as NK2 homeobox 5 (NKX2-5), T-box 5 (TBX5), NFATC1, GATA4, and SRY (sex-determining region Y)-box 9 (SOX9) [5, 6].

55.2.3 Maturation

The end result of EMT is the formation of the cardiac cushions, which will undergo maturation and form the cardiac valves. This process of maturation is not very well understood, but the mesenchymal cells formed by EMT will differentiate into fibroblasts that secrete specific ECM components necessary for valve formation [7].

The process of normal valve formation is the result of a concert of pathways and transcription factors that need to be tightly regulated. Much work has been done to understand the molecular bases of valve formation and abnormality, and while we

have uncovered a lot, many questions still cloud our understanding of normal and abnormal valve formation. The molecular pathway of TA is no exception, with many unknowns still obscuring our complete understanding of the exact pathological process.

55.3 Abnormal Valve Development: Underlying Molecular Pathways of TA/Univentricular Heart

Animal models for TA as well as genetic studies of patients with this condition have suggested that the two major families of secretory proteins that are involved in valve formation—TGF-ß/BMP and NOTCH—and their regulators and/or downstream target effectors are directly involved in the malformation of the tricuspid valve.

What follows is a discussion of the TGF-ß/BMP and the Notch pathways, their relation to tricuspid valve formation and TA, their overlap, and important downstream targets of both pathways that have been implicated in TA, namely, NFATC1 and Hey2.

Figure 55.1 illustrates how these different factors play a role in the heart in relation to the endocardium and the myocardium within the regions destined to become valves.

55.3.1 TGF-ß/BMP Family of Growth Factors

Aside from their vital role in heart development, the TGF-ß and BMP pathways play an essential role in embryonic development. In fact, the TGF-ß and the BMP subfamilies of secreted proteins are part of larger superfamily of growth factors known as the TGF-ß superfamily. This superfamily includes three major branches: the TGF-ß sensu stricto (TGF-ß in vertebrates), DVR (decapentaplegic-Vg-related, which includes BMP), and activin. These three different subfamilies share many characteristics such as the structure of the ligands, the receptors, the mechanism of action of the ligand-receptor complex, as well as the intracellular mediators of the ligands—the SMADs [8]. This similarity in the mechanism of action, especially in the SMAD mediators, will play an important role in the overlap between the BMP and the TGF-ß pathways as they relate to TA, as we shall discuss below.

Ligands of the TGF-ß superfamily require two receptors to function, TGF-ß receptors type I and II, both of which are receptor tyrosine kinases. The ligand binds to receptor type II and will induce the type II receptor to bind to a type I receptor and phosphorylate it. The phosphorylated type I receptor is now activated and will in turn phosphorylate and activate a "receptor-activated SMAD" molecule (R-SMAD) [9]. The R-SMAD represents the intracellular mediator of the ligand and is responsible for transmitting the TGF-ß or BMP signal into the nucleus.

In humans, there are more than 30 different ligands in the TGF-ß superfamily [10]. There are also seven type I receptors and five type II receptors [9]. A

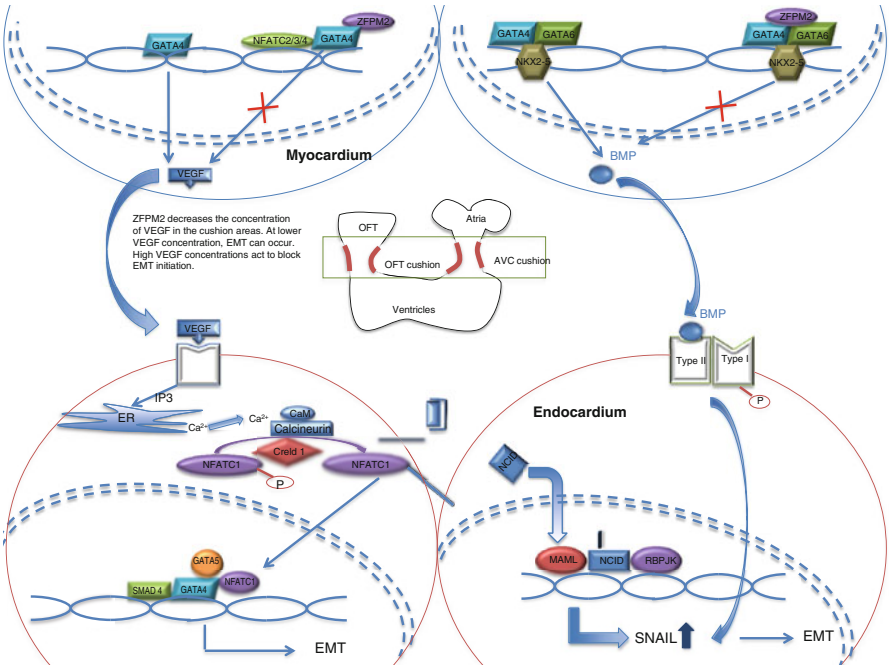

Fig. 55.1 The Notch receptor is present in endocardial cells prior to EMT and will bind to its ligand and release its NCID domain. This domain forms a nuclear complex with MAML and RBPJK and will upregulate SNAIL, which leads to EMT formation. Simultaneously, myocardial BMP2 signals will reach the endocardium and will stabilize the nuclear SNAIL signal. At the correct level, VEGF produced by the myocardium will bind to its receptor on the endocardium and result in an increase of Ca^{2+} from the ER via IP3. This Ca^{2+}, in concert with calmodulin, will activate calcineurin. Calcineurin will dephosphorylate NFATC1 and uncover its nuclear localization signal. It is believed that the step of NFATC1 dephosphorylation is also controlled by Creld1. Once in the nucleus, NFATC1 will bind to GATA4 and/or GATA5 among other proteins and will induce EMT

ligand-receptor complex can be made by numerous combinations of ligand, type I and type II receptors.

While the type II receptor determines the ligand specificity, the type I receptor determines the SMAD specificity [8]. Ultimately, BMP ligands result in the activation of SMAD1, SMAD5, and SMAD8, while the TGF-ß ligands result in the activation of SMAD2 and SMAD3 [9]. All R-SMAD molecules must then necessarily bind to cytoplasmic SMAD4 molecule to form a functional unit that will in turn enter the nucleus. Once in the nucleus, this SMAD4/R-SMAD functional unit will bind to specific transcription factors and regulate gene expression [9, 10]. Later on we will show that the SMAD-4 molecule, which links both the BMP and the TGF-ß pathways, interacts directly with GATA4, one of the most important regulators of valve formation whose cofactors have been implicated in TA. It is this link between GATA4 and SMAD4 that will tie the BMP and TGF-ß pathways to TA.

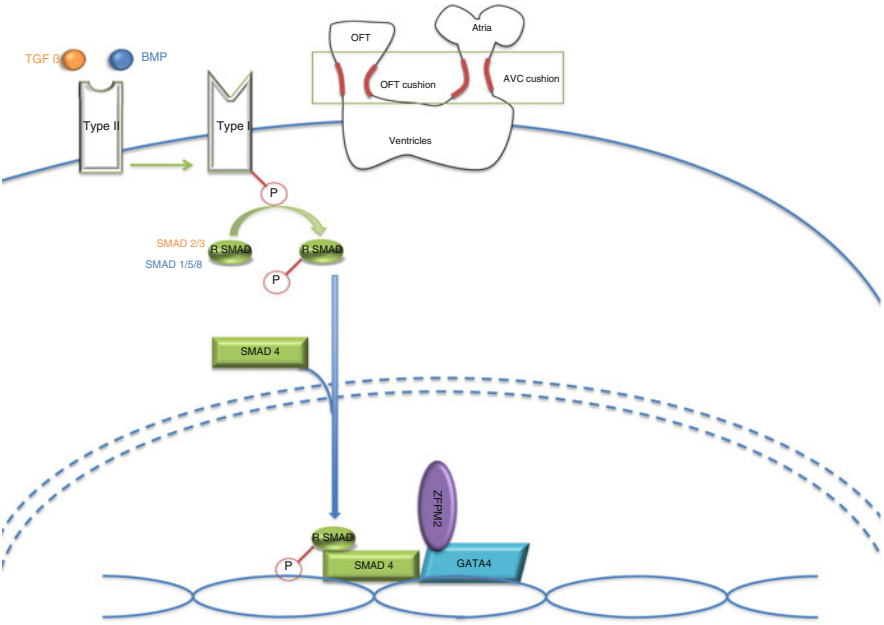

Fig. 55.2 TGF-ß or BMP ligand will bind to the type II receptor that will activate the type I receptor. The type I receptor will phosphorylate a particular R-SMAD molecule (SMAD2/3 for TGF-ß and SMAD 1/5/8 for BMP). This R-SMAD molecule will complex with a SMAD4 molecule to enter into the nucleus and interact with transcription factors such as GATA4

Figure 55.2 illustrates the similarities of the TGF-ß and the BMP pathways and their mechanism of action in the heart.

55.3.1.1 Role of TGF-ß Protein in Tricuspid Valve Formation

Although TGF-ß and BMP belong to the same superfamily and share many characteristics, they play distinct roles in tricuspid valve formation. These differences can be seen in the various functions that each pathway plays in EMT.

During embryogenesis, cells that are destined to form valves undergo three separate rounds of EMT, aptly named primary, secondary, and tertiary EMT. Each round of EMT is followed by a round of MET to reset the cells into the epithelial state in preparation for the next round of EMT. Primary EMT results in the formation of cardiac progenitor cells. Secondary EMT plays an important role in the formation of the cardiac tube. Finally, tertiary EMT results in valve formation [11]. TGF-ß and BMP play essential roles in tertiary EMT.

TGF-ß is one of the earliest molecules to be involved in EMT. Studies carried out in mice and chick embryos have shown that TGF-ß acts as an inductive stimulus for EMT, as well as a regulator of later steps in the EMT program. Studies on the various isoforms of TGF-ß in the chick embryo found that TGF-ß2 is essential for EMT initiation, while TGF-ß3 is essential for mesenchymal cell invasion into the ECM

[12]. In mice, the function of the TGF-ß genes was slightly different. Studies performed in mice using functional antibodies against different isoforms of TGF-ß concluded that TGF-ß1 and TGF-ß3 were not needed for EMT to occur. TGF-ß2, however, did play a role. In vitro studies showed that the number of mesenchymal cells that invaded the collagen assay upon TGF-ß2 antibody exposure was significantly reduced. Along the same lines, in vivo studies with *TGF-ß2*$^{-/-}$ mice showed an abnormality in EMT that resulted in hypercellular cushions [13].

Besides the TGF-ß ligand itself, the TGF-ß receptor has an important role in EMT (indicating perhaps that other pathways besides those activated by the TGF-ß ligand are at play). The importance of the TGF-ß receptor has been studied in mice and chick embryos. Studies in chick embryos showed that if TGF-ß receptor type II is blocked, EMT does not take place [6]. In mice, it appears that the TGF-ß ligand-receptor interaction is more complicated. In vivo studies showed that blocking TGF-ß receptor type II does not affect EMT. In vitro studies, on the other hand, showed that blocking the same receptor inhibited explanted tissue EMT. This implies that other compensatory mechanisms, possibly unrelated to the TGF-ß ligand, are able to make up for the loss of the receptor [5].

55.3.1.2 Role of BMP in Tricuspid Valve Formation

Although similar in importance to the TGF-ß pathway discussed above, BMP seems to have a more upstream role than that of TGF-ß in valve formation. Previous reports have shown that BMP2 is important in the initiation of the EMT process. Experiments done on mouse AV canal explants showed that in the absence of the myocardium, endocardial cells exposed to BMP2 are able to undergo EMT. Therefore, BMP2 released from the myocardial cells must be part of the inductive stimuli that kick off EMT in the endocardial cells. Furthermore, BMP2 resulted in an upregulation of TGF-ß in these cells, indicating that perhaps BMP2 is upstream of the TGF-ß pathway in EMT [5, 6]. BMP4 is more important in the process of valve maturation as opposed to EMT initiation [6]. BMP5, BMP6, and BMP7 have been investigated together in the mouse heart. Double knockout mice for BMP5 and BMP7 did not form a cardiac cushion, while double knockout mice for BMP6 and BMP7 showed a delay in the cardiac cushion formation that affected the outflow tract cushion more than it did in the AV cushion [6].

The effect of BMP on EMT can also be appreciated by blocking the BMP receptors. Indeed, blocking the BMP2 type I receptor in mice resulted in mice embryos that failed to undergo EMT and had a decrease TGF-ß expression—similar to BMP2 knockout mice [5].

55.3.1.3 The TGF-ß/BMP Pathway in TA: A Role for ZFPM2 and SMAD

While one can draw distinctions between the roles of TGF-ß and BMP in early valve formation, the fact that they belong to the same superfamily and therefore share a common mechanism of action means that these two pathways will overlap. They do so at the level of the SMAD molecules and more specifically SMAD4. Understanding the role of SMAD4 in both pathways and the role it plays alongside one of the

main regulators of valve formation (GATA4) is the key to understanding the roles of TGF-ß and BMP in TA.

The SMAD proteins play a vital role in the downstream pathway of both TGF-ß and BMP. After binding of either BMP or TGF-ß to a surface receptor, a series of events occurs that ultimately results in the activation of a ligand-specific R-SMAD molecule. SMAD4 will then bind to the activated R-SMAD molecule and translocate it into the nucleus [9, 10, 14]. Once in the nucleus, the SMAD4/R-SMAD complex interacts with other transcription factors, including the master regulator of cardiac development, the GATA4 protein. Studies have shown that disruption of this interaction could lead to CHD mainly related to atrioventricular septation and valve formation. In fact, mice double heterozygous for both genes die in utero because of atrioventricular septal defects. Furthermore, in vitro experiments show a strong physical and functional interaction between SMAD4 and GATA4 [15].

In short, the BMP and TGF-ß pathways must signal through SMAD4 to relay their message into the nucleus. SMAD4, in turn, interacts with several transcription factors, including GATA4. The way that all of this ties in with TA is through GATA4's transcriptional partner ZFPM2.

ZFPM2 (also known as FOG2) is a zinc finger protein with 8 zinc finger domains. It is highly expressed in the heart where it interacts with GATA4 and mediates its activity [16, 17]. *ZFPM2*$^{-/-}$ mice die in utero between days E13 and E14 from a cardiac phenotype that mirrors TA [18].

The molecular pathways that lead to TA are not yet well defined. We have at our disposal only pieces of the puzzle that seem to implicate an intricate relationship between upstream factors like TGF-ß and BMP and downstream targets like GATA4 ZFPM2 and SMAD4. The identification of transcriptional targets for the GATA4/SMAD4 and GATA4/ZFPM2 interactions would help establish a better genotype/phenotype correlation and a comprehensive mechanism that links the transcriptional outcome activities with the underlying defect.

55.4 The Notch-Hey2 Pathway

Besides the BMP and the TGF-ß pathways, the Notch pathway is one of the upstream regulators of EMT and valve formation [5, 6]. Not unlike the previous two pathways, the Notch pathway is vital for several cellular processes including differentiation and patterning. It distinguishes itself from the TGF-ß and the BMP pathways, however, by using ligands that are not secreted. The Notch pathway involves a membrane-bound receptor binding to a neighboring cell's membrane-bound ligand [19]. This makes the Notch signaling pathway contact dependent, unlike either the BMP or the TGF-ß signaling pathways.

There are four Notch receptors in mammals and they all share the same basic structure; an extracellular domain will bind to one of the five Notch ligands (Dll 1, Dll 3, Dll 4, Jag 1, and Jag 2), an intracellular domain (NICD) that detaches from the receptor and moves into the nucleus, and a transmembrane domain [19, 20].

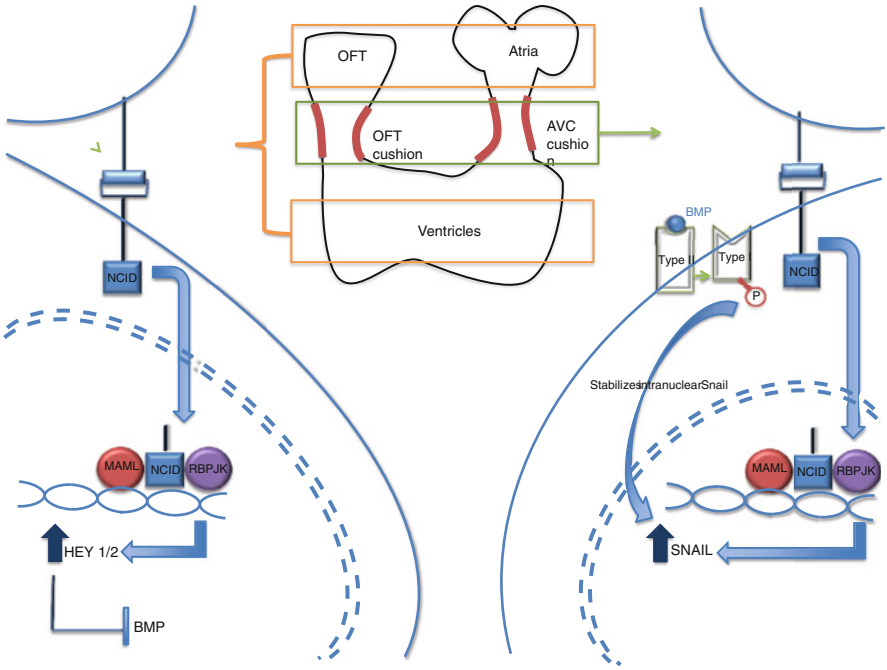

Fig. 55.3 After Notch binds to its ligand in a cell contact-dependent manner, it will release its NICD domain. This domain will travel into the nucleus and form a complex with MAML and RBPJK and upregulate different factors depending on what area of the heart this is taking place in. In the atria and ventricle (*left side* of the figure), the Notch pathway will result in the upregulation of HEY1/2 that will in turn block BMP signaling. This will work to inhibit EMT. In the cushion regions (*right side* of the figure), the Notch pathway results in the activation of SNAIL and will induce EMT. BMP will stabilize the SNAIL in the nucleus

After the Notch binds to its ligand, a series of reactions ensue that ultimately result in the detachment of the NICD and its translocation into the nucleus. Once in the nucleus, the NICD forms a complex with the RBPJK (Recombinant signal Binding Protein for immunoglobulin kappa J region) transcription factor. This NICD/RBPJK complex recruits the coactivator protein MAML (MAsterMind-Like), and this entire complex upregulates the expression of several downstream targets, including Hey2 and SNAIL. Figure 55.3 illustrates this contact-dependent Notch signaling pathway.

55.4.1 Role of Hey2 Notch in Tricuspid Formation and TA

Like TGF-ß and BMP, Notch also plays an important role in normal valve formation. The importance of the Notch pathway in normal tricuspid valve formation was realized in studies that showed severely dysmorphic cardiac cushions upon

inhibition of Notch in mice. Upregulation of Notch, on the other hand, results in hypercellular cushions [6]. Detailed spatial and temporal analysis of the expression of Notch during cardiac cushion development reveals an important role for Notch in the regulation of the EMT process in the tricuspid valves. Analysis of the spatial distribution of the Notch ligand, Dll4, just prior to EMT reveals its presence in high amounts in areas destined to become valves [21]. Predictably, Notch itself also was present in these atrioventricular canal (AVC) areas prior to EMT initiation. Furthermore, inhibition of Notch, either directly or by inhibiting its RBPJK transcription factor, resulted in endocardial cells that are unable to migrate into the cardiac jelly [19, 21], which indicates that Notch must play a role in EMT and tricuspid valve formation.

Besides allowing EMT to occur, the Notch signaling pathway is also important for patterning the premature cardiac cushion areas. It seems that some of the transcription factors activated downstream of Notch, specifically Hey1 and Hey2, determine which areas will undergo EMT by inhibiting essential EMT signals in the tissue in which they are present. Just prior to valve development in the mouse, Hey1 is present in the atrial myocardium and endocardium, and Hey2 is present in the ventricular endocardium. Thus, these downstream Notch cofactors inhibit EMT in the ventricle and atria and allow EMT to proceed only in the AVC and the OFT cushion regions where they are not present [21].

Unlike the relation between TGF-ß/BMP and TA, the relation between Notch and TA is more direct. The evidence that tied the Notch pathway to TA involved studies done on $Hey2^{-/-}$ mice. These mice mostly died in utero or survived to die shortly after birth. More important, however, are the shared cardiac defects among all mice with this genotype whereby 40% of them presented with tricuspid atresia [22].

55.4.2 Cross Talk Between the Notch and TGF-ß/BMP Pathways

Serving as a reminder of the intricacies involved in cardiac valve formation is the fact that the TGF-ß, the BMP, and the Notch pathways exhibit cross talk between them. Studies have shown that the Hey2 and Hey1 cofactors demarcate the boundaries of AVC and OFT cushion by downregulating BMP2 in all but these two areas in the heart [21]. Furthermore, it appears that high levels of BMP2 in the AVC areas maintain a high level of EMT specific genes, namely, the transcription factor Snail1. Coincidentally, Snail1 is also a downstream target of the Notch pathway, and Snail1 acts in a positive feedback loop with Notch [19].

There is also some evidence that links the Notch pathway to the TGF-ß pathway via R-SMAD molecules. Inhibition of the Notch pathway leads to a decrease in the SMAD3 levels within endothelial cells. Notch activation, on the other hand, leads to endothelial cell downregulation of SMAD1 and SMAD2 [20].

To highlight the complexities of the three pathways mentioned above, one should keep in mind that the spatial expression of the different ligands and receptors mentioned thus far is crucial. It appears that the Notch receptor is preferentially expressed in the endocardium during tricuspid valve formation, while its ligands are

present both in the endocardium and myocardium. Similarly, BMP signals, especially the BMP2 signal, are myocardial in origin [5, 20].

55.4.3 Other Downstream Targets: NFATc1 and the Tricuspid Valve

Just like the TGF-ß/BMP and the Notch pathways that can be tied to TA via their respective downstream targets, the GATA4/ZFPM2 and the Hey2, respectively, other downstream transcription factors have been implicated in TA. Chief among those is the NFATC1.

NFATC1 is a transcription factor that was initially implicated in T-cell activation. It belongs to the Rel/NF-kB family and has, since its discovery, been described to interact with several regulators of differentiation during embryogenesis [23]. NFATC1 is a cytoplasmic protein that moves into the nucleus to bind DNA and regulate gene expression upon its dephosphorylation by calcineurin, a calcium-calmodulin-dependent phosphatase [23, 24].

NFATC1 plays a role in valve development as shown by the *Nfatc1* knockout mice that fail to develop mature valve leaflets [25]. The role of NFATC1 in valve maturation has been corroborated by the fact that it interacts with several other transcription factors, including, but not limited to, the GATA zinc finger protein family [26]. During early valve formation, NFATC1 expression is restricted to endocardial cells in areas of the heart that are destined to become cardiac cushions [27]. After the cardiac cushions have formed, expression of NFATC1/calcineurin at day E11 in the endocardial cells is required for cardiac valve elongation and maturation [28]. In parallel, human genetic studies identified two compound heterozygous mutations in the *NFATC1* gene in a patient suffering from TA [23]. Cellular analysis revealed that the NFATC1 mutated proteins affected with this compound heterozygous mutation resulted in abnormal NFATC1 activity including decreased nuclear localization, decreased NFATC1 DNA-binding affinity, a subsequent decrease in calcineurin-induced transcriptional activity, and finally, decreased ability of NFATC1 to bind to other transcription factors such as GATA5 and HAND2—both of which play essential roles in cardiac valve development [23]. Similarly, a recent study in a family with TA identified a pathological mutation in *NFATC1* that resulted in a decrease in expression of downstream targets [29].

Several upstream signaling pathways besides calcineurin have been implicated directly in the regulation of NFATC1 including vascular endothelial growth factor (VEGF) and connexin 45, while others, including TGF-ß and BMP, have an indirect effect on NFATC1 [24, 30, 31]

Mice that are deficient for connexin 45 died in utero and had cardiac problems that were similar to *Nfatc1*$^{-/-}$ mice [32]. Furthermore, analysis of cardiac cells revealed that NFATC1 in these mice was mainly cytoplasmic and was unable to translocate into the nucleus [31].

Similarly, it has been shown that VEGF plays an important role in cardiac valve development by affecting NFATC1 activity. Indeed, cultures of chick endocardial cushion cells treated with VEGF had a significantly higher amount of nuclear

NFATC1 than cells without VEGF treatment. Ultimately, VEGF was shown to cause an increase in proliferation of these endocardial cushion cells by activating the calcineurin/NFATC1 pathway [30]. Mouse studies have recently identified cysteine rich with EGF-like domains 1 (Creld1), a risk gene for nonsyndromic atrial septal defects (ASD), as a regulator of NFATC1. Creld1-deficient mice had NFATC1 that maintained a phosphorylated state, which inhibited the nuclear translocation of NFATC1. Furthermore, Creld1-deficient mice did not respond to VEGF treatment, while control mice showed a normal NFATC1 response to VEGF, indicating that VEGF regulation of NFATC1 occurs through Creld1 [24].

As a testament to the complexities of the different pathways in valve formation and to our imprecise yet growing knowledge of these pathways, recent studies have identified a novel role of NFACT in the outflow tract (OFT) valve formation. There, it seems that NFATC1 is critical during two time points: the initiation of EMT and the maturation of the valves. At the first time point, NFATC1 plays a role similar to that discussed above. However, during the second time point, which occurs when the valves are beginning to mature, it seems that NFATC1 plays a different role. Then, it seems that NFATC1 is a critical factor in determining the cell fate by inhibiting endocardial cells from undergoing EMT and becoming mesenchymal cells. During the maturation phase, it seems that by inhibiting EMT, NFATC1 maintains cells in their endocardial nature. Here again one can note the overlap between the different pathways discussed thus far, as NFATC1 inhibits EMT during the maturation phase of the valves by downregulating SNAIL1 and SNAIL2. By downregulating these two factors, NFATC1 essentially blocks endocardial cells from becoming mesenchymal cells, thereby inhibiting EMT [33].

55.5 Animal Models

Initial animal models used to study TA were mice models. These mice were for the most part not created to study TA specifically but rather a different cardiac abnormality or normal cardiac or valve development. More recent animal models have included a pig model with evidence of tricuspid dysplasia/ tricuspid atresia [34].

55.5.1 Trisomy 16 Mouse

As early as 1985, the trisomy 16 mouse model was being recognized as a potential model to study the "endocardial cushion defect" observed in patients with Down's syndrome [35]. Though this model succeeded in recreating some of the cardiac phenotypes observed in humans who have trisomy 21, it had additional phenotypes that were seen in patients who suffer from microdeletions on chromosome 22, the reason being that the mouse chromosome 16 carries genes that are expressed on human chromosome 22 [35, 36].

Coincidentally, mice with trisomy 16 had features resembling human TA. Indeed, around half of the animals with trisomy 16 showed a muscular right atrial floor with

an atrioventricular junction that was connected exclusively to the left atrium with no right ventricular connection [36]. Other non-TA cardiac phenotypes observed in mice with trisomy 16 include a common atrioventricular junction, a lack of atrioventricular septation, and a lack of subpulmonary infundibulum formation [36].

55.5.2 Hey2 Mutant Mice

Another mouse model that has been used to study TA is the Hey2 mutant mouse. Hey2 is one of the downstream targets of the Notch signaling pathway, and it plays a role in the patterning of the cardiac endocardium prior to EMT. Transgenic mice were created with a mutated Hey2 protein that lacked three domains: the helix-loop-helix domain, the YXXW domain, and the orange domain.

There were no reported cardiac phenotypes in Hey2 heterozygous mice. Homozygous mice, however, consistently had numerous cardiac defects. The most common defect observed in homozygous mice was a ventricular septal defect (VSD). Other defects included an ASD and a TA-like phenotype where there was an absence of tricuspid valve formation or complete valve stenosis. These defects were present in about 40% of embryos with homozygous null mutations for Hey2, and there was thus partial penetrance depending on the genetic background [22].

55.5.3 ZFPM2 Mutant Mice

Deleting all eight exons of the *Zfpm2* gene resulted in mice that have been used as models to TA. *Zfpm2* heterozygous mice showed normal cardiac development. *Zfpm2*$^{-/-}$ homozygous mice however did not survive beyond day E13.5. Examination of the embryos showed several cardiac defects including pulmonary stenosis, VSD, ASD, TA, and a single AV valve that connected both atria to the left ventricle. The right ventricle was smaller in these animals, but the left ventricular compact zone was larger than in wild-type mice [18].

55.5.4 *SAP130* Mutant Pig

In an effort to expand the animal models of CHD, recent work has focused on the use of pigs to model heart disease. Pigs carry significant advantages over mice, not least of which is the ability to perform more invasive studies and hemodynamic characteristics that more closely resemble that of humans. Recent work has shown that a CRISPR introduced gene mutation in *SAP130* has produced pigs with tricuspid dysplasia and 1 pig with tricuspid atresia. The study itself was a proof of concept for the ability to model CHD in pigs, and the development of TA in some fetuses is encouraging with regards to our ability to use such models to better understand the molecular pathways of TA [34].

55.6 Conclusion

The variety of the phenotypes in each model and the overlap between the different phenotypes in the different models suggest that there is a great deal of overlap between different pathways in cardiac development, which makes understanding the molecular pathway of TA more challenging.

Among the various molecular pathways in TA, however, the TGF-ß/BMP pathway with its GATA4/ZFPM2 downstream target and the Notch pathway with its Hey2 downstream target seem to be of significant importance. In addition, it seems that NFATC1 is also a part of any story involving TA. And while the TGF-ß/BMP and the Notch pathways are essential for many other developmental origins, the secret to the molecular pathway of TA could lie with NFATC1. The role that NFATC1 plays in valve formation sets it aside from other factors. At the time that corresponds to valve formation, the presence of NFATC1 in the entire embryo is restricted to areas destined to become valves. This unique feature might just indicate that the holy grail of TA is NFATC1. And while it will not account for all the unknowns, it is entirely plausible that this transcription factor could serve as the thread that unravels the details of the molecular pathway of TA.

References

1. Runyan R, Markwald RR. Invasion of mesenchyme into three-dimensional collagen gels- a regional and temporal analysis of interaction in embryonic heart tissue. Dev Biol. 1983;95:108–14.
2. Krug E, Mjaatvedt C, Markwald RR. Extracellular matrix from embryonic myocardium elicits an early morphogenetic event in cardiac endothelial differentiation. Dev Biol. 1987;120:348–55.
3. Mjaatvedt C, Lerepa RC, Markwald RR. Myocardial specificity for initiating endothelial-mesenchymal cell transition in embryonic chick heart correlates with a particulate distribution of fibronectin. Dev Biol. 1987;119:59–67.
4. Runyan RP, Sharma J, Loeber R, et al. Signal transduction of a tissue interaction during embryonic heart development. Cell Regul. 1990;1:301–13.
5. Camenisch TD, Runyan R, Markwald RR. Molecular regulation of cushion morphogenesis. In: Harvey R, Rosenthal N, editors. Heart development and regeneration. London: Academic; 2010. p. 363–87.
6. Person A, Klewer SE, Runyan R. Cell biology of cardiac cushion development. Int Rev Cytol. 2005;243:287–335.
7. de Vlaming A, Sauls K, Hajdu Z, et al. Atrioventricular valve development: new perspectives on an old theme. Differentiation. 2012;84:103–16.
8. Herpin A, Lelong C, Favrel P. Transforming growth factor-beta-related proteins: an ancestral and widespread superfamily of cytokines in metazoans. Dev Comp Immunol. 2004;28:461–85.
9. Wakefield LM, Hill CS. Beyond TGFbeta: roles of other TGFbeta superfamily members in cancer. Nat Rev Cancer. 2013;13:328–41.
10. Massague J. TGFbeta signalling in context. Nat Rev Mol Cell Biol. 2012;13:616–30.
11. Thiery JP, Acloque H, Huang RY, et al. Epithelial-mesenchymal transitions in development and disease. Cell. 2009;139:871–90.

12. Boyer AS, Ayerinskas II, Vincent EB, et al. TGFb2 and TGFb3 have separate and sequential activities during epithelial–mesenchymal cell transformation in the embryonic heart. Dev Biol. 1999;205:530–45.
13. Azhar M, Runyan RB, Gard C, et al. Ligand-specific function of transforming growth factor beta in epithelial-mesenchymal transition in heart development. Dev Dyn. 2009;238:431–42.
14. Wrana JL. Signaling by the TGFbeta superfamily. Cold Spring Harb Perspect Biol. 2013;5: a011197.
15. Moskowitz IP, Wang J, Peterson MA, et al. Transcription factor genes Smad4 and Gata4 cooperatively regulate cardiac valve development. Proc Natl Acad Sci U S A. 2011;108: 4006–11.
16. Lu J, McKinsey TA, Xu H, et al. FOG-2, a heart- and brain-enriched cofactor for GATA transcription factors. Mol Cell Biol. 1999;19:4495–502.
17. Tevosian SG, Deconinck AE, Tanaka M, et al. FOG-2, a cofactor for GATA transcription factors, is essential for heart morphogenesis and development of coronary vessels from epicardium. Cell. 2000;101:729–39.
18. Svensson E, Huggins GS, Lin H, et al. A syndrome of tricuspid atresia in mice with a targeted mutation of the gene encoding Fog-2. Nat Genet. 2000;25:353–6.
19. de la Pompa JL, Epstein JA. Coordinating tissue interactions: notch signaling in cardiac development and disease. Dev Cell. 2012;22:244–54.
20. Garside VC, Chang AC, Karsan A, et al. Co-ordinating notch, BMP, and TGF-beta signaling during heart valve development. Cell Mol Life Sci. 2013;70:2899–917.
21. MacGrogan D, Nus M, de la Pompa JL. Notch signaling in cardiac development and disease. Curr Top Dev Biol. 2010;92:333–65.
22. Donovan J, Kordylewska A, Jan YN, et al. Tetralogy of Fallot and other congenital heart defects in Hey2 mutant mice. Curr Biol. 2001;12:1605–10.
23. Abdul-Sater Z, Yehya A, Beresian J, et al. Two heterozygous mutations in NFATC1 in a patient with tricuspid atresia. PLoS One. 2012;7:e49532.
24. Mass E, Wachten D, Aschenbrenner AC, et al. Murine Creld1 controls cardiac development through activation of calcineurin/NFATc1 signaling. Dev Cell. 2014;28:711–26.
25. Lange AW, Yutzey KE. NFATc1 expression in the developing heart valves is responsive to the RANKL pathway and is required for endocardial expression of cathepsin K. Dev Biol. 2006;292:407–17.
26. Nemer G, Nemer M. Cooperative interaction between GATA5 and NF-ATc regulates endothelial-endocardial differentiation of cardiogenic cells. Development. 2002;129:4045–55.
27. Armstrong EJ, Bischoff J. Heart valve development: endothelial cell signaling and differentiation. Circ Res. 2004;95:459–70.
28. Chang CP, Neilson JR, Bayle JH, et al. A field of myocardial-endocardial NFAT signaling underlies heart valve morphogenesis. Cell. 2004;118:649–63.
29. Li B, Li T, Pu T, et al. Genetic and functional analyses detect one pathological NFATC1 mutation in a Chinese tricuspid atresia family. Mol Genet Genomic Med. 2021;9(9):e1771. https://doi.org/10.1002/mgg3.1771.
30. Combs MD, Yutzey KE. VEGF and RANKL regulation of NFATc1 in heart valve development. Circ Res. 2009;105:565–74.
31. Kumai M, Nishii K, Nakamura K, et al. Loss of connexin45 causes a cushion defect in early cardiogenesis. Development. 2000;127:3501–12.
32. Graef IA, Chen F, Crabtree GR. NFAT signaling in vertebrate development. Curr Opin Genet Dev. 2001;11:505–12.
33. Wu B, Wang Y, Lui W, et al. Nfatc1 coordinates valve endocardial cell lineage development required for heart valve formation. Circ Res. 2011;109:183–92.

34. Gabriel GC, Devine W, Redel BK, et al. Cardiovascular development and congenital heart disease modeling in the pig. Am Heart Assoc. 2021;10(14):e021631.
35. Epstein CJ, Cox DR, Epstein LB. Mouse trisomy 16: an animal model of human trisomy 21 (down syndrome). Ann N Y Acad Sci. 1985;450:157–68.
36. Anderson RH, Webb S, Brown NA. The mouse with trisomy 16 as a model of human hearts with common atrioventricular junction. Cardiovasc Res. 1998;39:155–64.

Part XV

Ebstein Anomaly

Clinical Presentation and Therapy of Ebstein Anomaly

56

Nikolaus A. Haas, David J. Driscoll, and Silke Rickert-Sperling

56.1 Introduction

Ebstein anomaly is a rare congenital heart defect, accounting for less than 1% of cardiac malformations and occurring in approximately 1 out of 210,000 live births. It is characterized by an abnormality of the tricuspid valve, where the valve is positioned lower than normal in the right ventricle. Although primarily a tricuspid valve defect, the right ventricle itself is often structurally abnormal and weakened (myopathic).

56.2 Pathologic Physiology

The embryologic basis of Ebstein anomaly is failure of the tricuspid valve leaflets to delaminate from the ventricular muscle. Embryologically the tricuspid valve leaflets are part of the ventricular wall and become separate (delaminate) during development. If this process is disturbed, the leaflets stay connected to the ventricular wall. The septal leaflet is the least well delaminated. The anterior leaflet, albeit the most

N. A. Haas (✉)
Department of Pediatric Cardiology and Intensive Care, Ludwig Maximilians University, Munich, Germany
e-mail: Nikolaus.haas@med.uni-muenchen.de

D. J. Driscoll
Division of Pediatric Cardiology, Department of Pediatrics, Mayo Clinic College of Medicine, Rochester, MN, USA
e-mail: driscoll.david@mayo.edu

S. Rickert-Sperling
Cardiovascular Genetics, Charité – Universitätsmedizin Berlin, Berlin, Germany
e-mail: silke.sperling@charite.de

© The Author(s), under exclusive license to Springer Nature Switzerland AG 2024

S. Rickert-Sperling et al. (eds.), *Congenital Heart Diseases: The Broken Heart*,
Advances in Experimental Medicine and Biology 1441,
https://doi.org/10.1007/978-3-031-44087-8_56

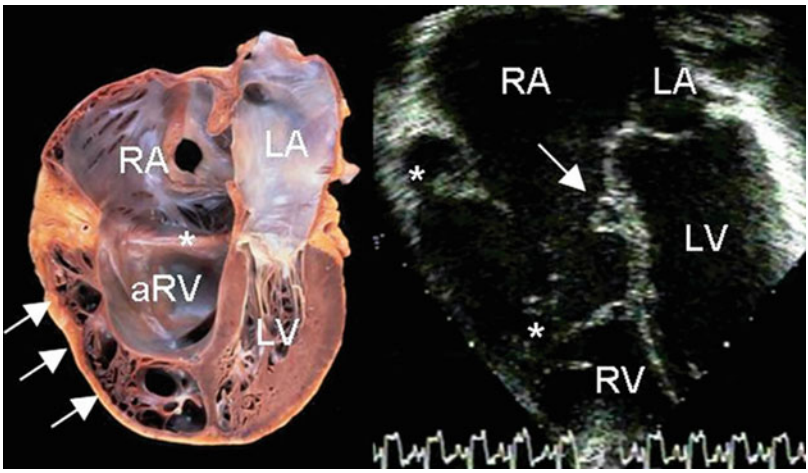

Fig. 56.1 Pathologic specimen of Ebstein anomaly (*left*) and echocardiographic image (*right*). The septal leaflet is plastered against the septum (failure of delamination), and the anterior leaflet is markedly enlarged and displaced into the right ventricle and tethered to the free wall of the right ventricle. There is a large atrial septal defect. *Arrows* on the left panel show thinned wall of right ventricle. *Arrow* on the right panel shows the hinge point where the septal leaflet is attached to the septum. Abbreviations: *RA* right atrium, *LA* left atrium, *aRV* atrialized portion of the right ventricle, *LV* left ventricle, *RV* right ventricle. * defines the enlarged anterior leaflet of the tricuspid valve

completely delaminated, is usually quite large but also may have tethered attachments to the right ventricular free wall. Thus, the apparent orifice of the tricuspid valve is displaced into the right ventricle. However, the true orifice is not displaced and the portion of the heart between the true and apparent orifice is the so-called atrialized portion of the right ventricle. The tricuspid valve annulus is enlarged and the leaflets show no coaptation, resulting in tricuspid regurgitation.

The abnormalities in Ebstein anomaly are not limited to the tricuspid valve. The right ventricle (Fig. 56.1) is not normal and always, to a greater or lesser degree, is myopathic. In some cases the left ventricle also may show evidence of fibrosis.

An atrial septal defect or stretched patent foramen ovale is present in 50–70% of cases, VSDs may exist, and 30% of cases are associated with a right-sided accessory bypass tract or Wolff–Parkinson–White (WPW) syndrome. Therefore, atrial arrhythmias and especially paroxysmal atrial tachycardias are common in patients with Ebstein anomaly. These can be associated with ventricular pre-excitation (WPW) or the dilated right atrium. Accessory conduction pathways should be identified and ablated during a preoperative electrophysiologic study. Ebstein anomaly of the tricuspid valve can commonly occur in congenitally corrected TGA.

The pathophysiology of Ebstein anomaly depends on the degree of dysplasia of the tricuspid valve, the degree of tricuspid valve insufficiency, or, in rare cases, tricuspid valve stenosis. In addition, determinants of clinical severity include the severity of right ventricular myopathy; the presence or absence of an interatrial

communication; the presence, absence, and degree of right ventricular outflow tract obstruction; and the presence or absence of ventricular pre-excitation.

56.3 Clinical Presentation

The presentation and clinical course of patients with Ebstein are quite variable and dependent upon the severity of the malformation. On one end of the spectrum, fetal hydrops and death can occur. On the other end of the spectrum, patients with mild forms of Ebstein anomaly can have a normal life span without medical or surgical intervention.

The classic presentation at birth is cyanosis and/or marked cardiomegaly. Newborns presenting with cyanosis do so because of right-to-left shunting through a patent foramen ovale (PFO) or atrial septal defect (ASD). In patients with a massive cardiomegaly, respiratory distress or even lung hypoplasia may be the leading picture. This may be accompanied by signs of congestive, mainly right sided, heart failure (hepatomegaly, edema, acidosis). Beyond the newborn period, patients may present because of the presence of a murmur, fatigue, dyspnea, cyanosis, atrial arrhythmias, or cardiomegaly discovered serendipitously.

56.4 Physical Examination

For patients with an ASD, cyanosis is usually apparent. When a neonatal pulse oximetry screening is in place, they should be picked up by lower than normal saturations.

Despite the presence of significant tricuspid insufficiency, because of the capacitance of the dilated right atrium, the jugular venous impulses usually are normal. The cardiac impulse may be quite diffuse as a result of cardiomegaly and a volume overloaded right ventricle. Classically, patients with Ebstein anomaly have been described as having a "quadruple rhythm." Rarely, if the valve is stenotic, a tricuspid diastolic murmur is present.

56.5 Diagnostic Imaging

Echocardiography is a key diagnostic tool for accurately diagnosing Ebstein's anomaly in neonates and children. It provides detailed information about the anatomy of the tricuspid valve, the degree of tricuspid regurgitation, and the presence of other associated malformations such as ASD/PFO, VSD, or cc-TGA. Echocardiography also allows for the estimation of right atrial size, right ventricular size and function, and left ventricular function. It can assess the degree and location of right ventricular outflow obstruction. Transthoracic echocardiography is usually sufficient for diagnosis in neonates and children.

Chest radiography often shows a characteristic picture with significant cardiomegaly occupying most of the chest.

Diagnostic cardiac catheterization is typically unnecessary in the era of echocardiography for the diagnosis of Ebstein's anomaly. However, it may be indicated for hemodynamic assessment in specific situations, especially when considering a bidirectional cavopulmonary shunt or in cases with depressed left ventricular function. Cardiac catheterization may also be performed to evaluate the pulmonary artery, exclude pulmonary hypertension, or perform balloon valvuloplasty for anatomic pulmonary valve stenosis. Electrophysiological studies may be necessary for symptomatic patients with WPW syndrome and associated tachycardias.

Magnetic resonance imaging (MRI) can be useful in adults and teenagers who present later in life to assess the size and function of the right and left ventricles and determine cardiac output. Computer tomography (CAT-scan) can provide similar anatomical details as MRI.

56.6 Treatment

The treatment approach for Ebstein's anomaly is determined based on several factors, including the degree of cardiomegaly, right ventricular size, tricuspid regurgitation, cyanosis resulting from right-to-left shunting, and the presence of arrhythmias. Neonates with severe hypoxemia and significant cardiomegaly pose particular challenges. Some neonates with severe tricuspid valve insufficiency and elevated pulmonary resistance may have "functional pulmonary atresia" without anatomical pulmonary atresia. These cases typically respond to prostaglandin (PGE1) administration. However, if there is anatomical pulmonary atresia or stenosis, a systemic-to-pulmonary shunt or balloon pulmonary valvuloplasty may be required. Most neonates will need intubation, mechanical ventilation, and measures to reduce pulmonary vascular resistance, such as high oxygen and inhaled nitric oxide. Pulmonary compression or hypoplasia may be present due to the massive cardiomegaly. Neonatal operation may be necessary if these interventions fail to improve the condition.

Infants without associated anomalies and less severe cardiomegaly, who can be weaned off PGE1 and/or nitric oxide and remain stable, may be considered for operative repair at a later stage when the risk of mortality is significantly lower than in the neonatal period.

The main goals of surgical intervention are to establish a competent and nonstenotic tricuspid valve, eliminate sources of right-to-left shunting, and reduce the size of the right atrium and atrialized right ventricle as necessary. Some patients may require ablation or division of an accessory pathway, while others may need a maze procedure to address atrial arrhythmias. Tricuspid valve repair is the preferred surgical approach if feasible. The Cone repair method, which involves surgically delaminating the tricuspid valve tissue from the ventricular wall to create a cone-like structure and fixing it at the normal tricuspid valve annulus, has become the surgical method of choice for tricuspid valve repair. Additionally, a Glenn operation may be

performed in patients with severely reduced right ventricular volume to relieve the volume burden on the right ventricle from superior vena cava drainage (referred to as 1 and ½ repair).

56.7 Outcome

The long-term outcome of patients with Ebstein's anomaly depends on factors such as postoperative tricuspid valve function, as well as the size and function of the right ventricle (RV) and left ventricle (LV). Recent studies have shown promising results, with a 30-day mortality rate of less than 10% and survival rates of approximately 85% at 10 years and 70% at 20 years. The freedom from reoperation rates at 1, 5, 10, 15, and 20 years were reported as 97%, 91%, 82%, and 70%, respectively, for patients who underwent Danielson-type valve repair or valve replacement.

More recent reports from various centers worldwide have confirmed the favorable outcomes of patients who underwent the "cone" reconstruction method. These patients experienced a lower early mortality rate of about 1–2% and higher rates of successful repair. Furthermore, they had very favorable mid-term outcomes with regards to residual or recurrent tricuspid regurgitation.

Human Genetics of Ebstein Anomaly

57

Farbod Sedaghat-Hamedani, Gregor U. Andelfinger, and Benjamin Meder

57.1 Background

Ebstein anomaly (EA) is a rare, congenital cardiac defect of the tricuspid valve with a birth prevalence between 0.5 and 1 in 20,000 [1]. It is characterized by displacement of the tricuspid valve toward the apex of the right ventricle (RV) and "atrialization" of the RV (Fig. 57.1) [2]. EA accounts for about 0.5% of all congenital heart diseases (CHD) [2]. Depending on severity of the defect and due to heterogeneity of the disease, patient's presentation varies from severe heart failure symptoms and arrhythmia in neonatal life to asymptomatic adults.

Left ventricular noncompaction cardiomyopathy (LVNC), atrial septal defect (ASD), patent foramen ovale (PFO), accessory conduction pathways (Wolff–Parkinson–White syndrome) and mitral valve prolapse are the most common heart diseases associated with EA [3, 4]. Bicuspid aortic valve, ventricular septal defect (VSD), pulmonary outflow obstruction, and patent ductus arteriosus (PDA) are further congenital heart diseases which can be associated with EA [4]. Familial recurrence and an association with structural genomic variation, including syndromic forms, point to a genetic influence in pathogenesis. Gene content of more commonly observed chromosomal imbalances suggests that multiple cardiac regulators can contribute to Ebstein anomaly. The current gene catalogue discussed

F. Sedaghat-Hamedani
Institute for Cardiomyopathies Heidelberg (ICH), University Hospital Heidelberg, Heidelberg, Germany

G. U. Andelfinger
QC, Canada

B. Meder (✉)
Institute for Cardiomyopathies Heidelberg, Universitätsklinikum Heidelberg, Innere Medizin III - Kardiologie, Angiologie und Pneumologie, Heidelberg, Germany
e-mail: benjamin.meder@med.uni-heidelberg.de

© The Author(s), under exclusive license to Springer Nature Switzerland AG 2024

S. Rickert-Sperling et al. (eds.), *Congenital Heart Diseases: The Broken Heart*,
Advances in Experimental Medicine and Biology 1441,
https://doi.org/10.1007/978-3-031-44087-8_57

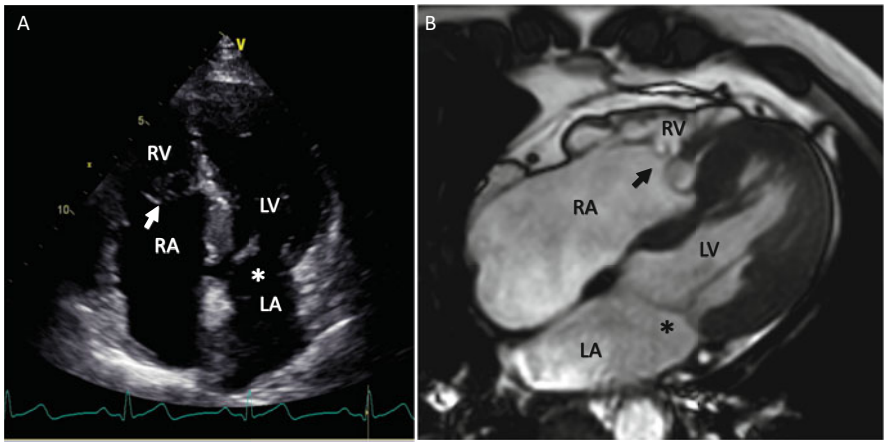

Fig. 57.1 Displacement of the Tricuspid Valve towards the Right Ventricle (RV). RA=Right Atrium; LV=Left Ventricle; LV=Left Atrium; * denotes the Mitral Valve

here suggests that diverse developmental pathways are affected in Ebstein anomaly and that variable expressivity and incomplete penetrance are commonly observed phenomena. It is very likely that the causal genes identified to date act in concert with modifiers, either environmental or (epi)genetic.

57.2 Genetic Background

The etiology of EA is still not completely clear. However, it is known that EA is genetically heterogeneous and can occur sporadically or familial or in association with other genetic syndromes [2, 4].

EA has been identified in association with rare mutations, chromosomal abnormalities, and copy-number variants (CNVs) [4]. Mutations in the sarcomeric protein myosin heavy chain 7 (*MYH7*) was reported in cases of combined LVNC and EA [5–7]. In a cohort of 141 unrelated probands with EA, mutations in *MYH7* were identified in 8 patients (6%) [8]. Among 8 mutation-positive probands, 6 had LVNC, whereas among 133 mutation-negative probands, none had LVNC. This suggests that *MYH7* mutations identified in EA cases are associated with LVNC and highlight the importance of genetic testing as well as evaluation of family members in this subset of patients [8]. Mutations in the cardiac transcription factors NK2 homeobox 5 (*NKX2–5)* and *GATA*-binding protein 4 (*GATA4*) have also been identified as cause of EA.

The occurrence of extracardiac anomalies in about 20% of cases with Ebstein anomaly has prompted systematic investigations of structural genomic variation as a potential cause. From case reports and patient series, a correlation of Ebstein anomaly with several disorders emerges; details are summarized in Table 57.1. Deletion in 1p36 and 8p23.1 has been reported as frequent chromosomal

Table 57.1 Summary of chromosomal imbalances reported in Ebstein anomaly

Chromosomal disorder	Proven or suspected causal gene(s)	References
Deletion 1p36	DVL1, SKI, RERE, PDPN, SPEN, CLCNKA, ECE1, HSPG2, LUZP1, WASF2, PRDM16, PRKCZ, UBE4B, MASP2	[2, 22–30]
Microdeletion 5q35	NKX2–5	[31]
Deletion 8p23.1	GATA4	[2, 32, 33]
Duplication 9p	Unknown	[34]
Deletion and duplication 11q	ETS1	[10]
Duplication 15q	Unknown	[35, 36]
Trisomy 18	Unknown	[37]
Deletion 18q21.3- > qter	NFATC1	[38]
Trisomy 21	Unknown	[39–44]

imbalances, and that likely candidate genes include *GATA4* and *NKX2*.5 [2, 9]. Furthermore rearrangements of the chromosomal region 11q (deletion or duplication) is likely to lead to EA as 46,XY,del(11)(11q21q23), and 47,XX,+der(22)t(11;22)(q23;q11.2) identified in patients with EA [10]. CNVs near the transcriptional repressor HEY1, a member of the NOTCH signaling pathway or CNVs close to genes involved in early myocardial development, including *NODAL*, *PDLIM5*, *SIX1*, *ASF1A,* and *FGF12,* were also reported in association with EA [4, 9].

Canine tricuspid valve malformation (CTVM) bears a striking resemblance to human Ebstein anomaly. It has been noted that this malformation is enriched in specific dog breeds, suggesting either founder effects or other strong influences of the genetic background. Genome-wide linkage analysis identified a CTVM susceptibility locus on dog chromosome 9 (CFA9) [11].

Syndromic forms of congenital heart disease also can be caused by single genes or be of unknown genetic origin. In a larger case series with 44 patients with Ebstein anomaly, 12 (27%) had syndromic presentation, and 7 of those had distinct disorders including CHARGE syndrome ($n = 2$), VACTERL association, Noonan syndrome, Kabuki syndrome, Holt–Oram syndrome, and Cornelia de Lange syndrome (one each) [2]. An additional two patients with CHARGE syndrome have been reported in the literature, both of which carry mutations in CHD7 (chromodomain helicase DNA binding protein 7), as well as one additional patient each with Kabuki syndrome, Holt–Oram syndrome, Noonan syndrome, Williams syndrome, and Ellis–van Creveld syndrome without mutation screening [12–17]. A single patient with thiamine-responsive megaloblastic anemia and Ebstein anomaly has been reported; interestingly, several other cardiac defects have been described in this syndrome, including one case of atrial standstill, which can be part of Ebstein syndrome [18, 19]. A relatively high number of patients with Ebstein anomaly and Down syndrome have been reported in the literature (Table 57.1); however, one has

to keep in mind that the denominator of all children born with trisomy 21 is much higher than for all other chromosomal imbalances listed here.

57.3 Management and Prognosis

Depending on patient's signs and symptoms the management and prognosis are varying. Asymptomatic patients can be managed under close follow-up. EA Patients with right heart failure (HF) should be treated like other right HF patients including diuretics and low sodium diet. Surgical therapies, e.g., tricuspid valve repair or replacement and reduction atrioplasty, are indicated in patients with EA in the presence of RV dilatation and progressive ventricular function impairment [3]. Electrophysiological evaluation and ablation should be performed in EA patients with Wolff–Parkinson–White syndrome, although these have lower success rates and higher risk of recurrence than patients with structurally normal heart [20, 21].

Without any treatment the prognosis of EA is poor and many symptomatic neonates with EA do not survive the first decade of life. The mortality among neonates is 29% at 1 year and 34% at 10 years [1]. However, with the improvement of medical therapy the prognosis of EA patients has improved. Updated prospective, long-term studies are essential for re-evaluation of outcomes of EA patients [4, 21].

References

1. Lupo PJ, Langlois PH, Mitchell LE. Epidemiology of Ebstein anomaly: prevalence and patterns in Texas, 1999-2005. Am J Med Genet A. 2011;155A(5):1007–14.
2. Digilio MC, et al. Ebstein anomaly: genetic heterogeneity and association with microdeletions 1p36 and 8p23.1. Am J Med Genet A. 2011;155A(9):2196–202.
3. Yuan SM. Ebstein's anomaly: genetics, clinical manifestations, and management. Pediatr Neonatol. 2017;58(3):211–5.
4. Giannakou A, et al. Copy number variants in Ebstein anomaly. PLoS One. 2017;12(12): e0188168.
5. Vermeer AM, et al. Ebstein anomaly associated with left ventricular noncompaction: an autosomal dominant condition that can be caused by mutations in MYH7. Am J Med Genet C Semin Med Genet. 2013;163C(3):178–84.
6. Sedaghat-Hamedani F, et al. Clinical genetics and outcome of left ventricular non-compaction cardiomyopathy. Eur Heart J. 2017;38(46):3449–60.
7. Kayvanpour E, et al. Clinical and genetic insights into non-compaction: a meta-analysis and systematic review on 7598 individuals. Clin Res Cardiol. 2019;108(11):1297–308.
8. Postma AV, et al. Mutations in the sarcomere gene MYH7 in Ebstein anomaly. Circ Cardiovasc Genet. 2011;4(1):43–50.
9. Sicko RJ, et al. Genetic variants in isolated Ebstein anomaly implicated in myocardial development pathways. PLoS One. 2016;11(10):e0165174.
10. de Lonlay-Debeney P, et al. Ebstein anomaly associated with rearrangements of chromosomal region 11q. Am J Med Genet. 1998;80(2):157–9.
11. Andelfinger G, et al. Canine tricuspid valve malformation, a model of human Ebstein anomaly, maps to dog chromosome 9. J Med Genet. 2003;40(5):320–4.
12. Corsten-Janssen N, et al. The cardiac phenotype in patients with a CHD7 mutation. Circ Cardiovasc Genet. 2013;6(3):248–54.

13. Yuan SM. Congenital heart defects in Kabuki syndrome. Cardiol J. 2013;20(2):121–4.
14. Tongsong T, Chanprapaph P. Prenatal sonographic diagnosis of Holt-Oram syndrome. J Clin Ultrasound. 2000;28(2):98–100.
15. Chang YC, et al. Common atrium with Ebstein's anomaly in a neonate with Ellis-van Creveld syndrome. Zhonghua Min Guo Xiao Er Ke Yi Xue Hui Za Zhi. 1995;36(1):50–2.
16. Wright NL, Summitt RL, Ainger LE. Noonan's syndrome and Ebstein's malformation of the tricuspid valve. Am J Dis Child. 1968;116(4):367–72.
17. Williams DA, Cook AL. An infant with Williams-Beuren syndrome and Ebstein anomaly. Cardiol Young. 2010;20(4):445–7.
18. Akbari MT, et al. Thiamine-responsive megaloblastic anemia syndrome with Ebstein anomaly: a case report. Eur J Pediatr. 2014;173(12):1663–5.
19. Lorber A, et al. Cardiac manifestations in thiamine-responsive megaloblastic anemia syndrome. Pediatr Cardiol. 2003;24(5):476–81.
20. Cappato R, et al. Radiofrequency current catheter ablation of accessory atrioventricular pathways in Ebstein's anomaly. Circulation. 1996;94(3):376–83.
21. Attenhofer Jost CH, et al. Ebstein's anomaly. Circulation. 2007;115(2):277–85.
22. Shimada S, et al. Microarray analysis of 50 patients reveals the critical chromosomal regions responsible for 1p36 deletion syndrome-related complications. Brain and Development. 2015;37(5):515–26.
23. Arndt AK, et al. Fine mapping of the 1p36 deletion syndrome identifies mutation of PRDM16 as a cause of cardiomyopathy. Am J Hum Genet. 2013;93(1):67–77.
24. Battaglia A, et al. Further delineation of deletion 1p36 syndrome in 60 patients: a recognizable phenotype and common cause of developmental delay and mental retardation. Pediatrics. 2008;121(2):404–10.
25. Goyette P, et al. Human methylenetetrahydrofolate reductase: isolation of cDNA mapping and mutation identification. Nat Genet. 1994;7(4):551.
26. Riegel M, et al. Terminal deletion, del(1)(p36.3), detected through screening for terminal deletions in patients with unclassified malformation syndromes. Am J Med Genet. 1999;82 (3):249–53.
27. Zaveri HP, et al. Identification of critical regions and candidate genes for cardiovascular malformations and cardiomyopathy associated with deletions of chromosome 1p36. PLoS One. 2014;9(1):e85600.
28. Rodriguez-Revenga L, et al. Cryptic chromosomal rearrangement screening in 30 patients with mental retardation and dysmorphic features. Clin Genet. 2004;65(1):17–23.
29. Thienpont B, et al. Left-ventricular non-compaction in a patient with monosomy 1p36. Eur J Med Genet. 2007;50(3):233–6.
30. Faivre L, et al. Prenatal detection of a 1p36 deletion in a fetus with multiple malformations and a review of the literature. Prenat Diagn. 1999;19(1):49–53.
31. Baekvad-Hansen M, et al. Delineation of a 2.2 Mb microdeletion at 5q35 associated with microcephaly and congenital heart disease. Am J Med Genet A. 2006;140(5):427–33.
32. Hutchinson R, Wilson M, Voullaire L. Distal 8p deletion (8p23.1----8pter): a common deletion? J Med Genet. 1992;29(6):407–11.
33. Paez MT, et al. Two patients with atypical interstitial deletions of 8p23.1: mapping of phenotypical traits. Am J Med Genet A. 2008;146A(9):1158–65.
34. Nakagawa M, et al. Ebstein's anomaly associated with trisomy 9p. Clin Genet. 1999;55(5): 383–5.
35. O'Connor R, et al. Pure duplication of the distal long arm of chromosome 15 with Ebstein anomaly and clavicular anomaly. Case Rep Genet. 2011;2011:898706.
36. Miller MS, et al. Ebstein anomaly and duplication of the distal arm of chromosome 15: report of two patients. Am J Med Genet A. 2005;139A(2):141–5.
37. Correa-Villasenor A, et al. Ebstein's malformation of the tricuspid valve: genetic and environmental factors. The Baltimore-Washington Infant Study Group. Teratology. 1994;50(2): 137–47.

38. van Trier DC, et al. Cardiac anomalies in individuals with the 18q deletion syndrome; report of a child with Ebstein anomaly and review of the literature. Eur J Med Genet. 2013;56(8):426–31.
39. Cyrus C, et al. Down syndrome with tandem 21;21 rearrangement and Ebstein's anomaly--a case report. Int J Cardiol. 2007;115(1):e58–60.
40. Siehr SL, et al. Ebstein anomaly and trisomy 21: a rare association. Ann Pediatr Cardiol. 2014;7 (1):67–9.
41. Silva SR, Bruner JP, Moore CA. Prenatal diagnosis of Down's syndrome in the presence of isolated Ebstein's anomaly. Fetal Diagn Ther. 1999;14(3):149–51.
42. Johnson CD, et al. Ebstein's anomaly in a patient with Down's syndrome. Bol Asoc Med P R. 1989;81(6):221–2.
43. Venturini E, et al. Ebstein's tricuspid anomaly and Down's syndrome. A clinical case report. Recenti Prog Med. 1992;83(10):556–8.
44. Leite Mde F, Gianisella RB, Zielinsky P. Intrauterine detection of Ebstein's anomaly and Down's syndrome. Prenatal diagnosis of a rare combination. Arq Bras Cardiol. 2004;82(4): 390–5.

Molecular Pathways and Animal Models of Ebstein's Anomaly

58

Bjarke Jensen, Gregor U. Andelfinger, and Alex V. Postma

Abstract

Ebstein's anomaly is a congenital malformation of the tricuspid valve characterized by abnormal attachment of the valve leaflets, resulting in varying degrees of valve dysfunction. The anatomic hallmarks of this entity are the downward displacement of the attachment of the septal and posterior leaflets of the tricuspid valve. Additional intracardiac malformations are common. From an embryological point of view, the cavity of the future right atrium does not have a direct orifice connected to the developing right ventricle. This chapter provides an overview of current insight into how this connection is formed and how malformations of the tricuspid valve arise from dysregulation of molecular and morphological events involved in this process. Furthermore, mouse models that show features of Ebstein's anomaly and the naturally occurring model of canine tricuspid valve malformation are described and compared to the human model. Although Ebstein's anomaly remains one of the least understood cardiac

B. Jensen
Department of Medical Biology, Amsterdam Cardiovascular Sciences, Amsterdam University Medical Centres, Amsterdam, The Netherlands

G. U. Andelfinger
Cardiovascular Genetics, Department of Pediatrics, CHU Sainte Justine, Université de Montréal, Montréal, QC, Canada

A. V. Postma (✉)
Department of Medical Biology, Amsterdam Cardiovascular Sciences, Amsterdam University Medical Centres, Amsterdam, The Netherlands

Department of Human Genetics, Amsterdam University Medical Centres, Amsterdam, The Netherlands
e-mail: a.v.postma@amsterdamumc.nl

© The Author(s), under exclusive license to Springer Nature Switzerland AG 2024

S. Rickert-Sperling et al. (eds.), *Congenital Heart Diseases: The Broken Heart*,
Advances in Experimental Medicine and Biology 1441,
https://doi.org/10.1007/978-3-031-44087-8_58

malformations to date, the studies summarized here provide, in aggregate, evidence for monogenic and oligogenic factors driving pathogenesis.

Keywords

Ebstein's anomaly · Tricuspid valve · NKX2-5 · Left ventricular noncompaction · Posterior leaflet · Hypoplastic left heart syndrome · Septal leaflet · Endocardial cushion · Mesenchyme · Atrioventricular canal · Epicardial-derived cells · EPDCs · Junctional myocardium · BMP · Alk2 · Alk3 · Bone morphogenetic protein · Canine tricuspid valve malformation · CTVM · GATA4 · TBX5 · Transforming growth factor beta · Labradors · Dogs · Mouse models · Knockout · Fog2 · PLD1 · AV canal

58.1 Introduction

Few cardiac malformations pose riddles as intriguing as Ebstein's anomaly for both the clinician and the basic researcher. The anatomic hallmarks of this entity are the downward displacement of the hinge-line of the septal and posterior leaflets of the tricuspid valve [1]. These leaflets are dysplastic and will often have excessive attachments to the ventricular wall. Characteristically, the anterior leaflet is typically hinged as in normal hearts but it may be enlarged and "sail-like." The downward displacement of the right-sided atrioventricular junction associates with tricuspid insufficiency and dilation of the right atrium [2]. The portion between the functional and anatomic valve annulus is termed "atrialized right ventricle." The right ventricle is dysfunctional. Because of considerable variation in the extent of valve displacement and the size and position of the tricuspid orifice, the severity of the setting varies substantially [3]. In more severe cases of Ebstein's anomaly, dysplasia of the septal leaflet can be so severe that only a small orifice from the right atrium to the right ventricle persists [4–6]. Associated anomalies, particularly secundum atrial septal defect and accessory atrioventricular (AV) pathways, are common, and an association with ventricular inversion (left-sided Ebstein's anomaly) is well known [7]. Left-sided anomalies including aortic and mitral valve anomalies as well as abnormal contraction of the left ventricle have been well documented during life and autopsy, including aortic valve malformations and left ventricular noncompaction (LVNC), which is better described as excessive trabeculation [8–16]. Malformation of the tricuspid valve with abnormal attachment of the septal leaflet is also common in hypoplastic left heart syndrome [17, 18].

The morphologic features of Ebstein's anomaly and associated malformations suggest that any genes involved in the pathogenesis of this disease might exert an influence on valve- and myocardium-specific developmental pathways (Chap. 57). Besides that Ebstein's anomaly exhibits features of perturbed normal development, such as the displaced valve hinge-line, it has been postulated that some features of the setting are in fact typical for the state of the normal tricuspid valve at 8 weeks of development, such as a small orifice and excessive myocardial tethering of the valve

[19]. This complex appearance may reflect both genetic and environmental effects, in addition to that, numerous tissues may be involved, including cushion mesenchyme, heart tube myocardium, chamber myocardium, endocardium and epicardially derived cells. Unfortunately, in comparison to other congenital heart diseases (CHD), there is a scarcity of both molecular data and animal models that can aid in the investigation of this interesting malformation.

58.2 Development of the Right Ventricular Inlet and Tricuspid Valve

Valve development is a highly conserved process [20]. It is initiated early in heart morphogenesis, and primitive cardiac valves arise after cushions are induced at the atrioventricular canal and the outflow tract regions already in the fourth week of gestation. Cushion formation is initiated by signals from the outer myocardial layer which induce the endocardium to undergo an epithelial-to-mesenchymal transition [21]. Mesenchymal cells then invade the underlying extracellular matrix of the cardiac jelly. This process determines the identity of the cushions, as well as safeguards the heart-tube like identity of the atrioventricular canal myocardium by keeping endocardial signaling at a distance [22]. The endocardial cushions of the AV canal have unique developmental properties and will fuse to form the atrioventricular septum. This divides the slit-like lumen of the atrioventricular canal into a left and a right channel, which will remodel and give rise to the mitral and tricuspid orifices respectively [23]. Mesenchyme from the endocardial cushions also will contribute to the formation of the inlet portion of the right ventricle [19].

It is important to note that before septation, the cavity of the future right atrium does not have a direct orifice to the developing right ventricle (Fig. 58.1)

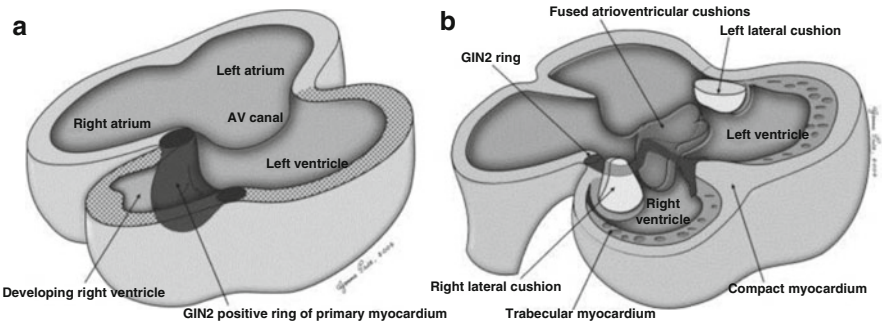

Fig. 58.1 (**a**) Location of the ring of musculature of the primary heart tube delineated by reaction to an antibody to the nodose ganglion of the chick. This is the myocardium of the so-called primary ring. (*AV* atrioventricular, *GIN2* antigen to chick nodose ganglion). (**b**) The first step in remolding of the primary ring occurs concomitant with appearance of the primary ventricular septum. As the apical parts of the ventricle balloon form the primary tube, the inferior part of the primary foramen deepens to form the right ventricular inlet component between the right atrium and the dorsal part of the developing right ventricle. At the same time, the cushions within the atrioventricular canal become draped across the inferior part of the forming ventricular septum (Adapted from [23])

[19, 24–26]. The formation of the tricuspid orifice and valve initiates in the sixth week of gestation and is thought to occur in two phases: first, the development of a connection between the right atrium and the right ventricle, and second, the formation of the valves and their suspension apparatus.

In the first phase, which occurs in the 6th and 7th week of gestation, the AV canal undergoes a proportional expansion which is mainly rightward, and to a lesser degree leftward [23, 27]. A channel is hereby maintained between the right atrium and the ventricle despite the thickening of the ventricular septum immediately below the AV canal [27]. The expansion the AV canal leads to the formation on the posterior-right of a myocardial ridge at the boundary between the AV canal and the embryonic right ventricle. This myocardial funnel then develops to become the "tricuspid gully" [19], which at this stage does not have any leaflets of the tricuspid valve yet. The major orifice of the developing tricuspid valve is parallel to the developing ventricular septum while perforations in the floor of the gully create an additional inferior opening [24]. With the appearance of the endocardial cushion, the lumen between the trabecular and compact layers of myocardium expand, leading to the formation of the anterosuperior and inferior leaflets during the seventh week of gestation. Delamination of the septal leaflet from the developing ventricular septum occurs much later during the twelfth week.

In the second phase, which occurs in the 8th week of gestation and extends into the fetal period [28], epicardially derived cells, myocardium and endocardial cushions all make contributions to the leaflets of the tricuspid valve [19, 24, 29]. Epicardially derived cells (EPDC) are known to contribute to the developing fibroblast population in the heart [30, 31]. EPDCs contribute to the development of the AV canal and the annulus fibrosus and populate the ventricular myocardial wall and interventricular septum [32, 33]. Using the mWt1/IRES/GFP-Cre mouse to trace the fate of EPDCs from embryonic day (ED) 10 until birth, Wessels et al. found the parietal AV leaflets have a very strong epicardial contribution, whereas the septal leaflet of the tricuspid valve (and all leaflets derived from the major cushions) hardly have any epicardial contribution [29].

In parallel to this process, the muscle masses of atrium and ventricle become largely disconnected by the fusion of the tissues of the atrioventricular sulcus (located at the epicardial side of the junctional myocardium) with those of the atrioventricular cushions (located at the endocardial side of the junctional myocardium). This fusion leads to the formation of fibrous insulating tissues at approximately 7 weeks of development in the anteromedial portion of the right atrioventricular junction and is largely completed around the 12th week of development. In the normal adult heart, the only remaining myocardial continuity between atrial and ventricular myocardium is the atrioventricular axis of conduction [25]. In Ebstein's anomaly, however, myocardial connections may be found between the right atrium and the right ventricle and between the proximal parts of the atrioventricular conduction axis and the ventricular septum, all of which may serve as substrates of ventricular pre-excitation and ventricular fibrillation [7].

Molecular pathways involved in the pathogenesis of Ebstein's anomaly are likely to impact the cellular and morphological events of tricuspid valve formation at very

early stages. Involved tissues may be, to various degrees, cushion mesenchyme, heart tube myocardium, chamber myocardium, endocardium and epicardially derived cells. Several signaling and transcription cascades are therefore prime candidates based on their spatiotemporal expression patterns or known functions in heart morphogenesis.

58.3 Mouse Models of Ebstein's Anomaly

Although several mouse models exist that replicate some aspects of Ebstein's anomaly, no single-gene model exhibiting all its features has been reported to date. This might have to do with the fact that the severity- and the spectrum of defects observed in CHD mouse models varies greatly, and is strongly dependent on the genetic background. Case in point, the spectrum of defects resulting from a reduction in Gata4 protein, which is crucial to heart development in human and mouse, is strongly dependent on the genetic background, as 24% of C57BL6/J mice and 70% of FVB mice carrying a Gata4 mutation show no phenotype [34]. Nonetheless, there are several mouse models that phenocopy (aspects of) Ebstein's anomaly. One of the major features of Ebstein's anomaly is abnormal development of the tricuspid valves. Though there are only two transgenic mouse models listed as Ebstein's anomaly (see below), there are about a dozen genes that when disrupted in mice associate with tricuspid atresia (e.g., CC2D2A, HEY2, LEFTY1, LEFTY2, MMP21, NKX2-5, PSME4, PLD1, SMAD6, ZFPM2) (see also Chap. 51). For the major part these genes are transcription factors, well known for their involvement in cardiac development. For example, tricuspid atresia is reported in Zfpm2 (friend of GATA 2 or FOG2) knockout mice, most likely secondary to impaired attenuation of endothelial-to-mesenchymal transition within the developing cushions [35, 36]. In contrast, the PLD1 gene does not encode a transcription factor and it is ubiquitously expressed, rather than being heart specific, and is involved in the hydrolysis of phosphatidylcholine which produces phosphatidic acid and choline. Nonetheless, mutations in the PLD1 gene gives rise to autosomal-recessive Ebstein's anomaly in humans [37], and PLD1 knockout mice have tricuspid valve regurgitation and an enlarged right atrium [38]. It turns out that PLD1 is also involved in endothelial–mesenchymal transition, an established pivotal early step in valvulogenesis [37], providing a possible mechanism whereby loss of PLD1 function may lead to tricuspid atresia.

However, the most faithful murine Ebstein's model to date is an Nkx2-5 (NK2 homeobox 5) p.Arg25Gly knockin allele, which mimics a mutation found in humans [39]. The human NKX2-5 p.Arg52Gly mutation destabilizes the homeodomain of this transcription factor, reduces DNA binding as well as homo- and heterodimerization with GATA4 and TBX5 [40]. In the 129Sv background, this knockin leads to a high penetrance of congenital heart disease, in particular ventricular septal defects (82%), atrioventricular septal defects (18%) and tricuspid valve anomalies (47%). In addition, all investigated knockin mice had excessive trabeculation, which has also been reported for Nkx2.5 heterozygous mice [41],

consistent with the association of NKX2.5 and excessive trabeculations in human [42]. Incomplete delamination was seen in all mice with tricuspid valve anomalies, with all hallmarks of Ebstein's anomaly in 8.5% of mice. Detailed molecular assessment and timelines of maldevelopment of the tricuspid valve have not yet been reported in this mouse. In keeping with other studies [43, 44], penetrance of different phenotypic aspects of those mice was highly dependent on the background. After one cross into the C57B6 background, attenuation of most defects was noted, with the exception of excessive trabeculation which still had a very high penetrance [39].

The second murine model that phenocopies much of Ebstein's anomaly is one in which GATA (GATA binding protein) 6-Cre driver mouse were used to conditionally delete Alk3 (BMPR1A) in the developing AV canal [45]. Interestingly, lineage analysis showed a clear contribution of AV canal cardiac myocytes to the future tricuspid mural and posterior leaflets, but not to the tricuspid septal leaflet. The mitral septal leaflet and the atrial border of the annulus fibrosus were also stained. When Alk3 was deleted in these cells, defects were seen in the same leaflets, i.e., the tricuspid mural leaflet and mitral septal leaflet were longer, the tricuspid posterior leaflet was displaced and adherent to the ventricular wall and the annulus fibrosus was disrupted resulting in ventricular pre-excitation. These defects provide in fact some overlap with Ebstein's anomaly and demonstrate that signaling by Alk3, the type 1a receptor for bone morphogenetic proteins, in the myocardium of the AV canal is required for the development of both the AV valves and annulus fibrosus, but they do not replicate the hallmark of the condition, namely, the apical displacement and nondelamination of the septal leaflet of the tricuspid valve. In addition, the authors observed variation in the extent of Cre-mediated recombination and defects of the tricuspid mural leaflet was identified in 36% of cGATA6-Cre/Alk3 mice and posterior hinge-line was displaced apically in one out of six investigated mice only. Conceivably, expression of Cre in the GATA6-Cre driver mouse may become progressively restricted in primary myocardium and thus insufficient to label all AV canal myocardial cells.

While good mouse models of Ebstein's anomaly are scarce, valuable data on the possible molecular pathways involved in Ebstein's anomaly have been gathered from murine models. Specifically, gain- and loss-of-function studies, tissue explant studies and expression patterns all point toward an important role of BMP (bone morphogenetic protein) signaling in endothelial–mesenchymal transformation of endocardial cushions. BMP2 is strongly expressed in AV cushions, whereas the major BMP receptors, including BmprII, Alk2 (Acvr1, activin A receptor, type 1), and Alk3 (Acvr3), are widely expressed in the entire heart, with no clear spatial restriction [46, 47]. In extrapolation of these results, it can be presumed that key processes possibly involved in Ebstein's anomaly are at least in part mediated through BMP signaling in the developing atrioventricular myocardium, including the processes leading to proper electric insulation of ventricles and atria [45]. Within the same morphological processes and molecular pathway, it was observed that positioning of the endocardial cushions in the ventricular lumen and formation of early trabeculae are part of one remodeling process which is under control of

TGF-β2 (transforming growth factor, beta 2) [48]. In the Tgf-beta2-KO mouse, remodeling of the early myocardium is disturbed as indicated by defective trabeculae formation, persistence of valvular myocardium, disturbed myocardial phenotypes and differential defects at left and right side of the AV canal [48]. Bmp2 and Tgf-beta2 themselves are under genetic control of Tbx (T-box) 20, disruption of which leads to defective AV canal myocardial and valve development [49]. Besides the role of connective tissues in proper electric insulation, genes such as Tbx2 and Notch are also required for the correct patterning of the AV canal myocardium such that it propagates the electrical impulse slowly [50, 51]. In mice with activated Notch signaling there was, besides accessory AV-connections, also excessive atrial myocardium on the tricuspid valve, which resembles an Ebstein's anomaly-like phenotype [51]. In conclusion, as seen in other mouse mutants, these observations suggest that the morphogenetic processes governing normal and abnormal tricuspid formation are likely to be under the control of a cooperative gene network [52].

58.4 Canine Tricuspid Valve Malformation as a Model for Human Ebstein's Anomaly

Ebstein's anomaly can naturally occur in mammals and is most frequently reported in dogs [53]. Specifically, canine tricuspid valve malformation (CTVM) can be seen as an Ebstein's dog model, as it is characterized by an apical displacement of the attachment of the tricuspid leaflets and adherence of the septal leaflet to the interventricular septum (Fig. 58.2). Other features include thickening of the valve leaflets, redundancy of the parietal leaflet and presence of a large, fused papillary

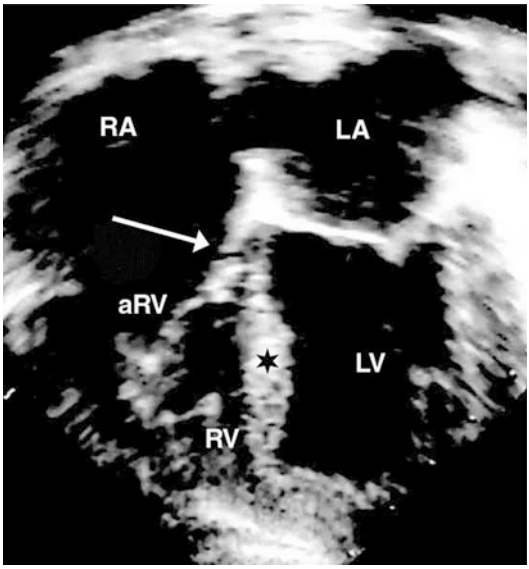

Fig. 58.2 Apical four-chamber echocardiogram in canine tricuspid valve malformation. *Arrowhead* downward displacement and abnormal adherence of the septal leaflet of the tricuspid valve [62]. *RA* right atrium, *LA* left atrium, *aRV* atrialized right ventricle, *RV* right ventricle, *LV* left ventricle, ★ interventricular septum

muscle rather than normal small, discrete muscles. Additional congenital heart defects in affected dogs have been described, including mitral valve abnormality [54–58]. CTVM has been most frequently identified in Labrador Retrievers, but it has been observed in other breeds as well [57, 59–62]. As in humans, the clinical picture varies, with severity in affected dogs ranging from asymptomatic, to premature death secondary to right heart failure [56, 61, 62]. In general, CTVM mimics the morphological and clinical picture of Ebstein's anomaly.

The availability of larger dog pedigrees and ascending genealogies from breeding documents has facilitated the genetic analysis of CTVM. There are three available genetic studies on CTVM in dogs, and all show clear evidence of its heritability. Two studies favor a recessive mode of transmission [59, 60] and one study demonstrates autosomal dominant transmission with reduced penetrance [63]. In this latter study, a total of 140 tested polymorphic markers excluded ~60% of the genome, with a suggestive linkage to canine chromosome 9 (CFA9) with a two-point LOD score of 1.56. Subsequently, fine mapping and linkage analysis yielded a maximum multipoint LOD score for the three most informative markers within the critical interval of 3.33, indicating odds of greater than 2000:1 that CTVM is linked to a locus on CFA9 (Fig. 58.3) [63]. Subsequent comparative mapping showed that this interval is homologous to a gene-rich region on human chromosome 17q, but a disease-contributing variant could not yet be isolated (Fig. 58.4) [64, 65]. The human region however does contain several genes that are involved in heart development and function, some of which might be candidates for CTVM or Ebstein's anomaly. Two genes stand out in particular, *TBX2* and *JUP*. TBX2 is a gene that encodes a transcription factor belonging to the family of T-box factor proteins that bind DNA. It is expressed in a variety of tissues and organs during embryogenesis. In the heart, as mentioned earlier, Tbx2 is required for the correct patterning of the AV canal myocardium and the induction of endocardial cushion formation [50, 51, 66] and both processes might be affected in Ebstein's anomaly. In human, mutations in TBX2 are associated with a syndromic cardiovascular and skeletal developmental disorder; heart phenotypes include double-outlet right ventricle and valvular pulmonic stenosis, among others [58]. The JUP gene encodes plakoglobin a major cytoplasmic protein and is present in adhering junctions, the desmosomes and the intermediate junctions. Mutations in this gene in humans give rise to arrhythmogenic right ventricular cardiomyopathy (ARVC), a disease specific to the right side of the heart, in which myocyte integrity is affected by loss of cell-cell adhesion [67]. In addition, mutations in JUP affect the structure and distribution of mechanical and electrical cell junctions. If, and how these genes might be involved in CTVM or Ebstein's anomaly needs further study.

CTVM also occurs in other dog breeds, for instance a single locus seems to control the predisposition in the Dogue de Bordeaux population in Israel toward both CTVM and subaortic stenosis [60]. It is unknown whether this locus is identical to the Labrador CTVM locus on CFA 9. Furthermore, in Labradors, two independent studies estimated CTVM heritability at 0.71 and penetrance at 68% [59, 63]. In addition, in Keeshonds, conotruncal defects (CTD) are oligogenic, with the strongest support for a locus on CFA9 (LOD 3.7) that fully overlaps with the CTVM locus

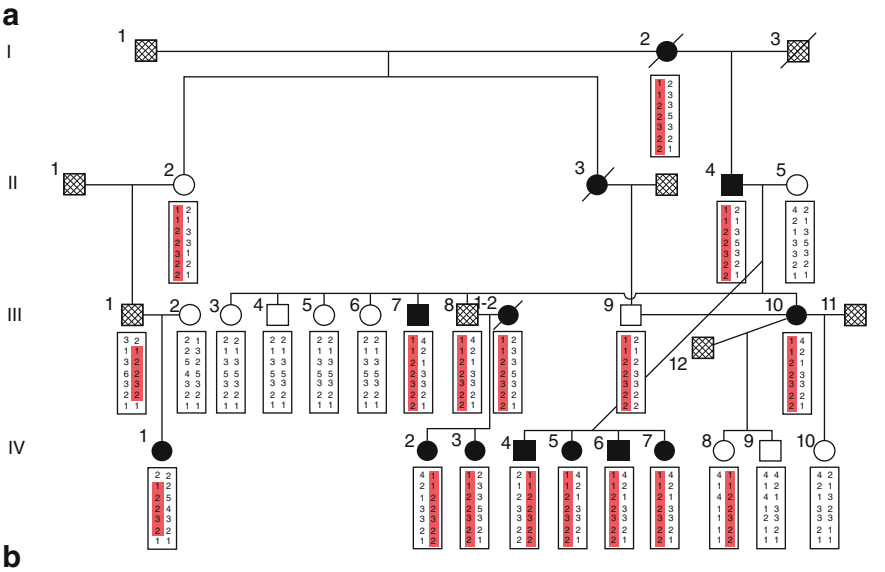

Fig. 58.3 (**a**) kindred CTVM1, (**b**) kindred CTVM2, (**c**) kindred CTVM3, (**d**) legend, (**e**) genotyped markers and map distances (*cR*). All affected dogs in kindreds CTVM2 and CTVM3 also fulfilled the diagnostic criteria for canine tricuspid valve malformation (CTVM). None of the dogs in the series reported here showed any other intra- or extracardiac malformation [62]

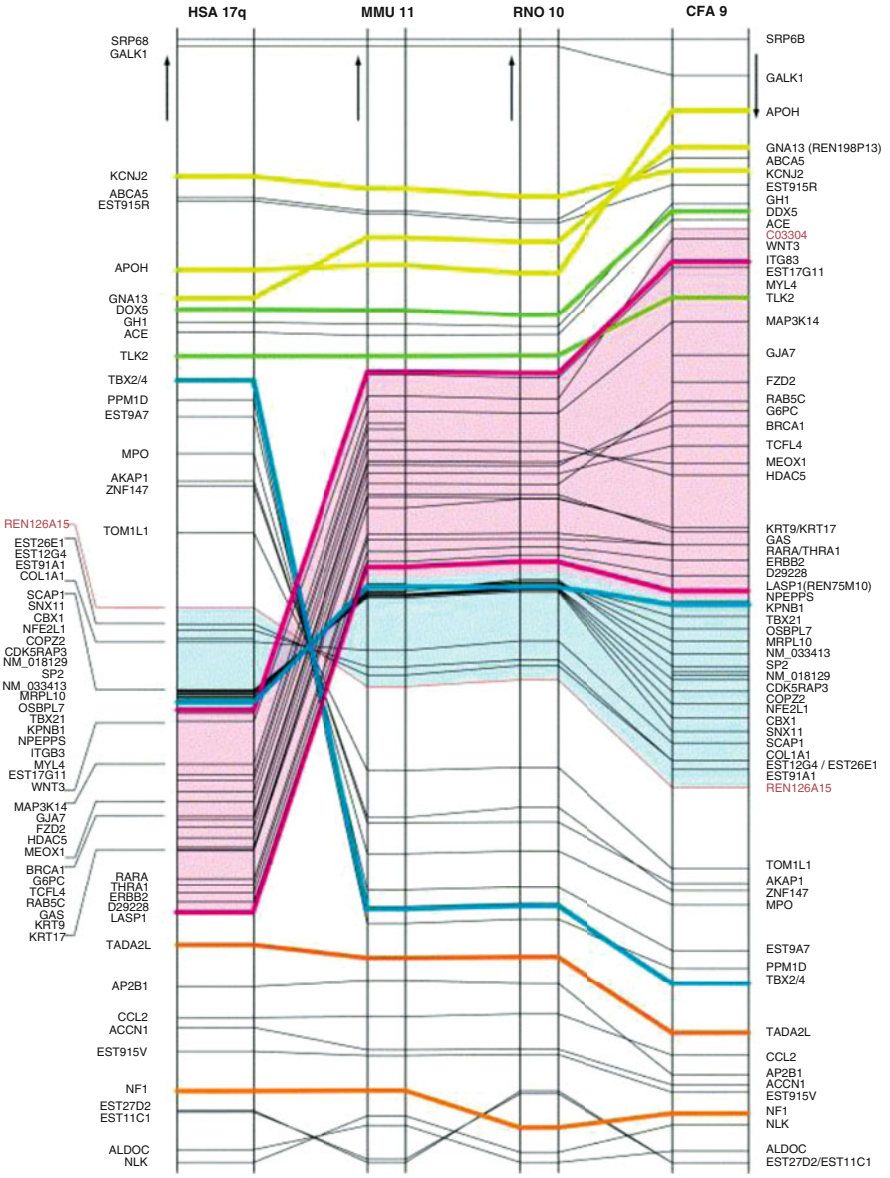

Fig. 58.4 *Horizontal axis*: human chromosome 17q (HSA17q) and its syntenic regions on mouse chromosome 11 (MMU11), rat chromosome 10 (RNO10), and dog chromosome 9 (CFA9). *Vertical axis*: Chromosomal positions of genes, with largest distances in individual species equalized to each other. Positions are drawn to scale. *Arrows* denote directionality from centromere to telomere. The recombinant markers for the ctvm interval, C03304 and REN126A15, are labeled by red lettering in the right-hand column. *Yellow*, *green*, *blue*, *purple,* and *orange lines* facilitate the identification of genes involved in important rearrangement events. *Pink* and *blue overlays* identify human chromosomal segments that undergo macroreversals in a multiple genome rearrangement scenario. Brackets group genes in densely mapped areas in respective order [64]

mapped in Labradors [68]. It is conceivable that breed-specific background effects in the Labrador, Keeshond and Dogue de Bordeaux dogs influence both penetrance and expressivity of CTVM, reminiscent of observations both in humans and mouse.

58.5 Conclusion

The molecular substrates of Ebstein's anomaly are still largely unknown. Nonetheless, the elements outlined above leave ample scope to consider several specific processes in the development of this condition. In general, cell populations that affect tricuspid valve development arise from epicardial, endocardial, mesenchymal and myocardial lineages. However, specific AV canal precursors for the tricuspid septal leaflet have not yet been identified. With regards to which molecular cascades govern the behavior of these cell populations, literature suggests that these include the TGF-β, Bmp2 and Notch signaling pathways, besides matrix proteins and transcription factors of the T-box family. There are some naturally occurring and transgenic animal models that mimic Ebstein's anomaly, although the phenotype and penetrance varies. Further study of these models might yield more insight into the molecular pathophysiological mechanism behind Ebstein's disease.

Acknowledgments GA is funded by the Canadian Institutes of Health Research and holds the Banque Nationale Research Chair in Cardiovascular Genetics.

References

1. Schreiber C, Cook A, Ho SY, Augustin N, Anderson RH. Morphologic spectrum of Ebstein's malformation: revisitation relative to surgical repair. J Thorac Cardiovasc Surg. 1999;117(1):148–55.
2. Qureshi MY, O'Leary PW, Connolly HM. Cardiac imaging in Ebstein anomaly. Trends Cardiovasc Med. 2018;28(6):403–9.
3. Possner M, Gensini FJ, Mauchley DC, Krieger EV, Steinberg ZL. Ebstein's anomaly of the tricuspid valve: an overview of pathology and management. Curr Cardiol Rep. 2020;22(12):157.
4. Leung MP, Baker EJ, Anderson RH, Zuberbuhler JR. Cineangiographic spectrum of Ebstein's malformation: its relevance to clinical presentation and outcome. J Am Coll Cardiol. 1988;11(1):154–61.
5. Rusconi PG, Zuberbuhler JR, Anderson RH, Rigby ML. Morphologic-echocardiographic correlates of Ebstein's malformation. Eur Heart J. 1991;12(7):784–90.
6. Zuberbuhler JR, Allwork SP, Anderson RH. The spectrum of Ebstein's anomaly of the tricuspid valve. J Thorac Cardiovasc Surg. 1979;77(2):202–11.
7. Sanchez-Quintana D, Cabrera JA, Picazo-Angelin B, Cabrera A, Anderson RH. Histological examination of the potential arrhythmic substrates in the setting of Ebstein's malformation. J Anat. 2020;237(1):155–65.
8. Petersen SE, Jensen B, Aung N, Friedrich MG, McMahon CJ, Mohiddin SA, Pignatelli RH, Ricci F, Anderson RH Bluemke DA. Excessive trabeculation of the left ventricle: JACC: cardiovascular imaging expert panel paper. Cardiovascular Imaging. 2023;16(3):408–425.
9. Attenhofer Jost CH, Connolly HM, O'Leary PW, Warnes CA, Tajik AJ, Seward JB. Left heart lesions in patients with Ebstein anomaly. Mayo Clin Proc. 2005;80(3):361–8.

10. Attenhofer Jost CH, Connolly HM, Warnes CA, O'Leary P, Tajik AJ, Pellikka PA, et al. Noncompacted myocardium in ebstein's anomaly: initial description in three patients. J Am Soc Echocardiogr. 2004;17(6):677–80.
11. Castaneda-Zuniga W, Nath HP, Moller JH, Edwards JE. Left-sided anomalies in Ebstein's malformation of the tricuspid valve. Pediatr Cardiol. 1982;3(2):181–5.
12. Daliento L, Angelini A, Ho SY, Frescura C, Turrini P, Baratella MC, et al. Angiographic and morphologic features of the left ventricle in Ebstein's malformation. Am J Cardiol. 1997;80(8): 1051–9.
13. Gerlis LM, Ho SY, Sweeney AE. Mitral valve anomalies associated with Ebstein's malformation of the tricuspid valve. Am J Cardiovasc Pathol. 1993;4(4):294–301.
14. Monibi AA, Neches WH, Lenox CC, Park SC, Mathews RA, Zuberbuhler JR. Left ventricular anomalies associated with Ebstein's malformation of the tricuspid valve. Circulation. 1978;57 (2):303–6.
15. Stähli BE, Gebhard C, Biaggi P, Klaassen S, Valsangiacomo Buechel E, Attenhofer Jost CH, et al. Left ventricular non-compaction: prevalence in congenital heart disease. Int J Cardiol. 2013;167(6):2477–81.
16. van Engelen K, Postma AV, van de Meerakker JBA, Roos-Hesselink JW, Helderman-van den Enden ATJM, Vliegen HW, et al. Ebstein's anomaly may be caused by mutations in the sarcomere protein gene MYH7. Neth Hear J. 2013;21(3):113–7.
17. Reyes A, 2nd, Bove EL, Mosca RS, Kulik TJ, Ludomirsky A. Tricuspid valve repair in children with hypoplastic left heart syndrome during staged surgical reconstruction. Circulation. 1997;96(9 Suppl):II-341–3; discussion II-4-5
18. Stamm C. The morphologically tricuspid valve in hypoplastic left heart syndrome. Eur J Cardiothorac Surg. 1997;12(4):587–92.
19. Lamers WH, Virágh S, Wessels A, Moorman AFM, Anderson RH. Formation of the tricuspid valve in the human heart. Circulation. 1995;91(1):111–21.
20. Lincoln J, Alfieri CM, Yutzey KE. Development of heart valve leaflets and supporting apparatus in chicken and mouse embryos. Dev Dyn. 2004;230(2):239–50.
21. Armstrong EJ, Bischoff J. Heart valve development: endothelial cell signaling and differentiation. Circ Res. 2004;95(5):459–70.
22. Bressan M, Yang PB, Louie JD, Navetta AM, Garriock RJ, Mikawa T. Reciprocal myocardial-endocardial interactions pattern the delay in atrioventricular junction conduction. Development. 2014;141(21):4149–57.
23. de Lange FJ, Moorman AFM, Anderson RH, Männer J, Soufan AT, Vries CG-d, et al. Lineage and morphogenetic analysis of the cardiac valves. Circ Res. 2004;95(6):645–54.
24. Kanani M, Moorman AFM, Cook AC, Webb S, Brown NA, Lamers WH, et al. Development of the atrioventricular valves: clinicomorphological correlations. Ann Thorac Surg. 2005;79(5): 1797–804.
25. Wessels A, Markman MWM, Vermeulen JLM, Anderson RH, Moorman AFM, Lamers WH. The development of the atrioventricular junction in the human heart. Circ Res. 1996;78 (1):110–7.
26. Wessels A, Vermeulen JLM, Virágh SZ, Kálmán F, Morris GE, Man NT, et al. Spatial distribution of "tissue-specific" antigens in the developing human heart and skeletal muscle. I. An immunohistochemical analysis of creatine kinase isoenzyme expression patterns: CK ISOENZYMES IN HUMAN MUSCLE. Anat Rec. 1990;228(2):163–76.
27. Faber JW, Hagoort J, Moorman AFM, Christoffels VM, Jensen B. Quantified growth of the human embryonic heart. Biol Open. 2021;10(2)
28. Sizarov A, Devalla HD, Anderson RH, Passier R, Christoffels VM, Moorman AF. Molecular analysis of patterning of conduction tissues in the developing human heart. Circ Arrhythm Electrophysiol. 2011;4(4):532–42.
29. Wessels A, van den Hoff MJB, Adamo RF, Phelps AL, Lockhart MM, Sauls K, et al. Epicardially derived fibroblasts preferentially contribute to the parietal leaflets of the atrioventricular valves in the murine heart. Dev Biol. 2012;366(2):111–24.

30. Dettman RW, Denetclaw W, Ordahl CP, Bristow J. Common epicardial origin of coronary vascular smooth muscle, perivascular fibroblasts, and Intermyocardial fibroblasts in the avian heart. Dev Biol. 1998;193(2):169–81.
31. Gittenberger-de Groot AC, Vrancken Peeters M-PFM, Mentink MMT, Gourdie RG, Poelmann RE. Epicardium-derived cells contribute a novel population to the myocardial wall and the atrioventricular cushions. Circ Res. 1998;82(10):1043–52.
32. Wessels A, Pérez-Pomares JM. The epicardium and epicardially derived cells (EPDCs) as cardiac stem cells: epicardially derived cells as cardiac stem cells. Anat Rec A: Discov Mol Cell Evol Biol. 2004;276A(1):43–57.
33. Zhou B, von Gise A, Ma Q, Hu YW, Pu WT. Genetic fate mapping demonstrates contribution of epicardium-derived cells to the annulus fibrosis of the mammalian heart. Dev Biol. 2010;338 (2):251–61.
34. Rajagopal SK, Ma Q, Obler D, Shen J, Manichaikul A, Tomita-Mitchell A, et al. Spectrum of heart disease associated with murine and human GATA4 mutation. J Mol Cell Cardiol. 2007;43 (6):677–85.
35. Flagg AE, Earley JU, Svensson EC. FOG-2 attenuates endothelial-to-mesenchymal transformation in the endocardial cushions of the developing heart. Dev Biol. 2007;304(1):308–16.
36. Svensson EC, Huggins GS, Lin H, Clendenin C, Jiang F, Tufts R, et al. A syndrome of tricuspid atresia in mice with a targeted mutation of the gene encoding Fog-2. Nat Genet. 2000;25(3): 353–6.
37. Lahrouchi N, Postma AV, Salazar CM, De Laughter DM, Tjong F, Piherova L, et al. Biallelic loss-of-function variants in PLD1 cause congenital right-sided cardiac valve defects and neonatal cardiomyopathy. J Clin Invest. 2021;131(5)
38. Ta-Shma A, Zhang K, Salimova E, Zernecke A, Sieiro-Mosti D, Stegner D, et al. Congenital valvular defects associated with deleterious mutations in the PLD1 gene. J Med Genet. 2017;54 (4):278–86.
39. Ashraf H, Pradhan L, Chang EI, Terada R, Ryan NJ, Briggs LE, et al. A mouse model of human congenital heart disease: high incidence of diverse cardiac anomalies and ventricular noncompaction produced by heterozygous *Nkx2-5* homeodomain missense mutation. Circ Cardiovasc Genet. 2014;7(4):423–33.
40. Kasahara H. Biochemical analyses of eight NKX2.5 homeodomain missense mutations causing atrioventricular block and cardiac anomalies. Cardiovasc Res. 2004;64(1):40–51.
41. Choquet C, Nguyen THM, Sicard P, Buttigieg E, Tran TT, Kober F, et al. Deletion of Nkx2-5 in trabecular myocardium reveals the developmental origins of pathological heterogeneity associated with ventricular non-compaction cardiomyopathy. PLoS Genet. 2018;14(7): e1007502.
42. Wilsbacher L, McNally EM. Genetics of cardiac developmental disorders: cardiomyocyte proliferation and growth and relevance to heart failure. Annu Rev Pathol. 2016;11:395–419.
43. Winston JB, Erlich JM, Green CA, Aluko A, Kaiser KA, Takematsu M, et al. Heterogeneity of genetic modifiers ensures normal cardiac development. Circulation. 2010;121(11):1313–21.
44. Winston JB, Schulkey CE, Chen I-BD, Regmi SD, Efimova M, Erlich JM, et al. Complex trait analysis of ventricular septal defects caused by *Nkx2-5* mutation. Circulation. 2012;5(3): 293–300.
45. Gaussin V, Morley GE, Cox L, Zwijsen A, Vance KM, Emile L, et al. Alk3/Bmpr1a receptor is required for development of the atrioventricular canal into valves and annulus Fibrosus. Circ Res. 2005;97(3):219–26.
46. Lyons KM, Pelton RW, Hogan BL. Organogenesis and pattern formation in the mouse: RNA distribution patterns suggest a role for bone morphogenetic protein-2A (BMP-2A). Development. 1990;109(4):833–44.
47. Roelen BA, Goumans MJ, van Rooijen MA, Mummery CL. Differential expression of BMP receptors in early mouse development. Int J Dev Biol. 1997;41(4):541–9.
48. Kruithof BPT, Kruithof-De-Julio M, Poelmann RE, Gittenberger-De-Groot AC, Gaussin V, Goumans M-J. Remodeling of the myocardium in early trabeculation and cardiac valve formation; a role for TGFβ2. Int J Dev Biol. 2013;57(11–12):853–63.

49. Cai X, Nomura-Kitabayashi A, Cai W, Yan J, Christoffels VM, Cai C-L. Myocardial Tbx20 regulates early atrioventricular canal formation and endocardial epithelial–mesenchymal transition via Bmp2. Dev Biol. 2011;360(2):381–90.
50. Aanhaanen WT, Boukens BJ, Sizarov A, Wakker V, de Gier-de Vries C, van Ginneken AC, et al. Defective Tbx2-dependent patterning of the atrioventricular canal myocardium causes accessory pathway formation in mice. J Clin Invest. 2011;121(2):534–44.
51. Rentschler S, Harris BS, Kuznekoff L, Jain R, Manderfield L, Lu MM, et al. Notch signaling regulates murine atrioventricular conduction and the formation of accessory pathways. J Clin Invest. 2011;121(2):525–33.
52. Bonyadi M, Rusholme SAB, Cousins FM, Su HC, Biron CA, Farrall M, et al. Mapping of a major genetic modifier of embryonic lethality in TGFβ1 knockout mice. Nat Genet. 1997;15(2):207–11.
53. Michaëlsson M, Ho S. World Scientific Publishing Company; 2000.
54. Chetboul V, Tran D, Carlos C, Tessier D, Pouchelon JL. Les malformations congénitales de la valve tricuspide chez les carnivores domestiques: étude rétrospective de 50 cas: Kongenitale Missbildungen der Trikuspidalklappe bei domestizierten Karnivoren: Retrospektive Studie von 50 Fällen. Schweiz Arch Tierheilkd. 2004;146(6):265–75.
55. Eyster GE, Anderson L, Evans AT, Chaffee A, Bender G, Johnston J, et al. Ebstein's anomaly: a report of 3 cases in the dog. J Am Vet Med Assoc. 1977;170(7):709–13.
56. Hoffmann G, Amberger CN, Seiler G, Lombard CW. Tricuspid valve dysplasia in fifteen dogs. Schweiz Arch Tierheilkd. 2000;142(5):268–77.
57. Kornreich BG, Moïse NS. Right atrioventricular valve malformation in dogs and cats: an electrocardiographic survey with emphasis on splintered QRS complexes. J Vet Intern Med. 1997;11(4):226–30.
58. Liu N, Schoch K, Luo X, Pena LDM, Bhavana VH, Kukolich MK, et al. Functional variants in TBX2 are associated with a syndromic cardiovascular and skeletal developmental disorder. Hum Mol Genet. 2018;27(14):2454–65.
59. Famula TR, Siemens LM, Davidson AP, Packard M. Evaluation of the genetic basis of tricuspid valve dysplasia in Labrador retrievers. Am J Vet Res. 2002;63(6):816–20.
60. Ohad DG, Avrahami A, Waner T, David L. The occurrence and suspected mode of inheritance of congenital subaortic stenosis and tricuspid valve dysplasia in Dogue de Bordeaux dogs. Vet J. 2013;197(2):351–7.
61. Adin D. Tricuspid valve dysplasia. St. Louis: Saunders Elsevier; 2008.
62. Wright K. Tricuspid valve dysplasia. St. Louis: Mosby Elsevier; 2011.
63. Andelfinger G, Wright KN, Lee HS, Siemens LM, Benson DW. Canine tricuspid valve malformation, a model of human Ebstein anomaly, maps to dog chromosome 9. J Med Genet. 2003;40(5):320–4.
64. Andelfinger G, Etter L, Dyment M, Hitte C, Galibert F, Kirkness E, et al. Radiation hybrid mapping and genomic organization of canine *TBX2* and *TBX4*: brief notes. Anim Genet. 2003;34(4):307–9.
65. Andelfinger G, Hitte C, Etter L, Guyon R, Bourque G, Tesler G, et al. Detailed four-way comparative mapping and gene order analysis of the canine ctvm locus reveals evolutionary chromosome rearrangements. Genomics. 2004;83(6):1053–62.
66. Singh R, Hoogaars WM, Barnett P, Grieskamp T, Rana MS, Buermans H, et al. Tbx2 and Tbx3 induce atrioventricular myocardial development and endocardial cushion formation. Cell Mol Life Sci. 2012;69(8):1377–89.
67. Asimaki A, Syrris P, Wichter T, Matthias P, Saffitz JE, McKenna WJ. A novel dominant mutation in plakoglobin causes arrhythmogenic right ventricular cardiomyopathy. Am J Hum Genet. 2007;81(5):964–73.
68. Werner P, Raducha MG, Prociuk U, Ostrander EA, Spielman RS, Kirkness EF, et al. The keeshond defect in cardiac conotruncal development is oligogenic1. Hum Genet. 2005;116(5):368–77.

Part XVI

Hypoplastic Left Heart Syndrome

Clinical Presentation and Therapy of Hypoplastic Left Heart Syndrome

59

Nikolaus A. Haas, David J. Driscoll, and Silke Rickert-Sperling

59.1 Introduction

Hypoplastic left heart syndrome (HLHS) is a complex congenital heart defect characterized by several abnormalities that result in a significantly underdeveloped left ventricle and severe hypoplasia of the ascending aorta, often leading to retrograde perfusion. These abnormalities include aortic valve atresia or severe stenosis, accompanied by a severely hypoplastic aortic valve annulus (Fig. 59.1). Mitral valve atresia, hypoplasia, and/or stenosis with a hypoplastic valve annulus with or without a ventricular septal defect can also contribute to the development of HLHS. Endocardial fibroelastosis and sinusoids may be present as well. The interatrial septum can either be closed or the foramen ovale severely stenotic. Other malformations, such as anomalous pulmonary venous drainage or variations of the systemic veins, may coexist. It is also common to observe a coarctation of the aorta in these cases.

N. A. Haas (✉)
Department of Pediatric Cardiology and Intensive Care, Ludwig Maximilians University, Munich, Germany
e-mail: Nikolaus.haas@med.uni-muenchen.de

D. J. Driscoll
Division of Pediatric Cardiology, Department of Pediatrics, Mayo Clinic College of Medicine, Rochester, MN, USA
e-mail: driscoll.david@mayo.edu

S. Rickert-Sperling
Cardiovascular Genetics, Charité – Universitätsmedizin Berlin, Berlin, Germany
e-mail: silke.sperling@charite.de

© The Author(s), under exclusive license to Springer Nature Switzerland AG 2024

S. Rickert-Sperling et al. (eds.), *Congenital Heart Diseases: The Broken Heart*,
Advances in Experimental Medicine and Biology 1441,
https://doi.org/10.1007/978-3-031-44087-8_59

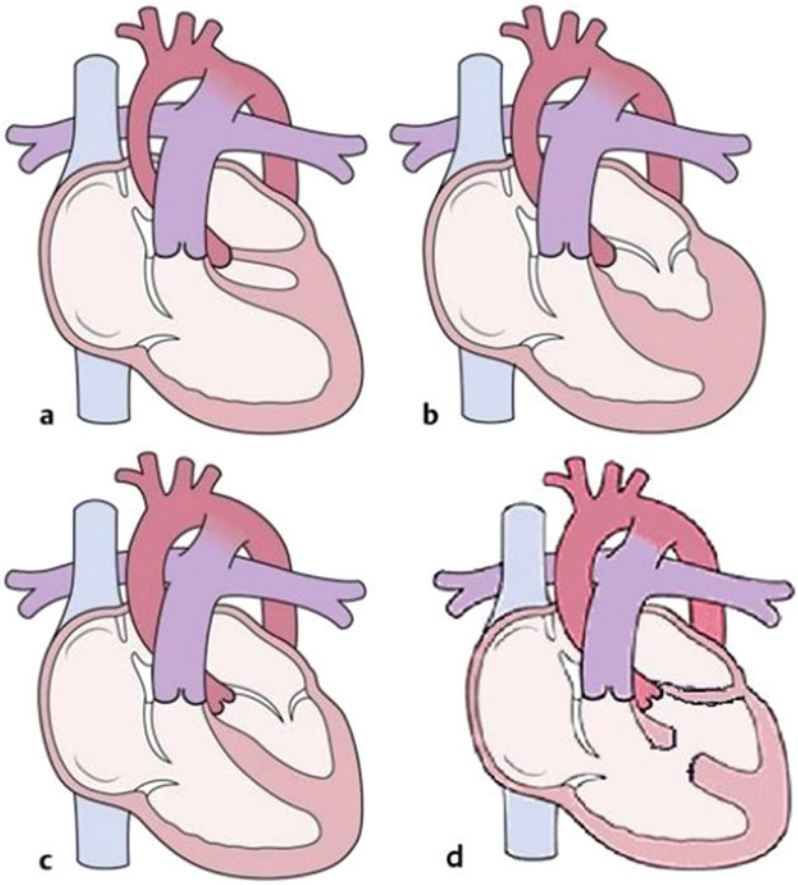

Fig. 59.1 Diagrammatic representation of HLHS. (**a**) Aortic valve atresia and mitral valve atresia; (**b**) Aortic valve atresia and normal mitral valve; (**c**) Aortic valve stenosis and normal mitral valve, (**d**) Aortic valve stenosis, mitral valve atresia and a ventricular septal defect

59.2 Pathologic Physiology

During fetal development, hypoplastic left heart syndrome (HLHS) does not typically interfere with the fetal blood supply, allowing normal somatic growth and overall tolerance of the defect. However, due to retrograde perfusion of the upper part of the body, children with HLHS may exhibit a slight reduction in head circumference and brain volume.

At birth, systemic blood flow relies on the right ventricle pumping blood into the pulmonary artery, which then distributes it to both the lungs and the aorta through a patent ductus arteriosus. Once again, the upper part of the body receives retrograde perfusion, which can be compromised if coarctation is present. When the ductus arteriosus closes, significant systemic organ ischemia occurs, ultimately leading to death.

In cases where the ductus arteriosus fails to close significantly, there is substantial transpulmonary recirculation of blood, resulting in an excessive volume load in the right ventricle. This leads to heart failure and pulmonary edema, which, if left untreated, can be fatal. However, there have been very rare reports of patients surviving into childhood due to the development of early pulmonary vascular obstructive disease, which restricts pulmonary blood flow and reduces the occurrence of pulmonary edema.

59.3 Clinical Presentation

Most infants with HLHS typically exhibit cyanosis and tachypnea shortly after birth. However, in some cases, the cyanosis may be mild and go unnoticed initially. These infants may then present at around 3–7 days of age in a state of cardiogenic shock, resembling the clinical picture of neonatal sepsis, as a result of the closure of the ductus arteriosus. Infants with a restrictive interatrial communication will present immediately after birth with respiratory failure.

59.4 Physical Examination

At birth, infants with HLHS often exhibit cyanosis, an increased right ventricular impulse, and a systolic murmur. When a general pulse oximetry screening is in place, most cases of HLHS can be detected by oxygen saturation levels below 94%. If the ductus arteriosus is restrictive, peripheral pulses may be diminished or absent. Tachypnea and other signs of congestive heart failure are common in affected infants. It is important to consider a diagnosis of HLHS in a 3- to 7-day-old infant presenting with a sudden onset of shock.

59.5 Diagnostic Imaging

Echocardiography is the primary diagnostic tool for accurately diagnosing all variants of hypoplastic left heart syndrome (HLHS) in neonates and children. It provides detailed information about the degree and location of left ventricular outflow tract obstruction, the size of the ascending aorta, the flow across the coarctation, and the patency of the patent ductus arteriosus (PDA). It also helps assess the interatrial communication, ruling out any potential obstruction (restrictive patent foramen ovale), and documenting pulmonary venous drainage, excluding total anomalous pulmonary venous return (TAPVR).

Cardiac catheterization is generally not necessary for the diagnosis of HLHS in the era of echocardiography. However, it may be required to define the anatomy of abnormal pulmonary venous drainage or to perform interventional procedures for palliation, such as balloon septostomy.

Magnetic resonance imaging (MRI) is not routinely used for the primary diagnosis or management of children with HLHS but may be helpful during follow-up care.

Computer tomography (CT) scans can provide similar anatomical details as MRI but with higher resolution for smaller vessels. In some cases, CT scans may be used instead of catheter investigation to define the anatomy of pulmonary venous drainage for detailed surgical planning.

59.6 Treatment

Neonatal management of hypoplastic left heart syndrome involves several steps to stabilize the patient and provide appropriate care.

The initial treatment is aimed at maintaining the patency of the ductus arteriosus using prostaglandin. Early diagnosis and initiation of prostaglandin in the delivery room are crucial. Intubation should be avoided if possible.

In cases where patients present in cardiogenic shock after closure of the ductus arteriosus, reopening the ductus using high doses of prostaglandin is necessary. Aggressive intensive care management is also required, including correction of acidosis, catecholamine support, ventilation, antibiotic therapy, and other supportive measures. If the interatrial septum is restrictive, a balloon septostomy may be performed.

Family counseling is an essential part of the management process. After initial stabilization, extensive and unbiased counseling should take place, involving the family in the decision-making process. Palliative care (comfort care) may be chosen for many patients with HLHS due to the historically unfavorable long-term outcomes. Palliative care includes discontinuing prostaglandin, extubation if ventilated, providing intravenous fluid therapy, administering adequate doses of morphine for pain management, and providing psychological support to the family.

Norwood Operation

The Norwood operation is a three-stage surgical approach used as a palliative management strategy for univentricular hearts like HLHS.

- Norwood stage 1 operation is typically performed at 2–5 days of age (Fig. 59.2). It involves reconstructing the aorta and pulmonary artery to establish unobstructed systemic perfusion, balanced pulmonary perfusion, and unobstructed pulmonary venous return. There are different modifications of this operation, but the goal is for the right ventricle to empty into the neoaorta. Pulmonary blood flow is supplied via a modified Blalock–Taussig shunt or the Sano modification.
- Norwood stage 2 operation is performed at around 4–6 months of age. It involves ligating the modified Blalock–Taussig shunt or the Sano shunt, repairing any distortions of the pulmonary tree, and performing a bidirectional Glenn anastomosis. This unloads the ventricle, but cyanosis may persist.
- Norwood stage 3 operation, also known as the modified Fontan operation, is performed at around 2–3 years of age. It involves using an extracardiac conduit from the inferior vena cava to the underside of the right pulmonary artery (Fig. 59.3). This further reduces cyanosis and aims to achieve nearly normal saturations.

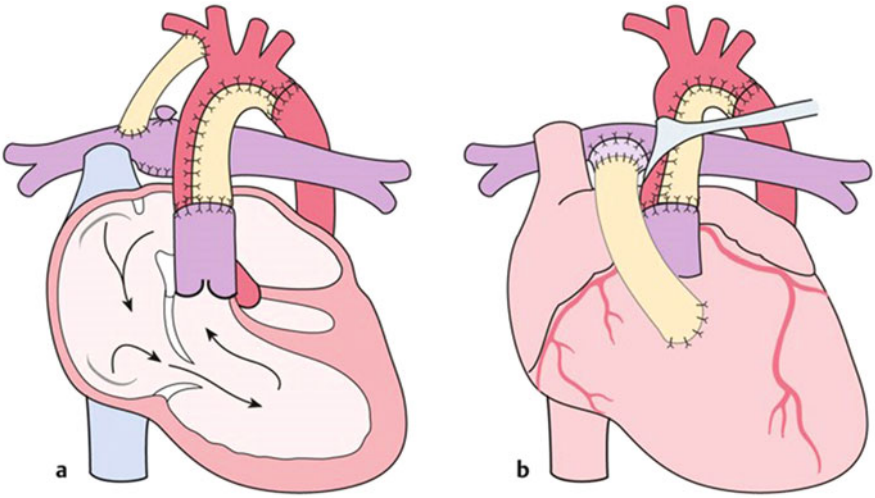

Fig. 59.2 Norwood stage 1 operation with modified Blalock–Taussig shunt (**a**) or Sano-Shunt (**b**). Reproduced from Kinderkardiologie, Georg Thieme Verlag, N. Haas, U. Kleideiter, 2011

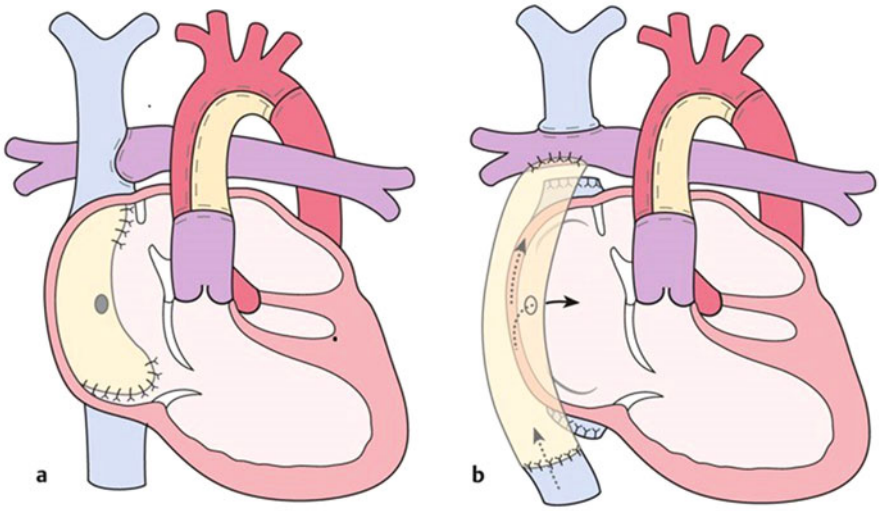

Fig. 59.3 Norwood stage 3 operation with total cavopulmonary anastomosis with lateral atrial tunnel (**a**) or extracardiac tunnel (**b**) in HLHS. Reproduced from Kinderkardiologie, Georg Thieme Verlag, N. Haas, U. Kleideiter, 2011

In some centers, a hybrid approach known as the "Giessen" approach may be performed instead of the Norwood I procedure. This involves interventional cardiac catheterization procedures to maintain systemic perfusion, surgical or interventional banding of the pulmonary arteries to reduce pulmonary blood flow and development

of pulmonary hypertension, and the creation of an unrestricted interatrial communication.

Cardiac Transplantation
Cardiac transplantation is an alternative treatment strategy for HLHS in infancy. However, it is often limited by the scarcity of organ donors, particularly outside of the United States. Cardiac transplantation carries its own risks, including rejection, infection, posttransplant lymphoproliferative disease, renal failure, and graft coronary artery disease.

59.7 Outcome

Hypoplastic left heart syndrome (HLHS) is recognized as one of the most severe forms of congenital heart disease. The surgical management of HLHS involves multiple stages, with varying mortality risks at each stage. The mortality rate from the first stage, the Norwood operation, can range from 5% to 40%, depending on the surgeon's experience and associated anomalies. In larger multi-institutional cohorts, the mortality rate is typically less than 25%. There is also a risk of interstage mortality, estimated to be around 5–10%, between the first and second stages (bidirectional Glenn anastomosis). The second stage carries an additional mortality risk of about 5–10%, and the third stage (modified Fontan operation) has a 3–8% risk of death.

Long-term survival for patients with HLHS after the Fontan operation is reduced, with estimated survival rates of 70–85% at 10 years postoperation, typically before puberty. However, exercise capacity continuously decreases, reaching approximately 50% of normal in ideal candidates. HLHS patients often have factors that pose challenges for the Fontan operation, such as a right systemic ventricle and tricuspid regurgitation, leading to a worsening long-term outcome. Many patients will eventually develop heart failure and may become candidates for cardiac transplantation. Long-term complications following the Fontan operation include atrial arrhythmias, protein-losing enteropathy, liver cirrhosis, hepatocellular carcinoma, plastic bronchitis, and left ventricular dysfunction.

In addition to the cardiovascular problems associated with HLHS, there is a significant proportion of patients who experience cerebral, psychiatric, psychosocial, and familial issues, even in cases classified as "hemodynamically uncomplicated" HLHS. These factors must be addressed and taken into consideration during parental counseling and long-term management.

Human Genetics of Hypoplastic Left Heart Syndrome

60

Constanze Pfitzer, Katharina R. L. Schmitt, and Woodrow D. Benson

Abstract

Hypoplastic left heart syndrome (HLHS) is a severe congenital cardiovascular malformation characterized by hypoplasia of the left ventricle, aorta, and other structures on the left side of the heart. The pathologic definition includes atresia or stenosis of both the aortic and mitral valves. Despite considerable progress in clinical and surgical management of HLHS, mortality and morbidity remain concerns. One barrier to progress in HLHS management is poor understanding of its cause. Several lines of evidence point to genetic origins of HLHS. First, some HLHS cases have been associated with cytogenetic abnormalities (e.g., Turner syndrome). Second, studies of family clustering of HLHS and related cardiovascular malformations have determined HLHS is heritable. Third, genomic regions that encode genes influencing the inheritance of HLHS have been identified. Taken together, these diverse studies provide strong evidence for genetic origins of HLHS and related cardiac phenotypes. However, using simple Mendelian inheritance models, identification of single genetic variants that "cause" HLHS has remained elusive, and in most cases, the genetic cause remains unknown. These results suggest that HLHS inheritance is complex rather than simple. The implication of this conclusion is that researchers must move beyond the expectation that a single disease-causing variant can be found. Utilization of

C. Pfitzer · K. R. L. Schmitt
Department of Congenital Heart Disease/Paediatric Cardiology, German Heart Center Berlin, Berlin, Germany
e-mail: constanze.pfitzer@dhzc-charite.de; katharina.schmitt@dhzc-charite.de

W. D. Benson (✉)
Department of Pediatrics, Herma Heart Center, Children's Hospital of Wisconsin, Medical College of Wisconsin, Milwaukee, WI, USA
e-mail: dbenson@mcw.edu

© The Author(s), under exclusive license to Springer Nature Switzerland AG 2024

S. Rickert-Sperling et al. (eds.), *Congenital Heart Diseases: The Broken Heart*,
Advances in Experimental Medicine and Biology 1441,
https://doi.org/10.1007/978-3-031-44087-8_60

complex models to analyze high-throughput genetic data requires careful consideration of study design.

Keywords

Hypoplastic left heart syndrome · HLHS · Hypoplasia · Left ventricle · Bicuspid aortic valve · BAV · Turner syndrome · Trisomy 18 · Smith–Lemli–Opitz syndrome · VACTERL association · CHARGE syndrome · Wolf–Hirschhorn syndrome · Rubinstein–Taybi syndrome · Noonan syndrome and Holt–Oram syndrome · Linkage analysis · Chromosome · Genome-wide association study · GWAS · GJA1 · NKX2–5 · Notch 1 · ERBB4 · ZIC3 · HAND1 · Copy-number variants · CNV · de novo · TBX5 · IRX1

60.1 Introduction: What Is HLHS?

Hypoplastic left heart syndrome (HLHS) is a severe form of congenital heart disease (CHD). As the name suggests, hypoplasia of the left ventricle (LV) resulting in a functional single ventricle is a cardinal feature, but the pathologic definition includes atresia or stenosis of both the aortic and mitral valves, along with hypoplasia of the ascending aorta. Intact ventricular septum and normally related great arteries are also factored in the definition [1–3]. A subclassification scheme, based on the pathologic anatomy of the aortic and mitral valves, is widely employed. Although emphasis has been on left-sided heart structures, dysplasia of both tricuspid and pulmonary valves often is reported [4–7]. Despite a similar approach to surgical management for hearts with LV hypoplasia, the HLHS definition used for studies of genetic discovery typically excludes anatomic variations of LV hypoplasia such as unbalanced atrioventricular septal defect and double-outlet right ventricle with mitral valve atresia. This exclusion is based on the belief that the developmental origins of these varied LV hypoplasia phenotypes differ from the origins of HLHS.

60.1.1 HLHS Prevalence

HLHS accounts for approximately 4–8% of all CHD, and the prevalence has been estimated from 0.06 to 1.20 with a median of 0.22 per 1000 live births [8, 9]. HLHS is viable in utero and rarely results in fetal loss. HLHS is slightly more common in males; however, there is no ethnic or geographical association. Despite live birth of ~2000 cases of HLHS annually, the burden to society is substantial. The direct costs, medical morbidity, and utilization of a disproportionate share of pediatric cardiac resources make HLHS a central problem in pediatric cardiology.

60.1.2 HLHS-Related Phenotypes

An increased prevalence of CHD in families identified by an HLHS proband was noted in the Baltimore-Washington Infant Study [9, 10]. Additional observations that first-degree relatives of HLHS probands had increased occurrence of bicuspid aortic valve (BAV) [9, 11] lead to the hypothesis that cardiac malformations characterized by obstruction to blood flow in the LV outflow tract are causally related. In addition to HLHS and BAV, these malformations include aortic valve stenosis and aortic coarctation (collectively referred to as left-sided malformations). Additional supportive evidence for a causal relationship stems from several other observations including (1) the association of underlying BAV with aortic stenosis in patients of all ages [12, 13], (2) longitudinal observations in the fetus that identified HLHS as part of the in utero natural history of aortic stenosis [14, 15], (3) occurrence of these defects in patients with Turner syndrome [16], and (4) findings of identical twins with discordant phenotypes of BAV and HLHS [17]. Further, BAV, HLHS, and other left-sided cardiac malformations have been shown to be heritable [17–19]. However, little is known of the size or extent of these effects. This may be an important consideration in the design of genetic discovery studies, i.e., can these phenotypes be pooled or should they be separately analyzed in order to minimize noise from phenotypic variation?

60.2 Genetic Studies of HLHS

Several lines of evidence support a genetic cause for HLHS. First, there are numerous reports linking occurrence of HLHS to chromosomal abnormalities, e.g., Turner syndrome (monosomy X) and Jacobsen syndrome (chromosome 11q deletion) [20, 21]. Less frequently, trisomy 18, Smith–Lemli–Opitz syndrome, VACTERL association, CHARGE syndrome, Wolf–Hirschhorn syndrome, Rubinstein–Taybi syndrome, Noonan syndrome, and Holt–Oram syndrome have been reported [22–25]. However, these reports need to be analyzed cautiously as lack of phenotype detail and variation in CHD phenotype criteria blurs the genotype-phenotype correlations. For example, LV hypoplasia observed in Noonan syndrome or Holt–Oram syndrome may be associated with unbalanced atrioventricular septal defect rather than HLHS.

A second line of evidence supporting genetic origins of HLHS is that heritability (h^2, a statistical measure of genetic effect size) indicates that HLHS is determined largely by genetic factors. In a family-based study where all participants were screened for CHD by echocardiography, Hinton et al. [17] determined HLHS heritability was very high. In addition, the recurrence risks for HLHS and any CHD were 8% and 22%, respectively. Further, a tenfold increase in bicuspid aortic valve was noted. McBride et al. [19] also found high heritability using a family-based analysis of phenotypically related left-sided heart malformations.

Further evidence comes from use of linkage analysis to identify genomic regions that encode genes influencing the inheritance of HLHS. Hinton et al. [26] used

nonparametric linkage analysis and identified two significant loci on chromosomes 10q22 and 6q23. These findings confirmed that nonsyndromic HLHS is genetically heterogeneous. Interestingly, ~21% of kindreds contributed to linkage at each locus, suggesting these loci account for a substantial number of HLHS cases. Further, a suggestive HLHS locus on 11q22, previously identified in a case of HLHS with a balanced translocation t [10, 11] (q24;q23), validated these analyses [27]. When the linkage approach was extended to a family-based cohort ascertained by either an HLHS or BAV proband, subset linkage analysis showed a significant improvement in the logarithm of odds (LOD) score at chromosome 14q23, providing evidence that some HLHS and BAV cases are genetically related [26]. In a family-based cohort ascertained by probands with left-sided malformations that included aortic valve stenosis, aortic coarctation, and HLHS, McBride et al. [28] found evidence for suggestive linkage to chromosomes 2p23, 10q21, and 16p12. They concluded that overlapping linkage peaks provide evidence for a common genetic etiology. Mitchell et al. [29] performed a genome-wide association study (GWAS) using a trio design where probands were ascertained by varied left-sided malformations including HLHS. Major findings included association at a chromosome 16 locus and suggestive association at loci on chromosome 3 and 10.

Several investigators have reported findings of genetic variants in single genes using mutation analysis of candidate genes in series of cases or small families. Genetic variants in connexin 43 (*GJA1*/*Cx43*) [30], NK2 homeobox 5 (*NKX2–5*) [31–33], Notch 1 (*NOTCH1*) [34, 35], and V-erb-B2 avian erythroblastic leukemia viral oncogene homolog 4 (*ERBB4*) [36] have been reported in HLHS. Ware et al. [37] identified patients with HLHS who had mutations in Zic family member 3 (ZIC3), a transcription factor associated with heterotaxy syndrome. More recently [38], patients with left-sided heart defects were found to be enriched for de novo variants in histone-modifying genes (H3K4me-H3K27me pathway); interestingly, patients with conotruncal defects and heterotaxy demonstrated similar enrichment. In addition to these reports of germinal mutations, there is a single report that identifies somatic mutations in heart and neural crest derivatives expressed 1 (*HAND1*) [39].

Genetic studies of HLHS patients have also evaluated copy-number variations (CNVs), which are genomic regions of DNA gains or losses >1000 base pairs [40–45]. CNVs are detectable as a result of recent advances in molecular cytogenetics, particularly using microarray-based methods. Utilizing such methods to scan the genome, it has become evident that a significant proportion of the normal healthy human genome harbors CNV of unknown medical significance. However, other CNVs, usually large and often *de novo*, are considered pathogenic. Several investigators have examined the role of CNV in CHD, and three recent family-based studies examine the role of CNV in HLHS. Hitz et al. [40] sought to determine the impact of structural genomic variation in multiplex families ascertained by a proband with a left-sided heart malformation including some cases with HLHS. They searched for unique or rare copy-number variations present only in affected members. Their findings indicate that unique CNVs contribute to at least 10% of left-sided heart malformations cases. Carey et al. [41] evaluated patients with single

ventricle, many of whom had HLHS. Putatively pathogenic CNVs had a prevalence of 13.9%, which was significantly greater than the 4.4% rate of such CNVs among controls. The authors concluded that pathogenic CNVs seem to contribute to the cause of single ventricle forms of CHD in ≥10% of cases and are clinically subtle but adversely affect outcomes in children harboring them. Warburton et al. [42] compared CNV rates in two types of CHD, HLHS versus conotruncal defects, and found no significant difference. However, they found a substantially higher rate of de novo CNVs in probands with CHD than in control families (9 vs. 2%). Among the de novo or rare inherited CNVs, there were 12 CNVs that the authors considered likely to be causally related to CHD.

Liu et al. gained novel insights and state an isolation of HLHS mutant mice and identification of genes causing HLHS by using mouse forward genetics [46]. Previous studies have shown, that mutations from seven HLHS mouse lines indicate a multigenetic enrichment in ten human chromosome regions, which are associated to HLHS [17, 28, 47]. Within their study, Liu et al. analysed mutations by CRISPR-Cas9 (***C****lustered* ***R****egularly* ***I****nterspaced* ***S****hort* ***P****alindromic* ***R****epeats-associated)* in *Sap130* and *Pcdh9* [46]. These are genes, which haven't been linked to CHD yet. In contrast, they report that Sap130 and Pcdha9 are digenic causes of HLHS. In addition, they found one subject with HLHS with Sap130 and Pcdha13 mutations and utilized mouse and zebrafish modeling to describe the possible phenotype. Within this model, Sap130 induced a left ventricular hypoplasia, whereas Pcdha9 spread the penetrance of aortic valve abnormalities, both characteristic HLHS defects. These insights induce a new model of a combinatorial genetic approach for the complex genetics of HLHS.

60.3 HLHS Exhibits Complex Inheritance

Taken together, these diverse studies provide strong evidence for genetic origins of HLHS and related cardiac phenotypes. Initially, analyses of pedigrees ascertained by an HLHS proband were interpreted as indicating simple Mendelian inheritance of HLHS [48]. However, review of literature indicates that despite considerable effort, identification of single genetic variants that "cause" HLHS has remained elusive. These results may indicate that HLHS inheritance is complex rather than simple, a finding concluded by several studies [26, 40]. The implication of this conclusion is that researchers must move beyond the expectation that a single disease-causing variant can be found. Although analytical methods to evaluate the effects of 2 or more genetic variants are well established, the ability to apply these methods in a high-throughput manner must be developed. Furthermore, researchers must realize that utilization of these more complex models requires careful consideration of study design and statistical power. Optimal approaches to discovering pathogenetic variants in complex diseases remain unclear [49].

60.4 Pathogenetic Mechanisms of HLHS

What types of genes might be involved in the genetic underpinnings of HLHS? Concepts of cardiac development have greatly influenced our understanding of the formation of the mesoderm derived, 4-chambered vertebrate heart. Human genetic studies have identified mutations in genes important for early heart formation that cause CHD, supporting the idea that these birth defects are caused by alterations during cardiogenesis [50–54]. There has been considerable interest in CHD such as HLHS, in which individual chambers or valves of the developing heart are selectively impaired [50]. A widely accepted hypothesis is that HLHS develops as a result of embryonic alterations in blood flow, such as premature narrowing of the foramen ovale [1] or aortic valve obstruction [55]. In this light, it is noteworthy that valve malformation is a prominent part of the HLHS phenotype as evidenced by the frequent occurrence of left- and right-sided valve dysplasia in HLHS probands and the presence of BAV in family members [17]. The "no-flow, no-grow" hypothesis of heart maldevelopment also is supported by studies in the embryonic chick heart, which alter blood flow during cardiac development [56]. An alternative hypothesis for HLHS etiology focuses on the summation of separate genetic modules. Recent studies have investigated chamber-specific regulatory mechanisms, e.g., TBX5 (T-box 5) and IRX1 (iroquois homeobox 1), leading to formation of morphologically, functionally, and molecularly distinct cardiac chambers [50, 51]. In this context, it has been suggested that LV hypoplasia may result from a primary defect in myocardial growth during development. Unfortunately, there are presently no experimental models of HLHS to elucidate the relative contribution of these two hypotheses, but defining the genetic underpinnings of HLHS should enlighten the debate.

60.5 Conclusion

While once uniformly lethal, for the past two decades, a three-staged surgical approach for HLHS has dramatically reduced mortality [57]. Despite this progress in clinical care, mortality and morbidity of HLHS remain significant. Further, progress in patient management has provided little insight into the cause of HLHS. This lack of knowledge has been a barrier to progress in risk appraisal and assessment of clinical outcomes. In addition, there has been limited information for reproductive decision making for both parents of children with HLHS and survivors of HLHS surgical intervention who are now reaching reproductive age. Further, without understanding the origins of HLHS, care of patients is based solely on clinical phenotype rather than the underlying mechanism of cardiac maldevelopment. Studies to date strongly support significant genetic underpinnings of HLHS. However, although numerous genetic abnormalities have been associated with HLHS, at this time it is not possible to reconcile all genetic findings into a comprehensive pathogenetic model. Together these genetic findings indicate genetic heterogeneity and complex inheritance of HLHS. Ultimately, we expect that

identification of genetic underpinnings may result in better understanding of outcomes. New biological insights into HLHS will facilitate development of alternative therapeutic strategies.

References

1. Lev M. Pathologic anatomy and interrelationship of hypoplasia of the aortic tract complexes. Lab Investig. 1952;1:61–70.
2. Noonan JA, Nadas AS. The hypoplastic left heart syndrome; an analysis of 101 cases. Pediatr Clin N Am. 1958;5:1029–56.
3. Tchervenkov CI, Jacobs JP, Weinberg PM, et al. The nomenclature, definition and classification of hypoplastic left heart syndrome. Cardiol Young. 2006;16:339–68.
4. Bharati S, Lev M. The surgical anatomy of hypoplasia of aortic tract complex. J Thorac Cardiovasc Surg. 1984;88:97–101.
5. Aiello VD, Ho SY, Anderson RH, Thiene G. Morphologic features of the hypoplastic left heart syndrome—a reappraisal. Pediatr Pathol. 1990;10:931–43.
6. Stamm C, Anderson RH, Ho SY. The morphologically tricuspid valve in hypoplastic left heart syndrome. Eur J Cardiothorac Surg. 1997;12:587–92.
7. Bharati S, Nordenberg A, Brock RR, Lev M. Hypoplastic left heart syndrome with dysplastic pulmonary valve with stenosis. Pediatr Cardiol. 1984;5:127–30.
8. Hoffman JI, Kaplan S. The incidence of congenital heart disease. J Am Coll Cardiol. 2002;39:1890–900.
9. Ferencz C, Rubin JD, McCarter RJ, et al. Congenital heart disease: prevalence at live birth. The Baltimore-Washington infant study. Am J Epidemiol. 1985;121:31–6.
10. Loffredo CA, Chokkalingam A, Sill AM, et al. Prevalence of congenital cardiovascular malformations among relatives of infants with hypoplastic left heart, coarctation of the aorta, and d-transposition of the great arteries. Am J Med Genet A. 2004;124:225–30.
11. Brenner JI, Berg KA, Schneider DS, Clark EB, Boughman JA. Cardiac malformations in relatives of infants with hypoplastic left- heart syndrome. Am J Dis Child. 1985;143:1492–4.
12. Roberts WC. The structure of the aortic valve in clinically isolated aortic stenosis: an autopsy study of 162 patients over 15 years of age. Circulation. 1970;42:91–7.
13. Roberts WC, Ko JM. Frequency by decades of unicuspid, bicuspid, and tricuspid aortic valves in adults having isolated aortic valve replacement for aortic stenosis, with or without associated aortic regurgitation. Circulation. 2005;111:920–5.
14. Hornberger LK, Sanders SP, Rein AJ, et al. Left heart obstructive lesions and left ventricular growth in the midtrimester fetus. A longitudinal study. Circulation. 1995;92:1531–8.
15. Makikallio K, McElhinney DB, Levine JC, et al. Fetal aortic valve stenosis and the evolution of hypoplastic left heart syndrome: patient selection for fetal intervention. Circulation. 2006;113:1401–5.
16. Surerus E, Huggon IC, Allan LD. Turner's syndrome in fetal life. Ultrasound Obstet Gynecol. 2003;22:264–2677.
17. Hinton RB Jr, Martin LJ, Tabangin ME, et al. Hypoplastic left heart syndrome is heritable. J Am Coll Cardiol. 2007;50:1590–5.
18. Cripe L, Andelfinger G, Martin LJ, Shooner K, Benson DW. Bicuspid aortic valve is heritable. J Am Coll Cardiol. 2004;44:138–43.
19. McBride KL, Pignatelli R, Lewin M, et al. Inheritance analysis of congenital left ventricular outflow tract obstruction malformations: segregation, multiplex relative risk, and heritability. Am J Med Genet A. 2005;134:180–6.
20. Madriago E, Nguyen T, McFerson M, et al. Frequency and outcomes of cardiac operations and catheter interventions in Turner syndrome. Am J Cardiol. 2012;110:580–5.
21. Mattina T, Perrotta CS, Grossfeld P. Jacobsen syndrome. Orphanet J Rare Dis. 2009;4:9.

22. Jongmans MJC, Admiraal RJ, van der Donk KP, et al. CHARGE syndrome: the phenotypic spectrum of mutations in the CHD7 gene. J Med Genet. 2006;43:306–14.
23. Schulz S, Fröber R, Kraus C, Schneider U. Prenatal diagnosis of hypoplastic left heart syndrome associated with Noonan syndrome and de novo RAF1 mutation. Prenat Diagn. 2012;32:1016–8.
24. von Elten K, Sawyer T, Lentz-Kapua S, Kanis A, Studer M. A case of Wolf-Hirschhorn syndrome and hypoplastic left heart syndrome. Pediatr Cardiol. 2013;34:1244–6.
25. von Elten K, Sawyer T, Lentz-Kapua S, Kanis A, Studer M. Novel *SMAD3* mutation in a patient with hypoplastic left heart syndrome with significant aortic aneurysm. Case Rep Genet. 2014;2014:591516.
26. Hinton RB, Martin LJ, Rame-Gowda S, et al. Hypoplastic left heart syndrome links to chromosomes 10q and 6q and is genetically related to bicuspid aortic valve. J Am Coll Cardiol. 2009;53:1065–71.
27. Guenthard J, Buehler E, Jaeggi E, Wyler F. Possible genes for left heart formation on 11q23.3. Ann Genet. 1994;37:143–6.
28. McBride KL, Zender GA, Fitzgerald-Butt SM, et al. Linkage analysis of left ventricular outflow tract malformations (aortic valve stenosis, coarctation of the aorta, and hypoplastic left heart syndrome). Eur J Hum Genet. 2009;17:811–9.
29. Mitchell LE, Agopian AJ, Bhalla A, et al. Genome-wide association study of maternal and inherited effects on left-sided cardiac malformations. Hum Mol Genet. 2014;24:265–73.
30. Dasgupta C, Martinez AM, Zuppan CW, et al. Identification of connexin43 (alpha1) gap junction gene mutations in patients with hypoplastic left heart syndrome by denaturing gradient gel electrophoresis (DGGE). Mutat Res. 2001;479:173–86.
31. Elliott DA, Kirk EP, Yeoh T, et al. Cardiac homeobox gene NKX2-5 mutations and congenital heart disease: associations with atrial septal defect and hypoplastic left heart syndrome. J Am Coll Cardiol. 2003;41:2072–6.
32. McElhinney DB, Geiger E, Blinder J, Benson DW, Goldmuntz E. NKX2.5 mutations in patients with congenital heart disease. J Am Coll Cardiol. 2003;42:1650–5.
33. Stallmeyer B, Fenge H, Nowak-Gottl U, Schulze-Bahr E. Mutational spectrum in the cardiac transcription factor gene NKX2.5 (CSX) associated with congenital heart disease. Clin Genet. 2010;78:533–40.
34. McBride KL, Riley MF, Zender GA, et al. NOTCH1 mutations in individuals with left ventricular outflow tract malformations reduce ligand-induced signaling. Hum Mol Genet. 2008;17:2886–93.
35. Garg V, Muth AN, Ransom JF, et al. Mutations in NOTCH1 cause aortic valve disease. Nature. 2005;437:270–4.
36. McBride KL, Zender GA, Fitzgerald-Butt SM, et al. Association of common variants in ERBB4 with congenital left ventricular outflow tract obstruction defects. Birth Defects Res A Clin Mol Teratol. 2011;91:162–8.
37. Ware SM, Peng J, Zhu L, et al. Identification and functional analysis of *ZIC3* mutations in heterotaxy and related congenital heart defects. Am J Hum Genet. 2004;74:93–105.
38. Zaidi S, Choi M, Wakimoto H, et al. De novo mutations in histone-modifying genes in congenital heart disease. Nature. 2013;498:220–4.
39. Reamon-Buettner SM, Ciribilli Y, Inga A, Borlak J. A loss-of-function mutation in the binding domain of HAND1 predicts hypoplasia of the human hearts. Hum Mol Genet. 2008;17:1397–405.
40. Hitz MP, Lemieux-Perreault LP, Marshall C, et al. Rare copy number variants contribute to congenital left-sided heart disease. PLoS Genet. 2012;8:e1002903.
41. Carey AS, Liang L, Edwards J, et al. Effect of copy number variants on outcomes for infants with single ventricle heart defects. Circ Cardiovasc Genet. 2013;6:444–51.
42. Warburton D, Ronemus M, Kline J, et al. The contribution of de novo and rare inherited copy number changes to congenital heart disease in an unselected sample of children with conotruncal defects or hypoplastic left heart disease. Hum Genet. 2014;133:11–27.

43. Payne AR, Chang S-W, Koenig SN, Zinn AR, Garg V. Submicroscopic chromosomal copy number variations identified in children with hypoplastic left heart syndrome. Pediatr Cardiol. 2012;33:757–63.
44. Iascone M, Ciccone R, Gallettid L, et al. Identification of de novo mutations and rare variants in hypoplastic left heart syndrome. Clin Genet. 2012;81:542–54.
45. Glessner JT, Bick AG, Ito K, et al. Increased frequency of de novo copy number variants in congenital heart disease by integrative analysis of single nucleotide polymorphism array and exome sequence data. Circ Res. 2014;115:884–96.
46. Lui X, Yagi H, Saeed S, et al. The complex genetics of hypoplastic left heart syndrome. Nat Genet. 2017;49(7):1152–9.
47. Martin LJ, Ramachandran V, Crpe LH, et al. Evidence in favor of linkage to human chromosomal regions 18q, 5q and 13q for bicuspid aortic valve and associated cardiovascular malformations. Hum Genet. 2007;121:275–84.
48. Shokeir MH. Hypoplastic left heart. Evidence for possible autosomal recessive inheritance. Birth Defects Orig Artic Ser. 1974;10:223–7.
49. MacArthur DG, Manolio TA, Dimmock DP, et al. Guidelines for investigating causality of sequence variants in human disease. Nature. 2014;508:469–76.
50. Bruneau BG. The developing heart and congenital heart defects: a make or break situation. Clin Genet. 2003;63:252–61.
51. Fishman MC, Olson EN. Parsing the heart: genetic modules for organ assembly. Cell. 1997;91:153–6.
52. Hinton RB, Yutzey KE, Benson DW. Congenital heart disease: genetic causes and developmental insights. Prog Pediatr Cardiol. 2005;20:101–11.
53. Small EM, Krieg PA. Molecular regulation of cardiac chamberspecific gene expression. Trends Cardiovasc Med. 2004;14:13–8.
54. Armstrong EJ, Bischoff J. Heart valve development: endothelial cell signaling and differentiation. Circ Res. 2004;95:459–70.
55. Fishman NH, Hof RB, Rudolph AM, Heymann MA. Models of congenital heart disease in fetal lambs. Circulation. 1978;58:354–64.
56. deAlmeida A, McQuinn T, Sedmera D. Increased ventricular preload is compensated by myocyte proliferation in normal and hypoplastic fetal chick left ventricle. Circ Res. 2007;100:1363–70.
57. Feinstein JA, Benson DW, Dubin AM, et al. Hypoplastic left heart syndrome: current considerations and expectations. J Am Coll Cardiol. 2012;59(1 Suppl):S1–S42.

Molecular Pathways and Animal Models of Hypoplastic Left Heart Syndrome

61

Hisato Yagi, Xinxiu Xu, George C. Gabriel, and Cecilia Lo

Abstract

Hypoplastic left heart syndrome (HLHS) is a severe congenital heart disease (CHD) with underdevelopment of left-sided heart structures. While previously uniformly fatal, surgical advances now provide highly effective palliation that allows most HLHS patients to survive their critical CHD. Nevertheless, there remains high morbidity and mortality with high risk of heart failure. As hemodynamic compromise from restricted aortic blood flow has been suggested to underlie the poor LV growth, this suggests the possibility of prenatal fetal intervention to recover LV growth. As such interventions have yielded ambiguous results, the optimization of therapy will require more mechanistic insights into the developmental etiology for HLHS. Clinical studies have shown high heritability for HLHS, with an oligogenic etiology indicated in conjunction with genetic heterogeneity. This is corroborated with the recent recovery of mutant mice with HLHS. With availability-induced pluripotent stem cell (iPSC)-derived cardiomyocytes from HLHS mice and patients, new insights have emerged into the cellular and molecular etiology for the LV hypoplasia in HLHS. Cell proliferation defects were observed in conjunction with metaphase arrest and the disturbance of Hippo-YAP signaling. The left-sided restriction of the ventricular hypoplasia may result from epigenetic perturbation of pathways regulating left–right patterning. These findings suggest new avenues for fetal interventions with therapies using existing drugs that target the Hippo-YAP pathway and/or modulate epigenetic regulation.

H. Yagi · X. Xu · G. C. Gabriel · C. Lo (✉)
Department of Developmental Biology, University of Pittsburgh School of Medicine, Pittsburgh, PA, USA
e-mail: cel36@pitt.edu

© The Author(s), under exclusive license to Springer Nature Switzerland AG 2024

S. Rickert-Sperling et al. (eds.), *Congenital Heart Diseases: The Broken Heart*,
Advances in Experimental Medicine and Biology 1441,
https://doi.org/10.1007/978-3-031-44087-8_61

Keywords

Hypoplastic left heart syndrome (HLHS) · Congenital heart disease (CHD) · Left ventricle (LV) · Left ventricular outflow tract obstruction (LVOTO) · Hippo signaling · Induced pluripotent stem cell-derived cardiomyocytes (iPSC-CM)

61.1 Introduction

Hypoplastic left heart syndrome (HLHS) is a severe structural heart defect that accounts for 30% of infant mortality associated with CHD [1–3]. It is characterized by underdevelopment of left-sided heart structures, including hypoplasia of the aorta (Ao), aortic and mitral valves, and left ventricle (LV). The resulting decrease in systemic cardiac output is incompatible with postnatal survival, and thus without treatment, HLHS is invariably fatal. However, surgical advances with a three-stage palliative surgical course now permit most infants with HLHS to survive their critical CHD, with many surviving to adulthood. Surgical palliation creates a pattern of blood flow that allows the right ventricle to serve as the systemic pumping chamber, and thus surgically palliated HLHS patients have a single pumping chamber and are said to have a systemic right single ventricle (SV) physiology. Despite the highly effective palliative surgeries, HLHS patients continue to suffer high risk of heart failure, with heart transplantation being the ultimate therapy. HLHS patients also exhibit high risk for poor neurodevelopmental outcomes that can include autism spectrum disorder, cognitive impairment, and other sociobehavioral deficits [4, 5]. Recent studies indicate these adverse neurodevelopmental outcomes are largely unrelated to hypoxic injury or surgical trauma, but rather are derived from patient intrinsic factors yet to be identified [6, 7].

61.2 Hemodynamics and the Developmental Etiology of HLHS

The hypoplastic LV in HLHS is commonly thought to arise secondary to having a hypoplastic aorta and/or aortic valve causing the reduction of blood flow to the LV under a “no flow-no grow” paradigm. Supporting such a hemodynamic model are various studies showing experimental manipulations restricting blood flow to the left side of the heart can cause hypoplasia of left-sided heart structures including the atria, ventricle, and aortic and mitral valve, yielding phenotypes reminiscent of the constellation of defects seen with HLHS. This was observed in chick embryos with obstruction of blood flow through the left atrioventricular canal or with left atrial ligation [8]. In the fetal sheep, hypoplasia of the LV and aortic and mitral valves are observed with balloon insertion in the left atrium to obstruct LV filling [9], or with catheter guided occlusion of the foramen ovale preventing normal right to left shunting of blood [10]. As fetal blood flow bypasses the lung with the RV output circulating through the ductus arteriosus, blood supply to the left side of the heart is

mediated by right to left shunting of blood through the foramen ovale. Thus observation that some human fetuses with HLHS have smaller foramen ovale is suggested as evidence for reduced blood flow contributing to HLHS [11]. As most HLHS patients are diagnosed before birth with noninvasive fetal ultrasound examination, this suggested the possibility of clinical intervention prenatally. Thus in utero balloon angioplasty has been employed to increase aortic blood flow in human fetuses diagnosed by echocardiography as having evolving HLHS [12]. The expectation is that increased blood flow would promote sufficient LV growth to allow surgical palliation with biventricular repair, and be associated with better long-term outcome. However, such prenatal interventions have thus far yielded ambiguous results, suggesting more studies are needed to investigate the molecular mechanism driving LV hypoplasia in HLHS [13, 14].

61.3 Complex Genetics Underlie the Genetic Etiology of HLHS

Extensive clinical evidence supports the genetic etiology for HLHS [15]. These studies have shown HLHS is genetically heterogeneous and is largely characterized by complex non-Mendelian genetics [16]. Given the complex genetic architecture, it is perhaps not surprising that so far only a few genes have been implicated to cause HLHS. Thus mutations in *GJA1* [17], *MYH6* [18], *NKX2–5* [19–21], *NOTCH1* [22, 23], *ERBB4* [24], *ZIC3* [25], *RBFOX2* [26], and *HAND1* [27] were reported to contribute to HLHS or closely related left ventricular outflow obstructive lesions (LVOTO). HLHS also has been reported in association with certain syndromic disorders including Turner syndrome [28], Jacobsen syndrome [29], trisomy 13 [30], and trisomy 18 [31]. As HLHS and other LVOTO lesions have been shown to be genetically linked and are often seen in conjunction with various extracardiac and brain anomalies including microcephaly [32], this suggests common molecular pathways underlie the pathogenesis of HLHS despite its genetic heterogeneity, Insights into these pathways may help to accelerate the innovation of new therapies for recovering LV growth in fetuses with HLHS.

61.4 Recovery of HLHS Mutant Mice

Mouse models have been invaluable for investigating the developmental etiology of a wide spectrum of CHD, but previously HLHS had not been observed in mice. It was suggested that the short gestation period of mice (18.5 days) may not be sufficient for the hemodynamic remodeling thought to mediate HLHS pathogenesis. This was disproven with the recovery of eight independent mouse lines with HLHS from a large-scale mouse mutagenesis screen [33]. Notable is the fact that these eight mouse lines shared no genes in common, indicating profound genetic heterogeneity, consistent with the clinical genetic findings. We further observed non-Mendelian transmission, indicating a multigenic etiology for HLHS, also consistent with findings from the human clinical studies. Together, this accounted for the previous

failure in using reverse genetic approaches in generating HLHS mutant mice. In contrast, the inherent design of a mutagenesis screen with more than 50 mutations per mouse and the high-throughput screening of a large number of mice (100,000) made it possible to recover rare combinations of mutations causing HLHS. Additionally, by conducting the screen using high-throughput fetal echocardiography with high CHD detection sensitivity/specificity, this further ensured the efficient recovery of HLHS mutant mice. Having genetic models of HLHS can greatly facilitate investigations into the developmental, and cell and molecular mechanisms contributing to HLHS.

61.5 Hemodynamic Uncoupling of LV Hypoplasia in HLHS Mutant Mice

Among the HLHS mutant lines recovered, the *Ohia* mouse line [33, 34] was analyzed in detail and documented to provide stable transmission of the HLHS phenotype. A spectrum of CHD phenotypic severity was observed comprising varying degrees of aorta hypoplasia, hypoplasia/atresia of the aortic and mitral valves, and with small muscle-bound LV of varying sizes (Fig. 61.1). Tracking growth and development of the heart using fetal echocardiography showed growth arrest of the left-sided heart structures in *Ohia* mutant mice by E13.5, even as right-sided heart structures continued to grow (Fig. 61.2a–d). LV contractility was markedly reduced (Fig. 61.2e). Further, in *Ohia* mutants, there was no restriction of the foramen ovale, which can be observed in some HLHS patients and has been suggested to contribute hemodynamically to the LV hypoplasia (Fig. 61.2f) [35, 36]. Hemodynamic uncoupling of LV hypoplasia was further indicated by the finding of hypoplastic LV with normal sized aorta, or hypoplastic aorta with normal sized LV in some *Ohia* mutant mice [33]. Together these findings suggest the LV hypoplasia in the *Ohia* HLHS mutant mice is cell autonomous and not of hemodynamic origin. Increasing aortic blood flow in this context is not likely to promote LV growth. Further mechanistic insights are needed before evidence-based therapy can be developed for fetal intervention to recover LV growth prenatally in human conceptuses with evolving HLHS.

61.6 Digenic Etiology for HLHS in *Ohia* Mutant Mice

The *Ohia* HLHS mouse line was analyzed in detail with extensive phenotype–genotype analysis. This led to the recovery of two mutations that together comprised a digenic etiology for HLHS: *Sap130* encoding a Sin3A associated chromatin modifying protein in the histone deacetylase (HDAC) complex [37], and *Pcdha9*, a cell adhesion protein in the protocadherin family [38] shown to cause HLHS. Mutations in these two genes in homozygosity can cause HLHS with incomplete penetrance. This was verified with analysis of mice bearing *Sap130* and *Pcdha9* mutations generated by CRISPR/Cas9 gene editing [33]. It is worth noting a

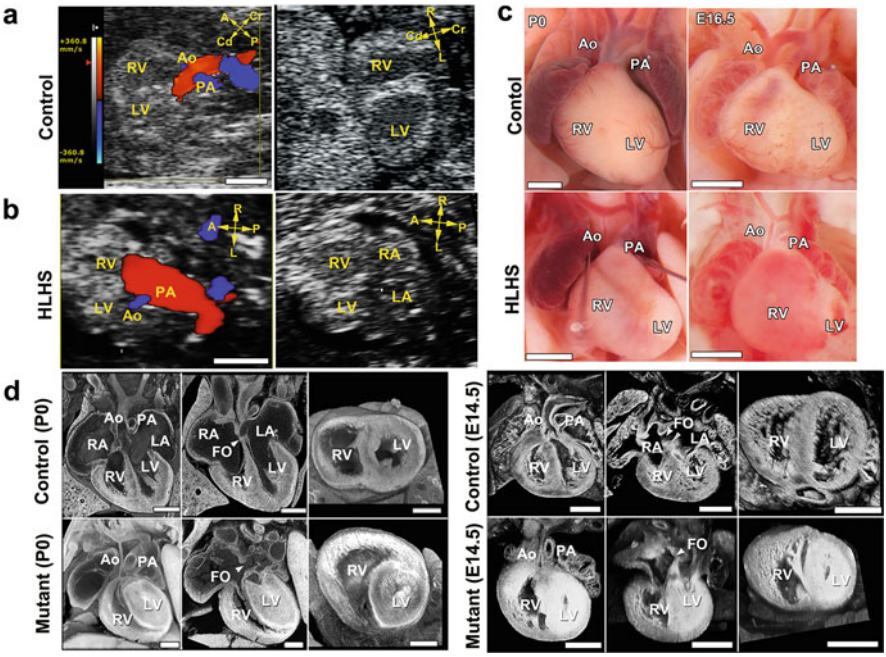

Fig. 61.1 *Ohia* HLHS phenotype. (**a**–**d**) HLHS phenotype in *Ohia* mutants. (**a**, **b**) Ultrasound color-flow imaging of normal fetus (**a**), showing robust flow from the aorta (Ao) and pulmonary artery (PA). In the HLHS mutant (**b**), the aorta showed only a narrow flow stream, whereas the pulmonary artery showed robust flow. 2D imaging revealed hypoplastic LV (**b**), as compared with the normal-sized LV in the control (**a**). (**c**) Newborn (P0) or E16.5 hearts from wild-type and HLHS mutants. Hypoplastic aorta and LV are visible in the HLHS mutant. (**d**) Histopathology showing the cardiac anatomy of HLHS mutant and littermate control at birth (P0) and E14.5. Compared with controls, the HLHS mutant exhibited hypoplastic aorta and aortic valve atresia, hypertrophied LV with no lumen, and mitral valve stenosis and patent foramen ovale (FO), arrowhead. LA, left atrium; RA, right atrium; LV, left ventricle; RV, right ventricle; A, anterior; P, posterior; L, left; R, right; Cr, cranial; Cd, caudal. Scale bars: a, b, 0.5 mm; c, 1 mm; d, 0.5 mm (From Liu et al., 2017)

previous genetic analysis of patients with HLHS has similarly pointed to a digenic model for HLHS [16].

While mice double homozygous for the *Sap130/Pcdha9* mutations have HLHS, mice homozygous for the *Sap130* mutation alone can exhibit isolated hypoplastic LV, indicating the LV hypoplasia is derived from the *Sap130* mutation. This was corroborated with the finding that *sap130a* zebrafish mutant embryos exhibited a small ventricle phenotype [33] during early development when the heart is comprised of only first-heart-field derivatives equivalent to the mouse LV progenitors (Fig. 61.3). In contrast, mice harboring only the *Pcdha9* mutation can exhibit bicuspid aortic valve (BAV), a phenotype often seen in conjunction with HLHS or in family members of HLHS probands [39]. These findings suggest HLHS is a composite lesion generated combinatorially with the *Sap130* mutation causing LV hypoplasia, while the *Pcdha9* mutation may drive the valvular defects.

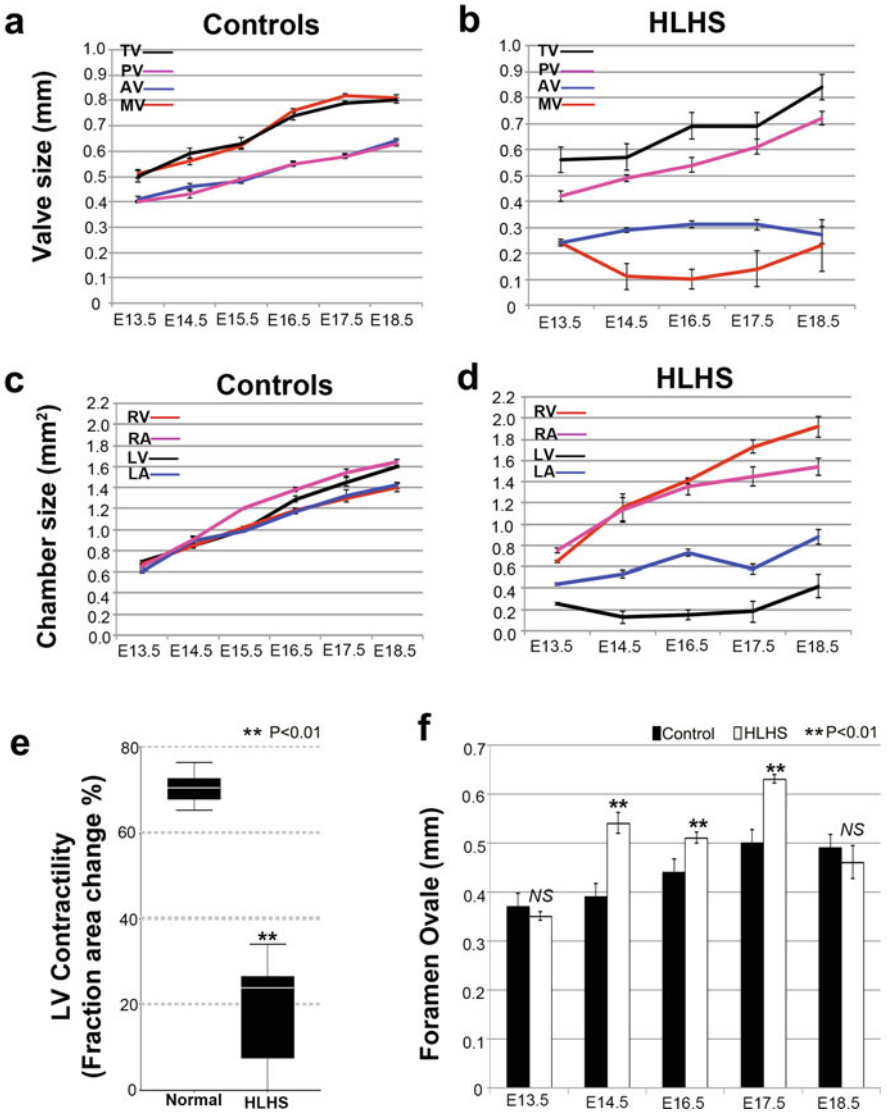

Fig. 61.2 Delineating cardiac development in *Ohia* HLHS mutants using fetal echocardiography (**a**–**d**). Developmental profile of the growth of cardiac valves and chambers in normal vs. HLHS embryos ($n = 15$ embryos per group). Data shown are mean ± s.e.m. LA, left atrium; LV, left ventricle; RA, right atrium, RV, right ventricle; MV, mitral valve, TV, tricuspid valve, AV, aortic valve, PV, pulmonary valve. (**e**) Fetal ultrasound measurements show LV contractility is decreased in HLHS mutant fetuses ($n = 15$ embryos per group). Data shown are median with interquartile range. Wilcoxon rank sum test, $P = 0.000003$. (**f**) Measurements of the foramen ovale (FO) showed FO size was not restrictive in HLHS mutants. Data shown are mean ± s.e.m. Unpaired Student's *t*-test: E13.5, $n = 12$ (control = 6, HLHS = 6) $P = 0.385$, $t = -0.908$, df = 10; E14.5, $n = 18$ (control = 12, HLHS = 6), $P = 0.000084$, $t = 5.222$, df = 16; E16.5, $n = 27$ (control = 15,

Deficiency in *Sin3A*, the protein to which Sap130 is bound, causes preimplantation lethality associated with genome instability [40, 41]. Reminiscent of this, the *Sap130* knockout mouse also dies at preimplantation. It is notable that Sin3A has been shown to be indispensable for the maintenance of stem cell pools [42], and in cooperation with Nanog, it provides for the maintenance of pluripotency [43]. Cells with homozygous loss of *Sin3A* exhibit cell proliferation defects with evidence of DNA damage and apoptosis [41]. Together these observations suggest the small LV phenotype in *Ohia* HLHS mutant mice may arise from a cell autonomous defect in the maintenance and propagation of the LV progenitors in the early embryo. In contrast, mutation in the protocadherin cell adhesion protein may perturb cell–cell adhesion to cause dysregulation of endothelial mesenchymal transition (EndoMT) essential for heart valve development. This could contribute to the aortic/mitral valve defects associated with HLHS. Thus HLHS is a CHD with a digenic etiology that combinatorially orchestrates a composite phenotype comprising a small LV accompanied by valvular defects.

61.7 LV Hypoplasia Associated with Cell Proliferation Defect and Increased Apoptosis

The *Ohia* mouse model made it possible to investigate the cellular and molecular basis for the LV hypoplasia in HLHS. Previous analysis of heart tissue from human HLHS fetuses indicated a cell proliferation defect [44]. Examination of the developmental profile of cardiomyocyte proliferation in *Ohia* HLHS mutant heart from E14.5 to term showed reduction in cell proliferation throughout development. Interestingly, this was observed in both the LV and RV, but the most marked reduction was seen in the LV and at the earliest stage examined (E14.5). Quantitative assessment by fetal echocardiography showed LV growth is arrested by E14.5 (Fig. 61.2). This cell proliferation defect was associated with accumulation of cells at metaphase, indicating blockage of anaphase progression. Concomitantly, apoptosis was elevated together with evidence of DNA damage response with increased γH2AX, all defects seen only in the LV. Thus, the small LV phenotype in *Ohia* mutants arises relatively early in development and is likely from the combined effects of reduced cell proliferation and blockage of mitosis due to inhibition of anaphase progression. It is worth noting that SAP130 ChIPseq analysis recovered *Cdc20* and *Bub3*, as SAP130 targets. These are two components of the mitotic checkpoint complex. Also identified as SAP130 targets are many proteins of the anaphase promoting complex (*Cdc16, Cdc20, Cdc27, Anapc1, Anapc4, Anapc5, Anapc7, Anapc13,* and *Anapc15*). Together these findings indicate metaphase arrest is likely mediated by activation of mitotic checkpoint control with inhibition of the

Fig. 61.2 (continued) HLHS = 12), $p = 0.001$, $t = 3.7$, df = 25; E17.5, $n = 21$ (control = 12, HLHS = 9), $P = 3.4633\text{E-}9$, $t = 10.262$, df = 19; E18.5, $n = 12$ (control = 6, HLHS = 6), $P = 0.453$, $t = -0.782$, df = 10. NS, not significant (From Liu et al., 2017)

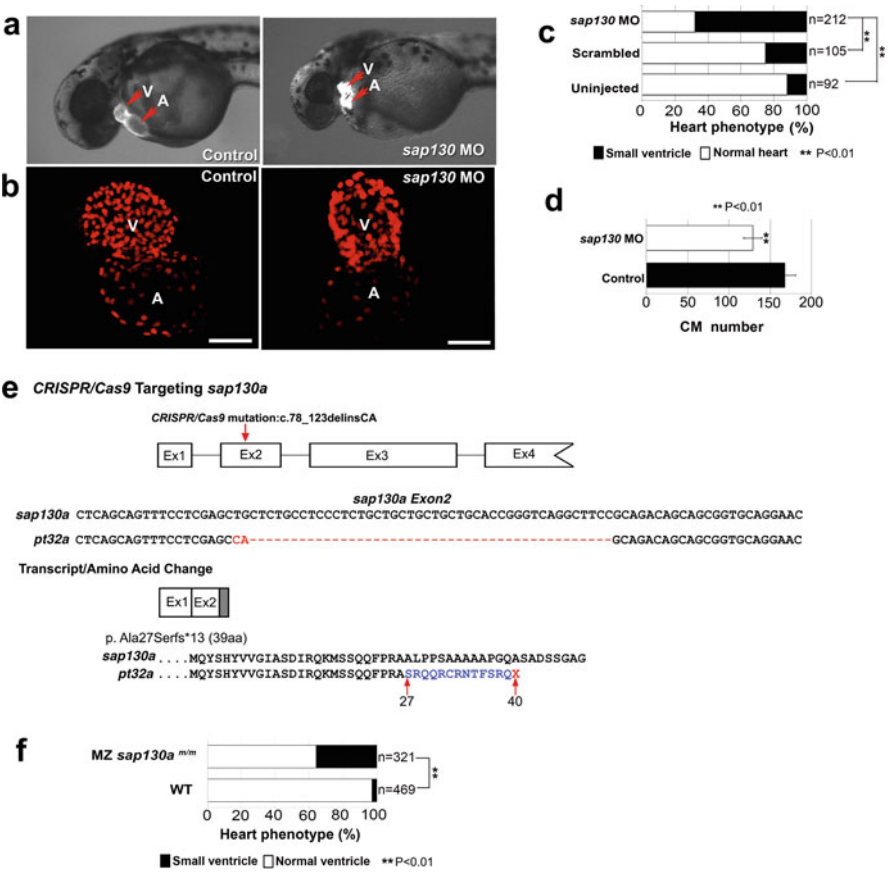

Fig. 61.3 Small ventricle in *sap130a* morpholino knockdown and CRISPR/Cas9-targeted *sap130a* mutant embryos. (**a**) *sap130a* morpholino (MO) knockdown in zebrafish embryos showed reduction in ventricle size (right panel) when compared to uninjected or scrambled MO injected embryos. (**b**) The smaller ventricle phenotype is readily visualized using DsRed cardiomyocyte nuclear labeling (Tg(5.7myl7:nDsRed2) in the ventricle at 72 hpf (bottom). (**c**) *sap130a* MO knockdown of zebrafish embryos at 5 ng MO ($n = 212$) resulted in small heart phenotype compared to scrambled ($n = 105$, Fisher's exact test, $P = 2.7601\text{E-}13$) and uninjected zebrafish embryos (**c**) ($n = 92$, Fisher's exact test, $P = 1.7789\text{E-}20$). (**d**) Quantification of DsRed2-labeled cardiomyocyte nuclei showed the *sap130a* MO knockdown (5 ng MO) zebrafish embryos ($n = 7$) had fewer cardiomyocytes compared to control uninjected ($n = 6$). Data shown are mean ± s.e.m. Unpaired Student's T-test, $P = 0.000132$, $t = 5.731$, $df = 11$. (**e**) CRISPR/Cas9 generated sap130a mutation with 2 bp insertion and 46 bp deletion in exon 2 in zebrafish mutant line pt32a is shown (red arrow), predicting a frameshift causing premature termination. (**f**) Homozygous maternal zygotic CRISPR/Cas9 *sap130a* mutant embryos showed small ventricle phenotype ($n = 321$) compared to wild-type zebrafish embryos ($n = 469$; Fisher's exact test, $P = 8.2846\text{E-}37$). It was necessary to F4 generate *sap130a* maternal zygotic mutant embryos, as *sap130a* is expressed as maternal transcripts. V, ventricle; A, atrium. Scale bar, 40 μm (From Liu et al., 2017)

anaphase promoting complex, accounting for the cell proliferation defect and increased apoptosis associated with the LV hypoplasia in *Ohia* HLHS mutant mice.

61.8 LV Hypoplasia and Hippo-YAP Signaling

Additional studies suggested the small LV phenotype in HLHS may involve disturbance of Hippo signaling, a pathway already well described to play an important role in regulating heart organ size, and cardiomyocyte proliferation [45, 46]. This pathway is highly evolutionarily conserved, playing an important role in the regulation of cell proliferation, apoptosis, and stem cell self-renewal. Hippo signaling is mediated by a kinase cascade regulating protein phosphorylation and the activation/inactivation-degradation of the transcriptional coactivators YAP and TAZ. When Hippo pathway is off, YAP/TAZ are stably maintained and are translocated into the nucleus where they form transcriptional complexes with TEADs to activate transcription of genes regulating cell proliferation and stem cell renewal. Analysis of induced pluripotent stem cell derived cardiomyocytes (iPSC-CM) from *Ohia* HLHS mutant mice and from HLHS patients showed abnormal activation of Hippo signaling with the loss of Yap1 nuclear localization [47] and reduced cell proliferation and increased apoptosis. This same finding in HLHS mice and patients despite the genetic heterogeneity would suggest a common mechanism driving the LV hypoplasia regardless of the specific genetic basis for the HLHS phenotype.

A role for SAP130 in the regulation of Hippo-YAP is indicated by the SAP130 ChIPseq analysis which also showed many genes in the Hippo pathway are SAP130 targets, including *Yap1*, *Wwtr1*(*Taz*), *Lats1/2*, *Mob1a/b*, *Sav1*, and *Tead1/2/3/4* (Fig. 61.4). YAP1 has been shown to regulate cardiomyocyte proliferation from the very earliest stages of mouse heart development, with YAP1 and TEAD observed to be strongly expressed and nuclear localized in the E8.5 myocardium [48]. *Nkx2.5*-Cre mediated cardiac-specific deletion of *Yap1* resulted in embryos with smaller hearts which is evident by E9.5 [46]. This was associated with 50% reduction in the number of cardiomyocytes and a significant reduction in proliferating cells in the heart [46]. These *Nkx2.5*-Cre deleted *Yap1* mutant embryos die by E10.5 from heart failure with thin myocardium. In a separate study, *Nkx2.5*-Cre deletion of a floxed *Sav1* allele, a Hippo pathway core component in the MST1/MST2 complex, resulted in cardiomegaly due to increase in the number of cardiomyocytes in the heart. This reflected the loss of Hippo signaling required to repress cardiomyocyte proliferation. As the heart enlargement affected the RV and LV equally, this indicated Hippo regulation of ventricular growth has no intrinsic "sidedness" [49]. This would point to a role for *Sap130* in specifying the sidedness associated with HLHS, perhaps via *Sap130* integration of pathways regulating left–right patterning and Hippo signaling.

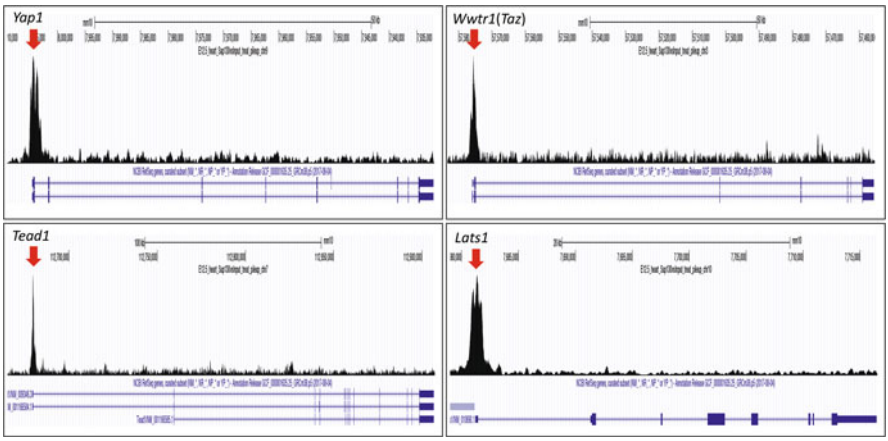

Fig. 61.4 Hippo pathway components identified as targets of Sap130. Chromatin Immunoprecipitation sequencing with Sap130 antibody showed peaks at transcription start sites (Red Arrow) for many Hippo pathway components, 4 of which are shown

61.9 Restriction of Defects to Left-Sided Heart Structures

The restriction of anatomical defects to the left side of the heart in HLHS is striking. The notable uniform fatality of HLHS patients in the absence of surgical palliation highlights the importance of bilateral asymmetry in the heart in ensuring efficient oxygenation of blood. Thus, the heart is the most left–right asymmetric organ in the body, with the left heart devoted to systemic circulation, while the right heart is devoted to pulmonary circulation. Left–right patterning of the body plan is established early in development with left-sided expression first of *Nodal,* followed by *Lefty1/2*, and finally the transcription factor *Pitx2*. Such left-sided *Nodal/Lefty/Pitx2* expression cascade can be detected in the posterior second heart field and anterior heart field cell lineages around the time of heart looping [50]. Interestingly, the SIN3A-HDAC repressor complex to which SAP130 is bound has been shown to interact with TET1, a DNA demethylase, causing demethylation of the *Lefty* promoter to activate transcription [42]. TET-mediated DNA demethylation has also been shown to regulate NODAL/LEFTY signaling required for gastrulation [51]. Depletion of the DNA methyltransferase *Dnmt1* in zebrafish or frog embryos can cause laterality defects, confirming the importance of epigenetic regulation in the specification of left–right patterning [52].

The involvement of epigenetics in left–right patterning and the LV hypoplasia in HLHS is also suggested by the interaction of the SIN3A/HDAC repressor complex with BRG1 in the SWI/SNF complex [53]. Perturbation of the SWI/SNF chromatin remodeling complex has been shown to cause left–right patterning defects [54]. The epigenetic regulation of left–right patterning could involve alteration in DNA methylation and/or chromatin and the perturbation of *Nodal/Lefty/Pitx2* expression.

Consistent with this model, the incidence of heterotaxy and other rare laterality related phenotypes, such as biliary atresia, is significantly elevated among patients with HLHS [55]. Using the *Ohia* mouse model, it will be possible to further investigate the role of the SIN3A-HDAC repressor complex in the epigenetic regulation of laterality and the left-sided heart defects in HLHS. Insights into the molecular mechanism by which LV hypoplasia emerges in HLHS will have important implications for the future development of new avenues of therapy with fetal intervention to recover LV growth prenatally. It should be noted that fetal intervention is likely critical given findings from the *Ohia* model indicated the LV hypoplasia is associated with depletion of early LV progenitors. Additionally, the proliferative potential of cardiomyocytes in the human heart is observed to be lost after birth, further suggesting the need for fetal intervention [56, 57].

61.10 Future Prospects

First described more than five decades ago [58, 59], HLHS has become a lesion that can be prenatally recognized and has several palliative treatment options. While surgical treatment of HLHS is performed in three stages with considerable success, without a clear understanding of its molecular causes [60], prenatal therapy has had limited success. Insights that have emerged from recent studies of HLHS mutant mice and HLHS patient derived iPSC-cardiomyocytes suggest new avenues for therapeutic intervention. It is worth noting compounds that can modulate Hippo-YAP signaling, DNA methylation, or HDAC activity are already available, with some in clinical trials for treatment of various diseases. Hence, this suggests the exciting prospects for future targeted therapies to recover LV growth in fetuses with evolving HLHS. Such interventions will require more detailed mechanistic studies to expand on these findings and to determine the generalizability of these findings to HLHS patients at large.

Acknowledgment This work is supported by funding from NIH HL142788 (to CWL) and AHA Career Development Award 847524 (to HY).

References

1. Garcia AM, Beatty JT, Nakano SJ. Heart failure in single right ventricle congenital heart disease: physiological and molecular considerations. Am J Physiol Heart Circ Physiol. 2020;318(4):H947–H65. https://doi.org/10.1152/ajpheart.00518.2019.
2. Driscoll DJ, Offord KP, Feldt RH, Schaff HV, Puga FJ, Danielson GK. Five- to fifteen-year follow-up after Fontan operation. Circulation. 1992;85(2):469–96. https://doi.org/10.1161/01.cir.85.2.469.
3. Gentles TL, Gauvreau K, Mayer JE, Jr., Fishberger SB, Burnett J, Colan SD, et al. Functional outcome after the Fontan operation: factors influencing late morbidity. J Thorac Cardiovasc Surg. 1997;114(3):392–403; discussion 4–5. https://doi.org/10.1016/s0022-5223(97)70184-3
4. Lloyd DF, Rutherford MA, Simpson JM, Razavi R. The neurodevelopmental implications of hypoplastic left heart syndrome in the fetus. Cardiol Young. 2017;27(2):217–23.

5. Sigmon ER, Oster M, Kelleman M, Susi A, Nylund C. Association of Congenital Heart Disease with autism: a case-control study. American Academy of Pediatrics Elk Grove Village; 2019.
6. Hansen JH, Rotermann I, Logoteta J, Jung O, Dütschke P, Scheewe J, et al. Neurodevelopmental outcome in hypoplastic left heart syndrome: impact of perioperative cerebral tissue oxygenation of the Norwood procedure. J Thorac Cardiovasc Surg. 2016;151 (5):1358–66.
7. Newburger JW, Sleeper LA, Bellinger DC, Goldberg CS, Tabbutt S, Lu M, et al. Early developmental outcome in children with hypoplastic left heart syndrome and related anomalies: the single ventricle reconstruction trial. Circulation. 2012;125(17):2081–91.
8. deAlmeida A, McQuinn T, Sedmera D. Increased ventricular preload is compensated by myocyte proliferation in normal and hypoplastic fetal chick left ventricle. Circ Res. 2007;100 (9):1363–70. https://doi.org/10.1161/01.RES.0000266606.88463.cb.
9. Fishman NH, Hof RB, Rudolph AM, Heymann MA. Models of congenital heart disease in fetal lambs. Circulation. 1978;58(2):354–64. https://doi.org/10.1161/01.cir.58.2.354.
10. Wong FY, Veldman A, Sasi A, Teoh M, Edwards A, Chan Y, et al. Induction of left ventricular hypoplasia by occluding the foramen ovale in the fetal lamb. Sci Rep. 2020;10(1):880. https://doi.org/10.1038/s41598-020-57694-4.
11. Feit LR, Copel JA, Kleinman CS. Foramen ovale size in the normal and abnormal human fetal heart: an indicator of transatrial flow physiology. Ultrasound Obstet Gynecol. 1991;1(5):313–9. https://doi.org/10.1046/j.1469-0705.1991.01050313.x.
12. Freud LR, McElhinney DB, Marshall AC, Marx GR, Friedman KG, del Nido PJ, et al. Fetal aortic valvuloplasty for evolving hypoplastic left heart syndrome: postnatal outcomes of the first 100 patients. Circulation. 2014;130(8):638–45.
13. Pickard SS, Wong JB, Bucholz EM, Newburger JW, Tworetzky W, Lafranchi T, et al. Fetal aortic valvuloplasty for evolving hypoplastic left heart syndrome: a decision analysis. Circ Cardiovasc Qual Outcomes. 2020;13(4):e006127.
14. McElhinney DB, Marshall AC, Wilkins-Haug LE, Brown DW, Benson CB, Silva V, et al. Predictors of technical success and postnatal biventricular outcome after in utero aortic valvuloplasty for aortic stenosis with evolving hypoplastic left heart syndrome. Circulation. 2009;120(15):1482–90.
15. Hinton RB Jr, Martin LJ, Tabangin ME, Mazwi ML, Cripe LH, Benson DW. Hypoplastic left heart syndrome is heritable. J Am Coll Cardiol. 2007;50(16):1590–5. https://doi.org/10.1016/j.jacc.2007.07.021.
16. McBride KL, Pignatelli R, Lewin M, Ho T, Fernbach S, Menesses A, et al. Inheritance analysis of congenital left ventricular outflow tract obstruction malformations: segregation, multiplex relative risk, and heritability. Am J Med Genet A. 2005;134(2):180–6.
17. Dasgupta C, Martinez AM, Zuppan CW, Shah MM, Bailey LL, Fletcher WH. Identification of connexin43 (alpha1) gap junction gene mutations in patients with hypoplastic left heart syndrome by denaturing gradient gel electrophoresis (DGGE). Mutat Res. 2001;479(1–2): 173–86. https://doi.org/10.1016/s0027-5107(01)00160-9.
18. Theis JL, Zimmermann MT, Evans JM, Eckloff BW, Wieben ED, Qureshi MY, et al. Recessive MYH6 mutations in hypoplastic left heart with reduced ejection fraction. Circ-Cardiovasc Gene. 2015;8(4):564–71. https://doi.org/10.1161/Circgenetics.115.001070.
19. Elliott DA, Kirk EP, Yeoh T, Chandar S, McKenzie F, Taylor P, et al. Cardiac homeobox gene NKX2-5 mutations and congenital heart disease: associations with atrial septal defect and hypoplastic left heart syndrome. J Am Coll Cardiol. 2003;41(11):2072–6. https://doi.org/10.1016/s0735-1097(03)00420-0.
20. McElhinney DB, Geiger E, Blinder J, Benson DW, Goldmuntz E. NKX2.5 mutations in patients with congenital heart disease. J Am Coll Cardiol. 2003;42(9):1650–5. https://doi.org/10.1016/j.jacc.2003.05.004.
21. Stallmeyer B, Fenge H, Nowak-Gottl U, Schulze-Bahr E. Mutational spectrum in the cardiac transcription factor gene NKX2.5 (CSX) associated with congenital heart disease. Clin Genet. 2010;78(6):533–40. https://doi.org/10.1111/j.1399-0004.2010.01422.x.

22. McBride KL, Riley MF, Zender GA, Fitzgerald-Butt SM, Towbin JA, Belmont JW, et al. NOTCH1 mutations in individuals with left ventricular outflow tract malformations reduce ligand-induced signaling. Hum Mol Genet. 2008;17(18):2886–93. https://doi.org/10.1093/hmg/ddn187.
23. Garg V, Muth AN, Ransom JF, Schluterman MK, Barnes R, King IN, et al. Mutations in NOTCH1 cause aortic valve disease. Nature. 2005;437(7056):270–4. https://doi.org/10.1038/nature03940.
24. McBride KL, Zender GA, Fitzgerald-Butt SM, Seagraves NJ, Fernbach SD, Zapata G, et al. Association of common variants in ERBB4 with congenital left ventricular outflow tract obstruction defects. Birth Defects Res A Clin Mol Teratol. 2011;91(3):162–8. https://doi.org/10.1002/bdra.20764.
25. Ware SM, Peng J, Zhu L, Fernbach S, Colicos S, Casey B, et al. Identification and functional analysis of ZIC3 mutations in heterotaxy and related congenital heart defects. Am J Hum Genet. 2004;74(1):93–105. https://doi.org/10.1086/380998.
26. Homsy J, Zaidi S, Shen Y, Ware JS, Samocha KE, Karczewski KJ, et al. De novo mutations in congenital heart disease with neurodevelopmental and other congenital anomalies. Science. 2015;350(6265):1262–6. https://doi.org/10.1126/science.aac9396.
27. Reamon-Buettner SM, Ciribilli Y, Inga A, Borlak J. A loss-of-function mutation in the binding domain of HAND1 predicts hypoplasia of the human hearts. Hum Mol Genet. 2008;17(10):1397–405. https://doi.org/10.1093/hmg/ddn027.
28. Lara DA, Ethen MK, Canfield MA, Nembhard WN, Morris SA. A population-based analysis of mortality in patients with turner syndrome and hypoplastic left heart syndrome using the Texas birth defects registry. Congenit Heart Dis. 2017;12(1):105–12. https://doi.org/10.1111/chd.12413.
29. Grossfeld PD, Mattina T, Lai Z, Favier R, Jones KL, Cotter F, et al. The 11q terminal deletion disorder: a prospective study of 110 cases. Am J Med Genet A. 2004;129A(1):51–61. https://doi.org/10.1002/ajmg.a.30090.
30. Martinez Crespo JM, Del Rio M, Gomez O, Borrell A, Puerto B, Cararach V, et al. Prenatal diagnosis of hypoplastic left heart syndrome and trisomy 18 in a fetus with normal nuchal translucency and abnormal ductus venosus blood flow at 13 weeks of gestation. Ultrasound Obstet Gynecol. 2003;21(5):490–3. https://doi.org/10.1002/uog.119.
31. Kukora S, Firn J, Laventhal N, Vercler C, Moore B, Lantos JD. Infant with trisomy 18 and hypoplastic left heart syndrome. Pediatrics. 2019;143(5) https://doi.org/10.1542/peds.2018-3779.
32. Glauser TA, Rorke LB, Weinberg PM, Clancy RR. Congenital brain anomalies associated with the hypoplastic left heart syndrome. Pediatrics. 1990;85(6):984–90.
33. Liu X, Yagi H, Saeed S, Bais AS, Gabriel GC, Chen Z, et al. The complex genetics of hypoplastic left heart syndrome. Nat Genet. 2017;49(7):1152–9. https://doi.org/10.1038/ng.3870.
34. Li Y, Klena NT, Gabriel GC, Liu X, Kim AJ, Lemke K, et al. Global genetic analysis in mice unveils central role for cilia in congenital heart disease. Nature. 2015;521(7553):520–4. https://doi.org/10.1038/nature14269.
35. Jantzen DW, Moon-Grady AJ, Morris SA, Armstrong AK, Berg C, Dangel J, et al. Hypoplastic left heart syndrome with intact or restrictive atrial septum: a report from the international fetal cardiac intervention registry. Circulation. 2017;136(14):1346–9. https://doi.org/10.1161/CIRCULATIONAHA.116.025873.
36. Taketazu M, Barrea C, Smallhorn JF, Wilson GJ, Hornberger LK. Intrauterine pulmonary venous flow and restrictive foramen ovale in fetal hypoplastic left heart syndrome. J Am Coll Cardiol. 2004;43(10):1902–7. https://doi.org/10.1016/j.jacc.2004.01.033.
37. Kadamb R, Mittal S, Bansal N, Batra H, Saluja D. Sin3: insight into its transcription regulatory functions. Eur J Cell Biol. 2013;92(8–9):237–46. https://doi.org/10.1016/j.ejcb.2013.09.001.
38. Wu Q, Maniatis T. A striking organization of a large family of human neural cadherin-like cell adhesion genes. Cell. 1999;97(6):779–90.

39. Teekakirikul P, Zhu W, Gabriel GC, Young CB, Williams K, Martin LJ, et al. Common deletion variants causing protocadherin-α deficiency contribute to the complex genetics of bicuspid aortic valve and left-sided congenital heart disease. Human Genetics Genomics Adv. 2021;2:100037.
40. Dannenberg JH, David G, Zhong S, van der Torre J, Wong WH, Depinho RA. mSin3A corepressor regulates diverse transcriptional networks governing normal and neoplastic growth and survival. Genes Dev. 2005;19(13):1581–95. https://doi.org/10.1101/gad.1286905.
41. McDonel P, Demmers J, Tan DW, Watt F, Hendrich BD. Sin3a is essential for the genome integrity and viability of pluripotent cells. Dev Biol. 2012;363(1):62–73. https://doi.org/10.1016/j.ydbio.2011.12.019.
42. Zhu F, Zhu Q, Ye D, Zhang Q, Yang Y, Guo X, et al. Sin3a-Tet1 interaction activates gene transcription and is required for embryonic stem cell pluripotency. Nucleic Acids Res. 2018;46(12):6026–40. https://doi.org/10.1093/nar/gky347.
43. Saunders A, Faiola F, Wang J. Concise review: pursuing self-renewal and pluripotency with the stem cell factor Nanog. Stem Cells. 2013;31(7):1227–36. https://doi.org/10.1002/stem.1384.
44. Gaber N, Gagliardi M, Patel P, Kinnear C, Zhang C, Chitayat D, et al. Fetal reprogramming and senescence in hypoplastic left heart syndrome and in human pluripotent stem cells during cardiac differentiation. Am J Pathol. 2013;183(3):720–34. https://doi.org/10.1016/j.ajpath.2013.05.022.
45. von Gise A, Lin Z, Schlegelmilch K, Honor LB, Pan GM, Buck JN, et al. YAP1, the nuclear target of Hippo signaling, stimulates heart growth through cardiomyocyte proliferation but not hypertrophy. Proc Natl Acad Sci U S A. 2012;109(7):2394–9. https://doi.org/10.1073/pnas.1116136109.
46. Xin M, Kim Y, Sutherland LB, Qi X, McAnally J, Schwartz RJ, et al. Regulation of insulin-like growth factor signaling by Yap governs cardiomyocyte proliferation and embryonic heart size. Sci Signal. 2011;4(196):ra70. https://doi.org/10.1126/scisignal.2002278.
47. Xu X, Jin K, Bais AS, Zhu W, Yagi H, Feinstein TN, et al. iPSC modeling shows uncompensated mitochondrial mediated oxidative stress underlies early heart failure in hypoplastic left heart syndrome. bioRxiv. 2021:2021.05.09.443165. https://doi.org/10.1101/2021.05.09.443165
48. Ota M, Sasaki H. Mammalian Tead proteins regulate cell proliferation and contact inhibition as transcriptional mediators of Hippo signaling. Development. 2008;135(24):4059–69. https://doi.org/10.1242/dev.027151.
49. Heallen T, Zhang M, Wang J, Bonilla-Claudio M, Klysik E, Johnson RL, et al. Hippo pathway inhibits Wnt signaling to restrain cardiomyocyte proliferation and heart size. Science. 2011;332(6028):458–61. https://doi.org/10.1126/science.1199010.
50. de Soysa TY, Ranade SS, Okawa S, Ravichandran S, Huang Y, Salunga HT, et al. Single-cell analysis of cardiogenesis reveals basis for organ-level developmental defects. Nature. 2019;572(7767):120–4. https://doi.org/10.1038/s41586-019-1414-x.
51. Dai HQ, Wang BA, Yang L, Chen JJ, Zhu GC, Sun ML, et al. TET-mediated DNA demethylation controls gastrulation by regulating lefty-nodal signalling. Nature. 2016;538(7626):528–32. https://doi.org/10.1038/nature20095.
52. Wang L, Liu Z, Lin H, Ma D, Tao Q, Liu F. Epigenetic regulation of left-right asymmetry by DNA methylation. EMBO J. 2017;36(20):2987–97. https://doi.org/10.15252/embj.201796580.
53. Sif S, Saurin AJ, Imbalzano AN, Kingston RE. Purification and characterization of mSin3A-containing Brg1 and hBrm chromatin remodeling complexes. Genes Dev. 2001;15(5):603–18. https://doi.org/10.1101/gad.872801.
54. Takeuchi JK, Lickert H, Bisgrove BW, Sun X, Yamamoto M, Chawengsaksophak K, et al. Baf60c is a nuclear notch signaling component required for the establishment of left-right asymmetry. Proc Natl Acad Sci U S A. 2007;104(3):846–51. https://doi.org/10.1073/pnas.0608118104.

55. Pradat P, Francannet C, Harris JA, Robert E. The epidemiology of cardiovascular defects, part I: a study based on data from three large registries of congenital malformations. Pediatr Cardiol. 2003;24(3):195–221. https://doi.org/10.1007/s00246-002-9401-6.
56. Zebrowski DC, Vergarajauregui S, Wu CC, Piatkowski T, Becker R, Leone M, et al. Developmental alterations in centrosome integrity contribute to the post-mitotic state of mammalian cardiomyocytes. elife. 2015;4:4. https://doi.org/10.7554/eLife.05563.
57. Bergmann O, Zdunek S, Felker A, Salehpour M, Alkass K, Bernard S, et al. Dynamics of cell generation and turnover in the human heart. Cell. 2015;161(7):1566–75. https://doi.org/10.1016/j.cell.2015.05.026.
58. Lev M. Pathologic anatomy and interrelationship of hypoplasia of the aortic tract complexes. Lab Investig. 1952;1(1):61–70.
59. Noonan JA, Nadas AS. The hypoplastic left heart syndrome; an analysis of 101 cases. Pediatr Clin N Am. 1958;5(4):1029–56. https://doi.org/10.1016/s0031-3955(16)30727-1.
60. Norwood WI, Lang P, Hansen DD. Physiologic repair of aortic atresia-hypoplastic left heart syndrome. N Engl J Med. 1983;308(1):23–6. https://doi.org/10.1056/NEJM198301063080106.

Part XVII

Cardiomyopathies

Clinical Presentation and Therapy of Cardiomyopathies

62

Nikolaus A. Haas, David J. Driscoll, and Silke Rickert-Sperling

62.1 Introduction

Cardiomyopathies are a group of diseases that primarily affect the heart muscle, leading to mechanical or electrical dysfunction of the heart. They can be categorized into primary and secondary forms. Primary cardiomyopathies can be further classified as congenital, acquired, or mixed. In terms of the heart muscle itself, there are five distinct types of cardiomyopathies: hypertrophic cardiomyopathy, dilated or congestive cardiomyopathy, restrictive cardiomyopathy, arrhythmogenic (right ventricular) dysplasia, and noncompaction cardiomyopathy. While cardiomyopathies primarily affect the heart, they can also have systemic manifestations, impacting other organs and potentially causing progressive debilitation, heart failure, or even death.

N. A. Haas (✉)
Department of Pediatric Cardiology and Intensive Care, Ludwig Maximilians University, Munich, Germany
e-mail: Nikolaus.haas@med.uni-muenchen.de

D. J. Driscoll
Division of Pediatric Cardiology, Department of Pediatrics, Mayo Clinic College of Medicine, Rochester, MN, USA
e-mail: driscoll.david@mayo.edu

S. Rickert-Sperling
Cardiovascular Genetics, Charité – Universitätsmedizin Berlin, Berlin, Germany
e-mail: silke.sperling@charite.de

© The Author(s), under exclusive license to Springer Nature Switzerland AG 2024

S. Rickert-Sperling et al. (eds.), *Congenital Heart Diseases: The Broken Heart*,
Advances in Experimental Medicine and Biology 1441,
https://doi.org/10.1007/978-3-031-44087-8_62

62.2 Hypertrophic Cardiomyopathy

62.2.1 Pathologic Physiology

Hypertrophic cardiomyopathy (HCM) is a condition characterized by an increase in myocardial thickness and disorganized growth of myocardial fibers (Fig. 62.1). It can manifest with or without obstruction of the left ventricular outflow tract, and when obstruction is present, it is referred to as "hypertrophic obstructive cardiomyopathy" (HOCM), previously known as idiopathic hypertrophic subaortic stenosis (IHSS) or asymmetric septal hypertrophy (ASH). In cases without outflow tract obstruction, it is termed "hypertrophic nonobstructive cardiomyopathy" (HCM or HNCM). The incidence of HCM is estimated to be around 1 in 500 individuals. Symptoms can include chest pain, shortness of breath, exercise intolerance, syncope, and sudden death, particularly among children and young adults under the age of 35. Notably, HCM is the most common identifiable nontraumatic cause of death on the athletic field. During exercise or physical exertion, the hypertrophied myocardium may experience inadequate myocardial perfusion, leading to myocardial ischemia. This compromised blood flow can trigger ventricular arrhythmias, including tachycardia, fibrillation, and potentially sudden cardiac death.

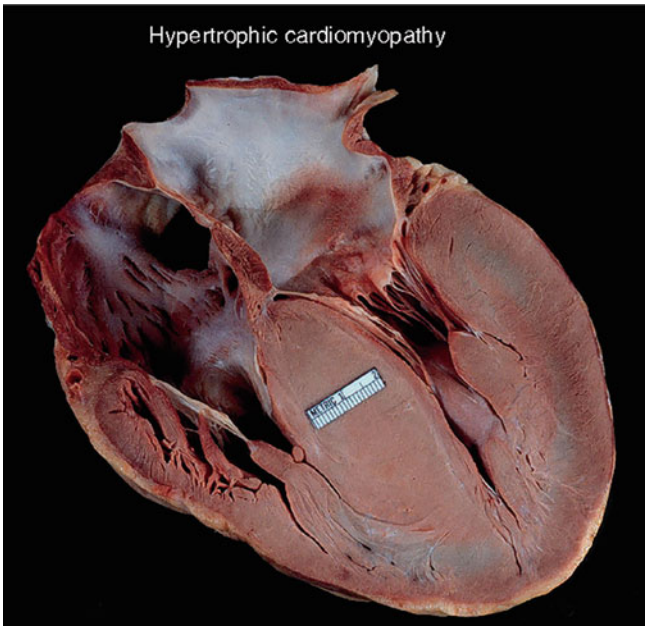

Fig. 62.1 Pathologic specimen of hypertrophic cardiomyopathy. Note the markedly thickened septum and left ventricular posterior wall (Reproduced or adapted from Driscoll, David, Fundamentals of Pediatric Cardiology, Lippincott Williams & Wilkins, 2006, with permission of the author and publisher)

62.2.2 Clinical Presentation

Patients with HC usually come to medical attention in one or more of the following ways: detection of a murmur, an abnormal electrocardiogram, from family screening or a positive family history, from evaluation of syncope, chest pain, palpitations, shortness of breath especially during exercise or out-of-hospital cardiac arrest.

62.2.3 Physical Examination

In patients with nonobstructive forms of hypertrophic cardiomyopathy (HCM), there is typically no characteristic murmur present. The physical examination may or may not reveal a prominent apical impulse and an S4 sound. However, it's important to note that in some cases, obstruction can be unmasked, leading to the appearance of a murmur. This can occur with maneuvers that lower systemic vascular resistance, such as inhaling amyl nitrate or assuming a standing position.

On the other hand, patients with obstructive HCM will often have a systolic ejection murmur. However, in subtle cases, it can be mistaken for an innocent flow murmur. Additionally, there may be a bifid pulse, which can be an indicator of underlying obstruction. It is crucial to conduct a detailed assessment of the family history, particularly looking for instances of unexplained death in otherwise healthy individuals, as this can provide important clues for diagnosing HCM.

62.2.4 Diagnostic Imaging

Echocardiography is an accurate diagnostic tool for assessing hypertrophic cardiomyopathy. It allows for the measurement of various parameters that aid in the diagnosis. One important finding is a septum thickness of greater than 15 mm in adults, which is considered pathognomonic for HCM. Diastolic dysfunction can also be observed, providing further evidence of the condition. Furthermore, echocardiography can detect mitral valve abnormalities, specifically systolic anterior movement (SAM) of the mitral valve, which is a common finding in HOCM. This movement of the mitral valve toward the left ventricular outflow tract can contribute to the obstruction of blood flow. In cases of HOCM, echocardiography can assess the gradient between the left atrium and aorta both at rest and under exercise. This evaluation helps to determine the severity of the obstruction and its impact on cardiac function during different levels of activity.

The ECG is used as screening method in athletes and will reveal signs of increased left ventricular muscle mass (Sokolov–Lyon index) and arrhythmias under exercise.

Cardiac catheterization was previously used to directly measure the LVOTO gradient and obtain endomyocardial biopsies to further specify the diagnosis.

However, with the noninvasive nature of echocardiography and its ability to accurately assess LVOTO gradients, the need for invasive procedures has diminished.

In cases of HOCM, certain interventional techniques, such as alcohol septal ablation, can be performed using cardiac catheterization. However, these procedures are not typically used for diagnostic purposes but rather for therapeutic interventions aimed at reducing the obstruction.

Magnetic resonance imaging (MRI) is a valuable tool in the evaluation of HCM, particularly in cases where echocardiography suggests the presence of the condition. MRI provides additional information that can aid in the diagnosis and management of HCM.

One of the advantages of MRI is its ability to detect atypical distributions of hypertrophy that may not be clearly visualized with echocardiography. It allows for a detailed assessment of myocardial thickness, including the measurement of septal thickness, which is a key diagnostic criterion for HCM. Furthermore, MRI can accurately calculate myocardial mass, providing quantitative data about the extent of hypertrophy.

Another important aspect that MRI can evaluate is the presence of myocardial scarring and fibrosis. This information is crucial as myocardial fibrosis is associated with an increased risk of arrhythmias and sudden cardiac death (SCD). By identifying areas of scarring or fibrosis, MRI helps in risk stratification and guides treatment decisions.

62.2.5 Treatment

In symptomatic patients with hypertrophic cardiomyopathy (HCM) who experience symptoms such as shortness of breath, exercise intolerance, and pulmonary congestion, medical treatment focuses on reducing cardiac muscle performance. This is typically achieved through the administration of beta-blockers and calcium channel inhibitors. It is important to note that other medications that affect preload and afterload are contraindicated in HCM. Lifestyle modifications are also recommended to minimize the risk of arrhythmias during exercise.

One of the most significant concerns in HCM is the increased risk of sudden death. Population-based studies have indicated that the annual risk of sudden death is around 1%. Although the ability to identify patients at high risk for sudden death is still limited, certain features have been associated with a higher risk. These include a diagnosis of HCM in childhood, septal thickness exceeding 30 mm, the presence of nonsustained ventricular tachycardia, failure of normal increase in systolic blood pressure during exercise, a family history of premature death associated with HCM, significant left ventricular outflow tract obstruction, and prior cardiac arrest.

The current treatment paradigm for HCM involves identifying patients at high risk for sudden death and implanting an automatic internal cardiac defibrillator (AICD) as a preventive measure. For symptomatic patients who are not at high risk for sudden death and do not qualify for AICD implantation, treatment with

beta-blockers or amiodarone may be considered to reduce the risk of malignant arrhythmias.

In cases where significant left ventricular outflow tract obstruction is present, surgical interventions such as myotomy/myectomy, endovascular radiofrequency ablation, or transcoronary transcatheter alcohol septal ablation (TASH) may be performed. There is increasing evidence suggesting that eliminating the obstruction can prolong life and alleviate symptoms in these patients.

62.2.6 Outcome

Untreated, hypertrophic cardiomyopathy carries a significant risk of death, estimated to be around 1% per year. However, there are interventions available that can reduce this risk and improve outcomes for affected individuals.

For patients with significant left ventricular outflow tract obstruction, surgical interventions such as myotomy/myectomy can be performed. These procedures aim to relieve the obstruction and improve blood flow, reducing the risk of complications and death.

In cases where patients are identified as being at high risk for sudden death based on certain criteria (as mentioned earlier), the implantation of an automatic defibrillator, also known as an implantable cardioverter-defibrillator (ICD), is recommended. An ICD is designed to detect and treat life-threatening arrhythmias, thus reducing the risk of sudden cardiac death.

In some cases, conservative management may prove ineffective in managing the symptoms and complications associated with HCM. In such situations, cardiac transplantation may be considered as a treatment option. Cardiac transplantation involves replacing the diseased heart with a healthy donor heart, offering a potential cure for end-stage HCM.

62.3 Dilated Cardiomyopathy

Dilated or congestive cardiomyopathy is characterized by the dilation of the left ventricle along with reduced systolic function (Fig. 62.2). A normal left ventricular ejection fraction typically ranges between 50% and 60%. When the ejection fraction falls below 50%, it is considered abnormal and may indicate the presence of dilated cardiomyopathy.

While dilated cardiomyopathy is generally rare in childhood, with an incidence of about 1–2 per 100,000 children, it is actually the most common form of cardiomyopathy in this age group. Diagnosing dilated cardiomyopathy in children can be challenging as its clinical presentation can overlap with acute myocarditis. Therefore, thorough diagnostic investigations are necessary to clarify the diagnosis and differentiate between these conditions.

The diagnostic workup for dilated cardiomyopathy may include various tests such as echocardiography, cardiac MRI, genetic testing, and endomyocardial

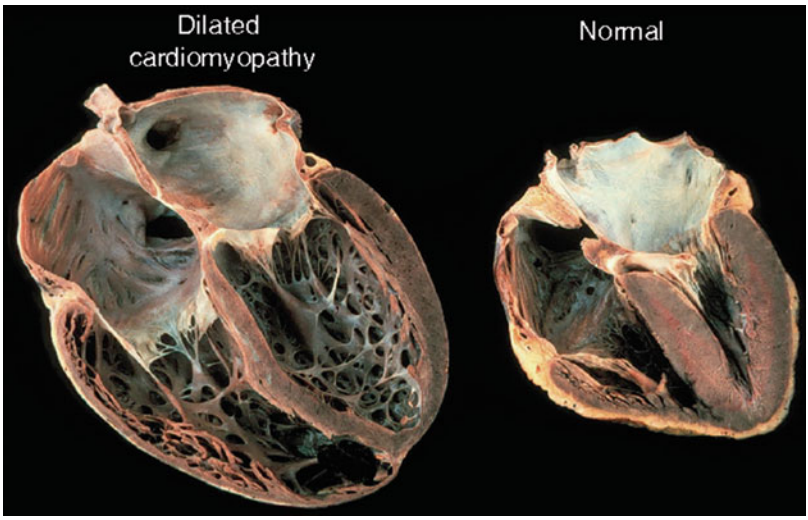

Fig. 62.2 Normal heart on the right compared to dilated cardiomyopathy on the left

biopsy. These investigations help assess the structural and functional abnormalities of the heart, identify potential underlying causes, and rule out other conditions that may mimic dilated cardiomyopathy.

62.3.1 Pathologic Physiology

Dilated cardiomyopathy (DCM) can arise from various specific disorders or can be classified as idiopathic when no specific cause is identified. Some of the known specific disorders associated with DCM include carnitine deficiency, beta-oxidation defects, alcohol or drug-induced damage (such as Adriamycin or cocaine), tachycardia-induced disorders, selenium deficiency, mitochondrial defects, myocarditis, coronary artery anomalies, thyrotoxicosis, storage diseases, amyloidosis, and postpartum cardiomyopathy, among others. It is also believed that in cases where no explanation for the cardiomyopathy is found, a prior unrecognized viral myocarditis might be the underlying cause. New gene mutations associated with DCM continue to be discovered, expanding our understanding of its genetic basis.

The genetic implications of DCM depend on the specific underlying cause. However, for idiopathic dilated cardiomyopathy, approximately 20–30% of individuals with DCM have family members who also exhibit abnormal ventricular function, suggesting a familial component.

In DCM, there is a progressive decline in muscular function, resulting in the thinning of the ventricular wall, ventricular dilation, mitral valve ring dilation, and mitral valve regurgitation. This leads to reduced forward blood flow across the aortic valve. Impaired cardiac function causes increased left atrial volume and pressure,

leading to pulmonary congestion and the clinical manifestation of symptoms such as shortness of breath and susceptibility to respiratory infections. Additionally, the elevated end-diastolic pressure can give rise to ventricular and supraventricular arrhythmias, posing a risk of sudden cardiac death.

62.3.2 Clinical Presentation

In infants and young children, dilated cardiomyopathy (DCM) can manifest with a murmur indicative of mitral valve insufficiency or present with symptoms of congestive heart failure. These symptoms may include failure to thrive, fatigue, excessive sweating, coughing, hepatomegaly (enlarged liver), and weak pulses. The impaired cardiac function and inadequate circulation can result in poor growth and development.

In older patients, the clinical presentation of DCM may include fatigue, shortness of breath, exercise intolerance, syncope (fainting), and/or arrhythmias. These symptoms are indicative of the reduced pumping capacity of the heart and compromised circulation, leading to limited exercise tolerance and an increased risk of arrhythmias.

62.3.3 Physical Examination

In patients with dilated cardiomyopathy (DCM), it is possible for some individuals to have mild or moderate forms of the condition and exhibit a normal physical examination. However, it is more common for DCM patients to have abnormalities during physical examination.

In infants, the physical examination may reveal signs of respiratory distress, such as tachypnea (rapid breathing), intercostal and/or subcostal retractions (visible inward pulling of the chest wall during breathing), tachycardia (elevated heart rate), sweating, and evidence of poor weight gain. The first heart sound is typically normal, while the second heart sound may be increased if there is associated pulmonary hypertension. A holosystolic mid-frequency murmur of mitral regurgitation and a diastolic gallop rhythm at the apex of the heart may be present. Other signs may include prolonged capillary refill time, peripheral cyanosis (bluish discoloration of the extremities), and a prominent chest shape known as "voussure cardiaque."

In older patients, similar auscultatory findings to infants may be present, including murmurs and gallop rhythm. However, retractions are less likely, and there may be the presence of pulmonary rales and crackles (abnormal lung sounds) on auscultation.

62.3.4 Diagnostic Imaging

Echocardiography is an essential diagnostic tool for establishing a diagnosis of dilated cardiomyopathy (DCM). It provides accurate information regarding the condition. Key findings on echocardiography include reduced ejection fraction, increased left ventricular dimensions during diastole and/or systole, and assessment of cardiac output through transaortic blood flow. It is crucial, especially in infants, to confirm the origin of both coronary arteries from the aorta and rule out anomalous origin of the left coronary artery from the pulmonary artery. Pulmonary artery pressure can also be assessed using tricuspid regurgitation.

Laboratory screening involves the measurement of certain markers to evaluate the severity of heart failure. BNP (beta natriuretic peptide) or pro-NT-BNP are commonly used markers in DCM. Other cardiac enzymes such as troponin T or CK-MB may be elevated in cases of inflammatory processes like myocarditis or ischemia.

The ECG is not typically specific to DCM, but it may reveal signs of "infarction" or severe ischemia in children with anomalous origin of the left coronary artery from the pulmonary artery (ALCAPA).

Cardiac catheterization is usually unnecessary for diagnosing DCM in the era of echocardiography. However, it may be essential if coronary artery abnormalities are suspected or to perform endomyocardial biopsies to determine specific treatable forms of DCM, such as eosinophilic myocarditis, and differentiate acute myocarditis.

Magnetic resonance imaging (MRI) can be helpful in the differential diagnosis of myocarditis and provides additional information. It can reveal areas of inflammation, edema, scarring, and other abnormalities using techniques such as late gadolinium enhancement.

62.3.5 Treatment

Treatment options for dilated cardiomyopathy (DCM) vary depending on the underlying cause of the condition. In secondary forms of DCM, addressing the primary problem is crucial. For example, infants with DCM due to anomalous origin of the left coronary artery from the aorta can have good outcomes if the condition is diagnosed early and corrective surgery is performed to reattach the coronary artery to the aorta. Similarly, patients with DCM secondary to carnitine deficiency can benefit from early diagnosis and appropriate treatment with carnitine replacement.

In cases of acute myocarditis, anti-inflammatory treatment such as immunoglobulins may be effective, and patients with tachycardia-induced cardiomyopathy typically show significant improvement once the underlying tachycardia is controlled.

Pharmacologic therapy for myocardial dysfunction has significantly advanced in the past 15 years. The main principles of management include reducing preload and afterload, providing inotropic support, modulating autoregulatory pathways that worsen myocardial energy consumption, and relieving secondary effects like

pulmonary congestion. Patients with depressed myocardial function should receive appropriate doses of ACE inhibitors, beta blockers, spironolactone, and diuretics. The role of digitalis in this context remains a subject of debate. Restrictive atrial communication can be introduced to decompress the left atrium and reduce pulmonary congestion, which has shown excellent clinical effects.

Experimental treatment options for DCM include intracoronary stem cell therapy has not proven beneficial so far. If routine medical therapy for heart failure fails, intensive care management with the use of phosphodiesterase inhibitors, calcineurin inhibitors, and left ventricular assist device support may be necessary. In such cases, listing the patient for cardiac transplantation is appropriate. DCM has become one of the leading causes for cardiac transplantation in childhood, adolescence, and young adulthood.

62.3.6 Outcome

In patients with idiopathic dilated cardiomyopathy (DCM) caused by myocarditis, an old rule of thumb suggests that approximately one-third of patients will experience improvement with normalization of ejection fraction, one-third will have a worsening condition leading to death, and one-third will survive but without a return to normal systolic function. In cases of genetically proven DCM, the disease typically progresses over time, often necessitating referral to a cardiac transplant program.

The survival rate for patients with idiopathic dilated cardiomyopathy varies between 50% and 70% over a five- to ten-year period. Several studies have shown that treatment with afterload-reducing agents, diuretics, beta blockers, and spironolactone can improve symptoms and potentially increase survival rates, although the extent of the benefit may vary among studies.

For patients who undergo cardiac transplantation, the 10-year survival rate is approximately 60% to 80%. It's worth noting that these statistics are general estimations and individual outcomes may vary based on various factors such as the patient's overall health, response to treatment, and access to medical care.

62.4 Restrictive Cardiomyopathy (RCM)

Restrictive cardiomyopathy (RCM) is a relatively rare form of cardiomyopathy characterized by abnormal diastolic function. The ventricles in RCM are stiff, which impairs relaxation and makes it difficult for the atria to fill the ventricles properly. As a result, atrial and end-diastolic pressures become elevated, leading to dilated atria. It is important to differentiate RCM from constrictive pericarditis, as they have distinct origins, treatment options, and prognoses.

RCM encompasses a heterogeneous group of myocardial diseases that can vary depending on the underlying pathogenesis. In adults, amyloidosis is the most common cause of RCM, followed by hemosiderosis and sarcoidosis. In children, the primary cause of RCM is often unknown, but it is frequently associated with

genetically linked cardiomyopathies. Endomyocardial fibrosis is primarily found in sub-Saharan Africa, while secondary RCM can be seen in conditions such as glycogen storage disease and mucopolysaccharidoses.

Clinical presentation in children with RCM typically includes symptoms of pulmonary congestion, shortness of breath, and reduced exercise capacity. Diagnosis is usually made through echocardiography, which reveals small ventricles and dramatically enlarged atria, resembling an "ice cone" appearance. Patients exhibit normal systolic function but impaired diastolic function. Cardiac MRI can also aid in confirming the diagnosis, and catheter investigation may reveal characteristic ventricular end-diastolic pressure curves. Endomyocardial biopsies are an option for further evaluation.

Treatment options for RCM in childhood are limited, with the main focus being on relieving symptoms of pulmonary congestion. Introducing a restrictive atrial communication to decompress the left atrium and reduce pulmonary congestion has shown reasonable clinical effects. Unfortunately, the prognosis for infants and children with restrictive cardiomyopathy is generally poor, and cardiac transplantation is often recommended soon after diagnosis.

62.5 Ventricular Noncompaction Cardiomyopathy (NCC)

For many years, clinicians have observed hearts with a distinctive appearance described as "feathery" or "embryonic." Another term used to describe this appearance is spongy myocardium. This condition is now recognized as left ventricular noncompaction (LVNC), which is believed to result from embryonic arrest during myocardial development. As the left ventricle forms, the myocardium typically undergoes compaction, eliminating deep crevices. In LVNC, deep intertrabecular recesses and excessive trabecularization are present, particularly at the apex of the left ventricle. LVNC is the third most common cardiomyopathy in children, following dilated cardiomyopathy (DCM) and hypertrophic cardiomyopathy (HCM). Several genetic malformations have been associated with LVNC, including Barth syndrome.

The extent of myocardium affected can vary greatly, ranging from localized cases involving the apex to more generalized forms. Consequently, the clinical presentation can vary accordingly. Generally, affected myocardium predisposes individuals to arrhythmias, clot formation, and decreased contractility. Studies have suggested that LVNC is a unique form of cardiomyopathy that can be associated with arrhythmias and sudden death. Severely affected cases may exhibit signs of heart failure and dilated cardiomyopathy. Other patients may present with clot formation and systemic embolism, while some may experience tachyarrhythmias and sudden cardiac death. The diagnosis of LVNC is typically made based on the echocardiographic appearance of the left ventricular myocardium, as well as MRI. However, distinguishing between normal and abnormal myocardium is not always clear-cut. Generally, LVNC is diagnosed when the proportion of trabecularization is more than

twice the thickness of the underlying ventricular wall (>66%) and consolidated myocardium to spongy myocardium is less than 30% in the affected area.

The prognosis for patients with LVNC varies depending on the presentation and extent of myocardium affected. Heart failure tends to progress over time, necessitating anticongestive treatment. Aggressive management of arrhythmias is crucial. In severe cases, cardiac transplantation may be necessary.

62.6 Arrhythmogenic Cardiomyopathy (ACM)

Arrhythmogenic cardiomyopathy (ACM), previously known as arrhythmogenic right ventricular dysplasia (ARVD) or cardiomyopathy (ARVC), is a genetically mediated cardiomyopathy characterized by potentially life-threatening ventricular arrhythmias and fibrofatty infiltration of the right ventricular myocardium, leading to fibrolipomatosis. Although it primarily affects the right ventricle, cases of left ventricular involvement have also been reported, prompting the abandonment of the name ARVC.

ACM has an estimated incidence of 1 in 10,000 in the US population and approximately 40 in 10,000 in Italy. It may account for up to 10% of unexplained sudden deaths in young individuals. ACM causes fibrofatty replacement of the myocardium, resulting in hypokinetic areas in the right ventricular free wall and associated arrhythmias originating from the right ventricle. Causative mutations have been primarily identified in genes that encode desmosomal proteins, including desmoplakin, plakophilin 2, desmoglein 2, desmocollin 2, and plakoglobin. There is some evidence suggesting that inflammation in response to viral infection and immune triggers may contribute to cardiac myocyte damage and necrosis. Additionally, ARVC has been observed in endurance athletes, such as high-performance bicyclists, even in the absence of desmosomal abnormalities. In these cases, excessive stress on the right ventricular wall during high-intensity exercise may be a contributing factor, resembling the pathophysiology seen in patients with tetralogy of Fallot and long-standing pulmonary regurgitation.

ACM is a significant cause of ventricular arrhythmias in children and young adults, predominantly affecting males. Approximately 30–50% of cases have a familial distribution, and sudden cardiac death during exercise may be associated with the condition. Therefore, some clinicians advise against vigorous exercise for patients with ACM, and family members of affected individuals should undergo screening for this condition.

Specific physical examination findings are usually absent, and sudden cardiac death in otherwise healthy family members may prompt consultation. Some patients may exhibit characteristic electrocardiogram (ECG) patterns, such as T-wave inversion in leads V1–3 and right bundle branch block in 90% of cases, as well as epsilon waves in 50% of cases. While echocardiography can sometimes be misleading, magnetic resonance imaging (MRI) and transvenous biopsies are more reliable diagnostic tools. Palpitations may be the initial symptoms, typically appearing in adolescence or early adulthood, with signs of ACM rarely detected in infancy.

The primary goal of therapy is to decrease the risk of sudden cardiac death. Sotalol is currently considered the preferred treatment for ventricular arrhythmias associated with ACM. Catheter ablation may be helpful in managing refractory arrhythmias. As ACM progresses over time, the myocardium weakens and dilates, with the right ventricle usually affected first. Clinical signs of right heart failure manifest earlier, along with arrhythmias. Patients with a history of cardiac arrest or potentially lethal arrhythmias may be treated with an automatic internal cardiac defibrillator (AICD). In severe cases, cardiac transplantation may be necessary.

Human Genetics of Cardiomyopathies

63

Arjan C. Houweling, Ronald H. Lekanne Deprez, and Arthur A. M. Wilde

Abstract

The identification of a disease-causing variant in a patient diagnosed with cardiomyopathy allows for presymptomatic testing in at risk relatives. Carriers of a pathogenic variant can subsequently be screened at intervals by a cardiologist to assess the risk for potentially life-threatening arrhythmias which can be life-saving. In addition, gene-specific recommendations for risk stratification and disease specific pharmacological options for therapy are beginning to emerge. The large variability in disease penetrance, symptoms, and prognosis, and in some families even in cardiomyopathy subtype, makes genetic counseling both of great importance and complicated.

63.1 Introduction

Approximately thirty years ago pathogenic variants in the beta cardiac myosin heavy chain (*MYH7*) gene were the first identified hereditary cause for hypertrophic cardiomyopathy [1]. Advances in genomic sequencing technologies have been enormous in recent years, currently even whole-genome sequencing in a diagnostic setting is feasible [2, 3]. The number of reported gene–disease relationships associated with cardiomyopathies has expanded enormously in recent years.

A. C. Houweling (✉) · R. H. Lekanne Deprez
Department of Clinical Genetics, Amsterdam University Medical Centers, University of Amsterdam, Amsterdam, The Netherlands
e-mail: a.houweling@amsterdamumc.nl

A. A. M. Wilde
Department of Clinical and Experimental Cardiology, Academic Medical Center, Amsterdam, The Netherlands

© The Author(s), under exclusive license to Springer Nature Switzerland AG 2024

S. Rickert-Sperling et al. (eds.), *Congenital Heart Diseases: The Broken Heart*, Advances in Experimental Medicine and Biology 1441,
https://doi.org/10.1007/978-3-031-44087-8_63

However, in many cases evidence supporting the gene–disease causality is very limited, confounding the value of detected variants. In an effort to clinically validate gene–disease relationships the NIH-funded Clinical Genome Resource (ClinGen) developed a framework to define and evaluate the clinical validity of gene–disease pairs for Mendelian disorders [4]. This gene–disease curation considers both human and experimental evidence reported in literature and uses an algorithm to weight the evidence to determine a gene–disease association (definitive, strong, moderate, limited, no evidence, refuted/disputed). The option of sequencing dozens of genes simultaneously not only improves detection of causal pathogenic variants, but also increases the chance of detecting variants of unknown significance (VUS) [5, 6]. Further complicating the translation of genotype to future personalized perspective and risk estimation is the observation that in many cases pathogenic variants in a specific gene are identified in patients with different forms of cardiomyopathy [7]. In addition, within a given family some carriers may be asymptomatic till old age whereas a relative with the exact same pathogenic variant may die in young adulthood due to a fatal arrhythmia. This phenomenon of variable penetrance is likely, at least in part, to be caused by disease modifying genetic factors (constituting a polygenic risk score). Studies aimed at unraveling the polygenic risk scores have begun to emerge and insights from these efforts are likely to have a clinical role in the near future [8]. However, as these modifiers remain to be identified in the field of cardiogenetics, everyone carrying a pathogenic variant is currently given the same recommendations.

The diagnosis of idiopathic cardiomyopathy is established in patients with a myocardial disorder in which the heart muscle is structurally and functionally abnormal in the absence of other (i.e., environmental or external) causal factors that can be detected in the patient's history (e.g., alcohol abuse in dilated cardiomyopathy (DCM)), physical examination (e.g., myotonia from myotonic dystrophy in DCM), cardiac investigation (major coronary artery disease in DCM) or other means [9]. This diagnosis by exclusion can be challenging, especially in DCM. When the terms idiopathic hypertrophic cardiomyopathy (HCM), DCM, arrhythmogenic (right ventricular) cardiomyopathy (ACM or ARVC), and noncompaction cardiomyopathy (NCCM) are used, it is meant that no clinical causal factors have been identified. This does not exclude the possibility that the cardiomyopathy is hereditary. Restrictive cardiomyopathy is not addressed in this chapter since its genetic basis (with the exception of amyloidosis) remains unclear.

63.2 Inheritance Pattern

Cardiomyopathies in general are thought to be monogenetic diseases. This means that a disease-causing (or actionable or pathogenic) variant in a single gene is the main causal factor in the development of the disease. In most cardiomyopathies, the inheritance pattern is autosomal dominant. Clues in a pedigree for autosomal dominant transmission are affected males and females in multiple generations and male-to-male transmission. X-linked and recessive transmission occur in rare

cardiomyopathy cases, but in those cases/families extra-cardiac signs are often present. An example of recessive inheritance is Naxos disease, named after the island of Naxos where the first cases were identified, which is arrhythmogenic right ventricular cardiomyopathy (ARVC) with woolly hair and palmoplantar hyperkeratosis (MIM# 601214). Fabry disease (MIM# 301500), a metabolic disease which causes HCM as well as acroparesthesia and renal failure, is inherited as an X-linked disorder. These so-called phenocopies are not extensively addressed in this chapter, but an overview can be found in Table 63.1.

Autosomal dominant inheritance is sometimes difficult to recognize from the pedigree. This is due to incomplete and age-related disease penetrance—especially in females—and to the large intra- and interfamilial variability of disease expression. Incomplete disease penetrance means that not all people with the causal variant develop a cardiomyopathy during life. In families with a cardiomyopathy penetrance increases with age but may not be complete [17, 18]. The laymen can interpret this phenomenon as the disease "is skipping a generation." The large variability means that not all people with the same cardiomyopathy have the same disease course or develop the same symptoms.

In autosomal dominant inheritance, one gene variant causes the disease. However, we also encounter patients with two or more causal variants. These variants can be located in the same gene on different alleles (compound heterozygous or homozygous) or in different genes (digenic). In HCM, the presence of two actionable variants is relatively frequent (about 3–5%). The presence of more than one pathogenic variant often is associated with a more severe phenotype: younger age of onset, more pronounced abnormalities on cardiac imaging (e.g., severe hypertrophy in HCM), and a higher risk of life-threatening arrhythmias [19–21].

63.3 Involved Genes

63.3.1 Hypertrophic Cardiomyopathy

Causal variants in HCM are almost exclusively located in genes encoding sarcomeric proteins. The sarcomere represents the basal contractile unit of striated muscles, such as cardiac muscle, and is made up of thick and thin filaments. During contraction, the thin filaments slide past the thick filaments, shortening the sarcomere. In about up to 60% of patients a disease-causing (pathogenic) variant can be detected [22]. Whenever a genetic cause for HCM is found, ~80% of disease-causing variants are identified in the *MYBPC3* and *MYH7* genes (Table 63.1). Many countries or populations have specific so called founder variants [23, 24]. These variants derive from a common ancestor and often comprise a large part of the detected variants in that country or population.

No clear genotype–phenotype correlations are present in HCM. Some correlations have been reported in large cohorts; however they cannot currently be used for prognosis or therapeutic options in the individual patient [11, 25]. The clinical validity of putative HCM associated genes was recently evaluated by the

Table 63.1 Genes for cardiomyopathies and cardiomyopathy phenocopies

Disorder/Gene	Frequency in phenotype (%)/ phenotype	Gene–disease curation[a]
HCM	**Frequency in phenotype (%)**	**Gene–disease curation[a]** [10]
MYBPC3	30–40%	Definitive
MYH7	30–50%	Definitive
TPM1, TNNT2, TNNI3, MYL2, MYL3, ACTC1	<5%	Definitive
CSRP3, JPH2, TNNC1	NA	Moderate
HCM phenocopies (mixed cardiac or syndromic)	**Phenotype**	**Gene–disease curation[a]** [11]
ABCC9	Cantu syndrome	Definitive
BAG3	Myofibrillar myopathy	Definitive
CACNA1C	Timothy syndrome	Definitive
CAV3	Caveolinopathy	Definitive
CRYAB	Alpha-B crystallinopathy	Definitive
DES	Desminopathy	Definitive
FHL1	Emery–Dreifuss MD	Definitive
FLNC	Myofibrillar myopathy	Definitive
PRKAG2	LVH/pre-excitation (Wolf–Parkinson–White syndrome)/ conduction disease	Definitive
PLN	HCM, DCM, ARVC	Definitive
LAMP2	Danon disease	Definitive
FXN	Friedrich ataxia	Definitive
GLA	Fabry disease	Definitive
PTPN11	Noonan, Leopard, CFC syndrome	Definitive
RAF1	Noonan, Leopard	Definitive
RIT1	Noonan syndrome	Definitive
TTR	Amyloidosis	Definitive
GAA	Pompe disease	Definitive
MYO6	Bilateral hearing loss	Definitive
SLC25A4	Mitochondrial disease	Definitive
ALPK3	Infant-onset	Strong
COX15	Leigh syndrome	Strong
ACTN2	LVH, LVNC, DCM, VF	Moderate
LDB3	Myofibrillar myopathy	Moderate
KRAS2	Noonan, Leopard, CFC syndrome	?
SOS1	Noonan	?
BRAF1	CFC syndrome	?

(continued)

Table 63.1 (continued)

Disorder/Gene	Frequency in phenotype (%)/ phenotype	Gene–disease curation[a]
MAP2K1	CFC syndrome	?
MAP2K2	CFC syndrome	?
HRAS	Costello syndrome	?
GDE	Glycogen storage disorder III	?
Mitochondrial (*MT-TI*)	LVH "plus" syndrome	?
DCM	**Frequency in phenotype (%)** [12, 13]	**Gene–disease curation[a]** [14]
TTN	14–25%	Definitive
MYH7	3%	Definitive
LMNA	5%	Definitive
FLNC	NA	Definitive
SCN5A	2–3%	Definitive
TNNT2	2%	Definitive
TNNC1	<1%	Definitive
DES	<1%	Definitive
PLN	2%	Definitive
RBM20	2%	Definitive
BAG3	NA	Definitive
DSP	NA	Strong
TPM1	<1%	Moderate
TNNI3	1%	Moderate
ACTC1	<1%	Moderate
ACTN2	1%	Moderate
NEXN	NA	Moderate
VCL	1%	Moderate
DCM phenocopies	**Phenotype**	**Gene–disease curation[a]**
LMNA	Emery–Dreifuss muscular dystrophy, Limb–Girdle muscular dystrophy type 1B	?
DMD	Duchenne/Becker muscular dystrophy	?
DES	Desminopathy	?
LDB3	Myofibrillar myopathy	?
TAZ	Barth syndrome	?
SGCD	Limb–Girdle muscular dystrophy type 2F	?
TCAP	Limb–Girdle muscular dystrophy type 2G	?
FKRP		?

(continued)

Table 63.1 (continued)

Disorder/Gene	Frequency in phenotype (%)/ phenotype	Gene–disease curation[a]
	Limb–Girdle muscular dystrophy type 2I	
TTN	Limb–Girdle muscular dystrophy type 2 J,	?
	Early-onset myopathy with fatal cardiomyopathy	
FKTN	Muscular dystrophy	?
BAG3	Progressive myofibrillar myopathy	?
HFE	Hereditary hemochromatosis	?
MYH7	Laing distal myopathy	?
DSP	Carvajal syndrome	?
DOLK	Congenital disorder of glycosylation	?
Mitochondrial	Kearns–Sayre syndrome	?
ARVC	**Frequency in phenotype (%)** [15]	**Gene–disease curation[a]** [16]
PKP2	20–46%	Definitive
DSG2	3–20%	Definitive
DSP	3–20%	Definitive
DSC2	1–15%	Definitive
JUP	<1% (higher in Naxos)	Definitive
TMEM43	<2% (higher in Newfoundland)	Definitive
PLN	<4% (higher in Netherlands)	Moderate
DES	<3%	Moderate
FLNC	<3%	?
NCCM	**Frequency in phenotype (%)**	**Gene–disease curation**
MYH7	21%	?
ACTC1, TNNT2, TNNI3, TPM1, PLN, DSP, LMNA, SCN5A, DTNA, MIB1, PRDM16, MYBPC3	NA	?
NCCM phenocopies	**Phenotype**	**Gene–disease curation**
TAZ	Barth syndrome	?
LDB3	Myofibrillar myopathy	?

[a]ClinGen website https://search.clinicalgenome.org/kb/gene-validity
? not curated by ClinGen for the disease–gene association
HCM, hypertrophic cardiomyopathy; *DCM*, dilated cardiomyopathy; *ARVC*, arrhythmogenic right ventricular cardiomyopathy; *NCCM*, noncompaction cardiomyopathy; *LVH*, left ventricular hypertrophy; *CFC*, Cardiofaciocutaneous; *NA*, not ascertained or <1%

ClinGen cardiovascular working group. Fifty-seven genes were selected based on their frequent inclusion in HCM panels and prior reports. Of these, only the "sarcomeric" genes *MYBPC3, MYH7, TNNT2, TNNI3, TPM1, ACTC1, MYL2,* and *MYL3* were categorized as definitive. The genes *CSRP3*, *TNNC1,* and *JPH2* were categorized as having moderate evidence [10]. These observations indicate that caution is important when interpreting variants in other putative HCM genes. Periodic reassessment of variants of unknown significance and of variants in genes with limited evidence supporting disease association over time is warranted.

63.3.2 Dilated Cardiomyopathy

In contrast to HCM, causal variants in DCM patients are found in a lower percentage of cases and are often unique for the family. The variant detection rate has however increased enormously by the relatively recent discovery of the Titin gene (*TTN*) encoding the largest protein in the human genome. In up to 25% of familial DCM cases (likely) pathogenic variants in *TTN* are reported [26]. Titin is highly expressed in the heart, where it regulates sarcomere contraction and signaling. Despite the fact that many variants in this gene are found, it is uncertain whether or not variants in *TTN* are pathogenic. This is partly because *TTN* missense variants are very common with 23 on average per individual in the Exome Variant Server database and because even truncation variants are frequently also found in healthy control populations (in up to 3% of individuals) [26]. In addition, loss of function variants in the filamin C gene (*FLNC*) were recently identified as an important cause of DCM [27, 28]. Other genes responsible for DCM encode proteins of the sarcomere, the nuclear envelope, the cytoskeleton, ion channels, desmosomes, and proteins involved in calcium homeostasis. In a recent case-control study in a cohort of 2538 patients, protein coding regions of 56 commonly tested genes were compared to both 912 healthy controls and a reference population of 60,706 individuals. Rare variants in 12 genes (*TTN, DSP, MYH7, LMNA, BAG3, TNNT2, TNNC1, PLN, ACTC1, NEXN, TPM1,* and *VCL*) were significantly enriched in DCM cases and potentially explained 17% of the cases [29]. The *FLNC* and *RBM20* genes were not evaluated in this study. Furthermore, a DCM causing effect by a loss of function mechanism has been identified for the *TTN*, *FLNC, SCN5A, BAG3, DSP, PLN, VCL,* and *LMNA* genes [30]. In addition, variants in a hot spot region of exon 9 of the *RBM20* gene play a key role in DCM [31]. Recently the ClinGen cardiovascular working group completed the literature curation of DCM-associated genes (see ClinGen website; https://clinicalgenome.org/affiliation/40035/) [14]. Fifty-one genes were curated. Of these, 19 genes have substantial evidence supporting a role in monogenic DCM, including 11 definitive (*BAG3, DES, FLNC, LMNA, MYH7, PLN, RBM20, SCN5A, TNNC1, TNNT2, TTN*), 1 strong (*DSP*), and 7 moderate (*ACTC1, ACTN2, JPH2, NEXN, TNNI3, TPM1, VCL*) evidence classification [14].

Genotype–phenotype correlations are present in DCM. DCM patients with an actionable variant in the *LMNA* (lamin A/C) gene almost all have conduction disease and are at higher risk of developing arrhythmic events [32, 33]. In addition, (likely)

pathogenic variants in *PLN, SCN5A, RBM20,* and *FLNC* have been associated with a higher risk of arrhythmias and/or severe heart failure [34, 35].

63.3.3 Arrhythmogenic Cardiomyopathy

The ClinGen cardiovascular working group recently completed the literature curation of ACM-associated genes (see ClinGen website https://search.clinicalgenome.org/kb/gene-validity). The *FLNC* gene was not evaluated. Out of 26 genes only eight genes obtained substantial evidence supporting a role in ACM [16]. Six genes had a strong evidence and were classified as definitive (*DSC2, DSG2, DSP, JUP, PKP2,* and *TMEM43)* the other two genes had moderate evidence (*DES* and *PLN*). Five of these genes encode for components of the cardiac desmosome: plakoglobin (*JUP*), desmoplakin (*DSP*), plakophilin-2 (*PKP2*), desmoglein (*DSG2*), and desmocollin-2 (*DSC2*); and three encode nondesmosomal proteins: transmembrane protein 43 (*TMEM43*), Desmin (DES), and *PLN*. Recently, truncating variants in *FLNC* were reported to cause ACM. Together, these nine genes have been reported to be responsible for 60–65% of all ACM cases [36–38]. The most frequently mutated gene is *PKP2*, with a detection rate up to of 46% [15, 39].

Genotype–phenotype correlations have been suggested in ACM. The presence of multiple causal variants has been associated with a more severe phenotype [40]. In addition, a founder mutation in *TMEM43* has been associated with a malignant phenotype in males [41]. Furthermore, pathogenic variants in *DSP* have been associated with a left dominant arrhythmogenic cardiomyopathy phenotype [42, 43].

63.3.4 Noncompaction Cardiomyopathy

NCCM is genetically heterogeneous. Most NCCM associated variants can be found in genes that encode for sarcomeric proteins, with *MYH7, MYBPC3,* and *TTN* as the most frequently involved genes. Little is known about specific genotype–phenotype correlations [44].

The exact causal mechanism is also unknown. It has been suggested to be the result of a block in embryonic trabecular development, but recent studies have identified pathogenic variant carriers with a normal heart who developed the noncompacted myocardium later in life [44].

63.4 Overlapping Phenotypes

Although in clinical evaluation the type of cardiomyopathy seems essential for the cardiologist and patient, in reality clear-cut specific cardiomyopathies are not always seen. In the last twenty years genetic testing has revealed that disease variability is large, and, also, that the same genes and even the same variants can give rise to different cardiomyopathies. Almost all combinations of cardiomyopathies have been

reported in families, but these combinations can also be present in a single patient at the same time or in consecutive order. Carriers of the Dutch *PLN* founder variant c.40_42del can have a clear isolated ARVC phenotype and may develop a clear DCM phenotype later in life [35] and HCM may progress to DCM [45]. In all types of cardiomyopathies treatment and prognosis are mainly determined by the results of cardiac evaluations and not by the results of the genetic test. Therefore, it is essential to be aware of the possibility of overlapping phenotypes in a patient or family, since it is unlikely that a patient with HCM with features of NCCM has two different diseases. In two recent genome wide association studies several genome-wide-significant susceptibility loci were identified for HCM and DCM. Several of these loci had opposing effects in HCM and DCM. These observations indicate that a polygenic risk score may account, at least in part, for the variable penetrance and overlapping phenotypes observed in cardiomyopathy [8, 46].

63.5 Genetic Testing and Counseling

Based on their association with malignant ventricular arrhythmias, the identification of a pathogenic variant in specific genes (*LMNA*, *FLNC, PLN*) may be considered in decisions on ICD implantation [47]. However, since in most cases no clear genotype–phenotype correlations are present, for the majority of patients the main benefit of finding the causal variant is that it provides a better option to detect relatives at risk for the cardiomyopathy, and associated life-threatening arrhythmias. The incomplete and age dependent disease penetrance in cardiomyopathies makes it difficult to identify the relatives at risk, and in case of normal echocardiographic findings the relative needs life-long follow-up. Finding the causal variant in a patient means that one can perform predictive DNA testing for healthy relatives. First-degree relatives are at 50% risk of having the causal variant. Carriers of the pathogenic variant are at risk of developing disease and are advised to undergo regular cardiac evaluations. Noncarriers are not at risk of developing the cardiomyopathy, do not need cardiac evaluations and can be discharged from (further) cardiological follow-up. In addition, the variant cannot be transmitted to their offspring, so they also are no longer at risk.

The Working Group on Myocardial and Pericardial Diseases of the European Society of Cardiology has given advice for the screening of asymptomatic relatives of a cardiomyopathy patient based on the presence or absence of a disease-causing variant in the family. This advice is summarized in Table 63.2. For most cardiomyopathies, they also advise discontinuing clinical screening for at risk relatives between age 50 and 60 years if no symptoms are present. Recent studies have shown, however, that disease still can become manifest after this age. For example, in HCM increased mortality is also present after age 50, which suggests that continued clinical screening is warranted in asymptomatic relatives [18, 48].

Table 63.2 General recommendations for cardiac evaluations in asymptomatic relatives of cardiomyopathy patients without clinical signs of disease (adapted from Charron et al.) [9]

	HCM[a]	DCM[a]	ARVC[a]	NCCM[a]
Asymptomatic relatives from families without a known causal variant				
Cardiac evaluation	ECG, echocardiography	ECG, echocardiography (and Holter-ECG if conduction disease in relative)	ECG, echocardiography, Holter-ECG, signal averaged ECG	ECG, echocardiography
Start of cardiac evaluation[a]	10–12 years	10–12 years	10–12 years	New-born
Frequency of cardiac evaluation[b]	10–20 years: Every 1–2 years >20 years: Every 2–5 years	10–20 years: Every 1–2 years >20 years: Every 2–5 years	10–20 years: Every 1–2 years >20 years: Every 2–5 years	<20 years: Every 1–3 years >20 years: Every 2–5 years
Variant carriers				
Cardiac evaluation	Initially ECG, echocardiography, exercise test, Holter-ECG; additional evaluations ECG and echocardiography	Initially ECG, echocardiography, exercise test, Holter-ECG; additional evaluations ECG and echocardiography (and Holter-ECG if conduction disease in relative)	Initially ECG, echocardiography, exercise test, Holter-ECG, signal averaged ECG; additional evaluations ECG and echocardiography, signal averaged ECG	Initially ECG, echocardiography, exercise test, Holter-ECG; additional evaluations ECG and echocardiography
Start of cardiac evaluation	10–12 years	10–12 years	10–12 years	New-born
Frequency of cardiac evaluation	10–20 years: Every year >20 years: Every 1–3 years	10–20 years: Every year >20 years: Every 1–3 years	10–20 years: Every year >20 years: Every 1–3 years	<20 years: Every year >20 years: Every 1–3 years

[a]Phenocopies are not covered here

[b]Screening at younger age must be considered if affected children are present in the family

63.6 Genetics of Cardiomyopathies in the Future

In the past years, efforts have successfully been directed at identifying novel disease-associated genes using NGS technologies including whole-exome sequencing. However, in many patients diagnosed with a cardiomyopathy, the genetic cause can still not be detected [49]. This may be due to the fact that many disease genes are still unknown, or that we are not able to interpret variants properly (e.g., variants that cause problems with RNA splicing or regulation of expression), but it can also be due to the fact that not all cardiomyopathies are monogenetic [8, 46]. In research we no longer frequently identify new causal genes that are disease causing in more than a few percent of the cardiomyopathy population—with the relatively recent exception of *TTN*. However, in addition to promising variants, more often one finds variants of unknown significance (VUS). These are genetic variants of which it is not known or not certain whether they can cause a cardiomyopathy or not, or add to disease expression as a modifier. Frequently more than one VUS in a single patient is identified and with expansion of NGS techniques to the entire exome or genome VUS are also found in genes previously not known to be associated with cardiomyopathies. Recent studies have shown that a number of variants previously annotated in literature and in databases as disease causing are now frequently found in healthy controls, which makes their causality extremely doubtful. These observations underline the importance of validating and updating knowledge on putative gene–disease relationships which will be a challenge for the near future. Personalized risk assessment based on knowledge of the polygenic risk score and environmental factors is also expected to play a role in future clinical care [8, 46, 50]. Promising novel pharmacological treatment strategies, based on the unraveling of the underlying mechanisms of disease, for patients with cardiomyopathies have recently began to emerge [51–53]. A good example of this are the encouraging results of a phase 3 trial for the treatment of symptomatic obstructive HCM with Mavacamten, a specific inhibitor of cardiac myosin ATP [54].

63.7 Conclusion

Many cardiomyopathy-associated genes have been identified in recent years allowing for family screening and eventual prevention of sudden cardiac death. NGS techniques have resulted in an increased yield of genetic diagnosis, but also add a new layer of complexity to genetic counseling due to the frequent detection of VUS. Validation of gene–disease relationships, reclassification of VUS, unraveling the polygenic risk factors allowing for personalized risk assessment, and the development of precision medicine based on genotype will be among the future challenges in the field of cardiomyopathies.

References

1. Geisterfer-Lowrance AA, et al. A molecular basis for familial hypertrophic cardiomyopathy: a beta cardiac myosin heavy chain gene missense mutation. Cell. 1990;62:999–1006.
2. Thaventhiran JED, et al. Whole-genome sequencing of a sporadic primary immunodeficiency cohort. Nature. 2020;583:90–5.
3. Turro E, et al. Whole-genome sequencing of patients with rare diseases in a national health system. Nature. 2020;583:96–102.
4. Strande NT, et al. Evaluating the clinical validity of gene-disease associations: an evidence-based framework developed by the clinical genome resource. Am J Hum Genet. 2017;100:895–906.
5. Christiaans I, Mook ORF, Alders M, Bikker H, Lekanne Dit Deprez RH. Large next-generation sequencing gene panels in genetic heart disease: challenges in clinical practice. Neth Heart J. 2019;27:299–303.
6. van Lint FHM, et al. Large next-generation sequencing gene panels in genetic heart disease: yield of pathogenic variants and variants of unknown significance. Neth Heart J. 2019;27:304–9.
7. van Spaendonck-Zwarts KY, van den Berg MP, van Tintelen JP. DNA analysis in inherited cardiomyopathies: current status and clinical relevance. Pacing Clin Electrophysiol. 2008;31 (Suppl 1):S46–9.
8. Harper AR, et al. Common genetic variants and modifiable risk factors underpin hypertrophic cardiomyopathy susceptibility and expressivity. Nat Genet. 2021;53:135–42.
9. Charron P, et al. Genetic counselling and testing in cardiomyopathies: a position statement of the European Society of Cardiology Working Group on Myocardial and Pericardial Diseases. Eur Heart J. 2010;31:2715–26.
10. Ingles J, et al. Evaluating the clinical validity of hypertrophic cardiomyopathy genes. Circ Genom Precis Med. 2019;12:e002460.
11. Miller RJH, et al. Defining genotype-phenotype relationships in patients with hypertrophic cardiomyopathy using cardiovascular magnetic resonance imaging. PLoS One. 2019;14: e0217612.
12. Hershberger RE, Hedges DJ, Morales A. Dilated cardiomyopathy: the complexity of a diverse genetic architecture. Nat Rev Cardiol. 2013;10:531–47.
13. Kayvanpour E, et al. Genotype-phenotype associations in dilated cardiomyopathy: meta-analysis on more than 8000 individuals. Clin Res Cardiol. 2017;106:127–39.
14. Jordan E, et al. An evidence-based assessment of genes in dilated cardiomyopathy. Circulation. 2021;144:7.
15. James CA, Syrris P, van Tintelen JP, Calkins H. The role of genetics in cardiovascular disease: arrhythmogenic cardiomyopathy. Eur Heart J. 2020;41:1393–400.
16. James CA, et al. An international evidence based reappraisal of genes associated with arrhythmogenic right ventricular cardiomyopathy (ARVC) using the ClinGen framework. Circ Genom Precis Med. 2021;14:e003273.
17. Groeneweg JA, et al. Clinical presentation, long-term follow-up, and outcomes of 1001 arrhythmogenic right ventricular dysplasia/cardiomyopathy patients and family members. Circ Cardiovasc Genet. 2015;8:437–46.
18. Lorenzini M, et al. Penetrance of hypertrophic cardiomyopathy in sarcomere protein mutation carriers. J Am Coll Cardiol. 2020;76:550–9.
19. Alsters S, et al. Fatal neonatal hypertrophic cardiomyopathy caused by compound heterozygous truncating MYBPC3 mutation. Neth Heart J. 2019;27:282–3.
20. Richard P, et al. Double heterozygosity for mutations in the beta-myosin heavy chain and in the cardiac myosin binding protein C genes in a family with hypertrophic cardiomyopathy. J Med Genet. 1999;36:542–5.
21. Lekanne Deprez RH, et al. Two cases of severe neonatal hypertrophic cardiomyopathy caused by compound heterozygous mutations in the MYBPC3 gene. J Med Genet. 2006;43:829–32.

22. Burke MA, Cook SA, Seidman JG, Seidman CE. Clinical and mechanistic insights into the genetics of cardiomyopathy. J Am Coll Cardiol. 2016;68:2871–86.
23. Adalsteinsdottir B, et al. Hypertrophic cardiomyopathy in myosin-binding protein C (MYBPC3) Icelandic founder mutation carriers. Open Heart. 2020;7:e001220.
24. Alders M, et al. The 2373insG mutation in the MYBPC3 gene is a founder mutation, which accounts for nearly one-fourth of the HCM cases in the Netherlands. Eur Heart J. 2003;24: 1848–53.
25. Lopes LR, et al. Novel genotype-phenotype associations demonstrated by high-throughput sequencing in patients with hypertrophic cardiomyopathy. Heart. 2015;101:294–301.
26. Schafer S, et al. Titin-truncating variants affect heart function in disease cohorts and the general population. Nat Genet. 2017;49:46–53.
27. Ader F, et al. FLNC pathogenic variants in patients with cardiomyopathies: prevalence and genotype-phenotype correlations. Clin Genet. 2019;96:317–29.
28. Ortiz-Genga MF, et al. Truncating FLNC mutations are associated with high-risk dilated and arrhythmogenic cardiomyopathies. J Am Coll Cardiol. 2016;68:2440–51.
29. Mazzarotto F, et al. Reevaluating the genetic contribution of monogenic dilated cardiomyopathy. Circulation. 2020;141:387–98.
30. Jordan E, Hershberger RE. Considering complexity in the genetic evaluation of dilated cardiomyopathy. Heart. 2021;107:106–12.
31. Refaat MM, et al. Genetic variation in the alternative splicing regulator RBM20 is associated with dilated cardiomyopathy. Heart Rhythm. 2012;9:390–6.
32. Akhtar M, Elliott PM. Risk stratification for sudden cardiac death in non-ischaemic dilated cardiomyopathy. Curr Cardiol Rep. 2019;21:155.
33. van Rijsingen IA, et al. Risk factors for malignant ventricular arrhythmias in Lamin a/c mutation carriers a European cohort study. J Am Coll Cardiol. 2012;59:493–500.
34. Peters S, Kumar S, Elliott P, Kalman JM, Fatkin D. Arrhythmic genotypes in familial dilated cardiomyopathy: implications for genetic testing and clinical management. Heart Lung Circ. 2019;28:31–8.
35. van der Zwaag PA, et al. Phospholamban R14del mutation in patients diagnosed with dilated cardiomyopathy or arrhythmogenic right ventricular cardiomyopathy: evidence supporting the concept of arrhythmogenic cardiomyopathy. Eur J Heart Fail. 2012;14:1199–207.
36. Brun F, et al. FLNC truncations cause arrhythmogenic right ventricular cardiomyopathy. J Med Genet. 2020;57:254–7.
37. Hall CL, et al. Filamin C variants are associated with a distinctive clinical and immunohistochemical arrhythmogenic cardiomyopathy phenotype. Int J Cardiol. 2020;307:101–8.
38. Hall CL, et al. RNA sequencing-based transcriptome profiling of cardiac tissue implicates novel putative disease mechanisms in FLNC-associated arrhythmogenic cardiomyopathy. Int J Cardiol. 2020;302:124–30.
39. van Tintelen JP, et al. Plakophilin-2 mutations are the major determinant of familial arrhythmogenic right ventricular dysplasia/cardiomyopathy. Circulation. 2006;113:1650–8.
40. Rigato I, et al. Compound and digenic heterozygosity predicts lifetime arrhythmic outcome and sudden cardiac death in desmosomal gene-related arrhythmogenic right ventricular cardiomyopathy. Circ Cardiovasc Genet. 2013;6:533–42.
41. Hodgkinson KA, et al. The natural history of a genetic subtype of arrhythmogenic right ventricular cardiomyopathy caused by a p.S358L mutation in TMEM43. Clin Genet. 2013;83:321–31.
42. Augusto JB, et al. Dilated cardiomyopathy and arrhythmogenic left ventricular cardiomyopathy: a comprehensive genotype-imaging phenotype study. Eur Heart J Cardiovasc Imaging. 2020;21:326–36.
43. Bhonsale A, et al. Impact of genotype on clinical course in arrhythmogenic right ventricular dysplasia/cardiomyopathy-associated mutation carriers. Eur Heart J. 2015;36:847–55.
44. van Waning JI, et al. Genetics, clinical features, and long-term outcome of noncompaction cardiomyopathy. J Am Coll Cardiol. 2018;71:711–22.

45. Cregler LL. Progression from hypertrophic cardiomyopathy to dilated cardiomyopathy. J Natl Med Assoc. 1989;81(820):824–6.
46. Tadros R, et al. Shared genetic pathways contribute to risk of hypertrophic and dilated cardiomyopathies with opposite directions of effect. Nat Genet. 2021;53:128–34.
47. Towbin JA, et al. 2019 HRS expert consensus statement on evaluation, risk stratification, and management of arrhythmogenic cardiomyopathy. Heart Rhythm. 2019;16:e301–72.
48. Christiaans I, et al. Manifest disease, risk factors for sudden cardiac death, and cardiac events in a large nationwide cohort of predictively tested hypertrophic cardiomyopathy mutation carriers: determining the best cardiological screening strategy. Eur Heart J. 2011;32:1161–70.
49. Almomani R, et al. Biallelic truncating mutations in ALPK3 cause severe pediatric cardiomyopathy. J Am Coll Cardiol. 2016;67:515–25.
50. Fatkin D, Huttner IG, Kovacic JC, Seidman JG, Seidman CE. Precision medicine in the Management of Dilated Cardiomyopathy: JACC state-of-the-art review. J Am Coll Cardiol. 2019;74:2921–38.
51. Green EM, et al. A small-molecule inhibitor of sarcomere contractility suppresses hypertrophic cardiomyopathy in mice. Science. 2016;351:617–21.
52. Stern JA, et al. A small molecule inhibitor of sarcomere contractility acutely relieves left ventricular outflow tract obstruction in feline hypertrophic cardiomyopathy. PLoS One. 2016;11:e0168407.
53. Yotti R, Seidman CE, Seidman JG. Advances in the genetic basis and pathogenesis of sarcomere cardiomyopathies. Annu Rev Genomics Hum Genet. 2019;20:129–53.
54. Olivotto I, et al. Mavacamten for treatment of symptomatic obstructive hypertrophic cardiomyopathy (EXPLORER-HCM): a randomised, double-blind, placebo-controlled, phase 3 trial. Lancet. 2020;396:759–69.

Molecular Pathways and Animal Models of Cardiomyopathies

64

Buyan-Ochir Orgil and Enkhsaikhan Purevjav

Abstract

Cardiomyopathies are a heterogeneous group of disorders of the heart muscle that ultimately result in congestive heart failure. Rapid progress in genetics, molecular and cellular biology with breakthrough innovative genetic-engineering techniques, such as next-generation sequencing and multiomics platforms, stem cell reprogramming, as well as novel groundbreaking gene-editing systems over the past 25 years has greatly improved the understanding of pathogenic signaling pathways in inherited cardiomyopathies. This chapter will focus on intracellular and intercellular molecular signaling pathways that are activated by a genetic insult in cardiomyocytes to maintain tissue and organ level regulation and resultant cardiac remodeling in certain forms of cardiomyopathies. In addition, animal models of different clinical forms of human cardiomyopathies with their summaries of triggered key molecules and signaling pathways will be described.

Keywords

Inherited cardiomyopathy · Mutation · Pathogenic variant · Common final pathway · Cardiomyocyte · Cardiac remodeling · Failing heart · Cardiac compensatory mechanisms · Fetal gene program · Cardiomyopathy animal model

B.-O. Orgil · E. Purevjav (✉)
Department of Pediatrics, The Heart Institute, Division of Cardiology, University of Tennessee Health Science Center, Memphis, TN, USA
e-mail: epurevja@uthsc.edu

© The Author(s), under exclusive license to Springer Nature Switzerland AG 2024

S. Rickert-Sperling et al. (eds.), *Congenital Heart Diseases: The Broken Heart*,
Advances in Experimental Medicine and Biology 1441,
https://doi.org/10.1007/978-3-031-44087-8_64

64.1 From Genetic Abnormality to Cellular Pathology and Cardiomyopathy: "Final Common Pathways"

It is widely accepted that inherited cardiomyopathies are a group of heterogeneous diseases of the heart muscle resulting from genetic alterations in cardiac myocytes, the chief contractile cell type in the heart [1]. The "Final common pathway" hypothesis elucidating the mechanisms of inherited cardiomyopathies, first described by Towbin et al. in the late 1990s, suggests that genes encoding proteins with similar functions and/or location or involved in the same pathway are responsible for a consistent cardiomyopathy phenotype with distinctive morpho/histological cardiac remodeling [2]. Further, disruption of particular protein pathways may intersect with other intracellular and intercellular pathways, resulting in an overlapping phenotype (Fig. 64.1). Apoptosis, necrosis, autophagy, gene expression changes, and metabolic and arrhythmogenic disturbances—which may present as the sole feature or as overlapping signs—result in definitive forms of cardiac remodeling including fibrosis, cardiomyocyte hypertrophy, and atrophy. Typically, molecular signaling activates associated compensatory responses and cooperates with genetic and/or environmental modifiers, stress or toxicity related that, in turn, may or may not influence the final cardiomyopathy phenotype.

According to the 2006 American Heart Association (AHA) classification and guideline statement, five types of inherited cardiomyopathies are distinguished based on morphological and clinical features: dilated cardiomyopathy (DCM), hypertrophic cardiomyopathy (HCM), restrictive cardiomyopathy (RCM), arrhythmogenic right ventricular cardiomyopathies (ARVC) or arrhythmogenic cardiomyopathies

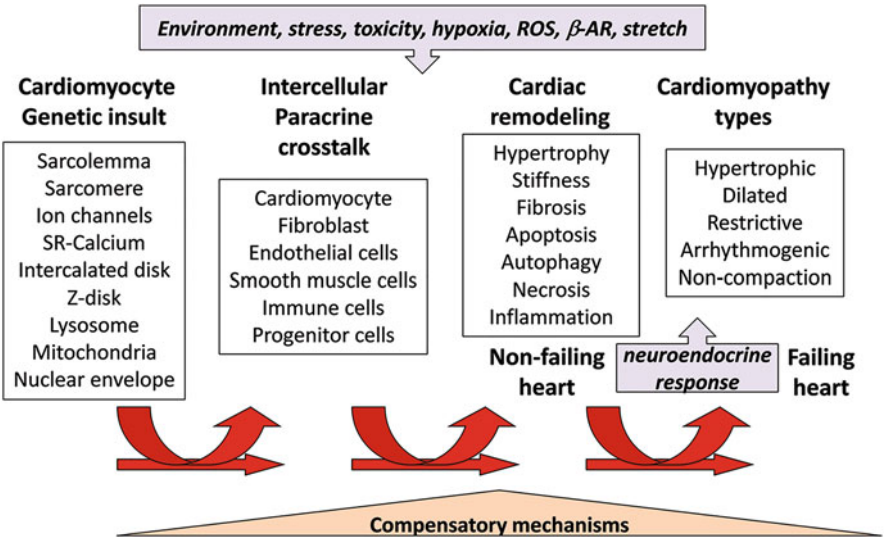

Fig. 64.1 "Final common pathway" hypothesis of the development of cardiomyopathy supplemented by intracellular and intercellular signaling

(ACM), and left ventricular noncompaction cardiomyopathy (LVNC) [3]. Due to the phenotypic heterogeneity presented in patients, LVNC has not been classified as a distinct cardiomyopathy by the European Society of Cardiology [4, 5]. Alterations in cellular morphology and size, gene expression patterns, and metabolic shifts in cardiomyocytes driven by genetic insult initially compensate and maintain cardiac function in the subtle, preclinical stages of cardiomyopathy; however, when compensatory mechanisms fail, additional paracrine signaling, neuroendocrine signaling, and other pathological pathways are activated on a tissue, organ or whole organism level, leading to congestive heart failure. Thus, inherited forms of cardiomyopathy, irrespective of the specific morpho/clinical condition, may or may not present signs of heart failure.

64.2 Compensatory Stress Regulators in Inherited Cardiomyopathy

In inherited cardiomyopathies, cellular pathology originates from the initial genetic assault; however, the phenotypic expression of the specific cardiomyopathy type will be distinguished later when the effects of cardiac remodeling are perceptible. Thus, individuals carrying gene mutations may not present clinical signs of cardiomyopathy until adulthood, supporting a temporal mechanism by which chronically altered cellular responses and cardiac remodeling lead to the clinically relevant cardiomyopathy phenotype. Cellular responses to maintain normal cardiomyocyte function include changes in Ca^{2+} transients and mechanotransduction, the number and sensitivity of sarcomeres, and shifts in metabolic processes and gene expression, including activation of fetal genes and non-coding microRNAs.

Calcium transients: Intracellular sarcoplasmic Ca^{2+} concentrations directly and critically control the contraction and relaxation of the sarcomere [6]. Two critical coupling on structural and functional levels must be balanced on every heartbeat to precisely control intracellular calcium cycling [7]. This process is controlled by activation of ion channels, G protein-coupled receptors (GPCRs), stretch-activated channels, the sarcoplasmic reticulum (SR), and many other biologic and chemical receptors and cellular organelles [8]. In the initial compensated period of genetic cardiomyopathy, contractility and heart rate are facilitated through altered key Ca-handling proteins and Ca^{2+} transients. However, if Ca^{2+} overload stress is sustained, this activates calmodulin-calcineurin, a serine/threonine phosphatase through dephosphorylation of NFAT (nuclear factor of activated T cells). Activated calmodulin-calcineurin then translocates into the nucleus, changing the gene expression and triggering abnormal contractility and pathological hypertrophy and remodeling [9].

Mechanotransduction signaling: Mechanotransduction is the complex intracellular mechanism of three different interrelated processes including mechanosensation, mechanotransmission, and mechanoresponse that allows the heart to adapt to new working conditions and recover normal function by regulating gene expression in response to a biomechanical stretch and stress [10]. Altered

stretch recruits the integrin-induced phosphorylation of focal adhesion kinase (FAK), activating the downstream Src signaling in cardiomyocytes [11]. The integrin–talin complex, components of the costamere, connects the sarcomere to the sarcolemma and extracellular matrix (ECM) through the Z-discs, which consist of numerous mechanosensitive proteins including muscle LIM protein (MLP), telethonin (TCAP), nebulette, myopalladin, cardiac ankyrin repeat protein (CARP), filamin C [12] and others. Mutations in all these costamere and Z-disc proteins induce pathological signaling pathways in response to sustained stretch and may initiate the development of cardiomyopathies [13, 14].

Metabolic substrate utilization: Fatty acids (FAs) and glucose are the energy substrates in normal adult heart to generate high-energy adenosine triphosphate (ATP) molecules for cardiac contraction and relaxation. In the healthy heart, phosphocreatine, a molecule smaller than ATP that is capable of rapidly diffusing through the myofibrils, is the main reserve source of ATP during acute stress [15]. In the initial compensatory stages of cardiomyopathy, the heart favors burning free FAs, which yield about three times more ATP molecules than glucose, but require more oxygen to metabolize [16]. Molecular sensors such as hypoxia-inducible factors (HIFs) [17], AMP-activated protein kinase (AMPK) [18], the mechanistic target of rapamycin (mTOR) [19], and the peroxisome proliferator–activated receptor (PPAR) family proteins detect changes in oxygen or energy levels and regulate downstream transcriptional, translational, posttranslational, or epigenetic modifications [20]. As contractility or relaxation is continuously altered, the demand for ATP increases, yet the levels of phosphocreatine are progressively reduced. In the decompensated stage of cardiomyopathy, energy substrate utilization shifts from FA oxidation (60% to 90%) to glucose burning (60% to 90%), a less efficient resource for producing energy [15], resulting in a circuit that limits cardiac performance.

Fetal gene program: The process of expressing the genes that are predominantly expressed during cardiac development is called fetal gene program [21]. This adaptive process is associated with a whole program of cell survival under stress and observed in a variety of pathophysiologic conditions such as hypoxia, ischemia, hypertrophy, and atrophy [22]. In adult cardiomyocytes, contractility is inversely proportional to levels of atrial natriuretic peptide (ANP), brain natriuretic peptide (BNP), β-Myosin heavy chain (β-MHC), and α-skeletal actin (α-SMA), genes that are normally expressed during embryogenesis [23]. During fetal development, α-MHC replaces β-MHC with lower ATPase activity and enhanced ATP use as the dominant transcript in cardiac muscle. Thus, decrease in the α-MHC/β-MHC ratio is used as a marker of fetal gene reactivation [24]. Secreted by the heart, circulating ANP and BNP in plasma induce diuresis and vasodilation *via* increasing intracellular cyclic guanosine monophosphate (cGMP) in target tissues including kidneys and blood vessels [25]. To compensate for increased myocardial wall stress, expression of these fetal genes is induced through immediate early genes (IEGs) encoding transcription factors such as c-Fos, c-Jun, Egr-1, c-Myc, Src, Ras, and mitogen-activated protein kinases (MAPKs). In addition, increase in expression of transcriptional factors such as GATA4, NKX2-5, MEF2, and SP1 is considered a

marker of fetal gene program reactivation [26]. A persistent activation of fetal gene program becomes insufficient to support cardiac structure and function at a certain point and may contribute to pathological hypertrophy and contractile dysfunction, independent of Ca^{2+} handling in the heart [27].

Intercellular crosstalk in the myocardium: Beside cardiomyocytes, composing approximately 56% of the adult murine heart, fibroblasts (27%), endothelial cells (7%), and smooth muscle cells (10%) reside in cardiac ECM containing numerous transient immune cells [28]. The interaction of cardiomyocytes with noncardiomyocyte cells as well as between all cells with each other occurs *via* direct cell–cell interactions in the heart and through ongoing reciprocal secretion of auto- and paracrine factors and all these crosstalk connections are essential in preserving normal cardiac function [29]. Cytokines such as interleukins (IL)-4, IL-6, IL-13 and many others, integrins, endothelin1 (ET1), bone morphogenetic proteins (BMPs), PECAM-1 also known as CD31, vascular endothelial growth factor (VEGF), VE-cadherin, endothelial cell-derived nitric oxide (NO), ANP, BNP, and transforming growth factor (TGF)β-3 are the major molecules—messengers that regulate the complex crosstalk processes, whereas genetic mutations may trigger pathological signaling between these messengers [30].

MicroRNAs: are short sequences of single-stranded RNAs that control expression of target genes that are involved in physiological and pathological myocardial adaptation to stress [31]. MicroRNAs function as a complex network in which specific binding sites located in the 3′ untranslated region (UTR) pairs with target messenger RNA (mRNA) to direct their posttranscriptional expression resulting in translational inhibition or, in some cases, mRNA degradation and subsequent downregulation of targeted corresponding proteins [32]. Many physiological and pathological processes are regulated by noncoding microRNAs in the heart such as cardiac development [33], physiological and pathological hypertrophy [34], cardiac regeneration [35], arrhythmias, and heart failure [36, 37].

64.3 Physiological and Pathological Cardiac Remodeling and Signaling Pathways in Genetic Cardiomyopathy

64.3.1 Cardiomyocyte Hypertrophy

Cardiomyocyte hypertrophy (increase in size) and atrophy (decrease in size) are the most common adaptive responses that occur when cardiac cells respond to multiple factors including genetic abnormalities [38, 39]. Two types of hypertrophy exist at the cellular level: concentric and eccentric [40]. Concentric hypertrophy is an increase in myocyte width-to-length ratios that occur as a result of addition of sarcomeres in parallel as physiological adaptive responses to keep pace with a hemodynamic and pressure demand [41]. Persistent stress may transform physiological hypertrophy into a pathological state when reduced volumes of ventricular chambers affect cardiac output (i.e., diastolic dysfunction), ultimately resulting in the development of heart failure [42]. In contrast, eccentric hypertrophy is an increase in

myocyte length-to-width ratios associated with increased end-to-end addition of sarcomeres, primarily associated with decreased force production with impaired contractile function (i.e., systolic dysfunction) with maladaptive remodeling and often associated with DCM and congestive heart failure [43]. Progression to pathological cardiac hypertrophy implicates many maladaptive processes involving cell death, fibrosis, alterations in calcium, mitochondrial and metabolic behavior, and disturbance in sarcomere and vascular function, leading to heart failure. In inherited cardiomyopathies, triggering of intracellular and extracellular hypertrophic signal-transduction pathways are dependent on the location of the genetic mutation. The major signal transduction cascades such as GPCRs, protein kinase B (PKB) or AKT, MAPK, necrosis factor alpha (TNF-α), microRNAs, and RNA-binding proteins have been shown to play a significant role in the development of pathological hypertrophy.

GPCR signaling: GPCRs are integral membrane proteins consisting seven membrane-spanning domains that are competent to respond to paracrine and autocrine factors including adrenergic factors, angiotensin II (AngII), and ET1 [44]. The sarcomere, when composed of mutant proteins, exhibits altered myofilament Ca^{2+} sensitivity, reduced ATP efficiency and inhibits the sequestration of Ca^{2+} from the cytosol causing cardiac dysfunction and arrhythmias [45, 46]. Further, mutation-induced contractile dysfunction causes activation of GPCR signaling by ET1 and AngII and increases the release of Ca^{2+} from the SR, activating calmodulin and NFAT [47, 48]. GPCR signaling is also associated with activation of the ERK (extracellular signal-regulated kinase) and AKT signaling pathways [49].

AKT signaling: Many adaptive processes in the heart such as protein synthesis, apoptosis, gene expression, and metabolism are regulated by phosphoinositide 3-kinase (PI3K) [50]. Activation of PI3K on the cardiomyocyte sarcolemma initiates activation of PKB/AKT [51]. When PKB/AKT-mediated phosphorylation of GSK3β (glycogen synthase kinase) inactivates it, hypertrophic transcriptional effectors including GATA4, β-catenin, c-Myc, and NFAT are activated within the heart [52]. Compensated hypertrophy and increased contractile efficiency is induced by AKT1 and AKT2 [53]; however, chronic activation of the PI3K/AKT pathway *via* mTOR may lead to pathological cardiac hypertrophy [54].

MAPK pathway: The MAPK family consists of four subfamilies of kinases: ERK1/2, c-Jun N-terminal kinases (JNK1-3), p38 kinases, and ERK5 that convert extracellular stimuli into a wide range of cellular responses [9]. MAPKs are highly regulated protein kinases that undergo phosphorylation steps to catalytically activate their kinase domain. In cardiomyocytes, MAPK signaling is initiated by GPCRs, insulin-like growth factor-1 (IGF-1) and fibroblast growth factor receptor (FGFR), TGFβ, and by cytokines, stretch, AngII or ET-1 [55]. When activated *via* the three-module cascade of phosphorylating kinases, MAPKs then translocate into the nucleus and activate transcription factors, resulting in reprogramming of cardiac gene expression.

Activated ERK1/2 stimulates the transcription of genes such as BNP and Elk-1 [56]. JNKs and p38 are activated mainly by inflammatory cytokines, ischemia, oxidative stress, heat shock, endotoxins, as well as secondarily by growth factors

and GPCR [57]. JNKs activation increases expression of ANP, α-SMA, TGFβ1, Elk-1, p53, and collagen type I in cardiac hypertrophy, and inhibits NFAT4, NFATc1, and signal transducer and activator of transcription-3 (STAT3). The p38 module promotes expression of proinflammatory cytokines such as IL-1β, TNF-α, and IL-6 through the integrin–FAK–Src-Ras pathway [58].

TNF-alpha: TNF-α is a cytokine that initiates an inflammatory response *via* coupling with TNF receptor and activating NF-κB, PKC, stress-activated protein kinases (SAPKs), and JNKs in response to stress [59]. Once activated, TNF-α triggers expression of matrix metalloproteinases (MMPs), a family of enzymes that degrade the ECM components [60]. Levels of TNF-α and MMPs have been found to be concordantly increased in DCM and the failing human heart [53]. The NF-kB cascade is initiated upon activation of NF-κB inducing kinase (NIK) and Ikappa B kinase (IKK) complex, triggering subsequent IkB-α degradation. Activated NF-κB translocates to the nucleus causing cardiac hypertrophy [61].

64.3.2 Cardiomyocyte Atrophy

Cardiac atrophy is a pathological event associated with mechanical and metabolic unloading of the myocardium resulting in death and loss of cardiomyocytes and degenerative remodeling of the heart [39] and is typically a result of maladaptive processes of apoptosis, necrosis, or excessive autophagy.

Apoptosis is the process also known as programmed cell death as defined by certain morphologic changes, such as DNA fragmentation, progressive cardiomyocyte atrophy, and death [62]. Apoptosis is induced *via* an intrinsic pathway by cytochrome *c* released from mitochondria or *via* an extrinsic pathway by activation of cell membrane-bound death receptors (such as Fas or TNF-α) by coupling with the corresponding cytokines or ligands [63, 64]. Both pathways ultimately activate downstream effector caspases. Induction of apoptosis plays a critical role in the transition from compensatory hypertrophy to decompensated heart failure [65]. As adult cardiomyocytes are terminally differentiated, apoptosis is detrimental to cardiac function not only due to cardiac myocyte loss but also by generating fibrosis and decreased heart compliance [66]. Many of the signaling pathways, including AKT and β-adrenergic stimulation with cytochrome *c* release from mitochondria [67], activation of Fas by up-regulated Fas ligand and TNF-α or degradation of cFlip, inhibitors of Fas, are common in the failing heart [68].

Necrosis, a premature death of cells, is typically a result of the unregulated digestion of cell components, rupture of plasma membrane, and eventual lysis of the cells due to activation of various death receptors, resulting in a tissue damage and remodeling [69]. There are different types of regulated necrosis that include necroptosis, pyroptosis, ferroptosis, and mitochondrial permeability transition (MPT)-dependent necrosis [70]. Among them, necroptosis and MPT-dependent necrosis have been shown to play important roles recently in cardiac remodeling and heart failure [71]. Necrosis is almost always detrimental due to loss of sarcolemmal integrity, uncontrolled release of cellular products and enzymes into the ECM,

and consequent inflammatory responses. The wave-front phenomenon of myocardial atrophy with pathological remodeling such as inflammation, fibrosis, hypertrophy, and ventricular dilation with preceded necrosis is well documented in human ARVC [72]. This genetically determined process extends from the epicardium toward the endocardium, resulting into progressive wall thinning in the right ventricle (RV), left ventricle (LV), or both with time commonly during end-stage disease [73]. The complex pathogenesis and underlying mechanisms have been associated in ARVC with disruption of sarcolemmal and desmosomal integrity *via* alteration of WNT-β-catenin pathways. In addition, peroxisome proliferator-activated receptors (PPARγ and PPARα) signaling and abnormal Ca^{2+} homeostasis *via* MPT may play important roles [74, 75].

Autophagy is a natural process of conserving and recycling of cytoplasmic components, thus playing important roles in cell survival by removing oxidated proteins and damaged subcellular components during stress [76]. Autophagy is controlled by sequential actions of autophagy-related genes (Atgs), such as Beclin1 (Atg6), microtubule-associated protein 1 light chain 3 or LC3 (Atg8), and class III PI3K that are responsible for vesicle elongation and conjugation [77, 78]. In contrast, the mTOR pathway or class I PI3K acts to inhibit autophagy. Although autophagy is a cytoprotective mechanism, proapoptotic factors released from the damaged mitochondria may lead to apoptotic cell death [79]. Several signaling pathways, reactive oxygen species (ROS), and increases in cytosolic Ca^{2+} levels not only trigger apoptosis, but potently induce autophagy. In the heart, excessive autophagy causes cell death and cardiac atrophy [78]. Thus, autophagy in the failing heart caused by DCM appears to be a sign of failed cardiomyocyte repair [80].

64.3.3 Cardiac Fibrosis

Interstitial and/or perivascular fibrosis as one of the major hallmarks of cardiomyopathies and is an independent predictor of adverse outcome due to disruption in excitation-contraction coupling (ECC) between cardiomyocytes causing arrhythmias. Fibrosis is also associated with an increase of myocardial stiffness and decrease in contractility with progression to LV systolic dysfunction [81, 82]. Fibrosis is primarily produced by resident fibroblasts in the heart; however, there is evidence for collagen production by cardiomyocytes [83]. There are two forms of fibrosis that exist: replacement and reactive myocardial fibrosis [84]. Several profibrotic factors are known to cause fibrotic responses in the heart. These factors include AngII, platelet-derived growth factor (PDGF), connective tissue growth factor (CTGF), and the renin-angiotensin-aldosterone system (RAAS) along with respective prominent downstream mediators such as TGFβ1, IL-1, IL-10, IL-11, and chemokines that in-turn recruit cell surface receptors, integrins, syndecans, and CD44 causing fibrosis in the heart [85].

Angiotensin II: AngII generated by angiotensin converting enzyme (ACE) from AngI directly induces a series of G protein- and non-G protein signaling cascades *via*

binding to angiotensin type 1 receptors (AT1-Rs) [47]. AT1-R-mediated NADPH oxidase activity leads to generation of ROS and increases SMAD2 levels, augmenting the nuclear translocation of phosphorylated SMAD3s [86, 87]. As a result, stimulated TGFβ induces fibroblast proliferation and differentiation into collagen-secreting myofibroblasts leading to cardiac fibrosis.

CTGF is a protein mainly expressed in fibroblasts in the healthy heart, but is also secreted by injured cardiomyocytes during cardiac remodeling [88]. Although a mouse heart with CTGF deletion and overexpression did not have a fibrotic phenotype [89], increased amounts of CTGF secreted by cardiomyocytes and myofibroblasts into the ECM in cardiac hypertrophy and heart failure have been shown to contribute to fibrosis as an autocrine factor [90].

TGFβ is a cytokine involved in regulation of many signaling pathways involved in cellular differentiation, homeostasis, cardiac fibrosis, and hypertrophy [91]. When TGFβ binds to its serine/threonine kinase receptors known as type I and type II TGF-β receptors (TβRs), the downstream SMAD signaling pathway activates to stimulate collagen production. TGFβ also signals through TGFβ-activated kinase 1 (TAK1) to activate ATF2 (activated transcription factor 2), MAPK, Rho GTPase, AKT, and FAK, which are directly correlated with cardiac hypertrophy and fibrosis [88, 92].

SMADs: SMAD proteins are a family of transcription factors that consist of 3 groups: receptor-activated (SMADs 1, 2, 3, 5, and 8), co-mediators (SMADs 4 and 10), and inhibitory (SMADs 6 and 7) [93]. Receptor-activated or phosphorylated SMADs associate with co-SMADs and then translocate to the nucleus, where they interact with transcriptional factors and co-activators and alter gene expression [94]. The best characterized members of the SMADs family are Smad2 and 3, which are shown to activate myofibroblast differentiation and stimulate ECM synthesis, inducing scar formation and organization [95].

Rho: Ras family G proteins regulate intracellular actin dynamics and formation of focal adhesions through Rho/ROCK signaling [96]. TGFβ and mechanical force promotes the nuclear translocation of myocardin-related transcription factor A (MRTF-A) in cardiac fibroblasts, inducing a myofibroblast-like cell type gene expression through Rho/ROCK signaling [88]. In addition, the Rho/Rho-kinase system has been shown to play a role in adipogenesis and desmosomal development by regulating expression of genes involved in Wnt signaling [97].

Kruppel-like transcription factors (KLF) is a large family of transcription factors that have three high-fidelity zinc-finger (ZNF) motifs with an important role in cell differentiation and tissue-development [98]. For example, KLF15, a negative regulator of cardiac fibrosis, inhibits the SMAD3 activity on the CTGF promoter [88, 99]. TGFβ down-regulates KLF15 in cardiac fibroblasts and myocytes, leading to fibrosis [100]. The other KLF member, KLF5, is up-regulated through AngII and activates TGFβ expression, thereby connecting AngII and TGFβ signaling in cardiac fibrosis [101].

64.4 Electrical Tissue Remodeling and Arrhythmogenesis

Electrophysiological remodeling in genetic cardiomyopathy occurs at the cellular and tissue levels and it is not fully understood how exactly these changes contribute to electrical instability and increased risk of arrhythmias. In cardiac muscle, the action potential initiated by sinoatrial node (SAN) cells spreads along the specialized complex formed by T (transverse)-tubule and terminal cisterna of SR known as a dyad [102]. Dyad accommodates the ECC of plasma membrane depolarization with activation of cardiomyocyte contraction [103]. Ca^{2+} homeostasis, ion channels located within the sarcolemma and intercalated discs, sarcomere Ca^{2+} sensitivity, and cell–cell coupling though gap junctions and desmosomes are all crucial components in regulating cardiac electrical remodeling [104].

Calcium cycling: Arrhythmogenesis is triggered through disturbance of the orchestrated interactions of key intracellular calcium-handling proteins of the myofilaments, T-tubule, and SR, including troponins and tropomyosin, dihydropyridine receptor (DHPR) cardiac $\alpha 1$, ryanodine receptor-2 (RyR2), calsequestrin, triadin, junctin, sarcoplasmic reticular Ca^{2+} ATPase 2 (SERCA2), and phospholamban and the comprehensive reviews were published by Kranias and Schartner groups [8, 103].

Sarcolemmal action potential (AP) prolongation, a result of down-regulation of repolarizing K^+ currents, an increase in late Na^+ current and changes in intracellular Ca^{2+} transport, contributes to the development of arrhythmias [105]. The cardiac Na^+ channel (Nav1.5) interacts differentially with either syntrophin–dystrophin complex at the lateral membrane or at the intercalated discs by synapse associated protein 97 (SAP97). For example, loss of Nav1.5 results in a significant lateral conduction velocity slowing and prolongation of AP with delayed repolarization in hearts of dystrophin-deficient *mdx* mouse models [106].

Decreased gap junction coupling, due to altered post-Golgi transport and down-regulation of connexin-43 (Cx43), leads to loss of electrical cell–cell coupling and slows conduction velocity [107, 108]. Reorganization of desmosomal proteins such as desmoplakin (DSP) and plakoglobin (JUP) is suggested to play a causal role in the development of arrhythmogenic and fibro-fatty remodeling in the heart *via* interfering the Wnt/β-catenin signaling [109]. Desmosomal protein plakophilin-2 (PKP2) also plays a role in expression of Nav1.5, affecting a sodium channel function in cardiomyocytes [110].

64.5 Failing Heart

A pathologic causative genetic insult followed by sustained maladaptive remodeling results in the development of decompensated cardiomyopathy when the failing heart is unable to keep up with the hemodynamic demands at all levels, from the molecule to the whole organism [111]. The genetic contribution to heart failure is complex and molecular cell level alterations of end-stage cardiomyopathy and heart failure respond to irreversible cardiac remodeling with significant changes in membrane

ion currents and intracellular Ca^{2+} metabolism, fibrosis, hypertrophic or atrophic remodeling, and cell death [112]. Cell–cell coupling abnormalities include reorganization of sarcolemma, gap junctions, and desmosomes, while cardiac function is significantly depressed with depleted force development and slowed relaxation [112, 113]. Recent advances in understanding of the pathogenesis and mechanisms underlying the development of heart failure in different types of cardiomyopathies have significant implications for prevention, diagnostics, and therapies of failing heart [114, 115].

64.6 Animal Models of Human Cardiomyopathies

Numerous small and large animal models have been developed to discover underlying novel pathogenic mechanisms as well as clarify known molecular and cellular mechanisms of cardiomyopathies discussed above. Characterization of the mechanisms of cardiomyopathies using animal models is challenging, owing to the complexity of techniques and heterogeneous disease-causing mechanisms and modulators of pathology. Recently discovered novel gene-editing technologies using ZFNs (zinc-finger nucleases), TALENs (transcription-activator like effector nucleases), and CRISPR-Cas (clustered regularly interspaced short palindromic repeats-CRISPR associated) genes enabled to rapidly generate precise and targeted changes in the genome of living cells [116]. Powerful tools for targeting mRNA such as RNA interference (RNAi) and morpholino knockdown remain as the most effective technologies for discovering and functionally studying novel cardiomyopathy candidate genes [117, 118]. Wide accessibility of transgenic, knockout and knock-in murine models has been one of the most successful approaches for studying genetic cardiomyopathies and disease progression on a whole-organism level. Table 64.1 summarize animal models of human cardiomyopathy with a focus on cellular location of the proteins/genes and associated cardiac remodeling, key genetic and molecular signaling exposed.

Hypertrophic cardiomyopathy models: Animal models of HCM mostly carry human mutations in sarcomeric protein-encoding genes such as α-MHC (β-MHC in humans), α-tropomyosin, troponins and myosin binding protein C (MyBP-C) and these models have demonstrated that some HCM associated mutations primarily enhance contractile properties with increased force generation, ATP hydrolysis, and actin–myosin sliding velocity, suggesting that the hypertrophy may not be a compensatory response to diminished contractile function [170]. However, models of HCM also show delayed myocardial relaxation that occurs before the onset of hypertrophy, suggesting that diastolic dysfunction is a direct consequence of HCM mutations that leads in compensatory LV hypertrophy [171]. Abnormal Ca^{2+} cycling in cardiomyocytes and altered Ca^{2+} sensitivity of myofilaments before overt histopathologic changes occur in the myocardium clearly linked to mutations in sarcomeric genes [172]. Myocardial fibrosis is a cellular substrate for high risk of cardiac arrhythmias and sudden cardiac death in HCM. Hearts from animal models of HCM progressively accumulate myocardial fibrosis in the same manner as human

Table 64.1 Animal models of human genetic cardiomyopathies and associated cardiac remodeling and molecular signaling

Cell	Gene	Human disease	Animal model	References	Remodeling	Signaling
Sarcolemma	Sarcoglycan delta (SGCD)	DCM	Mouse KO	Cordier et al. 2000 [119]	Focal necrosis, vascular spasm, fibrosis after stress	Destabilization of DGC, membrane permeability defect, Ca^{2+} imbalance
			Mouse KI S151A	Rutschow et al. 2014 [120]	Mild DCM	
	Sarcospan (SSPN)		Mouse KO	Araishi et al. 1999 [121]	Progressive DMD with extensive degeneration and regeneration.	Disruption of ECM-sarcolemma-cytoskeleton connection
	Laminin-a2 (LAMA2)		Mouse KO	Miyagoe-Suzuki et al. 2000 [122]	Dilation of ventricles	
	Dystrophin (DMD)	DMDBMDXL-DCM	Mouse	Sicinki et al. 1989 [123]	Dilated ventricles	Destabilization of DGC, actin—sarcolemma connection, Ca^{2+} alteration
			Zebrafish	Guyon et al. 2003.[124]	Mutant zebrafish are less active	
			Canine	Jones et al. 2004 [125]	DMD and DCM phenotype	
	Dystrobrevin alpha (DTNA)	DMD LVNC	Mouse KO	Yoshida 2000 [126]	Muscle dystrophy, mild cardiomyopathy	Alteration in cyclic GMP levels
	Caveolin3 (CAV3)		Mouse KO	Woodman et al. 2002 [127]	Hypertrophy, dilation, and reduced fractional shortening	ERK1/2 activation, Src
			Mouse TG P104L	Kuga et al. 2011 [128]	Hypertrophy with enhanced contractility, apoptosis	nNOS production, altered ER stress response
			Zebrafish KO	Nixon et al. 2005.[129]	Disruption of muscle differentiation, cardiac edema	Myoblast fusion defects
Sarcomere	Myosin heavy chain 7 (MYH7)	DCM HCM LVNC	Mouse TG R403Q	Kamisago et al. 2006 [130]	Cardiac dysfunction, myocyte disarray, hypertrophy, fibrosis.	
	Titin (TTN)	DCM, HCM	Zebrafish	Xu et al. 2002 [131]	Cardiac edema, poor contraction, normal sarcomeres are absent	Blockage of sarcomere assembly

	Tropomyosin (TPM1)	DCM	Mouse KO	Rethinasamu et al. 1998 [132]	Homozygous null mice are embryonic lethal (E8–E11.5)	
		DCM	Mouse TG E54K	Rajan et al. 2007 [133]	Dilated LV, impaired systolic, and diastolic functions	Decreased Ca^{2+} sensitivity and tension generation.
		HCM	Mouse TG E180G	Prabhakar et al. 2001 [134]	Fibrosis, concentric hypertrophy, and atrial enlargement	Increased myofilament Ca^{2+} sensitivity
		HCM	Mouse TG D175N	Muthuchamu et al. 1999 [135]	Myocyte disarray, hypertrophy, reduced contractility and relaxation	Thin filament enhanced Ca^{2+} sensitivity
	Troponin T (TNNT2)	Diverse CM	Mouse TG MyHC	TARDIFF et al. 1998 [136]	Mild hypertrophy, disarray, reduced number of myocytes	Multiple cellular mechanisms
			Mouse TG R92Q	Tardiff et al. 1999 [137]	Fibrosis, diastolic dysfunction, shorter sarcomere lengths, mitochondrial pathology	ANP and β-MHC induction, increased basal sarcomeric activation
			Zebrafish KO	Sehnert et al. 2002 [138]	Sarcomere loss and myocyte disarray	Dysregulation of thin filament expression
	Troponin I (TNNI3)	HCM	Mouse TG I145G	James et al. 2000 [139]	Cardiomyocyte disarray, diastolic dysfunction, fibrosis, cell death.	Increased sensitivity to Ca^{2+} and hypercontractility
			Rabbit TG R146G	Sanbe et al. 2005 [140]	Cardiomyocyte disarray, fibrosis and connexin43 dis-organization	Altered fractal pattern of the repolarization phase
			Mouse KO	Huang et al. 1999 [141]	Acute heart failure, shortened sarcomeres	Reduced Ca^{2+} sensitivity, elevated resting tension
	Myosin binding protein C (MyBPC)	HCM	Mouse TG	Yang et al. 1998 [142]	Disorganization of sarcomere and dysgenesis, pCa^{2+} force curve shift	Inefficient incorporation of truncated protein into sarcomere
			Mouse KO	Palmer et al. 2004 [143]	Severe HCM, reduced myofilament stiffness	Altered sarcomere shortening velocity
			Cat TG	Meurs, 2005 [144]	Sarcomeric disorganization	
Intermediate filaments	Desmin (DES)	DCM	Mouse TG R173del 179	Wang et al. 2001 [145]	Desmin network and myofibril alignment disruption, intra-SR granular aggregates	Blunted response to beta-agonist stimulation

(continued)

Table 64.1 (continued)

Cell	Gene	Human disease	Animal model	References	Remodeling	Signaling
			Zebrafish	Li et al. 2013 [146]	Disorganized muscles, small larvae, reduced swimming activity.	abnormal eccentric work
			Mouse KO	Milner et al. 1996 [147]	Loss of myofibrils lateral alignment, mitochondrial defects, necrosis	muscle architecture disruption and degeneration
Z-disc	Myopalladin (MYPN)	DCM HCM RCM	Mouse TG Y20C	Purevjav et al. 2012 [148]	Disrupted intercalated discs, hypertrophy and heart failure	Disruption of desmin, vinculin, DSP, and CX43
	Muscle LIM protein (CSRP3)	DCM	Mouse	Arber et al. 1997 [149]	DCM, hypertrophy and heart failure, disruption of cardiomyocyte cytoarchitecture.	Altered mechanosensation
	Nebulette (NEBL)	DCM	Mouse TG	Purevjav et al. 2010 [150]	DCM, mitochondrial abnormalities	Stretch induced alteration of Z-disc assembly
	Nexilin (NEXL)	DCM	Zebrafish	Hassel et al. 2009 [151]	Z-disc damage, heart failure	Stretch-induced Z-disc disruption
	Telethonin (TCAP)	DCM	Mouse KO	Knoll et al. 2011 [152]	Heart failure following biomechanical stress	Stress-induced modulation of nuclear p53
			Zebrafish	Zhang et al. 2009[153]	Deformed muscle structure and impaired swimming ability	Disruption of sarcomere-T-tubule interaction through ILK
	Cypher/ZASP	DCM	Mouse KO	Zhou et al. 2001 [154]	Ventricular dilation, Z-disc disruption, muscle weakness	α-actinin or other Z-line protein interactions
Iband	Cardiac ankyrin repeat protein (ANKRD1)	HCM DCM	Mouse TG α-MHC	Song et al. 2012 [155]	Attenuated cardiac hypertrophy to pressure overload and isoproterenol	Reduced TGF-β ERK1/2, MEK and Smad3 to pressure overload
			Mouse KO	Bang et al. 2014 [156]	No cardiac phenotype	
Gap junction	Connexin 43 (CX43)	ARVC	Mouse KO	Thomas et al. 1998 [157]	Conduction defects without gross pathology	Slowing of intercellular channels in sinoatrial node and ventricular conduction cells
			Mouse TG α-MHC	Ewart et al. 1997 [158]	Conotruncal defects, partial rescue of Cx43 KO mice	

Desmosome	Desmoplakin2 (DSP2)	ARVC	Mouse KO	Garcia-Gras et al. 2006 [75]	RV dilation, fibro-fatty infiltration, apoptosis, necrosis	Cell–cell contact disruption
			Mouse TG	Yang et al. 2006 [159]	RV dilation, fibrofatty infiltration, apoptosis	
	Plakophilin2 (PKP2)		Mouse KO	Grossmann et al. 2004 [160]		
	Desmocolin2 (DSC2)		Zebrafish	Heuser et al. 2006 [161]	Loss of desmosomal plaque and midlines, cardiac dysfunction	Cell–cell contact disruption
	Desmoglein2 (DSG2)		Mouse TG N271S	Pilichou et al. 2009 [162]	Arrhythmia, dilated ventricles, necrosis, atrophy, fibrosis, cell death,	Cell–cell contact disruption and cell atrophy due to necrosis
			Mouse TG	Krusche et al. 2011 [163]	Dilated LV, fibrosis, ventricular arrhythmias	
	Junctional plakoglobin (JUP)		Zebrafish KO	Martin et al. 2009 [164]	Decreased heart size, bradycardia, cardiac edema	Interference with Wnt/b-catenin
			Mouse KO	Kirchhof et al. 2006 [165]	VT, RV dilation, and dysfunction	
Costameres	Talin (TLN)	HCM	Mouse cKO	Manso et al. 2013 [166]	Blunted fibrosis and hypertrophy, and hypercontraction to pressure overload	Blunted ERK1/2, p38, Akt, and Gsk3 after mechanical stress
	Filamin C (FLNC)	DCM	Medaka zacrofish K1680X	Fujita et al. 2012 [167–169]	Enlarged heart, myocardial wall rupture, detachment of myofibrils from sarcolemma and intercalated discs, Z-disc destruction.	Disrupted structural integrity of cardiac and skeletal muscles against stress.
Nuclear envelope	Lamin A (LMNA)	DCM	Mouse KO N195K	Ho et al. 2013 [168]	Nucleocytoplasmic shuttling of Mlk1	Altered actin polymerization
			Mouse KO	Sullivan et al. 1999 [169]	Cardiac myocytes degeneration, patchy mineralization, atrophy	Emerin dislocation

DCM, dilated cardiomyopathy; *HCM*, hypertrophic cardiomyopathy; *RCM*, restrictive cardiomyopathy; *ARVC*, arrhythmogenic right ventricular cardiomyopathy; *LVNC*, left ventricular noncompaction cardiomyopathy; *XL-DCM*, X-chromosome linked DCM; *DMD*, Duchenne muscular dystrophy; *BMD*, Becker muscular dystrophy; *KO*, knock-out; *KI*, knock-in; *TG*, transgenic

patients [173]. Systems genetics analysis is an innovative approach that utilizes a large genetic reference population (GRP). Family of BXD mice derived from DBA/2J mouse, a natural model of HCM, has been used in systems genetics analysis for discovering modifier genes in cardiomyopathy [174, 175]. All these animal studies have continuously being utilized for developing targeted diagnostics and therapies in humans with HCM [176]

Dilated cardiomyopathy models: Animal models of DCM generally resemble human mutations in genes encoding cytoskeletal, and sarcolemmal and sarcomeric/Z-disc proteins and present with ventricular dilation, impaired contractility and thinning of the ventricular walls correlated with the loss of heart muscle mass and disorganization of muscle architecture [177]. Combination of arrhythmias and myocyte dysfunctions resembling human DCM are common features of animal models of DCM [178]. In addition, functional changes in nonmyocyte cells have been associated with fibrotic scars that stiffen the heart tissue and impede normal cardiomyocyte contractility [11]. Novel DCM mechanisms such as impaired Z-disc assembly and mechanosensation [179], sensitivity to apoptosis, abnormalities in myofibrillogenesis under metabolic stress, protein folding, inhibition of protein aggregation, and degradation of misfolded proteins have been explored [180].

Restrictive cardiomyopathy models: RCM is the least common but most lethal form of cardiomyopathy, where impaired ventricular relaxation and bi-atrial dilation due to increased stiffness of the myocardium and pressure in the ventricles overcome the changes in myofibrillar arrangement and cardiomyocyte gross abnormalities [181]. Most of animal models of RCM, similar to HCM, carry mutations in troponins as well as in titin, MYPN, and desmin intermediate filament [182].

Arrhythmogenic cardiomyopathy models: Many models of ARVC with mutations in genes encoding desmosomal (DSP, PKP, DSC, DSG, and JUP) and nondesmosomal proteins have been developed [183]. Nondesmosomal genes associated with ACM encode proteins expressed in SR, intermediate filaments, Z-discs, nuclear envelope, sarcolemma, and cellular adhesion junctions [184]. Structural and functional alterations include progressive diffuse or segmental loss of cardiomyocytes, probably due to cardiomyocyte apoptosis or necrosis, and replacement with fibrotic and adipose tissue. Fibro-fatty tissue primarily is seen in the RV with common LV and biventricular involvement in later stages of the disease [162]. Interestingly, knock-in mice carrying the p.S358L mutation in TMEM43 demonstrated disturbed intestinal and metabolic homeostasis that contributed to cardiac pathophysiology of ARVC5, a fully penetrant form of ACM, suggesting an importance of cardio-metabolic studies in mutation positive patients [185].

Left ventricular noncompaction cardiomyopathy models: Animal models of LVNC demonstrate spongiform ventricular myocardium with deep trabeculations regulated *via* signaling pathways driven by Notch [186] or Notch-related Mib1 [187], BMP [188], and TGF-β [189]. Other signaling related to LVNC phenotype include NKX2-5 and NFATC1 [190, 191]. Barth syndrome with featured LV

noncompaction caused by tafazzin (*TAZ*) mutations and tafazzin knockdown mice, created using a short-hairpin RNAi transgenesis, showed hypertrabeculation and noncompaction [192].

Animal genetic reference populations utilized for systems biology approaches: Overlap of the phenotypes is common in cardiomyopathies, and clinical characteristics may vary considerably among patients, even among family members who carry pathological mutation [193]. This variability is partially explained by modifier genes, however, the lack of widespread studies in identifying modifier genes persists due to significant variances in human lifestyle, stress and environment [194]. In fact, most genetically engineered animal models are created on a single fixed genetic background and therefore are often challenging to explain phenotype diversity seen in humans [195]. In this respect, several groups have utilized animal (rat and mouse) GRPs circumvent some limitations of human GWAS studies by integrating large multi "omics" with cardiac phenotypes using systems biology methods to identify significant genomic loci and modifier genes associated with human DCM, HCM, heart rate and cardiac conduction abnormalities [175, 196–199]. For example, roles of TNNI3K (troponin-I-interacting kinase) in controlling echocardiographic parameters and metabolism related phenotypes have recently been demonstrated by different groups using rodent GRPs [200, 201].

64.7 Summary

Recent advances in molecular biology, gene-editing techniques and systems biology and genetics methods have vastly improved the understanding of molecular mechanisms responsible for cardiomyopathies and cardiac dysfunction. The wide range of innovative technologies and techniques used in animal models *in vivo* has led to advances in our knowledge on the etiology, pathophysiology, and therapeutics of inherited cardiomyopathies. Mutant proteins in cardiomyocytes perturb cardiac function whether the prime distress occurs in the contractile apparatus or neighboring cellular complexes, yet persistent cellular stress leads to tissue, organ, and organism level pathology and pathophysiology.

References

1. Harvey PA, Leinwand LA. The cell biology of disease: cellular mechanisms of cardiomyopathy. J Cell Biol. 2011;194(3):355–65. https://doi.org/10.1083/jcb.201101100.
2. Bowles NE, Bowles KR, Towbin JA. The "final common pathway" hypothesis and inherited cardiovascular disease. The role of cytoskeletal proteins in dilated cardiomyopathy. Herz. 2000;25(3):168–75.
3. Maron BJ, Towbin JA, Thiene G, Antzelevitch C, Corrado D, Arnett D, et al. Contemporary definitions and classification of the cardiomyopathies: an American Heart Association Scientific Statement from the Council on Clinical Cardiology, Heart Failure and Transplantation Committee; Quality of Care and Outcomes Research and Functional Genomics and Translational Biology Interdisciplinary Working Groups; and Council on Epidemiology and

Prevention. Circulation. 2006;113(14):1807–16. https://doi.org/10.1161/CIRCULATIONAHA.106.174287.
4. Maron BJ. The 2006 American Heart Association Classification of Cardiomyopathies is the gold standard. Circ Heart Fail. 2008;1(1):72–6. https://doi.org/10.1161/circheartfailure.108.770826.
5. Elliott P, Andersson B, Arbustini E, Bilinska Z, Cecchi F, Charron P, et al. Classification of the cardiomyopathies: a position statement from the european society of cardiology working group on myocardial and pericardial diseases. Eur Heart J. 2007;29(2):270–6. https://doi.org/10.1093/eurheartj/ehm342.
6. Allen DG, Kurihara S. Calcium transients in mammalian ventricular muscle. Eur Heart J. 1980;1:5–15. https://doi.org/10.1093/eurheartj/1.suppl_1.5.
7. Eisner DA, Caldwell JL, Kistamas K, Trafford AW. Calcium and excitation-contraction coupling in the heart. Circ Res. 2017;121(2):181–95. https://doi.org/10.1161/CIRCRESAHA.117.310230.
8. Kranias EG, Bers DM. Calcium and cardiomyopathies. Subcell Biochem. 2007;45:523–37. https://doi.org/10.1007/978-1-4020-6191-2_20.
9. Heineke J, Molkentin JD. Regulation of cardiac hypertrophy by intracellular signalling pathways. Nat Rev Mol Cell Biol. 2006;7(8):589–600. https://doi.org/10.1038/nrm1983.
10. Swynghedauw B. Darwinian evolution and cardiovascular remodeling. Heart Fail Rev. 2016;21(6):795–802. https://doi.org/10.1007/s10741-016-9574-3.
11. Saucerman JJ, Tan PM, Buchholz KS, McCulloch AD, Omens JH. Mechanical regulation of gene expression in cardiac myocytes and fibroblasts. Nat Rev Cardiol. 2019;16(6):361–78. https://doi.org/10.1038/s41569-019-0155-8.
12. Frank D, Frey N. Cardiac Z-disc signaling network. J Biol Chem. 2011;286(12):9897–904. https://doi.org/10.1074/jbc.R110.174268.
13. Watkins H, Ashrafian H, Redwood C. Inherited cardiomyopathies. New Engl J Med. 2011;364(17):1643–56. https://doi.org/10.1056/NEJMra0902923.
14. Knoll R, Buyandelger B, Lab M. The sarcomeric Z-disc and Z-discopathies. J Biomed Biotechnol. 2011;2011:569628. https://doi.org/10.1155/2011/569628.
15. Neubauer S. The failing heart – an engine out of fuel. N Engl J Med. 2007;356(11):1140–51. https://doi.org/10.1056/NEJMra063052.
16. Ashrafian H, Frenneaux MP, Opie LH. Metabolic mechanisms in heart failure. Circulation. 2007;116(4):434–48. https://doi.org/10.1161/CIRCULATIONAHA.107.702795.
17. Cerychova R, Pavlinkova G. HIF-1, metabolism, and diabetes in the embryonic and adult heart. Front Endocrinol (Lausanne). 2018;9:460. https://doi.org/10.3389/fendo.2018.00460.
18. Hardie DG, Ross FA, Hawley SA. AMPK: a nutrient and energy sensor that maintains energy homeostasis. Nat Rev Mol Cell Biol. 2012;13(4):251–62. https://doi.org/10.1038/nrm3311.
19. Howell JJ, Manning BD. mTOR couples cellular nutrient sensing to organismal metabolic homeostasis. Trends Endocrinol Metab. 2011;22(3):94–102. https://doi.org/10.1016/j.tem.2010.12.003.
20. Huss JM, Kelly DP. Nuclear receptor signaling and cardiac energetics. Circ Res. 2004;95(6):568–78. https://doi.org/10.1161/01.RES.0000141774.29937.e3.
21. Razeghi P, Young ME, Alcorn JL, Moravec CS, Frazier OH, Taegtmeyer H. Metabolic gene expression in fetal and failing human heart. Circulation. 2001;104(24):2923–31. https://doi.org/10.1161/hc4901.100526.
22. Rajabi M, Kassiotis C, Razeghi P, Taegtmeyer H. Return to the fetal gene program protects the stressed heart: a strong hypothesis. Heart Fail Rev. 2007;12(3-4):331–43. https://doi.org/10.1007/s10741-007-9034-1.
23. Herron TJ, McDonald KS. Small amounts of alpha-myosin heavy chain isoform expression significantly increase power output of rat cardiac myocyte fragments. Circulation research. 2002;90(11):1150–2.

24. Lyons GE, Schiaffino S, Sassoon D, Barton P, Buckingham M. Developmental regulation of myosin gene expression in mouse cardiac muscle. J Cell Biol. 1990;111(6 Pt 1):2427–36. https://doi.org/10.1083/jcb.111.6.2427.
25. Nakagawa Y, Nishikimi T, Kuwahara K. Atrial and brain natriuretic peptides: hormones secreted from the heart. Peptides. 2019;111:18–25. https://doi.org/10.1016/j.peptides.2018.05.012.
26. Azakie A, Fineman JR, He Y. Myocardial transcription factors are modulated during pathologic cardiac hypertrophy in vivo. J Thorac Cardiovasc Surg. 2006;132(6):1262–71. https://doi.org/10.1016/j.jtcvs.2006.08.005.
27. Nagata K, Liao R, Eberli FR, Satoh N, Chevalier B, Apstein CS, et al. Early changes in excitation-contraction coupling: transition from compensated hypertrophy to failure in Dahl salt-sensitive rat myocytes. Cardiovasc Res. 1998;37(2):467–77.
28. Banerjee I, Fuseler JW, Price RL, Borg TK, Baudino TA. Determination of cell types and numbers during cardiac development in the neonatal and adult rat and mouse. Am J Physiol Heart Circ Physiol. 2007;293(3):H1883–91. https://doi.org/10.1152/ajpheart.00514.2007.
29. Takeda N, Manabe I. Cellular interplay between cardiomyocytes and nonmyocytes in cardiac remodeling. Int J Inflam. 2011;2011:535241. https://doi.org/10.4061/2011/535241.
30. Tirziu D, Giordano FJ, Simons M. Cell communications in the heart. Circulation. 2010;122(9):928–37. https://doi.org/10.1161/CIRCULATIONAHA.108.847731.
31. Catalucci D, Gallo P, Condorelli G. MicroRNAs in cardiovascular biology and heart disease. Circ Cardiovasc Genet. 2009;2(4):402–8. https://doi.org/10.1161/CIRCGENETICS.109.857425.
32. Valencia-Sanchez MA, Liu J, Hannon GJ, Parker R. Control of translation and mRNA degradation by miRNAs and siRNAs. Genes Dev. 2006;20(5):515–24. https://doi.org/10.1101/gad.1399806.
33. Thum T, Galuppo P, Wolf C, Fiedler J, Kneitz S, van Laake LW, et al. MicroRNAs in the human heart: a clue to fetal gene reprogramming in heart failure. Circulation. 2007;116(3):258–67. https://doi.org/10.1161/CIRCULATIONAHA.107.687947.
34. Care A, Catalucci D, Felicetti F, Bonci D, Addario A, Gallo P, et al. MicroRNA-133 controls cardiac hypertrophy. Nat Med. 2007;13(5):613–8. https://doi.org/10.1038/nm1582.
35. Hodgkinson CP, Kang MH, Dal-Pra S, Mirotsou M, Dzau VJ. MicroRNAs and cardiac regeneration. Circ Res. 2015;116(10):1700–11. https://doi.org/10.1161/CIRCRESAHA.116.304377.
36. Wahlquist C, Jeong D, Rojas-Munoz A, Kho C, Lee A, Mitsuyama S, et al. Inhibition of miR-25 improves cardiac contractility in the failing heart. Nature. 2014;508(7497):531–5. https://doi.org/10.1038/nature13073.
37. Romaine SP, Tomaszewski M, Condorelli G, Samani NJ. MicroRNAs in cardiovascular disease: an introduction for clinicians. Heart. 2015;101(12):921–8. https://doi.org/10.1136/heartjnl-2013-305402.
38. Frey N, Katus HA, Olson EN, Hill JA. Hypertrophy of the heart: a new therapeutic target? Circulation. 2004;109(13):1580–9. https://doi.org/10.1161/01.CIR.0000120390.68287.BB.
39. Baskin KK, Taegtmeyer H. Taking pressure off the heart: the ins and outs of atrophic remodelling. Cardiovasc Res. 2011;90(2):243–50. https://doi.org/10.1093/cvr/cvr060.
40. Sawada K, Kawamura K. Architecture of myocardial cells in human cardiac ventricles with concentric and eccentric hypertrophy as demonstrated by quantitative scanning electron microscopy. Heart Vessels. 1991;6(3):129–42. https://doi.org/10.1007/BF02058278.
41. Mihl C, Dassen WR, Kuipers H. Cardiac remodelling: concentric versus eccentric hypertrophy in strength and endurance athletes. Neth Heart J. 2008;16(4):129–33. https://doi.org/10.1007/BF03086131.
42. Seidman JG, Seidman C. The genetic basis for cardiomyopathy: from mutation identification to mechanistic paradigms. Cell. 2001;104(4):557–67.
43. Nakamura M, Sadoshima J. Mechanisms of physiological and pathological cardiac hypertrophy. Nat Rev Cardiol. 2018;15(7):387–407. https://doi.org/10.1038/s41569-018-0007-y.

44. Sadoshima J, Qiu Z, Morgan JP, Izumo S. Angiotensin II and other hypertrophic stimuli mediated by G protein-coupled receptors activate tyrosine kinase, mitogen-activated protein kinase, and 90-kD S6 kinase in cardiac myocytes. The critical role of Ca(2+)-dependent signaling. Circ Res. 1995;76(1):1–15.
45. Knollmann BC, Potter JD. Altered regulation of cardiac muscle contraction by troponin T mutations that cause familial hypertrophic cardiomyopathy. Trends Cardiovasc Med. 2001;11 (5):206–12. https://doi.org/10.1016/s1050-1738(01)00115-3.
46. Baudenbacher F, Schober T, Pinto JR, Sidorov VY, Hilliard F, Solaro RJ, et al. Myofilament Ca2+ sensitization causes susceptibility to cardiac arrhythmia in mice. J Clin Invest. 2008;118 (12):3893–903. https://doi.org/10.1172/JCI36642.
47. Mehta PK, Griendling KK. Angiotensin II cell signaling: physiological and pathological effects in the cardiovascular system. Am J Physiol Cell Physiol. 2007;292(1):C82–97. https://doi.org/10.1152/ajpcell.00287.2006.
48. Salazar NC, Chen J, Rockman HA. Cardiac GPCRs: GPCR signaling in healthy and failing hearts. Biochim Biophys Acta. 2007;1768(4):1006–18. https://doi.org/10.1016/j.bbamem.2007.02.010.
49. Wang J, Gareri C, Rockman HA. G-protein-coupled receptors in heart disease. Circ Res. 2018;123(6):716–35. https://doi.org/10.1161/CIRCRESAHA.118.311403.
50. Manning BD, Toker A. AKT/PKB signaling: navigating the network. Cell. 2017;169(3): 381–405. https://doi.org/10.1016/j.cell.2017.04.001.
51. Cantley LC. The phosphoinositide 3-kinase pathway. Science. 2002;296(5573):1655–7. https://doi.org/10.1126/science.296.5573.1655.
52. Sugden PH, Fuller SJ, Weiss SC, Clerk A. Glycogen synthase kinase 3 (GSK3) in the heart: a point of integration in hypertrophic signalling and a therapeutic target? A critical analysis. Br J Pharmacol. 2008;153(Suppl 1):S137–53. https://doi.org/10.1038/sj.bjp.0707659.
53. Condorelli G, Morisco C, Latronico MV, Claudio PP, Dent P, Tsichlis P, et al. TNF-alpha signal transduction in rat neonatal cardiac myocytes: definition of pathways generating from the TNF-alpha receptor. FASEB J. 2002;16(13):1732–7. https://doi.org/10.1096/fj.02-0419com.
54. Proud CG. Ras, PI3-kinase and mTOR signaling in cardiac hypertrophy. Cardiovasc Res. 2004;63(3):403–13. https://doi.org/10.1016/j.cardiores.2004.02.003.
55. Wang Y. Mitogen-activated protein kinases in heart development and diseases. Circulation. 2007;116(12):1413–23. https://doi.org/10.1161/CIRCULATIONAHA.106.679589.
56. Owens DM, Keyse SM. Differential regulation of MAP kinase signalling by dual-specificity protein phosphatases. Oncogene. 2007;26(22):3203–13. https://doi.org/10.1038/sj.onc.1210412.
57. Kim S, Iwao H. Activation of mitogen-activated protein kinases in cardiovascular hypertrophy and remodeling. Jpn J Pharmacol. 1999;80(2):97–102.
58. Aikawa R, Nagai T, Kudoh S, Zou Y, Tanaka M, Tamura M, et al. Integrins play a critical role in mechanical stress-induced p38 MAPK activation. Hypertension. 2002;39(2):233–8.
59. Vinay DS, Kwon BS. TNF superfamily: costimulation and clinical applications. Cell Biol Int. 2009;33(4):453–65. https://doi.org/10.1016/j.cellbi.2009.02.001.
60. Li H, Mittal A, Paul PK, Kumar M, Srivastava DS, Tyagi SC, et al. Tumor necrosis factor-related weak inducer of apoptosis augments matrix metalloproteinase 9 (MMP-9) production in skeletal muscle through the activation of nuclear factor-kappaB-inducing kinase and p38 mitogen-activated protein kinase: a potential role of MMP-9 in myopathy. J Biol Chem. 2009;284(7):4439–50. https://doi.org/10.1074/jbc.M805546200.
61. Gordon JW, Shaw JA, Kirshenbaum LA. Multiple facets of NF-kappaB in the heart: to be or not to NF-kappaB. Circ Res. 2011;108(9):1122–32. https://doi.org/10.1161/CIRCRESAHA.110.226928.
62. Valente M, Calabrese F, Thiene G, Angelini A, Basso C, Nava A, et al. In vivo evidence of apoptosis in arrhythmogenic right ventricular cardiomyopathy. Am J Pathol. 1998;152(2): 479–84.

63. Kataoka T, Budd RC, Holler N, Thome M, Martinon F, Irmler M, et al. The caspase-8 inhibitor FLIP promotes activation of NF-kappaB and Erk signaling pathways. Curr Biol. 2000;10(11):640–8. https://doi.org/10.1016/s0960-9822(00)00512-1.
64. Devin A, Lin Y, Liu ZG. The role of the death-domain kinase RIP in tumour-necrosis-factor-induced activation of mitogen-activated protein kinases. EMBO Rep. 2003;4(6):623–7. https://doi.org/10.1038/sj.embor.embor854.
65. Gill C, Mestril R, Samali A. Losing heart: the role of apoptosis in heart disease--a novel therapeutic target? FASEB J. 2002;16(2):135–46. https://doi.org/10.1096/fj.01-0629com.
66. Kim NH, Kang PM. Apoptosis in cardiovascular diseases: mechanism and clinical implications. Korean Circ J. 2010;40(7):299–305. https://doi.org/10.4070/kcj.2010.40.7.299.
67. Narula J, Pandey P, Arbustini E, Haider N, Narula N, Kolodgie FD, et al. Apoptosis in heart failure: release of cytochrome c from mitochondria and activation of caspase-3 in human cardiomyopathy. Proc Natl Acad Sci U S A. 1999;96(14):8144–9.
68. Torre-Amione G, Kapadia S, Lee J, Durand JB, Bies RD, Young JB, et al. Tumor necrosis factor-alpha and tumor necrosis factor receptors in the failing human heart. Circulation. 1996;93(4):704–11.
69. Khalid N, Azimpouran M. Necrosis. Treasure Island: StatPearls; 2021.
70. Tonnus W, Meyer C, Paliege A, Belavgeni A, von Massenhausen A, Bornstein SR, et al. The pathological features of regulated necrosis. J Pathol. 2019;247(5):697–707. https://doi.org/10.1002/path.5248.
71. Zhu H, Sun A. Programmed necrosis in heart disease: molecular mechanisms and clinical implications. J Mol Cell Cardiol. 2018;116:125–34. https://doi.org/10.1016/j.yjmcc.2018.01.018.
72. Sen-Chowdhry S, Syrris P, Prasad SK, Hughes SE, Merrifield R, Ward D, et al. Left-dominant arrhythmogenic cardiomyopathy: an under-recognized clinical entity. J Am Coll Cardiol. 2008;52(25):2175–87. https://doi.org/10.1016/j.jacc.2008.09.019.
73. Corrado D, Basso C, Thiene G, McKenna WJ, Davies MJ, Fontaliran F, et al. Spectrum of clinicopathologic manifestations of arrhythmogenic right ventricular cardiomyopathy/dysplasia: a multicenter study. J Am Coll Cardiol. 1997;30(6):1512–20. https://doi.org/10.1016/s0735-1097(97)00332-x.
74. Kim C, Wong J, Wen J, Wang S, Wang C, Spiering S, et al. Studying arrhythmogenic right ventricular dysplasia with patient-specific iPSCs. Nature. 2013;494(7435):105–10. https://doi.org/10.1038/nature11799.
75. Garcia-Gras E, Lombardi R, Giocondo MJ, Willerson JT, Schneider MD, Khoury DS, et al. Suppression of canonical Wnt/beta-catenin signaling by nuclear plakoglobin recapitulates phenotype of arrhythmogenic right ventricular cardiomyopathy. J Clin Invest. 2006;116(7):2012–21. https://doi.org/10.1172/JCI27751.
76. Glick D, Barth S, Macleod KF. Autophagy: cellular and molecular mechanisms. J Pathol. 2010;221(1):3–12. https://doi.org/10.1002/path.2697.
77. Yu L, Chen Y, Tooze SA. Autophagy pathway: cellular and molecular mechanisms. Autophagy. 2018;14(2):207–15. https://doi.org/10.1080/15548627.2017.1378838.
78. Liu H, Xie Q, Xin BM, Liu JL, Liu Y, Li YZ, et al. Inhibition of autophagy recovers cardiac dysfunction and atrophy in response to tail-suspension. Life Sci. 2015;121:1–9. https://doi.org/10.1016/j.lfs.2014.10.023.
79. Maiuri MC, Zalckvar E, Kimchi A, Kroemer G. Self-eating and self-killing: crosstalk between autophagy and apoptosis. Nat Rev Mol Cell Biol. 2007;8(9):741–52. https://doi.org/10.1038/nrm2239.
80. Nishida K, Kyoi S, Yamaguchi O, Sadoshima J, Otsu K. The role of autophagy in the heart. Cell Death Diff. 2009;16(1):31–8. https://doi.org/10.1038/cdd.2008.163.
81. O'Hanlon R, Grasso A, Roughton M, Moon JC, Clark S, Wage R, et al. Prognostic significance of myocardial fibrosis in hypertrophic cardiomyopathy. J Am Coll Cardiol. 2010;56(11):867–74. https://doi.org/10.1016/j.jacc.2010.05.010.

82. Chung H, Kim Y, Park CH, Kim JY, Min PK, Yoon YW, et al. Effect of sarcomere and mitochondria-related mutations on myocardial fibrosis in patients with hypertrophic cardiomyopathy. J Cardiovasc Magn Reson. 2021;23(1):18. https://doi.org/10.1186/s12968-021-00718-3.
83. Schram K, De Girolamo S, Madani S, Munoz D, Thong F, Sweeney G. Leptin regulates MMP-2, TIMP-1 and collagen synthesis via p38 MAPK in HL-1 murine cardiomyocytes. Cell Mol Biol Lett. 2010;15(4):551–63. https://doi.org/10.2478/s11658-010-0027-z.
84. Schalla S, Bekkers SC, Dennert R, van Suylen RJ, Waltenberger J, Leiner T, et al. Replacement and reactive myocardial fibrosis in idiopathic dilated cardiomyopathy: comparison of magnetic resonance imaging with right ventricular biopsy. Eur J Heart Fail. 2010;12(3):227–31. https://doi.org/10.1093/eurjhf/hfq004.
85. Frangogiannis NG. Cardiac fibrosis: cell biological mechanisms, molecular pathways and therapeutic opportunities. Mol Aspects Med. 2019;65:70–99. https://doi.org/10.1016/j.mam.2018.07.001.
86. Griendling KK, Sorescu D, Ushio-Fukai M. NAD(P)H oxidase: role in cardiovascular biology and disease. Circ Res. 2000;86(5):494–501. https://doi.org/10.1161/01.res.86.5.494.
87. Huang S, Chen B, Su Y, Alex L, Humeres C, Shinde AV, et al. Distinct roles of myofibroblast-specific Smad2 and Smad3 signaling in repair and remodeling of the infarcted heart. J Mol Cell Cardiol. 2019;132:84–97. https://doi.org/10.1016/j.yjmcc.2019.05.006.
88. Creemers EE, Pinto YM. Molecular mechanisms that control interstitial fibrosis in the pressure-overloaded heart. Cardiovasc Res. 2011;89(2):265–72. https://doi.org/10.1093/cvr/cvq308.
89. Accornero F, van Berlo JH, Correll RN, Elrod JW, Sargent MA, York A, et al. Genetic analysis of connective tissue growth factor as an effector of transforming growth factor beta signaling and cardiac remodeling. Mol Cell Biol. 2015;35(12):2154–64. https://doi.org/10.1128/MCB.00199-15.
90. Dorn LE, Petrosino JM, Wright P, Accornero F. CTGF/CCN2 is an autocrine regulator of cardiac fibrosis. J Mol Cell Cardiol. 2018;121:205–11. https://doi.org/10.1016/j.yjmcc.2018.07.130.
91. Shi Y, Massague J. Mechanisms of TGF-beta signaling from cell membrane to the nucleus. Cell. 2003;113(6):685–700.
92. Dolivo DM, Larson SA, Dominko T. Crosstalk between mitogen-activated protein kinase inhibitors and transforming growth factor-beta signaling results in variable activation of human dermal fibroblasts. Int J Mol Med. 2019;43(1):325–35. https://doi.org/10.3892/ijmm.2018.3949.
93. Hata A, Chen YG. TGF-beta signaling from receptors to Smads. Cold Spring Harb Perspect Biol. 2016;8(9). doi: https://doi.org/10.1101/cshperspect.a022061.
94. Hanna A, Humeres C, Frangogiannis NG. The role of Smad signaling cascades in cardiac fibrosis. Cell Signal. 2021;77:109826. https://doi.org/10.1016/j.cellsig.2020.109826.
95. Khalil H, Kanisicak O, Prasad V, Correll RN, Fu X, Schips T, et al. Fibroblast-specific TGF-beta-Smad2/3 signaling underlies cardiac fibrosis. J Clin Invest. 2017;127(10):3770–83. https://doi.org/10.1172/JCI94753.
96. Amano M, Fukata Y, Kaibuchi K. Regulation and functions of Rho-associated kinase. Exp Cell Res. 2000;261(1):44–51. https://doi.org/10.1006/excr.2000.5046.
97. Cristancho AG, Lazar MA. Forming functional fat: a growing understanding of adipocyte differentiation. Nat Rev Mol Cell Biol. 2011;12(11):722–34. https://doi.org/10.1038/nrm3198.
98. Kaczynski J, Cook T, Urrutia R. Sp1- and Kruppel-like transcription factors. Genome Biol. 2003;4(2):206. https://doi.org/10.1186/gb-2003-4-2-206.
99. Yuping Y, Hua C, Qing Z. Advances in the relationship between Kruppel-like factor 15 and cardiovascular disease research. Cardiovasc Endocrinol Metab. 2018;7(2):37–41. https://doi.org/10.1097/XCE.0000000000000140.

100. Wang B, Haldar SM, Lu Y, Ibrahim OA, Fisch S, Gray S, et al. The Kruppel-like factor KLF15 inhibits connective tissue growth factor (CTGF) expression in cardiac fibroblasts. J Mol Cell Cardiol. 2008;45(2):193–7. https://doi.org/10.1016/j.yjmcc.2008.05.005.
101. Shindo T, Manabe I, Fukushima Y, Tobe K, Aizawa K, Miyamoto S, et al. Kruppel-like zinc-finger transcription factor KLF5/BTEB2 is a target for angiotensin II signaling and an essential regulator of cardiovascular remodeling. Nat Med. 2002;8(8):856–63. https://doi.org/10.1038/nm738.
102. Lu F, Pu WT. The architecture and function of cardiac dyads. Biophys Rev. 2020;12(4):1007–17. https://doi.org/10.1007/s12551-020-00729-x.
103. Schartner V, Laporte J, Bohm J. Abnormal excitation-contraction coupling and calcium homeostasis in myopathies and cardiomyopathies. J Neuromuscul Dis. 2019;6(3):289–305. https://doi.org/10.3233/JND-180314.
104. Bers DM. Calcium cycling and signaling in cardiac myocytes. Annu Rev Physiol. 2008;70:23–49. https://doi.org/10.1146/annurev.physiol.70.113006.100455.
105. Wickenden AD, Kaprielian R, Kassiri Z, Tsoporis JN, Tsushima R, Fishman GI, et al. The role of action potential prolongation and altered intracellular calcium handling in the pathogenesis of heart failure. Cardiovasc Res. 1998;37(2):312–23. https://doi.org/10.1016/s0008-6363(97)00256-3.
106. Petitprez S, Zmoos AF, Ogrodnik J, Balse E, Raad N, El-Haou S, et al. SAP97 and dystrophin macromolecular complexes determine two pools of cardiac sodium channels Nav1.5 in cardiomyocytes. Circ Res. 2011;108(3):294–304. https://doi.org/10.1161/CIRCRESAHA.110.228312.
107. Glukhov AV, Fedorov VV, Kalish PW, Ravikumar VK, Lou Q, Janks D, et al. Conduction remodeling in human end-stage nonischemic left ventricular cardiomyopathy. Circulation. 2012;125(15):1835–47. https://doi.org/10.1161/CIRCULATIONAHA.111.047274.
108. Lambiase PD, Tinker A. Connexins in the heart. Cell Tissue Res. 2015;360(3):675–84. https://doi.org/10.1007/s00441-014-2020-8.
109. Saffitz JE. The pathobiology of arrhythmogenic cardiomyopathy. Ann Rev Pathol. 2011;6:299–321. https://doi.org/10.1146/annurev-pathol-011110-130151.
110. Cerrone M, Delmar M. Desmosomes and the sodium channel complex: implications for arrhythmogenic cardiomyopathy and Brugada syndrome. Trends Cardiovasc Med. 2014;24(5):184–90. https://doi.org/10.1016/j.tcm.2014.02.001.
111. Towbin JA, Bowles NE. The failing heart. Nature. 2002;415(6868):227–33. https://doi.org/10.1038/415227a.
112. Cahill TJ, Ashrafian H, Watkins H. Genetic cardiomyopathies causing heart failure. Circ Res. 2013;113(6):660–75. https://doi.org/10.1161/CIRCRESAHA.113.300282.
113. Rodriguez-Sinovas A, Sanchez JA, Valls-Lacalle L, Consegal M, Ferreira-Gonzalez I. Connexins in the heart: regulation, function and involvement in cardiac disease. Int J Mol Sci. 2021;22(9):4413. https://doi.org/10.3390/ijms22094413.
114. Seferovic PM, Polovina M, Bauersachs J, Arad M, Gal TB, Lund LH, et al. Heart failure in cardiomyopathies: a position paper from the Heart Failure Association of the European Society of Cardiology. Eur J Heart Fail. 2019;21(5):553–76. https://doi.org/10.1002/ejhf.1461.
115. Gigli M, Sinagra G, Mestroni L. Gene therapy in heart failure: the unexpected results from the CUPID 2 trial. G Ital Cardiol (Rome). 2017;18(2):101–5. https://doi.org/10.1714/2663.27295.
116. Knott GJ, Doudna JA. CRISPR-Cas guides the future of genetic engineering. Science. 2018;361(6405):866–9. https://doi.org/10.1126/science.aat5011.
117. Matson CW, Clark BW, Jenny MJ, Fleming CR, Hahn ME, Di Giulio RT. Development of the morpholino gene knockdown technique in Fundulus heteroclitus: a tool for studying molecular mechanisms in an established environmental model. Aquat Toxicol. 2008;87(4):289–95. https://doi.org/10.1016/j.aquatox.2008.02.010.
118. Shan G. RNA interference as a gene knockdown technique. Int J Biochem Cell Biol. 2010;42(8):1243–51. https://doi.org/10.1016/j.biocel.2009.04.023.

119. Cordier L, Hack AA, Scott MO, Barton-Davis ER, Gao G, Wilson JM, et al. Rescue of skeletal muscles of gamma-sarcoglycan-deficient mice with adeno-associated virus-mediated gene transfer. Mol Ther. 2000;1(2):119–29. https://doi.org/10.1006/mthe.1999.0019.
120. Rutschow D, Bauer R, Gohringer C, Bekeredjian R, Schinkel S, Straub V, et al. S151A delta-sarcoglycan mutation causes a mild phenotype of cardiomyopathy in mice. Eur J Hum Genet. 2014;22(1):119–25. https://doi.org/10.1038/ejhg.2013.97.
121. Araishi K, Sasaoka T, Imamura M, Noguchi S, Hama H, Wakabayashi E, et al. Loss of the sarcoglycan complex and sarcospan leads to muscular dystrophy in beta-sarcoglycan-deficient mice. Hum Mol Genet. 1999;8(9):1589–98. https://doi.org/10.1093/hmg/8.9.1589.
122. Miyagoe-Suzuki Y, Nakagawa M, Takeda S. Merosin and congenital muscular dystrophy. Microsc Res Tech. 2000;48(3-4):181–91. https://doi.org/10.1002/(SICI)1097-0029(20000201/15)48:3/4<181::AID-JEMT6>3.0.CO;2-Q.
123. Sicinski P, Geng Y, Ryder-Cook AS, Barnard EA, Darlison MG, Barnard PJ. The molecular basis of muscular dystrophy in the mdx mouse: a point mutation. Science. 1989;244(4912):1578–80.
124. Guyon JR, Mosley AN, Zhou Y, O'Brien KF, Sheng X, Chiang K, et al. The dystrophin associated protein complex in zebrafish. Hum Mol Genet. 2003;12(6):601–15.
125. Jones BR, Brennan S, Mooney CT, Callanan JJ, McAllister H, Guo LT, et al. Muscular dystrophy with truncated dystrophin in a family of Japanese Spitz dogs. J Neurol Sci. 2004;217(2):143–9.
126. Yoshida M, Hama H, Ishikawa-Sakurai M, Imamura M, Mizuno Y, Araishi K, et al. Biochemical evidence for association of dystrobrevin with the sarcoglycan-sarcospan complex as a basis for understanding sarcoglycanopathy. Hum Mol Genet. 2000;9(7):1033–40.
127. Woodman SE, Park DS, Cohen AW, Cheung MW, Chandra M, Shirani J, et al. Caveolin-3 knock-out mice develop a progressive cardiomyopathy and show hyperactivation of the p42/44 MAPK cascade. J Biol Chem. 2002;277(41):38988–97. https://doi.org/10.1074/jbc.M205511200.
128. Kuga A, Ohsawa Y, Okada T, Kanda F, Kanagawa M, Toda T, et al. Endoplasmic reticulum stress response in P104L mutant caveolin-3 transgenic mice. Hum Mol Genet. 2011;20(15):2975–83. https://doi.org/10.1093/hmg/ddr201.
129. Nixon SJ, Wegner J, Ferguson C, Mery PF, Hancock JF, Currie PD, et al. Zebrafish as a model for caveolin-associated muscle disease; caveolin-3 is required for myofibril organization and muscle cell patterning. Hum Mol Genet. 2005;14(13):1727–43. https://doi.org/10.1093/hmg/ddi179.
130. Kamisago M, Schmitt JP, McNamara D, Seidman C, Seidman JG. Sarcomere protein gene mutations and inherited heart disease: a beta-cardiac myosin heavy chain mutation causing endocardial fibroelastosis and heart failure. Novartis Found Symp. 2006;274:176–89.
131. Xu X, Meiler SE, Zhong TP, Mohideen M, Crossley DA, Burggren WW, et al. Cardiomyopathy in zebrafish due to mutation in an alternatively spliced exon of titin. Nat Genet. 2002;30(2):205–9. https://doi.org/10.1038/ng816.
132. Rethinasamy P, Muthuchamy M, Hewett T, Boivin G, Wolska BM, Evans C, et al. Molecular and physiological effects of alpha-tropomyosin ablation in the mouse. Circ Res. 1998;82(1):116–23.
133. Rajan S, Ahmed RP, Jagatheesan G, Petrashevskaya N, Boivin GP, Urboniene D, et al. Dilated cardiomyopathy mutant tropomyosin mice develop cardiac dysfunction with significantly decreased fractional shortening and myofilament calcium sensitivity. Circ Res. 2007;101(2):205–14. https://doi.org/10.1161/CIRCRESAHA.107.148379.
134. Prabhakar R, Boivin GP, Grupp IL, Hoit B, Arteaga G, Solaro RJ, et al. A familial hypertrophic cardiomyopathy alpha-tropomyosin mutation causes severe cardiac hypertrophy and death in mice. J Mol Cell Cardiol. 2001;33(10):1815–28. https://doi.org/10.1006/jmcc.2001.1445.

135. Muthuchamy M, Pieples K, Rethinasamy P, Hoit B, Grupp IL, Boivin GP, et al. Mouse model of a familial hypertrophic cardiomyopathy mutation in alpha-tropomyosin manifests cardiac dysfunction. Circ Res. 1999;85(1):47–56.
136. Tardiff JC, Factor SM, Tompkins BD, Hewett TE, Palmer BM, Moore RL, et al. A truncated cardiac troponin T molecule in transgenic mice suggests multiple cellular mechanisms for familial hypertrophic cardiomyopathy. J Clin Invest. 1998;101(12):2800–11. https://doi.org/10.1172/JCI2389.
137. Tardiff JC, Hewett TE, Palmer BM, Olsson C, Factor SM, Moore RL, et al. Cardiac troponin T mutations result in allele-specific phenotypes in a mouse model for hypertrophic cardiomyopathy. J Clin Invest. 1999;104(4):469–81. https://doi.org/10.1172/JCI6067.
138. Sehnert AJ, Huq A, Weinstein BM, Walker C, Fishman M, Stainier DY. Cardiac troponin T is essential in sarcomere assembly and cardiac contractility. Nat Genet. 2002;31(1):106–10. https://doi.org/10.1038/ng875.
139. James J, Zhang Y, Osinska H, Sanbe A, Klevitsky R, Hewett TE, et al. Transgenic modeling of a cardiac troponin I mutation linked to familial hypertrophic cardiomyopathy. Circ Res. 2000;87(9):805–11.
140. Sanbe A, James J, Tuzcu V, Nas S, Martin L, Gulick J, et al. Transgenic rabbit model for human troponin I-based hypertrophic cardiomyopathy. Circulation. 2005;111(18):2330–8. https://doi.org/10.1161/01.CIR.0000164234.24957.75.
141. Huang X, Pi Y, Lee KJ, Henkel AS, Gregg RG, Powers PA, et al. Cardiac troponin I gene knockout: a mouse model of myocardial troponin I deficiency. Circ Res. 1999;84(1):1–8.
142. Yang Q, Sanbe A, Osinska H, Hewett TE, Klevitsky R, Robbins J. A mouse model of myosin binding protein C human familial hypertrophic cardiomyopathy. J Clin Invest. 1998;102(7):1292–300. https://doi.org/10.1172/JCI3880.
143. Palmer BM, McConnell BK, Li GH, Seidman CE, Seidman JG, Irving TC, et al. Reduced cross-bridge dependent stiffness of skinned myocardium from mice lacking cardiac myosin binding protein-C. Mol Cell Biochem. 2004;263(1–2):73–80.
144. Meurs KM, Sanchez X, David RM, Bowles NE, Towbin JA, Reiser PJ, et al. A cardiac myosin binding protein C mutation in the Maine Coon cat with familial hypertrophic cardiomyopathy. Hum Mol Genet. 2005;14(23):3587–93. https://doi.org/10.1093/hmg/ddi386.
145. Wang X, Osinska H, Dorn GW 2nd, Nieman M, Lorenz JN, Gerdes AM, et al. Mouse model of desmin-related cardiomyopathy. Circulation. 2001;103(19):2402–7.
146. Li M, Andersson-Lendahl M, Sejersen T, Arner A. Knockdown of desmin in zebrafish larvae affects interfilament spacing and mechanical properties of skeletal muscle. J Gen Physiol. 2013;141(3):335–45. https://doi.org/10.1085/jgp.201210915.
147. Milner DJ, Weitzer G, Tran D, Bradley A, Capetanaki Y. Disruption of muscle architecture and myocardial degeneration in mice lacking desmin. J Cell Biol. 1996;134(5):1255–70. https://doi.org/10.1083/jcb.134.5.1255.
148. Purevjav E, Arimura T, Augustin S, Huby AC, Takagi K, Nunoda S, et al. Molecular basis for clinical heterogeneity in inherited cardiomyopathies due to myopalladin mutations. Hum Mol Genet. 2012;21(9):2039–53. https://doi.org/10.1093/hmg/dds022.
149. Arber S, Hunter JJ, Ross J Jr, Hongo M, Sansig G, Borg J, et al. MLP-deficient mice exhibit a disruption of cardiac cytoarchitectural organization, dilated cardiomyopathy, and heart failure. Cell. 1997;88(3):393–403.
150. Purevjav E, Varela J, Morgado M, Kearney DL, Li H, Taylor MD, et al. Nebulette mutations are associated with dilated cardiomyopathy and endocardial fibroelastosis. J Am Coll Cardiol. 2010;56(18):1493–502. https://doi.org/10.1016/j.jacc.2010.05.045.
151. Hassel D, Dahme T, Erdmann J, Meder B, Huge A, Stoll M, et al. Nexilin mutations destabilize cardiac Z-disks and lead to dilated cardiomyopathy. Nat Med. 2009;15(11):1281–8. https://doi.org/10.1038/nm.2037.
152. Knoll R, Linke WA, Zou P, Miocic S, Kostin S, Buyandelger B, et al. Telethonin deficiency is associated with maladaptation to biomechanical stress in the mammalian heart. Circ Res. 2011;109(7):758–69. https://doi.org/10.1161/CIRCRESAHA.111.245787.

153. Zhang R, Yang J, Zhu J, Xu X. Depletion of zebrafish Tcap leads to muscular dystrophy via disrupting sarcomere-membrane interaction, not sarcomere assembly. Hum Mol Genet. 2009;18(21):4130–40. https://doi.org/10.1093/hmg/ddp362.
154. Zhou Q, Chu PH, Huang C, Cheng CF, Martone ME, Knoll G, et al. Ablation of Cypher, a PDZ-LIM domain Z-line protein, causes a severe form of congenital myopathy. J Cell Biol. 2001;155(4):605–12. https://doi.org/10.1083/jcb.200107092.
155. Song Y, Xu J, Li Y, Jia C, Ma X, Zhang L, et al. Cardiac ankyrin repeat protein attenuates cardiac hypertrophy by inhibition of ERK1/2 and TGF-beta signaling pathways. PLoS One. 2012;7(12):e50436. https://doi.org/10.1371/journal.pone.0050436.
156. Bang ML, Gu Y, Dalton ND, Peterson KL, Chien KR, Chen J. The muscle ankyrin repeat proteins CARP, Ankrd2, and DARP are not essential for normal cardiac development and function at basal conditions and in response to pressure overload. PLoS One. 2014;9(4):e93638. https://doi.org/10.1371/journal.pone.0093638.
157. Thomas SA, Schuessler RB, Berul CI, Beardslee MA, Beyer EC, Mendelsohn ME, et al. Disparate effects of deficient expression of connexin43 on atrial and ventricular conduction: evidence for chamber-specific molecular determinants of conduction. Circulation. 1998;97(7):686–91.
158. Ewart JL, Cohen MF, Meyer RA, Huang GY, Wessels A, Gourdie RG, et al. Heart and neural tube defects in transgenic mice overexpressing the Cx43 gap junction gene. Development. 1997;124(7):1281–92.
159. Yang Z, Bowles NE, Scherer SE, Taylor MD, Kearney DL, Ge S, et al. Desmosomal dysfunction due to mutations in desmoplakin causes arrhythmogenic right ventricular dysplasia/cardiomyopathy. Circ Res. 2006;99(6):646–55. https://doi.org/10.1161/01.RES.0000241482.19382.c6.
160. Grossmann KS, Grund C, Huelsken J, Behrend M, Erdmann B, Franke WW, et al. Requirement of plakophilin 2 for heart morphogenesis and cardiac junction formation. J Cell Biol. 2004;167(1):149–60. https://doi.org/10.1083/jcb.200402096.
161. Heuser A, Plovie ER, Ellinor PT, Grossmann KS, Shin JT, Wichter T, et al. Mutant desmocollin-2 causes arrhythmogenic right ventricular cardiomyopathy. Am J Hum Genet. 2006;79(6):1081–8. https://doi.org/10.1086/509044.
162. Pilichou K, Remme CA, Basso C, Campian ME, Rizzo S, Barnett P, et al. Myocyte necrosis underlies progressive myocardial dystrophy in mouse dsg2-related arrhythmogenic right ventricular cardiomyopathy. J Exp Med. 2009;206(8):1787–802. https://doi.org/10.1084/jem.20090641.
163. Krusche CA, Holthofer B, Hofe V, van de Sandt AM, Eshkind L, Bockamp E, et al. Desmoglein 2 mutant mice develop cardiac fibrosis and dilation. Basic Res Cardiol. 2011;106(4):617–33. https://doi.org/10.1007/s00395-011-0175-y.
164. Martin ED, Moriarty MA, Byrnes L, Grealy M. Plakoglobin has both structural and signalling roles in zebrafish development. Dev Biol. 2009;327(1):83–96. https://doi.org/10.1016/j.ydbio.2008.11.036.
165. Kirchhof P, Fabritz L, Zwiener M, Witt H, Schafers M, Zellerhoff S, et al. Age- and training-dependent development of arrhythmogenic right ventricular cardiomyopathy in heterozygous plakoglobin-deficient mice. Circulation. 2006;114(17):1799–806. https://doi.org/10.1161/CIRCULATIONAHA.106.624502.
166. Manso AM, Li R, Monkley SJ, Cruz NM, Ong S, Lao DH, et al. Talin1 has unique expression versus talin 2 in the heart and modifies the hypertrophic response to pressure overload. J Biol Chem. 2013;288(6):4252–64. https://doi.org/10.1074/jbc.M112.427484.
167. Fujita M, Mitsuhashi H, Isogai S, Nakata T, Kawakami A, Nonaka I, et al. Filamin C plays an essential role in the maintenance of the structural integrity of cardiac and skeletal muscles, revealed by the medaka mutant zacro. Dev Biol. 2012;361(1):79–89. https://doi.org/10.1016/j.ydbio.2011.10.008.

168. Ho CY, Jaalouk DE, Vartiainen MK, Lammerding J. Lamin A/C and emerin regulate MKL1-SRF activity by modulating actin dynamics. Nature. 2013;497(7450):507–11. https://doi.org/10.1038/nature12105.
169. Sullivan T, Escalante-Alcalde D, Bhatt H, Anver M, Bhat N, Nagashima K, et al. Loss of A-type lamin expression compromises nuclear envelope integrity leading to muscular dystrophy. J Cell Biol. 1999;147(5):913–20. https://doi.org/10.1083/jcb.147.5.913.
170. Palmiter KA, Tyska MJ, Haeberle JR, Alpert NR, Fananapazir L, Warshaw DM. R403Q and L908V mutant beta-cardiac myosin from patients with familial hypertrophic cardiomyopathy exhibit enhanced mechanical performance at the single molecule level. J Muscle Res Cell Motil. 2000;21(7):609–20. https://doi.org/10.1023/a:1005678905119.
171. Wang L, Seidman JG, Seidman CE. Narrative review: harnessing molecular genetics for the diagnosis and management of hypertrophic cardiomyopathy. Ann Intern Med. 2010;152(8):513–20. https://doi.org/10.7326/0003-4819-152-8-201004200-00008.
172. Mosqueira D, Smith JGW, Bhagwan JR, Denning C. Modeling hypertrophic cardiomyopathy: mechanistic insights and pharmacological intervention. Trends Mol Med. 2019;25(9):775–90. https://doi.org/10.1016/j.molmed.2019.06.005.
173. Musumeci B, Tini G, Russo D, Sclafani M, Cava F, Tropea A, et al. Left ventricular remodeling in hypertrophic cardiomyopathy: an overview of current knowledge. J Clin Med. 2021;10(8):1547. https://doi.org/10.3390/jcm10081547.
174. Zhao W, Zhao T, Chen Y, Zhao F, Gu Q, Williams RW, et al. A murine hypertrophic cardiomyopathy model: the DBA/2J strain. PLoS One. 2015;10(8):e0133132. https://doi.org/10.1371/journal.pone.0133132.
175. Chen Y, Xu F, Munkhsaikhan U, Boyle C, Borcky T, Zhao W, et al. Identifying modifier genes for hypertrophic cardiomyopathy. J Mol Cell Cardiol. 2020;144:119–26. https://doi.org/10.1016/j.yjmcc.2020.05.006.
176. Gannon MP, Link MS. Phenotypic variation and targeted therapy of hypertrophic cardiomyopathy using genetic animal models. Trends Cardiovasc Med. 2021;31(1):20–31. https://doi.org/10.1016/j.tcm.2019.11.009.
177. Ross J Jr. Dilated cardiomyopathy: concepts derived from gene deficient and transgenic animal models. Circ J. 2002;66(3):219–24. https://doi.org/10.1253/circj.66.219.
178. McNally EM, Mestroni L. Dilated cardiomyopathy: genetic determinants and mechanisms. Circ Res. 2017;121(7):731–48. https://doi.org/10.1161/CIRCRESAHA.116.309396.
179. Vejandla RM, Orgil B-O, Alberson NR, Li N, Munkhsaikhan U, Khuchua Z, Martherus R, Azeloglu EU, Fuyi X, Lu L, Towbin JA, Purevjav E. Deficiency in nebulin repeats of sarcomeric nebulette is detrimental for cardiomyocyte tolerance to exercise and biomechanical stress. Am J Phys Heart Circ Phys. 2021;320(5):H2130–46. https://doi.org/10.1152/ajpheart.00732.2020.
180. Guo W, Schafer S, Greaser ML, Radke MH, Liss M, Govindarajan T, et al. RBM20, a gene for hereditary cardiomyopathy, regulates titin splicing. Nat Med. 2012;18(5):766–73. https://doi.org/10.1038/nm.2693.
181. Huang XP, Du JF. Troponin I, cardiac diastolic dysfunction and restrictive cardiomyopathy. Acta Pharmacol Sin. 2004;25(12):1569–75.
182. Liu X, Zhang L, Pacciulli D, Zhao J, Nan C, Shen W, et al. Restrictive cardiomyopathy caused by troponin mutations: application of disease animal models in translational studies. Front Physiol. 2016;7:629. https://doi.org/10.3389/fphys.2016.00629.
183. Padron-Barthe L, Dominguez F, Garcia-Pavia P, Lara-Pezzi E. Animal models of arrhythmogenic right ventricular cardiomyopathy: what have we learned and where do we go? Insight for therapeutics. Basic Res Cardiol. 2017;112(5):50. https://doi.org/10.1007/s00395-017-0640-3.
184. Gerull B, Brodehl A. Genetic animal models for arrhythmogenic cardiomyopathy. Front Physiol. 2020;11:624. https://doi.org/10.3389/fphys.2020.00624.
185. Orgil B-O, Munkhsaikhan U, Pierre JF, Li N, Fuyi X, Alberson NR, Johnson JN, Wetzel GT, Boukens BJD, Lu L, Towbin JA, Purevjav E. The TMEM43 S358L mutation affects cardiac

small intestine and metabolic homeostasis in a knock-in mouse model. Am J Phys Heart Circ Phys. 2023;324(6):H866–80. https://doi.org/10.1152/ajpheart.00712.2022.
186. D'Amato G, Luxan G, de la Pompa JL. Notch signalling in ventricular chamber development and cardiomyopathy. FEBS J. 2016;283(23):4223–37. https://doi.org/10.1111/febs.13773.
187. Luxan G, Casanova JC, Martinez-Poveda B, Prados B, D'Amato G, MacGrogan D, et al. Mutations in the NOTCH pathway regulator MIB1 cause left ventricular noncompaction cardiomyopathy. Nat Med. 2013;19(2):193–201. https://doi.org/10.1038/nm.3046.
188. Chen H, Shi S, Acosta L, Li W, Lu J, Bao S, et al. BMP10 is essential for maintaining cardiac growth during murine cardiogenesis. Development. 2004;131(9):2219–31. https://doi.org/10.1242/dev.01094.
189. Kodo K, Ong SG, Jahanbani F, Termglinchan V, Hirono K, InanlooRahatloo K, et al. iPSC-derived cardiomyocytes reveal abnormal TGF-beta signalling in left ventricular non-compaction cardiomyopathy. Nat Cell Biol. 2016;18(10):1031–42. https://doi.org/10.1038/ncb3411.
190. Pashmforoush M, Lu JT, Chen H, Amand TS, Kondo R, Pradervand S, et al. Nkx2-5 pathways and congenital heart disease; loss of ventricular myocyte lineage specification leads to progressive cardiomyopathy and complete heart block. Cell. 2004;117(3):373–86.
191. de la Pompa JL, Timmerman LA, Takimoto H, Yoshida H, Elia AJ, Samper E, et al. Role of the NF-ATc transcription factor in morphogenesis of cardiac valves and septum. Nature. 1998;392(6672):182–6. https://doi.org/10.1038/32419.
192. Phoon CK, Acehan D, Schlame M, Stokes DL, Edelman-Novemsky I, Yu D, et al. Tafazzin knockdown in mice leads to a developmental cardiomyopathy with early diastolic dysfunction preceding myocardial noncompaction. J Am Heart Assoc. 2012;1(2):jah3. https://doi.org/10.1161/JAHA.111.000455.
193. Sen-Chowdhry S, Syrris P, Pantazis A, Quarta G, McKenna WJ, Chambers JC. Mutational heterogeneity modifier genes and environmental influences contribute to phenotypic diversity of arrhythmogenic cardiomyopathy. Circ Cardiovasc Genet. 2010;3(4):323–30. https://doi.org/10.1161/CIRCGENETICS.109.935262.
194. Chandrasekera PC, Pippin JJ. The human subject: an integrative animal model for 21(st) century heart failure research. Am J Transl Res. 2015;7(9):1636–47.
195. Molenhuis RT, Bruining H, Brandt MJV, van Soldt PE, Abu-Toamih Atamni HJ, Burbach JPH, Iraqi FA, Mott RF, Kas MJH. Modeling the quantitative nature of neurodevelopmental disorders using collaborative cross mice. Mol Autism. 2018;9(1). https://doi.org/10.1186/s13229-018-0252-2.
196. Qingqing G, Mendsaikhan U, Khuchua Z, Jones BC, Lu L, Towbin JA, Biao X, Purevjav E. Dissection of Z-disc myopalladin gene network involved in the development of restrictive cardiomyopathy using system genetics approach. World J Cardiol. 2017;9(4):320. https://doi.org/10.4330/wjc.v9.i4.320.
197. Qingqing G, Fuyi X, Orgil B-O, Khuchua Z, Munkhsaikhan U, Johnson JN, Alberson NR, Pierre JF, Black DD, Dong D, Brennan JA, Cathey BM, Efimov IR, Towbin JA, Purevjav E, Lu L. Systems genetics analysis defines importance of TMEM43/ LUMA for cardiac- and metabolic-related pathways. Physiol Genomics. 2022;54(1):22–35. https://doi.org/10.1152/physiolgenomics.00066.2021.
198. Adriaens ME, Lodder EM, Moreno-Moral A, Šilhavý J, Heinig M, Glinge C, Belterman C, Wolswinkel R, Petretto E, Pravenec M, Remme CA, Bezzina CR. Systems genetics approaches in rat identify novel genes and gene networks associated with cardiac conduction. J Am Heart Assoc. 2018;7(21). https://doi.org/10.1161/JAHA.118.009243.
199. Orgil B-O, Fuyi X, Munkhsaikhan U, Alberson NR, Bajpai AK, Johnson JN, Sun Y, Towbin JA, Lu L, Purevjav E. Echocardiography phenotyping in murine genetic reference population of BXD strains reveals significant QTLs associated with cardiac function and morphology. Physiol Genomics. 2023;55(2):51–66. https://doi.org/10.1152/physiolgenomics.00120.2022.

200. Lodder EM, Scicluna BP, Milano A, Sun AY, Tang H, Remme CA, Moerland PD, Tanck MWT, Pitt GS, Marchuk DA, Bezzina CR. Dissection of a quantitative trait locus for PR interval duration identifies Tnni3k as a novel modulator of cardiac conduction. PLoS Genet. 2012;8(12):e1003113. https://doi.org/10.1371/journal.pgen.1003113.
201. Gu Q, Orgil B-O, Bajpai AK, Chen Y, Ashbrook DG, Starlard-Davenport A, Towbin JA, Lebeche D, Purevjav E, Sheng H, Lu L. Expression levels of the Tnni3k gene in the heart are highly associated with cardiac and glucose metabolism-related phenotypes and functional pathways. Int J Mol Sci. 2023;24(16):12759. https://doi.org/10.3390/ijms241612759.

Part XVIII

Arrhythmias

Clinical Presentation and Therapy of Arrhythmias

65

Nikolaus A. Haas, David J. Driscoll, and Silke Rickert-Sperling

65.1 The Normal ECG

The electrocardiogram (ECG) is one of the cornerstones of diagnostic investigations in pediatric or adult cardiology. The standard ECG includes 12 leads; there are 6 leads that are derived from electrodes from the arms and legs (Einthoven and Goldberger leads) and 6 precordial leads (Wilson leads).

The normal cardiac rhythm originates from the sinus node that is located at the junction of the superior vena cava and the right atrium (Fig. 65.1). The cells of the sinus node exhibit spontaneous depolarization which is the reason that those cells function as the primary pacemaker of the heart. Depolarization of these cells activates myocardial cells of the right atrium. Depolarization of atrial cells produces the "p-wave" of the ECG. The electrical activity of the atria reaches the ventricle by traveling through the atrioventricular node (AV) and the bundle of His. Conduction through the AV node is relatively slow and this accounts for the "PR" interval which is the isoelectric period on the ECG between the end of the p-wave and the q-wave of the QRS complex. The QRS complex represents the depolarization of the cells of the ventricles, and the T-wave represents the repolarization ventricular myocardium.

N. A. Haas (✉)
Department of Pediatric Cardiology and Intensive Care, Ludwig Maximilians University, Munich, Germany
e-mail: Nikolaus.haas@med.uni-muenchen.de

D. J. Driscoll
Division of Pediatric Cardiology, Department of Pediatrics, Mayo Clinic College of Medicine, Rochester, MN, USA
e-mail: driscoll.david@mayo.edu

S. Rickert-Sperling
Cardiovascular Genetics, Charité – Universitätsmedizin Berlin, Berlin, Germany
e-mail: silke.sperling@charite.de

© The Author(s), under exclusive license to Springer Nature Switzerland AG 2024

S. Rickert-Sperling et al. (eds.), *Congenital Heart Diseases: The Broken Heart*, Advances in Experimental Medicine and Biology 1441,
https://doi.org/10.1007/978-3-031-44087-8_65

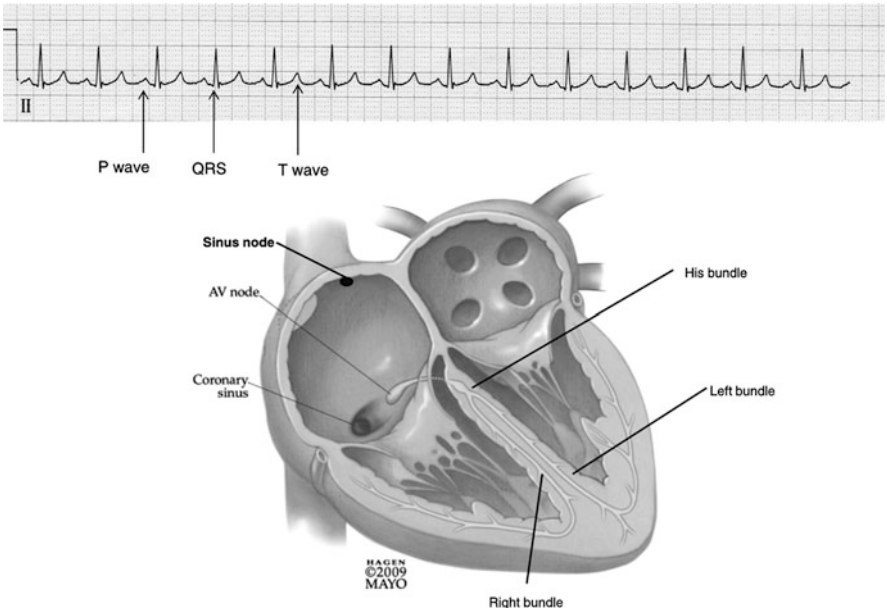

Fig. 65.1 Cardiac diagram depicting the electrical conduction system. Normal ECG

The electrical activity of each part of the heart is reflected in typical leads and so one can differentiate the affected part of the heart, for example in the case of ischemia, based on the typical ECG changes. Besides the arrhythmias, there are typical patterns of ECG changes that are linked to typical cardiac diseases such as infarction, myocarditis, pericarditis, or special forms of cardiomyopathies.

65.2 Introduction

Arrhythmias can be classified based upon the site of origin of the arrhythmia (supraventricular or ventricular), the heart rate of the arrhythmia (tachyarrhythmia or bradyarrhythmia), the function or dysfunction of the AV node (atrioventricular block or dissociation), or the underlying mechanism of the arrhythmia (reentry or bypass tract, automatic focus, ion channel defect).

Tachyarrhythmias originating from above the ventricles are termed supraventricular tachycardias and include various forms of atrial tachycardia, AV node reentry tachycardia, and tachycardia resulting from an accessory pathway (e.g., Wolff–Parkinson–White syndrome, Fig. 65.2). Atrial fibrillation and atrial flutter, technically, are supraventricular arrhythmias but usually are simply referred to as atrial fibrillation and atrial flutter. Tachyarrhythmias originating from the ventricles are termed ventricular tachycardias; they include ventricular fibrillation and are the most relevant tachycardias leading to sudden cardiac death (SCD).

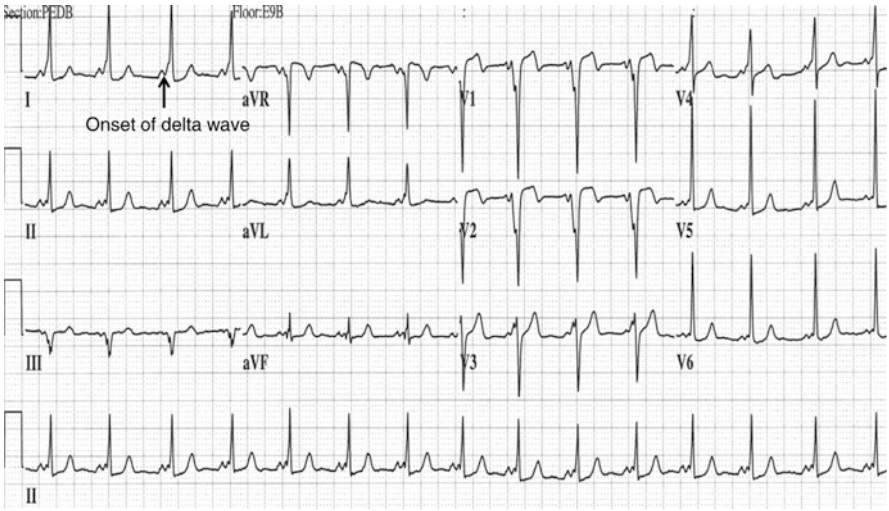

Fig. 65.2 This is an example of Wolff–Parkinson–White syndrome. Note the short PR interval and the delta wave (Reproduced or adapted from Driscoll D (2006) *Fundamentals of Pediatric Cardiology*. Lippincott Williams & Wilkins, with permission of the author and publisher)

Bradyarrhythmias (where the heart rate is too slow) can result from sinus node disease or AV node disease. In the latter case, the heart rate is slow because conduction through the AV node is abnormal. These bradyarrhythmias include first-, second-, and third-degree atrioventricular block. In first-degree atrioventricular block, the PR interval is prolonged but the heart rate is normal. In second-degree block, some, but not all, of the atrial beats are conducted to the ventricles, and in third-degree block, none of the atrial beats are conducted to the ventricle.

There are a number of arrhythmia syndromes that can be inherited, and these frequently can be associated with syncope, seizures, and sudden death. Many of these conditions result from mutations in genes encoding critical ion channels in the heart and will be discussed in this chapter.

65.3 Channelopathies

Channelopathies, a term coined by Dr. Michael Ackerman, occur in approximately 1 in 1000 individuals. These conditions, along with other inherited abnormalities of ion channels, can be caused by mutations in specific genes. Additionally, they can be induced or acquired as a result of other disorders, drugs, or toxins.

Mutations in genes encoding ion channels can lead to dysfunction in the ion channel subunits or their interacting proteins. Each type of channel is composed of subunits encoded by multiple genes. Depending on the specific mutation, the defect may affect ion selectivity, signal transduction, gating, or conductance of the channel. In cardiovascular physiology, the electrical impulse in heart cells relies on the

electrochemical gradient generated by ion channels. Cardiac channelopathies can cause altered repolarization, increasing the risk of malignant ventricular arrhythmias, syncope, and cardiac death.

The long-QT syndrome, a channelopathy, results in characteristic ECG changes that can be detected by surface ECG. There are different forms of the long QT syndrome, including Jervell and Lange–Nielsen syndrome and Romano–Ward syndrome. Other cardiovascular channelopathies include the short QT syndrome, Brugada syndrome, catecholaminergic polymorphic ventricular tachycardia (CPVT), Anderson–Tawil syndrome, Timothy syndrome, drug-induced torsades de pointes, progressive cardiac conduction disease or Lev-Lenegre disease, and familial atrial fibrillation.

65.4 Long QT Syndrome

Long QT syndrome (LQTS) is a channelopathy (Fig. 65.3) that affects the repolarization process. Initially, two forms were identified and named Jervell and Lange–Nielsen syndrome (autosomal recessive) and Romano–Ward syndrome (autosomal dominant). Subsequently, numerous mutations in 16 LQTS susceptibility genes have been discovered. The estimated incidence of LQTS ranges from 1 in 2500 to 1 in 7000 people. The majority of cases are caused by mutations in *KCNQ1* (LQT1), *KCNH2* (LQT2), and *SCN5A* (LQT3).

Traditionally, a prolonged QT interval on the electrocardiogram (ECG) served as the hallmark and diagnostic marker for LQTS. However, the introduction of genetic testing has revealed that 40–50% of patients who test positive for pathogenic mutations may have a normal QT interval on the ECG.

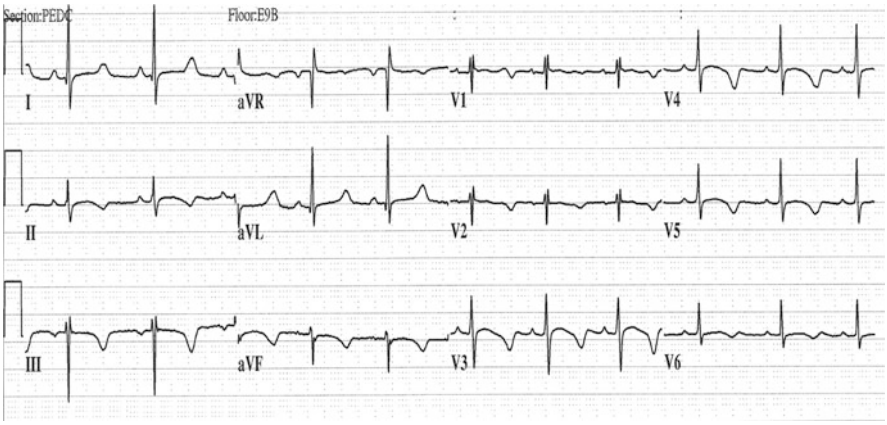

Fig. 65.3 This is an example of QT prolongation. Note that the T-wave is more distant from the preceding QRS than is normal (Reproduced or adapted from Driscoll D (2006) *Fundamentals of Pediatric Cardiology*. Lippincott Williams & Wilkins, with permission of the author and publisher)

LQTS increases the risk of typical ventricular arrhythmias, such as torsades des pointes, leading to transient loss of cardiac output and symptoms such as fainting, drowning, seizures, or cardiac death. These episodes are typically triggered by exercise or stress. Rare forms of LQTS may also be associated with deafness or muscle weakness. There are over 17 described genetic variations, with most LQTS cases being inherited in a dominant manner.

The hallmark sign is the prolongation of the QT interval, hence the name of the syndrome. However, there is significant overlap between the corrected QT interval (QTc) in normal individuals and patients with LQTS. The QTc is derived from Bazett's formula, where QTc = QT interval divided by the square root of the RR interval. In general, a QTc greater than 480 ms in postpubertal females or greater than 470 ms in postpubertal males raises the probability of LQTS. These values represent the 99th percentile for QT intervals. However, in the absence of a personal history of LQTS-triggered events or family history, the increased probability of LQTS remains below the tenth percentile chance. According to guidelines from the American Heart Association and American College of Cardiology, a QTc ≥450 ms in adult males and ≥ 460 ms in adult females is defined as a "prolonged QTc." However, approximately 50% of genetically confirmed LQTS patients will have a QTc value lower than these cutoffs, and 20% of normal individuals would exceed these cutoffs.

In addition to genetic testing, the clinical diagnosis of LQTS is based on a combination of family and personal history factors and ECG changes, as described by the Schwarz score (Fig. 65.4). A score of 0–1 indicates a low probability of LQTS, a score of 2–3 suggests an intermediate probability, and a score ≥ 4 indicates a high probability.

Treatment for all types of LQTS includes lifestyle modifications, appropriate antiarrhythmic therapy (such as beta blockers or sodium blocking agents), and, if necessary, the implantation of an ICD (implantable cardioverter-defibrillator). Other treatment modalities may involve surgical amputation of the left-sided ganglion stellatum to interrupt the cervical sympathetic pathways.

Corrected QT interval (QTc)	≥ 480 ms	3 points	QTc defined according to Bazett's correction
	460–470 ms	2 points	
	450 ms and male gender	1 point	
Torsades de pointes		2 points	
T-wave alternans		1 point	
Notched T-waves in at least 3 leads		1 point	
Low heart rate for age (children)		0.5 points	
Syncope	with stress	2 points	Cannot receive points both for syncope and Torsades
	without stress	1 point	
Congenital deafness		0.5 points	
Family history	Other family member with confirmed LQTS	1 point	Same family member cannot be counted for LQTS and sudden death
	Sudden cardiac death in immediate family member aged <30	0.5 point	
Score: 0–1 : low probability of LQTS; 2–3 : intermediate probability of LQTS; ≥ 4 : high probability of LQTS			

Fig. 65.4 The Schwarz score is a clinical scoring system used to assess the likelihood of Long QT Syndrome (LQTS). It combines family and personal history factors with ECG changes to determine the probability of LQTS. The score ranges from 0 to 9, with higher scores indicating a higher probability of LQTS

65.4.1 Rare Romano–Ward Syndrome (LQT4–6 and LQT9–16)

Romano–Ward syndrome encompasses various subtypes of Long QT Syndrome (LQTS) with distinct genetic mutations. LQTS 1 is the most prevalent subtype, accounting for approximately 30 to 35% of all cases, and it involves an affected potassium channel. LQTS 2 is the second most common form, affecting 25–30% of individuals, and also involves a potassium channel dysfunction. LQTS 3 is characterized by abnormalities in a sodium channel, and there is some overlap with the Brugada syndrome. Additionally, there are other variations known as LQTS types 4–6 and 9–16.

65.4.2 Jervell and Lange–Nielsen Syndrome

Jervell and Lange–Nielsen syndrome (JLNS) is a rare variant of LQTS. It was the first form of LQTS to be documented with an ECG recording in patients presenting with seizures and sudden cardiac death, along with profound sensorineural deafness affecting both ears. JLNS is characterized by a combination of LQTS 1 and LQTS 5, and individuals with this syndrome are at a higher risk of developing arrhythmias compared to other forms of LQTS.

65.4.3 Andersen–Tawil Syndrome (LQT7)

LQTS 7, also known as Andersen–Tawil syndrome (ATS), is characterized by three distinct clinical features. Firstly, there are ventricular arrhythmias resulting from prolonged QT interval. Secondly, periodic episodes of weakness or paralysis occur when potassium levels are low, known as hypokalemic periodic paralysis. Lastly, individuals with ATS may exhibit dysmorphic features, including facial and skeletal abnormalities. This syndrome is caused by mutations in the *KCNJ2* gene, which encodes a potassium channel protein. ATS represents a unique channelopathy that establishes a connection between cardiac and skeletal muscle excitability.

65.4.4 Timothy Syndrome (LQTS 8)

Timothy syndrome, also known as LQTS 8, is characterized by QT prolongation and the presence of lethal arrhythmias. Individuals with Timothy syndrome may also exhibit syndactyly (fusion of fingers or toes). Additional congenital heart defects such as Tetralogy of Fallot, ventricular septal defect (VSD), or hypertrophic cardiomyopathy (HCM) have been reported. Other associated features include immune deficiency, hypoglycemia, and cognitive disorders within the autism spectrum. Timothy syndrome is caused by a mutation in a calcium channel gene (*CACNA1C*), highlighting the role of calcium channels in the development of this condition.

65.5 Short QT Syndrome

Short QT syndrome (SQTS) is an extremely rare disease characterized by a shortened QT interval observed on the ECG, defined as a QTc $\leq$ 330–340 ms. It follows an autosomal dominant inheritance pattern and results from a gain of function in ion channels within the heart cells. Currently, approximately 6 variants influencing potassium influx and calcium outflux have been identified. Patients with short QT syndrome may present with symptoms such as sudden death, syncope, and palpitations. In some cases, atrial fibrillation may manifest in neonates. Many individuals affected by this condition have a family history of premature sudden death. Treatment typically involves the use of quinidine and the implantation of an ICD (implantable cardioverter-defibrillator).

65.6 Catecholaminergic Polymorphic Ventricular Tachycardia

Catecholaminergic polymorphic ventricular tachycardia (CPVT) is a condition associated with life-threatening arrhythmias, such as ventricular fibrillation or tachycardia, which typically occur during or after emotional or physical stress, including exercise. Common clinical presentations include dizziness, sudden blackouts, syncope, or sudden death. CPVT is primarily caused by a mutation in the RYR2 gene, which encodes the cardiac ryanodine receptor or calcium release channel. In rare cases, homozygous or compound heterozygous mutations involving *CASQ2*, which encodes calsequestrin, can also lead to CPVT.

Typically, CPVT is diagnosed in the second decade of life based on the patient's clinical history and confirmed through ECG monitoring during exercise, followed by genetic testing. Some individuals may exhibit sinus bradycardia or atrial fibrillation at rest. The incidence of CPVT is approximately 1 in 10,000 people, and it may account for about 10 to 15% of unexplained sudden cardiac deaths in young individuals.

Treatment options for CPVT include the use of beta-blockers to reduce sympathetic effects on the heart, often combined with flecainide, a class 1a antiarrhythmic drug. This combination has shown reliable results in preventing arrhythmias. Lifestyle modifications are also recommended. In cases where antiarrhythmic medication fails, sympathetic denervation may be indicated. Finally, an implantable cardioverter-defibrillator (ICD) may be considered for refractory cases.

65.6.1 Brugada Syndrome

Brugada syndrome is an autosomal dominant inherited ion channel disease with a variable incidence, estimated to be around 1 in 10,000 in Europe and higher in Asian countries. It primarily affects young, otherwise healthy men and typically manifests in the fourth decade of life. Diagnosis of Brugada syndrome is based on the characteristic ECG pattern, which includes ST segment elevation in leads V1–3

accompanied by a right bundle branch block (RBBB). This pattern may only appear under certain conditions such as fever, exercise, or triggered by certain events, including drugs. Dedicated tests, such as Ajmaline provocation tests, and specific ECG leads are used to confirm the diagnosis of the ECG changes. There is some overlap between Brugada syndrome and LQTS 3.

There are currently over 25 known susceptibility genes associated with Brugada syndrome, with loss-of-function mutations in the SCN5A sodium channel being the most common genetic cause, accounting for about 20% of cases. Brugada syndrome is associated with an increased risk of sudden death, and in Asia, it is believed to be the most common cause of natural death in young men under the age of 50, with different names given to this phenomenon in different Asian countries. Family screening plays a crucial role in identifying individuals at risk.

There is no specific antiarrhythmic treatment for Brugada syndrome, and therefore, lifestyle modifications are advised to reduce the incidence of serious arrhythmias. These modifications may include avoiding excessive alcohol consumption, certain medications, and early treatment of fever with paracetamol. Individuals at higher risk may be treated with an implantable cardioverter-defibrillator (ICD). Testing asymptomatic family members is recommended to identify potential carriers of the genetic mutation.

65.6.2 Lev-Lenègre Disease

Lev disease, also known as Lenègre disease or progressive cardiac conduction disease, is an acquired form of atrioventricular (AV) block characterized by idiopathic fibrosis and subsequent calcification of the AV node. It primarily affects the elderly population. There is also a variant of Lev disease known as Lenègre disease, which tends to present in younger patients. Both forms, including Lev-Lenègre disease, can be associated with a mutation on chromosome 3p21. The cardiac sodium channel gene, *SCN5A*, is located on chromosome 3p21, and several mutations in *SCN5A* have been linked to AV conduction block. It has been proposed that in Lenègre disease, a combination of haploinsufficiency (reduced gene expression) and aging contributes to a progressive decline in conduction.

65.6.3 Wolff–Parkinson–White Syndrome

Wolff–Parkinson–White (WPW) syndrome is a condition characterized by the presence of an accessory electrical pathway between the atria and ventricles, leading to a distinct ECG pattern with a shortened PR interval and a delta wave (Fig. 65.2). While the majority of WPW cases are sporadic without a known genetic background, a small number of cases are associated with a mutation in the *PRKAG2* gene, which can be inherited in an autosomal dominant fashion, making it possible for WPW syndrome to be familial in some instances.

The primary mechanism underlying WPW syndrome is the presence of this accessory pathway, which allows for early electrical transmission of atrial impulses

to the ventricles, resulting in the characteristic ECG findings. In addition to the ECG abnormalities, WPW syndrome may be associated with other congenital heart defects such as Ebstein's anomaly or congenitally corrected TGA, as well as other syndromes such as hypokalemic periodic paralysis. Clinically, WPW syndrome manifests as episodes of abrupt onset tachycardia with heart rates exceeding 200 beats per minute, leading to impaired stroke volume and symptoms such as dizziness, fainting, and syncope.

Treatment for WPW syndrome typically involves the use of antiarrhythmic medications to control and prevent episodes of supraventricular tachycardia. In some cases, electrophysiological studies may be performed to identify and selectively destroy the accessory pathway through a procedure called catheter ablation. Overall, the prognosis for individuals with WPW syndrome is generally good with appropriate management and treatment.

65.7 Diagnosis

In many cases, the type of arrhythmia can be ascertained from the surface electrocardiographic tracing. In rare cases, an intracardiac electrophysiologic study may be necessary to precisely define the type and underlying mechanism of the arrhythmia. In general, supraventricular arrhythmias are more benign than ventricular arrhythmias.

65.8 Treatment

The treatment of any arrhythmia depends upon an accurate definition of the type and mechanism of the specific arrhythmia. The spectrum of treatment includes observation, drug therapy, electrical or pharmacologic cardioversion, pacemaker insertion, radiofrequency ablation, automatic internal cardiac defibrillator, cardiac surgery, and in very unusual circumstances, cardiac transplantation. It is important to determine if an arrhythmia or an arrhythmia syndrome is potentially inheritable since, in those cases, it is critical to screen family members for the condition. It also is important to search for potentially inheritable arrhythmias in family members of subjects who have unexplained early or sudden death, drowning deaths, and other deaths that occurred in unusual circumstances.

65.9 Outcome

Outcome of treatment of arrhythmias depends upon the type of arrhythmia and whether it is an isolated arrhythmia or is associated with congenital heart disease or myocardial disease.

Human Genetics of Cardiac Arrhythmias

66

Eric Schulze-Bahr and Sven Dittmann

Abstract

Inherited forms of cardiac arrhythmias mostly are rare diseases (prevalence <1: 2000) and considered to be either "primary electrical heart disorders" due to the absence of structural heart abnormalities or "cardiac ion channel disorders" due to the myocellular structures involved. Precise knowledge of the electrocardiographic features of these diseases and their genetic classification will enable early disease recognition and prevention of cardiac events including sudden cardiac death.

The genetic background of these diseases is complex and heterogeneous. In addition to the predominant "private character" of a mutation in each family, locus heterogeneity involving many ion channel genes for the same familial arrhythmia syndrome is typical. Founder pathogenic variants or mutational hot spots are uncommon. Moreover, phenotypes may vary and overlap even within the same family and mutation carriers. For the majority of arrhythmias, the clinical phenotype of an ion channel mutation is restricted to cardiac tissue, and therefore, the disease is nonsyndromic.

Recent and innovative methods of parallel DNA analysis (so-called next-generation sequencing, NGS) will enhance further mutation and other variant detection as well as arrhythmia gene identification.

Keywords

Familial arrhythmias · Inherited arrhythmias · Ion channel · Primary electrical disorder · Long-QT syndrome · LQTS · Brugada syndrome · Catecholaminergic

E. Schulze-Bahr (✉) · S. Dittmann
Department of Cardiovascular Medicine, Institute for Genetics of Heart Diseases (IfGH), University Hospital Münster, Münster, Germany
e-mail: eric.schulze-bahr@ukmuenster.de

© The Author(s), under exclusive license to Springer Nature Switzerland AG 2024

S. Rickert-Sperling et al. (eds.), *Congenital Heart Diseases: The Broken Heart*,
Advances in Experimental Medicine and Biology 1441,
https://doi.org/10.1007/978-3-031-44087-8_66

polymorphic ventricular tachycardia · CPVT · Short-QT syndrome · SQTS · Idiopathic ventricular fibrillation · Sudden cardiac death · SCD

66.1 Introduction: Inherited Forms of Cardiac Arrhythmias

The field of cardiac arrhythmias and pathophysiologic insights into arrhythmogenesis has dramatically matured, driven, in the last two decades, by the in-depth understanding of inherited forms of arrhythmia. Components of cardiac ion channels have been identified that are the clues to cardiac action potential generation and inherited forms of primary electrical heart diseases.

Many identified pathogenic variants are "private" (i.e., family specific). Pinpoint protein regions of the native ion channel that cause ion channel dysfunction have been identified and may allow modification by drugs. Pathophysiological and common disease pathways can be recreated in patient-derived cellular models (human-induced pluripotent stem cells, hiPSCs) and transdifferentiated cardiomyocyte-like cells that share the patient's genetic setting and are subjected to comprehensive biomedical research.

Nearly every inherited arrhythmia is genetically heterogeneous. For some primary electrical disorders (PEDs) of the heart, more than 10 different genes or associated loci are known (e.g., long-QT syndrome, atrial or ventricular fibrillation). In addition, there is significant allelic heterogeneity (e.g., >300 different LQTS pathogenic variants). In contrast, in some PEDs the mutation detection rate ("sensitivity of a genetic test") is still low (e.g., atrial or ventricular fibrillation, 10–20%) raising the issue of clinical phenotypic conditions. Therefore, precise knowledge and recognition of the genetic forms of PEDs are essential, including differentiation from non-genetic forms. In the light of existing genetic heterogeneity, but also of unforeseen genetic complexity in known disease genes, next-generation sequencing (NGS) technologies will improve modern genetic diagnostics. Together with sufficient pathogenicity variant prediction, this parallelized gene analysis (e.g., several hundreds of genes for a distinct phenotype in a single analysis run) will further replace DNA analysis depending on Sanger sequencing approaches. However, apart from delineating the genomic complexity of monogenic cardiac disorders, it is likely that upon NGS analyses, cardiovascular genes not being previously linked to the patient's phenotype will be addressed and novel genes may be identified. Importantly, additional confirmatory research steps are required to establish a relationship between a novel gene and the phenotype (Table 66.1).

66.2 Congenital Long-QT Syndrome (LQTS)

LQTS is characterized by prolongation of the QT interval, typically measured in a baseline 12-lead or exercise ECG (recommended speed, 50 mm/s). These values have to be corrected for heart rate (by using Bazett's formula to drive the corrected

Table 66.1 Inherited forms of cardiac arrhythmias and implications of genetic testing

Disease	Mutation detection rate (sensitivity)	Implication of a pathogenic genetic finding		Reference
		Diagnostic	Therapeutic/ prognostic	
Long-QT syndrome (LQTS)	70–80%	+++	+++/+++	ClinGen MonDO: 0002442 [1]
Brugada syndrome (BrS)	20–30%	+	+/++	ClinGen MonDO: 0015263 [2]
Catecholaminergic polymorphic ventricular tachycardia (CPVT)	50–60%	+++	++/+	ClinGen MonDO: 0017990 [3]
Short-QT syndrome (SQTS)	25%	+	+/+	ClinGen MonDO: 0015263 [3]
Idiopathic ventricular fibrillation (IVF, SCA)	20–30%	++	++	[4, 5]
Early repolarization syndrome (ERS)	?	–	–/–	[6, 7]
Short-coupled torsade de pointes tachycardia (scTdP)	?	+	+/–	[8, 9]
Sinus node disease (SND)	?	–	+/–	
Cardiac conduction disease (CCD/PCCD)	10–20%	+	+/+	[10]
Atrial fibrillation	?	–	–/–	[10]
Sudden cardiac death, unclear (SIDS, SADS, SUDS, SUNDS, SCD)	10–30%	++		[11–16]

CCD, Cardiac conduction disease; *PCCD*, Progressive cardiac conduction disease; *SND*, Sinus node disease; *SADS*, Sudden arrhythmic death syndrome; *SCA*, Sudden cardiac arrest; *SCD*, Sudden cardiac death; *SIDS*, Sudden infant death syndrome; *SUDS*, Sudden unexpected death syndrome; *SUNDS*, Sudden unexpected nocturnal death syndrome

QTc value). A QTc of >450 ms (males) or >460 ms (females) is indicative of an LQTS, but there is overlap with the normal population. The presence of interventricular conduction delay such as complete right or left bundle branch block may limit the use of the QT interval. The QT interval can also be affected by many drugs. In contrast to congenital LQTS, drug-induced QT prolongation ("acquired LQTS") is often not genetic, and only in 10–15% of case can the drug be considered to have unmasked "hidden LQTS." For many physicians, recognition of LQTS and accurate QT interval measurements are still difficult [17].

Due to cascade family investigations and systematic genetic testing, it now has become clear that there are many LQTS mutation carriers without symptoms [18]. These asymptomatic but LQTS mutation-positive patients still have congenital LQTS, even though the term "syndrome" might be misleading. In a series of 1710 LQTS cases, the mean QTc interval was QTc 471 ± 45 ms, but a large portion had a normal QTc interval below 460 ms (genetic subtypes: 47% LQT1, 36% LQT2, and 35% LQT3) [18]. The overall risk for cardiac events or arrest might be lower and mainly is determined by the degree of QT interval prolongation and exposure to risk or event-triggering factors [19, 20]. A mutation analysis is essential not only in patients with evident LQTS but also in asymptomatic family members with normal QTc interval (i.e., <440–460 ms) who have a tenfold increased risk of cardiac events in comparison to non-carriers [19].

The type of mutation and the location of the mutation within the particular channel domains have been proposed to impact on the underlying biophysical defect and, subsequently, on severity of the disease [18, 21]. However, the clinical utility of such information has not yet been validated. The obvious variability of clinical presentation among carriers of the same LQTS mutation, even in the same family, initiated studies to investigate the role of single-nucleotide polymorphisms (SNPs) for disease modulation. So far, rare SNP alleles have been investigated in LQTS patients and in the general population and have been proposed to influence repolarization [22–24], but unlikely in drug-induced forms of QT interval prolongation [25]. Further studies are needed to show the impact on clinical decision-making upon SNP genotyping, since the overall effect of minor SNP alleles on the QTc interval usually is small (<5 ms).

In 2020, Adler et al. revalidated the disease causality and relationship of so far published gens for long-QT syndrome (LQTS) regarding the ClinGen requirements [1]. Only three genes (*KCNQ1*, chr. 11p15.5: ~35% of all cases; *KCNH2,* chr. 7q36.1: ~30%; and *SCN5A,* chr. 3p22.2: ~10–15%) identified with definitive evidence.

One additional gene is associated with syndromal forms of LQTS (+ extracardiac clinical signs): *CACNA1C (*definitive for Timothy syndrome) with moderate evidence for typical LQTS. Limited disease genes for typical LQTS are *KCNJ2* (but definitive for syndromal Andersen-Tawil syndrome), *KCNE1* (strong for atypical LQTS), and *CAV3*. Another four genes associated with atypical LQTS, where prolongation is connected with neonatal heart block of autosomal-recessive inheritance, had definitive or strong evidence (definitive: *CALM1* (calmodulin 1), *CALM2* (calmodulin 2), and *CALM3* (calmodulin 3); strong: *TRDN* (triadin)) [1]. In case of *KCNE2*, this gene was disputed for LQTS, but if secondary provoking factors are present, there is some evidence for atypical LQTS [26] (Table 66.2).

Pathogenic variants in *KCNQ1* as a cause for the LQT1 subtype lead to a decreased gene product level or altered gene product sequence. In consequence, this leads to loss of function by defects in ion permeation, channel gating, and channel trafficking. It has been noted that approximately 5–10% of genotype-positive LQTS patients have more than one pathogenic variant in the same or another LQTS-related gene [27, 28]. Digenic or biallelic disease appears to be

Table 66.2 Inherited forms of LQTS

Isolated (cardiac) forms ClinGen MonDO: 0002442			
LQTS	**Core genes (mutation detection rate > 1%)**	**Rare genes (<1%)**	**Reference**
	KCNQ1 (LQT1), KCNH2 (LQT2), SCN5A (LQT3)	*CACNA1C, CALM1, CALM2, CALM3, KCNE1, KCNJ2, (RYR2) TRDN* (autosomal rec.)	[1]
Syndromal forms			
	Gene	**Clinical signs**	**Mode of inheritance reference**
Jervell and Lange-Nielsen syndrome (JLNS)	*KCNQ1, KCNE1*	*Congenital hearing loss*	AR [1]
Timothy syndrome (TS)	*CACNA1C*	*Partial syndactyly, flat nasal bridge, low-set ears, small upper jaw, narrow upper lip, autism*	AD, sporadic [1]
Andersen-Tawil syndrome (ATS)	*KCNJ2*	*Periodic paralysis, short stature, scoliosis, deep-set ears, hypertelorism, broad nasal root, micrognathia, clinodactyly, brachydactyly, and syndactyly*	AD [1]

AD Autosomal dominant; *AR* Autosomal recessive

more penetrant with a more severe phenotype. Non-synonymous variants are responsible for the majority of *KCNQ1*-related LQTS cases, often by a dominant-negative effect and a more severe phenotype [29] than variants conferring haploinsufficiency. Of note, truncating variants including nonsense, frameshift, splice site, and structural variants (CNVs; multi exon deletions and a multi exon duplication (in-frame tandem repeat of exons 3–6, leading to duplication of the second to fifth transmembrane domains of the channel)) are rarely noted and also reported [27, 30, 31].

KCNQ1-related phenotypes can differ according to regionality with some regions associated with more malignant phenotypes; e.g., C-loop variants are suggested to be associated with a higher risk of sudden cardiac death [32].

KCNH2-related LQTS is due to decreased gene product level or altered gene product sequence. The disease mechanism is again a loss of function, similarly to the LQT1 subtype, and caused by both haploinsufficiency or a dominant-negative effect, i.e., of the mutant on the wild-type protein. About 60% of LQT2 pathogenic variants are non-synonymous variants; the remaining 40% are nonsense, frameshift, insertions, deletions, and duplications (intragenic tandem duplication) or involve a splice site. *KCNH2* variants account for approximately 30% of LQTS cases. Recently, Walsh et al. showed that non-truncating variants in *KCNH2* are enriched in the transmembranous encoding domains of ion channel and specific N-terminal

and C-terminal domains and have a >95% probability of pathogenicity [33]. Shimizu et al. reported on correlations between specific variant types, gene location, and clinical phenotype [34]: patients with non-synonymous variants in the transmembrane pore region have a significantly higher cardiac event rate than those with non-synonymous variants in the N-terminus, transmembrane non-pore, or C-terminus regions. It has been noted that approximately 10% of genotype-positive LQT patients have more than one pathogenic variant in one or more LQTS genes; biallelic or digenic pathogenic variants appear to be generally associated with a more severe phenotype with longer QTc intervals and a higher incidence of cardiac events.

In contrast, only an altered but not reduced gene product sequence of *SCN5A* causes long-QT syndrome of the subtype LQT3. The likely disease mechanism is gain-of-function. So far, over 200 pathogenic non-synonymous variants and in-frame deletions or insertions have been reported. The sodium current mediated by Nav1.5 consists of peak and late current components ($I_{Na\text{-}P}$ and $I_{Na\text{-}L}$), and thereby, gain-of-function variants were shown to enhance either $I_{Na\text{-}P}$ or $I_{Na\text{-}L}$, which can trigger life-threatening arrhythmias. *SCN5A*-related LQTS accounts for 5–10% of LQTS cases [35]. *SCN5A*-related LQTS can present with specific overlapping phenotypes: patients may have marked resting bradycardia, QT interval prolongation more pronounced during slow heart rate (which might explain why arrhythmic events occur more frequently at rest), a first cardiac event that is lethal, and onset after puberty [36].

If a non-synonymous *SCN5A* pathogenic variant has also in vitro loss-of-function properties, e.g., the p.Glu1784Lys variant which is a quite common one, a mixed phenotype with LQT3, conduction disease, and Brugada syndrome may result, with specific therapeutic requirements and challenges [37–39].

TRDN-related LQTS is a very rare subform due to an absent gene product level that is associated with an atypical presentation, mainly autosomal recessive, with extensive T-wave inversions in precordial leads V1 through V4, persistent or transient QT prolongation, and severe disease expression of exercise-induced cardiac arrest in early childhood. Biallelic loss-of-function variants in TRDN have also been associated with catecholaminergic polymorphic ventricular tachycardia (CPVT), and the term "triadin knockout syndrome" [40, 41] has been proposed. TRDN is expressed in both cardiac and skeletal muscle and undergoes extensive alternative splicing to produce several isoforms; only biallelic LoF variants affecting cardiac isoforms should be considered as pathogenic for this rare entity.

CALM-related LQTS is also caused by an altered gene product sequence by a likely dominant-negative effect; reducing the calcium-dependent inactivation of the calcium channel $Ca_{V1.2}$ results in increased inward calcium channel current (I_{CaL}) and repolarization delay. All three *CALM* genes have been classified as definitive for LQTS and moderate for CPVT [42]; all pathogenic variants are non-synonymous: at least 35 distinct non-synonymous variants have been identified and reported in the International Calmodulinopathy Registry [43, 44] including 11 (31%) in *CALM1*, 16 (46%) in *CALM2*, and 8 (23%) in *CALM3*. The majority of CALM variants are de novo. Clinical signs are a presentation in infancy or early childhood (up to 5 years); marked sinus bradycardia or atrioventricular block and QT prolongation; and,

predominantly in *CALM1* gene carriers, a mild-to-severe neurological impairment, including seizures, development delay, motor and/or cognitive disability.

Biallelic pathogenic variants (homozygous and compound heterozygous) in the *KCNQ1* gene cause JLNS due to absent gene product level or altered gene product sequence. Nonsense, frameshift, splice site, whole-exon deletions, and non-synonymous variants have been reported as pathogenic. One study compared clinical features of homozygous variant carriers with a residual I_{Ks} current (slowly activating delayed rectifier potassium channel/current) even as little as 10% which had QT prolongation but no hearing loss ("autosomal-recessive LQTS"), whereas those patients with complete absence of I_{Ks} had typical JLNS [45]. Also, *KCNE1* gene mutations may cause JLNS [46–49].

KCNJ2 pathogenic variants cause another syndromic form of LQTS, named Andersen-Tawil syndrome (ATS), through altered gene product sequence by non-synonymous changes and an in vitro loss of function of the Kir2.1 channel (I_{Kir}, inwardly rectifying potassium channel), either via trafficking or gating defects, a major component of the cardiac action potential repolarization phase. ATS is caused in 60–70% by pathogenic variants in the *KCNJ2* gene; patients show QT-U abnormalities, but not a typical QT prolongation, ventricular arrhythmias occurring after frequent, polymorphic premature ventricular complexes, and polymorphic non-sustained ventricular tachycardia. In addition, extracardiac manifestations include dysmorphic features and periodic paralysis with hypo- and hyperkalemic episodes in some patients. The disease penetrance appears to be high in families.

CACNA1C-related Timothy syndrome (TS) is caused by variants leading to altered gene product sequence. A recurrent, de novo, non-synonymous variant, (p. Gly406Arg) in the *CACNA1C* gene was initially described in 13 TS patients [50] 15863612 [51] and have been shown to result from a gain-of-function through impaired calcium channel inactivation. Clinical features of TS are QT prolongation, syndactyly, immune deficiency, seizures, congenital heart defects, cognitive abnormalities, learning difficulties, and intermittent hypoglycemia [52]. The encoded calcium channel protein has a complex genomic structure with tissue-specific, alternative splicing that may result—depending upon the localization of the pathogenic variant (e.g., exon 8/8A)—in alternate cardiac splice forms with atypical TS (e.g., a more severe cardiac phenotype and without syndactyly) [51, 53]. Other non-synonymous variants in *CACNA1C* have been also reported in association with isolated LQTS 26253506 [53–55], but so far, this gene has only moderate disease evidence for isolated LQTS according to the ClinGen Cardiovascular Domain Working Group [1].

66.3 Brugada Syndrome (BrS)

Brugada syndrome (BrS) is a rare, hereditary arrhythmia with a typical ECG that, however, can occur transiently or incidentally (e.g., during class 1 antiarrhythmics) and/or triggered by fever or vagotonia. BrS is characterized by specific ST-segment

elevations in the right precordial leads (V1-V3) [56]. The diagnostically key image is the so-called type 1 ECG, which is characterized by an ST-segment elevation (J-point elevation) of ≥2 mm in ≥1 lead accompanied by a descending ST segment and a symmetrical, negative T-wave. In the current ESC guidelines [57], Brugada syndrome is diagnosed in particular (expert class 1 recommendation) when a spontaneous type 1 ECG is present OR an inducible type 1 ECG (medication, fever, etc.) is present in a patient with sudden cardiac arrest or ventricular fibrillation. BrS is often associated with atrioventricular conduction disorder and corresponding ECG signs, as well as atrial and malignant ventricular arrhythmias. The latter may be relevant in unexplained, sudden deaths, where it may be underlying in about 20% of cases [58, 59]. The prevalence of BrS is potentially overestimated and given as 1 in 2000, with a higher prevalence in Asian countries. The symptomatic patients are usually men in the third to fourth decade of life [60].

Due to the limited specificity of drug provocation tests in the diagnosis of BrS and several, potential phenocopies (e.g., mechanical RVOT compression, myocardial ischemia, electrolyte imbalances, hyperthermia, drug intoxications) [61], a so-called Shanghai Diagnostic Score has been proposed, where other clinical features are taken into account in addition to the type 1 ECG [56]. A score of ≥3.5 points corresponds to a definitive diagnosis of BrS and a score of 2–3 points to a possible or suspected diagnosis. In the context of risk stratification, the genetic finding (presence of a *SCN5A* gene mutation) [62–64] but also other polygenic gene markers (SNPs) may play a role in the future [65, 66].

Like other hereditary forms of arrhythmia, BrS is genetically heterogeneous (locus heterogeneity). Over 40 genes were initially published or proposed as potentially disease-causing genes for BrS. According to the ClinGen evaluation, 20 of the 21 published disease genes have "limited" or "disputed" disease evidence [2]. Only genetic variants with a loss of function (about 2/3 non-synonymous variants of class 4 or 5 according to ACMG) or copy number variations (CNV; in 1–3%) of the cardiac sodium channel gene are responsible for 20–25% of BrS cases. In families with pathogenic *SCN5A* variants, penetrance is incomplete and age-dependent, with provocation tests (e.g., ajmaline test) in genetic trait carriers being positive with development of type 1 ECG. In addition to *SCN5A*, genetic and experimental data have been published in families with Brugada syndrome demonstrating that pathogenic variants in *RRAD* or *TMEM168* led to a reduction in cardiac inward sodium current (I_{Na}) analogous to *SCN5A* gene mutations [67, 68]. In addition, genome-wide association studies in patients with BrS identified several genetic loci with common, non-coding but potentially regulatory variants (so-called polygenic risk scores, PRS) that were associated with the different phenotype manifestation of the disease, response to the ajmaline test, or the development of cardiac events. The clinical evaluation of these additional genetic tests is currently underway.

In 2019, a study by Campuzano et al. examined variants in 42 possible Brugada genes with regard to their potential disease pathogenicity. This study concluded that apart from *SCN5A SLMAP*, *SEMA3A*, *SCNN1A,* and *SCN2B* should be included in the list of BrS-related disease genes [69] (Table 66.3).

Table 66.3 Inherited forms of Brugada syndrome

Isolated cardiac forms **ClinGen MonDO: 0015263**			
Brugada genes	**Core gene (mutation detection rate > 1%)**	**Rare genes (<1%)**	**Reference**
	SCN5A	*RRAD, TMEM168, SLMAP, SEMA3A, SCNN1A, SCN2B*	[2, 67, 68] [69]
Syndromal forms			
Unknown			

SCN5A-related Brugada syndrome is caused by a decreased gene product level or altered gene product sequence and loss of function as disease mechanism due to a variety of pathophysiologic mechanisms (e.g., decreased expression of cardiac sodium channel, Nav1.5, in the sarcolemma, expression of non-functional channels, or altered gating properties leading to a decreased I_{Na} sodium current (e.g., delayed activation or earlier or faster inactivation) [36]. *SCN5A* pathogenic variants are identified in 20–30% of cases of European ancestry [70, 71] and typically inherited in by autosomal dominant inheritance with incomplete, disease- and age-dependent penetrance [71–75]. Even in the face that loss-of-function is the main mechanism, the majority of pathogenic variants are non-synonymous and infrequently nonsense, frameshift, splice site, or 9 in-frame deletions/insertions [76].

RRAD-related Brugada syndrome (encoding the RAD GTPase) [67], *GSTM3*-related Brugada syndrome (encoding the glutathione S-transferase Mu 3; CNV with exon 8 deletion) [77]), and *TMEM168*-related Brugada syndrome (encoding the transmembrane protein 168) 32175648 [68, 78] were also recently discovered to impair cardiac sodium channel function. A genome-wide association study (GWAS) suggested additional, modifying genetic risk loci [65], and also a serum autoantibody profile may serve for risk profiling [79].

The *RRAD* variant p.Arg210His was first identified via whole-exome sequencing (WES) in a three-generation pedigree with five affected family members. The identified variant results in an BRGDA-typical electrical defect with reduced amplitude of I_{Na} (−40% in human-induced pluripotent stem cell-derived cardiomyocytes (hiPSC-CM)) possibly triggered by the regulation of the $Na_V1.5$ (encoded by *SCN5A*) expression at the protein level, coupled with cardiomyocyte cytoskeletal abnormalities [67]. In the same line, a knock-in mouse model carrying the p. Arg210His mutation showed a decrease of $Na_v1.5$ and Cx43 expression [80].

66.4 Catecholaminergic Polymorphic Ventricular Tachycardia (CPVT) and Calcium Release Deficiency Syndrome (CRDS)

Catecholaminergic polymorphic ventricular tachycardia (CPVT) is a potentially malignant and heritable arrhythmia syndrome characterized by bidirectional or polymorphic VT during physical or emotional stress [81, 82]. It is estimated to

affect 1 in 10,000 people with reported mortality rates as high as 30–50% by the age of 35 years when left untreated, although most patients will present before the age of 10 [83]. The baseline ECG is usually normal, but during exercise (heart rate > 120–140 bpm), typically monomorphic and later polymorphic or bidirectional premature ventricular beats (VES) occur. Some patients may have these during emotional rather than physical stress. Consequently, patients may experience syncope or cardiac arrest during a sustained polymorphic or bidirectional ventricular tachycardia or due to ventricular fibrillation (VF) that occurred secondarily. There are still differential diagnoses to be considered (e.g., arrhythmogenic cardiomyopathies (ACM), electrolyte disturbances, digitalis intoxication, VES at resting conditions).

The majority of CPVT cases (mutation sensitivity, 50–60%) were caused by heterozygous pathogenic variants in *RYR2* gene (ryanodine receptor 2, CPVT1) [84] that encodes the sarcoplasmic reticulum (SR) Ca^{2+} channel called ryanodine receptor because of its affinity for binding the alkaloid ryanodine. *RYR2* variants are inherited in an autosomal dominant manner, whereas *CASQ2* pathogenic variants are rare (approximately 5% of cases) and demonstrate autosomal-recessive inheritance [85, 86]. Patients with *RYR2* pathogenic variants have similar clinical courses than those without; recessive forms of CPVT are more severe and more resistant to β-blockers. In patients with no family history of CPVT, sporadic mutations are likely to be the cause and may occur.

Using the ClinGen gene curation framework, definitive disease genes for CPVT are *RYR2*, *CASQ2, TECRL*, and *TRDN* [3] where genes with moderate evidence for disease causation in CPVT were the three calmodulin genes (*CALM1, CALM2, CALM3*) 23040497 [44, 87, 88], *TRDN* (triadin), and trans-2,3-enoyl-CoA reductase-like gene (*TECRL*). Other genes were disputed (*KCNJ2*, *PKP2*, and *SCN5A*) or refused (ankyrin 2 [*ANK2*]) as causative for CPVT.

Most of the reported variants in *RYR2* are gain-of-function variants, but also a small part of loss-of-function variants are described. These loss-of-function variants are related to frameshifts, CNVs, and secondary haploinsufficiency. In 2014, a deletion of exon 3 of *RYR2* was reported, associated with left ventricular non-compaction (LVNC) [89]; a second report of a non-synonymous variant with familial cosegregation showed an unexpected clinical overlap between LVNC and atypical CPVT due to an in vitro loss of function [90] emphasizing the fact that also this functional effect may be associated with additional phenotypes. Furthermore, another *RYR2* gene variant reduced Ca2+ release and short-coupled ventricular torsade de pointes arrhythmias [8]. During the last few years, other pathogenic variants were characterized as RYR2 loss-of-function and variant carriers did not show typical, clinical CPVT signs (in particular exercise-induced arrhythmias) [91]. To separate these different RYR2 effects, the term Ca2+ release deficiency syndrome (CRDS) [92, 93] has been recently established as a novel RYR2-related phenotypic spectrum and inherited arrhythmia syndrome [94].

Results from genetic testing should still be interpreted with some caution and require careful bioinformatic justification, since due to the large size of the *RYR2* gene approximately 3% of healthy individuals harbor a rare protein-altering variant

Table 66.4 Inherited forms of catecholaminergic polymorphic ventricular tachycardia (CPVT)

Isolated (cardiac) forms **ClinGen MonDO: 0017990**			
CPVT genes	**Core genes (mutation detection rate > 1%)**	**Rare genes (<1%)**	**Reference**
	RYR2, CASQ2	*CALM1, CALM2, CALM3* *CASQ2, TRDN, TECRL* (autosomal rec.)	[3, 10]
Syndromal forms			
Unknown			

in their exome (see Exome Aggregation Consortium [95]) and thereby may raise, in case of a lower clinical pre-test probability for CPVT, the rate of false-positive results for *RYR2* variants (Table 66.4).

CASQ2 is an established gene for autosomal-recessive CPVT (the second most common genetic cause of the disease, responsible for up to 5% of cases). Recent reports have also associated monoallelic or heterozygous *CASQ2* variants with CPVT, but also in a larger family with CPVT and a cosegregating, heterozygous p.Lys180Arg variant [96]. Although the evidence for autosomal dominant inheritance is not completely definitive, available functional data suggests that disease is likely due to decreased gene product level or altered gene product sequence [97, 98]. While the current CASQ2 registry [97] provides evidence to support autosomal dominant *CASQ2* association with CPVT, the data should be still interpreted with some caution, due to precise clinical information of relatives and since several variants have also been described in gnomAD population with a minor allele frequency (MAF) being too high for a rare syndrome/CPVT (i.e., MAF $>1*10^{-5}$). The variants also included presumed nonsense-mediated decay-escaping C-terminal truncating variants and a splice region variant without a proven in vitro effect on splicing. In contrast to the high (97%) penetrance for homozygous/compound heterozygous individuals, penetrance for heterozygotes was only 33% although it is expected that the population level penetrance of *CASQ2* heterozygous variants will be lower still.

The disease mechanism in CALM-related CPVT is likely a dominant-negative effect caused by altered gene product sequence which reduces the calcium-dependent inactivation of the calcium channel CaV1.2, resulting in increased inward calcium channel current (I_{CaL}) and repolarization delay. All three *CALM* genes (*CALM1-3*) encode an identical 149 long amino acid protein, calmodulin; all variants with evidence of pathogenicity identified in the CALM genes are non-synonymous and affect amino acid residues in the EF-hand Ca^{2+} binding loop III and IV. The majority of CALM variants are de novo and present with a clinical early onset during childhood.

Absent gene product level and altered gene product sequence of TECRL is associated with CPVT by a loss-of-function. Reported variants include both homozygous and compound heterozygous inheritance, with a variety of variant types (splice donor variant, stop gained, exon deletion (exon 2), non-synonymous

variants), and a large duplication encompassing the entire *TECRL* gene, with an uncertain molecular consequence. These cases presented with phenotypic features typical of CPVT and some mild prolonged QT interval, especially after stimulation by epinephrine or exercise.

Absent gene product level and altered gene product sequence of TRDN is associated with CPVT. The disease mechanism appears to be loss of function. TRDN is rarely associated with CPVT, but several reports have described biallelic loss-of-function variants in cases. These include both homozygous and compound heterozygous variants, with a variety of variant types described—stop gained, frameshift, exon deletion (exon 2), intronic variants (with proven effect on splicing), and non-synonymous variants (proven to lead to degraded protein). Biallelic loss-of-function variants in TRDN have also been associated with LQTS with an atypical presentation (ClinGen: strong evidence). This "triadin knockout syndrome" can lead to variable phenotypes.

66.5 Short-QT Syndrome (SQTS)

Short-QT syndrome (SQTS) is characterized by a very short-QT interval, absence of the ST segment, and symmetric, tall T waves on the ECG (<330 ms, or < 360 ms and symptoms). It is a very rare cardiac ion channel disease (< 1: 10,000) that can be associated with syncope, paroxysmal atrial fibrillation, ventricular fibrillation, or sudden cardiac death [99, 100]. A few hundred cases are currently described; diagnostic criteria are according to .

- **HRS/EHRA/APHRS Consensus Recommendations** [101]: QTc ≤330 ms or QTc 330–360 ms + at least 1 additional diagnostic feature
- **ESC SCD Guidelines Consensus Recommendations** [102]: QTc ≤340 ms (Class 1 recommendation) or QTc 340–360 ms + at least 1 additional diagnostic feature
- **So-called Gollob criteria**, **SQTS score** [103]: ≥4 points (high probability), 2–3 points (intermediate probability)
- **ESC VA/SCD Guidelines Consensus Recommendations** [57]: QTc ≤ 320 ms or QTc 320–360 ms + gene mutation, family history, or survivor of sudden cardiac death (SCA) in ventricular tachycardia (VF, VT)

Clinical signs may be adrenergically mediated (increasing QTc shortening with higher heart rate) [104]; however, there are also SQTS patients where vagal-mediated paradoxical QTc interval shortening and symptoms of bradycardia occur [105]. Implantation of an ICD with/without quinidine therapy is recommended for high-risk patients, regardless of genetic status. In asymptomatic SQTS patients (± the familial pathogenic variant), hydroquinidine effectively prolonged QTc intervals [106, 107]. Life-threatening cardiac arrhythmias are equally common across different genotypes [105]. Syncope in male is more often than in females (24% versus 7%; $p = 0.01$) whereas its symptoms (like atrial flutter, atrial fibrillation, or palpitations)

not s [108]. SQTS is highly lethal with sudden cardiac arrest/sudden cardiac death (SCA/SCD) mostly being the first clinical manifestation in about 30% of SQTS patients [99, 109, 110]. First choice of therapy is implantable cardioverter defibrillator (ICD); quinidine can be an effective pharmacological therapy [57].

Exogenous causes or phenocopies with shortening of the QTc interval should be taken into account in the differential diagnosis and are caused, for example, by

- Congenital lactase deficiency, primary carnitine deficiency *(SLC22A5* gene), primary hyperparathyroidism, or Klinefelter syndrome (47, XXY)
- Acidosis, digitalis intoxication, hyperthermia, hyperkalemia, hypercalcemia, congenital adrenal hyperplasia, hyperthyroidism, vitamin A intoxication, milk-alkali syndrome
- Rufinamide (anti-convulsive), selective ATP potassium channel opener (pinacidil, levcromakalim)

SQTS is an autosomal dominant inherited disease. ClinGen expert panels came to the conclusion that only four genes can be described as disease-causing genes [3]. In addition to the potassium channel genes *KCNH2* (SQT1), *KCNQ1* (SQT2), and *KCNJ2* (SQT3), the cardiac chloride-bicarbonate exchanger AE3 encoded by *SLC4A3* is the main cause of SQTS. While *KCNH2* and *KCNQ1* were classified as definite and moderate genes, respectively; *KCNJ2* and *SLC4A3* are only classified as moderate so far. With regard to the *SLC4A3* gene, two families have been identified with the identical variant. Also, some syndromic cases have been noted with a *CACNA1C* loss-of-function variant [111].

Genetic testing in the case of SQTS is currently recommended for four genes, including 3 genes that can also cause LQTS. Based on current results, the *SLC4A3* gene is currently the main gene for SQTS (approx. 15%) [112, 113]. Genotype–phenotype relationships are only partially known due to the lack of identified patients [106].

An indicative molecular genetic finding (class 4 or 5 variant according to ACMG) is considered an important diagnostic feature in the international recommendations (Gollob score: 2 points). In about 20% of the index patients, such mutations can be detected (Table 66.5).

SLC4A3-related SQTS resulted from experimental models showing that the membrane anion exchange (bicarbonate vs. chloride) protein showed a reduced membrane localization of the mutant protein (harboring an amino acid exchange) leading to a loss of function by intracellular alcalinization and shortening of the cardiomyocyte action potential duration [113].

In contrast, *KCNH2*-related SQTS is due to a rare, but in SQT1 common, non-synonymous pathogenic variant (p.Thr618Ile or p.Asn588Lys) that showed pathophysiologically in several disease models (including human-induced pluripotent stem cell-derived cardiomyocytes and a rabbit animal model) [99, 115] a gain-of-function mechanism. Note, loss-of-function variants in *KCNH2* are associated with LQTS.

Table 66.5 Inherited forms of short-QT syndrome (SQTS) [3]

Isolated (cardiac) forms ClinGen MonDO: 0000453			
	Core genes (mutation detection rate > 1%)	**Rare genes (<1%)**	**Reference**
	KCNH2, KCNQ1, SLC4A3	*KCNJ2*	[3, 112, 114]
Syndromal forms			
Carnitine deficiency	*SLC22A5*	*Early childhood cardiomyopathy, muscle hypotension, failure to thrive, hypoglycemia, convulsion*	Autosomal dom. OMIM 212140

Also non-synonymous genetic variants in the *KCNJ2* gene have been identified in a small series of SQTS patients, including also two probands with a de novo variant (paternity not confirmed). Experimental evidence demonstrated these variants led to a gain of function of the late repolarizing, KCNJ2-encoded I_{K1} current in the heart, and abbreviation of the action potential duration [116, 117].

Almost all evidence for *KCNQ1*-related SQTS derived from a single non-synonymous variant (p.Val141Met) identified in 9 unrelated probands, presenting with severe bradycardia in utero or at birth and atrial fibrillation [102, 118–121]. For another variant in the *KCNQ1* gene, p.Val307Leu, detected in a 70-year-old patient with ventricular fibrillation and a short-QT interval, in vitro studies report a gain-of-function effect of mutant I_{Ks} channels [122]. Note, loss-of-function variants in *KCNQ1* are associated with LQTS.

66.6 Other Uncommon Forms of Inherited Arrhythmias

Familial forms of supra- and ventricular arrhythmia have been described. Genes [123] almost all entities [123–125] and recommendations for genotyping have been published [10, 126]. However, in contrast to the typical inherited arrhythmia syndromes mentioned before, there is no current evaluation by the ClinGen Board for these disorders and their potentially relevant disease genes. For many of these uncommon forms of inherited arrhythmias, there is currently little data on the mutation detection rate, i.e., the pathogenic variant fraction, and on possible genotype–phenotype correlations.

Genotyping is thereby less important due to the often low rate of positive findings (e.g., in supraventricular arrhythmias). However, in individual diseases, especially in potentially malignant forms of arrhythmia (e.g., IVF, unclear SCA, IVT), it can be relevant not only etiologically but also primarily prophylactically for biologically related family members. If there is a positive family history for one of the listed diseases, genotyping should be initiated (Table 66.6).

Table 66.6 Other uncommon forms of inherited arrhythmias

	Associated genes	Reference
Idiopathic ventricular fibrillation (IVF) **"sudden cardiac arrest" (SCA), SCD, SIDS, SU(N)DS** **Idiopathic ventricular tachycardia (IVT)**		
	Multi-gene panel investigation of cardiac ion channel and cardiomyopathy genes, selected bioinformatic panel	
Short-coupled torsade de pointes tachycardia (scTDP)		
	RYR2, SCN5A	[8, 9, 127–129]
Multifocal ectopic Purkinje-related premature contractions and related cardiomyopathy (MEPPC)		
	SCN5A	[130–133]
Early repolarization syndrome (ERS)		
	No validated or curated genes	[10]
Atrial fibrillation (ATFB) (idiopathic or familial)		
	SCN5A, KCNQ1, MYL4, TTN	[134, 135]
WPW syndrome with HCM/LVH		
	PRKAG2, *mitochondrial (Leigh syndrome)*	[136]
Cardiac conduction disease (CCD/PCCD)		
	SCN5A, TRPM4 *GJA5, SCN1B*	[137, 138]
Cardiac conduction disease (CCD/PCCD), syndromal form		
	LMNA, TNNI3K, *DES, DMD, DMPK, EMD, LAMP2, ZNF9, GLA, PRKAG2, NKX2-5, GJC1, TBX5, mitochondrial (37 gene)*	[10]
Sinus node disease (SND)		
	HCN4, KCNJ5, *GNB2, KCNQ1, RYR2, SCN5A*	[10, 138]
Sinus node disease (SND), syndromal form		
	LMNA, *CACNA1D, EMD, GNB5, SGOL1*	[10]

CCD, Cardiac conduction disease; *PCCD*, Progressive cardiac conduction disease; *SCA*, Sudden cardiac arrest; *SCD*, Sudden cardiac death; *SIDS*, Sudden infant death syndrome; *SUDS*, Sudden unexpected death syndrome; *SUNDS*, Sudden unexpected nocturnal death syndrome; *HCM/LVH*, Hypertrophic cardiomyopathy, left ventricular hypertrophy

66.7 Conclusions

In recent years, many cardiovascular diseases and the related, underlying genes responsible have been re-evaluated by ClinGen [139]. The advantages of this standardized method are obvious. International experts for the respective diseases and the associated genetics evaluate the genes already described for a disease. They clearly demonstrate which genes originally designated as disease-causing are to be classified as causal at the time the data are collected and which are not.

In parallel with current recommendations for genotyping of distinct cardiovascular disorders (including many arrhythmias) [10, 57, 126], also technical advances using next-generation sequencing techniques, i.e., massively parallel analysis of hundreds to thousands of cardiovascular genes, approach clinical reality, as well as the notion that some variants in established disease genes cannot be judged finally or currently as causative (ACMG class 3-variants, VUS).

However, there is also some criticism since the literature used for the evaluation often does not take into account actual database entries from ClinVar or other database. In addition, familial segregation studies are often incomplete. Also, the expert group is not always in 100% agreement and some in vitro data may not be so conclusive as reported, since overall, it may be difficult to compare the different experimental approaches and cellular systems for pathogenic assessment of mutant variants. Some variants are described with no demonstrated in vitro effect on cellular electrophysiology, while other publications describe the same variant with a potential significant effect.

In recent years, also significant copy number variations (CNV), such as large deletions or duplications, have been recognized during genetic analysis and should now be implemented as part of a comprehensive genetic analysis. On the other hand, balanced and unbalanced translocations, inversions, and complex rearrangements, for example, are more difficult to identify.

With emerging knowledge of the genomic complexity as well as improved understanding of regulatory variants for cardiovascular disorders that may lead to similar effects such as non-synonymous loss-of-function variants, cardiovascular genetics will continue to pave the way for personalized medicine, taking inherited patient information and the individual clinical profile further into account.

References

1. Adler A, Novelli V, Amin AS, et al. An international, multicentered, evidence-based reappraisal of genes reported to cause congenital long QT syndrome. Circulation. 2020;141:418–28.
2. Hosseini SM, Kim R, Udupa S, et al. Reappraisal of reported genes for sudden arrhythmic death: evidence-based evaluation of gene validity for Brugada syndrome. Circulation. 2018;138:1195–205.
3. Walsh R, Adler A, Amin AS, et al. Evaluation of gene validity for CPVT and short QT syndrome in sudden arrhythmic death. Eur Heart J. 2021;43:1500.
4. Mellor GJ, Blom LJ, Groeneveld SA, et al. Familial evaluation in idiopathic ventricular fibrillation: diagnostic yield and significance of J wave syndromes. Circ Arrhythm Electrophysiol. 2021;14:e009089.
5. Neves R, Tester DJ, Simpson MA, et al. Exome sequencing highlights a potential role for concealed cardiomyopathies in youthful sudden cardiac death. Circ Genom Precis Med. 2022;15:e003497.
6. Chen X, Barajas-Martinez H, Xia H, et al. Clinical and functional genetic characterization of the role of cardiac calcium channel variants in the early repolarization syndrome. Front Cardiovasc Med. 2021;8:680819.

7. Zhang ZH, Barajas-Martinez H, Xia H, et al. Distinct features of Probands with early repolarization and Brugada syndromes carrying SCN5A pathogenic variants. J Am Coll Cardiol. 2021;78:1603–17.
8. Fujii Y, Itoh H, Ohno S, et al. A type 2 ryanodine receptor variant associated with reduced Ca (2+) release and short-coupled torsades de pointes ventricular arrhythmia. Heart Rhythm. 2017;14:98–107.
9. Kimura M, Fujisawa T, Aizawa Y, et al. An RyR2 mutation found in a family with a short-coupled variant of torsade de pointes. Int J Cardiol. 2017;227:367–9.
10. Wilde AAM, Semsarian C, Marquez MF, et al. European Heart Rhythm Association (EHRA)/Heart Rhythm Society (HRS)/Asia Pacific Heart Rhythm Society (APHRS)/Latin American Heart Rhythm Society (LAHRS) Expert Consensus Statement on the state of genetic testing for cardiac diseases. Europace. 2022;24(8):1307–67.
11. Campuzano O, Sanchez-Molero O, Fernandez A, et al. Sudden arrhythmic death during exercise: a post-mortem genetic analysis. Sports Med. 2017;47:2101–15.
12. Huang L, Wu KH, Zhang L, et al. Critical roles of Xirp proteins in cardiac conduction and their rare variants identified in sudden unexplained nocturnal death syndrome and Brugada syndrome in Chinese Han population. J Am Heart Assoc. 2018;7(1):e006320.
13. Huang PS, Hsieh CS, Chang SN, et al. Prevalence of sudden arrhythmic death syndrome-related genetic mutations in an Asian cohort of whole genome sequence. Europace. 2020;22:1287–97.
14. Liebrechts-Akkerman G, Liu F, Van Marion R, et al. Explaining sudden infant death with cardiac arrhythmias: complete exon sequencing of nine cardiac arrhythmia genes in Dutch SIDS cases highlights new and known DNA variants. Forensic Sci Int Genet. 2020;46:102266.
15. Mak CM, Mok NS, Shum HC, et al. Sudden arrhythmia death syndrome in young victims: a five-year retrospective review and two-year prospective molecular autopsy study by next-generation sequencing and clinical evaluation of their first-degree relatives. Hong Kong Med J. 2019;25:21–9.
16. Tan HL, Hofman N, Van Langen IM, et al. Sudden unexplained death: heritability and diagnostic yield of cardiological and genetic examination in surviving relatives. Circulation. 2005;112:207–13.
17. Viskin S, Rosovski U, Sands AJ, et al. Inaccurate electrocardiographic interpretation of long QT: the majority of physicians cannot recognize a long QT when they see one. Heart Rhythm. 2005;2:569–74.
18. Mazzanti A, Maragna R, Vacanti G, et al. Interplay between genetic substrate, QTc duration, and arrhythmia risk in patients with long QT syndrome. J Am Coll Cardiol. 2018;71:1663–71.
19. Goldenberg I, Horr S, Moss AJ, et al. Risk for life-threatening cardiac events in patients with genotype-confirmed long-QT syndrome and normal-range corrected QT intervals. J Am Coll Cardiol. 2011;57:51–9.
20. Mazzanti A, Trancuccio A, Kukavica D, et al. Independent validation and clinical implications of the risk prediction model for long QT syndrome (1-2-3-LQTS-risk). Europace. 2022;24:614–9.
21. Roberts JD, Asaki SY, Mazzanti A, et al. An international multicenter evaluation of type 5 long QT syndrome: a low penetrant primary arrhythmic condition. Circulation. 2020;141:429–39.
22. Arking DE, Pulit SL, Crotti L, et al. Genetic association study of QT interval highlights role for calcium signaling pathways in myocardial repolarization. Nat Genet. 2014;46:826–36.
23. Kolder I, Tanck MWT, Postema PG, et al. Analysis for genetic modifiers of disease severity in patients with long-QT syndrome type 2. Circ Cardiovasc Genet. 2015;8:447–56.
24. Lahrouchi N, Tadros R, Crotti L, et al. Transethnic genome-wide association study provides insights in the genetic architecture and heritability of long QT syndrome. Circulation. 2020;142:324–38.
25. Behr ER, Ritchie MD, Tanaka T, et al. Genome wide analysis of drug-induced torsades de pointes: lack of common variants with large effect sizes. PLoS One. 2013;8:e78511.

26. Roberts JD, Krahn AD, Ackerman MJ, et al. Loss-of-function KCNE2 variants: true monogenic culprits of long-QT syndrome or Proarrhythmic variants requiring secondary provocation? Circ Arrhythm Electrophysiol. 2017;10:e005282.
27. Kapplinger JD, Tester DJ, Salisbury BA, et al. Spectrum and prevalence of mutations from the first 2,500 consecutive unrelated patients referred for the FAMILION long QT syndrome genetic test. Heart Rhythm. 2009;6:1297–303.
28. Tester DJ, Will ML, Haglund CM, et al. Compendium of cardiac channel mutations in 541 consecutive unrelated patients referred for long QT syndrome genetic testing. Heart Rhythm. 2005;2:507–17.
29. Moss AJ, Shimizu W, Wilde AAM, et al. Clinical aspects of type-1 long-QT syndrome by location, coding type, and biophysical function of mutations involving the KCNQ1 gene. Circulation. 2007;115:2481–9.
30. Adler A, Uppal S, Orr N, et al. First report of a large duplication of the KCNQ1 gene in a patient with long QT syndrome. Can J Cardiol. 2014;30:1249.e1245–7.
31. Eddy CA, Maccormick JM, Chung SK, et al. Identification of large gene deletions and duplications in KCNQ1 and KCNH2 in patients with long QT syndrome. Heart Rhythm. 2008;5:1275–81.
32. Barsheshet A, Goldenberg I, O-Uchi J, et al. Mutations in cytoplasmic loops of the KCNQ1 channel and the risk of life-threatening events: implications for mutation-specific response to β-blocker therapy in type 1 long-QT syndrome. Circulation. 2012;125:1988–96.
33. Walsh R, Lahrouchi N, Tadros R, et al. Enhancing rare variant interpretation in inherited arrhythmias through quantitative analysis of consortium disease cohorts and population controls. Genet Med. 2021;23:47–58.
34. Shimizu W, Moss AJ, Wilde AAM, et al. Genotype-phenotype aspects of type 2 long QT syndrome. J Am Coll Cardiol. 2009;54:2052–62.
35. Wilde AAM, Moss AJ, Kaufman ES, et al. Clinical aspects of type 3 long-QT syndrome: an international multicenter study. Circulation. 2016;134:872–82.
36. Wilde AAM, Amin AS. Clinical Spectrum of SCN5A mutations: long QT syndrome, Brugada syndrome, and cardiomyopathy. JACC Clin Electrophysiol. 2018;4:569–79.
37. Henrion U, Zumhagen S, Steinke K, et al. Overlapping cardiac phenotype associated with a familial mutation in the voltage sensor of the KCNQ1 channel. Cell Physiol Biochem. 2012;29:809–18.
38. Makita N, Behr E, Shimizu W, et al. The E1784K mutation in SCN5A is associated with mixed clinical phenotype of type 3 long QT syndrome. J Clin Invest. 2008;118:2219–29.
39. Veltmann C, Barajas-Martinez H, Wolpert C, et al. Further insights in the Most common SCN5A mutation causing overlapping phenotype of long QT Syndrome, Brugada Syndrome, and conduction defect. J Am Heart Assoc. 2016;5(7):e003379.
40. Altmann HM, Tester DJ, Will ML, et al. Homozygous/compound heterozygous Triadin mutations associated with autosomal-recessive long-QT syndrome and pediatric sudden cardiac arrest: elucidation of the Triadin knockout syndrome. Circulation. 2015;131:2051–60.
41. Clemens DJ, Tester DJ, Giudicessi JR, et al. International Triadin knockout syndrome registry. Circ Genom Precis Med. 2019;12:e002419.
42. Sondergaard MT, Sorensen AB, Skov LL, et al. Calmodulin mutations causing catecholaminergic polymorphic ventricular tachycardia confer opposing functional and biophysical molecular changes. FEBS J. 2015;282:803–16.
43. Crotti L, Spazzolini C, Nyegaard M, et al. Clinical presentation of calmodulin mutations: the International Calmodulinopathy Registry. Eur Heart J. 2023;44:3357–70.
44. Crotti L, Spazzolini C, Tester DJ, et al. Calmodulin mutations and life-threatening cardiac arrhythmias: insights from the International Calmodulinopathy Registry. Eur Heart J. 2019;40:2964–75.
45. Bhuiyan ZA, Wilde AAM. IKs in heart and hearing, the ear can do with less than the heart. Circ Cardiovasc Genet. 2013;6:141–3.

46. Schulze-Bahr E, Haverkamp W, Wedekind H, et al. Autosomal recessive long-QT syndrome (Jervell Lange-Nielsen syndrome) is genetically heterogeneous. Hum Genet. 1997;100:573–6.
47. Schulze-Bahr E, Wang Q, Wedekind H, et al. KCNE1 mutations cause jervell and Lange-Nielsen syndrome. Nat Genet. 1997;17:267–8.
48. Schwartz PJ, Spazzolini C, Crotti L, et al. The Jervell and Lange-Nielsen syndrome: natural history, molecular basis, and clinical outcome. Circulation. 2006;113:783–90.
49. Zhang M, D'aniello C, Verkerk AO, et al. Recessive cardiac phenotypes in induced pluripotent stem cell models of Jervell and Lange-Nielsen syndrome: disease mechanisms and pharmacological rescue. Proc Natl Acad Sci U S A. 2014;111:E5383–92.
50. Splawski I, Timothy KW, Sharpe LM, et al. Ca(V)1.2 calcium channel dysfunction causes a multisystem disorder including arrhythmia and autism. Cell. 2004;119:19–31.
51. Splawski I, Timothy KW, Decher N, et al. Severe arrhythmia disorder caused by cardiac L-type calcium channel mutations. Proc Natl Acad Sci U S A. 2005;102:8089–96. discussion 8086-8088
52. Sepp R, Hategan L, Bácsi A, et al. Timothy syndrome 1 genotype without syndactyly and major extracardiac manifestations. Am J Med Genet A. 2017;173:784–9.
53. Wemhoner K, Friedrich C, Stallmeyer B, et al. Gain-of-function mutations in the calcium channel CACNA1C (Cav1.2) cause non-syndromic long-QT but not Timothy syndrome. J Mol Cell Cardiol. 2015;80:186–95.
54. Boczek NJ, Ye D, Jin F, et al. Identification and functional characterization of a novel CACNA1C-mediated cardiac disorder characterized by prolonged QT intervals with hypertrophic cardiomyopathy, congenital heart defects, and sudden cardiac death. Circ Arrhythm Electrophysiol. 2015;8:1122–32.
55. Fukuyama M, Wang Q, Kato K, et al. Long QT syndrome type 8: novel CACNA1C mutations causing QT prolongation and variant phenotypes. Europace. 2014;16:1828–37.
56. Antzelevitch C, Yan GX, Ackerman MJ, et al. J-Wave syndromes expert consensus conference report: emerging concepts and gaps in knowledge. J Arrhythm. 2016;32:315–39.
57. Zeppenfeld K, Tfelt-Hansen J, De Riva M, et al. 2022 ESC guidelines for the management of patients with ventricular arrhythmias and the prevention of sudden cardiac death. Eur Heart J. 2022;43:3997.
58. Papadakis M, Papatheodorou E, Mellor G, et al. The diagnostic yield of Brugada syndrome after sudden death with normal autopsy. J Am Coll Cardiol. 2018;71:1204–14.
59. Tadros R, Nannenberg EA, Lieve KV, et al. Yield and pitfalls of Ajmaline testing in the evaluation of unexplained cardiac arrest and sudden unexplained death: single-center experience with 482 families. JACC Clin Electrophysiol. 2017;3:1400–8.
60. Milman A, Andorin A, Gourraud JB, et al. Profile of patients with Brugada syndrome presenting with their first documented arrhythmic event: data from the survey on arrhythmic events in BRUgada syndrome (SABRUS). Heart Rhythm. 2018;15:716–24.
61. Sreenivasan S, Monaghan M, Baranchuk A. Multifactorial Brugada phenocopy. JAMA Intern Med. 2018;178:872–3.
62. Honarbakhsh S, Providencia R, Garcia-Hernandez J, et al. A primary prevention clinical risk score model for patients with Brugada syndrome (BRUGADA-RISK). JACC Clin Electrophysiol. 2021;7:210–22.
63. Probst V, Goronflot T, Anys S, et al. Robustness and relevance of predictive score in sudden cardiac death for patients with Brugada syndrome. Eur Heart J. 2021;42:1687–95.
64. Yamagata K, Horie M, Aiba T, et al. Genotype-phenotype correlation of SCN5A mutation for the clinical and electrocardiographic characteristics of Probands with Brugada syndrome: a Japanese multicenter registry. Circulation. 2017;135:2255–70.
65. Barc J, Tadros R, Glinge C, et al. Genome-wide association analyses identify new Brugada syndrome risk loci and highlight a new mechanism of sodium channel regulation in disease susceptibility. Nat Genet. 2022;54:232–9.

66. Jimmy Juang JM, Liu YB, Julius Chen CY, et al. Validation and disease risk assessment of previously reported genome-wide genetic variants associated with Brugada syndrome: SADS-TW BrS registry. Circ Genom Precis Med. 2020;13:e002797.
67. Belbachir N, Portero V, Al Sayed ZR, et al. RRAD mutation causes electrical and cytoskeletal defects in cardiomyocytes derived from a familial case of Brugada syndrome. Eur Heart J. 2019;40:3081–94.
68. Shimizu A, Zankov DP, Sato A, et al. Identification of transmembrane protein 168 mutation in familial Brugada syndrome. FASEB J. 2020;34:6399–417.
69. Campuzano O, Sarquella-Brugada G, Fernandez-Falgueras A, et al. Genetic interpretation and clinical translation of minor genes related to Brugada syndrome. Hum Mutat. 2019;40:749–64.
70. Brugada J, Campuzano O, Arbelo E, et al. Present status of Brugada syndrome: JACC state-of-the-art review. J Am Coll Cardiol. 2018;72:1046–59.
71. Wijeyeratne YD, Tanck MW, Mizusawa Y, et al. SCN5A mutation type and a genetic risk score associate variably with Brugada syndrome phenotype in SCN5A families. Circ Genom Precis Med. 2020;13:e002911.
72. Chen Q, Kirsch GE, Zhang D, et al. Genetic basis and molecular mechanism for idiopathic ventricular fibrillation. Nature. 1998;392:293–6.
73. Kyndt F, Probst V, Potet F, et al. Novel SCN5A mutation leading either to isolated cardiac conduction defect or Brugada syndrome in a large French family. Circulation. 2001;104:3081–6.
74. Probst V, Wilde AAM, Barc J, et al. SCN5A mutations and the role of genetic background in the pathophysiology of Brugada syndrome. Circ Cardiovasc Genet. 2009;2:552–7.
75. Sarquella-Brugada G, Campuzano O, Arbelo E, et al. Brugada syndrome: clinical and genetic findings. Genet Med. 2016;18:3–12.
76. Kapplinger JD, Tester DJ, Alders M, et al. An international compendium of mutations in the SCN5A-encoded cardiac sodium channel in patients referred for Brugada syndrome genetic testing. Heart Rhythm. 2010;7:33–46.
77. Juang JJ, Binda A, Lee SJ, et al. GSTM3 variant is a novel genetic modifier in Brugada syndrome, a disease with risk of sudden cardiac death. EBioMedicine. 2020;57:102843.
78. Nguyen LKC, Shimizu A, Soh JEC, et al. Transmembrane protein 168 mutation reduces cardiomyocyte cell surface expression of Nav1.5 through αB-crystallin intracellular dynamics. J Biochem. 2021;170:577–85.
79. Chatterjee D, Pieroni M, Fatah M, et al. An autoantibody profile detects Brugada syndrome and identifies abnormally expressed myocardial proteins. Eur Heart J. 2020;41:2878–90.
80. Jajkiewicz C, Agnès T, Mickael D, et al. Molecular mechanisms of Brugada syndrome related to p.R211H mutation in RRAD gene. Arch Cardiovasc Dis Suppl. 2022;14:206–7.
81. Leenhardt A, Lucet V, Denjoy I, et al. Catecholaminergic polymorphic ventricular tachycardia in children. A 7-year follow-up of 21 patients. Circulation. 1995;91:1512–9.
82. Lucet V, Grau F, Denjoy I, et al. [Long term course of catecholaminergic polymorphic ventricular tachycardia in children. Apropos of 20 cases with an 8 year-follow-up]. Arch Pediatr. 1994;1:26–32.
83. Abbas M, Miles C, Behr E. Catecholaminergic polymorphic ventricular tachycardia. Arrhythm Electrophysiol Rev. 2022;11:e20.
84. Priori SG, Napolitano C, Tiso N, et al. Mutations in the cardiac ryanodine receptor gene (hRyR2) underlie catecholaminergic polymorphic ventricular tachycardia. Circulation. 2001;103:196–200.
85. Bhuiyan ZA, Hamdan MA, Shamsi ET, et al. A novel early onset lethal form of catecholaminergic polymorphic ventricular tachycardia maps to chromosome 7p14-p22. J Cardiovasc Electrophysiol. 2007;18:1060–6.
86. Lahat H, Eldar M, Levy-Nissenbaum E, et al. Autosomal recessive catecholamine- or exercise-induced polymorphic ventricular tachycardia: clinical features and assignment of the disease gene to chromosome 1p13-21. Circulation. 2001;103:2822–7.

87. Jiménez-Jáimez J, Palomino Doza J, Ortega Á, et al. Calmodulin 2 mutation N98S is associated with unexplained cardiac arrest in infants due to low clinical penetrance electrical disorders. PLoS One. 2016;11:e0153851.
88. Nyegaard M, Overgaard MT, Søndergaard MT, et al. Mutations in calmodulin cause ventricular tachycardia and sudden cardiac death. Am J Hum Genet. 2012;91:703–12.
89. Ohno S, Omura M, Kawamura M, et al. Exon 3 deletion of RYR2 encoding cardiac ryanodine receptor is associated with left ventricular non-compaction. Europace. 2014;16:1646–54.
90. Roston TM, Guo W, Krahn AD, et al. A novel RYR2 loss-of-function mutation (I4855M) is associated with left ventricular non-compaction and atypical catecholaminergic polymorphic ventricular tachycardia. J Electrocardiol. 2017;50:227–33.
91. Zhong X, Guo W, Wei J, et al. Identification of loss-of-function RyR2 mutations associated with idiopathic ventricular fibrillation and sudden death. Biosci Rep. 2021;41(4): BSR20210209.
92. Roston TM, Wei J, Guo W, et al. Clinical and functional characterization of ryanodine receptor 2 variants implicated in calcium-release deficiency syndrome. JAMA Cardiol. 2022;7:84–92.
93. Sun B, Yao J, Ni M, et al. Cardiac ryanodine receptor calcium release deficiency syndrome. Sci Transl Med. 2021;13:eaba7287.
94. Steinberg C, Roston TM, Van Der Werf C, et al. RYR2-ryanodinopathies: from calcium overload to calcium deficiency. Europace. 2023;25:euad156.
95. Lek M, Karczewski KJ, Minikel EV, et al. Analysis of protein-coding genetic variation in 60,706 humans. Nature. 2016;536:285–91.
96. Gray B, Bagnall RD, Lam L, et al. A novel heterozygous mutation in cardiac calsequestrin causes autosomal dominant catecholaminergic polymorphic ventricular tachycardia. Heart Rhythm. 2016;13:1652–60.
97. Ng K, Titus EW, Lieve KV, et al. An international multicenter evaluation of inheritance patterns, arrhythmic risks, and underlying mechanisms of CASQ2-Catecholaminergic polymorphic ventricular tachycardia. Circulation. 2020;142:932–47.
98. Wleklinski MJ, Kryshtal DO, Kim K, et al. Impaired dynamic sarcoplasmic reticulum Ca buffering in autosomal dominant CPVT2. Circ Res. 2022;131:673–86.
99. El-Battrawy I, Besler J, Liebe V, et al. Long-term follow-up of patients with short QT syndrome: clinical profile and outcome. J Am Heart Assoc. 2018;7:e010073.
100. Gussak I, Brugada P, Brugada J, et al. Idiopathic short QT interval: a new clinical syndrome? Cardiology. 2000;94:99–102.
101. Priori SG, Wilde AAM, Horie M, et al. HRS/EHRA/APHRS expert consensus statement on the diagnosis and management of patients with inherited primary arrhythmia syndromes: document endorsed by HRS, EHRA, and APHRS in May 2013 and by ACCF, AHA, PACES, and AEPC in June 2013. Heart Rhythm. 2013;10:1932–63.
102. Harrell DT, Ashihara T, Ishikawa T, et al. Genotype-dependent differences in age of manifestation and arrhythmia complications in short QT syndrome. Int J Cardiol. 2015;190:393–402.
103. Gollob MH, Redpath CJ, Roberts JD. The short QT syndrome: proposed diagnostic criteria. J Am Coll Cardiol. 2011;57:802–12.
104. Giustetto C, Scrocco C, Schimpf R, et al. Usefulness of exercise test in the diagnosis of short QT syndrome. Europace. 2015;17:628–34.
105. Raschwitz LS, El-Battrawy I, Schlentrich K, et al. Differences in short QT syndrome subtypes: a systematic literature review and pooled analysis. Front Genet. 2019;10:1312.
106. Hu D, Li Y, Zhang J, et al. The phenotypic spectrum of a mutation hotspot responsible for the short QT syndrome. JACC Clin Electrophysiol. 2017;3:727–43.
107. Mazzanti A, Maragna R, Vacanti G, et al. Hydroquinidine prevents life-threatening arrhythmic events in patients with short QT syndrome. J Am Coll Cardiol. 2017;70:3010–5.
108. El-Battrawy I, Schlentrich K, Besler J, et al. Sex-differences in short QT syndrome: a systematic literature review and pooled analysis. Eur J Prev Cardiol. 2020;27:1335–8.
109. Giustetto C, Di Monte F, Wolpert C, et al. Short QT syndrome: clinical findings and diagnostic-therapeutic implications. Eur Heart J. 2006;27:2440–7.

110. Giustetto C, Schimpf R, Mazzanti A, et al. Long-term follow-up of patients with short QT syndrome. J Am Coll Cardiol. 2011;58:587–95.
111. Endres D, Decher N, Rohr I, et al. New Cav1.2 channelopathy with high-functioning autism, affective disorder, severe dental enamel defects, a short QT interval, and a novel CACNA1C loss-of-function mutation. Int J Mol Sci. 2020;21:8611.
112. Christiansen MK, Kjær-Sørensen K, Clavsen NC, et al. Genetic analysis identifies the SLC4A3 anion exchanger as a major gene for short QT syndrome. Heart Rhythm. 2023;20: 1136–43.
113. Thorsen K, Dam VS, Kjaer-Sorensen K, et al. Loss-of-activity-mutation in the cardiac chloride-bicarbonate exchanger AE3 causes short QT syndrome. Nat Commun. 2017;8:1696.
114. Campuzano O, Fernandez-Falgueras A, Lemus X, et al. Short QT syndrome: a comprehensive genetic interpretation and clinical translation of rare variants. J Clin Med. 2019;8:1035.
115. Odening KE, Bodi I, Franke G, et al. Transgenic short-QT syndrome 1 rabbits mimic the human disease phenotype with QT/action potential duration shortening in the atria and ventricles and increased ventricular tachycardia/ventricular fibrillation inducibility. Eur Heart J. 2019;40:842–53.
116. Hancox JC, Du CY, Butler A, et al. Pro-arrhythmic effects of gain-of-function potassium channel mutations in the short QT syndrome. Philos Trans R Soc Lond Ser B Biol Sci. 2023;378:20220165.
117. Hancox JC, Whittaker DG, Du C, et al. Emerging therapeutic targets in the short QT syndrome. Expert Opin Ther Targets. 2018;22:439–51.
118. Hong K, Piper DR, Diaz-Valdecantos A, et al. De novo KCNQ1 mutation responsible for atrial fibrillation and short QT syndrome in utero. Cardiovasc Res. 2005;68:433–40.
119. Righi D, Silvetti MS, Drago F. Sinus bradycardia, junctional rhythm, and low-rate atrial fibrillation in short QT syndrome during 20 years of follow-up: three faces of the same genetic problem. Cardiol Young. 2016;26:589–92.
120. Sarquella-Brugada G, Campuzano O, Iglesias A, et al. Short QT and atrial fibrillation: a KCNQ1 mutation-specific disease. Late follow-up in three unrelated children. HeartRhythm Case Rep. 2015;1:193–7.
121. Villafañe J, Fischbach P, Gebauer R. Short QT syndrome manifesting with neonatal atrial fibrillation and bradycardia. Cardiology. 2014;128:236–40.
122. Bellocq C, Van Ginneken AC, Bezzina CR, et al. Mutation in the KCNQ1 gene leading to the short QT-interval syndrome. Circulation. 2004;109:2394–7.
123. Yuan SM. Fetal arrhythmias: genetic background and clinical implications. Pediatr Cardiol. 2019;40:247–56.
124. Musunuru K, Hershberger RE, Day SM, et al. Genetic testing for inherited cardiovascular diseases: a scientific statement from the American Heart Association. Circ Genom Precis Med. 2020;13:e000067.
125. Stiles MK, Wilde AAM, Abrams DJ, et al. 2020 APHRS/HRS expert consensus statement on the investigation of decedents with sudden unexplained death and patients with sudden cardiac arrest, and of their families. Heart Rhythm. 2021;18:e1–e50.
126. Schulze-Bahr E, Klaassen S, Gerull B, et al. Gendiagnostik bei kardiovaskulären Erkrankungen. Die Kardiologie. 2023;17:300–49.
127. Hirose S, Murayama T, Tetsuo N, et al. Loss-of-function mutations in cardiac ryanodine receptor channel cause various types of arrhythmias including long QT syndrome. Europace. 2021;24:497.
128. Kajiyama T, Miyazawa K, Kondo Y, et al. SCN5A mutation and a short coupled variant of Torsades de Pointes originating from the right ventricle: a case report. J Cardiol Cases. 2020;21:104–5.
129. Sonoda K, Ohno S, Shimizu Y, et al. SCN5A mutation identified in a patient with short-coupled variant of torsades de pointes. Pacing Clin Electrophysiol. 2020;43:456–61.

130. Calloe K, Broendberg AK, Christensen AH, et al. Multifocal atrial and ventricular premature contractions with an increased risk of dilated cardiomyopathy caused by a Nav1.5 gain-of-function mutation (G213D). Int J Cardiol. 2018;257:160–7.
131. Doisne N, Waldmann V, Redheuil A, et al. A novel gain-of-function mutation in SCN5A responsible for multifocal ectopic Purkinje-related premature contractions. Hum Mutat. 2020;41:850–9.
132. Gao X, Ye D, Zhou W, et al. A novel functional variant residing outside the SCN5A-encoded Nav1.5 voltage-sensing domain causes multifocal ectopic Purkinje-related premature contractions. HeartRhythm Case Rep. 2022;8:54–9.
133. Laurent G, Saal S, Amarouch MY, et al. Multifocal ectopic Purkinje-related premature contractions: a new SCN5A-related cardiac channelopathy. J Am Coll Cardiol. 2012;60:144–56.
134. Al-Azaam B, Darbar D. Atrial fibrillation in inherited channelopathies. Card Electrophysiol Clin. 2021;13:155–63.
135. Kim JA, Chelu MG, Li N. Genetics of atrial fibrillation. Curr Opin Cardiol. 2021;36:281–7.
136. Ahamed H, Balegadde AV, Menon S, et al. Phenotypic expression and clinical outcomes in a South Asian PRKAG2 cardiomyopathy cohort. Sci Rep. 2020;10:20610.
137. Guerri G, Krasi G, Precone V, et al. Cardiac conduction defects. Acta Biomed. 2019;90:20–9.
138. Porta-Sanchez A, Priori SG. Genetic abnormalities of the sinoatrial node and atrioventricular conduction. Card Electrophysiol Clin. 2021;13:625–39.
139. Tavtigian SV, Greenblatt MS, Harrison SM, et al. Modeling the ACMG/AMP variant classification guidelines as a Bayesian classification framework. Genet Med. 2018;20:1054–60.

Molecular Pathways and Animal Models of Arrhythmias

67

Tyler L. Stevens, Sara Coles, Amy C. Sturm, Catherine A. Hoover, Maegen A. Borzok, Peter J. Mohler, and Mona El Refaey

T. L. Stevens
The Dorothy M. Davis Heart and Lung Research Institute, The Ohio State University Wexner Medical Center, Columbus, OH, USA

Department of Physiology and Cell Biology, The Ohio State University Wexner Medical Center, Columbus, OH, USA

S. Coles
Division of Cardiology, Department of Medicine, Duke University Medical Center, Durham, NC, USA

A. C. Sturm
Genomic Medicine Institute, 23andMe, Sunnyvale, CA, USA

C. A. Hoover
Department of Biochemistry, Chemistry, Engineering and Physics, Commonwealth University of Pennsylvania, Mansfield, PA, USA

Department of Cellular and Molecular Medicine, University of Arizona, Tucson, AZ, USA

M. A. Borzok
Department of Biochemistry, Chemistry, Engineering and Physics, Commonwealth University of Pennsylvania, Mansfield, PA, USA

P. J. Mohler
The Dorothy M. Davis Heart and Lung Research Institute, The Ohio State University Wexner Medical Center, Columbus, OH, USA

Department of Physiology and Cell Biology, The Ohio State University Wexner Medical Center, Columbus, OH, USA

Department of Internal Medicine, Division of Cardiovascular Medicine, The Ohio State University Wexner Medical Center, Columbus, OH, USA

M. El Refaey (✉)
The Dorothy M. Davis Heart and Lung Research Institute, The Ohio State University Wexner Medical Center, Columbus, OH, USA

Department of Surgery, Division of Cardiac Surgery, The Ohio State University Wexner Medical Center, Columbus, OH, USA
e-mail: mona.elrefaey@osumc.edu

© The Author(s), under exclusive license to Springer Nature Switzerland AG 2024

S. Rickert-Sperling et al. (eds.), *Congenital Heart Diseases: The Broken Heart*,
Advances in Experimental Medicine and Biology 1441,
https://doi.org/10.1007/978-3-031-44087-8_67

Abstract

Arrhythmias account for over 300,000 annual deaths in the United States, and approximately half of all deaths are associated with heart disease. Mechanisms underlying arrhythmia risk are complex; however, work in humans and animal models over the past 25 years has identified a host of molecular pathways linked with both arrhythmia substrates and triggers. This chapter will focus on select arrhythmia pathways solved by linking human clinical and genetic data with animal models.

Keywords

Channelopathies · Action potential · Repolarization · *SCN5A* · Calcium · Brugada syndrome · Ventricular arrhythmias · atrial arrhythmias · Long QT syndrome · LQTS · *KCNQ1* · *KCNE2* · Reentry arrhythmias · Ankyrin-B · *ANK2* · Short QT syndrome · SQTS · *HERG* · *KCNJ2* · Arrhythmogenic Cardiomyopathy · ACM · Catecholaminergic polymorphic ventricular tachycardia · CPVT · Ryanodine receptor · *RYR2* · FKBP12.6 · Early repolarization syndrome · ERS · *KCNJ8*

67.1 Introduction

Over the past two decades, our understanding of arrhythmias and arrhythmia-associated pathways has increased with the advent of genetic research in congenital arrhythmias. These findings, when combined with clinical data, animal models, and newly emerging induced pluripotent stem cell (iPSC) data, have redefined the ability to diagnose and treat congenital and acquired forms of heart disease. Traditionally, congenital cardiac arrhythmias have been described as "channelopathies" in the context of the affected protein, most often an ion channel. It has also become relevant to address ion channel-associated gene products that support the structure and function of ion channels, as their role in the pathophysiology of arrhythmias is more relevant than previously recognized. Channelopathy mechanisms illustrated in large and small animal models have provided insight to the "trigger and substrate" basis of arrhythmias.

67.2 Ventricular Arrhythmias

67.2.1 Brugada Syndrome

Brugada syndrome (BrS) was initially described in 1992 as a disease characterized by right bundle branch block with ST segment elevation and is associated with fatal outcomes including syncope, malignant ventricular arrhythmia and sudden cardiac death (SCD) [1]. Although it is inherited as an autosomal dominant trait [2], the penetrance of Brugada syndrome is at a lower level compared to that of the

congenital long QT syndrome [3]. Brugada syndrome can be broken down into three major types of repolarization patterns, types 1, 2, and 3. Wilde et al. describes a detailed breakdown of the ECG characteristic of each type, where all types are characterized by a J wave amplitude ≥2 mm, and each specific type is further characterized based on specific T wave morphology, ST-T configuration, and ST segment elevation [4]. Example ECG traces for each subtype can be found in Fig. 67.1 [5].

Two primary pathogenic hypotheses have been suggested for Brugada syndrome involving early repolarization and late activation of ventricular myocytes. These two etiological theories are not mutually exclusive and have often demonstrated a mechanically heterogeneous disease. An important breakthrough in the ability to define the molecular pathways underlying arrhythmia disorders is the application of electrophysiology to single cardiomyocytes. This approach, pioneered for investigating neuronal membrane currents, utilizes glass micropipettes to measure the currents moving through a small membrane "patch." The technique can be utilized to measure populations of myocyte currents or modified to measure the movement of currents through single channels. Currents implicated in the arrhythmogenesis of Brugada syndrome include the fast inward sodium current (I_{Na}), transient outward potassium current (I_{to}), and the L-type calcium current ($I_{Ca,L}$).

To date, variants in more than 25 genes have been identified as pathogenic for Brugada syndrome [6]. Most notably, *SCN5A*, which encodes for the alpha-subunit of the $Na_v1.5$ voltage-gated Na^+ channel (I_{Na}), accounts for approximately 20% of Brugada syndrome patients [6, 7]. Several studies attribute conduction abnormalities in Brugada syndrome to Na^+ channel defects, the majority of them indicating a loss of function of $Na_v1.5$ [7, 8]. *Scn5a* $^{+/-}$ mice replicate phenotypes found in Brugada syndrome patients including atrial, atrioventricular, and ventricular conduction defects. Further, *Scn5a* $^{+/-}$ mice show reduced right ventricle expression of $Na_v1.5$ leading to reduced current, reduced upstroke velocity, and reduction of maximum right ventricle I_{Na} [9, 10]. These findings link mechanistic pathogenesis of Na^+ channels and the shortened epicardial action potential (AP) that gives rise to transmural current flow during the plateau phase of the AP, prolonged QT interval, and subsequent ST segment elevation in precordial leads as classically observed in ECGs of Brugada syndrome patients.

Pathogenic variants were identified in other genes linked to sodium channel. Specifically, variants were identified in *SCN1B*, *SCN2B* and *SCN3B* encoding the β subunits of the $Na_v1.5$. Variants in *SCN1B* affect the Na^+ channel function by impacting its trafficking and causing a reduction in I_{Na} [11]. Interestingly, the D211G variant in *SCN2B* is also a loss of function variant and was reported to reduce the cell surface expression of $Na_v1.5$ [12]. Variants in *SCN3B* were linked to loss of function of Na^+ channel and Brugada syndrome [13]. In addition, pathogenic variants in *SCN10,* which encodes the neuronal sodium channel $Na_v1.8$ were identified in a significant percentage of patients with the typical Brugada phenotype [14, 15]. Another distinct form of Brugada syndrome has been linked to glycerol-3-phosphate dehydrogenase 1-like gene (*GPD1L*), which may impact trafficking of the

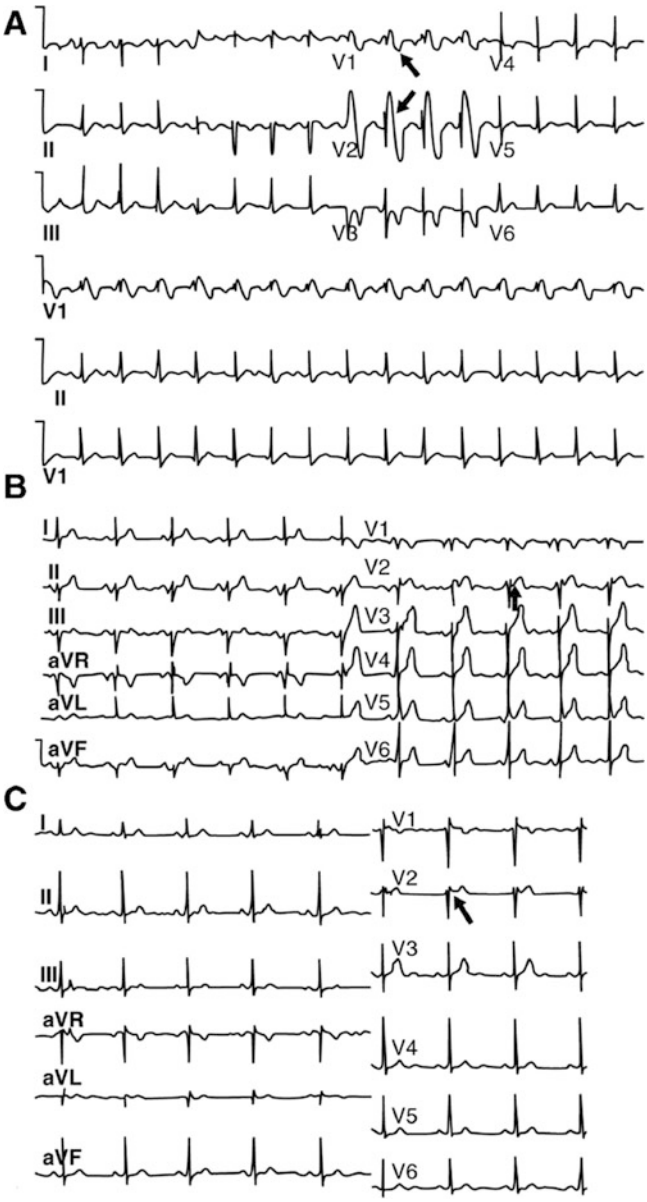

Fig. 67.1 Brugada electrocardiogram (ECG) patterns. (**a**) A diagnostic coved-type (type I) Brugada ECG pattern documented in a 9-year-old girl who presented with syncope and positive family history of BrS. Note the pattern resembling a right bundle branch block (arrows) in leads V_1 and V_2, with typical ST elevation. (**b**) Baseline ECG of a 58-year-old asymptomatic man with positive family history of BrS. Example of a type II saddleback Brugada ECG pattern. Genetic analysis revealed a mutation in the *SCN5A* gene. Note the saddleback-shaped patterns, with a high initial augmentation followed by an ST elevation greater than 2 mm in lead V_2. (**c**) Example of a baseline type III saddleback Brugada ECG pattern (arrow) documented in a 61-year-old asymptomatic man who was diagnosed on the basis of a positive result on class IC antiarrhythmic drug testing. Previously published, used with permission, from Coppola et al.

Na^+ channel. The *GPD1L* variant result in a partial reduction of I_{Na} and is associated with progressive conduction disease and a relatively good prognosis [16, 17]. Interestingly, variants in *RAN* guanine nucleotide release factor *(RANGRF)* gene were also linked to partial reduction in the I_{Na} and Brugada syndrome [18]. Finally, the gene for sarcolemmal membrane-associated protein (SLMAP), which is found in T-tubules and in the sarcoplasmic reticulum was also identified as a causative factor to the syndrome by impacting the $Na_v1.5$ trafficking [18].

Dysfunction of calcium channels in canine and rabbit cardiomyocytes has been associated with the pathogenesis of Brugada syndrome. A synergistic relationship between I_{Na} and $I_{Ca,L}$ is essential to an appropriate AP in ventricular epicardium; therefore, disruption of this synergism may permit the I_{to} current to limit the AP amplitude, allowing a second upstroke and an extrasystole resulting in polymorphic ventricular tachycardia. In subsequent studies with Brugada syndrome patients, an association between loss-of-function variants in calcium channel subunits and shorter than normal QT interval with ST segment elevation was identified [17, 19, 20]. Action potential heterogeneity was observed in canine ventricular cardiomyocytes with calcium channelopathy, displaying a deep phase 1 notch that inactivated the I_{Ca} allowing dispersion of repolarization, phase 2 reentry, and polymorphic ventricular tachycardia. On ECG, these canine models showed prolonged QT intervals, ST elevation, and developed T-wave alternans, supporting a close genotype–phenotype relationship with calcium channel dysfunction and Brugada syndrome.

Gain of function variants in genes regulating the outward potassium currents were interestingly reported in Brugada patients. Pathogenic variants in *KCND2, KCND3, KCNE3,* and *KCNE5* were all found in Brugada cases [17, 21, 22]. The potassium inwardly rectifying channel, subfamily J, member 8 (*KCNJ8*) gene that encodes Kir6.1 was also linked to reported cases. Specifically, a pathogenic variant (S422L-*KCNJ8)* was identified in a diagnosed case with Brugada syndrome [23]. In addition, four *KCNH2* variants, T152I, R164C, W927G, and R1135H were also identified in Brugada patients [24]. Finally, the gene for ATP-binding cassette, subfamily C, member 9 (*ABCC9*), which encodes the sulfonylurea receptor subunit 2 A (*SUR2A*) was identified as a susceptibility gene for Brugada syndrome [25].

The transient receptor potential melastatin protein number 4 (*TRPM4*) is a calcium-activated nonselective cation channel that is expressed in many tissues including the heart. Pathogenic variants were identified in *TRPM4* and were linked to Brugada syndrome [26]. A recent study using isolated myocytes from *Trpm4*$^{-/-}$ mice identified a novel role of *TRPM4* in the regulation of $Na_v1.5$ function [27]. Interestingly, Plakophilin-2 (*PKP2)*, the primary or more prevalent gene correlated with arrhythmogenic right ventricular cardiomyopathy (ARVC) was linked to Brugada syndrome in *PKP2* variants that displayed I_{Na} reduction [28]. The hyperpolarization activated cyclic nucleotide-gated potassium channel 4 (*HCN4*), which mediates the pacemaker (I_f) current in the heart has been reported in a few cases of Brugada syndrome. However, the exact pathophysiologic mechanism has yet to be determined [29, 30]. The Hes-Related Family BHLH Transcription Factor With YRPW Motif 2 (*HEY2*) was linked to Brugada cases and was found

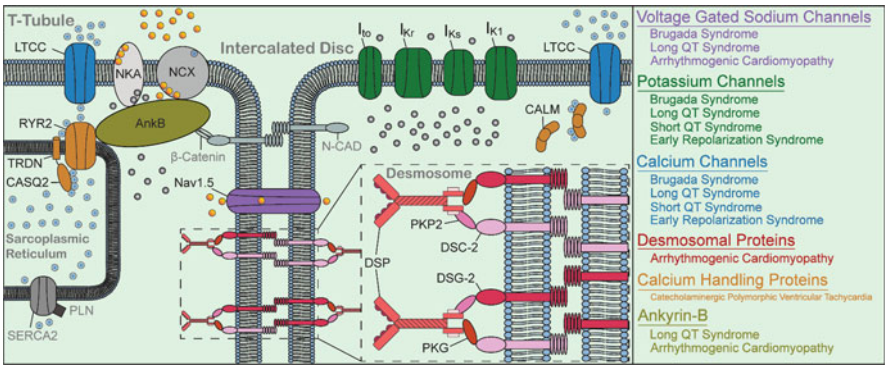

Fig. 67.2 Diagram of key proteins linked to arrhythmogenic disorders labeled with black text. Proteins are color coated based on categories. Panel links each protein category to their associated arrhythmogenic diseases, including voltage-gated calcium channel $Na_V1.5$, potassium channels (I_{kr}, I_{ks}, I_{to}, I_{K1}), L-type calcium channel (LTCC), desmosomal proteins (PKP2, DSP, DSG-2, DSC-2, PKG), Ankyrin B, and additional calcium handling proteins (TRDN, CASQ2, RYR2, CALM1/3)

to play a role in *SCN5A* expression [31, 32]. Finally, pathogenic variants in Semaphorin-3A precursor (*SEMA3A)* and fibroblast growth factor 12 (*FGF12*) were also identified and therefore both genes are included in Brugada syndrome diagnostic panels [18, 33].

While Brugada syndrome has been classically regarded as an electrical disorder and primarily linked to variants in genes encoding ion channel proteins, recent work has linked Brugada syndrome to variants identified in sarcomeric proteins. Importantly, studies have also identified an overlap with cardiomyopathy characteristics, including structural abnormalities [34, 35]. A variant identified in *TPM1* gene, which encodes the sarcomeric α-tropomyosin, was regarded as a predisposing cause of an overlap syndrome provoking both hypertrophic cardiomyopathy and Brugada phenotypes [36]. However, more studies are needed to validate and identify the exact role of *TPM1* in Brugada syndrome. Another report identified the association of Myosin Binding Protein C3 (*MYBPC3*) with Brugada syndrome for the first time [37]. Given the genetic complexity of many variants and the role of environmental factors in the manifestations of the phenotype, Brugada syndrome is more considered as an oligogenic disease rather than a monogenic disorder. A diagram of major proteins linked to Brugada syndrome, as well other arrhythmogenic disorders, is provided in Fig. 67.2.

67.2.2 Long QT Syndrome

As with many inherited arrhythmogenic diseases, the long QT syndrome (LQTS) phenotype involves ion channel proteins but can be precipitated via several different avenues of cellular dysfunction. Prolonged QTc intervals are derived from delayed

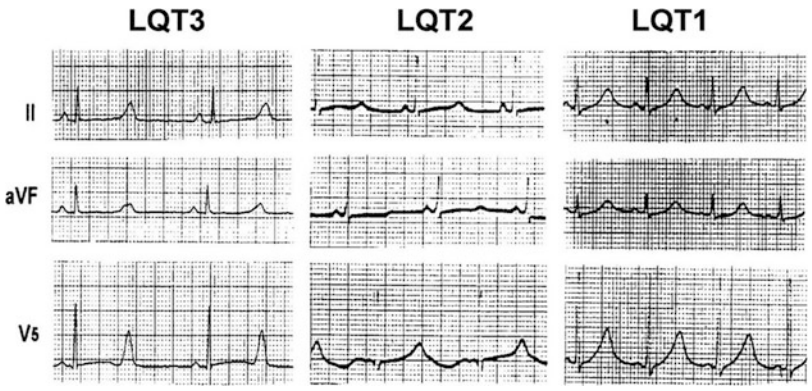

Fig. 67.3 Distinctive T-wave Pattern in the 3 Major LQTS Genotypes. T-wave morphology by LTQS genotype: LQT1: typical broad-based T-wave pattern (corrected QT [QTc] 570 ms); LQT2: typical bifid T-wave (QTc 583 ms); and LQT3: typical late-onset peaked/biphasic T-wave (QTc 573 ms) (Previously published, used with permission, from Goldenberg et al.)

repolarization of the ventricle due to either reduction in repolarizing currents or increase in depolarizing currents. This implicates loss-of-function mutations in K^+ channel subunits or gain-of-function mutations in Na^+ and Ca^{2+} channel subunits and their respective regulatory proteins.

LQTS can be classified into three major types (types 1–3). Each classification is based on the genetic variant associated with the disease progression, specifically *KCNQ1* for LQT1, *KCNH2* for LQT2, and *SCN5A* for LQT3 [38, 39]. Clinical diagnosis of LQTS can be assisted using the Schwartz scoring criteria. This takes into account QTc duration, T wave abnormalities, heart rate, syncope, family history, and other risk factors into consideration to determine the risk factor for LQTS [40]. Representative ECG traces for each major type of LQTS are provided in Fig. 67.3.

A host of variants have been identified in *KCNQ1*, most of which act to reduce I_{Ks} (the slow component of the cardiac delayed rectifier K^+ current) channel trafficking to the cell membrane, reduce I_{Ks} responsiveness to β-adrenergic signaling, or alter channel gating which all act to prolong the AP duration, producing a prolonged QT interval. I_{Ks} activation is governed by sympathetic stimulation, namely, protein kinase A (PKA) phosphorylation mediated by the AKAP targeting protein Yotiao. This pathway ensures rapid repolarization and a shortening of the AP during episodes of increased heart rate. Interruption of I_{Ks} and Yotiao association, as demonstrated in *KCNQ1* G589D and *KCNQ1*$^{-/-}$ mouse models, renders I_{Ks} insensitive to β-adrenergic stimulation, slowing repolarization and producing a prolonged QTc [41]. These findings support the hypothesis that LQTS1 patients with dysfunctional I_{Ks} channels are unable to appropriately respond to β-adrenergic stimulation and thus develop prolonged AP durations due to an inability to initiate repolarization and subsequently trigger arrhythmogenesis. Recently, a variant in *KCNQ1* Y587M was shown to cause a severe LQT phenotype due to aberrant trafficking of I_{Kr}

channels (rapidly activating component of the delayed rectifying potassium current), suggesting alternative molecular pathways for the development of LQTS resulting from variants in *KCNQ1* [42].

While in a state of decreased I_{Ks} and bradycardia, murine, rat, rabbit, and human data have shown that induction of early afterdepolarizations into the AP compromises membrane repolarization, prolonging the QT interval and subsequently triggering polymorphic ventricular tachycardia [41]. In fact, Several LQTS models develop early afterdepolarizations or action potential prolongation recovery by an increased L-type calcium channel and late I_{Na} currents resulting in oscillations of the membrane potential that can produce premature APs [41]. Additionally, canine and murine models have displayed amplification in transmural dispersion of repolarization heterogeneity, when modeled after reduced I_{Ks} as in LQT1. Some models suggest that ventricular M cells (middle layer of ventricular myocytes) are integral to the prolongation of ventricular repolarization due to their naturally low volume of I_{Ks} and resultant prolonged QT interval. [41]. Although implications of a coupled pathogenic mechanism involving both *KCNQ1* variants and I_{Ks}-deficient M-cell physiology have been made, these interactions are still unclear beyond potassium channel alpha subunits.

In addition, variants in other genes are associated with a disruption of I_{Ks} including *KCNE1,* which encodes the beta subunits of $K_V7.1$, and *AKAP9*, a PKA scaffolding protein, linked to LQT5 and 11, respectively. Although *KCNE1* variants are linked to LQT5, they have physiological implications similar to that of the *KCNQ1* variants. Moreover, variants impeding the association between KCNE1 and KCNQ1 result in decreased functionality of $K_V7.1$, resulting in prolonged QT interval and lengthened AP duration [43]. *KCNE1* variants have also been shown to have decreased binding affinity for PIP2. Disruption of the KCNE1-KCNQ1-PIP2 interaction reduces I_{Ks} activity, leading to QTc prolongation [44, 45]. LQTS may result from dysfunction in potassium channel accessory or beta subunits including *KCNE2*. *Kcne2* $^{-/-}$ mice display defects in AP and QT interval duration as well as defects in multiple repolarizing potassium currents [46, 47]. Mutations in the genes encoding proteins of the inward rectifier potassium channels are also linked to LQTS. Specifically, *KCNJ2* variants can result in LQT7 (Andersen-Tawil Syndrome) due to decreased affinity of the channel protein to bind PIP2 [48, 49]. Mutations in the gene encoding for the G protein coupled inwardly rectifying potassium channel are also linked to long QT syndrome - specifically, mutations in *KCNJ5* result in LQT13. Variants in *KCNJ5* have been shown to decrease trafficking of the protein to the cell membrane and decrease the amplitude of the inward rectifying potassium current [50]

While loss-of-function $Na_v1.5$ variants can cause Brugada syndrome, gain-of-function variants at the intracellular link between domains III/IV (DIII/IV) cause persistent I_{Na} during the AP plateau phase, resulting in delayed repolarization and prolonged QT. Mice homozygous or heterozygous for the $Na_v1.5$ ΔKPQ deletion display aberrant $Na_v1.5$ inactivation, persistent I_{Na}, and prolonged AP durations resulting in spontaneous ventricular arrhythmias [51]. *Scn5a*Δ/+ mice showed paradoxical transient AP prolongation upon abrupt acceleration of pacing rate that

favors the occurrence of early afterdepolarizations, demonstrating rate dependent arrhythmogenesis. This observation was due to the increased I_{Na}, causing sudden increase of sodium and calcium load so that during each AP, the increased SR calcium release activated a larger Na/Ca exchange current, favoring early afterdepolarizations and reentry arrhythmias [51]. These outcomes were confirmed by a second study using *Scn5a*Δ/+ mouse hearts, during which prevention of ventricular tachycardia was observed by decreasing dispersion of repolarization and suppressing early afterdepolarizations. Additionally, cardiomyocytes from transgenic N1325S mice showed delayed inactivation and generated a late persistent current, prolonged AP, and early afterdepolarizations resulting in the LQTS phenotype. Finally, models using induced pluripotent stem cell-derived cardiomyocytes (iPSC-CMs) harboring the *Scn5a*1798insAsp/+ variant demonstrated increased persistent I_{Na}, prolonged AP duration, and early afterdepolarizations at low pacing rates [6]. Interestingly, these phenotypic findings were replicated in iPSC-CMs from a human patient with a similar *SCN5A* 1795insAsp/+ mutation at the COOH terminus of $Na_v1.5$, evoking small, sustained currents similar to ΔKPQ variants. In addition to variants in *SCN5a,* variants in *SCN4B* and syntrophin alpha 1 (*SNTA1)* also result in increased late sodium currents, and are linked to LQT3 and LQT12, respectively [52].

Gain-of-function variants in calcium channel proteins such as *CACNA1C* are associated with LQT8 (Timothy Syndrome). Missense mutations in *CACNA1C*, which encodes for $Ca_v1.2$, a subunit of a voltage-gated calcium channel, interfere with the inactivation of the channel. Prolonged calcium current into the cell results in a prolonged QT interval [53, 54].

LQTS mechanisms are not limited to variants in genes encoding channel proteins; in fact, variants in genes encoding structural and regulatory proteins also result in LQTS. Specifically, loss-of-function variants in ankyrin-B (encoded by *ANK2*) in cardiomyocytes demonstrate a central role in the arrhythmogenesis of congenital LQTS4 or "ankyrin-B syndrome." In myocardium, ankyrin-B associates with Na/Ca exchanger (NCX) and Na/K ATPase (NKA) at the cell membrane [55]. Heterozygous ankyrin-$B^{+/-}$ mice displayed defects resulting in dysfunctional NKA channels and intracellular Na^+ accumulation, generating inhibition of NCX function, reduction of Ca^{2+} extrusion, and increase in intracellular Ca^{2+} [55]. Supporting this, human and mouse studies of *ANK2* loss-of-function mutations indicate polymorphic ventricular tachycardia immediately following increases in sympathetic tone as with exercise or stress; however, sinus bradycardia and QT prolongation are demonstrated primarily in patients with *ANK2* variants [6, 55]. Interestingly, the loss of family history in many *ANK2* variants and the incomplete penetrance of AnkB-associated cardiac phenotype strongly suggest the association of additional environmental and/or genetic factors in the development of the severe phenotype of many *ANK2* variants [56]. In addition, Calmodulin (CALM) variants have recently been shown to result in LQT14 and LQT15. Variants in *CALM1* and *CALM2*, which encode for calmodulin-1 and -2, respectively, are linked to a prolonged QT interval, ventricular arrhythmias, and atrioventricular block in infants. Many of these mutations impact the calcium-binding regions of calmodulin, which interferes with

calcium affinity, sodium and potassium currents, and calcium dynamics [57]. A diagram of major proteins linked to LQTS is provided in Fig. 67.2.

67.2.3 Short QT Syndrome

Short QT syndrome is a repolarization disorder characterized by a QTc below 340 ms on the electrocardiogram, atrial and ventricular arrhythmias and importantly a high risk of syncope and SCD [58]. The majority of short QT syndrome (SQTS) variants result from gain-of-function in potassium channel subunits or loss of function in calcium voltage-gated channels [59]; however, phenotypic plasticity has been noted in some forms of SQTS [8]. Penetrance in probands and murine models has demonstrated varying degrees of severity in QT shortening because of the effect of variant on associated subunits of the potassium channel. Representative ECG traces from a patient with SQTS previously published by Dewi et al. are provided in Fig. 67.4 [60].

Gain-of-function variants in *KCNH2,* which mediates I_{Kr}, have been closely associated with SQTS1. The hotspot variant (p.T618I) leads to a major gain of function in I_{Kr} and was identified in 18 cases of seven unrelated families [61]. Other variants have also been reported with a potential pathogenic role including, p.N588K (c.1764C>A), N588K (c.1764C>G) [62], p.I560T, [63], p.E50D [64], p.W927G [24], p.R1135H [65], and p.R164C [24]. Under normal physiologic conditions, *HERG* (human *ether-a-go-go*-related gene) allows timely repolarization of the ventricles and returns to resting membrane potential; however, N588K channels have been shown to increase the amplitude of I_{Kr} and shorten the AP duration

Fig. 67.4 ECG taken from a 65-y-old patient with SQTS; QT interval 240 ms, QTc 294 ms, previously published by Dewi et al.

resulting in arrhythmogenesis [66]. The introduction of a positive charge in the channel pore increases the energy requirement for channel inactivation, leading to a greater repolarization earlier in the AP and shorter refractory periods. This change leaves the ventricles susceptible to premature stimulation. Of note, changes in extracellular potassium concentrations do not produce a change in channel conductance, indicating a disruption in K^+ permeability as the primary pathogenic mechanism. Corderio et al. produced a mouse model showing that arrhythmogenesis may begin in SQTS1 when the shorter ventricular refractory period produced by short AP durations is combined with the longer Purkinje cell AP duration in the ventricles, producing a heterogeneous repolarization and resultant polymorphic ventricular tachycardia [66]. Interestingly, gain of function variants in (*KNCNQ1*), a key contributor to I_{Ks}, have also been linked to SQTS (SQTS2) [67].

Accelerated repolarization and shortened QT intervals also are associated with variants in *KCNJ2*, resulting in gain-of-function of the Kir2.1 channel protein. The Kir2.1 channel sustains resting membrane potentials, modulates cardiac excitability, and participates in determining the length of the QT interval by way of an inward rectifying current, I_{K1}, during the repolarization phase of the AP [68]. SQTS3 is characterized by an asymmetric T wave specific to an D172N Kir2.1 mutation demonstrating slow ascending and rapidly descending limbs [69]. The highly conserved 172 position is integral for normal channel blocking, but its function can be disrupted with an acidic to neutral residue change as seen in D172N, allowing an increased outward current shortening repolarization [69]. Guinea pig myocytes with overexpressed Kir2.1 channels produced an increased I_{K1} density, duplicating the gain-of-function pathogenic mechanism as seen in SQTS3. Moreover, increased outward current in mice overexpressing Kir2.1 showed an increased rate of change in membrane potential during the last phase of the AP producing a shortened repolarization and subsequent QT as seen in SQTS [69]. These changes were arrhythmogenic in both the ventricles and atria of transfected mice, inferring that the same mutation may increase risk for both ventricular and atrial fibrillations in an individual with SQTS3. Sporadic loss of function variants in *CACNA1C* (SQTS4) [19], *CACNB2* (SQTS5) [19] and *CACNA2D1* (SQTS6) [70] have also been reported. Importantly, Thorsen et al. 2017 identified a missense mutation in the anion exchanger (AE3)-encoding *SLC4A3* in two unrelated families diagnosed with SQTS [71]. A diagram of major proteins linked to SQTS is provided in Fig. 67.2.

67.2.4 Catecholaminergic Polymorphic Ventricular Tachycardia

Catecholaminergic polymorphic ventricular tachycardia (CPVT) is found in autosomal dominant, recessive, and idiopathic forms. The most common genetic mechanism for CPVT is autosomal dominant gain-of-function variants in the *RYR2* gene responsible for the assembly of the RYR2 or ryanodine receptor [8]. This protein controls the release of Ca^{2+} from the sarcoplasmic reticulum by way of L-type Ca^{2+} channel signaling and thus is central to the timely stimulation of sarcomeres that produce heart muscle contraction. Mutations in *RyR2* and associated proteins can

cause premature channel opening and Ca^{2+} release leading to delayed afterdepolarizations, bidirectional ventricular tachycardia, and ventricular fibrillation upon β-adrenergic stimulation [6]. Although about 70 *RYR2* variants have been identified, the mechanisms by which CPVT originates from these mutations can be largely attributed to the effects on RYR2 luminal Ca^{2+} sensitivity, binding to association proteins, sarcoplasmic reticulum Ca^{2+} load, and lowered initiation threshold [6].

CPVT is characterized by episodic syncope occurring either to physical stress, such as exercise, or emotional stress, with the absence of structural cardiac abnormalities. These episodes of syncope are generally caused by onset of ventricular tachycardia, potentially resulting in ventricular fibrillation and sudden cardiac death. A diagnosis can be made by studying a probands ECG both at rest and following a stress test through exercise. Additionally, genetic testing can be performed to identify variants in CPVT-associated genes. Typical treatments include the use of beta-blockers, which can be administered in conjunction with flecainide if necessary. Exercise restriction is often recommended, and an implantable cardioverter defibrillator (ICD) can be implanted if there is a history of recurrent cardiac arrest [72].

Several *Ryr2* R4496C knock-in mouse models show that β-adrenergic stimulation induces CPVT Ca^{2+} waves by increasing store overload-induced Ca^{2+} release (SOICR), producing a higher Ca^{2+} and lower sarcoplasmic reticulum Ca^{2+} levels during resting state, which are susceptible to the R4496C lowered Ca^{2+} wave initiation threshold. Additionally, Purkinje cells in this model were more vulnerable to changes in intracellular Ca^{2+} leading to early and delayed afterdepolarizations, inferring a significant role in CPVT arrhythmogenesis [6]. The heterogeneity of a single *RYR2* mutation was demonstrated by Loaiza et al. showing altered RYR2 cytosolic Ca^{2+} sensitivity, protein kinase A phosphorylation, and luminal Ca^{2+} modulation in V2475F mice [68, 73]. A gain of function *Ryr2* R176Q$^{/+}$ mouse model demonstrated calcium oscillations that resulted in baseline bradycardia and AV block, with inducible SCD following caffeine injections [74]. These oscillations were partially attenuated by suppressing the β- adrenergic pathway via Calmodulin-dependent protein kinase II (CaMKII) inhibition. Interestingly, recent *in vitro* studies examined additional RYR2 variants resulting in RYR2 degradation (G357S) or alterations to posttranslational modifications that result in sarcoplasmic reticulum (SR) calcium leak (D3638A) [75, 76]. An additional CPVT murine model identified a reduced binding affinity and decreased RYR2 association to FK506 binding protein (Fkbp12.6), responsible for stabilizing the RYR2. Dissociation of these proteins in FKBP12.6$^{-/-}$ mice was shown to destabilize the closed state of RYR2, allowing uncontrolled Ca^{2+} release and inducing ventricular tachycardia [77]. While it is clear the pathogenic mechanisms of specific CPVT mutations are varied, Loaiza et al. asserted that the production of delayed afterdepolarizations might be a point of convergence for *RYR2* mutations and the CPVT phenotype [73].

Outside of *RYR2*, variants linked to CPVT have been identified within triadin (*TRDN*), calsequestrin (*CASQ2*), and calmodulin genes, each providing novel insights into the underlying mechanisms of disease. CASQ2 and TRDN both play

an integral role in binding calcium within the SR and regulating calcium-induced calcium release. *Casq2* $^{-/-}$ mice displayed defects in the SR size and structure, as well as increased SR load that promotes calcium leak and polymorphic arrhythmias following catecholamine exposure [78]. Additionally, *CASQ2* variants D307H and R33Q were introduced into murine models, resulting in increased propensity for inducible arrhythmias, morphological changes to the SR/SR junction, and reduced TRDN expression. Both variants resulted in loss of CASQ2 protein expression via separate mechanisms, including autophagy (R33Q) and ER-associated degradation (E307H) [79, 80]. The well-characterized T59R *TRDN* variant, shown to prevent protein transport from the ER, was introduced into a *Trdn*-KO mouse [81]. Substantial loss of CASQ2 and TRDN were observed, as well as slight reductions in RYR2. This resulted in increased calcium sparks and decreased load, with decreased transient amplitude and rise time [81, 82]. Calmodulin is a calcium binding protein responsible for transducing multiple signaling pathways, including RYR2 binding and CaMKII activation. Select CPVT-linked variants within *CALM1/3* results in decreased C-terminal affinity for Ca^{2+} (N98S/A103V), as well as an inability to properly regulate RYR2 function (N98S/A103V/N54I), leading to more frequent calcium sparks, decrease in SR load, and increased propensity for inducible arrhythmias [83, 84]. An established *Calm1* N98$^{/+}$ murine model displayed basal bradycardia, prolonged QTc and QRS intervals, and increased arrhythmogenic events derived by increased L-type calcium induced β-adrenergic stimulation [85]. A breakdown of the major CPVT genes/variants is provided in Table 67.1 and Fig. 67.2.

67.2.5 Arrhythmogenic Cardiomyopathy

Arrhythmogenic Cardiomyopathy (ACM), also formerly named arrhythmogenic right ventricular cardiomyopathy/dysplasia (ARVC/D), is a primarily genetic form of heart disease originally believed to have right ventricular dominance. Recent evidence has identified left and biventricular dominant cases, leading to the usage of the term ACM over ARVC/D [90]. It is characterized by fibro-fatty infiltration of the ventricular myocardium, mild chamber dilation, increased propensity for ventricular arrhythmias and SCD. Unique to CPVT and other arrhythmogenic disorders, structural defects are apparent in ACM [91, 92]. An example cardiac MRI of an ACM patient can be found in Fig. 67.5 [93]. However, electrical abnormalities precede structural changes, referred as a "concealed phase" where ventricular abnormalities and SCD are commonly the first clinical manifestation of disease [94–96].

Approximately 16 genes are linked to ACM with identified disease-causing variants. Despite this distribution, the majority (85–90%) of variants are localized within desmosomal genes, particularly in *PKP2*, desmoplakin (*DSP*), and desmogelin-2 (*DSG2*) [91]. The desmosome is an essential protein complex localized at the intercalated disc (ID), providing structural integrity at the cardiomyocyte junction, and assists in protein recruitment and trafficking to the gap junction and other ID components. Indeed human tissue often shows ID

Table 67.1 Table of major CPVT variants, protein localization, functional changes, and related animal models

Gene	Protein	Localization/ structure	Key variants	Functional change	Animal models	References
RYR2	Ryanodine Receptor-2	SR membrane	R4496C	Gain of function/increased calcium sensitivity	R4496C *Ryr2* KI	[73, 74, 86–88]
			V2475F	Altered PKA phosphorylation/gain of function	V2475F *Ryr2* KI (homologous recombination)	
			R176Q	Gain of function	R176Q *Ryr2* KI	
			G357S	Reduced protein expression		
			D3638A	Conformation Change Altering PTMs (Hyperactivity)		
CASQ2	Calsequestrin-2	SR internal/ membrane	R33Q	Reduced Protein Expression (Autophagy)	R33Q *Casq2* KI	[78–80, 89]
			D307H	Reduced Protein Expression (ER-Associated Degradation)	D307H *Casq2* KI	
					Casq2 KO	
TRDN	Triadin	SR internal/ membrane	T59R	Reduced protein expression	T59R Transgenic (AAV) *Trdn*	[81, 82]
FKBP12.6	FK506-binding protein	SR membrane			FKBP12.6 KO (homologous recombination)	[77]
CALM genes	Calmodulin	Cytoplasm	*CALM1*-N98S	Altered RYR2 Regulation/Reduced Ca^{2+} interactions (C-terminal)	*Calm1* N98S CRISPR KI	[83, 84]
			CALM1-N54I	Altered RYR2 Regulation		
			CALM3-A103V	Reduced Ca^{2+} Interactions (C-terminal)		

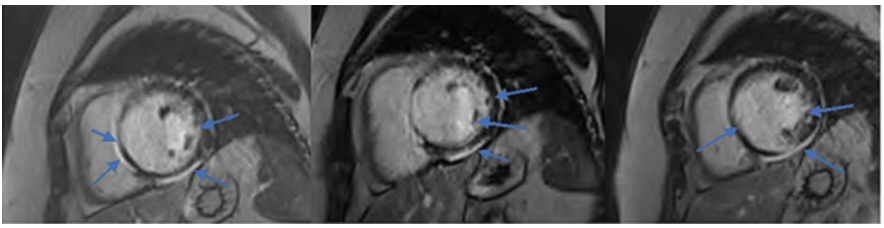

Fig. 67.5 Postcontrast cardiac MRI revealing fibrosis from the base of the left ventricle to the right ventricular septum, previously published by Mohamed et al.

remodeling and reduced ID protein expression, including desmosomal targets [97]. Outside the desmosome, most ACM-linked variants lie within structural proteins, such as lamin A/C, desmin, and α-T-catenin, or those that regulate electrical activity, including phospholamban and sodium channel $Na_v1.5$. A full list of ACM-linked genes and related mouse models is included in Table 67.2.

Despite a diverse genetic background, common proposed mechanisms of pathogenicity are shared between cases/genetic causes. Multiple studies have shown that connexin-43 (Cx43), an essential gap junction protein that promotes unidirectional AP propagation between cardiomyocytes via ion exchange, often has expression and activity changes in both human patients [104, 126] and animal models. Green et al. discovered multiple ACM-linked *DSP* variants that were shown to reduce Cx43 trafficking via reduced binding affinity to the trafficking microtubule end binding protein 1 (EB1) [127]. Later work by this group revealed loss of DSP, a common ACM feature, resulting in hyper-phosphorylation of Cx43 via a RAS-MEK-ERK dependent pathway, ending in Cx43 ubiquitination and degradation [128]. Reduced Cx43 expression was also identified in a *Dsg* KO murine model [109]. A *Pkp2* het KO murine model revealed increased Cx43 hemi channel activity and leakage that induced calcium sparks and arrhythmias prior to structural defects [98]. Outside Cx43, additional ion channel/pumps functional changes have been established. An inducible *Pkp2* homo KO mouse model resulted in decreased expression of calcium handling proteins (RYR2, $Ca_v1.2$, CASQ2) as well as AnkB, resulting in more frequent calcium sparks and inducible arrhythmias [99]. RYR2 T2809 phosphorylation and channel leakage was identified in the RV of the *Pkp2* het KO model in a following study [98]. $Na_v1.5$ levels have been shown to be reduced in select ACM cases [104], with multiple identified variants being presented as the genetic driver of ACM [129, 130]. Finally, the phospholamban variant R14del induces SERCA hyperphosphorylation via aggresome formation [131, 132].

Alterations in Wnt/β-catenin signaling have often been shown in ACM models, typically through mislocalization of the ID protein plakoglobin (PKG), a binding competitor of β-catenin and antagonist of the signaling pathway. Inactivation ultimately results in increased expression of adipogenic and fibrotic genes. Knockdown of *DSP* drives PKG mislocalization to the nucleus and suppresses Wnt/β-catenin signaling. Indeed, a *Dsp* KO mouse model revealed fibrosis and adipocyte content,

Table 67.2 Table of ACM-linked genes, localization within the cardiomyocyte, and associated animal models. Animal models listed are murine models unless otherwise indicated

Function	Gene	Protein	Localization/structure	Pathogenic variants[a]	Animal models	References
Desmosomal	*PKP2*	Plakophilin-2	ID/desmosome	171	Embryonic whole-body KO	[98–103]
					Tamoxifen-inducible cardiac specific KO(Het/Homo)	
					Transgenic S329X (αMHC)	
					Transgenic R735X (AAV injections)	
	DSP	Desmoplakin	ID/desmosome	86	Embryonic Whole-Body/Cardiac KO	[104–108]
					Mlc2v-Cre-inducible Cardiac KO	
					α-MHC-Cre-inducible Cardiac KO	
					Transgenic V30M (αMHC)	
					Transgenic Q90R (αMHC)	
					Transgenic R2834H (αMHC)	
	DSG2	Desmoglein-2	ID/desmosome	50	Embryonic Whole-Body KO	[109–114]
					Flp-Recombinase Whole-Body Fragmented DSG2	
					Transgenic (αMHC) N266S	
	DSC2	Desmocollin-2	ID/desmosome	42	Transgenic Overexpression model	[115, 116]
					Zebrafish Haploinsufficient model (c.631-2A→G)	
	JUP	Junction plakoglobin (PKG)	ID/desmosome	15	Embryonic Whole-Body KO	[109, 117–121]
					Tamoxifen-Inducible αMHC/MerCreMer Cardiac KO	
					αMHC-Cre Cardiac KO	
					Transgenic 2157del2	
	ANK2	Ankyrin B (AnkB)	Z-lines/T-tubules	–	*Ank2* (αMHC) Cardiac KO	[56]

Additional Structural	*CDH2*	N-Cadherin	ID/adherens junction	–	–	
	CTNNA3	α-T-catenin	ID/area composita	2	–	
	DES	Desmin	Intermediate filaments/ cytoskeleton	11	–	
	FLNC	Filamin C	Sarcomere/ID	–	–	
	LMNA	Lamin A/C	Nuclear envelope	16	–	
	TJP1	Zonula occludens 1 (ZO1)	ID/tight junction	–	–	
	TMEM43	Transmembrane protein 43 (LUMA)	Nuclear envelope/ID	3	S358L TMEM43 (αMHC Cre)	[122]
	TTN	Titin	Sarcomere	–	–	
Other	*PLN*	Phospholamban	Sarcoplasmic reticulum	4	R14del Homozygous (*Hprt* Cre)	[123]
	SCN5A	Sodium channel $Na_v1.5$	Cell membrane	–	–	

[a]Pathogenic variants determined through the ARVC database [124, 125]

along with chamber dilation and ventricular arrhythmias [105]. A key contributor to this pathway is GSK3β, which is responsible for degrading β-catenin and has been proposed to be a potential therapeutic target. Multiple studies have shown promising results of GSK3β inhibition, as both desmosomal (*Dsg* KO, *Jup*^{2157del2}) and nondesmosomal (*Ank2*-cKO, *Tmem43* S358L) ACM mouse models have shown increased β-catenin stability and improved phenotypes [56, 109, 122]. Outside the Wnt/β-catenin signaling, activation of the Hippo pathway via increased phosphorylation of targets NF2 and YAP has been shown to drive ACM progression in both a cellular model (HL1 PKP2:shRNA KD myocytes) and mouse lines (*Myh6:Jup, Nkx2.5-Cre:Dsp*$^{W/F}$) [97]. A diagram of major proteins linked to ACM is provided in Fig. 67.2.

67.2.6 Early Repolarization Syndrome

Increase of ventricular I_{to}, ATP-sensitive K+ current (I_{KATP}), or acetylcholine-regulated K+ current ($I_{K,Ach}$) current and decrease of $I_{Ca,L}$ and I_{Na} current are suspected in the arrhythmogenesis of early repolarization syndrome (ERS); however, the exact mechanism is still unknown [133]. ERS shares a close phenotype with Brugada syndrome as evidenced by its intermittent concomitant presentation in some patients, with diagnosis differentiating primarily on the area of the heart affected. Genotypes of ERS demonstrate heterogeneity and variants have been identified in at least six genes [134].

The *KCNJ8* Ser422Lys variant produces a gain-of-function of the Kir6.1 subunit causing decreased ATP sensitivity and increased I_{KATP}. This, along with an outward imbalance of potassium currents facilitated by increased I_{to} during bradycardia or $I_{K,Ach}$ during vagal influence in epicardium, can facilitate a shift in the transmural voltage gradient between endocardium and epicardium resulting in phase 2 reentry, amplification of the J wave, and polymorphic ventricular tachycardia. In whole cell patch clamp studies, left inferior ventricular epicardium demonstrated a higher susceptibility to ERS due to higher concentration of Kir6.1 and higher levels of I_{to} when coupled with known ERS mutations including *KCNJ8* [23, 135].

Similarly, the *KCND3* G307A variant produces a gain of function in K_v4.3, the alpha subunit to the I_{to} channel. The heterozygous variant ultimately results in ventricular fibrillation storm, with cultured cells showing increased K_v4.3 current density, slowed inactivation and recovery, with the effects exacerbated with two copies of the variant [136]. Variants within *SCN1Bβ* (S248R and R250T) have also been linked to ERS and shown to interact and regulate K_v4.3 activity. With similar effects toward I_{to} channel activity as the *KCND3* G307A variant, the proposed mechanism of pathogenicity was altered K_v4.3 interactions. Only the R250T variant, associated with a more severe phenotype, displayed increased interactions with K_v4.3 via Co-IP experiments [137].

Pathogenesis of ERS has also been attributed to loss-of-function variants in L-type calcium channels leading to a decreased inward Ca^{2+} current. Burashnikov et al. found that mutations in any one of three subunits of the L-type calcium channel

(LTCC), α1, β2, and α2δ, were found in patients with ERS; however, the β2 subunit was found in higher frequency associated with ERS [20]. Pharmacological loss of function in LTCC was modeled in canine hearts using verapamil, an LTCC blocker, and resulted in a net outward shift of current balance during the early AP phase, allowing phase 2 reentry and induction of ventricular arrhythmia. The same model demonstrated further loss of left ventricular epicardial AP dome and early repolarization morphology when verapamil and acetylcholine were infused together, inferring a parasympathetic role in arrhythmogenesis of ERS [138–140]. This result indicates the need for future investigation into the implications of bradycardia and circadian rhythms with regard to the arrhythmogenesis of ERS.

While the link between I_{ks}/I_{kr} activity changes and ERS remains questionable, select variants in *KCNE1*, essential for modulating the subunits of KCNQ1, have been identified in multiple families with ERS. The well characterized S38L variant results in decreased KCNE-1 protein levels, as well as mislocalization from the cell membrane to the cytosol. In addition, mislocalization of KCNE1 is observed from the cellular membrane to the cytosol. Due to this perturbed trafficking and mislocalization, I_{ks} levels are significantly reduced, believed to induce the ERS phenotype [141]. A diagram of major proteins linked to ERS is provided in Fig. 67.2.

67.3 Atrial Arrhythmias

Human atrial arrhythmias consist of atrial fibrillation, atrial flutter and many different forms of supraventricular tachycardia such as focal atrial tachycardia (FAT), AV-nodal reentry tachycardia, accessory pathways, multifocal or chaotic atrial tachycardia (MAT) etc.[142–145]. Atrial arrhythmias may result from defects in atrial size, alterations in atrial fibrosis, or defects in atrial excitability. Atrial fibrillation is the most common arrhythmic disorder seen and reported on the clinical setting in adults, and its incidence increases significantly with aging [146]. Animal models have been important in defining the pathways underlying these disparate phenotypes. While too many to detail in depth, protein classes with described mouse models linked with atrial fibrillation include models of G-protein-coupled receptor signaling, altered ion channel proteins and protein complexes, altered calcium homeostasis, defects in proteins involved in cardiac conduction (i.e., connexin 40), as well as defects in transcription factors, cytokines, and growth factors [147].

More evidence is growing on the link between the novel Coronavirus Disease (COVID-19) and the incidence of cardiovascular complications and arrhythmias. COVID-19, caused by severe acute respiratory syndrome Coronavirus (SARS-CoV2), has affected millions of people across the world. Recent reports have highlighted the occurrence of atrial arrhythmias in adult patients admitted to hospitals with COVID-19 [148–151]. Interestingly, the association between atrial fibrillation and viral infections such as COVID-19 can be explained by the inflammatory process and the inflammatory mediators accompanying the infection process [152]. However, there is limited data on the prevalence of new onset atrial fibrillation

as a result of the myocardial injury and inflammation accompanying the COVID-19. Therefore, more studies are needed to explain the exact pathophysiology of atrial arrhythmias/atrial fibrillation in the context of the COVID infection.

67.4 Conclusions and Future Perspectives

Identifying the pathogenic mechanisms of congenital cardiac arrhythmias has profound implications on the diagnosis, and treatment of these conditions. Importantly, studies in the last 15 years have revealed a pivotal subclass of arrhythmogenic mutations affecting nonion channel proteins, expanding the mechanistic substrates of "channelopathies," and therefore prompting augmented study in this area. The use of animal models has afforded an accurate framework for the investigation of human arrhythmias, providing improved insights into the clinical presentations of these diseases. In addition to animal models, human-induced pluripotent stem cells (hiPSCs) are on the rise as a model to study human arrhythmias. Patient-derived hiPSCs bring several advantages over other models, including that they retain the electrophysiological, molecular, and genetic properties of the patient's cardiomyocytes. This *in vitro* model is particularly useful for observing how the electrical current in cardiomyocytes is disrupted by the patient-specific mutations, as well as for high throughput drug development and therapeutic testing. However, this model does not come without its challenges. While hiPSCs do provide a good approximation of the clinical presentation of the arrhythmia under investigation, the correlation between *in vitro* and *in vivo* data is not strong and, in some cases, lacking completely. It is important to consider this as not a replacement but a complementary model to assess disease mechanisms.

Further understanding of genotype–phenotype relationships in the congenital arrhythmia syndromes will allow clinicians to more accurately screen, risk-stratify, and apply personalized therapy to patients across the globe. While mice, rabbits, and guinea pigs have served as primary models for human arrhythmia, atypical models including zebrafish offer exciting promise for our understanding of human disease [153]. Furthermore, computational approaches continue to offer high throughput and rapid evaluation of cardiac disease susceptibility [154].

Appropriate differentiation of cell types from transcription factors plays a key role in proper cardiac development, and misregulation can lead to congenital heart disease and arrhythmias. In fact, loss of the cardiac transcription factor Nkx2-5 has been shown to lead to conduction defects and inducible arrhythmias [155, 156], ultimately attributed to altered regulation of cell fate divergence in Purkinje fiber network morphogenesis [157]. Of note, common drivers of many arrhythmogenic disorders are either increased protein expression, or variants that result in hyperactivity of ion channels. A major barrier in targeting specific genes expressing malfunctioning ion channels is the possibility of off target effects. Amiodarone, a widely used antiarrhythmogenic drug, was analyzed using multiple dosages in mice, where it was determined to decrease the expression of many ion channel subunits, including genes that produce $Na_v1.5$, Cx43, $Ca_v1.2$, and multiple K^+ channel

subunits [158–160]. While it is an effective therapeutic, the lack of specificity provides potential risks to select patients. Therefore, recent studies have focused on studying the effects of micro RNAs in the heart and how they are misrelated in many heart disorders. Not only do microRNAs have been linked to essential transcription factors and methylated genes, but have also been directly linked toward targeting essential ion channel genes including potassium voltage-gated channel subfamily j member 2 and gap junction protein alpha-1 [161]. Future studies more thoroughly studying/targeting the transcriptional regulators of ion channels and other arrhythmia-linked genes are essential toward the improvement and development of effective personalized treatments.

While nearly all mouse and cellular models for arrhythmias are monogenic, it is essential to consider the diversity within the human genome and evaluate the complexities of the oligogenic background in arrhythmogenic disorders. As previously stated, Brugada syndrome is likely an oligogenic disease due to both an absence of an identified variant in ~80% of cases, and a lack of understanding in the interactions between rare and common variants with environmental factors [35]. ACM also has relatively low frequency of monogenic sporadic cases (~40%) [91, 94, 162, 163], with multiple sources identifying strong variability in phenotype due to incomplete penetrance and environmental factors [164, 165]. Even clinical ACM-variants introduced into murine models have been shown to lack a phenotype following cardiac stress, further suggesting ACM is not a monogenic disease [166]. Cases of SCD also have a diverse genetic background that often cannot be linked to a single variant, highlighting the complex links between disease progression and clinical variants [167]. While the complex genetic background makes producing effective models of arrhythmogenic disorders difficult, these models are still a useful tool to evaluate the effects of external/environmental factors and provide an effective first step toward the design and evaluation of future therapeutics. These findings emphasize the need to improve genetic testing to identify lower risk variants that may still be capable of causing disease in conjunction with additional variants. The ability to more effectively determine if rare or common variants may be pathogenic in conjunction is a vital next step to improve the development of arrhythmogenic animal models.

References

1. Brugada P, Brugada J. Right bundle branch block, persistent ST segment elevation and sudden cardiac death: a distinct clinical and electrocardiographic syndrome. A multicenter report. J Am Coll Cardiol. 1992;20(6):1391–6. https://doi.org/10.1016/0735-1097(92)90253-j.
2. Chen QY, Kirsch GE, Zhang DM, Brugada R, Brugada J, Brugada P, Potenza D, Moya A, Borggrefe M, Breithardt G, Ortiz-Lopez R, Wang Z, Antzelevitch C, O'Brien RE, Schulze-Bahr E, Keating MT, Towbin JA, Wang Q. Genetic basis and molecular mechanism for idiopathic: ventricular fibrillation. Nature. 1998;392(6673):293–6.
3. Priori SG, Napolitano C, Gasparini M, Pappone C, Della Bella P, Brignole M, Giordano U, Giovannini T, Menozzi C, Bloise R, Crotti L, Terreni L, Schwartz PJ. Clinical and genetic heterogeneity of right bundle branch block and ST-segment elevation syndrome: A

prospective evaluation of 52 families. Circulation. 2000;102(20):2509–15. https://doi.org/10.1161/01.cir.102.20.2509.
4. Wilde AA, Antzelevitch C, Borggrefe M, Brugada J, Brugada R, Brugada P, Corrado D, Hauer RN, Kass RS, Nademanee K, Priori SG, Towbin JA, Study Group on the Molecular Basis of Arrhythmias of the European Society of Cardiology. Proposed diagnostic criteria for the Brugada syndrome: consensus report. Circulation. 2002;106(19):2514–9. https://doi.org/10.1161/01.cir.0000034169.45752.4a.
5. Coppola G, Corrado E, Curnis A, Maglia G, Oriente D, Mignano A, Brugada P. Update on Brugada Syndrome 2019. Curr Probl Cardiol. 2021;46(3):100454. https://doi.org/10.1016/j.cpcardiol.2019.100454.
6. Hsiao PY, Tien HC, Lo CP, Juang JM, Wang YH, Sung RJ. Gene mutations in cardiac arrhythmias: a review of recent evidence in ion channelopathies. Appl Clin Genet. 2013;6:1–13. https://doi.org/10.2147/TACG.S29676.
7. Crotti L, Marcou CA, Tester DJ, Castelletti S, Giudicessi JR, Torchio M, Medeiros-Domingo-A, Simone S, Will ML, Dagradi F, Schwartz PJ, Ackerman MJ. Spectrum and prevalence of mutations involving BrS1-through BrS12-susceptibility genes in a cohort of unrelated patients referred for Brugada syndrome genetic testing: implications for genetic testing. J Am Coll Cardiol. 2012;60(15):1410–8. https://doi.org/10.1016/j.jacc.2012.04.037.
8. Abriel H, Zaklyazminskaya EV. Cardiac channelopathies: genetic and molecular mechanisms. Gene. 2013;517(1):1–11. https://doi.org/10.1016/j.gene.2012.12.061.
9. Martin CA, Zhang Y, Grace AA, Huang CL. Increased right ventricular repolarization gradients promote arrhythmogenesis in a murine model of Brugada syndrome. J Cardiovasc Electrophysiol. 2010;21(10):1153–9. https://doi.org/10.1111/j.1540-8167.2010.01767.x.
10. Martin CA, Zhang Y, Grace AA, Huang CL. In vivo studies of Scn5a+/- mice modeling Brugada syndrome demonstrate both conduction and repolarization abnormalities. J Electrocardiol. **2010**;43(5):433–9. https://doi.org/10.1016/j.jelectrocard.2010.05.015.
11. Watanabe H, Koopmann TT, Le Scouarnec S, Yang T, Ingram CR, Schott JJ, Demolombe S, Probst V, Anselme F, Escande D, Wiesfeld AC, Pfeufer A, Kaab S, Wichmann HE, Hasdemir C, Aizawa Y, Wilde AA, Roden DM, Bezzina CR. Sodium channel beta1 subunit mutations associated with Brugada syndrome and cardiac conduction disease in humans. J Clin Invest. 2008;118(6):2260–8. https://doi.org/10.1172/JCI33891.
12. Riuro H, Beltran-Alvarez P, Tarradas A, Selga E, Campuzano O, Verges M, Pagans S, Iglesias A, Brugada J, Brugada P, Vazquez FM, Perez GJ, Scornik FS, Brugada R. A missense mutation in the sodium channel beta2 subunit reveals SCN2B as a new candidate gene for Brugada syndrome. Hum Mutat. 2013;34(7):961–6. https://doi.org/10.1002/humu.22328.
13. Hu D, Barajas-Martinez H, Burashnikov E, Springer M, Wu Y, Varro A, Pfeiffer R, Koopmann TT, Cordeiro JM, Guerchicoff A, Pollevick GD, Antzelevitch C. A mutation in the beta 3 subunit of the cardiac sodium channel associated with Brugada ECG phenotype. Circ Cardiovasc Genet. 2009;2(3):270–8. https://doi.org/10.1161/CIRCGENETICS.108.829192.
14. Hu D, Barajas-Martinez H, Pfeiffer R, Dezi F, Pfeiffer J, Buch T, Betzenhauser MJ, Belardinelli L, Kahlig KM, Rajamani S, DeAntonio HJ, Myerburg RJ, Ito H, Deshmukh P, Marieb M, Nam GB, Bhatia A, Hasdemir C, Haissaguerre M, Veltmann C, Schimpf R, Borggrefe M, Viskin S, Antzelevitch C. Mutations in SCN10A are responsible for a large fraction of cases of Brugada syndrome. J Am Coll Cardiol. 2014;64(1):66–79. https://doi.org/10.1016/j.jacc.2014.04.032.
15. Fukuyama M, Ohno S, Makiyama T, Horie M. Novel SCN10A variants associated with Brugada syndrome. Europace. 2016;18(6):905–11. https://doi.org/10.1093/europace/euv078.
16. London B, Michalec M, Mehdi H, Zhu X, Kerchner L, Sanyal S, Viswanathan PC, Pfahnl AE, Shang LL, Madhusudanan M, Baty CJ, Lagana S, Aleong R, Gutmann R, Ackerman MJ, McNamara DM, Weiss R, Dudley SC. Mutation in glycerol-3-phosphate dehydrogenase 1 like gene (GPD1-L) decreases cardiac Na+ current and causes inherited arrhythmias. Circulation. 2007;116(20):2260–8. https://doi.org/10.1161/CIRCULATIONAHA.107.703330.

17. Antzelevitch C, Nof E. Brugada syndrome: recent advances and controversies. Curr Cardiol Rep. 2008;10(5):376–83. https://doi.org/10.1007/s11886-008-0060-y.
18. Ishikawa T, Sato A, Marcou CA, Tester DJ, Ackerman MJ, Crotti L, Schwartz PJ, On YK, Park JE, Nakamura K, Hiraoka M, Nakazawa K, Sakurada H, Arimura T, Makita N, Kimura A. A novel disease gene for Brugada syndrome: sarcolemmal membrane-associated protein gene mutations impair intracellular trafficking of hNav1.5. Circ Arrhythm Electrophysiol. 2012;5(6):1098–107. https://doi.org/10.1161/CIRCEP.111.969972.
19. Antzelevitch C, Pollevick GD, Cordeiro JM, Casis O, Sanguinetti MC, Aizawa Y, Guerchicoff A, Pfeiffer R, Oliva A, Wollnik B, Gelber P, Bonaros EP, Burashnikov E, Wu Y, Sargent JD, Schickel S, Oberheiden R, Bhatia A, Hsu LF, Haissaguerre M, Schimpf R, Borggrefe M, Wolpert C. Loss-of-function mutations in the cardiac calcium channel underlie a new clinical entity characterized by ST-segment elevation, short QT intervals, and sudden cardiac death. Circulation. 2007;115(4):442–9. https://doi.org/10.1161/CIRCULATIONAHA.106.668392.
20. Burashnikov E, Pfeiffer R, Barajas-Martinez H, Delpon E, Hu D, Desai M, Borggrefe M, Haissaguerre M, Kanter R, Pollevick GD, Guerchicoff A, Laino R, Marieb M, Nademanee K, Nam GB, Robles R, Schimpf R, Stapleton DD, Viskin S, Winters S, Wolpert C, Zimmern S, Veltmann C, Antzelevitch C. Mutations in the cardiac L-type calcium channel associated with inherited J-wave syndromes and sudden cardiac death. Heart Rhythm. 2010;7(12):1872–82. https://doi.org/10.1016/j.hrthm.2010.08.026.
21. Ohno S, Zankov DP, Ding WG, Itoh H, Makiyama T, Doi T, Shizuta S, Hattori T, Miyamoto A, Naiki N, Hancox JC, Matsuura H, Horie M. KCNE5 (KCNE1L) variants are novel modulators of Brugada syndrome and idiopathic ventricular fibrillation. Circ Arrhythm Electrophysiol. 2011;4(3):352–61. https://doi.org/10.1161/CIRCEP.110.959619.
22. Giudicessi JR, Ye D, Tester DJ, Crotti L, Mugione A, Nesterenko VV, Albertson RM, Antzelevitch C, Schwartz PJ, Ackerman MJ. Transient outward current (I-to) gain-of-function mutations in the KCND3-encoded Kv4.3 potassium channel and Brugada syndrome. Heart Rhythm. 2011;8(7):1024–32. https://doi.org/10.1016/j.hrthm.2011.02.021.
23. Barajas-Martinez H, Hu D, Ferrer T, Onetti CG, Wu Y, Burashnikov E, Boyle M, Surman T, Urrutia J, Veltmann C, Schimpf R, Borggrefe M, Wolpert C, Ibrahim BB, Sanchez-Chapula JA, Winters S, Haissaguerre M, Antzelevitch C. Molecular genetic and functional association of Brugada and early repolarization syndromes with S422L missense mutation in KCNJ8. Heart Rhythm. 2012;9(4):548–55. https://doi.org/10.1016/j.hrthm.2011.10.035.
24. Wang QI, Ohno S, Ding WG, Fukuyama M, Miyamoto A, Itoh H, Makiyama T, Wu J, Bai J, Hasegawa K, Shinohara T, Takahashi N, Shimizu A, Matsuura H, Horie M. Gain-of-function KCNH2 mutations in patients with Brugada syndrome. J Cardiovasc Electrophysiol. 2014;25(5):522–30. https://doi.org/10.1111/jce.12361.
25. Hu D, Barajas-Martinez H, Terzic A, Park S, Pfeiffer R, Burashnikov E, Wu Y, Borggrefe M, Veltmann C, Schimpf R, Cai JJ, Nam GB, Deshmukh P, Scheinman M, Preminger M, Steinberg J, Lopez-Izquierdo A, Ponce-Balbuena D, Wolpert C, Haissaguerre M, Sanchez-Chapula JA, Antzelevitch C. ABCC9 is a novel Brugada and early repolarization syndrome susceptibility gene. Int J Cardiol. 2014;171(3):431–42. https://doi.org/10.1016/j.ijcard.2013.12.084.
26. Liu H, Chatel S, Simard C, Syam N, Salle L, Probst V, Morel J, Millat G, Lopez M, Abriel H, Schott JJ, Guinamard R, Bouvagnet P. Molecular genetics and functional anomalies in a series of 248 Brugada cases with 11 mutations in the TRPM4 channel. PLoS One. 2013;8(1):e54131. https://doi.org/10.1371/journal.pone.0054131.
27. Ozhathil LC, Rougier JS, Arullampalam P, Essers MC, Ross-Kaschitza D, Abriel H. Deletion of Trpm4 alters the function of the Nav1.5 Channel in Murine cardiac myocytes. Int J Mol Sci. 2021;22(7):3401. https://doi.org/10.3390/ijms22073401.
28. Cerrone M, Lin X, Zhang M, Agullo-Pascual E, Pfenniger A, Chkourko Gusky H, Novelli V, Kim C, Tirasawadichai T, Judge DP, Rothenberg E, Chen HS, Napolitano C, Priori SG, Delmar M. Missense mutations in plakophilin-2 cause sodium current deficit and associate

with a Brugada syndrome phenotype. Circulation. 2014;129(10):1092–103. https://doi.org/10.1161/CIRCULATIONAHA.113.003077.
29. Ueda K, Hirano Y, Higashiuesato Y, Aizawa Y, Hayashi T, Inagaki N, Tana T, Ohya Y, Takishita S, Muratani H, Hiraoka M, Kimura A. Role of HCN4 channel in preventing ventricular arrhythmia. J Hum Genet. 2009;54(2):115–21. https://doi.org/10.1038/jhg.2008.16.
30. Wilde AA, Behr ER. Genetic testing for inherited cardiac disease. Nat Rev Cardiol. 2013;10(10):571–83. https://doi.org/10.1038/nrcardio.2013.108.
31. Bezzina CR, Barc J, Mizusawa Y, Remme CA, Gourraud JB, Simonet F, Verkerk AO, Schwartz PJ, Crotti L, Dagradi F, Guicheney P, Fressart V, Leenhardt A, Antzelevitch C, Bartkowiak S, Borggrefe M, Schimpf R, Schulze-Bahr E, Zumhagen S, Behr ER, Bastiaenen R, Tfelt-Hansen J, Olesen MS, Kaab S, Beckmann BM, Weeke P, Watanabe H, Endo N, Minamino T, Horie M, Ohno S, Hasegawa K, Makita N, Nogami A, Shimizu W, Aiba T, Froguel P, Balkau B, Lantieri O, Torchio M, Wiese C, Weber D, Wolswinkel R, Coronel R, Boukens BJ, Bezieau S, Charpentier E, Chatel S, Despres A, Gros F, Kyndt F, Lecointe S, Lindenbaum P, Portero V, Violleau J, Gessler M, Tan HL, Roden DM, Christoffels VM, Le Marec H, Wilde AA, Probst V, Schott JJ, Dina C, Redon R. Common variants at SCN5A-SCN10A and HEY2 are associated with Brugada syndrome, a rare disease with high risk of sudden cardiac death. Nat Genet. 2013;45(9):1044–9. https://doi.org/10.1038/ng.2712.
32. Veerman CC, Podliesna S, Tadros R, Lodder EM, Mengarelli I, de Jonge B, Beekman L, Barc J, Wilders R, Wilde AAM, Boukens BJ, Coronel R, Verkerk AO, Remme CA, Bezzina CR. The Brugada Syndrome susceptibility gene HEY2 modulates cardiac transmural ion channel patterning and electrical heterogeneity. Circ Res. 2017;121(5):537–48. https://doi.org/10.1161/CIRCRESAHA.117.310959.
33. Campuzano O, Sarquella-Brugada G, Fernandez-Falgueras A, Cesar S, Coll M, Mates J, Arbelo E, Perez-Serra A, Del Olmo B, Jorda P, Fiol V, Iglesias A, Puigmule M, Lopez L, Pico F, Brugada J, Brugada R. Genetic interpretation and clinical translation of minor genes related to Brugada syndrome. Hum Mutat. 2019;40(6):749–64. https://doi.org/10.1002/humu.23730.
34. Monasky MM, Pappone C, Piccoli M, Ghiroldi A, Micaglio E, Anastasia L. Calcium in Brugada Syndrome: questions for future research. Front Physiol. 2018;9:1088. https://doi.org/10.3389/fphys.2018.01088.
35. Monasky MM, Micaglio E, Ciconte G, Pappone C. Brugada Syndrome: Oligogenic or Mendelian disease? Int J Mol Sci. 2020;21(5):1687. https://doi.org/10.3390/ijms21051687.
36. Mango R, Luchetti A, Sangiuolo R, Ferradini V, Briglia N, Giardina E, Ferre F, Helmer Citterich M, Romeo F, Novelli G, Sangiuolo F. Next generation sequencing and linkage analysis for the molecular diagnosis of a novel overlapping syndrome characterized by hypertrophic cardiomyopathy and typical electrical instability of Brugada Syndrome. Circ J. 2016;80(4):938–49. https://doi.org/10.1253/circj.CJ-15-0685.
37. Pappone C, Monasky MM, Ciconte G. Epicardial ablation in genetic cardiomyopathies: a new frontier. Eur Heart J Suppl. 2019;21(Suppl B):B61–6. https://doi.org/10.1093/eurheartj/suz028.
38. Goldenberg I, Moss AJ. Long QT syndrome. J Am Coll Cardiol. 2008;51(24):2291–300. https://doi.org/10.1016/j.jacc.2008.02.068.
39. Moss AJ, Zareba W, Benhorin J, Locati EH, Hall WJ, Robinson JL, Schwartz PJ, Towbin JA, Vincent GM, Lehmann MH. ECG T-wave patterns in genetically distinct forms of the hereditary long QT syndrome. Circulation. 1995;92(10):2929–34. https://doi.org/10.1161/01.cir.92.10.2929.
40. Schwartz PJ, Crotti L. QTc behavior during exercise and genetic testing for the long-QT syndrome. Circulation. 2011;124(20):2181–4. https://doi.org/10.1161/CIRCULATIONAHA.111.062182.

41. Killeen MJ, Sabir IN, Grace AA, Huang CL. Dispersions of repolarization and ventricular arrhythmogenesis: lessons from animal models. Prog Biophys Mol Biol. 2008;98(2–3):219–29. https://doi.org/10.1016/j.pbiomolbio.2008.10.008.
42. Wu J, Sakaguchi T, Takenaka K, Toyoda F, Tsuji K, Matsuura H, Horie M. A trafficking-deficient KCNQ1 mutation, T587M, causes a severe phenotype of long QT syndrome by interfering with intracellular hERG transport. J Cardiol. 2019;73(5):343–50. https://doi.org/10.1016/j.jjcc.2018.10.011.
43. Nerbonne JM, Kass RS. Molecular physiology of cardiac repolarization. Physiol Rev. 2005;85(4):1205–53. https://doi.org/10.1152/physrev.00002.2005.
44. Wu X, Larsson HP. Insights into cardiac IKs (KCNQ1/KCNE1) channels regulation. Int J Mol Sci. 2020;21(24):9440. https://doi.org/10.3390/ijms21249440.
45. Li Y, Zaydman MA, Wu D, Shi J, Guan M, Virgin-Downey B, Cui J. KCNE1 enhances phosphatidylinositol 4,5-bisphosphate (PIP2) sensitivity of IKs to modulate channel activity. Proc Natl Acad Sci U S A. 2011;108(22):9095–100. https://doi.org/10.1073/pnas.1100872108.
46. Roepke TK, Kontogeorgis A, Ovanez C, Xu X, Young JB, Purtell K, Goldstein PA, Christini DJ, Peters NS, Akar FG, Gutstein DE, Lerner DJ, Abbott GW. Targeted deletion of kcne2 impairs ventricular repolarization via disruption of I(K,slow1) and I(to,f). FASEB J. 2008;22(10):3648–60. https://doi.org/10.1096/fj.08-110171.
47. Gordon E, Panaghie G, Deng L, Bee KJ, Roepke TK, Krogh-Madsen T, Christini DJ, Ostrer H, Basson CT, Chung W, Abbott GW. A KCNE2 mutation in a patient with cardiac arrhythmia induced by auditory stimuli and serum electrolyte imbalance. Cardiovasc Res. 2008;77(1):98–106. https://doi.org/10.1093/cvr/cvm030.
48. Mizusawa Y, Horie M, Wilde AA. Genetic and clinical advances in congenital long QT syndrome. Circ J. 2014;78(12):2827–33. https://doi.org/10.1253/circj.cj-14-0905.
49. Wallace E, Howard L, Liu M, O'Brien T, Ward D, Shen S, Prendiville T. Long QT Syndrome: Genetics and Future Perspective. Pediatr Cardiol. 2019;40(7):1419–30. https://doi.org/10.1007/s00246-019-02151-x.
50. Yang Y, Yang Y, Liang B, Liu J, Li J, Grunnet M, Olesen SP, Rasmussen HB, Ellinor PT, Gao L, Lin X, Li L, Wang L, Xiao J, Liu Y, Liu Y, Zhang S, Liang D, Peng L, Jespersen T, Chen YH. Identification of a Kir3.4 mutation in congenital long QT syndrome. Am J Hum Genet. 2010;86(6):872–80. https://doi.org/10.1016/j.ajhg.2010.04.017.
51. Nuyens D, Stengl M, Dugarmaa S, Rossenbacker T, Compernolle V, Rudy Y, Smits JF, Flameng W, Clancy CE, Moons L, Vos MA, Dewerchin M, Benndorf K, Collen D, Carmeliet E, Carmeliet P. Abrupt rate accelerations or premature beats cause life-threatening arrhythmias in mice with long-QT3 syndrome. Nat Med. 2001;7(9):1021–7. https://doi.org/10.1038/nm0901-1021.
52. Medeiros-Domingo A, Kaku T, Tester DJ, Iturralde-Torres P, Itty A, Ye B, Valdivia C, Ueda K, Canizales-Quinteros S, Tusie-Luna MT, Makielski JC, Ackerman MJ. SCN4B-encoded sodium channel beta4 subunit in congenital long-QT syndrome. Circulation. 2007;116(2):134–42. https://doi.org/10.1161/CIRCULATIONAHA.106.659086.
53. Bohnen MS, Peng G, Robey SH, Terrenoire C, Iyer V, Sampson KJ, Kass RS. Molecular pathophysiology of congenital long QT Syndrome. Physiol Rev. 2017;97(1):89–134. https://doi.org/10.1152/physrev.00008.2016.
54. Splawski I, Timothy KW, Decher N, Kumar P, Sachse FB, Beggs AH, Sanguinetti MC, Keating MT. Severe arrhythmia disorder caused by cardiac L-type calcium channel mutations. Proc Natl Acad Sci U S A. 2005;102(23):8089–96.; discussion 8086-8. https://doi.org/10.1073/pnas.0502506102.
55. Curran J, Mohler PJ. Coordinating electrical activity of the heart: ankyrin polypeptides in human cardiac disease. Expert Opin Ther Targets. 2011;15(7):789–801. https://doi.org/10.1517/14728222.2011.575363.
56. Roberts JD, Murphy NP, Hamilton RM, Lubbers ER, James CA, Kline CF, Gollob MH, Krahn AD, Sturm AC, Musa H, El-Refaey M, Koenig S, Aneq MA, Hoorntje ET, Graw SL, Davies

RW, Rafiq MA, Koopmann TT, Aafaqi S, Fatah M, Chiasson DA, Taylor MR, Simmons SL, Han M, van Opbergen CJ, Wold LE, Sinagra G, Mittal K, Tichnell C, Murray B, Codima A, Nazer B, Nguyen DT, Marcus FI, Sobriera N, Lodder EM, van den Berg MP, Spears DA, Robinson JF, Ursell PC, Green AK, Skanes AC, Tang AS, Gardner MJ, Hegele RA, van Veen TA, Wilde AA, Healey JS, Janssen PM, Mestroni L, van Tintelen JP, Calkins H, Judge DP, Hund TJ, Scheinman MM, Mohler PJ. Ankyrin-B dysfunction predisposes to arrhythmogenic cardiomyopathy and is amenable to therapy. J Clin Invest. 2019;129(8):3171–84. https://doi.org/10.1172/JCI125538.

57. Crotti L, Johnson CN, Graf E, De Ferrari GM, Cuneo BF, Ovadia M, Papagiannis J, Feldkamp MD, Rathi SG, Kunic JD, Pedrazzini M, Wieland T, Lichtner P, Beckmann BM, Clark T, Shaffer C, Benson DW, Kaab S, Meitinger T, Strom TM, Chazin WJ, Schwartz PJ, George AL Jr. Calmodulin mutations associated with recurrent cardiac arrest in infants. Circulation. 2013;127(9):1009–17. https://doi.org/10.1161/CIRCULATIONAHA.112.001216.
58. Pereira R, Campuzano O, Sarquella-Brugada G, Cesar S, Iglesias A, Brugada J, Cruz FES, Brugada R. Short QT syndrome in pediatrics. Clin Res Cardiol. 2017;106(6):393–400. https://doi.org/10.1007/s00392-017-1094-1.
59. Campuzano O, Sarquella-Brugada G, Cesar S, Arbelo E, Brugada J, Brugada R. Recent advances in short QT Syndrome. Front Cardiovasc Med. 2018;5:149. https://doi.org/10.3389/fcvm.2018.00149.
60. Dewi IP, Dharmadjati BB. Short QT syndrome: tThe current evidences of diagnosis and management. J Arrhythm. 2020;36(6):962–6. https://doi.org/10.1002/joa3.12439.
61. Hu D, Li Y, Zhang J, Pfeiffer R, Gollob MH, Healey J, Harrell DT, Makita N, Abe H, Sun Y, Guo J, Zhang L, Yan G, Mah D, Walsh EP, Leopold HB, Giustetto C, Gaita F, Zienciuk-Krajka A, Mazzanti A, Priori SG, Antzelevitch C, Barajas-Martinez H. The phenotypic spectrum of a mutation hotspot responsible for the short QT Syndrome. JACC Clin Electrophysiol. 2017;3(7):727–43. https://doi.org/10.1016/j.jacep.2016.11.013.
62. McPate MJ, Duncan RS, Milnes JT, Witchel HJ, Hancox JC. The N588K-HERG K+ channel mutation in the 'short QT syndrome': mechanism of gain-in-function determined at 37 degrees C. Biochem Biophys Res Commun. 2005;334(2):441–9. https://doi.org/10.1016/j.bbrc.2005.06.112.
63. Harrell DT, Ashihara T, Ishikawa T, Tominaga I, Mazzanti A, Takahashi K, Oginosawa Y, Abe H, Maemura K, Sumitomo N, Uno K, Takano M, Priori SG, Makita N. Genotype-dependent differences in age of manifestation and arrhythmia complications in short QT syndrome. Int J Cardiol. 2015;190:393–402. https://doi.org/10.1016/j.ijcard.2015.04.090.
64. Gollob MH, Redpath CJ, Roberts JD. The short QT syndrome: proposed diagnostic criteria. J Am Coll Cardiol. 2011;57(7):802–12. https://doi.org/10.1016/j.jacc.2010.09.048.
65. Itoh H, Sakaguchi T, Ashihara T, Ding WG, Nagaoka I, Oka Y, Nakazawa Y, Yao T, Jo H, Ito M, Nakamura K, Ohe T, Matsuura H, Horie M. A novel KCNH2 mutation as a modifier for short QT interval. Int J Cardiol. 2009;137(1):83–5. https://doi.org/10.1016/j.ijcard.2008.05.050.
66. Cordeiro JM, Brugada R, Wu YS, Hong K, Dumaine R. Modulation of I(Kr) inactivation by mutation N588K in KCNH2: a link to arrhythmogenesis in short QT syndrome. Cardiovasc Res. 2005;67(3):498–509. https://doi.org/10.1016/j.cardiores.2005.02.018.
67. Bellocq C, van Ginneken AC, Bezzina CR, Alders M, Escande D, Mannens MM, Baro I, Wilde AA. Mutation in the KCNQ1 gene leading to the short QT-interval syndrome. Circulation. 2004;109(20):2394–7. https://doi.org/10.1161/01.CIR.0000130409.72142.FE.
68. Miake J, Marban E, Nuss HB. Functional role of inward rectifier current in heart probed by Kir2.1 overexpression and dominant-negative suppression. J Clin Invest. 2003;111(10):1529–36. https://doi.org/10.1172/JCI17959.
69. Priori SG, Pandit SV, Rivolta I, Berenfeld O, Ronchetti E, Dhamoon A, Napolitano C, Anumonwo J, di Barletta MR, Gudapakkam S, Bosi G, Stramba-Badiale M, Jalife J. A novel form of short QT syndrome (SQT3) is caused by a mutation in the KCNJ2 gene. Circ Res. 2005;96(7):800–7. https://doi.org/10.1161/01.RES.0000162101.76263.8c.

70. Templin C, Ghadri JR, Rougier JS, Baumer A, Kaplan V, Albesa M, Sticht H, Rauch A, Puleo C, Hu D, Barajas-Martinez H, Antzelevitch C, Luscher TF, Abriel H, Duru F. Identification of a novel loss-of-function calcium channel gene mutation in short QT syndrome (SQTS6). Eur Heart J. 2011;32(9):1077–88. https://doi.org/10.1093/eurheartj/ehr076.
71. Thorsen K, Dam VS, Kjaer-Sorensen K, Pedersen LN, Skeberdis VA, Jurevicius J, Treinys R, Petersen I, Nielsen MS, Oxvig C, Morth JP, Matchkov VV, Aalkjaer C, Bundgaard H, Jensen HK. Loss-of-activity-mutation in the cardiac chloride-bicarbonate exchanger AE3 causes short QT syndrome. Nat Commun. 2017;8(1):1696. https://doi.org/10.1038/s41467-017-01630-0.
72. Napolitano C, Priori SG, Bloise R. Catecholaminergic polymorphic ventricular tachycardia. In: Adam MP, Ardinger HH, Pagon RA, Wallace SE, Bean LJH, Gripp KW, Mirzaa GM, Amemiya A, editors. GeneReviews®. Seattle, WA: University of Washington; 1993.
73. Loaiza R, Benkusky NA, Powers PP, Hacker T, Noujaim S, Ackerman MJ, Jalife J, Valdivia HH. Heterogeneity of ryanodine receptor dysfunction in a mouse model of catecholaminergic polymorphic ventricular tachycardia. Circ Res. 2013;112(2):298–308. https://doi.org/10.1161/CIRCRESAHA.112.274803.
74. Bezzerides VJ, Caballero A, Wang S, Ai Y, Hylind RJ, Lu F, Heims-Waldron DA, Chambers KD, Zhang D, Abrams DJ, Pu WT. Gene therapy for catecholaminergic polymorphic ventricular tachycardia by inhibition of Ca(2+)/Calmodulin-Dependent Kinase II. Circulation. 2019;140(5):405–19. https://doi.org/10.1161/CIRCULATIONAHA.118.038514.
75. Liu Y, Wei J, Wong King Yuen SM, Sun B, Tang Y, Wang R, Van Petegem F, Chen SRW. CPVT-associated cardiac ryanodine receptor mutation G357S with reduced penetrance impairs Ca2+ release termination and diminishes protein expression. PLoS One. 2017;12(9):e0184177. https://doi.org/10.1371/journal.pone.0184177.
76. Acimovic I, Refaat MM, Moreau A, Salykin A, Reiken S, Sleiman Y, Souidi M, Pribyl J, Kajava AV, Richard S, Lu JT, Chevalier P, Skladal P, Dvorak P, Rotrekl V, Marks AR, Scheinman MM, Lacampagne A, Meli AC. Post-translational modifications and diastolic calcium leak associated to the novel RyR2-D3638A mutation lead to CPVT in patient-specific hiPSC-derived cardiomyocytes. J Clin Med. 2018;7(11):423. https://doi.org/10.3390/jcm7110423.
77. Wehrens XH, Lehnart SE, Huang F, Vest JA, Reiken SR, Mohler PJ, Sun J, Guatimosim S, Song LS, Rosemblit N, D'Armiento JM, Napolitano C, Memmi M, Priori SG, Lederer WJ, Marks AR. FKBP12.6 deficiency and defective calcium release channel (ryanodine receptor) function linked to exercise-induced sudden cardiac death. Cell. 2003;113(7):829–40. https://doi.org/10.1016/s0092-8674(03)00434-3.
78. Katz G, Khoury A, Kurtzwald E, Hochhauser E, Porat E, Shainberg A, Seidman JG, Seidman CE, Lorber A, Eldar M, Arad M. Optimizing catecholaminergic polymorphic ventricular tachycardia therapy in calsequestrin-mutant mice. Heart Rhythm. 2010;7(11):1676–82. https://doi.org/10.1016/j.hrthm.2010.07.004.
79. Valle G, Boncompagni S, Sacchetto R, Protasi F, Volpe P. Post-natal heart adaptation in a knock-in mouse model of calsequestrin 2-linked recessive catecholaminergic polymorphic ventricular tachycardia. Exp Cell Res. 2014;321(2):178–89. https://doi.org/10.1016/j.yexcr.2013.12.014.
80. Valle G, Arad M, Volpe P. Molecular adaptation to calsequestrin 2 (CASQ2) point mutations leading to catecholaminergic polymorphic ventricular tachycardia (CPVT): comparative analysis of R33Q and D307H mutants. J Muscle Res Cell Motil. 2020;41(2–3):251–8. https://doi.org/10.1007/s10974-020-09587-2.
81. Cacheux M, Fauconnier J, Thireau J, Osseni A, Brocard J, Roux-Buisson N, Brocard J, Faure J, Lacampagne A, Marty I. Interplay between Triadin and Calsequestrin in the Pathogenesis of CPVT in the Mouse. Mol Ther. 2020;28(1):171–9. https://doi.org/10.1016/j.ymthe.2019.09.012.

82. Roux-Buisson N, Cacheux M, Fourest-Lieuvin A, Fauconnier J, Brocard J, Denjoy I, Durand P, Guicheney P, Kyndt F, Leenhardt A, Le Marec H, Lucet V, Mabo P, Probst V, Monnier N, Ray PF, Santoni E, Tremeaux P, Lacampagne A, Faure J, Lunardi J, Marty I. Absence of triadin, a protein of the calcium release complex, is responsible for cardiac arrhythmia with sudden death in human. Hum Mol Genet. 2012;21(12):2759–67. https://doi.org/10.1093/hmg/dds104.
83. Hwang HS, Nitu FR, Yang Y, Walweel K, Pereira L, Johnson CN, Faggioni M, Chazin WJ, Laver D, George AL, Cornea RL, Bers DM, Knollmann BC. Divergent regulation of ryanodine receptor 2 calcium release channels by arrhythmogenic human calmodulin missense mutants. Circ Res. 2014;114(7):1114–24. https://doi.org/10.1161/CIRCRESAHA.114.303391.
84. Gomez-Hurtado N, Boczek NJ, Kryshtal DO, Johnson CN, Sun J, Nitu FR, Cornea RL, Chazin WJ, Calvert ML, Tester DJ, Ackerman MJ, Knollmann BC. Novel CPVT-associated calmodulin mutation in CALM3 (CALM3-A103V) activates arrhythmogenic Ca Waves and Sparks. Circ Arrhythm Electrophysiol. 2016;9(8):e004161. https://doi.org/10.1161/CIRCEP.116.004161.
85. Tsai WC, Guo S, Olaopa MA, Field LJ, Yang J, Shen C, Chang CP, Chen PS, Rubart M. Complex Arrhythmia Syndrome in a knock-in mouse model carrier of the N98S Calm1 mutation. Circulation. 2020;142(20):1937–55. https://doi.org/10.1161/CIRCULATIONAHA.120.046450.
86. Cerrone M, Colombi B, Santoro M, di Barletta MR, Scelsi M, Villani L, Napolitano C, Priori SG. Bidirectional ventricular tachycardia and fibrillation elicited in a knock-in mouse model carrier of a mutation in the cardiac ryanodine receptor. Circ Res. 2005;96(10):e77–82. https://doi.org/10.1161/01.RES.0000169067.51055.72.
87. Kannankeril PJ, Mitchell BM, Goonasekera SA, Chelu MG, Zhang W, Sood S, Kearney DL, Danila CI, De Biasi M, Wehrens XH, Pautler RG, Roden DM, Taffet GE, Dirksen RT, Anderson ME, Hamilton SL. Mice with the R176Q cardiac ryanodine receptor mutation exhibit catecholamine-induced ventricular tachycardia and cardiomyopathy. Proc Natl Acad Sci U S A. 2006;103(32):12179–84. https://doi.org/10.1073/pnas.0600268103.
88. Aiba I, Wehrens XH, Noebels JL. Leaky RyR2 channels unleash a brainstem spreading depolarization mechanism of sudden cardiac death. Proc Natl Acad Sci U S A. 2016;113(33):E4895–903. https://doi.org/10.1073/pnas.1605216113.
89. Knollmann BC, Chopra N, Hlaing T, Akin B, Yang T, Ettensohn K, Knollmann BE, Horton KD, Weissman NJ, Holinstat I, Zhang W, Roden DM, Jones LR, Franzini-Armstrong C, Pfeifer K. Casq2 deletion causes sarcoplasmic reticulum volume increase, premature Ca2+ release, and catecholaminergic polymorphic ventricular tachycardia. J Clin Invest. 2006;116(9):2510–20. https://doi.org/10.1172/JCI29128.
90. Bennett RG, Haqqani HM, Berruezo A, Della Bella P, Marchlinski FE, Hsu CJ, Kumar S. Arrhythmogenic cardiomyopathy in 2018-2019: ARVC/ALVC or both? Heart Lung Circ. 2019;28(1):164–77. https://doi.org/10.1016/j.hlc.2018.10.013.
91. Stevens TL, Wallace MJ, Refaey ME, Roberts JD, Koenig SN, Mohler PJ. Arrhythmogenic cardiomyopathy: molecular insights for improved therapeutic design. J Cardiovasc Dev Dis. 2020;7(2):21. https://doi.org/10.3390/jcdd7020021.
92. Hoorntje ET, Te Rijdt WP, James CA, Pilichou K, Basso C, Judge DP, Bezzina CR, van Tintelen JP. Arrhythmogenic cardiomyopathy: pathology, genetics, and concepts in pathogenesis. Cardiovasc Res. 2017;113(12):1521–31. https://doi.org/10.1093/cvr/cvx150.
93. Mohamed S, Keane S, McNally C, Hayes J. A case report of biventricular arrhythmogenic cardiomyopathy in a middle-aged female. Cureus. 2022;14(1):e20885. https://doi.org/10.7759/cureus.20885.
94. Basso C, Corrado D, Marcus FI, Nava A, Thiene G. Arrhythmogenic right ventricular cardiomyopathy. Lancet. 2009;373(9671):1289–300. https://doi.org/10.1016/S0140-6736(09)60256-7.

95. Sen-Chowdhry S, Syrris P, McKenna WJ. Role of genetic analysis in the management of patients with arrhythmogenic right ventricular dysplasia/cardiomyopathy. J Am Coll Cardiol. 2007;50(19):1813–21. https://doi.org/10.1016/j.jacc.2007.08.008.
96. Nava A, Bauce B, Basso C, Muriago M, Rampazzo A, Villanova C, Daliento L, Buja G, Corrado D, Danieli GA, Thiene G. Clinical profile and long-term follow-up of 37 families with arrhythmogenic right ventricular cardiomyopathy. J Am Coll Cardiol. 2000;36(7):2226–33. https://doi.org/10.1016/s0735-1097(00)00997-9.
97. Chen SN, Gurha P, Lombardi R, Ruggiero A, Willerson JT, Marian AJ. The hippo pathway is activated and is a causal mechanism for adipogenesis in arrhythmogenic cardiomyopathy. Circ Res. 2014;114(3):454–68. https://doi.org/10.1161/CIRCRESAHA.114.302810.
98. Kim JC, Perez-Hernandez M, Alvarado FJ, Maurya SR, Montnach J, Yin Y, Zhang M, Lin X, Vasquez C, Heguy A, Liang FX, Woo SH, Morley GE, Rothenberg E, Lundby A, Valdivia HH, Cerrone M, Delmar M. Disruption of Ca(2+)i homeostasis and Connexin 43 hemichannel function in the right ventricle precedes overt arrhythmogenic cardiomyopathy in Plakophilin-2-deficient mice. Circulation. 2019;140(12):1015–30. https://doi.org/10.1161/CIRCULATIONAHA.119.039710.
99. Cerrone M, Montnach J, Lin X, Zhao YT, Zhang M, Agullo-Pascual E, Leo-Macias A, Alvarado FJ, Dolgalev I, Karathanos TV, Malkani K, Van Opbergen CJM, van Bavel JJA, Yang HQ, Vasquez C, Tester D, Fowler S, Liang F, Rothenberg E, Heguy A, Morley GE, Coetzee WA, Trayanova NA, Ackerman MJ, van Veen TAB, Valdivia HH, Delmar M. Plakophilin-2 is required for transcription of genes that control calcium cycling and cardiac rhythm. Nat Commun. 2017;8(1):106. https://doi.org/10.1038/s41467-017-00127-0.
100. Cruz FM, Sanz-Rosa D, Roche-Molina M, Garcia-Prieto J, Garcia-Ruiz JM, Pizarro G, Jimenez-Borreguero LJ, Torres M, Bernad A, Ruiz-Cabello J, Fuster V, Ibanez B, Bernal JA. Exercise triggers ARVC phenotype in mice expressing a disease-causing mutated version of human plakophilin-2. J Am Coll Cardiol. 2015;65(14):1438–50. https://doi.org/10.1016/j.jacc.2015.01.045.
101. Moncayo-Arlandi J, Guasch E, Sanz-de la Garza M, Casado M, Garcia NA, Mont L, Sitges M, Knoll R, Buyandelger B, Campuzano O, Diez-Juan A, Brugada R. Molecular disturbance underlies to arrhythmogenic cardiomyopathy induced by transgene content, age and exercise in a truncated PKP2 mouse model. Hum Mol Genet. 2016;25(17):3676–88. https://doi.org/10.1093/hmg/ddw213.
102. Grossmann KS, Grund C, Huelsken J, Behrend M, Erdmann B, Franke WW, Birchmeier W. Requirement of plakophilin 2 for heart morphogenesis and cardiac junction formation. J Cell Biol. 2004;167(1):149–60. https://doi.org/10.1083/jcb.200402096.
103. Cerrone M, Noorman M, Lin X, Chkourko H, Liang FX, van der Nagel R, Hund T, Birchmeier W, Mohler P, van Veen TA, van Rijen HV, Delmar M. Sodium current deficit and arrhythmogenesis in a murine model of plakophilin-2 haploinsufficiency. Cardiovasc Res. 2012;95(4):460–8. https://doi.org/10.1093/cvr/cvs218.
104. Gomes J, Finlay M, Ahmed AK, Ciaccio EJ, Asimaki A, Saffitz JE, Quarta G, Nobles M, Syrris P, Chaubey S, McKenna WJ, Tinker A, Lambiase PD. Electrophysiological abnormalities precede overt structural changes in arrhythmogenic right ventricular cardiomyopathy due to mutations in desmoplakin-A combined murine and human study. Eur Heart J. 2012;33(15):1942–53. https://doi.org/10.1093/eurheartj/ehr472.
105. Garcia-Gras E, Lombardi R, Giocondo MJ, Willerson JT, Schneider MD, Khoury DS, Marian AJ. Suppression of canonical Wnt/beta-catenin signaling by nuclear plakoglobin recapitulates phenotype of arrhythmogenic right ventricular cardiomyopathy. J Clin Invest. 2006;116(7):2012–21. https://doi.org/10.1172/JCI27751.
106. Gallicano GI, Bauer C, Fuchs E. Rescuing desmoplakin function in extra-embryonic ectoderm reveals the importance of this protein in embryonic heart, neuroepithelium, skin and vasculature. Development. 2001;128(6):929–41.
107. Lyon RC, Mezzano V, Wright AT, Pfeiffer E, Chuang J, Banares K, Castaneda A, Ouyang K, Cui L, Contu R, Gu Y, Evans SM, Omens JH, Peterson KL, McCulloch AD, Sheikh

F. Connexin defects underlie arrhythmogenic right ventricular cardiomyopathy in a novel mouse model. Hum Mol Genet. 2014;23(5):1134–50. https://doi.org/10.1093/hmg/ddt508.
108. Yang Z, Bowles NE, Scherer SE, Taylor MD, Kearney DL, Ge S, Nadvoretskiy VV, DeFreitas G, Carabello B, Brandon LI, Godsel LM, Green KJ, Saffitz JE, Li H, Danieli GA, Calkins H, Marcus F, Towbin JA. Desmosomal dysfunction due to mutations in desmoplakin causes arrhythmogenic right ventricular dysplasia/cardiomyopathy. Circ Res. 2006;99(6):646–55. https://doi.org/10.1161/01.RES.0000241482.19382.c6.
109. Chelko SP, Asimaki A, Andersen P, Bedja D, Amat-Alarcon N, DeMazumder D, Jasti R, MacRae CA, Leber R, Kleber AG, Saffitz JE, Judge DP. Central role for GSK3beta in the pathogenesis of arrhythmogenic cardiomyopathy. JCI Insight. 2016;1(5):e85923. https://doi.org/10.1172/jci.insight.85923.
110. Hermida A, Fressart V, Hidden-Lucet F, Donal E, Probst V, Deharo JC, Chevalier P, Klug D, Mansencal N, Delacretaz E, Cosnay P, Scanu P, Extramiana F, Keller DI, Rouanet S, Charron P, Gandjbakhch E. High risk of heart failure associated with desmoglein-2 mutations compared to plakophilin-2 mutations in arrhythmogenic right ventricular cardiomyopathy/dysplasia. Eur J Heart Fail. 2019;21(6):792–800. https://doi.org/10.1002/ejhf.1423.
111. Eshkind L, Tian Q, Schmidt A, Franke WW, Windoffer R, Leube RE. Loss of desmoglein 2 suggests essential functions for early embryonic development and proliferation of embryonal stem cells. Eur J Cell Biol. 2002;81(11):592–8. https://doi.org/10.1078/0171-9335-00278.
112. Kant S, Krull P, Eisner S, Leube RE, Krusche CA. Histological and ultrastructural abnormalities in murine desmoglein 2-mutant hearts. Cell Tissue Res. 2012;348(2):249–59. https://doi.org/10.1007/s00441-011-1322-3.
113. Pilichou K, Remme CA, Basso C, Campian ME, Rizzo S, Barnett P, Scicluna BP, Bauce B, van den Hoff MJ, de Bakker JM, Tan HL, Valente M, Nava A, Wilde AA, Moorman AF, Thiene G, Bezzina CR. Myocyte necrosis underlies progressive myocardial dystrophy in mouse dsg2-related arrhythmogenic right ventricular cardiomyopathy. J Exp Med. 2009;206(8):1787–802. https://doi.org/10.1084/jem.20090641.
114. Rizzo S, Lodder EM, Verkerk AO, Wolswinkel R, Beekman L, Pilichou K, Basso C, Remme CA, Thiene G, Bezzina CR. Intercalated disc abnormalities, reduced Na(+) current density, and conduction slowing in desmoglein-2 mutant mice prior to cardiomyopathic changes. Cardiovasc Res. 2012;95(4):409–18. https://doi.org/10.1093/cvr/cvs219.
115. Brodehl A, Belke DD, Garnett L, Martens K, Abdelfatah N, Rodriguez M, Diao C, Chen YX, Gordon PM, Nygren A, Gerull B. Transgenic mice overexpressing desmocollin-2 (DSC2) develop cardiomyopathy associated with myocardial inflammation and fibrotic remodeling. PLoS One. 2017;12(3):e0174019. https://doi.org/10.1371/journal.pone.0174019.
116. Heuser A, Plovie ER, Ellinor PT, Grossmann KS, Shin JT, Wichter T, Basson CT, Lerman BB, Sasse-Klaassen S, Thierfelder L, MacRae CA, Gerull B. Mutant desmocollin-2 causes arrhythmogenic right ventricular cardiomyopathy. Am J Hum Genet. 2006;79(6):1081–8. https://doi.org/10.1086/509044.
117. Li J, Swope D, Raess N, Cheng L, Muller EJ, Radice GL. Cardiac tissue-restricted deletion of plakoglobin results in progressive cardiomyopathy and activation of {beta}-catenin signaling. Mol Cell Biol. 2011;31(6):1134–44. https://doi.org/10.1128/MCB.01025-10.
118. Ruiz P, Brinkmann V, Ledermann B, Behrend M, Grund C, Thalhammer C, Vogel F, Birchmeier C, Gunthert U, Franke WW, Birchmeier W. Targeted mutation of plakoglobin in mice reveals essential functions of desmosomes in the embryonic heart. J Cell Biol. 1996;135(1):215–25. https://doi.org/10.1083/jcb.135.1.215.
119. Li D, Liu Y, Maruyama M, Zhu W, Chen H, Zhang W, Reuter S, Lin SF, Haneline LS, Field LJ, Chen PS, Shou W. Restrictive loss of plakoglobin in cardiomyocytes leads to arrhythmogenic cardiomyopathy. Hum Mol Genet. 2011;20(23):4582–96. https://doi.org/10.1093/hmg/ddr392.
120. Swope D, Cheng L, Gao E, Li J, Radice GL. Loss of cadherin-binding proteins beta-catenin and plakoglobin in the heart leads to gap junction remodeling and arrhythmogenesis. Mol Cell Biol. 2012;32(6):1056–67. https://doi.org/10.1128/MCB.06188-11.

121. Lombardi R, da Graca Cabreira-Hansen M, Bell A, Fromm RR, Willerson JT, Marian AJ. Nuclear plakoglobin is essential for differentiation of cardiac progenitor cells to adipocytes in arrhythmogenic right ventricular cardiomyopathy. Circ Res. 2011;109(12):1342–53. https://doi.org/10.1161/CIRCRESAHA.111.255075.
122. Padron-Barthe L, Villalba-Orero M, Gomez-Salinero JM, Dominguez F, Roman M, Larrasa-Alonso J, Ortiz-Sanchez P, Martinez F, Lopez-Olaneta M, Bonzon-Kulichenko E, Vazquez J, Marti-Gomez C, Santiago DJ, Prados B, Giovinazzo G, Gomez-Gaviro MV, Priori S, Garcia-Pavia P, Lara-Pezzi E. Severe Cardiac Dysfunction and Death Caused by Arrhythmogenic Right Ventricular Cardiomyopathy Type 5 Are Improved by Inhibition of Glycogen Synthase Kinase-3beta. Circulation. 2019;140(14):1188–204. https://doi.org/10.1161/CIRCULATIONAHA.119.040366.
123. Haghighi K, Kolokathis F, Gramolini AO, Waggoner JR, Pater L, Lynch RA, Fan GC, Tsiapras D, Parekh RR, Dorn GW, MacLennan DH, Kremastinos DT, Kranias EG. A mutation in the human phospholamban gene, deleting arginine 14, results in lethal, hereditary cardiomyopathy. Proc Natl Acad Sci U S A. 2006;103(5):1388–93. https://doi.org/10.1073/pnas.0510519103.
124. van der Zwaag PA, Jongbloed JD, van den Berg MP, van der Smagt JJ, Jongbloed R, Bikker H, Hofstra RM, van Tintelen JP. A genetic variants database for arrhythmogenic right ventricular dysplasia/cardiomyopathy. Hum Mutat. 2009;30(9):1278–83. https://doi.org/10.1002/humu.21064.
125. van der Velde KJ, Imhann F, Charbon B, Pang C, van Enckevort D, Slofstra M, Barbieri R, Alberts R, Hendriksen D, Kelpin F, de Haan M, de Boer T, Haakma S, Stroomberg C, Scholtens S, van de Geijn GJ, Festen EAM, Weersma RK, Swertz MA. MOLGENIS research: advanced bioinformatics data software for non-bioinformaticians. Bioinformatics. 2019;35(6):1076–8. https://doi.org/10.1093/bioinformatics/bty742.
126. Ng R, Manring H, Papoutsidakis N, Albertelli T, Tsai N, See CJ, Li X, Park J, Stevens TL, Bobbili PJ, Riaz M, Ren Y, Stoddard CE, Janssen PM, Bunch TJ, Hall SP, Lo YC, Jacoby DL, Qyang Y, Wright N, Ackermann MA, Campbell SG. Patient mutations linked to arrhythmogenic cardiomyopathy enhance calpain-mediated desmoplakin degradation. JCI Insight. 2019;5:e128643. https://doi.org/10.1172/jci.insight.128643.
127. Patel DM, Dubash AD, Kreitzer G, Green KJ. Disease mutations in desmoplakin inhibit Cx43 membrane targeting mediated by desmoplakin-EB1 interactions. J Cell Biol. 2014;206(6):779–97. https://doi.org/10.1083/jcb.201312110.
128. Kam CY, Dubash AD, Magistrati E, Polo S, Satchell KJF, Sheikh F, Lampe PD, Green KJ. Desmoplakin maintains gap junctions by inhibiting Ras/MAPK and lysosomal degradation of connexin-43. J Cell Biol. 2018;217(9):3219–35. https://doi.org/10.1083/jcb.201710161.
129. Te Riele AS, Agullo-Pascual E, James CA, Leo-Macias A, Cerrone M, Zhang M, Lin X, Lin B, Sobreira NL, Amat-Alarcon N, Marsman RF, Murray B, Tichnell C, van der Heijden JF, Dooijes D, van Veen TA, Tandri H, Fowler SJ, Hauer RN, Tomaselli G, van den Berg MP, Taylor MR, Brun F, Sinagra G, Wilde AA, Mestroni L, Bezzina CR, Calkins H, Peter van Tintelen J, Bu L, Delmar M, Judge DP. Multilevel analyses of SCN5A mutations in arrhythmogenic right ventricular dysplasia/cardiomyopathy suggest non-canonical mechanisms for disease pathogenesis. Cardiovasc Res. 2017;113(1):102–11. https://doi.org/10.1093/cvr/cvw234.
130. Erkapic D, Neumann T, Schmitt J, Sperzel J, Berkowitsch A, Kuniss M, Hamm CW, Pitschner HF. Electrical storm in a patient with arrhythmogenic right ventricular cardiomyopathy and SCN5A mutation. Europace. 2008;10(7):884–7. https://doi.org/10.1093/europace/eun065.
131. Te Rijdt WP, Asimaki A, Jongbloed JDH, Hoorntje ET, Lazzarini E, van der Zwaag PA, de Boer RA, van Tintelen JP, Saffitz JE, van den Berg MP, Suurmeijer AJH. Distinct molecular signature of phospholamban p.Arg14del arrhythmogenic cardiomyopathy. Cardiovasc Pathol. 2019;40:2–6. https://doi.org/10.1016/j.carpath.2018.12.006.

132. Te Rijdt WP, van Tintelen JP, Vink A, van der Wal AC, de Boer RA, van den Berg MP, Suurmeijer AJ. Phospholamban p.Arg14del cardiomyopathy is characterized by phospholamban aggregates, aggresomes, and autophagic degradation. Histopathology. 2016;69(4):542–50. https://doi.org/10.1111/his.12963.
133. Mercer BN, Begg GA, Page SP, Bennett CP, Tayebjee MH, Mahida S. Early repolarization syndrome; mechanistic theories and clinical correlates. Front Physiol. 2016;7:266. https://doi.org/10.3389/fphys.2016.00266.
134. Gussak I, Antzelevitch C. Early repolarization syndrome: a decade of progress. J Electrocardiol. 2013;46(2):110–3. https://doi.org/10.1016/j.jelectrocard.2012.12.002.
135. Medeiros-Domingo A, Tan BH, Crotti L, Tester DJ, Eckhardt L, Cuoretti A, Kroboth SL, Song C, Zhou Q, Kopp D, Schwartz PJ, Makielski JC, Ackerman MJ. Gain-of-function mutation S422L in the KCNJ8-encoded cardiac K(ATP) channel Kir6.1 as a pathogenic substrate for J-wave syndromes. Heart Rhythm. 2010;7(10):1466–71. https://doi.org/10.1016/j.hrthm.2010.06.016.
136. Takayama K, Ohno S, Ding WG, Ashihara T, Fukumoto D, Wada Y, Makiyama T, Kise H, Hoshiai M, Matsuura H, Horie M. A de novo gain-of-function KCND3 mutation in early repolarization syndrome. Heart Rhythm. 2019;16(11):1698–706. https://doi.org/10.1016/j.hrthm.2019.05.033.
137. Yao H, Fan J, Cheng YJ, Chen XM, Ji CC, Liu LJ, Zheng ZH, Wu SH. SCN1Bbeta mutations that affect their association with Kv4.3 underlie early repolarization syndrome. J Cell Mol Med. 2018;22(11):5639–47. https://doi.org/10.1111/jcmm.13839.
138. Koncz I, Gurabi Z, Patocskai B, Panama BK, Szel T, Hu D, Barajas-Martinez H, Antzelevitch C. Mechanisms underlying the development of the electrocardiographic and arrhythmic manifestations of early repolarization syndrome. J Mol Cell Cardiol. 2014;68:20–8. https://doi.org/10.1016/j.yjmcc.2013.12.012.
139. Sprung J, Laszlo A, Turner LA, Kampine JP, Bosnjak ZJ. Effects of hypothermia, potassium , and verapamil on the action potential characteristics of canine cardiac Purkinje fibers. Anesthesiology. 1995;82(3):713–22. https://doi.org/10.1097/00000542-199503000-00013.
140. Yoon N, Jeong HK, Lee KH, Park HW, Cho JG. Transmural conduction time in an early repolarization syndrome model. Exp Ther Med. 2020;20(4):3064–71. https://doi.org/10.3892/etm.2020.9061.
141. Yao H, Ji CC, Cheng YJ, Chen XM, Liu LJ, Fan J, Wu SH. Mutation in KCNE1 associated to early repolarization syndrome by modulation of slowly activating delayed rectifier K+ current. Exp Cell Res. 2018;363(2):315–20. https://doi.org/10.1016/j.yexcr.2018.01.030.
142. Jacquemart E, Bessiere F, Combes N, Ladouceur M, Iserin L, Gardey K, Henaine R, Dulac A, Cohen S, Belli E, Jannot AS, Chevalier P, Ly R, Clavier S, Legendre A, Petit J, Maltret A, Di Filippo S, Hascoet S, Marijon E, Waldmann V. Incidence, risk factors, and outcomes of atrial arrhythmias in adult patients with atrioventricular septal defect. JACC Clin Electrophysiol. 2022;8(3):331–40. https://doi.org/10.1016/j.jacep.2021.09.004.
143. Higuchi S, Sarcon A, Sternick EB, Sanchez-Quintana D, Anderson RH, Scheinman M, Hsia H. Isolated left-sided accessory pathway potential: the potential possibilities. JACC Clin Electrophysiol. 2021;7(10):1316–23. https://doi.org/10.1016/j.jacep.2021.05.011.
144. Scher DL, Arsura EL. Multifocal atrial tachycardia: mechanisms, clinical correlates, and treatment. Am Heart J. 1989;118(3):574–80. https://doi.org/10.1016/0002-8703(89)90275-5.
145. Marzlin KM, Webner C. Atrioventricular reentrant tachycardia. AACN Adv Crit Care. 2017;28(2):223–8. https://doi.org/10.4037/aacnacc2017151.
146. Jean-Pierre CGGKV. Atrial fibrillation in the elderly. In: Williamson D, editor. Drugs and aging, vol. 19. Springer; 2002. p. 819–46.
147. Riley G, Syeda F, Kirchhof P, Fabritz L. An introduction to murine models of atrial fibrillation. Front Physiol. 2012;3:296. https://doi.org/10.3389/fphys.2012.00296.
148. Yarmohammadi H, Morrow JP, Dizon J, Biviano A, Ehlert F, Saluja D, Waase M, Elias P, Poterucha TJ, Berman J, Kushnir A, Abrams MP, Rubin GA, Jou S, Hennessey J, Uriel N,

Wan EY, Garan H. Frequency of atrial arrhythmia in hospitalized patients with COVID-19. Am J Cardiol. 2021;142:52–7. https://doi.org/10.1016/j.amjcard.2021.01.039.
149. Bhatla A, Mayer MM, Adusumalli S, Hyman MC, Oh E, Tierney A, Moss J, Chahal AA, Anesi G, Denduluri S, Domenico CM, Arkles J, Abella BS, Bullinga JR, Callans DJ, Dixit S, Epstein AE, Frankel DS, Garcia FC, Kumareswaram R, Nazarian S, Riley MP, Santangeli P, Schaller RD, Supple GE, Lin D, Marchlinski F, Deo R. COVID-19 and cardiac arrhythmias. Heart Rhythm. 2020;17(9):1439–44. https://doi.org/10.1016/j.hrthm.2020.06.016.
150. Peltzer B, Manocha KK, Ying X, Kirzner J, Ip JE, Thomas G, Liu CF, Markowitz SM, Lerman BB, Safford MM, Goyal P, Cheung JW. Outcomes and mortality associated with atrial arrhythmias among patients hospitalized with COVID-19. J Cardiovasc Electrophysiol. 2020;31(12):3077–85. https://doi.org/10.1111/jce.14770.
151. Goyal P, Choi JJ, Pinheiro LC, Schenck EJ, Chen R, Jabri A, Satlin MJ, Campion TR, Nahid M, Ringel JB, Hoffman KL, Alshak MN, Li HA, Wehmeyer GT, Rajan M, Reshetnyak E, Hupert N, Horn EM, Martinez FJ, Gulick RM, Safford MM. Clinical characteristics of Covid-19 in New York City. N Engl J Med. 2020;382(24):2372–4. https://doi.org/10.1056/NEJMc2010419.
152. Guo Y, Lip GY, Apostolakis S. Inflammation in atrial fibrillation. J Am Coll Cardiol. 2012;60(22):2263–70. https://doi.org/10.1016/j.jacc.2012.04.063.
153. Milan DJ, Macrae CA. Zebrafish genetic models for arrhythmia. Prog Biophys Mol Biol. 2008;98(2–3):301–8. https://doi.org/10.1016/j.pbiomolbio.2009.01.011.
154. Glynn P, Unudurthi SD, Hund TJ. Mathematical modeling of physiological systems: an essential tool for discovery. Life Sci. 2014;111(1–2):1–5. https://doi.org/10.1016/j.lfs.2014.07.005.
155. Meysen S, Marger L, Hewett KW, Jarry-Guichard T, Agarkova I, Chauvin JP, Perriard JC, Izumo S, Gourdie RG, Mangoni ME, Nargeot J, Gros D, Miquerol L. Nkx2.5 cell-autonomous gene function is required for the postnatal formation of the peripheral ventricular conduction system. Dev Biol. 2007;303(2):740–53. https://doi.org/10.1016/j.ydbio.2006.12.044.
156. Tanaka M, Berul CI, Ishii M, Jay PY, Wakimoto H, Douglas P, Yamasaki N, Kawamoto T, Gehrmann J, Maguire CT, Schinke M, Seidman CE, Seidman JG, Kurachi Y, Izumo S. A mouse model of congenital heart disease: cardiac arrhythmias and atrial septal defect caused by haploinsufficiency of the cardiac transcription factor Csx/Nkx2.5, vol. 67. Cold Spring Harb Symp Quant Biol; 2002. p. 317–25. https://doi.org/10.1101/sqb.2002.67.317.
157. Choquet C, Kelly RG, Miquerol L. Nkx2-5 defines distinct scaffold and recruitment phases during formation of the murine cardiac Purkinje fiber network. Nat Commun. 2020;11(1):5300. https://doi.org/10.1038/s41467-020-19150-9.
158. Nattel S, Frelin Y, Gaborit N, Louault C, Demolombe S. Ion-channel mRNA-expression profiling: Insights into cardiac remodeling and arrhythmic substrates. J Mol Cell Cardiol. 2010;48(1):96–105. https://doi.org/10.1016/j.yjmcc.2009.07.016.
159. Bosch RF, Li GR, Gaspo R, Nattel S. Electrophysiologic effects of chronic amiodarone therapy and hypothyroidism, alone and in combination, on guinea pig ventricular myocytes. J Pharmacol Exp Ther. 1999;289(1):156–65.
160. Le Bouter S, El Harchi A, Marionneau C, Bellocq C, Chambellan A, van Veen T, Boixel C, Gavillet B, Abriel H, Le Quang K, Chevalier JC, Lande G, Leger JJ, Charpentier F, Escande D, Demolombe S. Long-term amiodarone administration remodels expression of ion channel transcripts in the mouse heart. Circulation. 2004;110(19):3028–35. https://doi.org/10.1161/01.CIR.0000147187.78162.AC.
161. Grunert M, Appelt S, Dunkel I, Berger F, Sperling SR. Altered microRNA and target gene expression related to Tetralogy of Fallot. Sci Rep. 2019;9(1):19063. https://doi.org/10.1038/s41598-019-55570-4.
162. Gandjbakhch E, Redheuil A, Pousset F, Charron P, Frank R. Clinical diagnosis, imaging, and genetics of arrhythmogenic right ventricular cardiomyopathy/dysplasia: JACC State-of-the-Art Review. J Am Coll Cardiol. 2018;72(7):784–804. https://doi.org/10.1016/j.jacc.2018.05.065.

163. Bhonsale A, Groeneweg JA, James CA, Dooijes D, Tichnell C, Jongbloed JD, Murray B, te Riele AS, van den Berg MP, Bikker H, Atsma DE, de Groot NM, Houweling AC, van der Heijden JF, Russell SD, Doevendans PA, van Veen TA, Tandri H, Wilde AA, Judge DP, van Tintelen JP, Calkins H, Hauer RN. Impact of genotype on clinical course in arrhythmogenic right ventricular dysplasia/cardiomyopathy-associated mutation carriers. Eur Heart J. 2015;36 (14):847–55. https://doi.org/10.1093/eurheartj/ehu509.
164. Karmouch J, Protonotarios A, Syrris P. Genetic basis of arrhythmogenic cardiomyopathy. Curr Opin Cardiol. 2018;33(3):276–81. https://doi.org/10.1097/HCO.0000000000000509.
165. Corrado D, Link MS, Calkins H. Arrhythmogenic right ventricular cardiomyopathy. N Engl J Med. 2017;376(15):1489–90. https://doi.org/10.1056/NEJMc1701400.
166. Hamada Y, Yamamoto T, Nakamura Y, Sufu-Shimizu Y, Nanno T, Fukuda M, Ono M, Oda T, Okuda S, Ueyama T, Kobayashi S, Yano M. G790del mutation in DSC2 alone is insufficient to develop the pathogenesis of ARVC in a mouse model. Biochem Biophys Rep. 2020;21: 100711. https://doi.org/10.1016/j.bbrep.2019.100711.
167. Jaouadi H, Bouyacoub Y, Chabrak S, Kraoua L, Zaroui A, Elouej S, Nagara M, Dallali H, Delague V, Levy N, Benkhalifa R, Mechmeche R, Zaffran S, Abdelhak S. Multiallelic rare variants support an oligogenic origin of sudden cardiac death in the young. Herz. 2021;46 (Suppl 1):94–102. https://doi.org/10.1007/s00059-019-04883-1.

Perspective

An Integrated Future for Congenital Heart Disease: Leveraging Knowledge for a Better Future

Deepak Srivastava

The fate of children with congenital heart disease (CHD) has been dramatically altered over the last 50 years, and that fate is poised once again to undergo paradigm-shifting advances. Clinical breakthroughs involving novel surgical and catheter-based approaches, as well as advances in cardiopulmonary bypass, imaging, and pre- and postoperative management have combined to result in major improvements in survival for many forms of CHD. In comparison with the revolutionary changes in surgical approach observed in the 1960s, 1970s, and 1980s, there have been considerably fewer fundamental changes in our approach to CHD over the last 20 years, although survival for complex CHD has steadily improved across all centers through refinement of surgical technique and clinical management. In contrast, in that time period there has been an explosion in our understanding of the genetic and developmental basis for CHD. Although this has yet to lead to significant changes in clinical care, one can begin to envision the path that will inevitably emerge that will lead to more tailored and informed approaches to intervention, prevention, and outcomes management. This textbook elegantly integrates knowledge of clinical anatomy with developmental biology, molecular biology, and human genetics in a way that marries the more recent basic advances with the rich history of clinical advances. Here, I will briefly synthesize how our greater foundation of knowledge and emerging technologies can be leveraged with clinical medicine to alter the natural history of CHD.

Emerging knowledge of the molecular biology underlying cardiac developmental events has led to a new understanding of CHD based more on etiologic origins during development than the ultimate anatomic findings or region affected at birth. For example, transposition of the great arteries and truncus arteriosus may both be conotruncal defects, but have vastly different embryologic origins. Similarly, a subset of double-outlet right ventricle (DORV) cases may be related to abnormal neural crest development, while a different subset may be due to abnormalities in the process of cardiac looping. The recognition that discrete pools of cardiac progenitor

© The Author(s), under exclusive license to Springer Nature Switzerland AG 2024

S. Rickert-Sperling et al. (eds.), *Congenital Heart Diseases: The Broken Heart*,
Advances in Experimental Medicine and Biology 1441,
https://doi.org/10.1007/978-3-031-44087-8

cells contribute to specific regions or structures and are selectively regulated by independent gene networks provides a molecular basis for understanding the origin for many forms of CHD. Advances in single cell biology have now revealed many more types of specialized progenitor and differentiated cells in the heart, each one potentially susceptible to unique perturbations resulting in specific forms of CHD. As we begin to leverage the power of modern human genetics and search for genetic variance that leads to CHDs, we will be able to identify the cell types most affected by genetic variance that may be contributing to developmental defects. Given these advances in the mechanistic basis for CHD, it is becoming imperative to properly classify CHD based on the etiologic origin, as those are the ones that would presumably share a genetic cause.

Indeed, the revolutionary advances in DNA sequencing over the last few years have begun to reveal an increasing role for genetic variants in the etiology of CHD. While ~45% of CHD can now be explained largely by genetic mutations, it is likely that this number will continue to increase as we are able to broadly sequence whole genomes from larger populations of CHD patients, along with their parents. Understanding how combinations of coding and non-coding genetic variants result in CHD will be essential and will likely reveal the cause of a significant percentage of unexplained disease. Furthermore, a correlation of coding and non-coding genetic variants to longer-term outcome variables should lead to identification of those at greatest risk for complications even after palliation. To date, the majority genes shown to contribute to CHD are involved in signaling and transcriptional events that alter gene expression in early cardiac progenitors, altering their fate and morphogenesis. A deeper interrogation of the precise mechanisms and gene networks by which these factors function will be essential to truly understand the cause and effect relationship with disease. Recent advances in understanding normal and abnormal development at the single cell transcriptomic and epigenetic level, coupled with artificial intelligence and systems biology approaches, promise to provide a comprehensive understanding of the specific cell types affected by genetic variance in the setting of CHD.

The ability to connect genetic variance with disease mechanism has been possible due to not only new developmental biology techniques, but also a combination of stem cell technology and novel tools for efficient gene editing in human cells. The challenges of deeply analyzing the consequences of disease mutations in relevant human cells have been overcome by induced pluripotent stem cell (iPSC) technology, which involves induction of pluripotency from adult somatic cells such as dermal fibroblasts or peripheral lymphocytes. Differentiation of iPSCs from patients enables scientists to interrogate the functional consequences of disease-causing variants in specific types of cardiomyocytes, conduction system, smooth muscle, or endothelial cells. Efficient gene-editing techniques using CRISPR can correct or introduce relevant mutations, facilitating direct cause and effect studies in human cells, and can also allow rapid introduction of human mutations into mice for more three-dimensional morphogenetic studies. By accurately modeling the defects underlying human disease, such platforms can then be utilized for drug discovery

to identify agents that could alter the fundamental defect, as well as the ongoing postnatal consequences of a congenital defect.

As the population of survivors with CHD grows and ages, we are beginning to see numerous comorbidities that may share etiologies with the cardiac morphologic defect. For example, poor neurodevelopmental outcomes have been observed in many patients with CHD as they reach school age and beyond. Growing evidence suggests that the same genetic variants that lead to a cardiac defect may also affect neurologic development or outcomes, rather than cyanosis or cardiopulmonary bypass being the primary culprit for the neurologic deficits. The potential to mitigate this effect is attractive, as significant neurologic development continues postnatally. Similarly, the age-dependent thickening and calcification observed in patients with bicuspid aortic valve is likely related to the primary molecular defect leading to the morphologic abnormality and could potentially be prevented by appropriate pharmacologic intervention postnatally, as has been shown in mice.

Heart failure is a rapidly expanding challenge in CHD survivors despite optimal surgical intervention. Novel technologies based on an understanding of cardiac developmental biology may allow regeneration of new heart muscle through conversion of existing fibroblasts within the heart into contractile cardiomyocytes, improving cardiac function. Other conditions such as septal defects may also benefit from the ability to create new muscle from neighboring cells that could be coaxed to expand and "fill-in" the defect. Furthermore, the recognition of fundamental differences in the developmental and molecular origins of right and left ventricular cardiomyoctes may allow conversion of the failing systemic right ventricle to a more left ventricle-like physiology, potentially mitigating the need for cardiac transplant in such conditions.

An ultimate, but long-term, goal of integrating a deep understanding of the etiology of CHD with clinical knowledge is to identify measures that might actually prevent the emergence of CHD even in those that are genetically predisposed. This would require knowledge of those parents genetically at risk to have offspring with CHD, the mechanisms by which those genetic variants predispose to disease, and identification of methods to safely modify the downstream pathways affected by the variants through the mother. This paradigm has been best demonstrated by the observation that maternal folic acid supplementation has dramatically lowered the incidence of neural tube defects. The recognition that most CHD is caused by heterozygous mutations that only reduce gene dosage slightly provides hope that relatively small changes in dosage of gene networks may be sufficient to overcome the disease threshold, ultimately preventing disease even in the presence of gene mutations. A combination of AI advances and larger-scale sequencing of parents and their children with CHD, combined with single cell gene network data should point to those individuals at greatest risk for having a child with CHD—and strategies to lower their risk.

Although we are poised to translate modern knowledge of CHD into novel therapies in the coming years, this will only occur in the setting of integrated teams that understand the clinical, developmental, molecular, and genetic

underpinnings of the disease process. The unique organization of this textbook promotes such an environment and will be a valuable tool in this critical effort. I am optimistic that over the next two decades, major leaps in addressing CHD will emerge from our deep understanding of biology, and those leaps will change the face of what remains a leading cause of childhood morbidity and mortality.

San Francisco, CA, USA Deepak Srivastava
April 2024

Index

A
Aberrant right subclavian artery (A-RSA), 687, 779–781, 783–787, 789, 855, 856
Acidosis, 620, 622, 756, 905, 934
Actin
  alpha-skeletal actin, 994
  cardiac actin, 105, 118, 487, 606
  filaments, 419, 421–425, 429
  smooth muscle actin, 282, 605, 608
Actinin, 419, 429
Action potential (AP), 79, 427, 428, 1000, 1059, 1061, 1063–1067, 1071, 1075
Activin A receptor (ACVR)
  ACVR1, 726, 780, 788, 789, 855, 920
  ACVR2B, 564, 633, 635, 686, 688, 708, 710
  ACVR3, 920
Adams-Oliver syndrome, 522, 524
Adenosine deaminase that acts on RNA (ADAR), 319
Adenosine diphosphate (ADP), 422, 424–427, 430, 431
Adenosine triphosphate (ATP), 367, 369–374, 376, 381, 388, 422, 424–427, 430, 431, 987, 994, 996, 1001, 1074
Adenylate cyclase, 287, 510, 512
Alagille syndrome (AGS), 523, 524, 634, 636, 765, 766, 876
Alcohol, 60, 63, 403–405, 409–411, 654, 968–970, 978, 1030
αB-crystallin, 980
Amphibians, 136, 217, 228, 230, 231
Andersen-Tawil syndrome (ATS), 1028
Angiotensin II (AngII), 384, 996, 998, 999
Ankyrin 2 neuronal (ANK2), 1065, 1072
Ankyrin repeat domain 1, cardiac muscle (ANKRD1), 595, 596, 1004
Anomalous origin of the left coronary artery, 801–803, 972
Anomalous venous connections, 482
Aorta
  ascending, 32, 34–36, 79–81, 210, 646–648, 653, 673, 741, 742, 753, 754, 764–766, 931
  overriding, 133, 647–649, 653
Aortic
  aorticopulmonary septal complex, 127, 132, 136
  arch, 26, 29, 36, 91, 128, 129, 131, 137, 207, 211, 215, 217, 219, 240, 254, 280, 349, 543, 624, 626, 647, 653, 665, 666, 674, 690, 703, 713, 741–759, 762–770, 778–789, 818, 835, 837–839, 842, 844–846, 854, 857, 878
  coarctation, 137, 349, 352, 513, 712, 763, 765–767, 769, 786, 939, 940
  stenosis, supravalvar, 741, 742, 763, 764, 766
  valve, 37, 90, 97, 275, 305, 498, 500, 539, 540, 542, 543, 545, 646, 652, 673, 741–746, 762, 764–766, 778, 799, 805, 839, 916, 939–942, 948, 952, 970
  valve atresia, 931, 932, 951
  valve, bicuspid (BAV), 57, 61, 241, 244, 246, 305, 323, 349, 352, 406, 742, 745, 748, 750, 762–767, 778, 779, 784, 787–789, 805, 806, 909, 939, 940, 942, 951
  valve replacement, 97, 746
  valve stenosis, 404, 741–747, 749–753, 755, 762–764, 939, 940
  valvotomy, 745, 758, 759
Apoptosis, 31, 38, 133, 211, 244, 324, 381, 385, 411, 441, 487, 488, 544, 654, 689, 766, 784–786, 859, 953–955, 992, 996–998, 1002, 1005, 1006
Array comparative genomic hybridization (Array-CGH), 442, 814

© The Author(s), under exclusive license to Springer Nature Switzerland AG 2024

S. Rickert-Sperling et al. (eds.), *Congenital Heart Diseases: The Broken Heart*,
Advances in Experimental Medicine and Biology 1441,
https://doi.org/10.1007/978-3-031-44087-8

Arrhythmias
atrial, 355, 464, 466, 502, 558, 594, 669, 670, 703, 874, 904–906, 1075
familial, 1046
fetal, 321
inherited, 1034, 1042, 1046–1047
lethal, 976, 1028
supraventricular, 971, 1024, 1031
ventricular, 756, 966, 975, 976, 985, 1005, 1026–1028, 1031, 1058–1075
Arrhythmogenesis, 320, 354, 999–1000, 1059, 1063, 1065, 1067, 1068, 1074, 1075
Arrhythmogenic right ventricular cardiomyopathy (ARVC), *see* Cardiomyopathy
A-RSA, *see* Aberrant right subclavian artery (A-RSA)
Arterial
pole, 9, 11, 12, 15, 24, 28–40, 79, 105, 108, 110, 113–115, 117, 118, 133, 146, 187, 193, 482, 646, 653, 689, 819, 853, 857
switch, 666–669, 808, 809
ASD, *see* Atrial septal defect (ASD)
Asplenia, 168, 700, 702, 703, 709–712, 732
Assay of transposase-accessible chromatin sequencing (ATAC-seq), 262
Atherosclerosis, 156, 320, 386, 762, 812–814
Atrial
appendage, 15, 18, 26, 88, 207, 538, 544, 605, 606, 700, 701, 703
fibrillation, 323, 464, 1024, 1026, 1029, 1067, 1075, 1076
isomerism, 113, 172, 596, 702–704, 710
situs, 171
Atrial natriuretic peptide (ANP), *see* Natriuretic peptide A (NPPA)
Atrial septal defect (ASD)
ostium primum, 60, 112, 461, 462, 464–466, 482, 483, 485, 489–490, 554, 556, 566, 574
ostium secundum, 60, 152, 461, 462, 482
sinus venosus, 461, 465
Atrioventricular
bundle, 22, 81, 186, 188
canal, 8, 9, 17, 19, 20, 22, 25–27, 31, 32, 40, 79, 80, 187, 191, 204, 219, 228–232, 234–236, 276, 473, 483, 498, 536, 538, 563, 565, 600, 631, 636, 764, 894, 917, 948
cushion, 17, 20, 26, 27, 40, 41, 60, 80, 147–149, 540, 722, 826, 918
junction, 11, 21, 27, 135, 203, 204, 207, 209, 228, 232, 234, 482, 483, 485, 487, 489–491, 897, 916, 918
node, 20, 22, 81, 186, 192–194, 230, 254, 260, 384, 799, 1023
valve, 27, 89, 232, 234, 236, 301, 554, 555, 647, 703, 869, 871, 877
Atrioventricular septal defect (AVSD)
complete, 555–558, 560, 574, 579
incomplete, 554, 577, 579
intermediate, 557, 566
transitional, 554
Atrogin-1, 286
Atrophy, 992, 994, 995, 997–998, 1005
Autophagy, 381, 441, 992, 997, 998, 1069, 1070
AVSD, *see* Atrioventricular septal defect (AVSD)

B

Ballooning model, 80
BCL6 corepressor (BCOR), 522, 523, 633
Beta(β)-catenin, 158, 190–192, 230, 278, 324, 353, 376, 822, 826, 857, 996, 1000, 1005, 1071, 1074
Biliary atresia, 168, 720, 957
Birds, 19, 22, 28, 30, 38, 118, 191–193, 215, 217, 229–232, 234
Blalock–Taussig shunt, 622, 934, 935
Blepharophimosis syndrome, 523
Bone morphogenetic proteins (BMPs)
BMP2, 109, 148, 191, 192, 276, 576, 823, 889, 891, 894, 895, 920, 921, 925
BMP10, 194, 274–276, 280
Bradyarrhythmias, 1024, 1025
Brain natriuretic peptide (BNP), 300, 972, 994–996
BRG1-associated factor (BAF)
BAF45C, 299, 352
BAF60C, 109, 352
Bromodomain and extra terminal (BET), 353–354
Brugada syndrome (BRGDA), 517, 1026, 1028–1030, 1058–1062, 1064, 1074, 1077

C

Caenorhabditis elegans, *see* Nematode
Calcineurin, 285–287, 562, 563, 565, 889, 895, 896, 973

Calcium, 173, 187, 189, 190, 228, 243, 244, 246, 247, 261, 286, 287, 320, 355, 387, 411, 419, 428, 472, 513, 516, 562, 565, 724, 725, 727, 730, 731, 734, 764, 983, 993, 996, 1000, 1028, 1029, 1059, 1061, 1062, 1064–1066, 1068–1071, 1074, 1075
Calcium channel, 228, 516, 968, 1028, 1061, 1062, 1064, 1065, 1074
Calcium channel voltage-dependent L type alpha 1C subunit (CACNA1C), 980, 1028, 1065, 1067
Calmodulin (CALM)
  CALM1, 1062, 1065, 1069, 1070
  CALM2, 1065
  CALM3, 1036–1038, 1042, 1043, 1070
  calmodulin-dependent kinase II (CaMKII), 287, 427, 1068, 1069
Calsequestrin (CASQ), 418, 419, 1000, 1029, 1068
Calsequestrin 2 (CASQ2), 1029, 1062, 1068–1071
Canine
  heart, 1075
  tricuspid valve malformation (CTVM), 911, 921–923
Cap-binding protein (CBP), 317
Cardiac
  arrhythmias, 345, 1001, 1058, 1076
  asymmetry, 168, 169, 171–175, 177–179
  catheterization, 96, 465, 501, 557, 590, 621, 622, 626, 666, 667, 704, 744, 749, 754, 758, 806, 838, 871, 906, 933, 935, 967, 968, 972
  conduction system, 18, 20, 79, 81, 93, 126, 134, 186–195, 230, 254, 258, 260, 273, 274, 279, 300, 345, 369, 370
  crescent, 8, 78, 79, 104, 107, 109, 114, 117, 173, 187, 189, 254
  cushions, 79, 115, 767, 887, 891, 893
  development, 6, 41, 58, 78–79, 202, 208, 210, 240, 241, 254, 256–259, 272–278, 289, 297, 300, 301, 305, 315, 320, 321, 323, 324, 342–345, 347, 352, 356, 368, 369, 399, 401–405, 407–412, 449, 469, 491, 507, 511, 512, 515, 537, 544, 546, 578, 595, 600–601, 609, 632, 635, 636, 689, 701, 766, 879, 881, 892, 897, 898, 919, 942, 952, 994, 995, 1076
  evolution, 175
  fibrosis, 284, 288, 353, 998–999
  jelly, 8, 9, 11, 15, 18, 31, 132, 146–148, 273, 276, 351, 887, 894, 917
  looping, 11, 14, 113, 133, 174, 204, 210, 299, 349, 352, 536, 538, 539, 675, 707, 732
  neural crest, 30, 32, 63, 80, 126, 133, 537, 542, 545, 651, 673
  progenitor cells, 78, 83, 103–119, 173, 174, 242, 248, 511, 577, 647, 689, 846, 876, 890
  septation, 78, 80, 81, 83, 246, 254, 301, 541, 577, 646, 779
  transcription factors, 62, 78, 191–193, 245, 246, 296–305, 408, 437, 468, 527, 632, 638, 707, 881, 910, 1076
  transplantation, 670, 802, 874, 936, 969, 973–976, 1031
Cardiac ankyrin repeat protein (CARP), 595, 596, 994, 1004
Cardinal veins, 11, 13, 20, 21, 26, 147, 594, 595, 600, 601, 603, 606, 607, 609–611
Cardio-facio-cutaneous syndrome, 471, 474
Cardiomegaly, 378, 905, 906, 955
Cardiomyocytes
  adult, 134, 277, 279, 282, 372–377, 379, 388, 389, 421, 423, 438, 995, 997
  atrial, 11, 15, 20, 25, 26, 189, 194, 235, 242, 246, 421, 438, 487, 539, 544
  embryonic, 8, 11, 18–20, 31, 78, 80, 187, 190, 276, 277, 367, 376, 388, 578
  ventricular, 15, 18–20, 22, 38, 78, 80, 187, 193, 194, 234, 242, 274, 284, 288, 346, 368, 377, 386, 487, 539, 544, 955, 1061, 1064, 1065
Cardiomyopathy
  arrhythmogenic right ventricular cardiomyopathy (ARVC), 922, 975, 978–980, 982, 985, 998, 1004–1006, 1061, 1073
  dilated cardiomyopathy (DCM), 318, 320, 323, 324, 352, 385, 403, 469, 487, 846, 969–974, 978, 980–983, 985, 996–998, 1002–1006
  dilated cardiomyopathy, idiopathic, 970, 973
  hypertrophic cardiomyopathy (HCM), 64, 137, 318, 345, 352, 403, 471, 521, 524, 769, 965–969, 974, 977–980, 982, 983, 985, 987, 1001–1006, 1028, 1062
  hypertrophic obstructive cardiomyopathy (HOCM), 966–968
  noncompaction cardiomyopathy (NCCM), 978, 982, 984, 985
  restrictive cardiomyopathy (RCM), 516, 965, 973, 974, 978, 1005, 1006

CAT, *see* Common arterial trunk (CAT)
Catecholaminergic polymorphic ventricular tachycardia (CPVT), 1026, 1029–1031, 1067–1070
Cat eye syndrome, 595, 631
Caval veins, 20, 43, 104, 108, 111, 112, 146, 147, 216, 219, 463, 482, 483, 486, 488, 601, 603, 608
Cbp/P300-interacting transactivator with Glu/Asp-rich carboxy-terminal domain 2 (CITED2), 510, 511
Cell-cell junctions, 418
Cell culture, 248, 346, 438, 439, 441, 487
Channelopathies, 1025–1026, 1028, 1058, 1061, 1076
CHARGE syndrome, 137, 350, 353, 472, 525, 574, 634, 636, 768, 843, 845, 911, 939
Char syndrome, 523
Chemical exposure, 407–408
Chemokine (C-X-C motif) ligand 12 (CXCL12), 159, 813
Chick embryo, 104, 134, 208, 217, 485, 540, 605, 726, 733, 822, 890, 891, 948
Chicken, 4, 24, 37, 175, 189, 232, 234, 235, 437, 441, 545, 609, 611, 779, 858
Chromatin
  immunoprecipitation (ChIP), 297, 304, 343, 446–448
  immunoprecipitation sequencing (ChIP-seq), 303, 343, 446, 956
  organization, 354, 355
  remodeling complex, 299, 342, 351, 355, 473, 956
  structure, 302–303, 351, 353, 355, 446
Chromodomain helicase DNA-binding protein 1 (CHD1), 513
Chromodomain helicase DNA-binding protein 7 (CHD7), 137, 342, 349, 350, 353, 472, 474, 522, 525, 634, 636, 763, 768, 843, 845, 911
Chronotropy, 428
Cilia
  cilia, motile, 173, 178, 564, 676, 711, 722, 725, 727–730, 733, 734
  ciliary genes, 595, 676, 708, 711–713
Ciona intestinalis, 83
Cis-regulatory elements, 296, 302–303, 448, 787
Clawed frog, 437, 707
Clonal analysis, 105, 111, 112, 115, 116, 118, 606, 649
Clustered regularly interspaced short palindromic repeats (CRISPR), 82, 240, 243, 244, 248, 439, 726, 897, 950, 954, 1070
CNV, *see* Copy number variation (CNV)
Coarctation, *see* Aortic, coarctation
Collagen, 280, 282, 283, 384, 441, 608, 764, 786, 887, 891, 997–999
Collagen type IV alpha 1 (COL4A1), 677, 813
Common arterial trunk (CAT), 542, 543, 647, 649–652, 674, 677, 686, 779, 780, 783, 786–789, 835, 854–860, 877
Common atrioventricular canal (CAVC), 301, 489, 490, 688
Common atrium, 8, 60, 149–151, 483, 536, 554, 556, 575, 594, 600, 601
Common ventricle, 601
Conduction
  block, 59, 192, 260, 513, 1025, 1030
  defects, 137, 370, 469, 769, 880, 904, 909, 1059, 1075, 1076
  disease, 195, 517, 770, 983, 986, 1025, 1026, 1030, 1061, 1076
  system, 17, 20–22, 40, 79, 81, 93, 107, 126, 134, 186–195, 230, 254, 260, 279, 298, 299, 368, 600, 1024
Congestive heart failure (CHF), 91, 464, 500, 502, 743, 748, 754, 756, 801, 837–839, 870–872, 933, 971, 993, 996
Connective tissue growth factor (CTGF), 279, 282, 283, 998, 999
Connexin 40 (GJA5), 370, 508, 513, 631, 632, 635, 813, 1075
Connexin 43 (GJA1), 130, 822, 825, 940, 1004
Contractile proteins, 246, 299, 345, 352
Contraction
  isometric, 425–426
  isotonic, 426–427
Copy number variation (CNV), 507, 508, 513, 519, 520, 567, 631, 674, 675, 707, 814, 881, 940, 941
Cornelia-de-Lange syndrome, 356, 525, 911
Coronary
  endothelial cells, 81, 827
  endothelium (CoE), 160, 161, 818
  sinus, 20, 21, 24, 26, 60, 88, 92, 146, 147, 160, 418, 462, 463, 465, 482–484, 486, 488, 489, 589, 594, 600, 601, 603, 608, 612, 799–809
  smooth muscle cells (CoSMC), 81, 161, 278, 826
  vascular anomalies, 812, 826
  vascular system, 156, 160, 161, 818, 822, 823

veins, 160, 418, 826
vessels, 22–24, 156–163, 429, 431, 814, 825, 826
Coronary artery
anomalies (CAA), 819, 821, 822, 824
disease, 156, 262, 299, 804, 813, 814, 936, 978
fistula, 805, 806
Costello syndrome, 524, 769, 981
Cri du chat syndrome, 631
Cripto, FRL-1, Cryptic family 1 (CFC1), 510, 512, 527, 564, 565, 634, 635, 675, 708, 710
Cyanosis, 60, 93, 94, 463, 464, 500, 501, 589, 619–621, 625–627, 663, 665, 669, 753, 756, 757, 837, 870, 872, 905, 906, 933, 934, 971
Cysteine-rich protein with EGF-like domains 1 (CRELD1), 560–563, 565, 567, 709, 713

D

DAN domain family member 5 (DAND5), 173, 724
Danio rerio, *see* Zebrafish
Defibrillator, 968, 969, 976, 1031, 1068
Desmocollin 2 (DSC2), 975, 982, 984, 1005, 1072
Desmoglein 2 (DGL2), 975
Desmoplakin (DSP), 975, 981–984, 1000, 1004, 1006, 1062, 1069, 1071, 1072
Dextrocardia, 170–173, 596, 700, 701, 703, 706, 708–713, 720, 722, 727
Dextro-transposition of the great arteries (d-TGA), 566, 626, 663–670, 672, 710, 711, 727
Diabetes, 60, 63, 386, 401–403, 408–411, 654, 677, 691–692, 789, 860
Diaphragmatic hernia, 318, 522, 523
DiGeorge syndrome (DGS), 61, 126, 136–137, 323, 507, 517, 518, 632, 633, 636, 674, 768, 843–845, 877
Dilated cardiomyopathy (DCM), *see* Cardiomyopathy
Dishevelled 1 (DVL1), 522, 524, 911
Dishevelled 2 (DVL2), 650, 686, 692
Dogs, 911, 921–925
Dorsal mesenchymal protrusion (DMP), 21, 25, 26, 60, 80, 111–113, 146–151, 230, 231, 483, 543, 574–580, 596, 604–606, 609, 611
Dorsal mesentery (DM), 148, 485, 732
Dorsal mesocardium, 9–11, 13, 25, 26, 107, 108, 146–149, 151, 482, 483, 485, 538, 575, 576, 594
DORV, *see* Double outlet right ventricle (DORV)
Double inlet left ventricle, 234, 538, 539, 869
Double outlet right ventricle (DORV), 131, 133, 136, 138, 171, 172, 208, 299, 347–349, 510, 512, 515, 516, 527, 542, 544, 623–627, 630–636, 638, 646–654, 672, 674–676, 684, 686, 688, 690, 704, 784, 786, 787, 789, 806, 858, 859
Down syndrome, 61, 247, 276, 491, 518, 524, 559–562, 564, 566–568, 574, 579, 631, 674, 911
Drosophila melanogaster, *see* Fruit fly
Duane-radial ray syndrome, 521
Ductus arteriosus, 81, 91, 128, 131, 214, 215, 403, 406, 595, 619, 622, 646, 665, 667, 743, 746, 748, 749, 753, 754, 778, 932–934, 948
Dynein, axonemal, heavy chain (DNAH)
DNAH5, 173, 177, 520, 708, 710, 712, 728–730
DNAH11, 177, 652, 687, 708, 712, 728, 730
D4 zinc and double PHD fingers family 3 (Dpf3), 299, 352

E

E1A binding protein p300 (P300), 297, 299, 300, 302, 303, 305, 347
Early repolarization syndrome (ERS), 1074–1075
Ebstein anomaly, 903–907, 909–912, 916–925
Echocardiography, 96, 97, 99, 176, 440, 464, 465, 501, 557, 590, 621, 622, 626, 665, 666, 699, 744, 749, 751, 754, 757, 758, 802, 806, 838, 871, 905, 906, 933, 939, 949, 950, 952, 953, 967–969, 972, 974, 975, 986
Ectoderm, 78, 109, 110, 127, 128, 130–132, 254, 344, 651, 690, 778, 782–784, 857
Ectomesenchymal cells, 127
Ectothermic vertebrates, 193, 202, 217, 229, 232, 235, 236
Edwards syndrome, 61, 518, 631
Elastin (ELN), 62, 519, 742, 763, 764, 766, 813
Electrocardiogram (ECG)
depolarization, 1000, 1023
PR interval, 1023, 1025, 1030
p-wave, 1023

Electrocardiogram (ECG) (*cont.*)
QRS complex, 1023
q-wave, 1023
repolarization, 1023, 1059, 1061
T-wave, 1023
Ellis-van Creveld syndrome (EVC), 876
Embryogenesis, 110, 174, 242, 261, 273, 319, 351, 352, 437, 440, 512, 523, 635, 687, 688, 710, 712, 778, 783, 786, 818, 858, 859, 890, 895, 922, 994
Embryonic node, 168, 169, 173, 174, 177, 720–725, 727–731, 733
Embryonic stem cells (ESC), 82, 301, 343
EMT, *see* Epithelial-to-mesenchymal transition (EMT)
ENCODE, 302, 303, 469–472, 764, 766, 786, 813, 822, 847, 848, 878, 1028, 1029
Endocardium, endocardial
endocardial cells, 32, 115, 132, 146, 161, 242, 246, 254, 272–276, 472, 487, 517, 562, 600, 823, 886, 887, 889, 891, 894–896
endocardial cushion, 19, 21, 26, 27, 31, 32, 38, 40, 41, 60, 80, 81, 148, 203, 204, 207, 275, 276, 280, 353, 461, 471, 483, 485, 490, 498, 538–541, 543–546, 554, 562, 574, 653, 673, 677, 762, 820, 854, 858, 877, 879, 895, 896, 917, 918, 920, 922
Endoderm, 9, 78, 107, 109, 110, 131, 132, 254, 300, 343, 542, 577, 651, 778, 782–784, 786, 788, 857, 878
Endothelin 1 (ET1), 132, 439
Endothelium, endothelial
endothelial cells, 79, 81, 106, 115, 119, 147, 159–161, 241, 244, 246, 255, 272–276, 278–283, 346, 366, 382–383, 440, 487, 488, 596, 601, 602, 611, 778, 783, 814, 827, 855, 857, 894, 995, 1092
endothelial-to-mesenchymal transition, 23, 129, 157, 243, 245, 275–277, 517, 646, 821, 887, 919, 953
Enhancers, 109–112, 192–194, 288, 296, 297, 299, 303, 343, 354, 355, 448, 472, 511, 578, 611, 648, 687, 688, 724, 879, 881
Environmental factors, 63, 262, 305, 388, 398, 399, 401, 408–410, 412, 567, 595, 630, 638, 684, 710, 767, 987, 1062, 1077
Epicardial-derived cells (EPDCs), 156–160, 545, 821–823, 825, 918
Epicardium, 22, 23, 37, 79, 81, 104, 115–117, 134, 156–163, 254, 274–278, 282, 418, 545, 821–823, 826, 877, 998, 1061, 1074
Epigenetics, epigenetic
epigenetic marks, 305, 342, 349, 351, 436, 446
epigenetic mechanisms, 247, 305, 374, 387, 399, 410, 411, 438, 636, 654, 957
epigenetic modification, 62, 342, 343, 350, 351, 356, 436, 994
epigenetic regulators, 288, 343, 350, 411, 632
Epigenome, 387, 445–448
Epithelial-to-mesenchymal transition (EMT), 23, 129, 130, 132, 157–159, 254, 274, 277, 278, 282, 470, 646, 653, 821–823, 886, 887, 889–894, 896, 897, 917
Erythroblastic leukemia viral oncogene homolog (ERBB)
ERBB2, 273, 274, 281, 368, 373, 380, 388
ERBB4, 273, 274, 281, 388, 940, 949
Excitation-contraction coupling (ECC), 427–429, 431–432, 998, 1000
Extracellular matrix (ECM), 18, 130, 132, 133, 146, 158, 244, 255, 272, 273, 279, 282, 283, 384, 386, 420, 575, 677, 732, 764, 786, 789, 821, 887, 890, 917, 994, 995, 997, 999
Extracellular signal-regulated kinase (ERK)
ERK1, 288
ERK2, 288
ERK5, 996

F

Fabry disease, 979, 980
Fetal gene program, 994, 995
Fetal heart, 211, 212, 214, 216, 241, 248, 254, 321, 370, 691, 692, 877
Fibrillin 1 (FBN1), 244, 522, 525, 767
Fibroblast growth factors (FGF)
FGF8, 109, 110, 115, 133, 611, 649, 651, 689, 690, 732, 733, 780, 783–785, 788, 855, 858
FGF9, 159, 826
FGF10, 109, 110, 112, 278, 578, 858
FGF16, 159, 243, 246, 277
FGF20, 159, 277
FGFR3, 520, 524, 858
Fibroblasts, 22, 81, 108, 127, 134, 160–162, 189, 194, 236, 241, 242, 255, 272–275, 277–280, 282–284, 301, 353, 366, 382–384, 386, 387, 438, 519, 522, 524, 578, 611, 783–784, 823, 858, 887, 918, 995, 996, 998, 999, 1062
Fibrofatty infiltration, 975, 1005
Fibronectin, 243, 245, 282, 321, 786

Fibrosis, 162, 212, 279, 280, 282–284, 287, 318, 345, 353, 354, 384, 904, 968, 974, 992, 996–999, 1001–1003, 1005, 1030, 1071, 1075
Final common pathway hypothesis, 992, 993
First heart field (FHF), 8, 9, 11, 19, 27, 104–107, 109, 112, 114, 116, 117, 119, 146, 187, 254, 258, 536, 538, 689
First heart sound, 464, 500, 621, 744, 748, 971
Fluorescence-activated cell sorting (FACS), 255, 259, 441
Fluorescence in situ hybridization (FISH), 61, 64, 442, 446, 766
Focal adhesion kinase (FAK), 826, 994, 997, 999
Folate
  folate-binding protein, 691, 787
  folate deficiency, 403, 410
  folic acid (FA), 63, 691, 787
  Folr1, 691, 780, 787
Fontan operation, 872–874, 934, 936
Forkhead box (FOX)
  FOXC1, 633, 677, 780, 786, 787, 855
  FOXC2, 109, 633, 780, 786, 787, 855
  FOXH1, 113, 633, 635, 675, 686–688, 724
  FOXJ1, 728
  FOXL2, 520, 523
Frank-Starling mechanism, 426
Frank-Ter Haar syndrome (FTHS), 635
Friend of GATA 2 (FOG2), 61, 632, 649, 878–879, 892, 919
Fruit fly, 83, 436, 437

G

Gallus gallus, *see* Chicken
Gap junctions, 130, 187, 191, 193, 228, 279, 282, 427–429, 513, 635, 677, 733, 822, 1000, 1001, 1004, 1069, 1071, 1077
Gastrocoel roof plate (GRP), 722
Gastrulation brain homeobox 2 (GBX2), 784–785
GATA binding protein (GATA)
  GATA4, 60, 62, 107, 109, 161, 191, 192, 228, 243, 244, 246, 281, 283, 288, 297, 298, 300–302, 344, 347, 352, 409, 410, 438, 468–470, 487, 507, 508, 510, 513, 514, 527, 542, 544, 563, 564, 596, 608, 611, 632, 633, 650, 707, 763, 770, 788, 844, 847, 848, 855, 878, 879, 881, 886, 887, 889, 890, 892, 895, 898, 910, 911, 919
  GATA5, 278, 300, 564, 565, 649, 763, 767, 788, 847, 889, 895
  GATA6, 60, 190–192, 283, 288, 300, 318, 520, 523, 542, 564, 565, 632, 633, 649, 780, 788, 844, 846–848, 855, 920
Genetic counseling, 64, 66, 638, 672, 845, 987
Genetic testing, 58, 63–66, 93, 767, 910, 969, 984, 985, 1026, 1027, 1029, 1068, 1077
Genome-wide association study/studies (GWAS), 59, 240, 262, 263, 443, 469, 638, 675, 762, 812, 814, 940
Genotyping technologies, 442–443
Glenn anastomosis, 934, 936
G-protein coupled receptors (GPCR), 428, 993, 996, 997
Great arteries, 82, 91, 127, 128, 131, 132, 169, 171, 172, 247, 323, 349, 404, 543, 623, 624, 626, 671–678, 683–692, 703, 710, 714, 727, 770, 778–781, 788, 789, 805, 806, 808, 809, 812, 819, 821, 824, 835, 836, 854, 856, 858, 870, 876, 938
Growth differentiation factor (GDF)
  GDF1, 633, 635, 675, 686, 687, 692, 708, 710, 724
  GDF3, 510, 512
Guinea pig, 210, 1067, 1076

H

Haploinsufficiency, 61, 62, 132, 305, 348, 353, 409, 469, 470, 472, 523, 525, 579, 632, 649, 765, 1030
Harvey rat sarcoma viral oncogene homolog (HRAS), 522, 524, 769, 981
Heart and neural crest derivatives expressed (HAND)
  HAND1, 27, 62, 116, 131, 194, 195, 243, 248, 296, 301, 544, 940
  HAND2, 27, 116, 131, 297, 298, 300, 301, 348, 632, 633, 780, 783, 789, 895
Heartbeat, 228, 418
Heart development, *see* Cardiac, development
Heart looping, *see* Cardiac, looping
Heart tube, 6–11, 13–15, 18, 20, 26, 27, 41, 78–83, 104, 105, 107, 108, 112–115, 117, 133, 146, 168–171, 173–175, 187–189, 193, 202, 203, 206, 228, 229, 254, 273, 276, 296, 298, 301, 536, 538, 539, 600–602, 611, 647–649, 651, 689, 724, 853, 877, 887, 917, 919
Hes family bHLH transcription factor 1 (HES1), 650

Hes-related family bHLH transcription factor with YRPW motif 2 (HEY2), 192, 321, 514, 515, 876, 879, 881, 886, 919, 1061
Heterotaxy, 63, 168, 171, 177, 178, 321, 349, 402, 489, 515, 521, 523, 526, 560, 563, 564, 566, 574, 587, 633–635, 638, 652, 675–677, 684, 687, 690, 692, 699–704, 706–714, 720–722, 724, 726–728, 732, 733, 940, 957
His bundle, 92, 230, 259, 260
His–Purkinje system, 92
Histological analysis, 440, 441, 578
Histone
  acetylase, 343
  acetylation, 342–344, 711
  acetyltransferase (HAT), 192, 297, 299, 300, 344, 347
  deacetylases (HDACs), 287, 288, 299, 300, 302, 344–346, 348, 352, 950, 956, 957
  deacetylation, 344–346
  demethylation, 354, 711
  HDAC1, 345
  HDAC2, 345–347
  HDAC3, 345–346, 354
  HDAC5, 287, 346
  HDAC7, 346
  HDAC9, 287, 346
  methylation, 347, 349, 410
  methyltransferase, 342, 347–349, 525, 766
  modification, 343, 344, 350, 351, 410, 446
  modifying genes, 711, 940
Histone 3 lysine 4 (H3K4), 349, 350, 711
Histone 3 lysine 9 (H3K9), 346
Histone 3 lysine 27 (H3K27), 349, 711
Histone 3 lysine 36 (H3K36), 348
HLHS, *see* Hypoplastic left heart syndrome (HLHS)
Holt-Oram syndrome (HOS), 469
Homeobox (HOX) transcription factors
  HOXA1, 112, 633, 649, 780
  HOXA3, 783, 784
  HOXB1, 111, 112, 780
  HOXD13, 843, 845
Human ether-a-go-go-related gene potassium channel 1 (HERG), 1066
Hyaluronan synthase 2 (HAS2), 510, 512
Hyperplasia, 204, 346, 371, 372
Hyperpolarization activated cyclic nucleotide-gated potassium channel 4 (HCN4), 107, 607, 1061
Hypertrophic cardiomyopathy (HCM), *see* Cardiomyopathy
Hypertrophic obstructive cardiomyopathy (HOCM), *see* Cardiomyopathy
Hypertrophy, 11, 61, 95, 244, 262, 272, 274, 279–289, 324, 344–346, 352, 353, 378, 382, 439, 464, 501, 617, 654, 749, 756, 758, 764, 768, 966, 968, 979, 982, 992–999, 1001–1005
Hypophosphatemia, 522, 525
Hypoplasia, 27, 126, 132, 190, 206, 208, 209, 215, 240, 245–246, 278, 321, 323, 345, 352, 472, 578, 621, 624, 653, 665, 701, 746–748, 763, 765, 767, 782, 783, 826, 843, 846, 847, 905, 906, 931, 938, 939, 941, 942, 948–951, 953–957
Hypoplastic left heart syndrome (HLHS), 208, 209, 211, 212, 214–216, 243–245, 321, 405, 406, 408, 587, 765, 843, 844, 871, 872, 916, 931–936, 938–943, 948–953, 955–957
Hypoxemia, 619, 620, 622, 906
Hypoxia, 212, 277, 281, 367, 368, 372–374, 381, 387, 403, 409–411, 472, 620, 752, 860, 994
Hypoxia signaling pathways, 409

I

IAA, *see* Interrupted aortic arch (IAA)
Immunohistochemistry, 441
Induced pluripotent stem cells (iPSC), 240–249, 438, 677, 955, 1058
Inferior vena cava (IVC), 87, 219, 462, 463, 589, 608, 703, 872, 873
Inositol requiring 80 (INO80), 351, 353
Inositol-1,4,5-triphosphate (IP3), 286
Inositol-1,4,5-triphosphate receptor (IP3R), 432
Inotropy, 428
In situ hybridization, 441, 723
Insulin-like growth factor 1(IGF1), 274, 279, 283–284, 287, 996
Intercellular communication, 279, 282, 389
Intercellular crosstalk, 995
Interrupted aortic arch (IAA), 132, 136, 137, 353, 542, 673, 674, 741, 753–755, 763, 767–768, 779–781, 783, 784, 786–789, 837–839, 843, 844, 855, 856
Interventricular communication, 490, 536, 539, 540
Interventricular septum (IVS), 41, 43, 79, 80, 117, 146, 219, 539, 544, 545, 646, 856, 918, 921

Ion channel, 8, 320, 345, 427, 514, 730, 880, 993, 1000, 1024–1026, 1029, 1058, 1062, 1071, 1075–1077
IP3 receptors (IP3Rs), 432
Iroquois homebox 4 (IRX4), 510, 511
Islet 1 (ISL1), 149, 189, 190, 241, 242, 298, 301, 510, 511, 577, 632, 633
Isomerism, 113, 172, 190, 489, 596, 687, 688, 700–704, 710, 724, 732
Ivemark syndrome, 703

J
Jacobsen syndrome, 138, 631, 939, 949
Jagged 1 (JAG1), 61, 522, 524, 631, 634, 636, 650, 763, 765, 766
Jatene procedure, 666–669
Jumonji (JMJD2A), 344, 347–348

K
Kabuki syndrome, 63, 349, 350, 472, 474, 525, 765, 766, 911
Kartagener syndrome, 526, 712, 728
Kaufman-McKusick syndrome, 560
Kinesins, 728
Knockin, 919
Knockout
  conditional, 731
  double, 891
Kruppel-like factor 2 (KLF2), 202
Kruppel-like factor 5 (KLF5), 999

L
Labradors, 922, 925
Lamb, 211, 212, 214
Lamin
  lamin A/C (LMNA), 355, 981–983, 985, 1005
  lamin B receptor (LBR), 520, 525
Larsen-like syndrome, 526
Laterality defects, 168, 171, 172, 178, 402, 515, 635, 638, 675, 688, 689, 709, 710, 712, 713, 720, 721, 723, 727–729, 731, 956
Lateral plate mesoderm (LPM)
  left, 174, 686, 687, 689, 722, 724, 726
  right, 174, 686, 687, 689, 723, 724, 726
Left atrium (LA), 21, 25–27, 79, 87–89, 91, 98, 104, 112, 135, 146–152, 170, 172, 188, 211, 212, 216, 219, 234, 254, 462, 482, 483, 485, 486, 488–490, 499, 501, 587–591, 595, 601, 603, 604, 606–608, 610–612, 646, 666, 668, 684, 699, 700, 703, 799, 806, 836, 870, 872, 897, 904, 921, 948, 951, 952, 967, 973, 974
Left–right axis, 80, 170, 173, 179, 675, 684, 687, 724, 726, 727
Left-right determination factor 1 (LEFTY1), 919
Left-right determination factor 2 (LEFTY2), 564, 566, 710, 919
Left-right patterning, 491, 560, 564, 609, 635, 692
Left-to-right shunt, 462, 499, 500, 664, 806
Left ventricle (LV), 8, 9, 11, 14–19, 22, 27, 31, 38, 40, 78, 81, 89, 91, 98, 104, 106, 107, 113, 117, 131, 135, 150, 170, 172, 173, 175, 187, 188, 208, 214, 215, 234, 245, 254, 272, 280, 296, 301, 349, 352, 418, 462, 486, 490, 498–501, 536, 538, 539, 541, 555, 589, 590, 623, 627, 646–648, 654, 663, 664, 667, 668, 671, 673, 684, 685, 689, 701, 741, 742, 765, 768, 781, 801, 806, 856, 873, 876, 897, 904, 906, 907, 916, 931, 938, 948, 951, 952, 969, 974, 998, 1071
Left ventricular noncompaction (LVNC), *see* Cardiomyopathy
LEOPARD syndrome, 126, 137, 634, 636, 812
Lev-Lenegre disease, 1026
Linkage analysis, 438, 442, 468, 635, 712, 814, 911, 922, 939, 940
Lithium, 401, 403, 406, 409, 411
Long QT syndrome (LQTS)
  QT prolongation, drug-induced, 1035
Lumenization, 594, 601
Lungfish, 230, 231
Lymphoid enhancer-binding factor 1 (LEF1), 578

M
Magnetic resonance imaging (MRI), 99–100, 176, 177, 213, 215, 440, 465, 501, 537, 557, 590, 621, 623, 626, 627, 666, 685, 733, 744, 749, 752, 754, 758, 759, 781, 806, 838, 856, 871, 906, 933, 934, 968, 969, 972, 974, 975, 1069, 1071
Mahogunin ring finger 1 (MGRN1), 489
Major aortopulmonary collateral arteries (MAPCA), 617, 620, 835, 871
Makorin ring finger protein 2 (MKRN2), 523, 526, 709, 714

Mammals, 6, 18, 19, 22, 28, 30, 38, 83, 107, 136, 157, 171, 175, 188, 191, 193, 215, 217, 229–235, 254, 296, 316, 346, 368, 371, 372, 374–377, 436, 540, 779, 892, 921
MAPK/ERK kinase (MEK)
MEK1, 288, 470, 471
MEK2, 288, 470, 471
MAPK pathway, 59, 996
Marfan syndrome (MFS), 246, 525, 767
Mass spectrometry (MS), 262, 448, 449
Mastermind-like 3 (MAML3), 526
Maternal
exposure, 63, 402–405, 706
infections, 403
stress, 404, 410, 439
Matrix metalloproteinases (MMP), 346, 709, 713, 732, 997
Mechanotransduction signaling, 993
Mediator complex subunit 13-like (MED13L), 675, 677
Medication
angiotensin-converting enzyme (ACE) inhibitor, 406
beta-blocker, 406, 1068
diuretics, 502
spironolactone, 973
Mesenchymal
cap, 20, 26, 27, 60, 149–150, 230, 470, 471, 474, 483, 485, 486, 539, 574–576
cells, 32, 36, 38, 80, 81, 148, 150, 156, 157, 244, 246, 258, 274, 277, 279, 282, 538, 546, 575, 578, 691, 822, 887, 890, 891, 917, 953
precursors, 231, 483, 574
protrusion, 27
Mesenchyme, 9, 13, 25, 28, 32, 35, 36, 78, 127, 129, 130, 133, 149, 150, 158, 174, 230, 231, 234, 348, 485, 545, 575, 576, 578, 602, 605, 606, 647, 651, 653, 689, 690, 778, 784, 820, 826, 857, 917, 919
Mesocardium, 9–11, 25, 26, 483, 485
Mesoderm, 7, 9, 104, 107, 117–119, 130, 169, 174, 187, 189, 190, 228, 241, 242, 248, 254, 273, 482, 485, 488, 515, 600, 652, 686–689, 722, 724, 782, 847, 857, 876, 942
Mesoderm posterior 1 homolog (MESP1), 105, 134, 241, 242, 510, 511, 514, 515, 520
Messenger RNA, *see* RNA
Metabolome, 448–449
Methylation
DNA, 303, 350, 387, 410, 446, 567, 630, 636, 956, 957
protein, 303, 342, 349
Methyl-CpG binding domain-based (MBD), 446
Methyltransferase, 158, 316, 317, 342, 347–350, 446, 472, 514, 517, 522, 525, 766, 956
Micro-computed tomography (micro-CT), 440
MicroRNAs, *see* RNA
Microtubule, 579, 728, 1071
Midline 1 (MID1), 523, 526
Mid-pharyngeal endothelial strand (MPES), 594, 596, 601, 602, 607, 611
Mitochondria, 346, 367, 368, 372, 373, 377, 384, 385, 388, 411, 424, 997, 998
Mitral
atresia, 468, 626, 872, 932, 938, 950
insufficiency, 464, 466, 556, 558, 873, 971
valve, 60, 79, 89, 90, 246, 461, 464, 465, 468, 490, 498, 499, 541, 554, 556–558, 623, 626, 748, 749, 762, 769, 846, 873, 876, 878, 886, 909, 938, 948, 950, 952, 967, 970, 971
Mixed-lineage leukemia protein 2 (MLL2), 349, 350, 522, 525, 766
Morphogen hypothesis, 728–730
Morpholino oligonucleotides (MO), 439, 954
Mouse
embryo, 8, 31, 32, 82, 104, 105, 108, 109, 115, 138, 160, 173, 174, 209, 210, 258, 441, 482, 539, 545, 596, 607, 609–611, 649–651, 687, 690, 722–724, 726, 727, 729, 781, 786, 788, 860
heart, 78, 79, 81, 106, 135, 136, 148, 169, 175, 176, 189, 258, 262, 305, 374, 484, 488, 540, 541, 648, 824, 891, 955, 999, 1000, 1065
models, 132, 133, 136, 137, 146, 149, 171, 178, 210, 211, 282, 381, 440, 469, 471–473, 482, 488, 489, 562, 568, 576, 579, 596, 608–610, 650, 654, 685–687, 689, 690, 692, 725, 779, 783, 785–787, 789, 821, 854, 858, 860, 886, 896, 897, 919–921, 949, 953, 957, 1063, 1067, 1068, 1071, 1074, 1075
Mowat-Wilson syndrome (MOWS), 470, 474
Msh homeobox (MSX)
MSX1, 240, 276, 348, 469, 470, 789, 855
MSX2, 276, 789, 855
Muenke syndrome, 524
Murmur, 94, 463, 464, 500–502, 556, 589, 620, 621, 626, 665, 743, 744, 748, 753, 756, 757, 806, 837, 838, 870, 871, 905, 933, 967, 971
Muscularization, 161, 485, 539, 540, 543, 823, 825

Mus musculus, *see* Mouse
Myocardialization, 27, 38, 133, 231, 544, 604–605, 611
Myocardin (Myocd), 302, 320, 324, 346
Myocarditis, 99, 969, 970, 972, 973, 1024
Myocardium
  atrial, 25, 78, 79, 111, 186, 190, 194, 606, 611, 894
  chamber, 79, 81, 187, 192, 194, 228, 230, 369, 463, 600, 608, 823
  compact, 18–20, 22, 156, 159, 208, 274, 367, 369, 372, 374, 545, 822, 823, 826, 918
  developing, 9, 10, 16, 18, 19, 25, 31, 40, 187, 190, 192, 193, 273, 274, 347, 368, 374, 410, 488, 544, 609, 822, 823, 918, 920, 1006
  junctional, 918
  outflow tract, 9, 17, 19, 28, 31–34, 36, 37, 78, 79, 105, 111, 187, 188, 228, 347, 542, 544, 648, 689–691, 722, 731, 821, 917, 966
  primary, 10, 17, 20, 24, 608, 920
  pulmonary trunk, 111, 118, 119, 133, 690
  sinus venosus, 79, 112, 188, 189, 227, 463, 601, 606, 611
  subpulmonary, 31, 34, 543, 648–650, 652, 653, 821
  venous pole, 78, 104, 111, 112, 115, 118, 119, 600, 606, 649
  ventricular, 9, 105, 107, 118, 156, 159, 192, 194, 255, 276, 301, 367, 487, 538, 544, 764, 821, 825, 826, 918, 974, 975, 1006, 1023, 1069
  working, 20, 186–193, 228, 235, 818
Myocyte enhancer factor 2C (MEF2C), 276, 297, 299, 300, 409, 577, 632
Myofibrils, 248, 419, 420, 428, 429, 473, 994, 1003–1005
Myogenesis, 110, 438
Myogenic differentiation factor (MyoD), 110, 117
Myosin-binding protein C (MYBPC3), 318, 422, 514, 516, 979, 980, 982–984, 1062
Myosin filaments, 419–422
Myosin heavy chain (MYH)
  MYH6, 59, 60, 243, 245, 299, 421, 468, 470, 510, 512, 514, 516, 880, 949
  MYH7, 243, 245, 246, 288, 421, 514, 516, 910, 977, 979–984, 1002

N
Natriuretic peptide A (NPPA), 187, 606, 880
Naxos disease, 979
Necrosis, 975, 992, 996–998, 1002, 1004–1006
Nematode, 436
Nephronophthisis (NPHP)
  NPHP2, 708, 712
  NPHP3, 708, 712
  NPHP4, 633, 635, 708, 714
Nervous system, 6, 11, 127, 130, 524, 763
N-ethyl-N-nitrosourea (ENU), 82, 439, 782, 827
Neural crest
  cells (NCC), 127, 129–131, 137, 138, 472, 690, 820, 821, 854, 857, 859, 860, 974
  cells, cardiac (CNCC), 126–138, 841, 842, 846, 847, 859
Neural tube, 108, 117, 127–131, 134, 354, 691
Neuregulin 1 (NRG1), 194, 273–275
Neurofibromatosis type 1 (NF1), 769
Next-generation sequencing (NGS), 256, 257, 343, 443–448, 451, 527, 849, 987
Nipped-B homolog (NIPBL), 356, 522, 525
Nitric oxide synthase 3 (NOS3), 487
NK2 homeobox 5 (NKX2-5), 109, 189, 191–195, 242, 243, 245, 246, 276, 298, 299, 301, 305, 348, 408, 409, 437, 438, 468–470, 472, 513, 514, 527, 577, 632, 649, 707, 844, 847, 848, 880, 881, 887, 910, 919, 940, 994, 1006
NK2 homeobox 6 (NKX2-6), 510, 511, 844, 848
NODAL, 409, 564, 566, 634, 635, 708, 710, 911
Nodal signaling, 112, 174, 175, 511, 512, 515, 565, 635, 686–688, 723–727, 729–734
Nodal vesicular parcels (NVP), 729, 730
Noncompaction, 244, 299, 515, 516, 545, 916, 965, 974–975, 978, 982, 984, 993, 1005–1007
Nonsense mediated decay (NMD), 314, 315, 318
Noonan-like syndrome, 524
Noonan syndrome, 59, 63, 137–138, 247, 471, 474, 524, 560, 574, 634, 636, 756, 763, 768, 769, 911, 939, 980
Norwood procedure, 934–936
NOTCH
  NOTCH1, 18, 60, 161, 191, 204, 243–245, 275, 298, 305, 347, 514, 515, 520, 524, 633, 650, 651, 724, 763, 764, 767, 940, 949
  NOTCH2, 321, 520, 524, 633, 636, 650, 724, 763, 766
Nuclear factor of activated T-cells (NFAT)
  NFATC1, 115, 242, 321, 509, 562, 563, 565–567, 878–880, 886–889, 895–896, 898, 911, 997, 1006
  NFATC2, 287
  NFATC3, 287

Nuclear lamina, 354
Nuclear magnetic resonance spectroscopy (NMR), 449
Nuclear receptor binding SET domain protein 1 (NSD1), 519, 522, 525
Nuclear receptor subfamily2/group F (NR2F2), 514, 515, 563, 564, 566
Nucleoporin, 355, 707, 709, 714
Nucleosome, 342, 343, 351, 448, 449, 711

O
Obesity, 63, 386, 401, 404
Oculofaciocardiodental syndrome, 522, 523, 633, 635
Okihiro syndrome, 521, 633
Opitz syndrome, 526
Outflow tract (OFT)
  cushions, 79, 80, 537, 540, 541, 646, 647, 652, 653, 689, 691, 722, 891, 894
  elongation, 646–648, 650–652, 654, 674
  morphogenesis, 131, 647, 651–653
  septation, 38, 126, 136, 254, 347, 647, 653, 654, 819, 821, 854, 856, 857, 860
  valve, 646, 650, 652, 854, 896
Outlet defects, 536, 544, 545
Oxidative stress, 372–374, 376, 377, 379, 381, 386, 409–411, 691, 860, 996
Oxygen consumption, 386, 424

P
Pacemaker, 81, 186–191, 228, 260, 427–429, 873, 1023, 1031, 1061
Paired box 3 (PAX3), 117, 651
Paired-like homeodomain 2 (PITX2), 112, 190, 409, 510, 511, 514, 515, 633, 652, 675, 707
Pallister–Killian syndrome, 518
Parathyroid gland, 127, 137
Partial anomalous pulmonary venous connections (PAPVC), 596
Partial anomalous venous return, 464, 521, 594, 703
Patau syndrome, 61, 518, 631
Patch closure, 465, 557
Patched 1 (PTC1), 580
Patent ductus arteriosus (PDA), 58, 91, 132, 138, 216, 318, 352, 403, 410, 513, 514, 516, 517, 523, 620, 621, 626, 663–665, 667, 743, 748, 752–756, 838, 843, 844, 871, 872, 876, 877, 909, 932, 933
Patent foramen ovale (PFO), 60, 152, 216, 233, 462, 468, 511, 663–666, 756, 904, 905, 909, 933, 951
Paternal exposure, 408
Pelger–Huet anomaly, 525
Persistent truncus arteriosus (PTA), *see* Common arterial trunk (CAT)
Peters plus syndrome, 525
Pharyngeal arch arteries (PAA), 9, 28, 30, 32, 115, 126, 127, 131, 646, 689, 778–786, 789, 853, 854, 857, 858, 860
Pharyngeal mesoderm, 78, 104, 118, 647
Phosphoinositide 3-kinase (PI3K), 996, 998
Phospholamban (PLN), 428, 980–985, 1000, 1071, 1073
Phosphorylation
  phosphorylation of RyR2s, 427
  phosphorylation sites, 423, 429
  protein kinase A phosphorylation, 1068
Photoactivatable ribonucleoside-enhanced cross-linking and immunoprecipitation (PAR-CLIP), 448
Plakoglobin (JUP), 419, 922, 975, 982, 984, 1000, 1005, 1006, 1071, 1072
Plakophilin 2 (PKP2), 975, 982, 984, 1000, 1005, 1061, 1062, 1069, 1072, 1074
Planar cell polarity (PCP), 13, 36, 115, 158, 159, 646, 650, 651, 675, 685–687, 731, 787, 822
Platelet-derived growth factor (PDGF), 278, 578, 597, 609, 653, 813, 998
Platelet-derived growth factor receptor (PDGFR), 822
Platelet endothelial cell adhesion molecule 1 (PECAM1), 242, 677
Plexin (PLXN), 595, 847, 848
Podoplanin (Pdpn), 600, 606, 607, 609, 826, 911
Pole, 28–39
Polycystin (PKD)
  PKD1, 730
  PKD2, 173, 709, 713, 730
Polysplenia, 168, 700, 702, 703, 709, 712, 732
Posterior leaflet, 916, 920
Post-transcriptional regulation, 289
Post-translational modifications, 354, 355, 730
Potassium channel genes (KCN)
  KCNE2, 1064
  KCNJ2, 1028, 1064, 1067
  KCNJ8, 1061, 1074
  KCNQ1, 1026, 1063, 1064, 1075
Potocki–Lupski syndrome, 519

PR domain containing 16 (PRDM16), 911, 982
Pre-B-cell leukemia homeobox 1 (PBX1), 651, 780, 788, 820, 855, 859
Premature translation termination codons (PTC), 318
Pressure overload, 162, 279–287, 373, 379, 381, 596, 1004, 1005
Primary atrial foramen, 482, 483, 485, 489
Primary atrial septum (PAS), 25–27, 60, 146, 149–152, 231, 232, 234, 482, 483, 485–488, 490, 574–576, 752
Primary cilia, 173, 177, 178, 579, 580, 711, 722, 725–727, 729, 730, 734
Primary cilia dyskinesia (PCD), 177, 178, 676, 711–713, 728
Primary electrical disorders (PEDs), 1034
Progenitor cells, 34, 36, 78, 80, 81, 83, 103–119, 157, 159, 161, 173, 174, 187, 191, 242, 248, 254, 272, 273, 296, 298, 301, 345, 356, 490, 611, 646, 648–653, 674, 689, 731, 821, 822, 842
Prostaglandin, 622, 665–667, 750, 753–755, 759, 838, 872, 906, 934
Protein kinase A (PKA), 287, 427–429, 1063, 1064, 1068, 1070
Protein kinase C (PKC), 286, 432, 997
Protein tyrosine phosphatase non-receptor type 11 (PTPN11), 59, 137, 471, 474, 522, 524, 560, 563, 564, 566, 763, 769, 980
Proteome, 262, 448–449
Pulmonary
  atresia, 94, 513, 515, 566, 596, 617–623, 650, 703, 711, 713, 742, 755, 835, 838, 844, 870, 906
  edema, 500, 589, 590, 933
  hypertension, 91, 94, 405, 463–466, 499–503, 556–558, 837, 906, 936, 971
  insufficiency, 755–759
  shunt, 906
  stenosis, 59, 60, 94, 97, 137, 301, 402, 463, 464, 471, 515, 524, 617, 621, 625, 626, 647, 649, 650, 653, 663, 665, 667, 703, 704, 756–759, 763, 768–770, 779, 789, 870, 880, 897
  trunk, 30, 32, 34–37, 79–81, 104, 111, 112, 115, 118, 119, 127–129, 132, 133, 172, 254, 646–649, 652, 653, 671, 673, 683–685, 690, 778, 787, 854, 859
  valve, 38, 81, 90, 91, 97, 211, 463–465, 500, 501, 557, 617, 618, 620–623, 646, 652, 653, 666, 668, 669, 673, 742, 745, 755–759, 768, 787, 938, 952
  valve replacement, 621, 626
  valve stenosis, 516, 742, 755, 756, 758, 759, 906
  vein, 20, 21, 25–27, 87, 104, 112, 146, 147, 230, 231, 461–463, 465, 483, 485, 486, 488, 587–591, 594–596, 601, 602, 604–612
  venous return, 408, 483, 485, 488, 521, 664, 668, 703, 872, 934
Pulmonary artery
  hypertension, 214, 500
  stenosis, 352, 471, 669, 871
Purkinje fiber, 79, 81, 134, 186, 188, 259, 260, 274, 1076

R
Ras/MAPK pathway, 524, 769
Rat, 377, 388, 437, 438, 488, 524, 1064
Rat sarcoma viral oncogene homolog/mitogen-activated protein kinase (RAS/MAPK), 636
Rattus norvegicus, *see* Rat
Reptiles, 217, 219, 230–235
Restrictive cardiomyopathy (RCM), *see* Cardiomyopathy
Retinaldehyde dehydrogenase 2 (RALDH2), 543, 858
Retinoic acid, 111–113, 116, 173, 241, 275, 352, 401, 404, 407, 409, 519, 609, 611, 636, 650, 677, 684, 690–691, 729, 787, 822, 823, 842, 858, 860
Retinoic acid inhibitors, 690
Rho-kinase, 432, 788, 823, 999
Ribonucleoprotein (RNP), 314, 320
Right atrial shunt, 554
Right atrium (RA), 15, 17, 25, 27, 40, 79, 87–89, 92, 104, 113, 135, 146, 147, 149–151, 170, 172, 186, 188, 209, 216, 219, 232, 234, 254, 418, 461–463, 483, 484, 486, 488, 490, 498, 499, 587–589, 594, 596, 600, 603, 606, 610–612, 636, 646, 648, 650, 666, 668, 684, 690–692, 700, 729, 765, 799, 806, 836, 870, 872, 873, 904–906, 916–919, 921, 951, 952
Right-to-left shunt, 501, 558, 619, 756, 837, 873
Right ventricle
  right ventricular hypertrophy, 501, 621, 756, 758
  right ventricular outflow tract obstruction (RVOTO), 406, 619, 622, 623, 627, 757, 871, 905

RNA
5´ end capping, 315–317
guanylyltransferase and 5´triphosphatase, 316
immature RNA, 314
mature RNA, 314
messenger RNAs (mRNAs), 138, 204, 255, 257, 262, 275, 283, 288, 289, 314, 315, 317–319, 322, 324, 410, 441, 445, 687, 856, 857, 995, 1001
microRNAs (miRNA), 288, 299, 303, 305, 317, 319, 322–324, 411, 445, 448, 993, 995, 996, 1077
miR-133, 288, 302, 303
miR-143, 302, 303
miR-145, 302, 303, 324
non-coding RNA, 283, 288, 302, 313–325, 410, 445, 469
polyadenylation, 317
poly-A site, 317
pre-mRNA splicing, 314, 317, 319–321
ribosomal RNAs, 319, 321
RNA editing, 314, 319
RNA maturation, 315
RNA methyltransferase, 316
RNA-seq RNA-binding proteins, 314, 996
small nuclear RNAs (snRNAs), 320, 321
small nucleolar RNAs (snoRNAs), 321
transfer RNAs (tRNAs), 319, 321
Robinow syndrome, 524
Ross procedure, 745
Rubella infections, 399, 403
Rubinstein–Taybi syndrome, 939
Ryanodine receptors (RYR)
RYR1, 419
RYR2, 419, 427, 431, 1000, 1029, 1062, 1067–1071
RYR3, 419

S
Saccharomyces
S. cerevisiae, 315, 317
S. pombe, 315
Sanger sequencing, 442, 443, 767
Sarcomere, 245, 374, 419–423, 426, 429, 473, 514, 516, 596, 597, 979, 983, 993–996, 1000, 1002, 1003, 1067, 1073
Sarcomeric proteins, 320, 468, 513, 516, 709, 714, 910, 979, 984, 1062
Sarcoplasmatic reticulum, 285, 286
Sarcoplasmic/endoplasmic reticulum calcium ATPase 2A (SERCA2A), 321
Second heart field (SHF)
development, 108, 273, 301, 491, 543, 564, 649, 651, 689
origin, 115
posterior, 649, 651
Second heart sound, 464, 500, 501, 621, 744, 757, 971
Semaphorin (SEMA)
SEMA3C, 111, 130, 131, 543, 780, 847, 848, 855, 857
SEMA3D, 488, 596, 611, 612
Semilunar valve, 90–91, 127, 132, 133, 499, 555, 623, 741–759, 762–770, 778–789, 835, 836
Senning/Mustard procedure, 668, 670
Septal leaflet, 90, 464, 545, 554, 556, 903, 904, 916, 918, 920, 921, 925
Septum
aorticopulmonary, 79, 80, 128, 841, 876
atrial, 20, 26, 60, 80, 111, 112, 149, 150, 172, 231–234, 461, 462, 465, 468–470, 472, 482, 483, 485, 487, 489, 490, 539, 554, 555, 604, 606, 611, 668
interventricular, 41, 43, 117, 170, 187, 188, 273, 302, 539, 544, 799
perimembranous, 489, 501
primum, 151
secundum, 152, 461, 485
Serum response factor (SRF), 109, 288, 297, 302, 346
SH3 and PX domains 2B (SH3PXD2B), 522, 525, 635
SHH, *see* Sonic hedgehog (SHH)
Short QT syndrome (SQTS), 1026, 1029, 1066–1067
Short stature homeobox 2 (SHOX2), 189, 190
Shroom family member 3 (SHROOM3), 709, 713, 714
Signal transducer and activator of transcription 3 (STAT3), 281, 997
Silencers, 303, 448
Simpson–Golabi–Behmel syndrome, 522, 525
Single nucleotide polymorphisms (SNPs), 301, 443, 446, 630, 631, 638, 675, 707, 813, 879, 881
Single ventricle, 216, 217, 245, 565, 623, 806, 869, 870, 872, 873, 938, 940, 941, 948
Sinoatrial node (SAN), 79, 81, 186–191, 259, 260, 427, 428, 607, 610, 1000, 1004
Sinuses of Valsalva, 90, 91, 808
Sinus node, 20, 91, 92, 230, 594, 607, 703, 704, 799, 1023, 1025
Sinusoidal veins, 88

Sinus venosus, 60, 81, 107, 112, 135, 146, 147, 160, 161, 187–190, 219, 227, 278, 461–463, 465, 468, 482, 488–489, 594, 600, 601, 603–607, 610, 611, 819
Sirtuins, 344, 346
Situs
  ambiguus, 699–704, 706, 708–711
  defects, 706–715
  inversus, 168, 175–178, 521, 526, 675, 676, 684, 699, 700, 702, 706, 708–714, 720–722, 724, 728, 733
  solitus, 168, 175, 176, 672, 675, 676, 684, 699, 700, 702, 712, 721, 728
Slit homolog 2 (SLIT2), 784
SMAD family member (SMAD)
  SMAD2, 516, 688, 708, 710, 711, 785, 788, 858, 889, 890, 894, 999
  SMAD3, 785, 813, 858, 889, 894, 999
  SMAD4, 297, 786, 886, 889–892
  SMAD6, 763, 767, 919
  SMAD7, 783
Small nuclear RNAs (snRNAs), *see* RNA
Small nucleolar RNAs (snoRNAs), *see* RNA
Smith-Lemli-Opitz syndrome, 474
Smoke, 405, 409
Smoothened (SMO), 277, 577, 580, 687, 726, 822
Smooth muscle cells (SMC), 24, 115–116, 160, 161, 241, 242, 244, 261, 346, 429–432, 605, 606, 608, 778, 823, 826, 857
Snail family zinc finger (SNAIL), 889, 893
SNPs, *see* Single nucleotide polymorphisms (SNPs)
Soc-2 suppressor of clear homolog (SHOC2), 474, 522, 524
Sodium channel voltage gated (SCN)
  SCN1B, 1059, 1074
  SCN2B, 1059
  SCN3B, 1059
  SCN4B, 1065
  SCN5A, 20, 22, 187, 193–195, 260, 305, 514, 517, 981–984, 1026, 1030, 1059, 1060, 1062, 1063, 1065, 1073
  SCN10A, 195, 305
Sonic hedgehog (SHH), 274, 277, 567, 568, 577, 609, 611, 687, 726–727, 729, 786, 858
Son of sevenless homolog 1 (SOS1), 244, 247, 474, 522, 524, 763, 769, 980
Sotos syndrome, 525
Spalt-like transcription factor (SALL)
  SALL1, 520, 521
  SALL4, 520, 521, 633
Splanchnic
  mesoderm, 78, 157, 482, 485, 488, 600, 601, 689
  plexus, 596, 601, 602, 607, 611
Splicing
  alternative, 314, 318, 320, 321, 324, 325, 445, 470
  spliceosome, 320
SRY (sex determining region Y)-box (SOX)
  SOX7, 507
  SOX9, 129, 137, 150, 283, 887
Stromal cell-derived factor 1 (SDF1), 813
Subclavian artery, 30, 61, 91, 131, 132, 136, 617, 622, 685, 747, 751–754, 768, 778, 781, 783, 787, 845, 856
Sudden cardiac death (SCD), 350, 623, 757, 759, 804, 805, 966, 968, 969, 971, 974–976, 987, 1024, 1028, 1058, 1066, 1068, 1069, 1077
Superior vena cava, 87, 88, 92, 147, 461, 462, 470, 588, 589, 606, 703, 806, 819, 872, 873, 907, 1023
SWI/SNF complex, 351–352, 956
SWI/SNF related matrix associated actin dependent regulator of chromatin (BRG1), 351–352, 956

T

Tachyarrhythmias, 191, 214, 974, 1024
T-box (TBX)
  TBX1, 61, 80, 109–114, 116–119, 132, 137, 299, 300, 302, 507, 509, 510, 513, 514, 519, 542, 543, 611, 619, 631–633, 636, 651, 653, 761, 768, 779, 780, 782–787, 821, 825, 842–844, 846, 848, 854–858, 860
  TBX2, 19, 20, 191–193, 235, 299, 300, 677, 921, 922
  TBX3, 19, 20, 25, 189–195, 229, 230, 260, 299, 300, 305, 521
  TBX5, 8, 27, 58, 109, 111–113, 190–195, 228, 232, 244, 246, 297–301, 305, 345, 352, 409, 449, 469, 474, 487, 510, 511, 514, 521, 522, 526, 527, 542, 544, 545, 560, 579, 595, 596, 609, 632, 633, 763, 769, 770, 826, 847, 880, 881, 887, 919, 942, 1047
  TBX15, 526
  TBX18, 8, 25, 111, 189–191, 299, 600, 606, 611, 732, 821, 822, 825
  TBX20, 192, 228, 243, 245, 297, 299–301, 469, 470, 510, 511, 542, 545, 632, 844, 846
Teratocarcinoma-derived growth factor 1 (TDGF1), 510, 512, 634, 635
Teratogens, 64, 399, 401, 408, 411, 630, 654, 706, 860

Tetralogy of Fallot (TOF), 60–62, 94, 111, 113, 136, 245, 301, 323, 324, 349, 352, 404, 490, 491, 499, 506, 512, 515, 527, 542, 617–627, 630–638, 646, 647, 649–652, 654, 674, 752, 756, 764, 768, 788, 806, 807, 812, 842–847, 849, 876, 975, 1028
TGA, *see* Transposition of the great arteries (TGA)
Thalidomide, 63, 399, 401, 407, 409, 410
Thick filament, 419, 420, 422–424, 429, 430, 432, 514, 979
Thin filament, 422, 424–426, 428–430, 432, 514, 516, 979, 1003
Third heart sound, 94
Thymus, 127, 136, 691, 784, 856
Thyroid gland, 127, 137
Timothy syndrome, 675, 980, 1026, 1028, 1065
Titin (TTN), 320, 419, 423, 429, 637, 981–984, 987, 1002, 1006, 1073
TOF, *see* Tetralogy of Fallot (TOF)
Total anomalous pulmonary venous connection (TAPVC), 594–597, 606–608, 611, 612
Total anomalous pulmonary venous return (TAPVR), 587–591, 596, 600–612, 701, 703, 933
Townes–Brock syndrome, 520
Trabeculation, 15–19, 24, 31, 41, 115, 205, 206, 210, 230–232, 235, 254, 272–275, 302, 351, 368, 539–541, 919
Transcription
  transcription activator-like effector nucleases (TALEN), 82, 439, 1001
  transcriptional network, 193, 194, 258, 296, 298, 301, 387, 632
  transcription factors, 7, 8, 27, 58, 59, 62, 78, 80, 83, 105, 107–110, 112, 117, 126, 129–131, 136, 137, 150, 158, 159, 162, 174, 177, 190–194, 228, 246, 275, 281, 283, 285, 287, 288, 296–303, 305, 318, 320, 344–346, 351, 387, 408, 409, 446, 510–511, 513–515, 521–523, 542, 546, 563, 577–579, 595, 608, 609, 611, 631–633, 635, 649, 650, 675, 677, 688, 689, 707–709, 714, 724, 728, 732, 764, 769, 770, 780, 783, 784, 786, 788, 789, 842, 846–848, 878–881, 886, 887, 889, 892–895, 898, 919, 925, 940, 956, 994, 996, 999, 1075–1077
Transcription factor AP-2 beta (TFAP2B), 318, 523, 633
Transcriptome, 107, 109, 116, 189, 257, 259, 262, 319, 321, 444–448, 814
Transforming growth factors (TGFs)
  TGFB2, 148, 691, 767, 780, 786, 860
  TGFBR1, 785, 858
  TGFBR2, 521, 707, 767, 781, 785, 786, 826, 858, 878
  TGFß, 242, 280, 288, 470, 510, 511, 514–516, 521, 675, 688, 710, 785–788, 858–860, 996, 999
  TGFß2, 158, 277, 786, 858
Transient receptor potential cation channel subfamily M member 4 (TRPM4), 1061
Translation, 248, 285, 289, 302, 314, 315, 317, 318, 322–324, 566, 860, 978
Transmembrane protein 43 (TMEM43), 982, 984, 1073
Transplantation, 82, 670, 720, 802, 936, 948, 969, 973–976, 1031
Transposition of the great arteries (TGA), 94, 171, 172, 215, 511, 542, 566, 626, 627, 647, 650–654, 664, 668, 669, 671–678, 683–692, 701, 703, 727, 767, 805, 806, 808, 809, 812, 821, 843, 845, 876, 877, 881, 904, 1031
Tricuspid
  atresia, 234, 405, 539, 869–874, 876–881, 886–898, 919
  valve, 60, 89, 90, 92, 463, 464, 468, 498, 499, 537–539, 542, 544, 545, 554, 556–558, 668, 757, 870, 877, 880, 886–888, 890, 893, 894, 897, 903–906, 909, 912, 917–921, 925, 952
Trisomy
  trisomy 13, 60, 61, 502, 518, 631, 949
  trisomy 16, 886, 896, 897
  trisomy 18, 61, 502, 518, 545, 631, 939, 949
  trisomy 21, 60, 61, 94, 489, 502, 518, 560, 561, 567, 574, 631, 638, 751, 768, 896, 912
Tropomyosin, 320, 422, 429, 1000, 1003
Troponin
  troponin C, 430
  troponin I (TNNI3), 516, 1003
  troponin T, 203, 972, 1003
Truncus arteriosus, *see* Common arterial trunk (CAT)
Tumor necrosis factor (TNF), 997
Turner syndrome, 61, 518, 631, 765, 787, 939, 949
Two-cilia hypothesis, 730, 731, 733

U
Ubiquitin
ubiquitination, 350, 609, 1071
ubiquitin proteasome system (UPS), 318
Ulnar–mammary syndrome, 521, 522
Univentricular heart, 215, 323, 506, 512, 677, 703, 869–881, 885–898, 934
Unroofed coronary sinus, 462

V
VACTERL, 684, 843, 845, 911, 939
V-Akt murine thymoma viral oncogene homolog (AKT)
AKT1, 285, 996
AKT2, 285, 996
Valsalva, 91, 802–805, 808, 819, 821
Valvuloplasty, 97, 742, 758, 759, 906
VANGL planar cell polarity protein 2 (VANGL2), 159, 650
Variants of unknown significance (VUS), 601, 709, 978, 983, 987
Vascular cell adhesion molecule 1 (VCAM1), 822
Vascular endothelial growth factor (VEGF)
VEGF-A, 274–277, 279, 281, 822, 823
VEGF-B, 274, 277, 281
VEGF-C, 274, 277, 281, 821
Vascular smooth muscle cells (VSMCs), 22, 24, 274, 277, 278, 605, 606, 609, 764, 784
Velocardiofacial syndrome, *see* DiGeorge syndrome (DGS)
Vena cava, 461, 600, 606, 700, 701, 703, 878
Venous pole, 12, 25–27, 78–80, 104, 107, 108, 110–112, 115, 117–119, 146–150, 173, 187, 228, 482, 483, 538, 575, 577, 594, 600, 601, 606, 608–611, 646, 649
Ventricular
arrhythmias, 100, 260, 756, 758, 759, 966, 975, 976, 985, 1026–1028, 1031, 1058–1075
conduction system, 17, 22, 186, 193–194, 230, 260
fibrillation, 812, 918, 1024, 1029, 1068, 1074
preexcitation, 904, 920
septation, 22, 39, 82, 217, 228, 229, 232, 234, 235, 537, 538, 541, 542, 544, 546
septum, 19, 22, 27, 38–41, 89, 186, 193, 217, 229–232, 234, 242, 472, 498, 536, 537, 539, 540, 542–546, 554–556, 663, 664, 666–668, 673, 742, 753, 755, 917, 918, 938, 1071
Ventricular septal defect (VSD)
inlet, 498, 502, 506, 536, 539, 540, 543–544, 554, 555
muscular, 94, 489, 498, 499, 501, 502, 512, 518, 519, 544–545
perimembranous, 498–502, 511, 516, 523, 539, 542, 545
supracristal, 402, 498, 506
Vertebrates, 7, 24, 82, 83, 118, 173, 175, 186, 188, 202, 217, 219, 227–230, 232, 235, 236, 255, 296, 302, 351, 353, 371, 372, 515, 542, 710, 711, 720, 731, 733, 818, 848, 879, 888, 942
Volume overload, 284, 499, 502, 756, 757
VSD, *see* Ventricular septal defect (VSD)

W
Whole exome sequencing (WES), 59, 64, 65, 445, 512, 514–517, 523, 563, 707, 710, 712, 713
Whole genome sequencing (WGS), 59, 64, 65, 445
Williams–Beuren syndrome, 519, 631, 742
Williams syndrome, 62, 352, 756, 764, 766, 911
Wingless-type MMTV integration site family (WNT)
WNT5A, 108, 112, 114, 242, 411, 520, 524, 650, 651, 675, 692, 783, 822, 857
WNT, canonical, 108, 242, 411, 650, 822, 857
WNT ligands, 278
Wolff-Parkinson-White syndrome (WPW), 904, 906, 1030, 1031
Wolf–Hirschhorn syndrome, 348, 519, 939

X
Xenopus laevis, *see* Clawed frog

Y
Yeast-two-hybrid (Y2H), 450

Z
Zebrafish, 83, 134, 135, 174, 175, 190, 191, 202–206, 210, 228, 230, 243, 245, 305, 348, 349, 352, 353, 368, 369, 371–379, 387, 388, 409, 411, 437, 439, 440, 511, 512, 517, 563, 609, 707, 710, 713, 722–724, 731–733, 779, 782, 783, 788, 854, 858, 879, 941, 951, 954, 956, 1002–1005, 1072, 1076
Zic family member (ZIC)
ZIC1, 129
ZIC2, 177

Zic family member (ZIC) (*cont.*)
ZIC3, 177, 321, 514, 515, 564, 565, 633, 635, 672, 686, 688, 708, 709, 780, 940, 949
Zinc finger nucleases (ZFN), 439
Zinc finger protein FOG family member 2 (ZFPM2), 61, 632, 649, 878–879, 881, 886, 891–892, 895, 897, 898, 919